

RRFM

EUROPEAN RESEARCH
REACTOR CONFERENCE **2012**



Transactions

Prague, Czech Republic
18 - 22 March 2012



AREVA

RRFM/IGORR 2012 Gold Sponsor



ENS CONFERENCE

organised in collaboration with:



International Group on Research Reactors



IAEA

International Atomic Energy Agency

© 2012
European Nuclear Society
Rue Belliard 65
1040 Brussels, Belgium
Phone + 32 2 505 30 54
Fax +32 2 502 39 02
E-mail ens@euronuclear.org
Internet www.euronuclear.org

ISBN 978-92-95064-13-3

These transactions contain all contributions submitted by 16 March 2012.

The content of contributions published in this book reflects solely the opinions of the authors concerned. The European Nuclear Society is not responsible for details published and the accuracy of data presented.



Programme Committee

Edgar Koonen, SCK-CEN, Belgium (Chairman)
Gilles Bignan, CEA/RJH, France (*IGORR Chair*)
Pablo Adelfang, IAEA, Austria
Helmut Böck, TU-Vienna, Austria
Vladimir Broz, NRI Rez, Czech Republic
Philippe Auzière, AREVA NC, France
André Chabre, CEA, France
Heiko Gerstenberg, TU-München, Germany
Andrea Borio di Tigliole, LENA / Università degli Studi de Pavia, Italy
Dominique Geslin, CERCA (AREVA Group), France
Istvan Vidovszky, AEKI, Hungary
José Marques, Instituto Tecnológico e Nuclear, Portugal
Gunter Damm, Jülich Research Center, Germany
Jacob de Vries, Delft Reactor Institute, The Netherlands
Stephen Curr, Rolls-Royce plc, United Kingdom
Peter Schreiner, GKSS Research Centre, Germany
Sandro Tozser, IAEA, Austria
Pascal Claude, AREVA, France (*IGORR*)
Douglas L. Selby, ORNL, United States (*IGORR*)
Jose Lolich, Balseiro Institute, Argentina (*IGORR*)
Danas Ridikas, IAEA, Austria (*IGORR*)



Monday 19 March 2012

2012 PROGRESS REPORT ON HEU MINIMIZATION ACTIVITIES IN ARGENTINA

Pablo Cristini, Liliana de Lio, Daniel Gil, Alfredo G. Gonzalez,
Marisol López, Oscar Novara, Horacio Taboada

COMISIÓN NACIONAL DE ENERGÍA ATÓMICA
Av. Del Libertador 8250 (1429) Buenos Aires, Argentina

An extension of the original CNEA-NNSA DoE contract for the RA-6 reactor core conversion was signed in March 2010 to enhance the final national HEU inventories minimization. Previously, CNEA reserved a small inventory of HEU for further R&D uses in fission chambers, neutronic probes and standards. This minimization comprises all fresh and irradiated HEU remnant inventories coming from fuels and Mo99 targets fabrication and irradiated HEU-oxides retained in production filters and solutions. Those inventories are being recovered, down-blended into LEU and purified or, in few cases and due to cost-benefit considerations, declared wastes.

CNEA has a R&D program focused on the development of the fabrication technology of U-Mo monolithic (Zry-4 cladding) miniplates to support the qualification activities of the RERTR program. Some monolithic 58% enrichment and LEU 8%Mo and U10%Mo miniplates and plates were and are being delivered to INL-DoE to be irradiated in the ATR reactor core. Full scale plates will take part of the ALT FUTURE irradiation at the BR II Belgium reactor.

CNEA, a worldwide leader on LEU technology for fission radioisotope production is providing Brazil with 1/3 of the national requirements on Mo99 by weekly deliveries. ANSTO is firmly producing several fission radioisotopes batches by week. During November and December 2011 the production in the new fission Mo-99 facilities of the Atomic Egyptian Agency (AEA) in Inshas Atomic Center, Egypt was demonstrated. To support these activities CNEA is refurbishing in Ezeiza Atomic Center a set of radiochemical cells where the spent LEU based material retained in the filters of the Mo99 production facility of CNEA along these last 10 years will be separated from wastes, recovered and purified to be reutilized in this or in other nuclear applications. CNEA is strongly committed to improve the diffusion of LEU target and radiochemical technology for radioisotope production and target and their process optimization.

Future plans include:

- Development of waste separation techniques optimization.
- Fabrication and delivering to INL to be irradiated in the ATR core of complementary U-8%Mo and U-10%Mo monolithic miniplates and development and fabrication of LEU very high density monolithic and dispersed U-Mo fuel plates with Zr cladding for the FUTURE-MONO experiment in the frame of the RERTR program.
- Optimization of LEU target and radiochemical techniques for radioisotope production and waste separation, recovery and purification of irradiated LEU inventories contained in fission Mo99 production filters..

1. Introduction:

In March 2010, a supplementary agreement between CNEA and NNSA-DoE to the original one - involving the RA-6 reactor core conversion and the exportation to the US of 42 SNF in terms of the SNF FRR Program- was signed by both parties. This was done in the frame of the efforts for

HEU minimization for civilian uses. From remaining HEU inventories, used in the past for fuel and target fabrication, a small amount of it for R&D purposes was reserved by CNEA (for further uses in fission chambers, neutronic probes and standards fabrication).

This minimization means the recovery, blending down and purification of fresh and irradiated HEU inventories contained in scraps from fuel and target fabrication and in fission Mo99 production filters, or the disposition as waste of those few inventories whenever its recovery is not advisable due to a cost-benefit consideration. These tasks are taking place and the corrected deadline is December 2013.

2. New tasks on HEU minimization

Previously it was informed about the inventories classification into 6 groups (see Table 1)

Description	Group Number	Form	U Mass (kg)	Enrichment	235 U Mass (kg)
Irradiated Mo-99 Targets And Solutions	1	Solid and Liquid	1.928	89.73%	1.73
UF6 Cylinder	2	Gas / Solid (UO₂F₂)	0.65	90.14%	0.59
Miscellaneous Solids (alloys, metal)	3	Solid	0.397	87.15%	0.346
Miscellaneous Solutions	4	Liquid	0.228	89.91%	0.205
Materials declared waste to dispose	5	Solid	0.505	89.97%	0.453
Ingot for MEU-Mo/Zr Miniplates Fabrication	6	Solid	0.344	88.66%	0.305
TOTAL			4.05		3.63

Tab. 1 HEU inventories

Regarding the progress of the tasks involved the present status can be seen in Table 2. Most of them are already finished.

Group 1 comprises the refurbishment of a radiochemical laboratory (LFR lab), licensing of two transport casks, for irradiated solutions and solids contained in cartridge filters, among of the proper recovery, downblending and purification of the HEU inventory in the hot cells of the LFR lab. This task is ongoing and the actualized deadline is December 2013.

Group 2 comprised the opening of a valve stucked 5A type cylinder containing a partial hydrolized UF6 inventory, and the recovery, downblending and purification of the HEU inventory into LEU. This task was finished on October 2010¹

Group 3 implied the downblending of an HEU-Al inventory through cast melting. This task was finished during September 2010.

Group 4 is made of several HEU solutions in aqueous and organic media. It was characterized and partially downblended and partially wasted. It finished on May 2011.

Group 5: this inventory will be managed as waste and located in a new storage site, expecting to finish this task by November 2012.

Group 6 included the blending down of a HEU ingot to 58% enrichment (at U235) to make ME U-10%Mo and U-8%Mo based miniplates with Zr cladding. The agreement includes the exportation to INL of miniplates for irradiation testing under the RERTR program. This task is being accomplished with a first delivery made in April, 2010 and a final second one scheduled for March 2012^{II}. Finally, the remaining 58% enrichment inventory will be downblended to LEU-10%Mo or LEU-8%Mo for full scale plate fabrication in the frame of the RERTR programme.

GROUP	DESCRIPTION	HEU MASS (Kg)	RECOVERED AND DOWNBLENDED (Kg)	DECLARED WASTE OR TO BE WASTED (Kg)
1	IRRADIATED MATERIAL	1,928	-	-
2	5A CYLINDER CONTAINING HEU-F6	0,649	0,628	0,021
3	SOLIDS	0,378	0,374	0,004
4	LIQUIDS	0,228	0,140	0,086
5	MATERIAL TO DECLARE WASTE	0,505	0	0,505**
6	HEU FOR MEU-Mo MINIPLATES & LEU-Mo PLATE FABRICATION	0,344	0,310*	0,034
TOTAL		4,032	1.452	0.650

Tab. 2 Recovery and downblending into LEU

3. R&D on VHD fuels

The development of CNEA miniplates using monolithic UMo alloy cores involves the use of the well known Zr alloy named Zircalloy-4 (Zry-4). Zry-4 is commonly used as nuclear fuels cladding for nuclear power plants. In this case Zry-4 is employed as cladding in top, cover and frame. The fuel material in the core is an alloy between Uranium (U) and Molybdenum (Mo) with different contents of Mo (between 7-10% wt/wt). These Mo percentages are enough to retain the gamma phase at low temperature but also not to penalize the reactor neutronics due to the capture cross section of Mo95 isotope. The fabrication process includes hot and cold co-rolling. Regarding hot co-rolling temperature between 575° - 660°C the presence of some amount of alpha plus delta phases were revealed by analyses. Also although hot rolling at 800-850°C takes place in gamma phase (with metastable bcc crystal structure), an important dog bone zone^{III} and Ux-Zry-Moz phases^{IV} were found. To avoid both drawbacks an intermediate temperature at 700°C was employed. Different rolling temperatures produced different effects:

- hot co-rolling at 650°C shows a thin interlayer, but no difference in the composition of the initial materials of cover, frame and fuel coupon.

- A small interlayer appear at the hot co-rolling at 700°C which is a little different from the 650°C, and a dog bone appeared at both coupon ends, but less relevant than the one observed at 800°C.

Rx, TEM, EDAX and microprobe analyses showed an interlayer between the Zry-4 covers and the UMo coupon, formed with UxZry and UxZryMoz phases, that are in concordance with other studies^V. Observed effects enabled improving the fabrication conditions.

Regarding the pack assembly it is essential to prevent gaps and oxygen presence as well as impurities by achieving an intimate fit between Zry-4 and UMo fuel components and clean surface contact. In other case that could be areas for potential debonds or undermine optimum bonding during pack reduction.

In all cases TIG welding was employed in the same conditions, and different kind of interlayers were observed. It can be concluded that this procedure do not contribute to the decomposition of the UxMo.

Conclusions: for plate hot co-rolled at 800°C a marked dog bone regions were observed at each end of plate with are characteristic of the ductility difference between the U-xMo alloy and Zry-4 at this temperature, but not roll speed effects were observed. This presence could be diminished by using a longer lead or ends, but not disappeared. No dog bone zone was observed in miniplates co-rolled at 650°C.

LEU target and radiochemical technology for Mo99 and other fission radioisotopes production:

It is by far the largest contribution of CNEA to HEU minimization for civilian uses. It was already informed about the circumstances of the final cutoff to HEU supply for Mo99 production and how CNEA found an adequate LEU replacement without changing its radiochemical technology.

CNEA has developed and is using high-density LEU-aluminum dispersion targets. The target meat has a density of 2.9 gU/cm³ obtained by increasing the ratio of uranium aluminide to aluminum in the target meat. The mass of U-235 in the target meat is about twice that of conventional uranium-aluminum alloy targets.

CNEA was able to convert to LEU-based production in the same set of hot cells that were being used for HEU-based production, without interrupting Mo-99 production. Targets are irradiated in the RA-3 reactor at CNEA's Ezeiza Atomic Center near Buenos Aires. Target processing is carried out in a hot cell facility at the Ezeiza site. Process wastes are also managed at the site.

CNEA's development showed that there are no technical barriers to conversion of fission Mo-99 production from HEU targets to LEU targets. Production using LEU targets is technically feasible and is being carried out by CNEA in Argentina and by the Australian National Nuclear Science and Technology Organisation. ANSTO is using CNEA's radiochemical technology and LEU targets to produce Mo-99.

This new LEU technology satisfies the most stringent requirements of quality for its use in nuclear medicine applications. Mo-99 purity has been consistently higher than that produced using HEU targets^[VI]. Also in September 2005, CNEA began the regular production of high quality fission I-131, a by-product of Mo-99 production, meeting also international quality standards.

HEU-LEU production process comparison costs reveal that this new technology has no significant overall cost of 10% ^[VII]. Due to the fact that CNEA was able to duplicate the LEU-based radioisotope weekly production rate, since 2010 provides Mo99 to Brazil covering 1/3 of the Brazilian market.

During November and December 2011 the production in the new fission Mo-99 facilities of the Atomic Egyptian Agency (AEA) in Inshas Atomic Center, Egypt was demonstrated. This achievement was the result of the collaboration between several technical groups of CNEA, INVAP and AEA involved in this task, like experts in Mo99 production, product quality control, design and facility building and radiochemical cells and laboratory equipment.

To support these activities CNEA is refurbishing a set of radiochemical cells where the spent LEU based material retained in the filters of the Mo99 production facility along these last 10 years will be separated from waste, recovered and purified to be reutilized in this or in other nuclear applications.

4. **Conclusions:**

FINAL HEU MINIMIZATION: CNEA is minimizing the remnants HEU inventories, both fresh and irradiated from fuel and target fabrication scraps and fission RI production solutions and filters. All these tasks are scheduled to finish during December 2012.

R&D ON LEU VHD FUELS: CNEA is actively supporting both R&D activities to achieve solutions for core conversions.

LEU TECHNOLOGY FOR FISSION RI PRODUCTION: No technical, quality or financial reasons make disadvantageous changing from HEU to LEU for fission Mo99 and other RI production. CNEA leads LEU based isotope production technology, and with INVAP built all LEU-based production systems in Australia and Egypt. This is by far the largest contribution of CNEA to the HEU minimization for civilian uses.

^I L. N. Aldave, H. Blanco Bello, A. A. Bonini, L. I. De Lio, L. A. Dell'Occhio, M. Falcón, T. Feijoo, A. Gauna, D. A. Gil, A. Rodriguez y J. Valdez. 2010 RERTR International Meeting, Lisbon, Portugal, 10-14 October 2010.

^{II} M.López, A. González, R. González, F. Rice, H. Taboada, D. Wachs. 2010 RERTR International Meeting, Lisbon, Portugal, 10-14 October 2010.

^{III} J. L. Snelgrove, G. L. Hofman, C. L. Trybus, and T. C. Wiencek. Development Of Very-High-Density Fuels By The Rertr Program. 19th International Meeting on Reduced Enrichment for Research and Test Reactors (RERTR). Seoul, Republic of Korea. October 7-10, 1996.

^{IV} M. K. Meyer, C. L. Trybus, G. L. Hofman, S. M. Frank, T. C. Wiencek. Selection and Microstructures of High Density Uranium Alloys. 20th International Meeting on Reduced Enrichment for Research and Test Reactors (RERTR) Jackson Hole, WY (US), 10 Oct 1997.

^V J. L. Snelgrove, G. L. Hofman, C. L. Trybus, and T. C. Wiencek. Development Of Very-High-Density Fuels By The Rertr Program. 19th International Meeting on Reduced Enrichment for Research and Test Reactors (RERTR). Seoul, Republic of Korea. October 7-10, 1996

^{VI} Durán, A. 2005. Radionuclide Purity of Fission Mo-99 Produced from LEU And HEU. A Comparative Study. 2005 International RERTR Meeting, Boston, Massachusetts, USA, November 6-10, 2005. Available at http://www.rertr.anl.gov/RERTR27/PDF/S8-3_Duran.pdf.

^{VII} Cestau D., A. Novello, P. Cristini, M. Bronca, R. Centurión, R. Bavaro, J. Cestau, E. Carranza. HEU and LEU cost comparison in the production of molybdenum-99. 2008 International RERTR Meeting, Washington, DC, USA, 5-9 October 2008, and Cestau D., A. Novello, P. Cristini, M. Bronca, R. Centurión, R. Bavaro, J. Cestau, E. Carranza. 2007. HEU and LEU comparison in the production of molybdenum-99. 2007 International RERTR Meeting, Prague, Czech Republic, Sep. 23-27, 2007. Available at http://www.rertr.anl.gov/RERTR29/PDF/6-4_Cestau.pdf

U.S. PROGRESS IN THE DEVELOPMENT OF VERY HIGH DENSITY LOW ENRICHMENT RESEARCH REACTOR FUELS

M.K. MEYER, D. M. WACHS, J.-F. JUE, D.D. KEISER, J. GAN, F. RICE,
A. ROBINSON, N.E. WOOLSTENHULME, P. MEDVEDEV

*Idaho National Laboratory
PO. Box 1625
Idaho Falls, ID 83415*

G.L. HOFMAN, Y.-S. KIM

*Argonne National Laboratory
9700 S. Cass Avenue
Argonne, IL 60439*

ABSTRACT

The effort to develop low-enriched fuels for high power research reactors began world-wide in 1996. Since that time, hundreds of fuel specimens have been tested to investigate the operational limits of many variations of U-Mo alloy dispersion and monolithic fuels. In the U.S., the fuel development program has focused on the development of monolithic fuel, and is currently transitioning from conducting research experiments to the demonstration of large scale, prototypic element assemblies. These larger scale, integral fuel performance demonstrations include the AFIP-7 test of full-sized, curved plates configured as an element, the RERTR-FE irradiation of hybrid fuel elements in the Advanced Test Reactor, reactor specific Design Demonstration Experiments, and a multi-element Base Fuel Demonstration. These tests are conducted alongside miniplate tests designed to prove fuel stability over a wide range of operating conditions. Along with irradiation testing, work on collecting data on fuel plate mechanical integrity, thermal conductivity, fission product release, and microstructural stability is underway.

1. INTRODUCTION

Analysis of the possibilities for very high enrichment fuel for converting the highest power research reactors began in 1996. Investigation of possible fuel phases converged quickly on uranium alloys stabilized in the gamma phase by molybdenum or a combination of niobium and zirconium, or molybdenum with a ternary element addition as the primary candidates. The RERTR-1 and RERTR-2 experiments were configured as a screening test of these fuels, and began irradiation in the Advanced Test Reactor in 1997. [i] Results of these experiments indicated superior performance of U-Mo fuel with more than 6 wt.% molybdenum over U-Nb-Zr. Global interest in eliminating the use of high-enriched uranium and the promising results from these experiments stimulated research around the world, and aggressive programs began to develop and deploy this technology. Although U-Mo itself has proven to be a robust fuel that is stable under irradiation to high burnup, challenges arose in implementing this fuel in aluminum-based research reactor fuel system operating at high power density. Unsatisfactory fuel plate swelling behavior in this system is caused by irradiation stability of the fuel/matrix interaction layer. [ii,iii,iv] Progress has been made using additives to the fuel matrix and coating of fuel particles to address this issue.

In the U.S., this problem and the requirement for very high uranium density led to the development of monolithic fuel technology as an alternative to dispersion fuel. Monolithic fuel is the primary candidate for U.S. LEU fuel development. As the U.S. program moves from the research phase toward qualification of these fuels, there have been many

successes and, as is to be expected, some issues uncovered related to scaling up of the process used for production of research quantities of fuel to fabrication of large, fully prototypic fuel elements.

2. STATE OF DEVELOPMENT OF U-Mo MONOLITHIC FUEL

Current major efforts in the development of monolithic fuel include the RERTR-12, AFIP-6 MkII, AFIP-7, and RERTR-FE irradiation campaigns. Additional information regarding these tests can be found elsewhere in these proceedings. [v] The state of development of U-Mo monolithic fuel is defined both by the results of these irradiation tests and the results of scaling the fabrication process to supply increasingly larger fuel plates with manufacturing tolerances meeting the requirements for production fuel elements.

The RERTR-12 test was designed to provide information on the fission rate and fission density dependence of fuel swelling to very high burnup ($>1 \times 10^{22}$ fissions/cm³), the effect of variations in the ratio of fuel and cladding thickness on irradiation performance, and information on blister threshold temperature as a function of fission density, irradiation conditions and fuel/clad thickness ratio. The RERTR-12 test includes 56 small fueled miniplates that envelope the anticipated LEU fuel operating conditions of U.S. high power research reactors. As of March 2012, this experiment is entering its fifth and final cycle of irradiation. Postirradiation examination of the first two test capsules is complete, and has been successful in providing data on the steady state irradiation behavior of U-Mo monolithic fuel.

Blister threshold testing conducted on miniplates prior to the RERTR-12 campaign resulted in a mean blister threshold temperature of 391°C ($\pm 27^\circ$) at a fission density of 4.25×10^{21} fissions/cm³, which is similar to uranium aluminide and uranium silicide dispersion fuel. Data from the RERTR-12 experiment, however, indicates a decrease in blister threshold temperature of approximately 100°C at equivalent burnups. The reason for this decrease is not fully understood, but may be caused by differences in the fabrication process used to produce these test specimens; this process was developed to minimize variations in areal fuel loading. The higher blister threshold temperatures measured in earlier experiments indicates that the currently observed low blister threshold temperature is not caused by a fundamental flaw in the U-Mo monolithic fuel system. An intensive effort is underway to fully understand the cause for this change in blister threshold temperature and actions that must be taken to correct it.

The AFIP-6 MkII experiment is a bounding test conducted at very high power density (surface heat flux > 500 W/cm²) designed to uncover any deficiencies in the performance of full-size fuel plates under these conditions. The AFIP-6 MkII experiment completed one long cycle of irradiation before an issue related to flow induced vibration was noted; this issue is currently being evaluated. The first fuel plate removed from the experiment was examined in the ATR canal, and appears to have performed well.

The AFIP-7 experiment was designed to provide engineering-scale performance data on monolithic fuel in an element configuration prototypic of that used in most research reactors. The AFIP-7 experiment consists of four plates with design very similar to Advanced Test Reactor plate five. The test successfully completed the planned two cycles of irradiation in the ATR. A specially designed channel probe was used to provide data on the dimensional stability of the fuel element coolant channels after each irradiation cycle to ensure that the fuel element configuration was dimensionally stable and verify that coolant channel dimensions did not change during irradiation because of fuel plate shape changes. This aspect of performance was confirmed by this test, removing an uncertainty in the use of monolithic fuel.

Fabrication of full-size fuel foils for the RERTR-FE demonstration element in ATR began in October of 2011. The RERTR-FE is a demonstration of a full-size element (sans burnable poison plates) in the ATR driver core. U-Mo foils for this demonstration must meet the rigorous dimensional specifications for use as ATR driver fuel elements. The required length of these foils (121.9 cm) and the tight fabrication tolerances resulted in a high foil rejection rate on the initial production runs. The process used to make U-Mo foils is currently being evaluated to improve the process yield and to ensure that fabrication is prototypic. Fabrication of RERTR-FE fuel plates continues to further refine the hot isostatic pressing and plate finishing and inspection processes.

After the completion of the RERTR-FE test, qualification of monolithic base fuel technology will proceed with DDE (Design Demonstration Experiments) for the U.S. university research reactors to demonstrate that the specific LEU fuel designs for these reactors are suitable for use. The Base Fuel Demonstration in the Advanced Test Reactor will be a multi-element test to provide assurance of consistent irradiation performance for larger scale production runs of fuel.

The RERTR-13 test, currently being irradiated in ATR, is the first in the series of 'complex' fuel tests to be conducted to inform the development of fuels with burnable poisons and complex geometries. The RERTR-13 test will provide basic data on the performance of B_4C and ZrB_2 burnable poisons, both as thin foils that could be incorporated in a cladding layer and dispersed along with U-Mo particles dispersion fuel.

Other important areas of development are progressing in support of fuel qualification. In particular, fuel modeling and measurement of mechanical and thermal properties are important tasks currently in progress. The discreet nature of the interface between the U-Mo foil and the aluminum cladding differs from that in a plate-type dispersion fuel. Fuel plate mechanical models are being developed to understand the evolution of the stress state in U-Mo monolithic fuel during operation. These models take into consideration the stress introduced during the fabrication process and how that stress evolves during irradiation due to swelling and creep. Initial thermal diffusivity measurements of irradiated U-Mo have been made and tensile measurements of prototypic U-Mo foils and bend tests of irradiated U-Mo are under way.

3. DISCUSSION & CONCLUSION

Development of new nuclear fuel systems requires a sustained effort. Because of the fuel operating environment and the long time for an experiment cycle to complete, development of commercially viable fuels routinely spans two decades or more. The nature of materials under irradiation increases the possibility for unexpected behaviors.

The occurrence of low blister threshold temperatures in the RERTR-12 experiment presents a significant new challenge in the understanding of the fuel system, but does not appear to be a fundamental flaw. The rapid scaleup of fuel fabrication technology from the bench scale to production of large prototypes with tight tolerances has resulted in a low production yield and the requirement to further develop the U-Mo foil fabrication process.

Despite these issues, there has also been significant forward progress in the development of U-Mo monolithic fuel. This progress includes confirmation of the stability of the coolant channel dimensions in a fuel element configuration and confirmation of good steady state fuel performance over a wide range of fission densities and fission rates.

Although some hurdles remain prior to fuel qualification, the development of monolithic fuel continues to be promising. The U.S. program is working to understand and correct the issues in fabrication and blister temperature performance that have been recently identified.

4. REFERENCES

- ⁱ S.L. Hayes, C.L. Trybus, M.K. Meyer, "Irradiation Testing of high-density Uranium Alloy Dispersion Fuels," Proceedings of the 1997 International Meeting on Reduced Enrichment for Research Reactors, ANL/TD/TM99-06, Argonne National Laboratory (1999).
- ⁱⁱ J.M. Hamy, P. Lemoine, F. Huet, B. Guigon, C. Jarousse, J.L. Emin,, "Status as of March 2004 of the French UMo Group Development Program," Transactions of the 8th International Topical Meeting on Research Reactor Fuel Management (2004).
- ⁱⁱⁱ A. Leenaers, S. Van Den Berghe, E. Koonen, L. Saannen, M. Verwerft, C. Jarousse, F. Huet, M. Trotbas, M. boyard, S. Guillot, "Post-irradiation Examination of Uranium-7wt% Molybdenum Atomized Dispersion Fuel," Transactions of the 8th International Topical Meeting on Research Reactor Fuel Management (2004).
- ^{iv} G.L. Hofman, Y.S. Kim, M.R. Finlay, J.L. Snelgrove, S.L. Hayes, M.K. Meyer, C.R. Clark, F. Huet, "Recent Observations at the Postirradiation Examination of Low-Enriched U-Mo Miniplates Irradiated to High Burnup," Transactions of the 8th International Topical Meeting on Research Reactor Fuel Management (2004).
- ^v N.E. Woolstenhulme, D.M. Wachs, M.K. Meyer, "Status Report and Future Plans Regarding irradiationTesting of Low-Enriched Monolithic Fuel Designs," these proceedings.

INTERNATIONAL CENTRES OF EXCELLENCE BASED ON RESEARCH REACTORS

K. ALLDRED, S.M. TOZSER, P. ADELFGANG

*International Atomic Energy Authority
Wagramer Strasse 5, A-1400 Vienna – Austria*

ABSTRACT

A number of high flux research reactors were, or will be constructed. Each of these high flux facilities has the potential to be an important regional or International Centre of Excellence based on Research Reactors (ICERR) and scientific hub for research and materials investigations. Some are so organized currently, but for many there is a strongly national focus and scope for a significant expansion of their international role. There are manifold benefits of an expanded international role both for the ICERR's themselves and for the institutes that affiliate with them. These benefits include increased utilization and financial stability, increased international prestige, and enhanced scientific resources and capabilities.

There are significant hurdles to obtaining the benefits from an expanded international role. For example, to achieve its full potential an ICERR must accommodate scientists from other nations, and include the plans and aspirations of the international community in the ICERR governance. The ICERR must also fully meet the national responsibilities for safety and security. Balancing these potentially conflicting requirements and finding a path through the organisational and legal issues is a significant challenge for any institute. The existing ICERR's therefore provide important case studies and examples of best practice that could inform the actions of other potential ICERR's.

This paper describes an IAEA initiative to encourage and support the formation of new ICERR's, strengthen existing ones, and increase training resources available to Member States. The initiative will seek to share best practice and facilitate meetings and technical exchanges between the existing and potential ICERRs, and between the potential ICERR's and potential subscribing or affiliating institutes.

1. Introduction

A number of high flux research reactors were, or will be constructed. Each of these high flux facilities has the potential to be an important regional or International Centre of Excellence based on Research Reactors (ICERR) and scientific hub for research and materials investigations, see Table 1. Some are so organized currently, but for many there is a strongly national focus and scope for a significant expansion of their international role.

Country	Facility	Neutron Spectrum
Belgium	BR2 / MYRRHA	Thermal
China	China Advanced Research Reactor (CARR)	Thermal
China	China Experimental Fast Reactor (CEFR)	Fast
France	Jules Horowitz Reactor	Thermal
Germany	FRM-II	Thermal
Holland	HFR	Thermal
Japan	Joyo	Fast
Japan	Monju	Fast
Kazakhstan	IGR	Thermal / Fast
Russia	SM-3	Thermal
Russia	MIR.M1	Thermal
Russia	BOR-60	Fast
Russia	Multifunctional fast neutron research reactor (MBIR)	Fast
USA	ATR	Thermal
USA	HFIR	Thermal

Tab 1: Examples of Existing and Planned High Flux Research Reactors

Several Member States are initiating or preparing for nuclear power programmes, and are faced with significant challenges for the timely development of the needed human resources. A framework of national competences must be rapidly developed both for the operational and the regulatory aspects of the nuclear power program. This includes establishing or strengthening academic institutions in the relevant disciplines and developing specific training facilities for programme managers as well as younger staff.

The IAEA has a new initiative on International Centres of Excellence based on Research Reactors (ICERR) that is intended to help Member States to create and sustain these competences. The ICERRs will be based on highly experienced organizations that have state-of-the-art nuclear reactor facilities and a broad range of world-class expertise. They will be able to accept international trainees and scientists to work at the ICERR (secondees) and participate in joint scientific and technical projects. The ICERR will fill the gap between academic education and commercial, product-specific training by providing “Nuclear Education” programs that offer direct experience of working in nuclear facilities in addition to formal training.

It is envisaged that the ICERRs will provide powerful options for sustainable competence building. They are important sources of expertise as well as examples of best practice for nuclear safety culture and programme management that will serve as valuable references for new nuclear programmes. In addition, the ICERR will provide a platform for ongoing joint research and peer-to-peer education. Affiliated institutions will be able to rapidly develop and sustain their own research programmes through their access to the ICERR’s physical and educational resources. Thus, by affiliating with one or more ICERRs, Member States embarking on new nuclear programs will have an opportunity to shorten learning curves, accelerate the human resources development effort and reduce its overall costs.

The new IAEA initiative will develop the ICERR concept, document the available ICERR capabilities, facilitate development of ICERR networks and integrate the ICERR option into the Agency’s support for the development of nuclear infrastructure, and nuclear education and training.

2. The ICERR Concept

An ICERR is a leading scientific centre that is open to international participation and welcomes scientists from other countries to work on joint or similar programs. An ICERR has the facilities, staff and programs to support the generation of one or more world class international competencies and development of new leading edge technologies.

There is no standard format for an ICERR; there are many viable options and it is expected that the structure will be tailored to meet the specific needs of each ICERR and its affiliates. However, common to all is a high performance research reactor employing best practices in nuclear safety, and with a range of ancillary hot cells and laboratories (eg for fuel and material investigations), services (eg fuel management, waste treatment), a broad spectrum of scientific and technical skills, and links to the nuclear energy industry. The ICERR will be at the heart of network drawing together the expertise, capabilities and facilities of the ICERR with those of the users and contributors from other countries, see Figure 1.

Specifically an ICERR will:

- Help research institutions from different countries to participate in the cutting edge science with access to the physical and technical resources of the centre and its projects;
- Create international scientific networks that enhance the capabilities of the affiliating institutions as well as the ICERR itself;
- Use collaboration as a means to achieve projects and develop science and expertise that otherwise may not be possible;
- Provide access to results (including created Intellectual Property) to participating members of joint projects;
- Lead innovative programmes, develop and share technologies, scientific concepts and experience, and design of installations;
- Train scientific and engineering personnel; and
- Have an intergovernmental support framework due to the sensitive technologies involved.



Fig 1: The ICERR Concept

It is envisaged that an ICERR's affiliates would purchase access to its operational capabilities through a subscription with predefined terms. This subscription would include an option to send staff to work at the ICERR and learn first-hand how nuclear facilities are organised, operated and regulated.

The ICERR concept is mutually beneficial, see the summary in Table 2. On one hand, the scientific base and prestige of the ICERR itself would be enhanced, and the ICERR would benefit from additional financial resources in the form of subscription revenues, as well as from access to the expanded technical capabilities of its network of affiliates. Such high flux facilities are expensive, and they are most effective when they are supported intellectually and financially by the World Community. With multilateral support they may be able to complete the needed studies more quickly and cost effectively, avoiding duplication of R&D investments and fragmentation of scientific effort.

On the other hand, the affiliated institutions and organisations would gain access to state-of-the-art research facilities and expertise at much lower cost, and more rapidly, than through development of their own, independent research facilities. This will provide the scientists in those countries with increased opportunities and greater access to the international scientific community, strongly leveraging the investments in the affiliation or participation. The affiliates would be able to accelerate and deepen the development of their own nuclear expertise at all managerial levels with the ICERR as a source of best practice. The affiliates would have opportunity to train staff through direct participation in experienced teams at the ICERR resulting in learning curves that are shorter and less prone to iteration. The affiliated research institutions would have also the opportunity to develop, and be recognised for, world-class technical specialties that support the programs at the ICERR.

In addition, each new, well-functioning ICERR will build confidence in the supra-national approach in which a few well-equipped, well-utilized, well-funded, safe and secure facilities can substitute for many comparatively isolated facilities with lower utilization and increased funding challenges.

3. Challenges to establishing an ICERR

Initiating or expanding an international role for research centre is not straightforward. There are a number of technical, administrative and legal challenges to be met and overcome.

For the centre operator, these challenges include defining mechanism to identify, access and sustain international funds and international partners. The sensitive technologies involved require the ICERR to be supported by intergovernmental agreements, especially in field of non-proliferation. The admittance of foreign staff to the ICERR operations must be properly managed to ensure the safe, secure and effective utilization of the reactor and its experimental installations. Clear rules for the development, protection and dissemination of IPR must also be developed.

Governments seeking to leverage participation in the ICERR to enhance their national programs must be willing to enact the necessary measures to protect nuclear technologies and recognise that the expected return on the investment in the ICERR will only be achieved through a sustained and actively managed national competence development programme. Issues such as the selection of the appropriate staff for participation in the ICERR and their subsequent retention within the national programmes need to be addressed.

Of course, these challenges are not new. The experience of research reactors with existing international programmes is highly informative, for example, Institute Laue Langevin in France, Halden in Norway, the OPAL reactor in Australia and the Jules Horowitz Reactor project in France. International scientific collaboration projects in other sectors also provide examples of best practice, including the larger projects such as ITER and CERN. The IAEA initiative will examine these experiences and incorporate the lessons learned into the new ICERR projects.

4. Proposed Activities

It is envisaged that activities under the IAEA ICERR initiative will follow three paths in parallel:

1. Development of the ICERR concept, including clear definitions of the role of the ICERR, the affiliates, and the IAEA. The challenges to an expanded international role will be identified together with best practices to meet them from the existing collaborative projects.
2. The IAEA will help to support initial secondment and training programs at ICERR's;
3. A publication in the IAEA's Nuclear Energy Series will be issued containing information on existing and proposed ICERR's and guidance on setting up or affiliating with an ICERR.

5. Launch Meeting

The launch meeting for the ICERR initiative will be held in Cadarache, France from 10th to 12th April 2012 to examine the user perspectives of ICERRs, including a top-level (national) view of likely user requirements, the lessons learned from previous international collaborative scientific facilities and projects, including the approaches taken to address their challenges and opportunities, and the strategy for further development of the ICERR concept.

6. Summary

The IAEA is launching an initiative to enhance the international role of high flux research reactors as International Centres of Excellence and provide an important new option for countries to accelerate and strengthen their development of national nuclear competences and provide a sustainable option for nuclear education and training. The initiative will examine best practices in international cooperation developed to date and use this to inform the definition, development, and support for the ICERR concept.

ICERR Operators	Involved Governments	Institutional Users / Affiliates	Industry
<u>Science and Technology</u>			
<ul style="list-style-type: none"> • Acquire or develop modern technologies • Sustainable development of national facilities and competences • Making optimal or better use of equipment and facilities • Prospects for future enhancement of the facility 	<ul style="list-style-type: none"> • National competence building • Accelerate development of nationally important technologies • Provide information on status and competency of partner MS – more confidence in a collaborative rather secretive programs 	<ul style="list-style-type: none"> • High level of investigations • Programs inherently comply with all major international standards • Access to results of joint programs and investigations 	<ul style="list-style-type: none"> • Developing, gaining access to modern technologies • Monitor technology directions and future markets
<u>Financial</u>			
<ul style="list-style-type: none"> • Making it easier to find and/or justify funding • Potential income generation from international projects and programs 	<ul style="list-style-type: none"> • Reduced costs of competence building • Cost effectiveness of research 	<ul style="list-style-type: none"> • Cost effectiveness of research and decreased cost of investigations through collaborations with other users. • Acquiring and/or developing modern technologies 	<ul style="list-style-type: none"> • Cost effectiveness of research
<u>Human resources development</u>			
<ul style="list-style-type: none"> • Increased opportunity for scientific achievement for staff and students 	<ul style="list-style-type: none"> • Accelerated competence building • Stronger national competences 	<ul style="list-style-type: none"> • Opportunity for scientific achievement for staff / students 	
<u>Prestige</u>			
<ul style="list-style-type: none"> • Leadership in international projects and programs • Involved in worldwide activities in the nuclear field 	<ul style="list-style-type: none"> • Prestige of involvement in international projects / programs • Build public confidence in nuclear technologies 	<ul style="list-style-type: none"> • Recognition of involvement in international projects / programs 	

Tab 2: Summary of Benefits of ICERR'

The Jules Horowitz Reactor: A new high Performances European MTR (Material Testing Reactor) with modern experimental capacities: Toward an International Centre of Excellence

G. BIGNAN, X. BRAVO, P.M. LEMOINE

*French Atomic Energy Commission - Nuclear Energy Directorate
Cadarache and Saclay Research Centres - France*

Corresponding author: gilles.bignan@cea.fr

ABSTRACT

The Jules Horowitz Reactor (JHR) is a new Material Testing Reactor currently under construction at CEA Cadarache research centre in the south of France. It will represent a major Research Infrastructure for scientific studies dealing with material and fuel behaviour under irradiation (and is consequently identified for this purpose within various European road maps and forums; ESFRI, SNE-TP...). The reactor will also be devoted to medical Isotopes production.

The reactor will perform R&D programs for the optimization of the present generation of NPP, support the development of the next generation of NPP (mainly LWR) and also offer irradiation possibilities for future reactors.

JHR is fully optimised for testing material and fuel under irradiation, in normal and non-normal conditions:

- With irradiation loops producing the operational condition of the different power reactor technologies,

- With high thermal and fast flux capacity to address existing and future NPP needs.

JHR is designed, built and will be operated as an international user-facility open to international collaboration. This results in several aspects:

- a partnership with the funding organisations gathered within a consortium.

- The preparation of the JHR International Program (JHIP) as an OECD project open to non-members of the JHR consortium.

It will answer needs expressed by the scientific community (R&D institutes, TSO...) and the industrial companies (Utilities, Fuel Vendors...).

Consequently the JHR facility is in total agreement with the concept of International Centre of Excellence defined by the IAEA as a scientific hub for cutting edge research and materials investigations (multilateral support to complete cost effective studies avoiding fragmentation of scientific effort, access to developing countries to such state of the art research reactor facilities, supra national approach....)

This paper gives an up-to-date status of the construction and of the developments performed to build the future experimental capacity and will particularly focus on proposed operating rules of JHR as an International Centre of Excellence on Research Reactors as defined by the IAEA.

1. Introduction

European Material Testing Reactors (MTR) has provided an essential support for nuclear power programs over the last 40 years within the European Community. However, these Material Test Reactors (MTRs) will be more than 50 years old in this decade and will face increasing probability of shut-down due to the obsolescence of their safety standards and of their experimental capability. Such a situation cannot be sustained long term since “nuclear energy is a competitive energy source meeting the dual requirements for energy security and the reduction of greenhouse gas emissions, and is also an essential component of the energy mix” [1].

Associated with hot laboratories for the post irradiation examinations, MTRs are structuring research facilities for the European Research Area in the field of nuclear fission energy.

MTRs address the development and the qualification of materials and fuels under irradiation with sizes and environment conditions relevant for nuclear power plants in order to optimise and demonstrate safe operations of existing power reactors as well as to support future reactor design:

- Nuclear plants will follow a long-term trend driven by the plant life extension and management, reinforcement of the safety, waste and resource management, flexibility and economic improvement.
- In parallel to extending performance and safety for existing and coming power plants, R&D programs are taking place in order to assess and develop new reactor concepts (Generation IV reactors) that meet sustainability purposes.
- **In addition, for most European countries, keeping competences alive is a strategic cross-cutting issue;** developing and operating a new and up-to-date research reactor appears to be an effective way to train a new generation of scientists and engineers.

This analysis was already made by a thematic network of Euratom 5th FP, involving experts and industry representatives, in order to answer the question from the European Commission on the need for a new Material Testing Reactor (MTR) in Europe [2].

This entire preparatory work leads to the fact that the **JHR research infrastructure has been identified on the ESFRI Roadmap since 2008.**

2. The JHR project in this context

JHR will offer modern irradiation experimental capabilities to study material & fuel behaviour under irradiation. JHR will be a flexible experimental infrastructure to meet industrial and public needs within the European Union related to present and future Nuclear Power Reactors.

JHR is designed to provide high neutron flux (twice as large as the maximum available today in MTRs), to run highly instrumented experiments to support advanced modelling giving prediction beyond experimental points, and to operate experimental devices giving environment conditions (pressure, temperature, flux, coolant chemistry, ...) relevant for water reactors, for gas cooled thermal or fast reactors, for sodium fast reactors, ...

These objectives require representative tests of structural materials and fuel components as well as in-depth investigations with "separate effects" experiments coupled with advanced modelling.

For example, the JHR design accommodates improved on-line monitoring capabilities such as the fission product laboratory directly coupled to the experimental fuel sample under irradiation.

As a modern research infrastructure, JHR will contribute to the development of expertise and know-how, and to the training of the next generation of scientists and operators with a positive impact on nuclear safety, competitiveness and social acceptance. The JHR is mainly designed to meet these technical objectives.

As another important objective, **the JHR will contribute to secure the production of radioisotope for medical application. This is a key public health stake.**

JHR, as a future international User Facility, is driven by an international consortium gathering industry (Utilities, Fuel vendors...) and public bodies (R&D centres, TSO, Regulator...).

CEA is encouraging by this consortium to enlarge its membership and in 2011 a new member enter JHR consortium: the Israel Atomic Energy Commission (IAEC).

The present members list of JHR consortium is the following:

CEA (France), EDF (France), AREVA(France), Euratom, SCK.CEN (Belgium), UJV (Czech Republic), VTT(Finland), CIEMAT(Spain), Vattenfall (Sweden), DAE(India), IAEC (Israël).

We also have to quote a bilateral agreement with JAEA (Japan) regarding JHR access.

The JHR facility description and the development of the first experimental capacity is described in detailed in previous RRFM and IGORR conferences (see for examples ref [3], [4],[5] and [6]) and we just give here a short update status before focusing on a description of JHR as an International Centre of Excellence following IAEA Initiative.

3. JHR update status

The construction of JHR which was started in 2007 is going-on in a nominal way (foreseen first criticality end of 2016-ready for operation in 2017):



Fig1: View of the Building site end of 2011

4. JHR Safety: an innovative approach

The JHR differs from the previous generation of reactors by incorporating the safety analysis right from the design phase, based on a modern reference system and methodology; in particular those used in contemporary projects such as the EPR a GEN3 NPP under construction in Finland, China and France.

The methodological safety approach for the JHR is summarised, highlighting various innovative aspects and the specific design features of the new experimental reactor.

Then, some of the initial design choices and options are detailed, coming directly from this innovative approach and feedback from existing reactors.

The JHR Safety approach has been presented in detail at the IAEA Conference in Rabat last November 2011 and some examples of incorporating Safety from the design phase are described in this reference [7].

5. JHR as an IAEA International Centre of Excellence on Research Reactor (ICERR)

Building an International User Facility: In parallel to the construction of the reactor, the preparation of an international community around JHR is continuing; this is an important topic because, as indicated in the introduction, building and gathering a strong international community in support to MTR experiments is a key-issue for the R&D in nuclear energy field. Consequently, CEA is welcoming scientists, Engineers (called Secondees) from various organisations/institutes who are integrated within the JHR team for a limited period of time (typically one year) for various topics such as physics studies for the development of the experimental devices (neutron physics, thermo-hydraulic...) and/or for support to the future Operator (Safety Analysis, I-C&C...).

As described in the IAEA paper on this present conference (K. Alldred et al) the new initiative of the Agency to launch the ICERR concept is intended to help Member States willing to go on Nuclear Technology via the setting-up of a Research Reactor to create and sustain key-competences.

Actually, between the academic training and the “commercial training linked to a product” there is a need for **setting-up a framework for Nuclear Education “in the field”** using modern High-Performances Infrastructures dedicated to the training of future seniors scientists, Engineers...for the benefits of decision-makers in countries wishing to develop Nuclear Energy. These scientists invited to an ICERR for getting this Nuclear Education are called Secondees as described above.

The ICERR will provide Nuclear Education “in the field” that offer direct experience of working in nuclear facilities and provide training opportunities that fill the gap between academic education and commercial-product specific training. This will allow Secondees to learn about best practices in Material and Fuel Science, Nuclear Safety, Reactor Operation, Nuclear Technologies, Fuel management, Wastes Management, ancillary Hot Cells and Laboratories and so on. It also means that the hosting country has enough qualified staff to tutor in a good way the secondees.

JHR provides an informative model for potential ICERR as well as options for access to its own research facilities and training resources.

Building an international joint program: the JHIP (Jules Horowitz International Program): According to the consortium agreement, JHR is aimed to become a user reactor at international level on the model of the Halden Reactor Project with multinational project and proprietary experiments. Consequently, CEA is preparing, with the support of the OECD/NEA, a joint program called Jules Horowitz International Programme (JHIP) which has been thought with the strategic scope to address fuel and material issues of common interest that are key for operating plants and future NPP (mainly focused on LWR).

The CEA proposals mainly deal with fuel safety and reliability (LOCA and source Term experiments addressing fission products release in a variety of fuel failure conditions).

The target is to get a nearly completed JHIP OECD agreement by mid-2012 in order to launch scientific programs up to 2013.

6. Conclusion

As indicated, JHR building is going-on in a nominal way and its first criticality is scheduled for the end of 2016. This facility – regarding the experimental capacity - is already open and will be more and more so to international collaboration. It is clear that within a context of nuclear renewal, the JHR will be a key infrastructure in the European Research Area for R&D in support to the use of nuclear energy and can play a key-role on the new IAEA Initiative regarding the setting-up of International Centres of Excellence on Research Reactors.

7. References

- [1] The Green Paper, “Towards a European Energy Security Strategy”, published by the European Commission in November 2000
- [2] FEUNMARR, Future European Union Needs in Material Research Reactors, 5th FP thematic network, Nov. 2001 – Oct 2002
- [3] The Jules Horowitz Reactor Project:” A new High Performances European and International Material Testing Reactor for the 21st century”- G. Bignan, D.Iracane Nuclear Energy International publication (NEI-Dec 2008)
- [4] “Sustaining Material Testing Capacity in France: From OSIRIS to JHR”
G. Bignan, D. Iracane, S. Loubière, C. Blandin CEA (France) IGORR 2009 Conference (Beijing)
- [5] The Jules Horowitz Reactor: A new European MTR (Material Testing Reactor) open to International collaboration: Description and Status
G.Bignan; P. Lemoine; X. Bravo CEA (France) –RRFM 2011- Roma
- [6] “The Jules Horowitz Reactor: A new European MTR open to International collaboration”
Gilles Bignan et al, IGORR 2010 (Knoxville TN –ORNL- September 2010)
- [7] The Jules Horowitz Reactor: A new European MTR (Material Testing Reactor) open to International collaboration: Update Description and focus on the modern safety approach.
G. Bignan et al –IAEA International Conference on Research Reactors: Safe Management and Effective Utilization (Rabat- November 2011)

A NEW METHOD OF PRODUCING U(Mo) PARTICLES FOR MATERIAL TESTING REACTORS (MTR)

G. CHAMPION^(1,2), J. ALLENOU^(1,2), M. PASTUREL, O. TOUGAIT

¹*Sciences chimiques de Rennes, UMR-CNRS 6226, Université de Rennes 1, Campus de Beaulieu, 35042 Rennes, France*

X. ILTIS, F. CHAROLLAIS, M.C. ANSELMET

²*CEA, DEN, DEC, Cadarache, 13108 Saint-Paul-Lez-Durance, France*

ABSTRACT

Uranium-molybdenum powders can be obtained via several routes such as different kinds of atomisation, grinding or hydriding-dehydriding processes. Each of these techniques leads to particular powder properties correlated to their manufacturing process. However, all these methods imply at a certain point of their fabrication process, a “melting-solidification” step which is believed to play a predominant role in the behaviour of the fuel under high irradiation conditions. In this paper, a new way of producing γ -U(Mo) particles from a “chemical reduction-agglomeration” process is introduced. Typical microstructure and morphological characteristics of the resulting powders are presented and discussed in comparison with the atomised powder particles that are currently the more industrially advanced product.

1. Introduction

Necessity of using low enriched uranium fuel for previous and future material testing reactors (MTR) has led to the development of a dense composite material based on an U(Mo) alloy. This composite material is made of γ -U(Mo) particles embedded in an aluminium based matrix.

Behaviour under irradiation of such a fuel has shown a strong dependency on both (i) the composition and nature of the matrix, (ii) the fabrication method of these γ -U(Mo) particles. Currently three different main methods are available for γ -U(Mo) fabrication. The first and the most easily available on an industrial scale is the atomisation process which produces spherical shaped particles, with small sized grains, exhibiting a non-homogeneous content of molybdenum (at the grain scale level) and a very small internal porosity volume fraction [1]. The second one is the grinding method which leads to highly defective microstructures, no internal porosity and elongated shaped particles [2]. These two methods and the corresponding different microstructural properties led to different gas retention features under high irradiation conditions [3-4]. The third method of producing γ -U(Mo) particles that can be found in the open literature is based on a multi-steps “hydriding - dehydriding” process. Particles produced via this last method are planned to be tested under irradiation (within the RERTR program) and one may suppose a different gas retention behaviour according to their different microstructural characteristics [5].

An innovative method of producing γ -U(Mo) particles via a “chemical reduction-agglomeration” process known as metallothermy is described hereafter [6-7]. Thanks to this method, microstructural characteristics and morphological aspects of the powder, different from those obtained by the previous processes can be achieved and will be discussed particularly in comparison with the powder particles obtained by an atomisation process.

2. Fabrication of γ -U(Mo) powder particles

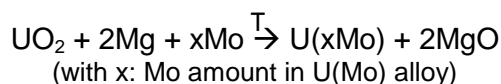
The metallotherapy process consists of the reduction of an oxide compound by a metallic precursor at given pressure and temperature. This reaction can only be performed under very specific conditions that are defined by the free standard enthalpy of formation (also called the Gibbs free energy change ΔG) of the different elements and their oxides, as represented by the Ellingham diagram [8]. According to this diagram, only a few metals can reduce the uranium dioxide.

2.1. From metallotherapy to magnesiotherapy

Magnesium has been chosen to reduce UO_2 for several reasons:

- firstly, it is known that the metallotherapy reaction is highly exothermic [9-10], this is even truer when the difference between the two Gibbs free energy change ΔG is large: Mg is the closest element that can reduce UO_2 on a large range of temperatures,
- secondly, Mg is the metal the most available, the cheapest and the easiest to handle among the other possibilities (Be, Th and Ca).

The metallotherapy reaction can thus be referred to as “reaction of magnesiotherapy” and is as follows:



During the magnesiotherapy reaction, the uranium dioxide is reduced into metallic uranium, and, in a molybdenum rich environment, U(Mo) powder particles can be produced. Simultaneously, the magnesium oxidises to give magnesia as a by-product.

From the Ellingham diagram, this reaction is possible in a large range of temperatures: $[T_{\text{ambient.}} \text{ to } 1400^\circ\text{C}]$. However, an appropriate temperature must be selected in order to achieve the reaction in a realistic timeline frame. Details of the experimental procedure, tools and materials used to achieve γ -U(Mo) powder particles are described hereafter.

2.2. Experimental procedure

The magnesiotherapy reaction is a process activated with temperature, where two main events take place: the chemical reduction of the uranium dioxide and the “agglomeration” of the just fabricated particles. In order to optimise these two reactions, the reactive elements must be arranged in a specific way.

2.2.1. The “chemical reduction” reaction

This first reaction is carried out by producing a green compact, using a hand press, made of uranium dioxide and molybdenum powders (respective mean particles sizes: 30 μm and 3 μm) which are previously mechanically mixed up (Figure 1). This procedure will serve three main purposes:

- obtain an object which is easy to handle,
- ensure that UO_2 , once reduced, is homogeneously surrounded by molybdenum particles to give an U(Mo) alloy free of Mo rich areas,
- allow the transformation of magnesium in gas or liquid state, as expected for the reduction of the uranium dioxide with the presence of numerous paths within the pellet.

Once the “chemical reduction” reaction took place, a heat treatment is necessary. Its purpose is to create agglomerates of several U(Mo) powder particles. Time and temperature are chosen to achieve the desired bondage strength, agglomerates size distribution and porosity level.

2.2.2. The “agglomeration” reaction

During this heat treatment, the characteristics of the green body have a predominant role: it gives some cohesion between the powder particles. As the formation of agglomerates depends also on diffusion and proximity between the different sized particles, this step can

be optimised. First results with time frames ranging from 24 to 48 hours and temperatures ranging from 900 to 1100 °C are described in the following sections.

All along these two reactions, the different materials are placed into a molybdenum crucible which is arc-welded under an argon atmosphere to avoid mainly the evaporation of Mg. This crucible is introduced into a sealed silica tube to minimise once more the oxidation of the later.

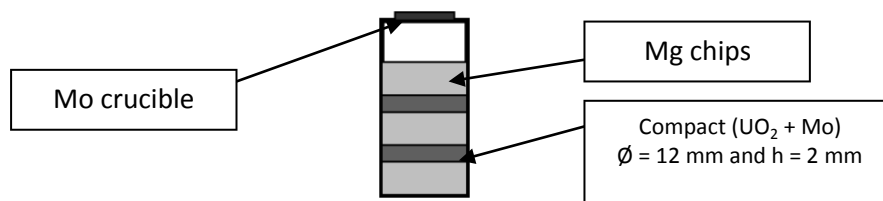


Figure 1. Schematic representation of the filled molybdenum crucible.

2.2.3. Obtaining the final product

As previously mentioned, the magnesiothermy process gives a by-product “MgO” that is mixed to the U(Mo) powder particles. A final cleaning step is then necessary. For now, diluted chloride acid is used to get rid of the magnesia to obtain pure U(Mo) powder particles. Some development regarding this last issue is undergoing. Since the final product is still in a form of a pellet, most of the remained magnesium chips can also be easily removed.

3. Results

In this section, powders obtained by magnesiothermy are systematically compared with the atomised ones, in terms of particles size distribution and structural, morphological and microstructural characteristics.

3.1. Particles size distribution

Size distributions of particles manufactured via the two processes have been measured by laser granulometry; results are illustrated in Figure 2.

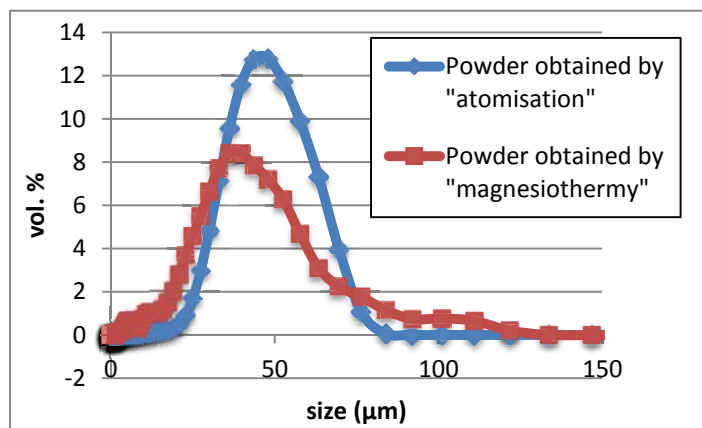


Figure 2. Size distribution for particles produced via an atomisation process and a magnesiothermy process (48h - 950 °C).

The atomised powder was supplied by the Korea Atomic Energy Research Institute (KAERI) and used by AREVA-CERCA for manufacturing the IRIS 4 plates [11]. Its granulometry range was obtained by mixing two sieved powders ([0-40 µm] and [40-125 µm]) and is typical of that used by fuel plates manufacturers. The powder directly issued from the magnesiothermy process (without any crushing or sieving step) exhibits a very similar particle size distribution, with almost the same medium range size (about 50 µm), despite of the presence of particles larger than 100 µm (which could be easily eliminated by sieving).

3.2. Structural characterisation

It is well known that the behaviour of U(Mo) fuel under irradiation is optimised when the crystallographic state corresponds to the cubic (and isotropic) γ -U form (bcc). An atomised powder (Figure 3b) and a powder synthesised by magnesiothermy (Figure 3a) have been characterised by X-Ray diffraction, revealing that both powders only exhibit the γ -U(Mo) phase.

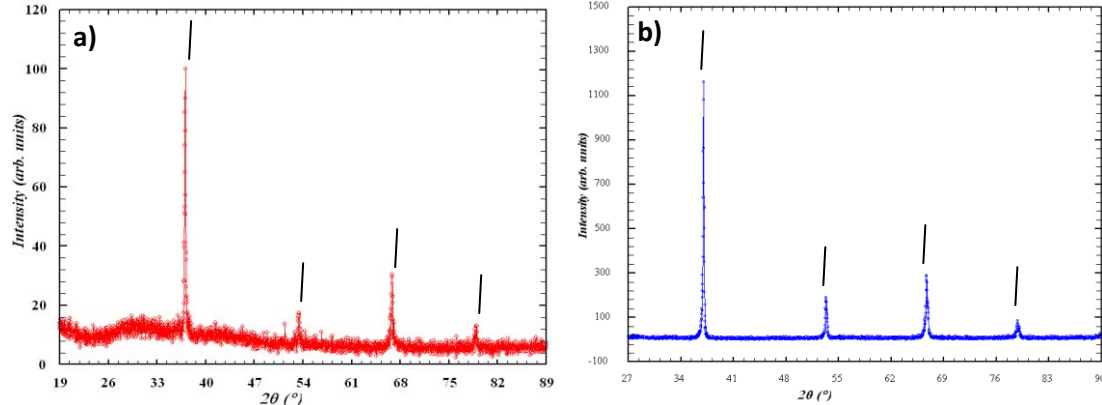


Figure 3. X-ray diffraction diagrams for powders produced via a) magnesiothermy (24h - 1000 °C) and b) atomisation; γ -U(Mo) characteristic peaks are indicated by black lines.

3.3. Morphological characterisation

Figure 4 compares the morphological characteristics of the two types of powders. It clearly illustrates the more irregular shape of the “magnesiothermy” one, with a certain tendency to the agglomeration (more or less marked, depending on the annealing conditions and easily removable by a gentle crushing).

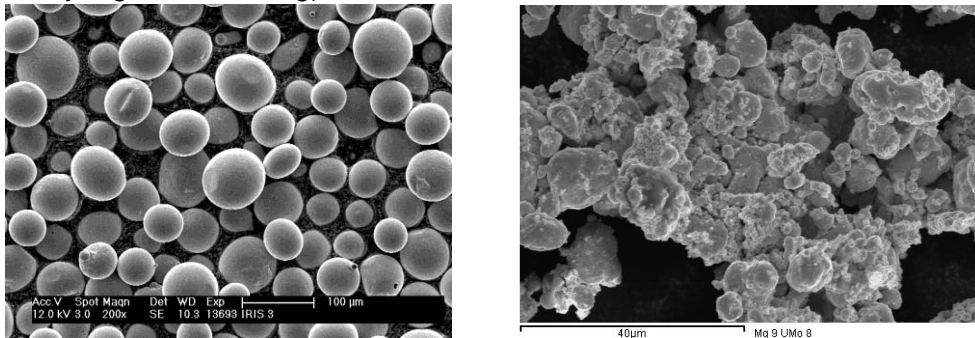


Figure 4. Scanning electron micrographs of morphological characteristics of γ -U(Mo) powders produced via a) atomisation and b) magnesiothermy (1000 °C - 24 h).

3.4. Microstructural characterisation

Chemical etching performed on the atomised particles (cf. Figure 5a) reveals two cellular microstructures, columnar or equiaxed, which is specific to the atomisation process and shows the direction of solidification. Long sized columnar grains (around 10 μ m) and almost no intragranular porosity can be noticed. Particles obtained by magnesiothermy exhibit small (about 1 μ m) equiaxed grains, even at their periphery: see Figure 5b (encircled area).

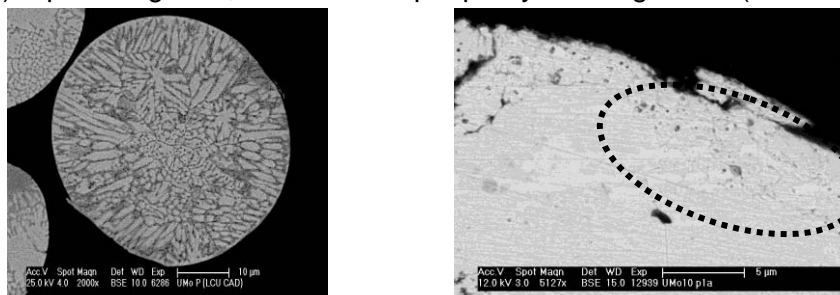


Figure 5. Scanning electron micrographs of polished and chemically etched γ -U(Mo) powders produced via a) atomisation and b) magnesiothermy.

Another feature really distinguishes this type of powder from the atomised one: the presence of small closed porosities. They can be observed in Figure 6a, on a partly ion etched particle and in Figure 6b, on a mechanically polished one. Their size is of the order of a few tenths of micrometre, their density varies with the fabrication conditions (especially the annealing temperature and duration) and they seem to be mainly intragranular. First data give a porosity that ranges in size between 0 and 3 μm for a volume fraction around 2%.

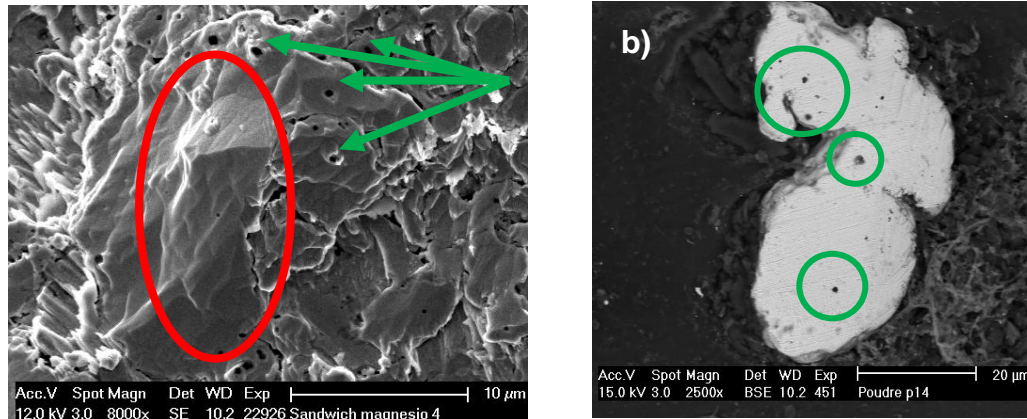


Figure 6. Scanning electron micrographs of powders obtained via magnesiothermy (24h - 1100°C), a) after ion etching and b) in cross section after polishing (grains and grain boundaries are pointed out in red, porosity in green).

3.5. Composition characterisation

The homogeneity of repartition of Mo in the particles directly influences the stability of γ -U(Mo) phase and, thus, its behaviour during the plate manufacturing process and the irradiation. In atomised particles, it has been shown by neutron diffraction that two γ -U(Mo) phases, with different lattice parameters are respectively present at cell boundaries and cell interior regions [12]. The occurrence of these two phases is a consequence of a molybdenum microsegregation process during the solidification (lower molybdenum content close to grain boundaries compared to the cell interior regions).

In order to evaluate the homogeneity of the molybdenum repartition, in a powder synthesised by magnesiothermy, punctual EDS analyses were performed across some particles. Figure 7 and Table 1 give an example of results. They show that the molybdenum is homogeneously distributed in the U(Mo) particles, at the scale of this type of measurement (i.e. about 1 μm^3). Indeed, the standard deviation of the molybdenum content is less than 1 wt%.

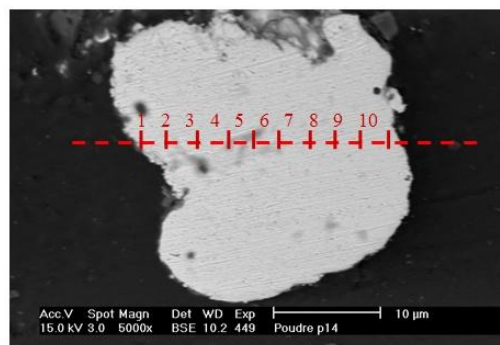


Figure 7. Position of EDS measurement points across a γ -U(Mo) particle produced by magnesiothermy (24h – 1100°C).

Elements	1	2	3	4	5	6	7	8	9	10	Average	Standard deviation
Mo (wt.%)	13,16	13,23	13,37	12,09	12,92	13,28	13,43	12,44	12,68	13,62	13,02	0,48
U (wt.%)	86,84	86,77	86,63	87,91	87,08	86,72	86,57	87,56	87,32	86,38	86,98	0,48

Table 1. Values of Mo and U concentrations at different points across a γ -U(Mo) particle obtained by magnesiothermy (24h – 1100°C).

3.6. Process operating parameters

Several parameters can be adjusted during the atomisation and the magnesiothermy processes in order to tailor the main powder particle characteristics:

- Concerning the (rotating disk) atomisation process: the particle size distribution and the particle shape can be controlled respectively by the flow rate of the melted alloy and the type of disk used to disintegrate this liquid. Other operating parameters such as diameter or rotation speed of the disk and nature of the atmosphere used to atomise the powders have also an influence on the final product [13].
- Concerning the chemically reduced powder: several operating parameters have an influence, on the powder size distribution (such as the pressure used to obtain the UO_2/Mo green compact, the initial particle size distributions of UO_2 and Mo), on the particle sizes (duration and type of the heat treatment, heating ramp rate), and on the γ -phase stability (cooling rate) for a given reaction temperature. Stoichiometric ratios used to calculate the added magnesium quantity also have an effect on the final product characteristics.

Moreover, in both cases, process operating conditions allow the production of $\text{U}(\text{Mo},\text{X})$ powders, which is not the case for instance for the “hydriding – dehydriding” process. For example, $\text{U}(\text{Mo},\text{Ti})$ powders were already obtained by magnesiothermy, with satisfactory results in terms of chemical homogeneity of the particles.

4. Discussion and conclusion

From these different powder and process properties and from several Post Irradiation Examinations (PIE) carried out in programs such as IRIS or RERTR, it is possible to draw up first assumptions concerning the general behaviour of a powder obtained by magnesiothermy compared to an atomised one.

4.1. Discussion concerning an eventual fuel plate fabrication

Taking into account the particular shape of the powders obtained by magnesiothermy, two main assumptions can be exposed:

- Fuel plate fabrication using magnesiothermy powders might be easier. Indeed, particles produced via an atomisation process route, are perfectly spherical and show a tendency to roll and agglomerate into the cladding material (even if no dog-bone effect is pointed out) during fabrication. Ground powders, on the other hand, have a non-uniform shape and are difficult to handle during hot rolling, leading to dog-bone effects. The requirements for an easy fuel plate fabrication step would be a compromise between these two behaviours, with a powder exhibiting morphological properties in between. Powders produced via the magnesiothermy process, that are agglomerates showing a “polyhedral - almost spherical” shape would be more advantageous from a fuel plate manufacturing point of view.

- As fabricated meat porosity could also be more advantageous. Atomised powders give a small amount of porosity with a rate around 3 vol% and fuel plates made of ground powders, contain around 10 vol% porosity. Fuel plates using the chemically reduced powder would consequently be situated again in between with a final porosity ranged between 3 and 10 vol%. This porosity might be very useful in order to act as a reservoir for fission gas products created under irradiation and might thus postpone the pillowing effect of the fuel element.

4.2. Discussion concerning the behaviour under irradiation

From the microstructural and composition characteristics of the powder obtained by magnesiothermy, two assumptions can be made:

- The presence of internal porosity would be interesting in order to influence the fission gases retention or their mobility inside the particles under irradiation, all the more reason that this type of porosity is located within the particles, where fission products appear.
- The homogeneous repartition of the molybdenum which is a consequence of the absence of the solidification phenomenon might help the stability of the γ phase during fuel plate fabrication.

4.3. Conclusion

An innovative method of producing γ -U(Mo) powder particles excluding the “melting-solidification” step has been presented. Main characteristics of the magnesiothermy process and obtained powders have been discussed in comparison with the atomisation process. Several differences have been noticed, particularly in terms of:

- structure/microstructure: the magnesiothermy process is potentially an asset in optimising the γ -U(Mo) alloy stability and swelling properties via an homogeneous distribution of Mo within the particles and grain boundaries and the presence of an intragranular porosity,
- morphology: the magnesiothermy process is supposed to supply powder particles that meet the requirements for an optimised fuel plate manufacturing by hot rolling.

These last assumptions need to be confirmed through several complementary studies such as High-Temperature X-Ray diffraction (HT-XRD), neutron diffraction analyses aimed to evaluate the γ -U(Mo) alloy stability.

References

- [1] K.H. Kim et al. "Characterization of U-2 wt% Mo and U-10 wt% Mo alloy powders prepared by centrifugal atomization", J. Nucl. Mater. 245 (1997) 179-184.
- [2] C.R. Clark et al. "Fuel powder production from ductile uranium alloys", Proceedings of Reduced Enrichment for Research and Test Reactors (RERTR), Sao Paulo, Brazil, Oct. 18-23, 1998.
- [3] S. Van den Berghe et al. "Transmission electron microscopy investigation of irradiated U-7 wt%Mo dispersion fuel", J. Nucl. Mat. 375 (2008) 340-346.
- [4] A. Leenaers et al. "Irradiation behavior of ground U(Mo) fuel with and without Si added to the matrix", J. Nucl. Mater. 412 (2011) 41-52.
- [5] L. Olivares et al. "Manufacturing and characterization of LEU dispersion miniplates based on hydride UMo powders", Proceedings of Reduced Enrichment for Research and Test Reactors (RERTR), Beijing, China, Nov. 1-5, 2009.
- [6] J. Allenou, F.Charollais, M. Brothier, X. Iltis, O. Tougait, M. Pasturel, H. Noël, "Poudre d'un alliage à base d'uranium et de molybdène utile pour la fabrication de combustibles nucléaires", Demande de brevet français n° 10 61319 du 28/12/2010.
- [7] J. Allenou, M.Brothier, F. Charollais, X. Iltis, O. Tougait, M. Pasturel, H. Noël, "Procédé de préparation d'une poudre d'un alliage à base d'uranium et de molybdène", Demande de brevet français n° 10 61320 du 28/12/2010.
- [8] P. Desré et al. "Thermodynamique des matériaux: équilibre des phases et métastabilité", Ed. EDP Sciences, 2010.
- [9] S. Luidold et al. "Production of niobium powder by magnesiothermic reduction of niobium oxides in a cyclone reactor", Inter. J. Refr. Metals and Hard Mater. 25 (2007) 423-432.
- [10] P. Rojas et al. "Processes to obtain metallic uranium from UF₆", Proceedings of Reduced Enrichment for Research and Test Reactors (RERTR), Beijing, China, Nov. 1-5, 2009.
- [11] M. Ripert et al. "Results of the IRIS 4 irradiation in OSIRIS reactor: oxidised U-Mo particles dispersed in Al (with 0 or 2,1%Si)", Proceedings of Reduced Enrichment for Research and Test Reactors (RERTR), Beijing, China, Nov. 1-5, 2009.
- [12] J.M. Park et al. "Neutron diffraction analyses of U-(6-10 wt.%)Mo alloy powders fabricated by centrifugal atomization", J. Nucl. Mat. 397 (2010) 27-30.
- [13] B. Champagne et al. "REP atomization mechanisms", Powder Metal. Inter. 16 (1984) 125-128.

STUDY OF SI AND ZRN COATED UMO ATOMISED PARTICLES USING HIGH ENERGY XRD

T. ZWEIFEL¹, H. PALANCHER, A. BONNIN, F. CHAROLLAIS

CEA, DEN, DEC

F-13108 St Paul Lez Durance Cedex – France

A. LEENAERS, S. VAN DEN BERGHE

SCK•CEN

Boeretang 200, B-2400 MOL – Belgium

R. JUNGWIRTH, W. PETRY

Forschungsneutronenquelle Heinz Maier-Leibnitz (FRM II), Technische Universität München,
D-85747 Garching bei München, Germany

P. LEMOINE

CEA, DEN, DISN

Saclay, F-91191 Gif-sur-Yvette – France

ABSTRACT

Within the SELENIUM project, the behaviour of Si (0.6 μm) and ZrN (1 μm) coated atomized UMo powders has been analysed after plate manufacturing and thermal treatments using high energy X-ray diffraction.

It is demonstrated that this coating does not influence the destabilisation of the UMo particles but strongly limit the growth of the UMo/Al interaction layer under thermal treatments. This last result supplement recent heavy ion experiments performed on the SELENIUM fuel plates.

1. Introduction

In the framework of the SELENIUM project, two innovative solutions have been developed for improving the in-pile irradiation performances of UMo/Al nuclear fuels. They are based on physical vapour deposition (PVD) of either ZrN or Si on UMo atomised particles [1, 2].

The manufacturing feasibility of fuel plates containing such coated UMo particles has been demonstrated by AREVA-CERCA using depleted/natural UMo atomized powders. The SCK•CEN will test the in-pile behaviour of the corresponding LEU full size plates. This experiment should start in April 2012 in the BR2 reactor.

To supplement previous SEM/EDX characterizations of the coated powders in fresh fuel plates [3], and annealed UMo/Al compacts [4], the crystallographic composition of these materials has been investigated by high energy X-ray diffraction [5,6].

2. Experimental methods

a. Sample preparation

Depleted/natural UMo atomised powder was coated by PVD with either 1 μm thick ZrN or 0.6 μm Si.

¹ Also at Forschungsneutronenquelle Heinz Maier-Leibnitz (FRM II), Technische Universität München, D-85747 Garching bei München, Germany

From these starting materials (UMo(Si) and (UMo(ZrN)) and from regular (uncoated) UMo atomised powder, 5 compacts made with pure Al powder as a matrix have been prepared and 4 ones further annealed, the last one being kept as a reference [4]. Annealing conditions for each sample are:

- 340°C for 130 days
- 450°C for 4 hours
- 550°C for 2 hours
- 550°C for 4 hours.

Destructive examinations by SEM and EPMA are already available on these samples [4].

From these compacts 1 mm thick samples have been cut.

Moreover from the as-manufactured SELENIUM fuel plates (UMo(Si)/Al and UMo(ZrN)/Al), 10×10 mm² samples have been cut and the cladding being subsequently removed by mechanical polishing.

After manufacturing either at SCK•CEN (coated powder production) or at AREVA-CERCA (fuel plate production), the final preparation of these 17 samples has been performed at TUM/FRM II. Table 1 recaps the characteristics of the samples analysed by HE-XRD.

	UMo powders	UMo compacts					Fuel plates
		Un-annealed	340°C for 130 days	450°C for 4 hours	550°C for 2 hours	550°C for 4 hours	
UMo		x	x	x	x	x	
UMo(Si)	x		x	x		x	x
UMo(ZrN)	x	x	x	x	x	x	x

Table 1: SELENIUM samples characterised using HE-XRD.

b. Data acquisition

HE-XRD measurements have been performed at the ESRF (Grenoble, France) on the ID15B beamline using a 87keV X-ray beam which has a size of about 0.3×0.3mm². At least 20 locations per sample have been characterized in transmission mode.

Data have been analysed using with the FullProf software which uses the Rietveld method. At least 10 phases have been taken into account in the refinement. These phases are: α-U (destabilisation of UMo fuel), two γ-UMo phases (with different Mo content), UC (contamination induced during casting of the UMo ingots), as well as UO₂ (native oxide layer on the surface of the fuel kernel), UAl₃ (resulting from interaction fuel matrix), U₆MoAl₄₃ (resulting from interaction fuel matrix), U₂Mo (resulting from annealing), and U(Mo,Al)₂ (resulting from interaction fuel matrix), Si (coating), ZrN (coating) which may be found in the surrounding layer of the UMo particles, and finally the Al matrix itself.

In all measured patterns presented in this paper, the background has been removed.

3. Experimental results

a. Si and ZrN coated powders (UMo(Si) and UMo(ZrN))

The patterns measured on the coated UMo particles confirm that no destabilisation of γ-UMo phase has occurred during the PVD process. Indeed no trace of α-U has been found in both samples as usually observed in as-fabricated UMo atomised powder [7]. Note the asymmetry of γ-UMo Bragg lines as shown in Figure 1-A for the (310)-direction: this observation is in agreement with the presence of two γ-UMo phases related to Mo-depleted zones in the vicinity of grain boundaries. Indeed difference in the Mo content of γ-UMo phase will cause a shift in lattice parameter.

Moreover some contaminations have been identified in the UMo particles. As already reported for fuel plates, the UC and UO_2 phases have been detected within the expected concentration range (about 1 and 0.3 wt% respectively) [5, 8]. However the PVD treatment did not induce an important oxidation. The presence of Al (1wt%) is more surprising but could be the result of a contamination during preparation.

Finally the presence of a last phase must be noted (see Figure 1-B); it has not been possible to determine its nature up to now. However complementary measurements (μ -XRD) have demonstrated that this phase was not located in the outer shell of the UMo particle but rather in the core [8].

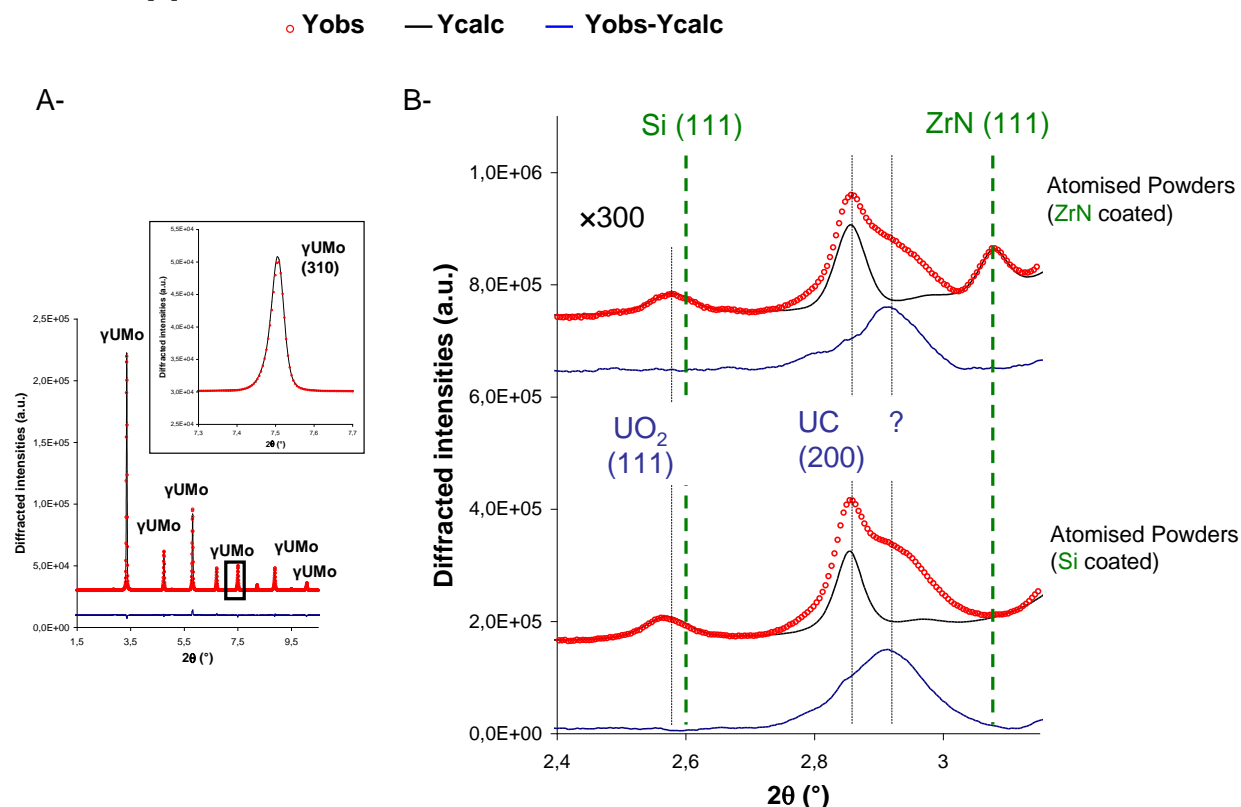


Figure 1: HE-XRD patterns collected on UMo(Si) and UMo(ZrN) powders (A-) and zooms in the [2.4;3.2] 2θ range. Red circles represent measured data, whereas black and blue lines indicate calculated and difference (between observed and calculated data) patterns, respectively.

On top of the results obtained on the UMo particle core, these HE-XRD measurements can also be sensitive to the coatings (see Figure 1-B). It must be reminded that a measurement of the UMo powder granulometry is required to convert the measured weight fractions into coating thicknesses [6,8]. The results of such measurement on SELENIUM powders being not yet available, it has been chosen here to consider for the thickness calculations the granulometry of UMo powders used for manufacturing IRIS plates.

In the case of Si deposition, it has not been possible to assess the presence of the Si phase (Fd-3m, $a_0=5.43$ Å). Indeed the peaks of this phase systematically overlap with the UO_2 broad ones thus making a definitive conclusion difficult.

It has been shown that the Si quantity in a 0.6 μm thick Si coating is equivalent to that found in the meat of a UMo/Al(Si) fuel plate with a matrix containing 5wt%Si [9, 2]. Considering that the matrix fraction in the meat is about 13wt% (in conventional 8 $\text{gU}\cdot\text{cm}^{-3}$ UMo/Al fuel plates), the Si weight fraction in this UMo powder should yield about 0.5wt%. However HE-XRD pattern simulations have demonstrated that such a quantity of crystalline Si is not present in the analysed powder.

In the case of ZrN coatings, Bragg lines can be unambiguously attributed to the ZrN cubic structure (Fm-3m, $a_0=4.08$ Å). The amount of this phase (about 1.2wt%) is however lower than expected if one considers both the measured thickness (1 μm) and density (about 6.8 $\text{g}\cdot\text{cm}^{-3}$). The presence of amorphous ZrN could thus not be fully excluded.

b. Full size fuel plates

The destabilisation ratios observed in the two analysed fuel plates (UMo(Si)/Al and UMo(ZrN)/Al) are low but in agreement with those reported for fuel plates manufactured under similar conditions [6]. The weight fraction of the α -U phase in the UMo particle core (α -U_ratio) is close to 14wt%.

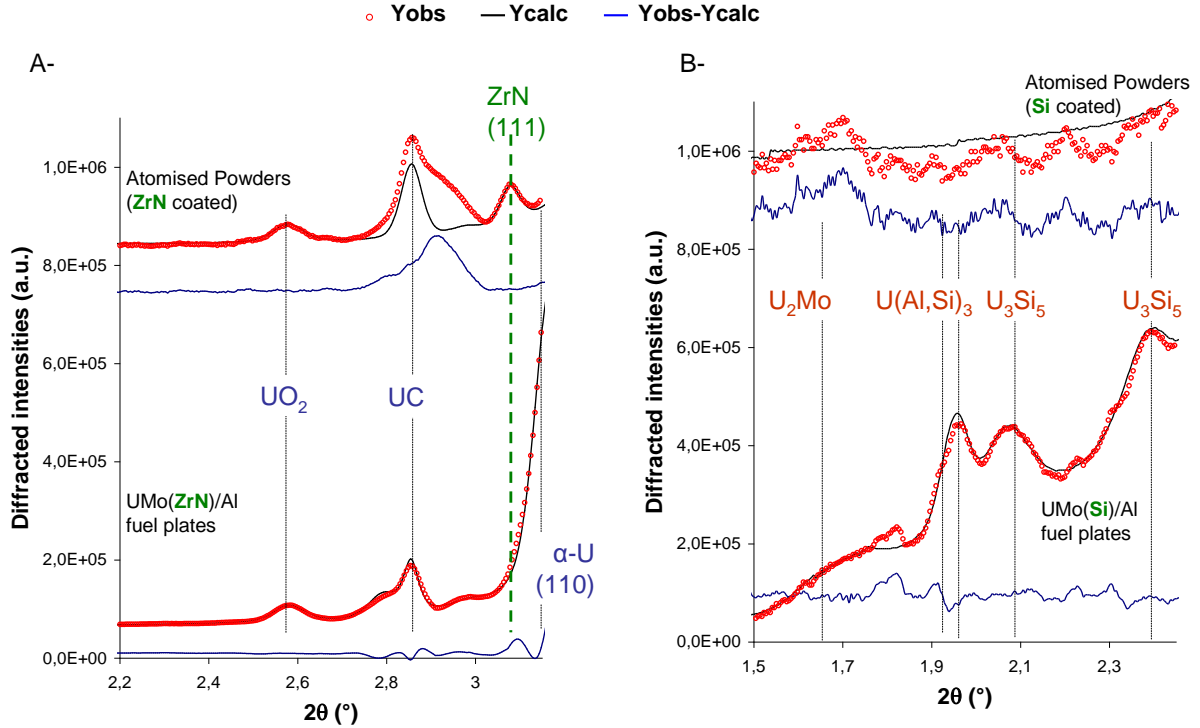


Figure 2: Comparison between HE-XRD patterns collected on UMo(ZrN)/Al (A-) and UMo(Si)/Al (B-) as manufactured fuel plates and as coated powders. Zooms are shown for two different 2θ ranges ([2.2; 3.1] (A-) and [1.5; 2.5] (B-))

The HE-XRD measurements on the as-fabricated UMo(ZrN)/Al fuel plate do not enable the study of the ZrN crystal structure. The reason is that ZrN's most intense peaks overlap with the α -U Bragg lines which exhibit a higher intensity.

The analysis of the UMo(Si)/Al fuel plate is much more fruitful. HE-XRD measurements definitely show the presence of two uranium Silicide phases:

- $U(Al,Si)_3$ with two lattice parameters (4.16\AA and 4.21\AA),
- A distorted U_3Si_5 phase.

Note that these phases were not present in the UMo(Si) powders and are those usually found in the Silicon rich diffusion layer (SiRDL) obtained in UMo/Al(Si) fuel plates after manufacturing [EFUTURE and IRIS plates, 6] as well as in UMo/AlSi7 [10] or UMo/Si [11] diffusion couples. This analysis is furthermore in full agreement with the SEM/EDX characterisations which have highlighted the growth of a SiRDL in these UMo(Si)/Al fuel plates [3]. However it must be stressed that the amount of these $U(Al,Si)_3$ and U_3Si_5 crystalline phases (about 0.3wt%) is lower than the one obtained for fuel plates containing 4-6wt% Si in the matrix [6]. It equals to the SiRDL amount measured in the IRIS4_2.1%Si fuel plate. Using these HE-XRD measurements, the Si concentration is evaluated to 51at%.

Three hypotheses can be proposed to explain this result:

- A larger amount of amorphous phases would be present in the SiRDL of UMo(Si)/Al than in UMo/Al(Si) plates; indeed macroscopic HE-XRD measurements are only sensitive to the crystalline phases in the SiRDL and very recent TEM characterisations conclude on the presence of amorphous compounds in this IL [12],
- A fraction of the Si has not reacted with Uranium to grow the SiRDL,
- The granulometry of the UMo atomised powder used for producing this UMo(Si)/Al fuel plate would be much larger than the one selected of IRIS/E-FUTURE fuel plates.

c. Compacts

In this section, the UMo loading and destabilisation ratios will be first described and the influence of a given protective layer on the growth of the UMo/Al interdiffusion layer (IL) will be then discussed.

The analysis of HE-XRD patterns collected on the 13 compacts has demonstrated that the U loading was particularly low compared to fuel plates. For example, Al weight fractions in compacts has been found to be about 80wt% instead of 13wt% in conventional 8 gU.cm⁻³ UMo/Al fuel plates [6]. As a consequence of the low UMo powder amount in the analysed samples, the composition of the coatings became very difficult to analyse. They will not be discussed in this paper.

The composition of the UMo particles core derived from HE-XRD patterns is in large agreement with the U-8Mo TTT curve (see Figure 3-A). Indeed, whatever the coating (see Figure 3-B), the destabilisation products are mainly:

- U₂Mo and α -U for compacts annealed at the two lowest temperatures (340 and 450°C),
- γ -UMo and α -U for compacts annealed at 550°C.

In the IL between Al and destabilised γ -UMo atomised particles, three main phases have been identified: UAl₃, U₆Mo₄Al₄₃ and UAl₂ as expected from literature [5,13]. From Figure 4, it is clear that both ZrN and Si coatings are very efficient in limiting the growth of the UMo/Al IL. Indeed for thermal treatments at 550°C, if a thick IL has been measured in UMo/Al compacts, almost no IL could be found in UMo(Si)/Al and UMo(ZrN)/Al annealed under the same conditions. Note that no significant amount of IL has been detected neither in UMo/Al nor in UMo(Si)/Al compacts annealed at 340 and 450°C: the presence of a thick oxide layer in these compacts may also explain this low reactivity. UMo(ZrN)/Al compacts are significantly less affected by the presence of UO₂.

These HE-XRD measurements therefore confirm not only SEM/EPMA analyses on these annealed compacts but also recent heavy ion irradiation experiments performed on the related fuel plates [3].

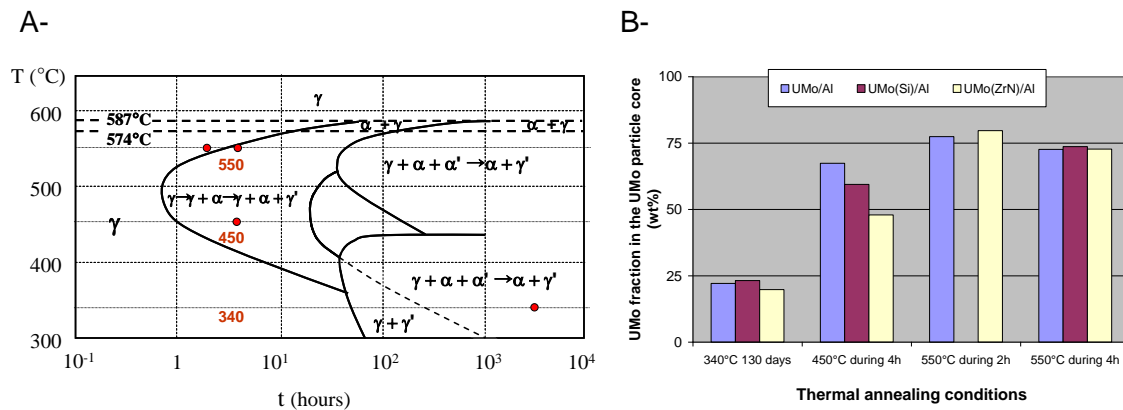


Figure 3: Destabilisation of the γ -UMo phase in the analysed compacts.

Superimposition of the compact annealing conditions (red circles) with the U-Mo8 TTT curve taken from [14] and references therein (A-).

Normalised UMo fraction in the particle core after annealing as determined by HE-XRD (B-). Note that only the UMo(ZrN)/Al compact annealed at 450°C during 4h exhibits a destabilisation ratio different from the other compacts annealed in the same conditions (more work is undergoing to understand this difference).

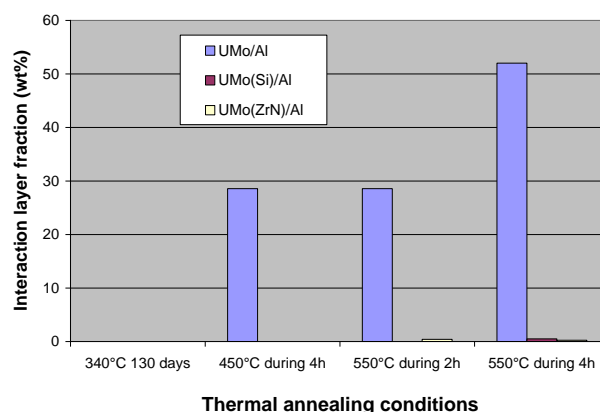


Figure 4: Normalised UMo/Al interaction layer weight fractions in compacts

4. Conclusions

In this paper, Si and ZrN coated atomized UMo powders, full size test plates and compacts were considered. The effects of different annealing conditions were examined by high energy X-ray diffraction.

For the coated powders, the PVD sputtering process is shown to avoid both destabilisation of the γ -UMo phase and surface oxidation of the UMo particles. Moreover, evidence has been provided for the presence of the crystalline ZrN in the UMo(ZrN) powders.

Concerning UMo(ZrN)/Al full size plate, it has been impossible using these macroscopic measurements to state on the presence of the ZrN phase. On the contrary, $U(Al,Si)_3$ and U_3Si_5 compounds have been detected in UMo(Si)/Al as fabricated fuel plates using HE-XRD thus confirming the presence of a regular SiRDL in these samples. Both Uranium Silicide phases have not been detected in the powders.

Investigations performed on UMo/Al, UMo(Si)/Al and UMo(ZrN) compacts have demonstrated that the 1 μ m ZrN coating as well as 0.6 μ m Si coatings are very efficient for preventing the growth of an IL under thermal annealing.

More local measurements (TEM or even nano-XRD) would be required to better describe the coating crystallographic composition.

Acknowledgments

This work was supported by a combined grant (FRM0911) of the Bundesministerium für Bildung und Forschung (BMBF) and the Bayerisches Staatsministerium für Wissenschaft, Forschung und Kunst (StMWFK).

References

- ¹ S. Van den Berghe, A. Leenaers, C. Detavernier, RRFM 2011, Rome, Italy.
- ² S. Van den Berghe, A. Leenaers, C. Detavernier, RRFM 2010, Lisbon, Portugal.
- ³ R. Jungwirth, T. Zweifel, H.-Y. Chiang, W. Petry, S. Van den Berghe, A. Leenaers, RERT2011, Santiago, Chile.
- ⁴ A. Leenaers, S. Van den Berghe, C. Detavernier, RRFM 2011, Rome, Italy.
- ⁵ A. Bonnini, H. Palancher, V. Honkimäki, R. Tucoulou, Y. Calzavara, C.V. Colin, J-F. Bérrar, N. Boudet, H. Rouquette, J. Raynal, C. Valot, J. Rodriguez-Carvajal, Zeit. Krist. Proc. (2011) 1, 29-34.
- ⁶ H. Palancher, A. Bonnini, V. Honkimäki, T. Buslaps, M. Grasse, B. Stepnik, T. Zweifel, J. Alloys and Compounds, (2012) accepted; A. Bonnini, H. Palancher, F. Charollais, MC. Anselmet, V. Honkimäki, P. Lemoine, RRFM2011, Rome, Italy.
- ⁷ J. M. Park, H. J. Ryu, K.H. Kim, D. B Lee, Y. S. Lee, J. S. Lee, B. S. Seong, C. K. Kim, M. Cornen, J. Nucl. Mater. 397 (2010) 27–30.
- ⁸ A. Bonnini, H. Palancher, P. Cloetens, H. Suhonnen, V. Honkimäki, in preparation.

-
- ⁹ S. Van den Berghe, A. Leenaers, E. Koonen, L. Sannen, *Advances in Science and Technology* (2010) 73, 78–90.
- ¹⁰ J. Allenou, H. Palancher, X. Iltis, M. Cornen, O. Tougait, R. Tucoulou, E. Welcomme, Ph. Martin, C. Valot, F. Charollais, M.C. Anselmet, P. Lemoine, *J. Nucl. Mater.* 399 (2010), 189-199.
- ¹¹ A. Leenaers, S. Van den Berghe, W. Knaepen, C. Detavernier, submitted in *Solid State Sciences*.
- ¹² B. Yao, E. Perez, D.D. Keiser Jr., J.-F. Jue, C.R. Clark, N. Woolstenhulme, Y. Sohn, *J. Alloys and Compounds*, 509, 9487-9496.
- ¹³ H. Palancher, R. Tucoulou, P. Bleuet, A. Bonnin, E. Welcomme, P. Cloetens, *J. Appl. Crystallogr.* 44, (2011) 1111-1119.
- ¹⁴ F. Mazaudier, C. Proye, F. Hodaj, *J. Nucl. Mater.* 377 (2008) 476–485.

UPDATE ON FUEL DEVELOPMENT OF MONOLITHIC UMo CORE Zr ALLOY CLADDING MINIPLATES AND PLATES

M. LÓPEZ, A.G. GONZALEZ, H. TABOADA

Nuclear Fuel Cycle Management, National Commission of Atomic Energy (CNEA)

Libertador 8250 (CP 1429), Buenos Aires, Argentina

ABSTRACT

In the frame of the RERTR program and since 1978 the National Atomic Energy Commission of Argentina (CNEA) has been deploying an intense activity on high density fuel developments 1, 2). In particular and since 2004, the monolithic U-Mo fuel core concept was specially developed in CNEA.

Several efforts have been made on the UMo monolithic core with Zirconium alloy based cladding concept, which is a promising, low cost, simple known technology one. An update of the results found during this development with miniplates and plates is shown in this work.

1. Introduction

During a considerable time many studies on Uranium-Molybdenum alloys were done and demonstrated that are good candidates for research reactors fuel performance (3, 4), this material has a good requiring in high density and good irradiation performance at high burn up. Clearly depending on the amount of Mo content there is a compromise between the capability to stabilize gamma phase U and acceptable U density and parasite neutron capture by Mo95 isotope for the fuel.

In the National Commission of Atomic Energy (CNEA – Argentina) many experiments were done with monolithic fuels, employing zircalloy-4 as frame and covers to avoid the well known interaction between Uranium and aluminum. During those experiments a special material in the interlayer where Mo, U and Zr appear were observed. In general, the presence of Molybdenum in U-Mo alloy stabilizes gamma phase, on the other hand Zirconium presence lowers its stability.

The process employed to obtain the miniplates involved the hot co-rolling of Zry-4 (as cladding) and UMo alloy (the fuel material in the core) which percentage of Molybdenum (Mo) includes 7, 8 and 10 % (%wt/wt). This Mo content (3, 4) is enough to retain the gamma phase at low temperature but also not to penalize the reactor neutronics due to the capture cross section of Mo95 isotope.

Regarding hot co-rolling temperature between 575° - 660°C the presence of some amount of alpha plus delta phases were revealed by analyses. Also although hot rolling at 800-850°C takes place in gamma phase (with metastable bcc crystal structure), an important dog bone zone (5) and $U_xZr_yMo_z$ phases (6) were found. To avoid both drawbacks an intermediate temperature at 700°C was employed.

2. Experimental Procedures

The miniplates were made by picture and frame process, employing as fuel different alloys of UMo (7, 8 and 10% of Mo) and covered by Zry-4. These materials were assembled and TIG welded at external borders, after that they received a hot co-rolling treatment at different temperatures (650°, 750° and 800°C).

The UMo alloys were melted in an induction furnace inside a zirconia-ytria crucible and poured into a graphite mold. The time employed to obtaining the alloy was 20 minutes, with 400 mbar Ar of pressure, employing a power of 5-20 Kw, and a temperature from 25 to 1550°C. Three Argon cleaning process at 300 mbar was made. The ingot obtained was cut in order to obtain coupons of 1 mm of thickness, and both, frame and coupons were polished to 120. The welded sandwich was hot co-rolled in seven or more steps up to the total deformation required to reach the final dimensions of the U-Mo foil: 0,14 mm thick.

2.1 Microprobe analysis.

Some specimens were subjected to microanalysis in a microprobe with Cameca SX50 standards. These results can be observed in the figure 3 a).

TEM and EDAX analysis were made too and different growing of the interlayer was observed.

The results obtained for both methods were coincident.

3. Results

In the work under different rolling temperatures produces different effects and it can be seen clearly in the figure 1-a).

Figure 1 show a thin interlayer, but no difference in the composition of the initial materials of the cover, frame and fuel coupon, this figure correspond to a hot co-rolling at 650°C.

Figure 2 show a small interlayer at the hot co-rolling at 700°C and the composition is a little different from the 650°C, and a dog bone appeared at both coupon ends, less than the one observed at 800°C.

Figure 3-d) shows the radiography, the TEM and EDAX analysis and the microprobe analysis where it can be observed an interesting interlayer between the Zry covers and the UMo coupon, it can be seen clearly that new compounds are formed with composition of U_xZr_y and $U_xZr_yMo_z$, that are in concordance with other studies [7] .

This comparison enables improving the fabrication conditions.

4. Discussion

Regarding the pack assembly it is essential to prevent gaps and oxygen presence as well as impurities by achieving an intimate fit between Zry-4 and UMo fuel components and clean surface contact. In other case, those could be areas for potential debonding which could undermine optimum bonding during pack reduction.

In all cases TIG welding was employed in the same conditions, and different kind of interlayers was observed. It can be concluded that this procedure do not contribute to the decomposition of the U_xMo .

For plate hot co-rolled at 800°C a marked dog bone regions were observed at each end of plate with are characteristic of the ductility difference between the U-xMo alloy and the Zry-4 at this temperature, but no roll speed effects was observed. This observation could be diminished but not disappeared if it is used a longer lead or ends. Not dog bone was observed at 650°C.

5. Figures

Figure 1

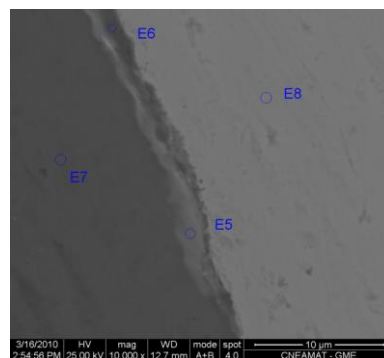


Fig. 1-a) Micrograph of U7Mo - 650°C miniplate –

Point E5 shows the presence of U-Zr, E6 U-Mo-Zr, E7 Zr, E8 U-Mo

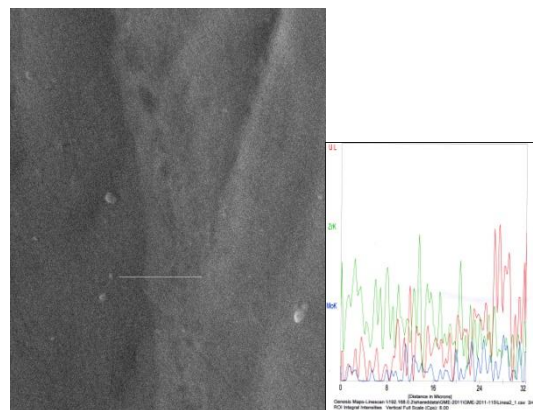
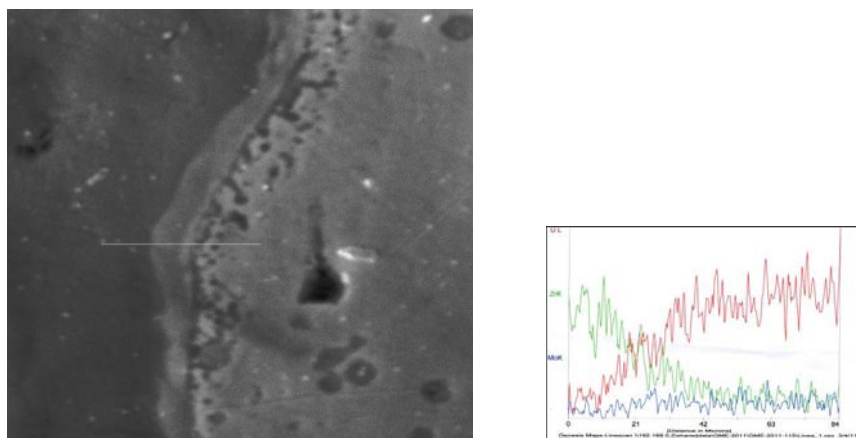


Fig. 1- b) Details of the composition on line of the interlayer

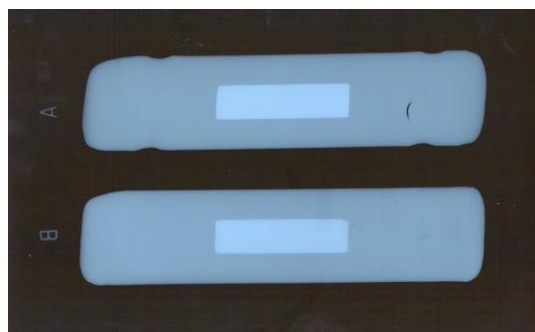
Figure 2



Relative composition of a line at 700°C

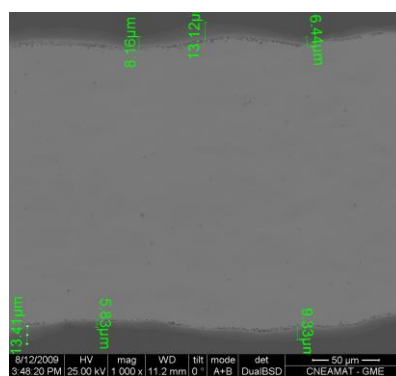
Figure 3

Figure 3 – a)



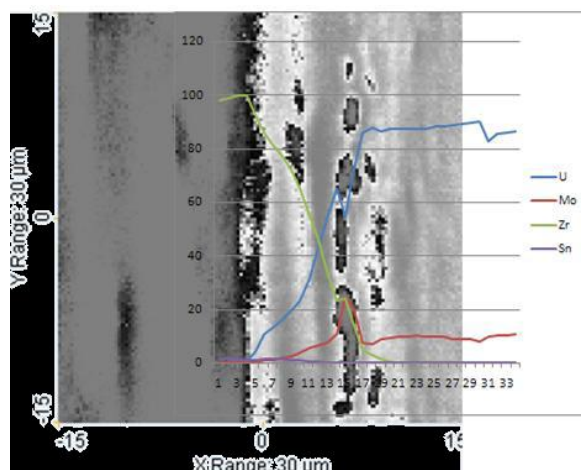
Radiography of a miniplate co-rolled at 800°C

Figure 3 – b)



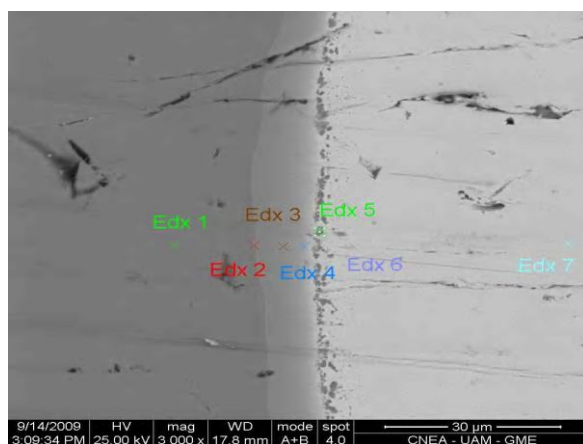
Micrography of the interlayer of miniplate 3-a)

Figure 3- c)



Microprobe composition of interlayer – Miniplate 3-a)

Figure 3-d)



EDAX analysis of miniplate 3-a)

Points 1 and 2: presence of Zr; Point 3: presence of Zr/U

Point 4: presence of Zr/U/Mo; Point 5: presence of Zr/Mo

Points 6 and 7: Presence of UMo

6. References

- [1] M. López, E.E. Pasqualini. Increasing the performance of U-Mo Fuels Abstracts. Presented at the 2004 International RERTR Meeting.
- [2] M. López, A. Gonzalez, R. Gonzalez, F. Rice, H. Taboada, D. Wachs. Monolithic U-Mo Based Plate Development New Findings, Fuel Development - Fuel Fabrication Technology. Presented at the 2010 International RERTR International Meeting, Portugal, 10-14 October 2010.

[3] M.S. Farkas, A.A. Bauer, F. A. Rough, The Constitution of Delta-Phase alloys of the System Uranium-Zirconium-Molybdenum`, Transaction of the Metallurgical Society of Aime, 215: 685-669 (1959).

[4] G.L. Hofman, A. E. Ray, `Design of High Density Gamma-Phase Uranium Alloys for LEU Dispersion Fuel Applications The 1998 International Reduced Enrichment for Test Reactor conference, October 18-23 (1998).

[5] J. L. Snelgrove, G. L. Hofman, C. L. Trybus, and T. C. Wiencek. Development of Very-High-Density Fuels by the Rertr Program. 19th International Meeting on Reduced Enrichment for Research and Test Reactors (RERTR). Seoul, Republic of Korea. October 7-10, 1996.

[6] M. K. Meyer, C. L. Trybus, G. L. Hofman, S. M. Frank, T. C. Wiencek. Selection and Microstructures of High Density Uranium Alloys. 20th International Meeting on Reduced Enrichment for Research and Test Reactors (RERTR) Jackson Hole, WY (US), 10 Oct 1997.

[7] E. Perez, B. Yao, D.D. Keiser Jr., Y.H. Sohn. Microstructural analysis of as-processed U-10 wt.%Mo monolithic fuel plate in AA6061 matrix with Zr diffusion barrier. Journal of Nuclear Materials (2010).

PROCESSING WINDOW DESIGN FOR U ALLOYS

D.A. LOPES, T.A.G. RESTIVO*, R.G. GOMIDE

LABMAT, Centro Tecnológico da Marinha em São Paulo, 18560-000 Iperó SP, Brazil.

A.F. PADILHA

Depto. Engenharia Metalúrgica e de Materiais, Escola Politécnica -USP, 05508-030 São Paulo, Brazil.

* corresponding author. Tel.:+5515 97814776, fax.:+5515 3229 8181; thomaz.restivo@usp.br

ABSTRACT

Nuclear fuels composed by uranium metal alloys in monolithic and dispersed forms have been considered for research and power reactors due to their density properties and fast heat transfer. The U-Nb-Zr and U-Mo alloys are the most promised systems for plate type fuel elements owing to its broad gamma-phase stable field, which shows higher ductility and isotropic behaviour, allowing extensive fabrication capability. Heat treatment processes are often employed to stabilize gamma-phase regarding one take in account the complexity of the transformation kinetics and the effect of impurities on the actual alloy behaviour and microstructure. Therefore, a thoroughly knowledge of transformation-temperature-time (TTT) diagrams is needed for design the process to obtain high quality products to be applied for nuclear purpose. Conversely to the conventional TTT diagram tracing, the work employs new tools, like drop calorimetry, as a complementary method to the dilatometry and X-ray diffraction. The former can detect enthalpies of heating and transformation from ambient up to selected isotherms while the dilatometer is used to scan for sample volume changes related to phase transformations. The resulted TTT diagram shows the gamma-phase temperature and time ranges stability for the alloys, driving the possible forming process schemes. The U-7.5Nb-2.5Zr alloy case has shown two processing windows under gamma-phase stability ranges at about 200°C and 400°C. The high temperature condition can be sustained up to 30 minutes. Some expected and new transitions findings are analysed besides the reaction enthalpies leading to clarify the actual transformation mechanisms for this alloy. One high temperature transformation path was detected to occur above 650°C. The U-10Mo alloy has shown slower transformation kinetics, expanding the magnitude of time scale.

Keywords: uranium alloy, TTT diagram, drop calorimetry, dilatometry.

1. Introduction

Nuclear fuels composed by uranium metal alloys in monolithic and dispersed forms have been considered to research and power reactors due to their density properties and fast heat transfer. Among several candidates, U-Nb-Zr and U-Mo alloys are the most promised systems for plate type fuel elements owing to its broad gamma-phase stable field. This fact allows extensive fabrication capability since cubic gamma-phase shows good plasticity, higher strength and elongation. Heat treatment processes are often employed to stabilize gamma-phase. However, the complexity of the transformation kinetics and the effect of impurities play an important whole on the actual alloy behavior and microstructure. Exogenous impurities are easily picked up during uranium metallurgical reduction, melting and casting. Therefore, a thoroughly knowledge of transformation-temperature-time (TTT) diagrams is mandatory for design the process and obtain high quality products.

Uranium metal occurs in three allotropic forms from the ambient temperature to the melting point: alpha-phase (α), which structure is orthorhombic, stable up to 661 °C; beta-phase (β), a tetragonal crystal structure, from 661 °C to 769 °C; gamma-phase (γ), a body-centered cubic structure, from 769 °C up to the melting point [1-3]. In addition to the three allotropic forms, many alloy systems subjected to quenching from the γ equilibrium field or subsequent annealing show transitions to a variety of metastable supersaturated phases arising from martensitic and diffusional mechanisms [2]. In general, the phase transformation of U-rich alloys systems follow the sequence: $\gamma \rightarrow \gamma^s \rightarrow \gamma^o \rightarrow \alpha'' \rightarrow \alpha' \rightarrow \beta \rightarrow \alpha$.

The technological interest is to retain the γ -phase at room temperature or a very similar structure like γ^s .

Rapid quenching the alloy U-7.5Nb-2.5Zr (Mulberry) from the high-temperature γ -phase field suppresses diffusional decomposition, resulting in the formation of supersaturated metastable γ^s phase. These phase generally exhibit better combinations of strength and ductility than the unalloyed uranium [4]. In addition, the presence of alloying elements in supersaturated solid solution substantially improves their corrosion resistance. Annealing this alloy in temperatures below the γ -phase field causes the phase decomposition into two new ones: $\gamma_3 + \alpha$. This reaction is driven by diffusion, being analogous to pearlite in steels, where alternating platelets of essentially alloy-free α uranium and alloy-enriched γ_3 is formed [4]. This two-phase structure exhibit somewhat higher strength and low ductility. In spite of this well-known knowledge on U alloys, there are rather few recent publications on the field [5-7]. Most part of the articles is older and should be reviewed through new techniques and concepts.

The U-10Mo alloy is a hypoeutectic composition of the binary system, undergoing a primary nucleation of alpha phase and subsequently an eutectoid decomposition at 565 °C resulting in alpha-uranium phase and the intermetallic phase MoU₂ (δ). The transformations show less sensitivity on quenching rate which enable the retention of gamma-phase with low cooling rates [8].

The knowledge on the transformation mechanisms and how long this phase transitions occur is essential for satisfactory processing of nuclear fuel plates. The alloy TTT diagram can anticipate the behavior for testing process schedules. Numerous studies of the alloying behavior and transformation characteristics of uranium base alloys have appeared literature during the past years [8-10]. However, significant differences still exist between existing investigations, making further experiments necessary. Apart to the troublesome microstructure and hardness analyses normally employed to build TTT diagrams, the authors propose calorimetric and dilatometric complementary methods applied over up-quenching mode. The advantage of such approach is the close heat cycle simulation to be used in the actual thermomechanical forming, driving to the establishment of process windows. X-ray diffraction analyses are also employed to strengthen the results.

2. Experimental

The U-7.5Nb-2.5Zr and U-10Mo alloys were melted in plasma and induction furnaces under purified argon. Alloy compositions were analyzed by ICP spectrometer: U-7.4Nb-2.3Zr and U-9.5Mo. The main impurities detected are Al, Fe and Cu rated to 1200 ppm total. The uranium alloy was heat treated at 1000 °C for 5 hours followed by water-quenching to obtain a solid solution γ -phase stabilized structure. Some homogenized alloy samples were also annealed at 300 °C and 500 °C for 6 hours to form the γ decomposition phases. Specimens were prepared by diamond polishing down to 1 μ m. These polished samples were analyzed by X-ray diffraction (Shimatzu XRD-6000, CuK α , 40kV) at 2 θ range from 20° to 80° and a scan rate of 0.02°/min. The calorimetric analyses were carried out at a Setaram quasi-Calvet MHTC model with both drop sensor and parallel DSC crucibles with alumina as the reference material. The DSC type allows scanning on cooling (10 down to 1 °C/min) the temperature and determining heat flow direction of transformation reactions for finned samples. By its turn, the samples are introduced into the drop captor down to the calorimeter cell under a stable temperature. The experiment scheme consists on dropping a NIST SRM720 sapphire standard and after a U alloy piece in six isotherms from 200 °C up to 700 °C. Sample mass weighed from 245 mg to 1025 mg. Since the standard enthalpy is known, the calorimeter constant can be evaluated at the respective temperature by the relation:

$$(H(T) - H(T_0))/S = K \quad (1),$$

where S is the endothermic peak integer with dimensions μ V.s, and K the constant [mW/ μ V]. The K values were used for the determination of heat change of dropped U alloy samples from 25°C up to the isothermal temperature, being maintained constant for 6 hours after drop to detect later peaks.

Square samples about 4mm length were analyzed in a dilatometer (Setaram Setsys

TMA) from room temperature up to 800°C (2hrs. isotherm) under heating rates of 40, 20, 10 and 5 °C/min in an argon atmosphere. The temperature determinations in all techniques were picked up by their onset values.

3. Results and Discussion

The X-ray diffraction profiles of both alloys showed a γ -stabilized quenched from 1000°C in room temperature as the starting phases. Heat treating isothermal-annealed samples of U-7.5Nb-2.5Zr and U-10Mo at 300 °C and 500 °C are shown in Fig. 1. For Mulberry alloy, The 300 °C annealed sample display diffraction profile identified as α'' characterized by a doublet at about $2\theta = 40^\circ$ [11]. Two phases were identified at 500 °C annealed sample (Fig. 1b) where well defined peaks of α -phase coexist with γ_3 cubic structure reflections shifted toward higher angles regarding γ -phase. U-10Mo alloy X-ray profile is unchanged after 300 °C treatment (Fig. 1c) while the 500 °C annealed sample profile (Fig.1d) discloses still a large amount of γ -phase besides noticeable reflections of α and δ (MoU_2) phases.

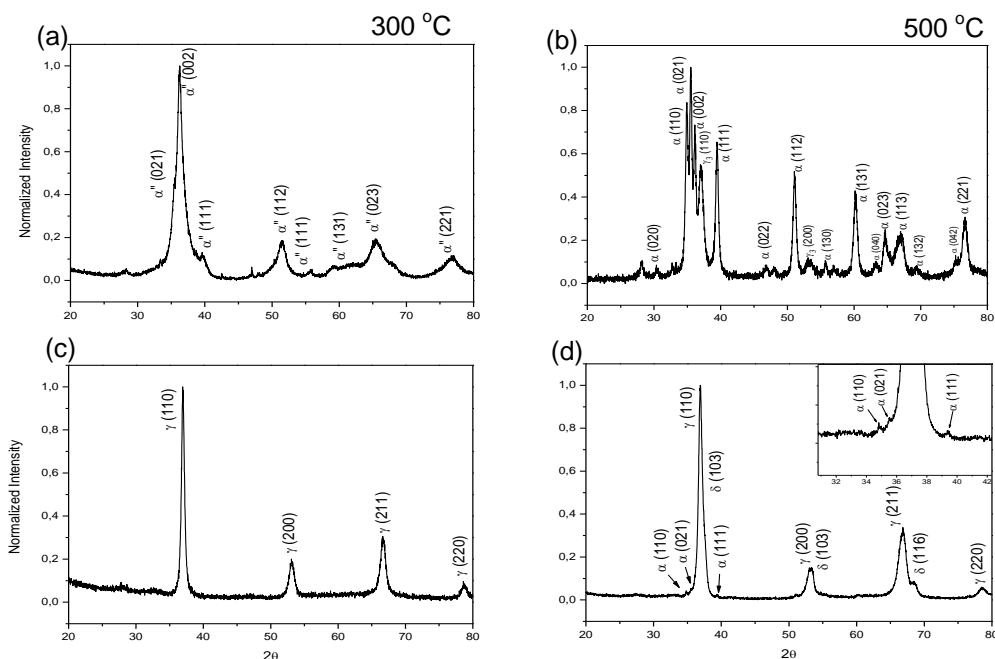


Fig 1. X-ray profiles for heat treated U-Nb-Zr (a,b) and U-Mo (c,d).

Examples of a drop calorimeter analyses are shown in Fig. 2. Peak integration provides the enthalpy change from ambient to the cell temperature. The total heat may include the enthalpy of heating and some possible transformations, if they are fast. For slower transformations, the related peaks and baseline drifts occur afterwards during the remaining isotherm. The onset temperature at 493 °C isotherm for U-7.5Nb-2.5Zr (Fig 2b) indicates the transformation end point of the endotherm, corresponding to 100% phase conversion. The calorimetry results for U-10Mo alloy has also shown relevant drifting and peaks as shown in Fig 2 c, d. New earlier transformations were detected in dropping experiments as a strong baseline change after the drop peak, which could be assigned to a second order transformation into γ -phase.

The calorimetric search of transformation points is aided by plotting the enthalpy of heating versus temperature (Fig. 3). Fitting the curve $\Delta H \times T$ shows for the U-7.5Nb-2.5Zr alloy that the peaks at about 500 and 600 °C are respectively more endo/ exothermic than the general point trend meaning there are two overlapped fast transformations inside the measured area. Similar shifts are not observed for the U-10Mo alloy which justifies the hypothesis of a second order transformation. The related onset time point cannot be exactly determined in these cases once the drop peaks are far more strong and takes place along 11

minutes. Therefore, the considered points were set at 2/3 of the peak duration.

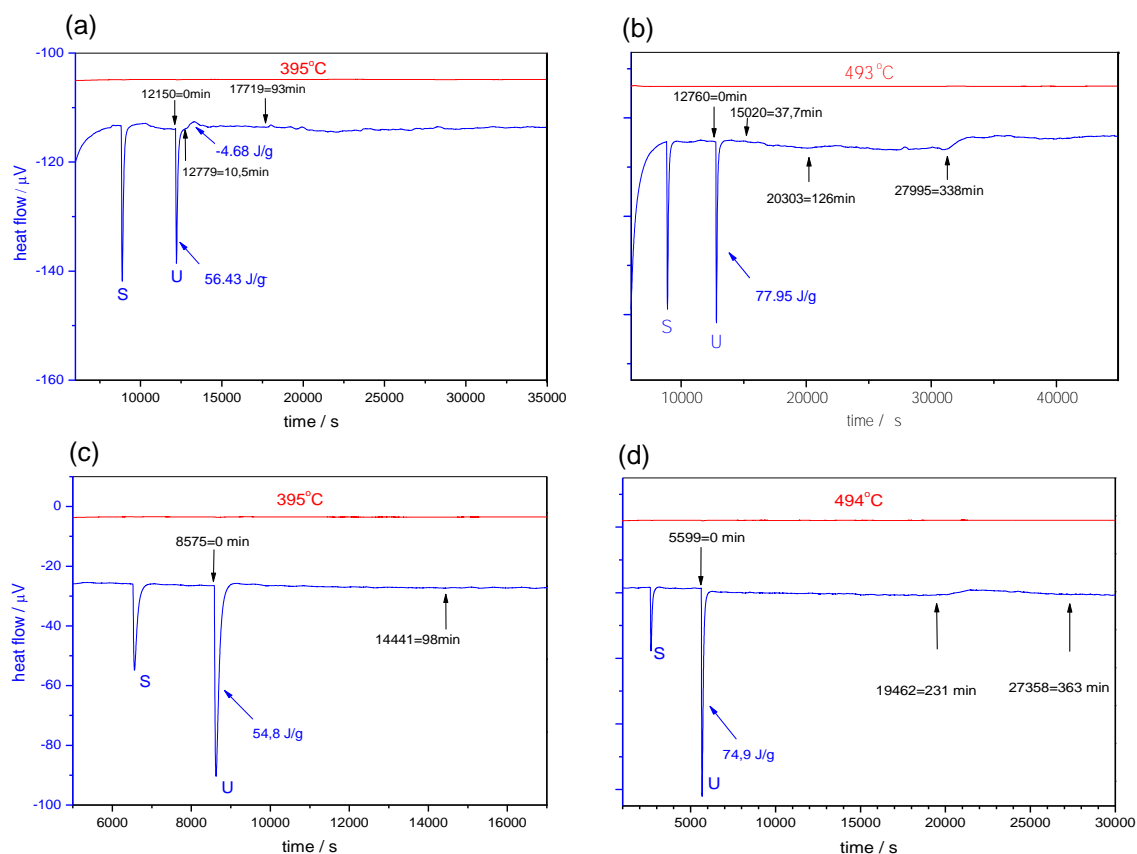


Fig 2. Drop calorimeter runs simulating up-quenching: U-7.5Nb-2.5Zr (a,b) and U-10Mo (c,d); drops: S = sapphire; U = uranium alloy

One approach to identify the actual phases is to take in account the dilation characteristics expected to each transformation, linking them to expansive or shrinkage behavior. Dilatometric results is shown in Fig. 4 for both systems at heating rates of 5 °C/min and shows a sequence of shrinkage and expansion for both alloys in the temperatures ranged from 370 °C up to 580 °C defining TTT boundaries data points. The dilatometric and calorimetric results are compiled in TTT diagram drawings for both alloys in Fig. 5. The dilatometric curves of U-7.5Nb-2.5Zr alloy has shown some expansion onset points at high temperature, suggesting there is a new transformation boundary. By its turn, the U-10Mo second order transformation points detected by calorimetry are included as a dashed line on the corresponding TTT diagram.

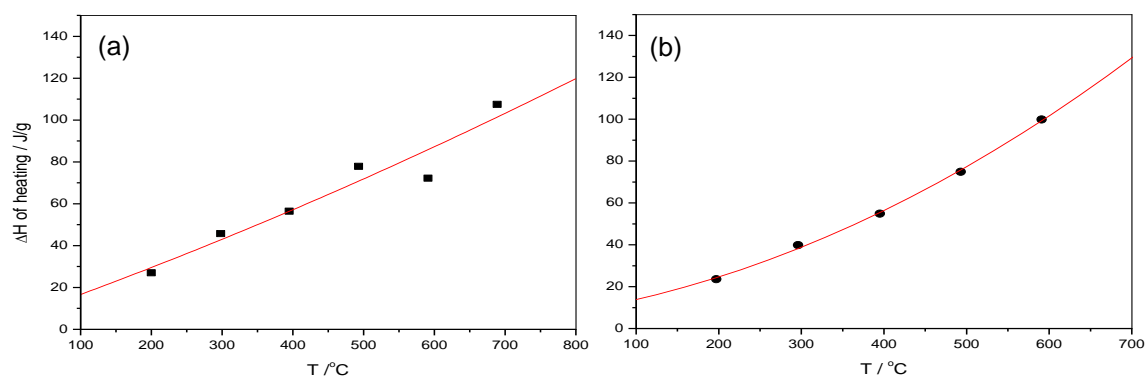


Fig. 3. Enthalpy of heating determined by drop calorimetry; U-7.5Nb-2.5Zr (a) U-10Mo (b).

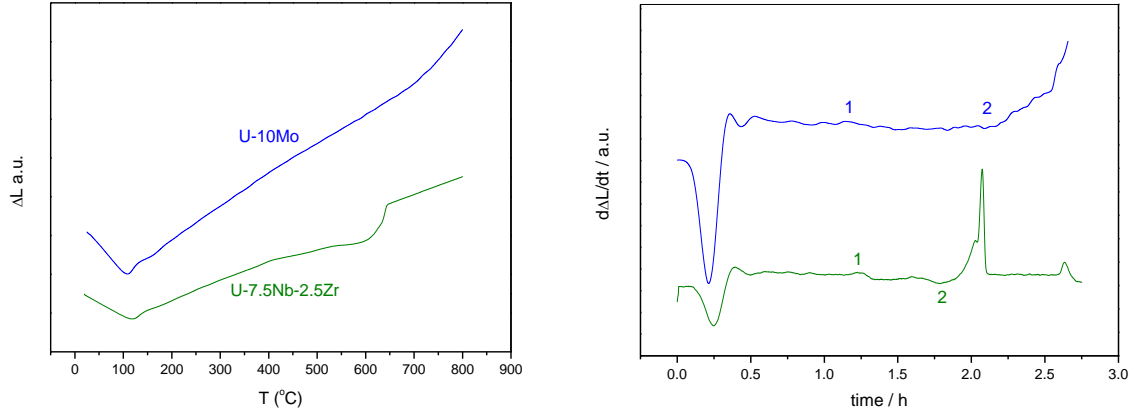


Fig. 4. Dilatometric analysis of U-7.5Nb-2.5Zr and U-10Mo alloy: ΔL curves (left) and the respective $d\Delta L/dt$ derivatives for heating rate 5°C/min.

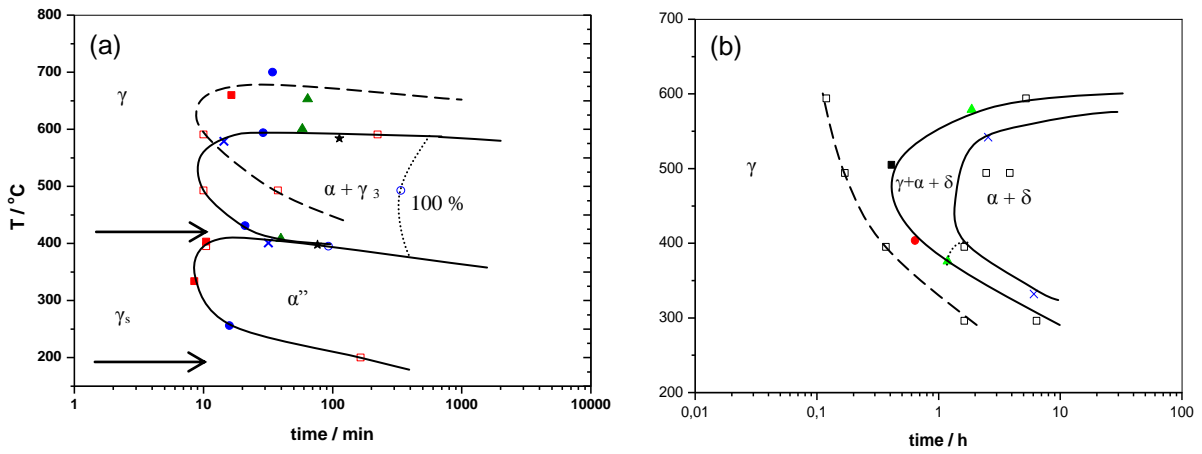


Fig. 5. TTT diagram drawings for U-7.5Nb-2.5Zr (a) and U-10Mo (b); calorimetry (hollow) and dilatometry (filled); x points refers to scanning calorimeter sensor; the two arrows represent the suggest processing windows.

The TTT diagram for U-7.5Nb-2.5Zr alloy displays low temperature transformations lines at longer times when comparing to previous diagrams in literature [8]. Under careful conditions, the γ -phase workability can be retained for 30 min at 400 °C or at about 200°C for longer times, being these some likely process windows for the alloy. Drawing the field boundaries among the data points suggest, inversely to the literature previous diagram, the upper limit of α'' is not a horizontal line, but rather a descending one over longer times. U-10Mo TTT demonstrates the alloy is far less restrictive regarding γ -phase decomposition, being the most critical condition found at about 500°C.

4. Conclusions

The TTT diagrams of U-7.5Nb-2.5Zr and U-10Mo alloys were determined by calorimetry and dilatometry combined techniques under up-quenching mode. In the first case, the processing windows can be set for long times at 200 °C and up to 30 minutes at 400 °C. The second alloy diagram displays extensive γ -phase stability region. The complementary calorimetric approach was proved as a useful tool in addition to dilatometry in order to provide further information, including transformation energies, as well as it consists on a more fast technique than the traditional ones.

The authors acknowledge the CNPq, CAPES and FINEP councils of MCT Ministry.

References

- [1] G. L. Hofman, A short note on high density fuels, ANL Bulletin, Argonne, Illinois, 1996.
- [2] W. D. Wilkinson, Uranium metallurgy Vol. II. Interscience Publishers, 1st edition, New York, USA, p. 867-1261, 1962.
- [3] W. D. Wilkinson, Uranium metallurgy Vol. I. Interscience Publishers, 1st edition, New York, USA, p. 02-217, 1962.
- [4] K. H. Eckelmeyer, Uranium and uranium alloys. in: Metals Handbook, volume 2. Tenth ed. Ohio, USA: ASM International, 1990.
- [5] A. Ewh, E. Perez, D. D. Keiser and Y. H. Sohn. J. of Phase Equil. and Diff., 31 [3] p. 216, 2010.
- [6] C.B. Basak, R. Keswani, G.J. Prasad, H.S. Kamath, N. Prabhu. J. of Alloys and Compounds. 471 (2009) 544.
- [7] D. E. Burkes, C. A. Papesch, A. P. Maddison, T. Hartmann, F. J. Rice. J. of Nucl. Mater. v. 403, p. 160-166, 2010.
- [8] Gerard L. Hofman and Mitchell K. Meyer. Design of high density gamma-phase uranium alloys for LEU dispersion fuel application. Proceeding of RERTR Meeting, São Paulo, oct. 1998.
- [9] C. W. Dean, Y – 1 6 9 4; Union Carbide Corporation-Nuclear Division, Oak Ridge Y-12 Plant, Oak Ridge, Tennessee; October 24, 1969.
- [10] P. E. Repas R. H. Goodenow R. F. Hehemann. Technical Report AMRA CR 63-02/I, 82p., 1963.
- [11] W. Lehmann, R. F. Hills. J. of Nucl. Mater. v. 2 , p. 261, 1960.

OPAL ENGINEERING STRATEGIES TO MANAGE NEUTRON GUIDE SEAL LEAKS

C. HUMPHREY* and P. METCALF

*Australian Nuclear Science and Technology Organisation (ANSTO)
Locked Bag 2001, Kirrawee DC, NSW 2234 Australia*

*Corresponding author: chris.humphrey@ansto.gov.au, P: +61 2 9717 7094, F: +61 2 9717 9228

ABSTRACT

In the first two years following hot commissioning of the OPAL Reactor in 2006 light water leaks were detected in all five (5) bellows leak detection chambers of the helium guide cooling system. These seals form part of the primary LOCA barrier for the reactor pool. To date no water has been detected past the double metallic C-seals of the neutron beam assemblies into the assembly boxes.

This paper reports strategies implemented by the OPAL Engineering group to manage current leak rates and deal with any future escalation of leaks. These include: changes to the reactor control and monitoring system to enable ongoing reactor operation, automation of the drainage operation, installation of a pool water leak recycling system, design provisions for helium back pressurisation and in-pool mechanical collar seals.

The systems approved and implemented on the reactor ensure that leaked water is drained from the inter seal void space to limit pressure on the inner seal. The system includes remote real time indication and warnings of leak rates and is capable of handling leak rates up to 0.5 m³/h. By automatically recycling the water drainage, the system has reduced plant radioactive liquid waste discharges and operator dose rates to ALARA.

1. Introduction

The Open Pool Australian Light-water (OPAL) research reactor is a 20 MW_t multi-purpose facility primarily for neutron beam research and medical/industrial isotope production.

The core of 16 plate-type fuel assemblies of LEU (19.75%) is light water (H₂O) cooled and moderated with a heavy water (D₂O) reflector contained in a cylindrical zircalloy Reflector Vessel (RVE) located at the bottom of the 12.6 m deep Reactor Pool (RPO).

There are five (5) neutron beam assembly penetrations through the RPO to the RVE that contain the tangential guides for transport of different energy range neutrons from the core to instrument users. Two are cold neutron beam assemblies (CG-1/2/3, CG-4), two thermal neutron beam assemblies (TG-1/2/3, TG-4) and one assembly for a future hot beam (HB-1/2).

The neutron beam assemblies are filled and cooled by helium gas from the Inner Neutron Guide Helium Cooling System (INGHCS). This system serves to remove gamma deposition heating to prevent thermal damage to the guide super mirror surfaces and to detect leakage of water from either the RPO or RVE. Since the neutron beam assemblies are at core height and form part of the RPO boundary their integrity forms part of the pool LOCA barrier.

A cross section of the beam assembly from the RPO to the RVE is given in Figure 1.

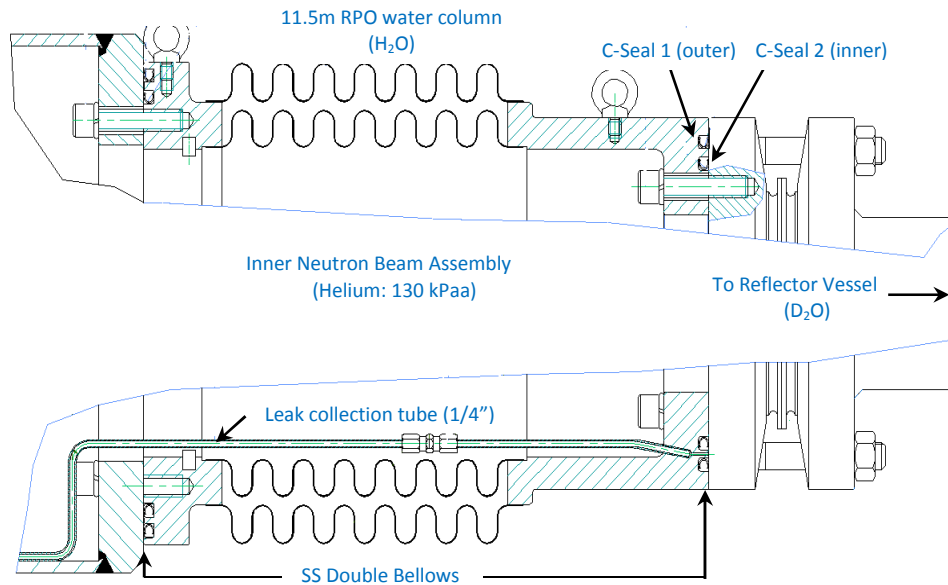


Figure 1: Inner neutron beam assembly - schematic

This figure shows the double metallic bellows and C-seals of the inner part of the beam assembly. There are two C-seals on both the RVE wall and RPO wall with one leak collection tube joining the inter-seal space per assembly. C-seal 1 (outer) and C-seal 2 (inner) together constitute the primary LOCA barrier. For 'defence in depth' an independent secondary LOCA barrier (not shown) consisting of an aluminium plate window bolted to the reactor face is installed for each beam assembly.

Light water pool leaks are detected by: (1) Level switches connected to each inter-seal space collection tube in the facility basement (bellows seals). (2) Gas dew point sensors and level switches connected to the helium atmosphere of each beam assembly (box seals).

2. Leak-rate History

Following OPAL first criticality in Aug 2006, full power commissioning in Nov 2006 and the initial period of early operation leaks were detected by control room alarms from the level switches in all five (5) bellows seals of the INGHCS. These are the chambers that collect water from the inter seal space of the double metallic C-seals of the beam bellows. Dates of discovery are in Table 1:

Seal	Discovery Dates
TG-4	Aug 2007
CG-4	July 2008
TG-1/2/3 and HB-1/2	Sept 2008
CG-1/2/3	Oct 2008

Table 1: Seal leakage discovery

In each instance the water was confirmed to be pool light water and not heavy water from the RVE. To date no water has been detected via either sustained high humidity of the helium or via the level switches connected to the inner neutron beam assemblies (box seals); thus LOCA barrier 1 is still intact.

Since discovery the objective has been to drain water that has leaked past C-seal 1 in a timely manner to reduce the potential for RPO water to back-up into the pipe and place increased demand on C-seal 2.

Figure 2 presents a summary of leak rate data for each beam assembly over the last 4 years. Of note is that leak rates increased during 2008/2009 and began to stabilise in 2010/2011 while the leak rate steadily rises and falls over the monthly power/shutdown/refueling reactor operating cycle. CG-1/2/3 and TG-4 represent the most significant leak sites.

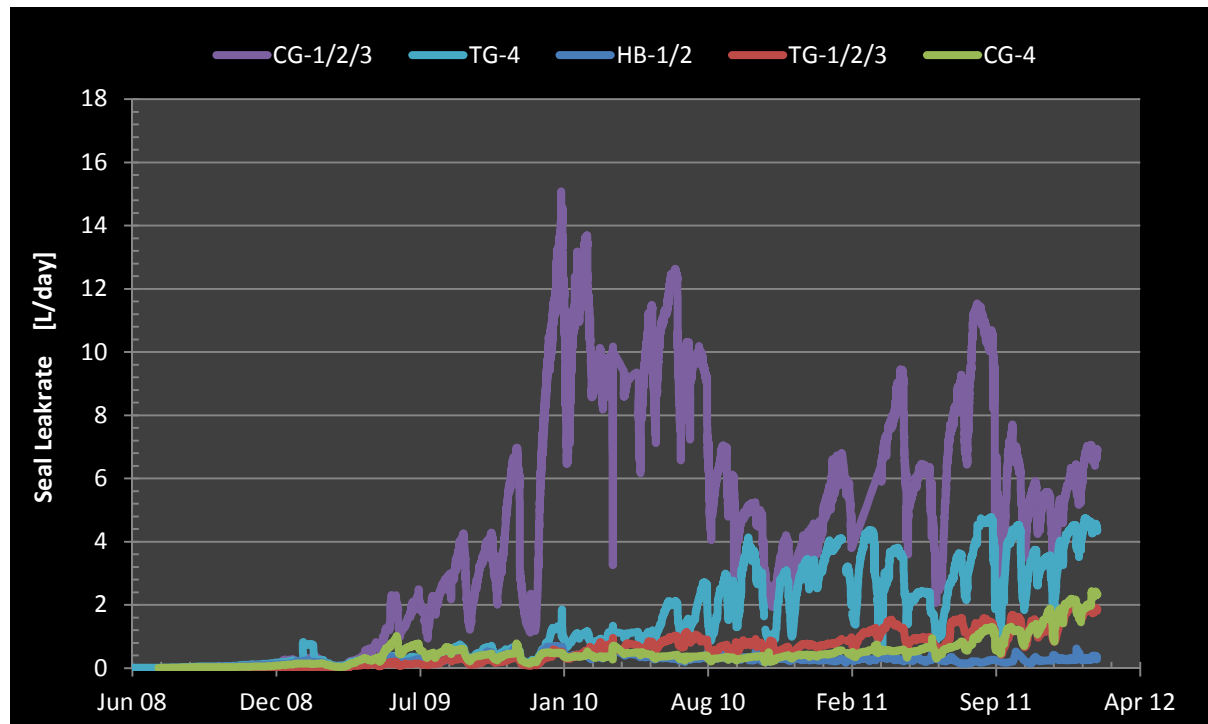


Figure 2: Neutron beam assembly – bellows seal leak-rate data

3. Mitigation Strategies

A range of strategies have been considered since discovery of the leaks each with differing levels of complexity and risk. The goal has been to safely allow for continued reactor operation with ongoing leak rate monitoring and strategy implementation at fixed triggering rates. Triggering ranges for different strategies agreed between ANSTO and primary reactor vendor INVAP S.E are:

Combined Seal Leak Rate [L/day]	Strategy
< 10	Automatic Drainage
10 – 100	Recycling System
>100	Helium Pressurisation
>> 100	Mechanical Collars

Table 2: Triggering Ranges for Mitigation Strategies [1]

3.1 RCMS Bank Insertion Removal

Implemented in Dec 2008 this change removed the Reactor Control and Monitoring System (RCMS) 'Bank Insertion' (controlled automatic shutdown function) from the five (5) level switches of the bellows seals. This enabled continued reactor operation whilst reducing the time critical task for operators to drain water before it reached the switches. The 'Bank Insertion' function for the five (5) level switches of the box seals was not altered. These serve the function of detecting large beam assembly leaks as required by the OPAL safety case [2]. Maintenance plans have also been implemented to perform a monthly visual check of these last five switches prior to start-up post refueling and an 18 monthly switch functional test.

Implemented in June 2009 this engineering modification project provided an automatic drainage system for the leaked water in the bellows seals to eliminate manual drainage and hence reduce dose rates to plant operators. The dose rate in the drainage area is ~ 150 $\mu\text{Sv/h}$ with manual drainage resulted in a collective dose of ~ 20 μSv per operation. The frequency of drainage at this time was up to 7 times/24 h period.

The system installed consisted of a series of 24V_{DC} solenoid valves controlled by the RCMS on a signal from the high level switches of the leakage collection chamber. Vacuum breakers were also installed to the vent lines to aid in free gravity drainage of the RPO water which was piped into the active liquid waste (B-line) system. The RCMS was programmed to record the drainage volume and frequency for leak rate tracking. This change had the outcome of eliminating operators doses received from manual drainage in line with ALARA principles.

Installed in Nov 2011 this engineering modification project designed jointly by ANSTO/INVAP involves recycling/recirculating leaked water from the bellows seals to the RPO via the existing pools hot water layer system. The modification was classified as a nuclear safety category 2 plant change by ANSTO and included an independent risk analysis in the form of a FMECA.

The installation to the INGHCS includes a new stainless steel pressure vessel, pump, valving and pipework. New instruments include two level switches for control of the pump and high level warning level switch; dedicated flow-meters (0.5 – 5.0 L/h) for each seal; local pressure indicators; and under/over pressure protection devices. The solenoid valves installed as part of the automatic drainage change have been retained. The system is sized for continuous duty of leak-rates up to 0.5 m³/h (12,000 L/day) with an overflow to the B-line active liquid waste network. The small 3φ pump of 0.55 kW is powered from a new cubicle installed in an existing MCC with LCS near the pump. A simplified P&I diagram of the INGHCS Recirculation System is given in Figure 3.

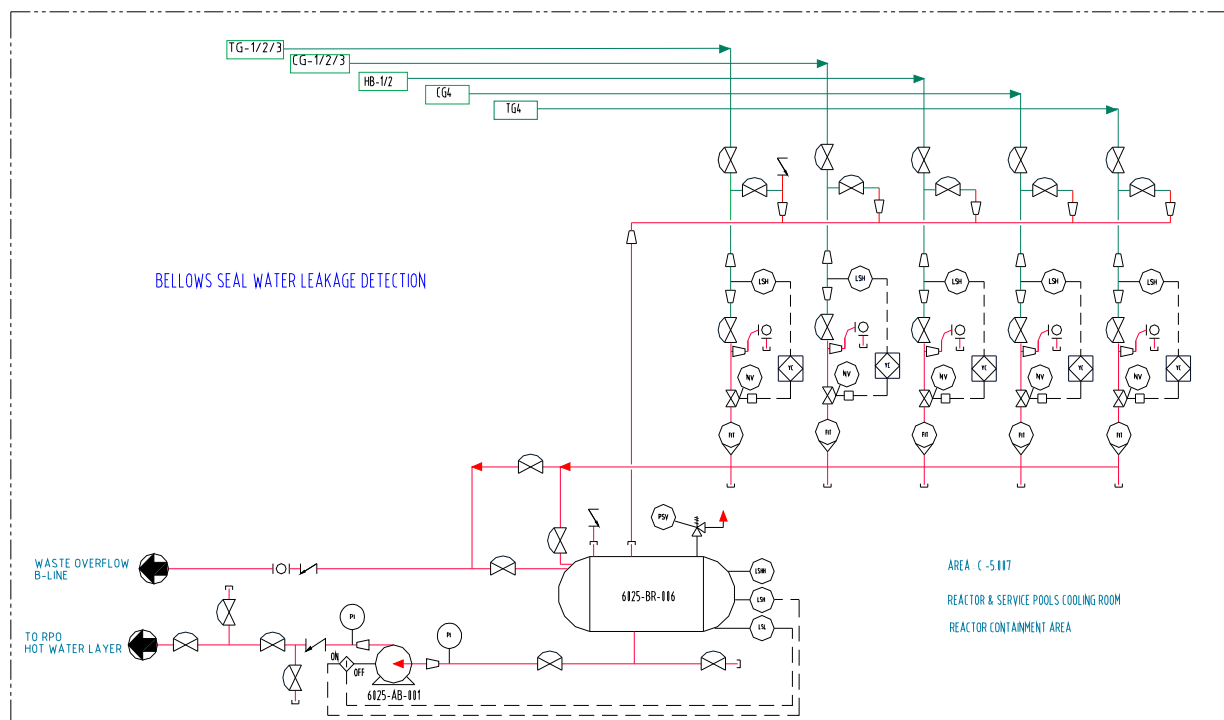


Figure 3: INGHCS Recirculation System – simplified P&I diagram

The system has two modes, 'Batch Discharge' or 'Continuous Discharge' with each bellows leak collection chamber being able to operate independently in a different mode depending on the leak rate over time. Mode transition is remotely performed from the RCMS by the configuration of the solenoid valves. In this way the system is capable of monitoring and draining both small and larger leaks into the future.

3.4 Helium Pressurisation

A concept design has been completed for helium pressurisation into the INGHCS Recirculation System to reduce the differential pressure in the space between the C-seals and the hydrostatic column of the RPO, see Figure 1. The design includes pressure protection devices for the guides in the event of over-pressurisation due to the breaking of the inner C-seal. This strategy has not been implemented on the reactor to date as leak rates remain relatively low.

3.5 Mechanical Collars

Based upon the success of mechanical clamps with graphite seals to rectify leaks on the RVE in Nov 2009 [3] INVAP S.E has prototyped mechanical closure collars for use in the RPO for both the RPO and RVE bellows flanges focusing on the CG-1/2/3 in-pool position.

Work has included laboratory bench tests of two collar designs and special underwater tooling for removal of in-pool obstacles (bellows cover, eye-bolts, and metal strip/s). A detailed 3D model of the in-pool area and a physical dry model for trial installation of collars from a distance of 8 m were completed in Feb 2011.

4. Conclusion

Since discovery of the neutron beam assembly bellows seal leaks in 2008 a range of management strategies have been developed to enable continued safe reactor operation. Plant changes implemented on the OPAL Reactor have been completed without any additional unscheduled reactor shutdowns and have resulted in doses to the operations group being reduced to ALARA, and discharges off-site via the active liquid waste network to be minimised. The online instrumentation provides the OPAL Engineering group with data to monitor the rates of water leakage past the first C-seal and plan for any future interventions.

5. Acknowledgements

Diego Arruda from INVAP S.E for support with design and installation works of the INGHCS Recirculation System.

6. References

- [1]. *Carlos Durione*, INVAP (May 2009), Beam Tubes Bellows Seal Leak Analysis, RRRP-0400-EBEIN-090-A.
- [2]. OPAL Safety Analysis Report, ANSTO Rev 01, Chpt 11 – Reactor Utilisation.
- [3]. *Russell Thiering*, ANSTO (Sept 2010), OPAL Reflector Vessel – Repairs Options to Mitigate Light Water Leaks, IGORR 13 Proceedings.

UPDATING THE IAEA DATA BASE ON RESEARCH REACTOR AGEING AND AGEING MANAGEMENT

(RRFM2012-A0110)

H.-J. ROEGLER
Independent Consultant
Bonn, Germany

At 2010 RRFM, the results of the 2008/09 IAEA Initiative on Research Reactor (RR) Ageing and Ageing Management have been presented¹. All information on RR Ageing has been compiled in an IAEA Database, accessible from all members of the RR Community. In 2011 IAEA contracted for an update of that data base which comprised (a) confirmation of the data provided in 2008/09 or (b) update of those data by the further experience gained since or (c) supplementary contributions on matters at the RRs reporting 2008/09 already or (d) new contributions from those RRs which had not participated last time.

In total 102 RRs have replied, a number exceeding the 77 from 2008/09 distinctly and can be considered as a success of IAEA's efforts to make the existing know how on RR ageing available to the entire RR community. The respective Database has been updated in 2011. The paper will highlight issues during collection of data and statistics of the results and their origins from the 2008/09 initiative and its 2011 update.

Everybody of the Research Reactor (RR) Community is aware that most of the operating RRs have aged. Also it is assumed that everybody of this community has knowledge of the many efforts of the IAEA for fighting ageing. These IAEA efforts are basically twofold: By numerous publications² the Agency has provided that guidance and support for the procedures and organization of structures at an RR in order to fight and minimize consequences of ageing and/or prevent effects of ageing endangering continuous operation or safety of the RR. On the other hand the Agency started already 1995³ to collect and compile existing experience from ageing and its fighting and curing to make that technical information available to the entire community. There are also quite some supplementary initiatives and actions by the Agency under other headlines which overlap with fighting ageing substantially, such as: (i) maintenance and repair, (ii) modernization and refurbishment, (iii) backfitting and re-licensing, (iv) upgrading, (v) surveillance and in-service inspections, and (vi) safety reviews.

This contribution will not deal with the publications for guidance and support, but with the existing knowledge on RR ageing and its provision to the RR Community. As mentioned, the

¹ H.-J. Roegler, Findings from Working for the IAEA Initiative on Research Reactor Ageing and Ageing Management, Transactions RRFM 2010, Marrakech, March 2010

² As examples may serve: IAEA-Safety Standard DS412: Ageing Management for Research Reactors; ISaG-2007: IAEA Activities for safe long term operation; IAEA-TECDOC-792: Management of Research Reactor Ageing; IAEA-TECDOC-1625: Research Reactor Modernization and Refurbishment; IAEA-TECDOC-1263: Application of non-destructive testing and in-service inspection to research reactors; IAEA-TECDOC-1387: Safety Considerations for Research Reactors in Extended Shutdown; IAEA-TRS-443: Understanding and Managing Ageing of Material in Spent Fuel Storage Facilities; IAEA-DS-382: Safety Guide on Ageing Management

³ 1995-Technical Meeting at Geesthacht, Germany with more than 100 participants; see Geesthacht-Proceedings; GKSS 95/E/51, containing 52 contributions on ageing

Agency started together with the German GKSS Research Centre a first attempt for members helping members of the RR Community to exchange their knowledge and experience on ageing and mitigating and/or curing the respective effects.

Early in 2009, during an Expert Commission Meeting at the Agency, it has been decided to start a more systematic approach for collecting RR Community's knowledge, this time in categories of systems and ageing mechanisms, all based on one IAEA template (structure as per Table 1) which had to be completed for participation. Moreover, the IAEA contracted for a person in charge of that initiative (the author).

Now the hard work began: contacting any and all RRs worldwide + convincing the operators on the value of participation, at first a value mainly for all other operators, but balanced by access to the information of very many other RRs.

Among the main difficulties of that job were finding valid Email addresses of all the 250 RRs, distinguishing the various names of some RRs from all the others, convincing one staff to reply to a person being not from the Agency, etc.

All this was done in 2009 and the 77 RRs⁴ having replied out of 133 being approached completed 152 templates with 249 times naming an ageing system. All these templates have been compiled in an initial version of the IAEA data base⁵. These figures⁶ are mentioned here as they were the starting point for the 2011 update of the initiative which had 2 main reasons for taking place:

Many of the 2009 templates reported of cases which had not been closed. Search for reasons were ongoing, authorities evaluation or repair action were pending, conclusions not been drawn for further management of ageing, all that being information the Agency wanted to collect supplementary to what has been reported already.

The participation rate of 77 out of about 250 operating RRs was less than what seemed to be possible to get, even when considering that all contributions being voluntary. Already in the 2010 reporting⁵ reasons for not-participating had been guessed: (i) fears of the respective authorities when publishing the ageing; (ii) lack of permission from owner/operator on publishing such "sensitive" data; (iii) fears of the anti-nuclear public; (iv) rejection of the entire idea of sharing such knowledge, and (v) language problems preventing dealing with the template and the not-adequately-simple background. The most extreme reply ever was: *"We do not have an ageing management program, because we do not have the funding for such a thing. We fix things when they break. That is unfortunately the nature of our business here due to monetary constraints. For me to fill out your template with something that is irrelevant is not worth your time, or ours. We also do not necessarily wish to have this information be publicly available."* Being rather harsh in its wording, however the reasoning for non-participating is fully understandable. That RR will not be the only-one thinking that way. And the anger with view to budget constraints had been

⁴ There were additional replies from authorities and industry dealing with RR technology and components, in total five only, distinctly below expectation.

⁵ The data base can be found under <http://www.iaea.org/OurWork/ST/NE/NEFW/AD/index.html>; responsible officer at IAEA is Mr. Edward Bradley <e.bradley@iaea.org>

⁶ The results of the 2009 initiative have been presented at 2010 RRFM at Marrakesh (see Footnote No. 1)

expressed frequently by those participating, too. Fortunately the statement did not condemn the initiative, but wants to see the experience compiled.

In 2011, a second run was finally started for the mentioned reasons and led to broadening of the basis of the information and the data base by now 90 RRs replying in 2011, either (a) confirming their 2009-input as still valid or (b) updating/renewing it or (c) completing further (new) templates. Well, the increase does not sound that great, but when considering that 24 RRs were new participants, it surely is. The gap between 90 (2011-replying) and 102 (totally participating)⁷ is originating from 12 RRs which did not confirm their 2009-input in 2011, but which will stay in the data base with the remark “unconfirmed in 2011”. It is worth to repeat: the total number of RRs having participated in the initiative is 102 which are 65 % of all RRs having been approached during both phases of the initiative. Table 2 shows a comparison between the 2009 and 2011 results.

The content, i. e. the distribution of the cases in terms of concerned RR systems and mechanisms is mainly changed by the larger number of cases (493 versus 367 in 2009; 34 % increase) than by any substantial redistribution. Nevertheless the most actual results (including very late contributions from 2012) have to be presented to the RR community together with highlighting some deductions.

The basic outcome is a 76×13 matrix (about 1000 boxes) loaded with 495 cases, what means that the majority of boxes is empty (see Figure 1). Despite the very many boxes one easily discovers a ‘Himalaya’-region consisting of obsolescence at the systems reactor protection, accident instrumentation, operational I&C and the Mount Everest: control console.

This first observation is clearly reflected when summing up the systems and look at the mechanisms only (Figure 2): obsolescence (K) is dominating, followed by corrosion (G) and mechanical displacement/fatigue/wear... (D). When one takes the mechanism: changes in requirements / acceptable standards as a special type of obsolescence together with “real” obsolescence, 190 cases fall into this dominant box. The radiation induced ageing (A) is of some size, but far from being dominant.

If one looks from the other side to that case matrix, i. e. from the systems, the 76 systems provide a rather diffuse spectrum (Figure 3). However, one notices the peaks at ‘Primary (44) and Secondary (33) Cooling’ and at ‘Reactor Protection (33)’. If however one sums up the groups in which these systems are structured, there are 3 dominant system groups: Reactor Block & Fuel (121), I&C (116), and Cooling (90). The entire rest has to live with comparably modest 154 nominations.

At this point of discussions of the result the author wants to pinpoint the grey area within Figure 3 with its disturbing 18 nominations in 9 subsystems. The entire RR Community and the Agency are aware of the underutilization of very many RRs. In so far it is surprising that the experimental and utilization devices/facilities have not aged as the RRs. As experimental facilities need modernization more frequently, the reason for the few nominations might be that either the

⁷ This number is even higher if those are added which responded but rejected the idea of participating or did not finish the process of completing one or more templates.

operator of an RR is less sensitive to this equipment or experimental facilities are exchanged/renewed/updated often⁸.

Back to some more statistical data: There are two parameters of the participating RRs worth to look at: Age and power. As the color in the background of the age-plot (Figure 5) indicates, the age structure is depressing. This time a separate box for RRs between 50 and 55 years had to be introduced which was not there in the 2009-paper. However the author found a nice and positive statement from a Dutch authority saying (1992)⁹: “*Age of reactors should, as age in human life, not only be seen as a disadvantage: early designs were conservative, robust, simple, straightforward – without today’s highly sophisticated safety insights but with comfortable safety margins in many areas*”. What a positive attitude to our ageing plants. Generally, structure of age does not show any surprise and the reply rate is rather independent from the age of the RR. This is also true for the non-confirming plants; no special age dependence.

Changing to the power dependence of the participants and non-participants (Figure 4), the result is similar: no specific dependence of reply rates from power, also for non-confirmation.

After having not found any significance in the age and power plots, a last attempt is made with view to regional differences (Table 3): The results in the table present a comparison between 2009 and 2011 and split the replies in regions additionally. The comparison from 2009 to 2011 clearly demonstrates the progress in the US by reply rate increasing from 35% to 51%. Still, Western Europe, Asia + Australia, and South America beat that rate and Africa is in that range as well, but in 2009 the US had been distinctly at the end of the queue. However, the main reason for discussing the regional distribution is Eastern Europe and especially Russia. The author has put a lot of efforts on contacting Russian Nuclear Research Centers, as he did at the US, but the outcome was disappointing: 29% reply rate in Eastern Europe (including Russia) and meager 8% from Russia itself. After having performed that effort, the author saw 2 reasons being responsible for that poor result: the Internet as established in Russia and language problems. Nowhere emails were bouncing back that frequently as from Russian centers. Far more than half having been mailed did so and one is never sure whether the address (already hard to find out) is wrong or outdated or the server has aged or is exhausted. Beyond that, if answering at all, replies need a long time to wait for. As mostly no replies came and with the knowledge of foreign language abilities in Russia generally, the author concludes that is neither fair nor prudent to expect aged staff speaking English sufficiently nor is it helpful to rely on English only when trying to be successful in Russia¹⁰. Thus, templates in more than one language should not be excluded generally.

Another statement has to be made to the term ‘Ageing Management’. Although without statistical proof, the author assures the readers that only very few templates mention or report on existence and/or experience of Ageing Management Systems at their RRs. That does not say that they have no way of managing ageing at their plant, but may be different from what the supportive documents of the Agency recommend. Obviously, there is still room for improvement, but one also needs to consider the quotation from above on that subject.

⁸ The author doubts the frequent exchange or modernization and recommends a separate focus on ageing of experimental facilities as a support in terms of underutilization. Without awareness of a potentially massive deficit in this area underutilization cannot be fought at all.

⁹ The statement is quoted from Nuclear Europe Worldscan 11-12/1992

¹⁰ This is true for other countries as well (e. g. PROC), but did not show that clear as for Russia

All in all, by working twice on the subject matter, the author learned a lot about minor and major problems of ageing RRs, also rather young-ones, and he learned it from very many nice members of the RR Community. The author admits that it took some pressure sometimes to get the replies, but it was done for the community who now has a data base which provides experience to about any type of ageing and respective contact person(s) easy to access via mail or telephone (Skype is not included unfortunately; worth to consider for the next update, at least voluntarily).

Finally, the author wishes to thank all participants from 2009 and 2011 without whom this paper would not have been written and presented and no data base would have been established.

Table 1: Brief on the template structure

Very brief RR details / data / description
 Max. 3 ageing problems per template permitted
 No enrichment conversions & no photographs
 Classification of the ageing issue / experience
 (13 mechanisms, 76 systems in 9 groups)
 2 blocks of requested information
 (description of issue; description of actions)
 Targeted questions on ageing case & its curing, e. g.
 ► on safety relevance
 ► on means / budget
 ► on support from outside the RR
 ► on authorities involvement
 Contact address for the RR / the ageing issue

Table2: IAEA Ageing Initiative-2009 vs 2011

Item	2009	2011
RRs approached	133	158 + 5
Mails per RR approached	xxxx	9.2 (1405)
Av. (total) age of RR approached	39.5 a	41.4 a (6540)
RRs replying +	77 = 58 %	90 = 57 % + 4 ¹¹
Mails per replying RR	xxxx	9.3 (934)
Av.(total) age of RR replying	37.8 a	40.7 a (4107)
RRs with unconfirmed contrib.	n/a	+ 12 = 102
Completed templates	155	205 (58 new) +3
Mentioned "cases of ageing"	364 (367)	490 (493)

¹¹the non-bold numbers are non-RR contributors

Fig. 1: 2011-Ageing Case Matrix

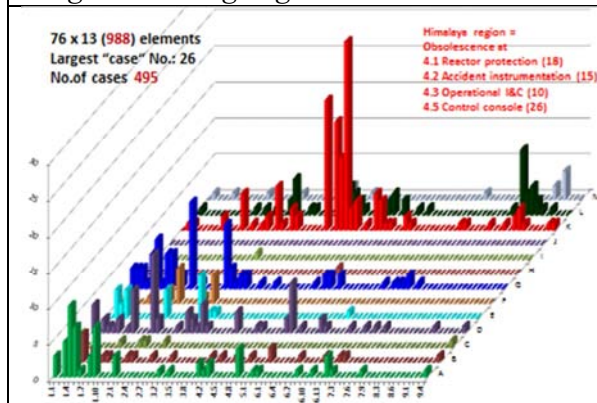


Fig. 2: Frequency of named Ageing Mechanisms

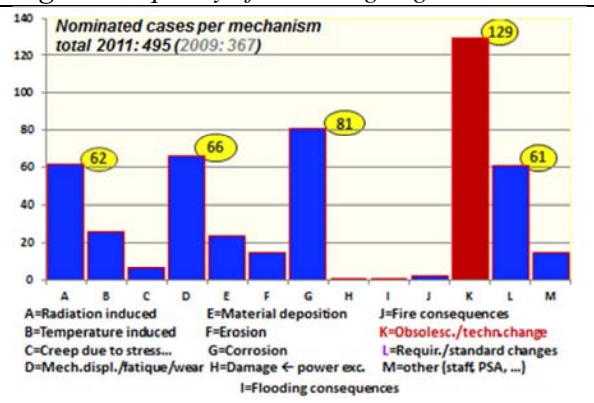


Fig.3: Named Ageing Cases per System

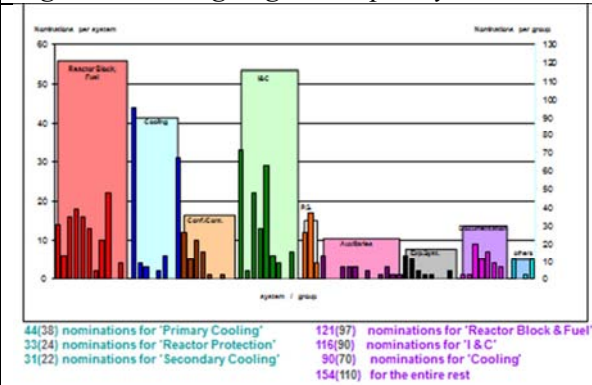


Fig. 5: Replies & Non-replies versus RR Age

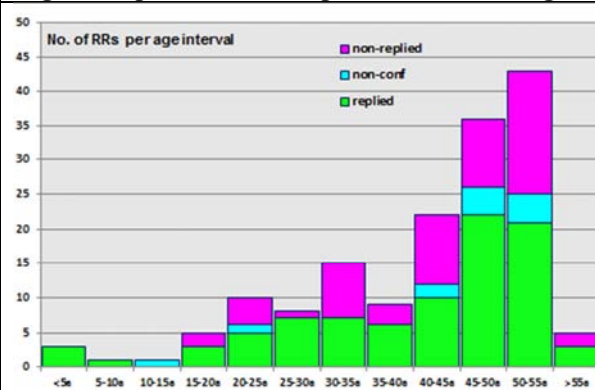


Figure 4: Replies & Non-replies vs RR Power

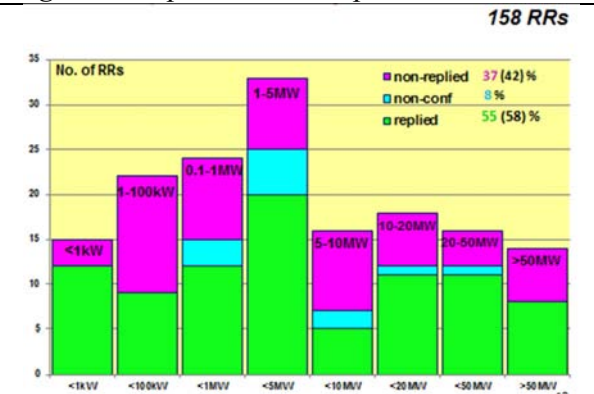


Table 3: Regional (& Institutional) Differences

2011+2009

- General Success Rate of the 2 Initiatives

World RRs	88 / 158 = 56 %	77 / 133 = 58 %
-----------	-----------------	-----------------
- Number of RRs approached / replied / %

W-Europe	19 / 28 = 68%	28 / 48 = 58%
Asia+Australia	24 / 33 = 73%	22 / 37 = 59%
America (N+S)	20/39 + 10/13 = 51+77%	37+12 / 13+8 = 35/67%
Africa	5 / 10 = 50%	4 / 7 (9) = 57%
E-EU (Russia)	10/35 (2/25) = 29 (8) %	
- Number of Institutions approached

Industry	for conf. only 1 / 2 = 50%	1 / 9 = 11%
Authorities	for conf. only 3 / 3 = 100%	4 / 10 = 40%

THE BERYLLIUM REFLECTOR MANAGEMENT PROGRAMME AT SAFARI-1 RESEARCH REACTOR

B.J. STEYNBERG, M. DE KOCK, J.W.H. VLOK
*SAFARI-1 Research Reactor, South African Nuclear Energy Corporation (Necsa)
Pelindaba – South Africa*

ABSTRACT

On 18th March 1965, SAFARI-1, the first research reactor in South Africa, achieved criticality, and on 10th April that year it reached full power at the initial design for 6.25 MW_{th} – later increased to 20 MW_{th}. The purpose of this reactor was initially for R&D, but throughout its operational history there were additional uses such as PWR fuel testing and lately more emphasis on the production of ⁹⁹Mo, other radioisotopes and neutron transmutation doping of Si. The high utilisation (more than 300 full power days per year) and the safe operation of the reactor are mission critical factors for SAFARI-1. An Ageing Management Programme was implemented to limit long term reactor downtime, and one of the priority projects on this programme was the implementation of a beryllium (Be) reflector management programme. The Be reflector elements had been in the core since the reactor start-up in 1965.

The Be reflector management programme entailed six phases:

- The theoretical evaluation of the old Be reflector elements for remaining functionality. This was done to determine the necessity and urgency for replacing the Be reflector elements.
- The specification and procurement of the new Be reflector elements. Available commercial supply of nuclear grade Be was evaluated and the appropriate procurement processes were followed.
- The replacement of the Be reflector elements in the reactor core. A structured approach was followed by forecasting via the use of MCNP calculations the impact of the new Be reflector elements in the core on the neutronic parameters, followed by the experimental determination of this impact. The results of this structured approach made possible the replacement of all the Be reflector elements all at once.
- The development of a Be reflector in-core management programme. The new Be reflector elements were captured in a programme of regular rotation (orientation and position) in the core.
- The evaluation of the old Be reflector elements which were removed. Dimensional tests were done and compared with the predicted values. Data gathered in this process were captured in a database to build up a knowledge base to assist in understanding the behaviour of the Be reflector elements in an irradiation environment.
- The disposal of the old Be reflector elements. Initial storage would be wet storage in the reactor pool, but a long term dry storage strategy must be developed.

1. Introduction

SAFARI-1, the sole research reactor in South Africa, is characterized as a multi-purpose tank-in-pool reactor. The initial design allowed for a thermal power rating of 6.25 MW – with the possibility to later increase the power rating. On the 18th of March 1965 the reactor achieved criticality, and the full initial design power of 6.25 MW_{th} was first reached on 10th of April 1965. The power rating of SAFARI-1 was later increased to a thermal power of 20 MW.

This facility is a high neutron flux reactor that is light water moderated and cooled as well as Be and light water reflected. The reactor has an 8 x 9 core lattice which currently contains 26 fuel assemblies and 6 fuel-follower control rod assemblies. The remaining lattice positions are filled by 8 solid aluminium spacer elements, 9 hollow aluminium elements (hosting isotope production thimbles), 4 solid lead shield element, and 19 Be reflector elements (some hollow and some solid) which are used to enhance the neutron flux density by reducing neutron leakage.

The purpose of this reactor was initially for R&D, but throughout its operational history there were additional uses such as PWR fuel testing and lately more emphasis on the production of ⁹⁹Mo, other radioisotopes and neutron transmutation doping of Si. The reactor has been in operation for 47 years and is recognised as a high utilized reactor, with more than three

million MWh of operations since the reactor went critical in 1965. In order to ensure safe and continual operation it was decided to invest in the life extension of SAFARI-1. Currently, an Ageing Management Programme (AMP) is underway at SAFARI-1 and as part of this programme the Be reflector elements were replaced since they were never replaced before.

2. Theoretical Evaluation

A theoretical evaluation was done to assess the condition of the Be reflector elements. Mechanisms that contributed to ageing of SAFARI-1's Be reflector elements are:

- Changes of the material properties due to neutron irradiation – also negatively impacting the ductility of Be.
- Creep or stresses due to pressure build-up of gaseous atoms. This can contribute to bowing or swelling of material.
- Damage due to operational events.

The following replacement guidelines were encountered during a literature search:

- HFR at Petten replaced their Be reflector elements (type S-200-F) after a fast fluence of approximately $5 \times 10^{22} \text{ n.cm}^{-2}$;
- BR2 adopted an upper limit of $6.4 \times 10^{22} \text{ n.cm}^{-2}$, for future replacements;
- Missouri reactor based their replacement on the power (MWd) accumulated before they observed cracks in the Be reflector elements (type S-200-F) for the first time.

The abovementioned fast fluence values seems rather high if compared to other reported observations on mechanical property changes:

- Fluence of $10^{20} \text{ n.cm}^{-2}$ lead to reduction of ductility at irradiation temperatures of $<100 \text{ }^{\circ}\text{C}$;
- Be irradiated to a fluence of $10^{21} \text{ n.cm}^{-2}$ and tested at a temperature $<100 \text{ }^{\circ}\text{C}$, exhibits increased yield strength and zero ductility.

The initial material specification of the SAFARI-1 Be reflector was unknown, and was assumed to be of type S-200-E. Neutronic calculations were performed using MCNP5 and MCNPX with the CINDER module. Based mostly on a representative HEU core, indicate that fluence of between approximately 6×10^{21} and $3 \times 10^{22} \text{ n.cm}^{-2}$ could be expected at various localised sections in the Be reflector elements. It is thus evident that the accumulated fast fluence in the SAFARI-1 Be reflector elements did not exceed the Petten criteria, but sections in all of them exceed the zero ductility criteria, as mentioned above.

The swelling behaviour of Be, for irradiations at temperatures below $75 \text{ }^{\circ}\text{C}$, as a function of fast fluence were calculated and the maximum swell was found to be less than 0.45 mm, versus a maximum allowable swell of 0.98 mm North/South and 1.14 mm East/West. Although there were concerns about the accuracy of the theoretical evaluation, it was evident that none of the reflectors were theoretically close to the swell limit.

However, practically the geometrical deformation of some of the Be reflector elements through bowing, swelling and limited mechanical damage (handling, wear and tear) lead to problems being experienced with core loading. This came to a head when in November 2010 the core could not be loaded. These loading problems were then resolved by:

- Replacement of the severely bent Be reflector elements in three positions and the reshuffle of the Be reflector elements in other positions;
- Polishing of the grid plate element ports;
- Exchanging one fuel element (physical damage of the end adaptor) with another one;
- The total unpack of the core and components was put on hold with only limited core changes done until the replacement of the Be reflector elements was completed.

This resulted in a high priority project to replace the Be reflector elements.

3. Specification and Procurement

When specifying Be reflector material, it is important to consider the impurities, isotropy and tensile strength of the material. In order to source Be for the new reflectors, a literature study was done to address the type of impurities as well as the maximum concentration that can be tolerated from a neutronic view. To capitalise on the excellent absorption characteristics of the material, it is of the utmost importance to keep the impurity levels of the high absorber elements to a minimum. Discussions with various international recognised suppliers of high quality Be, lead to an impurity specification. The total impurity content when converted according to ASTM-C1233-03 to an Equivalent Boron Content (EBC) is limited to a maximum of 10 ppm.

Type S-65-H Be reflector material was specified for the SAFARI-1 reactor. To ensure the continual and safe operation of the reactor, ten solid elements, ten hollow elements and 100 plugs were purchased from the Be manufacturer Materion Brush Beryllium & Composites.

Selection and supplier approval was performed in two stages:

- A quality system audit on the supplier; and
- A source inspection and a final acceptance inspection of the Be reflector elements at the supplier before shipping.

Once the new Be reflector elements were received, they were visually inspected, and subjected to a baseline dimensional characterisation under water. This information was necessary for the future dimensional characterisation and management of the Be reflector elements over their lifetime.

4. Replacement of Be Reflector Elements

Prior to the loading of the new Be reflector elements into the core, neutronic calculations were performed to determine if it was safe to replace all the Be reflector elements at once. Results indicated an insignificant change of the reactivity worth between the two cores (old poisoned Be reflector elements versus new Be reflector elements).

However, to confirm this assessment it was decided to do the Be replacement during a shutdown in October 2011 in steps and to do measurements of the reactivity worth:

Step 1: Obtain a stable critical bank with a previous cycle xenon free core at low power for at least 15 minutes.

Step 2: Increase the reactor power to 2 MW for 30 minutes irradiating C and Ni foils to obtain the fluxes, and then shut the reactor down.

Step 3: Use the same core and replace only two of the two old Be reflector elements with two new Be reflector elements. Obtain a stable critical bank at the same power as step 1 for at least 15 minutes and then shut the reactor down.

Step 4: Comparison of the measured reactivity worth with the calculated reactivity worth showed a small acceptable difference of 3 cents.

Step 5: Replace all except two of the old Be reflector elements with new Be reflector elements. (Two positions retained their old hollow Be reflector elements due to the RINGAS system installed in it – these remaining two old elements will be replaced as soon as the required maintenance on the RINGAS system can be done). Then obtain a stable critical bank at the same power as step 1 for at least 15 minutes.

Step 6: Increase the reactor power to 2 MW for 30 minutes irradiating C and Ni foils to obtain the fluxes, and then shut the reactor down.

Step 7: Comparison of the measured reactivity worth with the calculated reactivity worth showed a small acceptable difference of 5 cents.

Step 8: This gave confirmation that the initial calculations were reliable and it was decided to continue operation with the full load of new Be reflector elements. The new core was then loaded and the reactor was restarted for a normal 20 MW operations cycle.

5. Be Management Programme

During its lifetime the Be reflector elements will be exposed to neutron damage (inducing swelling, bowing and embrittlement) and fatigue and wear (causing displacement, material damage, deformation, surface deterioration and dimensional changes). This necessitates the periodic replacement of the Be reflector elements, and a Be Management Programme was established at SAFARI-1 to ensure:

- The availability of a complete irradiation history of the Be reflector elements at any point in time;
- The establishment of a knowledgebase to assist in the understanding of the behaviour of the Be reflector elements in an irradiated environment;
- The extension of the lifetime of the Be reflector elements (managing the ageing of the elements).

In order to achieve this, the following actions and practices were put in place:

- Periodic geometric deformation measurements, and comparison of these results with the baseline dimensional measurements taken at receipt of the Be reflector elements (see point 3 above);
- Tracking and recording the accumulated fast fluence history of each of the Be reflector elements in the core;
- Monitoring of tritium levels (kBq/l) in the primary water to assist in the detection of crack formation (It is assumed that no / low tritium is released during normal operations due to the low temperature at the reactor);
- Periodic visual inspection of the Be reflector elements;
- Periodic positional and rotational shuffling of the Be reflector elements in the core to ensure a more even accumulation of fluence over time;
- The above data and history is captured in a database as part of SAFARI-1's fuel management software program, and will be used to develop end-of-life criteria for the Be reflector elements.

6. Evaluation of Old Be Reflector Elements

As part of the knowledgebase, and to assist in the understanding of the behaviour of the Be reflector elements within a radiation environment, the geometric deformation of some of the old decommissioned Be reflector elements were measured. Measurements were performed with the same measurement tool which was used to do the dimensional analysis of the newly received Be reflector elements (see point 3 above). The following were concluded from these measurements:

- Bowing and / or swelling were detected to some extent on all of the Be reflector elements measured – for some elements up to 5 mm.
- Some Be reflector elements swelled to such extent that it closed the gap between adjacent elements. This is a confirmation of the core loading problems experienced.
- In most cases the swelling in one direction was substantially more than the swelling in the other direction. It is expected that this is indicative of the direction of neutron fluence and the fact that there was no (or low) rotational or positional change in the life of the Be reflector elements.

As it is not known where these Be reflector elements were located in the core during their lifetime, it is difficult to make any other conclusive remarks.

7. Disposal Strategy

Disposal of the old Be reflector elements will be via intermediate and final storage and will be handled in two separate phases. Phase 1 is the intermediate storage of the old Be reflector

elements in a vertical position in a specially manufactured aluminium rack designed for housing these Be reflector elements, housed in the reactor pool.

The decommissioned Be reflector elements cannot be stored in the reactor pool indefinitely, and for this reason the final disposal path needs to be identified. It is essential to plan for the disposal of waste and in this case the decommissioned Be reflector elements. Be waste is a liability for the facility due to financial and environmental implications and this liability must be discharged through a responsible final disposal. Phase 2 will action the final disposal of the old Be reflector elements. The following sources of information will be explored:

- IAEA Technical Report Series no. 441, "Management of Problematic Waste and Material Generated during the Decommissioning of Nuclear Facilities";
- Information published by the Irradiated Be Disposal Workshop held during May 2002;
- Information gathered at the 4th ISMTR and the at the 6th Specialist Meeting on Recycling of Irradiated Beryllium, during December 2011.

Characterisation of the Be waste is crucial in determining the final waste disposal strategy and need to be done. At this stage it looks as if surface storage may be the most plausible method of disposal of SAFARI-1's decommissioned Be reflector elements. A container for dry storage of the reflector is currently being investigated.

8. Conclusions

Due to ageing the 47 year old Be reflector elements of the SAFARI-1 research reactor had to be replaced. Although a theoretical evaluation did not conclusively indicate the need for urgent replacement, operational problems experienced in November 2010 necessitated the urgent replacement. It was subsequently proven through geometric dimensional measurements that bowed and swelled Be reflector elements caused the core loading problems experienced.

In order to manage the ageing of the new Be reflector elements installed during October 2011, a Be Management Programme was developed. Benefits to be gained from this programme are the knowledge obtained from the behaviour of Be reflector elements within an irradiation environment as well as the life extension of the elements.

The disposal strategy of the Be waste will be done in two phases – first as an interim wet storage in the reactor pool, followed by probably dry surface storage in a purpose made container.

References

1. M Belal, "Beryllium Replacement – Verification of the Predicted Neutronic Core Performance", Necsa report RRT-SAFA-REP-11031.
2. M Belal and WJ Strydom, "Beryllium Replacement Evaluation", Necsa report RR-REP-10/32.
3. M Belal and WJ Strydom, "The Status of the Beryllium Reflector in the SAFARI-1 Research Reactor", International Conference on Research Reactors, November 2011.
4. M de Kock, "Beryllium Management Program", Necsa report CMS No 009550.
5. M de Kock, "Procedure for Beryllium Management", Necsa report RR-OPR-7009.
6. M de Kock et al, "SAFARI-1 Research Reactor Beryllium Reflector Element Replacement, Management and Relocation", 4th ISMTR, December 2011.
7. HJ Stander et al, "Replacement of Core Beryllium Reflector for the SAFARI-1 Research Reactor", IAEA Workshop, October 2011.

APPLICATION OF A FAULT SCHEDULE TO THE PERIODIC SAFETY REVIEW OF THE OPAL DETERMINISTIC SAFETY CASE

M SUMMERFIELD

Leader, Technical Support Group, Reactor Operations

Australian Nuclear Science and Technology Organisation (ANSTO)

Locked Bag 2001, Kirrawee DC, NSW 2234 Australia

ABSTRACT

When granting the Facility Licence, Operating Authorisation for the OPAL reactor, the Australian nuclear regulator ARPANSA imposed a licence condition that a periodic safety review (PSR) should be performed at least once every 10 years, with the first to be completed within 2 years of the completion of commissioning. This first PSR has recently been completed and this paper focusses on the review of the deterministic safety assessment and specifically the application of a fault schedule to:

1. Assess the scope and extent of postulated initiating events considered in the deterministic safety assessment.
2. Determine the adequacy of the levels of defence in depth provided for postulated initiating events.
3. Identify any shortcomings in either of the above.

In addition, it is ANSTO's intent to revise the existing deterministic safety analysis to incorporate the fault schedule and this paper describes this process and discusses the benefits that are anticipated to result from it. For example, it is expected that a fault schedule will facilitate operations and support staff interrogating and understanding the deterministic safety assessment.

The paper also outlines the methodology by which the fault schedule was developed and provides guidance to those who may wish to apply the same methodology to their own nuclear facility.

1 Introduction

The Facility Licence, Operating Authorisation for the OPAL reactor granted by the Australian nuclear regulator ARPANSA imposed a licence condition that a periodic safety review (PSR) should be performed at least once every 10 years, with the first to be completed within 2 years of the completion of commissioning. This first PSR has recently been completed, using IAEA Safety Standard NS-G-2.10: Periodic Safety Review of Nuclear Power Plants as a guide in the absence of any internationally recognised standards or guides relating to performing a PSR for a research reactor.

The IAEA guidance divides a PSR into fourteen Safety Factors with Safety Factor 5 covering the deterministic safety analysis. The objective of the Safety Factor 5 is to "*review of the deterministic safety analysis is to determine to what extent the existing deterministic safety analysis remains valid when the following aspects have been taken into account: actual plant design; the actual condition of SSCs and their predicted state at the end of the period covered by the PSR; current deterministic methods; and current safety standards and knowledge. In addition, the review should also identify any weaknesses relating to the application of the defence in depth concept*". In the context of the PSR for OPAL (i.e. a PSR of a relatively new research reactor), this objective was simplified to be a "review of the deterministic analysis is to determine the adequacy of the current deterministic safety case as presented in the OPAL Safety Analysis Report (SAR), taking into account operating

experience since start-up and particularly, events that have occurred both within OPAL and at other facilities”.

The generic elements of the PSR of the deterministic safety analysis normally consist of the following seven elements:

- a. A compilation of the existing deterministic safety analyses and their assumptions.
- b. Limits and permitted operational states.
- c. Anticipated operational occurrences.
- d. Postulated initiating events (for the existing safety analyses and a comparable list for a modern reactor).
- e. Analytical methods and computer codes used in the existing deterministic safety analyses and comparable methods for a modern reactor, including validation.
- f. Radiation doses and limits on radioactive releases for accident conditions.
- g. Guidelines for deterministic safety analyses, including guidelines for single failure criterion, redundancy, diversity and separation.

Rather than trying to address each one of these elements separately, the methodology adopted for the PSR was the development of a comprehensive Fault Schedule for OPAL separate to the existing deterministic safety analyses that would address the first four of these elements simultaneously. It was also intended that the development of a comprehensive Fault Schedule for OPAL would have additional ongoing benefits for OPAL as described further in this paper.

2 Definition of a Fault Schedule

A Fault Schedule is defined in UK HSE Nuclear Safety Directorate Technical Assessment Guide T/AST/44 to be “*list of initiating faults, together with the protection systems provided to prevent the release of radioactive material*”. Appendix 3 of this Technical Assessment Guide contains a more detailed definition in a summarised and paraphrased form as follows:

“A fault schedule is a comprehensive schedule of initiating events which have the potential to give rise to a radiological release, together with the corresponding lines of protection. Categories of fault need to be identified for the fault schedule. For reactor plant twelve categories are identified, each category being broken down further into individual initiators.”

Also stated in this Technical Assessment Guide is the following explanation of the role of the fault schedule”

“The fault schedule plays a central role in distilling the safety analysis. Its purpose is to record the plant’s protection against the faults foreseen. A good fault schedule acts as a compact pointer to the analysis and protective measures, as a springboard for further analysis and as a compact record of the protection provided. It is developed in different degrees of detail as the safety case evolves. This is an iterative process. The objective of the supporting safety analysis is to demonstrate that the plant has adequate protection against the faults foreseen.”

As such, a Fault Schedule is more than just a listing of initiating events or faults, it is a tool that enables verification of the adequacy of the deterministic safety case and facilitates understanding. This latter point is particularly important when the Fault Schedule is incorporated into the SAR as it will (hopefully) make the SAR itself more user-friendly and encourage its use by all staff, not just those responsible for maintaining and/or updating the safety case.

3 The OPAL Fault Schedule

In the case of the Fault Schedule prepared as part of the PSR for OPAL, Table 1 of IAEA Safety Standard 35-G1 and the existing listing of postulated initiating events as identified in the OPAL SAR were used as bases. Initially, the OPAL Fault Schedule was subdivided into the 13 groups of initiating events consistent with the existing listing but during the course of development, it became apparent that a revised arrangement into 12 groups of initiating events would be more appropriate. These 12 groups are:

- Loss of electrical power supplies.
- Reactivity Insertion Accidents (RIA).
- Loss of Flow Events (LOFA).
- Loss of Heat Sink (LOHS).
- Loss of Coolant Accident (LOCA).
- Loss of heavy water.
- Erroneous handling or failure of equipment or components related to Fuel Assemblies.
- Special internal events.
- Loss of systems or supporting services.
- Utilisation events.
- Spurious actuation of safety systems.
- External events.

The group covering utilisation events was further subdivided into three parts to cover irradiation targets, the Cold Neutron Source (CNS) and the neutron beam facilities. A separate group covering the loss of systems or supporting services was considered appropriate as the way that this was dealt with in the existing SAR was considered to be deficient. A separate group covering human factors was not considered appropriate since human factors are identified as a potential cause of the initiating event where appropriate.

The OPAL Fault Schedule was tabulated with the following columns; fault ID, fault description, nominal; fault frequency, causes/effects/means of prevention, means of protection/mitigation – reactor safety functions (e.g. reactivity control, core cooling, decay heat removal and Containment), limiting or bounding and comments. These columns are described further below:

- a. An event ID is given to facilitate cross-referencing within the Fault Schedule and in/out of the Fault Schedule (e.g. in the actual safety analysis).
- b. The event description is generally self-explanatory. It should be noted that some initiating events may have a number of sub-events covering different scenarios that are, in practice, just variations of the same event. This is one of the benefits of a fault schedule in that it enables all events and scenarios to be explicitly identified and considered rather than implicitly as is often the case in many SARs.
- c. A nominal frequency is identified for each initiating event. This nominal frequency is not definitive and is only provided for indicative purposes so that the reader or user can appreciate the likelihood of each initiating event.
- d. Causes/effects/means of prevention are identified in a single column in the OPAL Fault Schedule. This was on the basis that for OPAL, it was not considered beneficial at this time to differentiate between the cause of an initiating event, the effect of an initiating event, or the means of prevention.
- e. With the exception of the initiating events associated with utilisation, the four sub-columns under means of protection/mitigation relate to four key OPAL reactor safety functions; criticality, core cooling, decay heat removal and containment and identify what means are available following the initiating event to fulfil those safety functions.

Note that the IAEA safety standards refer to three basic safety functions (sub-criticality, [decay] heat removal and confinement of activity) but for the OPAL Fault Schedule, it was considered more appropriate to separate core cooling from decay heat removal so as to differentiate between the passive, inherent safety features associated with core cooling (i.e. natural circulation cooling) and the active systems associated with decay heat removal to the ultimate heat sink.

- f. In the case of the initiating events associated with utilisation, the key safety functions relate to the specific utilisation activity under consideration. For irradiation targets, the key safety functions are target integrity, target cooling, target decay heat removal and containment; for the CNS, they are reactor core integrity, CNS integrity/cooling, CNS vacuum containment and deuterium containment; and for the neutron beam facilities, the key safety functions are reactor safety and radiation safety.
- g. The limiting or bounding column identifies whether an initiating event is the limiting event (e.g. it bounds other similar events), or is bounded by another event. This column means that it is relatively easy to track those initiating events that are or should be considered in more detail and those that are covered elsewhere.
- h. The comments column is self-explanatory.

The completed Fault Schedule was contained in the PSR report and the intention is for it to be incorporated into the OPAL SAR. In this way, the Fault Schedule will facilitate operations and support staff in their understanding the deterministic safety assessment rather than having to trawl through pages of text.

4 Results of the Review

The review concluded that in general, the deterministic safety case for the OPAL reactor as presented in SAR adequately takes into consideration the range of design basis initiating events that could impact safety. In the case of a number of initiating events, it has been determined that the deterministic safety case as presented in the SAR could be improved or clarified through the explicit (rather than implicit), consideration of initiating events and that an appropriate methodology for doing so would be the use of a tabulated fault schedule as used in the review.

A number of initiating events were also identified that need to be specifically incorporated and addressed in SAR that are not currently covered. In some cases, the SAR needs to contain an appropriate justification for the new event to be considered beyond design bases rather than an accident analysis, whilst for others, appropriate safety case justifications are contained in other parts of the SAR or in various supporting safety submissions.

5 Fault Schedule: Options for Other Users

As may be evident from the above description of the OPAL Fault Schedule, there are a number of options available when developing a fault schedule. Some of the more significant of these are discussed below.

- a. An option is whether to identify a nominal frequency for each initiating event. As indicated, this enables the reader or user to appreciate the likelihood of each initiating event. However, its inclusion can also be a distraction from the principal function of the fault schedule (i.e. being compact pointer to the analysis and protective measures, as a springboard for further analysis and as a compact record of the protection provided) as too much effort can be devoted to discussions regarding the appropriateness of the nominal frequencies identified.
- b. Fault schedules may have causes, effects and means of prevention identified as separate columns or may combine one or more of these aspects in the event

description. The combined option used in the OPAL Fault Schedule is simpler to develop but can be more confusing to the reader. Using separate columns enables the effects and means of prevention can be directly related to the cause but the disadvantage is that it can lead to too much detail being included in the fault schedule, again resulting in a distraction from the principal function of the fault schedule.

- c. The level of detail provided in the fault schedule is also a difficult balance between ensuring sufficient understanding whilst avoiding undue repetition. For example, the OPAL Fault Schedule does not identify every individual cause, effect or means of prevention for every event. This was on the basis that trying to identify every possible cause for many initiating events (e.g. every cause by which off-site electrical power supplies could be lost) would expand the fault schedule unnecessarily without any real benefit. Similarly, identifying standard means of prevention, such as high quality of construction, operator training and the use of approved procedures/instructions, is not generally beneficial except where special or dedicated provisions are in place (e.g. specific inspections of Fuel Assemblies).
- d. Determining the relevant safety functions applicable to the facility is important as they may vary depending upon the specifics of the reactor design. For example, as identified above, the OPAL Fault Schedule considers core cooling and decay heat removal separate safety functions but other options would be to stay with the single safety function of decay heat removal as identified by the IAEA or split this function into short-term and long-term cooling.
- e. The relevant safety functions may also be dependent on the chosen initiating event groupings. In the case of the OPAL Fault Schedule, the safety functions identified for the utilisation events (i.e. those associated with the irradiation facilities, the CNS and the neutron beams) are different to those identified for the reactor.

Other options include separate columns identifying protection interlocks, primary and secondary reactor protection system trip signals, claims on operator intervention. As such, the actual content and format of a fault schedule may be customised to the needs of the user and the specific facility under consideration with the aim of being a compact means of identifying the postulated initiating events considered in the design of the facility and the means of protection provided with respect to those faults.

6 Conclusions

A Fault Schedule was developed for OPAL as a way of reviewing and assessing the OPAL deterministic safety assessment as part of the Periodic Safety Review. The Fault Schedule was successful, demonstrating that in general, the deterministic safety case for the OPAL reactor as presented in SAR adequately takes into consideration the range of design basis initiating events that could impact safety. The Fault Schedule was also successful in identifying a number of areas where the deterministic safety case for the OPAL reactor could be improved through the explicit identification of initiating events and the inclusion of some additional initiating events.

The inclusion of the Fault Schedule into the OPAL Safety Analysis Report will also be beneficial to the ongoing operation of the reactor through facilitating operations and support staff in their understanding the deterministic safety assessment.

STATUS OF FULL SCALE MONOLITHIC UMO PLATE AND ASSEMBLY FABRICATION METHODS AND EQUIPMENT

J.M. WIGHT, R.E. JOHNSON
Uranium Processing & Research Reactors
Babcock & Wilcox Nuclear Operations Group
1570 Mount Athos Rd., Lynchburg, VA – USA

ABSTRACT

Recent GTRI Fuel Development fabrication contracts were executed for the AFIP-7 and AFIP-6 MKII irradiation experiments. Both experiments include full scale monolithic UMo fuel plates. AFIP-7 was the first full scale monolithic UMo assembly with multiple curved plates swaged into an assembly. A discussion of the development activities, the methods used for fabrication, the inspection of the plates, and the assembly of plates (including results) are included. Lessons learned from the experiments and current plans for implementation of best practices are outlined. Current plans for future GTRI Fuel Fabrication Capability demonstration assemblies and implementing an interim UMo foil production facility are also included.

1. Introduction

The Global Threat Reduction Initiative (GTRI) has an ongoing program to convert domestic and international civilian research reactors from HEU to LEU which includes the development of the high density fuel alloy of uranium–molybdenum (UMo)^[1]. One aspect of the development of the UMo fuel is irradiation testing. The purpose of the irradiation testing is to ensure the expected performance of the new fuel type. The AFIP-6 and the AFIP-7 fuel development experiments are irradiation tests which represent a more prototypic scale of the research reactors for which they are being developed ^[2]. In the last year, the AFIP-7 and AFIP-6 MKII assemblies were fabricated at Babcock & Wilcox (B&W) in Lynchburg, Virginia. Due to irradiation issues with the first AFIP-6 assembly, the AFIP-6 MKII test was a repeat assembly.

The AFIP-6 MKII assembly consisted of a fuel plate which measured 1143 mm X 56.8 mm with fuel meat dimensions of 571.5 mm X 34.9 mm. Each finished fuel plate was subsequently assembled into a single side rail.

The AFIP-7 assembly consisted of four fuel plates which measured 1016 mm X 62.8 mm with fuel core dimensions of 965.2 mm X 58.8 mm. Each fuel plate was then formed to a radius of 90.3 mm and assembled into a side rail and end fittings were attached to both ends.

Each of the plates followed the same basic operations to produce an acceptable plate. Those operations and the equipment utilized to perform these steps are outlined in the following paragraphs.

2. UMo Foils

The foils used for these experiments were UMo foils clad in pure Zr through the roll bonding process. Each foil was properly sized to the correct width prior to shipping due to foil sizing

limitations at B&W. The foils supplied for the AFIP-7 experiment were fabricated at the Y-12 National Security Complex (Y-12) and the Los Alamos National Laboratory (LANL). Each of the suppliers shipped 6 foils for use as finished plates and archive samples. The foils supplied for the AFIP-6 MKII fabrication campaign were fabricated at the Idaho National Laboratory (INL). Four (4) foils were provided for the AFIP-6 MKII experiment with 2 foils planned for use as archive samples.

2.1. Foil Preparation

When each foil is received at B&W, it is sampled to verify uranium (U) and U-235 weight percent. The typical sample is a 1.25 cm long trimming sheared from each end of the foil. That sample is then sheared in half to produce four samples for each foil. Subsequent analysis of the four foils produces an average U total weight percent and U-235 weight percent which is then applied to the foil for calculating the uranium content. The samples are sheared on a ~30 cm wide bench shear designed for the shearing of thin metal.

After sampling results have been obtained, the foils' Zr surface is polished on each side to remove any debris and oxide buildup. The foils are polished utilizing a Bosch cordless oscillating tool equipped with a Buehler polishing pad and 30 micron diamond paste. It takes approximately 20 minutes to polish both sides of the foil to achieve the desired surface finish.

Each foil is trimmed to length according to the requirements in the respective experiment drawing. After final sizing, inspections of the foil include: identification of visual defects, final mass, final width, length, and thickness measurements. The thickness measurements are obtained in prescribed locations according to the specification to allow proper correlation to final plate thickness and radiography measurements.

3. UMo Foil Cladding

Each UMo foil, deemed acceptable for use, is clad with the aluminum (Al) alloy, Al-6061, to encapsulate the fuel. This cladding process is performed using the Hot Iso-static Press (HIP) process. The process employs high temperature (~560°C) and high pressure (~100 MN/m²) held for approximately 90 minutes to bond the Al-Al and the Al-UMo surfaces to clad the foil and create the UMo fuel plate^[3].

3.1. HIP Can Pre-Assembly

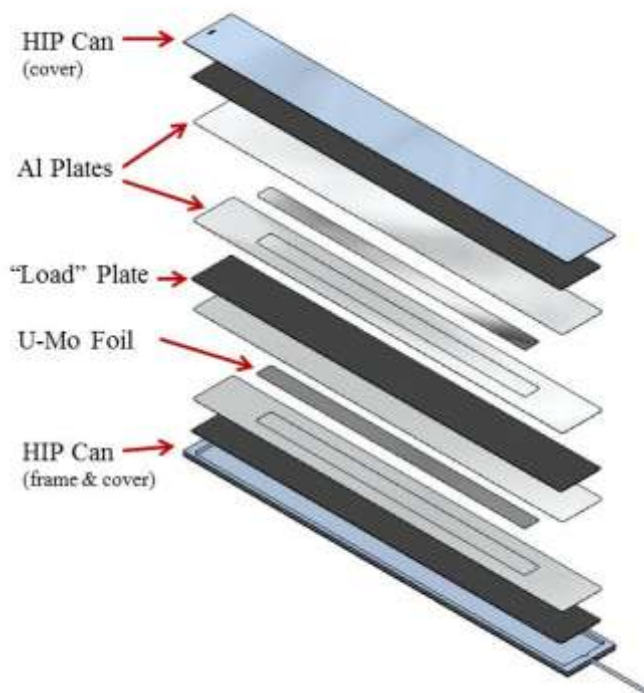
Foils and aluminum plates are stacked inside HIP cans which are sealed and evacuated to create an atmosphere inside the pressurized HIP chamber which is under vacuum. HIP cans utilized for AFIP-7 and AFIP-6 MKII were sized to allow for 2 finished plates per HIP can assembly (see Figure 1). The HIP can is fabricated from 304 stainless steel to reduce welding porosity and thus provide a consistent seal for the vacuum. A HIP can assembly consists of 4 parts: a frame, 2 covers, and a bake-out tube. Additionally, 2 or 3 steel "load" plates, used to separate the finished fuel plates, are fabricated to fit inside the frame. Prior to placing the Al cladding and UMo foils into the HIP can, the can parts are processed to a "pre-assembly" stage.

The pre-assembly of a HIP can includes a detergent wash of all the assembly parts to remove any debris and oil followed by a wipe down with alcohol. The bake-out tube is welded into a predrilled hole in the frame from the inside. Subsequently, one cover is welded to one side of the frame. The welding is performed using the GTAW process with an autogenous weld procedure. The steel "load" plates are coated with colloidal graphite suspended in isopropanol (Neolube No. 1) to prevent the Al from bonding to the steel.

The Al cladding for the UMo foil includes a set of 2 pieces of Al: a cover plate and a pocket plate. The Al cladding is procured at a thickness of ~ 1.8 mm to allow for sufficient plate

thickness to size the plate after HIP processing. After sizing the Al plates, by shearing, to fit in the HIP can, the pocket plate is fabricated by machining a pocket larger than the size of the intended foil and approximately 0.4 mm deep into the plate. Each cover plate and pocket plate surface intended for bonding to the UMo foil is then prepared by taking a stainless steel wire brush and abrading both the pocketed and un-pocketed surfaces. After brushing, each plate is detergent washed in the same manner as the HIP can pre-assembly, then etched in a Nitric acid solution for less than 30 seconds. After cleaning, the parts are wrapped in paper to ensure cleanliness prior to HIP can assembly.

Fig 1. HIP Can Assembly



3.2. HIP Can Assembly

The Al cladding, UMo foils, and steel load plates are assembled one piece at a time into the HIP can pre-assembly, as shown in Figure 1. A steel load plate is placed in the bottom of the HIP can pre-assembly. Then an Al pocket plate is wiped with alcohol and placed into the can. The first foil is wiped with alcohol, visually examined for defects, and then placed into the pocket centering the foil in the pocket as much as possible (see Figure 2). The Al cover plate is wiped with alcohol, and then carefully placed on top of the foil to prevent the foil from moving out of the pocket during the rest of the HIP can loading procedure. Another load plate is placed into the can and the process is repeated for a second plate. The third load plate is placed into the can if space is available in the frame. If there is insufficient space to allow the stainless steel HIP can cover to lay flat on the top of the assembled HIP can, then the third load plate is omitted, and the last Al cover is coated with Neolube to prevent the Al from bonding to the stainless steel.

Fig 2. Example of HIP Can Assembly



The stainless steel cover is placed on the assembled HIP can and tack welded to ensure proper fit up. Then the cover is seal welded to the frame using the same weld procedure as identified previously. To ensure the fidelity of the welds, the bake-out tube of the HIP can assembly is attached to a He leak detection system. This system, which is equipped with a roughing vacuum pump, allows for the detection of very small amounts of He. A pump down time of ~15-30 minutes is used to fully evacuate the HIP can assembly. Once a base vacuum has been achieved, a hand wand is used to spray He around the welds to identify any leaks in the HIP can. Any leaks that are identified can be re-welded and rechecked.

3.3. HIP Processing

Upon acceptance of the welds, the HIP can is placed into a furnace for a bake out, while maintaining vacuum integrity. The primary role of the bake out procedure is to drive off any residual moisture and/or contaminants. The bake-out is performed at ~300°C for 3 hours. The assembly is allowed to cool in the furnace until it is able to be handled. Then the pack is removed from the furnace to cool down to room temperature, while remaining under vacuum. To fully seal the HIP can, the bake out tube is heated with a jeweler's torch to cherry red (~900°C) then crimped in three places. A fourth crimp, farthest away from the can, is made which is then cut and quickly seal welded to complete the HIP can assembly sealing process.

The completed HIP can assembly is placed into the HIP. The HIP is processed at the parameters cited above. Upon completion of the successful HIP run, the HIP can covers have collapsed inwardly onto the contents of the assembly and the UMo foils have been clad in Al creating the UMo plate.

4. UMo Plate Processing

UMo fuel plates are removed from the HIP can, sized to length and width, and then machined to final thickness. The final plate follows most of the same quality assurance inspections as the current HEU fuel plates including: ultrasonic testing (UT), x-ray, dimensional, and visual inspections.

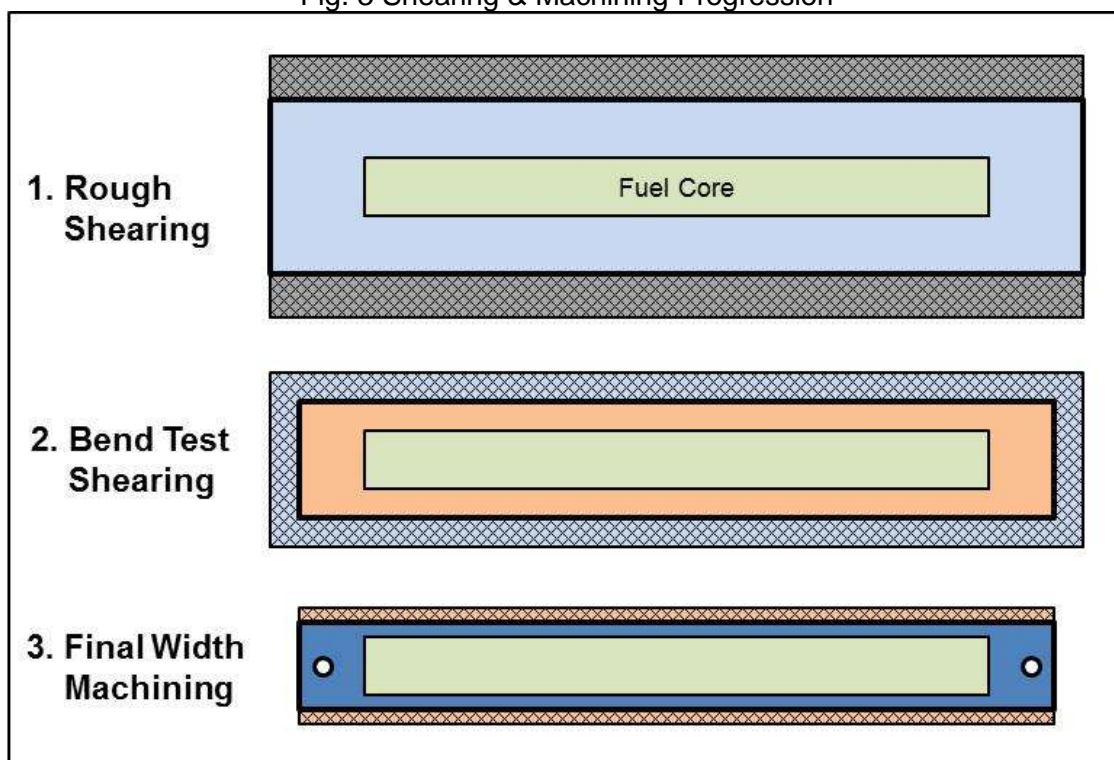
4.1. HIP Can Disassembly

The HIP can assembly is opened by sawing off the ends of the can with a band saw and machining the long edges of the can on a horizontal mill. Due to the toughness of stainless steel, the machining process is slow and the opening of a HIP can normally takes 4-6 hours. As the can is dis-assembled, proper attention is given to the ID of the can and location of the plate in the assembly to maintain ID's of the foils/plates. If traceability is in question, radiography can be employed to reveal foil shearing attributes (ie. corner notches) which can be compared with HIP can assembly records to determine foil identification.

4.2. Plate Sizing

Plate sizing is a multi-step process beginning with rough shearing (see numbered steps in Figure 3). The rough edges of the plate are removed (1), then samples for destructive bend testing are obtained (2). Bend test samples are used to perform a destructive test to ensure adequate bonding. After shearing, the plate is examined under a fluoroscope to locate the fuel core region. The fluoroscope is equipped with a punching device which creates holes in the plate aligned with the centerline of the fuel core. These locating holes are subsequently used for machining the plate to final width (3). The plate is machined to width on a straddle milling machine. This machine allows for machining both edges of a plate at the same time. After machining to width, the plate is sheared to final length.

Fig. 3 Shearing & Machining Progression



During the AFIP-7 fabrication campaign, it was determined that the fluoroscope was not fully adequate for centering UMo cores which were at the maximum fuel zone (foils that were overly wide or had excessive camber). To minimize errors associated with the centerline punching, an additional step to check the centerline by film radiography was added. This allowed for the introduction of a "offset" to ensure that the machining of the width of the plate was done in accordance with the true centerline of the fuel. This improvement has increased the success rate of the UMo plates through the edge clad inspection.

4.3. Plate Thickness Machining

The plate is machined to thickness after checking the cladding thickness over the fuel using the UT system. The plate is machined to thickness on a horizontal milling machine equipped with a tool which is wide enough to cut the entire width of the fuel plate. The plate is secured to a vacuum chuck, under the rotating cutter, and is traversed from one end of the plate to the other to machine the plate to the proper thickness on each side. After machining, the finished fuel plate is processed through the routine plate inspections outlined above.

5. Future Work

Fabrication development for UMo plates will continue with the fabrication of the ATR-FE experiment, and design demonstrations elements for the MIT, MURR, and NBSR reactors^[2]. As new opportunities to reduce operations and increase reliability are identified, they will be evaluated for implementation.

Newly funded work includes the engineering of a Limited Production Facility for UMo fuel plates including the fabrication of foils. It is anticipated that UMo coupons will be supplied for B&W to roll the foils and bond the Zr to the UMo. A demonstration of the foil rolling process is planned for 2013.

Based on the experience with fabricating experiments for GTRI and recent cost studies, it has been determined that additional fabrication process development should occur in the HIP process, specifically with the HIP can design. This includes designing a HIP can that:

- Has minimal waste
- Can be easily fabricated and easily opened
- Can produce a plate that is at near final thickness

By identifying design changes in the HIP can that lead to less waste, easier assembly and dis-assembly, and the minimization or elimination of the plate machining, significant increases in plate yields and decreases in plate cost can be achieved. Current efforts to develop these design changes are being pursued to determine their effectiveness. As design changes are implemented, additional demonstrations of the fabrication methods will be conducted.

6. References

- [1] D.M Wachs, et al., "High Density Fuel Development for Research Reactors", September 2007, Global 2007 – Advanced Nuclear Fuel Cycles and Systems.
- [2] N. E. Woolstenhulme, et al., "Design and Testing of Prototypic Elements Containing Monolithic Fuel", October 2011, RERTR 2011 Conference.
- [3] B.H. Park, et al., "INL HIP Plate Fabrication", February 2010, INL/EXT-10-17792.

ION IRRADIATION OF UMO/AL FUEL SAMPLES WITH 7WT% AND 12WT% SI INSIDE THE MATRIX (E-FUTURE II)

R. Jungwirth, T. Zweifel¹, H.-Y. Chiang, W. Petry
Forschungsneutronenquelle Heinz Maier-Leibnitz (FRM II)
Technische Universität München, Lichtenbergstr. 1, 85747 Garching – Germany

F. Charollais^(a), P. Lemoine^(b)
(a)CEA, DEN, DEC, Cadarache, F-13108 Saint-Paul-Lez-Durance, France
(b) CEA, DEN, DISN, Saclay, F-91191 Gif-sur-Yvette, France

Y. Calzavara, H. Guyon
ILL, 6 rue Jules Horowitz, F-38042 Grenoble Cedex 9 – France

S. Van den Berghe, A. Leenaers, E. Koonen
SCK-CEN, Boeretang 200, B-2400 Mol – Belgium

B. Stepnik, C. Jarousse
AREVA-CERCA, 10, Rue Juliette Récamier, F-69456 Lyon Cedex 06 - France

ABSTRACT

The addition of Si to the Al matrix of UMo/Al fuel results in the formation of a protective Si rich layer (SiRL) at the UMo/Al interface. However, this protective layer disappears during irradiation which subsequently leads to the formation of a conventional UMo/Al diffusion layer (IDL).

Within the framework of the E-FUTURE experiment of the LEONIDAS group, plates with 4wt%Si and 6wt%Si inside the Al matrix (powder mixture) have been irradiated in the BR2 reactor. However, these plates suffered from abnormal swelling in the high power regions.

A subsequent test (E-FUTURE II) will include plates with 7wt%Si and 12wt%Si (Al-Si "alloy" and "mixed" powder).

Recently it has been found that no IDL occurred after heavy ion irradiation inside fuel plates prepared with UMo powder coated with 600nm Si or 1000nm ZrN (SELENIUM fuel).

Samples from the E-FUTURE II test plates have been irradiated with Iodine at 80MeV to an integral fluency of 1×10^{17} ions/cm² which is the same fluency that has been used for the SELENIUM samples. This paper presents the results of the SEM/EDX analysis of non-irradiated and irradiated E-FUTURE II samples. These results are compared to data obtained earlier on heavy ion irradiated samples.

1. Introduction

The addition of some wt% Si to the Al matrix enhances the in-pile performance of dispersion UMo/Al nuclear fuels by retarding the undesired UMo/Al interaction and/or changing the properties of the interaction phase [1,2,3]. Since Si has a higher chemical affinity for U than Al [4], a silicon rich layer (SiRL) forms at the interface between the UMo and the Al already during plate production leaving a Si depleted zone around the UMo particles behind [5,6]. This SiRL retards the conventional UMo/Al interdiffusion during irradiation. However, a conventional UMo/Al interaction layer occurs as soon as the SiRL cannot maintain a sufficiently high Si

¹ Also at CEA, DEN, DEC, Cadarache, F-13108 Saint-Paul-Lez-Durance, France

concentration in the interaction layer [7].

It has therefore been decided by the LEONIDAS group to irradiate 4 test fuel plates with 4wt% and 6wt%Si addition inside the matrix in the BR2 reactor under severe conditions. The test was called E-FUTURE. However, first post irradiation examinations of the irradiated plates showed unacceptable high swelling in the high burn-up region [8]. It has therefore been decided to launch a subsequent test called E-FUTURE II that will include 4 test fuel plates with increased Si content (7wt%Si and 12wt%Si), differences in the matrix Si distribution (Al-Si mixed powder or Al-Si alloyed powder) and different heat treatment [9].

In this paper, the behavior of three of those samples with 7wt%Si (Al-Si alloy), 12wt%Si (Al-Si mixed powder) and 12wt%Si (Al-Si alloy) during heavy ion irradiation will be presented. The findings will be compared to heavy ion irradiated samples with lower Si addition to the matrix [7,20,21] and to samples prepared with UMo powder coated with Si [10, 11, 12, 13].

2. Experimental

Samples taken from three different test full-size fuel plates fabricated with atomized natural-U7Mo KAERI powder and Al matrices with different Si content have been provided by AREVA-CERCA in the framework of the LEONIDAS project [9]. The U loading inside the samples is 8gU/cm³, the cladding is AG3NE. During fabrication, the samples have been heat treated for 2 hours at 425°C to promote the SiRL growth. More details on the production parameters, the sample specifications and on the fresh fuel state can be found in [14]. A list of the examined samples is given in Tab. 1.

Small pieces (~1x1cm²) have been cut from the test fuel plates. The cladding has been removed on one side using abrasive paper and a cascade of diamond polishing paste (9µm - 1µm grain size) to access the meat layer.

One sample of each kind has been irradiated with iodine at 80MeV perpendicular to the surface at the Maier-Leibnitz tandem accelerator in Garching, Germany, until an integral fluency of 1x10¹⁷ ions/cm² was reached. The irradiation temperature was around 200°C (sample holder temperature ~5mm beside the irradiated area). The penetration depth of the iodine ions inside UMo is ~6µm, inside Al ~12µm [15]. It has been shown before that such irradiation conditions cause comparable effects to in-pile irradiation [16, 17,18].

These irradiation conditions are the same as in previous communications [7,19,20]. In particular the same conditions as during the ion irradiation of SELENIUM fuel samples have been used [18].

After irradiation, the samples were sectioned through the irradiated area. One of the pieces has been embedded into an epoxy resin and the cross section has been polished using abrasive Si-free disks and a cascade of diamond polishing paste (9 µm-1 µm). Afterwards, some atomic layers of gold have been deposited on the samples to increase the SEM/EDX contrast. SEM/EDX analyses have been carried out using a ZEISS EVO MA 25 microscope equipped with a ultra-dry silicon drift EDX detector from Thermo Fisher. Standardless EDX analysis has been used.

Plate number	Al-Si matrix		Heat treatment	
	Si content [wt%]	Production method	Temperature [°C]	Duration [hours]
7-A-425_2	7	Alloy	425	2
12-M-425_2	12	Mixture		
12-A-425_2	12	Alloy		

Tab. 1: List of examined samples [14].

3. Results

3.1. 7wt%Si – alloyed powder matrix

A SEM inspection including EDX analysis of sample 7-A-425_2 before irradiation revealed the microstructure expected from samples prepared with alloyed Al-Si powder (compare Fig. 1): Small Si precipitates ($\sim 1\mu\text{m}$ diameter) are finely dispersed inside the matrix. A SiRL has formed around most UMo particles thereby leaving behind a zone depleted in Si around the UMo particles. The Si content of the SiRL is $\sim 45\text{at\%Si}$ (EDX analysis). The thickness of the SiRL reaches up to $2\mu\text{m}$, however, the mean thickness is lower [14]. A minority of the UMo particle surface is however not protected at all or only by a very thin SiRL (thickness below 500nm). It is noteworthy that insufficiently protected parts are also found very near of Si precipitates inside the matrix – no Si depleted zone is visible at those spots.

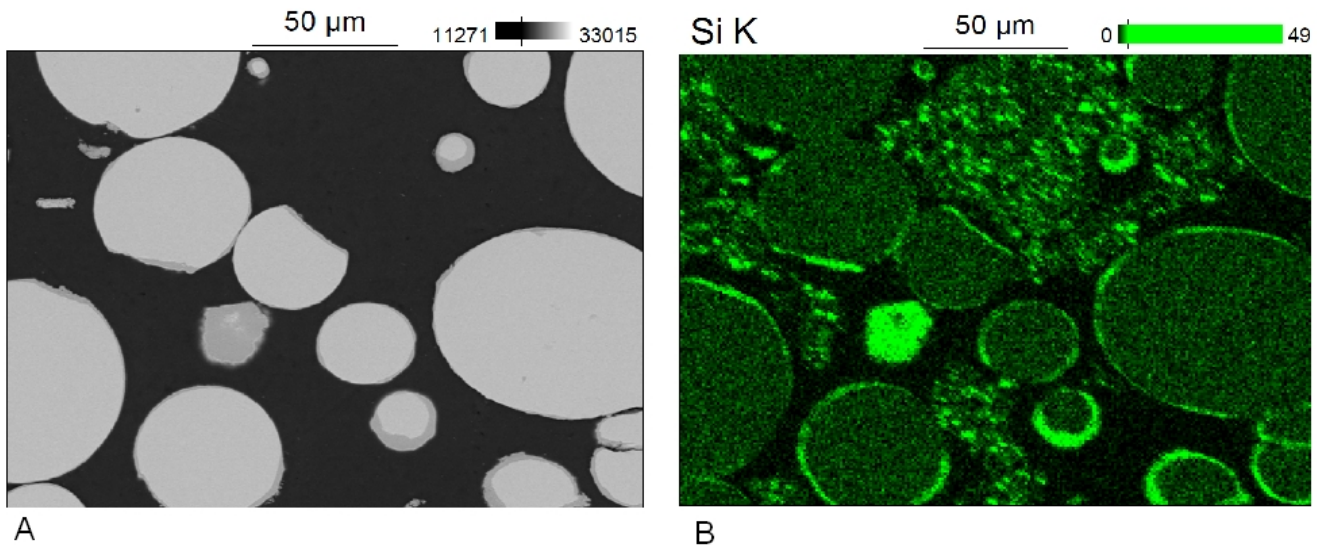


Fig. 1: BSE-image (A) and EDX K- α map (B) of the sample 7-A-425_2 before irradiation. Small Si precipitates are finely dispersed inside the matrix. A SiRL formed around the UMo particles leaving a Si depleted zone behind.

Fig. 2 shows a BSE image of cuts through the irradiated part of the sample. Fig. 2-A shows the case where the particle has been protected by a sufficiently thick SiRL. No IDL has formed at this spot. However, the Si content of the SiRL has decreased to between 0at\% and 20at\% as it has been determined by EDX analysis, depending on the spot analyzed and the initial SiRL thickness. This also can be seen in terms of differences in the gray level contrast. Fig. 2-B shows the case where the particle was not sufficiently protected. A conventional IDL has formed. The IDL itself is Si free. Since only a depth of $5\text{--}12\mu\text{m}$ inside the sample has been affected by the ion beam, it can not be concluded whether Si particles inside the matrix nearby the IDL have influenced the irradiation behavior or not.

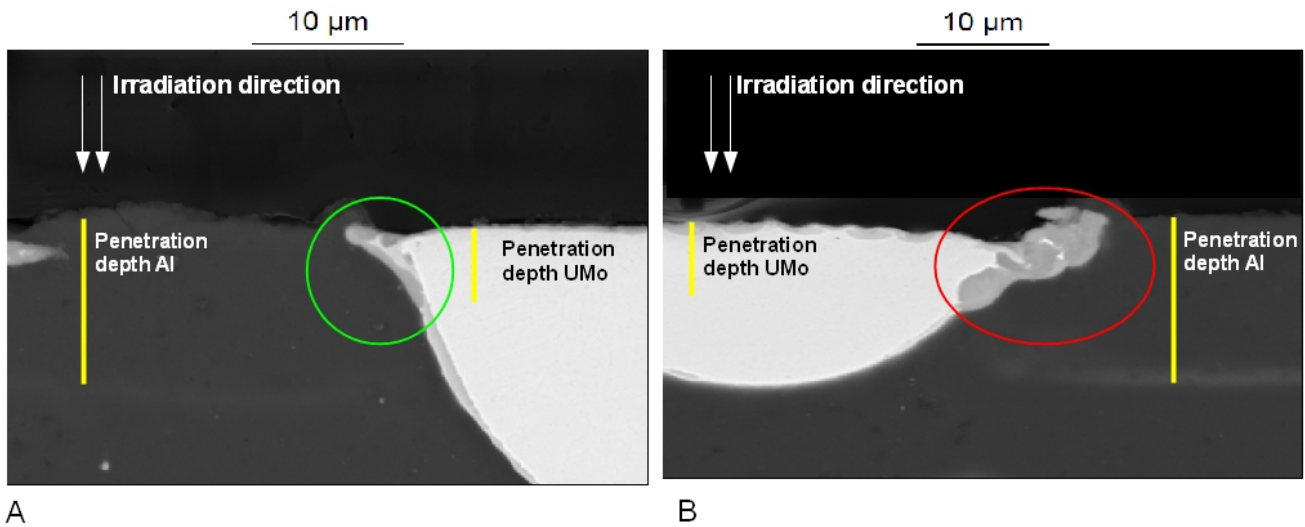


Fig. 2: BSE image of two irradiated UMo particles of sample 7-A-425_2. A sufficiently thick SiRL (A, green circle) completely suppressed the IDL formation. Insufficiently protected particles (B, red circle) are affected by conventional IDL formation.

3.2. 12wt%Si – mixed powder matrix

A SEM/EDX analysis of sample number 12-M-425_2 showed the expected microstructure of UMo/AlSi samples prepared with mixed Al-Si powder – compare Fig. 3. Big Si particles are dispersed inside the matrix. The size of the Si particles is in accordance with the size of the Si powder that has been used to prepare the Al-Si mixture. Furthermore, a SiRL has grown at the interfaces between the UMo and the Al. Note that the SiRL is not very well visible in Fig. 3-B due to the dominant Si content of the Si particles. Again, the SiRL shows strong thickness variations. Although some spots of the UMo particle surface are only hardly or not at all covered by a SiRL it can reach a thickness of 3µm and even more in other locations and most of the UMo particle surface is protected. Its Si content is found to be about 45at%, similar to what has been found in the alloy case. The occurrence of a SiRL correlates roughly with the presence of Si particles nearby. In contrast to what has been found on the samples prepared with alloyed Al-Si powder, no Si depleted zone is visible around the UMo particles. However, especially very small Si particles (<1µm diameter) have not been found near the UMo particles in contrast to big Si particles (some µm diameter) that are found anywhere inside the matrix. It can be concluded that similar to what has been observed on samples prepared with Al-Si alloyed powder, the small Si particles have been consumed when located near the UMo particles.

Fig. 4 shows a cross section through the irradiated part of the sample. A conventional Si free IDL formed at spots that were not sufficiently protected by a SiRL (red circle). A thick SiRL (green circle) suppressed the IDL formation. However, it suffered from Si depletion to between 0at% and 30at% (EDX analysis), depending on the analyzed spot and the initial thickness of the SiRL. This can also be seen from the gray level contrast in Fig. 4. Since the Si particles inside the matrix were rather big and the volume affected by the ion beam was small, once more it can not be definitely concluded to which extent nearby Si particles influenced the IDL formation.

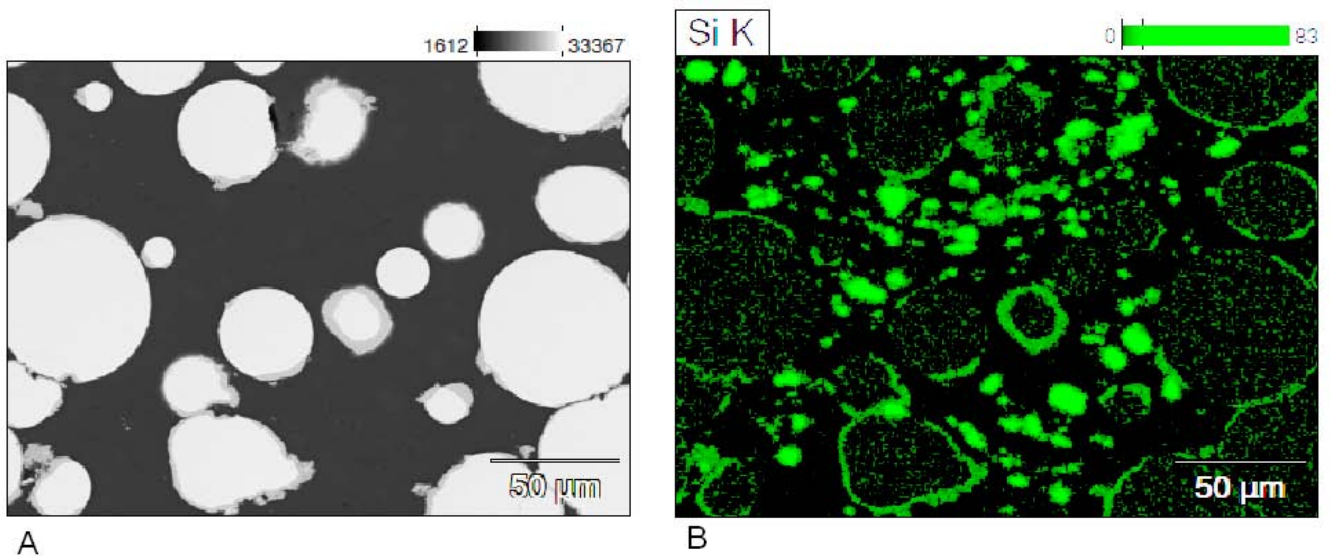


Fig. 3: BSE-image (A) and EDX K- α map (B) of the sample 12-M-425_2 before irradiation. Big Si powder particles are visible inside the matrix. A SiRL has formed around the UMo particles. Due to the dominant Si content of the Si particles, the contrast has been enhanced to make the SiRL more visible.

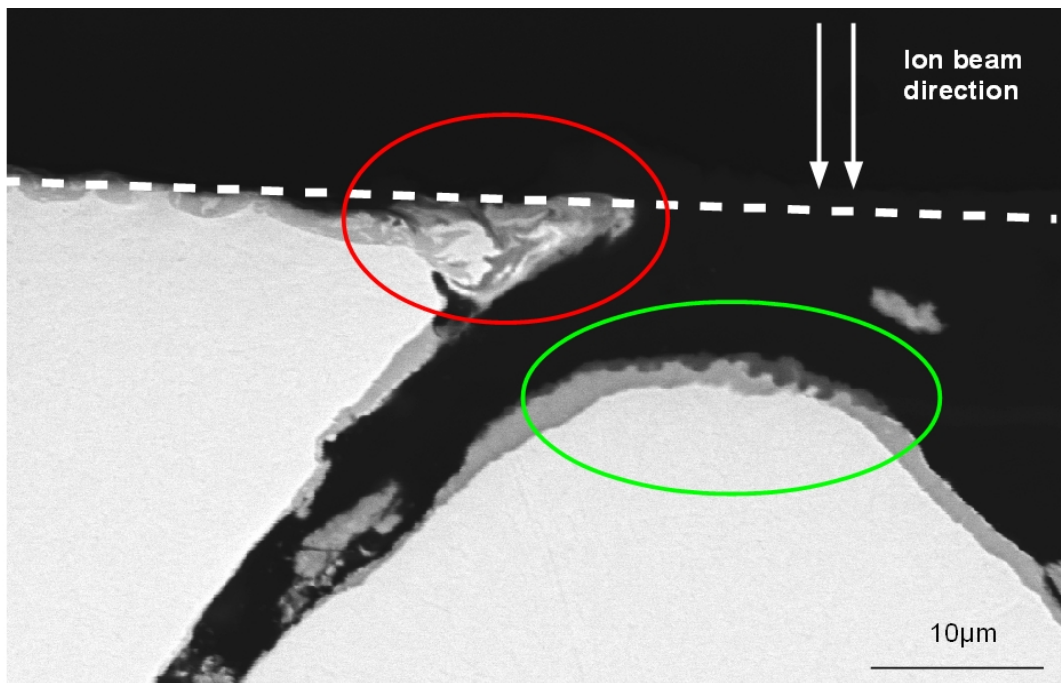


Fig. 4: Irradiated part of sample 12-M-425_2. A conventional Si free IDL formed at positions not sufficiently protected by a SiRL (red). A thick SiRL got attacked by diffusion (green) but suppressed the formation of a conventional IDL.

3.3. 12wt%Si – alloyed powder matrix

Fig. 5 shows a SEM image (A) and an EDX map on the Si-K- α line (B) of the non-irradiated sample 12-A-425_2. Similar to what has been found on sample 7-A-425_2, the Al matrix itself contains numerous fine Si precipitates (diameter $<1\mu\text{m}$). Furthermore, a SiRL formed around the UMo particles leaving a zone depleted in Si precipitates around the UMo particles behind. Again, the SiRL thickness varies on one and the same particle. The maximum thickness is about $3\mu\text{m}$ and the Si content is about 45at%. As before, there are also some parts that are hardly or even not at all protected by a SiRL. The unprotected spots are also found near Si precipitates inside the matrix, i.e. the Si from the matrix sometimes did not diffuse towards the UMo. No Si depleted zone can be observed in these cases.

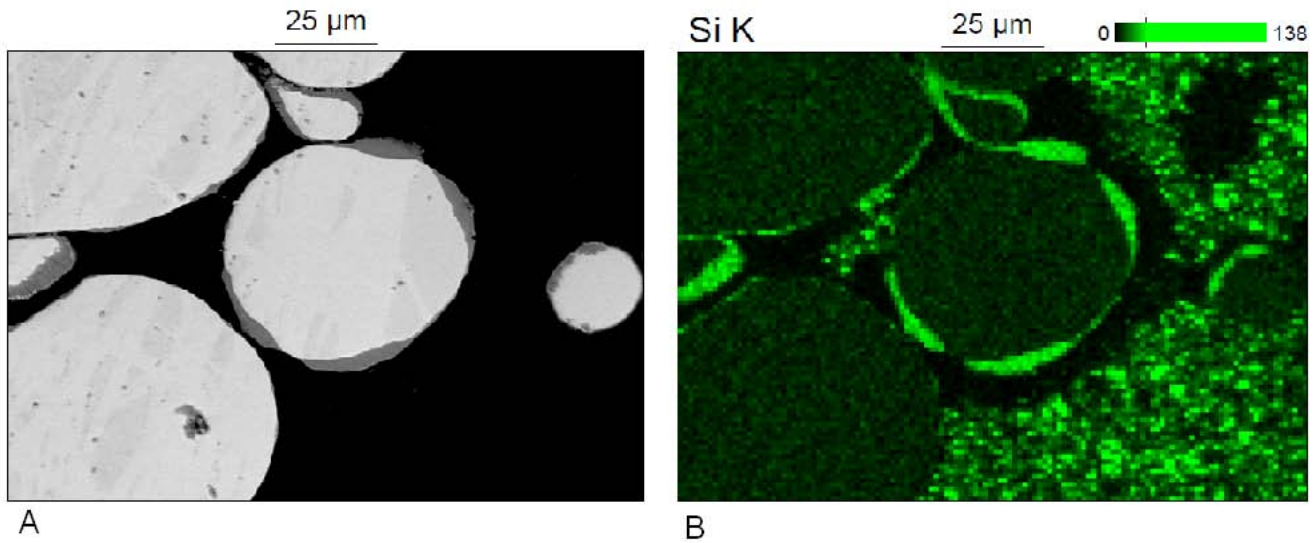


Fig. 5: BSE-image (A) and EDX K- α map (B) of sample 12-A-425_2 before irradiation. A SiRL has formed around the UMo particles leaving a zone depleted in Si precipitates around the UMo behind.

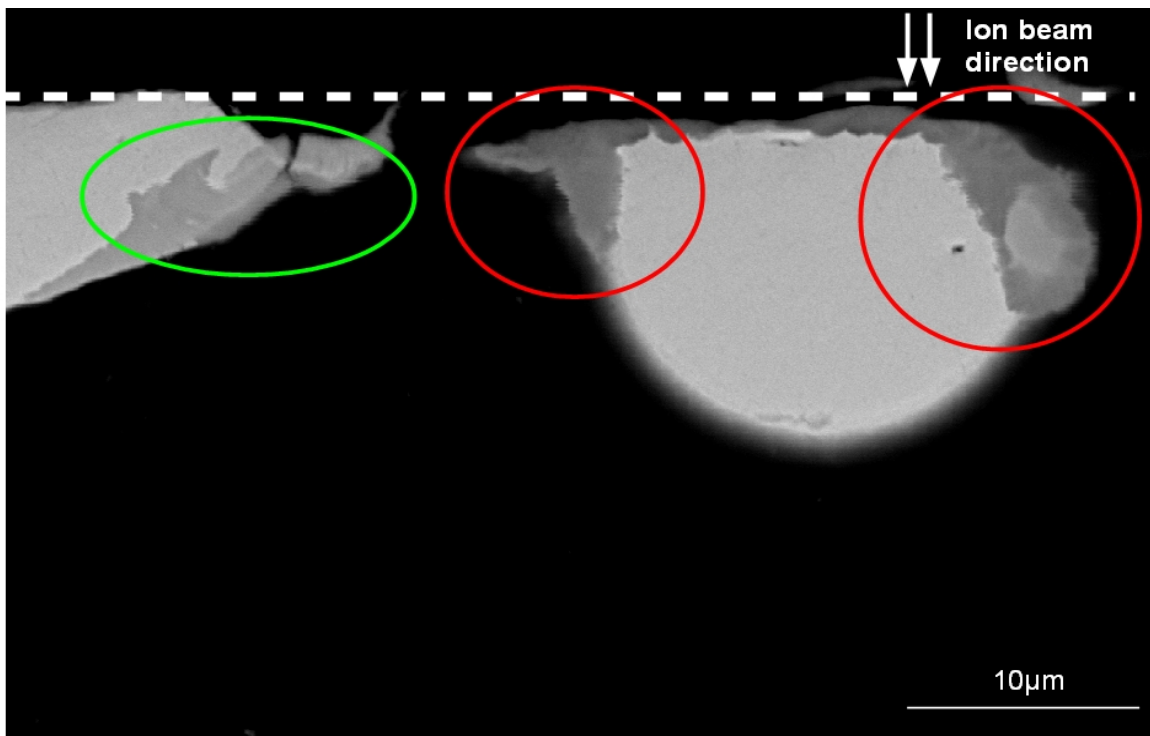


Fig. 6: BSE image of the irradiated part of sample 12-A-425_2. Particles protected by a SiRL have not been affected by an IDL formation. In contrast, a conventional IDL formed at spots insufficiently protected.

A cross section through the irradiated area of sample 12-A-425_2 is shown in Fig. 6. Again, A conventional IDL developed in cases where the particle was not or insufficiently protected by a SiRL (red circles). The IDL is in general Si free in these cases. In contrast, a thick SiRL suppressed the formation of an IDL. Thereby the SiRL was attacked by diffusion and the Si content was decreased as it has been determined by EDX analysis and can also be seen by the gray level contrast on the BSE image in Fig. 6 - green circle. The absolute values of the Si content vary strongly between 0at% and 30at% depending on the analyzed spot and the initial SiRL thickness. An influence of nearby Si precipitates can not finally be deduced from the existing data due to geometrical limits.

4. Summary and conclusions

Three UMo/Al samples containing 7wt%Si (Al-Si alloy) and 12wt%Si (Al-Si alloy and Al-Si mixed powder) inside the matrix have been examined before and after irradiation with heavy ions. Based on our SEM/EDX analysis the pre-irradiation state of all three samples is similar. A SiRL with a maximum thickness of 2-3 μm developed around most UMo particles inside all three samples. The Si content is about 45at%. However, the SiRL shows thickness variations in all three cases and there are spots on the UMo particles that are not protected at all or only protected by a thin SiRL. However, with the more accurate HE-X-ray analysis conducted at the ESRF it was possible to differentiate the Si content and the SiRL fraction of the respective samples [14].

In case Al-Si alloy powder has been used to create the matrix (7wt% and 12wt% Si), small Si precipitates are visible inside the matrix. However, around the UMo particles, the Si precipitates have dissolved and the Si has migrated towards the UMo forming the SiRL thereby leaving a Si depleted zone behind.

In case mixed Al-Si powder has been used (12wt%Si), big Si particles are visible everywhere inside the matrix. The presence and thickness of the SiRL roughly correlates with the presence of nearby Si particles. On first view there is no zone depleted in Si visible around the UMo particles. However, small Si particles with a diameter below 1 μm are only found some microns away from the UMo. It can therefore be assumed that these have been consumed and the Si has migrated towards the UMo particle forming the SiRL.

Especially in case of sample 7-A-425_2 and 12-A-425_2, there are some spots that are not covered by a SiRL although they are in direct contact with a matrix rich in Si precipitates, i.e. no Si depleted zone is present around the UMo particles. It can be suspected that at those spots a dense and very thin ($\sim 100\text{nm}$) U-oxide or U-nitride layer was present on the UMo surface hampering surface wetting and isolating the UMo from the Si rich matrix what results in suppressing the formation of a SiRL by diffusion. Indeed a layer with a thickness of $\sim 100\text{nm}$ has been found between the SiRL and the Al matrix at some spots inside all three samples, compare Fig. 7. Since the layer has almost the same gray level contrast as UMo, it was not possible to resolve it directly. The composition of the layer could not be determined definitely by EDX analysis. A similar effect has been observed previously on samples containing 2wt%Si (alloy) and 5 and 7wt%Si (mixed powder) and a similar heat treatment. In those samples, in areas where a dense oxide layer was present on the UMo surface, no SiRL was found at these spots. However, as soon as the oxide layer revealed cracks, a SiRL formed between the UMo and the oxide layer. It has been concluded that the cracks inside the oxide layer make path for the diffusion of the Si from the matrix towards the UMo which finally results in the formation of the SiRL [21].

The irradiation behavior of all three samples was similar. At spots that were protected by a thick SiRL the formation of a conventional IDL has been suppressed. However, the Si content of the SiRL was reduced during irradiation. At spots that were not protected by a SiRL a conventional, Si free IDL formed during ion irradiation. This seems to be a general behavior, there were no differences visible within the three examined samples that allow preference of one sample over the others.

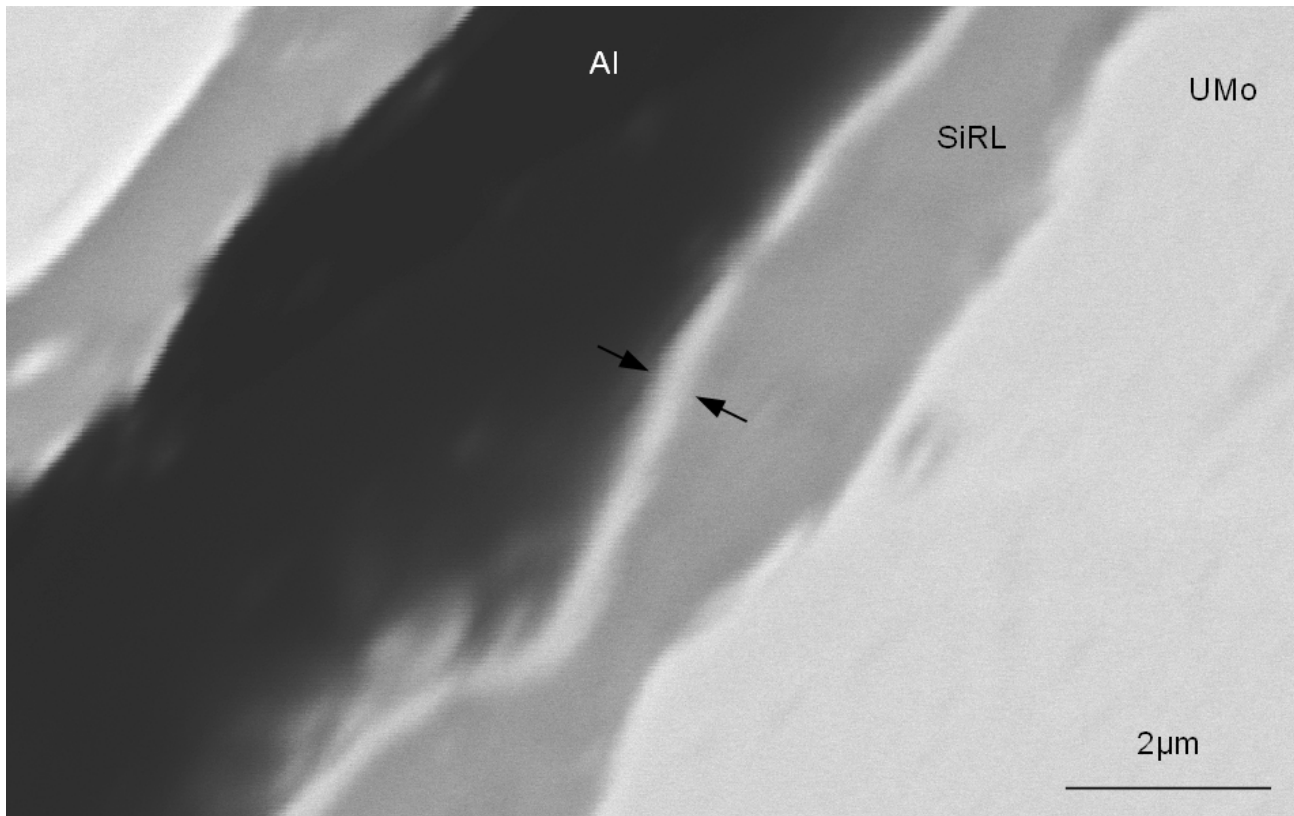


Fig. 7: BSE image of a spot where a layer (arrows) is present between the SiRL and the Al matrix.

The influence of Si precipitates nearby the UMo particles during irradiation on the IDL formation process remains uncertain since the volume affected by the ion beam is on the one hand very small and on the other hand the irradiation has been carried out perpendicular to the sample surface, i.e. the ion track inside the sample was often almost parallel to the location of the Si and the curvature radius of the UMo particle. Since during in-pile irradiation the Si inside the matrix probably will influence the IDL formation, no final conclusion which composition will show the best in-pile behavior is possible from this heavy ion irradiation test.

Compared to other samples with Si addition inside the matrix (2, 5 and 7wt%Si) [7,21] or sputtered Si layers (300nm and 600nm Si) on the UMo without Si addition to the matrix [11,13,18] that have been irradiated before under similar conditions it is found that:

- The thickness of the SiRL in case of 2.1wt%Si (alloyed matrix) and 5wt% and 7wt%Si (mixed powder matrix) is usually below 1µm, i.e. below the thickness that has been observed in this work. However, the Si content of the SiRL is found the same by EDX (~45at%Si). Also, the coverage of the UMo particles with a SiRL appears to be comparable. Nevertheless the overall SiRL fraction inside the samples examined previously and during the current study differs, as has been determined by HE-X-ray analysis [14,22]. The SiRLs with at thickness below 1µm have been consistently dissolved during heavy ion irradiation [7,21]. The samples examined here therefore show a superior irradiation performance compared to those samples.
- In case of 300 nm Si deposited on the UMo particles, no dense SiRL has developed around the UMo during plate fabrication. The Si agglomerated at some spots forming a SiRL (thickness <1µm) with a Si content of about 20-30at% whereas a Si content of ~45at% has been found during the current study. Furthermore, important parts of the UMo particles remained unprotected. In consequence an up to 5µm thick IDL developed around the UMo when affected by the ion beam [11,13,18]. The three samples

examined during the present study clearly show a better irradiation behavior than the sample prepared with 300 nm Si coated UMo powder.

- In case of 600 nm Si deposited on the UMo, a dense SiRL developed around all UMo particles. The thickness of the SiRL reached up to 2µm, the Si content of the SiRL was about 40-45at%. Both values are comparable to the findings during the current study. The coverage of the UMo with the SiRL is at least the same as found here. As a consequence of the different approach to form the SiRL there are no Si precipitates remaining inside the matrix. Note that this is not necessarily a disadvantage: Inside the IRIS-TUM sample prepared with 2.1wt%Si, all the Si from the matrix has reacted with the UMo to form the SiRL phase [21, 22]. As a matter of fact, the plate showed superior in-pile performance [23].

During heavy ion irradiation of the sample prepared with 600nm Si covered UMo, no IDL occurred at spots protected by a SiRL - what was usually the case. It can be concluded that the pre-irradiation state of the SiRL and the performance during heavy ion irradiation of this sample and the samples from the current study are very close. Therefore it is not possible to promote one approach over the other.

5. Outlook

Although the samples prepared with 12wt%Si inside the matrix in framework of the E-FUTURE II experiment and the samples prepared with sputtered layers on the UMo surface (Si and ZrN) in the framework of the SELENIUM project [10,11] showed most promising behavior during first out-of-pile studies [13,14,18] only in-pile irradiation can prove its final suitability. Although it would make the plate production process more complex, the next step could be to combine the strengths of both techniques: i.e. creating a SiRL by sputtering Si on the UMo particles or passivating the UMo surface by application of a nitride layer (e.g. ZrN, UN, TiN [24, 25]) and adding some wt%Si inside the matrix.

In case of sputtered Si in combination with Si inside the matrix there is on the one hand some Si inside the matrix to cover spots with a SiRL during plate fabrication that have not been sufficiently covered by sputtering before. However, most of the particles will already be covered with a SiRL. Therefore Si from the matrix will not diffuse at most spots towards the UMo, i.e. no Si free zone will be created around the UMo particles. This can be of advantage during in-pile irradiation at high burn-ups when the SiRL has been consumed by the growing IDL. As a consequence of the combination of both methods there will be Si particles sufficiently close to the UMo to influence the IDL formation and not only some µm away, as it is the case for fuel prepared with alloyed Al-Si powder only.

The situation is different in case of nitride covered surfaces in combination with Si inside the matrix. It has been shown that a dense nitride layer (ZrN, TiN) completely suppresses an IDL formation [18,24]. However, as soon as there are cracks inside the nitride layer a conventional IDL grows at those spots. Si precipitates inside the matrix may help to overcome this problem in two different ways: (i) In case there are cracks present inside the nitride coating already during plate fabrication the Si will diffuse from the matrix towards the cracks and form a protective SiRL at those spots. (ii) In case cracks occur in the nitride layer during in-pile irradiation there will be Si precipitates in direct contact with the UMo particles that influence the beginning growth of an IDL.

It needs to be evaluated after the irradiation test results are available if the presence of some locations where a classical IDL forms is detrimental to the overall plate behavior.

Acknowledgments

This work was supported by a combined grant (FRM0911) of the Bundesministerium für Bildung und Forschung (BMBF) and the Bayerisches Staatsministerium für Wissenschaft, Forschung und Kunst (StMWFK). Furthermore, the authors are grateful to the staff of the MLL tandem accelerator for the outstanding support during our beam times.

-
- [1] A. Leenaers, S. Van den Berghe, W. Van Renterghem, F. Charollais, P. Lemoine, C. Jarousse, A. Röhrmoser, W. Petry, "*Irradiation behavior of ground U(Mo) fuel with and without Si added to the matrix*", Journal of Nuclear Materials, 412, p.41, 2011
- [2] D.D. Keiser, A.B. Robinson, J.-F. Jue, P. Medvedev, D.M. Wachs, M.R. Finlay, "*Microstructural development in irradiated U-7Mo/6061 Al alloy matrix dispersion fuel*", Journal of Nuclear Materials, 393, p.311, 2009
- [3] M. Ripert, S. Dubois, P. Boulcourt, S. Naury, P. Lemoine, "*RIS-3 Experiment Status and result of thickness increase*", RRFM 2006, Sofia, 2006
- [4] H.J. Ryu, Y.S. Kim, G.L. Hofman, J.M. Park, C.K. Kim "*Heats of formation of (U,Mo)Al₃ and U(Al,Si)₃*", Journal of Nuclear Materials, 358, p52, 2006
- [5] X. Iltis, F. Charollais, M. Anselmet, P. Lemoine, A. Leenaers, S. Van den Berghe, E. Koonen, C. Jarousse, D. Geslin, F. Frery, H. Guyon, "*Microstructural Characterization of the E-Future Fresh Fuel Plates*", RERTR 2010, Lisbon, Portugal, 2010
- [6] X. Iltis, J. Allenou, H. Palancher, F. Charollais, "*Characterization of IRIS-3 as-fabricated Plates (Before Irradiation)*", Appendix to technical report INL/EXT-10-17972 by Porter et.al., 2010
- [7] R. Jungwirth, H. Breitzkreutz, W. Petry, A. Röhrmoser, W. Schmid, H. Palancher, C. Bertrand-Drira, C. Sabathier, X. Iltis, N. Tarsien, C. Jarousse, "*Optimization of the Si content in UMo/AlSi fuel plates*", RERTR 2009, Beijing, 2009
- [8] S. van den Berghe, Y. Pathoen, A. Leenaers, E. Koonen, F. Charollais, P. Lemoine, Y. Calzavara, H. Gyuon, "*Results of the non-destructive analysis of the E-FUTURE U(Mo)-Al(Si) fuel plates of the LEONIDAS program*", RERTR 2011, Santiago de Chile, Chile, 2011
- [9] F. Charollais, P. Lemoine, Y. Calzavara, H. Gyuon, E. Koonen, S. van den Berghe, C. Jarousse, D. Geslin, "*LEONIDAS U(Mo) dispersion fuel qualification program: progress and perspectives*", RERTR 2011, Santiago de Chile, Chile, 2011
- [10] S. Van den Berghe, A. Leenaers, C. Detavernier, "*SELENIUM fuel: Surface engineering of U(Mo) particles to optimize fuel performance*", RRFM 2010, Marakesh, 2010
- [11] S. Van den Berghe, A. Leenaers, C. Detavernier, "*Coated particle production in the selenium project*", RRFM 2011, Rome, 2011
- [12] A.L. Izhutov, V. Alexandrov, A. Novosyolov, V. Starkov, A. Sheldyakov, V. Shishin, V. Iakovlev, I. Dobrikova, A. Vatulin, G. Kulakov, V. Suprun, "*The main results of investigation of modified dispersion LEU U-Mo fuel tested in the MIR reactor*", RERTR2010, Lisbon, 2010
- [13] A. Leenaers, S. Van den Berghe, C. Detavernier, "*Out-of-pile study on the influence of Si present as coating layer or matrix element on the U(Mo)-Al interaction*", RRFM 2010, Rome, 2011
- [14] H. Palancher, X. Iltis, A. Bonnin, F. Charollais, S. van den Berghe, B. Stepnik, Y. Calzavara, "*Leonidas E-FUTURE II: Characteristics of the fresh fuel plates*", RRFM 2012, Prague, Czech Republic, 2012
- [15] J. Ziegler, *Stopping and Range of Ions in Matter, SRIM*, 2011
- [16] N. Wieschalla, A. Bergmaier, P. Böni, K. Böning, G. Dollinger, R. Großmann, W. Petry, A. Röhrmoser, J. Schneider, "*Heavy ion irradiation of UMo-Al dispersion fuel*", Journal of Nuclear materials, 357, p191, 2006
- [17] H. Palancher, N. Wieschalla, P. Martin, R. Tucoulou, C. Sabathier, W. Petry, J.-F. Berar, C. Valot, S. Dubois, "*Uranium-Molybdenum nuclear fuel plates behavior under heavy ion irradiation An X-ray diffraction analysis*", Journal of nuclear materials, 385, p449, 2009

-
- [18] R. Jungwirth, T. Zweifel, H.-Y. Chiang, W. Petry, S. Van den Berghe, A. Leenaers, “*Heavy ion irradiation of UMo/Al samples with protective Si and ZrN layers (SELENIUM)*”, RERTR 2011, Santiago de Chile, Chile, 2011
- [19] R. Jungwirth, W. Petry, H. Breitzkreutz, W. Schmid, H. Palancher, A. Bonnin, M. Grasse, C. Jarousse, B. Stepnik, “*Screening of different UMo/Al samples: Protective oxide layers, Ti addition to the matrix and ternary U-Mo-X alloys*”, RRFM 2011, Rome, Italy, 2011
- [20] R. Jungwirth, W. Petry, H. Breitzkreutz, W. Schmid, H. Palancher, C. Jarousse, “*Study of heavy ion irradiated UMo/Al miniplates: Si and Bi additions into Al and UMo ground powders*”, RRFM 2010, Marrakech, Morocco, 2010
- [21] R. Jungwirth, “*Irradiation behavior of modified high-performance nuclear fuels*”, Doctoral thesis, Technische Universität München, 2011
- [22] H. Palancher, A. Bonnin, V. Honkimäki, T. Buslaps, et al., “*Quantitative crystallographic analysis of as-fabricated full sized UMo/Al(Si) nuclear fuel plates*”, J. Alloys and Compounds, accepted, 10.1016/j.jallcom.2012.02.010; A. Bonnin, H. Palancher, F. Charollais, M.C. Anselmet, V. Honkimäki, P. Lemoine, Proceedings of RRFM 2011, Rome, Italy, March 20-24, 2011
- [23] A. Leenaers, S. V. den Berghe, W.V. Renterghem, F. Charollais, P. Lemoine, C. Jarousse, A. Röhrmoser, W. Petry, “*Irradiation behavior of ground U(Mo) fuel with and without Si added to the matrix*”, Journal of nuclear materials 412 (2011) 41-52
- [24] H. Y. Chiang, R. Jungwirth, T. Zweifel, W. Schmid, W. Petry, F. Kraus, “*Interactions Between UMo/Al Fuel and Diffusion Barriers, Nb and TiN, Under Heavy Ion Irradiation*”, RERTR 2011, Santiago de Chile, Chile, 2011
- [25] J. Yang, W. Cho, Y. Jeong, J. M. Park, C. K. Kim, “*Fabrication and Characterization of the Uranium Nitride Layer Coated U-Mo Spherical Particles*”, RERTR 2011, Santiago de Chile, Chile, 2011

LEONIDAS E-FUTURE : Results of the Destructive Analyses of the U(Mo)-Al(Si) Fuel Plates

A. Leenaers - J. Van Eyken - S. Van den Berghe - E. Koonen
SCK•CEN, Boeretang 200, B-2400 Mol – Belgium

F. Charollais^(a) - P. Lemoine^(b)
^(a)CEA, DEN, DEC, Cadarache, F-13108 Saint-Paul-Lez-Durance, France
^(b)CEA, DEN, DISN, Saclay, F-91191 Gif-sur-Yvette – France

Y. Calzavara - H. Guyon
ILL, 6 rue Jules Horowitz, F-38042 Grenoble Cedex 9 – France

C. Jarousse - B. Stepnik
AREVA-CERCA, 10, Rue Juliette Récamier, 69 456 Lyon Cedex 06 - France

D. Wachs^(a) - A. Robinson^(a)
^(a)Idaho National Laboratory, P.O. Box 1625, Idaho Falls, ID 83415 – USA

ABSTRACT

The LEONIDAS program is aimed at the qualification of the U(Mo)-Al(Si) dispersion fuel for the use in high power conditions. The first experiment of the program, called E-FUTURE, was performed to select the Si concentration and fuel plate heat treatment parameters for further qualification. It consisted of the irradiation of 4 distinct (4% and 6% Si, 2 different heat treatments) full size, flat fuel plates in the BR2 reactor (470 W/cm² peak BOL power, ~70% peak burn-up). After the irradiation, the E-FUTURE plates were examined non-destructively and found to have blistered in the high burn-up positions.

The destructive post-irradiation examinations (PIEs) of these plates are expected to yield further insight in the cause of this blistering and the underlying mechanisms related to the fuel-matrix interaction. The examinations include scanning electron microscopy (SEM) and electron probe microanalysis (EPMA). The results of this work and their interpretations in function of fuel behavior are presented in this paper.

1 Introduction

The LEONIDAS program [1, 2] is aimed at the qualification of the U(Mo)-Al(Si) dispersion fuel for the use in high power conditions. The first experiment of the program, designated E-FUTURE, was performed to select a Si concentration and fuel plate heat treatment parameters for further qualification.

The E-FUTURE experiment consisted of the irradiation of four full size, flat U(Mo)-Al(Si) dispersion fuel plates having a matrix of either 4 or 6 wt% Si mixed with pure Al. During fabrication, the fuel plates were submitted to different heat treatments. Some details of the experiment can be found in Table 1. When added to the Al matrix at room temperature, Si will be mainly present in the form of precipitates because of its low solubility in Al. During the annealing of the fuel plates, some of the Si will be thermally transported from the matrix to the fuel kernel surfaces [3, 4, 5, 6, 7], producing preformed U-Mo-Al-Si layers around the fuel particles. The presence of Si in the interaction product, enhanced by the preformed Si rich layers reduces the detrimental effects of the interaction between uranium and aluminum.

The E-FUTURE irradiation experiment was intended to show the best combination of added Si concentration and heat treatments during plate production. Although the experiment has shown a good behavior of the U(Mo) fuel up to a burn-up of $\sim 65\%$ ^{235}U and a positive influence of a higher Si content (6 wt % Si), an abnormal swelling has been measured in the highest burn-up region of each plate [2, 8]. A marked difference exists in blister size between the plates having 4 or 6 wt% Si in the matrix, with a clearly better behavior for the latter plates.

Microstructural analysis is performed on several samples cut from the fuel plates in an attempt to find a possible explanation for the blistering, to confirm the positive effect of a higher Si content in the matrix and to formulate recommendations for further development.

2 Plate fabrication and irradiation history

The 4 full sized fuel plates in the E-FUTURE experiment consist of 8gU/cc atomized U7wt%Mo particles dispersed in an Al-Si matrix (table 1). The matrix is a mixture of Al with either 4 or 6 wt% Si and two different cladding types were used (AlFeNi or AG3NE). The plates were heat treated under different time/temperature conditions during manufacturing, to promote the Si diffusion from the matrix towards the fuel kernels.

The E-FUTURE plates were irradiated at BR2 for 3 cycles resulting in 77 total effective full power days (EFPD). The maximum power at BOL was $>450\text{W}/\text{cm}^2$ as shown in table 1. Due to the absence of burnable poisons, there was a gradual reduction in power with irradiation time, reaching a value of around $250\text{ W}/\text{cm}^2$ at EOL. A local maximum burn-up of $\sim 70\%$ ^{235}U is attained over the full fuel cycle.

Before the start of the last irradiation cycle, plate 6111 was turned 180° with respect to its long axis. Since the hottest position is located at the edge of the fuel plates, this effectively put the high power position during the last cycle at the opposite edge for this plate. It furthermore caused the average and peak power of that plate to be higher during the last cycle compared to the other plates.

Plate Id.	U7MC4111	U7MC4202	U7MC6111	U7MC6301
	Fabrication data			
Cladding	AlFeNi	AG3NE	AlFeNi	AG3NE
Si % in Al matrix	4%	4%	6%	6%
Thermal treatment	425 °C – 2h	475 °C – 2h	425 °C – 2h	475 °C - 4h
	Irradiation data			
Mean BU (% ²³⁵ U)	48.3	48.1	47.1	47.5
Max BU (% ²³⁵ U)	71.3	71.3	68.7	71.4
Peak Heat Flux (W.cm ⁻²)	457	453	465	472

Table 1 Fabrication and irradiation data of the fuel plates of the E-FUTURE experiment.

After the irradiation and cool-down time, the E-FUTURE plates were transported from BR2 to the Laboratory for High and Medium Activity (LHMA) for PIE.

The non-destructive analysis showed [2, 8, 9] that all 4 plates have important swelling in the highest burn-up region, with three of them (4111, 4202 and 6111) showing a clear blistering in the swollen area. Plate 6301 (6%Si - 475°C - 4h) is the least affected. The plate thickness measurements are summarized in table 2.

Plate number	Maximum plate thickness (μm)	Reported as-built plate thickness (mm)	Maximum swelling (%)
U7MC4111	3045	1.29	138
U7MC4202	3390	1.29	165
U7MC6111	2345	1.28	84
U7MC6301	1842	1.29	44

Table 2 Plate thickness measured on the BONAPARTE measuring bench.

Oxide thicknesses in the top and bottom parts for all fuel plates are around 5-7μm, while in the high burn-up area, it increases to 25-35. The thickness of the oxide layer in the blister areas is significant higher but they are not further interpreted considering the sensitivity of the measuring tool (Eddy Current) to defects in the investigated object [9].

From the plates several samples were cut according to the scheme presented in figure 1.

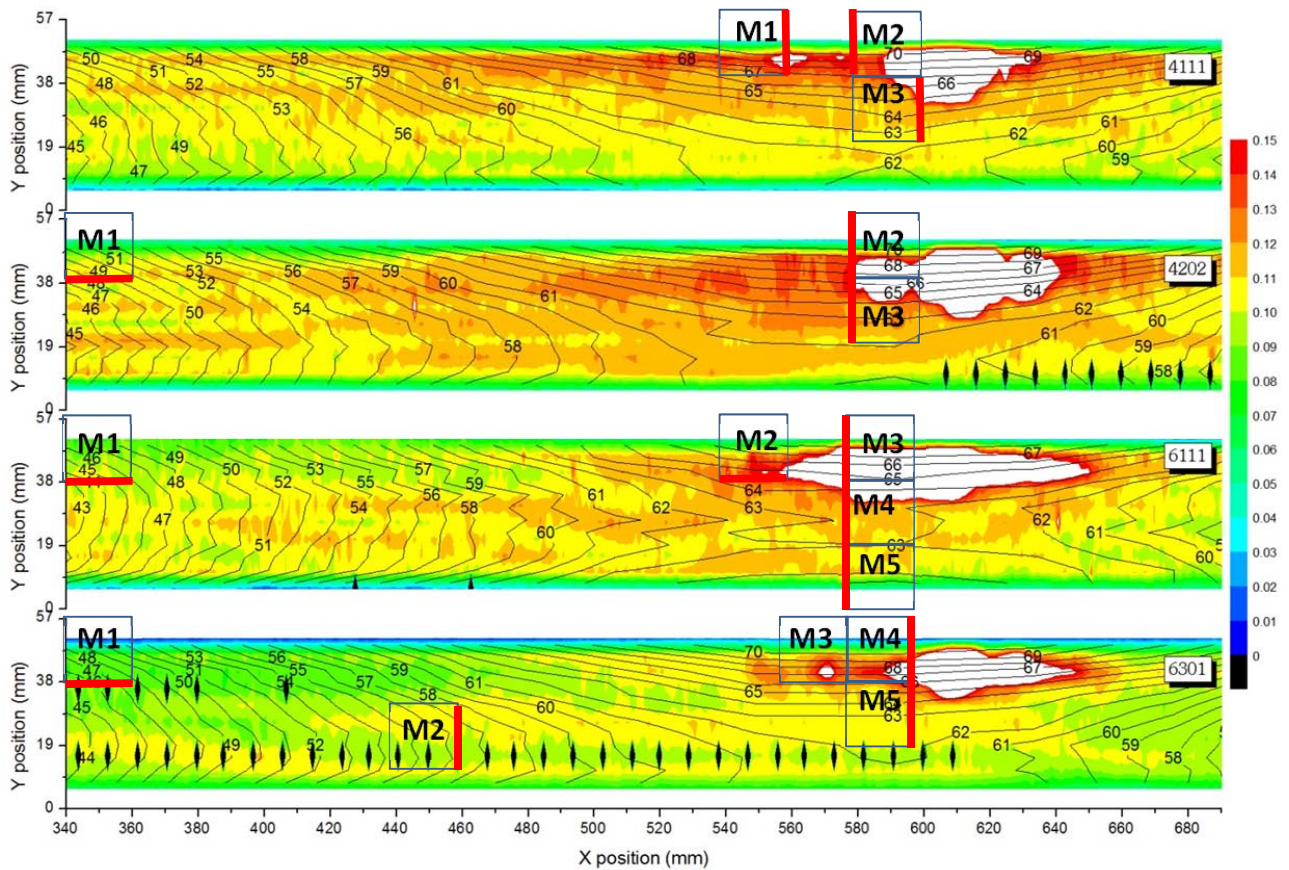


Figure 1 Cutting scheme for the E-FUTURE plates. Contour plot of the swelling-to-burn-up ratio over the central (blistered) part of the fuel plate. The color scheme is adapted to show the blistered areas, which have a Sw/BU ratio >0.15 [8, 9]. The polishing planes are indicated in red.

The samples are embedded (hot mounting) and polished. The polished surfaces of the samples are indicated by red lines in figure 1.

3 Post irradiation examination

All samples were subjected to scanning electron microscopy (SEM) while only a few were additionally analyzed with electron microprobe analysis (EPMA).

In figure 2, a collage of SEM images across the (partly) width of fuel plate 6111 (samples M3 and M4) illustrates the formed blister. This image is comparable to the observation in the deformed fuel plate of the FUTURE experiment (U7Mo dispersed in a pure Al matrix, irradiated for 40 EFPD's, max heatflux 340 W/cm^2 , final BU 29 % ^{235}U) [10].

Detailed SEM images show that at a location away from the blister (6111M4, fig. 2.1 and 2.2), thick interaction layers (IL) have formed but occasionally also small IL's can be observed.

Inside the fuel kernels, numerous fission gas (FG) bubbles can be observed. Also at the interface between fuel kernel surface and IL, small FG bubbles have developed. In between touching fuel kernels, somewhat larger voids are starting to form. These voids become larger when moving more towards the blister (6111M4 fig. 2.3 and 2.4). At this location, also crescent moon shaped voids at the interface between the IL and the matrix can be seen.

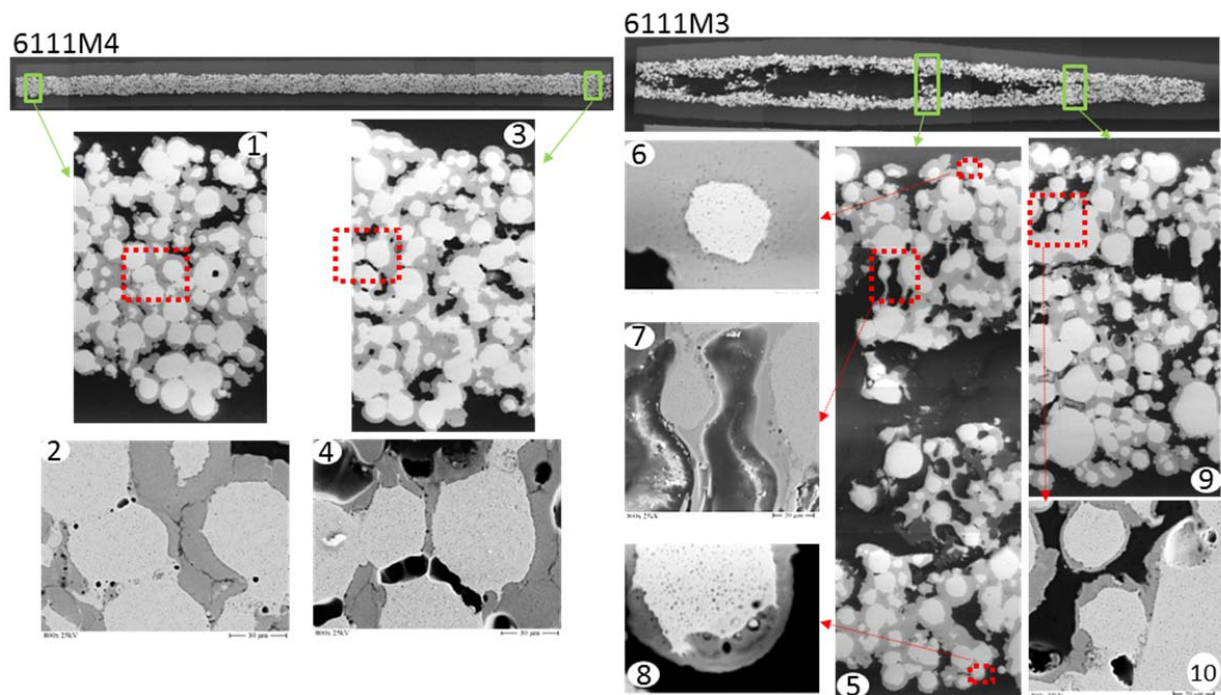


Figure 2

The composite SEM image of the blister (6111M3) shows that the cladding is unaffected (also in thickness), but a deformation of the meat has occurred. Although protective measures have been taken, some of the meat from the center is most probably pulled out during sample preparation. Since the detailed images show no extensive swelling of the fuel kernels or severe increase in IL thickness (even some AlSi matrix is still observed), the void in the center is probably resulting from a mechanical instability (buckling).

A detailed image (fig. 2.7) shows in the central part of the meat, some deformation of the fuel particles (from circular to elongated shapes) and especially of the matrix. This could again indicate mechanical instability and/or that a steep local increase in the temperature (due to low conductivity). Fig. 2.6 shows numerous FG bubbles in the interaction layer and inside the fuel particle. Irregularities in IL thickness and surface of the fuel kernel can frequently be seen (fig. 2.2, 4, 8, and 10) and is usually related to the presence of Si in or close to the IL. This will be confirmed by EPMA measurements.

Moving away from the blister towards the frame, the thickness of the IL seems to decrease (?). This is commonly attributed to the constraints that are applied to the meat and the better cooling conditions found at this location. Still, a lot of voids can be seen either in between IL and matrix or adjacent to the fuel kernel surface / in between fuel kernels.

3.1 Plate 6301 sample M2

Data : 6 wt% Si in matrix, heat treatment 475 °C – 4 h, AG3NE cladding

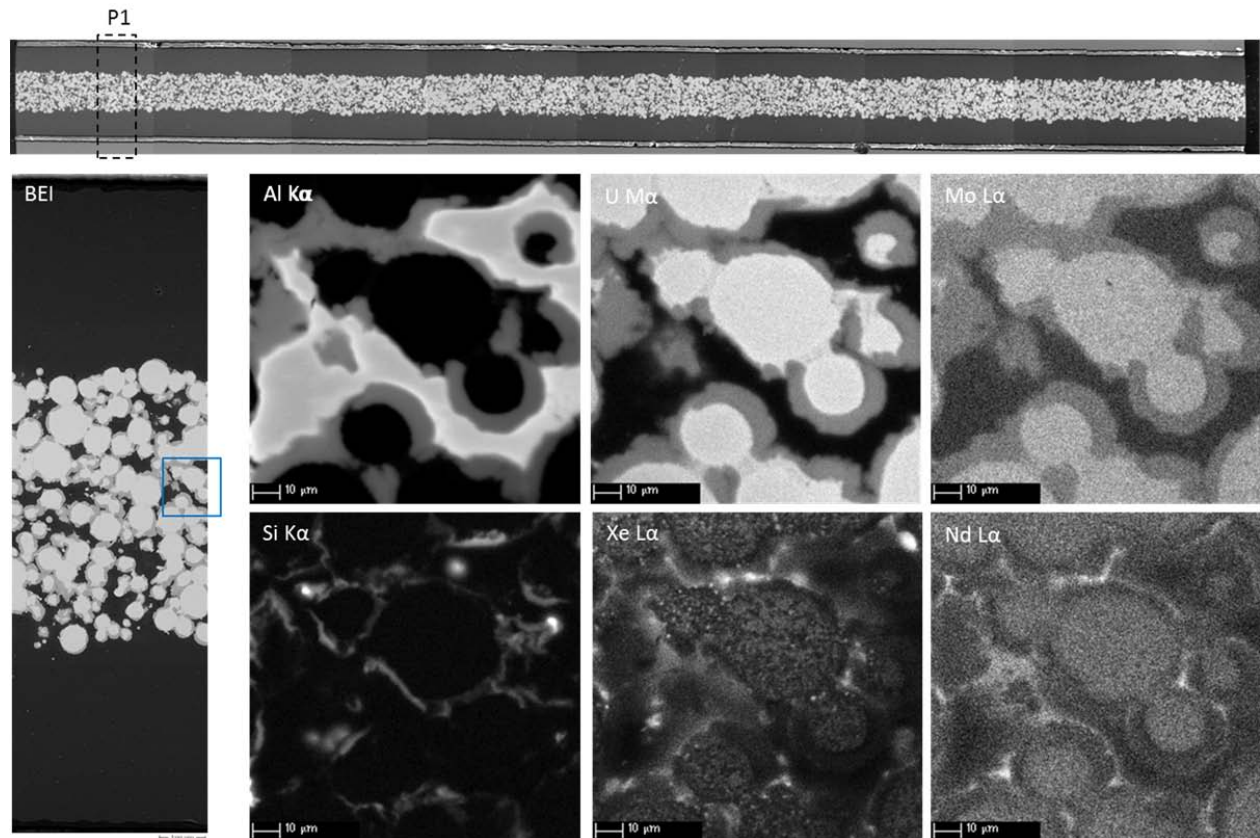


Figure 3 Collage of images covering the whole sample and a composition of backscattered electron images (BEI) over the width of the sample. Of the area outlined in blue on the BEI Al K α , U Ma, Mo La, Si K α , Xe La and Nd La X-ray maps are collected.

From all samples measured with EPMA, this sample is located at a higher burn-up position (average 58.6 % ^{235}U) but 140 mm away from the blister.

The BEI in figure 3 shows that at this position relatively thin IL's have formed and plenty of matrix is still available. The X-ray images (Al, U, Mo and Si) show that the thickness of the IL is very inhomogeneous. At any location on the fuel kernel surface where Si is observed in the mapping, only little interaction phase has formed. The irregular shape of the fuel kernels can also be related to the presence of Si. Occasionally some Si particles can still be observed in the matrix (spots in the Si map).

At locations where a thicker IL has formed, the fission products have been swept up by the growing IL, forming the typical halo. Where Si is present, no fission product halo can be observed and only the injection of the FP into the matrix is measured.

Inside the fuel kernels, some patches of Xe are observed corresponding to individual cells in the cellular kernel structure, indicating that the fission gas is still present as nanobubbles in those cells. Stable, SEM-visible (>100nm) fission gas bubbles have also formed inside some of the cells and on the cell boundaries, which are less stable due to their lower Mo content. However, also large Xe bubbles have formed either at the interface of the IL and the matrix (e.g. top right

corner), in between touching IL's or near the surface of the fuel kernel at those locations where a Si rich layer has formed.

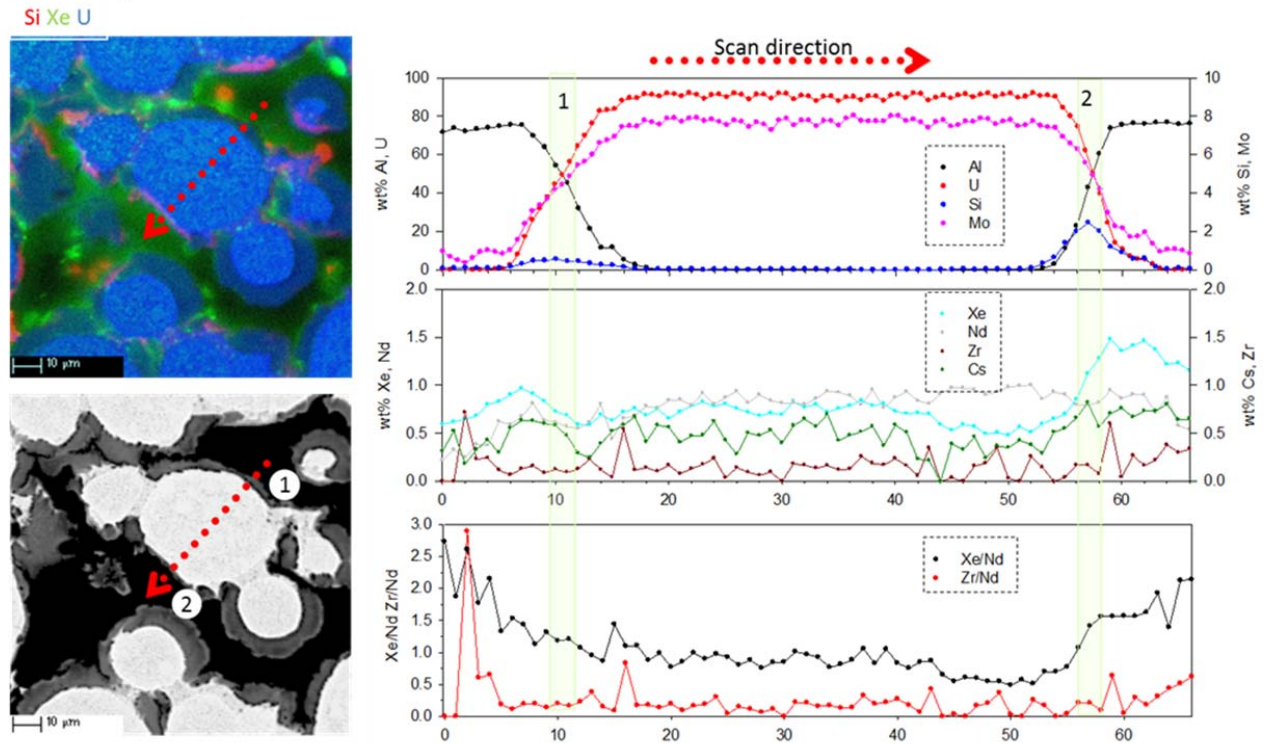


Figure 4 The red arrow on the combined Si, Xe and U X-ray map and absorbed current image, indicates the position of the quantitative linescan.

A quantitative linescan (fig. 4) is taken over a fuel kernel at a position where only a minor IL has formed. In the layers, a small quantity of Si can be found (below 3 wt%). The Xe and Nd signals increase after the IL but no peak intensity related to a halo, is observed. The ratio Xe/Nd inside the fuel kernel is below 1.8 (theoretical ratio [11]), indicating the precipitation of fission gas in bubbles. As these bubbles are opened during sample preparation, their gas content is not measured by EPMA. Only when the bubble are sufficiently small or the Xe is atomically dissolved, this effect can be neglected in the interpretation. Outside the fuel kernel, the ratio is higher and approximately around 1.4. The ratio Zr/Nd is constant, indicating a stationary behavior of Zr. The value of Zr/Nd is below the theoretical expected amount of 1.1 ([11]) and should be attributed to measurement error (calibration). The absolute value of Zr measured might be incorrect but the error is consistent over the whole linescan and therefore the relative interpretation is valid.

From several other linescans (total of ~ 100 measuring points) , an average composition of Al : 41.7 wt% , Si : 1.9 wt%, Mo : 4.8 wt% and U 51.1 wt% has been determined for the interaction layer. In the IL's, a minimum Si content of 0.8 at% and a maximum of 5.4 at% was found. This leads to a typical Al+Si/U+Mo atomic ratio 6.

3.2 plate 4202 sample M3

Data : 4 wt% Si in matrix, heat treatment 475 °C – 2h, AG3NE cladding

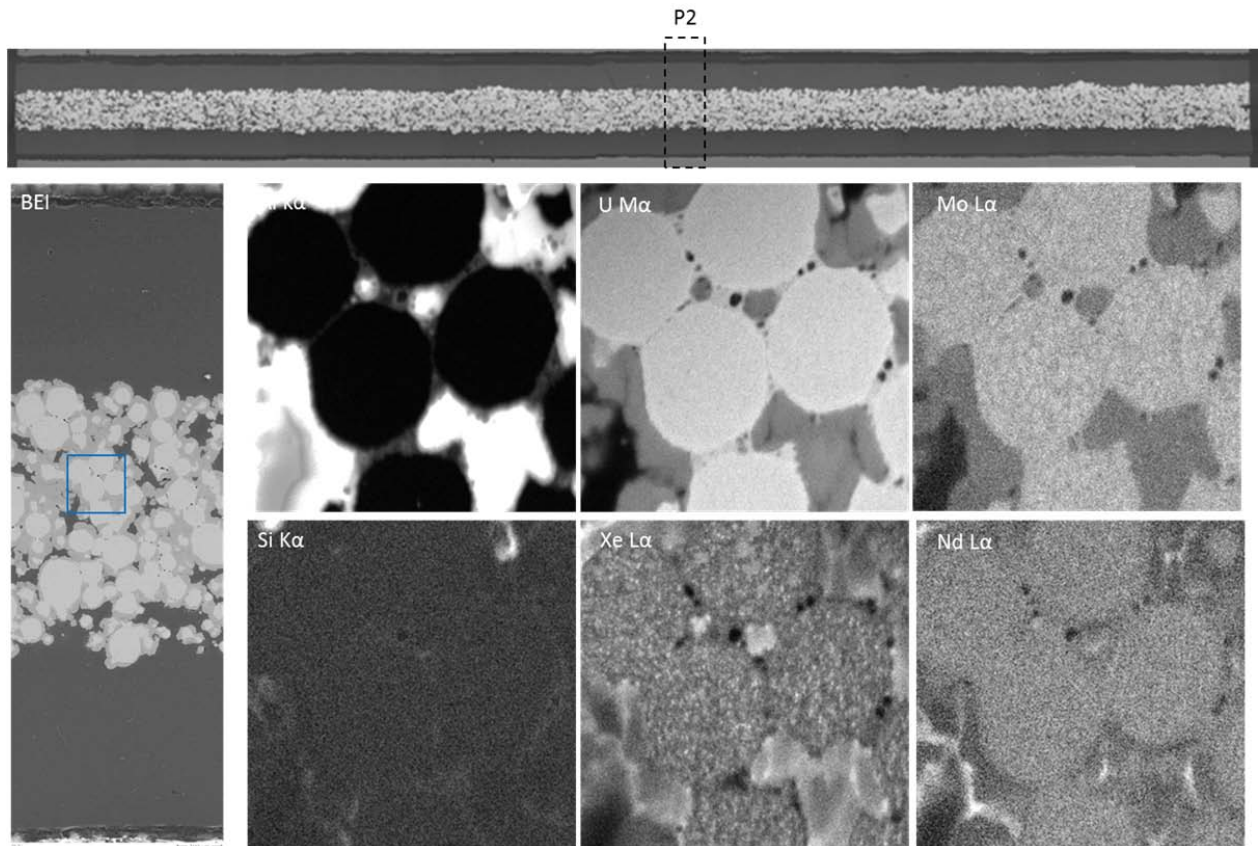


Figure 5 Collage of images covering the whole sample and a composition of backscattered electron images (BEI) over the width of the sample. Of the area outlined in blue on the BEI Al $K\alpha$, U $M\alpha$, Mo $L\alpha$, Si $K\alpha$, Xe $L\alpha$ and Nd $L\alpha$ X-ray maps are collected.

This sample has an average burn-up of 63.5 % ^{235}U and is located adjacent to the deformation. As a result of the slightly higher burn-up compared to the previous sample (6301M2), thicker IL's have formed and the amount of residual matrix has been reduced (fig.5).

The Si X-ray map shows that only very thin Si rich layers have formed and almost no Si particles can be seen in the matrix.

At the interface of the IL and the matrix (or in-between touching IL's), an accumulation of fission products (Xe, Nd) forming a halo, can be observed. It should be noted that in-between touching fuel kernels or even adjacent to the fuel surface, larger voids appear. Inside the fuel kernels, only a few Xe patches can still be seen (e.g. in kernel at top of image). The numerous visible Xe bubbles indicate that most of the nanobubbles have precipitated out.

The quantitative linescan and X-ray maps show that a Si particle (U shaped) is very close to the fuel particle but still an IL has formed (zone 1). In between the particle and the IL, the fission product halo is observed. The IL in zone 3 contains a larger amount of Si and it is also followed by a fission product halo.

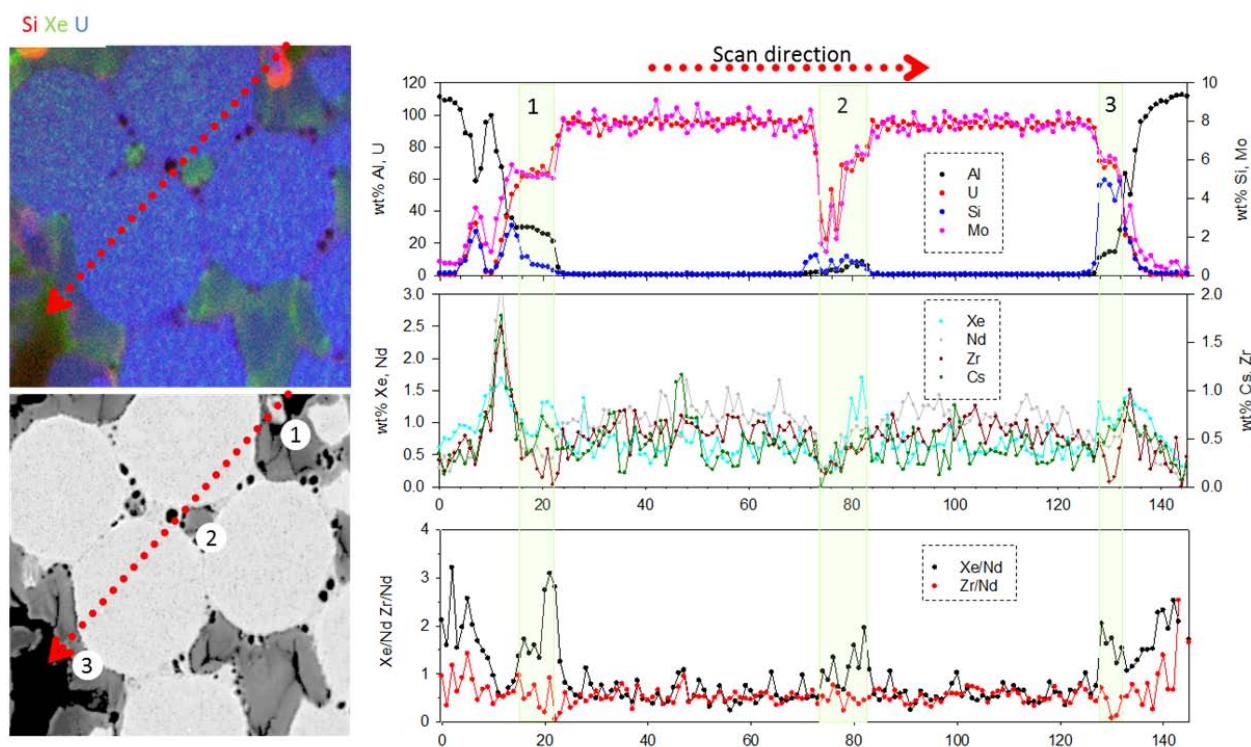


Figure 6 The red arrow on the combined Si, Xe and U X-ray map and absorbed current image, indicates the position of the quantitative linescan

The location of the IL's can be seen in the Xe/Nd ratio. In the IL this ratio is around 1.8 while inside the kernels a ratio of approximately 0.5 is measured which is due to venting of Xe during sample preparation. This shows that no Xe is released from the IL and that no large bubbles have formed, otherwise the ratio would be lower.

The Zr/Nd ratio shows a flat profile and amounts around 0.6 which is close to the theoretical value (0.8). This implies again the very stable and stationary behavior of Zr.

From several quantitative linescans (e.g. fig. 6) obtained on this sample, an average composition of the IL was deduced : Al : 25.6 wt% , Si : 2.6 wt% , Mo : 5.1 wt% and U 60 wt%. In the IL's, a minimum Si content of 2.8 at% and a maximum of 19.9 at% was found. This results in an (Al+Si)/(U+Mo) ratio of 3.1.

3.3 plate 6111 sample M4

Data : 6 wt% Si in matrix, heat treatment 425 °C – 2 h, AlFeNi cladding

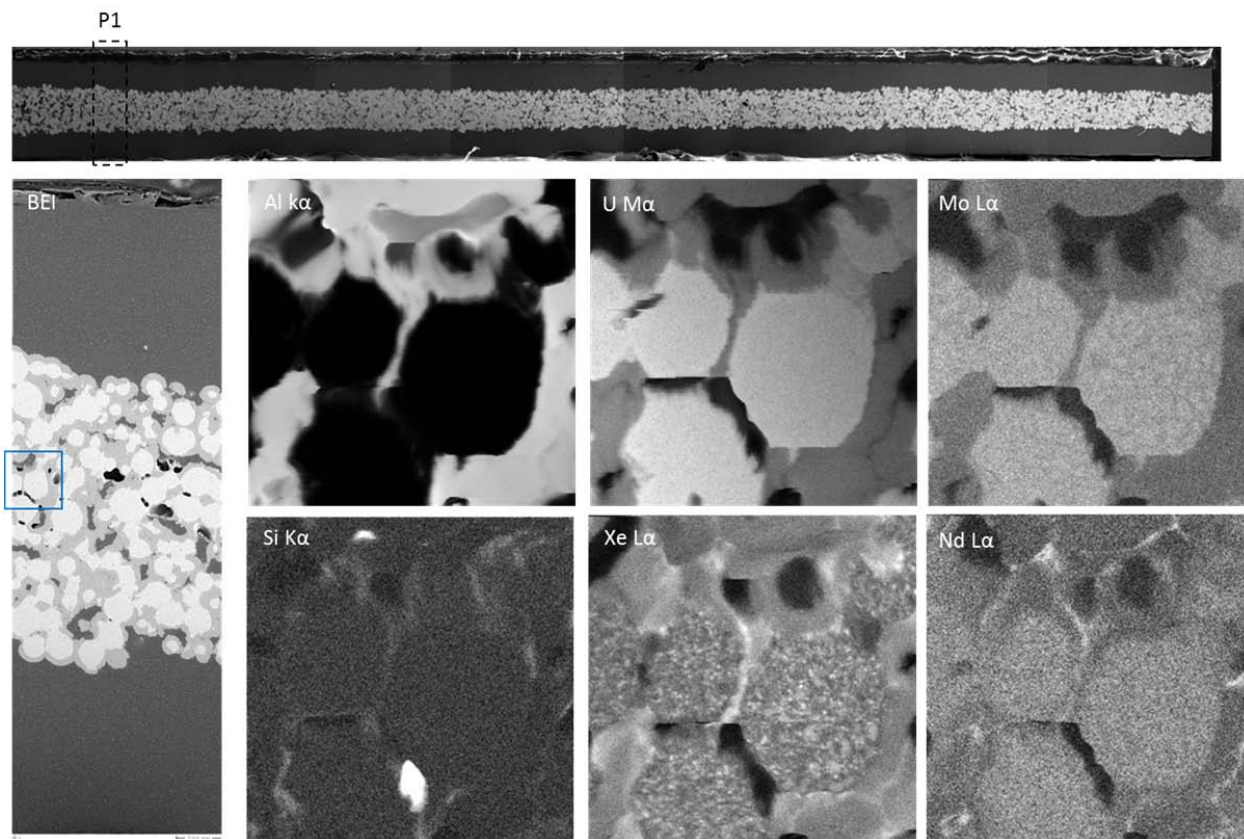


Figure 7 Collage of images covering the whole sample and a composition of backscattered electron images (BEI) over the width of the sample. Of the area outlined in blue on the BEI Al K α , U M α , Mo L α , Si K α , Xe L α and Nd L α X-ray maps are collected.

This sample also originates from a position close to the blister. The average burn-up is 64 % ^{235}U . The backscattered images (fig. 7) over the width of the samples shows voids in the meat but not the typical crescent moon shaped ones that are usually located at the interface IL and matrix. Here, the voids are more often located near the fuel surface ('underneath' the interaction layer) or in-between kernels. Thick IL's surround the fuel particles and only little matrix is left. From the Si X-ray map, the higher initial Si content of 6 wt% is clearly seen. Moreover, in one of the 'voids' observed with SEM, a remaining Si particle is measured. It might thus be that some of the voids observed in-between fuel particles, are resulting from pull out (of Si particles) during sample preparation.

A quantitative linescan is obtained across the fuel particle and the Si particle squeezed in-between. It is noted (also from the X-ray map) that no interaction occurred between the Si

particle and U(Mo). It cannot be excluded that this Si rich particle was in fact introduced in an existing void during sample preparation, which would explain the lack of interaction as well.

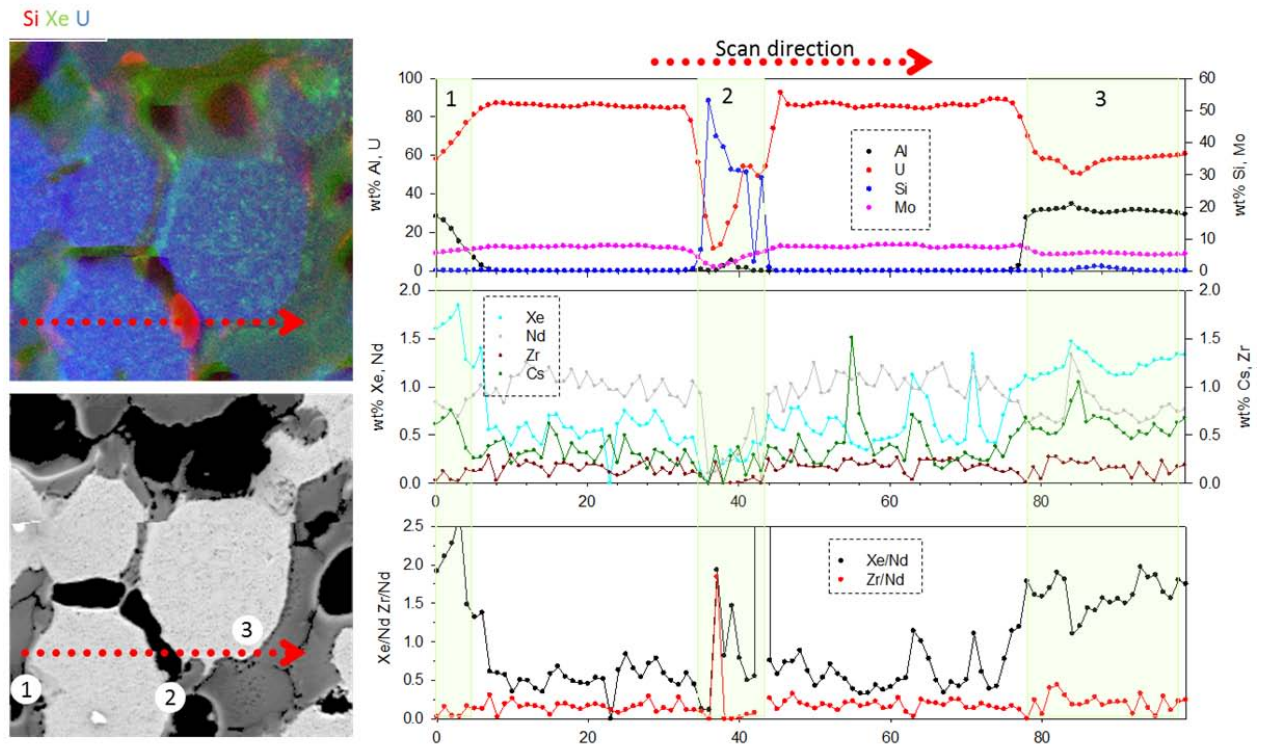


Figure 8 The red arrow on the combined Si, Xe and U X-ray map and absorbed current image, indicates the position of the quantitative linescan.

From several quantitative linescans (e.g. fig. 8) obtained on this sample an average composition of the IL was deduced : Al : 31.7 wt% , Si : 0.7 wt%, Mo : 5.1 wt% and U 58.5 wt% . This result in an atomic ratio Al+Si/Mo+U of 3.8. In the IL's, a minimum Si content of 0 at% and a maximum of 8.9 at% was found.

3.4 Plate 6301 sample M5

Data : 6 wt% Si in matrix, heat treatment 475 °C – 4 h, AG3NE cladding

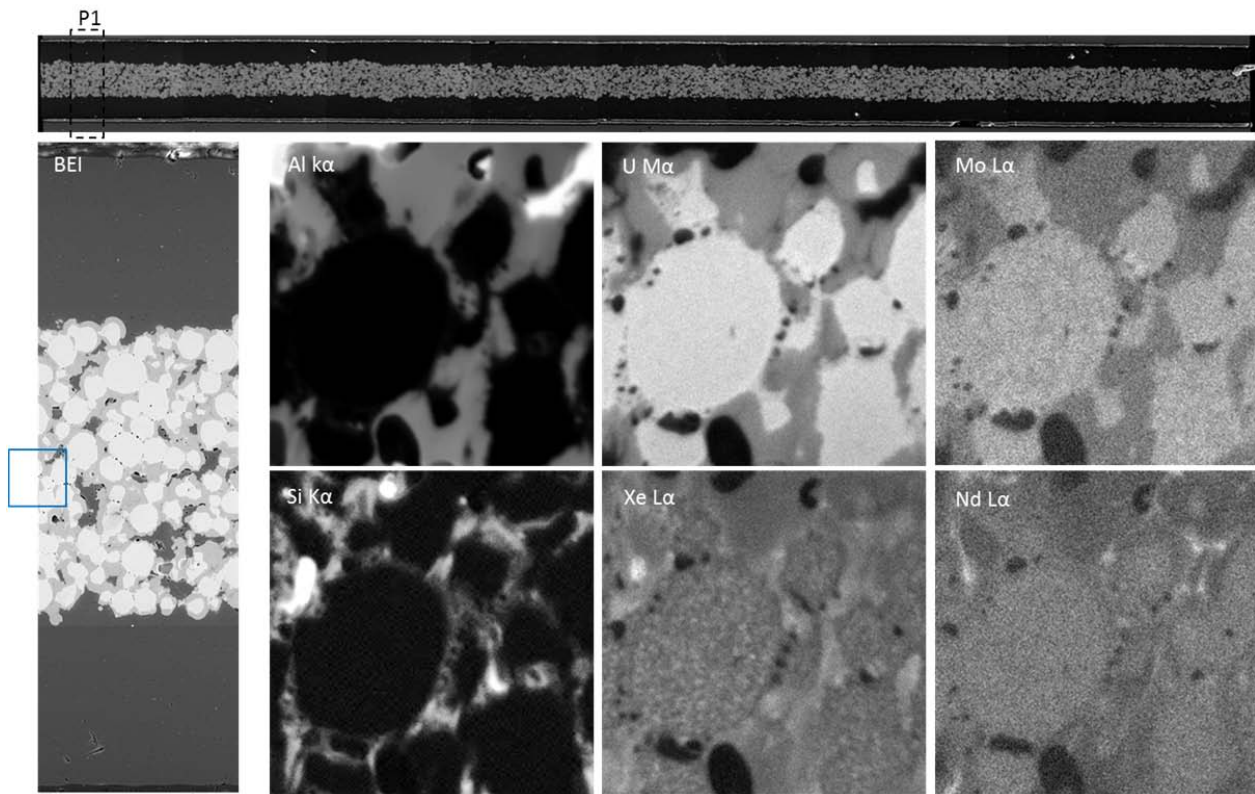


Figure 9 Collage of images covering the whole sample and a composition of backscattered electron images (BEI) over the width of the sample. Of the area outlined in blue on the BEI Al K α , U M α , Mo L α , Si K α , Xe L α and Nd L α X-ray maps are collected.

This sample is retrieved from a position close to the observed blister on fuel plate 6301 and has an average burn-up of 65 % ^{235}U .

The backscattered images (fig. 9) show that the meat still contains some matrix and that several larger voids have formed. Similar to the previous described samples (4202M3 and 6111M4) these voids are mostly located in-between fuel particles or adjacent to the fuel kernel surface. The higher Si content in this plate and the higher annealing temperature are reflected in the Si X-ray map. Almost all fuel particles are surrounded by a Si rich layer and occasionally some original Si particles can still be observed.

Looking in more detail, it can be seen that larger Xe bubbles have formed in the Si rich layer, but most of them were opened and vented during sample preparation. These could be the precursors of the larger voids, presumably formed as a result of the mechanical instability of this microstructure as the temperature increases further.

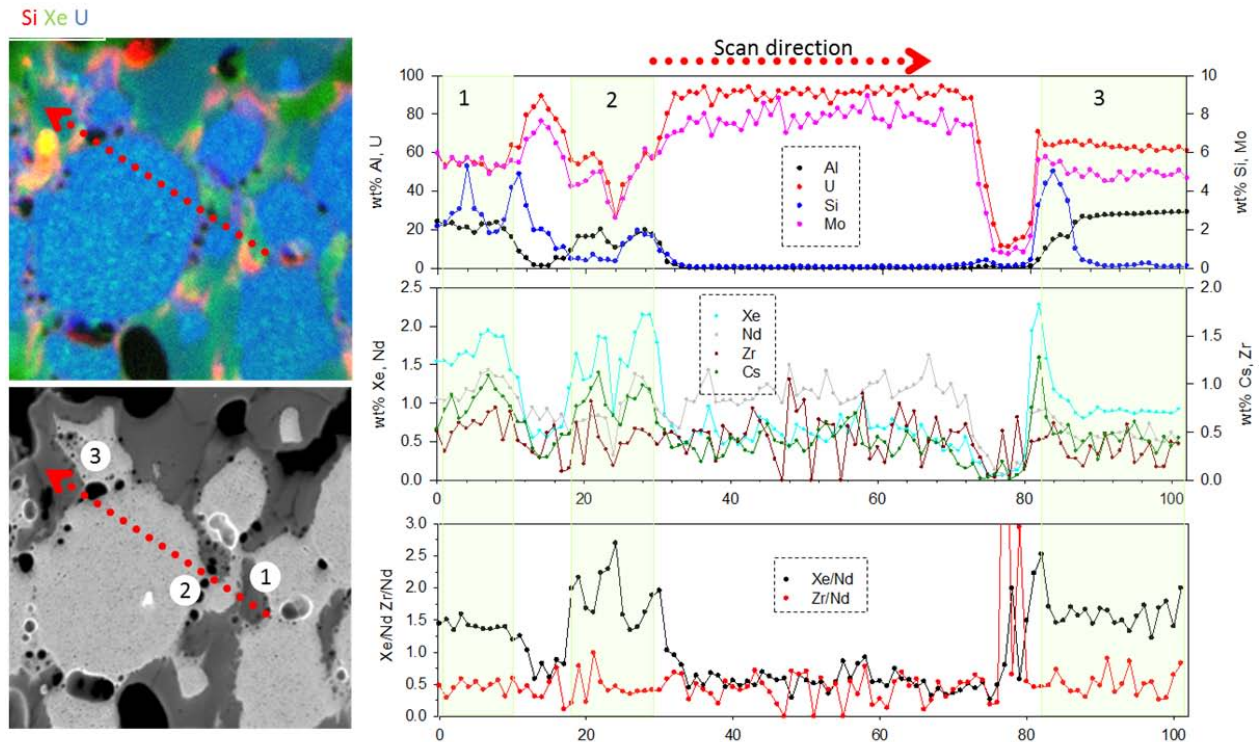


Figure 10 The red arrow on the combined Si, Xe and U X-ray map and absorbed current image, indicates the position of the quantitative linescan.

From the quantitative linescans (e.g. figure 10) the average composition of the IL was measured to be : Al : 25.9 wt% , Si : 2.2 wt%, Mo : 5.2 wt% and U 57.5 wt%. In the IL's, a minimum Si content of 1.4 at% and a maximum of 11.1 at% was found

The Xe/Nd inside the fuel kernels is far below the expected value of 1.8, indicating release (venting) of Xe from the fuel. Inside the IL, no release occurred. The Zr/Nd profile is flat and on average is close to the expected value of 0.84 [REF].

4 Analysis

	Temp (°C)	Al (σ) (wt%)	Si (σ) (wt%)	Mo (σ) (wt%)	U (σ) (wt%)	$\frac{Al+Si}{U+Mo}$ (σ)
6301M2	Away from blister	41.7 (4.6)	1.9 (1.1)	4.8 (0.3)	51.1 (4.4)	6.0 (0.9)
4202M3	Close to blister	25.6 (2.9)	2.6 (2.3)	5.1 (0.2)	60.0 (5)	3.1 (0.5)
6111M4	Close to blister	31.7 (6.6)	0.7 (1.1)	5.1 (0.6)	58.5 (6.5)	3.8 (1.2)
6301M5	Close to blister	25.9 (2.8)	2.2 (1.3)	5.2 (0.2)	57.5 (4)	3.4 (0.4)

Table 3 Summary of measured IL composition in the different fuel plates

In table 3, a summary is given of the measured composition of the IL. It should be stressed that the values are the average of several measurement points (>10 for each value).

The ratio Al+Si/U+Mo was calculated for all samples resulting in composition of the IL of (U+Mo)(Al+Si)₃ to (U+Mo)(Al+Si)₄ for sample 4202M3, 6111M4 and 6301M5 while for sample 6301M2 this becomes (U+Mo)(Al+Si)₆. This may be related to the lower temperatures seen at this location since the latter sample is located away from the max flux plane where the deformation occurred and has thus seen a lower heat flux [12] and less degradation of the thermal conductivity.

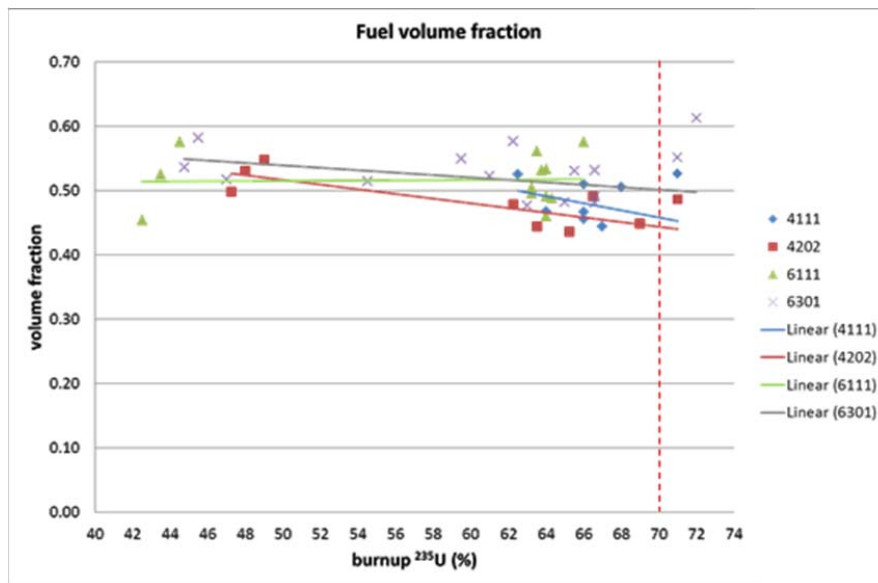


Figure 11 Surface fraction occupied by the fuel (FG bubbles included).

The surface/volume fraction occupied by the different phases in the meat (fuel, IL and matrix) have been calculated by image analysis performed on the SEM images. In figure 11,12 and 13 the fraction occupied by respectively the fuel, IL and matrix is plotted as function of the burn-up.

The outliers visible above a burn-up of 70 % ²³⁵U, are due to the formation of big voids in the meat (possibly at least partially resulting from pull out of material) and were excluded for further interpretation. On the remaining points a linear regression analysis was performed and a trend line was plotted, even if it is known that the IL growth is not strictly linear in function of burn-up

It is observed that the trend lines for the fuel fraction for all plates have a rather horizontal profile. This constant volume fraction is explained by the compensation of the fuel kernel swelling by the consumption due to interaction phase formation. There seems to be a slight downwards tendency of the fraction above 60 % ²³⁵U burn-up. This trend is more explicit for the 4XXX (4% Si added) then for the 6XXX (6% Si added) plates.

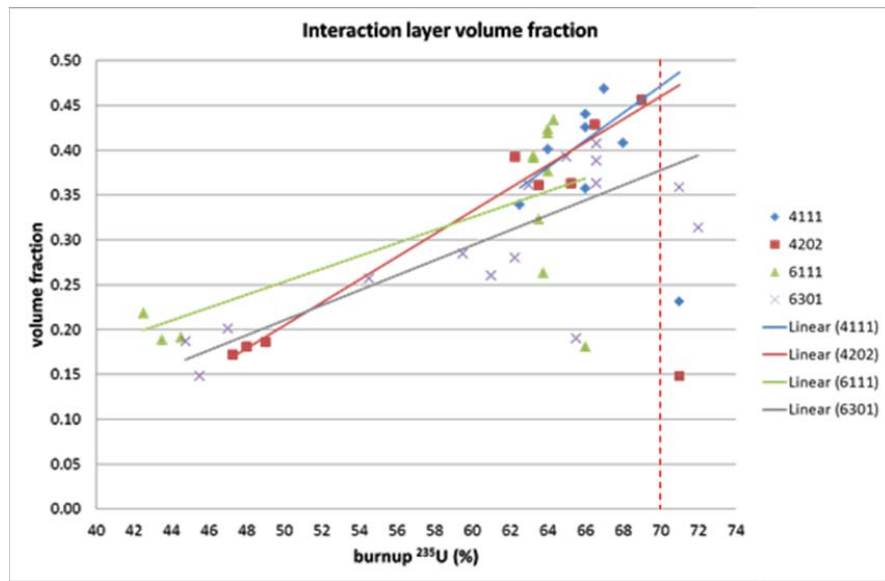


Figure 12 Surface fraction occupied by the interaction layer.

The difference between the 4XXX and 6XXX plates is even more obvious in the plot of the fraction occupied by the interaction layer. The trend lines for the 4111 and 4202 show a steeper increase then the ones for the 6111 and 6301 plates. The difference between the trend lines for the 6111 and 6301 plate furthermore can be interpreted to show an effect of the annealing temperature/time : the treatment of the 6301 plate was at a higher temperature and longer time (475 °C/4h) then plate 6111 (425°C/2h) resulting in more Si rich preformed layers acting as diffusion barrier during irradiation [6].

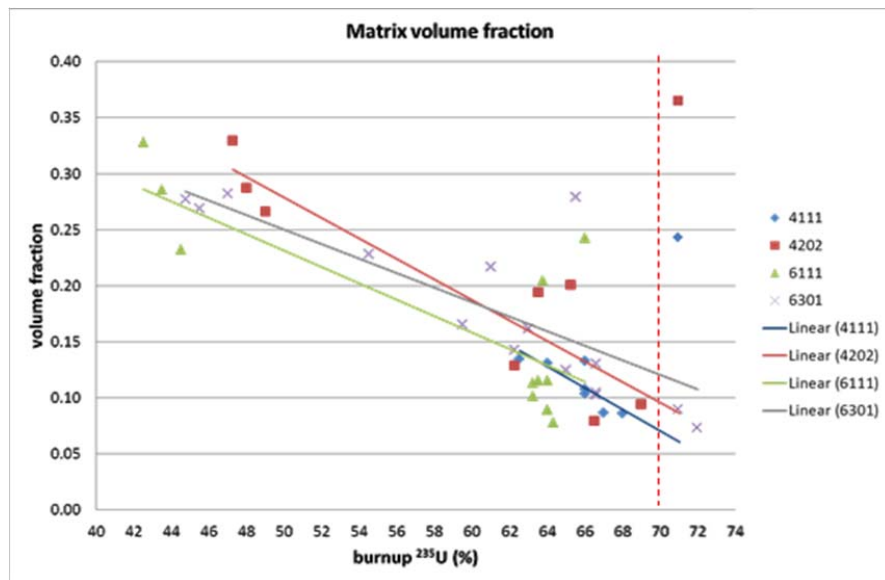


Figure 13 Surface fraction occupied by the AlSi matrix

The mirror image is logically seen in the plot of the surface fraction occupied by the matrix. Less matrix should be consumed in plate 6301 compared to 6111. Similar for fuel plate 4202 opposed to plate 4111.

Plates 4XXX show a steeper decrease in surface fraction occupied by the matrix than the 6XXX plates.

From this graph, one may deduce that blistering will occur when the matrix fraction becomes less than 10% of the total volume. This observation should be handled with care, since it is unknown what amount of matrix was consumed during the phase under irradiation after the blister was formed (higher temperatures).

5 Oxide layer thickness measurements

The SEM images were also used to measure the oxide layer thickness on the cladding surface. Unfortunately (and probably due to sample preparation) not all oxide layers were still intact. Several measurement were performed on each position of all samples on as well on the engraved as on the other side of the plate. The average value obtained is compared to the average oxide thickness measured with Eddy Current (NDT) [8, 9] and presented in figure 14.

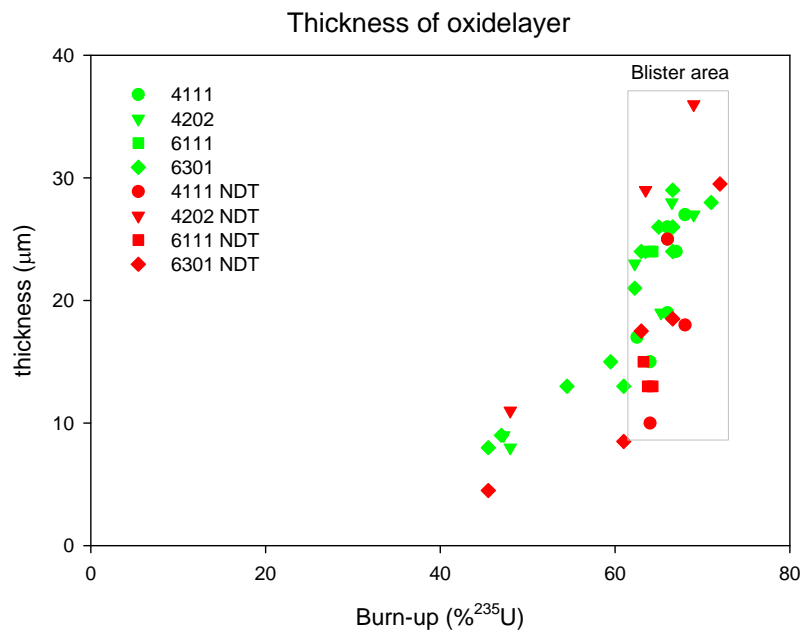


Figure 14 Oxide layer thickness measured on all samples with SEM/image analysis (green) and Eddy Current (red).

As X axis, the burn-up of the samples has been selected only to show the evolution of the oxide layer thickness as function of how close the samples are to the blister area (or the highest heat flux area).

Figure 14 shows a good correlation between the EC and SEM based measurements. Any deviation in layer thickness should be attributed to the difference in local (SEM) and global (EC) measurements.

6 Conclusion

Destructive analysis of the E-FUTURE plates confirm that show stable behavior up to a burn-up of 60 % ^{235}U , the fuel plates. At higher burn-up, the formation of voids mostly in-between fuel kernels or adjacent to the kernel surface is observed. Even in the deformed area (blister) the fuel show stable behavior and no excessive growth of the formed interaction layer is seen. The plastic deformation observed in the meat indicates that the fuel plates have suffered a mechanical instability (buckling) but the reason for this cannot be pin pointed.

EPMA measurements show that fission gas has been released from the fuel but in all samples Xe bubbles, and in some cases even patches of Xe nanobubbles, are observed in the fuel kernel.

From the calculation of the volume fractions occupied by the different phases, the positive effect of a higher Si amount added to the matrix and the higher annealing temperature can be derived unambiguously.

References

- [1] F. Fréry, H. Guyon, E. Koonen, S. Van den Berghe, P. Lemoine, F. Charollais, C. Jarousse and D. Geslin in: Proceedings of the 32nd International Meeting on Reduced Enrichment for Research and Test Reactors (RERTR), Lisbon, Portugal (2010).
- [2] F. Charollais, P. Lemoine, Y. Calzavara, H. Guyon, E. Koonen, S. Van den Berghe, B. Stepnik, C. Jarousse and D. Geslin in: Proceedings of the 33rd International Meeting on Reduced Enrichment for Research and Test Reactors (RERTR), Santiago, Chile (2011).
- [3] D. D. Keiser, A. B. Robinson, J. F. Jue, P. Medvedev, D. M. Wachs and M. R. Finlay, Journal Of Nuclear Materials, 393 (2) (2009) 311-320.
- [4] Y. S. Kim, G. Hofman and A. B. Robinson in: Proceedings of the International Topical Meeting on Research Reactor Fuel Management (RRFM), Vienna, Austria (2009).
- [5] R. Jungwirth, H. Breitzkreutz, W. Petry, A. Rohrmoser, W. Schmid, H. Palancher, C. Bertrand-Drira, C. Sabathier, X. Iltis, N. Tarisien and C. Jarousse in: Proceedings of the 31th International Meeting On Reduced Enrichment For Research And Test Reactors (RERTR), Beijing, China (2009).
- [6] X. Iltis, F. Charollais, M. C. Anselmet, P. Lemoine, A. Leenaers, S. Van den Berghe, E. Koonen, C. Jarousse, D. Geslin, F. Frery and H. Guyon in: Proceedings of the 32th International Meeting on Reduced Enrichment for Research and Test Reactors (RERTR), Lisbon, Portugal (2010).
- [7] M. Ripert, S. Dubois, P. Boulcourt, S. Naury and P. Lemoine in: Proceedings of the 10th International Topical Meeting on Research Reactor Fuel Management (RRFM), Sofia, Bulgaria (2006).
- [8] S. Van den Berghe, A. Leenaers and Y. Parthoens in: Proceedings of the International Meeting On Reduced Enrichment For Research And Test Reactors (RERTR), Santiago, Chili (2011).
- [9] S. Van den Berghe, Y. Parthoens, A. Leenaers, E. Koonen, V. Kuzminov, F. Charollais, P. Lemoine, C. Jarousse, H. Guyon, D. M. Wachs and A. B. Robinson, to be submitted to JNM, (2011).
- [10] A. Leenaers, S. Van den Berghe, E. Koonen, C. Jarousse, F. Huet, M. Troabas, M. Boyard, S. Guillot, L. Sannen and M. Verwerft, J. Nucl. Mater., 335 (2004) 39-47.
- [11] RSICC Computer Code Collection Origen 2.2., Oak Ridge National Laboratory CCC-371/ORIGEN 2.2 Code Package (Calculation performed by Dr. F. Jutier, SCK•CEN), June 2002.
- [12] A. Savchenko, A. V. Vatulin, I. V. Dobrikova and I. Konovalov in: Proceedings of the 10th International Topical Meeting on Research Reactor Fuel Management (RRFM), Sofia, Bulgaria (2006).

MICROSTRUCTURAL ANALYSIS OF IRRADIATED U-MO FUEL PLATES: RECENT RESULTS

D. D. KEISER, JR., D. M. WACHS, M. K. MEYER, A. B. ROBINSON, P. MEDVEDEV,
AND G. A. MOORE

*Nuclear Fuels and Materials Division, Idaho National Laboratory
P. O. Box 1625, Idaho Falls, Idaho 83403 USA*

ABSTRACT

Chemical interactions between U-Mo fuel particles and Al or Al alloy matrices can negatively impact the performance of an irradiated fuel plate, and in some cases can cause fuel plate failure. One possible remedy for this phenomenon is to replace the Al or Al-Si matrix in the dispersion fuel with another material that exhibits limited interaction with U-Mo alloys during fuel plate fabrication and irradiation. Mg is one material that meets this requirement, since U and Mg are immiscible. To test the effectiveness of using Mg as the matrix in U-Mo dispersion fuel, a fuel plate (R9R010) was tested in the RERTR-8 experiment. This paper describes how the fuel plate was fabricated, the results of the microstructural analysis that was performed on the fuel plate after irradiation, and how the observed microstructure compares to those for fuel plates with Al-2Si or AA4043 (≈ 4.5 wt% Si) matrix that were tested as part of the AFIP-1 experiment. Particular focus is given to any fuel/matrix interactions that may have occurred during irradiation. Generally, the tested RERTR-8 fuel plate exhibited good irradiation performance, with negligible interaction between the U-7Mo fuel particles and the Mg matrix. Whereas, the AFIP-1 fuel plates with Al-2Si and AA4043 matrices exhibited areas in the fuel meat where the matrix was completely consumed.

1. Introduction

The United States Reduced Enrichment for Research and Test Reactors (RERTR) Fuel development program is actively developing low enriched uranium (LEU) fuels for the world's research reactors that are currently fueled by uranium enriched to more than 20% ^{235}U [1]. One type of fuel being developed is a U-7Mo dispersion fuel with Al-Si alloy matrix. Early on, a U-7Mo dispersion fuel with pure Al matrix was pursued as an option for an LEU fuel, but interaction between the fuel and matrix resulted in the production of phases that did not exhibit favorable performance during irradiation [2]. One possible solution to this fuel/matrix interaction (FMI) was for Si to be added to the matrix of a dispersion fuel to reduce FMI and to "stabilize" any interaction products that develop [3]. Yet, recently it has been determined that at aggressive reactor conditions even dispersion fuels with Al-Si alloy matrix that contain up to 4.5 wt% Si will develop excessive fuel/matrix interaction at aggressive reactor conditions [4].

From a fuel performance standpoint, it would be beneficial if FMI could be eliminated during irradiation of U-7Mo dispersion fuels. One possible matrix material that may exhibit negligible interaction with U-Mo alloys is Mg. Based on the U-Mg phase diagram, U and Mg are immiscible and should display negligible interaction during fabrication and irradiation [5]. Due to this fact, Mg has been identified as a potential matrix material for use in inert matrix nuclear fuels [6], and in fact, there is experience using Mg matrix U-Mo dispersion nuclear fuels in Russian LWRs that dates back to the 1950's [6].

Early on, the RERTR program identified Mg as a possible matrix material for U-Mo dispersion fuels [7]. A fuel plate with Mg matrix was successfully fabricated [8] and tested [9] as part of the RERTR-3 experiment, with a positive result (i.e., no FMI was observed) [10]. As a result, a fuel plate was tested at more aggressive conditions in the RERTR-8 experiment [11]. This paper will discuss the fabrication, testing, and microstructural characterization results for a U-7Mo/Mg fuel plate that was tested as part of the RERTR-8 experiment to relatively aggressive irradiation conditions. Particular focus will be given to the microstructural development within the fuel meat and any evidence of FMI that can be identified using optical metallography and observations will be compared to what has been observed in irradiated AFIP-1 fuel plates that had Al-Si alloy matrices with 2 or 4.5 wt.% Si.

2. Experimental

2.1 Fuel Plate Fabrication

Initially, 58% enriched U-7Mo powder was prepared from cast alloy rods via centrifugal atomization in an argon atmosphere glove box. The particle size distribution of the powder utilized is provided in the table below.

Table 1. U-7Mo particle size distribution.

Size					
Mesh		μm		Mass (g)	%
-100	+200	-150	+75	30.773	81.2%
-200	+230	-75	+63	2.658	7.0%
-230	+325	-63	+45	2.992	7.9%
-325		-45		1.480	3.9%
				37.903	100%

U-7Mo/Mg compacts were prepared at 6 gU/cm^3 uranium density via uniaxial pressing in an argon atmosphere glove box. 133.4 KN of pressing force was used to obtain ~98% dense compacts. The Mg powder used was 99.8% purity, -325 mesh, Alfa Aesar Stock #10233. The nominal compact size was 0.4 cm thick x 1.5 cm wide x 1.8 cm long. A 36.8 vol% U-7Mo powder blend mix was used to establish the target 6 gU/cm^3 fuel loading in the 1.0 cm^3 compacts prepared.

The preparation of the rolling assembly involved placing a U-7Mo/Mg compact into a machined cavity in the face of a 0.6 cm-thick AA6061 plate. The base plate/compact was then covered with a 2.3 cm-thick AA6061 cover plate (see Fig 1). Friction Stir Welding (FSW) was used to bond the cover plate to the base plate. Prior to compact loading and assembly welding, the aluminum plates were chemically cleaned using the following steps: 12M NaOH bath, demineralized water rinse, ~30% nitric acid etch/desmutt, second demineralized water rinse, and a final rinse using ethanol.

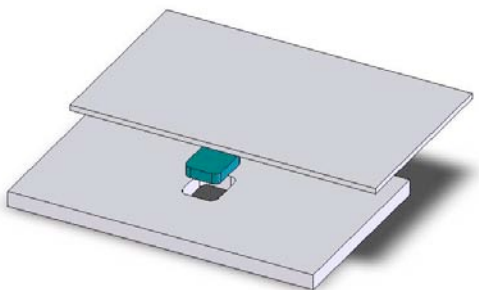


Figure 1. Mg-matrix dispersion fuel pellet laminate construction.

Hot rolling was conducted using a two-high Fenn rolling mill. The rolling assembly was preheated at 420°C for seven minutes prior to the first pass. Four five-minute reheats were performed between passes thereafter. A total of eleven passes were used to establish a final plate thickness of 0.14 cm; ~15% thickness reduction per pass. The nominal dimensions of the fuel zone region were 8.1 x 1.9 x 0.06 (cm).

Shearing was used to obtain 2.5 cm x 10.2 cm miniplates. The final thickness UT image of the R9R010 plate indicated less than a desired 50% signal transmission. Subsequently, the plate was hot pressed for 20 minutes at 420°C and 6000 psi, resulting in an improved UT signal. An optical image of the as-fabricated R9R010 fuel plate microstructure is presented in Fig. 2, which reveals some interaction between the Mg and the AA6061 cladding and pull-out of some U-7Mo particles. No evidence of interaction between the U-7Mo particles and the Mg matrix can be ascertained.

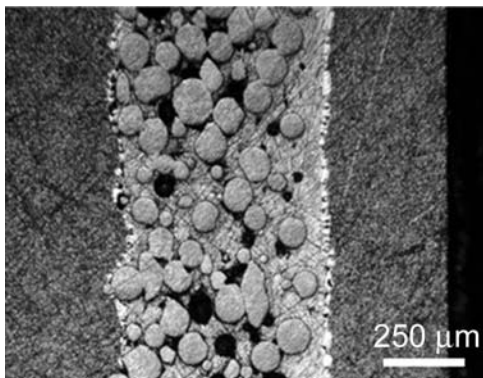


Figure 2. An optical image of a cross section of as-fabricated U-7Mo/Mg matrix miniplate. Some U-7Mo particle are pulled out during sample polishing. A narrow interaction layer exists between the fuel meat and the cladding.

2.2 Irradiation Testing

The RERTR-8 experiment was conducted to test 6 gU/cm³ U-Mo dispersion fuels using enriched uranium (58.2% U-235) to control the power density of the fuel. The average burnups were between 50 and 90% LEU equivalent at the end of irradiation. The fuel plates were positioned edge-on to the core, and as a result had a neutron flux gradient across the widths of the fuel plates. The R9R010 fuel plate came out of the reactor in March of 2006 after 90 effective full power days of irradiation. The irradiation conditions at low and high flux locations of the fuel plate are enumerated in Table 2. For comparison, the irradiation conditions are listed

for two plates tested in the AFIP-1 experiment, one with Al-2Si matrix and the other with AA4043 matrix (≈ 4.5 wt% Si).

Table 2. Irradiation conditions at low and high neutron flux locations for fuel plate R9R010 (U-7Mo/Mg), which was tested in the RERTR-8 experiment, and AFIP-1 fuel plates 1T2 with Al- 2 wt% Si matrix and 1B5 with AA4043 matrix (≈ 4.5 wt.% Si).

Sample		Heat flux, W/cm ²		Temperature, °C		Burnup, fissions (f) /cm ³	Average fission rate density, fissions/cm ³ -s
		BOL	EOL	BOL	EOL		
R9R010	High flux	405.5	359.4	145.2	171.3	5.5×10^{21}	11.0×10^{14}
	Low flux	273.9	246.3	118.8	126.5	3.7×10^{21}	7.4×10^{14}
1T2 (Al-2Si)	High flux	270.0	121.6	137.5	106.8	5.1×10^{21}	3.7×10^{14}
	Low flux	189.9	115.5	108.9	98.6	4.0×10^{21}	2.9×10^{14}
1B5 (AA4043)*	High flux	272.8	116.0	148.8	101.5	5.0×10^{21}	3.6×10^{14}
	Low flux	209.6	136.6	112.3	101.9	4.4×10^{21}	3.2×10^{14}

* AA4043 composition: 4.53Si-0.14Fe-0.09Cu-0.04Ti-0.01Zn-0.008Mg-bal Al.

2.3 Microstructural Characterization

For as-irradiated fuel plates, optical metallography (OM) is performed in a hot cell on a transverse cross section taken from the mid-plane. Both low and high magnification images are generated to identify any features of interest that may be present in the fuel plate microstructure. A more detailed description of the microstructural characterization of AFIP-1 fuel plates can be found in Ref. [4].

3. Results and Discussion

OM images of the microstructure observed at the transverse cross section taken at the midplane of fuel plate R9R010 are presented in Figure 6. Significant sample pull-out was observed in the fuel plate microstructure. At the interface, between the fuel meat and the cladding, the interaction zone that was present in the fuel plate after fabrication could be resolved. Negligible FMI was observed at the interface between the U-7Mo fuel particles and the Mg matrix, and this potentially resulted in the significant pullout of U-7Mo particles during sample polishing. The negligible FMI was observed even at the highest flux side of the fuel plate where the temperature approached 170°C, the fission density was around 5.5×10^{21} f/cm³, and the average fission rate density was around 11.0×10^{14} f/cm³ s. For comparison, OM images of the microstructure for the less-aggressively irradiated AFIP-1 fuel plates with Al-2Si and AA4043 (approx. 4.5 wt% Si) matrices are presented in Figures 7 and 8, respectively. For the high-flux side of the 1T2 (Al-2Si) fuel plate, where the peak temperature was around 137°C, the burnup was 5.1×10^{21} f/cm³, and the average fission rate density was 3.7×10^{14} f/cm³ s, complete consumption of the matrix was observed. For the high-flux side of the 1B5 (AA4043) fuel plate, where the the peak temperature was around 148.8°C, the burnup was 5.0×10^{21} f/cm³, and the average fission rate density was 3.6×10^{14} f/cm³ s, almost complete consumption of the matrix was observed. This indicates that even in the case where a U-7Mo/Mg fuel plate is irradiated under more aggressive conditions than are fuel plates with up to 4.5 wt% Si in an Al-

Si matrix, much less interaction can be expected. In fact, the amount of interaction for a U-7Mo/Mg fuel plate is negligible based on OM images.

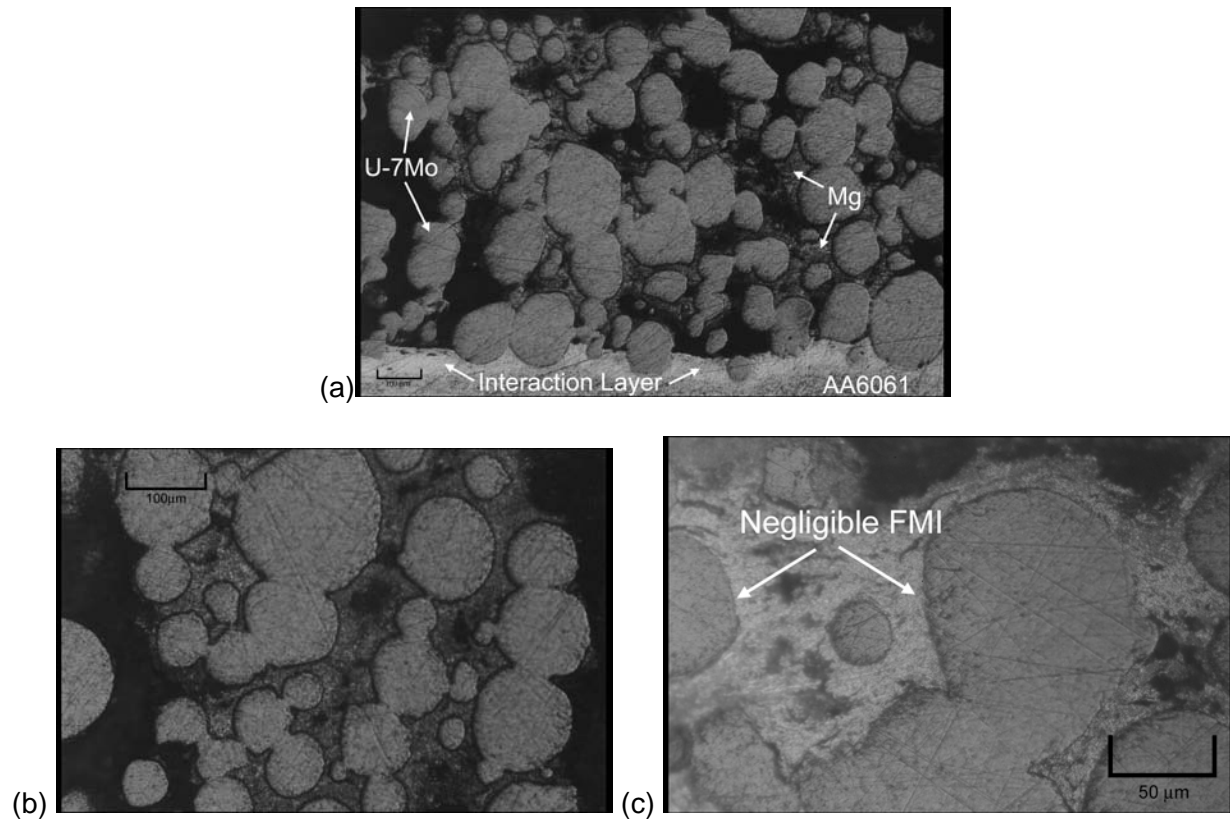


Fig. 6. A representative low-magnification optical micrograph (a) of the R9R010 fuel microstructure and representative higher magnification images (b,c) showing the negligible FMI that occurred at the U-7Mo/Mg interfaces during irradiation. The black areas are voids left behind due to sample pull-out during polishing. These images are representative of the microstructures observed at the low- and high-flux sides of the fuel plate.

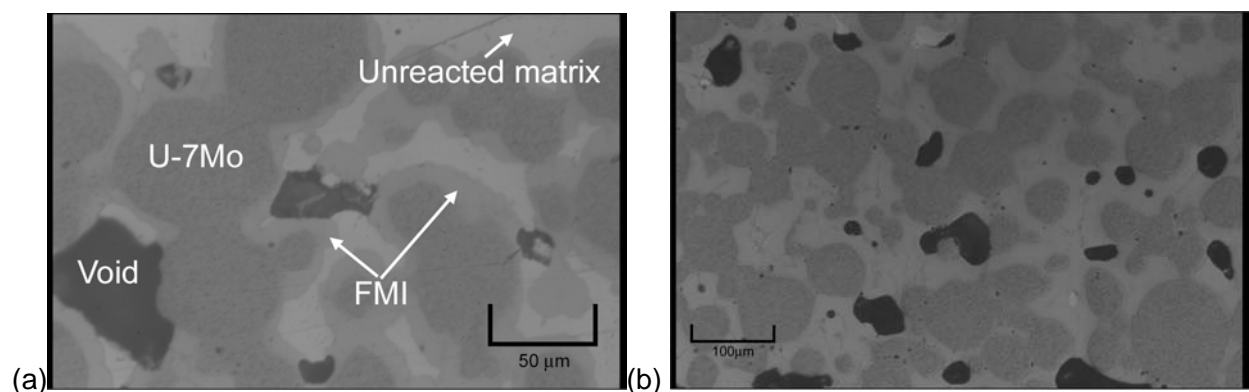


Fig. 7. Optical micrographs taken at a transverse cross section taken at the midplane for fuel plate 1T2 (U-7Mo/Al-2Si) from the AFIP-1 experiment at (a) the low-flux side and (b) the high-flux side. The black regions are porosity where similar porosity was observed in the as-fabricated fuel.

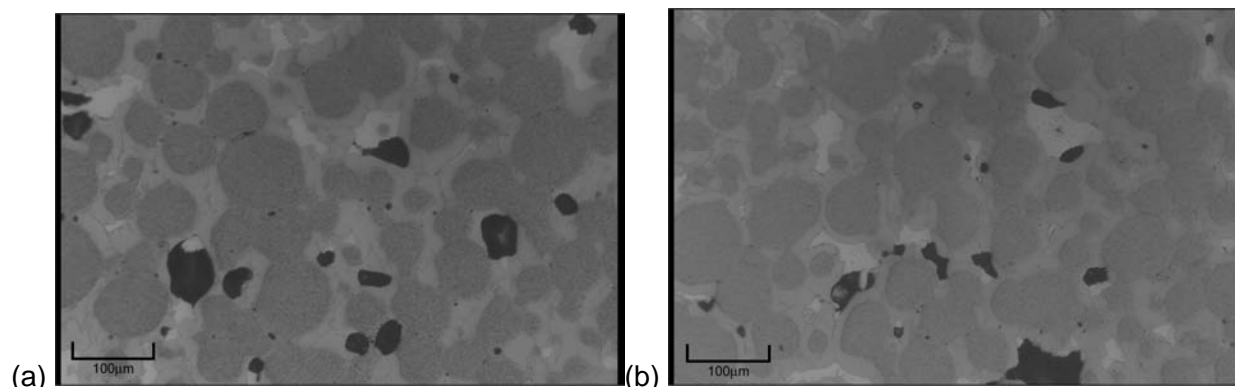


Fig. 8. Optical micrographs taken at a transverse cross section taken at the midplane for fuel plate 1B5 (U-7Mo/AA4043) from the AFIP-1 experiment at (a) the low-flux side and (b) the high-flux side. The black regions are porosity, where similar porosity was observed in the as-fabricated fuel. The dark phase is U-7Mo alloy, the medium contrast phase is interaction layer, and the brightest phase is unreacted AA4043 matrix.

4. Conclusions

Based on the microstructural characterization of U-7Mo dispersion fuel plates with Al-2Si, AA4043, or pure Mg as the matrix that were irradiated at relatively aggressive irradiation conditions in the AFIP-1 or RERTR-8 experiments, the interaction of fuel and matrix, which can limit the irradiation performance of a fuel plate, can potentially be eliminated by employing pure Mg as the matrix in the fuel zone.

Acknowledgments

This work was supported by the U.S. Department of Energy, Office of Nuclear Materials Threat Reduction (NA-212), National Nuclear Security Administration, under DOE-NE Idaho Operations Office Contract DE-AC07-05ID14517. Personnel in the Hot Fuel Examination Facility are recognized for their contributions in destructively examining fuel plates. Yeon Soo Kim is acknowledged for his assistance in collecting references for this paper.

References

- [1]. D. Wachs et al., Proc. of *GLOBAL 2007*, Boise, ID, September 9-13, 2007.
- [2]. A. Leenaers et al., *J. Nucl. Mater.* 335 (2004) 39-47.
- [3]. Y. S. Kim et al., Proc. of the RERTR-2005 International Meeting, Boston, MA, 2005.
- [4]. D. D. Keiser, Jr. et al., Proc. of the RERTR-2010 International Meeting, Lisbon, Portugal, 2010.
- [5]. T. B. Massalski, Ed, *Binary Alloy Phase Diagrams*, Vol. II, ASM International, Materials Park, OH (1990).
- [6]. International Atomic Energy Agency, "Viability of Inert Matrix Fuel in Reducing Plutonium Amounts in Reactors", IAEA-TECDOC-1516, August, 2006.
- [7]. J. L. Snelgrove, et al., Proc. of the RERTR-1996 International Meeting, Seoul, Republic of Korea, 1996.
- [8]. T. C. Wiencek, et al., Proc. of the RERTR-1998 International Meeting, Sao Paulo, Brazil, 1998.
- [9]. S. L. Hayes, et al., Proc. of the RERTR-1999 International Meeting, Budapest, Hungary, 1999.
- [10]. M. K. Meyer, et al., Proc. of the RRFM-2006 International Meeting, Sofia, Bulgaria, 2006.
- [11]. G. L. Hofman, et al., Proc. of the RRFM-2008 International Meeting, Hamburg, Germany, 2008.

Recrystallization and Swelling of U-Mo Fuel during Irradiation

YEON SOO KIM, G.L. HOFMAN
*Nuclear Engineering, Argonne National Laboratory
9700 South Cass Ave, Argonne, IL 60439 USA*

JIN SIK CHEON
*Korea Atomic Energy Research Institute
989-111 Daedeok-daero, Yuseong, Daejeon, 305-353, Republic of Korea*

ABSTRACT

A semi-theoretical model for U-Mo swelling by fission gas bubble growth was developed considering the fuel recrystallization kinetics observed in the U-Mo samples irradiated in the RERTR-1, -2, -3, -4, and -5 tests. The recrystallization kinetics was expressed by the Avrami equation that contains terms of fission density (or burnup), fission rate, Mo content, and extent of cold-work during sample fabrication. The end-of-life fission gas bubble swelling was calculated by integration of the swelling rate with respect to fission density. Then, the total fuel swelling was calculated adding the solid fission product swelling to the gas bubble swelling. The predicted total swelling was consistent with the measured data.

1. Introduction

U-Mo fuel swelling is composed of two parts: One that is induced by solid fission products including liquid fission products, and the other by fission gas bubbles. The solid fission products induced swelling is proportional to burnup (or fission density). The fission gas bubble swelling, however, is dependent upon factors including Mo content, fission rate, fabrication process, as well as fission density. The effect of temperature is negligible at the typical temperature ranges where research and test reactors are operated ($< 250\text{ }^{\circ}\text{C}$) [1].

The effect of the above mentioned factors is manifested by so called “recrystallization,” by which the as-fabricated fuel undergoes grain-refinement that effectively increases grain boundaries. Inter-granular fission gas bubble swelling, i.e., fission gas bubble formation and growth at the grain boundaries, is much larger than the intragranular fission gas bubble swelling. Hence, fission gas bubble swelling is enhanced by recrystallization in fuel with an increased grain boundary density. The fission gas bubble swelling rate can be expressed by quantifying and formulating the recrystallization kinetics of U-Mo fuel [2]. The recrystallization process at hand is similar to typical transformation reactions such as a new phase formation and, therefore, may be described by a phenomenological equation such as the Avrami equation [3]. The overall fission gas bubble swelling can be predicted by integration of the swelling rate, determined by the recrystallized volume fraction, with respect to fission density.

In this paper, measured data for recrystallized volume fraction of U-Mo fuel irradiated in the RERTR-1 through -5 tests are presented. The expressions developed for the kinetics of fuel recrystallization to predict fission gas bubble swelling are also provided. A method to predict the fuel overall swelling is also presented.

* Work supported by US Department of Energy, Office of Global Threat Reduction, National Nuclear Security Administration (NNSA), under Contract DE-AC-02-06CH11357. The submitted manuscript has been authored by a contractor of the U. S. Government under contract NO.DE-AC-02-06CH11357. Accordingly, the U. S. government retains a nonexclusive royalty-free license to publish or reproduce the published form of this contribution, or allow others to do so, for U.S. Government purposes.

2. Irradiation test data

Recrystallized volume fractions of fuel tested in RERTR-1, -2, -3, -4, and -5 were measured on the SEM images of fracture surfaces. Evolution of recrystallization in atomized U-Mo fuel is observable as a function of fission density as shown in series of images in Fig. 1.

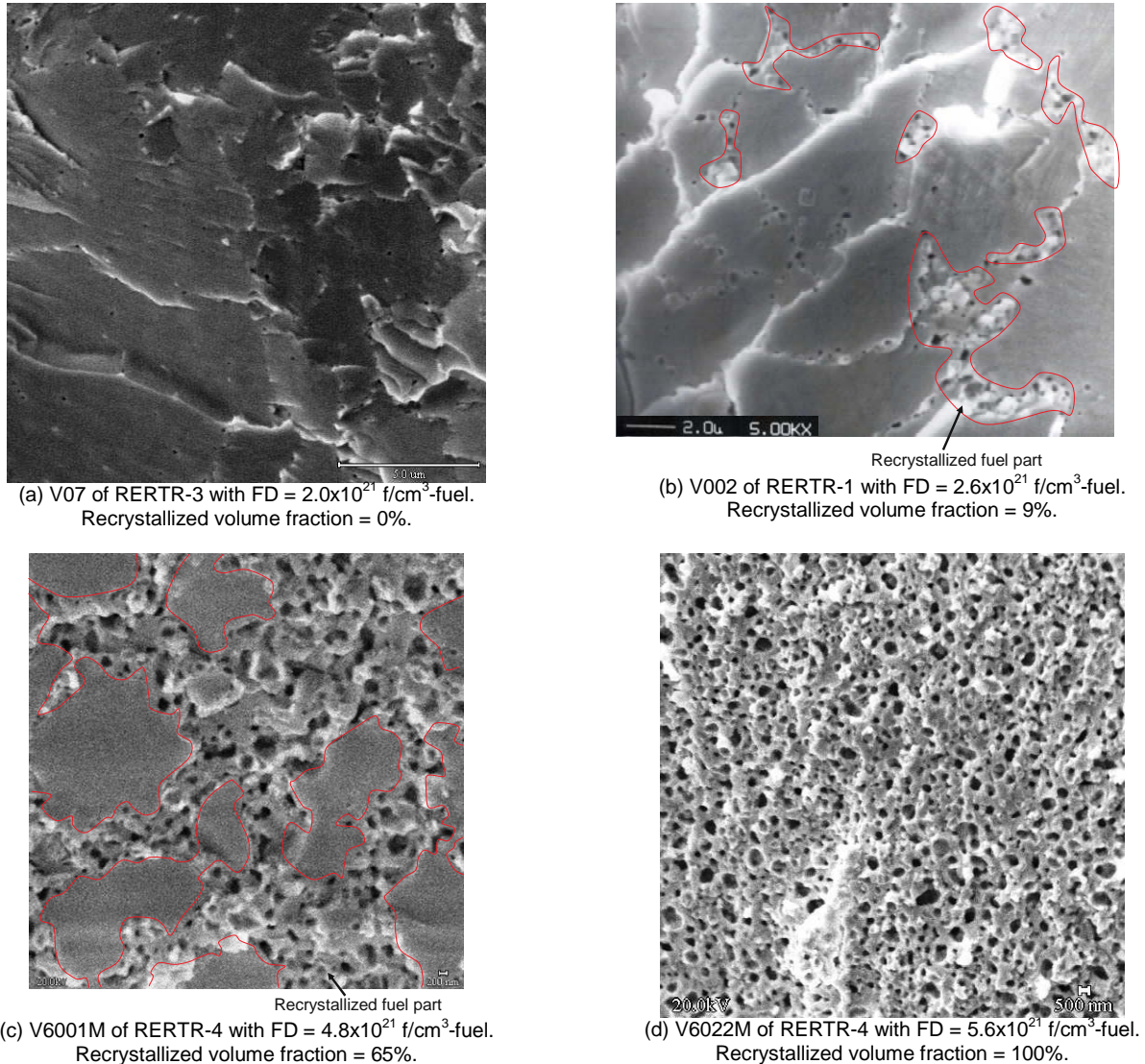


Fig. 1 SEM images of U-10Mo showing evolution of recrystallization with fission density.

Recrystallization enhances fission gas bubble swelling by the following mechanism:

- Pre-recrystallization stage (Fig. 1(a)): For the atomized U-10Mo, recrystallization does not appear until the fission density of $2.0 \times 10^{21} \text{ f/cm}^3\text{-fuel}$. The fission gas swelling rate in this stage is lowest.
- Recrystallization stage (Fig. 1(b) and Fig. 1(c)): When the density of fission-induced interstitial loops increase, grains undergo recrystallization. Recrystallization starts to take place at the grain triple points and later propagates along the preexisting grain boundaries [4]. As a result, the original grain subdivides, producing more grain boundaries. Fission gas

bubbles form in the grain boundaries with a much higher rate than the grain interior [1,5], so the fission gas bubble swelling rate increases.

- Post-recrystallization stage (Fig. 1(d)): At a fission density of 5.6×10^{21} f/cm³-fuel, atomized U-10Mo shows full recrystallization. The fission gas swelling rate in this stage is the highest.

The measured recrystallized fuel volume fractions for atomized and ground U-10Mo are shown in Fig. 2.

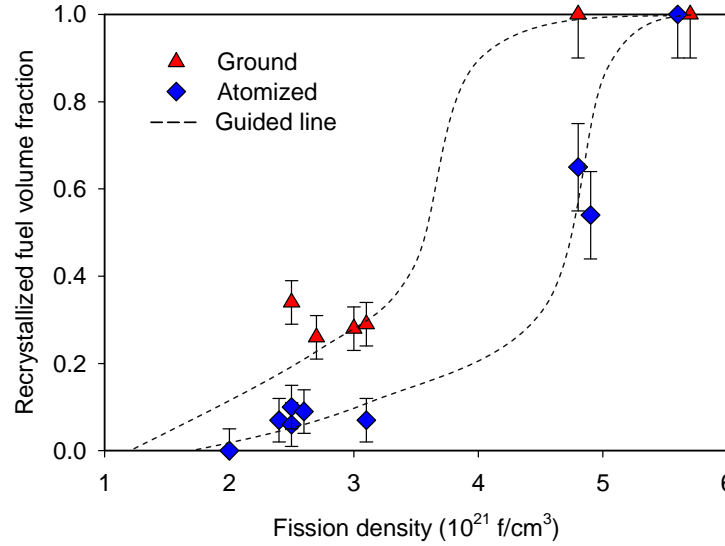


Fig. 2 Recrystallized fuel volume fraction for U-10Mo.

Measured fission gas bubble swelling data from the RERTR-3, -4, and -5 are shown in Fig.3. Data only for atomized U-10Mo samples are included for consistency. A detailed description of the measurement method of fission gas bubble swelling is given elsewhere [5].

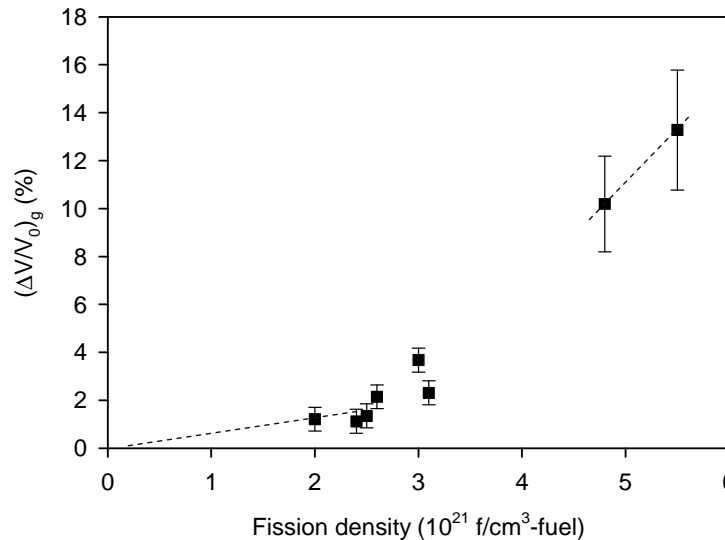


Fig. 3 Fission gas bubble swelling data for atomized U-10Mo. The fission gas bubble swelling with two distinctively different rates at pre-recrystallized and post-recrystallized regimes are marked with guided lines.

Overall fuel swelling was obtained by measuring the before and after U-Mo foil thicknesses of monolithic-foil-fuel plates to validate the recrystallization model. The reason to focus on monolithic fuel samples was because the data acquisition process for this type sample is

simpler than the dispersion sample. A more detailed description of the measurement method is given elsewhere [1].

The fuel swelling by the solid (plus liquid) fission products was given by a function of fission density [1] as follows:

$$\left(\frac{\Delta V}{V_0}\right)_s = 4.0 f_d, \quad (1)$$

where f_d is the fission density in 10^{21} f/cm³-fuel.

Fuel swelling by fission gas bubbles can be assessed by subtracting the solid fission product swelling from the total swelling according to Eq. (2). The result is summarized in Table 2.

$$\left(\frac{\Delta V}{V_0}\right)_f = \left(\frac{\Delta V}{V_0}\right)_s + \left(\frac{\Delta V}{V_0}\right)_g \quad (2)$$

where $\left(\frac{\Delta V}{V_0}\right)_f$, $\left(\frac{\Delta V}{V_0}\right)_s$ and $\left(\frac{\Delta V}{V_0}\right)_g$ are the total fuel swelling, fuel swelling by solid fission products and fuel swelling by fission gas bubbles, respectively.

Table 1 Fuel swelling measurement data

Test	Plate ID	Foil thickness before irradiation (mm)	Fission density (10^{27} f/m ³)	Measured $(\Delta V/V_0)_f$ (%)	Estimated $(\Delta V/V_0)_s$ by Eq.(1) (%)	Estimated $(\Delta V/V_0)_g$ by Eq. (2) (%)
RERTR-6	L1F040	0.25 ^a	3.0	13	12.0	1.0
RERTR-6	L1F100	0.25	3.0	17	12.0	5.0
RERTR-6	L2F030	0.5	2.6	12	10.4	1.6
RERTR-7	L1F140	0.25	4.4	25	17.6	7.4
RERTR-7	L1F120	0.25	4.8	28	19.2	8.8
RERTR-7	L2F040	0.5	2.7	13	10.8	2.2
RERTR-9	L1F34T	0.25	7.0	42	28.0	14.0
RERTR-9	L1P05A	0.25	6.3	30	25.2	4.8
RERTR-9	L1P04A	0.25	5.1	25	20.4	4.6
RERTR-9	L1F26C	0.25	6.0	34	24.0	10.0
RERTR-9	L1F32C	0.25	5.8	32	23.2	8.8
RERTR-9	L1P09T	0.25	6.8	43	27.2	15.8

^a The uncertainty in foil thickness is 0.005 mm.

3. Kinetics of Fuel Recrystallization

In order to express the recrystallization mechanism, the Avrami equation [3] is applied as follows:

$$V_{rx} = 1 - \exp[-K(F - F_0)^n] \quad (3)$$

where V_{rx} is the recrystallized fuel volume fraction, K is the recrystallization reaction constant, F is the fission density, F_0 is the fission density below which recrystallization does not occur, and n is the Avrami exponent dependent on the nucleation and growth mechanism.

Data fitting of the constants is explained below.

3.1 Constant K

The reaction constant K in the present case is governed by two factors: fission rate and Mo content. The fission rate factor is obtained by using U-10Mo samples with similar fission densities but with different fission rates. The Mo content factor is obtained by a linear interpolation between U-10Mo and U-7Mo data. K is then fixed by multiplication of the two factors.

$$K = K_0 [0.125(\dot{f} - 2.5) + 1][0.67(10 - x_{Mo}) + 1] \quad (4)$$

where K_0 is a fitting constant, \dot{f} is the fission rate in 10^{14} f/cm³-fuel-s, and x_{Mo} is the Mo content in wt.%.

3.2 Constant F_0

The incubation fission density F_0 is dependent on fuel type. The ground powder samples show shorter incubation periods than the atomized powder samples. The ground powder samples have higher dislocation densities and grain boundaries due to larger cold work. The extent of cold work is directly correlated with the hardness: the more cold work, the higher hardness. Hardnesses of atomized powder and foil U-Mo are similar and lower than ground powder. Therefore, it can be deduced that the ground powder has higher cold work than the atomized powder and foil while these two have similar cold work.

The measured data for recrystallized fuel volume fraction indeed show a result consistent with this reasoning (Fig. 2). Consequently, fission gas bubble swelling for atomized powder and foil fuels are tentatively considered the same until sufficient measurement data are available to compare.

Taking logarithm twice and rearranging Eq. (3) gives

$$\log(-\ln(1 - V_{rx})) = \log(K) + n\log(F - F_0) \quad (5)$$

Using the measured data in Fig. 2, $\log(-\ln(1 - V_{rx}))$ was plotted against $\log(F)$. Data fitting yields two straight lines: one for ground powder fuel and the other for atomized powder. The intercepts with the abscissa give F_0 . The values found this way are 1.38×10^{21} f/cm³-fuel and 1.67×10^{21} f/cm³-fuel for ground powder fuel and atomized powder fuel, respectively.

3.3 Exponent n

The similar method as in the previous section was used to find the exponent n . The measured data (V_{rx}) were plotted in terms of $\log(-\ln(1 - V_{rx}))$ against $\log(F - F_0)$. Data fitting gives a straight line as shown in Fig. 4. The slope of the line, which is equal to n , is 2.615 and the intercept with the ordinate is -0.987, which fixes K_0 given in Eq. (4) as 0.1.

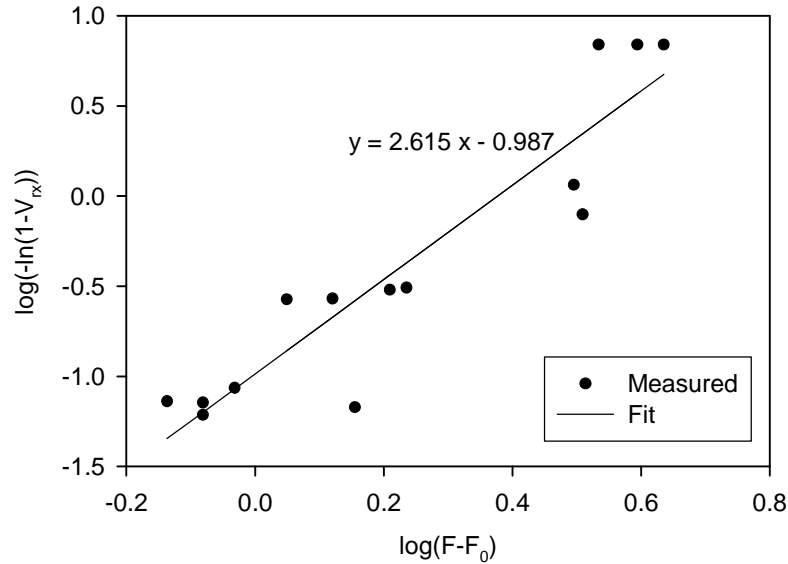


Fig. 4 Kinetics of recrystallization of U-10Mo during irradiation.
 $y = \log(-\ln(1-V_{rx}))$ and $x = \log(F-F_0)$.

3.4 Comparison of measured and predicted V_{rx}

The validity of the prediction model for recrystallized fuel volume fraction was examined by comparing with the measured data in Fig. 5. In general, the prediction was fair with the measured.

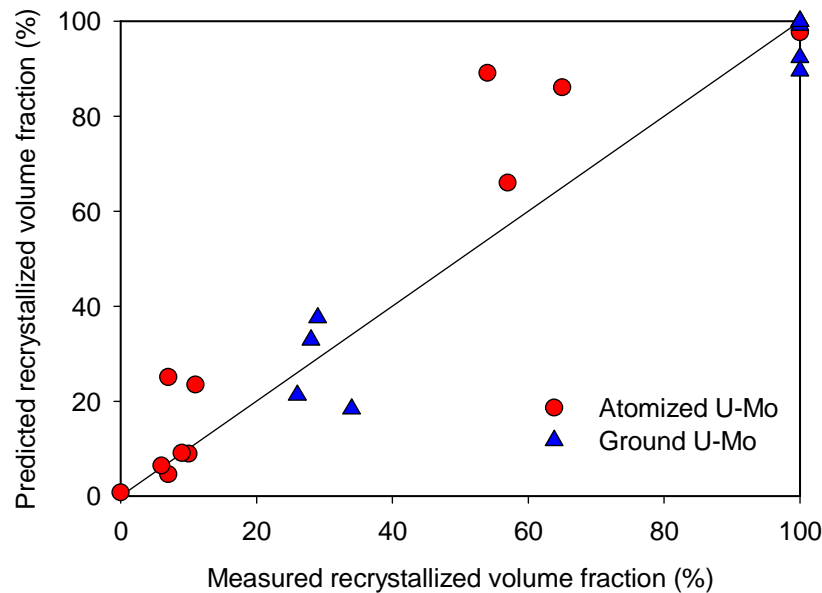


Fig.5 Comparison of the predicted and measured data of recrystallized volume fraction.

Although the comparison shows an overall trend of consistency, there are some data points inconsistent with prediction. The source of measurement errors is due to the uncertain boundaries between the recrystallized and unrecrystallized region. The possible sources of prediction errors lie in the use of life-averaged fission rates, inhomogeneous distribution of defects during fabrication, and differences in as-fabricated grain size.

4. Fission gas bubble swelling

4.1 Fission gas bubble swelling rates

4.1.1 Pre-recrystallization stage

Fission gas bubble swelling is due to bubble nucleation and growth in the grain boundaries. Fission gas bubbles increase in number and size with increasing fission density. The sample shown in Fig. 1 (a) is an example to illustrate fission gas bubble swelling in this stage. The fission gas bubble swelling rate in this stage is a linear function of fission density. From the data shown in Fig. 2, the fuel swelling rate by fission gas bubbles for this stage can be found using the data with fission density of up to $\sim 2 \times 10^{21}$ f/cm³-fuel. Hence, the fuel swelling rate by fission gas bubbles is data-fitted as

$$\left(\frac{\dot{\Delta V}}{V_0} \right)_{g,0} = 0.6\% \text{ per } 1 \times 10^{21} \text{ f/cm}^3\text{-fuel} \quad (6)$$

4.1.2 Post-recrystallization stage

In this stage, fuel is fully recrystallized. This stage begins at a fission density higher than $\sim 5 \times 10^{21}$ f/cm³-fuel but lower than 5.5×10^{21} f/cm³-fuel (see Fig. 3). The swelling rate by fission gas bubbles for this stage is high due to increased grain boundaries. The fuel swelling rate can be assessed using the fission gas bubble swelling data at measured in this stage. By data fitting of the fuel swelling rate by fission gas bubbles, the following rate is obtained:

$$\left(\frac{\dot{\Delta V}}{V_0} \right)_{g,rx} = 4.4\% \text{ per } 1 \times 10^{21} \text{ f/cm}^3\text{-fuel} \quad (7)$$

4.1.3 Recrystallization stage

In this stage, fuel is partially recrystallized. Hence, the swelling rate by fission gas bubbles is composed of the lower rate in the pre-recrystallized fuel part and the higher rate in the recrystallized fuel part as follows:

$$\left(\frac{\dot{\Delta V}}{V_0} \right)_{g,m} = (1 - V_{rx}) \left(\frac{\dot{\Delta V}}{V_0} \right)_{g,0} + V_{rx} \left(\frac{\dot{\Delta V}}{V_0} \right)_{g,rx} \quad (8)$$

where V_{rx} is given in Eq. (3), $\left(\frac{\dot{\Delta V}}{V_0} \right)_{g,0}$ and $\left(\frac{\dot{\Delta V}}{V_0} \right)_{g,rx}$ are given in Eqs. (6) and (7), respectively.

Rearranging Eq. (8) gives:

$$\left(\frac{\dot{\Delta V}}{V_0} \right)_{g,m} = \left(\frac{\dot{\Delta V}}{V_0} \right)_{g,0} + \left[\left(\frac{\dot{\Delta V}}{V_0} \right)_{g,rx} - \left(\frac{\dot{\Delta V}}{V_0} \right)_{g,0} \right] V_{rx} \quad (9)$$

4.2 Accumulated gas bubble swelling

The accumulated swelling by fission gas bubbles can be obtained by integration of Eq. (8) with respect to fission density as

$$\left(\frac{\Delta V}{V_0}\right)_g = \int_0^F \left\{ \left(\frac{\dot{\Delta V}}{V_0}\right)_{g,0} + \left[\left(\frac{\dot{\Delta V}}{V_0}\right)_{g,rx} - \left(\frac{\dot{\Delta V}}{V_0}\right)_{g,0} \right] V_{rx} \right\} dF \quad (10)$$

Or

$$\left(\frac{\Delta V}{V_0}\right)_g = \left(\frac{\dot{\Delta V}}{V_0}\right)_{g,0} F + \left[\left(\frac{\dot{\Delta V}}{V_0}\right)_{g,rx} - \left(\frac{\dot{\Delta V}}{V_0}\right)_{g,0} \right] \int_0^F V_{rx} dF \quad (11)$$

Integration of Avrami equation in Eq. (11) is performed by inserting V_{rx} given in Eq. (3) and by changing the lower integration end to the incubation fission density for recrystallization, F_0 , as follows:

$$\int_0^F V_{rx} dt = F - F_0 + \frac{\Gamma(1/n, K(F - F_0)^n) - \Gamma(1/n, 0)}{nK^{1/n}} \quad (12)$$

The evaluation of the upper incomplete gamma functions can be performed using commercially available computer software. Prediction of the total fuel swelling given in Eq. (2) can be made once the accumulated swelling by fission gas bubbles is found from Eq (11). Comparison of the prediction result with the measured data for foil fuel samples given in Table 1 confirms the validity of the modeling (Fig. 6).

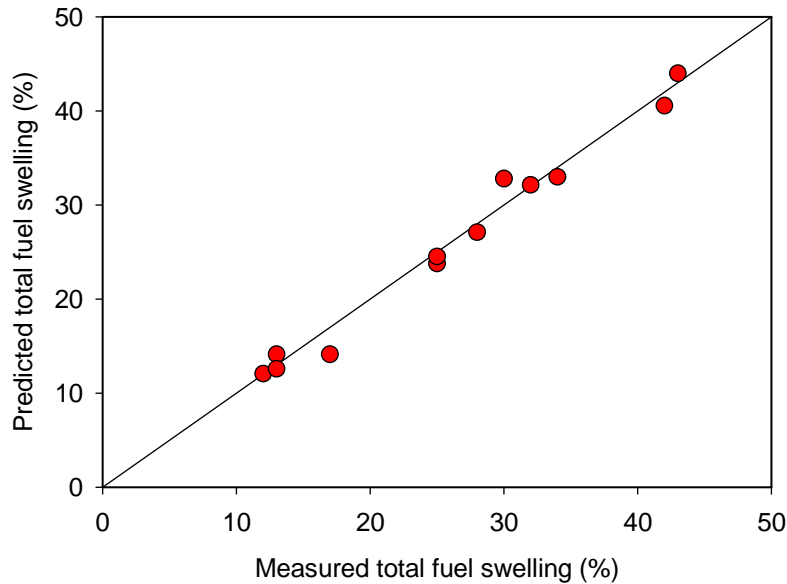


Fig. 6 Comparison between predicted and measured fuel swelling of U-Mo

5. Conclusion

Fission gas bubble swelling of U-Mo is closely related to fuel recrystallization (or grain refinement). The fission-induced recrystallization of fuel enhances gas bubble swelling rate after an initial incubation period. In order to find swelling kinetics, recrystallization kinetics must be known. Recrystallized fuel volume fractions were measured using samples from RERTR-1, -2, -3, -4, and -5 irradiation tests that have various Mo content, fission rate, and fission density and fabrication method. The effect of fission density, fission rate, Mo content, and extent of cold-work was parametrically examined and fitted to the Avrami equation. The Avrami equation, recrystallization kinetics correlation, was employed to express the fission gas bubble swelling rate. The post-irradiation fission gas bubble swelling is predicted by integration of the swelling rate with respect to fission density. Comparison between the model predictions and measured data showed consistent results.

Acknowledgments

The authors thank Mr. Adam Robinson at Idaho National laboratory for the use of plate thickness data used to obtain fuel swelling data given in Table 1. This work was supported by the U.S. Department of Energy, Office of Global Threat Reduction (NA-21), National Nuclear Security Administration, under Contract No. DE-AC-02-06CH11357 between UChicago Argonne, LLC and the Department of Energy.

References

- [1] Y.S. Kim, G.L. Hofman, J. Nucl. Mater., 419 (2011) 291.
- [2] J. Rest, J. Nucl. Mater., 349 (2006) 150.
- [3] M. Avrami, J. Chem. Phys., 7 (1939) 1103.
- [4] J. Rest, G.L. Hofman, Proc. Mat. Res. Soc. Mtg., Boston, MA, 2000.
- [5] Y.S. Kim, G.L. Hofman, J. Rest, G.V. Shevlyakov, ANL-08/11, Argonne National Laboratory, 2008. Available from: <http://www.osti.gov/bridge/>
- [6] C.R. Clark, Unpublished data, Argonne National Laboratory, 2002.
- [7] D.E. Burkes, R. Prabhakaran, T. Hartmann, J. Jue, F.J. Rice, Nucl. Eng. Design, 240 (2010) 1332.

RRFM 2012 – 16th INTERNATIONAL TOPICAL MEETING ON RESEARCH REACTOR FUEL MANAGEMENT

March 18-22, 2012
Prague, Czech Republic

AREVA INVOLVEMENT IN UMO FUEL MANUFACTURING AND RESEARCH TEST REACTOR FUEL TREATMENT

B. STEPNIK, M. GRASSE
AREVA-CERCA

Les Berauds, B.P. 1114, F-26104 Romans Cedex – France

D. GESLIN, C. JAROUSSE
AREVA-CERCA

10, rue Juliette Récamier, F-69456 Lyon Cedex 06 – France

A. TRIBOUT-MAURIZI, F. LEFORT-MARY
AREVA NC

Tour AREVA - 1, Place Jean Millier, F-92084 Paris, La Défense – France

D. ODE, A. JUVENELLE, N. REYNIER-TRONCHE
CEA Marcoule

BP 17 171, 30 207 Bagnols sur Cèze – France

ABSTRACT

AREVA has been involved in UMo fuel developments since 1999 in the framework of the GTRI program carried out under the auspices of US DOE. Initially, AREVA focused on the development of a suitable UMo solution for the needs of the reactor. Now, AREVA is starting to consider the future manufacturing production phase, which will make it possible to anticipate the reliable and economic delivery of UMo fuel assemblies.

The road is long and there's still some way to go in order to achieve the goal which relies on the qualification and use of UMo fuel. Thanks to the cooperative effort made by AREVA with its partners such as CEA and European reactors, the program to bridge the gap from R&D level to full manufacturing production has been taken into consideration at each step, ensuring a better understanding of the challenge to upscale the production.

In the first part of this paper, the AREVA-CERCA involvement in fuel manufacturing for research reactors will be presented. After a historical account of the manufacturing results obtained through the plate production used for the IRIS and LEONIDAS irradiation programs, a pre-industrial production program is presented and discussed.

The second part of this paper will present AREVA NC's involvement in fuel treatment for research reactors. AREVA-La Hague has wide experience in power reactor spent fuel treatment and is continuing to look at the feasibility of recycling RTR (Research Test Reactor) spent fuels. The paper will describe the current experience of AREVA La Hague in UAl spent fuel treatment and its intention to make the treatment of the various types of fuels such as U₃Si₂ fuel or UMo fuel feasible on an industrial scale.

1. Introduction

AREVA is a worldwide nuclear power-generating company which addresses the whole nuclear cycle for the nuclear power plants. Heavily involved in the Research Test Reactor (RTR) field, dedicated AREVA subsidiaries are partners of their customers throughout the fuel cycle: RTR design and construction, fuel manufacturing, transportation, spent fuel treatment.

Since 1999, AREVA has been engaged in a complete UMo program called FUMOG, for French UMo Group [1], [2]. The program has managed the common efforts of CEA and AREVA group, in the framework of the GTRI conversion program intended to qualify the use of UMo dispersed fuel, including its treatment. Since then, AREVA has been continuously endeavouring, together with associated partners, to challenge the unexpected adverse behaviour observed during UMo irradiation campaigns. These efforts are consistent with the international UMo fuel development work. The addition of Silicon (Si) to the UMo fuel is the promising improvement currently being tested.

Since 2005, AREVA's La Hague plant has been building up a wide experience in RTR UAl fuel back-end treatment. UAl fuels are in the process of treatment. In the case of Si-rich RTR fuel, U_3Si_2 or UMo+Si, the technological feasibility of the back-end treatment is not yet proven. Common CEA and AREVA NC R&D programs are in progress to study the La Hague capability to treat Si-rich fuels.

This paper provides technical and industrial information on UMo fuel manufacturing and Si-rich RTR fuel back-end treatment.

2. AREVA UMo fuel manufacturing

AREVA-CERCA is a research reactor fuel manufacturer which, over the last 50 years, has produced more than 70 fuel and target designs, from simple to complex designs made of UAl_x, U_3Si_2 , UZrH_x, UMo, etc

2.1. UMo fuel manufacturing approach

Projects are underway to take into consideration the customer's needs as well as state of the art international technology and industrial feasibility.

Over the years, strong partnerships have been built with the RTRs, mainly but not exclusively with the European ones. These partnerships have led to common projects and collaboration agreements. This allows good understanding of the RTR and fuel manufacturer constraints. The customer benefits are highly optimized fuel and high reactivity, allowing compliance with the scheduler constraints.

Partnerships have also been created with research centres to track and test the new international technological developments in the fuel manufacturing field. The customer benefits are up-to-date high performance fuels.

The fuel prototypes are developed by a manufacturer which always keeps the future manufacturing production in mind. The prototypes are built and tested in full size geometry allowing the technical feasibility to be investigated. The prototypes are produced using the production equipment in industrial conditions. This provides a demonstration of industrial feasibility and direct feedback from the production staff providing continuous optimization along the project.

2.2. UMo fuel manufacturing experience

For 15 years, AREVA-CERCA has deployed the industrial approach outlined above. More than one hundred UMo fuel plate prototypes have been produced. The first worldwide UMo element was built. The UMo fuel plate prototypes were irradiated in 8 RTR experiments and others are in preparation (E-FUTURE II [3], SELENIUM [4]...). This means more than one irradiation experiment every two years. Figure 1 presents an overview of this UMo fuel development contribution.

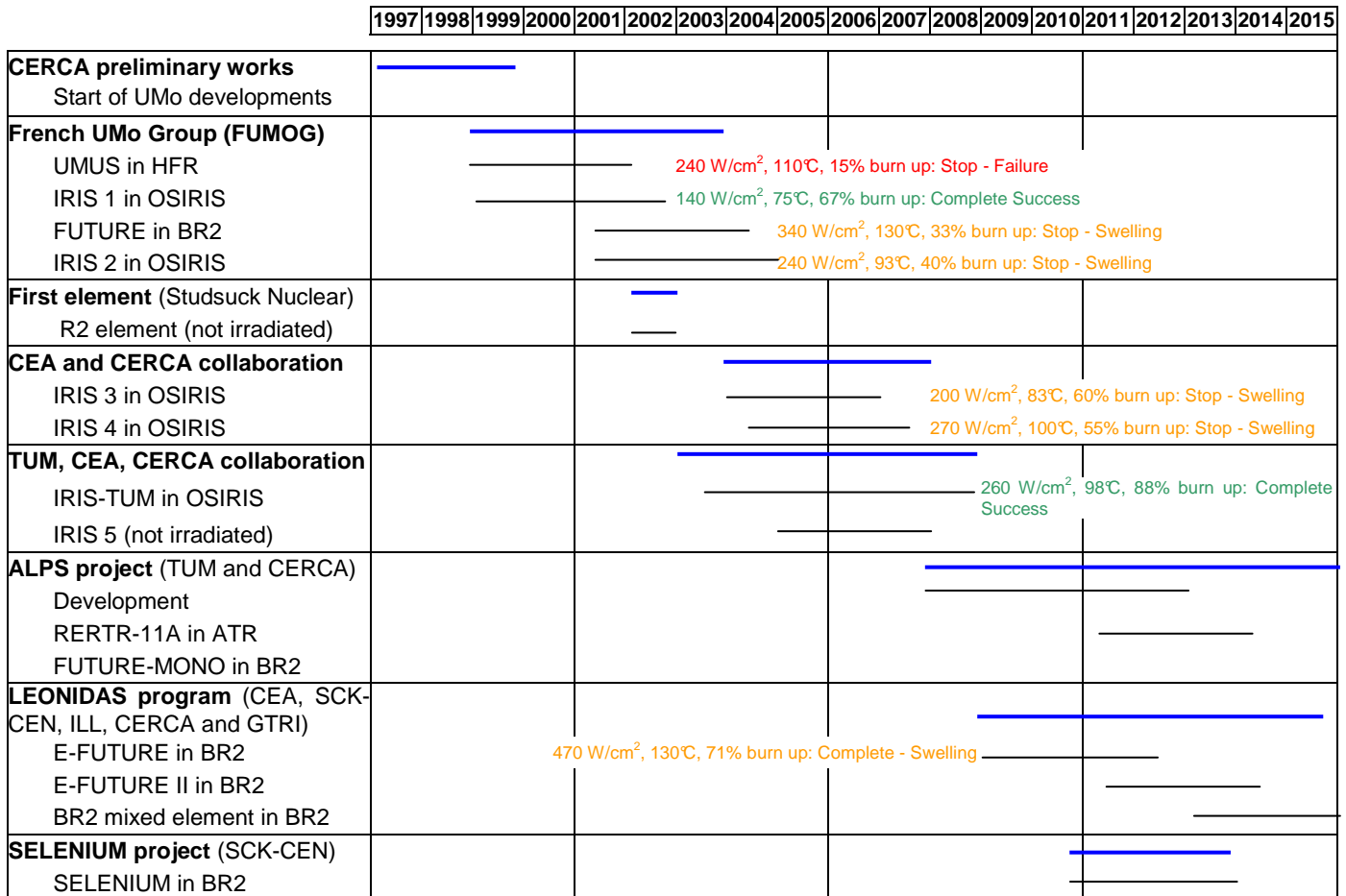


Fig 1. Schedule of the international UMo fuel development programs in which AREVA-CERCA has been involved (The duration takes into account the design, manufacturing, irradiation and PIE phases)

In 1997, UMo manufacturing was launched in AREVA-CERCA, on an internal budget. Preliminary tests were performed to evaluate UMo manufacturing with reference to standard specifications [5], [6], [7]. This demonstrated the technical feasibility of dispersion UMo fuel manufacturing as well as the leak of an industrial option to produce UMo particles.

During the 1999-2004 period, the UMo dispersed fuel studies were carried out by the French UMo Group (FUMOG) [1], [2]. It was evidenced that the production of ground UMo powder cannot be realized on an industrial scale. The mastering of UMo dispersion fuel plate manufacturing, using either ground UMo powder or KAERI atomized UMo powder up to 8 gU/cm^3 loading, embedded in a pure Aluminium (Al) matrix, was demonstrated. These were the UMUS, IRIS 1, FUTURE, IRIS 2 experiments [8]. Moreover, in 2002, the first UMo assembly in the world was manufactured for the R2 reactor [9]. The production of curved fuel plate was demonstrated for UMo powder embedded in pure Al matrix up to 8 gU/cm^3 .

However, this fuel exhibits unexpected adverse behaviour under irradiation tests [10]. The tentative solution for reducing this effect, applied worldwide, is Si incorporation into dispersed fuels. All the

irradiation tests have shown that Si incorporation delays the unexpected adverse behaviour observed during UMo irradiation campaigns [11], [12]. However, it is not yet enough for high performance research reactor conditions (i.e. 450 W/cm² and 50% ²³⁵U average burnup value) and experiments are currently in progress with higher Si contents.

Since 2004, UMo dispersion fuels have been manufactured with increasing Si contents. Three kinds of Si incorporation have been tested: (1) matrix made by powder mixtures of pure Al powders and pure Si powders, (2) matrix made by AlSi alloy powders and (3) UMo particles coated by Si embedded in a matrix of pure Al powders.

The first step was to test the matrix made by powder mixtures of pure Al powders and pure Si powders: 0.3 wt% Si in the IRIS 3 experiment [13], 4 %wt, 6 %wt Si in E-FUTURE experiment [14] and 12 wt% Si in the E-FUTURE II experiments [3]. The industrial feasibility of flat fuel plate manufacturing was demonstrated for UMo powder embedded in an Al+Si powder mixture up to 12 wt% up to 8 gU/cm³.

Secondly, the matrix made by AlSi alloy powder was tested: 2 wt% Si in IRIS 3 [13], IRIS 4 [15] and IRIS-TUM [16] experiments; and 7 wt% and 12 wt% Si in E-FUTURE II experiment [3]. The industrial feasibility of flat fuel plate manufacturing was proved for UMo powder up to 8 gU/cm³ and embedded in AlSi alloy powders lower than or equal to 2 wt%. Industrial feasibility was not established for Si contents greater than or equal to 7 wt%. The AlSi alloy becomes hard and brittle when the Si content increases. Applied heat treatments can decrease this effect, but not fully eliminate it [17]. Non-conformances occur during the rolling process and the yield rate decreases critically. A significant R&D program has to be deployed in order to demonstrate or rule out the industrial feasibility of this solution.

In a third step, the UMo coated by Si embedded in pure Al matrix was tested in 0.3 and 0.6 µm Si thickness layers in the SELENIUM experiment [4]. The industrial feasibility of flat fuel plate manufacturing was demonstrated for UMo powder up to 8 gU/cm³ coated with Si layer. However, the industrial feasibility of applying Si coating to UMo powder has not been investigated. Considering this solution, it is important to obtain perfect continuous layers of Si around the UMo particle. New manufacturing and associated inspection method are arising [18]. Today, the Si layer is obtained by Physical Vapour Deposition on small batches under laboratory conditions. The upscaling of this process has not been investigated, but even achievable it seems to be long and complex.

In parallel, since 2005, an UMo monolithic fuel investigation program is being conducted through TUM and AREVA-CERCA collaborative ventures [19], [20]. The program rules out as scheduled and irradiation of mini-plates and full size are scheduled in the coming months.

2.3. UMo fuel manufacturing production

Thanks to the approach followed, the long experience acquired and the expected promising irradiation results of E FUTURE II , the time to further analyze UMo production at industrial scale production is reached.

The industrial-scale production of UMo fuels will call for the handling of large UMo quantities. The regulation aspects, safety licences, storage capacities and transportation issues will need to be adapted accordingly.

It has been proved that ground UMo powder production cannot be realized on an industrial scale. Thus, AREVA-CERCA is making plans to operate an industrial-scale UMo powder production capacity in its facility. Contacts are being developed with UMo powder technology owners in order to make full assessments of the UMo powder technologies available. The assessments will need to cover several aspects as: adaptation to the French safety regulations, production capacity

(redundancy, reliability, operability and maintainability), quality assurance (repetitiveness, impurity level) and must be economically relevant.

Si-rich UMo plate manufacturing production is still to be addressed. As detailed above, manufacturing production feasibility has not yet been demonstrated for some option designed with high Si-rich UMo fuel. In this context, the irradiation results of the E-FUTURE II [3] and SELENIUM [4] experiments are of tremendous interest. They will need to discriminate between the three kinds of Si incorporation tested for UMo fuel to find the one which can operate in high performance research reactor conditions. Following E FUTURE II PIE, and the final down selection of the UMo fuel option, the program to bridge the industrial production gap will be defined and launched accordingly to the reactors conversion timeframe.

Assessment of the technical available option to produce UMo particles at industrial scale will start this year.

3. AREVA experience in RTR spent fuel treatment

3.1 AREVA experience in treatment of RTR UAl fuels

AREVA has long experience in the industrial-scale treatment of RTR UAl fuel. As of 2012, over 23tHM of U-Al type RTR fuels have been treated at AREVA's facilities in France. At the Marcoule site, 18tHM have been treated, and since 2005, over 5 tHM of U-Al type fuel have been successfully treated at La Hague [21].

The treatment process as performed at the La Hague facility is summarized in the figure below.

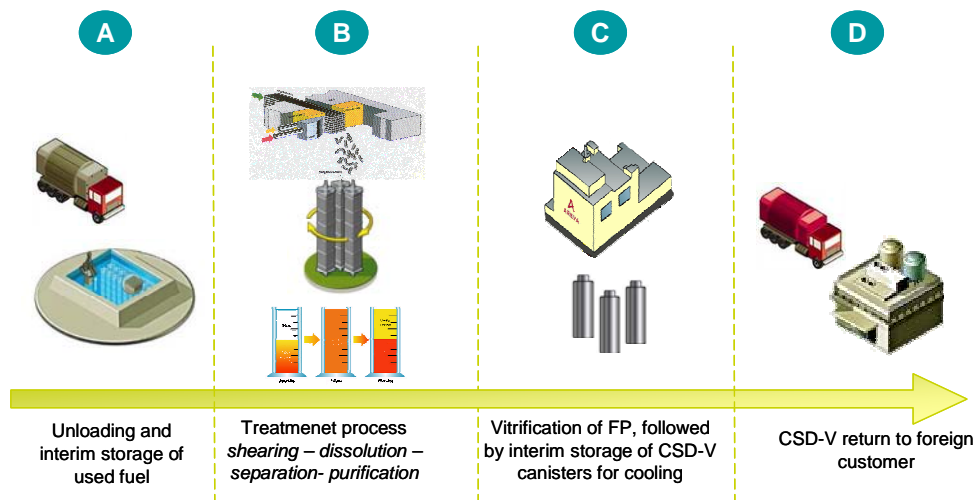


Fig 2. Schematic view of the RTR fuel treatment process

The RTR fuel treatment process of the La Hague plant includes the following steps:

- A- The reception and cooling step: once the fuel is received at La Hague plant, it is placed in interim storage pools for cooling. This cooling or deactivation decreases the radioactivity of the fission products substantially.
- B- The dissolution step: the fuel is introduced into the existing dissolver through a pit specially designed for RTR fuel. The dissolution is realized in a hot nitric acid solution. At this step, the process is limited by the aluminium concentration to 35-40g aluminium / L, to manage the risk of precipitation into aluminium nitrate.

The resulting solution is then diluted with the solution coming from the dissolution of the UOx fuel (power reactor fuel).

C- The extraction step: Uranium and plutonium are extracted from the solution by a liquid-liquid extraction process. Several extraction cycles in pulsed columns, mixer-settler banks, or centrifugal extractors are necessary to meet the end-product specifications.

At the end of these cycles, the following solutions are generated:

- a solution specifically containing the uranium
- a solution specifically containing the plutonium
- a solution containing the fission products and the minor actinides. This solution is then “vitrified”, i.e. conditioned into a stable, homogeneous and durable glass matrix, and encased in a standard canister, called “Vitrified Universal Canister” (UC-V). The UC-Vs are then stored in a specific interim storage facility at La Hague site for cooling.

D- The UC-Vs are returned to the foreign customer.



Fig. 3. Picture of a vitrified Universal Canister, “UC-V”

The RTR fuel treatment goes through every process step of the La Hague plant, from fuel storage and treatment to vitrification, including the analytical laboratories and waste processing. The specific characteristics of RTR fuel required specific demonstration, by example:

- lay-out : the implementation of the pit in the existing dissolver was a challenge because of the limited place available in the cell,
- mechanical: gravity feeding of the dissolution pit from the maintenance cell had to be demonstrated for long term use,
- chemical: the risk of crystallization of aluminium had to be managed properly,
- safety, criticality : the management of the risk of criticality in the dissolution pit had to be demonstrated, taking into account the high uranium enrichment.

Currently, the overall rate of the treatment is limited by the amount of aluminium contained in the active glass. Research and development is on-going to increase the amount of aluminium coming from the RTR fuel, by decreasing the amount of aluminium oxide coming from the non-active glass added for the vitrification.

3.2. Status of R&D on treatment of silicide RTR fuels

Silicide fuel is made of aluminium alloy mixed with U_3Si_2 particles. It was qualified for use in reactors during the 1980s under the RERTR program (Reduced Enrichment for Research and Test Reactors) in order to reduce the proliferation risk (less than 20 wt% ^{235}U), and has been used more and more extensively in RTRs since the end of the 20th century.

The treatment of silicide fuel is studied with the objective of following the same treatment process at La Hague as the one for UAl fuel and to adapt it to the specific characteristics of silicide.

The research programs conducted through the collaboration between AREVA and CEA focused on the acquisition of USi dissolution data in nitric acid and especially on the Si behaviour and its possible impact on the recycling process steps: dissolution, centrifugation and extraction. Indeed, for the UAl dissolution step, the concentration of silicide is limited to 0.4% of aluminium mass, or a maximum concentration of 160mg/L in the dissolution solution. In the USi case, the quantity of silicide is ten times greater.

Dissolution tests on unirradiated plate sections in nitric acid media resulted in complete dissolving of uranium and quantitative silicon precipitation as hydrated silica. Additional tests were carried out on thermally treated plates to simulate more closely the physical and chemical behaviour in the spent fuel. The reference conditions defined by these tests were then tested on spent fuel plate segments from the French SILOE reactor. Experiments with spent fuel were performed in the Atalante facility of CEA/Marcoule. It allowed the results obtained on unirradiated plates to be validated.

The silicic acid $\text{Si}(\text{OH})_4$ formed during dissolution polymerized to yield hydrated silica gel; this gel may hamper the liquid/liquid extraction performance and induces a risk of equipment fouling. The challenge of the R&D program currently in progress is to manage this gel in the process. The process can be directly adapted to USi fuel by a simple dilution to limit the quantity of silicide in the plant, but the treatment capacity would be affected. Thus, it appears that silicide fuel can be treated on a small scale, and AREVA and CEA are investing in R&D to improve the process up to an industrial scale.

Another option consists in using the centrifugation step existing in the La Hague plant for UOX treatment, in order to separate the silicide gel from the clarified solution which could then be treated in the separation process as for UAl fuel. This option is currently being investigated to give an industrial-scale response to the treatment of silicide fuel. The R&D program has already demonstrated the ability of the centrifugation step to properly separate the silicide gel from the dissolution solution. As the feasibility of the process has now been assessed, the challenge of the current program is to optimize the different steps and to demonstrate that the silicide gel will not accumulate in the La Hague equipment and will not affect the overall process performance once mixing with UOX solutions has been carried out [22].

3.3. Treatment of RTR UMo fuel

There are two specific characteristics of U-Mo fuel that will have an impact on back end options as compared to U-Al type RTR fuels, and in particular the feasibility of treatment options: the presence of molybdenum, and the presence of silicide.

The proposed scheme, as for the UAl fuels, would consist in dissolution in a nitric acid medium followed by dilution of the obtained solution into standard UOX fuel dissolution solutions before treatment by the PUREX process.

In 2005, within the scope of an AREVA-CEA cooperation, the CEA conducted a research and development program focussing on the dissolution step [23]. Dissolution tests were conducted on non-irradiated U-Mo powder with an Mo content of 7% to determine the necessary conditions for successful dissolution of the UMo fuel. Aluminium concentration was found to have an impact on the solubility of molybdenum. The conclusion of the tests was thus that the Al concentration should be less than 15 g/L in order to obtain a clear and stable dissolution solution (instead of 40 g/L for UAl fuels). The optimal dissolution conditions were then qualified with UMo plates irradiated inside the French Osiris reactor. Further studies would be necessary to optimize this point related

to the treatment capacity, and to determine the conditions for the extraction and waste conditioning steps, but the treatment R&D program stopped at that time due to the difficulties encountered by the fuel development.

Due to that, as the UMo fuel hadn't achieved the expected performance in reactor, Si was reinserted into the fuel composition, in addition to molybdenum. The industrial treatment of UMo fuels is thus directly linked to the R&D program in progress to optimize the silicide fuel treatment, and the possibility of adding the centrifugation step has to be considered, in relation with the quantity of silicide which will be added. Furthermore, some additional points have to be evaluated by R&D:

- Cross-impact of Mo and Si at the dissolution step, that is optimization of dissolution conditions related to the treatment scheme after dissolution. This R&D program has to be conducted on unirradiated and irradiated plates.
- Behaviour at the centrifugation step if necessary
- Impact of molybdenum on liquid-liquid extraction
- Impact of molybdenum on the vitrification step,
- Validation of the process treatment at laboratory scale with irradiated material, if necessary.

4. Conclusion

For many years, AREVA has been involved in Research and Testing Reactors (RTR) fuel manufacturing and RTR spent fuel treatment. The manufacturing production and the spent fuel treatment of these fuels are important issues for RTR operators.

Currently, within more than 15 years of participation in the development of a reliable UMo fuel system, AREVA-CERCA can be considered as a reliable partners in UMo projects. Since 1997, AREVA-CERCA has always financially contributed to improve UMo fuel manufacturing through internal dedicated R&D budget and in participating to the founding of the program requested in the frame of the international GTRI efforts.

The design of UMo dispersed fuel has reached a high level of complexity. From all the Si-rich UMo dispersed fuel designs tested, the industrial feasibility of the matrix made of Al+Si powder mixture has been demonstrated, but this is not the case for the industrial feasibility of the matrix made of AlSi alloy and UMo coated particles. For the latter, upscaling to industrial production looks like being a long process where several technical, economic and safety challenge will have to be addressed.

AREVA-CERCA is willing to discuss with any interested partners to proceed for setting up the necessary technology to produce reliably the fuel of the future for the benefits of customers and the community.

In this context, the irradiation results of the E-FUTURE II [3] and SELENIUM [4] experiments are of tremendous interest and will provide the necessary data set for the final UMo design option. for high performance research reactor conditions.

The other issue in the fuel cycle for RTR operators is spent fuel recycling.

For many years now, AREVA NC has acquired a wide industrial experience in RTR UAl fuel treatment at its La Hague plant.

To make the treatment of the various types of RTR fuel such as U_3Si_2 fuel and UMo fuel feasible, AREVA NC is thinking about an industrial scenario at the La Hague plant.

The technical feasibility of silicide fuel treatment is now being assessed; nevertheless, additional research and development is in progress to define the operating conditions corresponding to industrial-scale treatment. Silicide is a major risk for the plant which has to be considered in order to define the best way to manage it. Some answers are expected in 2012.

The same treatment scheme should be applied to UMo, in addition a specific R&D program has to be conducted to take into account both molybdenum and Si. The launching of this program will be dependent on the development of the UMo fuel, and the choice of the scheme will depend on the quantity of silicide added, but AREVA NC recommends a quantity as low as possible.

AREVA NC is now working on the definition of industrial treatment scenarios making it possible to treat the various types of materials such as UAl, USi and UMo RTR fuel on the current line (with or without modification) or on a new line to be designed at the La Hague plant. These scenarios will depend on the quantity and types of RTR fuels to be treated and AREVA NC is building a business plan adapted to the RTR customers for end 2012.

Thus, AREVA NC is suggesting a common collaboration with customers in order to reach a good understanding of customer requirements.

5. References

- [1] H. Vacelet, P. Sacristan, A. Languille, Y. Lavastre, M. Grasse, "Irradiation of full size UMo plates", RERTR 1999, Budapest, Hungary, 3-8 October 1999
- [2] A. Languille, JP. Durand, A. Gay, "New high density MTR fuel; the CEA-CERCA-COGEMA development program", RRFM 1999, Bruges, Belgium, 28-30 March 1999
- [3] B. Stepnik, M. Grasse, D. Geslin, C. Jarousse, F. Charollais, P. Lemoine, Y. Calzavara, H. Guyon, E. Koonen, S. Van den Berghe, "Leonidas UMo dispersion fuel qualification program: progress and perspectives highlight on the E-FUTURE II fuel plate manufacturing", RRFM 2012, Prague, Czech Republic, 18-22 March 2012
- [4] S. Van den Berghe, A. Leenaers, C. Detavernier, "Coated particle production in the SELENIUM project", RRFM 2011, Rome, Italy, 20-24 March 2011
- [5] JP. Durand, Y. Lavastre, M. Grasse, "LEU fuel development at CERCA – Status as of October 1997 – Preliminary developments of MTR plates with UMo fuel", RERTR 1997. Jackson Hole, Wyoming, USA, 5-11 October 1997
- [6] JP. Durand, JC. Ottone, M. Mahe, G. Ferraz, "LEU fuel development at CERCA -Status as of October 1998", RERTR 1998, Sao Paulo, Brazil, 18-23 October 1998
- [7] JP. Durand, B. Maugard, A. Gay, "Technical ability of new MTR high density fuel alloys regarding the whole fuel cycle", RRFM 1998, Bruges, Belgium, 29-31 March 1998
- [8] JM. Hamy, P. Lemoine, F. Huet, B. Guigon, C. Jarousse, JL. Emin, "Status as of march 2004 of the French UMo group development program", RRFM 2004, Munich, Germany, 21-24 March 2004
- [9] JP. Durand, F. Obadia, C. Jarousse, Y. Lavastre, M. Grasse, JM. Falgoux, U. Lindelöw, "Manufacturing and licensing of lead test assembly for the R2 reactor", RRFM 2003, Aix en Provence, France, 9-12 March 2003
- [10] G.L. Hofman, Y.S. Kim, H.J. Ryu, J. Rest, D.M. Wachs, M.R. Finlay, "Attempt to solve the instability in the irradiation behavior of low enriched u-mo/al dispersion fuel", Proceedings of RRFM 2006, Sofia, Bulgaria, 30 April-3 May 2006.
- [11] A. Leenaers, S. Van Den Berghe, W. Van Renterghem, F. Charollais, P. Lemoine, C. Jarousse, A. Röhrmoser, W. Petry, "Irradiation behaviour of ground U(Mo) fuel with and without Si added to the matrix", J. Nucl. Mater. 412, 2011, 41-52.
- [12] Y.S. Kim, G.L. Hofman, A.B. Robinson, "Effect of Si addition in Al in U-Mo/Al dispersion plates: observations from side-by-side irradiations from RERTR-6, -7A, -9A and -9B", Proceedings of RRFM 2009, Vienna, Austria, 22-25 March 2009.

- [13] M. Ripert, V. Marelle, X. Iltis, H. Palancher, C. Valot, F. Charollais, MC. Anselmet, X. Tiratay, P. Lemoine, S. Van den Berghe, A. Leenaers, C. Jarousse, "Synthetic review of the IRIS 3 experiment", RRFM 2011, Rome, Italy, 20-24 March 2011
- [14] F. Charollais, P. Lemoine, Y. Calzavara, H. Guyon, E. Koonen, S. Van den Berghe, C. Jarousse, D. Geslin, "LEONIDAS U(Mo) Dispersion Fuel Qualification Program : Progress and Perspectives", RERTR 2011, Santiago, Chile, 23-27 October 2011
- [15] F. Charollais, M. Ripert, MC. Anselmet, P. Boulcourt, X. Tiratay, P. Lemoine, C. Jarousse, "IRIS program : IRIS4 first results", RRFM 2009, Vienna, Austria, 22-25 March 2009
- [16] W. Petry, A. Röhrmoser, P. Boulcourt, A. Chabre, S. Dubois, P. Lemoine, C. Jarousse, JL. Falgoux, S. Van den Berghe, A. Leenaers, "UMo full size plat irradiation experiment IRIS-TUM – A progress report", RRFM 2008, Hamburg, Germany, 2-5 March 2008
- [17] A. Leenaers, S. Van den Berghe, A. Robinson, C. Detavernier, "Al-Si matrix : mixture or alloy – an annealing study", Proceedings of RERTR 2011, Santiago, Chile, 23-27 October 2011.
- [18] X. Iltis, H. palancher, A. Bonnin, F. Charollais, S. Van den Berghe, B. Stepnik, Y. Calzavara, "LEONIDAS E-FUTURE II : Characteristics of the fresh fuel plates", RRFM 2012, Prague, Czech Republic, 18-22 March 2012
- [19] C. Jarousse, P. Lemoine, P. Boulcourt, W. Petry, A. Röhrmoser, "Last manufacturing results of monolithic UMo full size prototype plates", RERTR 2006, Cape Town, South Africa, 26 October -3 November 2006
- [20] C. Jarousse, L. Halle, W. Petry, R. Jungwirth, A. Röhrmoser, W. Schmid, "FRM II and AREVA-CERCA common effort on monolithic UMo plate production", RRFM 2009, Vienna, Austria, 22 – 25 March 2009
- [21] E. Hélaine, P. Bernard, JL. Emin, D. Lepoittevin, F. Gouyau, "Research and test reactor fuel treatment at AREVA NC La Hague", RRFM 2007, Lyon, France, 12-14 March 2007
- [22] N. Reynier Tronche et al., Uranium silicide RTR fuel : Dissolution and extraction studies, RRFM 2012, Prague, Czech Republic, 18-22 March 2012
- [23] N. Herlet, G. Ferlay, JP. Cancausse, A. Juvenelle, "Reprocessing UMo spent fuel: dissolution experiments on non-irradiated and irradiated materials", RRFM 2005, Budapest, Hungary, 10-13 April 2005

FACTORS AFFECTING THE DECISION TO DECOMMISSION A RESEARCH REACTOR IN INDONESIA

DJAROT S. WISNUBROTO

*National Nuclear Agency of Indonesia – BATAN
Kuningan Barat, Mampang Prapatan, Jakarta – INDONESIA*

ABSTRACT

There are many factors that has to be considered on the decision to decommission this reactor, for example obsolescence, low performance, recent demography change, and recent finding of the earthquake potential source near the reactor location. The demography of Bandung city is rapidly changed, and the surrounding area of the reactor may be fully populated in the near future, so it may be not suitable to operate research reactor in that area. The recent earthquakes in Java island in the last 5 year, and new finding of the earthquake potential source called Lembang fault 10 km from the site made BATAN evaluate the safety of that reactor. However the decision for decommissioning is not easy due to the lack of infrastructures such as on the strategy of radioactive waste management, i.e. the presence radioactive waste storage facility is not capable to handle waste generated by the decommissioning. Another problem is, that some materials can not be carry directly to the waste storage facility about 100 km from the reactor due to the high radiation dose, so it will wait for some time for decay. While the spent fuels may be repatriated to the United States. On the regulations, BAPETEN finally published chairman decree on the decommissioning of nuclear reactors on 2009 as a basic regulation to move forward.

1. Introduction

Indonesia has 3 research reactors, the biggest is the 30 MW MTR-type multipurpose reactor at Serpong Site, and two TRIGA-type research reactors, the first one is 1 MW located at Bandung Site and the second one is a small reactor of 100 kW at Yogyakarta Site. The TRIGA MARK II research reactor at Bandung site was reaching its first critical core in 1964 and operated at maximum power of 1000 kW since 1971. The reactor was upgraded into 2 MW power level successfully in October 2000. This means that the TRIGA Reactor in Bandung has been operated for 48 years and will then be an object for the decommissioning programme in the near future. In order to anticipate the decommissioning programme for research reactor as well as other nuclear facilities, the Indonesian National Nuclear Energy Agency (BATAN) establishes a Division specially performing research and development work as well as services in the field of decontamination and decommissioning of nuclear devices and or nuclear facilities at the Radioactive Waste Technology Center (RWTC) at Serpong Site, 30 km southwest from Jakarta. This paper discusses the factors affecting the decision to decommission a research reactor in Indonesia using recent information including demographic and seismic datas.



Figure 1. The Bandung TRIGA MARK II Research Reactor .

2. Analysis

In the nuclear industry there are many reasons for facility shutdown and subsequent decommissioning. For research reactors these may include obsolete technology or process, lack of business need or support for continued operation, licensing and regulatory changes,

incidents and accidents, legal and political operational constraints, change of site use and stakeholder pressure. While the decision making process leading to either plant closure or continued operation will be plant specific [1].

2.1. The age and obsolescence

Generally the old age of research reactor is not only the main reason to decommission, many examples show that where there is a need for the future use of a reactor, the design and age related problems can be fixed so that the reactor can be operated for a longer period of time. For the older 47 year old FRG-1 Germany the neutron flux was increased and other measures were used to significantly increase its use [2]. The operating organization now believed that FRG-1 can be operated, resulting in over 50 years of operation. The HIFAR research reactor in Australia began operation in 1958. Although originally designed exclusively for materials testing, it was modified over the years to allow for medical radioisotope production, neutron scattering research and irradiations services. It was decided to decommission HIFAR because of the construction of a replacement research reactor with enhanced capabilities [3]. However other reasons such as change of land use or public pressure specially opposing the operation of nuclear facilities in certain location leading to decommissioning of research reactors.

Research reactor in Bandung can not be said to be old, because since its first criticality at 1964, the reactor has been modified several times. The reactor was upgraded from 250 kW to 1000 kW in 1971 and to 2000 kW in 2000. Only civilian building from the beginning has not changed, this may be a weak point after Lembang fault found not far from the reactor. The reactor has an authorization for operation until year 2016. However, the reactor has been shutdown since 2004 due to some technical problems, such as core bubbling, and detection of fission products in cooling tower. The operators are striving to accomplish the problems, while BATAN also considers about the decision on decommissioning.

2.2. Demography

The demography of Bandung city is rapidly changed, and the surrounding area of the reactor may be fully populated in the near future, so it may be not suitable to have a nuclear research reactor in that area. The population of Bandung City where reactor located in the year 2010 was 2.393.633 people, with the population density in that year was 14,228 per square kilometer, and population growth rate of 1.65% per year [4], so it can be predicted that within the next few years then Bandung become a very crowded city. The location of the reactor is adjacent to the Bandung zoo and not far away from the residential area. Although, up to now there is no public opposition with that nuclear facility but sooner or later they may be questioning about the status of the reactor.

2.3. Seismic situation

The recent earthquakes in Java island in the last 5 year, and new finding of the earthquake potential source called Lembang fault 10 km from the site made BATAN evaluate the safety of that reactor. The Lembang Fault is a large active fault situated less than 15 km from the major population centre of Bandung. Geological evidence has suggested that large earthquakes have occurred on this fault in the past, and therefore may occur in the future [5]. The map below shows a simulation of what scientists believe is the largest earthquake that could occur on the fault. It is clear that this event would cause widespread damage but it is still not known how likely such an event would be. BATAN consider seriously with recent finding by the geologist, and this fault may be able to produce an earthquake with a magnitude of 6 to 7. So this is an other important factor that decommissioning in the near future may not be inevitable, because 50 years ago there were not requirement for such as seismic conditions. However some scientists argue that by modify the building of the reactor than the damage due to the earthquake may be avoided. Discussion is still in progress how to handle this seismic issue.

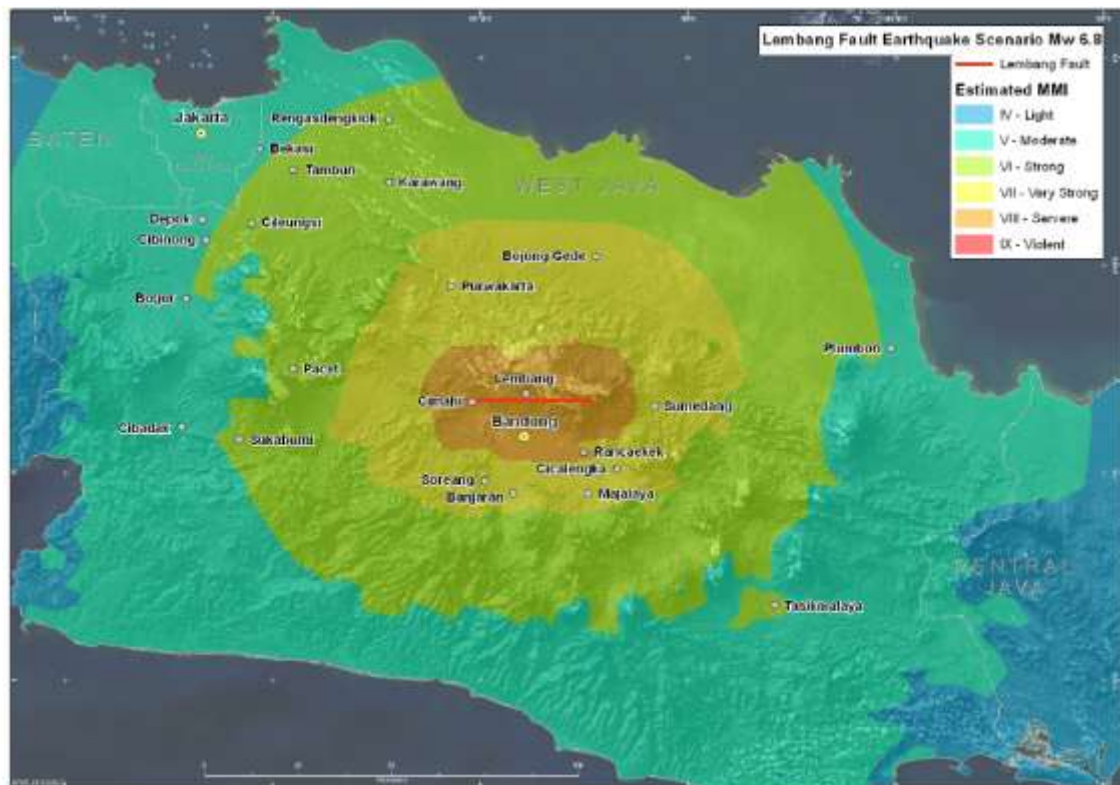


Figure 2. Lembang fault near Bandung City, and its earthquake scenario [5].

2.3. Regulation

In recent progress, nuclear regulatory agency of Indonesia (BAPETEN) is concerned about aspects of decommissioning that involve nuclear and radiation safety, and also gives special attention to safety assessments, waste management evaluations and risk evaluations for decommissioning activities. Early decommissioning planning is now under Indonesian Regulation (BAPETEN Chairman Decree 2009) [6]. It should be noted that new facilities are now required to address decommissioning aspects in order to receive authorization to operate. The regulatory process for decommissioning differ from that required for reactor operation. Special regulatory arrangements required for waste management because of the increased volumes and types of waste generated during commissioning. Also, regulatory issues arise concerning removal of spent fuel from the reactor or site.

The regulatory body requires decommissioning to be carried out in discrete, approved phases; and it ultimately approves release of the facility or site, as appropriate (for either restricted or unrestricted use). Approval of decommissioning projects by the regulatory body is now required by government regulation. However the regulation lack of the clearance/release criteria for unrestricted use of materials, buildings and sites.

A general regulatory trend today is to encourage the completion of decommissioning of research reactors as soon as possible after final shutdown. In particular for research reactors, an additional argument for immediate dismantling is that the decommissioning waste volumes are generally much smaller than for nuclear power plants and can be easily accommodated in storage facilities if disposal repositories are not available. However, in addition to safety considerations, the choice of strategy is influenced by political and other realities.

2.4. Funding

One of the most significant considerations in the decision of decommissioning is funding. Funding considerations include both estimated costs and the availability of financial resources. The funding of decommissioning strategy option studies is very important to ensure that a full range of viable decommissioning strategies is identified. The 'do nothing' strategy, which has been observed in the past in several countries, often occurs by default.

For Indonesia, the research reactors are owned by the government, no funding provisions are made in the course of the reactor operation and funds are allocated by the government only after permanent shutdown. One of the problems on the decommissioning is that, developing countries such as Indonesia usually give the budget priority to the productive sectors, so the government may be reluctant to give budget for the decommissioning program, may be the most practical decision is just extended shutdown while waiting for better economical situation in the future. .

2.5. Site reuse

The usual objective of decommissioning in the past was to achieve the release of the nuclear site with no subsequent uses foreseen in the near term. A more recent development is the realization that the land and facilities associated with the decommissioned reactor may be of value, and consideration of site reuse could be beneficial and therefore be incorporated into the decommissioning plan. For example, immediate dismantling may be desirable in order to deploy existing resources for a different use. Reactor staff may be usefully re-employed at the converted facility. Also, much equipment, such as hot cells and cranes, may be used for other purposes. For these and other reasons it is not uncommon for reactor operating organizations to implement immediate and selective decommissioning policies in order to convert the facilities for reuse. Indonesia considers the facilities to be decommissioned to serve an educational and historical purpose such as the FR-2 reactor situated at the Karlsruhe research centre in Germany that is currently being used as a museum [7]. It is more common, however, for deferred dismantling to occur by default, usually due to a lack of funds.

2.6. Waste and spent fuel managements

The availability and capability of radioactive waste management facilities is extremely important to the selection of an appropriate decommissioning strategy. Because of their experimental nature it is not unusual for a wide variety of radionuclides or physical-chemical forms to be found in the solid and liquid wastes of particular research reactors. Indonesia does not yet have an approved low level waste repository. Interim storage space for dry active wastes on-site may be limited, and acceptance criteria is not available for the storage of some waste. The presence radioactive waste storage facility is not capable to handle waste generated by the decommissioning. Another problem is, that some materials can not be carry directly to the waste storage facility about 100 km from the reactor due to the high radiation dose, so it will wait for some time for decay. So BATAN must build the waste storage facility, preparation for the aproprate transportation carrier, and setup the reactor site as the temporary storage facility. In that cases immediate dismantling may not be a viable strategy. While the spent fuels may be repatriated to the United States. If not, they will be moved to the interim storage for spent fuel (ISSF) facility in Sepong area.

2.7. Stakeholders involvment

In the past, activities of nuclear facilities was usually dealt with by institutional parties, typically nuclear operating organizations and regulatory bodies. Addressing the information and communication requirements for all stakeholders involved and interested in a decommissioning project has become significant. The public has become increasingly interested in decommissioning plans. This interest has resulted in enhanced scrutiny and review of projects, particularly by safety and environmental regulatory bodies with direct responsibility for granting project approvals, and also by government officials who require detailed information to keep abreast of the broader interests and issues raised by their constituents. BATAN must begin to communicate with stakeholders such as safety and envirnomenal regulatory bodies, government and political Figures, and even the public who have an interested in decommissioning. Although experience has shown that efforts to educate the public on nuclear matters are only moderately successful in achieving public acceptance. However, experience has also shown that bringing the various interest groups together in a common forum where they are kept well informed and where they can make

inputs to planning and proposed actions can be very effective in improving public acceptance of a proposed action.

2.6. Human resources

The Bandung reactor have been upgraded two time, so the operators have gained experiences on dismantling and decontamination, but unfortunately some of these skilled staffs are retired and in the next 5 years they will be retired all. This make the decision of decommissioning tend to choose deferred dismantling that more expensive than immediate dismantling. Unlike deferred dismantling, a strategy that involves immediate dismantling takes advantage of the expertise of existing staff. Conversely the availability of skilled human resources for deferred or future projects is a serious concern.

3. Conclusions

The Bandung TRIGA Mark II reactor first reached critically in 1964, which means that the reactor has been operated for about 47 years. Since its first criticality, the reactor has been modified several times. The reactor was upgraded from 250 kW to 1000 kW in 1971 and to 2000 kW in 2000. No decision has yet been made on the decommissioning of the reactor, but it is expected that in the near future it will be decommissioned. There are many factors that has to be considered on the decision to decommission the Bandung reactor. Among the important factors are obsolescence, demography, seismic condition, regulations, stakeholder communication, fund, and waste management. The demography of Bandung city is rapidly changed, and the surrounding area of the reactor may be fully populated in the near future, so it may be not suitable to operate research reactor in that area in the near future. The new finding of the earthquake potential source called Lembang fault 10 km from the reactor site made BATAN evaluate the safety of that reactor. The presence radioactive waste storage facility is not capable to handle waste generated by the decommissioning. Another problem is, that some materials can not be carry directly to the waste storage facility about 100 km from the reactor due to the high radiation dose, so it will wait for some time for decay. So BATAN must build the waste storage facility, preparation for the appropriate transportation carrier, and setup the reactor site as the temporary storage facility. While the spent fuels may be repatriated to the United States. If not, they will be moved to the interim storage for spent fuel (ISSF) facility in Sepong area. On the human resources, unfortunately some of these skilled staffs are retired and in the next 5 years they will be retired all. On the regulations, BAPETEN finally published chairman decree on the decommissioning of nuclear reactors on 2009 as a basic regulation to move forward. Finally, discussion with the stakeholders on the decision of decommissioning using the factors above is very important.

4. References

- 1) International Atomic Energy Agency, "Decommissioning of Research Reactors: Evolution, State of the Arts, Open Issue", Technical Report Series No.446, Vienna, (2006).
- 2) LARAIA, M., DLOUHY, Z., "Strategies and trends for nuclear reactors", Regulator Aspects of Decommissioning (Proc. Joint EC-IAEA-OECD/NEA Workshop Rome, 1999), Agenzie Nazionale per la Protezione dell' Ambiente, Rome (2000).
- 3) AUSTRALIAN GOVERNMENT, NUCLEAR SAFETY COMMITTEE, Comments to the CEO of ARPANSA Relating to the Decommissioning of HIFAR, ARPANSA, Yallambie, Victoria (2004), www.arpansa.gov.au/pubs/nsc/hifar.pdf
- 4) BPS, Indonesia Statistics 2010, Jakarta (2011) www.bps.go.id
- 5) Government of Indonesia, Earthquake Map of Indonesia 2010, Jakarta (2010).
- 6) National Nuclear Regulatory Agency, BAPETEN Chairman Decree No.4/2009 on the Decommissioning of Nuclear Reactor, Jakarta (2009).
- 7) BRENK SYSTEMPLANUNG, Stilllegung und Rückbau kerntechnischer Anlagen (Decommissioning and Dismantling of Nuclear Installations), Aachen, Germany (2000).

INSPECTION OF THE REACTOR TANK AND INTERNALS AT THE TRIGA FIR 1

I. AUTERINEN, A. KOSKINEN, P. KIVELÄ, J. HELIN, A. TUHTI
*VTT Technical Research Centre of Finland
Otakaari 3, FI-02044 VTT, Espoo – Finland*

ABSTRACT

According to the ageing management system at FiR 1 a thorough inspection of the reactor tank has to be performed every five years. Such inspection was performed in 2011 using improved methods and a more exhausting coverage of the tank and the beam tubes. A remotely controlled high resolution camera was used to inspect the seams of the aluminium tank. Also the core support structures and the beam tube bellows and collars were inspected. The visual inspection was performed by a qualified team from the WesDyne TRC from Sweden. The thickness of the tank wall was inspected by a VTT inspection team using an ultrasonic measurement device. The methods and results of this inspection campaign will be reported.

1. Introduction

FiR 1 -reactor is a TRIGA Mark II type research reactor manufactured by General Atomics (San Diego, CA, USA). The FiR 1 started operation in 1962, reactor power was increased in 1967 from 100 kW to 250 kW, and in 1982 the reactor instrumentation was renewed. In 1996-1997 the reactor building was completely renovated and the ventilation and reactor cooling systems were replaced.

Boron Neutron Capture Therapy (BNCT) work dominates the current utilization of the reactor. The weekly schedule allows still three days for other purposes such as isotope production, neutron activation analysis as well as education and training [1]. The operating licence of the reactor was extended for the period 2011 to 2023 by the government of Finland in December 2011.

According to the ageing management system at FiR 1 a thorough inspection of the reactor tank has to be performed every five years. Such inspection was performed in 2011 using improved methods and a more exhausting coverage of the tank and the beam tubes. The previous inspection had been performed five years before and also the nuclear regulatory body in Finland STUK required that the inspection results should be available for them when they gave their statement of the safety of the reactor for the ministry of employment and the economy for the processing of the continuation of the operating licence.

2. The inspection plan

Following parts of the reactor tank and internals were selected for inspection:

1. Welds of support structures.
2. Surface of the tank, including welds
3. Abnormality on the bottom of the tank (slight swelling/protrusion area).
4. Welds of thermal column.
5. The bellow in the tangential beam (bolts, nuts, bands).
6. Outer surface of the tangential beams.

These parts are indicated in Fig. 1 a and b.

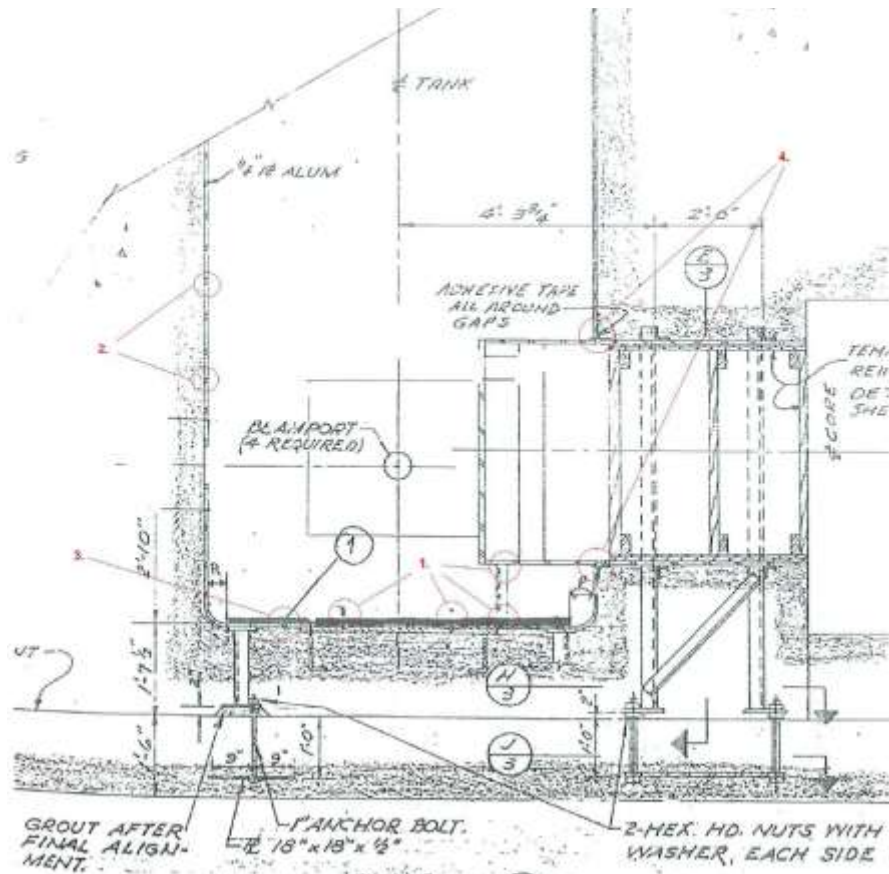


Fig 1a. Parts of the reactor tank and internals to be inspected are numbered from 1 to 6.

3. Inspection methods

Visual inspection using high resolution video camera was selected as the main method. The tank wall thickness was measured using ultrasound. Also eddy current measurements were originally considered, but after receiving the results of the visual inspection and the ultrasonic measurements this was considered unnecessary.

A plastic mould was originally considered for determining the abnormality on the bottom of the tank. But when the cause (depressions of the tank support legs) for these became clear in the visual inspection, the moulds were not needed anymore.

Table 1. Summary of the inspection plan.

	Visual	Ultrasonic	Mould
Tank welds	X		
The inner surface of the tank	X	X	
Abnormality on the bottom of the tank	X	X	(X)
Beam tubes	X		
outer surface	X		
collars	X		
collar bolts and nuts	X		

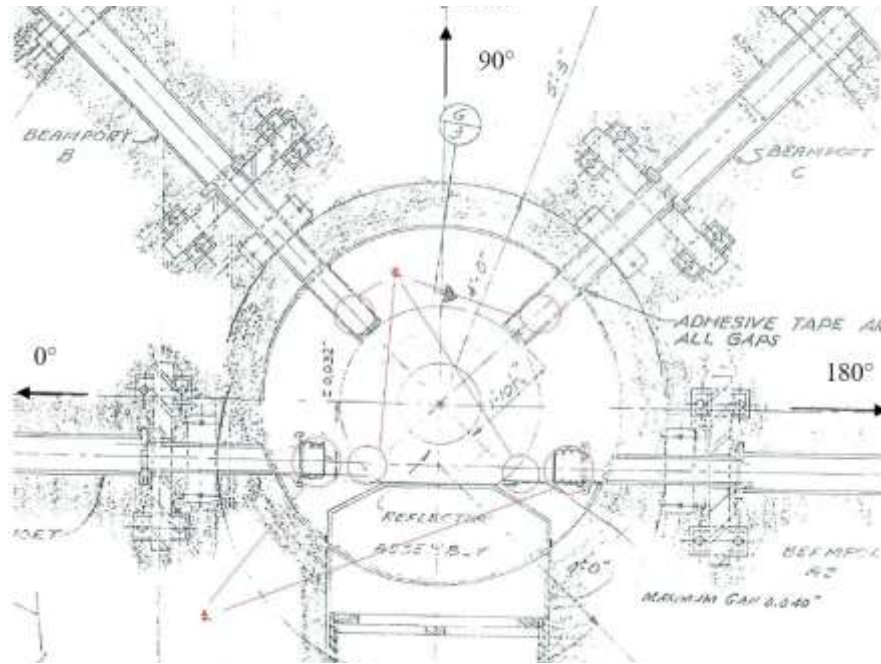


Fig 1b. Parts of the reactor tank and internals to be inspected are numbered from 1 to 6.

3.1 Visual inspection

Visual inspection was to be performed to specified welds, bottom of the tank (overview) and to other specified items (support structure welds, the bellow in the tangential beam tubing, bands, bolts, nuts). Weld inspections were planned to include all the weld intersections and at least 50 % of the welds otherwise (could also be 100 %). Visual inspection was to be carried out using suitable underwater camera and other equipment and the inspectors were required to be qualified for visual inspections according to EN 473.

WesDyne TRC AB (Sweden) was selected to perform the visual examination.

They used the N470-PTZ Underwater Pan & Tilt Color Camera (Ahlberg Electronics AB, Sweden). Some main characteristics of the camera are:

- Zoom ratio 4.1 – 73.8 mm
- Minimum object-to-lens distance 5 mm (at 4.1 mm)
- Zoom X72 (X18 optical, X4 digital)
- Close-range focusing, high resolution
- Resolution more than 460 lines

Both video and still pictures were recorded. The recording and camera control equipment were in a half size freight container located outside the reactor building. The camera cable was long enough to reach to the bottom of the reactor tank. The inspector was in the container with audio connection to the camera operator at the reactor tank.

3.2 Ultrasonic inspection

Ultrasonic (UT) inspection was to be carried out using manipulator and other suitable equipment for bringing the probe to the point of interest. Extent of the UT inspection was to be determined after visual inspection (if there were some abnormalities that need more than VT inspection). Main task was to determine the thickness of the tank wall in the bottom of the tank including the sites of the observed abnormalities.

The VTT NDT team qualified for UT inspections according to EN 473 (level 2) was selected to perform the UT inspection. UT-inspection was performed as thickness measurement with a straight beam probe 5MHz V110 Panametrics 0.25" and Krautkrämer USM 35.

4. Observations

4.1 Visual inspection

All planned targets were reached with the camera. Due to the good speed of the weld inspection all welds of the tank were inspected and recorded.

The main observations were:

Beam tubes

The locking bolts on the beam tube collars were found to be corroded.

Bulges

Four bulges were observed on the tank floor. The bulges were identified to be original and caused by the tank support leg pressure plates.

Debris

Debris was found on the reactor tank floor.

Epithermal Column

Impact marks and excess weld was observed on the Epithermal Column.

Tank Inner surface

Scratches and wear marks were observed on the surface of the tank walls.

Tank Welds

Porosity was observed on the circumferential and vertical welds of the reactor tank.

The visual inspection took totally three days including setting up the equipment and putting it back for transport.



Fig 2. Rosted beamtube collar bolt.



Fig 3. One of the bulges caused by the tank support leg pressure plates.

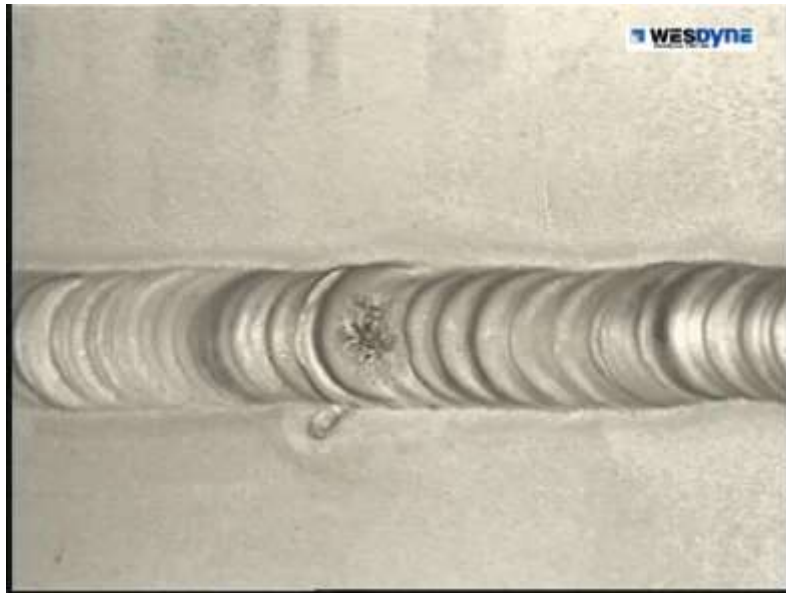


Fig 4. Porosity of a weld.

4.2 Ultrasonic inspection

The thickness of the tank aluminium wall was measured at several tens of locations at the bottom of the tank including the sites of the observed abnormalities. No changes in the thickness were observed.

5. Conclusions

In the visual inspection irregularities were observed in the tank welds. . These have been created in the manufacturing phase and have been stable since then and are not critical for the integrity of the tank. Also normal wear and tear was observed, but again not critical for the integrity of the tank. These could be avoided by more careful moving and supporting of equipment inside the tank, like tank side fuel rags.

The high quality pictures made it possible to identify the bulges in the bottom of the tank as depressions caused by tank support legs.

Ultrasonic measurements showed no changes in the thickness of the tank wall.

The high quality pictures confirmed corrosion in several of the tangential beam tube collar bolts. Some bolts are so much corroded that it calls for corrective actions.

References

1. Auterinen I, Salmenhaara S.E.J, The 250 kW FiR 1 TRIGA Research Reactor - International Role in Boron Neutron Capture Therapy (BNCT) and Regional Role in Isotope Production, Education and Training, Research Reactors: Safe Management and Effective Utilization - Proceedings of an international conference held in Sydney, Australia, 5-9 November 2007, Proceedings of an International Conference organized by the International Atomic Energy Agency (IAEA), IAEA-CN-156, 2008.
http://www-pub.iaea.org/MTCD/publications/PDF/P1360_ICRR_2007_CD/datasets/I.H.%20Auterinen.html

RELIABILITY AND REACTOR UTILIZATION IMPROVEMENTS AT HIGH FLUX ISOTOPE REACTOR (HFIR)

R. A. CRONE, L. R. BROWN, C. D. BRYAN, E. L. GRIFFIS

*Research Reactors Division, Oak Ridge National Laboratory
Building 7917, Oak Ridge, Tennessee, 37831-6398*

Notice: This submission was sponsored by a contractor of the United States Government under contract DE-AC05-00OR22725 with the United States Department of Energy. The United States Government retains, and the publisher, by accepting this submission for publication, acknowledges that the United States Government retains, a nonexclusive, paid-up, irrevocable, worldwide license to publish or reproduce the published form of this submission, or allow others to do so, for United States Government purposes.

ABSTRACT

The mission of HFIR is to provide safe, reliable, and efficient HFIR operation to support the neutron science mission. HFIR and supporting facilities are used for neutron scattering, isotope production and research, materials irradiation studies, neutron activation analysis, and gamma irradiation.

The HFIR is a 46 year old research reactor. In 2007, a Reliability and Risk Management Program was initiated to enable long-term safe, reliable, and efficient HFIR operation beyond 2040. The structured systematic approach of the RRM program has allowed the identification and mitigation many long-term ageing and degradation threats to Systems, Structures, and Components, avoiding unanticipated failures and increasing plant reliability and predictability.

In addition to the Reliability effort that has yielded 98% predictable operations, isotopes and materials irradiation programs have expanded and upgrades to the neutron activation analysis and gamma irradiation programs have been initiated.

This paper describes the processes used to increase the reliable operation of HFIR and the utilization of all of the reactor's capabilities.

Development of a Sustainable Risk & Reliability Management Program

Historically HFIR operation was focused on maximizing runtime for isotope production and neutron scattering, not predictable operations. After 35 years of operation, there were several years of unreliable operation that included numerous unplanned shutdowns and startup delays caused by equipment reliability issues. Neutron science upgrades made over the last five years have resulted in increased demand by the scientific community, making a focus on predictability essential to accommodate the growing user base.

In 2007, a Reliability and Risk Management Program was initiated to improve long-term safe, reliable, and efficient HFIR operation in order to support the neutron science mission beyond 2040. The initial phases of the reliability program development included:

- management team benchmarking trips to power reactors;
- engagement of staff to identify existing reliability threats;
- review of existing nuclear power industry guidance and tools related to reliability;
- establishment of a partnership with the Electric Power Research Institute; and
- consultations with reliability and risk management subject matter experts.

The HFIR management plan (focused on people, processes, and equipment) relies upon the Reliability and Risk Management Program as the method in determining work priorities to ensure the availability and predictability of the reactor. The Reliability program has established four goals; understand current threats and potential future threats to reliability, ensure resolutions to threats are implemented and, by ongoing re-examination, ensure new threats are not created.

Reliability Program Goal 1: Understand current threats to reliability

Four processes are in place to understand the current threats to plant reliability and understand the risk of these issues.

The Plant Health Committee is tasked with monitoring plant performance and taking actions necessary to improve plant reliability. The committee is comprised of members of the management team and first line supervisors. Items routinely presented to the committee include: system health reports, condition monitoring reports, outage critiques, post-job reviews, reliability treat tracking, 3-year plan updates, personnel safety improvements, and emergent issues.

System health reports (Figure 1) consolidate information from a number of sources to create a snapshot of the health and reliability of the system. These semi-annual reports for 16 system groupings are designed to identify potential system threats in a comprehensive and actionable format.

Each system grouping is reported on by a team with members from engineering, maintenance, operations, and nuclear safety. Information contained in the report includes: system health indicators, recommendations for resolution, issues and concerns resolved since last report, system reliability concerns including spare parts deficiencies, open safety basis items, planned work activities, system configuration and material condition walk-downs, and a summary of overall system health.

SYSTEM HEALTH REPORT		REV: 3	HWMP-2020.1 Page 1 of 3
Equipment and Installation Systems 60-0001 - New DPF Gas HEATS 60-0002 - Special Handling for Refuel (SAR) 60-0003 - Fuel Gas System 60-0004 - Steam Distribution 60-0005 - Condensate System 60-0006 - Air		Reporting Period: 1/2020 - 6/2020	
SYSTEM HEALTH INDICATORS		PREVIOUS REPORT	CURRENT
OPERATIONS	Engineered Shutdowns during the reporting period	0	0
	Open Operator Work Orders	0	1
	Open Control Room Deficiencies	0	0
	Open Standard Annotations	0	0
	Engineered Limiting Conditions for Operation (ELCO) Entries	1	0
MAINTENANCE	Surveillance Test Procedures (STP) in the Second 3 of 3s	0	0
	Open Corrective Work Orders	0	12
	Open Corrective Work Order Backlog (greater than 90 days)	0	0
	Service Preventive Maintenance (PM)	0	0
	Condition Monitoring Analysis - equipment Issues Identified	0	1
DESIGN/ENGINEERING	Open Design Modifications (i.e., DS, ACR, SCM and NCR)	22	20
	Open Drawings	14	14
	Open Temporary Modifications	0	0
	Design Modifications Open 30-day and/or 120-day Closed	2	0
	Modifications and Fabrications proceeding at risk	N/A	0
NUCLEAR SAFETY	Work in Progress (WIP) incidents	N/A	1
	Potentially Inadequate Safety Analysis Determinations (PISAD)	N/A	0

Figure 1: System Health Report Cover Page

System health indicators (Figure 2) are part of the system health reporting process conducted on 16 system groupings semi-annually. Operations, maintenance, engineering, and nuclear safety indicators are used to highlight past achievement and predict future performance allowing trends within the indicators for a system grouping to be identified as well as trends across systems for the specific indicators. Indicators are consolidated, trended, and reported to Plant Health Committee.

SYSTEM HEALTH BY SYSTEM GROUP		SYSTEM HEALTH INDICATORS															
Report of: Overall Reporting 1st - December 2019		Report of: Overall Reporting 1st - December 2019															
System Grouping		Engineered Shutdowns	Open Operator Work Orders	Open Control Room Deficiencies	Open Standard Annotations	Engineered Limiting Conditions for Operation (ELCO) Entries	Surveillance Test Procedures (STP) in the Second 3 of 3s	Open Corrective Work Orders	Open Corrective Work Order Backlog (greater than 90 days)	Service Preventive Maintenance (PM)	Condition Monitoring Analysis - equipment Issues Identified	Open Design Modifications (i.e., DS, ACR, SCM and NCR)	Open Drawings	Open Temporary Modifications	Design Modifications Open 30-day and/or 120-day Closed	Modifications and Fabrications proceeding at risk	Work in Progress (WIP) incidents
60-0001 - New DPF Gas HEATS		0	0	0	0	1	0	0	0	0	0	0	0	0	0	0	0
60-0002 - Special Handling for Refuel (SAR)		0	0	0	0	0	0	0	0	0	0	0	0	0	0	0	0
60-0003 - Fuel Gas System		0	0	0	0	0	0	0	0	0	0	0	0	0	0	0	0
60-0004 - Steam Distribution		0	0	0	0	0	0	0	0	0	0	0	0	0	0	0	0
60-0005 - Condensate System		0	0	0	0	0	0	0	0	0	0	0	0	0	0	0	0
60-0006 - Air		0	0	0	0	0	0	0	0	0	0	0	0	0	0	0	0
60-0007 - New DPF Gas HEATS		0	0	0	0	1	0	0	0	0	0	0	0	0	0	0	0
60-0008 - Special Handling for Refuel (SAR)		0	0	0	0	0	0	0	0	0	0	0	0	0	0	0	0
60-0009 - Fuel Gas System		0	0	0	0	0	0	0	0	0	0	0	0	0	0	0	0
60-0010 - Steam Distribution		0	0	0	0	0	0	0	0	0	0	0	0	0	0	0	0
60-0011 - Condensate System		0	0	0	0	0	0	0	0	0	0	0	0	0	0	0	0
60-0012 - Air		0	0	0	0	0	0	0	0	0	0	0	0	0	0	0	0
60-0013 - New DPF Gas HEATS		0	0	0	0	1	0	0	0	0	0	0	0	0	0	0	0
60-0014 - Special Handling for Refuel (SAR)		0	0	0	0	0	0	0	0	0	0	0	0	0	0	0	0
60-0015 - Fuel Gas System		0	0	0	0	0	0	0	0	0	0	0	0	0	0	0	0
60-0016 - Steam Distribution		0	0	0	0	0	0	0	0	0	0	0	0	0	0	0	0
60-0017 - Condensate System		0	0	0	0	0	0	0	0	0	0	0	0	0	0	0	0
60-0018 - Air		0	0	0	0	0	0	0	0	0	0	0	0	0	0	0	0

Figure 2: System Health Performance Indicators

The HFIR Top Ten list prioritizes equipment deficiencies impacting HFIR operations and is included in system health reports as a distinct set of performance indicators.

Reliability Program Goal 2: Identify and mitigate potential future threats

The Aging Management Program was developed based on guidance from the United States Department of Energy, the nuclear power industry, and the International Atomic Energy Agency. The program focuses on improving long-term reliable operation addressing both active and passive equipment.

- Passive equipment includes reactor vessel and pool liner, primary coolant system pressure boundary piping, confinement ducting, and select electrical components. This equipment is monitored through a variety of internal processes and individual aging management plans which identify degradation mechanisms, appropriate condition monitoring, and techniques for extending operation, repair/replacement plans, and remaining life/cost estimates.
- Active equipment that is life-limiting and involves major work scope requiring additional resources for extended outage time outside the scope of the normal annual budget is managed by the HFIR plant life extension (PLEX) infrastructure upgrade plan. PLEX items (Figure 3) are treated as individual upgrade projects and integrated into the routine operations and maintenance work plans.



Figure 3: PLEX Refurbishments & Improvements have Increased Predictability

The Preventative Maintenance Optimization (PMO) methodology used at HFIR focuses on improving maintenance effectiveness and equipment reliability by comparing existing maintenance activities and frequencies with nuclear power industry practices. The outcomes of PMO included:

- a shift to a more condition based maintenance philosophy,
- extension of frequency of many intrusive “overhaul” time-based tasks,
- removal of several time-based tasks that provided little to no benefit relative to cost, and
- significant improvements in resource utilization allowing the redeployment of existing resources to execute more planned equipment upgrades.

Condition monitoring of equipment parameters is performed to identify significant changes that may be indicative of a developing failure. Condition monitoring technologies used at HFIR include: vibration, lube oil, thermography (Figure 4), and ultrasonic. Data and analysis are reported each reactor operating cycle for the purpose of communicating recognized trends and allowing maintenance to be scheduled before failure occurs.

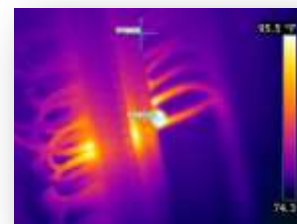


Figure 4: Thermography Image of Control Circuit Loose Wire

Reliability Program Goal 3: Track and implement resolutions to threats

The Plant Health and Reliability Action Tracking (PHRAT) system provides a comprehensive means of identifying and tracking reliability threats. Built-in categorization tools provide the ability to focus on specific areas (e.g., system vulnerabilities, critical spares, plant life extension upgrades, Operations top-ten list). Periodic status updates ensure management awareness of issues critical to plant reliability.

The HFIR 3-Year Plan is a rolling graphical representation of major work scope and related activities for future operating and outage cycles focused on ensuring HFIR availability and predictability. The plan is regularly updated to reflect status and work priorities adjustments to mitigate reliability threats and accommodate user needs.

The RRD Integrated Work Plan quantifies work scope and necessary resources required to implement United States Department of Energy and stakeholder priorities, as reflected in the HFIR management plan. It incorporates operations, maintenance, plant life extension upgrades, and other requirements in an integrated fashion that allows prioritization and risk management.

Reliability Program Goal 4: Avoid introducing new threats to reliability

The Reliability-Focused Design Process integrates general safety and reliability principles as well as design considerations for system reliability into the existing plant modification process. Design considerations for system reliability include:

- Design to avoid single point vulnerabilities
- Design with maintainability in mind
- Design to provide flexible control systems
- Design the system to be as simple as practical
- Design components to meet the requirements of their application
- Consider spare parts and consumable needs required by the design

Increased Utilization and Science Output

Over the past 5 years, HFIR has made deliberate efforts to increase reactor utilization and to add capabilities that benefit scientific programs; some examples include:

- Successful commissioning of the HFIR Cold Source with two small-angle neutron scattering instruments, cold triple-axis spectroscopy, and neutron imaging.
- Redesign of target rod experiment holder resulting in a ten-fold increase in material and isotope irradiation capacity
- Upgraded detectors and facility infrastructure in the neutron activation analysis lab which is particularly useful in assessing non-proliferation monitoring samples collected by the IAEA.
- Added a gamma irradiation facility (Figure 5) utilizing HFIR spent fuel core with 1×10^8 Rad/hr capabilities allowing for very fast replication of long-term radiation effects used in environmental qualification testing capabilities.



Figure 5: Gamma Irradiation Facility

These efforts have resulted in dramatic increases in utilization (Figure 6) over the past 2 years, and current projections indicate that even more irradiations are anticipated in the coming years.

Last year's marked increase in reactor utilization included:

- 173 Neutron Scattering and Material Science Publications
- 436 Materials Irradiations
- 585 Neutron Activation Analysis Irradiations
- 98 Commercial and Medical Isotope Irradiations
- 1,300 Users conducted 730 Unique Neutron Scattering Experiments

The increase in utilization is a result of several factors. First, proactive efforts to better understand the science programs currently performing research at HFIR were initiated. Working closely with these programs brings knowledge of the HFIR facilities directly to the scientists making decisions on what types of irradiations they wish to pursue. Additionally, an outreach program for disseminating information about HFIR through various conferences, user facilities and meetings around the world has been implemented.

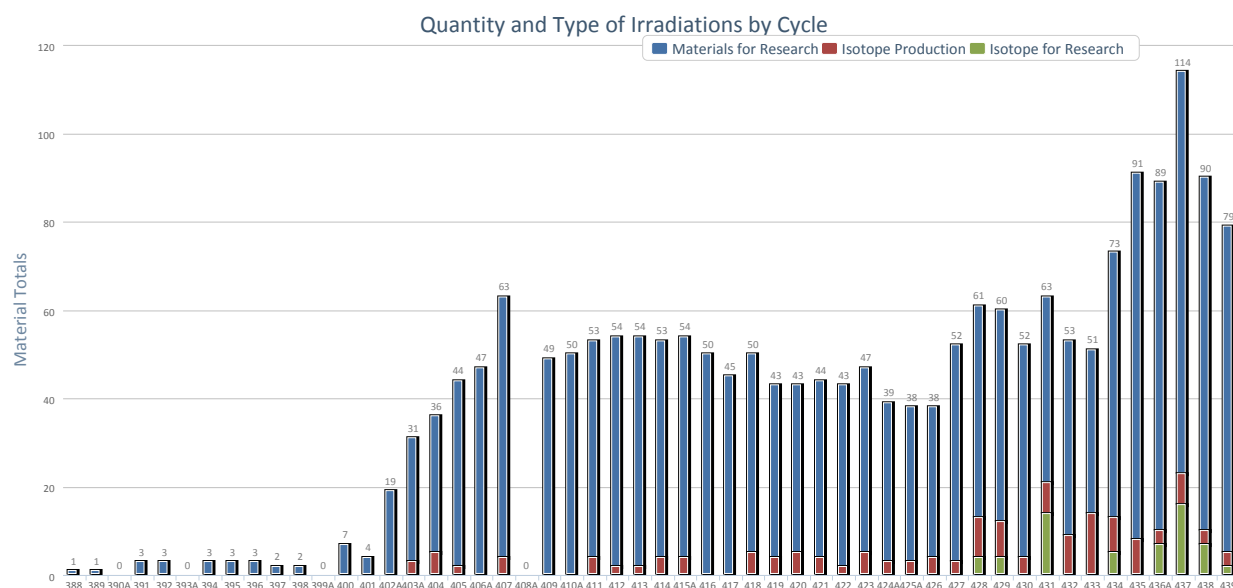


Figure 6: Illustration of Increase in Material and Isotope Irradiations

Outcomes of Implementation of the Risk and Reliability Management Program

Since 2007, reactor predictability has been >98% due to reliability program implementation and the resulting plant equipment upgrades. The tools are now in place to support safe, reliable, and efficient HFIR operations beyond 2040.

And finally, the most important factor in our increased utilization is our ability to accurately plan and predict reactor cycles for several years; a direct result of the reliability program.

Conclusion: It is possible to improve reliability at a research reactor by applying targeted reliability principles with established goals and alignment of resources.

STATUS OF AGEING MANAGEMENT PROGRAM FOR HANARO

JIN-WON SHIN, JUNG-HEE LEE, HYUNG-KYOO KIM, AND HOAN-SUNG JUNG

HANARO Management Division, Korea Atomic Energy Research Institute

989-111 Daedeok-daero, Yuseong-gu, Daejeon 305-353, Korea

ABSTRACT

HANARO is a 30 MW open pool type research reactor which has been operated for 16 years since its initial criticality in February 1995. It has been used for nuclear material testing, radioisotope production, neutron transmutation doping, nuclear activation analysis, and neutron scattering experiments. The plant life time is expected to be much more than the design lifetime by a safety reassessment based on realistic data and maintenance activities for an ageing management. Three kinds of system inspections, which consist of Surveillance Inspection (SI), Periodic Inspection (PI) and In-Service Inspection (ISI), are performed to maintain the system, structures, and components (SSCs) of the reactor in a safe condition. According to the results of inspections, many kinds of maintenances have been performed in appropriate ways. Maintenance activities are for correction, prevention, and ageing management program.

1. Introduction

HANARO is a 30 MW open-pool type multi-purpose research reactor which is operated by KAERI, the Korea Atomic Energy Research Institute. The initial criticality was achieved in Feb. 1995 and has been utilized for various purposes.

As key activities of our ageing management, three kinds of system inspections, which consist of Surveillance Inspection (SI), Periodic Inspection (PI) and In-Service Inspection (ISI), are performed to maintain the system, structures and components (SSCs) of the reactor in a safe condition. The SI is for the safety grade components and should be accompanied by a quality assurance procedure, while the PI is for non-safety grade and not necessarily mandatory. The ISI is carried out for the ASME Sec. III components such as reactor structures, reactivity control units, and safety related piping systems. According to the results of inspections, many kinds of maintenances have been fulfilled in appropriate ways. The corrective and preventive maintenances for the primary cooling system, the

primary purification system, and the reflector cooling system were performed. The vibration monitoring system for the above 3 systems has been constructed for the predictive maintenance. The fission chambers were replaced and the electric system for the power supply was overhauled for the preventive maintenance. The safety diagnosis and reinforcement for an effective life management and the safety of the building structures such as the reactor building, stack, secondary cooling system equipment room and cooling tower were performed. The upgrade of the instrumentation and control system has been carried out gradually since 2001 to overcome ageing and obsolescence problem. The conducted ISIs, maintenance activities and the future plan of the ageing management for HANARO are presented in this paper.

2. Maintenance history

The SI and PI were done according to the fixed interval periodically. The ISIs were carried out for the ASME Sec. III components such as reactor structures, reactivity control units, and safety related piping systems. According to the results of inspections, many kinds of maintenances have been fulfilled in appropriate ways. Maintenance activities are for correction, prevention and ageing management program. The major activities for system maintenance were in Table1.

Year	Activities
1996	- Replacement of a secondary pump(P3)
1997	- Installation of a hot water layer system
1999	- Replacement of heat exchanger plate(HX1, HX2)
2000	- Replacement of filler for cooling tower
2002	- Installation of a Window-based Operator Work Station
2003	- Overhaul of diesel generator
2004	- Measurement of reactor vessel inner-shell straightness and visual inspection of SOR/CAR and fuel channels - Overhaul of a primary cooling pump(P2)

	<ul style="list-style-type: none"> - Removal of scale in the secondary side of primary heat exchangers(HX2) - Overhaul of a reflector pump(P2)
2005	<ul style="list-style-type: none"> - Installation of a steel compartment to confine D₂O reflector system components - Replacement of entrance doors to the reactor hall for physical protection - Extended endurance test of SOR for life extension - Overhaul of a primary cooling pump(P1) - Removal of scale in the secondary side of primary heat exchangers(HX1) - Overhaul of a reflector pump(P2) - Replacement of the UPS system
2006	<ul style="list-style-type: none"> - Replacement of NaI detectors with delayed neutron detectors for a failed fuel detection system - Installation of gamma ion chambers for power measurement and a trip signal replacing the thermal power measurement system - Overhaul of the compressed air system - Safety review and repair of the reactor building and cooling tower buildings
2007	<ul style="list-style-type: none"> - Upgrade OWS to integrate the FTL system - Installation of two large tanks in the reactor hall for the temporary storage of pool water - Re-structuring of the user rooms in the reactor hall for the improvement of fire-resistance - Installation of a voltage sag compensator to prevent the reactor trip

	<p>due to a momentary interruption of electric power</p> <ul style="list-style-type: none"> - Overhaul of the electrical system - Replacement of filler of cooling tower
2008	<ul style="list-style-type: none"> - Replacement of two neutron detectors(RPS-B, RRS-A) - Repair of most welding areas of service water supply piping line
2009	<ul style="list-style-type: none"> - Upgrade OWS to integrate the CNS system
2010	<ul style="list-style-type: none"> - Replacement of three neutron detectors((RPS-A,C, RRS-B)
2011	<ul style="list-style-type: none"> - Overhaul of a reflector pump(P1) - Replacement of two secondary pumps(P1,P2)

Table1 Major maintenance activities

3. Ageing management program

Ageing management is performed in two categories, a normal scheduled maintenance for obsolesced structures, systems and components and a special maintenance for a physically aged SSCs. Problems by obsolescence can be expected by experiences and information from the markets and peers. And ISI and special inspection can monitor effects and performances of physical ageing of the SSCs.

The purpose of an ISI is to assess the status of reactor structures, systems and components related to safety in terms of an ageing effect. Several mechanical structure and components in HANARO are classified into ASME code Section III components which require ISI during a reactor operation. The period of ISIs is in table 2.

Component	Inspection Item	Period
Reactor Structure & Beam tube	Visual inspection - reactor structure & beam tube	5 year
	Measurement of vertical straightness - inner shell of reflector tank	10 year
	Measurement of diameter - fuel flow tube	10 year

RCU	Visual inspection - CAR & SOR	5 year
	Wear inspection - carriage and track	10 year
	Measurement of diameter - shroud tube	10 year
Neutron detector	Torque test	5 year

Table 2 ISI plan for the reactor and RCU

Hanaro is developing ageing management matrix based on the maintenance history and ISI results. And it will include results of special inspection and assessments such as periodic safety review which will be done in near future.

4. Conclusions

Many activities for a corrective maintenance and an ageing management including upgrading of the SSCs have been conducted during 16 years. And also the ISI program for HANARO was performed for the purpose of safe operation and lifetime assessment of the reactor. The ageing management is deployed as a management program already. And more systematic and effective program will be developed using an ageing matrix which includes comprehensive history data for operation and maintenance of HANARO.

5. References

- [1] IAEA SSG-10, "Ageing Management for Research Reactor"(2010)
- [2] H.K. Kim, H.S. Jung et al, "Ageing management status of hanaro research reactor",
Proceeding of the ICONE17,USA (2008)

Reactivity effects and restart after a longer maintenance break of research reactor FRM II

A. Röhrmoser,

A. Kastenmüller, R. Schätzlein, A. Pichlmaier

Forschungsneutronenquelle Heinz Maier-Leibnitz (*FRM II*),
Technische Universität München, D-85747 Garching, Germany

ABSTRACT

Extraordinary reactivity effects and the restart topic had to be dealt with after a one year maintenance break of the research reactor Heinz Maier-Leibnitz (FRM II). After the first criticality in 2004 and then 25 cycles of regular reactor operation in five years of 52, later 60 days each, an extended maintenance break was scheduled for the replacement of one beam and one irradiation tube of the reactor. Both changes were supposed to influence the core reactivity, although the effect was calculated to be only marginal in both cases. The maintenance was also used for improvement in the thermal coupling between the secondary and tertiary cooling circuits of the reactor, thereby reducing the coolant temperature back to the primary circuit by about 3 K.

When restarting FRM II in October 2011 with a fresh fuel element a very clear reactivity loss was observed. This manifested itself such that the control rod had to be withdrawn significantly further than usual (about 4.4cm) and a clearly reduced control rod driveway for the first month of operation at nominal power of 20 MW. For the 2nd half of the 60 days cycle #26 the control rod followed the typical route of the previous cycles, however at a slightly lower position.

The reactivity loss at the beginning of cycle #26 has been caused by a pronounced neutron poisoning through He-3 build-up in the central beryllium moderator during the one year maintenance break. The lowered temperature of the primary coolant gives a very small reactivity gain.

Detailed neutronics calculations will be presented, which clearly explained and predicted the different effects for the cycle #26.

1 Introduction

The research reactor FRM II of the Technische Universität München (TUM) has been designed to provide a maximal thermal neutron flux outside of the core at moderate 20 MW thermal power and an operation of at least 50 days per fuel element [1]. This is achieved by placing a very compact core in a large moderator tank with heavy water (HW) and cooled by light water (LW). The reactor is running now since 2004 and fulfilled all design expectations. The cycle length could be increased to 60 full power days (FPd) per element in 2008, thus consuming some design reserve of core reactivity.

With the end of the 25th cycle of FRM II in October 2010 and after more than 5 years of regular operation a first maintenance period was scheduled to allow for improvements on both the reactor operations as well as the scientific users side. This work deals with particular reactivity influences after this maintenance break and explains the effects through detailed neutronics calculations. These were required to safely restart and explain the behaviour of the reactor after one year.

2 Replacement of two tubes

One beam and one irradiation tube of the reactor had to be replaced during the maintenance break. Both exchanges were supposed to influence the core reactivity, although the effect is calculated to be negligibly small in both cases.

2.1 Inclined beam tube SR-11

The beam tube SR-11 is the only inclined beam tube in use at FRM II. It houses the positron source at FRM II. The beam tube is quite exceptionally in its nose, being not transparent for thermal neutrons but instead extremely absorbing with a 5mm thick cup of cadmium. The isotope Cd^{113} has a large absorption cross section for thermal neutrons and produces hence energetic γ -rays, which in turn are converted into positron/electron pairs. After 25 cycles the isotope Cd^{113} was calculated to be very widely burnt and can no more guarantee the intense positron beam. The total beam tube had to be replaced and this opportunity was also taken to redesign and optimize the nose itself. To achieve this goal, a large number of calculations by use of real geometry code MCNP [2] were carried out, here for a typical mid of cycle (MOC) situation.

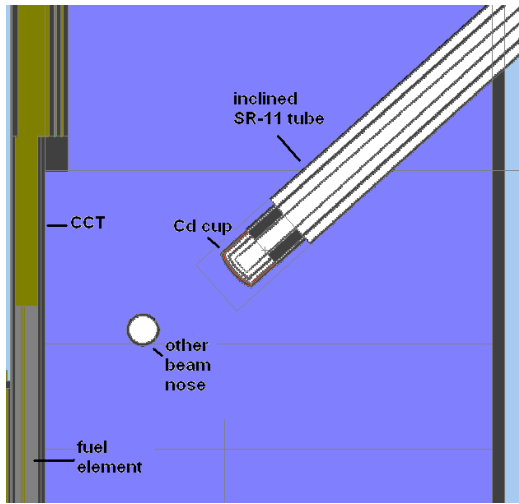
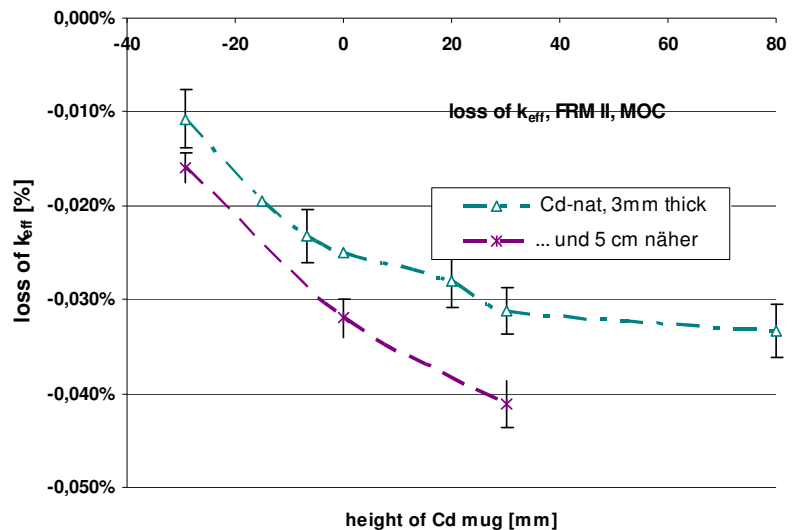


Fig. 2: calculated reactivity influence of the new inclined beam tube SR-11 at FRM II as a function of the Cd cup height; the new extends 5 cm closer to the fuel element.

Fig. 1: vertically inclined beam tube SR-11 of FRM II with a strongly absorbing nose of Cd in the heavy water tank- At the far left side the central channel tube (CCT) with a part of the fuel element is recognizable. The new tube extends 5 cm closer to the fuel element and has a modified Cd nose.



One major result was the prediction of a very tiny extra loss in reactivity with the beam nose 5 cm closer in comparison to the actual end position for several designs of the Cd nose. Because of the very tiny effect of maximum $\Delta k_{\text{eff}}=0.0001$ extra measures for the calculation had to be introduced to achieve the data of Fig. 2. This is more typical for an installation remote in the heavy water tank and remote from the core.

The final design for the tip of the tube was then a Cd-cup enriched in Cd^{113} and less high, 5 cm closer to the fuel element with the goal for higher flux output on positrons.

2.2 High flux irradiation thimble

The high flux irradiation tube of FRM II was originally designed for neutron activation and detection of very fast decaying products, but now it is the only irradiation tube in FRM II that is left free for other purposes. With the planned irradiation of LEU targets this thimble shall support a facility that shall become important for future at FRM II. The thimble is located vertically in the heavy water tank at a radius of 45 cm reaching down to the core mid plane (CMP). It had to be extended 74 cm to the bottom for the new purpose. The new thimble is no longer filled with light water from the reactor pool but He gas filled instead, to avoid a reactivity lack in comparison to the former situation.

Table 1:

Calculated reactivity effect of the new extended beam tube in comparison to the situation before 2011.

	k_{eff}	σ	Δk_{eff}	σ
former tube	1,00145	0,00005		
extended 74 cm, He	1,00157	0,00003	0,00011	0,00006
extended 74 cm, LW	1,00015	0,00003	-0,00131	0,00006

Also for this case a very small reactivity gain was calculated with $\Delta k_{\text{eff}} = +0.0001 \pm 0.00006$ for the thimble replacement in 2011. But with light water instead He filling for the new thimble the value would be pronounced negative with $\Delta k_{\text{eff}} = -0.0013 \pm 0.00006$.

The same procedure with storing neutron histories at a surface covering the installation somewhat distant from the core in the heavy water could be used. With extra calculations the focus was brought on the disturbance of this installation, comparing the two cases old and new installation, even a very tiny value Δk_{eff} is conceivable on a usual computer.

3 Reactor restart

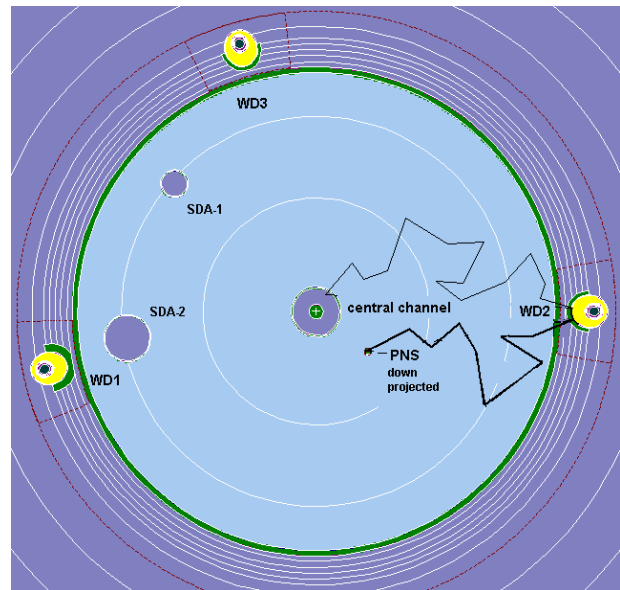
3.1 Restart neutron source after 1 year maintenance break

When restarting FRM II, as in any other reactor, some operational restrictions have to be met. One criterion is a minimum detector signal, measured simultaneously at three detectors before movement of the central control rod (CR) is allowed.

3.1.1 Detectors

Fig. 3.

Horizontal cut through the whole D₂O moderator tank and its environment at the bottom of the tank; here all three detectors (WD1,2,3) were cut as well as the central channel (CCT) for the primary coolant. At a radius of 45 cm the primary neutron source (PNS) is located at the height of the core and above it there is arranged a stack of SbBe pellets, that serve as a secondary source. The picture is taken from a simulation with the program MCNP, which calculates detector signals for fission neutrons of the core as well as from the primary and secondary source. For the latter secondary source an axial distribution was found by help of an extra activation calculation with the same code.



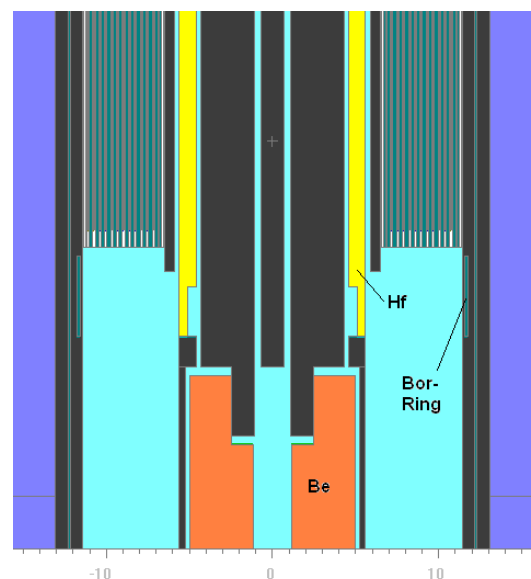
Three online wide range detectors (WDs) are distributed nearly equidistantly outside the D₂O moderator tank at about 2m distance from the core. The most restricting case at start up is with 'all shut down rods (SRs) withdrawn and the CR totally down', where all three WDs must reach the value 1.5 n/s and $5 \cdot 10^{-8} \%$ power level'. The number of neutrons from spontaneous fission of a fuel element is extremely small and could never serve this purpose. Hence other sources have to be inserted for start up.

3.1.2 Starter sources

FRM II has a primary and a secondary neutron source for a reactor restart at a radius of 45 cm from the central axis (cmp. also fig. 3).

1. The primary starter source Cf-252, which had reached 3fold the natural half-life after 8 years in a vertical thimble next to the core. This still means a high value of neutron strength, but standing alone this would not allow a reactor start any more (s. Fig. 5).
2. The secondary source of FRM II works on base of the $\text{Be}^9(\gamma, n)^9\text{Li}$ reaction, provided by a mixture of natural Sb and Be in pellets located in the same thimble above the primary source. During reactor power the Sb-123 isotope sees a high neutron flux and forms Sb-124 with a half-life of 60.3 days, providing the necessary high energy γ 's. The actual reactor pause reached finally one year, 6 times the half-life of Sb-124. Only a few % of the strength of the source were left.
3. A usual starter source is the partly burnt core through (γ, n) reactions. For the case with lost strength for external starter sources this is also an option after a clearly longer break for reactors with beryllium (Be) reflectors. FRM II has also an inside moderator (IM) part of Be. The IM is moved into the core while withdrawing the control rod (CR) during fuel burn up, what makes it difficult for use at start up, where the CR is fully inserted and the Be block is below and fully outside the fuel element. The CR shields the $\text{Be}(\gamma, n)$ reaction by blocking efficiently (long living) fission product γ 's and also blocks the few remaining neutrons on the foreseen way back to the fuel element.

Fig. 4:
Vertical cut situation at the bottom of the fuel element and the hafnium control rod in its down position. The beryllium follower is placed below the fuel element. High energetic core- γ 's from long living fission products can reach the Be unscattered only from a very small area. For starting the reactor that way the Hf CR in down position is further a clear obstacle as well as the neutronic shielding by the light water of the central channel



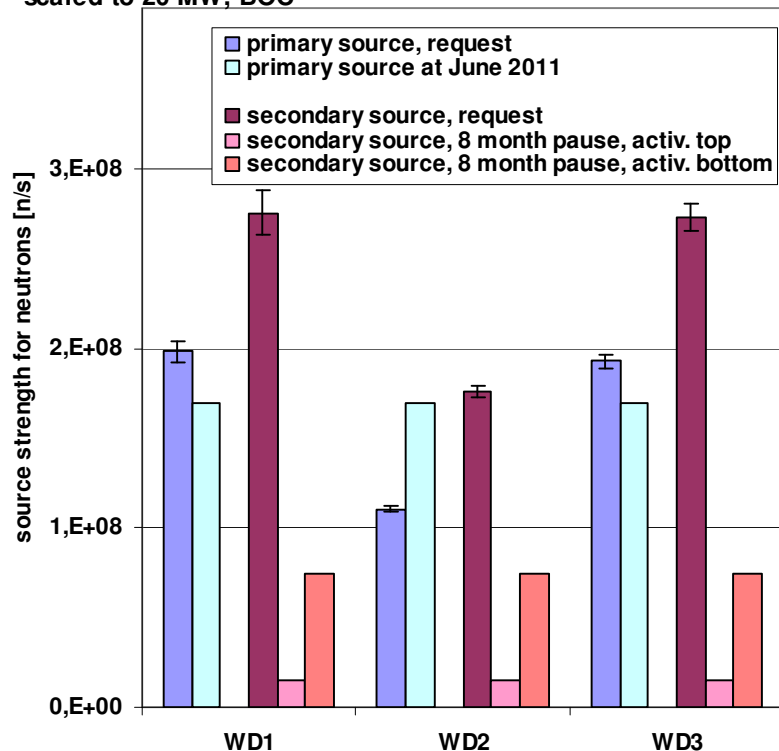
Option 3 was the foreseen start case at FRM II in 2011 but it could not be tested in the past stand alone, since there were always present and very sufficient so far the two external sources. The question that arose when the maintenance break before reactor became longer than expected was: “how much contributes each source to the detector signals and should be really started with option 3, a rather burnt fuel element instead of the fresh one?” The final answer of the theoretical analysis was:

- Starting with a burnt element is not an option for FRM II after a longer break because of the particular geometrical situation at restart.
- In the situation of 2011 one had to start with the remaining strength of the two external sources when using a fresh element. In CR down position the missing reactivity with a burnt fuel element is about twice the new element case, meaning that the multiplication of any external source is only about half of the value with a fresh element

There were very clear predictions for the detector signals resulting from the residual strength of each source. This is illustrated in Fig. 5, where first is shown the necessary strength of the two external sources to reach the minimum detector signal value $5 \cdot 10^{-8}$ % power level'. The primary source can guaranty this value at stat up conditions only at detector WD2 and hardly at the two others without support from the SbBe source. In June this would have been rather sufficient in the sum, but in October 2011 the SbBe source has seen extra 4 month pause and could contribute no more than very subordinate.

Fig. 5:
requirement and actual strength of the two starter sources FRM II in June 2011 for the criterion $5 \cdot 10^{-8}$ % power' at the three WDs (in relation to the case ,full reactor power of 20 MW), case 'start calibrations range', all ,shut down rods withdrawn, CR total inside core'.

starter sources FRM II, requirements for power signal $5E-10$ at WDs and actual estimations, scaled to 20 MW, BOC



And even more stringent than the first criterion $5 \cdot 10^{-8}$ % power' is the second one '1.5 ct/s' at any detector, as indicated when comparing protocol data of the last reactor start ups. Because of the results of this analysis in 2011 [8], it was asked for a temporary permission to start cycle #26 with a requirement of only 1ct/s. The necessity of this was clearly confirmed when the reduced count rates were just about reached at WD1 and WD3 when restarting with a fresh element.

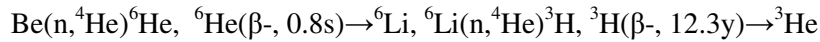
It shall be mentioned, that a very ingenious method had to be elaborated to come to the final estimations. A lot of support came with the 3d reactor model for the program MCNP [3], which calculates detector signals for fission neutrons of the core as well as from the primary and secondary sources. The primary source is well known, for the secondary source an axial activation distribution was found by help of an extra neutron flux calculation with the same code. For the yields of photo neutrons caused by γ -sources MCNP has clear support since version 4C2 [4], what helped again very much to quantify the secondary source contributions as well as to reveal a future lack with starting FRM II after a longer break with a burnt element.

3.2 Reduced reactivity at restart after one year maintenance break

When restarting FRM II in October 2011 with a fresh fuel element no criticality could be obtained at the usual critical position of the CR with a new fuel element. Obviously something yet unaccounted had changed in comparison to all former start ups with a fresh element, reactivity was obviously missing.

A first attempt for explanation with a polluted heavy water, caused during the emptying and refilling of the D_2O tank during the maintenance could be ruled out due to the measured cleanness of the D_2O . The reactivity loss caused by the replacement actions with one beam and one irradiation tube was expected to be clearly negligible, as described. Was something incorrect? Even assuming light water having penetrated into the replaced irradiation tube by a leak, would have caused not more than a small loss in k_{eff} (s. Table1).

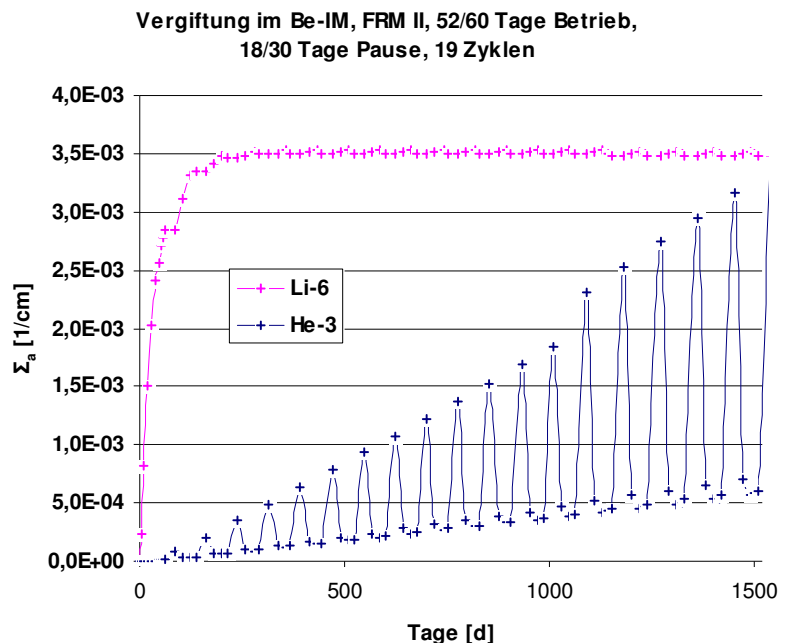
As the most plausible explanation it was identified a poisoning of the beryllium moderator (IM) with ^3He ($\sigma_{\text{th}} = 5330 \text{ b}$), what is produced through β -decay of the Be activation product tritium with $T_{1/2}=12.3 \text{ years}$.



This effect was already studied in principle for FRM II and documented in the annual report 2009 [5]. There were given diagrams for the top and the bottom part of the IM (s. original diagram Fig. 6 for the Be-IM top part in Picture 4) clearly showing the build-up of the macroscopic absorption cross section in the Be-IM through decay off tritium to ^3He during the short reactor stops of usually 2 or 3 weeks. There the poisoning is still of small effect for any start up, but linearly increasing with the number of cycles. At the end of any cycle remains a very small poisoning, but also increasing with reactor operations time. A closer survey of those diagrams and linearly extrapolating to a break of one year gave convincing indications for a remarkable poisoning in the beryllium with He-3 after one year stop.

Fig. 6:

Poisoning in the top part of the Be IM after 52/60 days of full power, calculated for the first 19 fuel element operations in an ideal cyclic manner. The absorption cross section contribution of He-3 in the Be goes clearly up during the typical reactor stops of 2 or 3 weeks and the peak increases also with each operations cycle. When linearly extrapolating to an operations break of 50 weeks the contribution of He-3 will have increased dramatically after 25 cycles.

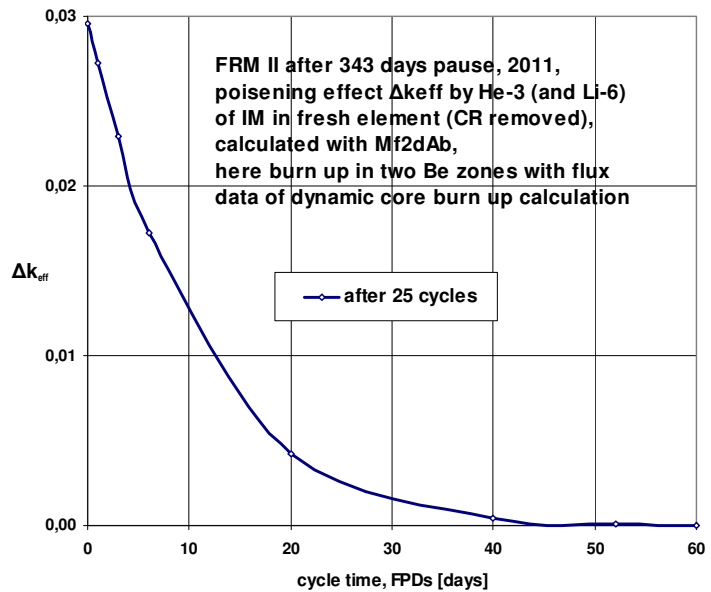


The qualitative explanation was not regarded sufficient evidence by the reactor operation responsible and it was requested a quantitative estimation with a calculation before the next attempt for further pulling the CR. So the reactor physicist was asked for a reliable simulation, which would predict the new critical control rod position. Thanks to a very modular system on base of RSYST[&] the module sequence Mf2dAb [6] (the one that gave already the results as outlined in fig. 6) could be modified over night for a further simulation up to 25 operations cycles and a stop afterwards of 343 days. Taking into account the basic poisoning of the Be-IM, the simulation predicted a 4½ cm higher CR in comparison to the critical position for the last cycle #25 after usual 3 weeks of FRM II pause (s. Fig. 6). And this was found to be absolute correct, when starting then nearly without delay.

Without being pressed for time so much following calculations with the same procedures gave further results. A total reactivity loss through the poisoning of the Be of $\Delta k_{\text{eff}}=0.030$ was calculated with totally inserted Be-IM (since at critical position the lower part of the Be is out of the core, the disturbance is somewhat smaller there, cmp. above). As outlined in fig. 6 the poisoning, caused by the stop itself, will disappear mainly during the first half of full power operation and totally after 50 days of the cycle.

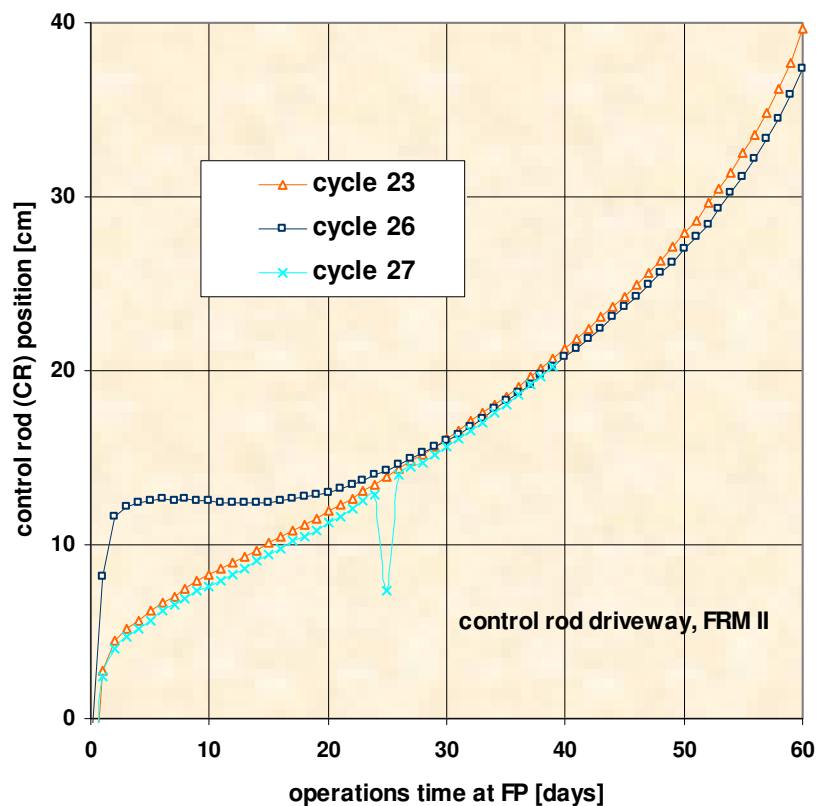
[&] A modular system for a wide variety of nuclear reactor calculations on base of RSYST, IKE Stuttgart, 1980's.

Fig. 7:
poisoning influence by He-3, Mf2dAb of
fresh fuel element in FRM II on value k_{eff}
when CR removed in calculation after 343
days pause in 2011 after 25 cycles of opera-
tion



During this 2011 cycle this manifested itself in an increase of the control rod position for first criticality by 4½ cm, a higher value the first days and then a very flat CR route for the first 3 weeks of operation at nominal power of 20 MW (s. figure 7). For the 2nd half of the 60 days cycle #26 the control rod followed the route of all previous cycles, however slightly lower at the end. At the actual running cycle #27 the He-3 poisoning influence is not pronounced because of the break of only 4 weeks and a slightly lower CR route seen at the end of cycle #26 continued in the first half of cycle #27.

Fig. 8:
driveway of CR of FRM II
during the last no-stop cycle #23
and the new cycle #26 starting in
October 2011 respectively the
actual running cycle #27.



The maintenance was also used for improvement in the thermal coupling between the secondary and tertiary cooling circuits of the reactor, thereby reducing the coolant temperature back to the primary circuit by $\Delta T = 3\text{ K}$. An analysis with [7] suggests all together a gain of only $\Delta k = 0.0003$ at 3K reduced temperature at primary and moderator coolant circuit, what would correspond to a 5-6mm lower end position of the CR after 60day FP operation. In fact cycle #26 ended lower (and #23 higher) than usual, but in the range of spread of CR end positions of actually 12 cycles with 60 FPd.

SUMMARY

During a one year maintenance break at research reactor FRM II one beam and one irradiation tube were replaced with new dimensions. The reactivity influence was expected to be nearly zero. Instead a big loss was realized when trying to go to power after the one year operations pause. This could be very well and quantitatively explained in very short time thanks to a very modular system describing a variety of reactor physical aspects under full power operation. Here a pronounced poisoning by He-3 in the Beryllium was identified as the clear cause. The poisoning could not be registered at the very first actions during start up, where the control rod of FRM II is totally down and the beryllium outside the core without reactivity influence. But when going to power by pulling the CR the poisoning manifests itself in a clear higher critical position of the CR. During the cycle the extra He-3 poisoning disappears totally, as predicted. The driveway of the cycle #26 in 2011 was finally slightly lower than usual, what corresponds to a small gain in reactivity by reducing the coolant temperature in the primary and moderator circuit by about 3 K, caused by better thermally coupling the secondary and tertiary cooling circuits of the reactor during the maintenance break in 2011.

After photonuclear studies for different options of start up sources for FRM II it was decided to start again with a fresh fuel element in Oct. 2011 and a temporarily permission for slightly reduced count rates at the three low power detectors. The practice confirmed this.

REFERENCES

- [1] "Physics of the Munich Compact Core Design", RERTR Conference 1988, San Diego, K. Böning, W. Gläser, A. Röhrmoser
- [2] "MCNP - A General Monte Carlo N-Particle Transport Code, Version 4C", LA-13709-M (April 2000), authored by J. F. Briesmeister
- [3] "Core Model of new German Neutron source FRM II", Nuclear Engineering and Design, June 2010, A. Röhrmoser
- [4] "New MCNP4C2 Features, Photonuclear physics", Los Alamos National Laboratory, Jan. 2001, J. Hendrix, M. White's doctoral dissertation integrated
- [5] "Neutronical Evaluations for operation of FRM II", Yearly Report of Operation of FRM II, 2009
- [6] „Neutron physical optimization and layout of a research reactor of moderate power with aim for high flux for beam tube experiments“, A. Röhrmoser, PhD thesis work at TU Munich, 1991, physics department
- [7] "Siede- und Temperaturkoeffizienten der Kompaktkernanordnung des geplanten FRM-II", A. Röhrmoser, internal report at TU Munich, March 1990
- [8] „Anfahrquellen FRM II, Anforderung und Ist-Stärke 2011“, internal report, FRM II, A. Röhrmoser, June 2011

New / Updated Safety Requirements from Nuclear Research Installations Operators in the Russian Federation

Alexander Sapozhnikov

Federal Environmental, Industrial and Nuclear Supervision Service of Russia (Rostekhnadzor),
109147 Moscow, Taganskaya, 34, Russia

ABSTRACT

The report is devoted to status of safety requirements and their development as a result of licensing, peer reviews, inspections, investigations of incidents and technical meetings on improvement of national safety norm, rules and regulations for Nuclear Research Installations (NRIs)¹ in the Russian Federation.

1. Introduction

The safety requirements currently in force in the Russian Federation are being developed as accumulation of scientific and technical knowledge and experience of Nuclear Research Installations use starting from the first in Eurasia research reactor F-1 (24 KWt, Moscow, 25 December 1946) and the First in the World Nuclear Power Plant AM (30 MWt, Obninsk, 27 June 1954). The purpose of the report is to show up-to-day safety requirements in the Russian Federation and their further perfection resultant changing of the legislation in the field of nuclear energy use, needs of development of nuclear energy, technology and science as well as lessons learned from operating experience of NRIs.

2. Genesis of safety requirements to NRIs in Russian Federation

The NRIs' safety background being in force till the late 90s reflected the level of technology of NRIs creation, achieved in the late 70's of past century. Two safety principals have been declared forming the strategy of defence-in-depth: 1) accident prevention, and 2) accident mitigation. The requirements to structure of protective barriers and levels have been presented in safety regulations. Protective levels have determined: 1) requirements to systems of normal operation; 2) requirements to safety systems designed specifically to fulfill safety functions in case of disturbances of normal operation, 3) requirement to the methods and means of accident mitigation. The system of technical and organizational measures defence-in-depth concept consists of five levels. Later on the necessity to improve the safety reference basis for NRIs was determined by increased park of NRIs, deployment of advanced NRIs, enhancement of the safety criteria and principles. To further decrease potential hazard the inherent safety characteristics are being envisaged in the design and construction of NRIs, including the following: increase of operational parameter margins; decrease of process variables; choice of proper structural materials; decrease of reactivity margin; use of degenerative feedback and self-quenching of possesses; use of passive components in protection systems that do not need a power supply; providing of inertial process with enough time for personnel intervention to prevent cliff edge effects leading to severe accident. It was also necessary to develop and implement the requirements and procedures for the NRI's nuclear materials safeguard, methods of NRIs safety assessment (independent expertise), guarantee the loss compensation due to possible accidents.

¹ NRIs – nuclear facility consisting of research reactor (RR) or critical assemble (CA) or subcritical assemble (SCA) and complexes of structures, systems, components and experimental facilities with incorporated workers (personnel) within territory defined by design (NRI site) for utilization of neutrons and ionizing radiation for research purposes.

Reactor facility – NRI that composed a research reactor (RR) in structure; Critical Stand (CS) – NRI that composed a critical assemble (CA) in structure; Subcritical Stand (SCS) – NRI that composed a subcritical assemble (SCS) in structure

Formidable national park of research facilities, which have different construction, power and utilization, has motivated graded approach to nuclear safety requirements and development of different nuclear regulations for RRs, excluding pulse RRs, (1975), for pulse RRs (1977), for CA (1978), and for SCA (1975). Since the Federal Law on the Use of Atomic Energy № 170-FZ was put in force in 1995 safety requirements NRIs were analyzed for compliance with new legislation and the reference levels developed by IAEA.

3. Reference level of safety requirements to NRIs in Russian Federation

At present the state system of nuclear safety regulations is developing in accordance with the international obligations of the Russian Federation concerning nuclear safety and security as well as civil liability for nuclear damage. Structure of Federal Norms and Rules (FNR) includes two levels of documents and safety requirements [1]:

- General provisions for safety ensuring of each type of the facilities using atomic energy (Nuclear Power Plant - NPP, Nuclear Research Installation - NRI, Nuclear Installation on Ships - NIS, Nuclear Fuel Cycle Facility - NFCF, Radioactive Sources - RS)

- Regulatory documents pertaining to types of activity:

- ⇒ Common for all types of nuclear facilities including requirements on external impact (NP-064-05), requirements on design and safe operation of equipment and pipelines of nuclear facilities (PNAE G-7-008-89), on radiation safety (NRB-99/2009, OSPORB-99/2010), on account and control of nuclear materials (NP-030-05), on account and control of radioactive substances and radwastes (NP-067-2005), on physical protection of nuclear materials, facilities and storages (Degree of Government of Russian Federation from 19 July 2007, № 456), on nuclear fuel storage and transportation (NP-061-05), and other.

- ⇒ Specific requirements for each category of nuclear facilities (NPP, NRI, NIS, NFCF, RS) including quality assurance, siting, design, safety justification, commissioning, operation, emergency preparedness, decommissioning.

The brief description of updated and new safety requirements are given below.

4. Updated and new safety requirements to NRIs in Russian Federation.

4.1. General Provisions on Safety of Nuclear Research Installations, NP-033-11

The document belongs to higher level of safety regulations and determines the main principles and general requirements to safety at all stages of NRI life time: design, siting, construction, putting in operation, operation and decommissioning. The first version of document entitled "General provisions for safety assurance of research reactors", OPB-IR 94, 1995, had been developed taking into account the safety principles for nuclear power plants (OPB-88) and had been applied only to RRs. The document included classification of structures, systems and components (SSC), safety requirements to RR's design, commissioning, put in operation and operation, measures to protect personnel and public in case of emergency, general provisions for decommissioning. The second version of the document NP-033-01, 2002, has been applied to all categories of NRIs. The last version of the document NP-033-11, 2011, includes safety requirements to contents of "Technological Regulations of NRI" that shall contain design limits and operating conditions as well as the list of obligatory operation procedures. The requirements to subcriticality of NRI in the temporary shutdown regime and long-term shutdown regime have been specified. The main specifics concerning the shutdown modes briefly described below:

- Temporary shutdown regime - the mode of NRI operation necessary for maintenance, including planned renewal, test of efficiency of systems, important to safety, fitting out of new experimental facilities/devices and preparation of experimental researches. In this mode the subcriticality (shutdown margin) shall be provided not less 2 % regardless of position of safety rods.

- Long-term shutdown regime - the mode of NRI operation including preservation of some systems and equipment and maintenance of NRI during the time when experimental researches at NRI is not being planned. At decision making about NRI transition in a mode of long-term shutdown regime operating organization shall develop the measures which would

provide NRI safety in a mode of long-term shutdown regime and prevent untimely ageing of SSC, including corrosion of fuel cladding in the NRI core and/or in storage. In this mode the subcriticality (shutdown margin) shall be provided not less 5 % and excluded power supply to drives of control system, experimental facilities/devices and fuel loading.

- Final shutdown regime - the mode of NRI operation to prepare NRI for decommissioning, including removal of nuclear material from the reactor core and its removal from NRI site.

The graded approach is reflected in FNR considering the scope of nuclear safety requirements. The majority of NRIs were designed, built, put in operation on the basis of the first versions of nuclear safety regulations developed in second half of 70s last century in former USSR for RRs, pulse RRs, CA and SCA. These documents were in force more than twenty years and were revised in 1995 in parallel with development of "General provisions for safety assurance of research reactors", OPB-IR 94. Since the "General provisions on safety of NRIs" (NP-033-01) was put in force in 2002 the nuclear safety regulations were harmonized and new versions of nuclear safety regulations for RRs (NP-009-04), for pulse RRs (NP-048-03); for CS (NP-008-04) and SCS (NP-059-05) were put in force.

4.2. Nuclear safety regulations for research reactors, NP-009-04

The document contains engineering requirements to the reactor core configuration and its parameters, to experimental facilities, to primary cooling circuit, to normal control system, important to safety, and to emergency control systems. They contain safety requirements to start-up and power operation modes, safety requirement for handling with nuclear materials and fuel. The list of obligatory safety documents that shall be developed for RR is attached in NP-009-04. As distinct from nuclear safety requirements to reactor of power plants documents includes the requirements to experimental facilities/devices, specific requirements to control and protection system that shall prevent potential failures of the experimental facilities and the reactor core, requirements to carry out an experimental work and other features specific for operation of RRs.

4.3. Nuclear safety regulations for pulse reactors, NP-048-03

Pulse reactor acts a short interval of time but with high power. Specific of pulse reactor consists in prompt neutron kinetics. As opposed to RRs with steady-state neutron flux the pulse reactors have not any limits for insertion of positive reactivity in the reactor core. Distinguish two types of pulse reactors: self-quenching burst (aperiodic) and with reactivity modulation, batch-type (repetitively pulse, periodic) reactors. The safety requirements to design take into account features of both mentioned types including pulse reactors with dissolved fuel (solution) pulse reactors. In some designs two coupled reactor cores are used with corresponding control systems and protection system.

4.4. Nuclear safety regulations for critical stands, NP-008-04

The document establishes requirements to the design of critical assemble and engineering systems of the CS, requirements to technical-organizational measures of their operation. Specifics of critical stand operation follows from very frequent changing of equipment and the core reconfigurations that is being carried out as often as each start-up of the installation. The graded approach is applied to modifications of SSC according to their safety significance:

- reconstruction – changing of SSC that results to changing of established in the design initiating events of design basis accidents (DBAs), beyond design basis accidents (BDBAs), and a list of limits and conditions of safety operation and the new safety assessment report shall be developed in result;

- modernization - changing of SSC that results to correction of the existing limits and conditions of safety operation of CS and amendment of SAR of CS (for instant replacement of SSC or installation of new one) shall be developed in result;
- modifications of critical assemble (its replacement or reconfiguration) within parameters of critical assemblies that have been foreseen in the design of stand and justified in SAR;
- changing of SSC that do not have an impact on determined limits and conditions of CS safety operation;
- changing of SSC that do not impact on safety CS.

4.5. Nuclear safety regulations for subcritical stands, NP-059-05

The specific of safety requirements to subcritical stands (SCS) as compare with critical stands (CS) consists in scope of used control and protection system and components. For instance if the effective reproduction of SCS less than 0,98 it is possible to operate installation without the neutron flux control channels and scram rods. Otherwise the technical and organizational safety requirements are closed to safety requirements for CS.

4.6. Nuclear safety regulations for subcritical electronuclear neutron generator (accelerator driven system -ADS)

The specific of subcritical electronuclear facility excludes self-sustaining nuclear reaction. An interest for design of such installations is being determined by possibility to resolve two problems simultaneous: to generate electricity and to utilize radiation waste. The design of subcritical electronuclear plant is at research study and engineering development. In addition to subcritical electronuclear neutron generator the research of space nuclear power installation and thermonuclear research installation are carrying out at present.

4.7. Requirements to content of safety analysis report of NRIs, NP-049-03

The general requirements, requirements to structure and content of SAR, including assessment of DBA and BDBA, are established. The SAR of NRI shall be submitted to Rostekhnadzor in the set of safety justifying documents for siting, commissioning and operation of NRI, and it is used for personnel training, development of technological regulations and other operating documentation.

4.8. Requirements to the quality assurance program of NRIs, NP-042-02

The document establishes a set of technical-organizational quality requirements having effect on safety. Requirements have been developed on the basis of the Federal law "On the use of Atomic Energy ", Federal Norms and Rules in view of IAEA recommendations and standards of the International Organization for Standardization (ISO).

4.9. Provisions on Investigation and reporting of the operational violations at nuclear research installations, NP-027-10

The document determines categorization of operational events, the order of event investigation and registration, appointment of committee for event investigation, contents of reportable information and procedure for event notification, requirements to event reporting. As compared with the previous version NP-027-01 to the document was added the requirements to investigation and registration events at NRI in decommissioning.

4.10. Requirements to content of plans of actions for personnel protection in case of an accident at nuclear research installations, NP-075-06

The document determines the requirements to contents of Emergency Plan that has to be developed by Operating Organization to protect personnel of NRI in case of an accident, also arrangements to ensure implementation of this plan. According to document's requirements at the site with a few NRIs the Emergency Plan have to be developed and implemented at each facility in constituent of the General Emergency Plan of the Operating Organization.

4.11. Consideration for external impact of natural and man-induced origin on nuclear energy facilities, NP-064-05

The document includes requirements to assess external impact of natural and man-induced origin at stages of designing, siting, construction, putting in operation, operation and decommissioning including extending storage under control of nuclear energy facilities.

4.12. Urgent protective action planning zone and precautionary action zone of radiation facilities. Conditions of operation and justification of boundaries, (SP CZZ and ZN-07)

The functional purpose of urgent protective action planning zone (UPZ) is the protective barrier providing a level of safety of the population at normal operation of radiation object. The document defines sanitary requirements for establishment of UPZ and precautionary action zone (PAZ), justification of their sizes depending on category of potential radiation risk of the facility, and it also regulates conditions of usage of these zones and measures to secure safety of the population and an environment.

4.13. Radiation Safety Norms NRB-99/2009

Establishes basic dose limits, permissible dose exposure to ionizing radiation of population in line with Federal Law "On Radiation Safety of Population".

4.14. General sanitary rules for ensuring of the radiation safety, OSPORB-99/2010

The document establishes requirements for people protection from harmful impact of all kind of ionizing radiation exposure. The document includes categorization of facilities sites regarding potential radiation hazard:

- category 1- off-site radiological hazard potential beyond UPZ,
- category 2- off-site radiological hazard potential within UPZ,
- category 3 - on-site radiological hazard potential only,
- category 4 - no radiological hazard potential beyond the facility hall and associated experimental facility areas.

Categorization of facility's potential radiation hazard is used to set requirements for NRI site, UPZ and PAZ, arrangement of radiation monitoring, emergency response measures.

4.15. Strengthening of safety requirements to NRIs

The reference basis for safety regulations of NRIs in Russian Federation has not any contradiction with recommendations of the Code of Conduct on the Safety of Research Reactors and IAEA standards. At present the activity is being continued to improve safety requirements of following FNR:

- Safety rules for decommissioning of nuclear research installations, NP-028-01, concerning details on:
 - ⇒ Structure and content of safety assessment report for NRI decommissioning;
 - ⇒ Structure and content of principal decommissioning programme (plan);
 - ⇒ Structure of the decommissioning database created at the stage of NRI in operation.
- Requirements to quality assurance program:

⇒ “General-purpose requirements to quality assurance program of objects of nuclear energy use” – new.

The following new FNR are being completed in 2012:

⇒ “Release of research installation site from regulatory control” (since decommissioning was completed) – new: IAEA recommendations;

⇒ “Requirements to the set and content of the documents to comprehensive survey of NRI for extension of its operating life” – new: the document is being developed to advance provisions of «Requirements to justification of possible extension of assigned operating life of nuclear facilities», NP-024-2000;

⇒ “Requirements to the periodic safety review of NRIs” – new: IAEA recommendations;

⇒ “Administrative regulation to perform by the Federal Environmental, Industrial and Nuclear Supervision Service the state service of granting permits to personnel of facilities to carry out activities in the sphere of the use of atomic energy” – new: instead of 5th regulations for different objects of nuclear energy use (NPP, NRI, NIS, NFCF, RS), that include requirements to qualification of personnel.

Fukushima-Daiichi NPP accident initiated the complementary target safety assessments [2] not only NPP but NRIs as well including reassessment of the following:

- Capability to assure safety at external impact of extreme natural and man-induced factors and their combinations;

- Efficiency and sufficiency of existing equipment and administrative measures to manage beyond design basis accidents, mitigation of their consequences and to prevent cliff edge effects and severe accident.

Results of complementary target safety assessments to improve safety requirements are considered in the separate paper at the present conference.

5. Conclusion

Operating experience at NRIs in the Russian Federation emphasizes the following aspects of strengthening of the safety requirements:

1.1. Improvement of the ageing management programme for SSC and first of all systems that carry out the fundamental safety functions;

1.2. Clarification and engineering development of nuclear safety requirements to NRIs of new types;

1.3. Emergency preparedness to severe BDBAs.

References

[1] The list of legislative acts and normative documents related to sphere of activity of Federal Environmental, Industrial and Nuclear Supervision Service of Russia P-01-01-2009, the order of Rostekhnadzor from 17 March 2010 № 178.

[2] The proposal by the WENRA Task Force about “Stress tests” specifications (21 April 2011) (<http://www.wenra.org/extra/pod/>).



Tuesday 20 March 2012

CALCULATIONS FOR THE IR-8 REACTOR CONVERSION TO LEU FUEL

D. ERAK, V. NASONOV, Y. PESNYA, A. TALIEV, Y. DUBOVSKIY

*NATIONAL RESEARCH CENTRE «KURCHATOV INSTITUTE»
NRC KI, 1, Akademika Kurchatova Sq., 123182 Moscow, Russia*

The IR-8 pool type research reactor of NRC KI was commissioned in 1981 for carrying out fundamental and applied researches in various areas of science and technique.

As a part of the RERTR program NRC “Kurchatov Institute” with financial support from U.S. Department of Energy studies the feasibility of conversion of the IR-8 reactor from HEU to LEU fuel. Argonne National Laboratory provides analytical support to the work in the performance of the analysis tasks for analysis verification purposes.

A detailed full-scale mathematical models (3D) of the IR-8 reactor from HEU (90% enrichment) and/or LEU (19.7% enrichment) fuel were created for precision neutronic calculations using the MCU-PTR code, implements the Monte-Carlo method. The code was verified and validated (V&V) and now the procedure of certification by Rostekhnadzor (Russian regulation body) is carried out.

As a reference time to determine of the IR-8 parameters the beginning of the equilibrium cycle of the reactor was selected. The loadings of the reactor IR-8 with HEU fuel for the equilibrium cycles of its operation were determined. All the necessary calculations for the gradual replacement of HEU to LEU fuel with subsequent output of the IR-8 reactor at the equilibrium cycle mode of partial loads were carried out. The neutronic and thermal-hydraulic parameters were determined for the equilibrium cycles of the IR-8 reactor with HEU (IRT-3M FAs, UO_2) and LEU (IRT-3M FAs, U-9%Mo) fuel.

1. Introduction

After finishing the calculating analysis of neutronic and thermal-hydraulic characteristics of the IR-8 reactor [1] with HEU [2] NRC “Kurchatov Institute” under the RERTR program began to study the calculated characteristics of the reactor with LEU fuel [3]. Three types of FAs with LEU fuel were examined: IRT-4M, IRT-3M and IRT-U [4]. IRT-3M FA with U-9%Mo LEU was chosen for the further investigations of the IR-8 conversion. Detailed full-scale models of the reactor with this fuel were created for neutronic calculations using MCU-PTR code [5]. The ASTRA [6] code was used for thermal-hydraulic calculations of the IR-8 reactor.

A strategy of the reactor conversion to LEU fuel in the regime of partial reloading was determined.

2. Brief description of the IR-8 reactor

The IR-8 is a pool type research reactor with power up to 8 MW. It uses light water as moderator, coolant and top shield. The IR-8 core consists of 16 IRT-3M FAs with tubular elements of square cross section. The fuel is UO_2 90% enrichment. The core and beryllium reflector are placed in the vessel on the supporting grid near bottom of the pool at ~11 m depth. The 13 rods with boron carbide absorber are used as control rods of CPS.

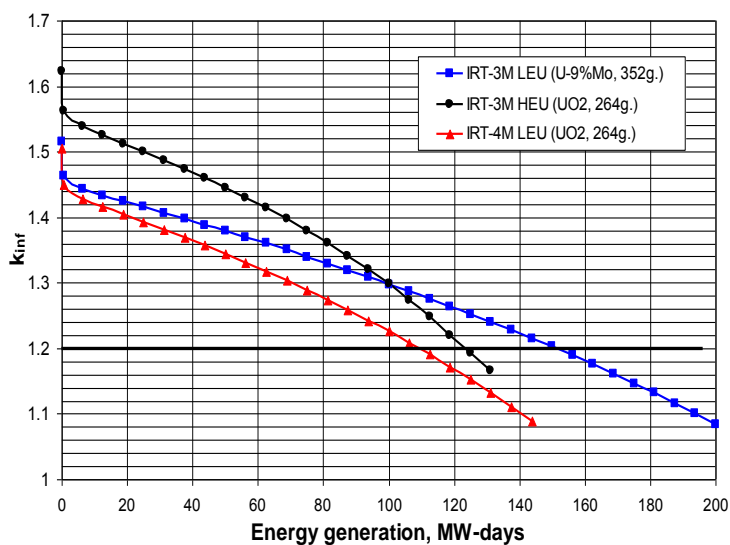
There are 12 horizontal experimental channels (beam tubes) in the reactor for carrying out fundamental and applied researches in various areas of science and technique. The IR-8 reactor construction provides possibility of installation of many vertical experimental channels (VEC) for irradiation of fuel, of structural materials and other are fulfilled.

Presently the reactor operates up to 6 MW power (average $\langle N_{\text{reactor}} \rangle = 5$ MW).

3. The choice of FA with LEU fuel for the IR-8 reactor conversion

Three variants of IRT type FAs with LEU were analyzed: IRT-4M (UO₂), IRT-3M (U-9%Mo) from tubular fuel elements and also IRT-U (U-9%Mo) from rod fuel elements. FAs with tubular fuel elements are used at the IR-8 reactor since 1965 (FA IRT-M, -2M). IRT-3M FAs (90% enrichment) are used since 1981. A great experience of operation and calculations of tubular FA has been accumulated. These assemblies have shown their high reliability even when the fuel burn-up is over 60%. Besides that FA with tubular fuel elements were tested hydraulically and velocities in them are well known [7]. Therefore, it was decided not to consider IRT-U FA for the IR-8 conversion.

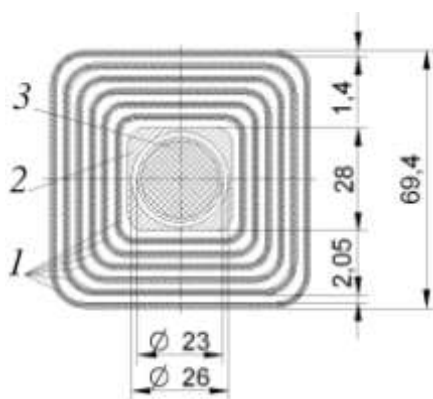
The results of calculated determination of changing multiplication factor for an infinite lattice of the reactor (k_{inf}) with such FAs from energy generation are shown on Fig. 1. At IRT-3M FA with HEU fuel burn-up ~ 58% achieved with FAs energy generation values to 125 MW-days. At this burn-up the value of k_{inf} =1.2.



This value of k_{inf} for IRT-3M FA with LEU corresponds to energy generation equals to 150 MW-days and burn-up ~49%, and for IRT-4M FA – energy generation is 110 MW-days and burn-up ~48%.

Calculated analysis showed that IRT-4M FA does not provide the necessary duration of the reactor cycle, which was achieved by using IRT-3M FA 90% enrichment (Fig. 2, Table. 1).

Fig. 1 Change of K_{inf} from energy generation of FA
($N_{FA} = \langle N_{reactor} \rangle / 16 = 5 \text{ MW} / 16 = 312.5 \text{ kW}$)



1 – fuel elements;
2 – channel of the CPS rod; 3 – CPS rod
Fig. 2. Cross section of IRT-3M
FA with control rod

FA	IRT-3M	IRT-3M
Fuel enrichment, %	90	19.7
²³⁵ U content, g	264	352
Fuel meat thickness, mm	0.4	0.5
Active length of meat, mm	600	600
Fuel meat composition	UO ₂ -Al	U- 9%Mo
Uranium density in the meat, g/cm ³	1.07	5.2
Cladding material	Al alloy CAB-1	Al alloy CAB-1
Cladding thickness, mm	0.5	0.45
Number of fuel elements in FA	6	6
Heat-exchange surface, m ²	1.42	1.38

Tab. 1: The main parameters of IRT-3M type FA

4. Neutronic parameters of the reactor

As a starting loading for the calculating output of the reactor in the equilibrium cycle the loading # 35 with HEU fuel (Fig. 3) is selected. In this loading two IRT-3M FAs with 19.7% enrichment instead of two "fresh" FA 90% enrichment are loaded (Fig. 4).

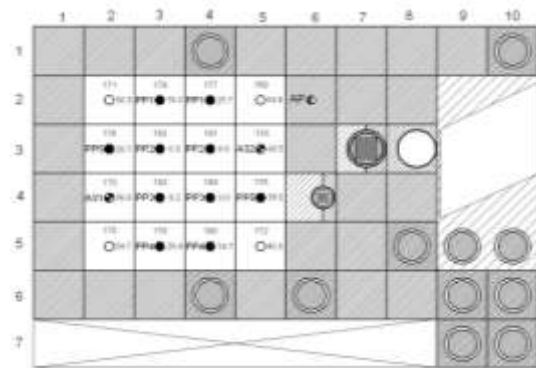


Fig. 3. Configuration of the IR-8 loading # 35 (HEU fuel).

Excess reactivity – 8.2 % $\Delta k/k$

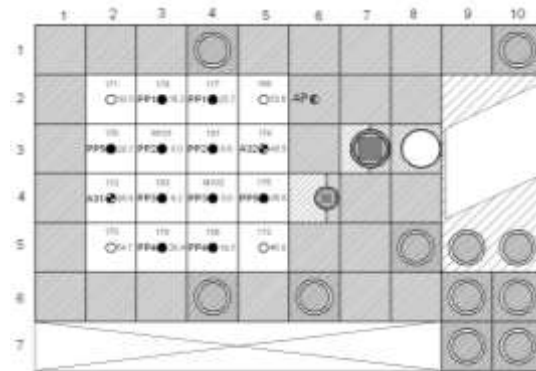


Fig. 4. Configuration of IR-8 loading # 1M (14 FA with HEU and 2 FA with LEU fuel)

Excess reactivity – 7.5 % $\Delta k/k$

After that, calculations were carried out for output the reactor into the equilibrium cycle. The same scheme as for the equilibrium cycle with HEU fuel was used. As a starting time the cycle length which was preliminary determined during the calculations of infinite lattice was used. Further this value was adjusted by means of calculation so that the values of excess reactivity at the end of equilibrium cycles were the same for HEU and LEU cores. Thus, the reactor was outputted into the equilibrium cycle (Fig. 5) and the main neutronic parameters of this cycle were determined (Tab. 2).

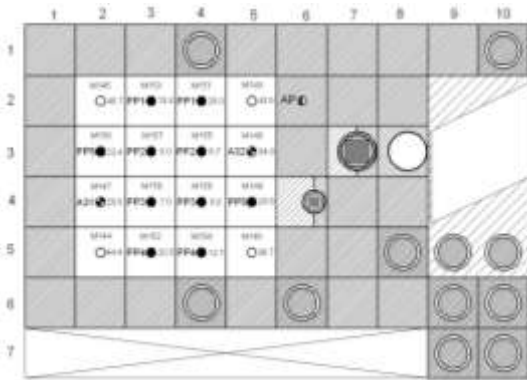
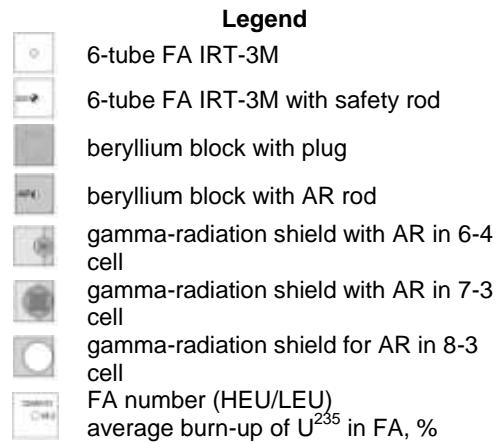


Fig. 5. Configuration of IR-8 loading #29M (16 FA with LEU fuel).

Excess reactivity – 7.1 % $\Delta k/k$

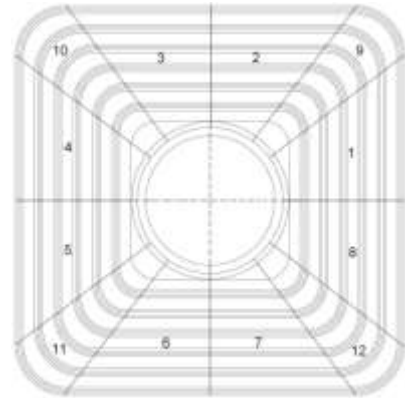
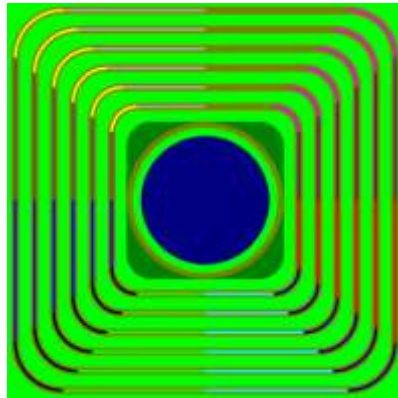
Parameter	Value		Parameter	Value	
	HEU	LEU		HEU	LEU
Reactor power, MW	6		Reactor power, MW	6	
Uranium enrichment, %	90	19.7	Max. thermal neutron flux, $cm^{-2} s^{-1}$:		
^{235}U loading in FA, g	264	352	- in the core (2-2 cell)	$1.1 \cdot 10^{14}$	$7.1 \cdot 10^{13}$
Cycle length, FPD's	41.7	48.3	- in the reflector (cell 2-1)	$1.2 \cdot 10^{14}$	$9.4 \cdot 10^{13}$
Cycles per year	4.0	3.45	- on the beam tube end face	$1.0 \cdot 10^{14}$	$8.9 \cdot 10^{13}$
FA consumption per year	8.0	6.9	- in the VEC	$5.3 \cdot 10^{13}$	$5.0 \cdot 10^{13}$
Excess reactivity, % $\Delta k/k$:			Max. fast ($E > 0.5$ MeV) neutron flux in the AR (6-4 cell), $cm^{-2} s^{-1}$		
- the beginning of cycle	8.2	7.1		$2.0 \cdot 10^{13}$	$1.9 \cdot 10^{13}$
- the end of cycle	1.8	1.8			

Tab. 2. Main neutronic parameters of the IR-8 reactor

5. Thermal-hydraulic parameters of the reactor

To increase the accuracy of the calculations and for taking into account the azimuthally irregularities within the FA as well as across the core at the calculating model all fuel elements of FA were additionally divided into 12 sectors by azimuth (Fig. 6). Thus, the number of registration zones with fuel increased from 2880 to 34560.

Calculations for determining the fuel burn-up for the equilibrium cycles for the reactor operating in the regime of partial reloading of two FAs with azimuthally divided fuel elements were carried out. (loadings # 29M÷37M). At the beginning of the reactor operating cycle #36M the core was consisted of only FAs with azimuthally divided fuel.



Cross section of the calculating model with the partition of FA into 12 sectors

Numbering of the sectors

Fig. 6. Calculating model of IRT-3M FA with LEU

For determining thermal-hydraulic parameters of the reactor with LEU fuel two starting loadings of the reactor equilibrium cycle were analyzed. In the first case two “fresh” FAs were loaded into 3-4 and 4-3 cells (loading #37M) and in the second case “fresh” FAs were loaded into 3-3 and 4-4 cells (loading #36M). Both loadings were examined in xenon-free and equilibrium xenon concentrations states. For these loadings power densities for all fuel zones were calculated. Basing on obtained results the most thermally stressed FAs were determined and thermal-hydraulic calculations were carried out. The most thermally stressed was the beginning of the equilibrium cycle with “fresh” FAs in 3-3 and 4-4 cells. The maximum of power density located in an external fuel element of the FA in 3-2 cell in sector #3 on the border with a beryllium reflector (Fig. 7).

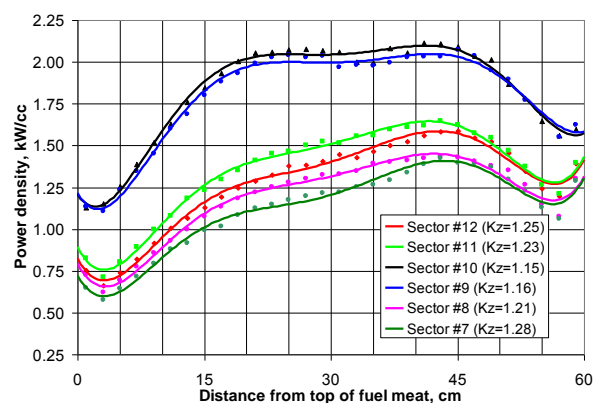
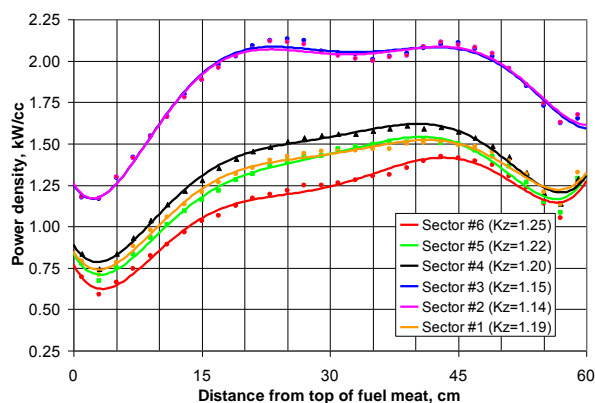


Fig. 7. Distribution of power density on the height of the fuel element

Main thermal-hydraulic parameters of the reactor equilibrium cycle are shown in Tab 3. Reactor power is 6 MW.

Parameter	Value	Parameter	Value	
			HEU	LEU
Coolant flow, l/s: through the reactor/all FAs	208/105	Power of FA in the most thermally stressed cell, kW	432	466
Coolant velocity in the gaps FA (average), m / s	2.4	Maximum calculating power density in meat, MW/m ³	2580	2130
Coolant pressure at the core inlet, MPa	0.186	Maximum heat flux on the surface of fuel elements, kW/m ²	477	516
Pressure drop across the core, MPa	0.022	Maximum design temperature on the surface of fuel elements, °C	93	92
Coolant temperature at core inlet, °C	до 50	The temperature of onset nucleate boiling (ONB), °C	130	131
Coolant temperature rise in the reactor, °C	6.9	Safety margin to onset nucleate boiling (ONB)	1.87	1.93

Tab. 3. Thermal-hydraulic parameters of the IR-8 reactor

5. Conclusion

Neutronic and thermal-hydraulic parameters of the equilibrium cycles of the IR-8 reactor operation with LEU fuel were obtained by means of calculations. Comparison of the results with parameters of the reactor operation with HEU showed that:

- Maximum fast ($E > 0.5$ MeV) neutron flux:
 - reduced up to 4% in ECs of the first row of the reflector;
 - almost the same in ECs of the core, VECs and beam tubes.
- Maximum heat neutron flux reduced up to:
 - 5% in VECs; -10% in beam tube ends; -19% in ECs of the reflector first row;
 - 12 % in the AR samples; -37% in ECs of the core.

For partial compensation of neutron flux decreasing due to the conversion to LEU fuel the replacing of “poisoned” removable beryllium blocks is necessary. Operation of the reactor with LEU fuel (IRT-3M, U-9%Mo) is possible at the power of up to 8 MW. All this allow to make a conclusion about technical feasibility of the IR-8 reactor conversion to LEU fuel.

Appreciation

Authors would like to thanks colleagues from ANL Jordi Roglans-Ribas, Nelson A. Hanan and Patrick L. Garner for expert assistance and analytical support during the entire complex of works on the calculated justification of the reactor IR-8 conversion to LEU fuel feasibility.

6. References

- [1] Ryazantsev E.P., Nasonov V.A., Egorenkov P.M. et al. Contemporary Status and Employment Perspectives of the IR-8 Reactor of RRC KI. International Scientific Conference "Research Reactors in the XXI Century." Moscow, June 20-22, 2006. Ed. NIKIET, M., 2006.
- [2] Nasonov V.A., Erak D.Y., Taliev A.V., Pesnya Y.E., Dubovskiy Y.M. The ongoing status of the project on feasibility studies for the conversion of the IR-8 reactor to LEU fuel. Proceedings of the 2011 International Meeting on RRFM. Roma, Italy, March 20 – 24, 2011.
- [3] Pesnya Y.E., Erak D.Y., Nasonov V.A., Taliev A.V. Neutronic parameters of the IR-8 reactor core consisting of IRT-3M type FAs with U-9%Mo LEU fuel being analyzed. Proceedings of the 2011 International Meeting on RERTR. Santiago, Chile, October 23-27, 2011.
- [4] Nasonov V.A., Ryazantsev E.P., Taliev A.V., Egorenkov P.M. The Work under “The Program Reduced Enrichment of Fuel for Research Reactors” to 19.7% in RRC “Kurchatov Institute” – Atomic Energy, 2010, v.108, is. 3, p. 299-303.
- [5] Alexeev N.I., Gomin E.A., Marin S.V., Nasonov V.A., Shkarovsky D.A., Yudkevich M.S. MCU-PTR Code for Precision Calculation of Pool and Tank Types Research Reactors. - Atomic Energy, vol. 109, is. 3, 2010, p. 123-129.
- [6] Taliev A.V. Modernized ASTRA code for thermal calculation of research reactor FAs consisting from tubular coaxial fuel elements. Preprint IAE-6405/5, Moscow, 2006.
- [7] Nasonov V.A., Ryazantsev E.P., Taliev A.V., Yashin A.F. Water velocities determination in the gaps of IRT-3M and IRT-4M FA. Atomic Energy, 2011, v.110, is. 6, p. 317-321.

Extended studies of FRM II core conversion with UMo dispersive fuel at a prolonged fuel element

A. Röhrmoser, H. Breitzkreutz, W. Petry

Forschungsneutronenquelle Heinz Maier-Leibnitz (*FRM II*),
Technische Universität München, D-85747 Garching, Germany

ABSTRACT

Studies for the conversion of the compact core of FRM II were done with UMo dispersive fuel at a somewhat prolonged fuel element. The main reason for this prolongation is to regain reactivity losses through reduced fuel enrichment below 50%. One constraint at any conversion study is to fulfil at least the cycle time of the current reactor in order to avoid major penalties beside unavoidable losses in neutron flux levels.

With a new burn up procedure based on 3d-calculations of the core and its surrounding, the relative flux output at different beam tubes directly can be calculated now. The flux losses will be very dependant on the beam or irradiation tube of regard (between 14% and 1% at thermal beam tubes and at irradiation channels).

Another reason for extending the core is to reduce the heat load of the cold source from the core and the cooling power for its liquid D₂.

It shall be shown a physical and technical evaluation of a core with dispersive fuel UMo7 at a maximum density of 8gU/cc and 30% enrichment. The study explores feasibility limits by means of a fuel zone enlarged in height, meat thickness and through a changed central channel. No changes to major systems of the reactor like control (CR) and shut down (SR) rods are deemed necessary. Nevertheless, the major question that remains is about the licensing for the extended fuel element.

1 Introduction

The multiple purpose research reactor FRM II of the Technische Universität München (TUM) has been designed to provide a maximal thermal neutron flux outside of the core [1]. This is achieved by placing a very compact core in a large moderator tank with heavy water (HW) and cooled by light water (LW). The enrichment of the used silicide fuel U₃Si₂ is 93% U235 (HEU) with a relatively high density of uranium, both design measures to achieve the necessary core reactivity for an operation of at least 60 days at moderate 20 MW power with the small fuel element. More than 90% of the U235 mass are embedded between the plates at a density of 3.0 gU/cm³, the rest at the half density and located outside to reduce local power densities. First criticality was achieved in spring 2004 and routine operation, i.e. user service started in 2005. The reactor fulfilled all design expectations and operates actually with its 27th fuel element. The life cycle could be even increases to 60 full power days (FPDs) per element, thus consuming some of the design reserve of core reactivity.

With receipt of the nuclear license to operate FRM II, TUM engaged in a R & D program to develop high density fuel in order to reduce the enrichment of the FRM II fuel element, as far as this is technically and economically feasible. Any scenario to convert the FRM II would have to keep the reactor power constant at 20 MW. Without changing the whole D₂O moderator tank with all its installations and its shutdown rods, the core geometry must remain unchanged. This is necessary not only to avoid a complete new licensing procedure, but also to prevent a reactor shutdown period of many years and tremendous cost.

The R & D program of TUM to qualify a highest density fuel concentrates on UMo alloys with 7 – 10 wt% Mo, hereby joining international efforts. Today two scenarios for the qualification of fuel assemblies made out of this alloy are considered, UMo powder dispersed in an Al matrix with densities up to 8 gU/cm³ and monolithic UMo foils with a density of 15–16 gU/cm³. With the maximum density of disperse UMo fuel research reactors of highest performance in Europe as well US can be converted to lower enriched fuel, however LEU (Low Enriched Uranium, < 20 % enrichment) can not be reached. Monolithic fuel with its higher density principally allows the conversion of a greater number of high performance research reactors. However the fuel is still on a long way for qualification and industrial production of monolithic fuel, in particular with thickness or density gradients, has yet to be proven.

For FRM II, the very high density UMo fuel has the most potential for a down grading of the enrichment below 50%. One of our contributions based on monolithic fuel was a principal design study for a FRM II core and ended up with the proposition of a thickness gradient of the monolithic UMo foils [4] instead of a simple density grade step actually, both measures to avoid too high local powers and temperatures.

A careful study of the neutronical and thermohydraulical evolution during operation is the base for a final license for FRM II with a modified core in general. Besides all the fabrication questions with monolithic fuel, a thickness gradient is another severe challenge for such fuel plates, that have to withstand high irradiation levels and flow turbulences during operation at maximum temperatures of about 100°C.

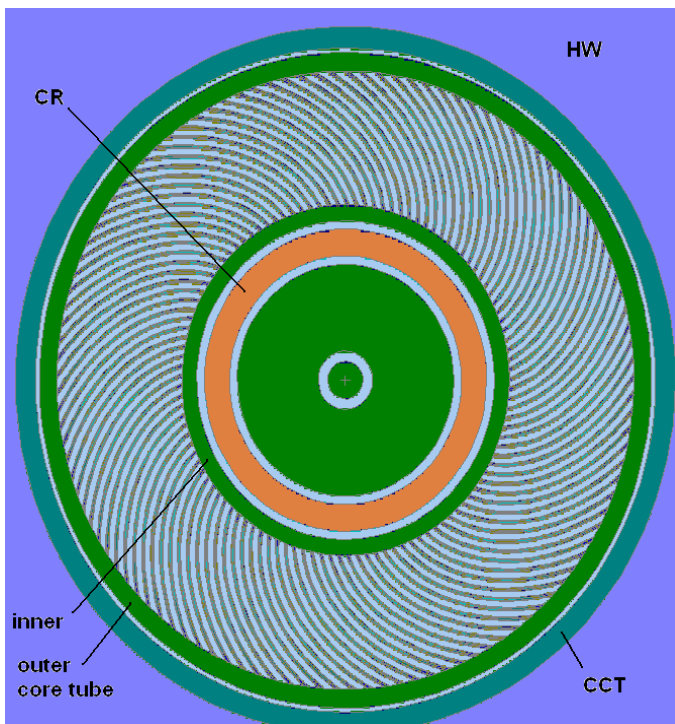


Fig. 1:

Horizontal cross section views of compact fuel element of FRM II in the vessel of HW (D₂O, dark blue). The element contains 113 plates actually and also in the low enriched case of this study. The green rings are all of material AlMg3 and mean (from out- to inside) the central core tube (in the low enriched case of this study zircaloy with 6.5mm thickness instead 8mm), the outer and inner element tube, the Al-filler of the control rod (CR, light red) of Hafnium material. The light blue areas mark the light water of the primary coolant circuit.

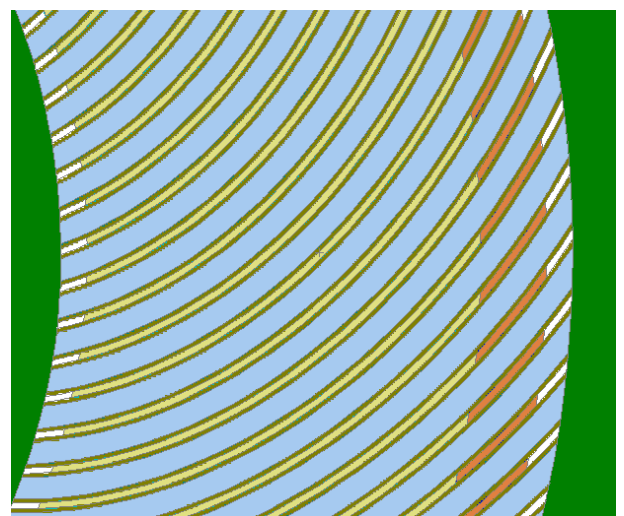


Figure 1b:

horizontal view, zoomed for an area of the fuel plates between inner and outer element tube as calculated in 3d-geometry. The involutes shaped fuel plates provide a constant width of the cooling channels and contain the fuel in two different uranium densities, outside (orange) with half of the inner U density (yellow). The cladding is of material AlFeNi and the frame (white) is of AlMg2. The fuel element is shown with measures as calculated.

This is why the dispersive fuel with a constant fuel thickness in the plates is our first class selection as long as the fabrication and irradiation questions with monolithic fuel are not clearly mastered. Our stud-

ies with unchanged geometry showed clearly too high local power values at the outer edge with dispersive UMo fuel, although the density stepping was kept [3]. Any solution has to address the cooling topic first.

The present study wants to explore feasibility limits for FRM II with such a dispersive fuel, it is supposed an uranium densities of 8.0 g/cm^3 for UMo dispersive fuel with 7wt% natural Mo, a fuel that was already studied in full size plate irradiations by TUM itself [5]. The core geometry has to be adapted as far as possible, but without restricting the save operation of the reactor and therefore avoiding changes to the control and shut down systems. Besides a small width-increase another remaining degree of freedom for conversion studies is the height of the active zone, i. e. the length of the fuel plates. Other parameters are in principle the fuel plate thickness and, with clear limitations, also the coolant channel thickness. The aim is to achieve the lowest enrichment level possible under the given boundary condition for FRM II reactor without too high losses for user operation.

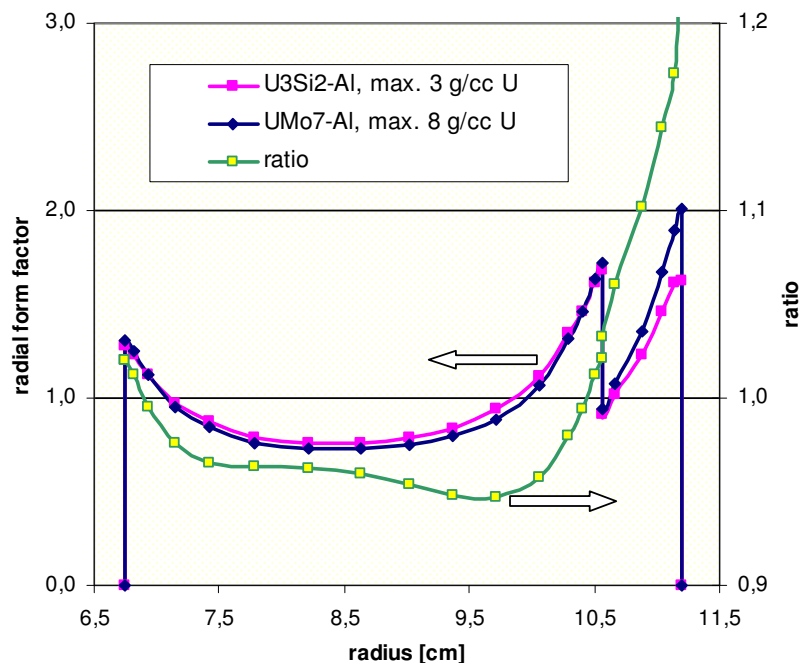
However, we need to emphasize that some of the changes discussed here may raise licensing issues regarding FRM II as the reactor in general. A requirement for a completely new license is not acceptable. While the discussed solution is feasible from a physics point of view, it is highly questionable if the scenario presented here can be realized in the very end within legal boundary conditions, and therefore, if the proposed lower enrichment level can be reached.

2 UMo dispersive calculations for FRM II

Challenges with regard to this new UMo fuel are the increase of the power density form factor of the reactor core because of the much stronger neutron absorption with the much higher U load and accordingly, of the maximum fission density in the fuel meat which is expected to be limited by about 2 or $2.3 \cdot 10^{21} \text{ cm}^{-3}$. Other concerns are the reduced thermal conductivity in the molybdenum fuel and the tolerable maximum fuel temperatures.

2.1 Calculations with UMo dispersion fuel, former results

Fig. 2:
Calculated radial power form factors in FRM-II at BOL with $\text{U}_3\text{Si}_2\text{-Al}$ HEU fuel as currently used, with UMo-Al dispersive MEU fuel and the comparison of the two cases (ratio = change in form factor).
The graph is originally from 2005 [3].



TUM did principal neutronics calculations for a 50% enriched fuel in original core geometry [3]. The result was that the density in the UMo fuel must be at least 7.5 g/cm^3 to keep the cycle length of 60d. The radial power form factor increased from 1.69 inside to a much worse value of 2.01 outside in an area that should have the hot stream filaments (s. Fig. 2 from 2005). Taking this much less fortunate power density distribution into account, it was obvious, that several measures had to be undertaken for an element with reduced enrichment to bring this most important factor for reactors operation in order again.

From the users point of view with that first estimation (50% enriched UMo in 100% original geometry) the maximum thermal flux at about a radius of 22 cm was depressed by about 8.0%, slightly dependent on the operations time of the cycle.

2.2 Calculational procedures

Major topics for core conception are the start reactivity and the reactivity loss and, indivisible from these, the power and neutron flux distribution in and out of the fuel element during the whole core burn-up.

2.2.1 Design calculations for FRM II

TUM developed a very detailed and complex module sequence Mf2dAb to cover all neutron physics aspects of the full fuel cycle of the reactor concept in 2d-cylindrical symmetry (r,z). It led finally to the core design of FRM II [2] with a single fuel element. A lot of adjustments were performed for the purpose of most precise predictions of the core performance during a full fuel element cycle. For instance, the movement of the control rod was introduced as a search parameter at fixed $k_{\text{eff}}=1.0$ into the 2d-neutronics code. It showed up that this is not so important for persueing criticality during burn up, but to predict local fission density values correctly.

2.2.2 MonteBurns calculations

Most of the former, complicated data preparation procedures and approximations can be bypassed today by use of 3d models and point data for cross sections. As computer power has exploded in the last 25 years and MonteCarlo (MC) methods for individual particle transport can be exploited intensively. In combination with a burn-up module, coupled codes allow a comparable tracing of flux and power profiles, covering the full core cycle. Several adaptations with respect to discrete energies and geometrical meshing are no more necessary. Furthermore, the capability to do burn-up calculations in 3d with real beam tubes in the moderator can be explored now, too. For this purpose, studies with the MCNP-ORIGEN2.2 coupled version of MonteBurns2 of LANL [6] were performed. This work will show mainly results obtained through this very powerful methodology, presented already for FRM II [7]. There were used mainly ENDF/B-VI data sets for the studies.

2.2.2.1 MCNP models

In 2003, an extensive review of the former MCNP model was done. From now on, the core was always calculated heterogeneous. In the HW tank, 11 beam tubes, one cold and one hot source and multiple irradiation channels penetrating from the top, were updated to the 'as-built'-situation. This MCNP model '3dMod_FRM2k' could finally be used for studying azimuthal effects like disturbances to the 2d symmetric model in the power distribution [8].

For principal comparison studies and to allow a direct comparison to the deterministic 'design case' model, a MCNP model with 2d-symmetric built-in components was also cut out. It is identical in all aspects with the 3dMod_FRM2k only with the exception, that in the D₂O moderator tank all the UIs are diluted in particular zones.

2.2.2.2 Burn up

For the burn-up calculations, the MonteBurns code was modified to allow for 50 zones, meaning 8*6 (axial*radial) core zones and 2 burn-up zones for a boron ring in a 2d-cylindrical symmetry (r,z) model for principal comparison studies. Hereby all relevant operational aspects can be covered. To allow extra predictions, especially for flux levels at specific beam tubes, it can be finally run for preselected core geometries a real 3d-model. For this model, the modified code allows for three azimuthal zones or 5*3*3 (axial*radial*azimuthal) core zones +5 extra burn-up zones for a boron ring and some extra burnable inserts.

Incorporating a search mode for positioning of a movable structure like the CR, as done in the classical module sequence Mf2dAb, is less straight-forward choice here due to the stochastic manner of this system and computationally expensive. Nevertheless, TUM has implemented such a feature within its X² framework and shown the feasibility [10]. However, in this study the repositioning of the CR is done

directly for the time steps to be processed, getting results that can be very well compared and only with some preparations work of the user beforehand.

2.3 Parameters for core geometry

The most stringent condition for this study is the embedding in the current situation of the reactor with no changes supposed to major systems like control and shut down rods. The CR has a driveway of ± 41 cm, even though during routine operation only somewhat more than half of this driveway, the upper range between about -7cm and +41 cm, is used. The shut down rods come very close to the outer radius $r_a=13.1$ cm of the central channel tube (CCT) when requested for a very sharp shut down of the reactor (SCRAM).

In any case, the core needs more fuel volume. To achieve this, several measures are necessary to approach an optimum for a fuel element with lower enrichment and much higher uranium load levels. Because of the very confined situation of the FRM II core, several smaller contributions must be summed up to achieve a greater gain in volume.

2.3.1 Core height

As already discussed, as a remaining degree of freedom for conversion appears the core height, here is a small variation conceivable. The fuel element is delivered as a whole together with its structure for suspension in the central channel tube, allowing in principle for a longer fuel element to regain reactivity and reduce local power levels. In this study, the active height was extended 6 cm to the bottom, since this is the only way without a need for changing the control rod (CR) system. Currently, the CR is moved till the top position during a full operation cycle (begin BOC, end EOC). In case the fuel element is extended to the top, it would no more be possible to fully move the inner Beryllium moderator (100 cm height) of the CR completely into the fuel zone, yielding a loss of reactivity and operation time for the reactor.

2.3.2 Plate thickness

Other degrees of freedom to increase the fuel volume are the fuel plate thickness and, with clear limitations, also the coolant channel thickness. The latter value was not changed in this study, since it seems to be very close to an optimum even in the case of lower enrichment.

For the studies here the cladding was reduced from 0.38mm to 0.3mm, an approach that has to be verified by the fabricator. Further reductions seem to be rather optimistic and are not regarded here. The gain of two times the difference in thickness (0.16mm) is used for the fuel layer, thus extending from 0.6mm to 0.76mm. While maintaining the overall plate thickness and also the current value of 2.2 mm thickness for the coolant channel gap between the plates, the number of plates is also unchanged to the current situation (113).

2.3.3 Central channel tube

The studies showed that it is necessary to have somewhat more flow area for the coolant water in the core. The CCT tube has now a thickness of 8mm and consists of the material AlMg3. When thinking of an exchange of this tube by the reactor material zircaloy, that shows excellent irradiation behavior, the same structural stiffness can be reached in comparison to now with a thickness of the tube of only 5 or 6 mm. Here it was supposed a zircaloy CCT tube for FRM II of 6.5mm thus remaining at a retained value. The current water gap of 1.5mm between CCT and fuel element might also be reduced, as it has no active cooling purpose and 1mm should be sufficient as space buffer. All together the active zone gains 2mm in outer radius and 6% in volume. And zircaloy with its lower absorption cross section than AlMg3 is favorable with respect to core reactivity and performance at this very high flux level location.

We want to emphasize again, that such a change to one of the central components of FRM II will require extra licensing procedures, which may also prevent such a solution from having opportunity for realization.

2.3.4 Total uranium mass

At a 76 cm high active zone instead of actual 70 cm, one gains then all together 53% in volume for the fuel. Taking the high U density of 8gU/cc with UMo instead of maximum 3.0gU/cc with the current dispersive fuel, the increase in uranium mass is 410%, meaning that the fuel element would contain 33 kg uranium instead of 8.1kg now.

Geometry	HEU / real	30% enr., L=76cm	gain in volume
meat thickness	0.6 mm	0.76 mm	26.7 %
cladding thickness	0.38 mm	0.30 mm	
cooling channel (CC) thickness	2.2 mm	2.2 mm	
number of plates	113	113	
active element height	70 cm	76 cm	8.6 %
inner radius of CC	6.5 cm	6.5 cm	
outer radius of CC	11.45 cm	11.65cm	5.7 %
fuel free gap inside/outside	0.25 cm	0.25 cm	
outer radius outer core tube	12.15 cm	12.35 cm	
CCT inner radius	12.3 cm	12.45 cm	
CCT outer radius	13.1 cm	13.1 cm	
CCT material in calculation	AlMg3	Zirkaloy	
volume 'meat'	2.960 l	4.302 l	45.3 %
mass U-235	7.54 kg	9.51 kg	
mass uranium total	8.11 kg	31.7 kg	
Neutronics			
cycle length at 20 MW thermal power after	60 days	60 days	
k_{eff} BOC,	1.133	1.117	
k_{eff} EOC, only 3*5(*3) radial/axial/(azimuthal) burn up	1.0076±0.0002	1.0070±0.0003	
Fission density maximum (plate of 5mm*5mm) EOC	1.8 10 ²¹	<1.3 10 ²¹	
Thermal hydraulics, calculation NBK			
pressure drop over element	5.3 bar	5.3 bar	
flow velocity of LW between plates	16 m/s	15.4 m/s	
mass flow of LW through fuel element	274 kg/s	277½ kg/s	
max. heat flux at plate surface (hot point)	369 W/cm ²	336 W/cm ²	
hot point at plate surface, conservative heat transfer	96.0°C	95.4°C	
safety value, local voiding S_{onb} at minimum	2.57	2.62	
safety value S_{fi} against flow instability	4.24	4.43	

Table 1: Comparison of the basic data of current HEU fuel element with the proposal for a 30% enriched element for FRM II

3 Results for the reactor

It shall be again emphasized, that all results with a new fuel element must be directly compared with the actual values of the current one.

3.1 Reactivities, safety

The radial dimensions of the core are totally unchanged from outside as well as from inside.

3.1.1 Control rod

The overall reactivity grasp and the differential reactivity of the CR are slightly lower than now. Consequently, the CR will use a greater span of its current driveway during normal operation.

First there is only an upper value for the moving speed of the CR, this should not have a new regulatory implication for reactor operation by the CR. And secondly there is the request, that the CR alone must keep any core situation very clearly below criticality and this is met even with the longer fuel element at unchanged CR system.

3.1.2 Shut down rod system

Any aspect of reactivity worth of the SRs during a 'scram' is very comparable to the current situation, and this is the case for comparison of the safety. The total reactivity grasp of the SRs in the final down position can be again slightly lower than now with a longer core.

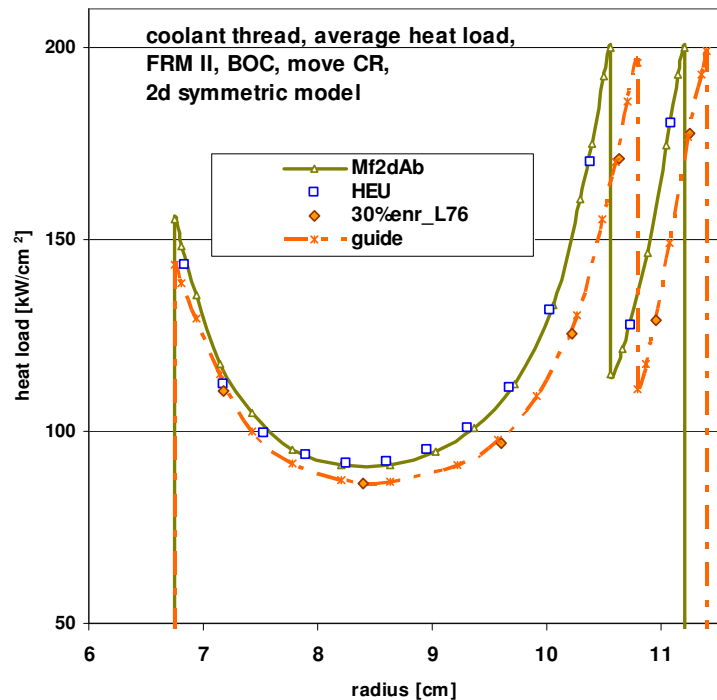
3.2 Reactivities during operation cycle

The main result of the calculations procedure MB, which is described shortly above, can be appointed the necessary of an enrichment of only 30% to achieve the same burn up of 1200 MWDs in total for the extended core. Of course, the presented solution is not the result of a single guess but rather of a long series of optimisation steps not shown here. Especially the problem of too high local power values from former calculations with unchanged core geometry was the guide for finding a less enriched fuel element for FRM II that also solves the operational constraints like safety values against voiding in the cooling channels. This once more underlines the necessity of taking neutronic and thermal hydraulic factors into account at the same time.

3.3 Core cooling

Fig. 3:

Heat load for coolant filaments over the radius in the coolant channels, calculated for the current HEU fuel and the 30% enriched case, both at BOL. The outer radius of the uranium zone was enlarged by 2 mm, gaining 6% in area for cooling channels at the active zone. The outer fuel zone with lower U density became slightly smaller, so that the hot streaming filament is always clearly inside the core.



It is regarded a basic requirement for the safety of FRM II, that the hot streaming filament is always clearly inside the core at a deeply negative value for the local void-reactivity worth. Such a hot stream filament must not be located at the outer edge of the cooling channel. Because of the cold stream filament at the edge, this is already very well guaranteed if the inner peak (speaking with Figure 3) has nearly the same height as the outer one, as it is the case with the current HEU fuel. For this purpose, the grading of the uranium density that was originally located 6.4 mm inside of the outer radius (end of fuel) was slightly reduced to 6 mm. This way the outer fuel zone with lower U density became slightly smaller, pulling the inner peak up the height of the outer one.

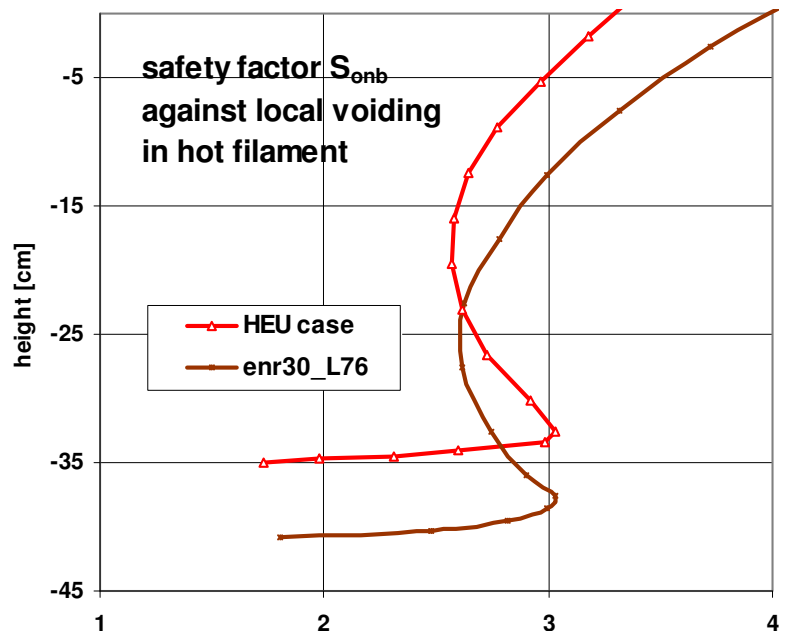
Thermal hydraulic calculations were carried out using the in-house developed code NBK [9], which is tailored especially for the involute shaped plates and channels of the fuel element. Starting from Fig. 3, it might appear that the hot stream filament is still located at the outer edge of the plate. However, NBK calculations using 30 stream filaments show that the hot filament is located further inside, near the density jump (compare Fig. 4). The reason for this is the lateral heat transport in the plates into the direction of the cold stream filaments. Conservative thermal hydraulic assumptions like ‘no mixing of the coolant filaments’ were used, together with a moderate choice for the convective heat transfer correlation identical in both NBK calculations. We have shown before [10] that modern CFD codes like Ansys CFX predict considerably lower cladding surface temperatures and therefore even higher safety margins. However, experimental validation for CFX is still missing.

The operation conditions were taken nominal with 20MW and 5.3 bar pressure loss over the element. As a result the absolute values of total heat load at the radial maxima are now comparable to the actual HEU case.

If we assume the same outer pressurizing conditions with the existing primary pumps, some small differences in values like the local pressure at the hot points appear with the NBK calculation, the overall water throughput being nearly untouched (s. Table 1). The only clear difference that arises is a general lower flow velocity with a prolonged fuel element in the primary coolant circuit (here 15,4 m/s instead of 16 m/s at nominal conditions between the fuel plates)[&]. The hot spots in temperature are calculated to be the same with a maximum value of 96°C at the plate surface.

Fig. 4:

Calculated safety factor S_{onb} against local voiding in comparison of the current HEU case to the 30% enriched element study for the hot stream filament 23 in this thermo-hydraulic NBK calculation with 30 filaments in total. Some conservative assumptions as for the convective heat transfer correlation at nominal operation conditions (20MW, 5.3 bar pressure loss) were the same in both cases. NBK was fed with the most unfortunate power distribution at BOC, calculated with the 3d-MCNP model at reactor start with a fresh fuel element.



[&] We are aware, that any relicensing will be addressed by any flow changes, what may hinder a simple replacement of the current fuel element by the one discussed here.

Although differences in local flow conditions and the most unfortunate power distributions at BOC are supposed for both cases, the safety factor S_{onb} against local voiding is again comparable to the actual case, being 2.62 for the new 30% enriched element instead of 2.57 for the HEU case under nominal operational conditions. Assuming more severe off-normal conditions, the safety factor S_{onb} converges even more. The lower values S_{onb} at the end are not the relevant ones for the overall assessment of the reactor, because of their very small axial extent of a few mm and the missing axial heat flow in the plates, which is not calculated in NBK. The very narrow peaks are flattened when scaling to local heat flux and safety values. CFX calculations, which utilize the necessary 3D heat transfer in the cladding, have confirmed this [10].

Concerning the safety value S_{fi} against flow instability after Forgan/Whittle, the 30% enriched element of this study shows up some preference - bearing in mind possible limitations when assuming the same outer pressurizing conditions.

3.4 Fission densities

Without closer regard, it is that the fission densities in a 50% increased fuel volume are lower than with the current fuel, in average as well as for any maximum. The distribution has a tendency towards more homogeneity than in the more compact case with HEU. The maximum fission density is now found at the outer edge of the high density region at a height 10 cm below fuel element mid plane with a value of below $1.3 \times 10^{21} \text{ f/cm}^3$.

4 Results for the users

With the new procedure based on 3d-calculations of the core and its surrounding the relative flux output at different beam tubes can now be calculated directly and it shows up that the flux losses will be very dependant on the beam or irradiation tube of regard. But beforehand a general discussion of the flux losses is appropriate.

4.1 Flux loss in the HW tank in general

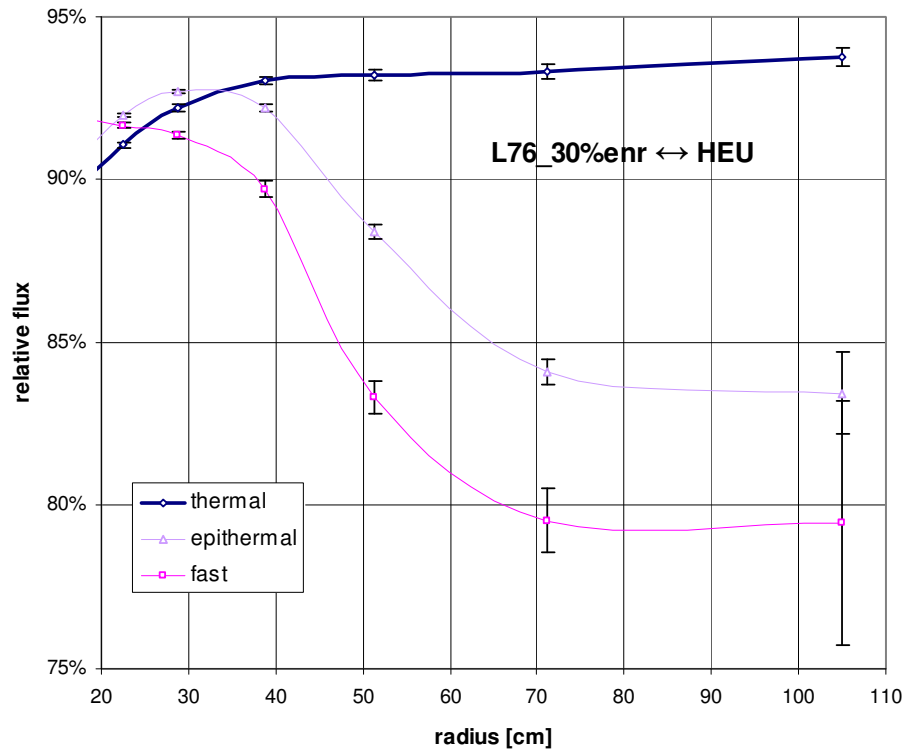
The following results are in comparison to the actual HEU case as a function of radius, averaged over the full height of $\pm 35 \text{ cm}$ around the core mid plane and therefore including the complete area in the HW tank that is relevant for nearly all user installations of FRM II. They are shown in Fig. 5 for mid of cycle (MOC).

- The thermal flux values are most important since thermal neutrons are most relevant for the experiments carried out at FRM II. While it is true that, in fact, a huge number of experiments utilize cold neutrons with 3 or 4 times slower velocities, those come from the cold neutron source (CNS) and represent just a remoderated fraction of Φ_{th} down to the cold flux Φ_{c} . This averaged loss in Φ_{th} in comparison to the actual HEU case is about 8% at a typical beam nose position at radius 30cm, decreases down to 7% till the radius 50cm and finally to 6% till the HW tank wall.
- The fast flux Φ_{s} reaches a rather constant level of 91% of the HEU value outside the core. This is mainly because of the more distributed neutron source term due to the extended fuel element. Further away from the core, Φ_{s} loses more and more. At a radius of 50cm Φ_{s} is then 85% in relative value and 80% at greater radius, but there the flux is already a very clean thermal one.
- The loss for the intermediate flux lies rather in between the values for the thermal and the fast flux.

The loss in fast flux is not a restriction for the neutron source, the loss in Φ_{s} is at any radius higher than the loss in thermal flux. For beam tube applications this is not a disadvantage, instead the opposite could be problematic. In general, it can be stated that the situation with disturbance by fast neutrons for thermal beam tubes will not become worse with the clearly lower enriched fuel element.

Fig. 5:

Calculated relative loss on neutron flux in the HW tank of FRM II as a function of radius averaged over the full height of ± 35 cm around the core mid plane. Both calculations were done with the 3d-MCNP model for the mid of cycle (MOC) situation after a burn up of 30 days with 3d burn up model of MB (MonteBurns); the MOC situation is the best snap-shot moment to show an average loss over a full cycle.

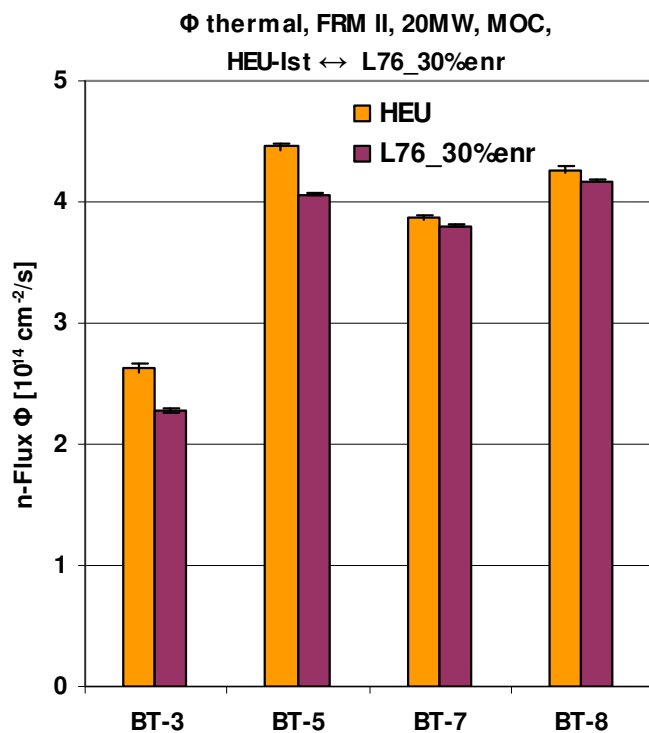


4.2 Thermal beam tubes

The vertical location of the thermal beam tubes is rather distributed at FRM II. For comparison we regard the beam tubes BT-3 at a height 30cm above core mid plane (CMP), beam tube BT-5 at CMP and 20 cm below CMP, the beam tubes BT-7 and BT-8. Because of the in average lowered position of the fuel element in the core, different values of loss in thermal output for the thermal beam tubes are found, meaning a smaller loss for the low lying tubes and a higher loss for the top tube BT-3 (see Fig. 6).

Fig. 6:

Calculated loss on thermal flux at the thermal beam tubes of FRM II, calculated with the 3d-MCNP model for the mid of cycle (MOC) situation after a burn up of 30 days with 3d burn up model of MB (MonteBurns); the MOC situation is the best snap-shot moment to show an average loss over a full cycle.



The most far-reaching consequences from a decline of the thermal neutron flux have experiments which are scarce in neutrons from their discriminating nature, i. e. those who are taking only an extremely low part of the neutron phase space arriving at the sample. These are mainly the three axis spectrometers (TAS). At FRM II, those TAS instruments with thermal neutrons are located at the beam tubes BT-5 and BT-7. Losses of 9% and 2% are calculated for them with the new core situation. On the other side there is a high loss of about 14% at BT-3, where the strain scanning instrument STRESS-SPEC is located. And it is one of the most popular and overbooked instruments. The low lying beam tube BT-8 provides neutrons for two diffractometers; like BT-7, they both would see a loss of about 2%, because of the low position in the HW tank.

4.3 Cold source beam tubes

Of real interest is also the situation for the flux at the cold neutron source (CNS), which provides neutrons for 19 out of a total of 30 instruments. At the radius of 40 cm of the CNS the loss in thermal flux will be about 7% (cmp. fig.1).

The CNS radial position in the HW tank is again something unchangeable for FRM II, but the high heat load of the CNS, resulting from the close neighbourhood to the core, can be reduced by moving the fission power somewhat away from the CNS. This is the case for the core of this study, which is now extended to the bottom away from the CNS. In general it must be expected to be advantageous to remove heat load from the CNS for the pronounced cold neutron usage at FRM II. But any possible gain under actual cooling conditions, currently under closer study at FRM II, is yet hard to predict.

4.4 Hot beam tube

Some extra regard needs the case for the hot neutrons of also low lying beam tube BT-9. The heat load from the core is more distributed over the core height due to the extension. But it is also more to the bottom now, what could compensate and help to achieve the same hot temperature at the hot source and hot neutron flux for the diffractometers at beam tube BT-9.

4.5 Irradiation positions

A comparison of the situation at the different irradiation positions at FRM II can be obtained the same way as for the beam tubes using the 3d model discussed before.

Although such an analysis was not performed in detail for this work, it can be stated, that because of the tendency to suffer of higher location in the HW tank, the loss for most positions will be comparable to the high lying beam tube BT-3. However, one of the most important irradiation locations is the remote silicon doping facility. It will suffer only 6% loss. A loss of this magnitude is at the border of what could be understood as "marginal", but seems inevitable with a fuel element with reduced enrichment for FRM II. Another facility that shall become important in the future for irradiations at FRM II is the irradiation of LEU targets for the production of Mo-99 for medical use. It is located in a beam tube that was prolonged to the bottom of the HW tank during the shut-down period in 2011 for this purpose. This irradiation facility will have a loss of 5% with the 30% enriched fuel element of this study.

SUMMARY

We presented a physical and technical evaluation of 30% enriched fuel element for FRM II based on dispersive fuel UMo7 at a maximum density of 8gU/cc. The study was kept on a conservative embedding regarding the current physical situation of the reactor with no changes necessary to major operational systems like control (CR) and shut down (SR) rods. The fuel element was extended 6 cm to the bottom and the inner diameter of the element and the outer diameter of the central channel tube were kept in the study.

All safety values of the reactor should be met at a comparable level to the current HEU fuel element. Especially for the cooling aspects, some geometric changes had to be introduced, as far as

the very restricted outer dimensions for a new element could allow. Finally safety criteria for the coolant flow are found comparable to the actual case.

The relative flux output at different beam tubes was calculated. The expected losses are very dependent on the beam or irradiation tube of regard, between 1% and 14% at thermal beam tubes and at irradiation channels.

Nevertheless the major question that remains is about the licensing for the new fuel element with respect to the extended core. Such legal aspects might well turn out to be show-stopper. Any final solution for FRM II with a new and clearly reduced enrichment will need to be further investigated for licensing with more tools than done in this conversion study, regarding also transient behaviour of the reactor.

ACKNOWLEDGEMENT

This work has been supported by a combined grant (FRM0911) from the Bundesministerium für Bildung und Forschung (BMBF) and the Bayerisches Staatsministerium für Wissenschaft, Forschung und Kunst (StMWFK).

REFERENCES

- [1] “Physics of the Munich Compact Core Design”, RERTR Conference 1988, San Diego, K. Böning, W. Gläser, A. Röhrmoser
- [2] „Neutron physical optimization and layout of a research reactor of moderate power with aim for high flux for beam tube experiments“, A. Röhrmoser, PhD thesis work at TU Munich, 1991, physics department
- [3] “Reduced Enrichment Program for the FRM II, Status 2004/05”, 9th International Topical Meeting on Research Reactor Fuel Management, RRFM 2005, Budapest, A. Röhrmoser, W. Petry, N. Wieschalla
- [4] “Reduced enrichment program for FRM II, actual status & a principal study of monolithic fuel for FRM II”, 10th International Topical Meeting on Research Reactor Fuel Management, A. Röhrmoser, W. Petry, RRFM 2006, Sofia
- [5] “UMo full size plate irradiation experiment IRIS-TUM – a progress report”, 12th International Topical Meeting on Research Reactor Fuel Management, RRFM 2008, Hamburg, W. Petry, A. Röhrmoser, P. Boulcourt, A. Chabre, S. Dubois, P. Lemoine, Ch. Jarousse, J.L. Falgoux, S. van den Berghe, A. Leenaers
- [6] “MonteBurns (2), an Automated Multi Step Monte Carlo Burnup Code System”, LA-UR-99-4999, Los Alamos National Laboratory, distributed by RSICC or NEA
- [7] “FRM II, New burn up calculations”, RERTR Conference 2010, Lisboa
- [8] “Core Model of new German Neutron source FRM II”, Nuclear Engineering and Design, June 2010, A. Röhrmoser
- [9] “Fuel plate temperatures during operation of FRM II” , 14th International Topical Meeting on Research Reactor Fuel Management, A. Röhrmoser, RRFM 2009, Vienna
- [10] Neutronics and Thermohydraulics of High Density Cores at FRM II Core Model of new German Neutron source FRM II”, H. Breikreutz, 2011, PhD thesis work at TU Munich, physics department

ATR LEU Monolithic Foil-Type Fuel with Integral Cladding Burnable Absorber – Neutronics Performance Evaluation

Gray S. Chang
Idaho National Laboratory
2525 N. Fremont Ave.
Idaho Falls, ID 83415-3870

ABSTRACT

The Advanced Test Reactor (ATR), currently operating in the United States, is used for material testing at very high neutron fluxes. Powered with highly enriched uranium (HEU), the ATR has a maximum thermal power rating of 250 MW_{th}. Because of the large test volumes located in high flux areas, the ATR is an ideal candidate for assessing the feasibility of converting HEU driven reactor cores to low-enriched uranium (LEU) cores. The burnable absorber – ¹⁰B, was added in the inner and outer plates to reduce the initial excess reactivity, and to improve the peak ratio of the inner/outer heat flux. The present work investigates the LEU Monolithic foil-type fuel with ¹⁰B Integral Cladding Burnable Absorber (ICBA) design and evaluates the subsequent neutronics operating effects of this proposed fuel designs. The proposed LEU fuel specification in this work is directly related to both the RERTR LEU Development Program and the Advanced Test Reactor (ATR) LEU Conversion Project at Idaho National Laboratory (INL).

1. Introduction

The Advanced Test Reactor (ATR) at the Idaho National Laboratory (INL) is a high power density and high neutron flux research reactor operating in the United States. Powered with highly enriched uranium (HEU), the ATR has a maximum thermal power rating of 250 MW_{th} with a maximum unperturbed thermal neutron flux rating of 1.0×10^{15} n/cm²-s. The conversion of nuclear test reactors currently fueled with HEU to operate with low-enriched uranium (LEU) is being addressed by the reduced enrichment for research and test reactors (RERTR) program.

The scope of this work is to assess the feasibility of converting the ATR HEU fuel to LEU fuel while retaining all key functional and safety characteristics of the reactor. Using the current HEU ²³⁵U enrichment of 93.0 % as a baseline, this study will evaluate the LEU uranium density required in the fuel meat to yield an equivalent K-eff between the ATR HEU core and an LEU core after 150 effective full power days (EFPD) of operation with a total core power of 115 MW. A lobe power of 23 MW is assumed for each of the five lobes. Then, the LEU ²³⁵U loading that yields an equivalent K-eff as the HEU ²³⁵U loading will be used to predict radial, axial, and azimuthal power distributions. ¹⁰B loading for LEU case studies will have 0.635 g in the LEU fuel meat at the inner 2 fuel plates (1-2) and outer 2 fuel plates (18-19), which can achieve peak to average ratios similar to those for the ATR reference HEU case study. The investigation of this paper shows the optimized LEU Monolithic (U-10Mo) Foil-type with Integral Cladding

Burnable Absorber (ICBA) (MF-ICBA) case can meet the LEU conversion objectives. The heat rate distributions will also be evaluated for this core and used to predict the core performance as it relates to the current Upgraded Final Safety Analysis Report (UFSAR) and the associated Technical Safety Requirements (TSRs).

2. ATR Full Core Model and MCWO – Fuel Burnup Analysis Tool

The ATR CIC-1994 (NT-3 of Cycle 103A-2) core configuration was chosen to build the ATR MCNP full core model in this work. For the detailed Cycle 103A-2 core configuration data refers to Table 1 in Reference 1. The detailed validation of the full core plate-by-plate MCNP model is in Reference 2. This model is used to optimize the ^{235}U and minimize ^{10}B loading in the LEU core by minimizing the K-eff differences with respect to the HEU core after 150 EFPD of operation with a total core power of 115 MW (23 MW per lobe).

The fuel burnup analysis tool used in this study consists of a BASH (Bourne Again Shell) script file that links together the two FORTRAN data processing programs, m2o.f and o2m.f. [3] This burnup methodology couples the Monte Carlo transport code MCNP [4,5] with the radioactive decay and burnup code ORIGEN2. [6] The methodology is known as Monte Carlo with ORIGEN2, or MCWO. [7] The MCWO fuel burnup analysis tool uses MCNP-calculated one-group microscopic cross sections and fluxes as input to a series of ORIGEN2 burnup calculations. ORIGEN2 depletes/activates materials and generates isotopic compositions for subsequent MCNP calculations.

3. ATR HEU Reference Case and LEU MF-ICBA Models Description

The typical ATR 7F fuel element (FE) was chosen in the HEU reference case model. The detailed 19 plate FE model with burnable absorbers is described in Section 3.1. Then, the proposed LEU Monolithic Foil-type and Integral Cladding Burnable Absorber (MF-ICBA) detailed FE model is described in Section 3.2.

3.1 Detailed ATR 7F Fuel Element Model

The ATR 7F FE was chosen as the reference HEU Case-A in this study. Table 4 in Ref. 2 shows the nominal ^{235}U and ^{10}B loadings for each fuel plate of the 7F FE. In the 7F fuel element, all 19 fuel plates are loaded with 93% enriched uranium in an aluminum matrix to a total of 1075 g U-235. The eight outer plates (plate-1 to plate-4 and plate-16 to plate-19) contain boron as a burnable poison for a total of 0.66 g ^{10}B .

The detailed, full core MCNP ATR model was used to perform the evaluation of the ATR reference HEU case with burnable absorber ^{10}B at the beginning of cycle (BOC) condition. Then, MCWO was used to evaluate the fuel cycle performance versus the EFPD using the following assumptions:

- Each nominal operating cycle was 50 EFPD, followed immediately by a seven day outage.
- Each 50 EFPD cycle was subdivided into 5 EFPD time step intervals.

- The OSCC positions were set to 105°.
- The resultant MCNP-calculated tallies were normalized to a core source power of 115 MW.

3.2 LEU Monolithic Foil-type and Integral Cladding Burnable Absorber Detailed FE model

A LEU monolithic fuel design with varied fuel meat thickness in the four inner plates (plate-1 to plate-4) and four outer plates (plate-16 to plate-19) was recommended in Ref. [2]. However, those LEU fuel designs did not include the 10B loading minimization. Because the 10B (n, α) reaction will produce Helium-4 (He-4), which can degrade the LEU foil fuel (U10Mo) type fuel performance. An alternative burnable absorber loading option – Integral Cladding Burnable Absorber (ICBA) is proposed in this study. In monolithic plates the fuel-cladding interface is protected with Zr diffusion barrier. Therefore an addition of layer of burnable absorber (5 mil) in ICBA was proposed, where the burnable absorber ^{10}B can be totally separated from not only the LEU foil-type fuel meat, but also from the fuel-cladding Zr diffusion barrier.

The optimization was achieved by reducing the fuel meat thickness as well as loading the two inner/outer plates with 0.635 g of ^{10}B in LEU ICBA Case. The isotopic concentration of ^{10}B in the boron of the burnable absorber is 20 wt%. The ^{10}B loading specification of ICBA in plates-1, -2, -18, and -19 are tabulated Table 1. The optimized LEU fuel plate specifications for the ICBA Case are given in Table 2. Table 2 shows that the nominal fuel meat thickness is 0.0330 cm (13 mil). The varied four inner plates (plate-1 to plate-4) fuel meat thicknesses are 0.0203 cm (8 mil), 0.0203 cm (8 mil), 0.0354 cm (10 mil), and 0.0305 cm (12 mil), respectively. While the varied 4 outer plates (plate-16 to plate-19) fuel meat thicknesses are 0.0305 cm (12 mil), 0.0354 cm (10 mil), 0.0203 cm (8 mil), and 0.0203 cm (8 mil), respectively. The detailed FE-18 model of LEU monolithic foil type ICBA Case is shown in Figure 1. The detailed MF-ICBA FE-18 with 4 fuel plates with 10B (Plates-1 to -2 and -18 to -19) are plotted in Figure 2.

Table 1. Integral Cladding Burnable Absorber (ICBA) with Boron-10 Specification.

ICBA	Boron-10	Thickness	ICBA	Boron-10
ICBA ID	g/cc	mil.	Vol. (cc)	Mass (g)
ICBA-01	0.008	5	6.888	0.058
ICBA-02	0.020	5	7.332	0.149
ICBA-18	0.008	5	13.663	0.111
ICBA-19	0.022	5	14.138	0.317
Total			42.021	0.635

Table 2. LEU Monolithic (U10Mo) Foil-type with ICBA (Boron-10) Specification.

LEU	Fuel Meat	Thickness	Fuel meat	U-235	Boron_10 Mass	U-235
Plate ID	Total U g/cc	mil.	Vol. (cc)	Mass (g)	(g)	Density (g/cc)
Plate-1	15.21	8	10.947	32.876	0.058	3.00
Plate-2	15.21	10	11.660	35.016	0.149	3.00
Plate-3	15.21	10	15.367	46.150	0	3.00
Plate-4	15.21	11	16.153	48.512	0	3.00
Plate-5	15.21	13	22.030	66.162	0	3.00
Plate-6	15.21	13	23.057	69.247	0	3.00
Plate-7	15.21	13	24.087	72.339	0	3.00
Plate-8	15.21	13	25.123	75.450	0	3.00
Plate-9	15.21	13	26.150	78.536	0	3.00
Plate-10	15.21	13	27.178	81.623	0	3.00
Plate-11	15.21	13	28.205	84.707	0	3.00
Plate-12	15.21	13	29.237	87.805	0	3.00
Plate-13	15.21	13	30.257	90.869	0	3.00
Plate-14	15.21	13	31.293	93.981	0	3.00
Plate-15	15.21	13	32.315	97.049	0	3.00
Plate-16	15.21	10	25.655	77.049	0	3.00
Plate-17	15.21	10	26.444	79.417	0	3.00
Plate-18	15.21	9	21.789	65.439	0.111	3.00
Plate-19	15.21	8	22.544	67.704	0.317	3.00
Total			449.490	1349.931	0.636	

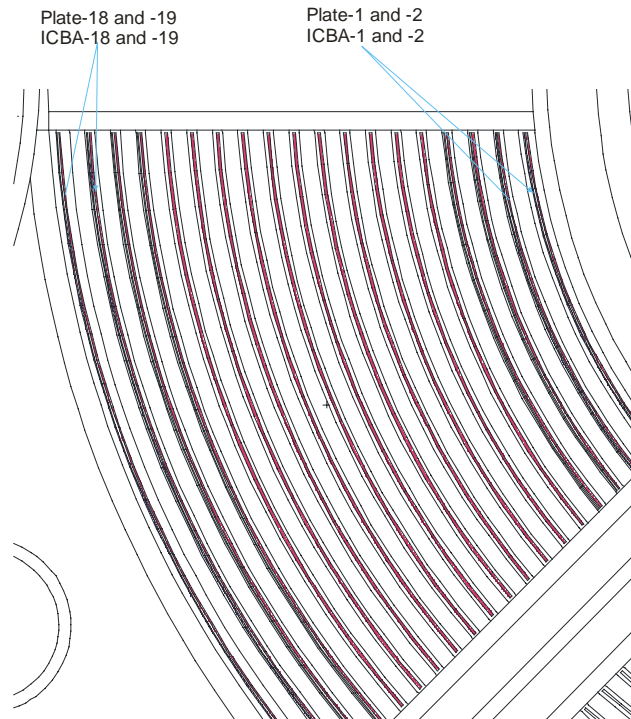


Figure 1. Monolithic foil-type with ICBA fuel element detailed configuration.

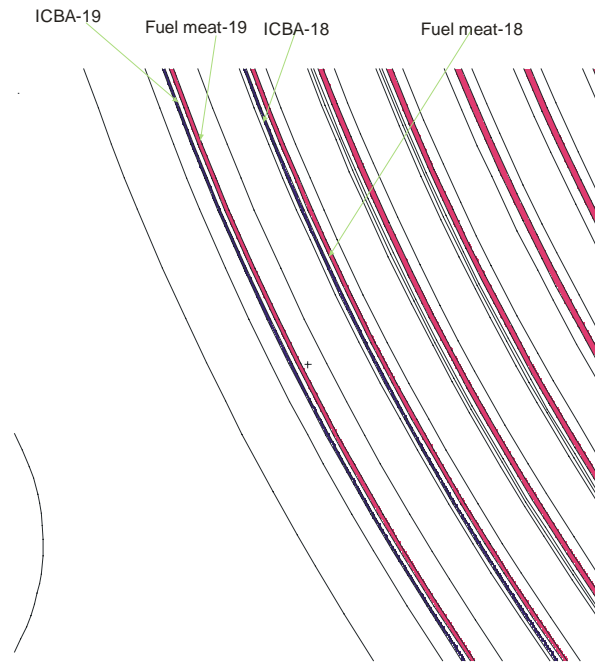


Figure 2. LEU ICBA and Fuel meat plates-18 and -19 detailed configuration.

4. HEU Reference Case and LEU Monolithic foil-type with ICBA Fuel Neutronics Performance Evaluation

Based upon the comparison between Case-A and Case-B relative heat flux L2AR profiles, the ^{235}U contents and fuel meat thickness of the inner/outer plates were evaluated and optimized in order to reduce the difference of K-eff profiles versus EFPD and LEU fuel peak heat flux L2AR. The LEU fuel loading was optimized such that the L2AR at the four inner/outer plates closely matches the ATR reference HEU Case-A.

The optimization was based upon a comparison of the MCWO-calculated K-eff versus EFPD and the radial power L2AR profile for various LEU fuel and ^{10}B loading schemes. In order to reduce the ^{10}B depletion impact on the fuel plate performance, ^{10}B was modeled in the two inner plates (plate-1 and plate-2) and two outer plates (plate-18 and plate-19). The LEU fuel (^{235}U enrichment 19.7wt%) loading schemes included varying parameters such as fuel meat thickness within the monolithic U10-Mo LEU fuel type as Case-B.

4.1 HEU Reference Case and LEU MF-ICBA Radial Fission Power Profiles Versus Burnup

The above tables, Table 1 and Table 2, summarize the fuel and ^{10}B minimization loading parameter variations that resulted in the flattest radial fission heat profile while still maintaining sufficient reactivity within the LEU core. Not surprisingly, the optimal LEU fuel loading is similar to the HEU reference case. The optimal LEU fuel loading has thinner plates at the inner/outer plate positions. For the purposes of determining the feasibility of HEU to LEU

conversion, the present study demonstrates a satisfactory loading scheme to achieve acceptable reactivity for three nominal 50 EFPD fuel cycles as well as maintain the radial heat flux L2AR profile.

The MCWO fuel burnup analysis code was used to calculate the relative radial plate fission power heat flux for the HEU Case-A and LEU Case-B at the beginning of the first cycle (BOC), 1st End of Cycle (EOC), 2nd, and 3rd EOC. For Fe-18 at BOC, the respective peak heat fluxes L2AR for Case-A and Case-B were determined to be 1.25 and 1.20, respectively, as shown in Figure 3. Figure 3 also indicates that HEU Case-A and LEU Case-B have a very similar fission power density profiles.

Results for Case-A and Case-B at the 1st, 2nd, and 3rd EOC are plotted in Figures 4, 5, and 6. These plot demonstrates that Case-A and Case-B yield very similar radial L2AR profiles versus burnup. Figures also indicate that the fission power density profiles are flattened toward the discharged burnup. These studies indicate that the LEU radial L2AR profiles can achieve flattened profiles bounded by HEU reference Case-A by varying fuel meat thickness of the inner/outer 2 plates. However, the fission power density (W/cm^3) L2AR profiles for the LEU cases with varied fuel meat thickness produced larger peaks within the inner/outer plates. This power density peaking will not result in a large, undesirable heat flux profile.

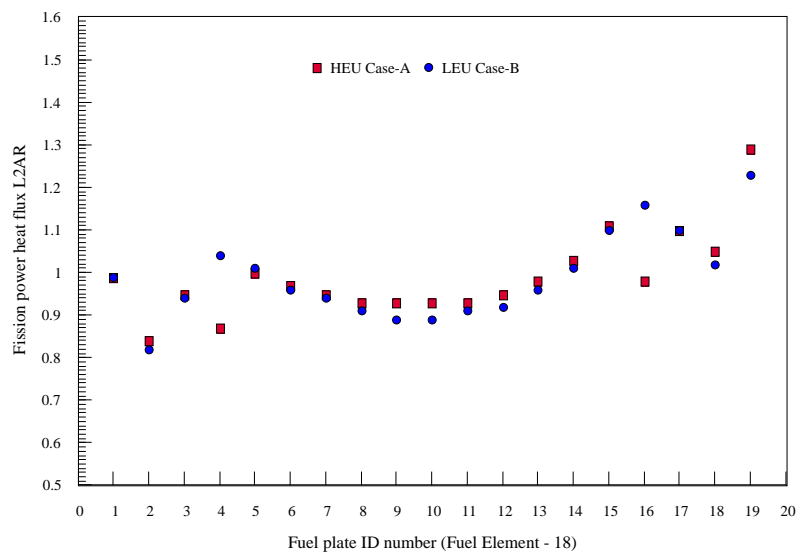


Figure 3. Fission power heat flux L2AR radial profiles for HEU Case-A and optimized LEU Case-B at BOC.

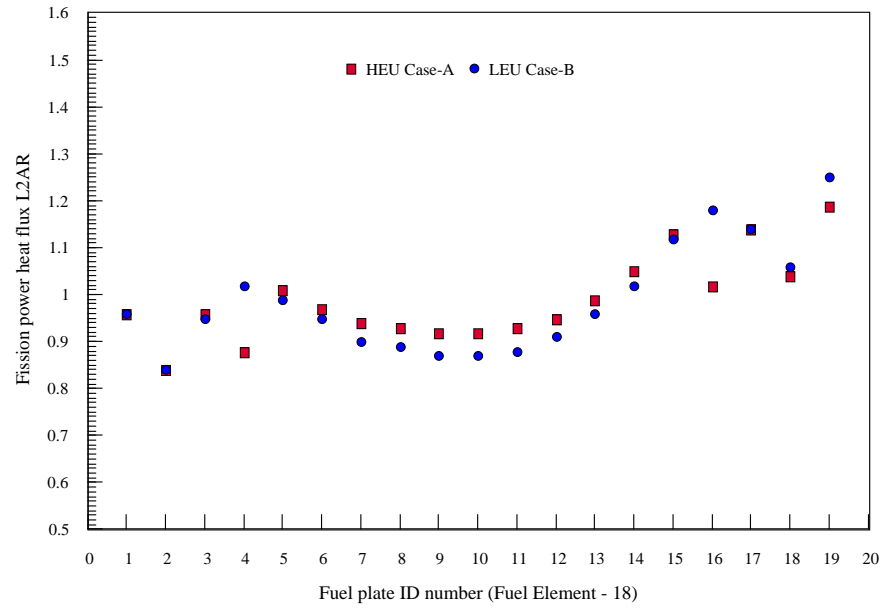


Figure 4. Fission power heat flux L2AR radial profiles for HEU Case-A and optimized LEU Case-B at 1st EOC.

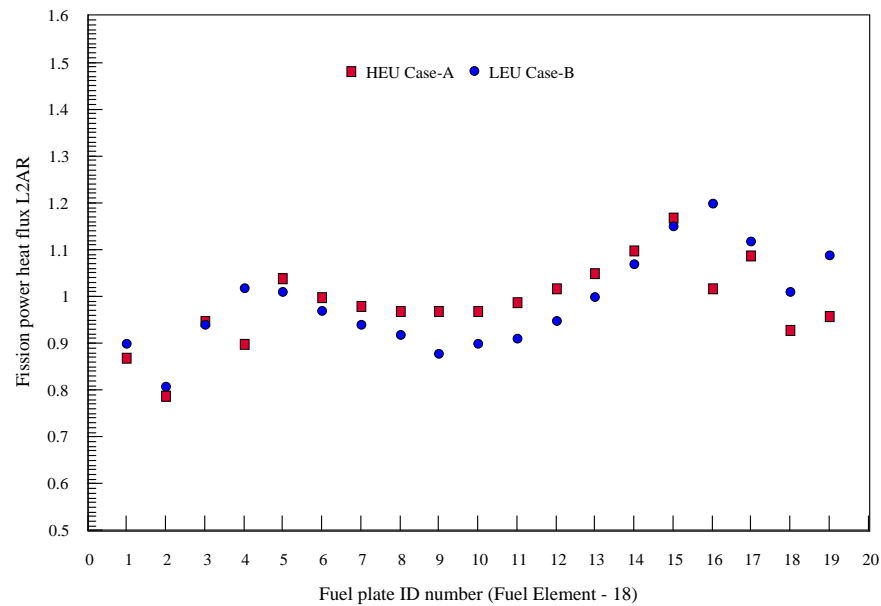


Figure 5. Fission power heat flux L2AR radial profiles for HEU Case-A and optimized LEU Case-B at 2nd EOC.

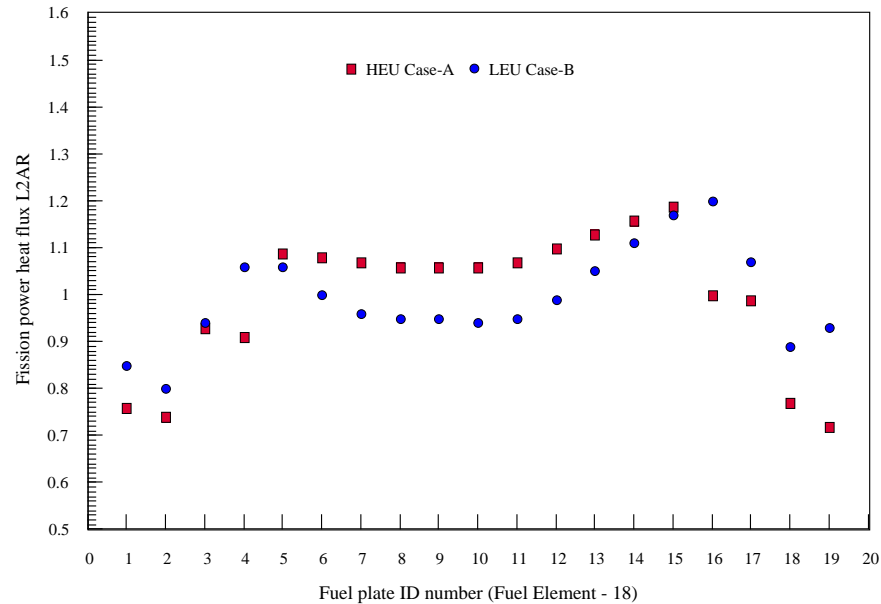


Figure 6. Fission power heat flux L2AR radial profiles for HEU Case-A and optimized LEU Case-B at 3rd EOC.

4.2 HEU Reference Case and Optimized LEU Case K-eff versus EFPD

Using the optimized LEU fuel loading, the MCWO-calculated K-eff for LEU Case-B as a function of EFPD as compared to the ATR reference HEU Case-A is shown in Figure 7. Note that the LEU fuels contain 80.25 wt% U-238, which can be transmuted to Pu-239. Although the LEU cases have a lower K-eff at the BOC when compared with HEU Case-A, the LEU cases sustain operation for the same EFPD as HEU Case-A (150 EFPD). The K-eff of HEU Case-A with and without ^{10}B at BOC are 1.1025 and 1.1969, respectively, which represents a hold-down reactivity of \$9.94. While, the K-eff of LEU Case-B with and without ^{10}B at BOC are 1.0625 and 1.1389, respectively, which represents a hold-down reactivity of \$8.77. The Figure 9 indicates that Case-A and Case-B has a small K-eff difference toward the end of three cycles EFPDs.

For a typical ATR new core fuel loading consists of about 1/3 fresh, 1/3 once-burnt at 1st EOC, and 1/3 twice-burnt at 2nd EOC fuel elements. Although the K-eff of all 40 fuel elements approaching the discharged burnup is about 0.988, which is less than 1. We believe (In phase-II, the LEU fuel cycle performance analysis will validate it in detailed analysis.) that the typical new core fuel loading can provide an adequate K-eff for the complete cycle operation.

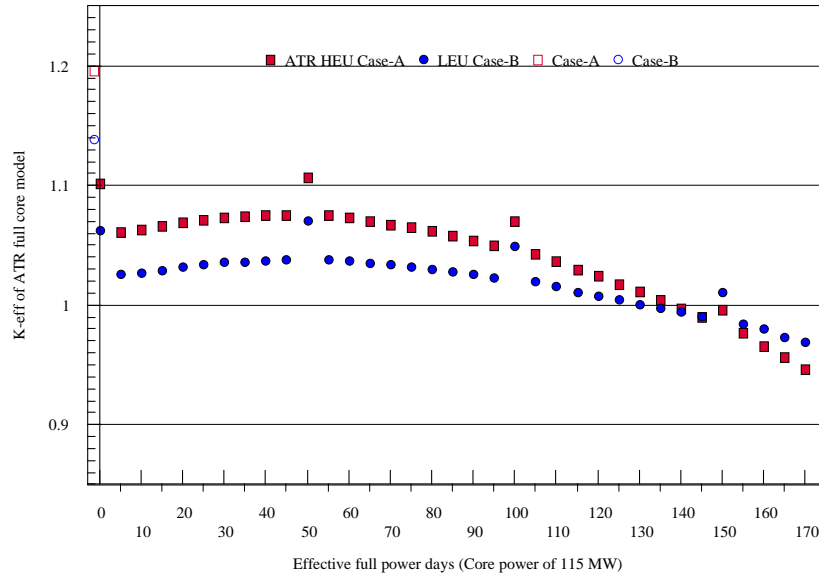


Figure 7. MCWO-calculated K-eff versus EFPD for ATR reference HEU Case-A and optimized LEU Case-B.

5. Conclusion and Recommendations

The detailed plate-by-plate MCNP ATR full core model used in this study handles complex spectral transitions at the boundaries between the plates in a straight forward manner. The MCWO-calculated K-eff versus EFPD results indicate that LEU Case-B provide adequate excess reactivity versus burnup while providing fission heat profiles similar to the ATR reference HEU Case-A. The LEU core conversion designer will be able to optimize the ^{235}U fuel loading so that the K-eff and relative radial fission heat flux profile are similar to Case-A. To achieve the flattened heat flux profile, the LEU monolithic core designer can fix the ^{235}U enrichment of 19.75wt% and vary the thickness of the four inner/outer plates, as well as adjust the amount of burnable absorber in the two inner/outer plates. The investigation of this paper shows the optimized LEU Monolithic (U-10Mo) case can all meet the LEU conversion objectives. As a result, it has been concluded that LEU core conversion for the ATR is feasible.

For the reference HEU 7F and LEU MF-ICBA cases, the BA is used not only to hold-down the initial excess reactivity, but also flatten the radial heat flux profile. Because the ^{10}B (n, α) reaction generates ^4He gas, which can potentially degrades the fuel plate performance. An alternative complex LEU MF fuel design with Integral Side-plate Burnable Absorber (ISBA), Cadmium (Cd), is currently undergoing a more in depth evaluation. As we know, if we put BA in side-plates, it only hold-down the initial excess reactivity. Then, using the fuel meat thickness variation approach in outer and inner four plates to flatten the radial plates profile to meet the LEU conversion project requirements. This ISBA design locates the BA in the side-plates, which physically separates the BA from both the fuel meat and the cladding, and takes advantage of the fact that the Cd (n, γ) reaction does not produce ^4He gas. A preliminary proposed complex MF-

ISBA can achieve a flattened fuel plate radial power profile by reducing the thickness of the fuel meat of the inner/outer plates. The complex LEU MF-ISBA fuel design can be shown to meet all the ATR LEU conversion operational and safety requirements in the LEU complex fuel design Phase-II.

The proposed LEU fuel specification in this work is directly related to both the RERTR LEU Development Program and the ATR LEU Conversion Project at INL. The LEU core designer can use the detailed plate-by-plate MCNP ATR full core model to optimize the ^{235}U loading by either minimizing K-eff differences with respect to the HEU core during the 150 EFPD of operation at a total core power of 115 MW (23 MW per lobe), or by reducing the higher L2AR of heat flux at the inner/outer plates. However, to demonstrate that the LEU core fuel cycle performance can meet the UFSAR safety requirement, a further study will be necessary in order to investigate the detailed radial, axial, and azimuthal heat flux profile variations versus EFPD. In addition, the safety parameters such as void reactivity and Doppler coefficients, control components worth (outer shim control cylinders, safety rods and regulating rod), and shutdown margins between the LEU cores need to be evaluated in depth.

6. References

- [1] G. S. Chang, M. A. Lillo, "MCWO Neutronics Analysis of RERTR Full Element Demonstration in Position 38 of the ATR," Idaho National Laboratory ECAR-1357, Rev. 1, June 2011.
- [2] G. S. Chang, M. A. Lillo, R. G. Ambrosek (retired), 'Neutronics and Thermal Hydraulics Study for Using a Low-Enriched Uranium Core in the Advanced Test Reactor 2008 Final Report,' INL/EXT-08-13980, June 2008.
- [3] G. S. Chang, "MCWO - LINKING MCNP AND ORIGEN2 FOR FUEL BURNUP ANALYSIS," Proceedings of 'The Monte Carlo Method: Versatility Unbounded In A Dynamic Computing World,' Chattanooga, Tennessee, April 17–21, 2005, on CD-ROM, American Nuclear Society, LaGrange Park, IL (2005).
- [4] Tim Goorley, Jeff Bull, Forrest Brown, et al., "Release of MCNP5_RSICC_1.30," MCNP Monte Carlo Team X-5, LA-UR-04-4519, Los Alamos National Laboratory, November 2004.
- [5] X-5 Monte Carlo Team, "MCNP—A General Monte Carlo N-Particle Transport Code, Version 5," Volume I (LA-UR-03-1987) and Volume II (LA-CP-0245), Los Alamos National Laboratory April 24, 2003 (Revised 6/30/2004).
- [6] G. Croff, "ORIGEN2: A Versatile Computer Code for Calculating the Nuclide Compositions and Characteristics of Nuclear Materials, Nuclear Technology," Vol. 62, pp. 335-352, 1983.

- [7] G. S. Chang and J. M. Ryskamp, "Depletion Analysis of Mixed Oxide Fuel Pins in Light Water Reactors and the Advanced Test Reactor," Nucl. Technol., Vol. 129, No. 3, p. 326-337 (2000).
- [8] Safety Analysis Report, "Safety Analysis Report for the Advanced Test Reactor," Idaho National Laboratory, SAR-153, Nov. 2003.

REACTIVITY PERFORMANCES OF TWO PROTOTYPES HEU FUEL ELEMENTS WITH CADMIUM WIRES IRRADIATED IN THE BR2 REACTOR

S.KALCHEVA, G. VAN DEN BRANDEN AND E.KOONEN

*SCK•CEN, BR2 Reactor Department
Boeretang, 2400 Mol – Belgium*

ABSTRACT

Two prototypes HEU fuel elements with cadmium wires have been manufactured and irradiated during five BR2 operation cycles in 2011 under the BR2 Conversion Project. The purpose of these irradiations was to investigate the effect of the replacement of the standard burnable absorbers (B_4C and Sm_2O_3) in the fuel meat by cadmium wires located in the grooves of the aluminium stiffeners of a standard BR2 fuel element. A detailed MCNPX 2.7 geometry and burn-up model has been developed and implemented for evaluation of the performance graph of the reactivity evolution vs. mean U5 burn-up in the HEU-Cd elements. A Nuclear Measurement Program for the determination of the reactivity effect of the HEU-Cd fuel elements relatively to a standard fresh BR2 HEU fuel element has been conducted in the shutdown of each operation cycle. MCNPX predictions for the reactivity effects of fresh as well as for burnt HEU-Cd fuel elements were in a good agreement with the measurements.

The overall conclusion is that the two cadmium-wired fuel elements behaved as expected. Therefore it can be concluded that the Cd wires are qualified as another type of burnable absorber for the BR2 driver fuel.

1. Introduction.

Upfront to the neutronic conversion feasibility evaluations in the framework of the BR2 conversion project, an optimization of the burnable absorber for the future LEU fuel system had to be performed. In this optimization project, the nature, quantity (or density, if applicable), geometrical form and localization in the fuel assembly of the burnable absorber have been studied [1-3].

For all conversion studies, the current fuel element geometry (number of fuel plates, plate and water gap thicknesses) is preserved in order to avoid significant changes in the thermal-hydraulics characteristics of the reactor. The cladding material (AG3NE) is also preserved mainly to avoid any new corrosion issue. Therefore two main characteristics of the BR2 fuel element design remained to be studied: the fuel meat type and the type of burnable absorber. The results of these studies have been reported at the RERTR'08 conference [1]. The final choice made for the new burnable absorber is: 36 Cd wires in the 12 grooves of the 3 Al side-plates of the standard BR2 fuel element. The optimum diameter for the different fuel types is: $\varnothing = 0.4 - 0.5$ mm for U-7Mo LEU 7.5 - 8.5 gU_{tot}/cc. The basic computational tool used in all studies is the Monte Carlo automatic burn-up code MCNPX 2.7 [4].

Up to now the needed LEU fuel system for the conversion of the BR2 reactor (high density U-Mo dispersed fuel) has not been yet qualified. Therefore a similar optimization study of the burnable absorber has been conducted for the current HEU fuel [1-3]. The present paper gives the results of the irradiation project HEU-Cd [5] which has been carried out in BR2 for the qualification of Cd-wires as burnable absorbers for the standard HEU driver fuel element, in the framework of the BR2 conversion project.

2. The use of burnable absorbers at BR2.

Burnable absorbers (aka poisons) are isotopes with high neutron absorption cross section. In the case of BR2 such poisons are incorporated in the fuel meat of a standard driver fresh fuel element. The purpose is to lower the initial reactivity at the beginning of the cycle, to reduce the control rod motion range during operation and to extend the burn-up (GWd/MTU) at discharge of the fuel element, which leads to reduction of the fresh fuel consumption. The burnable absorbers will capture neutrons and transmute all along the irradiation of the fuel element and should optimally be completely consumed at the burn-up of discharge of the fuel element, in order to limit the reactivity penalties.

At BR2 another major benefit of the use of burnable absorbers is the constitution of a 'large' inventory of fuel elements with various partial burn-ups. This allows to adapt the local irradiation conditions not only by modifications of the configuration but also by adaptations of the burn-up of the driver fuel in particular channels.

Since 1969 BR2 uses HEU fuel under the form of UAl_x grains dispersed in an aluminum matrix with a combination of burnable absorbers, boron under the form of B₄C and samarium under the form of Sm₂O₃, homogeneously mixed in the fuel meat.

2.1 Choice of suitable burnable absorbers for LEU.

BR2 is presently engaged in the qualification of high density LEU fuel, suitable for the conversion of the reactor. Right at the beginning of the project the issue of the burnable absorbers was reconsidered. Boron and samarium had been optimized for the present dispersed HEU fuel under the form of aluminide. Even if one would like to maintain the same combination of absorbers, the respective densities would have to be reviewed. Up to now nobody has yet tested to introduce burnable absorbers into the meat of high density dispersed fuels. In particular this has never been done for U-Mo fuels and there is also no intention by fuel developers to do so up to the present time.

The fuel manufacturer advises to remove the burnable absorbers from the meat. Mixing burnable absorbers in the fuel meat causes a major problem for the recovery of discarded fuel material which arises under various forms during the fabrication. This recovery is not possible due to the presence of those absorbers in the meat and therefore all discarded material has to be considered as fabrication scrap. Successful mixing burnable absorbers into the meat of a high density dispersed fuel matrix certainly would require additional development work.

Therefore other issues for the nature and localization of the burnable absorber for the new LEU fuel system had to be considered. The basic criteria for choice of optimal burnable absorber material are: 1. efficiency (high macroscopic absorption cross section); 2. the daughter isotopes of the burnable poison should have small absorption macroscopic cross section compared to the cross section of their precursor; 3. high melting point (more general: 'structural stability'); 4. commercial availability and manufacturing feasibility. Based on these criteria, the following burnable absorbers were considered: cadmium, gadolinium, boron, and erbium. Europium and hafnium have not been considered as candidates for burnable absorber since their daughter isotopes have high absorption cross sections. Samarium alone burns up too quickly and is only useful in combination with another absorber. Dysprosium would have the required characteristics but it is not commercially available in sufficient quantities, or not at an acceptable price.

2.2 Optimization of burnable absorber nature and geometry.

The nature and quantity (or density, if applicable) of the absorber(s) must be optimized. The criteria to guide the optimization are: 1. enhanced fuel utilization (maintain/increase burn-up at discharge); 2. extended core lifetime (maintain/increase cycle length); 3. flattened reactivity evolution (maintain/reduce present displacement evolution of the control rods); 4. the safety criteria (with respect to the Technical Specifications [6]).

Since a burnable absorber impact on neutronics also depends on its location and geometry, it was necessary to study different configurations. The Global Threat Reduction Initiative (GTRI) fuel development program had not considered, by the time these analyses were performed, the use of burnable absorbers homogeneously mixed in the aluminium matrix for the U-Mo-Al fuel system. Therefore, it was necessary to consider the use of lumped burnable absorbers for the future LEU fuel element. Three types of burnable absorber designs have been considered: 1) wires inserted in the grooves of the side plates where fuel plate are wedged, 2) plates inserted in the side plates, and 3) homogeneously mixed boron in the bulk of the aluminium side plates (this option was later discarded by the fuel manufacturer). Figure 1 illustrates the geometry of the first two designs.

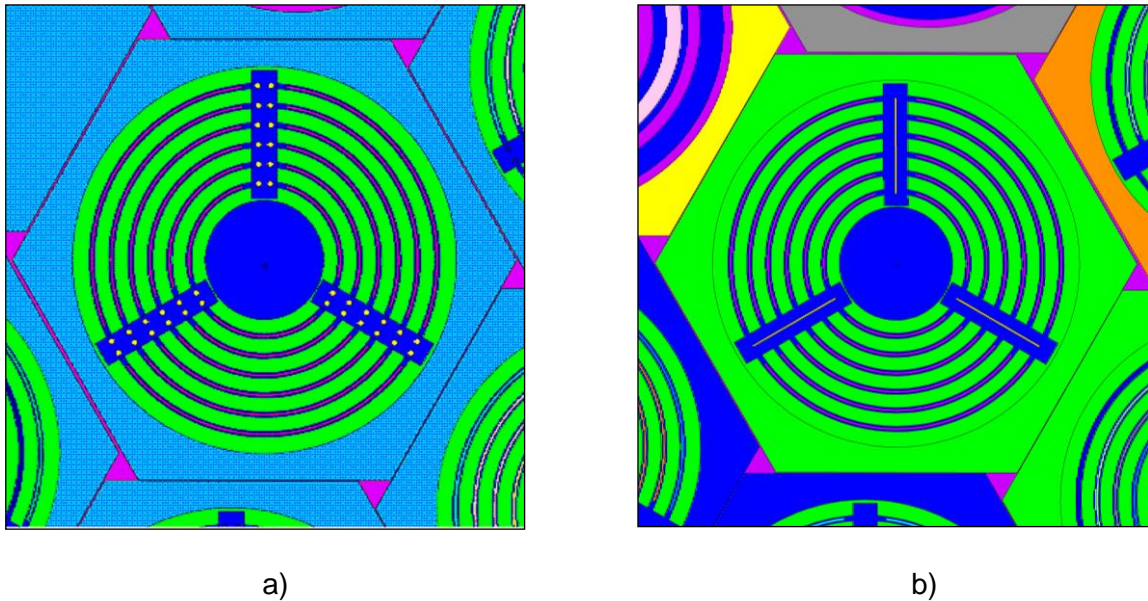


Figure 1. Lumped burnable absorber geometries considered: a) in 36 wires or b) in 3 slabs in the aluminium side plates.

A comparative analysis of the burn-up was performed for several burnable absorber candidates: Cd, Gd_2O_3 , Er_2O_3 , Sm_2O_3 and B_4C . The highest burnable absorber burn-up was obtained using cadmium and 10% less burn-up was obtained for gadolinium. Boron and samarium achieved a burn-up about two times lower while erbium achieved the lowest burn-up. Based on these analyses, it was decided that cadmium was the most appropriate choice for the burnable absorber for the proposed LEU fuel element.

2.3 MCNPX 2.7.0 calculations of poison burn-up

BR2 uses the automatic burn-up code MCNPX 2.7 for criticality and depletion calculations [4]. The detailed whole core geometry model of the BR2 reactor contains a detailed 3-D fuel distribution and a detailed 3-D beryllium poisons (helium-3, lithium-6 and tritium) distribution. Additionally, a detailed 3-D modeling of the cadmium poison in the wires has been applied in order to take into account the axial and radial cadmium burn-up evolution. A comparison of the burn-up in the cadmium wires in HEU-Cd fuel element with the burn-up of the mixed in the fuel meat poisons (boron and samarium) in the standard BR2 HEU fuel is given in Fig. 2. The poison burn-up is presented by two different ways. Fig. 2a shows the cadmium depletion, expressed as the change of the poison concentration vs. U5 depletion:

$$B_c^p[r.u.] = \frac{c_p(0) - c_p(B^5)}{c_p(0)} \quad (1)$$

The burn-up on Fig. 2b is expressed as the change of the absorption macroscopic cross section of the poison vs. U5 depletion:

$$B_\Sigma^p[r.u.] = \frac{\Sigma_p(0) - \Sigma_p(B^5)}{\Sigma_p(0)} \quad (2)$$

Where: $B_c^p[r.u.]$ is the poison depletion in relative units; $B_\Sigma^p[r.u.]$ is the poison burn-up expressed by the poison absorption macroscopic cross section; $c_p(0)$ is the fresh poison concentration; $c_p(B^5)$ is the poison concentration corresponding to B^5 depletion of U-235; $\Sigma_p(0)$ and $\Sigma_p(B^5)$ are the absorption macroscopic cross sections in fresh and in burnt poison, which are calculated using the burn-up option of MCNPX 2.7.

Figure 2a shows that in beginning of irradiation cadmium is depleted much faster than boron and practically is totally burnt after 1,5-2 BR2 irradiation cycles (at about 20% U5 depletion). However, Fig. 2b shows that the cadmium absorption during the first cycle is slower than the boron absorption which explains the absence of minimum in the reactivity evolution curve (see Fig. 3 in further Sect. 2.4). The evolution of the macroscopic absorption cross sections in the different poisons is compared in Figure 2c. As can be seen, the absorption macroscopic cross section of cadmium is significantly lower than the macroscopic cross sections of the standard poisons (boron and samarium). This is the reason for the higher reactivity effect of the fresh and low burnt HEU-Cd fuel element (see Fig. 6 in further Sect. 5.4). The calculations in Figure 2 have been performed for wire diameter $\varnothing = 0.4$ mm, however the general trend of the curves will not change for higher wire diameter (e.g. $\varnothing = 0.5$ mm). Only the absolute values of the macroscopic cross sections will change and the curves of the cadmium burn-up and macroscopic cross section will be closer to the corresponding boron curves.

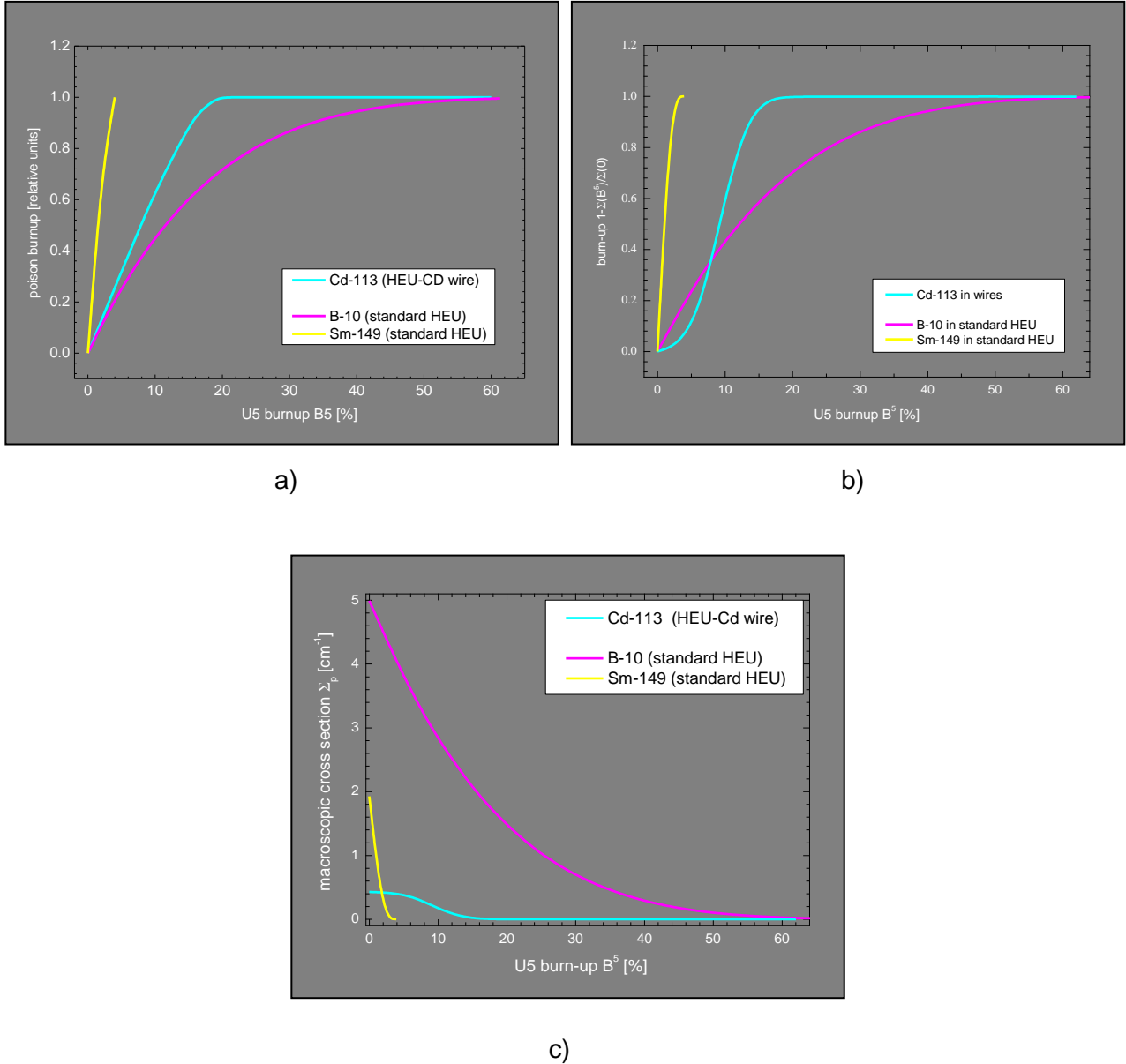


Figure 2. MCNPX 2.7.0 calculations of poison depletion (a) and poison burn-up (b) vs. U5 depletion in HEU-CD FE and in a standard BR2 HEU FE; macroscopic cross section (c).

2.4 Optimization of Cd-wire diameter.

The wire diameter for different fuel types (HEU and LEU) has been optimized on the basis of the reactivity excess at beginning of cycle (and corresponding critical position of the control rods) and control rods motion during operation. Figure 3 shows comparison of CR motion during typical BR2 operation cycle for several different fuel types: 1. Standard BR2 HEU fuel; 2. HEU fuel with cadmium wires; 3. LEU (UMo) fuel with cadmium wires. A typical BR2 reactor core load was used for all calculations. Two wire diameters of \varnothing (Cd)=0.4 mm and \varnothing (Cd)=0.5 mm are compared. The advantage of a smaller wire diameter (0.4 mm) is the prolonged cycle length, however the reactivity excess at BOC is too high (too low critical position of the control rods). This can be compensated by increasing the wire diameter. However, the larger the wire diameter, the slower is the cadmium burn-up, which will shorten the cycle length. A well optimized, slightly larger diameter (0.5 mm) will be sufficient to respect the shutdown margin at BOC and at the same time will not jeopardize the cycle

length. The cycle length for a fuel (HEU or LEU) with \varnothing (Cd)=0.5 mm will be shorter compared to \varnothing (Cd)=0.4 mm, but still significantly longer compared to the standard HEU fuel with mixed poisons.

The final choice made for the new burnable absorber is the following: 36 Cd wires in the 12 grooves of the 3 Al side-plates of the standard BR2 fuel element. The optimum diameter for the different fuel types is: $\varnothing = 0.5$ mm for the UAI HEU (1.3 gUtot/cc); $\varnothing = 0.5$ mm for U-7Mo LEU (8.5 gUtot/cc); $\varnothing = 0.4$ mm for U-7Mo LEU (7.5 gUtot/cc).

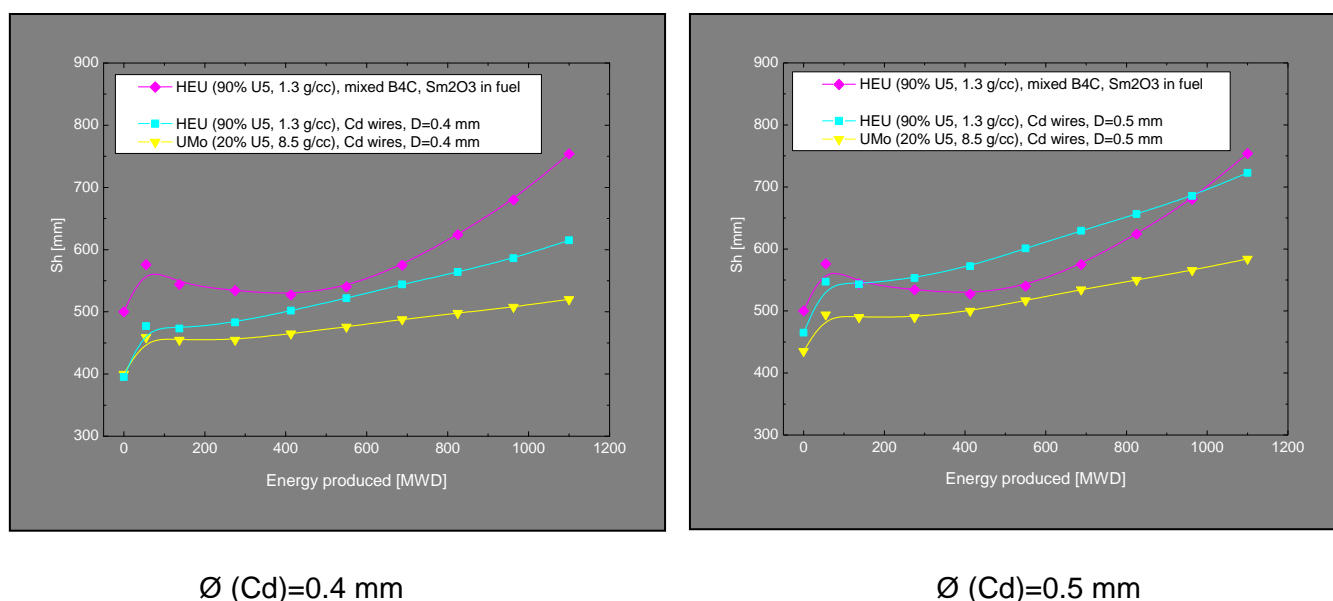


Figure 3. Comparison of CR motion during typical BR2 operation cycle for different fuel types: HEU and LEU fuels with cadmium wires vs. standard BR2-HEU fuel with mixed boron and samarium poisons in the fuel meat.

3. Manufacturing of prototypes for testing of new absorbers with HEU. Fabrication, commissioning and delivery.

A contract was signed with AREVA-CERCA for the redesign of the standard BR2 fuel element in order to allow the insertion of the Cd-wires within the grooves of the stiffeners. This effort is described in [3]. An Al-cladding has been added for the Cd-wires in order to prevent leaching of the Cd in the primary water [5]. Two elements (of the type HEU-Cd) have been fabricated. They have been "commissioned" in various stages (flat plates, incurved plates, assembly of the fuel element with particular attention to the insertion of the Cd wires within the grooves of the stiffeners) just like standard BR2 fuel elements.

The fuel manufacturer attested feasibility but informed that that some 'minor' design changes are required to accommodate the wires (these design changes are described in [3]). Fig. 4a (which gives a detail of the element cut represented in Fig.1a) shows schematically the stiffener design with the grooves for Cd-wires and one fuel plate:

- the important lengths AA and D remain unchanged;
- the total width of the stiffeners is increased from 5.58 mm to 6.80 mm;
- the total width of the fuel plates is reduced by less than 1.8 mm (1.72 – 1.8);

- the maximum width of the fissile meat in the plates is reduced by less than 0.9 mm (0.82 – 0.9), but the nominal width of the fissile meat remains unchanged: this is possible because of the progress in technological know-how by the fuel manufacturer;
- all other geometrical characteristics and dimensions of the fuel element remain unchanged.
- Figure 4b shows the general views of the fabricated HEU-Cd fuel elements.

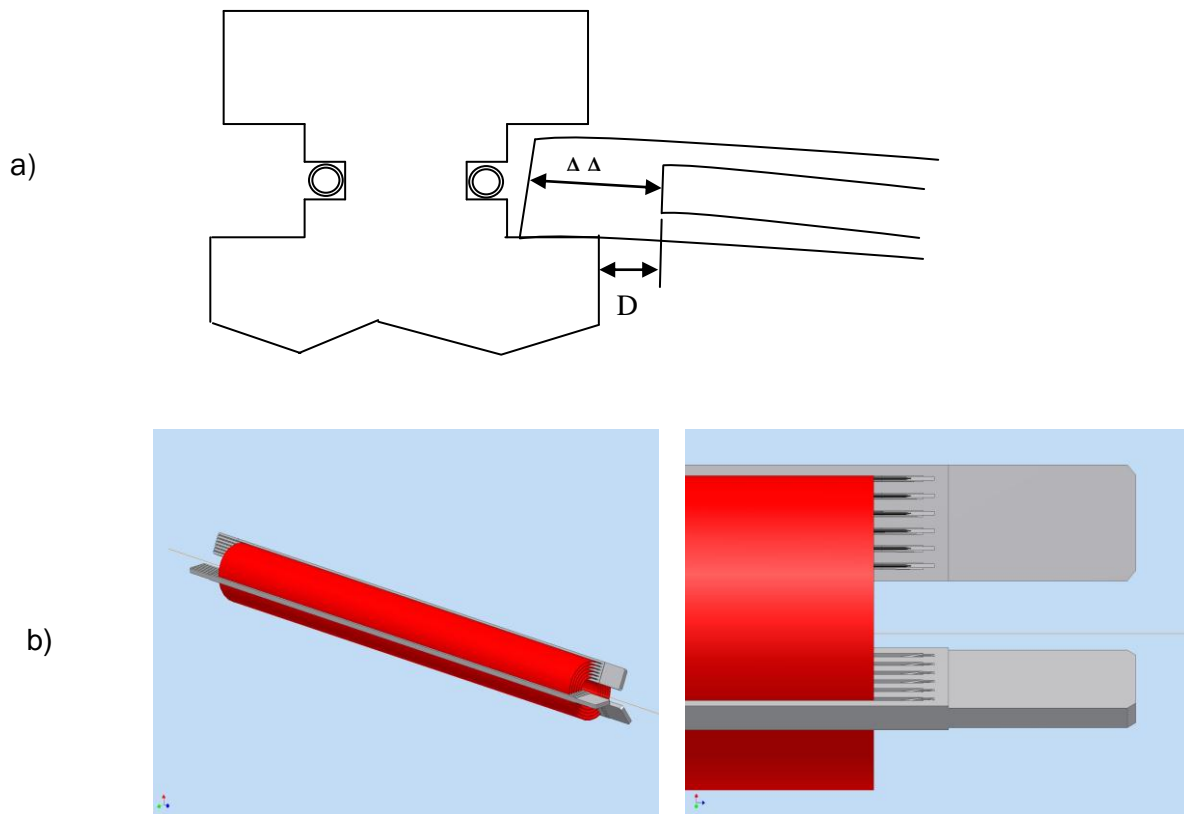


Figure 4. a) Diagram of the stiffener design; b) Views of BR2 fuel element with sheathed cadmium wires (AREVA-CERCA).

4. Irradiation history (power, heat flux, burn-up).

The chosen burnable absorbers (Cd-wires) must be 'qualified' and authorized in order to introduce them in the manufacturing of the lead-test assemblies (LTA's), prototypes of the future LEU BR2 driver fuel elements. The purpose of the HEU-Cd irradiation project was to determine the influence of the replacement of burnable absorbers (B_4C and Sm_2O_3) in the fuel meat of a standard BR2 fuel element by cadmium wires in the grooves of the side-plates/stiffeners [5].

Two prototype HEU fuel elements with cadmium wires have been manufactured for irradiation in the BR2 reactor. The irradiation campaign started in the 1st cycle of BR2 in 2011 and lasted for the remaining part of the year. One element was loaded in channel C199 and one element was loaded in channel G180. C-type channels are conventionally used for loading fresh fuel elements. The second cadmium-wired fuel element was loaded in a G-

channel (having a lower power than a C-channel) to obtain at the end of cycle 01/2011 a cadmium-wired fuel element with a small(er) burn-up.

The two HEU-Cd fuel elements have followed the same irradiation scheme as the standard BR2 driver fuel elements: 4 – 5 cycles depending on the burn-up reached after the 4th irradiation cycle. The two HEU-Cd elements being quite similar to the standard BR2 fuel elements (see the evaluation made in [2], in particular with respect to power peaking factors and the results of the first hydraulic measurement campaign further on in this report), they can be irradiated up to the authorized limit of 470 W/cm².

The objectives of these irradiations are essentially: 1. the qualification of the manufacturer; 2. the verification of the thermo-mechanical stability under irradiation of the design with Cd-wires in the grooves of the stiffeners; 3. The adequacy of the cadmium wires to serve as burnable absorbers.

5. Reactivity effects of HEU-Cd.

The nuclear measurements have determined the reactivity difference of the cadmium-wired fuel elements with respect to the standard fuel elements. As anticipated, the fresh cadmium wired fuel elements have a positive reactivity with respect to a fresh standard fuel element. The reactivity difference depends on the reactor channel in which the cadmium-wired element is placed. The renormalization of the reactivity effects for different channels and different burn-ups has been the subject of the reactivity measurements for both elements.

5.1 Choice of reactor channels for irradiation of HEU-Cd.

Before start of the irradiation of the two HEU-Cd wired fuel elements, detailed MCNPX 2.7 whole core models have been prepared for each reactor configuration of the BR2 cycles operated in 2011 with detailed 3-D geometry description of the wires in order to take into account the axial and radial cadmium burn-up evolution. The irradiation of the two HEU-Cd fresh fuel elements started in the cycle 01/2011A.3, and continued during the following cycles 02/2011A.5, 03/2011A.3, 04/2011A.1 and 05/2011A.2. The irradiation channels for each specific cycle have been carefully chosen in order to obtain various burn-ups at the end of each irradiation cycle. This information can be found in Table I.

Table I. Summary information about the reactor channels loaded with the two HEU-Cd fuel elements and MCNPX predicted burn-ups at BOC for the BR2 cycles in 2011.

Cycle	HEU-Cd1			HEU-Cd2		
	BR2 channel	U5 burn-up at BOC [%]	Cd burn-up at BOC [%]	BR2 channel	U5 burn-up at BOC [%]	Cd burn-up at BOC [%]
01/2011A.3	C-199	0	0	G-180	0	0
02/2011A.5	C-199	14	84	D-120	6	39
03/2011A.3	D-120	30.5	100	C-199	20	98
04/2011A.1	D-300	42.0	100	B-60	34.2	100
05/2011A.2	Not loaded	52.9 (end of irradiation history)	-	G-180	47.2	100
01/2011A.1	—	—	—	Not loaded	52.9 (end of irradiation history)	

5.2 Nuclear Measurement Program (NMP) for determination of the reactivity effects of HEU-CD.

The irradiation of the cadmium-wired fuel elements in the BR2 reactor resulted in the gradual increase of the burn-up level of each fuel element. The objective of the nuclear measurements was to obtain the evolution of the reactivity of the cadmium-wired fuel element as a function of burn-up. The reactivity effect of each element was measured at the start of a reactor cycle. All measurements were made in one and the same channel C199 to achieve maximum possibilities to compare. Due to the fact that only two fuel elements were available, the reactivity measurements were made with different reactor loads.

The zero power nuclear measurements before the full power operation of each cycle in 2011 consisted of the following steps:

1. Assembly of a suitable reactor load for the full power operation. One of the cadmium-wired elements, HEU-Cd1 loaded in channel C199. Measurement of the critical height of the control rods.
2. Replacement of the cadmium-wired fuel element HEU-Cd1 in channel C199 by the other HEU-Cd2 fuel element. Measurement of the critical height of the control rods.
3. Replacement of the cadmium-wired fuel element HEU-Cd2 in channel C199 by a fresh standard BR2. Measurement of the critical height of the control rods.

To determine the reactivity effect more quantitatively, the critical height had to be converted to reactivity [\$], which was determined by positive period measurement. Taking into account that the above described measurements lasted several days, a correction for the ^3He poisoning had to be done. Details about the NMP can be found in [7].

5.3 Reactivity effects of HEU-Cd FE: MCNPX predictions vs. measurements.

After finalizing the evaluations for the expected irradiation conditions for the new reactor core configuration, calculations of the reactivity effects of the HEU-Cd fuel elements have been performed by MCNPX prior to the measurements at each BOC using the corresponding cadmium and fuel burn-ups as shown in Table I. The reactivity effect of a HEU-Cd fuel element has been determined relatively to the reactivity of a fresh HEU standard BR2 fuel element for location in one and the same channel C199 of the BR2 reactor. After that the reactivity effects of the HEU-Cd fuel elements have been determined by measurements in the same manner as the calculations according to the NMP [7]. Fig. 5 shows the comparison of the measured reactivity values (corrected for ^3He poisoning) with the calculated values by the MCNPX code. Both, calculations and measurements, confirmed the anticipated form of the reactivity performance graph of fuel elements with cadmium wires. Taken into account the uncertainties of the used measurement, calculation and analysis methods (critical height, positive period measurements), as well as the fact that the elements were measured in different reactor loads, the measured and calculated results correspond very well.

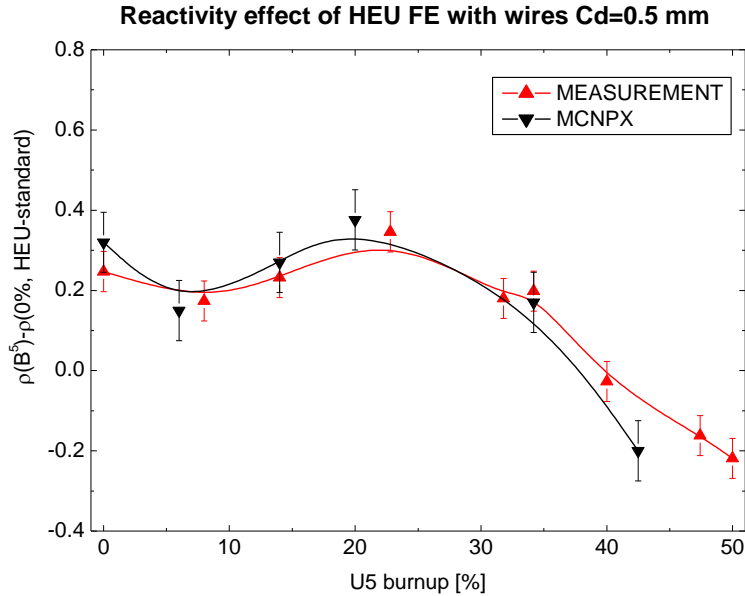


Figure 5. Reactivity effects of HEU-CD fuel elements: MCNPX predictions vs. measurements.

5.4 MCNPX calculations of reactivity effect of HEU-Cd vs. standard HEU.

The measurement of the reactivity effects of the HEU standard BR2 fuel elements were not included in the NMP during 2011 (due to insufficient time during preparation for the cycle before the start-up). Therefore, MCNPX comparative calculations of the reactivity performance graphs for both, HEU standard and HEU-Cd fuel elements with \varnothing (Cd)=0.5 mm have been performed using one and the same load of the cycle 02/2011A.5. The reactivity effects of a fresh and a burnt fuel element were determined relatively to the reactivity of a fresh HEU standard BR2 fuel element for location in one and the same channel C199. Fig. 6 shows the comparison of the reactivity performance graphs. Both fuel elements, HEU standard and HEU-Cd with \varnothing (Cd)=0.5 mm have almost identical performance for U5 burn-up higher than 10%. For burn-ups, lower than 10%, the reactivity of the HEU-Cd fuel element is higher than the reactivity of the standard HEU fuel element. This is due to the lower cadmium absorption macroscopic cross section in comparison with the standard poisons (boron and samarium), see Fig. 2c.

The reactivity performance for wire diameters: \varnothing (Cd)=0.4 mm and \varnothing (Cd)=0.6 mm are also depicted on Fig. 6. This graph shows that the choice of \varnothing (Cd)=0.6 mm will give a poorer reactivity performance. Cd-wires with \varnothing (Cd)=0.4 mm would give better reactivity performance during irradiation (higher reactivity than the standard fuel element), which could result in a longer cycle length. For the wires with \varnothing (Cd)=0.5 mm result in a reactivity performance most comparable to the one of the standard BR2 fuel and also allow to respect the minimum shutdown margin [6] at beginning of cycle.

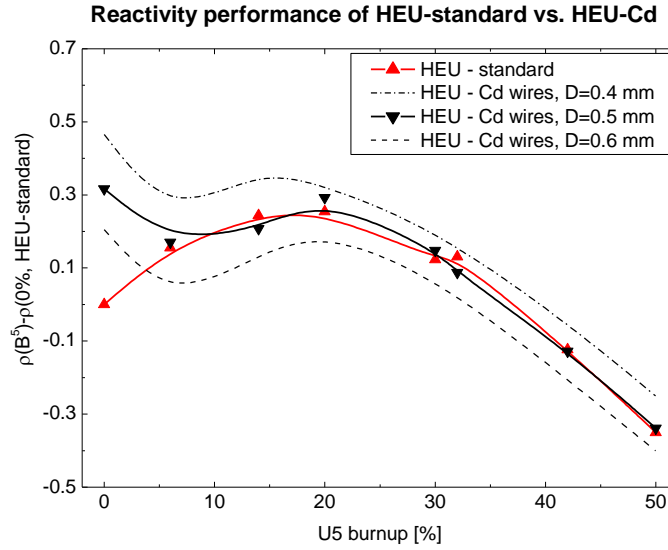


Figure 6. Reactivity performance of HEU-Cd fuel element vs. HEU standard BR2 fuel element: MCNPX 2.7 calculations.

6. Hydraulic measurements, wet sipping, chemical analysis of primary water.

6.1 Hydraulic measurements.

Although the replacement of burnable absorbers in the fuel meat by cadmium wires in the stiffeners only resulted in slight changes in the design of the fuel elements, the replacement could have an influence on the hydraulic characteristic of a fuel element because the water gap area is slightly reduced. The influence was however anticipated to be very small. To evaluate the hydraulic characteristics a hydraulic measurement program has been executed before, during and after the full power operation of the reactor. The prime goal of the hydraulic measurements was the comparison between the pressure drop Δp over a cadmium-wired fuel element and a standard fuel element. The secondary goal was the establishment of the pressure drop curve Δp over a fuel element (standard and cadmium-wired) as a function of the flow rate for different operational parameters, e.g. temperature, burn-up, with respect to the criterion for the minimum pressure drop $\Delta p \geq 2.1 \text{ kg/cm}^2$ as described by the Technical Specifications [7].

Figure 7 shows the evolution of the pressure difference Δp over a fuel element as a function of the primary volumetric flow rate Q as measured by FRCA4-1301 for a standard BR2 HEU fuel element (B710) in reactor channel C161 and for a cadmium-wired fuel element (BCd1) in reactor channel C199 [8]. This figure also shows the evolution of the pressure difference over the reactor as measured by DPRCA4-1301 as a function of the primary volumetric flow rate. The hydraulic measurements have shown that from a hydraulic point of view there is no difference between a cadmium-wired fuel element and a standard fuel element. The pressure difference over the fuel element at the nominal flow rate (DPRCA4-1301 = 3.2 kg/cm^2 with correspondingly FRCA4-1301 = $6830 \text{ m}^3/\text{h}$) is: 2.28 kg/cm^2 for the cadmium wired fuel element; 2.26 kg/cm^2 for the standard fuel element. The difference between both values is therefore 0.02 kg/cm^2 and much smaller than the criterion of 0.2 kg/cm^2 [6]. Based on these results the irradiation of the cadmium-wired fuel elements at nominal power of BR2 was authorized.

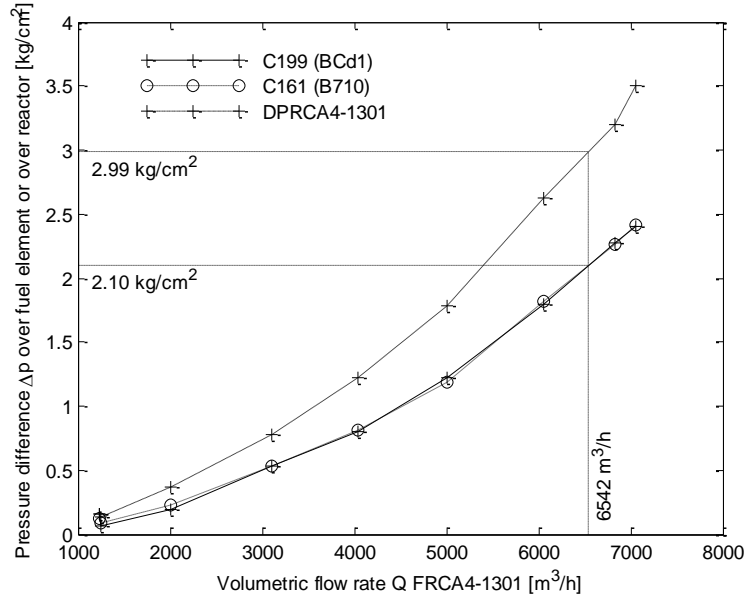


Figure 7. Evolution of the pressure difference over a fuel element and over the reactor as a function of the primary volumetric flow rate Q for a standard fuel element B710 in reactor channel C161 and for a cadmium-wired fuel element in reactor channel C199.

6.2 Primary water composition.

In case of failure of the cladding of the cadmium wires and leaching of the cadmium, the presence of cadmium wires might, although very unlikely, have an influence on the primary water quality [5]. To determine if there is release of cadmium from the cadmium-wired fuel elements, the composition of the primary water was subject to a follow-up during reactor operation. Water samples were taken with a frequency of three times a week for spectrometric analysis. The two cadmium isotopes followed were: ^{115}Cd : detection limit $1.3 \text{ Bq/ml} = 1 \times 10^{-8} \text{ ppb}$; ^{117}Cd : detection limit $2.5 \text{ Bq/ml} = 3 \times 10^{-10} \text{ ppb}$. During the whole full power operation the activity of both isotopes in the primary water was below the detection limit.

6.3 Visual inspection. Wet sipping.

After each cycle the two HEU-Cd elements have undergone visual inspection and a wet-sipping test like the standard BR2 fuel elements. The cadmium-wired fuel elements were subject to standard visual inspection before and after loading. The cadmium-wired elements were subject to a standard 48 h. wet-sipping test after each irradiation cycle. The wet-sipping water samples are examined for the presence of four fission products: ^{133}Xe , ^{131}I , ^{134}Cs , ^{137}Cs .

7. Conclusions.

The nuclear measurements have determined the reactivity difference of the cadmium-wired fuel elements with respect to the standard fuel elements. As anticipated, the fresh and low burnt cadmium-wired fuel elements have a positive reactivity effect with respect to a fresh standard fuel element.

MCNPX calculations have shown that for U5 burn-ups higher than 10%, the reactivity performance of the cadmium-wired fuel element with diameter \varnothing (Cd)=0.5 mm is almost identical to the reactivity performance of a standard BR2 fuel element.

The hydraulic measurements have shown that from a hydraulic point of view there is no difference between a cadmium-wired fuel element and a standard fuel element. This is true for the pressure difference as a function of flow, as a function of time and as a function of temperature.

During reactor operation no cadmium release was detected in the primary water. Visual inspection at the moment of unloading showed no anomalies. Wet sipping of the fuel elements after unloading the reactor elements showed no fission product release by the cadmium-wired elements.

Summarised, the two irradiated cadmium-wired fuel elements behaved as expected. With the exception of the anticipated reactivity difference, the cadmium-wired fuel elements have an identical behaviour with respect to standard fuel elements.

References

1. S. Kalcheva, E. Koonen and B. Guiot, "Optimized Burnable Absorber for the BR2 Reactor", *RERT 2008 – 30th International Meeting On Reduced Enrichment For research And Test Reactors*, October 5-9, 2008, Washington D.C., USA.
2. B. Guiot, "Improved BR2 Fuel Cycle With Optimized Burnable Absorber", Master Thesis, Mentors: E.Koonen, S.Kalcheva, Promoter: Prof. J.M.Noterdaeme, BNEN, SCK, Belgium. August, 2008.
3. N. Franck, S. Kalcheva and E. Koonen, "Cd wires as burnable poison for the BR2 fuel element", *Proceedings of the 13th Int. Topical Meeting on Research Reactor Fuel Management*, Vienna, Austria, March (2009).
4. MCNPX, Version 2.7.0, LANL, LA-UR-11-02295. April, 2011.
5. E. Koonen, "HEU-Cd: Update on the status of the project. Report for CEE examination", BR2 Reactor, SCK•CEN, December 2010.
6. E. Koonen, F. Joppen, B. Wellens, G. Van den Branden. Reactor BR2: Dossier 72. S 7680. Volume 3: Technische Specificaties, November 2009.
7. G. Van den Branden, "Nuclear measurements of HEU-Cd elements for cycle 01/2011 to 05/2011, BR2 Reactor, SCK•CEN, February 2012.
8. G. Van den Branden, "Nuclear and Hydraulic Measurements HEU-Cd elements", BR2 Reactor, SCK•CEN, January 2011.

NEUTRON DIFFRACTION ANALYSIS OF HIGH BURNUP LEU FUEL FROM NRU

D.F. SEARS, N. WANG

*Atomic Energy of Canada Limited
Chalk River Labs, Chalk River, Ontario K0J1J0 – Canada*

R. ROGGE, I.P. SWAINSON¹, R. DONABERGER

*National Research Council Canada
Canadian Neutron Beam Centre, Chalk River, Ontario K0J1J0 – Canada*

ABSTRACT

Al-U₃Si dispersion fuel has been used in the NRU reactor for almost two decades, and it has performed well, with stable swelling behaviour and no defects linked to the LEU fuel material. However, little is known about the phase composition and crystal structure of extruded Al-U₃Si fuel pins after irradiation to high burnup in the NRU reactor. AECL and NRC have developed the capability to perform neutron diffraction measurements on highly radioactive fuel samples using shielded apparatus on the C2 neutron diffractometer at NRU. This paper discusses diffraction measurements that were recently performed to assess the crystal structure of irradiated Al-U₃Si fuel from an NRU fuel rod. Samples were taken from different regions of the fuel rod that operate under different linear power, temperature and burnup conditions, to help assess the effect of these key operating parameters on fuel structure stability. Irradiated fuel samples with operating fuel temperatures ranging from 92 to 188 °C and burnups ranging from 63 to 90 atom% ²³⁵U were tested. Measurements using a monochromatic neutron beam with $\lambda \sim 1.33 \text{ \AA}$ show the only diffraction evidence of a crystalline phase is from the Al matrix, indicating that the U₃Si fuel particles and U-Si-Al reaction products that form during irradiation have become amorphous. The results provide a better understanding of the U₃Si fuel behaviour under neutron irradiation and help to characterize the spent LEU fuel that has accumulated in Canada from almost two decades of NRU operation.

1. INTRODUCTION

Uranium-silicide dispersion fuels are used extensively in research reactors that have converted from HEU to LEU fuel. In most designs, the fuel is fabricated as a metal-matrix-composite containing uranium silicide particles dispersed in an Al matrix, sheathed with Al cladding. The highest density compound in the U-Si binary system, U₃Si ($\rho = 15.4 \text{ g/cm}^3$), is used as the dispersed phase in reactors such as NRU and HANARO that use extruded rod or pin-type fuels developed in Canada. The second highest density compound in the U-Si system, U₃Si₂ ($\rho = 12.2 \text{ g/cm}^3$), is used predominantly in reactors that employ plate-type fuel (e.g., MTRs). Differences have been noted in the fission-gas bubble growth and swelling behaviour of these two fuel types under irradiation. In the early stages of the LEU development program, these differences were attributed to the crystal structure stability under irradiation; specifically, it was thought that U₃Si₂ remains crystalline while U₃Si becomes amorphous and swells excessively [1]. Although stable swelling and good behaviour were observed in fuel irradiations in NRU [2,3], persistent concerns about breakaway swelling in U₃Si limited its application to extruded rods, and emphasis shifted to the use of U₃Si₂ in plate-type fuels. Later work showed that U₃Si₂ also becomes amorphous under neutron irradiation [4], and subsequently differences in swelling behaviour were attributed to excess free volume in amorphous compounds [5]. More recent studies [6] have focused on the interdiffusion between the Al matrix and the uranium silicide particles, and the resulting reaction product(s) that form an interfacial layer around the particles, to help explain the observed differences in the swelling behaviour of the two silicide fuel types.

¹ Currently at Canadian Centre for Nuclear Innovation, 121 Research Drive, Saskatoon, SK S7N 1K2, Canada

There have been several diffraction studies of silicide fuel materials irradiated to low burnup in neutron and ion irradiation facilities [7-10], but scant information exists on the phase characterization of Al-U₃Si dispersion fuel elements that have been irradiated to high burnup under typical in-reactor operating conditions in NRU. Al-U₃Si fuel has been used in the NRU reactor for almost two decades, and it has performed well, with stable swelling behaviour and no defects linked to the fuel material itself. Some of the success in NRU could be attributed to the robust design of the extruded pin-type fuel where the thick, finned Al-cladding provides superior restraint to the swelling fuel core (compared to that provided by the thin cladding in plate-type fuels). It was speculated that differences in operating conditions, specifically in-reactor temperature, fission rate and fission density, may effect a transition from irradiation-induced amorphization to recrystallization and contribute to the satisfactory behavior. Difficulties in developing alternative LEU fuels based on UMo, and the recent trend towards adding Si to stabilize the interfacial layer that forms between the UMo and the Al matrix, have prompted renewed interest in high density U₃Si fuel and the stable reaction product that forms with Al. Also, given the significant quantity of Al-U₃Si fuel that has accumulated in Canada since NRU was converted from HEU to LEU in the early 1990's, it is considered important to fully characterize the irradiated material to support future efforts to disposition the spent fuel.

2. PREVIOUS WORK

AECL and NRC-CNRC have developed a Pb-shielded cell to safely perform neutron diffraction analysis on highly irradiated fuel materials. This unique facility at Chalk River has previously been successfully used for the examination of UMo-Al dispersion fuels that were irradiated in NRU [11]. These studies were conducted as a function of fuel-phase composition, burnup, and axial position along the UMo-Al fuel elements. They gave unique information on the irradiation behaviour of the γ phase UMo alloy, and the reaction products that form between the UMo fuel particles and Al matrix. This previous work provided evidence that the reaction layers that form as a result of the interaction of the Al matrix with the γ phase fuel particles are largely crystalline and have the same structure as the binary UAl_x compounds ($x = 2, 3, 4$), with the predominant reaction product being isostructural to UAl₃ [12]. Ion bombardment studies [13] produced similar results. In contrast, TEM measurements [14, 15] and other assessments [16] showed amorphous reaction products developed in Al-UMo plate-type fuels that operated at lower temperature. Subsequent work on the annular end regions of UMo-Al fuel elements that operated at lower temperature in NRU showed no diffraction peaks from the U-Mo-Al reaction products indicating that the material was amorphous [17]. It is inferred that the central regions of the test fuel in NRU exceeded the temperature limit for amorphous to crystalline transformation. The current work investigates whether similar changes occur in Al-U₃Si fuel.

3. EXPERIMENTAL

The nominal fuel composition is Al-61 wt% U₃Si with the U enriched to 19.75% ²³⁵U. Samples were examined and characterized in the hot cells prior to the diffraction experiment. Each specimen was mounted, ground and polished using standard procedures developed for silicide fuel (wet grinding on SiC papers, coarse polishing on diamond paste followed by final polishing on silica suspension). The microstructures were examined in the as-polished condition and photographed, with special attention to the U₃Si particles, the surrounding reaction layers, the core/cladding interface and the cladding surface oxide layer. Dimensions were measured with the aid of image analysis software.

A thin slice of fuel from an end sample was mounted, polished and examined in the shielded SEM facility (JEOL JXA 840A). The SEM was operated at a beam voltage of 25 kV with currents ranging from 20 to 55 nA. Spot compositions, X-ray maps and line scans were obtained using WDX analysis.

Samples were cut from different axial regions of the fuel rod to see if the effects of temperature and burnup caused different structural changes, as they had in our previous UMo-Al experiments [11, 12]. Four samples were selected, one each from the inlet and middle of a fuel element (401-9) and from the middle and outlet end of another element (393-12). At the rod limiting power of 2.1 MW in NRU, the maximum cladding surface temperature is ~ 130 °C and the maximum fuel centerline temperature is ~ 188 °C (calculated using fresh fuel properties). At the inlet end (bottom), where the bulk coolant temperature is ~ 35 °C, the nominal cladding surface and fuel centerline temperatures are 65 and 92 °C, respectively. At the outlet end (top), the cladding surface and fuel centerline temperatures are 94 and 120 °C, respectively. Thermal ionization mass spectroscopy was used to measure the U isotopic ratios to determine the burnup achieved (see Table 1). The finned Al cladding was removed

from the fuel element by machining until the fuel core was exposed. Cylindrical samples ~ 5.5 mm diameter x 10 mm long were then machined from the fuel core. Figure 1 shows the element during machining and the core sample after machining to final size.

Sample ID (Element#, location)	MWh/kgIHE	Atom% ²³⁵ U Burnup
(401-9, Outlet/Top)	2539	63.4%
(401-9, Middle)	3676	89.5%
(393-12, Middle)	3675	89.8%
(393-12, Inlet/Bottom)	2558	64.1%

Tab 1. Fuel burnups based on the measured U isotopic ratios.

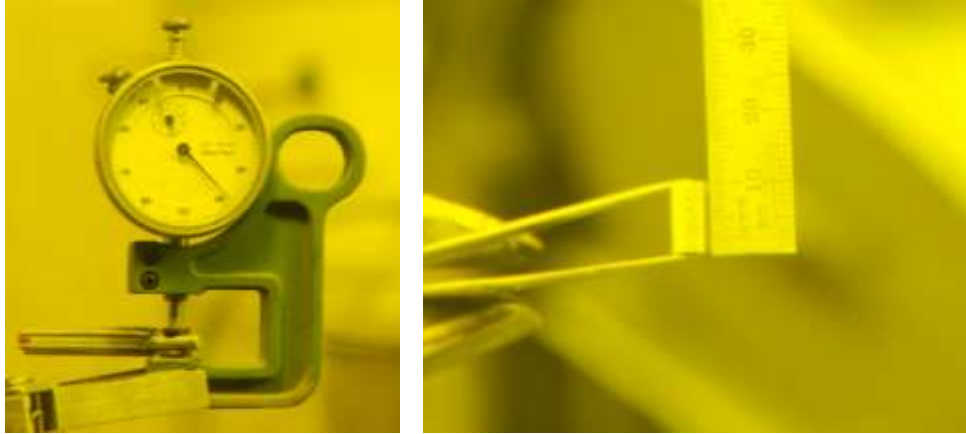


Fig 1. Irradiated Al-U₃Si fuel with cladding machined from core (left) and after final size (right).

Neutron diffraction data were collected on neutron powder diffractometer C2 at room temperature. The C2 diffractometer consist of an 800-wire BF₃ detector, each wire 0.1° apart from the next, so that a diffraction pattern of any 80° 2θ in the maximum operating range of 3–110 ° 2θ can be recorded at one time. The stage is centered with a dummy sample in the beam prior to the main experiment. The wavelengths and 2θ₀ (the zero-angle error) are calibrated using the Si standard NIST 640c.

The active fuel is loaded into a specially designed V can that is custom designed to fit both the fuel sample and inside the shielded cell. V has an almost zero coherent scattering length and its contribution to a powder diffraction pattern is usually very low. Cd (a strong neutron absorber) strips are added to the top and the bottom of the V can; these are used to set the upper and lower incident beam masks (“jaws”).

The Pb-shielded cell, which contains the V can and a fuel sample, has a removable plug to allow the incident neutron beam onto the sample, and a “window” that allows the diffracted neutrons out of the cell and towards the detectors; this window is also made of Pb, can be cranked open remotely, and defines 20–100° 2θ with respect to the incident beam. No part of the diffractometer needs to move during these measurements, which aids the safety case. For the present work, the wavelength of the monochromatic neutron beam, λ, is ~1.33 Å. The structure refinements were carried out with GSAS.

4. RESULTS AND DISCUSSION

Figure 2 shows the cross section of a NRU fuel element and the typical microstructure of the fuel core at the midplane region (393-12, middle). The oxide layer on the cladding surface is ~30 μm, the core is tightly bonded to the cladding and the fuel particle distribution is consistent with previous work [3]. The higher magnification images in Figure 2 show the microstructure at the core centre, mid-radius and periphery. During irradiation, the Al matrix reacts with the U₃Si particles to form a U-Si-Al interfacial layer around the particles. The interfacial layers are typically thicker in the mid-plane than in the end regions due to the higher local heat ratings, temperature and burnup in the former. The radial profile of the interaction layer thickness follows that of the radial temperature distribution. In midplane sample 393-12, the interfacial layers measured ~7 μm at the core periphery and ~12 μm at the centre. The corresponding U-Si-Al interfacial layer thickness measurements from each sample are summarized in Table 2. Estimates of the average volume fraction occupied by the interfacial

layers range from 8% at the inlet end to 18% at the midplane, sufficient to be detected by NDA if the material is crystalline. In the high burnup regions some of the particles have started to agglomerate. Small fission gas bubbles are visible in the kernels of the particles, but with no gross bubble coalescence and growth. In contrast, the interfacial layer lacks visible fission gas bubbles except near the reaction front with the fuel kernel.

Sample ID (Element#, location)	Fuel/Matrix Interaction Layer Thickness (μm)			
	Core Centre	Mid-Radius	Periphery	Range (min-max)
(401-9, Outlet)	7.2	6.7	6.4	3.6 - 11.8
(401-9, Middle)	14.1	11.5	7.9	4.8 - 24.4
(393-12, Middle)	11.8	10.6	6.9	5.4 - 20.6
(393-12, Inlet)	4.1	4.2	3.8	2.9 - 6.9

Tab 2. Thickness of fuel/matrix interfacial layer.

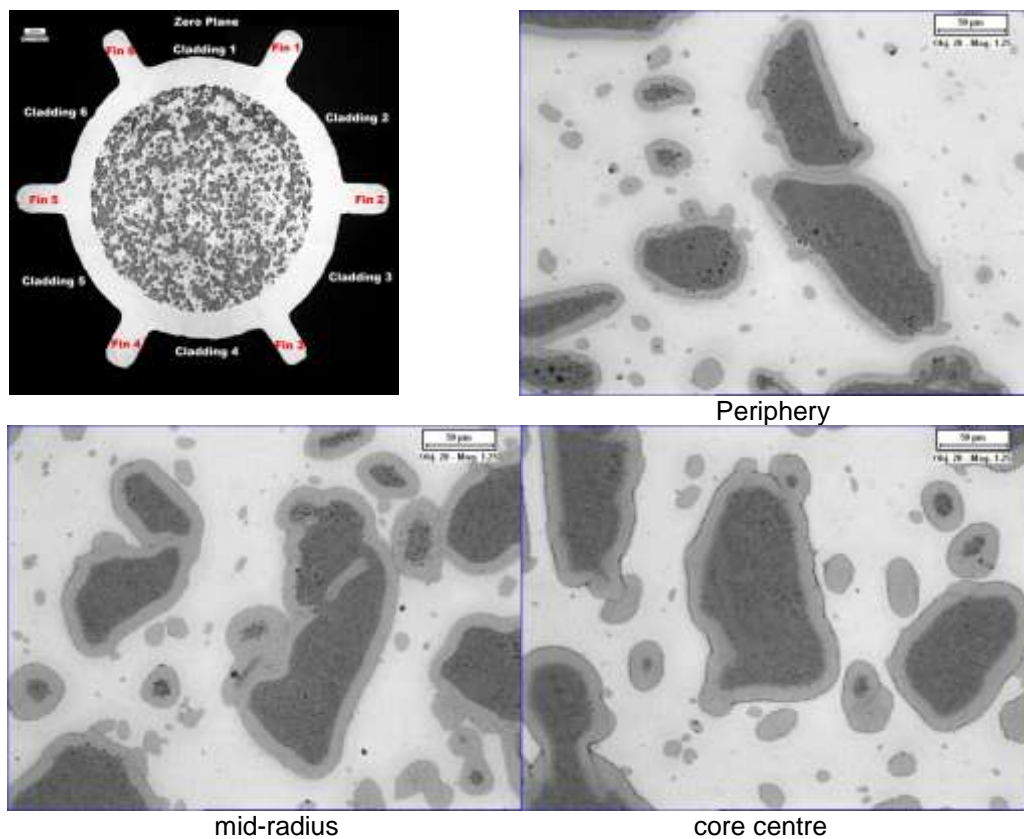


Fig 2. Typical fuel core microstructure near mid-plane of element 393-12 after 90 at% burnup; matrix Al (white), U-Si-Al interfacial layer (grey), U_3Si (dark grey), fission gas bubbles (back circles).

Figure 3 shows an SEM image of the irradiated fuel from an end sample (64% burnup) and a corresponding WDX line scan from the Al matrix across the U_3Si particle and the surrounding interfacial layer. The semi-quantitative line scan indicates the composition of the fuel particle kernel has an average U/Si ratio ~ 2.9 , close to the theoretical value of 3 for the nominal U_3Si composition. WDX spot analysis of the reaction layers surrounding the fuel particles show (Al,Si)/U ratios from about 2 to 5.4. This spans the range for $\text{U}(\text{Al,Si})_x$ where $x = 2-4$.

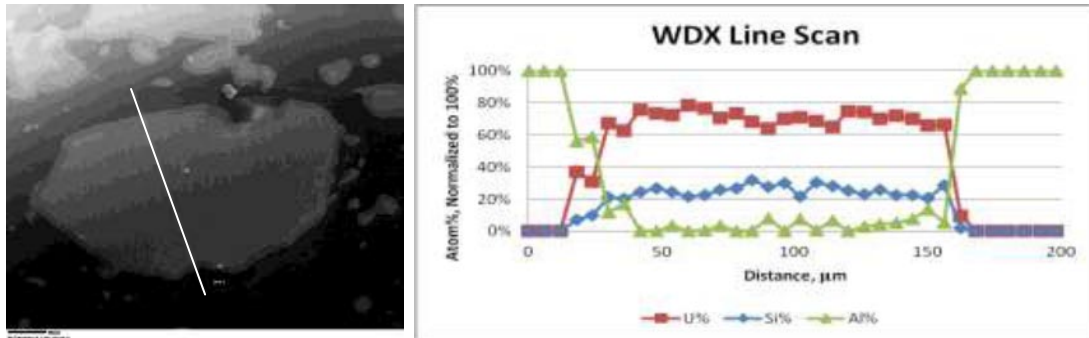


Fig 3. Left: SEM image showing path of line scan across U₃Si fuel particle (grey), interfacial layer (dark grey) and Al matrix (black) from end of fuel element 393-12 (64% burnup); Right: elemental line scan across a fuel particle, showing at% U, Si and Al, normalized.

Figure 4 shows the diffraction results. A sample of as-manufactured NRU fuel was used as the basis to compare the effects of burnup and temperature. As seen in Figure 4a, the calculated pattern fits the observed diffraction pattern well: the observed pattern is a composite of the two major phases, the Al matrix and the U₃Si phase. Minor contributions include U₃Si₂ (usually < 1 vol%), and also very minor contributions from the V can itself. The major systematic differences between the observed and calculated patterns lie in the fit to the intensity of the Al peaks: these differences are due to the extrusion texture that we have not corrected for. Figure 4b shows the fitted diffraction pattern of a sample cut from the midsection of an irradiated rod (90 at% burnup); it is not possible to discern Bragg peaks from U₃Si or U-Si-Al reaction products.

Figure 5 shows a composite figure taken with $\lambda \sim 1.33 \text{ \AA}$ in which all the fuel samples, from the top, bottom, and midsections of irradiated rods, are rescaled (to arbitrary scales) so that they can be overlayed. Apart from a drop-off in intensity in the background below $\sim 25^\circ 2\theta$ for one sample, there is no significant difference between these diffraction patterns. (This difference in background at low 2θ was probably due to a maladjustment of a boron shield on the scattered side, and is not likely to be due to the sample.)

Most evident is that all the diffraction patterns from the samples that have been subjected to 63-90 at% burnup plot on top of one another. The only strong Bragg peaks that remain are from Al. The other trace peaks correspond to V. A broad hump appears with a maximum near $30^\circ 2\theta$; it is likely that this represents the maximum in the scattered signal from the amorphized uranium silicide.

The crystalline Al phase in the diffraction patterns corresponds to the matrix material. The U-Si-Al intermetallic phases are either amorphous or, if they are crystalline, of such a low proportion in the bulk that they are not visible in the neutron diffraction pattern. This contrasts strongly with our earlier work on UMo-Al dispersion fuel, where uranium-aluminide phases were seen as significant crystalline phases in the diffraction patterns of those irradiated fuels.

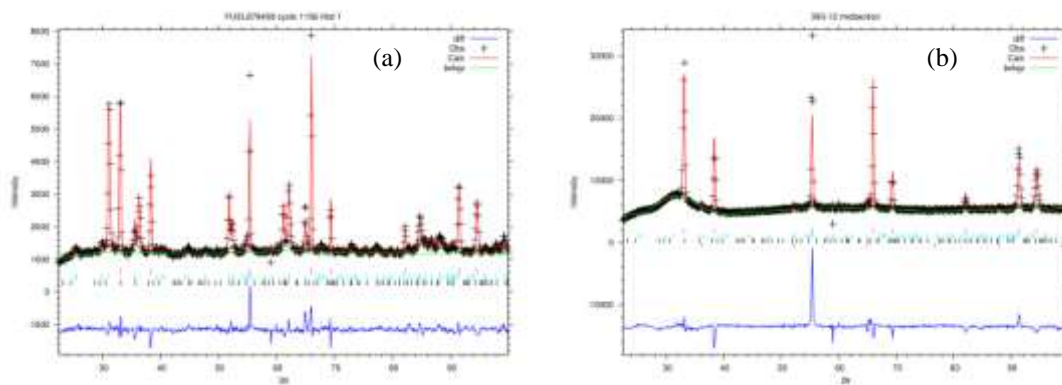


Fig 4. Observed data (crosses), Rietveld fits (smooth line), underlain by their difference (observed-calculated) plot (continuous line). (a) Unirradiated NRU fuel. (b) Irradiated NRU fuel from the midsection of rod 393-12 (90 at% burnup). The tick marks under the patterns represent calculated positions of peaks and are, from top to bottom, Al, U₃Si, U₃Si₂, and in (b) an additional set to represent V.

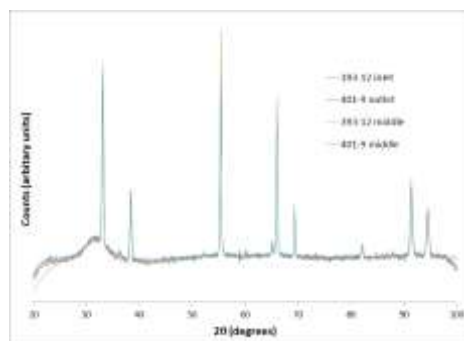


Fig 5. Rescaled data of four different fuel samples from the bottom, middle and top sections of NRU fuel irradiated to high burnup (63-90 at%).

5. SUMMARY AND CONCLUSION

Irradiated fuel samples from NRU with burnups ranging from 63 to 90 at% ^{235}U have been characterized using optical metallography, SEM/WDX and shielded neutron diffraction analysis. WDX analysis indicate the composition of the fuel particle kernel is consistent with the nominal U_3Si composition, and analysis of the U-Si-Al reaction layers surrounding the fuel particles show the (Al,Si)/U ratios ~ 2 -5.4. After irradiation to high burnup in NRU, the only evidence of a crystalline phase is that from the Al matrix material, indicating that the U_3Si and U-Si-Al components of the dispersion fuel have become amorphous. Given the long operating history of these fuels in NRU, it is apparent that loss of crystallinity of U_3Si in Al dispersion fuels is not associated with any negative consequences in performance. The results help to improve our understanding of the Al- U_3Si fuel behaviour under prototypical operating conditions in NRU and help to characterize the spent LEU fuel that has accumulated in Canada from almost two decades of NRU operation.

6. REFERENCES

- [1] G.L. Hofman, J. Nucl. Mater. 140 (1986) 256-263.
- [2] D.F. Sears, in: Proc. Int'l Meeting on Reduced Enrichment for Research and Test Reactors, 1991.
- [3] D.F. Sears, N. Wang, in: Proc. Int'l Meeting on Reduced Enrichment for Research and Test Reactors, Jackson Hole, Wyoming, USA, (1997).
- [4] R.C. Birtcher, J.W. Richardson and M.H. Mueller, J. Nucl. Mater. 230 (1996) 158-163.
- [5] G.L. Hofman and Y. S. Kim, Nucl. Eng. Technol. 37 (2005) 299.
- [6] Y.S. Kim and G. Hofman, J. Nucl. Mater. 410 (2011) 1-9.
- [7] M.L. Bleiberg, L.J Jones, Trans. Met. Soc. AIME 212 (1958) 758
- [8] B. Bethune, J. Nucl. Mater. 31 (1969) 197
- [9] R.C. Birtcher and L.M. Wang, Mat. Res. Soc. Symp. Proc. Vol. 235 (1992) 467.
- [10] R.C. Birtcher, J.W. Richardson, M.H. Mueller, J. Nucl. Mater. 244 (1997) 251-257.
- [11] K. Conlon and D. Sears, in: Proc. 10th Topical Meeting on Research Reactor Fuel Management (European Nuclear Society), Sofia, Bulgaria, (2006).
- [12] K. Conlon and D. Sears, in: Proc. 11th Topical Meeting on Research Reactor Fuel Management (European Nuclear Society), Lyon, France, (2007).
- [13] H. Palancher et. al. in: Proc. 10th Topical Meeting on Research Reactor Fuel Management (European Nuclear Society), Sofia, Bulgaria, (2006).
- [14] S. Van den Berghe, W. Van Renterghem, A. Leenaers, J. Nucl. Mater. 375 (2008) 340-346
- [15] J. Gan, D.D. Keiser, D.M. Wachs, A.B. Robinson, B.D. Miller, T.R. Allen, J. Nucl. Mater. 396 (2010) 234-239.
- [16] H.J. Ryu, Y.S. Kim and G.L. Hofman, J. Nucl. Mater. 385 (2009) 623-628.
- [17] D.F. Sears et al., in: Proc. Int'l Meeting on Reduced Enrichment for Research and Test Reactors, Beijing, China, (2009).

EVALUATION OF THE CONSERVATIVE ASSUMPTIONS - THE CORE INVENTORY AND CONSEQUENCES

M. BELAL, H. VAN GRAAN and H. SEALS

South African Nuclear Energy Corporation, Necsa, P.O.Box 582, Pretoria 0001, South Africa

ABSTRACT

The detailed assessment of the core source term and the consequences were performed within the framework of the safety reassessment of the SAFARI-1 research reactor. One of the related aspects to the re-assessment is the core inventory calculations and its application to the dispersion assessment. In estimating the core inventory, calculations are performed with some degree of simplifications and adding conservatism to each step throughout the process, from the inventory calculations to its application and models that correlate the nuclide release fractions. In this paper we evaluate the conservative assumptions to calculate the core inventory and dose to the public, and provide comparisons with a realistic core inventory. The evaluation groups the important nuclides by similar transmutation behaviour. This grouping provides a reference to the results of the consequence assessment that identifies dominant nuclides to the dose, therefore, the applicability of the conservative assumptions and margins developed were determined. Moreover, the application of the core source term to the consequence assessment was discussed. A hypothesised whole core and single fuel element damage were assumed and standard and specific sets of release fractions were used. The results indicated that, for the whole core damage, the conservative method produce conservative activity values for the dominant nuclides provided that nuclides with a high removal rate have a proper conservative assumption, and the single fuel damage found to be sensitive to this application and may not lead to a conservative dose.

1. Introduction

The safety assessment requires bounding values in order that consequence results have a conservative bias. Conservative assumptions are used in the calculation of the core inventory and its application to the consequence assessment to determine bounding inventories. In references [1,2], several important conclusions have been drawn from a realistic evaluation of core inventories as opposed to the conservative evaluation. Firstly, the fuel inventory source terms can be calculated reasonably well using analytical methods. Secondly, the source terms tend to be grossly overestimated in the conservative assessments. Moreover, it was shown that the fission product inventories are strongly dependent on the reactor power and burn-up, neutron flux distribution in the core, operating history and fuel management. These core operating parameters are considered to realistically estimate the fission inventory. Also it was recommended that this may only be used if it results in bounding inventories [1,2].

In this paper we evaluate the conservative assumption to calculate the core inventory and the related consequences. We calculate the core inventory realistically using the above recommendations also considering the spectral distribution in the core. Furthermore, the transmutation behaviour of all important nuclides was evaluated and grouped by similar characteristics. This grouping provided a reference to the results of the consequence assessment that identifies dominant nuclides to the dose. Therefore, margins developed due to the conservatism in the core inventory were determined, and correspondence to a bounding value of the core inventory was established.

In this approach, ORIGEN2.2 [3] code was used to calculate the core source term, and core specific ORIGEN libraries were calculated with MCNP [4]. In the consequence assessment, different sets of release fractions were applied to these core source terms and PC-

COSYMA [5] was used to determine the consequence of an event. Examining the final dose consequence provides insight into how the applied conservatism in the core source term affects the public dose. Additionally, a comparison of release fractions applied for SAFARI-1 and the published fractions [1] is shown.

2. Core Inventory Calculations

In calculating the source term, a certain nuclides are extracted according to a classification of important nuclides that is presented in [1], due to their high volatility and health impact associated with exposure. The list of nuclides is shown in table 1 of reference [1].

The rate at which the nuclide X_i changes as a function of time is described as follows:

$$\frac{dX_i}{dt} = \sum_{j=1}^N l_{ij} \lambda_j X_j + \phi \sum_{k=1}^N f_{ik} \sigma_k X_k - (\lambda_i + \phi \sigma_i) X_i \quad eq. 1 \text{ ref. [2]}$$

Where ϕ is the flux, λ_j the decay constant of nuclide j to i , σ_k the production cross section of nuclide i and $(\lambda_i + \phi \sigma_i)$ is the removal of nuclide i by natural decay or absorption. This system of equations is solved in ORIGEN2 by employing the matrix exponential method.

The practice in calculating the so called conservative source term is to use an average core spectrum to develop ORIGEN2 one group cross section library and the core highest flux experienced by a fuel element. This is used to deplete the fuel to one cycle, two cycles and up to nine cycles (nine cycles represents the fuel residence time in the core in case of SAFARI-1 reactor). Each of these nine inventories is then multiplied by number of fuel elements to represent the total number of fuel elements in the core. Due to the nature of the transmutation process (production and removal by absorption or decay), this assumption may not necessarily lead to a conservative source term, see equation 1. The consequence assessment reveals the nuclides that are the main contributor to the public dose. These nuclides' activity values are not necessarily conservative values in a source term calculated in this manner. Thus an iterative procedure may be required to evaluate the assumptions against the final concentration of these dominant nuclides.

A more realistic source term was calculated as a reference to evaluate the conservative assumption. Each fuel element was depleted with its specific spectrum and flux value it experiences in the equilibrium core of SAFARI-1 at its respective position occupied during the fuel cycle. The equilibrium core fuel management strategy is followed to the end of cycle for the final core inventory. In both realistic and conservative source terms, the number of fuel elements, irradiation and decay times were preserved.

In addition an important difference between the realistic and conservative assumptions is the cumulative fission rates of the actinides. This contributes to the production of the fission products, namely 0.86, 0.72 and 0.78 are the Realistic/Conservative ratios for U-235, Pu-239 and U-238, respectively.

In order to understand the differences between the conservative and the realistic source terms, the production and removal of each nuclide were studied and grouped by similar characteristics. Table 1 shows the grouping of these nuclides according to their transmutation behaviour. The activity of each fission product could be determined from equation 2. This represents the production by fission and absorption by nuclides of the same atomic number. The production by decay modes such as alpha decay is not presented in the equation, nevertheless, 30% of Cs-137 production in the conservative ST is contributed by such decay chains.

$$A_i = \lambda_i \cdot \left(\sum_{k=1}^5 f_k \sigma_{f_k} \phi N_k + \sum_{k=1}^n \sigma_{\gamma_k} \phi N_k \right) \cdot \frac{(1 - e^{-(\sigma_{\gamma_i} \phi + \lambda_i)t})}{(\sigma_{\gamma_i} \phi + \lambda_i)} \quad eq. 2$$

From Table 1, I-131 nuclides group features production by U-235 fission and removal by the natural decay. Besides that, U-235 contributes by nearly 95% to the total number of fissions. Therefore, the U-235 fission rate dominates the final I-131 concentration. Thus the conservative method generates the conservative I-131 activity value.

The Xe-135 nuclides group features a production by U-235 and removal by absorption and natural decay. The cumulative U-235 fission rate and Xe-135 removal rate results in a low Xe-135 concentration in the conservative source term.

The I-129 nuclides group features a long half life and a relatively high removal by absorption. Due to the long half life, the production by U235 and Pu239 to the I-129 parent fission products constitutes 100% and 83% respectively in the realistic and conservative source terms, and the fission products with a higher and lower mass numbers that are transmuted into I-129, such as U-235(n, f)Te-128(n, γ)Te-129(β^-)I-129 chain, constitutes the rest.

The same applies to the Cs134 nuclide group except that it is a shielded nuclide and has a considerable contribution by Cs-133 neutron capture. The Cs137 group is similar to the I-129 group except that $\lambda \gg \phi \sigma_{\gamma}$.

Tab 1: The nuclides grouping by similar characteristics, and the realistic to conservative activity ratios of the important nuclides

	Group characteristics	Production	$\sum_{i=1}^n \sigma_{\gamma_i} \phi N_i$	$\frac{(1 - e^{-(\sigma_{\gamma} \phi + \lambda)t})}{(\sigma_{\gamma} \phi + \lambda)}$	Real./Cons. (x# of nuclides)
Group 1 (I-131)	$\lambda \gg \phi \sigma_{\gamma}$ $\lambda \ll \Delta t$	U235(n, f)	--	~1.0	0.86 (x45)
Group 2 (Xe-135)	$\lambda < \phi \sigma_{\gamma}$ $\lambda \ll \Delta t$		--	1.29	1.12 (x1)
Group 3 (I-129)	$\lambda \ll \phi \sigma_{\gamma}$ $\lambda \gg \Delta t$	U235(n, f) + (n, γ)	0.76	1.19	0.78 (x4)
Group 6 (Cs-137)	$\lambda \gg \phi \sigma_{\gamma}$ $\lambda \gg \Delta t$		0.90	~1.0	0.78 (x13)
Group 4 (Cs-134)	$\lambda \geq \phi \sigma_{\gamma}$ $\lambda \gg \Delta t$		0.1	1.02	0.1 (x1)
Group 5 (Cs-136)	$\lambda \gg \phi \sigma_{\gamma}$ $\lambda \leq \Delta t$		0.72	0.98	0.45 (x4)

The above procedure was applied to the single fuel inventories (maximum burn-up and highest inventory) and Table 2 shows the conservative margins of nuclides that dominates the short and long term doses for a single fuel damage (see Figure 5).

Tab 2: The realistic to conservative ratio of dominant nuclides - single fuel element damage

Radionuclide	Real./Cons. ratio	
	Max. Burn-up	Highest Inventory
I-131	1.38	0.83
Cs-137	0.88	2.95

3. Consequence Assessment

A severe accident case was hypothesised and the conservative source term and the realistic source terms were used as input to a dose analysis. Both long term doses (over a period of 50 years) and short term doses (integrated over 7 days) were reported at 1 km from the

release point. Conservative weather conditions and a typical representative person for the Pelindaba site were assumed for all cases.

3.1.1 Core Damage - Standard Release Fractions

A release fraction is the fraction of the source term that is released into the environment and is dependent on the accident conditions. The release fractions are applied according to the chemical and physical properties of radionuclides, particularly volatility. They are obtained from temperature and burn-up correlations derived from the literature. According to thermal hydraulic analysis of the SAFARI-1 core, core damage occurs at 834°C. For the standard set of release fractions a burn-up of 50% was assumed.

Table 3: Release Fractions assumed for the Core Damage Event at 50% Burn-up

Radionuclide Grouping	Release Fraction
Iodine group	0.939
Noble gases	1.0
Cesium group	0.082
Tellurium group	0.021
Ruthenium group	0.002
Actinides	0.001
Others	0.1

For the total core damage, the total effective dose calculated from the realistic source term for the long term and the short term doses were 77% and 84% of the conservative doses, respectively.

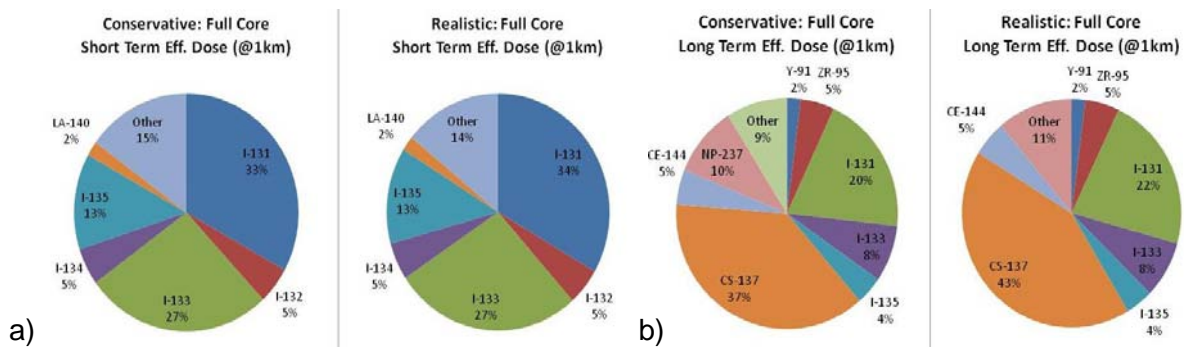


Figure 1: Breakdown of Public Dose per Radionuclide a) the short term dose and b) the long term dose

From Fig. 1, I-131 dominates the short term doses and Cs-137 and I-131 dominate the long term doses. This corresponds well with the production and removal findings that indicate that the conservative method will produce conservative activity values for these nuclides.

3.1.2 Core Damage - Other Reactors Release Fractions

The standard set of release fractions can be compared with the release fractions used in other reactors that use plate type Al clad fuel as described in [1]. There are significant differences in the release fractions for Cesium, accounting for the significant differences in the long term doses. Release fractions used for this comparison are listed in Table 5 and the dose comparison is provided in Figure 2.

Table 5: Release Fractions for core damage events [1]

Reactor Name	Radionuclide Grouping	Release Fraction
RRR (OPAL)	Noble gases	1.0
	I, Cs, Rb	0.3
	Te, Ru	0.01
SILOE	Noble gases	1.0
	I, Te, Cs, Br	0.5
	Other	0.01
ASTRA	Noble gases	1.0
	I, Te, Cs	0.27
	Ba, Sr, Ru	0.03
	Other	0.001

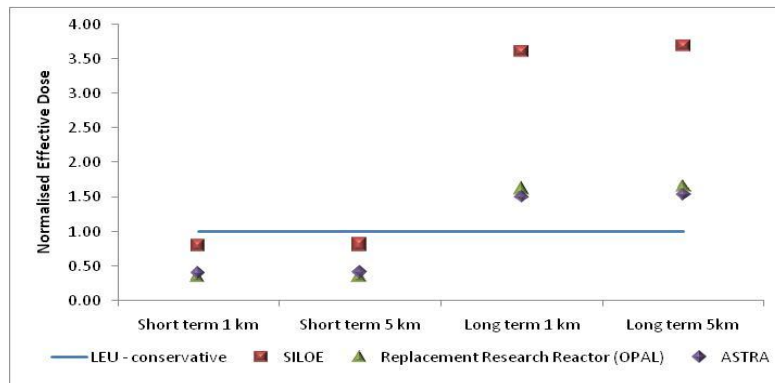


Figure 2: Comparing the Standard Set of Release Fractions with those for other reactors using plate type Al clad fuel.

Therefore, the margins in the core source term are determined by comparing the realistic and conservative sources of the dominant nuclides with the reference to groupings in Table 3. Margins of 14% for the short term dose and 22% for the long term dose are seen. Moreover, depending on the selection of the release fraction, this may add additional margin to the final dose.

3.2.1 Single Fuel Damage - Standard Release Fraction

A total core melt event is very improbable. A less severe accident may involve the damage to a single fuel element. This accident scenario is more sensitive to the method applied to calculate the source term. As part of the iteration to determine the margin of conservatism in the source term described earlier, four single element source terms were assessed:

- Conservatively calculated element with highest inventory
- Conservatively calculated element with highest burn-up
- Realistically calculated element with highest inventory
- Realistically calculated element with highest burn-up

The same release fractions, weather conditions, end points and representative person were considered for the dose analysis. Fig 3 shows that the two realistic source terms are about 1.3 times the reference conservative source term (Conservative, maximum burn-up) in the short term. In the long term, the conservatively calculated source term with the highest inventory gives a higher effective dose than the reference conservative case. This corresponds well with the production and removal findings (see Table 2).

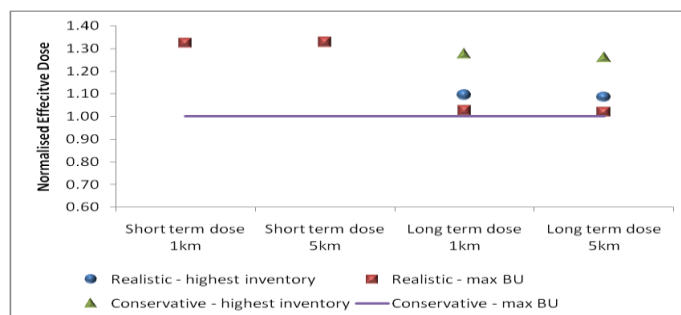


Fig 3. Relative Effective Dose with the Standard Set of Release Fraction

The dominant nuclides for the realistic highest inventory case are Cs-137 (43%) and I-131(22%). This shows that the conservative method of calculating source term does not always result in a conservative dose.

It should be noted however, that for the dose analysis in Fig 3, the release fractions were identical. This is significant because for the source terms with the highest inventories, the burn-up values are much lower than the value of 50% used to derive the release fractions in Table 3.

3.2.2 Single Fuel Damage - Specific Release Fraction

Source specific release fractions were derived using the burn-up values that correspond to the source terms calculated as show in Table 4.

Table 4: Release Fractions derived from burn-up correlations at 834°C

	Burn-up(%)	Iodine group	Noble gases	Cesium group	Tellurium group	Ruthenium Group	Actinides	Other
Realistic - highest inventory	31.8	0.865	0.997	0.057	0.013	0.001	0.001	0.100
Realistic - max BU	58	0.963	1.000	0.092	0.024	0.002	0.001	0.100
Conservative - highest inventory	11	0.802	0.995	0.038	0.007	0.001	0.001	0.100
Conservative - max BU	65	0.979	1.000	0.101	0.026	0.002	0.001	0.100

Fig 3 shows the relative doses when the release fractions based on the burn-up of each fuel element are applied. In this case the highest inventory elements yield lower doses.

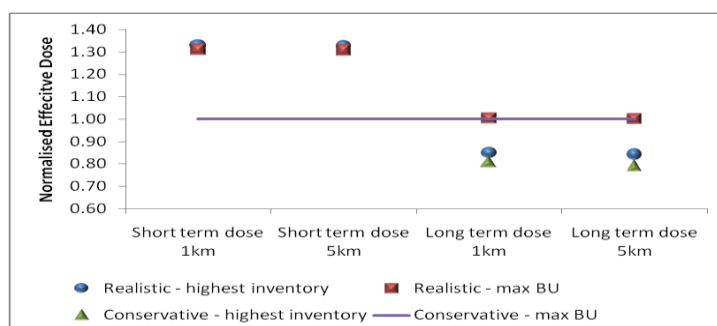


Fig 4. Relative Effective Doses with Source Term Specific Release Fractions

Fig 4 shows the radionuclide breakdown for the effective dose from all pathways (individual Release Fractions). This figure indicates the importance of Cs-137 and I-131 that is a driver for conservative assumptions for calculating the core source term. (The radionuclide distribution for the standard release fractions and those of the individual release fractions do not differ significantly.)

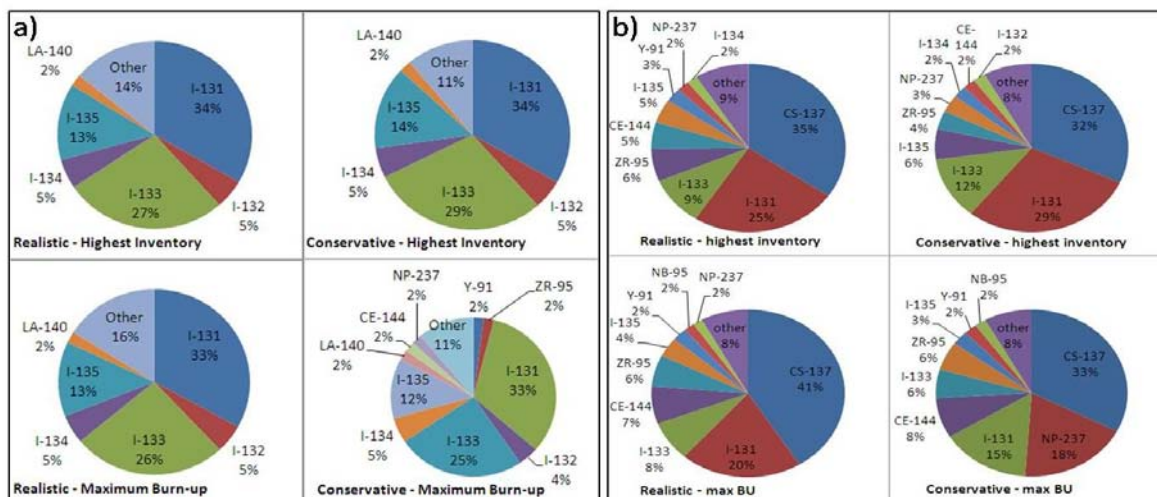


Fig 5. Radionuclide breakdown for a) the short term dose and b) the long term dose from all pathways (individual release fractions)

4. Conclusions

The conservative assumption in calculating the core source term was evaluated and was found to result in a 17% higher activity concentration in the total core inventory. However, nuclides such as Xe-135 do not result in a conservative value due to the removal rate that is four orders of magnitude higher than the fission rate, which may cause a considerable effect on the production and removal balance.

The dominant nuclides to the final dose belong to the I-131 and Cs-137 groups with the same transmutation behaviour. These groups had 14% and 22% conservative margins, however, a small modification to the in-core fuel management or the conservative procedure could lead to non-conservative value, due to the close removal rate of I-131 to the U-235 and Pu-239 fission rates. While the Cs-137 group has a removal rate that is two orders of magnitude lower than the fission rate, it could be assumed that this group will always result in a conservative value. This is due to the monotonic increase of the removal rate with the fission rate. Therefore, some cores that feature more pronounced spectral distribution may lead to a misleading conservative assumption and should be examined. This could be approached by an engineering judgment and an iterative procedure between the core inventory calculation and the consequence assessment to identify dominant nuclides to the final dose.

Moreover, although there may be fuel elements with a higher inventory than the fuel element with the maximum burn-up, the effect of the burn-up on the release fraction is more significant on the final dose.

5. References

- [1] IAEA Safety Reports Series 53, "Derivation of the Source Term and Analysis of the Radiological Consequences of Research Reactor Accidents", IAEA, 2008.
- [2] OECD NUCLEAR ENERGY AGENCY, "Nuclear Reactor Accident Source Terms", OECD, Paris (1986).
- [3] ALLEN G. CROFF, "ORIGEN2: A Versatile Computer Code for Calculating the Nuclide Compositions and Characteristics of Nuclear Materials", Oak Ridge National Laboratory, Chemical Technology Division, P. O. Box X, Oak Ridge, Tennessee 37831, 1983.
- [4] LANL, "MCNP — A General Monte Carlo N-Particle Transport Code, Version 5", X-5 Monte Carlo Team, 2008.
- [5] J Brown et. al, "PC-COSYMA", version 2.02.

IRSN ASSESSMENT OF OPERATING CONDITIONS ANALYSIS FOR PERIODIC SAFETY REVIEWS ON FRENCH RESEARCH REACTORS

M. AUZAS, F. GUPTA, M. CORBEL, T. BOURGOIS

Institut de Radioprotection et de Sûreté Nucléaire

B.P. 17, 92262 Fontenay-aux-Roses, France

ABSTRACT

As technical support organisation of the French Nuclear Safety Authority (ASN), the French Institute for Radiological protection and Nuclear Safety (IRSN) has to critically examine safety analysis provided by French operators in the frame of Periodic Safety Reviews (PSR). This paper presents the approach implemented by the IRSN to assess French PSR and particularly the approach used to assess "Operating Conditions Analysis" applied by the operator to demonstrate the reactor operation safety. This analysis consists, on the basis of postulated initiating events (PIE), in identifying and classifying accident sequences into categories depending on the occurrence probability notably on the robustness of the related preventive lines of defence. For each category, the operator verifies the compliance of the most severe accident sequences effects with safety objective of the category. In this context, the main objective of the IRSN assessment is to verify the robustness and the independence of the lines of defence implemented in application of the defence in depth principle. The outcomes of the French research reactors: ORPHEE, EOLE and MINERVE are given to illustrate this IRSN approach.

1. Introduction

To evaluate the safety state of French research reactors, the French Nuclear Safety Authority (ASN) requires from the operators a Periodic Safety Review (PSR). In accordance with ASN requirements [1] and IAEA guidelines [2], the operator performs a conformity check of the facility and a safety reassessment. He also analyses the experience feedback of the facility and of similar facilities (French or foreign). As technical support organisation of the French Nuclear Safety Authority (ASN), the French Institute for Radiological protection and Nuclear Safety (IRSN) has to critically examine these safety analysis provided by French operators. These analysis focus notably on external and internal hazards, the reactor operation safety, the safety of fuel storage and handling operations, radiological protection of workers and the confinement towards the environment.

For operation safety reassessment, the operator now performs an "Operating Condition Analysis" to take into account the practical experience of safety analysis at the present time (initially used for the PWR and applied since the 2000s to the research reactors). It is a new approach which has not been applied at the design stage for the French research reactors currently operating and which consists in studying the robustness of the lines of defence associated to the events likely to occur on the facility, from normal conditions to accident conditions (more and more severe) [3].

The main subject of this paper is to present this approach and the related IRSN assessment. Outcomes from the latest PSR assessment of the ORPHEE, EOLE and MINERVE research reactors, regarding the reactor operation safety, are given in order to detail it. This paper is in line with a previous article (referenced [4]) which focuses on the approach implemented by the IRSN for a technical assessment of PSR (organisation, procedures...).

2. The approach of Operating Conditions Analysis

To characterize the potential impact of the facility on the public, the operator verifies that the consequences of the events likely to occur on the facility are within limits called “safety objectives”. These objectives differ according to the occurrence probability of these events: higher is the probability lower must be the consequences.

The Operating Conditions Analysis consists in:

- ⤴ postulating initiating events in spite of preventive arrangements,
- ⤴ defining and evaluating the related accident sequences (ex: lines of defence, core damage and related radiological effects on populations),
- ⤴ categorizing the accident sequences, in terms of occurrence probabilities (normal operation, operating incidents, accidents) - a safety objective has been previously defined for each category,
- ⤴ verifying the compliance, for each category, of the most severe accident sequences effects with related safety objectives.

2.1 Initiating events census

The designation of initiating events consists in identifying events (ex: equipment failure or human error) likely to impact the two following reactor safety functions: core cooling and reactivity control¹.

2.2. Definition and classification of accident sequences

Accident sequences are defined from the PIE and assuming the failure of the safety systems/procedures specifically implemented to limit the consequences of the PIE. The additional failure has to be applied on an active safety system or a safety procedure required to manage the accident sequence. These accident sequences are classified into categories depending on the occurrence probability. The classification is based on the evaluation of the robustness of the lines of defence implemented to prevent the accident sequence. For example, the sequences resulting from the failure of one line of defence qualified as “medium” can be classified in the incidental category and those resulting from the failure of a “high” line of defence can be classified in the accidental category. The events resulting from failures of several lines of defence are usually classified in the “risk limitation” category.

2.3. Characterization of accident sequences and verification of compliance with safety objectives

Then, for each category, the operator selects the most severe accident sequences compared with the related core damage and estimated them. These estimations can be completed with the evaluation of the related radiological effects on populations. Finally, the compliance of these estimated effects with the related safety objectives of each category is verified. The evaluation of the consequences of the accident is performed with computer codes with penalizing assumptions (ex: higher possible cooling speed in case of inadvertent cooling of moderator).

¹ A list of initiating events classified into different categories of risks is presented in the AIEA guide referenced [5].

3. IRSN safety assessment of Operating Conditions Analysis illustrated with some outcomes regarding the ORPHEE, EOLE and MINERVE reactors

3.1 Assessment of the list of PIE and of the robustness of the related lines of defence

The purpose of IRSN assessment is first to verify the completeness and the relevance of the list of PIE and related accident sequences presented by the operator but mainly to verify the adequacy and the robustness of the lines of defence implemented to prevent the occurrence of the PIE and to limit the consequences of the related accident consequences.

Concerning, the evaluation of the lines of defence, the first step is to identify, for each accident sequence, the provisions of prevention, detection and mitigation of the consequences (which are the lines of defence). The second step is to evaluate the robustness of each provision (line of defence). This evaluation takes notably into account:

- ⤴ design requirements of equipments in order to verify :
 - ⤴ consideration of external hazards (particularly the seism),
 - ⤴ reliability of detection systems (redundancy and the diversity of measured parameter),
- ⤴ manufacturing requirements in order to verify the manufacturing quality of equipments: their adequacy and their good conditions regarding their operations, notably through findings from technical inspections at the factory and from design control before operation,
- ⤴ exploitation requirements in order to verify:
 - ⤴ the efficiency of procedures of safety actions implemented to prevent damage on the reactor core regarding the initial design of the equipments,
 - ⤴ the good adequacy of periodic test procedures regarding the safety action which have to be ensured (good safety parameter tested, frequency of tests),
 - ⤴ the findings from periodic tests and maintenance realised on the safety equipments (verification of their state, their performance and their operability),
 - ⤴ the findings from non destructive testing to verify the good state of the related structure,
- ⤴ findings from the conformity check:
 - ⤴ the adequacy of the design state and the related efficiency compared with the present moment,
 - ⤴ experience feedback from the reactor operation and from events occurred in the facility (or similar facilities) since the latest safety review notably to estimate the level of reliability of equipments in order to identify non-conformities or dysfunctions which could lead to others possible recurrent events.

For example, for the accident of the ORPHEE reactor “Inadvertent control rod withdrawal”, IRSN analysed the robustness of protection arrangement against overspeed of the withdrawal. In his safety demonstration, the operator has taken into account for the speed of rod withdrawal, the “speed threshold” i.e for which the safety action (declutch of the drive motor) is engaging. However, the IRSN analysis of periodic tests performed for this protection and particularly the related procedure, revealed that the mechanical declutch of the motor is not really tested. In this way, IRSN recommended to the operator to define new arrangements in order to really control the overspeed protections or to change his safety demonstration taking into account a failure of these protections and hence consider the maximal speed physically possible for control rods withdrawal events.

In this way, IRSN verifies that the safety equipments required to manage an event sequence are operational under the related accidental conditions what it makes possible to estimate their behaviour in this sequence. Moreover, IRSN verifies also, with this robustness assessment, that the additional failure on safety action (see paragraph 2.2) considered by the operator in the sequence of events, is independent of the PIE, is applied on the most penalizing moment and is the most severe additional failure for the safety analysis. However, according to the age of research reactors, some previous elements used by the IRSN to evaluate the robustness of lines of defence are no longer available (loss of information with the time in the facility). In this case, IRSN has to ask from the operator² additional tests or controls (destructive or non destructive) in order to verify that the design, manufacturing and exploitation requirements are ensured. Without this information, the related lines of defence will be considered by IRSN with a low level of reliability regarding their robustness.

Considering the previous element, the IRSN robustness assessment of lines of defence related to the EOLE and MINERVE reactors³, comes to the conclusion that the provisions implemented to prevent and limit consequences from an reactivity accident are sufficiency robust considering the main following lines of defence [4]:

- ✧ the reactor operation rules which impose notably a maximum super-criticality for each reactor (ex: $\beta/2$ for the EOLE reactor) in order to limit the core reactivity and which impose other safety standard like the worth of the control rods with a minimum anti-reactivity requirement,
- ✧ different checks performed by workers before initiating a sub-critical approach (ex: checks on core loading with different fuel compositions and on safety standard),
- ✧ the sub-critical approach which allows to detect (if the previous items fail) a core configuration error, by the extrapolation method of the sub-critical approach curves which reveals, in this case, a too or not enough reactive core before the end of the approach (whose the procedure is stopped in order to search and correct the related error before initiating again a new sub-critical approach).

Concerning ORPHE reactor⁴, IRSN concluded that the lines of defence regarding notably cooling accidents (ex: fuel assembly blockage), seism (likely to involve a loss of coolant resulting from damage on core cooling circuit) and electrical power supply loss (likely to involve a loss of forced convection by the loss of electrical power of primary pumps) which could lead to core damage, are various and quite robust since they rely mainly on conception arrangements and passive equipments designed as regard to seismic loads, such as:

- ✧ an emergency scram on various parameters (ex: abnormal pressure or temperature in the core, loss of electrical power),
- ✧ flywheels on the pumps of the primary coolant circuit that ensure a sufficient flow in the core for a few time,
- ✧ a weak residual power so that the core can be cooled by natural convection, with the opening of natural convection dampers (without electrical power supplies, i.e. a passive operation) which allows core cooling with the pool water,
- ✧ the conception of the primary coolant circuit which is contained in several leaktight bunkers, situated mainly above the pool, so that core uncovering is impossible in case of a rupture on the primary coolant circuit.

² This request was made thanks to formal questionnaires (technical dialogue with the operator) during the IRSN assessment of ORPHEE reactor safety review [4].

³ Critical mock-up of 100 W dedicated to the neutronic studies.

⁴ Pool type reactor of 14 MW designed mainly to produce thermal neutron beams dedicated to the study of materials structure and energy states of condensed matter.

3.2 Assessment of the compliance of the accident sequences effects with safety objectives

The IRSN assessment of this compliance consists in verifying:

- ⤴ the bounding conditions and the related uncertainties associated with the initial parameters of accident sequences,
- ⤴ the uncertainties resulting from the computer codes used to simulate the sequence of events and the related effects,
- ⤴ the assumptions considered to assess core damage and the related radiological effects on populations.

Most of time the safety objectives are applied regarding the fuel integrity.

For example from the IRSN assessment of core damage evaluation of EOLE and MINERVE reactors, IRSN requested to the operator to justify the values of neutronic parameters (ex: temperature coefficient, Doppler coefficient, void coefficient) used in his simulation of the most severe accident sequences studied and compounded by a total failure of emergency scram. The operator undertook to provide this justification [4].

4. Conclusion

Considering the previous elements, the reactor operation safety is based on the exhaustiveness of the list of PIE and the robustness of the lines of defence involved in the accident sequences. The assumptions used for the evaluation of the consequences of the most severe accident sequences selected have to be verified too.

In this way, the operating conditions analysis allows to conclude on the sufficiency of the number of the lines of defence regarding the sequence of events, on their adequacy with the different levels of defence in depth principle (good distribution between prevention, detection and limitation levels) and finally on their robustness.

5. References

- [1] FRENCH NUCLEAR SAFETY AUTHORITY, "ASN requirements for Periodic Safety Reviews on nuclear facilities operated by the CEA", DGSNR/SD3-CEA-05 (2005).
- [2] INTERNATIONAL ATOMIC ENERGY AGENCY, Safety of Research Reactors: Safety Requirements, Safety standards series, ISSN 1020-525X No. NS-R-4, Vienna (2005).
- [3] LIBMANN, J., "Safety nuclear elements", Edition: EDP Sciences (2000).
- [4] AUZAS, M., GUPTA, F., "Approach implemented by IRSN for the assessment of PSR on French RR", IAEA-CN-188, Morocco (2011) (Int. Conf. Morocco, 2011).
- [5] INTERNATIONAL ATOMIC ENERGY AGENCY, Safety Assessment of Research Reactors, Safety standards series, ISSN 0074-1892 No. 35-G1, Vienna (1994).

EXPERIMENTAL AND ANALYTICAL STUDIES ON THE SIPHON BREAKERS IN RESEARCH REACTOR

KWON-YEONG LEE ^{*}, KYOUNGWOONG SEO, DAE YOUNG CHI, JUHYEON YOON

*Fluid System Design Division, Korea Atomic Energy Research Institute
1045 Daedeok-daero, Yuseong-gu, Daejeon, 305-353, Republic of Korea*

SOON HO KANG

*Mechanical Engineering Department, Pohang University of Science and Technology
77 Cheongan-ro, Nam-gu, Pohang, Kyungbuk, 790-784, Republic of Korea*

MOO HWAN KIM

*Division of Advanced Nuclear Engineering, Pohang University of Science and Technology
77 Cheongan-ro, Nam-gu, Pohang, Kyungbuk, 790-784, Republic of Korea*

ABSTRACT

An investigation is carried out to understand siphon break phenomena inside a large pipe of research reactors. In open pool-type research reactor, the pool water itself is the ultimate heat sink. Therefore, the siphon breakers shall limit the pool water drain by the siphon effect when a postulated pipe break occurs below the reactor core position. A siphon break test is performed in POSTECH. The test facility is designed to be very large size with 16-inch main steel pipe to consider the real situation in research reactors. Preliminary siphon break line/hole tests are performed from an undershooting height viewpoint. The results show that the water drain by siphon is ceased when the air inflow through the siphon breaker is sufficient. The undershooting height increases as the size of siphon breakers decreases. An analytical model based on Bernoulli equation is developed and compared with experimental data. This model is capable of predicting the siphon break phenomena and the undershooting height roughly.

1. Introduction

In research reactor, the reactor core is cooled by a natural circulation through some opening valves to the reactor pool after the primary cooling pump is turned off. The pool water itself is the ultimate heat sink of the residual heat. So, it is very important to guarantee the pool water level is upper than a minimum level in the nuclear safety point of view. In open pool-type research reactor, however, a component of a system can be installed below the core level due to the component purpose. Then, the pool water is drained below the core by siphon effect and the core can't be cooled by the natural circulation any more when a postulated pipe break occurs below the reactor core position. Therefore, the system should install a siphon breaker to limit the pool water drain during and after all postulated initiating events.

Neil and Stephens [1] performed an experimental study to understand the siphon break phenomena in Idaho State University. The facility consisted of 500-gallon upper tank (1.89 ton), 4 inch acrylic pipe downcomer, 3/4 inch anti-siphon inlet air line, and 1323cm full distance. The flow orifice hole diameters is 17.25 to 48.26 mm for water and 2.39 to 6.45 mm for air. Three different modes of siphon break performance were described in their experimental results; Zero sweep-out mode, Partial sweep-out mode, and Fully sweep-out mode. Mode transitions from Fully sweep-out mode to Partial sweep-out mode and Partial

sweep-out mode to Zero sweep-out mode were shown as orifice hole diameter for water increased. As air orifice larger, there was faster transition between modes. In Zero sweep-out mode, the anti-siphon air accumulated in the downcomer as a giant bubble at the top of the downcomer. In Partial sweep-out mode, a significant fraction of air was swept out from the downcomer through the water orifice. In Full sweep-out mode, the air was being sweep out from the downcomer almost as fast as it was being sucked into the apex.

Sakurai [2] developed a calculation program SBAP (Siphon Breaker Analysis Program) for the above mentioned Zero sweep-out mode. It was assumed that the sucked air through siphon break valve is staying the upper part of the downcomer and perfectly separated from water, and the air is not swept out until the downcomer is fully filled with air. An experiment with 15 cm diameter downcomer and 4 cm diameter siphon break valve was also performed to verify the developed program. The program predicted the experimental results well.

For research reactors, a main pipe for primary cooling is designed as a large size to minimize the system pressure loss and to consider a Net Positive Suction Head (NPSH) for the cooling pump. In the large size pipe, the siphon phenomena could not be broken with a small size siphon breaker if the pipe break size is large.[3] The phenomena may be the Fully sweep-out mode. Unfortunately, the program SBAP is only for the Zero sweep-out mode, so it couldn't be applied to design the siphon breaker in research reactor. Besides, previous experiments were conducted for the siphon breakers in relatively small pipes.

In this paper, preliminarily experimental and analytical studies are performed to investigate the siphon break phenomena in a large pipe. For applying the practical design, the experimental facility is manufactured with the same scale of the general research reactor. The analytical model is based on Bernoulli equation.

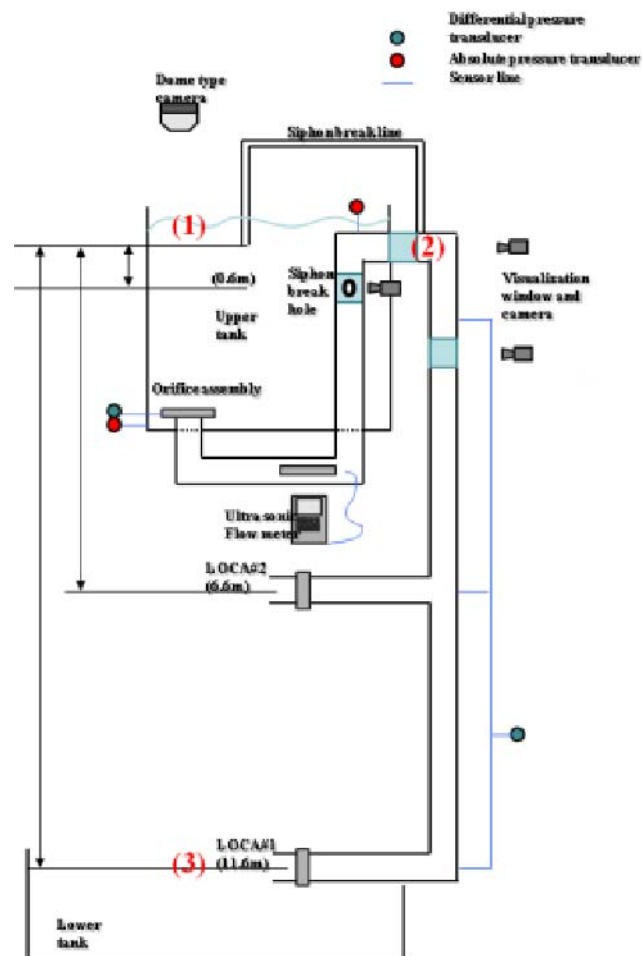


Figure 1. Schematic diagram of experimental facility

2. Experiment

A siphon break test is performed in Pohang University of Science and Technology (POSTECH)[4]. The schematic diagram of the test facility is shown in Figure 1. It consists of an upper tank, a lower tank, a return pump, all the necessary interconnecting pipes, valves and instruments. In order to consider the real situation in a research reactor, its size is decided to be very large with 12.5m width x 6.5m length x 16.5m height. The upper tank has about 60-tons of water capacity with 4m width x 3.6m length x 4m depths and the lower tank is a role of a reservoir with sufficient volume. The return pump is operated to raise water from the lower tank to the upper tank. 16-inch main steel pipe is connected and pass through the upper tank. To simulate pipe ruptures, two pipe break positions and three pipe break sizes are selected as variables. For siphon break line tests, 2.5 to 0.5-inches siphon break lines are connected to the apex of main pipe outside pool. And 30 to 55-mm siphon break holes are given on the main pipe inside pool for siphon break hole tests.

At this moment, preliminary tests have been conducted and an undershooting height of pool water level is mainly considered. In the experiment, the water drain by siphon phenomena is ceased when the air inflow through the siphon break line is sufficient. But siphon is not blocked until the pool water is entirely exhausted for 3.35m of the pool water depth below the siphon break line when the size of siphon breakers is less than 1-inch. Generally, the undershooting height increases as the size of siphon break line/hole decreases and the pipe break size increases as shown in Figures 2(a) and 3(a). Here, the undershooting height is defined to the difference between the end of the siphon break line and the final pool water level after the siphon breaking.

3. Analytical model

As an air volumetric flow rate through siphon breaker increases, the siphon is quickly breaking and the undershooting height decreases. To consider air flow effect, a resistance coefficient K of siphon breakers would be used.[5] From the definition of K , the air velocity is as below;

$$v = \sqrt{\frac{2\Delta P}{\rho K}} \quad (1)$$

Then, the volumetric flow rate is calculated as below;

$$\dot{Q} = Av = A\sqrt{\frac{2}{\rho K}} \cdot \sqrt{\Delta P} = F \cdot \sqrt{\Delta P} \quad (2)$$

Here, F is defined as an air flow rate factor and the values of siphon breakers in this experiment are summarized in Table 1. Also, ΔP is the differential pressure between the inner side of 16-inch main pipe near the siphon breakers and the atmosphere.

Siphon breakers		K	Area (m ²)	$F \equiv A\sqrt{\frac{2}{\rho_{air}K}}$
Line (inch)	2.5	6.87	0.00374	0.00228
	2	5.73	0.00222	0.00122
	1.5	4.63	0.00139	0.00070
Hole (mm)	55	2.68	0.00238	0.00190
	50	2.67	0.00196	0.00158
	45	2.64	0.00159	0.00128
	40	2.60	0.00126	0.00102
	35	2.60	0.00096	0.00079
	30	2.48	0.00071	0.00059

Here, air density 1.161 kg/m³ at 300K and 100kPa is used.

Table 1. Air flow rate factor

Next, the inner pressure of main pipe is dependent on the liquid flow. From the Bernoulli equation[6] among the positions (1), (2), and (3) in Figure 1, the velocity of position (3) and the pressure of position (2) are as below;

$$P_1 + \frac{1}{2} \rho v_1^2 + \rho g h_1 = P_2 + \frac{1}{2} \rho v_2^2 + \rho g h_2 = P_3 + \frac{1}{2} \rho v_3^2 + \rho g h_3 \quad (3)$$

$$v_3 = \sqrt{2g(h_1 - h_3)} = \sqrt{2g \cdot \Delta h} \quad (4)$$

$$P_2 = \frac{1}{2} \rho (v_3^2 - v_2^2) + \rho g (h_3 - h_2) = \frac{1}{2} \rho \left(1 - \frac{A_3^2}{A_2^2}\right) v_3^2 - \rho g (h_2 - h_3) \quad (5)$$

Because the distance between position (2) and (3) is constant, ΔP has a below relationship from equations (4) and (5);

$$\Delta P \propto \left(1 - \frac{A_3^2}{A_2^2}\right) \cdot \Delta h \quad (6)$$

Then, from equations (2) and (6), the air flow rate has a relationship as below;

$$\therefore \dot{Q} \propto F \cdot \sqrt{\left(1 - \frac{A_3^2}{A_2^2}\right) \cdot \Delta h} \quad (7)$$

Therefore, the effects of hydrostatic head and pipe break size are reflected in the below equations, respectively;

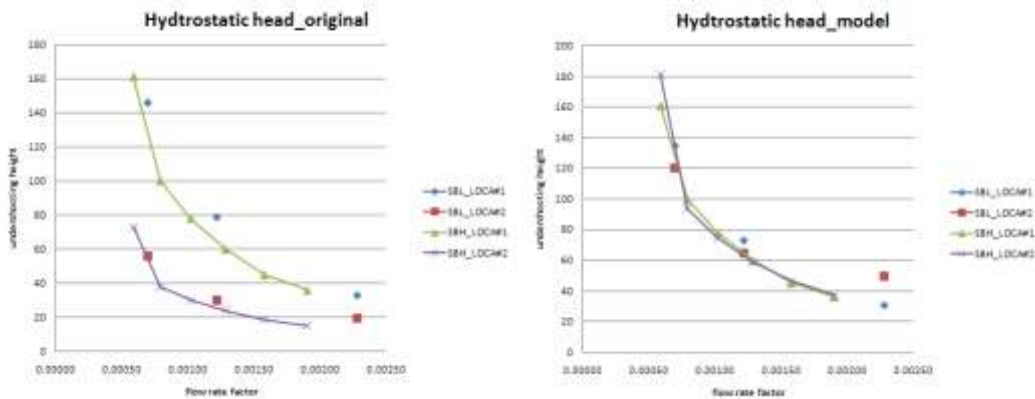
$$water_side \bullet air_side = \frac{\Delta h_b}{\Delta h_a} \bullet \left(\frac{\Delta h_b}{\Delta h_a}\right)^{1/2} = \left(\frac{\Delta h_b}{\Delta h_a}\right)^{3/2} \quad (8)$$

$$water_side \bullet air_side = \frac{A_{3,b}}{A_{3,a}} \bullet \left(\frac{A_2^2 - A_{3,b}^2}{A_2^2 - A_{3,a}^2}\right)^{1/2} \quad (9)$$

Finally, the form of analytical model for undershooting height prediction is as below;

$$y = f(F(a)) \left(\frac{\Delta h_b}{\Delta h_a}\right)^{3/2} \left\{ \frac{A_{3,b}}{A_{3,a}} \bullet \left(\frac{A_2^2 - A_{3,b}^2}{A_2^2 - A_{3,a}^2}\right)^{1/2} \right\} \quad (10)$$

Figure 2(b) shows the prediction results of the model considering the hydrostatic head effect. For $f(F(a))$, the function of siphon break hole test results at pipe break position #1 is used. It shows that the model predicts well the experimental data. Figure 3(b) shows the results considering the effect of pipe break size, and the function of siphon break line test results in 10 inch pipe break size is used for $f(F(a))$. The prediction by the model has some deviation from the experimental data.



(a) Results of experiment

(b) Results of model

Figure 2. Undershooting height comparison regarding siphon breaker type and pipe break position with 10-inch pipe break size

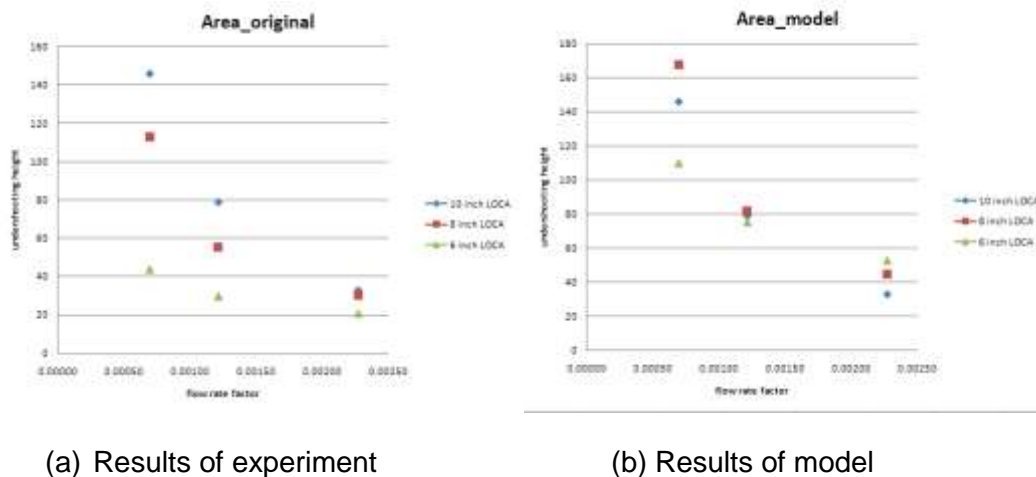


Figure 3. Undershooting height comparison regarding pipe break size at pipe break position #1

4. Conclusion

An investigation is carried out to understand siphon break phenomena that are very complicated due to transient and turbulent two-phase flow. The siphon breakers shall limit the pool water drain by the siphon effect when a postulated pipe break occurs below the reactor core position. A siphon break experiment is performed with a large facility consisted of an upper tank, a lower tank, a return pump, all the necessary interconnecting pipes, valves and instruments. For 16-inch main steel pipe, 2.5 to 0.5-inches siphon break lines and 30 to 55-mm siphon break holes are tested. The water drain by siphon phenomena is ceased when the air inflow through the siphon break line is sufficient. But siphon is not blocked until the pool water is entirely exhausted when the size of siphon breakers is small. An analytical model based on Bernoulli equation is developed. This model can predict the undershooting height roughly. We have a plan to improve it to be more elaborate model and verify it with POSTECH and Idaho experimental data regarding different main pipe size.

5. References

- [1] Neil, D. T., Stephens, A. G., "Siphon breaker design requirements – Final report", DOE/ER/12820-T1, 1993
- [2] Sakurai, F., "Study for Improvement of Performance of the Test and Research Reactors", JAERI-Research 99-016, 1999
- [3] Seo, K.W., Lee, K.Y., Yoon, H.G., Jeong, N.G., Park, Y.C., Chi, D.Y., Yoon, J.H., "Estimation on a Siphon Breaker Type of a Research Reactor", KNS Spring Meeting, Taebaek, Korea, May 26-27, 2011
- [4] Kang, S.H., Ahn, H.S., Kim, J.M., Lee, K.Y., Seo, K.W., Chi, D.Y., Kim, M.H., "Experimental study of siphon breaking phenomenon in real scale reactor design", KNS Fall Meeting, Gyeongju, Korea, October 27-28, 2011
- [5] CRANE Co., "Fluid of fluids through valves, fittings and pipes", 1988
- [6] Munson, B.R., Young, D.F., and Okiishi T.H., "Fundamentals of fluid mechanics", 1990

CORROSION MANAGEMENT FOR SECONDARY COOLING PIPING OF MULTI PURPOSE REACTOR 30MW GA SIWABESSY INDONESIA

Geni Rina Sunaryo

*Center for Reactor Technology and Nuclear Safety (PTRKN-BATAN), Bldg. 80, Puspiptek Area,
Serpong, Tangerang, 15310, INDONESIA.
Email : genirina@batan.go.id*

ABSTRACT

The previous activity on coupon corrosion experimental that has been immersed into the secondary cooling water of Indonesia Multi Purpose Research Reactor GA Siwabessy 30 MW, leads to do the further work for understanding the scientific background. Furthermore, on the previous paper, it has been described also the effectiveness of oxy and non oxy biocide agent on suppressing the total numbers of bacteria, aerobe and non-aerobe bacteria, and also the effectiveness of inhibitor on suppressing the corrosion rate. In fact, the inhibitor is added into the secondary water together with both biocide agent. Therefore the analyses or understanding the effect of those anti microbe chemicals into the secondary water with inhibitor in it, on suppressing the corrosion rate of carbon steel pipe, at room temperature, is the objective of present experiment and will be described in this paper. The corrosion rate is determined by using the potentiostate. The test specimen is made from carbon steel, diameter of 16 mm and thickness of 8mm, and be polished up to the grid of 2000. The media is antimicrobial with various concentrations that are added into 60 ppm inhibitor solution. The conductivity, dissolved oxygen and pH of the each solution are being analyzed. From the experimental results it is known that the corrosion rate of carbon steel is suppressed significantly by the adding of inhibitor, and moreover the dissolved oxygen concentration also is being suppressed by the inhibitor. The pH shows constant for all the experimental condition. The oxidizing agent addition up to 40ppm suppresses the corrosion rate of carbon steel from 0.7 ± 0.02 Mpy to 0.5 ± 0.02 Mpy. However, the non oxidizing agent does not give significant effect. Even the antimicrobial will not give any significant effect on corrosion rate of carbon steel, but the excess concentration of antimicrobial may lead another problem of deposition. It is because of there is a chemical balance temperature dependency in the water, so the optimum concentration is important to be applied. Furthermore, higher concentration of addition may not be economically efficient.

Key words: Corrosion, inhibitor, oxidizing agent, non oxidizing agent

I. INTRODUCTION

Research Reactor GA SIWABESSY is a multipurpose domains for fundamental and applied science, industry, human health care and environmental studies, as well as nuclear energy applications and the development of nuclear science and technology related human resources. It is located in Serpong area, Tangerang, Indonesia and has a power of 30 MW. A continue operation has to be carefully assessed, especially from the material structure point of view[1-4], in 25 years operation.

This research reactor is having two cooling systems, primary and secondary. The primary cooling system uses demineralized water, very low conductivity, in the purpose to maintaining the primary structure integrity as long as designed life.

The secondary system apply raw water as water cooling which is coming from the PUSPIPTEK tap water, which is only being pretreated by depositing method, and no further process. Stainless Steel and aluminium are the material used in the primary system, and

carbon steel is the most material used for secondary system. Therefore, to suppressing the corrosion rate, the inhibitor is being added in a certain concentration. The anti microbe and anti scaling also are being added to suppress the scaling formation and microbial growth that may induce the microbial induce corrosion. The inhibitor, anti scale and anti microbe solution concentration applied into the secondary water are recommended by the company. However, the actual scientific understanding that backgrounding the recommended concentration has not yet been understood. Therefore, some research activities have been started in the objective related.

The preliminary coupon corrosion surveillance results, bacteria identification, effectiveness of antimicrobe on suppressing the numbers of bacteria and the effect of inhibitor on suppressing the corrosion rate on carbon steel have been reported on the previous conference.[1-2] However, how far is the influence of antimicrobe on affecting the corrosion rate is still not yet known. Therefore, it becomes the objective of this paper. The experimental results on understanding well the effect on antimicrobe on corrosion rate will be described. Methodologies applied are corrosion rate determination for carbon steel by electrochemically with variation of inhibitor and antimicrobe solutions. The related conductivity and dissolved oxygen were done by applying the conductivitometry and oxygenmetry.

II. METHODOLOGY

Sample is made by carbon steel with the thickness of 8 mm and diameter of 16 mm, mounted, grinded and sanded by using sandpaper of grid 220, 400, 800, 1000 up to 2000. The sample is being held by using the sample holder (Fig.1.a) and then immersed in the solutions. Corrosion rates are measured electrochemically (Fig.1.b). As solutions, variate concentration of inhibitor only up to 150ppm, inhibitor of 60 ppm plus oxy and anti oxy microbial agent with concentration up to 40 ppm each, mix of 60 ppm inhibitor plus 20 ppm for both anti microbial agent are made. The corrosion rate is being measured for the duration of 15 minutes each. The dissolved oxygen is measured by using oxygenmeter for every solutions. Conductivity also is being measured for all solutions.



Figure 1. Potensiostate for measuring corrosion rate [5]

III. RESULTS AND DISCUSSIONS

The effect of inhibitor on corrosion rate of carbon steel has been reported elsewhere.[1] The corrosion rate decrease from 1.6 ± 0.02 Mpy and start to be in a constant value of 0.7 ± 0.02 Mpy in a range concentration of inhibitor as 60-100 ppm.

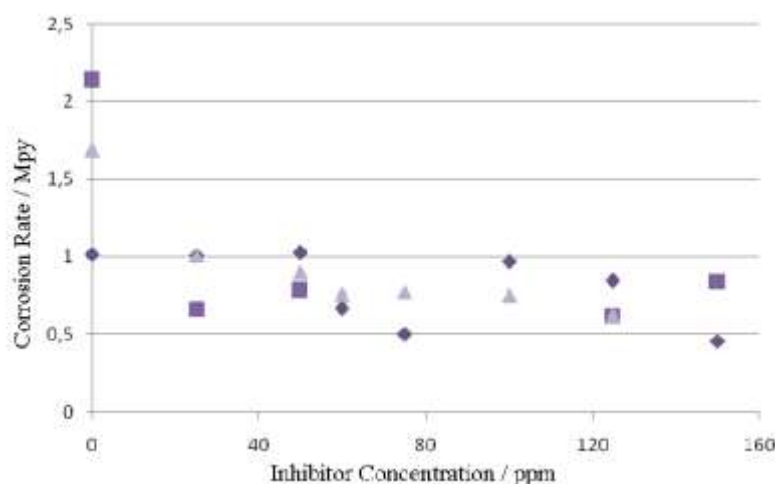


Figure 2. The corrosion rate dependence on concentration of inhibitor at room temperature for carbon steel material, from three times measurements (■, ▲, ◆) [5]

The inhibitor used is having the zinc chloride and phosphate acid with the active compound as orthophosphate with concentration of 5-10% w/v. Zinc may act as a cathodic inhibitor that influence the cathodic reaction by forming Zn(OH)_2 and then reduce the oxygen (Fig. 2). Therefore, it may suppress the oxidation of Fe. Finally, it suppresses the corrosion rate, in the medium of neutral basic.

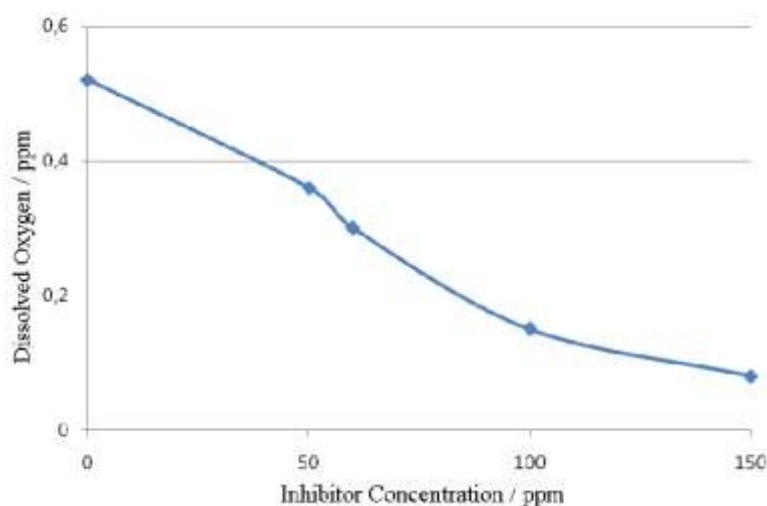


Figure 3. The effect of inhibitor on suppressing the dissolved oxygen in water at room temperature.[5]

Orthophosphate is an anodic inhibitor, that conjugate with monovalent and bivalent ions to form thin layer on the surface material as a protection.

The addition of non oxy biocide agent into 60 ppm inhibitor solutions do not affect the corrosion rate any further. However, the addition of oxy biocide agent suppress the corrosion rate becoming 0.5 ± 0.02 Mpy (Fig. 4). However, the pH shows constant for all the experimental condition. The conductivity seems to be suppressed a bit by the existence of oxy and non oxy biocide up to 20ppm, but it goes constant for the higher concentration of both biocides.

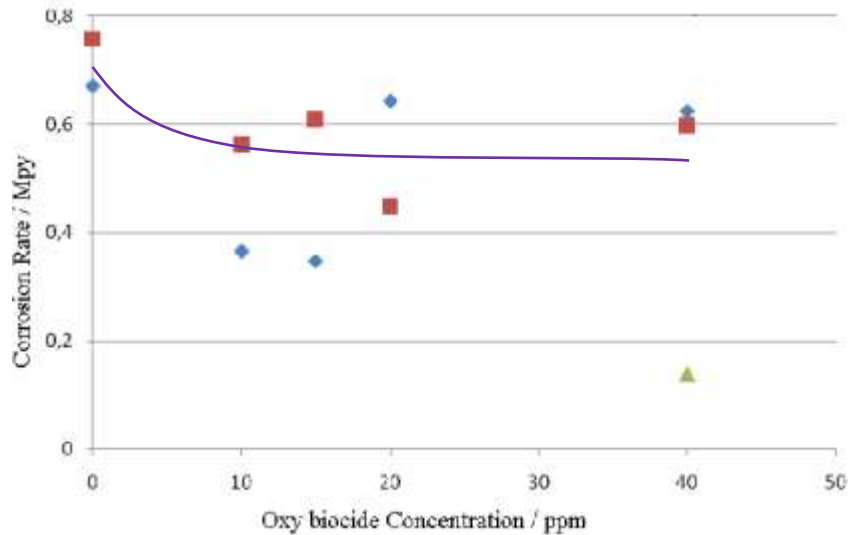


Figure 4. The corrosion rate dependence on concentration of oxy biocide agent for carbon steel material at room temperature, from three times measurement (♦,■,▲) [5]

The dissolved oxygen decrease by adding up the oxy bio agent, but not significantly for non oxy agent (Fig. 5)

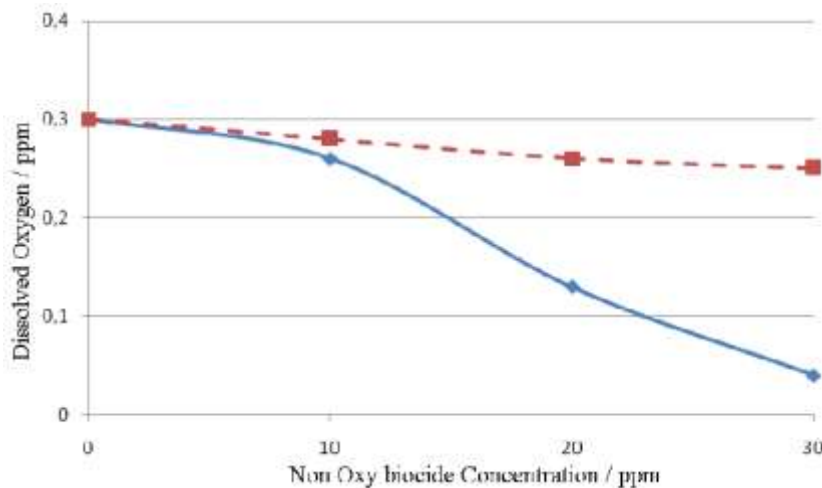


Figure 5. The dissolved oxygen dependence on concentration of non oxy biocide (---) and oxy biocide agent (—) at room temperature.[5]

The oxy biocide agent contain sodium hypochlorite that may kill the microbe that live on the surface of the material. It can not get through the sticky layer that caused by microbial activity. Therefore, oxy biocide agent can not kill microbe that live under the sticky layer. That's why the non oxy biocide agent is needed.

The non oxy biocide agent is an organic compound that may avoid the microbe immunity toward sodium hypochlorite and may kill microbe perfectly. Hence, it may suppress the mucus formation because of the microbe activity. The non oxy biocide contain isothiazolin, that biodegradable, that may give no significant effect to the environment for low concentration. But, high concentration (800 ppm) may cause eye irritation. The non oxy biocide is adding up into the secondary cooling water in the start and end operation of secondary cooling system. However, it should be noted since the application of oxy biocide should be afforded by non oxy biocide paralelly, so the appropriate concentration must be considered for not poisoning the environment.

Base on the above experimental results, the non oxy biocide agent of 10 ppm seems to start giving a good suppressing on corrosion rate and no further significant effect for higher

concentration. The oxy biocide of 20 ppm is giving a good result on suppressing the concentration of dissolved oxygen, and then affect the lower corrosion rate. But, the higher concentration of oxy biocide agent will not give any further effect on suppressing corrosion rate. Hence, it may only cost higher, economically.

Even the antimicrobial will not give any significant effect on corrosion rate of carbon steel, but the excess concentration of antimicrobial may lead another problem of deposition. It is because of there is a chemical balance temperature dependency in the water, so the optimum concentration is important to be applied. Furthermore, higher concentration of addition may not be economically efficient.

IV. CONCLUSION

The corrosion rate of carbon steel is suppressed significantly by the adding of inhibitor, and moreover the dissolved oxygen concentration also is being suppressed by the inhibitor. The pH shows constant for all the experimental condition and conductivity doesn't change significantly in all experimental solutions. The oxidizing agent addition up to 40ppm suppresses the corrosion rate of carbon steel from 0.7 ± 0.02 Mpy to 0.5 ± 0.02 Mpy. However, the non oxidizing agent does not give significant effect. Even both biocide do not show any significant effect on corrosion rate of carbon steel, but the excess concentration of both biocide should be considered, due to chemical balance that has temperature dependency in the water.

V. REFERENCES

- [1] "Secondary Cooling Water Quality Management for Multi Purpose Reactor 30MW GA Siwabessy Indonesia", RRFM-Rome, 2011.
- [2] "Analisis Kandungan Mikroba di Pendingin Sekunder RSG-GAS 30MW", Prosiding seminar PTAPB, Yogyakarta, 2011.
- [3] Aplikasi Program *Corrosion Surveillance* untuk kolam penyimpanan reaktor RSG-GAS, TKPFN-seminar, Surabaya 2010.
- [4] GENI RINA SUNARYO. SRIYONO. DIYAH ERLIANA, International Conference on Research Reactors: Safe Management and Effective Utilization, Sydney, Australia, 5-9 November 2007, "Water Chemistry Surveillance for Multi Purpose Reactor 30 MW GA Siwabessy, Indonesia".
- [5] "Pengaruh senyawa antimikroba terhadap Laju Korosi Pipa Baja Karbon", skripsi S1, Herry Sander Pranoto, STTN, 2011.

ACKNOWLEDGMENT

Many thanks to Mr. Iman Kuntoro, as a director of PTBIN-BATAN for his permission to use the facility and also highly appreciate to Herry Sanders who helped a lot for the experimental works during his present in PTRKN-BATAN.

STATUS REPORT AND FUTURE PLANS REGARDING IRRADIATION TESTING OF LOW ENRICHED MONOLITHIC FUEL DESIGNS

N.E. WOOLSTENHULME, D.M. WACHS, M.K. MEYER

Idaho National Laboratory

P.O. Box 1625, Idaho Falls, ID 83415 – USA

ABSTRACT

The US fuel development team has performed numerous irradiation tests on small to medium sized specimens containing low enriched uranium fuel designs. The team is now focused on qualification and demonstration of the uranium-molybdenum monolithic base fuel design and has begun testing prototypic elements containing this fuel. The team has also commenced irradiation of proposed complex fuel designs, which contain burnable absorbers, in order to enable conversion of all remaining US high power research reactors. The current status of these activities is presented and future plans are discussed to exhibit the overall methodology employed by the fuel development team for gathering data, maturing technology, and demonstrating performance of low enriched monolithic fuel designs.

1. Introduction

The Global Threat Reduction Initiative Convert program (GTRI-convert) employs the Fuel Development (FD) “pillar” to mature Low-Enriched Uranium (LEU) fuel technology in order to enable conversion of High Power Research Reactors (HPRR) to use of LEU fuels ^[1]. The GTRI-convert program also employs the Fuel Fabrication Capability (FFC) and Reactor Conversion pillars, whom are responsible for commercial fabrication deployment and reactor conversion efforts, respectively. The FD pillar has overseen design, fabrication, irradiation, and examination of numerous tests on specimens containing LEU fuels. To enable the three nearest term HPRR conversions, including the Massachusetts Institutes of Technology Reactor (MITR), University of Missouri Research Reactor (MURR), and National Bureau of Standard Reactor (NBSR), the FD pillar is currently focused on qualification of the “Base Fuel Design” ^[2]. The Base Fuel Design consists of uranium-10 wt% molybdenum alloy (U-10Mo) in the form of a rectangular monolithic foil, with thin zirconium interlayers, clad in aluminum alloy-6061 by hot isostatic press ^[3] as seen in Figure 1.

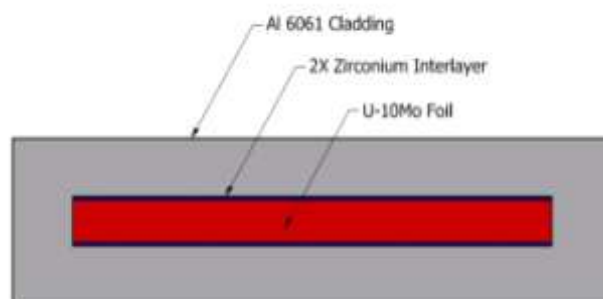


Figure 1: Base Fuel Design

The cornerstone for development of these fuel forms are irradiation testing campaigns. These campaigns provide a framework for fabrication technology development and production of test specimens for both fresh fuel characterization and Post Irradiation Examination (PIE). Irradiation testing campaigns, which are dedicated to development of the

Base Fuel Design, have progressed through the technology life cycle and have begun the design and irradiation of prototypic fuel elements ^[2].

In addition to the Base Fuel Technology, the FD pillar has also been tasked to develop “complex” fuel technology in order to enable conversion of the Advanced Test Reactor (ATR) and the High Flux Isotope Reactor (HFIR). Feasibility evaluations demonstrate that graded fuel meat will be required for HFIR LEU fuel plates ^[4]. Furthermore, analyses suggest that Integral Cladding Burnable Absorbers (ICBA's) may be required for both ATR and HFIR fuel plates ^{[5][6]}. These intricacies constitute complex fuel designs which will, like the Base Fuel Design, require technology maturation. The FD pillar has recently commenced irradiation campaigns regarding complex fuel technology and is currently advancing their future plans regarding complex fuel development. Conceptual complex fuel designs can be seen schematically in Figure 2.

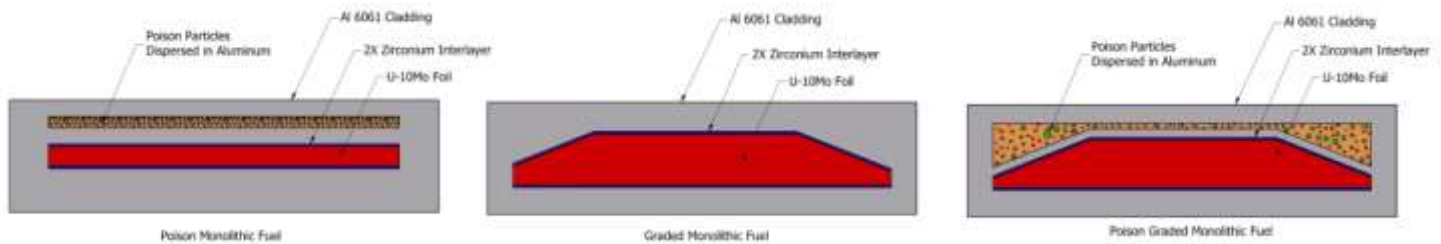


Figure 2: Conceptual Complex Fuel Designs

The FD pillar employs the methodology set forth in the ASME-NQA-1 technology life cycle ^{[7][8]}. Generally speaking, this is consistent with the NASA Technology Readiness Level (TRL) ^[1] method as well. Both of these call for a graded approach to development of technologies. In regards to irradiation testing, this approach is accomplished via successive irradiation campaigns as seen in Table 1.

Table 1: Irradiation Testing General Progression

NQA-1 Tech. Life Cycle	TRL Level	Base Fuel Campaigns (MITR, MURR, NBSR)	Complex Fuel Campaigns (ATR)	Complex Fuel Campaigns (HFIR)	Key Objectives
Basic Research	TRL-4	RERTR-8 thru -10	RERTR-13	RERTR-15	Identify fundamental phenomena (scientific test)
					Screen designs based on micro-scale behavior
					Bench-scale fabrication development
Applied Research	TRL-5	RERTR-12, AFIP-3 thru -7	RERTR-14, AFIP-8 series	AFIP-9 series	Identify application-based phenomena
					Scale-up fabrication development
					Down-select based on macro-scale behavior
Development Work	TRL-6	RERTR-FE/BFD, DDE's, LTA's	ATR LTA's	DDE-HFIR, HFIR LTA's	Confirm prototypic performance (engineering test)
Qualification	TRL-7				Fabrication qualification
Production	TRL-8	Reactor Conversion			Deployment

2. Base Fuel Irradiation Testing

The RERTR-1 through -10 Basic Research campaigns employed relatively small fuel plate specimens whose primary purpose was to advance bench scale fabrication development

and provide the performance data needed to select the most promising designs. The base fuel design was eventually selected for dedicated testing in the RERTR-12 Applied Research campaign. Irradiation of this experiment is currently underway. Generally speaking, the RERTR-12 campaign is considered a more scientific test as it is designed to identify fundamental phenomena within a large spectrum of irradiation conditions. For example, several RERTR-12 specimens can be accommodated in the irradiation vehicle and irradiated under various fission rates and fission densities. The small specimen size also facilitates whole-specimen PIE activities such as volumetric swelling by way of immersion density and testing for blister threshold and fission product release behavior.

Other Applied Research campaigns are typically designed to address specific engineering-scale phenomena. For example, the AFIP-7 irradiation was recently completed to exhibit performance of full-size base fuel design specimens in a formed, or curved, condition assembled in a prototype element configuration. This enabled key data to be gathered regarding the evolution of coolant channel gaps by way of in-canal channel gap probe. Other AFIP campaigns, such as the AFIP-6 series, were designed to exhibit performance of large-specimens at high powers and also to enable high resolution in-canal ultrasonic characterization for plate swelling and fuel-to-clad bonding data. The AFIP-6 MKII experiment is currently under irradiation. ^[2]

Eventually the Base Fuel Design will be demonstrated in prototypic configurations as “Development Work” campaigns. These include the RERTR Full Element (FE) and RERTR Base Fuel Demonstration (BFD), both which employ the Base Fuel Design in ATR driver fuel, and the Design Demonstration Experiments (DDE’s) to be irradiated in test reactors such as the ATR and the Belgium Reactor-2 ^[2]. Since each HPRR has proposed a distinct geometric configuration of the Base Fuel Design (see Figure 3), three separate DDE campaigns will be performed under reactor-specific prototypic conditions to address MITR, MURR, and NBSR. All of the aforementioned Development Work campaigns are currently in various phases of pre-irradiation design. Completion of these irradiation campaigns will serve as predecessors to the use of Lead Test Assemblies (LTA’s) and production LEU elements in HPRR’s fuel cycles.

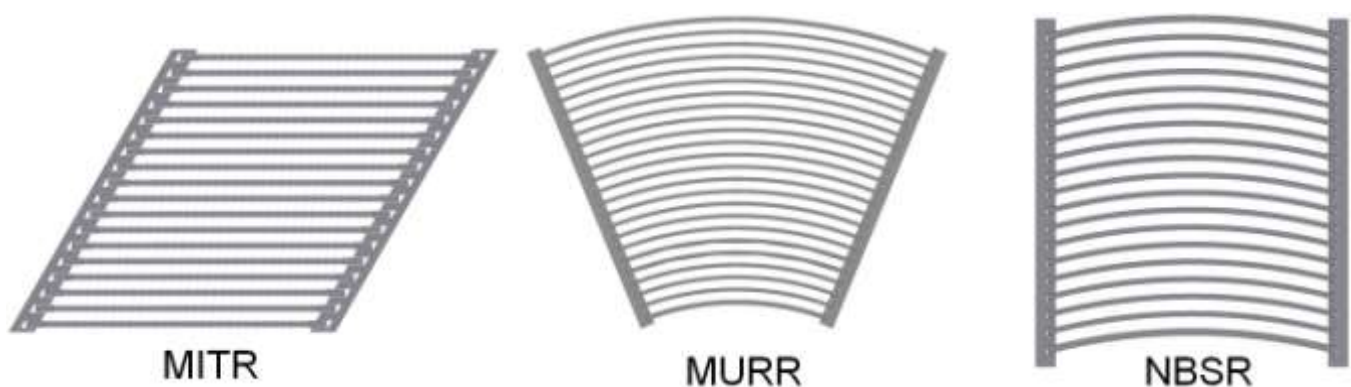


Figure 3: Cross Sections Views of NRC Regulated HPRR Fuel Elements

3. Complex Fuel Irradiation Testing

While the current conversion chronology calls for conversion of complex HPRR’s following base fuel HPRR’s ^[9], the general urgency associated with all reactor conversions, in addition to the economics of concurrent production of LEU-Mo fuel for all HPRR’s, provide strong incentives to accelerate the complex phase of the fuel development program. Currently, the FD pillar is maturing these plans with special attention given to the irradiation testing campaigns. Like the series of Base Fuel irradiation campaigns, the complex fuel

development program will follow the same progression as outlined in Table 1. Two sequences of irradiation tests are proposed for ATR and HFIR to address highly poisoned ICBA's and graded fuel meats, respectively

A series of irradiation tests are planned for the ATR complex fuel design. The RERTR-13 Basic Research irradiation campaign, which was designed to test various ICBA designs, is the first of these and is currently under irradiation. It will be followed by Applied Research campaigns including the RERTR-14 and the AFIP-8 tests which are analogous to the RERTR-12 and the AFIP-6, respectively ^[1]. It is worth noting that if forthcoming ATR LEU core design activities are successful in relocating burnable poisons to non-fueled hardware, then this series of irradiation test will likely be realigned or abandoned. Ultimately, the first elements to employ the final ATR LEU design will be irradiated as LTA's in the ATR.

A similar series of irradiation tests are proposed for the HFIR complex fuel design. The RERTR-15 Basic Research irradiation campaign is proposed to test small-scale graded fuel meats fabricated under different methods and parameters. An Applied Research RERTR-16 campaign may also be performed for HFIR complex fuel design as a separate effects test. However, most of the engineering-scale phenomena pertaining to HFIR fuel must be captured at large scale (e.g. "involute" plate forming, axial constraint by welding). These design features will be exhibited in the AFIP-9 series of Applied Research campaigns ^[1] as well as the DDE-HFIR Development Work campaign. The first assemblies to employ the final HFIR LEU design will be irradiated as lead test cores in the HFIR.

Due to the innate differences between the U-Mo monolithic and more traditional dispersion type fuels, the monolithic development campaigns have always expended significant effort in development of fabrication and quality control methods ^[10]. This trend is expected to continue into the complex fuel campaigns; particularly in regards to monolithic foils of non-rectangular cross-section such as those proposed for HFIR. In some cases, base fuel fabrication development activities were performed prior to full establishment of the FFC pillar. As a result, potential disparities between the final commercial process and those used for fabrication of irradiation testing specimens still pose some schedule related risk to the conversion program.

Since the FFC pillar is now well established, a more integrated approach to fabrication development is being recommended for complex fuel campaigns in order to mitigate this type of risk. For example, it is proposed that the fabrication development campaigns be chaired by a fabrication experts committee, composed of technical leads from GTRI-convert pillars, in order oversee the process of reviewing, selecting, and executing proposed fabrication methods. This process would be iterated with each successive fabrication campaign with an increasing emphasis on full-size demonstration, prototypic specifications, and commercial viability. The results of each fabrication, fresh fuel characterization, and PIE campaigns will feed the database used for selection of the final complex fuel designs and fabrication process.

4. Conclusions

The FD pillar has performed and will continue to perform irradiation tests on the base fuel design in a methodology consistent with consensus standards as well as former LEU fuel development programs ^[11]. Each Applied Research and Development Work irradiation campaign is purposed to accomplish distinct and necessary goals. These technical deliverables are necessary to enable HPRR conversion to LEU fuels. Ultimately, each of these campaigns is necessary for the LEU fuel qualification and reactor licensing bases. It is acknowledged that when the technical deliverables of these irradiation campaigns are compromised, then the campaign will likely require re-performance (e.g. AFIP-6 MKII) or its

technical objectives must be accomplished in another campaign. Future plans for complex fuel technology development are being developed and will follow the same general methodology to ensure that each HPRR has a sound bases for operation using these fuel designs.

5. References

- [1] D.M. Wachs, "RERTR Fuel Development and Qualification Plan", rev 5, 07/05/2011, INL external report INL/EXT-05-01017.
- [2] N.E. Woolstenhulme, D.M. Wachs, and M.K. Meyer, "Design and Testing of Prototypic Elements Containing Monolithic Fuel", Proceedings of the RERTR 2011 International Meeting, Santiago, Chile, October 23-27, 2011.
- [3] A.B. Robinson et al., "Irradiation Performance of U-Mo Alloy Based 'Monolithic' Plate-Type Fuel – Design Selection", INL external report INL/EXT-09-16807, Aug. 2009.
- [4] G. Ilas, R.T. Primm, III, "Fuel Grading Study on a Low-Enriched Uranium Fuel Design for the High Flux Isotope Reactor", March 31, 2010, ORNL/TM-2009/223/R1.
- [5] G. S. Chang, M. A. Lillo, R. G. Ambrosek, "Neutronics and Thermal Hydraulics Study for Using a Low-Enriched Uranium Core in the Advanced Test Reactor 2008 Final Report", June-2008, INL/EXT-08-13980.
- [6] R.T. Primm, III, et al., "Assumptions and Criteria for Performing a Feasibility Study of the Conversion of the High Flux Isotope Reactor Core to Use Low-Enriched Uranium Fuel", February 2006, ORNL/TM-2005/269.
- [7] "Quality Assurance Requirements for Nuclear Facility Applications", ASME NQA-1-2008, Part IV, Subpart 4.2.
- [8] "Applying Quality Assurance Requirements to Research and Development Activities", rev 3, 8/12/2010, INL Document LWP-13016.
- [9] J. Cleary, "U.S. HPRR Conversion Program Predecessors & Successors Report", 1-26-12.
- [10] N.E. Woolstenhulme, G.A. Moore, D.M. Perez, D.M. Wachs, "Development of Quality Assurance Methods for Low Enriched Fuel Assemblies", Proceedings of the RRFM-2010 International Meeting, Marrakech, Morocco, March 21-25, 2010.
- [11] NRC (Nuclear Regulatory Commission), 1988, "Safety Evaluation Report related to the Evaluation of Low-Enriched Uranium Silicide-Aluminum Dispersion Fuel for Use in Non-Power Reactors," NUREG-1313, July 1988.

OVERVIEW OF THE GTRI FUEL FABRICATION CAPABILITY

D.E. BURKES

*Systems Engineering and Integration Division, Pacific Northwest National Laboratory
P.O. Box 999, Richland, WA 99352 USA*

H. LONGMIRE

*Y-12 National Security Complex
P.O. Box 2009, Oak Ridge, TN 37831-8112 USA*

D. DOMBROWSKI

*Materials Science and Technology Division, Metallurgy (MST-6)
Los Alamos National Laboratory, PO Box 1663, Los Alamos, NM 87545 USA*

L. COLE

*Idaho National Laboratory
P.O. Box 1625, Idaho Falls, ID 83415-3855 USA*

ABSTRACT

The Fuel Fabrication Capability (FFC) is part of the U.S. Department of Energy's (DOE) National Nuclear Security Administration (NNSA) Global Threat Reduction Initiative (GTRI) Convert Pillar system. The FFC is primarily responsible for the establishment of a fabrication process for the low-enriched uranium-molybdenum fuel currently under development for supply to the U.S. High Performance Research Reactors. At present, the effect of changing fuel fabrication variables on U-Mo fuel performance is not fully understood. It is likely that the foil production process will change with continued scale up and commercial deployment, leading to changes in the fuel/clad interface structure and the fresh fuel microstructure. This paper will provide an overview of the current progress and the path forward that the U.S. FFC is taking towards development and demonstration of a prototypic fuel fabrication process. More specifically, the paper will address progress that has been made over the last six months in the area of technology development.

1. Introduction

The Global Threat Reduction Initiative's (GTRI) Fuel Fabrication Capability (FFC) has been tasked with the establishment and deployment of a fabrication process for the low-enriched uranium-molybdenum (LEU-Mo) monolithic fuel that is currently under development for supply to the U.S. research and test reactor community. The FFC has been designed to bridge fuel fabrication scope and interest between industry (both national and international), the U.S. Nuclear Regulatory Commission, multiple U.S. national laboratories, and reactor operators and stakeholders. Currently, the FFC is focusing much of its efforts on technology maturation and scale-up of reference processes that have been defined by the GTRI Fuel Development project. This emphasis revolves around three key criteria: (i) establishing the ability to meet throughput demands, (ii) keeping costs as low as reasonably possible, and (iii) ensuring a quality product. At present, the effect of changing fuel fabrication variables on U-Mo monolithic fuel performance is not fully understood. Furthermore, it is likely that the foil production process will continue to evolve with scale-up and commercial deployment. This paper will address the areas that the FFC is focusing on to better understand the impacts of fuel fabrication variables on the resultant fuel plate characteristics, based upon a traditional approach to fuel design qualification and licensing.

The traditional approach to fuel design qualification and licensing consists of three main phases: Development, Qualification, and Commercialization. These phases are often not

performed serially, and feedback loops must exist to ensure that the three criteria discussed above are addressed and met. This traditional relationship between fuel development (design) and fuel fabrication is illustrated in Fig. 1. The focus of this presentation will of course be on those areas that tend to fall within the red circle.

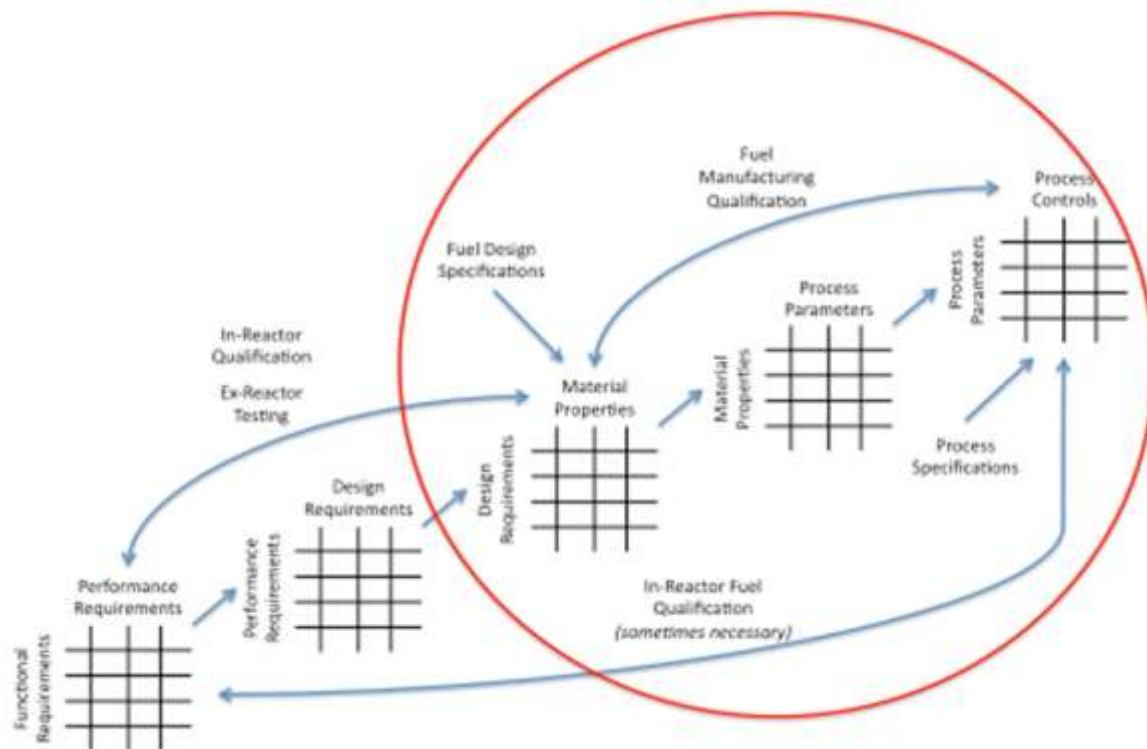


Fig. 1. Traditional relationship between fuel development and fuel fabrication with appropriate feedback loops.

2. Phase I – Development

The Development phase of fuel fabrication is primarily associated with defining the fundamental fuel and cladding material characteristics and properties. Many of these properties are dictated by the design requirements of the fuel itself. For example, grain size, homogeneity, and texture might all be important properties that contribute to swelling and burn-up uniformity during irradiation as defined by the design requirements. The uniformity and thickness of a diffusion barrier, such as zirconium, might be important to ensure that the fuel-clad interface remains stable under irradiation, also defined by the design requirements. The mechanical properties of such an interface may be important to ensure that the integrity of the fuel plate is maintained throughout its service lifetime and so on.

Furthermore, certain material characteristics and properties can drive the selection of fabrication methods. Impurities that are either present in the feedstock material or that are introduced during alloying and casting operations can limit subsequent fabrication steps, e.g. rolling of ingots to produce foils. The desired fuel materials performance characteristics and shelf life may guide the design of the rolling process and/or the rolling schedule to be employed. These properties, combined with the fuel design requirements and specifications, should be used to formulate a “best guess” for process parameters. Thus, fabrication studies, typically conducted at the bench scale, to correlate fabrication parameters with fuel characteristics and properties must be conducted. It is important to point out that this phase will deal primarily with the technical considerations of the fuel, and will be less focused on the three guiding criteria for fuel fabrication qualification. There are numerous examples that document the work conducted during the development phase of the GTRI program (see for example References 1-3).

3. Phase II – Qualification

The Qualification phase of fuel fabrication is primarily associated with establishing a clear understanding of how fabrication parameters and/or product specifications affect the fuel's performance. During this phase, certain adjustments to the process may be required to meet one or more of the three FFC guiding criteria. For example, during the development phase, different processing methods can be investigated with multiple subsets associated with each method, i.e. arc melting, vacuum induction melting, microwave melting, etc., again focusing primarily on the technical impacts rather than quality, cost, and efficiency. During the qualification phase, processes must be accepted, driven by the ability of those processes to meet the product specifications (i.e. a combination of fuel design requirements and specifications). Specific parameters that are unique to the accepted process should be investigated, i.e. whether enrichment downblending and alloying with Mo is conducted in a single step, whether a depleted uranium-molybdenum master alloy is used to downblend the enriched material, the form of molybdenum used in the alloying step, certain rheological parameters, etc. Once the specific processing parameters are known, certain process controls can be defined and further tested to demonstrate that the process is able to reliably produce a quality product that meets the design specification requirements and characteristics of the fuel. Process specifications and tolerances are also developed during this time. Associated with this phase and the definition of the fuel fabrication process are fuel inspection and test methods. It is desirable to avoid introducing new or complicated inspection and test methods for this new fuel type, as this contributes directly to the overall cost of the product. An example of one such study that is currently being performed is provided in Fig. 2.

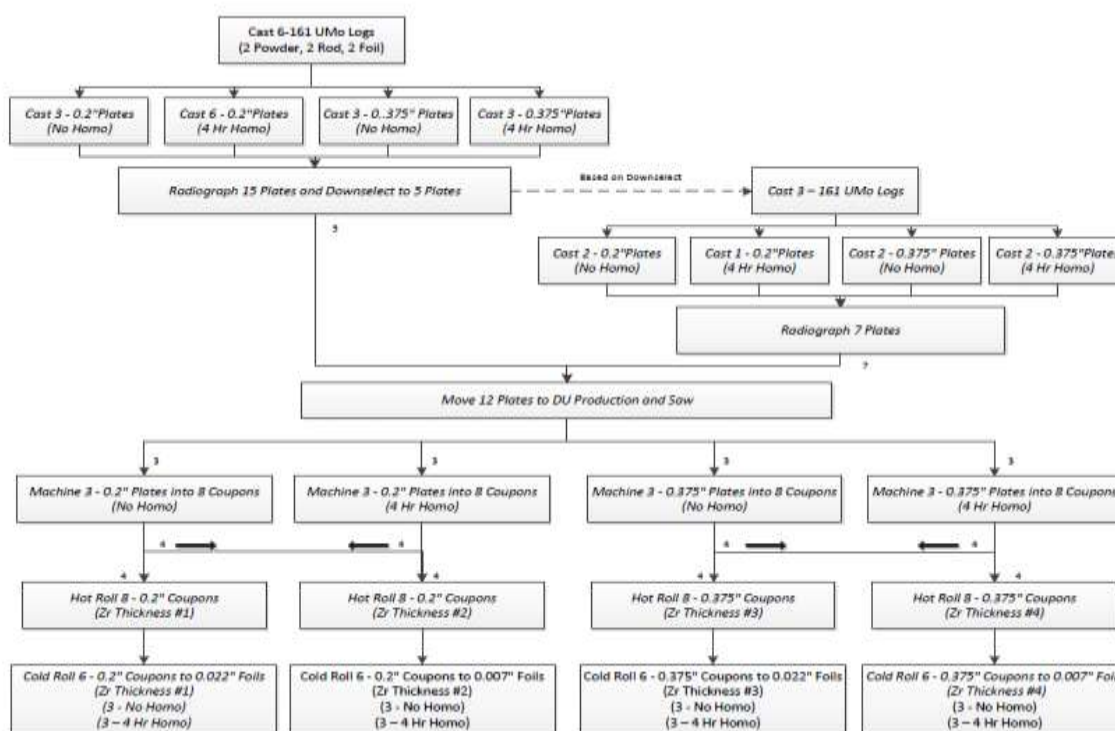


Fig. 2. Example of a parametric study to assess how fabrication parameters and/or product specifications relate to the design requirements of the fuel (i.e. performance). Note that (") represents 1 inch or 2.54 cm.

For the study presented in Fig. 2, a number of different processing options are evaluated, i.e. whether a homogenization treatment is performed or not, utilizing thick coupons as opposed to thin coupons, alloying with Mo powder versus Mo foil, etc. The intent of the

study is to relate the end product characteristics with choices made in upstream processes. In this manner, optimized or alternative processes and technologies can be compared against the “baseline” to effectively evaluate their potential and attractiveness, without impacting the fuel design requirements and specifications in a negative manner. There are a number of optimized and alternative processes being evaluated by the FFC to meet the guiding criteria and compare to the “baseline”, including but not limited to:

- DU-Mo Master Alloy Demonstration - It is hypothesized that such a master alloy/down-blend approach will eliminate some of the current issues associated with alloying and downblending in a single step (i.e. homogeneity of Mo and ²³⁵U). There may also be cost benefits realized by performing this step in a specialized depleted uranium facility.
- Optimization of Coupon Preparation Methods – Machining of coupons is a time intensive process and generates a significant amount of scrap that may not be recoverable. Alternatives to machining are being investigated, including both chemical and less time intensive mechanical processes.
- Foil Annealing Demonstration – Rolling of ingots to produce foils is not a straightforward process, especially in terms of foil homogeneity and uniformity. Vacuum annealing is being investigated as one method to help reduce curvature and flatness issues in cold-rolled foil. The process may also result in increased process yields for rolling thin U-Mo foils.
- Hot Isostatic Pressing (HIP) Can Optimization – Efforts to produce near-net shape fuel plates within a HIP can are being investigated. This will result in minimized final machining of fuel plates to size. Further, optimized HIP can designs that use less material, therefore resulting in less waste, or that are re-usable are being investigated. Both investigations will likely contribute to decreased costs and increased product throughput.
- Can-Less HIP Demonstration – This process promises to reduce manpower associated with make-up of steel HIP cans and reduce waste generated by a canned process, while increasing the throughput by a factor of 4 to 5, all of which directly result in decreased product costs. In addition, the method potentially shows enhanced grain growth along the bond line that is more typical of roll-bonded fuel plates.

In the end, the qualification effort must demonstrate that the process specifications, inspection and test methods will yield a high quality fuel product that meets the fuel design specifications. This phase is typically conducted at the pilot-scale, such that the feedback loop remains open and adjustments to the fuel fabrication process can be made relatively easily (i.e. different equipment, specifications, tolerances). However, if modifications to a process become significant then in-reactor fuel performance data will need to be generated as necessary to validate the qualification basis. An example of such a modification is the application of zirconium for a monolithic fuel design where the current basis is built upon Zr-coated monolithic foils produced by a co-rolling process [4]. It should be stressed that this is not always necessary, as solid characterization efforts on both unirradiated and irradiated materials can sometimes fulfill this requirement (i.e. Phase I of this approach).

4. Phase III – Commercialization

The Commercialization phase of fuel fabrication will demonstrate that the prototypical fuel can be fabricated, meeting all three FFC guiding criteria, and adequately performs within the operational envelope that has been defined. This is often conducted through fabrication and

irradiation of a Lead Use/Test Assembly. At this point, the fabrication process has been finalized through process and product specifications, as indicated in Fig. 1. Appropriate process controls have been determined and are in place to ensure product quality. Commercialization is the final step in fuel manufacturing qualification, and should link directly with qualification of fuel performance.

In the case of the GTRI program, this will be conducted via reactor specific Design Demonstration Experiments (DDEs) and the Base Fuel Demonstration. These demonstration experiments will be irradiated in reactors that are not necessarily the end user (i.e. ATR, BR-2, etc.), but under conditions that are representative of normal fuel operation (i.e. MITR, MURR, NBSR, etc.). This aspect of the program represents a slight departure from the traditional approach to research reactor fuel design qualification and licensing, but is just as robust. The choice of which process to build a fuel performance database upon (i.e. the left side of Fig. 1) can have significant impacts to commercialization of a fuel fabrication process, specifically with regards to cost and efficiency (i.e. the right side of Fig. 1). Issues such as accountable waste recycling volumes and associated recycle costs and process yield rates should be considered and addressed even as early as the Development phase, if at all possible.

5. Conclusions

The approach of the GTRI FFC to establish and deploy a fabrication process for the low-enriched uranium-molybdenum monolithic fuel that is currently under development for supply to the U.S. research and test reactor community has been presented. The FFC is currently transitioning from a Development phase to a Qualification phase. Technologies and process steps that are currently being considered and evaluated to ensure that the LEU-Mo monolithic fuel is of high quality and safe to use and can be made efficiently have been briefly discussed. The approach towards process improvement and optimization has also been briefly discussed.

6. References

1. D.E. Burkes *et al.*, "Fresh Fuel Characterization of U-Mo Alloys," RERTR 2008 – 30th Int. Meeting on Reduced Enrichment for Research and Test Reactors, Washington, DC (2008).
2. E. Perez *et al.*, "Microstructural Analysis of As-Processed U-10 wt% Mo Monolithic Fuel Plate in AA6061 Matrix with Zr Diffusion Barrier," *J. Nucl. Mater.* **402** (2010) pp. 8-14.
3. P. Lemoine and D. Wachs, "High Density Fuel Development for Research Reactors," Global 2007 – Advanced Nuclear Fuel Cycles and Systems, Boise, ID (2007).
4. G.A. Moore *et al.*, "Development Status of U10Mo Monolithic Fuel Foil Fabrication at the Idaho National Laboratory," RERTR 2010 – 32nd Int. Meeting on Reduced Enrichment for Research and Test Reactors, Lisbon, Portugal (2010).

INTERNATIONAL TOPICAL MEETING ON RESEARCH REACTOR FUEL MANAGEMENT (RRFM) - GLOBAL THREAT REDUCTION INITIATIVE'S U.S.-ORIGIN NUCLEAR MATERIAL REMOVAL PROGRAM: 2012 UPDATE

C. E. Messick, J. J. Galan

*Foreign Research Reactor Spent Nuclear Fuel Acceptance Program
U.S. Department of Energy, National Nuclear Security Administration
Office of Global Threat Reduction, Washington, D.C. 20585—United States of America*

Abstract

The *Nuclear Weapons Nonproliferation Policy Concerning Foreign Research Reactor Spent Nuclear Fuel*, adopted by the United States Department of Energy (DOE), in consultation with the Department of State (DOS) in May 1996, scheduled to expire May 12, 2016, to return research reactor fuel until May 12, 2019 to the U.S. is in its sixteenth year. This paper provides a brief update on the program, part of the National Nuclear Security Administration (NNSA), and discusses program initiatives and future activities. The goal of the program continues to be recovery of U.S.-origin nuclear materials, which could otherwise be used in weapons, while assisting other countries to enjoy the benefits of nuclear technology. The NNSA is seeking feedback from research reactor (RR) operators to help us understand ways to include eligible RRs who have not yet participated in the program.

1. Introduction

This paper presents the U.S. Department of Energy's (DOE) Foreign Research Reactor (FRR) Spent Nuclear Fuel (SNF) Acceptance Program, (the Acceptance Program), which is part of NNSA's Office of Global Threat Reduction (GTR). After an initial discussion of program history, contract issues are discussed. Planning issues are then set out to incorporate lessons learned from recent shipments in order to help FRRs understand issues which can affect their SNF disposition project. The final discussion topic regards DOE's efforts to advance the goals of the Acceptance Program, including recent changes to the program and with a conclusion that the Acceptance Program desires to work with FRRs to plan for shipment of their eligible spent fuel as early as possible.

2. Acceptance Program Metrics

The Acceptance Program, now in the sixteenth year of implementation, has completed Fifty eight (58) shipments to date, safely and successfully, and another is expected to be completed in the summer of 2012. Thirty countries have participated so far, shipping a total of 9261 fuel elements to the United States for management at Department of Energy (DOE) sites in South Carolina and Idaho, pending final disposition in a geologic repository. Forty five (45) of the Fifty eight (58) shipments contained aluminum-based spent nuclear fuel from research reactors and were placed into storage at the Savannah River Site (SRS) in South Carolina. Four (4) shipments have been forwarded on to the Y-12 National Security Complex, since the fuel was

fresh or slightly irradiated and eligible for receipt at that facility. The remaining eight (8) shipments consisted of Training, Research, Isotope-General Atomics (TRIGA) type fuel and were placed into storage at the Idaho National Laboratory (INL). The most recent shipment was completed without incident in February. During the remaining calendar year (February - December 2012), the program is planning to receive three shipments of SNF from other locations. It's important to note that some of the program's accomplishments were specifically identified at the 2010 Nuclear Security Summit and more will be announced at the 2012 Seoul Nuclear Security Summit to be held in Seoul, South Korea. None of this could have been accomplished without the cooperation of all of our partners.

3. Contractual Requirements

3.1 Contract and Contract Extensions

Many reactor operators had existing contracts to allow shipment of their SNF to the United States. If these reactor operators have not completed a contract extension or renewed their contract to allow shipments past 2011, a contract extension or renewal to authorize future shipments will be required. If the initial contract expired in 2011 without signing an extension, a new contract will be required. Reactor Operators who desire to ship under this program and do not have a modified contract should contact the Acceptance Program office to negotiate a new contract to authorize participation.

Please be aware that a Revised Fee Policy was published by DOE on January 31, 2012. Any contract modifications, renewals and all new contracts will be subject to the terms of the Revised Fee Policy. The Revised Fee Policy is further discussed below.

3.2 Contract Implementation

Each research reactor that returns SNF to the United States through the Acceptance Program enters into a contract with DOE. It is very important that the contracting parties clearly understand all of the provisions in the contract. Contract requirements are usually described in detail prior to the first shipment. As time passes and personnel change, some understanding may be lost, so it is very important to review the contract and ask questions if there is any doubt about requirements. Compliance with all contract requirements must be maintained. Further discussions on contract requirements can always be addressed to the Acceptance Program office. One important article which has been misunderstood in the past involves compliance with U.S. government regulations restricting public disclosure of any shipping plans, shipment information, or individual details comprising such plans or information. Compliance with this article is an important obligation to ensure security for all shipment activity. Any press release made prior to the material reaching the final storage site, even after the ship reaches international waters on the way to the United States, is a violation of the contract and makes the security of the shipment more vulnerable. Premature release of shipment related information also violates the U.S. Nuclear Regulatory Commission regulations under which the shipments are authorized. Also, The Convention on Physical Protection of Nuclear Material entered into by states which support the Acceptance Program requires that each state protect the confidentiality of this information. Our ability to continue this program depends on our customers following this critical and agreed-to process.

3.3 Contract Appendix Changes

Making changes to SNF after the Appendix A data has been accepted may require a new or revised Appendix A and cause either delays or re-evaluation of the data. Any changes to the authorized material after the data is submitted for evaluation must be approved in advance. The calculations that provide the safety basis for accepting the material are made from the data submitted and almost every possible change could result in the need to repeat these calculations prior to approving the material as acceptable. This adds to the cost and schedule of receipt preparations and may result in the inability of DOE to accept the material on the Reactor Operator's schedule if the required safety documents cannot be completed prior to the scheduled shipping date. Reactor operators need to understand that the fuel assemblies must be identified exactly as indicated in the Appendix A and that no changes may be made after the data is submitted.

3.4 Revised Fee Policy

DOE is continuing to try to keep the reactor operator's cost to participate in the Acceptance Program low as possible, however, because of the increase in operational costs of receiving and managing SNF, on January 31, 2012 DOE issued the **Revised Fee Policy for Acceptance of Foreign Research Reactor Spent Nuclear Fuel From High-Income Economy Countries** (77 FR §4807). This is the first fee increase since the fee policy was established in 1996.

A synopsis of the revision:

- The first phase took effect January 31, 2012; and the fee for receipt of LEU fuel increased from no higher than \$3,750 per kg of total mass to \$5,625 per kg of total mass. The fee for SNF shipments containing HEU remains the same.
- The second phase will be implemented automatically on January 1, 2014 and the fee for the receipt of LEU fuel will increase from \$5,625 per kg of total mass to \$7,500 per kg of total mass and for HEU fuel, the fee for the receipt of HEU fuel will increase from no higher than \$4,500 per kg of total mass to \$6,750 per kg of total mass.
- The third phase will be implemented automatically on January 1, 2016, and the fee for the receipt of HEU fuel will increase from \$6,750 per kg of total mass to \$9,000 per kg of total mass.
- DOE is also implementing a new minimum fee of \$200,000 per shipment of any type and amount of eligible SNF to reflect a minimum cost of providing acceptance services, this fee took effect January 31, 2012.
- The fee for return of TRIGA fuel will be the same as that of aluminum based fuel.

In the case where a reactor operator already has a signed and executed contract, DOE intends to negotiate an equitable adjustment to the fee in accordance with this revised fee policy.

Reactor operators and Acceptance Program participants should carefully review the Revised Fee Policy to determine the effects of this revision. If you have any questions, please contact the Acceptance Program office.

4. Focus on Early Planning

The Acceptance Program focuses on the planning and implementation of research reactor spent fuel shipments to the United States in support of worldwide nuclear nonproliferation efforts, while allowing other countries to enjoy the benefits of nuclear technology. Along with shipment logistics, the GTR office continues to address many other issues of programmatic importance.

4.1 Shipment Scheduling

It is always important that DOE clearly understands the intentions of all reactor operators so that our planning can be well integrated and supported to meet the reactor operator's needs. It is also important to submit the required fuel data as early as possible in order to allow adequate time for the receiving site to perform necessary reviews and prepare for receipt and storage. Early availability of this data is also important for use in verifying transport package license requirements or submitting for a license amendment, when required. Budget limitations have been known to challenge implementation of shipping plans for our customers and DOE. Similarly, the DOE receiving facilities also face increasing challenges in providing resources to receive material, particularly when reactor operator's shipping plans are not known in time to request funding. In addition, continuing budgetary pressure has limited the ability of DOE to continue to operate every facility full time. This decrease in operational availability may further limit flexibility. The Acceptance Program staff will be happy to answer questions about scheduling or clarify what type of information is needed to facilitate receipt of fuel.

Shipment delays impact DOE's ability to maintain a regular schedule of operations and adequate resources for the receipt facility. The FRRs are strongly encouraged to continue shipping as early as possible and maintain original schedules where possible. Deferring shipments when spent fuel is available for shipping could result in changes to DOE's ability to support the receipt of fuel when a shipment is desired by the reactor operator. Also, as the Acceptance Program approaches the end of the policy period, a large amount of shipments are expected. DOE may be required to exercise its authority to limit receipts to specific customers with the greatest need.

4.2 Insurance Issues

Insurance issues have been a recurring problem for reactor operators in high-income economy countries who participate in joint shipments. Nuclear liability insurance associated with ocean transport has the potential to adversely affect the total cost of shipping. This occurs because the shippers are sometimes required to have overlapping insurance coverage and may also have different requirements for minimum coverage. It is important for reactor operators to plan early for the required coverage and determine how to provide coverage in the least expensive manner. Consideration should be given for reactor operators entering into a joint shipment to coordinate in obtaining their nuclear liability insurance with the same pool or under a joint contract, where possible, in order to mitigate overlapping insurance costs. Recently, we have experienced better results for some customers with aggressive coordination. It is also important to be conscious of this potential problem and budget for any added cost that cannot be mitigated.

4.3 Cask License Review

The Acceptance Program enjoys very good working relationships with U.S. Nuclear Regulatory Commission (NRC) and U.S. Department of Transportation (DOT) staffs and wishes to take every measure possible to respect these relationships by ensuring that cask license applications are timely and complete. DOE meets periodically with NRC and DOT to discuss planned shipments and forecast the support required to meet the needs of the Acceptance Program and our customers. Because there are limited NRC and DOT resources for review of cask licenses, our customers need to provide adequate time in the preparation process, scheduling for early application for review and approval of cask licenses.

5. Efforts to Improve and Accelerate

The Acceptance Program has now well passed its midpoint with only four years remaining on the extended policy period plus a three year window to allow for cool down and shipment. More than ever, DOE and reactor operators need to work together to schedule shipments as soon as possible, to optimize shipment efficiency over the remaining years of the program. Countries interested in participating in the Acceptance Program should express their interest as soon as possible so that fuel and facility assessments can be scheduled and shipments may be entered in the long-term shipment forecast. New and current Acceptance Program participants should also coordinate with DOE at least 18 - 24 months in advance to ensure DOE can meet the reactor operator's plans and needs. Accelerated schedules are possible if there are no significant issues or changes from past shipments such as a change in fuel type or fuel condition. However, decreasing resources and coordination requirements with other agencies such as the NRC and DOT have the potential to limit DOE's capability to support these accelerated schedules. Specifically, the Acceptance Program may not be able to accommodate a large number of requests at the end of the program, particularly from geographically isolated regions.

5.1 Source Recovery

Several recent shipments of SNF have provided an opportunity for radioactive sources associated with the U.S. Radiological Remove division of GTR to be transported to the U.S. on the same vessel used to ship SNF. This is an excellent opportunity for the customer or other organizations in the customer's country or surrounding countries to dispose of unwanted radioactive sealed sources, particularly sources that cannot be transported by air. The DOE generally provides the ocean transport without charge when the ocean-going vessel is funded and managed by DOE. However, for vessels funded by other organization, the organization that is charged with dispositioning these sources also should coordinate with the organizations managing and funding the ocean-going vessel.

DOE sponsors a program to recover excess and unwanted radioactive sealed sources. Traditionally, the program has dealt largely with americium-241 and plutonium sources. Because of heightened concerns about the potential that radioactive sources may be diverted to use in a dirty bomb, DOE is moving aggressively to include other isotopes of concern. DOE is currently emphasizing larger excess sources containing cobalt-60 and cesium-137, such as medical irradiators. The DOE is also considering a campaign to manage large numbers of small obsolete sources, examples of which are cesium-137 brachytherapy sources, and various radium-226, americium-241, and other sources. To be considered, institutions must register their material with Los Alamos National Laboratory.

Reactor operators and other Stakeholders should consider this opportunity and also communicate with and assist in any coordination within their country or region. To learn more and register online, please visit osrp.lanl.gov.

5.2 Coordination with Other Programs

A primary goal of the Acceptance Program is to support worldwide nonproliferation efforts by disposition of HEU which contains uranium enriched in the United States. Integral to this process is the U.S. assistance offered in helping reactor operators convert their cores to low enriched uranium (LEU) as the reduced enrichment fuels become qualified and available. In addition, DOE plays a strategic role in ensuring a supply of enriched uranium for fuel fabrication.

In the Acceptance Program, the primary goal is intertwined with the missions of the Reduced Enrichment for Research and Test Reactors (RERTR) Program and the Enriched Uranium Operations group from DOE's Y-12 National Nuclear Security Complex in Oak Ridge, Tennessee. DOE's Acceptance Program staff remains committed to working with staff in other program offices within DOE to assist in smooth transition of core enrichment level and a steady supply of fuel.

6. Conclusion

The United States remains committed to supporting worldwide nonproliferation goals while assisting other countries to enjoy the benefits of nuclear technology such as those for which this program was designed. The programmatic goal is to accept eligible fuel as soon as possible to allow additional opportunities for all potential reactor operators that desire to participate in the Acceptance Program. Reactor operators are strongly encouraged to work closely with technical points-of-contact in order to ensure shipping schedules are accurate and achievable. The GTR staff hopes to work with all remaining eligible research reactors to plan for shipments of their eligible spent fuel as early as possible. DOE/NNSA continues to support research reactor operators' needs and would be happy to meet any interested parties to discuss the program.

COATINGS FOR INCREASED CORROSION RESISTANCE OF ALUMINIUM-CLAD SPENT FUEL IN WET STORAGE

S.M.C.FERNANDES, O.V.CORREA, J.A.DE SOUZA, L.V.RAMANATHAN,

*Materials science and Technology Center,
Instituto de Pesquisas Energéticas e Nucleares- IPEN
Av. Prof. Lineu Prestes 2242, Cidade Universitaria
05508-000 São Paulo. Brazil.*

ABSTRACT

Corrosion protection of spent RR fuel for long term wet storage was considered important, primarily from the safety standpoint and the use of conversion coatings was proposed in 2008. This paper presents the results of: (a) on-going field tests in which un-coated, boehmite, hydrotalcite (HTC) and cerium modified boehmite as well as HTC coated Al alloy coupons were exposed to the IEA-R1 reactor spent fuel basin for durations of up to 9 months; (b) HTC coating preparation at room temperature; (c) evaluation of corrosion resistance of aluminium alloy AA 1100 and AA 6061 specimens coated with different types of boehmite and HTC. In the field studies the HTC coated coupons were the most corrosion resistant. The cerium modified HTC coated specimens showed marked increase in pitting corrosion resistance, both in laboratory and the field tests, indicating its potential for use as a protective coating of spent Al-clad RR fuels.

1. Introduction

Most of the wet storage facilities for spent aluminium-clad research reactor (RR) fuel have water quality management programmes, to prevent and/or reduce degradation of the fuel cladding. Pitting corrosion has been identified as the main form of degradation that could cause cladding failure and release of fissile material, contaminating thereby the storage facilities. It has been shown that maintenance of water parameters within specified limits does not prevent pitting corrosion of the fuel cladding, due to synergism between many basin water parameters that affect corrosion of aluminium and its alloys [1,2]. Hence, it was considered imperative that some form of corrosion protection be given to stored spent RR fuel. Use of conversion coatings is a well established corrosion control technique and it has been extensively used in many industries to control the corrosion of various metals. In recent years, rare earth compounds have been used in corrosion protection systems for aluminium alloys [3]. Having observed the formation of cerium hydroxide films on Al alloys immersed in solutions containing cerium compounds as inhibitors, other chemical treatments have been proposed to form rare earth based conversion coatings on Al alloys [4-6]. Use of conversion coatings to protect spent Al-clad RR fuel assemblies was proposed in 2007 and the results of preliminary laboratory and field investigations carried out at IPEN in Brazil, revealed that cerium hydroxide coating increased the corrosion resistance of Al alloys [7,8]. The investigations were subsequently extended to include boehmite, hydrotalcite (HTC), cerium modified boehmite and cerium modified HTC coatings on Al alloy surfaces. Inclusion of cerium modified boehmite coatings was motivated by the fact that this type of Al hydroxide covers the surface of spent RR fuel. HTC is lithium aluminium-nitrate-hydroxide hydrate and it forms on Al alloys immersed in an appropriate alkaline lithium salt solution [9]. Immersion of Al alloys in such solutions result in formation of a polycrystalline barrier film composed mainly of HTC like compounds. Further studies were carried out recently to obtain HTC coatings at room temperature, as opposed to the previous set of studies where HTC coating were prepared from solutions at 95 °C.

This paper presents the results of: (a) field studies in which uncoated, boehmite coated, HTC coated, cerium modified boehmite and cerium modified HTC coated Al alloy coupons were exposed to the IEA-R1 reactor spent fuel basin for 6 and 9 months; (b) HTC coating preparation from different aqueous solutions; (c) evaluation of corrosion resistance of aluminium alloy AA 1100 and AA 6061 specimens coated with different types of boehmite and HTC.

2. Methods and materials

Aluminium alloys AA 1100 and AA 6061 (Table 1) were used in the laboratory and field tests. The field test procedure consisted of preparing Al alloy coupons, stacking the coupons in racks, immersion of the racks in the spent fuel section of the IEA-R1 research reactor in IPEN, Brazil, for 6 and 9 months, removal of the racks followed by disassembly and examination of the coupons [1].

Tab 1. Chemical composition of aluminium alloys (wt%)

Alloy	Cu	Mg	Mn	Si	Fe	Ti	Zn	Cr
AA 1100	0.16	<0.1	0.05	0.16	0.48	0.005	0.03	0.005
AA 6061	0.25	0.94	0.12	0.65	0.24	0.04	0.03	0.04

Coupons 10 cm in diameter and 3 mm thick of the two alloys were treated by immersion in solutions and under conditions shown in table 2. The coupon stacking sequence in the racks from top to bottom consisted of untreated, HTC coated, boehmite coated, HTC-Ce coated and boehmite-Ce coated. The surface features of the uncoated and coated coupons exposed for 6 and 9 months were examined with an optical microscope.

Tab 2. Solutions and conditions used to prepare coatings on Al alloys.

Solution	Purpose	Composition of solution and conditions
1	Degrease	25 g/L Na ₂ SiO ₃ ; 25 g/L Na ₂ CO ₃ ; 65 °C; 2 min.
2	Deoxidize	10% HNO ₃ ; 3% NaBrO ₃ ; 55 °C; 3 min.
3	Form boehmite	Deionized water; 97-100 °C; 5 min.
4	Incorporate Ce in boehmite	0.1% CeCl ₃ ; 97 °C; pH 4; 5 min.
5	Form HTC	6.9g/L LiNO ₃ ; 28.3 g/L KNO ₃ ; 2.4 g/L LiOH; 0.06 g/L NaAlO ₂ ; 98 °C; pH 12; 10 min.
6	Form HTC	0.1M Li ₂ CO ₃ ; LiOH; Al; pH 12; 15 min; R.T.
7	Form HTC	6.9g/L LiNO ₃ ; 28.3 g/L KNO ₃ ; 2.4 g/L LiOH; 2.5 g/L K ₂ S ₂ O ₈ ; 0.06 g/L NaAlO ₂ ; 98 °C; pH 12; 10 min.
8	Incorporate Ce in HTC	10 g/L Ce (NO ₃) ₃ ; 30% H ₂ O ₂ ; R.T.; 5 min.

In the laboratory tests HTC coatings were deposited on AA 1100 and AA 6061 specimens from solutions 5, 6 and 7 of Table 2. The composition, morphology and extent of corrosion protection provided by these coatings to the substrate were determined. The electrochemical behaviour of uncoated and coated specimens was determined from anodic potentiodynamic polarization measurements carried out with a standard 3-electrode arrangement in 0.1 M NaCl, using a saturated calomel reference electrode. The motivation for these tests was to obtain a HTC coating at room temperature, mainly to facilitate the process to coat spent fuels. Some of the HTC coated specimens were further treated by immersion in solution 8 of Table 2 to incorporate cerium.

3.Results and discussion

3.1 Laboratory tests

The main features of the coatings formed from the different solutions are summarized in Table 3. The coatings were identified by x-ray diffraction analysis. The surfaces treated in the nitrate, carbonate and carbonate + cerium solutions revealed intersecting blade or rod like HTC crystallites that formed a continuous layer across the surface. The coatings formed inside pits and recesses that developed during pre-treatment of the substrate. Scanning electron micrographs of HTC coatings on the Al alloys from the nitrate and carbonate solutions are shown in Fig. 1. Below the outer layer a dense layer of amorphous or nanocrystalline lithium aluminate forms [9]. The coating thickness varied with the substrate alloy, bath composition, age of the bath and immersion time. Typical coating thickness after 10 minutes of immersion was ~2 μm .

Tab 3. Aluminium alloy surface features following treatment in different solutions. (vide table 2 for solution composition; RT – room temperature)

Alloy AA	Coating solution and conditions			Surface features
	Solution	°C	Main anion	
1100	5	95	NO ₃	HTC forms – well defined crystallites
6061	5	95	NO ₃	HTC forms and Mg ₂ Si detected
1100	6	RT	CO ₃	HTC forms and surface etched
6061	6	RT	CO ₃	HTC and Mg ₂ Si detected
1100	7	95	NO ₃ + S ₂ O ₈	No HTC
6061	7	95	NO ₃ + S ₂ O ₈	No HTC, Mg ₂ Si detected
1100	5 + 8	RT + RT	CO ₃ + CeO ₂	HTC forms and surface etched
6061	5 + 8	RT + RT	CO ₃ + CeO ₂	HTC forms and surface etched.

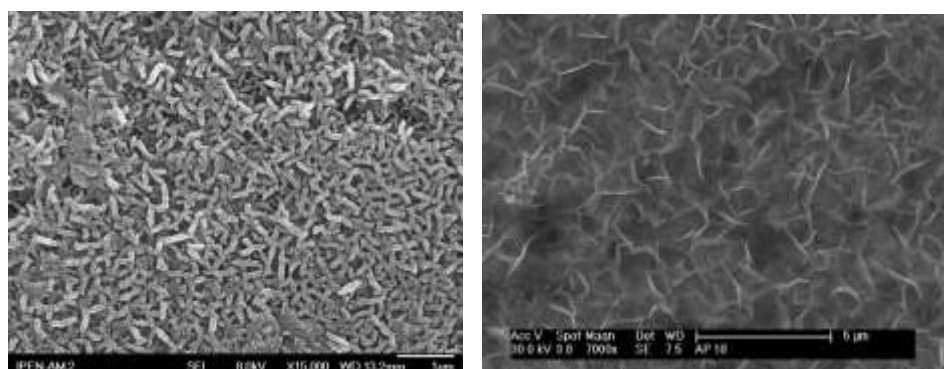


Fig 1. Micrographs of: (a) HTC on AA 6061 from NO₃ solution at 95 °C
(b) HTC on AA 1100 from CO₃ solution at RT + Ce impregnation

The electrochemical behaviour alloy AA 6061, with or without the coatings revealed differences in the anodic as well as the cathodic polarization curves. Table 4 summarizes the corrosion potential (E_{corr}), the pitting potential (E_{pit}) and the corrosion current densities (i_{corr}) of the AA 6061 specimens with the different coatings. The E_{pit} of the untreated specimen was very close to its E_{corr} signifying active corrosion and with boehmite coating, the E_{pit} increased to -650 mV. Cerium modified boehmite increased E_{pit} even more to -600 mV, indicating increased pitting corrosion resistance upon introduction of Ce. A HTC layer on the alloy surface resulted in an even more marked increase in the pitting resistance by increasing the E_{pit} from -750 to -580 mV. This increase in pitting resistance of the alloy with a HTC coat was further enhanced by modifying the HTC with Ce. The E_{pit} increased significantly to -420 mV. The cathodic current density of the AA 6061 specimen in 0.1 M NaCl decreased by an order

of magnitude upon coating it with either boehmite or HTC. The difference in the i_{corr} between the boehmite coated and the HTC coated specimens was slight with no marked change even with the introduction of Ce into the coating. The open circuit or corrosion potential E_{corr} of AA 6061 increased to almost the same extent with formation of boehmite or HTC. Modification of either coating with Ce increased E_{corr} to again the same extent.

Tab 4. Corrosion current (i_{corr}), corrosion potential (E_{corr}) and pitting potential (E_{pit}) of alloy AA 6061 in 0.1M NaCl

Surface condition	i_{corr} (mA.cm ⁻²)	E_{corr} (mV vs SCE)	E_{pit} (mV vs SCE)
None	1.5×10^{-6}	- 760	- 750
Boehmite	2.0×10^{-7}	- 711	- 650
Boehmite + Ce	3.5×10^{-7}	- 754	- 600
HTC	3.5×10^{-7}	- 718	- 580
HTC + Ce	4.0×10^{-7}	- 764	- 420

3.2 Coupons exposed to IEA-R1 reactor spent fuel section.

The coupons were removed from the racks, rinsed, decontaminated, dried and examined visually and with an optical microscope. The top surface of the untreated coupons revealed more pits compared to the bottom facing surface of the same coupon, indicating the influence of settled solids on the top surfaces.

Tab 5. Surface features of coupons exposed to the IEA-R1 reactor spent fuel section.

Alloy	Coating	Surface features after exposure for	
		6 months	9 months
AA 1100	None	Dark, many pits	Dark; Many pits
	HTC	Few stains, no pits.	Few stains, no pits.
	Boehmite	Bright, no pits.	Bright, no pits
	HTC + CeO ₂	Few stains, no pits,	Few stains, no pits.
	Boehmite + CeO ₂	Bright, no pits.	Bright, no pits.
AA 6061	None	Dark, few pits.	Very dark, few pits.
	HTC	Dark, stained, no pits.	Dark, stained, no pits.
	Boehmite	No pits.	No pits.
	HTC + CeO ₂	No pits.	No pits.
	Boehmite + CeO ₂	No pits.	No pits.

The main features of the coupons exposed for 6 and 9 months to IEA-R1 spent fuel basin is summarized in table 5. It is evident that the boehmite and HTC coated coupons of the two alloys revealed no pits on either side after 9 months of exposure to the spent fuel section of the IEA-R1 reactor, where as the untreated coupons revealed many pits of varying size.

4. General discussion

The laboratory and field tests have indicated the marked increase in corrosion resistance of Al alloys coated with boehmite and HTC. The corrosion resistance was further enhanced by modifying the two types of coatings with cerium dioxide. In the context of eventually protecting Al-clad spent RR fuels during long term wet storage, the coating process for irradiated fuels would be facilitated if treatments were to be carried out at room temperature. In this context, protecting with HTC coatings modified with cerium is the obvious choice. The HTC layer imparts pitting corrosion protection by acting as a physical barrier between the solution and the surface. The mechanism by which the cerium modified HTC imparts

protection is considered to be 'active corrosion protection', analogous to chromium coatings. This involves release of Ce ions from the coating, transport of Ce ions through the solution and its action at defect sites to stifle corrosion. It has been speculated that if a Ce^{4+} bearing inorganic coating contacts a solution, soluble Ce^{4+} is released into the solution. When these ions encounter reducing conditions, like those associated with exposed bare metal at coating defects, it reduces to Ce^{3+} , which forms an insoluble hydroxide and precipitates. The precipitated cerium hydroxide at the defect then stifles further corrosion.

5. Conclusions

1. Hydrotalcite (HTC) coatings on AA 1100 and AA 6061 alloys were prepared from nitrate baths at 95 °C and carbonate baths at room temperature.
2. The cerium modified HTC and boehmite coatings increased markedly the pitting resistance of the two alloys.
3. Coupons of the two types of alloys coated with boehmite and HTC when exposed to the IEA-R1 reactor spent fuel section for 9 months did not reveal any pits whereas the uncoated coupons of the two alloys revealed many pits.
4. Coating HTC on Al alloys from carbonate baths at room temperature followed by cerium modification from a nitrate bath, also at room temperature, is a simple process that can be tailored and scaled-up to protect radioactive spent Al-clad RR fuel assemblies for long term wet storage.

6. References

1. Corrosion of Research Reactor Aluminium Clad Spent Fuel in Water", IAEA - TRS 418, (2003).
2. L.V. Ramanathan, R. Haddad, P. Adelfang and I. Ritchie, Corrosion of Spent Aluminium-clad Research Reactor Fuel – Synergism in the Role of Storage Basin Water Parameters, Proceedings of 12th International topical meeting on Research Reactor Fuel Management (RRFM), Hamburg, Germany, (2008).
3. B.R.W. Hinton, D.R. Arnott and N.E. Ryan, Mater. Forum 9, 162, (1986).
4. D.R. Arnott, N.E. Ryan, B.R.W. Hinton, B.A. Sexton and A.E. Hughes, Appl. Surf. Sci., 22/23, 236, (1985).
5. M. Dabalà, L. Armelao, A. Buchberger and I. Calliari. Appl. Surf. Sci., 172, 132, (2001).
6. A.E. Hughes, S.G. Hardin, K.W. Wittel, P.R. Miller, in the Proceedings of the NACE meeting: Corrosion/2000, Research topical Symposium: Surface Conversion of Aluminum and Aluminum alloys for Corrosion Protection, Orlando, USA, (2000).
7. S.M.C.Fernandes, O.V.Correa, J.A.de Souza and L.V.Ramanathan, Lanthanide based conversion coatings for long term wet storage of aluminium-clad spent fuel, Proceedings of 14th International topical meeting on Research Reactor Fuel Management (RRFM), Marrakech, Morocco, (2010).
8. S.M.C.Fernandes, O.V.Correa, J.A.de Souza and L.V.Ramanathan, Protective coatings for wet storage of aluminium-clad spent fuel, Proceedings of 15th International Topical Meeting on Research Reactor Fuel Management (RRFM), Rome, Italy, (2011).
9. W. Zhang and R.G.Buchheit, Corrosion, vol.58, 7, 591, (2002).

EDUCATION AND TRAINING ON ISIS RESEARCH REACTOR

F. FOULON, B. LESCOP

*National Institute for Nuclear science and Technology
CEA Saclay Research Center, 91191 Gif-sur-Yvette, France*

X. WOHLEBER

*OSIRIS Operations Division, Nuclear Reactors and Services Department
CEA Saclay Research Center, 91191 Gif-sur-Yvette, France*

F. MALOUCH

*Reactors Studies and applied Mathematics Section (SERMA)
CEA Saclay Research Center, 91191 Gif-sur-Yvette, France*

ABSTRACT

Today, ISIS research reactor is an essential tool for the Education and Training programs organised by the National Institute for Nuclear Science and Technology. A large panel of training courses (duration ranging from 3 to 24 hours) have been developed on ISIS reactor. The training courses are included, both in academic degree programs and continuing education courses for professionals at French and Internationals level. In 2011, the Education & Training activity represented around 360 hours distributed over 70 working days. This paper presents the ISIS research reactor, the training courses and the Education and Training programs that have been developed with its use. It gives an example of the use of the reactor to establish correlation between measured core reactivity changes and calculations carried out with neutronic codes. Finally, it shows that low power research reactors are very powerful tools for the development of the human resources needed by the nuclear programs.

1. Introduction

From 2004 till 2006, ISIS research reactor went through a major refurbishment program in order to convert the reactor activity to education and training. Since 2007, ISIS reactor became an essential tool for the Education and Training (E&T) programs organised by the National Institute for Nuclear Science and Technology (INSTN) in replacement of ULYSSE reactor that was operated from 1961 till 2007 by the INSTN. In order to provide to students and professionals a high level of knowledge and qualification in disciplines related to nuclear reactors, a large panel of training courses have been developed on ISIS reactor. The training courses are included, both in academic degree programmes and continuing education courses for professionals at French and International levels.

After a presentation of ISIS reactor, we present the training courses that have been developed on ISIS reactor. We describe their use in the E&T programs from the INSTN. In addition to the operational aspects that are studied in the training courses, we show that simple experiments carried out on the reactor can be used to illustrate the reactor physics. As an example, the measurement of changes in the core reactivity resulting from the removal of experimental devices can be correlated to neutron calculations carried out with neutronic codes. In conclusion, we report on the feedback obtained from the trainees showing that low power research reactors are very powerful tools for the development of the human resources needed by the nuclear programs.

2. ISIS reactor characteristics

ISIS research reactor is located on the CEA Saclay site. It belongs to the same nuclear facility as OSIRIS reactor [1]. Both reactors are open core pool type reactors and exhibit the same core characteristics (size and configuration of the core, fuel and rod characteristics). However, from the thermo-hydraulic point of view, ISIS reactor has a nominal power of 700 kW, while OSIRIS can be operated up to 70 MW.

The pool of ISIS reactor is 7 meter deep. The core has a horizontal section of 62 cm x 70 cm and a height of 65 cm. It is composed of an Aluminium container with 56 cases which is included in a zirconium alloy container. The core is composed of 38 fuel assemblies, 6 control rods, 7 Beryllium assemblies, as well as 5 experimental cases (see Figure 1).

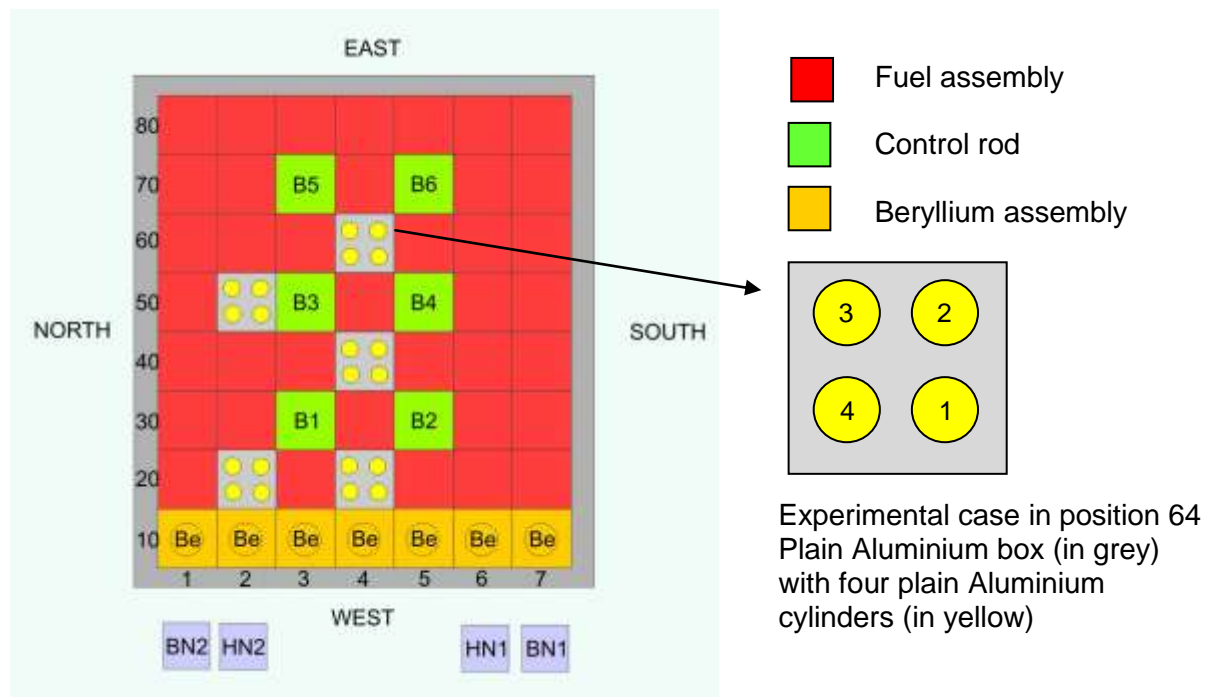


Fig. 1 : Schematic of the ISIS core

The MTR (Material Testing Reactor) type fuel, in silicide U_3Si_2Al form, is enriched at 19.75%. The active part of the fuel assembly has a height of 65 cm. The reactor is equipped with six control rods (B) with hafnium for the neutron capture. Beryllium assemblies, placed on one side of the core, are used both as a neutron reflector, to reduce the neutron leakage, and as the starting neutron source through (γ , n) reactions. The reactor is equipped with 4 neutron detection systems that are placed in metallic tubes found above the top of the core on the Beryllium assemblies' side (namely BN1, BN2, HN1 and HN2 in figure 1).

The experimental cases can be used to place devices to be irradiated or tested (instrumentation, samples to be activated, test fuel, ...). In its basic state, a case is filled with a plain aluminium box which exhibits the same dimension as a fuel assembly and contains four plain aluminium cylinders (28 mm in diameter). Each cylinder can be removed separately to introduce small samples or devices in the core. Such experimental cases can be used to modify the core reactivity by removing successively the four cylinders and eventually the whole box. The corresponding change in core reactivity can be then correlated to core reactivity change calculated by the mean of neutronic codes.

Above the core a stainless steel chimney separates the water from the primary water loop from the rest of the pool. Up to 50 kW, the reactor can be operated under natural convection in the chimney. Above 50 kW, the reactor is cooled through the primary water loop (flow rate 50 m³/h) which is in its turn cooled through the use of two heat exchangers from the secondary loop.

3. Training courses developed on ISIS reactor

From 2004 till 2006, ISIS reactor went through a major refurbishment of the control system and the control room in order to convert the reactor to E&T activities. After refurbishment and testing, the reconfigured ISIS reactor was licensed by the Regulatory Body and from March 2007, ISIS reactor became the main reactor used by CEA for E&T activities. A large panel of experiments, which are shown in figure 2, have been developed for the E&T programs organized by the INSTN. These experiments are integrated in nine courses, each course with duration of 3 hours.

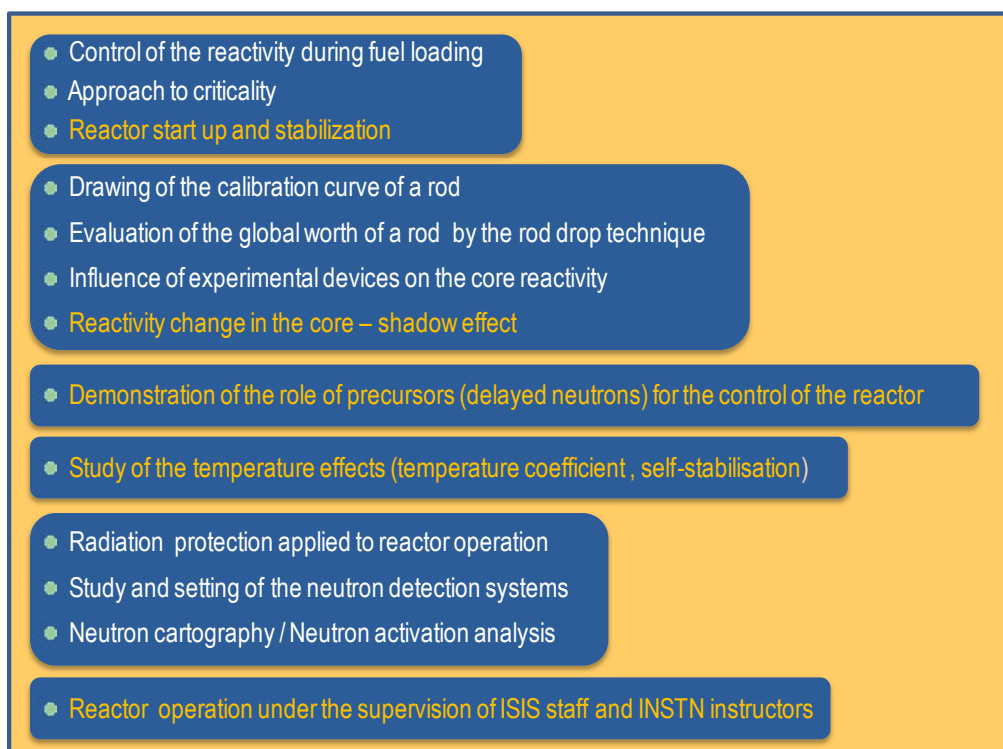


Fig. 2 : Content of the training courses developed on ISIS reactor

4. E&T Programs using ISIS reactor

Since 1956, the INSTN has always been promoting the use of laboratory work and training courses carried out on nuclear facilities in order to complete the theoretical courses. It was established that from a pedagogical point of view training courses on nuclear facilities and, in particular, on nuclear reactors was needed to ensure a practical and comprehensive understanding of the reactor principle and operation. Thus, today, whenever it is needed training courses on ISIS reactor are integrated in E&T programs from the INSTN.

The INSTN is involved both in academic programs and continuing education courses for professionals. The training courses on ISIS reactor are integrated in academic programs such as:

- an International Master in Nuclear Energy (<http://www.master-nuclear-energy.fr>),

- a one year specialisation course in Nuclear Engineering for engineers,
- Nuclear Engineering modules of various Masters and Engineer's degrees,
- Master's programmes of three Swedish Universities.

Concerning continuing education (www-instn.cea.fr), the training courses on ISIS reactors are addressed to a wide public that includes researchers, engineers, technicians and personnel from the Regulatory Body. They are integrated in such programs:

- a 8 week compulsory course for the operators of the French Research Reactors,
- 1 to 4 week regular courses related to the principles, the operation, the safety and the neutronic of nuclear reactors,
- 1 to 12 week courses organised to respond to the specific need of the nuclear industry and nuclear programs.

The latter, includes courses that have been developed on request for the personal of the French regulator body, for young engineers from the Italian company ENEL, for project managers of the Vietnamese company EVN (Electricity of Vietnam), or for teachers and professors from several Polish Universities ("train the trainers" course).

Depending on the public and on the pedagogic goals, the trainees follow programs that exhibit from 3 up to 24 hours of training courses on ISIS reactors. Every year, about 400 trainees participate to the training courses on ISIS reactor. E&T activity on ISIS research reactor represents about 360 hours distributed over 70 working days. One third of this activity concerns international courses that are taught in English. With an increase in the need for E&T, especially at an international level, the E&T activity on ISIS reactor could easily be increased up to 600 hours distributed over 120 working days.

5. Specific experiments on ISIS reactor

The training courses listed in § 3 are mainly intended to give a practical experience related to the principles and operation of nuclear reactors. In addition, training courses on ISIS reactor can also be used to respond to a specific need of academic and vocational programs. As an example, the study of the changes in core reactivity resulting from the removal of devices from the core in the experimental cases shown in figure 1 can be correlated to neutron calculations carried out with neutron calculations.

For this experiment, the reactor is operated at a constant power, the reactor being kept critical. As a result of the removal of Aluminium devices and their replacement by water, the reactivity effect related to the local change in the moderation volume is compensated by the movement of the control rod B6. Using the calibration curve of this rod (about 8 pcm per mm) the corresponding change in core reactivity is found.

For neutron calculation, the positions of the control rods and the real load in fuel assemblies are taken into account. A differential calculation with and without aluminium cylinder (replaced by water) gives the change in reactivity $\Delta\rho$ induced by the removal of the device according to:

$$\Delta\rho \text{ (pcm)} = 10^5 \text{Ln} \frac{k_{eff}(\text{water})}{k_{eff}(\text{Al device})}$$

where k_{eff} is the effective multiplication factor.

The $\Delta\rho$ of a device is calculated by using the OSIRIS core two-dimensional diffusion code developed by CEA. This code solves the diffusion equation using finite-difference method, applicable in 2-dimensional Cartesian coordinates and 4-energy group formalism. For safety reasons, these **Operation calculations** are conservative and generally over-estimate the real change in core reactivity.

Reference neutron calculations are also performed using the TRIPOLI-4 3-dimensional continuous-energy Monte Carlo transport code [2], developed by CEA and extensively validated according to reactor dosimetry benchmarks.

The following table shows the measured and calculated $\Delta\rho$ obtained when unloading in position 64 (see figure 1): (1) the cylinder number 1, (2) the four cylinders and (3) the box equipped with the 4 cylinders.

Removed devices	Measured $\Delta\rho$ (pcm)	2D Operation calculation - $\Delta\rho$ (pcm)	3D Reference calculation - $\Delta\rho$ (pcm)
1 Cylinder (number 1)	15 \pm 10 (1 σ)	40	28
4 Cylinders	252 \pm 10 (1 σ)	518	264
4 Cylinders + Box	49 \pm 10 (1 σ)	95	Not calculated

When removing 1 or 4 cylinders, the increase in the core reactivity is explained by the increase in the neutron moderation since the volume initially occupied by Aluminium is filled with water. At this stage the reactor is sub-moderated. When removing the box (+4 cylinders), the decrease in the core reactivity is explained by the increase in the capture of neutrons since, locally, the reactor has reached an over-moderated configuration. We observe a good correlation between the experimental and the calculated values of $\Delta\rho$, especially for the 3D reference calculation which is less conservative than the 2D operation calculation. Thus simple experiments carried out on ISIS reactor can be used to illustrate and validate neutron calculations made by the trainees.

6. Conclusion

Today, E&T represent the major activity of the ISIS Research Reactor. The training courses are integrated both in academic and vocational programs. The feedback obtained from the trainee's shows that hands-on experience on a research reactor has an invaluable impact on the trainees and ensures comprehensive understanding of the reactor principle and operation that cannot be gained only with theoretical courses associated with the use of simulators. Thus the INSTN is continuously promoting the use of the training courses on ISIS reactor in its E&T programs as they appear to be a very powerful tool for the development of the human resources needed by the nuclear industry and the nuclear programs.

7. References

[1] "The OSIRIS Reactor", CEA/Saclay Center.
http://den-dans.extra.cea.fr/en/Phoce/Vie_des_labos/Ast/ast_ssttheme.php?id_ast=66

[2] "Overview of TRIPOLI-4 version-7 Continuous-energy Monte Carlo Transport Code," Trama J.-C., Malvagi F., Petit O., Hugot F.X., Lee Y.K., Huot N., Dumonteil E., Zoia A., Brun E., Mazzolo A., International Congress on Advances in Nuclear Power Plants 2011 (ICAPP 2011), Nice, France, May 2-5, 2011.

MULTIDISCIPLINARY NUCLEAR SCIENCE AND ENGINEERING RESEARCH AND EDUCATION AT THE PENN STATE UNIVERSITY RADIATION SCIENCE AND ENGINEERING CENTER

K. ÜNLÜ

*Radiation Science and Engineering Center, Pennsylvania State University
University Park, PA 16802 - USA*

ABSTRACT

The Radiation Science and Engineering Center (RSEC) facilities at the Pennsylvania State University include the Penn State Breazeale Reactor (PSBR), gamma irradiation laboratories (In-pool Irradiator, Dry Irradiator, and Hot Cells), Radioanalytical Applications Laboratory, Neutron Beam Laboratory, Graphite Pile Laboratory, Radiochemistry Teaching Laboratory and various radiation detection and measurement laboratories. The PSBR, which first went critical in 1955, is the longest continuously operating university research reactor in the United States. The PSBR is a 1 MW, TRIGA with moveable core in a large pool and with pulsing capabilities. The RSEC facilities are heavily used for nuclear science and engineering research and education. Examples of innovative applications of neutron beam techniques for multidisciplinary nuclear science and engineering research at the RSEC will be presented.

Penn State offers undergraduate and graduate programs in nuclear science and engineering. Currently, 245 junior and senior undergraduate and 59 graduate students are enrolled in the Nuclear Engineering Program. Additionally approximately 90 graduate students are taking nuclear engineering courses for the MSc. degree program through the PSU World Campus. Several laboratory classes are held in the RSEC. A brief discussion of the educational programs at the RSEC, especially a new nuclear security education program, will also be presented.

1. Introduction

The Penn State Breazeale Reactor (PSBR) at the Radiation Science and Engineering Center (RSEC) is a 1 MW TRIGA Mark III reactor with pulsing capabilities. The moveable core at PSBR has no fixed reflector and is located in a 24 ft deep pool with ~71,000 gallons of demineralized water. A variety of dry tubes and fixtures are available in or near the core for irradiations. When the reactor core is placed next to the D₂O tank and graphite reflector assembly near the beam port locations, thermal neutron beams become available. In steady state operation at 1 MW, the thermal neutron flux is 1×10^{13} n/cm²sec at the edge of the core and 3×10^{13} n/cm²sec at the central thimble. The peak flux during a maximum pulse is $\sim 6 \times 10^{16}$ n/cm²sec with a pulse half width of ~10 msec.

The PSBR, the centerpiece of the RSEC, first went critical in 1955 and is the longest continuously operating university research reactor in the United States. The Nuclear Regulatory Commission renewed the PSBR's license for an additional 20 years in November 2009. A significant redesign of the core-moderator/beam port is currently underway to make full use of the PSBR's capabilities and to establish state-of-the-art neutron beam facilities.

2. Multidisciplinary Research at the Radiation Science and Engineering Center

Some recent research projects that utilize the neutron beam laboratory at the RSEC are listed below. Most of these are multidisciplinary in nature and involve other faculty members and graduate students from within the college of engineering, other colleges, other universities, national laboratories, and industry. The projects include: Neutron-Induced Soft Error Rate Measurements of Semiconductor Memories; Soft Error Analysis Toolset Development; Time-of-Flight Neutron Depth Profiling; Study of Water Distribution and Transport in a Polymer Electrolyte Fuel Cell Using Neutron Imaging; Neutron Imaging System Improvements; Neutron Transmission Measurements and Neutron Radioscopy for Borated Metals and other Borated Materials; Neutron Intercepting Semiconductor Chip Development; Neutron Beam Characterization with Neutron Chopper; Neutron Beam Modeling; Cold Neutron Source Design; and Fission Track Analysis. In addition to neutron beam laboratory activities several projects related to Neutron Activation Analysis and Thermal and Fast Neutron Irradiation continue at the RSEC. Brief descriptions of two research projects and key publication lists are given below.

2.1 Neutron-Induced Soft Error Rate (SER) Measurements of Semiconductor Memories

Soft errors are transient circuit errors caused due to excess charge carriers induced primarily by external radiation. Radiation directly or indirectly induces localized ionization that can flip the internal values of the memory cells. Our current study tries to characterize the soft error susceptibility for different memory chips working at different technology nodes and operating voltages. This study intends to observe the effect of ^{10}B and thermal neutrons on soft error rate. The PSBR is used as the neutron source in experiments in order to investigate the effect of ^{10}B on SER. The experimental setup consists of a custom circuit board interfaced with a computer through a GPIB card (Fig 1). The board has off-the-shelf SRAM memory chips and is controlled through a LabVIEW interface. The controlling application consists of simple routines to read and write a user-specified value across all of the memory. During the readout, it compares the written value to the value in each address. The circuit board is secured in the beam cave and connected to a PC outside using a 25-ft cable. This configuration allows for continuous read-write and for changing the operating conditions without interrupting the experiment.

The setup described above allows for accelerated testing of semiconductor memory devices with thermal neutrons. Different memories (16-kbit and 4-Mbit) from several vendors were evaluated at various supply voltages and reactor power levels. Linear increases in the SER were observed for corresponding decreases in voltage. For examining the statistical accuracy of the accelerated tests, they were performed at various reactor power levels. Since reactor power and flux at the exit of the beam port are directly correlated, changing the reactor power effectively changes the neutron flux impinging on the test sample; hence the SER is expected to increase. It has been verified that the SER increases as the reactor power increases. This multidisciplinary research involves faculty members and graduate students from nuclear engineering, computer science and engineering, and scientists from AMD/Spansion/Cerium laboratories. Further measurements and analysis results were published, and key publications are given in References [1,2].

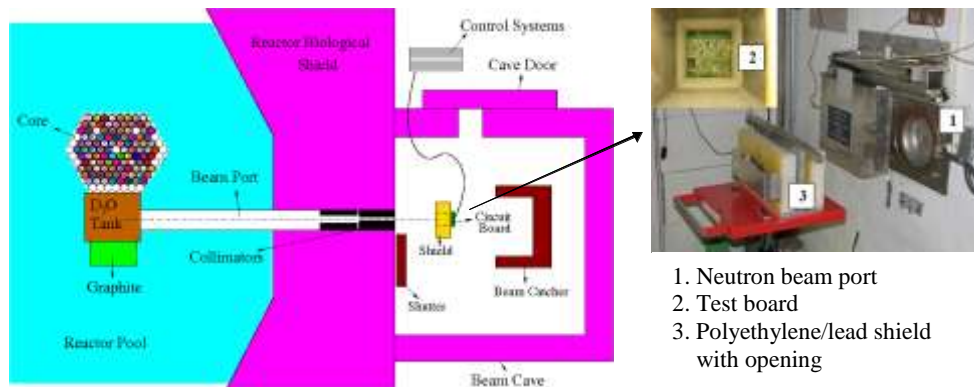


Fig 1. (Left) Simplified layout of the test board, (Right) test chip placed in front of the beam tube with the polyethylene/lead shield for thermal neutron testing.

2.2 Time-of-Flight (TOF) Neutron Depth Profiling

Neutron depth profiling (NDP) is a near-surface analysis technique to measure the spatial distribution of certain light isotopes of technological importance in substrates with low neutron affinity. Upon neutron absorption, certain light isotopes emit a charged particle, either a proton or alpha particle depending on the isotope, and a recoil nucleus. The particle emission is monoenergetic and isotropic. As the charged particle and the recoil move in the substrate, they lose kinetic energy through nuclear and coulombic interactions with host atoms. The amount of energy lost can then be correlated to the distance traveled by the particles, which is an indication of the depth at which the particles are created. Conventional NDP is based on the direct measurement of particle energies by charged particle detectors, mostly by silicon surface barrier detectors, passivated implanted planar silicon (PIPS) detectors or PIN photodiodes. A picture of the RSEC conventional NDP setup is shown in Fig 2. Conventional NDP has been used extensively for obtaining the depth profile of light elements in various fields. However, in tandem with the advances in scientific and technological applications, depth profiling with higher resolutions has become a necessity. Neutron depth profiling has reached the limits of resolution that can be attained by conventional techniques, limited by the use of charged particle semiconductor detectors. This limitation can be overcome, however, through a technique called time-of-flight neutron depth profiling (TOF-NDP). TOF-NDP eliminates the semiconductor detector and employs microchannel plates (MCP) for particle detection in time-of-flight configuration (Fig 3). Figures 4 and 5 illustrate the results of an NDP experiment performed with an Intel wafer with borophosphosilicate glass at the RSEC. Note that the measured particle energy carries information about the distance alpha particles traveled in the matrix before they hit the surface of the detector, i.e., the more energy they have the closer they are to the surface. Our preliminary measurements with TOF NDP indicates that it will provide up to a five times better resolution than the conventional NDP, which will make the depth-vs-concentration measurements of ultra shallow junction devices possible. This improvement will have a significant impact on the silicon industry as the dimensions of micro devices decreases. This multidisciplinary research involves faculty members and graduate students from nuclear engineering, as well as scientists from the Advanced Micro Devices/Cerium

Laboratory and NIST. Further measurements and analysis results were published and key publications are given in References [3,4].



Fig 2. Conventional NDP setup at the RSEC neutron beam laboratory.

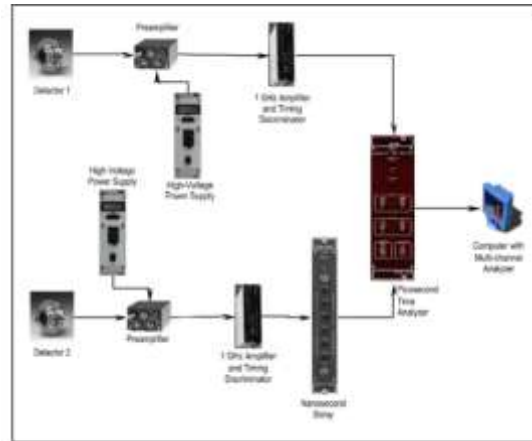


Fig 3. Equipment block diagram of TOF-NDP at RSEC neutron beam laboratory.

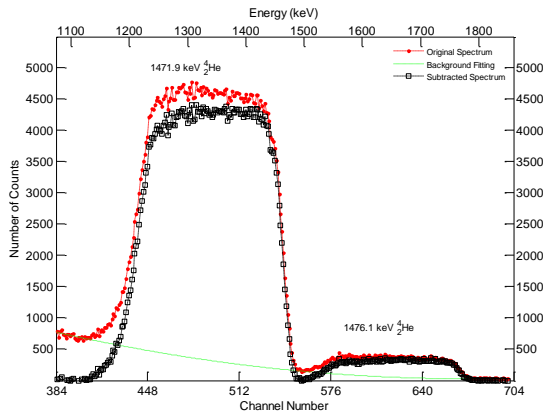


Fig 4. Alpha peaks from the $^{10}\text{B}(n,\alpha)^7\text{Li}$ reaction in Intel SAE2 BPSG wafer.

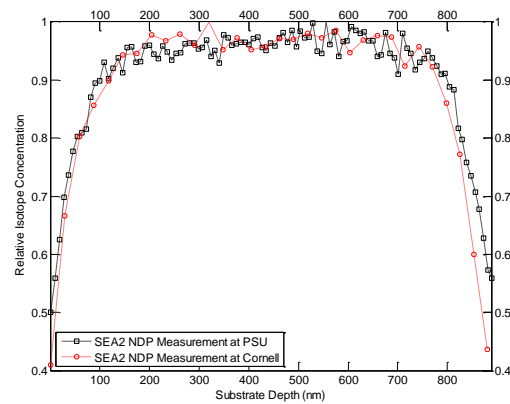


Fig 5. NDP measurements of Intel SEA2 BPSG sample; comparison of NDP done at Penn State and Cornell.

3. Nuclear Science and Engineering Education Programs at Penn State

The Penn State Nuclear Engineering Program is one of the leaders in nuclear science and engineering education in the United States. Our program is consistently ranked as one of the top five programs in the USA. This is mostly due to our reputation in graduate and undergraduate studies. Currently, 245 junior and senior undergraduate and 59 graduate students are enrolled in the Nuclear Engineering Program. Additionally, approximately 90 graduate students are taking nuclear engineering courses for the MSc. degree program through the PSU World Campus. Within PSU's nuclear science and engineering curriculum, several laboratory classes are held at the RSEC. These courses include, the radiation measurements and detection laboratory, radiochemistry laboratory, reactor physics laboratory, reactor operation and testing, and nuclear reactor core design synthesis. Typically about 30 faculty and staff members, 40 graduate students and over

250 undergraduate students use the RSEC facilities for education, research and service activities every year. These numbers represent a usage by 17 departments and/or programs in four colleges at Penn State. About 60 individuals from 23 different industries and research organizations, and other universities use the RSEC facilities yearly. In addition, the continuing education program and tours accommodate over 3,000 visitors per year.

Additionally, the PSU is currently working collaboratively with the Massachusetts Institute of Technology (MIT), and Texas A&M University (TAMU) on the development and implementation of the US National Nuclear Security Administration (NNSA), Global Nuclear Reduction Initiatives (GTRI), nuclear security education curriculum. The GTRI helps achieve the US Department of Energy's nuclear security goal to prevent the acquisition of illicit radioactive material for use in weapons of mass destruction (WMD) and other acts of terrorism. This organization has recognized a national need for university-level nuclear security education. To achieve this goal PSU, MIT and TAMU are contracted to develop a comprehensive nuclear security program within these universities. The development and pilot teaching of these courses are underway and they will be fully integrated within all three universities by 2014.

4. Summary

The Penn State Nuclear Engineering Program is one of the leaders in nuclear science and engineering research and education in the United States. Redesign and implementation of the core-moderator assembly, five new beam ports with a cold neutron source is currently underway. New beam ports would be geometrically aligned with the core-moderator assembly for optimum neutron output. The research areas envisioned for the RSEC's new neutron beam port/beam facility are for mostly cutting-edge nuclear and materials science research. Some examples include: a Mesitylene-based Cold Neutron Source and Cold Neutron Prompt Gamma Activation Analysis for neutron focusing research, materials characterization and determination of impurities in historically or technologically important materials; a Neutron Powder Diffractometer for structural determination of materials; and a Triple Axis Diffractometer to train students on neutron diffraction and perform preliminary structural determinations of materials. In addition to our research programs, Penn State offers undergraduate and graduate programs in nuclear science and engineering. Several laboratory classes held in the RSEC. PSU is currently working collaboratively with TAMU and MIT on the development and implementation of the National Nuclear Security Administration Nuclear Security Education curriculum.

5. References

- [1]. R. RAMARANAYARAN, V. DEGALAHAL, R. KRISHNAN, J. S. KIM, V. NARAYANAN, Y. XIE, M. J. IRWIN, K. ÜNLÜ, "Modeling Soft Errors at Device and Logic Level for Combinational Circuits," IEEE Transactions on Dependable and Secure Computing, 24, Sept 2007.
- [2]. K. ÜNLÜ, N. VIJAYKRISHNAN, S. M. ÇETINER, V. DEGALAHAL, M. J. IRWIN, "Neutron-Induced Soft Error Rate Measurements in Semiconductor Memory," Nucl. Instr. and Meth. A (2007).
- [3]. S.M. CETINER, K. ÜNLÜ, G.DOWNING, "Development and Applications of Time-of-Flight Neutron Depth Profiling," Journal of Radioanalytical and Nuclear Chemistry, Vol. 276, No. 3 (2008).

[4]. S. M. ÇETİNER, K. ÜNLÜ, "Depth profiling of boron in ultra-shallow junction devices using Time-of-Flight Neutron Depth Profiling (TOF-NDP)," Nucl. Instr. and Meth. A (2007).

DESIGN IMPROVEMENT OF IN-PILE TEST SECTION FOR PRESSURIZED WATER LOOP IN HANARO

J.T. HONG, H.Y. JEONG, S.H. AHN, C.Y. JOUNG, B.S. SIM, J.M. LEE

*Department of Research Reactor Utilization, KAERI
Daedeok-daero 989-111, Yuseong-gu Daejeon – Republic of Korea*

ABSTRACT

The Fuel Test Loop (FTL) established at HANARO (High-flux Advanced Neutron Application Reactor) is a pressurized water loop used to carry out fuel and material irradiation tests in steady-state operating conditions of a PWR and CANDU. The FTL is composed of an OPS (Out Pile System) and IPS (In-Pile test Section). The OPS includes several process systems such as the main cooling water system, emergency cooling water system, penetration cooling water system, letdown, makeup and purification system, waste storage and transfer system, intermediate cooling water system, sampling system, etc. The IPS including the test fuels is to be loaded into the IR-1 position in the HANARO core. The IPS can accommodate the maximum 3 pins of PWR fuel and has instruments such as a thermocouple, LVDT, and SPND to measure a fuel's performance during a test. The FTL coolant is supplied to the IPS at the required temperature, pressure and flow conditions that are consistent with the test fuel. The nuclear heat generated within the IPS is removed by the main circulating coolant.

In this paper, the design improvement of the IPS used for the fuel irradiation is introduced. The design improvement is performed in consideration of the experimental results of the PWR fuel irradiation during the FTL commissioning stage. The design for the safe withdrawal of the test rig from outer pressure vessel, and the design for an improvement of the workability of the sealing process are improved. The experimental results with mock-up devices for the design improvement are introduced. The improved design will be used as a standard design of the IPS in HANARO.

1. Introduction

HANARO (High-flux Advanced Neutron Application Reactor) in KAERI has a pressurized water loop called a Fuel Test Loop (FTL), which consists of an in-pile test section (IPS) and an out-pile system (OPS).

The OPS controls the test condition in the IPS such as pressure, temperature, and quality of the main cooling water. The OPS consists of a process system and an I&C (Instrumentation and Control) system. The process system includes the main cooling water (MCW) system, emergency cooling water (ECW) system, penetration cooling water (PCW) system, letdown, makeup and purification (LMP) system, waste storage and transfer (WST) system, intermediate cooling water (ICW) system, test loop sampling system, and IPS inter-space gas filling and monitoring system. The process system manages the operation of the cooling system such as the normal and emergent circulation of the coolant, the control of temperature, pressure and flow condition of the coolant, and the control of the volume, purification, and chemical quality of the coolant. The I&C system includes a safety control system and a non-safety control system. It manages process systems related with safety, shut down of the HANARO at the abnormal operating condition and acquisition & storage of data signals from the sensors installed in the IPS.

The IPS is located in the IR-1 irradiation hole of the HANARO core to test the neutron irradiation characteristics and the thermal hydraulic characteristics of the nuclear fuel under the same condition with the commercial nuclear power plant [1-3]. The IPS consists of the IPS

head, flow divider, test fuel carrier, and double pressure vessel. The inlet and outlet of cooling water are connected with the IPS head, and the flow of cooling water is divided by the flow divider. The test fuel carrier is a supporting structure, which has 3 fuel rod pins with several instruments such as a thermocouple, SPNDs, and a LVDT to measure the temperature, pressure, and neutron flux. The double insulated pressure vessel filled with neon gas insulates the IPS from the HANARO pool.

Based on the experimental report of the irradiation test of high burn-up PWR fuels at HANARO, it needs to change some designs of the IPS to safely withdraw the test fuel carrier from the pressure vessel and to improve the workability of the sealing process. Therefore, the mechanical design change of the IPS has been considered and passed the verification test using a mock up. The changed design will be used as a standard design of the IPS in HANARO.

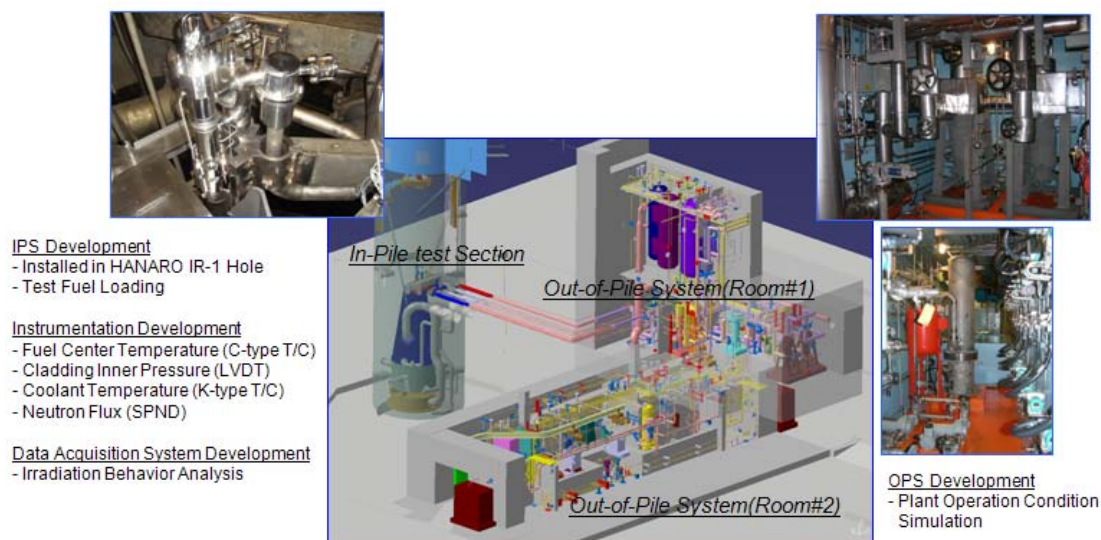


Fig 1. Fuel Test Loop in HANARO

2. Safe withdrawal mechanism

Because, coolant with high pressure and temperature is circulated in the IPS, all components of the IPS should have sealing structures. Therefore, it is not easy to disassemble the test fuel carrier from the pressure vessel due to the resistant pressure of the sealing components. In addition, the sealing components can cause transient status by releasing from each other. In particular, a big shock is generated due to the sealing components during the withdrawing process of the inner assembly from the pressure vessel as shown in Fig 2. Fig 3 shows a sectional view of the IPS head part. As shown in Fig 3, O-rings are installed at the pressure boundary between the inner assembly and the pressure vessel to seal the coolant while running the test rig. The O-rings generate resistance friction force when withdrawing force is induced on top of the inner assembly. Then, the inner assembly is rapidly withdrawn when the friction force of the O-ring disappears by detaching from the surface of the pressure vessel. At that moment, a big shock accompanying a certain sound is generated due to the pressure difference between the internal region of the IPS and the pool of HANARO. Because HANARO is an open-pool type reactor, there are some potential problems. First, the sudden withdrawal of the inner assembly generates bubbles in the pool. Also, the uncontrolled movement can damage the test rig and fuel pin. In a worst case, it can damage the reactor components, or the coolant can be spouted out. Therefore, equipment or a structure that compensates the shock generated by the pressure difference is needed.

As shown in Fig 4, two jacking bolts are added on the top flange part of the inner assembly to compensate the shock. When withdrawing the inner assembly from the pressure vessel, after loosening the six fastening bolts, the jacking bolts are fastened alternately. The inner assembly is

then smoothly withdrawn from the pressure vessel guided by the jacking bolts so as not to move abruptly.

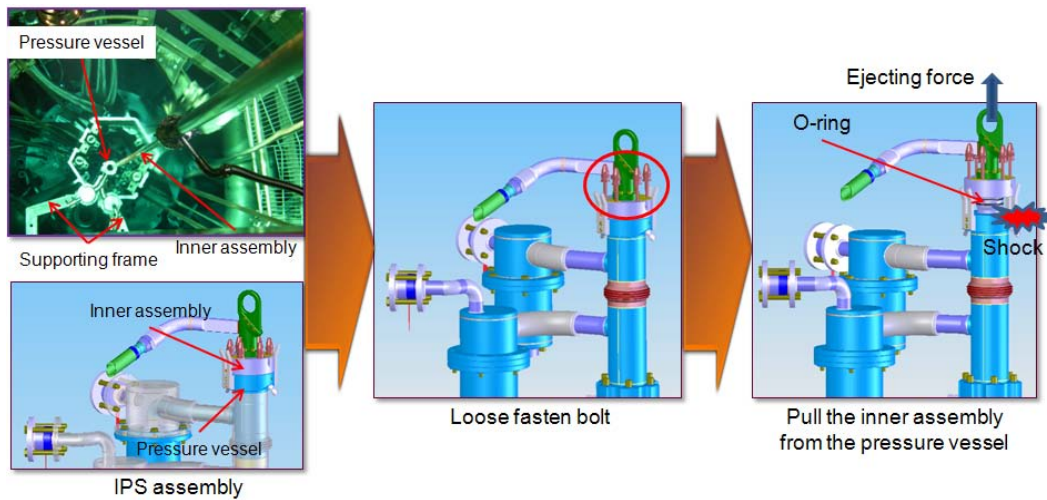


Fig 2. Withdrawal process of the inner assembly from the pressure vessel

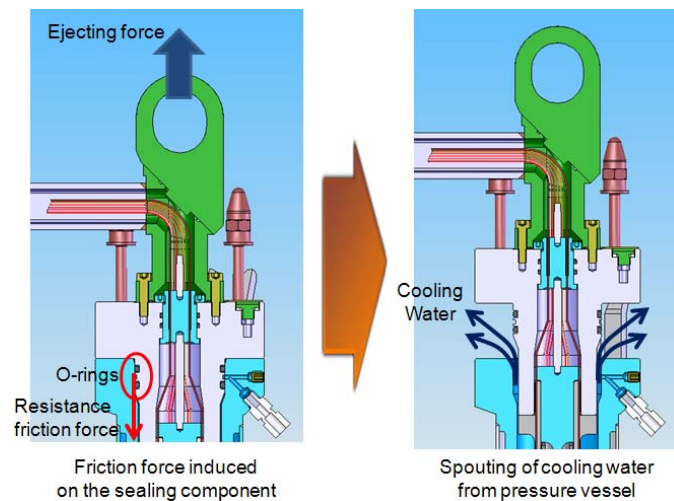


Fig 3. Section view of the sealing part of IPS

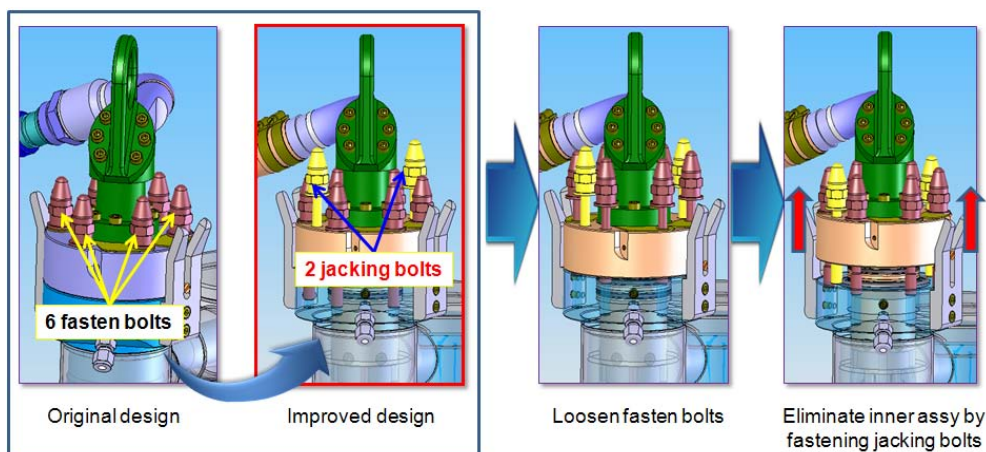


Fig 4. Operating mechanism of jacking bolts

As shown in Fig 5, an withdrawal experiment of the inner assembly has been carried out at HANARO with mock up equipment made with an improved design. During the test, there was no shock or noise from the sealing components. Therefore, it is verified that adding two jacking bolts works well to decrease the shock induced on the IPS.

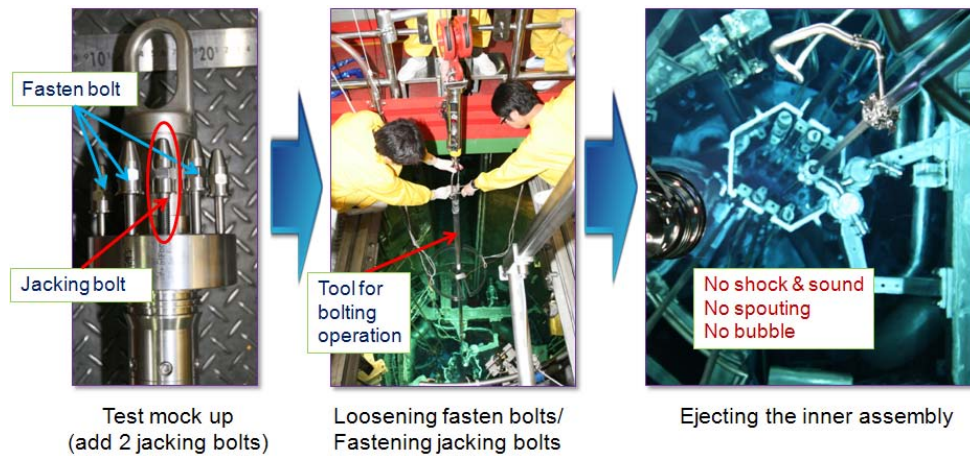


Fig 5. Withdrawal experiment of the inner assembly at HANARO

3. Mechanical sealing of instrumentation feedthrough

For instant measurement of the fuel performance during the irradiation test, 15 sensors such as thermocouples, LVDTs, and SPNDs are installed in the IPS. The sensors detect signals from the fuel rod and deliver them to the measuring device located in the outside of the IPS through MI cables (Diameter 1.0mm, Length 1600mm). Therefore, MI cables pass through the pressure boundary and need to be sealed out. Because the sheath of an MI cable has a 0.08mm thickness and made of AISI 316L, it is general to use a brazing process as a sealing method [4]. As shown in Fig 6, the brazing process of the instrumentation feedthrough part consists of three steps: protection of the inner assembly in the protection module, lifting of the module upside down, and a brazing process. However, because the inner assembly is 5290mm long, it is too difficult and time consuming to prepare for the brazing process. In addition, the brazing process is irreversible, and the whole inner assembly should be scrapped out if the brazing process fails in sealing or if the MI cables are damaged. Then, the cost becomes double. Therefore, a mechanical sealing method that can replace the brazing process is considered.

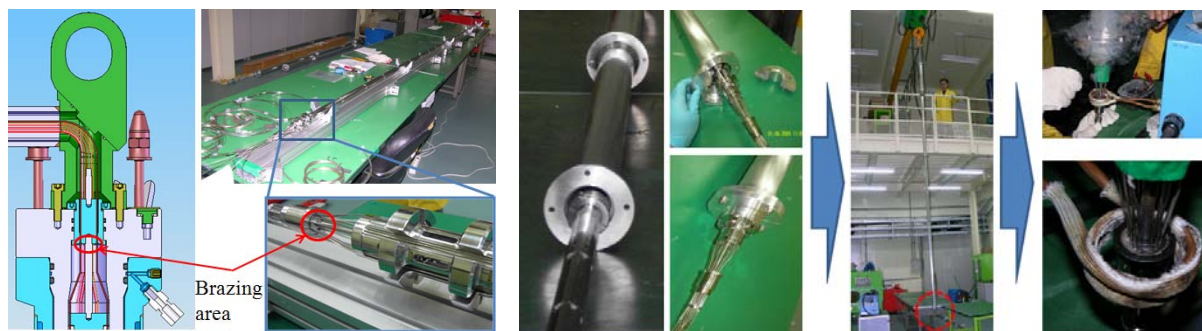


Fig 6. Brazing area of the inner assembly and brazing process

3.1 Preliminary test of graphite sealant

Generally, graphite is broadly used as a sealing material due to its compressibility and high sealing performance. If it is possible to use in sealing the feedthrough part of the test rig, it can simplify the whole assembly process and increase the reliability of sealing due to its reworkability. To check the sealing performance of graphite, a simple test mockup was made by welding the top flange with a sealing plug (M32x2) as shown in Fig 7. When compressive stress is induced on the graphite by adding the fastening torque on the sealing plug, the graphite is deformed and seals out the pressure boundary.

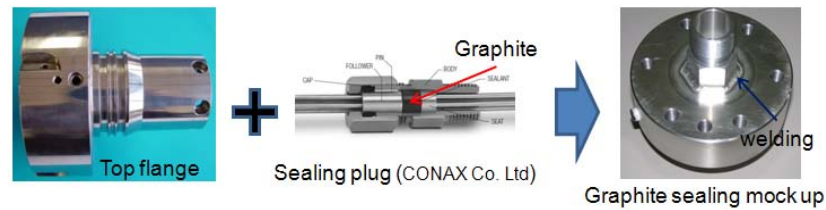


Fig 7. A test mockup of mechanical sealing

According to ASME section III and section V, it is necessary to pass the sealing criteria such as a hydraulic pressure test and helium leak test. Because the design condition of the IPS is 17.5MPa and 350°C, it should endure more than 22.5MPa (125% of design pressure) of hydraulic pressure and detect less than 5×10^{-9} torr · liter / sec (more conservative criteria than that of the ASME code) of helium detection ratio [5,6].

To check the sealing performance of the mockup, test devices for a hydraulic pressure test and helium leak test were developed. As shown in Fig 8, the hydraulic pressure should be induced by a manual pump and helium is detected by using the ASM310.

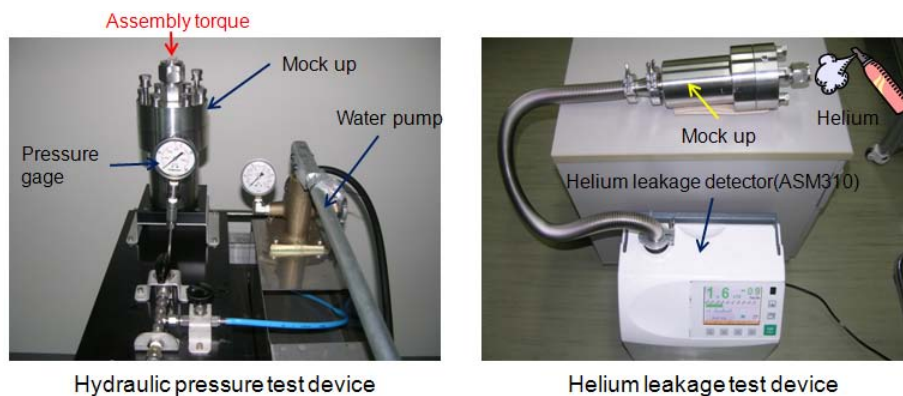


Fig 8. Equipment for sealing performance test

The sealing performance was checked while increasing the assembly torque. As a result, it satisfied the hydraulic sealing criterion (no pressure drop, no leakage) above 183 N·m of the assembly torque.

A helium leakage test was carried out to check whether helium gas passes through the graphite sealant at 1×10^{-3} torr of the vacuum state. When spraying helium gas at one side of the vessel, if a helium detector (ASM310) connected with the opposite side of the vessel indicates a helium gas of more than 5×10^{-9} torr · liter / sec, it fails the helium leak test. As a result, when graphite is compressed at more than 237 N·m of the assembly torque, it passes the helium leak test.

From the above preliminary test result, it is verified that the graphite can have sufficient sealing performance in the test rig above a certain compressive force.

3.2 Design modification of the IPS

Based on the preliminary test results, the design of the instrumentation feedthrough part is modified as shown in Fig 9. From the original brazing type design, the internal design of the top flange and the sealing plug are changed to fit to the graphite seal. In addition, supporting components including a guide pin were removed and two components such as a sealing piston and a bottom piece were added to deliver compressive force on the graphite. A testing mockup was fabricated with the modified design. Then, sealing process will be as follows:

First, a bottom piece which instrumentation cables are passed through is placed on the internal basis of the top flange. Second, a certain amount of flake graphite is put on the bottom piece using a funnel. Third, a sealing piston which instrumentation cables are passed through is placed on top of the flake graphite. Fourth, compressive stress is induced on the graphite by fastening the pressure plug contacted on top of the sealing piston. Fifth, repeat the above

process from the first because packing volume to seal out is not enough with a single process. Using the test mockup, sealing experiment is being carried out.

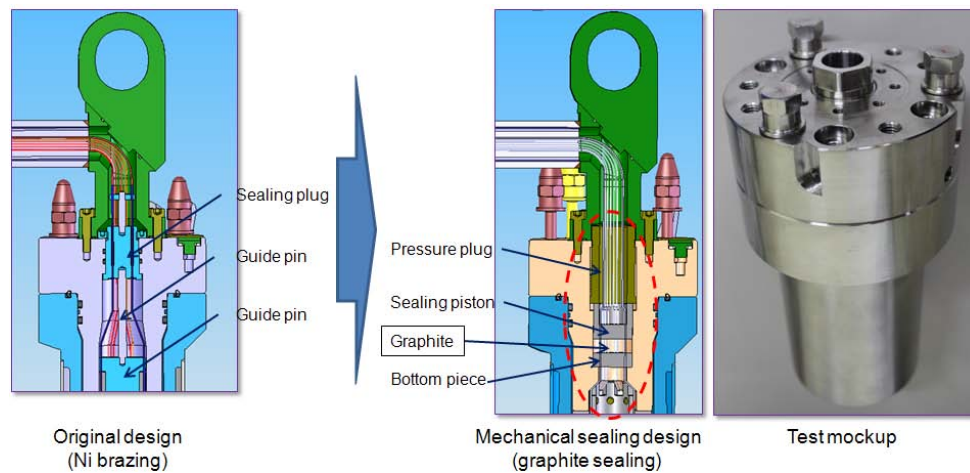


Fig 9. Design change of instrumentation feedthrough part and its mockup

4. Conclusion

In this study, the design modification of the inner assembly part of the IPS has been carried out to improve the safety and working efficiency. First, two jacking bolts are added to the flange part of the inner assembly to decrease the shock generated while withdrawing the inner assembly. This helps the cooling water not spatter out of the pool and improves safety. Second, brazing at the feedthrough part of the instrumentation cables is replaced with a mechanical sealing design. Graphite is placed on the pressure boundary and compressed with a bolt-typed pressure plug to seal out the cooling water. A sealing performance test was carried out with a hydraulic pressure pump and helium leak detector. It satisfied all the design criteria in the preliminary test and a mockup test is being carried out. The modified design will be applied to make a new IPS to carry out an irradiation test at the loop.

5. References

Please number your references and cite them in brackets. The list of references should be at the very end of your manuscript under the section heading "References".

- [1] S. H. Ahn, et. al., Proc. of the 3rd International Symposium on Material Testing Reactors, (2010) Operation of fuel test loop for irradiation test of PWR fuels in HANARO.
- [2] S. H. Ahn, et. al., Proc. of the 2008 Water Reactor Fuel Performance Meeting, (2008) Fuel test loop in HANARO
- [3] S. H. Ahn, et. al., J. of the Korean Institute of Plant Engineering, (2010) Vol.15, No.3, 99-105
- [4] G. Srinivasan, et. al., J. Mater. Process. Technol., (2008) Vol.198, 73-76
- [5] ASME Boiler and pressure vessel code, Sec III, "Testing", Subsection NB-6000, 2003
- [6] ASME Boiler and pressure vessel code, Section V, "Non Destructive Examination," Subsection V-1080, 2003

THE IN-CORE EXPERIMENTAL PROGRAMME AT THE MIT RESEARCH REACTOR

G.E. KOHSE, L-W. HU

*Nuclear Reactor Laboratory, Massachusetts Institute of Technology
138 Albany St., Cambridge, MA 02139 – USA*

ABSTRACT

The MIT Research Reactor (MITR) is owned and operated by MIT and is now licensed and operating at 6 MW, uprated from the original 5 MW. The reactor power density and spectrum are similar to those in typical light water power reactors. This makes the MITR an extremely useful test bed for a wide range of materials and fuels research in support of current generation and advanced power reactors. The in-core experimental programme currently utilizes three types of experimental facilities: a high temperature water loop that can be operated at pressurized water reactor (PWR) or boiling water reactor (BWR) conditions, a flexible, general purpose in-core irradiation space for inert gas environment irradiations at temperatures up to 900 °C, (in-core sample assembly – ICSA) and an experimental fuel irradiation facility. In addition to these currently operating facilities (which fully utilize the available in-core experimental space), a very high temperature irradiation facility (HTIF) for irradiations in the range of 1200-1400 °C has been demonstrated. A new irradiation is planned for this facility during the next year.

The pressurized water loop is currently operating under PWR conditions for on-going tests of SiC/SiC composite tubing that has been proposed as a replacement for Zircaloy™ cladding material for commercial PWR and BWR service. Twenty to thirty 10-cm long tube samples can be tested in the in-core space. Post-irradiation examination (PIE) includes weight loss measurements, visual inspections, SEM, thermal diffusivity measurements and burst tests for mechanical property evaluation. Non-destructive PIE can be performed at intervals with samples returned to the reactor for further exposure. The longest exposed specimens currently operating in the reactor have approximately three years of full-power equivalent exposure. An irradiation of MAX phases materials was recently completed in the ICSA facility. PIE is currently underway at Savannah River National Laboratory. A test to assess the irradiation performance of liquid-metal-bonded zirconium hydride fuel is in progress in the fuel irradiation facility. The samples are instrumented with centerline and clad thermocouples for real time evaluation of fuel thermal conductivity and periodic cover gas sampling is used to assess fission gas release and detect clad failure.

1. Introduction

The Massachusetts Institute of Technology (MIT) Research Reactor (MITR) is a 6 MW, tank-type reactor operated by the interdepartmental Nuclear Reactor Laboratory (NRL). The reactor is located on the MIT campus in Cambridge, Massachusetts, USA. It is the second research reactor to operate at the site and achieved first criticality in 1974. The power was recently uprated from the original 5 MW license after replacement of cooling towers and the primary heat exchanger to accommodate the increased power level. Activities at the reactor include teaching and training, medical irradiations, neutron activation analysis, neutron imaging and beam optics experiments and a very active program in materials and fuels development using a variety of in-core experimental facilities. An overview of the

experiments recently completed or currently underway in this in-core program is the focus of this paper.

The MITR is a very useful test bed for this type of experimentation due to the similarity of the in-core flux and spectrum to those of typical light water power reactors. In-core facilities typically have peak thermal flux of $2\text{--}3 \times 10^{13} \text{ n/cm}^2\text{-s}$ and peak fast flux of up to $10^{14} \text{ n/cm}^2\text{-s}$, $E > 0.1 \text{ MeV}$. There are twenty-seven fuel element positions of which three are available for installation of in-core experiments as shown in the photograph presented in Figure 1. The top of the core shown in Figure 1 is approximately 3 m below the surface of the coolant surface and 3.5 m below the reactor lid upper surface. Connections to in-core experiments are typically made through the lid or the upper section of the core tank, which is approximately 2 m in diameter. The area adjacent to the upper core tank is accessible even during full power reactor operation, facilitating the operation and maintenance of in-core facilities. A wide variety of experiments has been performed in these facilities. This paper discusses three facilities that are in current or near-term future use: a pressurized water loop, a general purpose inert gas irradiation facility that can operate up to 900°C , and a fuel test facility for irradiation of instrumented rodlets of liquid-metal-bonded zirconium hydride fuel. In each case the facility is briefly described followed by presentation of an experiment utilizing the facility.

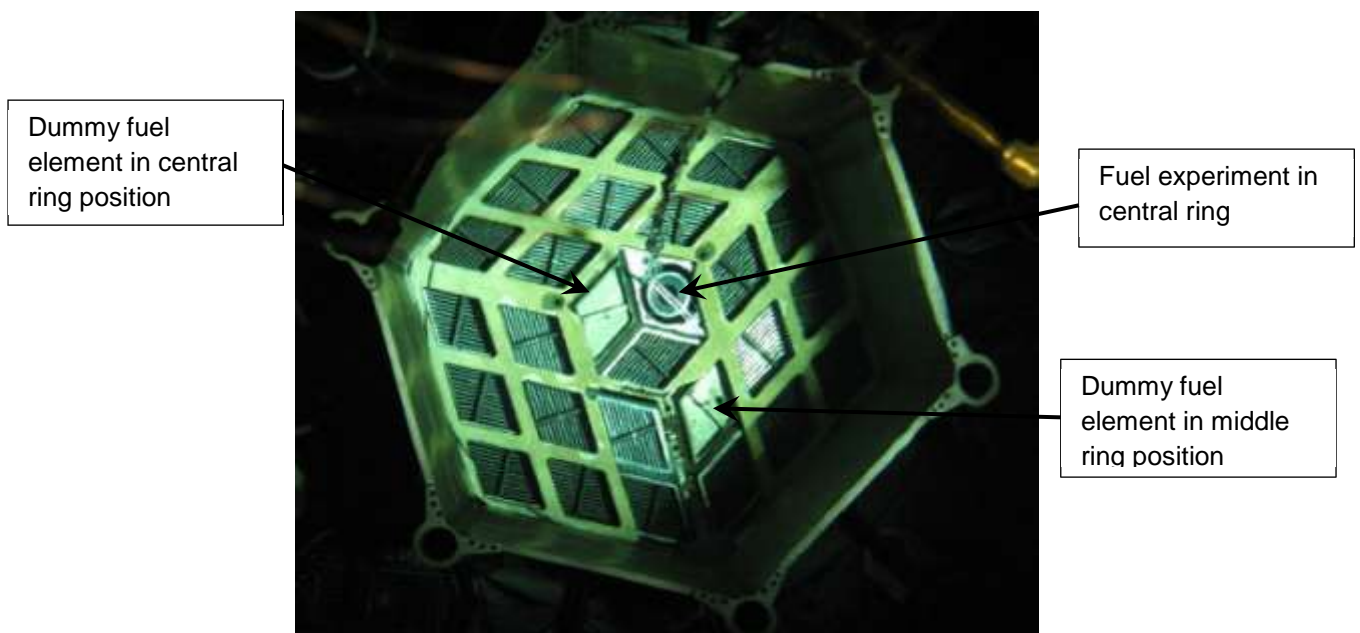


Figure 1. A photograph showing the MITR core with a fuel experiment installed and the other two in-core experimental positions occupied by solid dummy elements as indicated.

2. Pressurized water loop

Water loops at conditions representative of both pressurized water reactors (PWRs) and boiling water reactors (BWRs) have been operated in the MITR for a variety of purposes since the late 1980s. The loop currently installed and in use operates at temperatures up to 300°C and pressure sufficient to prevent boiling at any point in the loop. It is designed for in-core exposure of material samples and is currently being run at PWR chemistry conditions (hydrogen overpressure, boric acid and lithium hydroxide added). The loop is installed through the reactor core tank lid into a dedicated dummy fuel element that positions it in the reactor core. It consists of an outer aluminium containment tube with a gas-filled gap to

thermally isolate the high-temperature and pressure titanium autoclave. An external flow loop outside the reactor core tank consisting of a circulating pump and heater provides high temperature coolant which circulates over the samples positioned in core (see below for a typical set of samples and fixturing). Coolant chemistry is maintained by let-down of a fraction of the coolant to a clean-up and control system. Coolant temperatures and pressures, reactor power and coolant chemistry parameters such as dissolved gas content are monitored and logged.

This system has been in use for several years for on-going tests of SiC/SiC composite tubing that has been proposed as a replacement for Zircaloy™ cladding material for PWR and BWR service. Typical fixturing used to position tube samples in core is shown in Figure 2. Several capsules such as those shown are typically installed in the in-core section of the autoclave, which is approximately 4 cm in inside diameter with about 50 cm of active core height. Sample modules have also been installed above core to allow direct comparison between irradiated and unirradiated samples exposed in otherwise identical conditions. Twenty to thirty tube specimens can be exposed simultaneously in core and the samples can be removed from the reactor periodically for examination and then returned for further exposure. Samples to investigate the viability of bonding methods for sealing fuelled rods in commercial application have also been irradiated. The modular capsule system is flexible in allowing samples of different sizes and geometries to be tested and permitting adjustment of the test matrix as material performance is determined or new materials become available.



Figure 2. SiC/SiC tube sample fixturing. On the left is a partially assembled capsule showing tube samples positioned over the holder tubes and flux monitor wires. An assembled capsule is shown on the right with a flow shroud in place over the specimens between the top and bottom spacers.

Extensive discussion of the results of these experiments is beyond the scope of this paper, but it should be noted that this work has contributed to the improvement of SiC/SiC composite tubes for cladding applications and the demonstration of viability of the best performing materials up to 2-3 years of accumulated exposure. Irradiation has been found to

affect corrosion rates, mechanical behaviour, and the survival of a number of proposed bond methods. Available post-irradiation examination (PIE) techniques include weight measurements, tube burst testing, xenon flash thermal diffusivity measurements and scanning electron microscopy on intact, sectioned and burst tested samples.

3. Controlled temperature inert gas irradiation facility

Like the loop facility, this facility is installed in core using a dedicated dummy fuel element. It consists primarily of a titanium tube of approximately 5 cm diameter that extends from the core position to the gas space at the top of the reactor core tank. The tube itself does not penetrate the core tank boundary but gas lines and thermocouples (and other types of instrumentation connections, if necessary) are fed through the upper section of the reactor core tank. The in-core sample assembly (ICSA) tube has an S-bend to prevent irradiation streaming. Samples are loaded and unloaded through the flanged upper closure of the ICSA and can be loaded from or unloaded into a shielded transfer cask if necessary. The current ICSA is designed for high temperature operation based on nuclear heating of the sample capsules and additional “susceptor” material (generally titanium) if necessary. By adjusting the capsule mass and the width of the gas gap between the sample capsules and the cooled thimble wall design temperatures ranging up to the approved maximum temperature of 900 °C can be achieved. By adjusting the proportions of helium and neon in the mixed cover gas temperature can be controlled over a range of several hundred degrees for typical capsules at full reactor power. This allows target temperatures to be adjusted to compensate for uncertainty in the thermal design and variations in reactor power. This is illustrated in Figure 3.

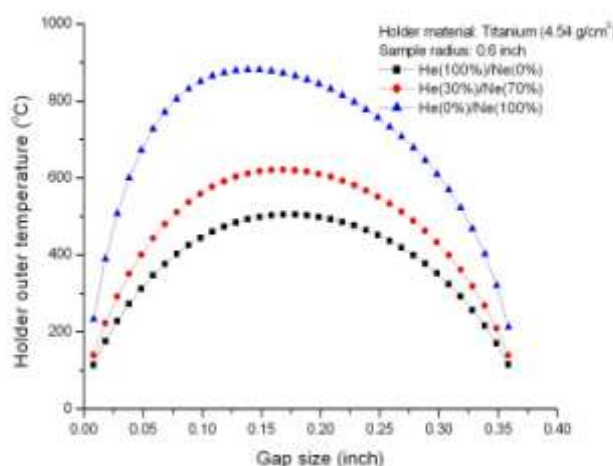


Figure 3. Calculated sample holder outer temperature for a range of gap sizes and helium/neon mixtures at a constant sample holder mass.

This system was used for a recently completed irradiation of a large number of samples of MAX phases materials. Three types of samples were irradiated: resistivity measurement bars, flat “dog-bone” tensile test samples and transmission electron microscopy disc samples. By adjusting the capsule masses and gas gaps two different irradiation temperatures (approximately 350 and 700 °C) were provided simultaneously. Post irradiation examination of these materials is on-going at Savannah River National Laboratory. The

facility will next be used for irradiation tests of fibre-optic sensors at temperatures between 500 and 800 °C.

4. Hydride fuel irradiation facility

As a research reactor, the MITR technical specifications do not allow irradiation of fuel in an independently cooled loop. A license amendment was obtained in 2004 to allow irradiation of up to 100 g of ^{235}U or equivalent in a facility that rejects heat passively to the reactor primary coolant, with the proviso that double encapsulation must be provided. To meet these requirements, while operating the test fuel at temperatures representative of a power reactor, the design shown in Figure 4 is used. The space between the titanium capsule and the rodlet cladding is filled with lead bismuth eutectic (LBE) to provide reliable thermal contact. The combined thermal resistance of the LBE gap and the titanium capsule is sufficient to raise the clad temperature to approximately 350 °C. Thermal design is based on MCNP calculations of the heat generation rate to meet goals for centreline temperature and clad temperature. The sample shown in Figure 4 has a thermal conductivity probe supplied by Idaho National Laboratory, other samples have centreline thermocouples and all samples have clad surface thermocouples for on-line thermal conductivity measurement. The cover gas is sampled periodically for fission gas content and the irradiation is stopped if levels rise above expected baseline values. Up to three rodlet capsules as shown can be installed in the in-core position, and they can be installed and removed independently.

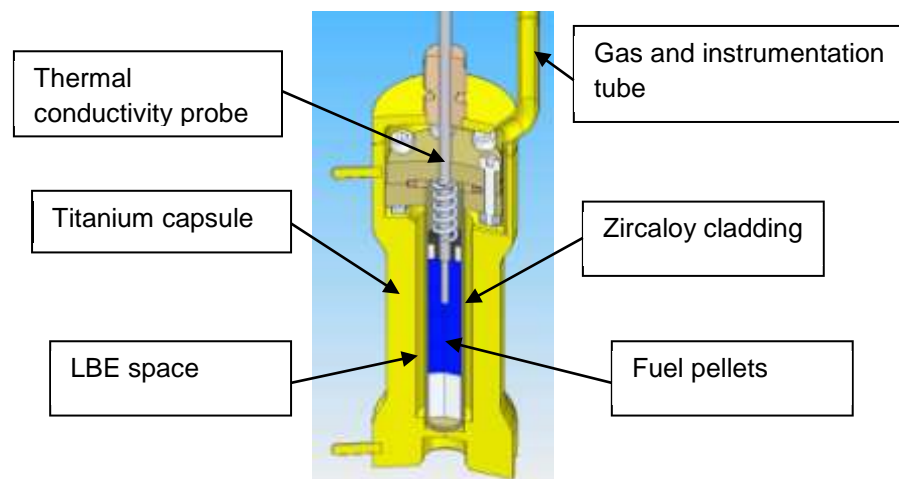


Figure 4. Cutaway view of the hydride fuel rodlet irradiation capsule. LBE fill is used to thermally couple the fuel rod surface to the titanium capsule.

Three rodlets have been tested to burnups from approximately 2.5 – 5 MWd/kgU. Two of these rodlets were removed from irradiation due to increases in the fission product release rate, while the third was removed due to mechanical problems with the irradiation system. Two more rodlets are available for irradiation, following which all rodlets will be shipped to Idaho National Laboratory for PIE.

5. Summary

The MITR has a vigorous on-going programme of in-core experiments using a combination of versatile general purpose facilities and custom-designed, special purpose experiments. These experiments, undertaken with partners from industry, academia and the national laboratories, generate data to support materials and fuel advances for current generation and advanced power reactors.

ADVANCED TEST REACTOR NATIONAL SCIENTIFIC USER FACILITY PARTNERSHIPS

F. M. MARSHALL, J. B. BENSON, J. I. COLE, M. C. THELEN

*ATR NSUF Office, Idaho National Laboratory
995 University Boulevard, Idaho Falls, ID 83401, USA*

T.R. ALLEN

*Engineering Physics Department, University of Wisconsin
1500 Engineering Drive, Madison, WI 53706, USA*

1. Introduction

In 2007, the Advanced Test Reactor (ATR), located at Idaho National Laboratory (INL), was designated by the U. S. Department of Energy (DOE) as a National Scientific User Facility (NSUF). This designation made test space within the ATR and post-irradiation examination (PIE) equipment at INL available for use by approved researchers via a proposal and peer review process. The goal of the ATR NSUF is to provide researchers with the best ideas access to the most advanced test capability, regardless of the proposer's physical location.

Goals of the ATR NSUF are to define the cutting edge of nuclear technology research in high temperature and radiation environments, contribute to improved industry performance of current and future light water reactors, and stimulate cooperative research between user groups conducting basic and applied research. As part of meeting each of these three goals, the ATR NSUF has developed a broad educational program aimed at increasing the number of researchers knowledgeable about reactor experimentation, post irradiation examination techniques, and material radiation effect fundamentals.

Since its inception, the ATR NSUF has expanded its reactor test space, obtained access to additional PIE equipment, taken steps to ensure the most advanced post-irradiation analysis possible, and initiated an educational program and digital learning library to help potential users better understand the critical issues in reactor technology and how a test reactor facility could be used to address this critical research. To date, 40 research projects have been awarded to 19 universities and four laboratories.

Recognizing that INL may not have all the desired PIE equipment, or that some equipment may become oversubscribed, the ATR NSUF established a Partnership Program. This program invited universities to nominate their capability to become part of a broader user facility. Several universities and two national laboratories have been added to the ATR NSUF with capability that includes reactor-testing space, PIE equipment, and ion beam irradiation facilities. This paper will discuss the research capabilities that are available to the ATR NSUF user community.

2. Facility Capability Summary

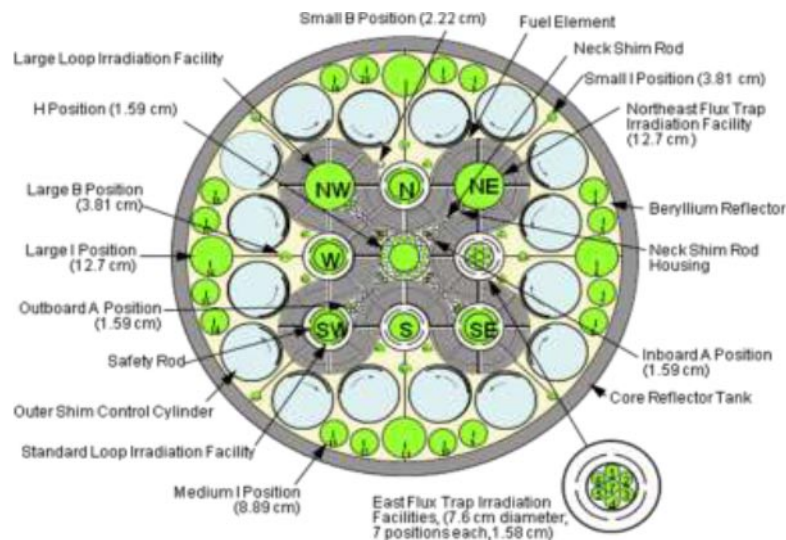
Several facilities are available for the ATR NSUF user community. Some of these are at the INL and many more are available through the ATR NSUF Partnership Program.

2.1 Advanced Test Reactor

The ATR is a pressurized, light-water moderated and cooled, beryllium-reflected, enriched uranium fueled reactor with a maximum operating power of 250 MW_{th}. It has operated continuously since 1967, to test materials and fuels in support of light water reactors (LWRs) and more advanced reactor designs. The ATR core cross section, shown in Figure 1, consists of 40 curved aluminum plate fuel elements configured in a serpentine arrangement around a three-by-three array of large irradiation locations in the core or flux traps, where the

peak thermal flux can reach 1.0×10^{15} n/cm²-sec, and peak fast flux ($E > 1.0$ MeV) 5×10^{14} n/cm²-sec. This core configuration creates five main reactor power lobes (regions) that can be operated at different powers during the same operating cycle. Along with the nine flux traps (large irradiation positions), there are 66 irradiation test positions ranging in diameter from 1.27 to 12.7 cm and all 122 cm long.

Figure 1. ATR core cross section.



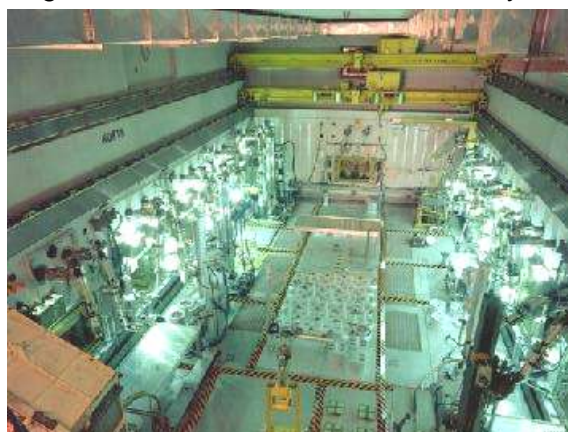
There are four primary experiment configurations in the ATR - static capsule, instrumented lead, pressurized water loop and the Hydraulic Shuttle Irradiation System (HSIS). Experiments must remain in the ATR for the entire duration of the operating cycle (average length of 49 days), except for experiments performed in the HSIS. The HSIS enables small volume, short duration, irradiations to be performed in the ATR.

The ATR building also houses the ATR Critical (ATRC) facility, which is a low power (5 kW maximum), full-size replica of the ATR, and is used to evaluate an experiment's potential impact on the ATR core, by measuring experiment control rod worths, reactivities, and void/temperature reactivity coefficients before inserting an experiment into the ATR.

2.2 Post-Irradiation Examination Capabilities

Post-irradiation examination (PIE) capabilities are available to ATR NSUF users at numerous facilities at the INL, including the Hot Fuel Examination Facility (HFEF). Figure 2 is a photograph of the interior of the HFEF.

Figure 2. Hot Fuel Examination Facility



These facilities house equipment and processes used for nondestructive examination, sample preparation, chemical, isotope, and radiological analysis, mechanical and thermal property examination, and microstructure property analysis. The HFEF also houses a 250 kW TRIGA reactor, two beam tubes, and two separate radiography stations for neutron radiography as well as the capability to prepare any material and fuel samples for the various examinations.

2.3 University Partner Capabilities

In addition to the capabilities of the INL facilities, the ATR NSUF has facilitated access to the facilities described below for the ATR NSUF user community through the Partnership Program. The objective of the Partnership Program is to offer a wider range of experimental facilities than is available at INL to the ATR NSUF user community, as well as to enable increased utilization of the partner facilities. Experimenters may need to use more than one facility to accomplish their research objectives, and, for awarded projects, the ATR NSUF will coordinate the work at the different facilities. This is also expected to enhance cooperation opportunities between the users and the partner facility research teams.

2.3.1 Massachusetts Institute of Technology (MIT)

The MIT reactor is a 5 MW_{th} tank-type research reactor with three positions available for in-core fuel and materials experiments in water loops at pressurized water reactor/boiling water reactor conditions, high-temperature gas reactor environments at temperatures up to 1400°C and fuel tests at LWR temperatures have been operated and custom conditions can also be provided. Fast and thermal neutron fluxes are up to 1×10^{14} and 5×10^{14} n/cm²-s, respectively.

2.3.2 North Carolina State University (NCSU)

The NCSU PULSTAR reactor is a 1 MW_{th} research reactor, fueled by uranium dioxide pellets in zircaloy cladding. The fuel provides response characteristics that are similar to commercial LWRs, which allows teaching experiments to measure moderator temperature, power reactivity coefficients, and Doppler feedback.

Nuclear Services laboratories at NCSU offer neutron activation analysis, radiography, imaging, instrumentation testing, and positron spectrometry capabilities. Additionally, the NCSU PULSTAR reactor facility offers a selection of dedicated irradiation beam port facilities with capabilities for neutron powder diffraction, neutron imaging, intense positron source and ultra-cold neutron source. An intense positron source has been developed to supply a high rate positron beam to two different positron/positronium annihilation lifetime spectrometers.

2.3.3 University of Michigan (UM)

The UM Irradiated Materials Complex (IMC) houses laboratories and hot cells for conducting high-temperature mechanical property, corrosion and stress corrosion cracking experiments on neutron irradiated materials in an aqueous environment and for characterizing fracture surfaces after failure.

The 1.7 MV Tandatron accelerator in the Michigan Ion Beam Laboratory at UM offers controlled temperature proton irradiation capabilities with energies up to 3.4 MeV as well as heavy ion irradiation.

2.3.4 Illinois Institute of Technology (IIT)

The Materials Research Collaborative Access Team (MRCAT) beamline at Argonne National Laboratory's Advanced Photon Source (APS) offers synchrotron radiation experiment

capabilities, including x-ray diffraction, x-ray absorption, x-ray fluorescence and 5 μm spot size fluorescence microscopy.

2.3.5 University of Nevada, Las Vegas (UNLV)

The Radiochemistry Laboratories at UNLV's Harry Reid Center for Environmental Studies offer metallographic microscopy, x-ray powder diffraction, Rietveld analysis, SEM and STEM, electron probe microanalysis, and x-ray fluorescence spectrometry.

2.3.6 University of Wisconsin at Madison (UW-M)

The Characterization Laboratory for Irradiated Materials at the UW-M can be used for SEM and STEM on neutron-irradiated materials. Capabilities also include sample preparation by grinding and polishing.

A 1.7 MV terminal voltage tandem ion accelerator at UW-M features dual ion sources for producing negative ions with a sputtering source or using a radio frequency plasma source. The analysis beamline is capable of elastic recoil detection and nuclear reaction analysis.

2.3.7 University of California at Berkeley (UCB)

At the UCB Nuclear Engineering laboratory, nanoindenter capabilities are available for testing on low radioactive samples. The nanoindenter has two load ranges, is housed in an environmental controlled enclosure, and is equipped with a high power optical microscope and an automated lens change to allow accurate positioning of indents on a sample.

2.3.8 Oak Ridge National Laboratory (ORNL)

The High Flux Isotope Reactor (HFIR) provides a high flux (up to 5×10^{15} n/cm²-s thermal) material irradiation test capabilities are similar to those available at the ATR. In-core irradiations are performed for medical, industrial, and isotope production and research on severe neutron damage to materials.

The Low Activation Materials Development and Analysis Laboratory (LAMDA) facility at ORNL is a set of multipurpose laboratories for evaluation of materials with low radiological activities. Testing capabilities include tensile, fracture toughness, electrical diffusivity, optical microscopy, microhardness, thermal diffusivity, etc. Samples must have gamma/beta activity corresponding to a dose of less than 60 mR/hr (at one foot).

2.3.9 Purdue University

Purdue's Interaction of Materials with Particles and Components Testing (IMPACT) experimental facility was designed to study in-situ dynamic heterogeneous surfaces at the nano-scale exposed to varied environments that modify surface and interface properties. In-situ techniques used in the IMPACT experiment include: low-energy ion scattering spectroscopy (LEISS), direct recoil spectroscopy, X-ray photoelectron spectroscopy (XPS), Auger electron spectroscopy (AES), EUV (13.5-nm) reflectometry (EUVR), EUV photoelectron spectroscopy (EUVPS), and mass spectrometry.

2.3.10 Pacific Northwest Nuclear Laboratory (PNNL)

PNNL's Material Science and Technology Laboratory includes advanced characterization and testing facilities for both non-radioactive and radioactive structural materials for nuclear power systems, both fission and fusion materials. The characterization includes all types of microscopy, including TEM, SEM, and Optical. Mechanical property testing is available for both hot and cold samples. A high-temperature furnace on a test frame is located in a large

walk-in fume hood in one of the labs for testing dispersible ceramics. A high-precision density apparatus is available for irradiated materials.

The Radiochemical Processing Laboratory (RPL) at PNNL houses specialized facilities for work with microgram-to-kilogram quantities of fissionable materials and megacurie activities of other radionuclides. These provide a platform for radiochemical process development, chemical and physical separations, radiomaterial characterization, radioisotope research, reactor dosimetry and radioactive and hazardous waste management.

2.3.11 Center for Advanced Energy Studies (CAES)

The CAES facility, located in Idaho Falls, Idaho, is a collaboration between the INL and three Idaho universities - Idaho State University, University of Idaho, and Boise State University. It houses a nanoindenter, atomic force microscope, Focused Ion Beam (FIB), Field Emission Gun Scanning Transmission Electron Microscope (FEG-STEM), and local electron atom probe for characterization of low-level radioactive materials.

3. Proposal Options

Researchers can gain access to the ATR NSUF facilities described above through several proposal options: open calls (offered twice each year), Rapid Turnaround Experiments (RTEs), which are expected to be of shorter duration than full irradiation experiments, and special focus calls (e.g., for the APS only). Proposal submittals are completed through the web site at <http://atrnsof.inl.gov/> and all proposals received are subject to a peer-review process before selection. An accredited U.S. university or college must lead proposals for open call experiments; collaborations with other organizations are encouraged. Any U.S.-based entities, including universities, national laboratories, and industry can propose research that would use the MRCAT beamline at the APS or would be conducted as an RTE. A new feature in 2012 is the collaboration with DOE's Nuclear Energy University Program (NEUP), allowing a researcher to submit a single proposal through the NEUP system to perform a research project that may also need access to the ATR NSUF facilities.

4. Education Program

The objective of the ATR NSUF education program is to establish a cadre of nuclear energy researchers, facilitating the advancement of nuclear science and technology through reactor-based testing. ATR NSUF uses focused internships, fellowships, and faculty/student exchanges to encourage faculty and student access to cutting-edge and one-of-a-kind tools for conducting reactor-based research in nuclear science and technology, fuels, and materials. Researchers gain access to key mentors, world-class facilities, and equipment. From these collaborations, a new text book on irradiation test planning and execution is in development. Additional outreach activities include university seminars, faculty exchanges, and an annual User Week to enable users and potential users to understand more about the ongoing research and collaboration opportunities. A major emphasis of all ATR NSUF education programs is to allow for maximum interaction and researcher access to the critical components of the nation's experimental nuclear research infrastructure.

5. Acknowledgements

This work was supported by the United States Department of Energy (DOE) under DOE Idaho Field Office Contract Number DE-AC07-05ID14517.

International Conference on Research Reactors IGORR-RRFM.
Prague (Czech Republic), March 2012.

Criticality of the PIK reactor

K.A. KONOPLEV

*Department of Reactor Physics and Technology, B.P. Konstantinov
Petersburg Nuclear Physics Institute
Orlova Roscha, 188300, Gatchina - Russia*

ABSTRACT

After a long period of construction, in 2011 the PIK reactor was loaded for the first time and went critical on February 28, 2011. The reactor is designed primarily for research using extracted neutron beams. At 100 MW, PIK is high-power by research reactors standards. High power and special design provide a record-setting neutron flux density in the extracted beams. The reactor is equipped with sources of ultra-cold, hot and cold neutrons, and it can cover the entire range of possible energies.

The reflector tank is equipped with a numerous flanges for installation of horizontal, inclined and vertical channels. To install instruments on the neutron beams, the reactor is surrounded by a wide circular hall and has an adjacent building – the neutron guide hall. Scientific instruments are also installed on the inclined channels in a separate experimental hall. It is expected that this will allow accommodating up to 50 devices. Six vertical channels in the reflector and one in the core can be used for irradiation.

The unperturbed thermal neutron flux reaches $1.2 \cdot 10^{15}$ n/cm²s in the reflector and $5 \cdot 10^{15}$ n/cm²s in the neutron trap in the core.

The scientific program covers a wide range of possible research on neutron beams of both fundamental and applied nature.

The experimental capabilities of the PIK reactor are at least as good as those of the best beam reactor of the world – the HFR reactor at the International Institute Laue-Langevin (Grenoble, France). There is no doubt that the completion of the PIK project will fully satisfy the needs of all organizations in Russia that are interested in using neutron methods for researches. PIK reactor could serve as the core of a new international neutron research center like the one in Grenoble.

The PIK research reactor is located in Gatchina (Leningrad region) at the Petersburg Nuclear Physics Institute.

In Russia, the situation with research reactors designed for physics researches is very complicated. Essentially, there are only four medium-power reactors (flux of less than $4 \cdot 10^{14}$ n/cm²s), and they do not fully comply with the requirements of modern physics experiments. The exception is the recently upgraded IBR-2 reactor at JINR (Dubna); this is a pulsed reactor with a mean power of 2 MW, which is clearly insufficient for the wide range of experiments that require accumulation of a large number of events. In this regard, the completion of the PIK research reactor complex is quite an important task.

1. Introduction

The name “PIK reactor” is well-known to the neutron scattering community. It should become another source of powerful neutron beams along with such centres as ILL in Grenoble, the FRM 2 reactor in Munich, and NIST in the USA. The long wait for this 100 megawatt reactor led to some pessimism among expected users, and therefore the physical start-up should demonstrate to the users that it is time to start preparing for experiments.

The need for new extracted neutron beams is clearly indicated by the heavy competition for requests to conduct research on extracted neutron beams and the large number of new tasks that could be solved with their help. One may say that there is a neutron “drought”.

At 100 MW, PIK is very powerful by research reactor standards. It provides a $1.2 \cdot 10^{15}$ n/cm²s thermal neutron flux in the heavy water reflector and a $5 \cdot 10^{15}$ n/cm²s flux in the neutron trap in the centre of the core. The reactor is equipped with neutron guides leading out from the cold neutron source and from heavy water. The neutron guides enter the neutron guide hall whose rear wall which is located 100 m away from the active core. The reactor should be equipped with a source of hot neutrons and a source of ultracold neutrons. In addition, a low-temperature loop for irradiation of different materials is being designed.

2. Reactor

The reactor was designed to get a 10^{15} n/cm²s undisturbed thermal neutron flux in the reflector. This level of flux is required in the part of the reflector with the experimental channels for extracted neutron beams. Such parameters can be obtained using SM2 type fuel elements [1] and a reactor with a 50 l core volume and 100 MW power. Manufacture of SM2 type fuel elements is well-established. There exists extensive experience with this type of fuel element at core loads of around 8 MW per liter, and it has been tested at up to 10 MW/l.

With the selected core parameters, i.e. 50 l core volume and 100 MW power, the energy release non-uniformity coefficient (Kv) needs to be on the order of 3. Given adequate cooling, this provides an adequate margin for stable operation. Fuel element parameters are shown in Table 1.

Table 1. PIK reactor fuel element

- enrichment – 90%
- fuel – UO₂ in a copper-beryllium matrix
- density of uranium in the matrix – 2.2 g/cm³
- cladding – stainless steel, 0.16–0.17 mm
- concentration of U-235 in the core – 600 g/l

Cross-shaped fuel element has a stainless steel can and is twisted for positioning in fuel assembly. The stainless tube is filled with the ceramic matrix (Fig. 1). To reduce Kv, profiled fuel loading is used around the central channel. The core is loaded with three types of fuel assemblies (Fig. 2).

The active core is encased in a double-walled stainless steel vessel. The gap between the walls is used for cooling the part of the vessel adjacent to the core. The core is cooled with light water at a pressure of 50 bar (Table 2), while heavy water under a pressure of 16 bar circulates in the gap between the vessel walls. Incidentally, monitoring the concentration of heavy water in the gap between the walls allows one to detect microcracks in the vessel wall, despite the fact that microcracking is impossible according to calculations.

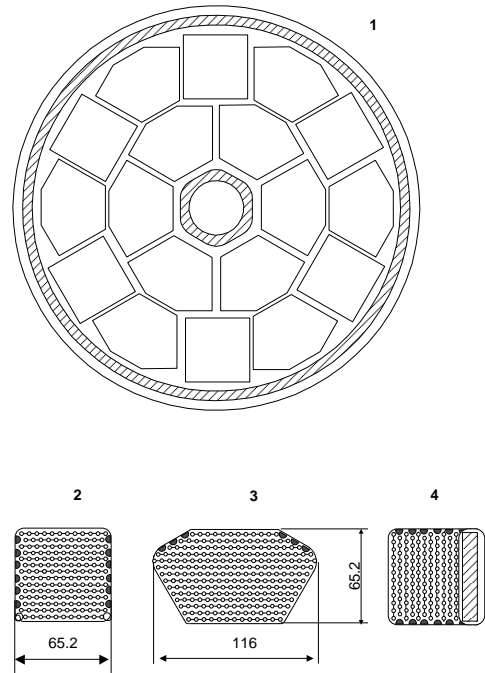
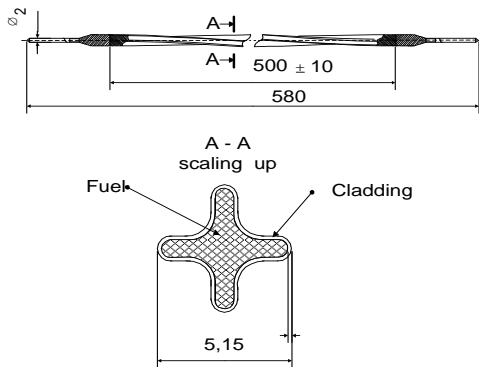


Figure 1. Fuel element

Figure 2. Fuel assemblies of the PIK reactor

One may note that the chosen scheme of cooling the core with light water and using a heavy water reflector has become dominant among recent beam reactor models.

The reactor is controlled using a central hafnium body in the form of two apart draw cylinders which are driving from the bottom, and europium oxide control rods in the reflector which are driving from the top. Reactor controls have a reactivity margin of $11 \beta_{\text{eff}}$. Cold core reactivity, when fully loaded with fresh fuel, is $17 \beta_{\text{eff}}$.

The reactor vessel and the reflector tank are located in a 15 meter deep shaft filled with water (Fig. 3). There are three types of experimental channels: horizontal, inclined, and vertical. The horizontal channels pass tangentially to the core, except for one which is radial (Fig. 4).

Table 2. Cooling circuits

First circuit

Coolant – H_2O

Pressure – 50 bar

Flow – $2400 \text{ m}^3/\text{hour}$

Input/output – $50/85 \text{ }^\circ\text{C}$

Reflector

Moderator – D_2O

Pressure – 6 bar

Diameter – 2.4 m

Height – 2 m

Gap between vessel walls

Coolant – D_2O

Pressure – 16 bar

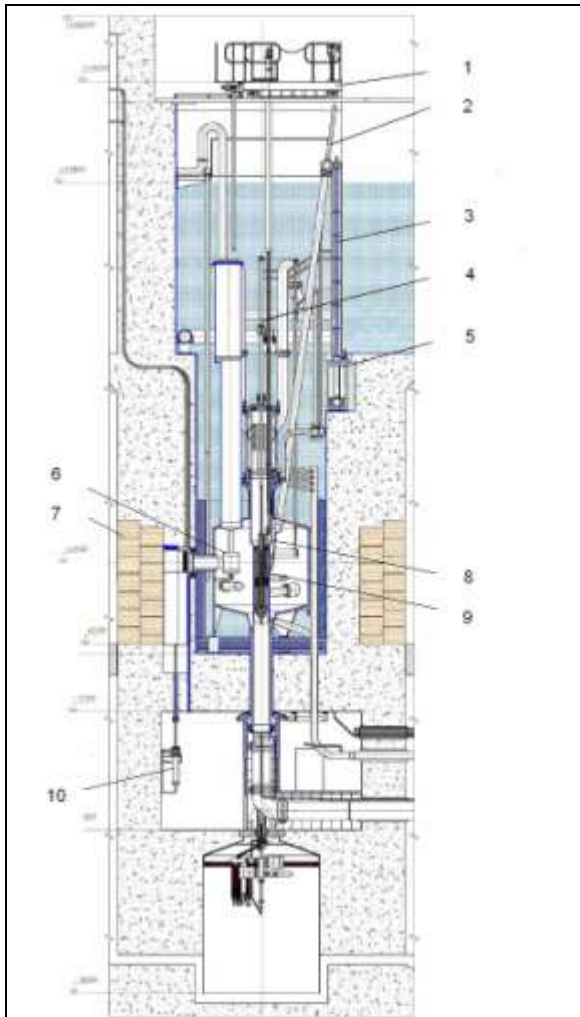


Figure 3. PIK reactor vertical cross-section

- 1 – loading machine
- 2 – control rod drive
- 3 – water seal
- 4 – central channel (CEC)
- 5 – loading drum
- 6 – cold neutron source
- 7 – disassemblable shielding
- 8 – control rod
- 9 – reactor core and vessel
- 10 – gate drive for horizontal channel (HEC)

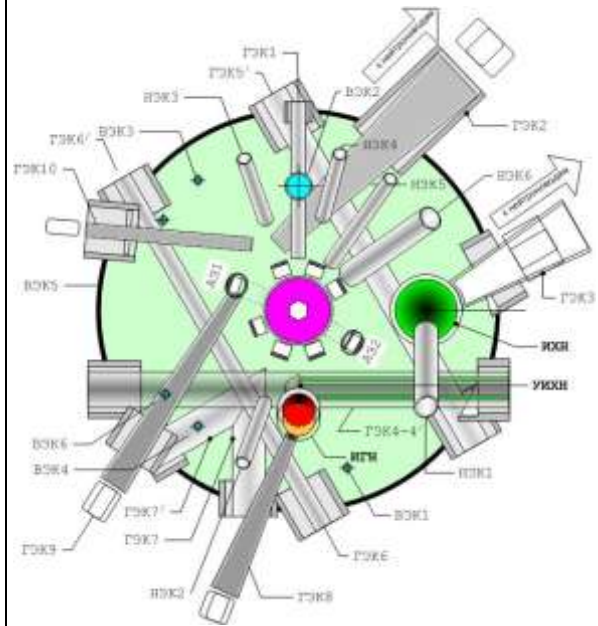


Figure 4. Experimental channels

3. First criticality

Neutron physics calculations of reactor startup were carried out with the aid of MCNP and MCU software. The calculated model was experimentally tested on a critical assembly in the form of a full-scale model of the PIK reactor.

Due to the above-mentioned difference between the reactivities of the fully loaded active core ($17 \beta_{\text{eff}}$) and reactor controls ($11 \beta_{\text{eff}}$), only 12 fuel assemblies were loaded. The remaining six positions for fuel assemblies were loaded with aluminum dummies (Fig. 5).

Loading was carried out with the use of a $4.56 \cdot 10^7$ n/s startup neutron source in the central channel. In addition to the standard instrumentation, detectors were taken from the critical assembly and installed in approximately the same places where they had been in the critical assembly. This allowed us to make an initial assessment of the power achieved. The power limit was set at 100 W and total energy production limit at under 100 W-hours. This restriction was

necessary because afterwards, manual work had to be performed on unloaded fuel assemblies. After the first 6 fuel assemblies, fuel loading was carried out one assembly at a time, controlled by the inverse multiplication method (Fig. 6).

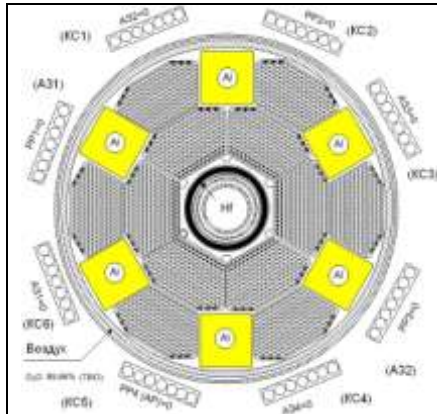


Figure 5. Core fuel loading

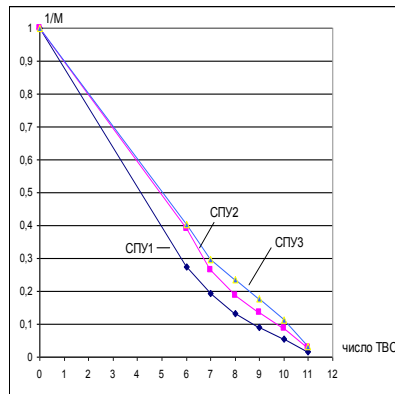


Figure 6. Inverse multiplication curves

Criticality was achieved at 16:23 on February 28, 2011.

Effectiveness of reactor controls was determined by the method of shooting the rods and by measuring the asymptotic period of acceleration:

$$\rho / \beta_{\text{eff}} = \frac{n_0 \sum_i a_i / \lambda_i}{\int n(t) dt}$$

n_0 – initial count rate;

a_i – relative output of the i -th group;

λ_i – decay constant of the i -th group;

$\int n(t) dt$ – integral count.

Asymptotic period of acceleration measurements used a step of $+0.2 \beta_{\text{eff}}$.

The integral characteristics were calculated by the method of reactivity compensation on different rods. The reactivity of the central control body was measured to be $10.7 \beta_{\text{eff}}$; preliminary calculations for its reactivity at first criticality conditions had given a value of $11.7 \beta_{\text{eff}}$. For controls in the reflector, the measured values are closer to the calculated ones, and for almost all 8 rods are within the margin of error. The calculated reactivity values on average coincided with the measured ones; their ratio was 1.03. The deviations were caused by small differences between the reactor geometry used in the numerical model and the real reactor, such as the position of some of the controls in the reflector. While comparing integral curves for upper and lower hafnium cylinders, it was found that the hafnium cylinders were shifted by up to 10 mm from the medial plane of the active core.

The main conclusion is that the measured weights of controls are in accordance with the requirements of the design. The calculated control positions at criticality coincided with the measured ones within the margin of error.

Neutron flux in the reactor channels of the reactor was measured by irradiation of activation detectors at several specific points. The distribution of energy release in the active core was recorded by measuring the activity of individual fuel elements in a disassemblable fuel assembly. Measurements of ^{140}La activity in the fuel elements were also used to estimate the power of the reactor.

Thermal neutron flux density in the central channel is shown in Figure 7.

One may note that all the above comparisons of measured values with calculations are for the calculations that were performed before the criticality experiment. After correcting for the

differences between the model of the reactor used in calculations and the constructed reality, the agreement between measured and calculated values became much better.

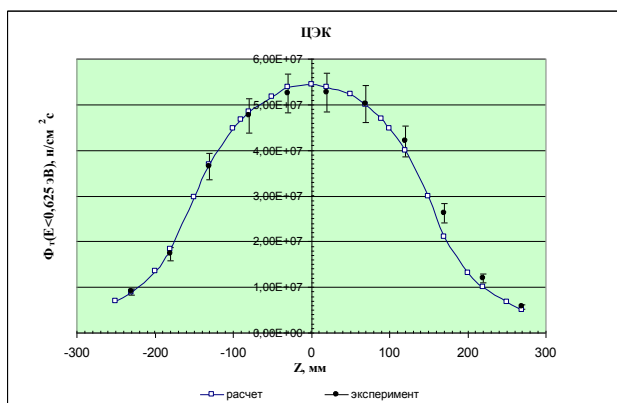


Figure 7. Thermal neutron flux density in the central channel

4. Preparation for power startup

The first criticality experiment was performed before the reactor was fully ready for increasing power up to the projected level. The system supplying power from a separate substation to the pumps of the first, second, and third circuits is not yet ready; neither are the emergency diesel generators. The holding tanks for emergency discharge and temporary storage of radioactive liquids are currently under construction.

Scientific equipment for work on neutron beams is being developed with the participation of several nuclear research centres, and the research programme is being refined at the same time.

The design of the reactor was developed by VNIPIET in the role of the general planner and ENTEK in the role of the chief designer under the scientific guidance of the PNPI.

This report uses materials kindly provided by participants in the preparation and execution of PIK first criticality, first and foremost by S.L. Smolsky and A.S. Zakharov. The author is deeply grateful to all of them.

References

1. V.A. Zikanov, V.A. Starkov, A.V. Klinov, V.M. Sviatkin.
The SM-2 high-flux reactor and its role in the development of nuclear science and technology.
Dmitrovgrad, 2011, NIIAR.

BRIEF DESCRIPTION ON LOW POWER COMMISSIONING IN CARR

LU ZHENG, XIAO SHIGANG, YUAN LUZHENG

*China Institute of Atomic Energy,
102413, Beijing, P.R. China*

ABSTRACT

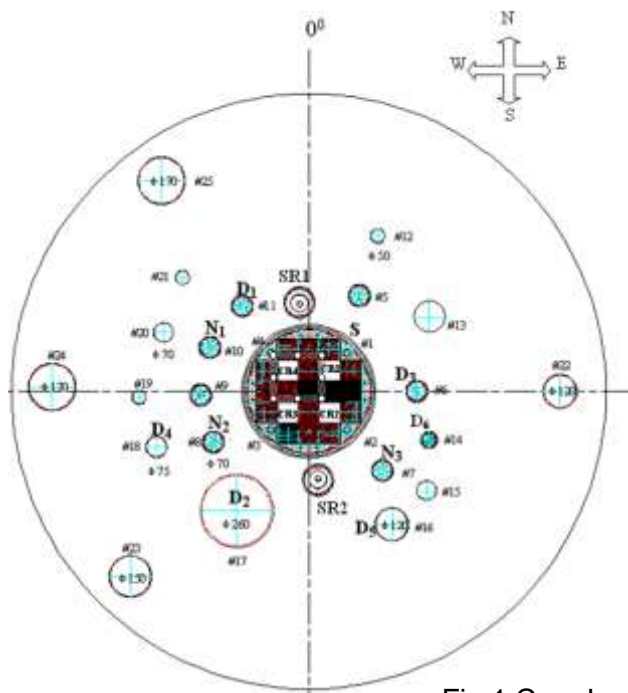
All low power physics experiments on CARR have been finished and will enter the power raising commissioning phase soon. Having successfully reached the first critical, CARR has conducted comprehensive measurements for its characteristics under low level power, such as, measurement on reactor's excess reactivity, calibration of control rod worth, measuring the shutdown margin in condition of control rod(s) stuck, these data and characteristics parameters obtained possess the vital significance for safe operation of the reactor later. In addition, power distribution in core under cold condition and both axial and radial relative thermal neutron flux distribution in many vertical channels have been measured by using activated gold foils, the results obtained provide important parameters significant information for reactor's safe operation, accident analysis and utilization research within irradiation channels. CARR's low level power commissioning on reactor physics, the results of experiments are well consistent with that of neutronics design, indicating that the neutronics design of CARR was well done and successful.

1.The First critical Experiment

The extrapolation method has been adopted for CARR's first critical experiment. It includes two stages, first the number of fuel assembly extrapolation and followed by the position height of control rod extrapolation. Fig.1 shows the core lay out of the first critical experiment.

The loading order of the fuel assemblies is shown in Fig.2. The initial condition of the core contains 4 fuel follower control rods and 17 dummy assemblies with depleted uranium. The first loading of fuel assemblies is the half of the minimum critical quantity calculated theoretically. And then, conduct the extrapolation at each step of taking away one dummy assembly and replaced by one standard fuel assembly till the difference of core fuel assembly quantities between loaded and extrapolated is less than one, insert all control rods to the core bottom, end the number of fuel assembly extrapolation. Now add one more fuel assembly and begin to conduct the position height of control rod extrapolation by slowly raising the control rod one by one to, according to 1/3 principle, one third of the pre-estimated height. When extrapolated values of 3 counting channels are consistent within 1mm, finish the position height extrapolation and prepare to make the transition for super critical. For performing this, first taking away the start-up neutron source, successively raising control rods one by one to the extrapolated height obtained, while closely pay attention to the changing of counting rate, once the counting begins increasing, indicate the reactor successfully getting critical and transiting to super-critical. Fig. 3 shows the counting rate change curve of CARR during super critical transition.

CARR goes first critical at the load of 9 fuel assemblies. Fig. 4 and Fig. 5 show respectively the curves of fuel assembly number extrapolation and control rod position height extrapolation. The experiments are completely consistent with theoretical calculation results. The critical position of control rods is 651 mm by subcritical extrapolation and 644 mm by super critical interpolation, the error of k_{eff} between theoretical calculation and experiment is just 0.75%.



S (#1 channel) Neutron source
 N1 ~ N3 (#10, #8, #7 channels)
 Count tube for start-up
 D1 ~ D3 (#11, #17, #6 channels)
 Ion. Chambers for start-up
 D4 ~ D6 (#18, #16, #13 channels)
 Ion. Chambers for C&P system

Fig.1 Core Lay Out of CARR

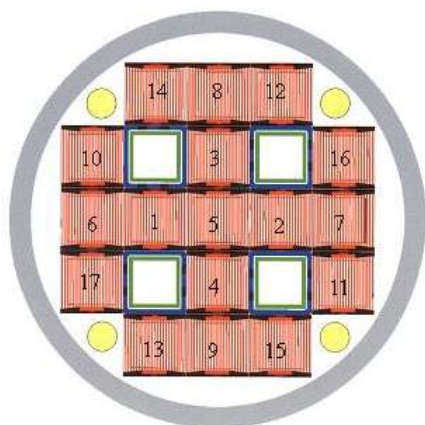


Fig. 2 Loading fuel order for the first critical experiment

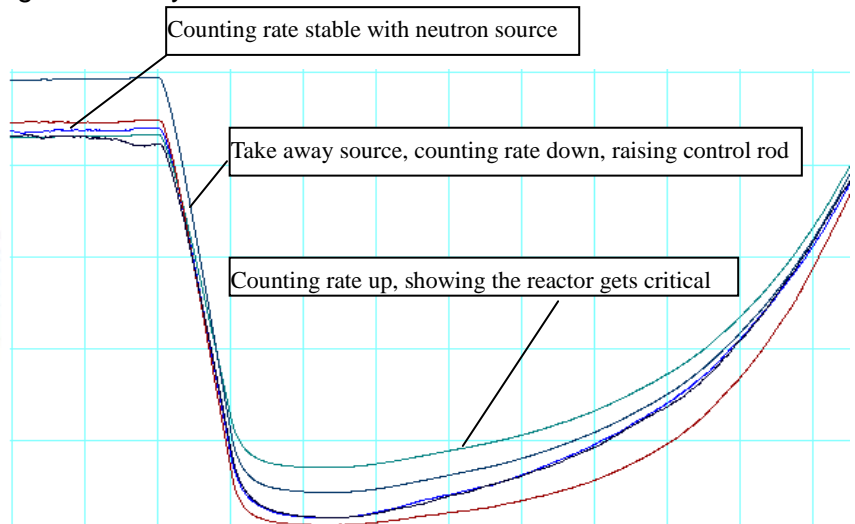


Fig. 3 Count-rate changing curve in the first critical process

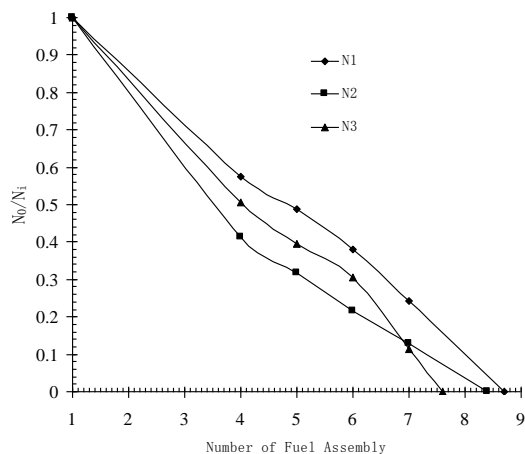


Fig. 4 The curve of fuel assembly number extrapolation

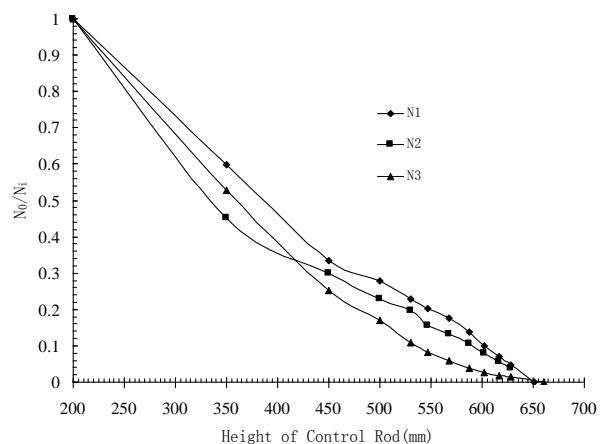


Fig. 5 The extrapolation curve for control rod height

2. Measurement for reactivity

The reactivity measurement covers measurements of excess reactivity, worth curve of control rod bank, regulating rod worth curve, control rods worth and reactor shut down margin.

2.1 Excess reactivity measurement

CARR possesses quite large excess reactivity. The total excess reactivity can be obtained by measuring the reactivity worth of each standard fuel assembly added from the minimum critical loading to full loading and by making appropriate correction with theoretical calculation. To assure the creditability of the measuring results, both periodic method and rod-dropping method are adopted. The measuring results are shown in Table 1.

Table 1: The measuring results of excess reactivity

	Periodic	Rod-dropping	Theoretical
Excess reactivity (mk)	180.97	182.03	184.60

1) In periodic method, when one assembly added, assuming that the efficiency of control rod bank in the vicinity of critical position keeps the same as before its loading, the reactivity worth corresponding to the change of control rod bank critical positions before and after the fuel loading can be obtained by linear interpolation. This value is approximately considered as the reactivity of newly added fuel assembly with certain error, and more, the reactivity measured in this way is under the condition of control rods existing in core instead of “net core” reactivity.

2) In rod-dropping method, the reactivity of newly added assembly is measured using the single control rod worth curve in relevant loading condition. Still this is the value under the condition of control rod existing in the core, it is required to correct into net core one by theoretical calculation. It may result in accumulated error because such correction is carried out after each step of fuel assembly adding.

Both results measured are consistent with the theoretical one in 2%. Compare to periodic method, the result of rod-dropping method is closer to the real one because of its net core correction. So, the excess reactivity of CARR measured is 182.03mk.

2.2 The worth curve measurement for control rod bank

Due to the large quantity of control rod bank worth, it is very difficult to measure the value under full loaded for CARR. Therefore, the rod-dropping method was adopted to measure the control rod bank worth for the part below the critical height of each given loading beginning with the minimum critical loading, i.e., from 9 to 17 assembly loadings 9 control rod bank values are measured and after theoretical correction the control rod bank worth curve under full loading between 234mm~646mm can be obtained. Under full loading core, the control rod bank worth measured by rod-dropping method below the critical height is 142mk, the excess reactivity measured is 182.03mk, so the total control rod bank worth of CARR is 324.03mk. Fig. 6 shows the worth curve of control rod bank. From Fig. 6, good consistency is shown between experimental and theoretical results which can fully indicate the accuracy of theoretical calculation and verification for the design software. For the part of control rod bank worth which has not been measured by experiment, the theoretical calculation result may be used as reference with quite good consistency expected.

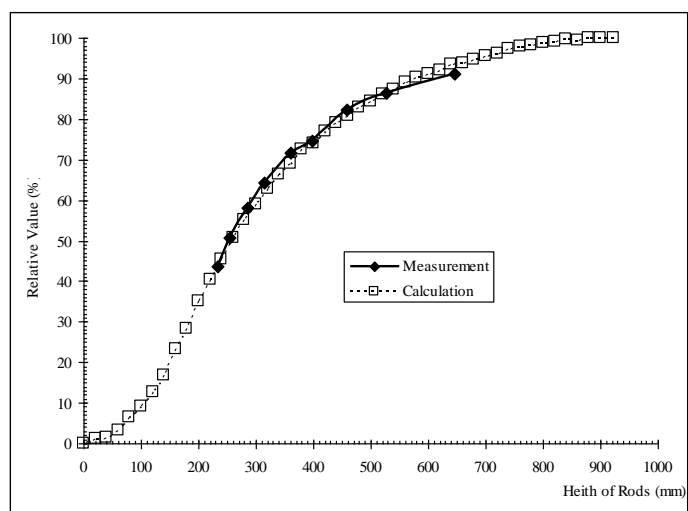


Fig. 6 The worth curve of control rod bank

2.3 The efficiency curve measurement for regulating rod

Under full fuel loading condition, completely withdraw CR3 to the core top and insert CR1 to the core bottom, let the reactor get critical with CR2 and CR4. Then keep the height of CR2 and CR4, gradually raising CR1 with the compensation of inserting CR3. The reactivity worth of CR1 at different heights can be measured by rod-dropping method.

During the experiment, keep the CR2 and CR4 at the height of 156mm, when CR3 completely inserted, the CR1 is raised from the bottom to height 650 mm. So the integrated worth curve of CR1 below 650 mm has been obtained as shown in Fig. 7. This efficiency curve of the regulating rod could be used as an important reference in later experiments and operation in spite of data lack over 650 mm with quite low value.

The linear section of CR1 worth is 220mm~380mm. In experiments which require the linear section as reactivity calibration, it is required to make the CR1 enter the linear section by adjusting the height of CR2 and CR4. The theoretical calculation for the regulating rod dropping was done using the real positions resulted from the experiment. Again good consistency is shown which has given the verification for theoretical calculation method and model.

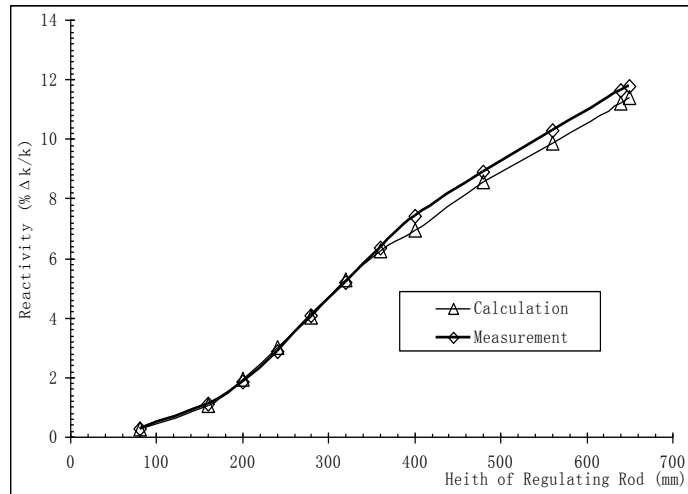


Fig. 7 The efficiency curve of regulating rod

2.4 Control rod worth measurement

Rod dropping method was adopted to measure various control rod worth in CARR. Table 2 shows the results measured.

Table 2: Control rod worth measuring results

Control rods Data items	SR1	SR2	SR1&2	CR1	CR2	CR3	CR4
Measured(% $\Delta k/k$)	-1.04	-0.97	-2.13	-13.14	-12.12	-11.73	-12.38
Calculated(% $\Delta k/k$)	-1.20	-1.12	-2.30	-13.45	-12.77	-11.99	-12.76
Relative error (%)	15.38	15.46	7.98	2.36	5.36	2.22	3.07
Design values(% $\Delta k/k$)	1.264		2.660	12.287			

Notes: The calculated values listed are calculated with real experimental positions. Design values are the parameters of net core without critical adjusting in neutronics design.

In Table 2, though the relative error of single safety rod worth is rather big between measuring result and calculated one, the absolute value deviation is not so large. This may be caused by two factors: one is that the precise requirement on k_{eff} calculation is quite high due to small worth of single safety rod, a little deviation in k_{eff} will result in rather large error; the other is that the layout of three ionization chambers used for measuring the reactivity worth is reasonable uniform from the whole core view but not from the single safety rod which may bring out some unfavorable effect on measuring results. The relative error of the total worth of two safety rods or each single rod worth of 4 regulating/compensating rods is obviously less than that of single safety rod, which, on some extents, explain the effect of two factors mentioned above.

Except the safety rods, the relative errors of control rods worth between calculated and measured are within 2%~6%, it indicates that during the neutronics design when taking into account the shutdown margin the consideration of 10% calculated error on control rod worth is reasonable and conservative.

2.5 The shutdown margin measurement

The measurements for shutdown margin of all rods dropping and one rod stuck out are performed using rod-dropping method. The results are shown in Table 3.

Table 3: Shutdown margin experiment results

CRs Condition Data items	CR1 stuck	CR2 stuck	CR3 stuck	CR4 stuck	CR1~CR4 dropped	All 6 rods dropped
Measured(% $\Delta k/k$)	-2.97	-3.35	-3.68	-3.47	-13.29	-17.21
Calculated(% $\Delta k/k$)	-3.198	-3.659	-4.058	-3.696	-14.476	-18.807
Relative error(%)	7.68	9.22	10.27	6.51	8.92	9.28

Notes: The calculated values listed are calculated with real experimental positions.

When the largest worth control rod CR1 was stuck at the core top position, the minimum shutdown margin of the reactor is -2.97% $\Delta k/k$, in neutronics design this value was -2.98% $\Delta k/k$ if taking into account the control rod worth calculation error, it shows very good consistency and meets the control rod stuck principle. Calculation with real experimental rod positions indicates that the maximum deviation of k_{eff} with the experiment is only 0.5%. In initial loading condition of cold core without xenon poisoning, the shutdown margin for dropping 4 regulating/compensation rods is -13.29% $\Delta k/k$, while for dropping all 6 control rods -17.21% $\Delta k/k$, which concludes that the reactivity shutdown margin of CARR under normal operation condition is enough and suitable.

3. Relative measurements for thermal neutron flux

The activated gold foils are used for measuring the thermal neutron flux distribution in reactor core and vertical channels in heavy water tank. The comparisons of measuring results of reactor core with theoretical calculation values are shown in Fig. 10. It indicates that the trend of measured and calculated curves is consistent on the whole, the deviation is mainly caused by their difference of critical control rod bank heights.

4. Measurement of power non-uniform factors

The measurement of relative power distribution was performed under the cold core condition and the power non-uniform factors were obtained, shown in Table 4. The whole core power non-uniform factor measured is less than that of calculated, which means that using the theoretical value as the input of accident analysis is safe and conservative and the uniformity of core power distribution in CARR meets the safety requirement under normal operation condition and accident condition.

Table 4: The results of power non-uniform factors measurement

	Calculated	Measured
Radial non-uniform factor F_r	1.164	1.156
Axial non-uniform factor F_z	2.352	2.358
Local non-uniform factor F_l	1.054	1.046
Whole core non-uniform factor F_n	2.886	2.851

5. Conclusion

The Results of low power commissioning indicate that all characteristics of CARR are in good consistency with that of neutronics design, which can conclude that the neutronics design of CARR was well done and successful.

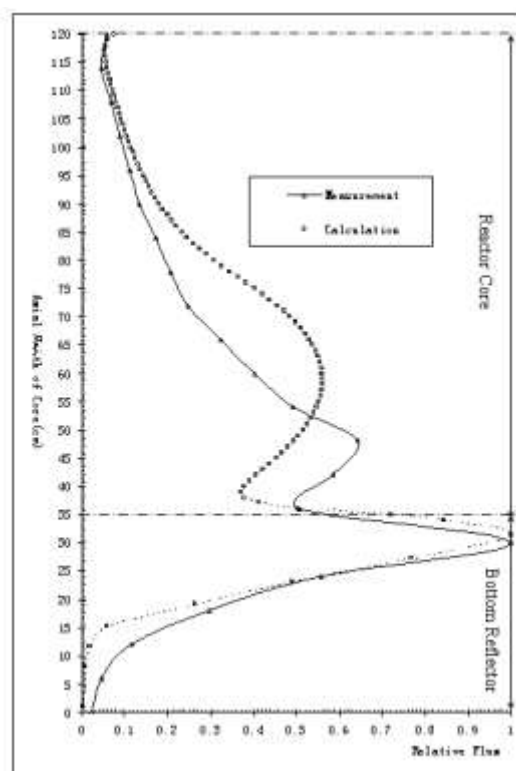


Fig. 10 Relative distribution of thermal neutron flux in central core axis

EXPERIMENTAL DEVICES IN JULES HOROWITZ REACTOR DEDICATED TO THE MATERIAL STUDIES IN SUPPORT TO THE CURRENT AND FUTURE NUCLEAR POWER PLANTS

C. COLIN, J. PIERRE, C. BLANDIN, C. GONNIER

DEN / DER / SRJH, CEA, Centre de Cadarache, 13108 Saint Paul lez Durance, FRANCE

D. MOULIN

DEN / DTN / STPA, CEA, Centre de Cadarache, 13108 Saint Paul lez Durance, FRANCE

M. AUCLAIR, F. ROZENBLUM

DEN / DRSN / SIREN, CEA, Centre de Saclay, 91191 Gif sur Yvette, FRANCE

Before their uses in industrial nuclear power plants (NPP), materials and fuel have to follow a long qualification process with different stages of screening, selection, qualification, optimization, processing, lifetime assessment and safety tests. These studies are most of the time associated with a complex multi-physical modelling of the materials' behaviours. It requires well controlled and instrumented irradiation experiments in material testing reactors (MTR). Considering the long term needs of this kind of experiments and the ageing of the present MTRs in Europe, it was decided to construct a new high performance MTR. The Jules Horowitz Reactor (JHR), under construction, will answer to these issues, in support of the current NPP (Gen.II, Gen.III), as well as of investigations related to future reactor systems. The aim of this presentation is to describe the main devices under development at CEA and dedicated to the material irradiations in JHR reactor. In-core and in reflector devices will be presented, corresponding to large ranges of temperature and neutrons flux of the irradiation conditions. A special attention focuses on the improvement of the thermal stability and gradients of the interest zones in samples despite strong γ heating and on an improvement of the instrumentation devoted to the experiments. Some specific devices will be described such as equipments designed to the qualification of reactor pressure vessel RPV steels, to the study of the stress corrosion cracking assisted by irradiation phenomena (IASCC), or to the studies of creep-swelling of structural materials.

1. Introduction

A good knowledge of the phenomena controlling the nuclear materials behaviours is required to justify their selections, optimisations and their uses in nuclear power plants (NPP). It is necessary to develop a good predictive material modelling, associated with a large experimental database at different scales and recovering closest as possible range of reactors conditions. But at the end of the process, this approach must be supplemented and validated by an experiment, of course well controlled, in a nuclear reactor environment like in material testing reactors (MTR). The aim of this paper is not to discuss the current and future situation of the nuclear energy, but it is obvious that it will be an essential component of the energy mix. The experimental irradiations in MTRs have to be continued to justify safety or to increase lifetime of the current NPP as well as to develop the future reactor systems [1]. On the other hand, it should be noted that the existing MTRs in Europe are or will be more than 50 years old in the next decade and so, they will be probably shut down in few years. Thus for example, because of its ageing, OSIRIS is planned to be shut down in less than ten years [2].

2. The JHR facility

Within this framework, it has been decided to launch the construction of the Jules Horowitz Reactor, implemented in Cadarache. The JHR characteristics have already been exposed elsewhere [3, 4, 5, 6, 7, 8], but the main points are resumed below. The Jules Horowitz Reactor (JHR) is a tank pool MTR with a maximum thermal power designed at

100MW. Its design allows a large experimental capability (around 20 experiments at the same time) inside the reactor core, close to the fuel with high fast neutron flux and outside the reactor core, in the reflector with higher thermal neutron flux : it is possible to perform irradiations in the core which will provide high damage rates (up to 15 dpa/year) in materials samples, while also carrying out in the reflector zone irradiations on fuel rods on displacement systems with precise positioning for example. The primary circuit which cools the fuel elements in the core will be lightly pressurized (12 bars). The reflector blocks, made of Beryllium, will be cooled by a forced water circulation connected to the reactor pool. The JHR is also designed to produce medical radio elements. Several equipments will be implemented in the reactor building and be used in support to the experimental programs:

- ❖ Hot cells in the nuclear auxiliary building will allow the preparation and examination of devices before and after irradiation. It will be possible to proceed to the first simple post irradiation examinations (PIE) of the irradiated samples. These on-site PIE programs will be of course completed by destructive examinations programs in dedicated hot cell laboratories, like LECl for materials in Saclay or LECA-STAR for fuel in Cadarache.
- ❖ Non destructive examination systems (spectrometry γ , X tomography, neutron imaging system) are foreseen in the pools and in the hot cells.
- ❖ Specific laboratories will also be set up in the installation for various uses: a fission product lab, a chemistry lab and a dosimetry lab

In the reactor building, the reactor pool is surrounded by several cubicles to receive instrumentation and control systems of each irradiation devices, linked by a system of fluid pipes and cables. The figure 1 presents the whole of the systems.

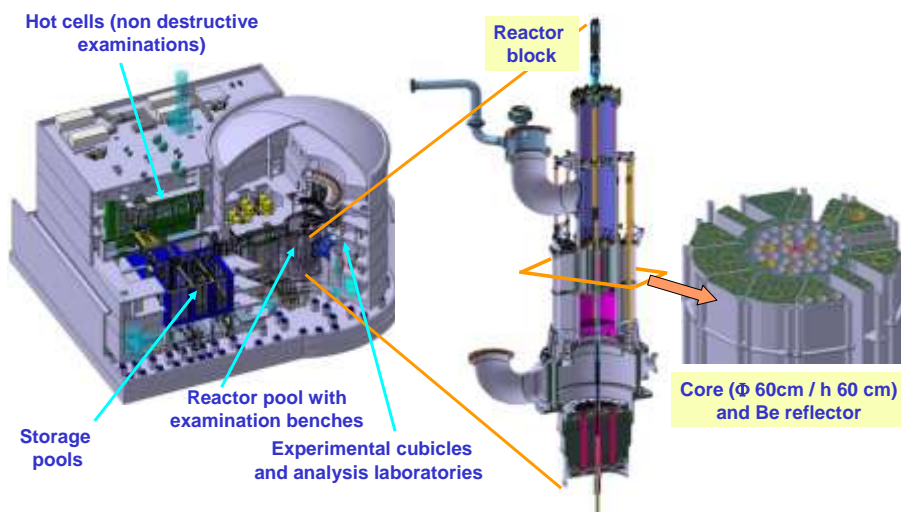


Figure 1 - Views of the main systems in the JHR facility and view of the reactor core.

3. Neutron performances

The core of the reactor can house up to 10 experimental devices distributed on three rings: 7 in small locations of 37 mm diameter and 3 in larger locations of 91 mm diameter. The reflector can also receive devices with 20 fixed positions, mainly of 100mm diameter but there will be one location of 200mm diameter. On figure 1, we can also see 6 water channels distributed around the reflector, where displacement systems will receive specific devices, a priori dedicated for fuel irradiations. Many calculations were performed to estimate neutron flux levels, by TRIPOLI 4.7 associated with JEFF-3.1 nuclear data library and considering a start-up fuel configuration (U_3Si_2 fuel and 70MW of core thermal power).

In this configuration, the highest fast flux in the core is $3.7 \cdot 10^{14} \text{ n.cm}^{-2}.\text{s}^{-1}$ ($E > 1\text{MeV}$). This allows reaching damage rates about 9dpa/year on the first ring. The corresponding γ heating is 12W.g^{-1} in stainless steel. Of course, on the third ring, flux levels are lower: $2 \cdot 10^{14} \text{ n.cm}^{-2}.\text{s}^{-1}$ ($E > 1\text{MeV}$) and 9W.g^{-1} . In the reflector, the fast flux level is in the range from $2 \cdot 10^{13}$ up to $2 \cdot 10^{11} \text{ n.cm}^{-2}.\text{s}^{-1}$ ($E > 1\text{MeV}$) and γ heating from 1.5 up to 0.2 W.g^{-1} according to the distance

to the reactor tank. The figure 2 underlines the evolution of the neutron spectra in the JHR core up to its reflector.

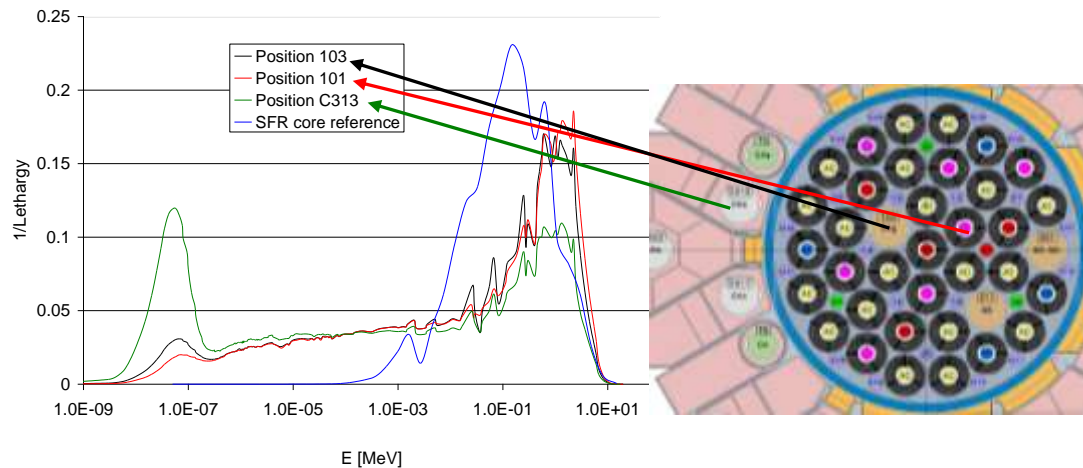


Figure 2 – Different neutron spectra met in JHR.

4. Experimental devices: material irradiations

Technological irradiations carried out in MTRs are in support of the current NPP, as well as of investigations related to future reactor systems. Because of the planned transition between the Gen II-III and Gen IV nuclear power reactors and considering the roadmap for the JHR deployment, CEA chose to mainly first develop new irradiation devices in support of LWR type reactors. Of course, the high technical skills of OSIRIS staff and its evident know-how is important for the setting-up and the design of the experimental capacity of the JHR. The two operating teams are working closely for the design of the new irradiation devices. This paper will expose the materials irradiation devices, which are at this moment under development at CEA. Another paper in this conference will present the JHR devices dedicated to the nuclear fuel irradiations [9].

4.1 MICA

The MICA device (Material Irradiation Capsule) has the same performances than the current CHOUCA test device widely used in OSIRIS reactor, i.e. irradiation of various geometries of samples in NaK (up to 450°C) or gas (up to 1000°C). These test devices are mainly foreseen for in core irradiations where fast flux can reach up to 9dpa a year (at 70 MW). Since adaptation studies were necessary to fit to JHR and a couple of years were available before the manufacturing of first batch of MICA, additional studies have been launched in two main directions:

- the specificities of JHR, in terms of test devices outline dimensions, lead to an advanced integrated head of device. The main defined constraints are the handling procedure and the co-activity in the reactor pool during the few days of refuelling (inter cycles). The nowadays design embeds the gas circuits control components (valves, pressure sensors, connection) and the current electrical connections (instrumentation and electrical heating). These numerous modifications, compared to former CHOUCA device, lead to manufacture a prototype of a MICA head completed late 2011 and tested in 2012: easiness of changing sensors, plugging/unplugging actions, tests with remote manipulator arms, tightness of circuits...
- the multipurpose carrier that MICA represents leads to keep most of widely former concepts that made CHOUCA devices successful but improve their thermal behaviour in order to meet the requirements, particularly in temperature precision and gradients mastering. The previous technological solutions chosen for the CHOUCA electrical elements have been reassessed to make the additional electrical heating more predictable in terms of modelling. Moreover, a special effort will be done in the determination of reactor gamma heating with qualification measurement during the start-up phase of JHR.

4.2 CALIPSO

The CALIPSO device (in-Core Advanced Loop for Irradiation in Potassium Sodium) meets the original need of a low temperature axial gradient (a maximum of 8 °C) all along the sample holding, in liquid metal coolant (NaK), up to 450°C for a first step of development, and up to 600°C in a second phase. The locations of such devices are the same than MICA devices. The design is based on an embedded thermo hydraulic loop, including a heater, an electromagnetic pump and an exchanger. The setting of each parameter (power of heater, flow of the pump and efficiency of exchanger) leads to a full control of the thermal conditions inside the test device and in particular in the sample location. The most difficult component turns out to be the pump, mostly because of dimensional and density of integration. Different technical solutions have been tested at the late 2011, and for mid 2012 the final prototype should be operational.

The layout of such a liquid metal coolant loop has been done in the past, particularly for fast reactor samples irradiations. Nevertheless, these former devices had an external loop very restrictive for both handling and safety point of view. Because safety rules became more rigorous and handling in JHR more time-consuming, CALIPSO with its embedded coolant loop represent a real innovative test device.



Design



Prototype

Figure 3 – CALIPSO pump

4.3 OCCITANE

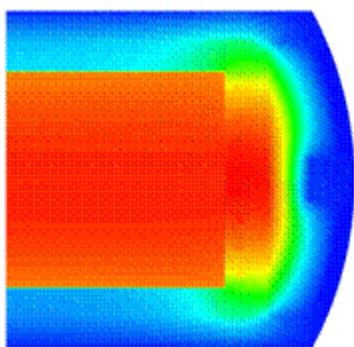


Figure 4 – Thermal calculation in OCCITANE device at 0.6W/g.

In the field of pressure vessel steels of NPPs, irradiations are carried out to justify the safety of this 2nd containment barrier and to improve its lifetime. CEA is designing a hosting system named OCCITANE (Out-of-Core Capsule for Irradiation Testing of Ageing by Neutrons), which will allow irradiations in an inert gas at least from 230 to 300°C. It will be implemented in the JHR reflector and reach damage rate about 100mdpa/year ($E > 1\text{MeV}$). The associated instrumentation will include at least thermocouples and dosimeters as close as possible to the samples. OCCITANE is based on IRMA device of OSIRIS. The design studies consist mainly in decreasing thermal gradient in the sample area (figure 4) and in integrating the capsule to the JHR environment.

4.4 Corrosion loop

Due to ageing of the NPPs, stainless steel core components undergo increasing radiation doses, which enhance their susceptibility to local corrosion phenomena, known as irradiation-assisted stress corrosion cracking (IASCC) [10]. Cold laboratories can study and model SCC phenomena; but to really be representative of LWR environments, these studies

need integral tests to take into account irradiation effects (radiation dose and flux) in MTRs. To answer to these industrial needs and in collaboration with DAE teams (India), CEA has just begun the design of a LWR corrosion loop, which will be located in the JHR reflector close to the tank. Its design will integrate the operational experience accumulated by the existing corrosion loops in cold laboratories at CEA and of course by the existing MTRs. A special attention will relate to the instrumentation associated with this device and will be based on the conclusions of the European program MTR+I3 [11].

4.5 About Gen IV

Right now, CEA anticipates the fourth generation research program; a first analysis of the SFR or GFR irradiation needs for materials and fuels has been performed. Accordingly, some feasibility studies have begun in order to prepare future irradiations in JHR. As example, CEA studies the feasibility of a transmutation capsules, of an in-core high temperature device with a large capacity, of metal liquid loops,...

5. Conclusions

The Jules Horowitz Reactor, even if it follows in the continuity of OSIRIS Reactor, has been designed with improved nuclear performances as well as handling constraints. Therefore all test devices, and in particular those foreseen in material irradiation, take into account the peculiarities of the JHR. Moreover, the constant improvements of modelling induce the associated qualification experiments to more accuracy and representing appropriately the modelling conditions. Thus, intense efforts of development are on progress on test devices design to match to requirements and provide around experimental samples accurate, mastered and reproducible physical and chemical conditions.

References

- [1] D. Iracane, and al., "Jules Horowitz Reactor: a high performance material testing reactor," *Comptes Rendus Physique*, vol. 9, pp. 445 – 456, 2008.
- [2] F. Rozemblum, and al., "Irradiation rigs in material testing reactor from OSIRIS to JHR," in *Fontevraud 7*. Avignon, France: SFEN, 26-30 September 2010.
- [3] M. Boyard, and al., "The Jules Horowitz Reactor core and cooling system design." Gaithersburg: IGORR 10, September 2005.
- [4] J. Dupuy, and al., "Jules Horowitz Reactor: general layout, main design options resulting from safety options, technical performances and operating constraints." Gaithersburg: IGORR 10, September 2005.
- [5] C. Pascal, and al., "Jules Horowitz Reactor: experimental capabilities." Gaithersburg: IGORR 10, September 2005.
- [6] G. Bignan, and al., "The Jules Horowitz Reactor: a new european MTR open to international collaboration, description and status." Knoxville, IGORR 13, September 2010.
- [7] D. Parrat and al., "Non-destructive examination benches and analysis laboratories in support to the experimental irradiation process in the JHR" Knoxville IGORR 13, Sept. 2010.
- [8] P. Roux, and al., "The MADISON experimental hosting system in the future Jules Horowitz Reactor." Knoxville - TN - USA: IGORR 13, September 19-24 2010.
- [9] T. Dousson and al., "Experimental devices in JHR dedicated to the fuel studies in support to the actual and future nuclear power plant." Prague: IGORR 14, March 18-22 2012.
- [10] M. Postler and al., "The influence of corrosion potential on stress corrosion cracking of stainless steels in PWR primary coolant environment," in *Electrochemistry in LWR*: , Eds. R. Bosch and al., , EFCP no. 49, 2007, pp. 107–121.
- [11] J. Dekeyser, et al., "Integrated infrastructure initiatives for material testing reactor innovations," *Nuclear Engineering and Design*, vol. 241, no. 9, pp. 3540 – 3552, 2011

SUPERCRITICAL-WATER EXPERIMENTAL SETUP FOR IN-PILE OPERATION

M. MILETIĆ

Czech Technical University in Prague, Department of Nuclear Reactors, marija_miletic@live.com

M. RŮŽIČKOVÁ, R. FUKAČ

Research Centre Rez Ltd., Rez, Czech Republic, ruz@cvrez.cz

I. PIORO, L. GRANDE

University of Ontario Institute of Technology, Oshawa, Ontario, L1H 7K4, Canada, Igor.Pioro@uoit.ca

ABSTRACT

The main goal of the Generation-IV nuclear-energy systems is to address fundamental research and development issues, which are necessary to establish the viability of next-generation reactor concepts to meet future needs for clean and reliable energy production. Generation-IV reactor concepts are being developed to use more advanced materials, coolants and higher burn-ups fuels, while keeping nuclear reactors safe and reliable.

One of the six Generation-IV concepts is a SuperCritical Water-cooled Reactor (SCWR), which continues the utilization of well-known light-water-reactor technologies. The Research Centre Rez Ltd. has taken part in a large European joint-research project dedicated to Generation-IV light-water reactors with motivation to contribute to the fundamental research and development of SCWRs by designing and building a test facility called “SuperCritical Water Loop (SCWL)”.

The main objective of this loop is to serve as an experimental facility for in-core and out-of-core corrosion studies of structural materials, testing and optimization of suitable water chemistry for future SCWRs, studies of water radiolysis at supercritical conditions, performance of bundle designs and nuclear fuels.

SCWR coolant is an aggressive medium. Fuel-channel materials must comply with temperature-design criteria to ensure safety. The industry accepted limit for the fuel centerline temperature is 1850°C, and the design limit for sheath (clad) temperature is up to 850°C. Preliminary material investigations have been conducted with existing Nuclear Power Plant (NPP) fuel-channel materials and uranium dioxide (UO₂) fuel within SCWR conditions. This study indicated that the fuel centerline temperature of UO₂ may exceed the industry accepted limit. Zirconium alloys are a popular choice for sheath materials in current NPPs due to low thermal-neutron absorption. However, corrosion rates increase significantly beyond 350 – 500°C, which make this alloy unsuitable for SCWRs. Therefore, alternative fuels and new sheath materials have to be defined and tested within the SCWR conditions.

This paper summarizes the concept of the SCWL, its design, utilization and first results obtained from non-active tests already performed within the supercritical-water conditions.

1. Introduction

The demand for clean, non-fossil-based electricity is growing. Therefore, the world needs to develop new nuclear reactors with higher thermal efficiencies in order to increase electricity generation and decrease detrimental effects on the environment. The current fleet of Nuclear-Power Plants¹ (NPPs) is classified as Generation II and III. Just a limited number of Generation III+ reactors, mainly, Advanced Boiling Water Reactors (ABWRs), operate in some countries. However, all these designs (related only to water-cooled reactors) are not as energy efficient because their operating temperatures and pressures are relatively low, i.e., below 350°C for a reactor coolant and even lower for a steam-power cycle (286°C at a pressure of 7 MPa). Currently, a group of countries, including Canada, European Union (EU), Japan, Russia, USA and others have initiated an international collaboration to develop the next-generation nuclear reactors (Generation-IV) and corresponding to that NPPs. The ultimate goal of developing such reactors is to increase NPP thermal efficiencies from 30 - 35% to 45 - 50%, which is the current level of advanced thermal power plants (supercritical-pressure coal-fired and natural-gas combined-cycle power plants). This increase in thermal efficiency would result in a higher production of electricity compared to current Pressurized-Water-Reactor (PWR) or Boiling-Water-Reactor (BWR) technologies per 1 kg of uranium.

However, accounting that the vast majority of modern power-nuclear reactors are water-cooled reactors we consider an SCWR concept as the most viable option for further development. Concepts of nuclear reactors cooled with water at supercritical pressures were mainly studied in the USA and Russia as early as the 1950s and 1960s [1]. After a 30-year break, the idea of developing nuclear reactors cooled with supercritical water became attractive again as the ultimate development path for water cooling. Many countries (Canada, China, Germany, Japan, South Korea, Russia, USA and others) have started to work in this direction. However, none of these concepts is expected to be implemented in practice before 2020 – 2025.

The main objectives of using supercritical water in nuclear reactors are to: 1) Increase thermal efficiency of modern NPPs from 30 – 35% to about 45 – 50%, 2) Decrease capital and operational costs and hence, decrease electrical-energy costs, and 3) Allow for the co-generation of hydrogen through thermochemical cycles.

SCW NPPs will have much higher operating parameters compared to NPPs (a pressure of about 25 MPa and an outlet temperature up to 625°C), and simplified flow circuit, in which steam generators, steam dryers, steam separators, etc. can be eliminated. Also, higher supercritical-water temperatures allow direct thermochemical production of hydrogen at low cost [2].

The design of SCW nuclear reactors is seen as a natural and ultimate evolution of today's conventional water-cooled reactors [1]. Development of SCWRs is based on the following four known technologies: 1) modern PWRs, which operate at pressures of 15 – 16 MPa, i.e., rather high pressures; 2) BWRs, which have a once-through or direct-cycle design; 3) modern supercritical turbines with pressures about 23.5 - 38 MPa and inlet temperatures up to 625°C, which have been successfully operating at coal-fired thermal-power plants for more than 50 years (see Fig. 1); and 4) nuclear steam reheat with outlet steam temperatures well beyond the critical temperature of water (up to 550°C), but at pressures below the critical pressure (3 – 7 MPa), which was implemented in some experimental reactors to increase the gross thermal efficiency of NPP (for details, see Fig. 2 and Table 1) [3].

¹ In 2012, 435 power reactors are operating around the world including 388 water-cooled reactors: 270 PWRs, 84 BWRs, 47 Pressurized Heavy-Water Reactors (PHWRs), and 15 Light-water Graphite-moderated Reactors (LGRs) or RBMKs; 17 Gas-Cooled Reactors (GCRs) and Advanced GCRs (AGRs) (both types cooled with subcritical carbon dioxide), and 2 SFR.

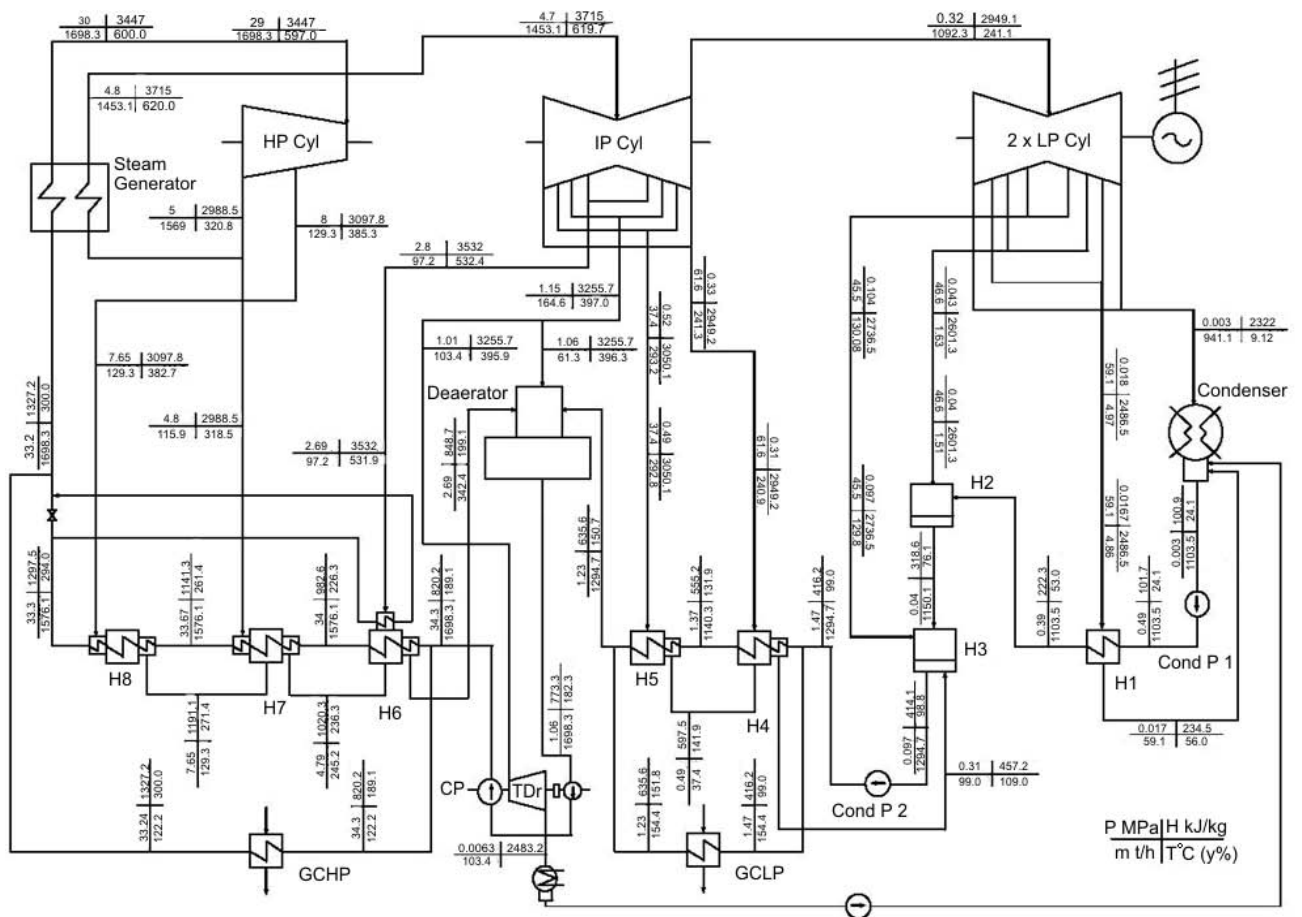


Fig. 1. Single-reheat-regenerative cycle 600-MW_{el} Tom'-Usinsk thermal power plant (Russia) layout [5]: Cyl – Cylinder; H – Heat exchanger (feedwater heater); CP – Circulation Pump; TDr – Turbine Drive; Cond P – Condensate Pump; GCHP – Gas Cooler of High Pressure; and GCLP – Gas Cooler of Low Pressure.

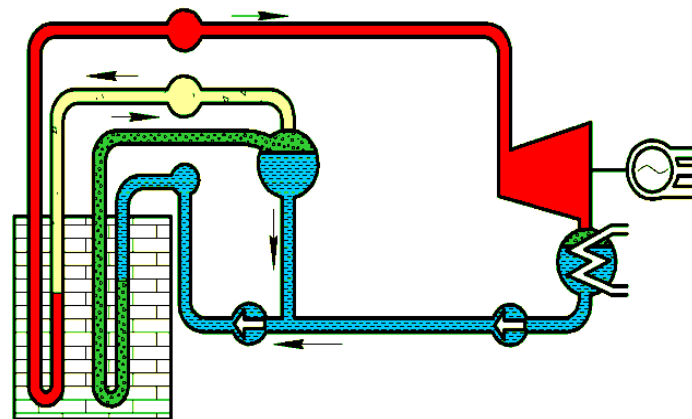


Fig. 2. Beloyarsk NPP (Russia) reactors schematic: Unit 2 with direct steam cycle (courtesy of Dr. Yurmanov, NIKIET, Russia):



Parameters	Before SRChs installation	After SRChs installation
Electrical power [MW_{el}]	60 – 70	100 – 105
Steam inlet pressure [MPa]	5.9 – 6.3	7.8 – 8.3
Steam inlet temperature [$^{\circ}\text{C}$]	395 – 405	490 – 505
Exhaust steam pressure [kPa]	9 – 11	3.4 – 4.0
Water mass flowrate (1 st loop) [kg/h]	1400	2300 – 2400
Pressure in steam separators [MPa]	9.3 – 9.8	11.8 – 12.7
Gross thermal efficiency [%]	29 – 32	35 – 36
Electrical power for internal needs [%]	10 – 12	7 – 9

Table 1. Average parameters of Beloyarsk NPP Unit 1 before and after installation of Steam-Reheat Channels (SRChs) [3].

In general, the SCWR concepts follow two main types, the use of either: (a) a large reactor pressure vessel (Fig. 3) with a wall thickness of about 0.5 m to contain the fuelled reactor core, analogous to conventional PWRs and BWRs, or (b) distributed pressure tubes or channels analogous to conventional CANDU^{®2} nuclear reactors. In general, mainly thermal-spectrum SCWRs are currently under development worldwide. However, several concepts of fast SCWRs are also considered [4].

1.3. Pressure-vessel SCWRs

The pressure-vessel SCWR concept is developed in China, EU, Japan, Russia and some other countries (Fig. 3). This type of reactor uses a traditional high-pressure circuit layout. However, due to significantly reduced flow rates (at supercritical conditions flow rates can be up to 8 times less than those in current reactors), high outlet temperatures and high heat fluxes significant fuel-sheath temperature non-uniformities may appear, which in turn can lead to sheath damage. Another challenge associated with pressure-vessel SCWRs is the manufacturing of pressure vessel due to quite large wall thickness. Also, in pressure-vessel reactors nuclear steam reheat at subcritical pressures is not possible inside a reactor. More information on thermal and fast pressure-vessel SCWRs can be found in the latest book [4].

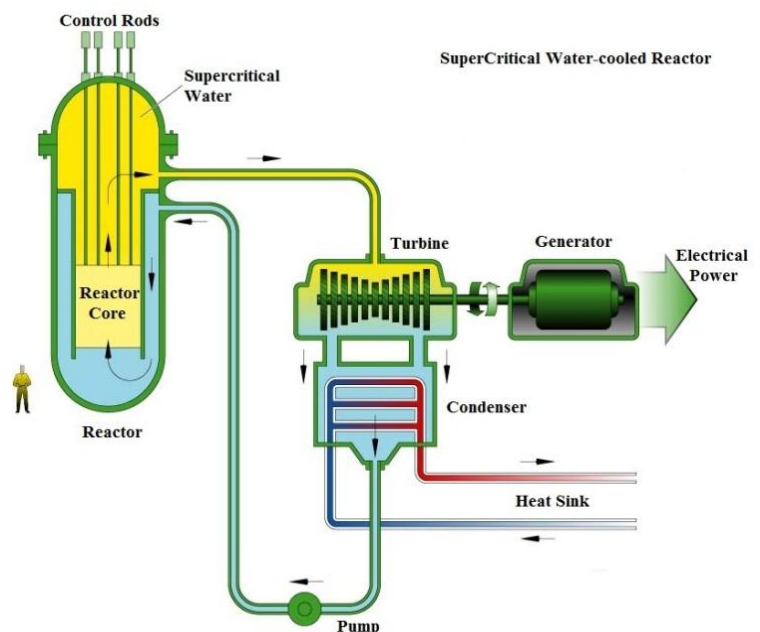


Fig. 3. Pressure-vessel SCWR schematic (courtesy of DOE USA).

1.4. Pressure-channel SCWRs

The pressure-channel SCWR designs are developed in Canada (Fig. 4) and Russia [1]. Within those two main classes, pressure-channel reactors are more flexible to flow, flux and density changes than pressure-vessel reactors. In addition, nuclear steam reheat can be implemented inside a pressure-channel SCWR based on the experience obtained from

² CANDU[®] (CANada Deuterium Uranium)

operating experimental BWRs in 60's and 70's (see Fig. 2, Table 1), which makes it completely suitable to modern supercritical direct single-steam-reheat-cycle turbines. All these factors make it possible to use the experimentally confirmed, better solutions developed for these reactors. One of them is channel-specific flow-rate adjustments or regulations. Also, a pressure tube at such pressures will have a wall thickness of about 10 – 15 mm (see Figs. 4 and 5) compared to about 400 – 500 mm for a pressure vessel. Therefore, a design whose basic element is a channel, which carries a high pressure, has an inherent advantage of greater safety than large vessel structures at supercritical pressures.

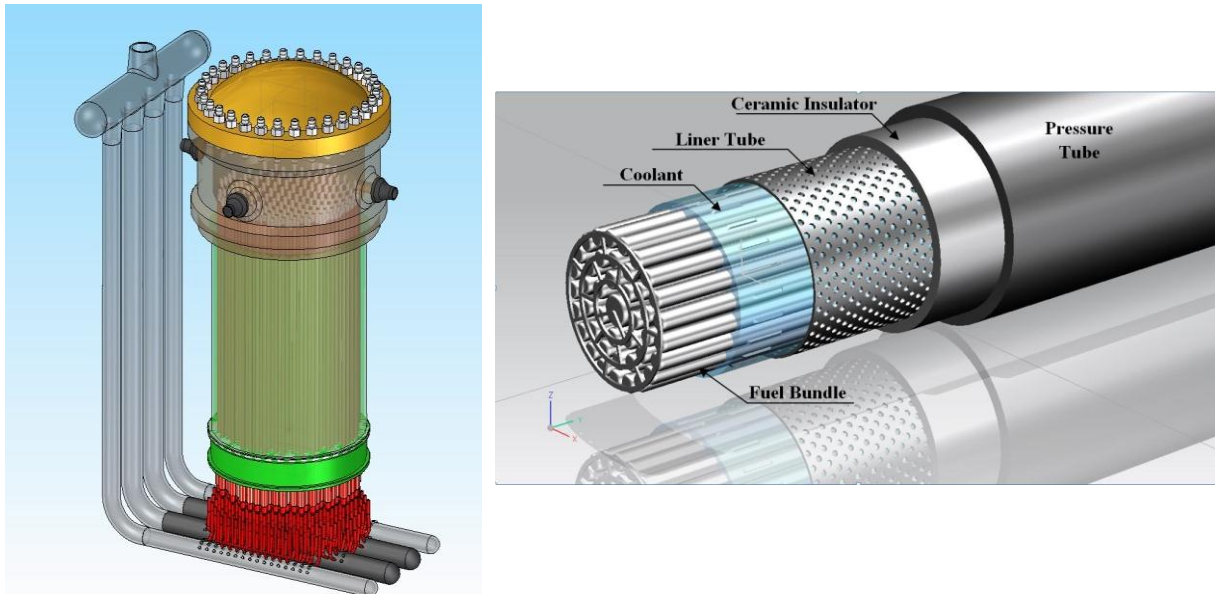


Figure 4. Left is the vertical core-configuration option (courtesy of AECL) and figure on the right represents the High-Efficiency Channel (HEC) with ceramic insert (AECL design) (drawing prepared by W. Peiman, UOIT).

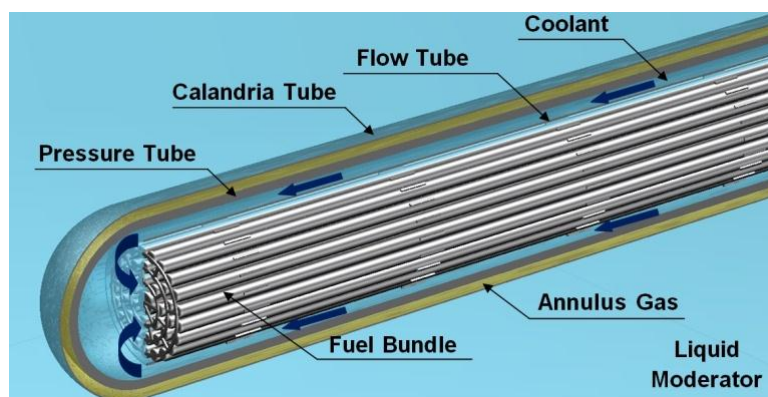


Fig 5. Re-Entrant Channel (REC) with annulus gas as thermal insulation for SCWR with liquid moderator (drawing prepared by W. Peiman, UOIT).

The major problem for SCWRs development is reliability of materials at high pressures and temperatures, high neutron flux and aggressive medium such as supercritical water. Unfortunately, up till now nobody has tested candidate materials at such severe conditions. Some candidate materials proposed by Russian scientists include Ferritic/Martensitic (F/M) steels, austenitic stainless steels, and nickel alloys (Inconels) for fuel sheath temperatures up to 600, 650, and 700 – 750°C, respectively [6]. Therefore, testing candidate materials and water chemistry within operating conditions of SCWRs (pressures 24 – 26 MPa;

temperatures 280 – 625°C and neutron flux about or higher than 10^{18} n/m²s) in an in-pile supercritical-water loop is the most important task of today.

A preliminary study of a generic PT-type SCWR showed that a centerline temperature of the uranium-dioxide fuel can be higher than that in modern water-cooled reactors (see Figure 6). Therefore, conventional fuels such as UO₂, MOX and ThO₂ have to be tested at higher temperatures for a possible use in SCWRs.

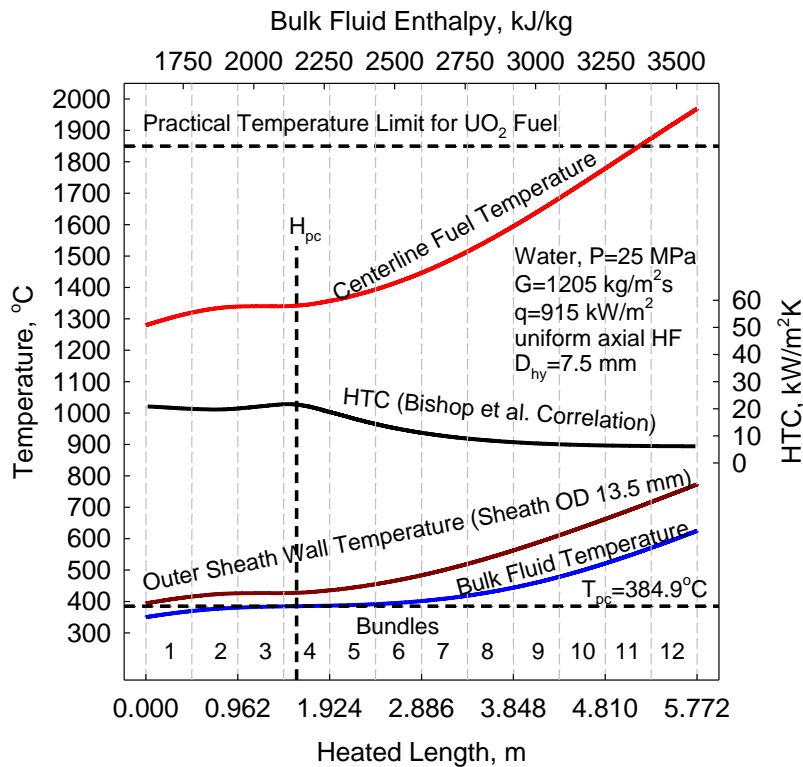


Fig. 6. Temperature and HTC profiles along heated length of fuel channel (fuel centerline temperature based on average thermal conductivity of UO₂).

In regard to nuclear fuels, a potential fuel must have a high melting point, high thermal conductivity, good irradiation, mechanical stability, and chemical compatibility with the sheath and the coolant [7]. These requirements eliminate various nuclear fuels categorized as metallic fuels, because of their low melting point, high irradiation-induced creep, and high irradiation swelling [7]. On the other hand, ceramic fuels have promising properties, which make these fuels suitable candidates for SCWRs and other high-temperature applications.

For a steady-state analysis at normal operating conditions, melting point and thermal conductivity are the most important thermophysical properties of a fuel. The thermal conductivity of the fuel governs the rate of heat-transfer removal from the fuel at specific conditions, while the melting point of the fuel determines the margin between an operating temperature and the melting point of the fuel. Consequently, these two factors influence the design of a fuel bundle as well as the selection of a fuel [21]. Thus, a higher thermal conductivity and melting point would allow increasing the thermal power generated per fuel bundle compared to that associated with a fuel, which has a lower thermal conductivity or melting point.

The UO₂ has been used as a fuel of choice in most commercial nuclear reactors such as PWRs, BWRs, CANDU reactors, etc. As shown in Fig. 7, thermal conductivity of UO₂ is between 2 and 3 W/m K within the operating temperature range of SCWRs. Table 2 lists basic properties of several selected fuels at 0.1 MPa and 25°C [8-14].

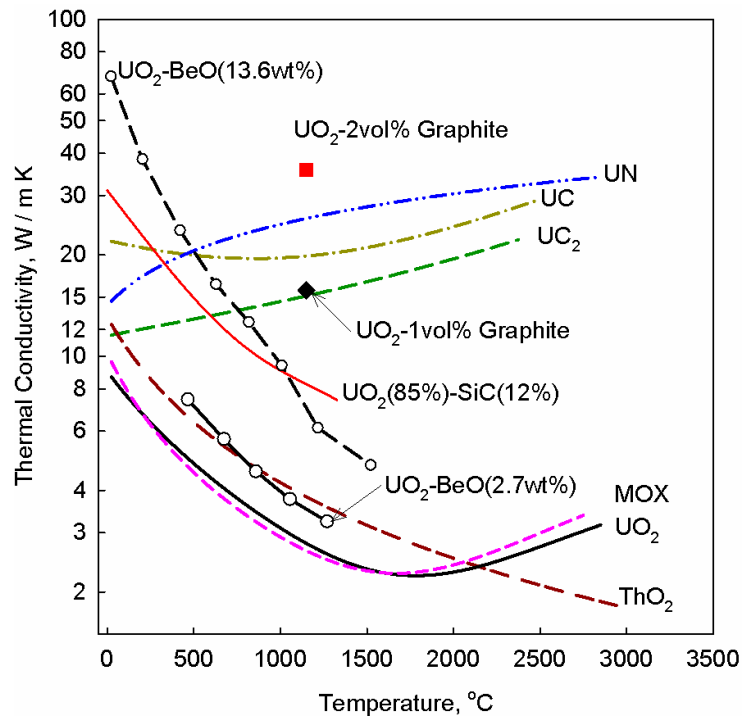


Fig. 7. Thermal conductivities of UO_2 , UN, UC and UC_2 , UO_2 plus graphite-fiber fuels as function of temperature [8-16].

Thoria or thorium dioxide (ThO_2) and Mixed OXide (MOX) are candidates for SCWR fuels, because of their resource availability. Uranium fuel is used in the majority of reactors. Thoria and MOX fuels supplement depleting uranium reserves. Thoria has the highest melting point among the nuclear fuels (see Table 2) and has an ability to use an open or a closed fuel cycle. MOX is the most sustainable fuel option since it is composed of irradiated fuel and promotes recycling of used fuel thus decreasing fuel wastes. Both Thoria and MOX have been used in test and even in some power reactors.

Another advantage of using ThO_2 and MOX is that are both proliferation compliant. Thoria does not produce plutonium and other transuranics elements compared to uranium cycles. MOX fuel has an ability to dispose of plutonium produced from weapons programs and from Light Water Reactor (LWR) fuel. This reprocessing reduces a stockpiling of plutonium in waste facilities. Moreover, ThO_2 and MOX have slightly higher thermal conductivity compared to that of UO_2 .

In spite of the fact that all the examined high thermal-conductivity fuels, i.e., alternative fuels such as UC, UC_2 and UN, showed significantly lower fuel centreline temperatures than those shown by the conventional low thermal-conductivity fuels (see Figs. 8 and 9), their other properties and behaviour are not well known. As a result, other factors such as a volumetric swelling, chemical compatibility, structural stability and thermal-shock resistance of these high thermal-conductivity fuels need to be taken into consideration.

Property	Unit	UO_2	MOX ³	ThO_2	UC	UC_2	UN
Molecular Mass	amu	270.3	271.2	264	250.04	262.05	252.03
Theoretical density	kg/m^3	10960	11,074	10,000	13,630	11,680	14,420
Melting Point	°C	2847±30	2750	3227±150	2507	2375	2850±30
Heat Capacity	J/kg	235	240	235	203	233	190

³MOX – Mixed Oxides ($\text{U}_{0.8}\text{Pu}_{0.2}$) O_2 , where 0.8 and 0.2 are the molar parts of UO_2 and PuO_2 .

Property	Unit	UO ₂	MOX ³	ThO ₂	UC	UC ₂	UN
	K						
Heat of Vaporization	kJ/kg	1530	1498	-	2120	1975±20	3325
Thermal Conductivity	W/m K	8.7	7.8 ⁴	9.7	21.2	11.57	14.6
Linear Expansion Coefficient, ×10 ⁻⁶	1/K	9.75	9.43	8.9 ⁵	10.1	18.1 ⁶	7.52
Electric Resistivity, ×10 ⁻⁸	Ω·m	7.32	-	-	250	120	146
Crystal Structure	-	FCC	FCC	FCC	FCC	BCT, <i>t</i> <1820°C FCC, <i>t</i> >1820°C	FCC

Table 2. Basic properties of selected fuels at 0.1 MPa and 25°C [8-16].

In regards to enhanced thermal-conductivity fuels, UO₂–BeO is the most suitable candidate. However, it should be noted that enhanced thermal-conductivity fuels are under development right now, and there is not enough information available about their properties and behaviour at irradiation and within supercritical conditions. Therefore, it is more likely that as the first stage conventional fuels will be used in SCWRs. Thus, in-pile and out-of-pile experiments with conventional fuels within the SCWR operating conditions are of significant importance for further development of these advanced reactors.

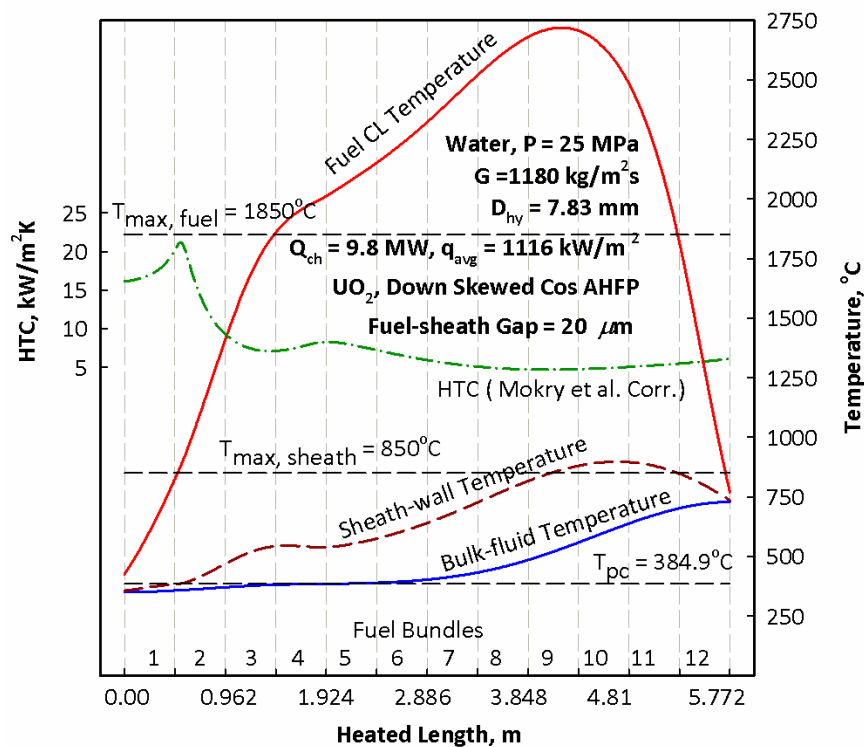


Fig. 8. Temperature and HTC profiles for UO₂ fuel at downstream-skewed cosine axial heat-flux profile (AHFP).

⁴ at 95% density

⁵ at 1000°C [18]

⁶ At 1000°C [18]

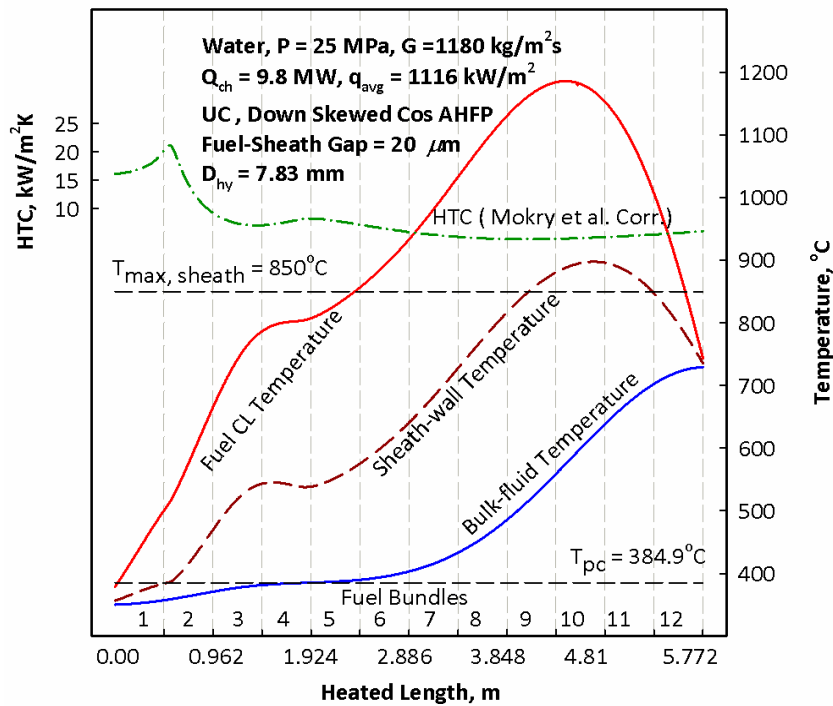


Fig. 9. Temperature and HTC profiles for UC fuel at downstream-skewed cosine AHFP.

2. Supercritical-water experimental setup for out-of-pile operation

Research Centre Rez Ltd. built the SCWL as a part of an European joint research project, called High Performance Light Water Reactor Phase 2 (HPLWR Phase 2) co-funded by the European Commission [19]. The loop is designed for operation inside research reactor LVR-15 in the Research Centre Rez Ltd. The major objective is using this experimental facility for corrosion studies of materials, studies of radiolysis in supercritical water and water chemistry optimization. The research reactor LVR-15 is located at the Research Centre Rez Ltd. in Rez; it is a light-water moderated and cooled tank reactor with forced-circulation cooling system. Since 2011, the reactor is entirely operated with low-enriched uranium fuel. Thermal neutron flux is about $1.5 \times 10^{18} \text{ n/m}^2\text{s}$ and fast flux is $2.5 \times 10^{18} \text{ n/m}^2\text{s}$. Average inlet water temperature is 43°C , and the outlet temperature is 48°C .

The following subsections summarize a basic design of the test loop with supercritical water, especially, focusing on the irradiation channel, which will be inserted inside the LVR-15 reactor core in the future for an in-pile operation of the loop. The SCWL loop will widen today's knowledge mainly in behavior of materials in supercritical water under irradiation conditions and will provide data for extending the radiolysis model from sub-critical to supercritical conditions. In the future, the loop shall also be equipped with a loading device for tests of materials on susceptibility to Irradiation Assisted Stress Corrosion Cracking (IASCC). The following groups of materials can be considered for testing: (i) austenitic stainless steels, (ii) ferritic/martensitic (F/M) steels and (iii) Ni-alloys; several steels are ODS (Oxide Dispersion Strengthened). However, ODS steels are under development, and Ni-based alloys are unacceptable for core structures due to high parasitic absorption of nickel. Water-chemistry regimes chosen for tests are the Normal Water Chemistry (NWC) simulated in autoclaves by additions of $\sim 150 \text{ ppb}$ oxygen, and Hydrogen Water Chemistry (HWC) – pure water with $\sim 30 \text{ cc/kg}$ hydrogen [20].

2.1. SCWL loop overview

The SCWL is a closed loop with forced circulation. It consists of the irradiation channel (which is to be located inside the LVR-15 reactor core) and auxiliary circuits next to the reactor in the reactor hall. The temperature and pressure in the testing area of the irradiation channel are 600°C and 25 MPa, correspondingly. Due to construction materials limitations for nuclear experimental devices, where the maximum surface temperature of material is 500°C for austenitic stainless steel, the target parameters inside the SCW irradiation channel can be achieved only in a restricted volume of the test section.

The SCWL loop consists of the following auxiliary circuits:

- Primary circuit: Irradiation channel, Regeneration exchanger, Cooler, Main circulating pump, Electrical heater, and Pressurizer
- Purification system
- On-line water-chemistry measurement system
- Sampling system
- Dousing system
- Cooling circuits (secondary and tertiary)
- System of organized leakage, and
- Control system and electrical installation

A scheme of the SCWL loop is shown in Fig. 10.

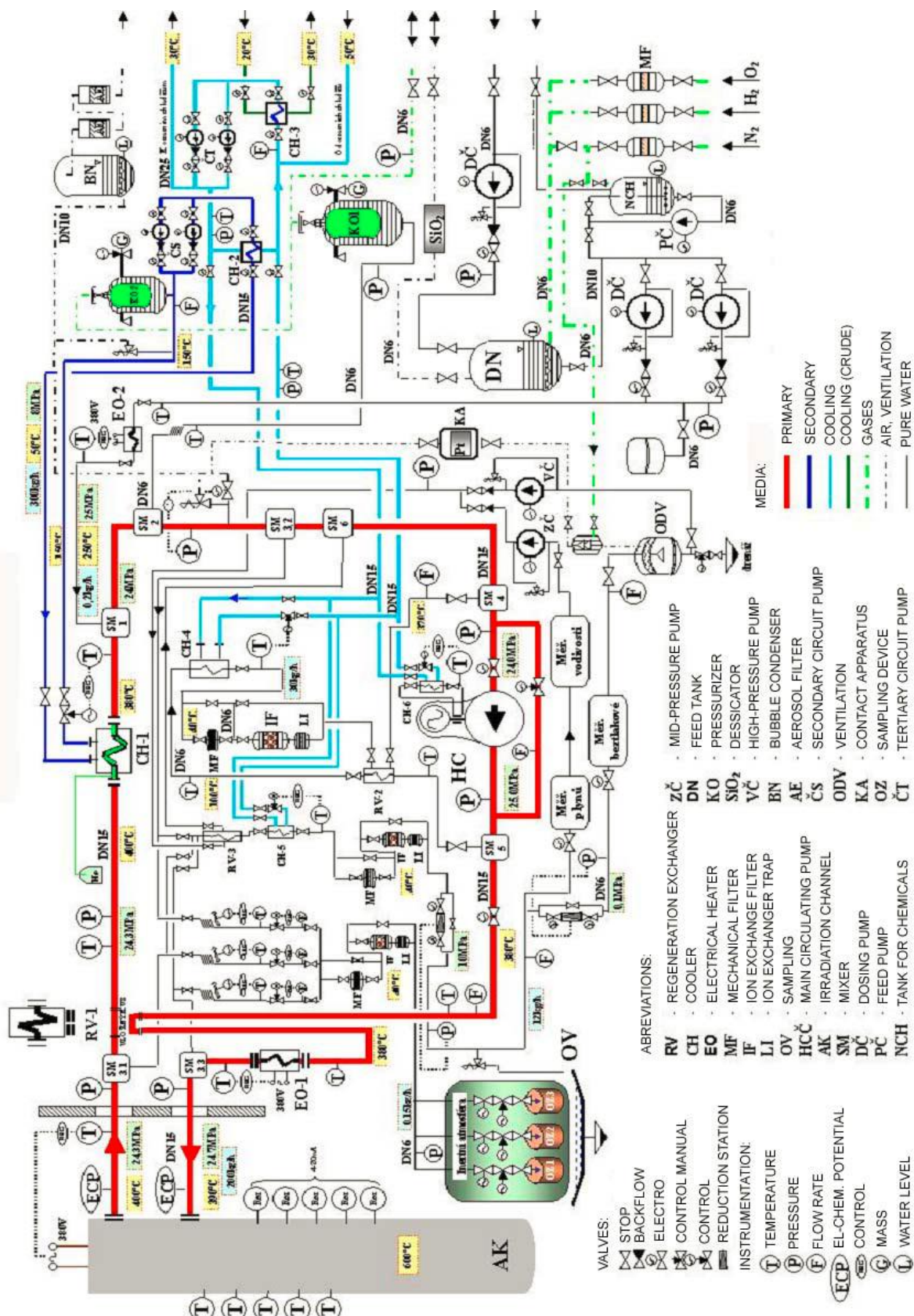


Fig. 10. Technological layout of auxiliary circuits of SCWL loop [19].

2.2. Irradiation channel description

The main part of the SCWL is its irradiation channel. The channel is a pressure tube positioned in the grid of the research reactor, being held in place by means of an aluminium “spacer”, which also provides thermal isolation of the pressure tube from reactor water.

The channel internals are formed by a headpiece with inlet and outlet tubes, several coaxial tubes (providing and directing the flow), heat exchanger, electrical heater, isolation elements and numerous fixing and stabilizing elements. The heat exchanger is placed above the sample area and is used to reach the test temperature inside that area. It is made of 36 stainless steel tubes 3×0.2 mm; six of these tubes are occupied by wiring of the electrical heating (see Fig. 12). This heat exchanger serves as recuperator that keeps the water temperature (and the wall surface temperature of the pressure tube) below the allowed limit of $\sim 450^{\circ}\text{C}$, which is the maximum operating temperature for pressure boundaries of nuclear experimental facilities. The recuperator together with complementary electrical heating, and eventually γ -heating while the reactor is in operation, serve to achieve the desired temperature inside the sample area, i.e., 600°C . The γ -heating of the LVR-15 reactor is estimated to reach ~ 17 kW for the SCWL. After leaving the sample area, water by-passes the electrical heater and enters the recuperator and finally exits the channel through the headpiece. Actual dimensions are 57-mm diameter and ~ 5000 -mm length.

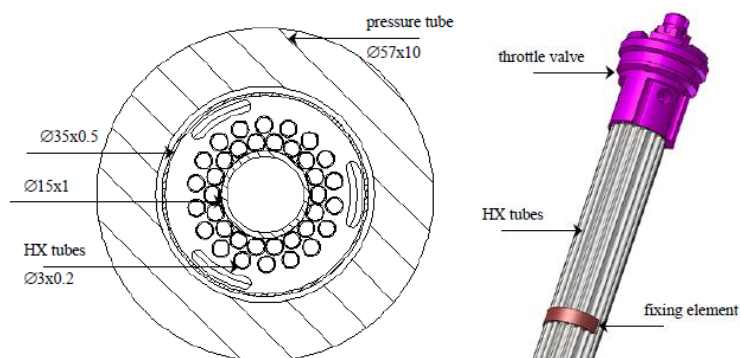


Fig. 11. Cross-section of the irradiation channel in the location of the regeneration exchanger and regeneration exchanger design [19].

The scheme of the flow through the irradiation channel is shown in Fig. 12.

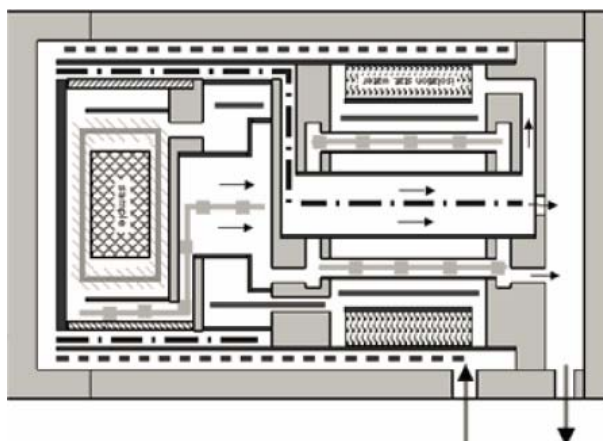


Fig. 12. Scheme of water flow through irradiation channel of SCW loop [20].

Additional heat source inside the irradiation channel is provided by an electrical heater, which power is limited by the available space inside the channel to ~ 15 kW.

2.3. Performed Tests

Phase I- trial period

During the first phase of SCWL testing, the main goal was to achieve operating parameters inside the loop and to compare calculated and simulated parameters with actual measurements. In the test section inside the irradiation channel, where the maximum parameters should have been reached, temperature of 550°C at 25 MPa was achieved [20]. The maximum design temperature of 600°C was not achieved due to the electrical heating, which was set to operate at 50% of nominal power, because of its malfunctioning limitations. Nevertheless, it has been adequately demonstrated that the expected maximum temperature of 600°C can be achieved with the available electrical power.

Phase II- loop non-active operation

The second phase of SCW testing was divided into two parts: 1) primary circuit testing and 2) irradiation channel testing.

The first tests were performed in dummy irradiation channel, where thermohydraulic losses were simulated. Pseudocritical point at 25 MPa was overcome by several degrees in primary circuit at inlet to the irradiation channel. The tests revealed minor flow instability and consequently temperature instability in the primary circuit. Consequently, a control valve was re-designed in order to improve regulating characteristics; and after repeating the tests, no flow instabilities occurred.

For the second test, the designed internals were inserted into the irradiation channel, a new headpiece with wiring was attached to thermocouples, and heating elements were connected to the channel [20]. This test followed the objective to achieve the maximum design temperature in the channel focusing also on water flow through the channel's internal parts and temperature distribution.

In order to reach the required temperature, water-flow optimization had to be performed by splitting the flow. Temperature distribution inside the channel is shown in Fig. 13.

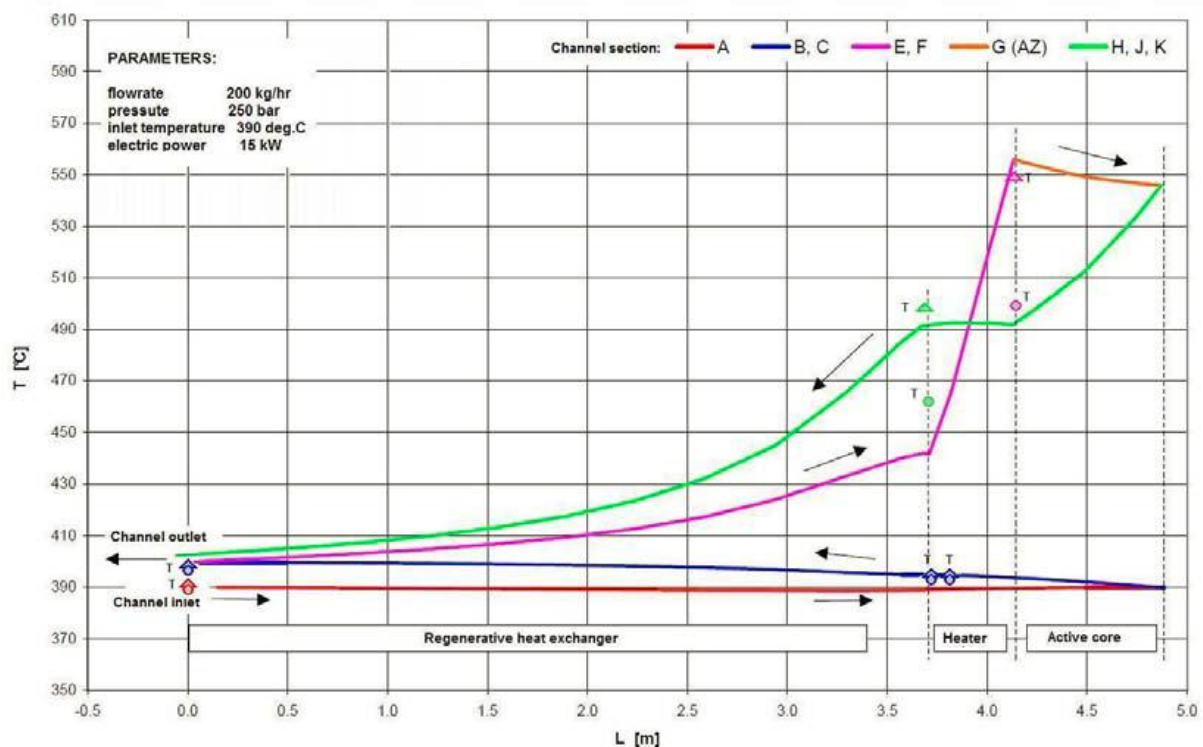


Fig. 13. Temperature distribution in irradiation channel – comparison of calculated and measured values* [20].

* Marked points represent real data measured during tests. Circle points represent temperature distribution at 200 kg/h flow rate through the channel and triangular points represent temperature distribution at flow splitting and with heating power reserve.

The heating power had to be limited due to unresolved problems with heating power control system. However, there was a very good agreement between calculated and measured data. Other measured parameters during this test are presented in Fig. 14.

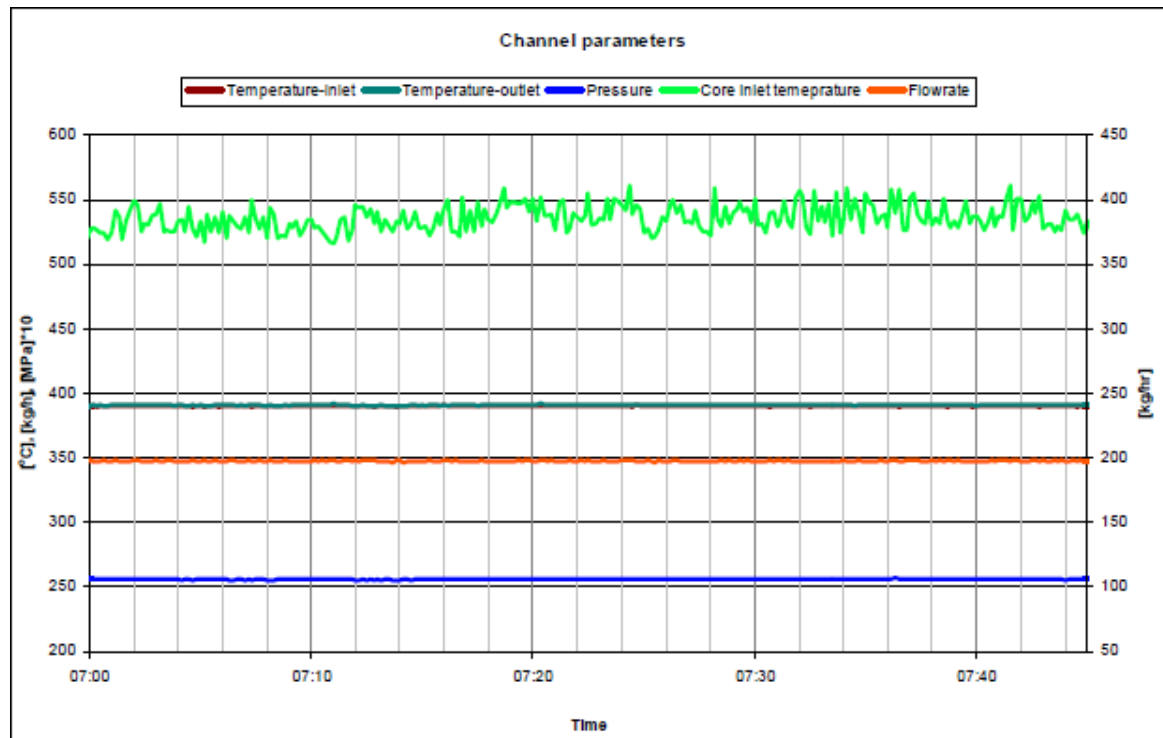


Fig. 14. Supercritical parameters in the SCWL during the non-active testing.

3. Conclusions

Accounting on the vast majority of water-cooled nuclear-power reactors in the world SCWR concepts are considered as the most viable option for Generation-IV reactors in many countries. Therefore, currently these high thermal-efficiency reactors are under development worldwide. The major problem for further development of SCWRs is reliability of materials, water chemistry and behavior of fuels at high temperatures and pressures, high neutron flux and aggressive medium such as supercritical water.

Therefore, to speed up these studies the SCWL was built at the Research Centre Rez Ltd. The SCWL is a unique facility, actually, one of the first such facilities in the world. Performed tests and obtained results from this loop will help in the future in understanding the supercritical state of water and utilization of that medium inside a nuclear reactor. Supercritical water is widely used in coal-fired thermal-power plants, but until today no one nuclear reactor operates with it. Therefore, research in this area, especially, building and operating the experimental device, which can be tested inside the reactor, will also help to understand better supercritical-water reactors as part of Generation-IV concepts. Planned tests in the SCWL loop within the area of corrosion, radiolysis and water chemistry in supercritical state of water will give enormous amount of data, which are necessary for designing and licensing SCW reactors in the future.

Recently, the SCWL loop irradiation channel was designed and tested at Research Centre Rez Ltd. This step was a big challenge considering the lack of information in this field, and technical limitations inside the loop itself such as space, maximum temperature, flow rate, etc., plus also very strict safety issues. After the first out-of-pile tests, we were able to justify a proper design of the irradiation channel, and it was verified that design parameters ($P = 25$ MPa and $T = 600^{\circ}\text{C}$) will be reached in the test section during in-pile testing. In the future it is planned that out-of-pile testing will continue for achieving the designed temperature of 600°C , and subsequently experiments with specific specimens of materials will be performed, consequently leading to the in-pile testing of the SCWL loop inside the LVR-15 research reactor.

Nomenclature

P	pressure, MPa
T	temperature, $^{\circ}\text{C}$
ν	specific volume, m^3/kg
ρ	density, kg/m^3

Subscripts

cr	critical
el	electrical

Abbreviations and Acronyms

AGR	Advanced Gas-cooled Reactor
ABWR	Advanced Boiling Water
AECL	Atomic Energy of Canada Limited
BCT	Body-Centered Tetragonal
BWR	Boiling Water Reactor
CANDU	CANada Deuterium Uranium
DOE	Department Of Energy
DPA	Displacement Per Atom
ECh	Evaporative Channel
FCC	Faced-Centered Cubic
F/M	Ferritic/Martensitic
GCR	Gas-Cooled Reactor
GFR	Gas-cooled Fast Reactor
GIF	Generation IV International Forum
HEC	High-Efficiency Channel
HPLWR	High Performance Light Water Reactor
HTC	Heat Transfer Coefficient
HWC	Hydrogen Water Chemistry
LFR	Lead-cooled Fast Reactor
LGR	Light-water Graphite-moderated Reactor
LVR-15	Light Water Reactor in Rez
MSR	Molten Salt Reactor
NIKIET	Russian acronym for RDIPE
NPP	Nuclear Power Plant
NWC	Normal Water Chemistry
ODS	Oxide Dispersion Strengthened
PHWR	Pressurized Heavy-Water Reactor
PWR	Pressurized-Water-Reactor
RBMK	Russian Acronym for Channel Reactor of High Power
REC	Re-Entrant Channel
SCC	Stress Corrosion Cracking
SCWL	Supercritical Water Loop
SCWR	SuperCritical Water-cooled Reactor
SFR	Sodium-cooled Fast Reactor
SRCh	Steam-Reheat Channel

St. St.	Stainless Steel
UC	Uranium Carbide
UC ₂	Uranium dicarbide
UN	Uranium Nitride
UOIT	University of Ontario Institute of Technology
UO ₂	Uranium dioxide
UO ₂ -BeO	Uranium dioxide plus Beryllium Oxide
VHTR	Very High Temperature Reactor

References

- [1] Pioro, I.L. and Duffey, R.B., Heat Transfer and Hydraulic Resistance at Supercritical Pressures in Power Engineering Applications, ASME Press, New York, NY, USA, 2007, 334 pages.
- [2] Naterer, G., Suppiah, S., Lewis, M., & Pioro, I. (2009). Recent Canadian advances in nuclear-based hydrogen production and the thermochemical Cu-Cl cycle. Int. J. of Hydrogen Energy (IJHE), 34, 2901-2917.
- [3] Saltanov, Eu. and Pioro, I., 2011. World Experience in Nuclear Steam Reheat, Chapter in book "Nuclear Power - Operation, Safety and Environment", Editor: P. Tsvetkov, INTECH, Rijeka, Croatia.
- [4] Oka, Y, Koshizuka, S., Ishiwatari, Y., and Yamaji, A., 2010. Super Light Water Reactors and Super-Fast Reactors, Springer, 416 pages.
- [5] Kruglikov, P.A., Smolkin, Yu.V. and Sokolov, K.V., 2009. Development of engineering solutions for thermal scheme of power unit of thermal power plant with supercritical parameters of steam, (In Russian), Proc. Int. Workshop "Supercritical Water and Steam in Nuclear Power Engineering: Problems and Solutions", Moscow, Russia, October 22–23, 6 pages.
- [6] Rodchenkov, B.S. and Yarmolenko O.A., 2009. Constructional materials for graphite-moderated reactors on supercritical parameters, (In Russian). Proc. Int. Workshop "Supercritical Water and Steam in Nuclear Power Engineering: Problems and Solutions", Moscow, Russia, October 22–23, 16 pages.
- [7] Chow, C. K. and Khartabil, H.F., "Conceptual Fuel Channel Designs for CANDU-SCWR", Journal of Nuclear Engineering and Technology, Vol. 40, 2008, pp. 1–8.
- [8] IAEA, "Thermophysical Properties of Materials for Nuclear Engineering: A Tutorial and Collection of Data", Vienna, Austria, 2008.
- [9] Kirillov, P.L., Terent'eva, M.I. and Deniskina, N.B., "Thermophysical Properties of Nuclear Engineering Materials", third ed. revised and augmented, Izdat Publ. House, Moscow, Russia, 2007.
- [10] Frost, B. R., "The Carbides of Uranium", Journal of Nuclear Materials, Vol. 10, 1963, pp. 265-300.
- [11] Cox, D. and Cronenberg, A., "A Theoretical Prediction of the Thermal Conductivity of Uranium Carbide Vapor", Journal of Nuclear Materials, Vol. 67, 1977, pp. 326-331.

- [12] Lundberg L. B. and Hobbins, R. R., "Nuclear Fuels for Very High Temperature Applications", Intersociety Energy Conversion Engineering Conference, San Diego, USA, 1992.
- [13] Leitnaker, J. M., and Godfrey, T. G., "Thermodynamic Properties of Uranium Carbide", Journal of Nuclear Materials, Vol. 21, 1967, pp. 175-189.
- [14] Khan, J. A., Knight, T. W., Pakala, S. B., Jiang, W. and Fang, R., "Enhanced Thermal Conductivity for LWR Fuel", Journal of Nuclear Technology, Vol. 169, 2010, pp. 61-72.
- [15] Solomon, A. A., Revankar, S., & McCoy, J. K. "Enhanced Thermal Conductivity Oxide Fuels." US Department of Energy, 2005 Project No. 02-180.
- [16] Ishimoto, S., Hirai, M., Ito, K. and Korei, Y. (1996). "Thermal Conductivity of UO₂-BeO Pellet." Journal of Nuclear Science and Technology, Vol. 33, 1996, No. 2, pp.134-140.
- [17] Gingerich, K. A., "Vaporization of Uranium. Mononitride and Heat of Sublimation of Uranium", Journal of Chemical Physics, Vol. 51, Iss. 10. 1969, pp. 4433-4439.
- [18] Bowman, A. L., Arnold, G. P., Witteman W. G. and Wallace, T. C., "Thermal Expansion of Uranium Dicarbide and Uranium Sesquicarbide", Journal of Nuclear Materials, Vol. 19, 1966, pp. 111-112.
- [19] Ruzickova, M., Hajek, P., Smida S., Vsolak, R., Petr, J., Kysela J. "Supercritical water loop design for corrosion and water chemistry tests under irradiation", The 3rd Int. Symposium on SCWR – Design and Technology, March 12-15, 2007, Shanghai, China.
- [20] Ruzickova, M., Vsolak, R., Hajek, P., Zychova, M., and Fukac, R. The supercritical water loop for in-pile materials testing", The 5th Int. Sym. SCWR (ISSCWR-5) Vancouver, British Columbia, Canada, March 13-16, 2011.
- [21] L. Leung, "Effect of CANDU bundle-geometry variation on dryout power", Proc. of ICONE-16, Paper #48827, p.8, ASME, Orlando, Florida, USA, (2008).



Jules Horowitz Reactor Project

Experimental Devices in Jules Horowitz Reactor dedicated to the fuel studies in support to the actual and future nuclear power plant

*Th. DOUSSON^(a), P. ROUX^(a), C. GONNIER^(a),
L. FERRY^(a), S. GAILLOT^(b), D. PARRAT^(c)*

*French Alternative Energies and Atomic Energy Commission (CEA²)
Nuclear Energy Division, Reactor Studies Department*

^aCEA, DEN-DER, building 225, CEA Cadarache, BP1, F-13108 Saint Paul lez Durance. FRANCE.

^bCEA, DEN-DTN, building 204, CEA Cadarache, BP1, F-13108 Saint Paul lez Durance. FRANCE.

^cCEA, DEN-DEC, building 151, CEA Cadarache, BP1, F-13108 Saint Paul lez Durance. FRANCE.

ABSTRACT

At the start-up of the Jules Horowitz reactor there will be a set of loops and capsules adapted to PWR and BWR conditions in order to test all kinds of LWR fuels:

- The first device **MADISON** (**M**ulti-rod **A**daptable **D**evice for Irradiations of experimental fuel **S**amples **O**perating in **N**ormal conditions) will reproduce the normal operating conditions of LWR power reactors (PWR, BWR or VVER, depending on the experimental need). It can be devoted to selection, characterisation or qualification experiments for up to height instrumented fuel rods.
- The second device, **ADELINE** (**A**dvanced **D**evice for **E**xperimenting up to **L**imits **I**rradiated **N**uclear fuel **E**lements) will be able to test a single experimental rod up to its operating limits. The first version, also called ADELINE “ramps” will allow clad failure during test protocol where as in the long term a second version will be dedicated to the post-failure behaviour coupled with a fission product laboratory.
- The third device, **LORELEI** (**L**ight water, **O**ne **R**od **E**quipment for **L**OCA **E**xperimental **I**nvestigations) is a capsule-type device and will perform experiments corresponding to accidental situations that may lead to limited fuel damage (including limited fuel fusion). This will occur with experiments reproducing the dewatering and the quenching phase of a LOCA sequence.

After a short reminder of the experimental service offer of the Jules Horowitz Reactor, this paper is firstly focused on the expected performances of each device and on their technical description as well as their associated experimental process.

1. Introduction - Experimental service offer of the Jules Horowitz Reactor

The Jules Horowitz (JHR) Material Testing Reactor will be operated from 2016 as an international user's facility on the CEA Cadarache site in the field of materials and fuels behaviour studies under neutron flux and also for medical applications with radio-isotopes production. To perform these types of irradiations, the JHR facility is designed to be flexible and adaptable to various requests in very large domains concerning type of samples (fuel or materials), neutron flux and spectrum, type of coolants and large thermal hydraulics conditions (LWR, Gen IV,...). A more detailed presentation of the project status is given in ref [1].

The main specific features of the JHR related to its experimental capability will be (cf. ref [2]):

- A high neutron fast flux within the core up to 10^{15} n/cm²/s (perturbed flux above 0.1MeV), and a high neutron thermal flux in the reflector (non perturbed flux up to 5.10^{14} n/cm²/s).
- High quality power ramp experiments up to 700 W/cm/min on one of the six displacement systems located around the core.
- Radiochemistry and dosimetry laboratories and in the long term a fission product analysis laboratory
- A set of hot cells, for recovery and management of fuel or material samples,
- Examinations capabilities that allow performing final checks before irradiation, post irradiation follow-up controls with a short delay and non-destructive examinations in dedicated hot cells.

This paper describes three types of devices dedicated to LWR fuel studies. These devices will be loaded on displacement systems located on the reflector of the core. These systems can move towards or from the core tank. They allow implementing easily and quickly linear power variations on the sample, and reaching representative power level and/or FP inventory (see fig. 1).

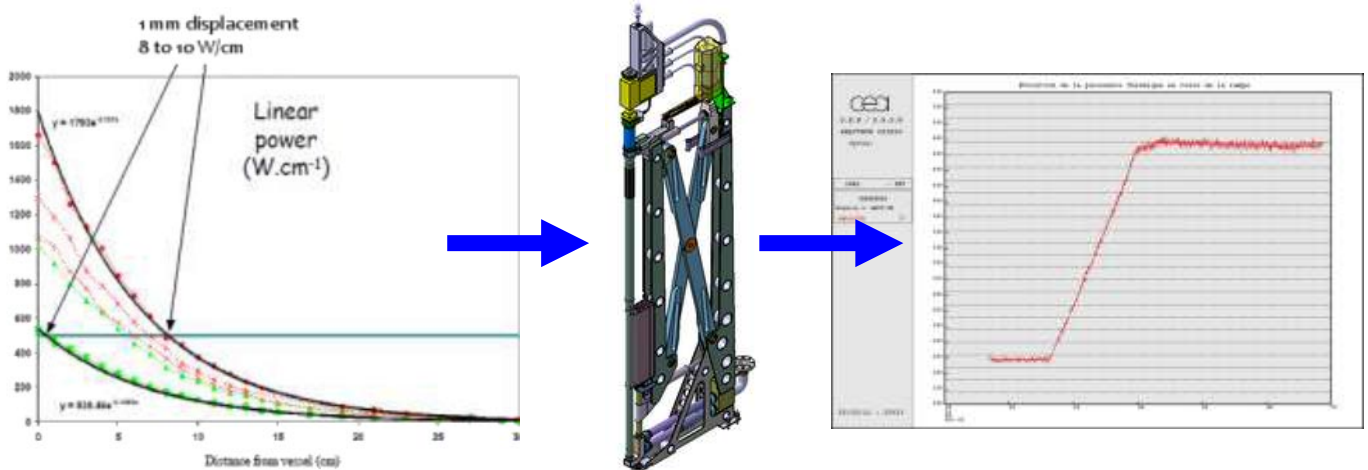


Fig. 1: Example of linear power variation made possible thanks to a speed control of the displacement system

The maximum speed of withdrawal is 50 mm/s. The total stroke of the displacement systems is 350 mm.

Such a concept is convenient for the operation (easy to handle, even during the operating cycle of the core) and for the safety (the safe back position and the off normal conditions of the device are not directly coupled to the core operations).

The JHR experimental processes of these devices will also take advantage from the non-destructive examination (NDE) benches, present in the facility, aiming at improving the experiment quality through NDE on full devices or sample holders by:

- Initial check of the experimental load status just before the beginning of irradiation (after transportation, assembling in JHR hot cell or insertion in the device),
- Adjustment of the experimental protocol after a first irradiation run at low power (sample evolution, power adjustment...),
- On the spot monitoring of the sample state after a test on the close-by gamma-X tomography stand (see fig.2) located in the reactor pool and with limited handlings (e.g. geometrical changes after an off-normal transient, quantification of short half-life fission product distribution...).



Fig. 2: Device on the gamma-X tomography stand

These three experimental equipments will make it possible to explore the fuel behaviour under different conditions: normal conditions, operating limits conditions and accidental situations.

2. MADISON device (normal conditions)

This experimental device will allow performing irradiations of LWR fuel samples when no clad failure is expected. Consequently, the experimental conditions will correspond to the normal operation of power reactors (steady states or slow transient that can take place in power plants) cf. ref [3].

An ability to reproduce operating conditions of power reactor plants

This experimental device is made of an in-pile part (holding the fuel samples) and situated on a displacement device of the JHR. This system allows an on-line regulation of the fuel linear power on the samples. Thanks to the high level of thermal neutron flux in the JHR reflector, this is possible to perform irradiation on high Burn Up samples at high linear power (this is possible to reach 400W/cm for a Burn Up of 80GW.d/t for a common UO₂ fuel of initial enrichment 4,95%: see fig 3).

The in-pile part is connected to a water loop providing thermal-hydraulics conditions expected for a given experimental program. The water loop will allow reproducing the thermal-hydraulics conditions of power reactors in term of water loop pressure, temperature, fluid velocity. In addition, in order to satisfy the need from all utilities and research institutes from the nuclear industry, the experimental device can adapt to conditions from all types of LWR reactor plant technologies (PWR, BWR or VVER). For the case of PWR reactor experiments, it will be possible to operate the water loop in normal conditions up to 160 bars and 320°C.

The water loop also allows a continuous regulation of chemical conditions thanks to a specific chemical analysis system and a water treatment system. Usual chemical conditions of power plants can be reproduced as well as specific chemical conditions (depending on customer needs).

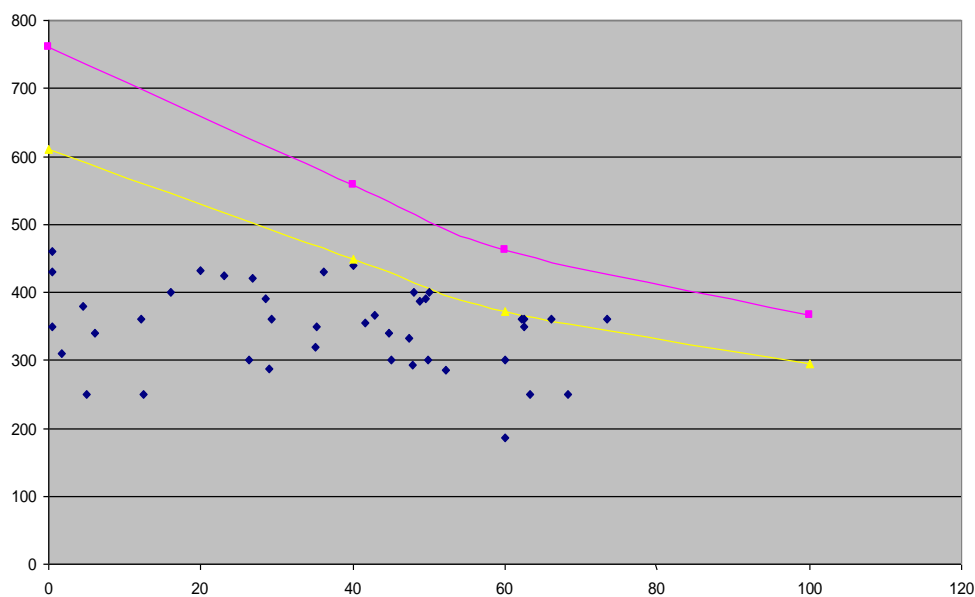


Fig. 3: Fuel linear power in function of Burn Up for a UO₂ fuel (4,95% enriched): Comparison of former PWR fuel experiments performed in MTR (blue dots) with MADISON performances: On pink curve the results are best estimate and on yellow curve, a margin of 20% is taken on the performances

A large and flexible hosting capacity

In order to satisfy the large range of experimental needs from the nuclear industry, the test section of the in-pile part has a very large volume. This will allow loading a large panel of sample holders.

Regarding the hosting capacity, of the MADISON device, it will be flexible enough to adapt to high embarking capacity sample holders (up to 8 samples) with low instrumentation or low embarking capacity sample holders (up to 1 sample), highly instrumented.

This flexibility in the hosting capacity offers customers the possibility to perform several types of experiments:

- Selection experiments: to irradiate numerous innovative samples in identical conditions and select the most promising products.
- Characterisation experiments: to irradiate few samples (1 or 2) with a lot of instrumentation and measure on-line physical properties of the products under neutron flux.
- Qualification experiments: to irradiate several samples under representative conditions of power reactors, in order to check if the products have adequate behaviour before using in power plants.

High performance instrumentation

The MADISON device will provide high performance instrumentations currently used in the nuclear industry. The first irradiation rig version will have a carrying capacity of 4 samples (with a maximum of 2 sensors per samples) and will be flexible enough to be operated with 2 samples (highly instrumented).

Some instruments will be fixed on the water loop and will measure on-line water loop thermal-hydraulics conditions (pressure, temperature, water flow, chemistry), and neutron flux conditions (thermal neutron flux, fast neutron flux). In addition, the design of the test section will allow an on-line measurement of the thermal balance in the test section that will provide a fuel samples linear power with 5% precision.

Some instruments will be implemented on the fuel samples. For that purpose, 5 tight connectors will be implemented on the sample holder to allow the plug-in of specific instruments. At present, the following instrumentation can be easily used in the first MADISON sample holder to be manufactured for the JHR start up:

- Fuel central temperature
- Clad temperature
- Clad elongation
- Fuel stack elongation
- Fuel plenum pressure

A second version of the MADISON sample holder is under investigation that will be based on the previous irradiation rig, but it will be limited to two rod samples equipped with diameter gauge.

3. ADELIN device (operating limits conditions)

Objectives of the ADELIN irradiation loop

The experimental LWR ADELIN loop which will soon start to be manufactured will be able to reproduce various experimental irradiation scenarios with experimental fresh or pre-irradiated fuel rods, such as:

- Power ramp tests,
- Rod internal over-pressurization ("lift-off"),
- Rod internal free volumes gas sweeping,

- Fuel centre melting conditions approach.

It will be a one rod experiment where clad failure will be allowed during the test protocol.

A first version will be mainly dedicated to power ramps testing. This will make it possible to continue the service offer and to operate with an experimental quality at least as good as the one already offered by ISABELLE1 loop in OSIRIS reactor. That means a qualified thermal balance and a good precision of the clad failure time and consequently a good knowledge of the linear power inducing the failure. Moreover, some enhancement will be added in order to make a quantitative clad elongation measurement during the power transient and to manage multiple experiences during a reactor cycle. This device can easily be upgraded in order to manage highly instrumented experiments with fuel and clad temperature measurement and fission gas release measurement.

In the long term, a second version will be dedicated to the post-failure behaviour coupled with a fission product laboratory.

ADELINE typical experimental scenario and performances

The device will accept different fuel samples types:

- PWR (including VVER type) and BWR fuel pellets from 5.5 mm up to 14 mm of diameter
- UO_2 fuels up to 12% enrichment of U5
- MOX fuels up to 20% ratio of Pu/(U+Pu)
- Rod length up to 600 mm
- Fresh fuel as well as high burnup fuel up to 120 GWd/t

The experimental sequence is envisaged in the following way (see fig. 4):

- A low power plateau that may last from one day to one week where it will be possible to maintain a clad temperature of 330°C ($\pm 10^\circ\text{C}$) while the linear power of the sample will be kept as low as 100 W/cm. Of course any higher value for this plateau will be allowed.
- A linear power ramp at a continuous rate ranging between 100 W/cm/min and 700 W/cm/min. During this increase of power, the clad surface temperature will be stabilized at $T_{\text{sat}} + \Delta T_{\text{sat}}$ as soon as the sample reaches 350 W/cm at its peak level.
- A high power plateau that may last 24 hours at a linear power up to 620 W/cm at the sample peak level.

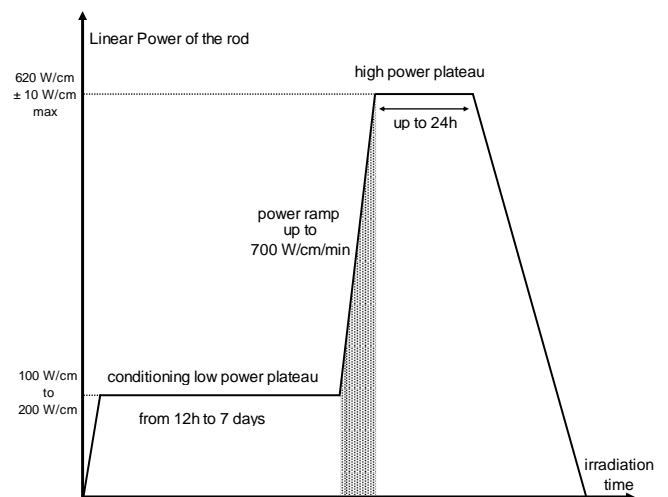


Fig. 4: standard power ramp test profile

If a failure of the clad were to occur during one of the last two phases, it would not necessary lead to the stop of the experiment. Indeed, the decision to end the experiment will be based on a certain level of contamination of the loop, not on clad failure detection.

Description of the loop

The loop is composed of two parts (see fig. 5):

An in-pile section, loaded on the displacement system, is subjected to the flux. It is composed of the following components:

- The containment made up of a strength tube and a light surrounding tube both in Zircaloy,

- The instrumentation holder containing the environment sensors and the so-called “jet pump” flow amplification system,
- The sample holder including the instrumented test rod to be tested,

The internal structures and the process are regulated thermally by the fluid in the loop. The fluid is injected from the out-of-pile section by circulation pumps operating simultaneously to obtain an overall flow rate of 50 g/s (called “inducing flow rate”). The fluid flows through a flow rate injection module used to re-entrain part of the flow in the test line and thus amplify the inducing flow rate. The amplification factor is around 4 to 5, resulting in a “useful” flow rate (also called “induced flow rate”) in the test channel of 200 g/s.

An out-of pile section is located in a 30 m² metallic liner covered cubicle close to its piping penetration. It includes the fluid circuit and the equipment needed to reproduce the thermal hydraulic conditions of the in-pile section.

The pressurization control is based on a simultaneous use of charging pumps and a depressurisation valve. The temperature control is done by the use of a 30 kW heater in the device head and a 40 kW heat exchanger in the cubicle. This main heat exchanger is cooled down by the experimental secondary cooling system of the facility and its convenient location (instead of inside the reactor pool) makes it possible to totally by-pass it in order to carry out energy saving during low power plateau phases.

A low pressure and low temperature system is installed in parallel of a part of the main loop. It mainly includes the filtration, the loop chemistry and coolant monitoring modules.

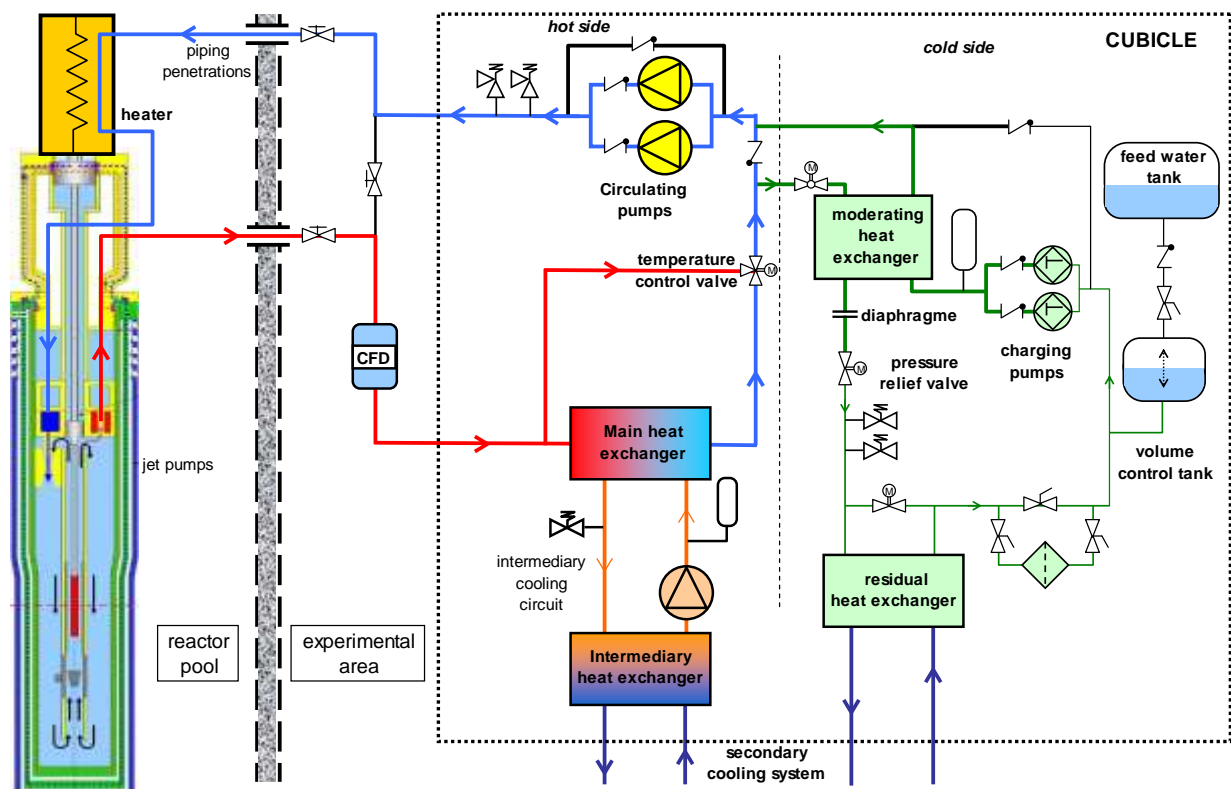


Fig. 5: Schematic diagram of the loop

Key features:

Easy and fast recovery of the sample:

An underwater transfer station has been designed in order to load and retrieve the sample holder without disconnecting the ADELIN device. It will avoid periods of unavailability of the experimental device due to its transfer toward the hot cells. This new tool will make possible to manage 3 to 4 ramp tests during a reactor cycle (about 25 days long).

High instrumented experiments:

The sample may be instrumented with a fuel centreline thermocouple and a cladding thermocouple. Moreover two capillary tubes connected to the top and the bottom free volumes of the rod may be used to sweep the gases (fission product and He) released by the fuel and to route them to the fission product laboratory in the JHR experimentation area.

Good accuracy of the thermal balance:

With an inlet temperature greater than 250°C at 160 bar and a fluid velocity greater than 0.8 m/s the thermal balance will be based on a differential temperature measurement greater than 20°C allowing a ± 10 W/cm accuracy on the peak linear power value at 620 W/cm.

4. LORELEI device (accidental situations)

The purpose of LORELEI device is investigating the behaviour (thermal-mechanical and radiological consequences) of LWR fuel rods under “Loss Of Coolant Accident” conditions. It will be situated in a reflector position on a displacement system of the JHR. The objective is not to simulate the thermal-hydraulic phenomena during the LOCA sequence but to simulate the clad burst conditions: temperature, pressure difference (internal /external pressure)

This equipment will consist in a pressurized (up to 130 bars) in-pile thermo-siphon able to cool a unique fuel sample with thermal conditions representative of current LWR power reactors (see fig. 6). It will be equipped with a gas injection able to rapidly empty the test device in order to simulate the dry-out of the fuel rod during the LOCA transient. A neutron screen can be used to flatten the neutron flux profile along the fuel sample. An electrical heater implemented in the sample holder will allow getting a homogeneous temperature distribution and will act as a dynamic thermal insulation in order to get representative adiabatic conditions; it will be switched-on at least during the initial heating, up to the clad burst (initial heat-up rate will be about 10 to 20°C/s). The high temperature phase (up to about 1200°C) will be monitored by adjusting the rod power with the displacement system. During this phase, the electrical heater will be switched-off in order to increase the heat losses and to prevent any temperature escalation due to the steam – zirconium reaction). At last, water can be re-injected in the device to simulate the quenching process.

A typical experimental process in this device will consist in a preliminary re-irradiation of the sample (several days with maximum linear power of 200W/cm) in order to produce a representative Fission Product inventory. It will continue with a dry out of the fuel sample simulating the Loss of coolant, a heat up phase of the fuel and a quenching by water injection.

This device will allow investigating ballooning and burst of the fuel cladding (the inner pressure of the fuel rod can be monitored to that purpose), clad corrosion phenomena (oxidation and hydriding), post quench behaviour and fission gas release (to that purpose, the device will be connected to the Fission Product laboratory).

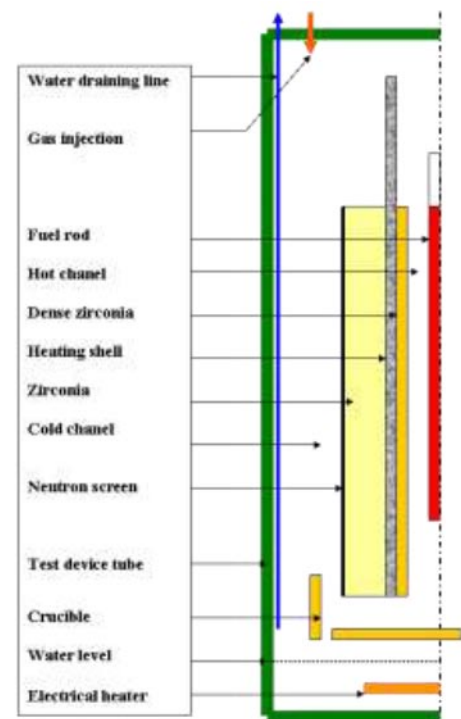


Fig. 6: LORELEI test device

This test device design is based on the “Griffon test device” which has been used in the SILOE reactor for the “FLASH program” (dedicated to LOCA). The design and the manufacturing of the test device are made in collaboration with the “Israel Atomic Energy Commission”, the last organization which joined the JHR consortium. The end of the test device manufacturing phase is foreseen in 2018.

5. Conclusion

As indicated in this paper, the experimental capacity for testing fuel under irradiation stays an important topic and CEA is maintaining significant R&D programs to improve the performances of the experiments (especially putting innovation on the experimental devices such as on-line instrumentation...). The combination of these three types of device will allow studying the fuel behaviour under any kind of operation conditions.

This continuous process leads to a strong feedback from the operation of OSIRIS (ISABELLE loop for ADELIN, GRIFFONOS for MADISON and LORELEI devices) and is of primary importance for the design of the hosting experimental systems of JHR and its NDE benches.

References

- [1] G.Bignan, X. Bravo, P.M.Lemoine, B.Maugard.
The Jules Horowitz Reactor: A new European MTR (Material Testing Reactor) open to International collaboration: Update Description and focus on the modern safety approach.
IAEA International Conference on Research Reactors: Safe Management and Effective Utilisation, 14-18 November, Rabat, Morocco
- [2] D. Parrat, G. Bignan, J.P. Chauvin, C. Gonnier
The future Jules Horowitz MTR:
A major European research infrastructure for sustaining the international irradiation capacity
9th International Conference on WWER Fuel Performance, Modelling and Experimental Support
17 – 24 September 2011, Burgas, Bulgaria.
- [3] P. Roux, C. Gonnier, D. Parrat, C. Garnier
The MADISON experimental hosting system in the future Jules Horowitz Reactor
13th IGORR meeting
September 2010 Knoxville, USA

Sudan Plans for a First Research Reactor: Driving Forces, Present Status and Way Ahead

M.H. Eltayeb¹, M. M. Eltayeb¹, S.A. Talha², A.M.E. Hassan¹, H. I. Gibrreel¹, A. Ibrahim¹, A.Y. Elamin¹, A. Ahmed¹, W.A. Abd Elbagi¹, M.E. Elhibir¹, S. Kamel¹, M. Ibrahim¹

- 1) Sudan Atomic Energy Commission*
- 2) Sudan Ministry of Electricity and Dams*

E-mail: tcsaec@gmail.com

Abstract:

Sudan Atomic Energy Commission (SAEC) is receiving assistance from the International Atomic Energy Agency (IAEA) to carry out a feasibility study for introducing Sudan first nuclear research reactor. The ultimate aim of establishing the reactor facility is to strengthen the national infrastructure for nuclear science and technology, support higher education and professional training programmes for nuclear applications and services and explore the possibility for the production of short lived radioisotopes for various applications in the fields of medicine, geology, agriculture, industry, environmental studies and non-destructive testing. The IAEA has provided Sudan with draft questionnaire for technology and safety infrastructure evaluation that is in addition to the IAEA publications in this regard.

A survey team has been established at SAEC and has studied the relevant IAEA documents and questionnaires. A further questionnaires dossier was developed after identifying the potential users of the proposed NRR. This dossier was designed for each individual organization and comprises questionnaires related to available and potential utilizations, identified groups and persons, human resource (HR) for acquisition, HR for operation and construction, infrastructure support for construction and operation, Legal, nuclear regulatory and physical security framework. Each subgroup of the survey team was assigned to a couple of organizations. An action plan with detail timeline was developed for the first three. It is expected that by analysing and interpreting the to-be-collected information together with a survey of the available NRRs, a detailed strategy plan with clear optimum utilization of the Sudan proposed NRR will be prepared. This plan will be the road map and together with the feasibility study where the 20 issues of the IAEA milestones approach will be addressed, constitute the full document to be submitted to the decision makers so as to make an informed decision for building a nuclear research reactor facility.

Sudan Atomic Energy Commission has concluded a memorandum of understanding with the Chinese Atomic Energy Institute for the establishment of research reactors in Sudan. An independent nuclear regulatory body, which, indeed will profit from the research reactor in strengthening its personnel capabilities, was established by a ministerial decree. Moreover, Sudan University for Science and Technology, through its newly established, Nuclear Engineering Department will, also, benefit from the research reactor project. In addition, the research reactor will form an ideal facility to train personnel from Sudan Ministry of Electricity and Dams for its nuclear power project.

Introduction:

Research reactors have played and continue to play a key role in the development of the peaceful uses of atomic energy. Their contribution to medicine, agriculture, industry, environmental sciences and education and training of scientists and engineers is well documented.

There are, currently, 672 constructed reactors around the globe from which 234 are operational. Research reactors underutilization forms one of the major problems facing the continuation of their operation. In that sense, IAEA has published a TECDOC on strategic planning for research reactors, to provide the rationale for a strategic plan, outline the methodology of developing such a plan and then gives a model that may be followed [TECDOC 1212]. Moreover, aging of research reactors and the need for refurbishment is an additional challenge which jeopardizes the availability of their products in the market.

Driving forces:

Sudan is planning to acquire its first RR to cover a broad range of possible applications and to promote the development of scientific research and technological development as well as to foster regional collaborative efforts in these areas. The establishment of the reactor in Sudan will also enable Sudan to acquire its own scientific base and fairly skilled cadres particularly as it embarks on launching of Nuclear Power Program. In addition to that, it will, also, help in strengthening the infrastructure for nuclear science and technology in the

country, providing technical facilities in the form of equipment and research tools to support higher studies and professional training programs, research, applications and services in nuclear science and technology at the Sudanese universities and scientific research centers. Moreover, establishment of the research reactor in Sudan will provide a training tool for manpower required for the management and operation of the nuclear power reactor for electricity production, which is presently under consideration. Furthermore, RR will help Sudan to produce short-lived radioisotopes for applications in several fields, including medicine, geology, agriculture, industry, environmental studies and non-destructive testing, particularly in the oil, sugar, cement, electricity production and various other industries. In this way it is expected to save resources that are currently used for the import of such radioisotopes from abroad.

Present status:

Sudan has concluded a project with IAEA with the objective of developing a RR strategic plan. For that purpose, SAEC has formed a project team with clear terms of reference for developing the strategic plan. The project team has established a work plan, and used the IAEA safety guides and standards and draft questionnaires for technology and safety infrastructure evaluation. The collection of data was followed by a fact finding mission conducted by IAEA. Lack of finance has created a major obstacle for the team to complete its work. Consequently, neither sufficient data was collected nor analyzed. Some fifty six personnel from different organizations have attended different activities in the field of nuclear reactors. The activities included scientific visits, technical meetings, workshops,

training courses and fellowships. Additionally, SAEC has signed a memorandum of understanding with China Institute for Atomic Energy (CIAE) for the purpose of establishing research reactors in Sudan and to help Sudan in developing the relevant human resources.

Way ahead:

Sudan has, recently, established a TC project with IATA with the following objectives:

- To establish the safety and technical infrastructures needed for establishment of the first research reactors in the country, including development of expertise and capabilities in research reactor project management and control, regulatory supervision of the research reactor and its ancillary facilities and safe operation and maintenance of the research reactor.
- To develop and review key specifications in preparation for contract placement and implementation.
- To ensure that the plans to achieve the infrastructure development milestones are integrated into the research reactors project.

SWOT analysis:

Strengths

- Understanding of customer needs
- Open communication channels with stake holders

- Long experience with the radiation applications in Sudan
- Very good collaboration with IAEA

Weaknesses

- Lack of qualified personnel
- Absence of government commitment
- Lack of regulatory requirements

Opportunities

- Providing Sudan first NPP personnel with training.
- Provide a training tool for the students from the reactor engineering department.
- Providing NAA services for the Oil industry.
- Provide a research tool for higher education institutes.

Threats

- Absence of government commitment through the life time of the facility and beyond
- Lack of the legislative and regulatory framework development.
- Lack of long term financial resources.

Scientific Upgrades at the Oak Ridge National Laboratory High Flux Isotope Reactor

D. L. SELBY, A. B. JONES, and L. CROW

** Instrument and Source Design Division
Oak Ridge National Laboratory
Building 7964K, Oak Ridge, Tennessee 37831-6476*

Notice: This submission was sponsored by a contractor of the United States Government under contract DE-AC05-00OR22725 with the United States Department of Energy. The United States Government retains, and the publisher, by accepting this submission for publication, acknowledges that the United States Government retains, a nonexclusive, paid-up, irrevocable, worldwide license to publish or reproduce the published form of this submission, or allow others to do so, for United States Government purposes.

ABSTRACT

In the early 1990's a decision was made to proceed with a long term plan to greatly increase the scientific capabilities of the High Flux Isotope Reactor (HFIR), particularly in the field of neutron scattering. Since the upgrade program was last reported on at IGORR several new cold neutron instruments have been added. In addition to the new instruments, major upgrades have been completed for the two Small Angle Neutron Scattering instruments by replacing their detectors with new helium-3 tube detectors. This upgrade is expected to provide as much as a factor of 5 to 10 increase in performance for many experiments performed on these instruments. Finally, there are still ongoing discussions for a future upgrade that would add a second cold source and Guidehall with 9 associated new instruments.

1. Introduction

As reported in IGORR papers in 2003, 2005, 2007, and 2010 a program was initiated just over 10 years ago to significantly improve the scientific capabilities of all four neutron beams at the Oak Ridge National Laboratory (ORNL) High Flux Isotope Reactor (HFIR). This paper will focus on developments associated with these upgrades since the last IGORR meeting.

2. History and Description of the High Flux Isotope reactor

ORNL submitted a proposal for the construction of the HFIR to the Atomic Energy Commission in March 1959 and approval to proceed with construction was received in July of that year. The reactor design was completed in 1960 and construction began in June of 1961. Initial criticality was achieved on August 25, 1965 and full power normal operation (100 MW) was initiated in 1966. Since that time, the HFIR has operated for 440 fuel cycles (fuel cycle length of 21 to 27 days depending on the power level and experiments loaded in the core region).

Figure 1 provides a layout of the reactor core, beryllium reflector and the four beam tubes. At the 85 MW full power operating condition the peak total neutron flux in the central flux trap for a typical target loading has been measured to be $\sim 4.0 \times 10^{15}$ n/(cm²-s) with a thermal to nonthermal ratio of ~ 1.7 . The peak thermal flux in the beryllium reflector is $\sim 1.4 \times 10^{15}$ and occurs near the tips of the beam tubes. The neutron thermal to nonthermal ratio in the reflector ranges from around 1 to 30. There are three tangential beam tubes and one radial beam tube that start near the peak flux in the beryllium reflector and penetrate the reactor pressure vessel. The modifications to these four beam lines and the thermal and cold neutron instruments are the focus of the scientific upgrades that have been performed at the reactor facility.

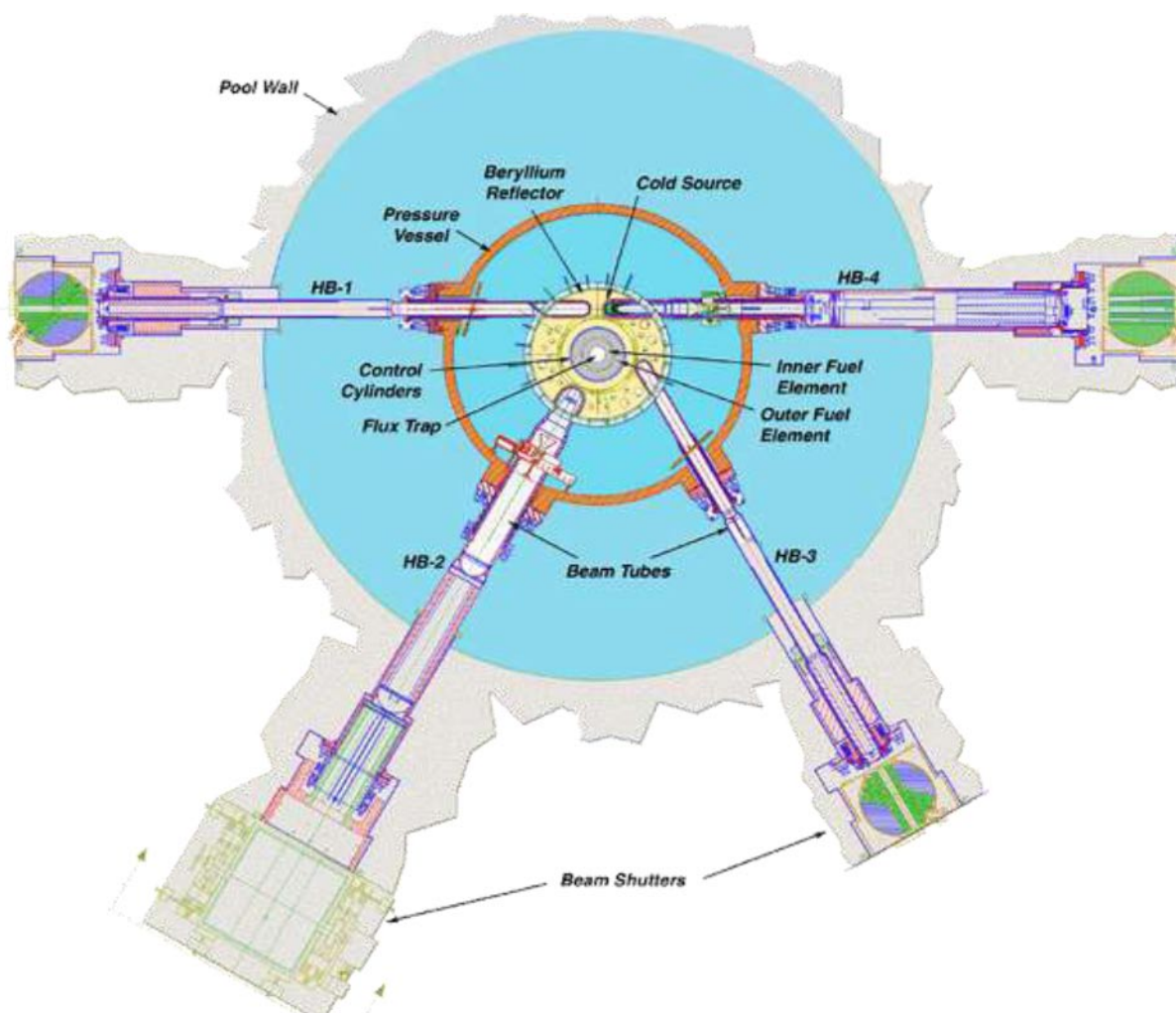


Figure 1: Layout of HFIR Reactor Core, Reflector, and Beam Tubes

3. New Cold Triple Axis Spectrometer

Since the last IGORR meeting the installation and commissioning of a new Cold Triple Axis Spectrometer (CTAX) have been completed; and in May of 2011 the HFIR Neutron Instrument Configuration Control Committee approved the transition from Commissioning to Normal Operation for this instrument. The instrument was incorporated into the formal user program for the last three cycles of FY 2011. This instrument which is located on cold guide 4 (CG-4) is shown in Figure 2. The instrument has been built through a collaboration effort between Oak Ridge National Laboratory, Brookhaven National Laboratory, and the University of Tokyo. The CTAX instrument is primarily being used for analysis of low-energy excitations and for studying magnetic effects in materials. Although CTAX has been in the user program for just over a half a year, the instrument is already oversubscribed by about a factor of 2.5 (i.e. beam time available for 2 proposals for every 5 submitted) and the user base for this instrument is still growing. Many interesting materials, including the new family of Fe-based superconductors, multiferroics, thermoelectrics, quantum magnets, etc, have already been studied on CTAX, taking advantage of a low instrument background rate and high energy resolution. One of the first technical papers based on research performed on this instrument has been submitted to *Physical Review* (*Magnetic interactions in the multiferroic phase of $\text{CuFe}_{1-x}\text{Ga}_x\text{O}_2$ ($x = 0.035$) refined by inelastic neutron scattering with uniaxial-pressure control of domain structure* by Taro Nakajima, Setsuo Mitsuda, Jason T. Haraldsen, Randy S. Fishman, Tao Hong and Noriki Terada).



Figure 2: New Cold Triple Axis Spectrometer (CTAX) on Beam Line CG-4

4. New Neutron Beam Test Stations

In 2008 a decision was made to build 4 neutron beam test stations at the CG-1 beam location. CG-1A would be used to test new neutron instrument techniques including spin-echo concepts. CG-1B would be used to align samples for use at both HFIR and SNS instruments and serve as a general purpose test beam. CG-1C and CG-1D would be used to develop new optics and neutron imaging techniques. Three of the four beam lines (CG-1A, CG-1B, and CG-1D) are now operational and heavily used. Although these beamlines were not intended to be added to the formal DOE user program, the high intensity [flux of 4×10^9 neutrons/(cm²-s) over an energy band of 0.8 to 10 Å (127 – 0.81 meV at end of the neutron guide] of these beams has resulted in a number of requests to use them from outside ORNL. As a result, formal requests for beam time on these test stations have been accepted and there were over 50 unique users allocated beam time at CG-1 in FY 2011.

5. New Single Crystal Diffractometer Instrument

In 2008 a project was initiated to build a single crystal diffractometer instrument at a beam position on CG-4 that uses image plates as the active detector mechanism. This instrument, called IMAGINE, is similar to the LADI-3 instrument at ILL and the KOALA instrument at the OPAL reactor. IMAGINE will be used to pinpoint light atoms, including hydrogen atoms, in supra and macromolecule crystallographic structures. Anticipated areas of research include bioenergy, biomedical, and pharmaceutical sciences where atomic information is critical to understanding essential underlying biochemical processes. Figure 3 shows a recent image of the neutron beam at the IMAGINE instrument shutter and Figure 4 shows a 3D model of the layout of the IMAGINE beam line. One of the unique features of this beamline and a difference from the above mentioned instruments is its neutron optics

system that uses elliptical mirrors, neutron filters and a flat mirror concept developed by the neutron optics group at ORNL to capture and focus the available neutrons at the sample position while maintaining an acceptable neutron divergence angle. Theoretically this concept should provide a neutron flux at the instrument almost a factor of 40 greater than that which would be obtained from a conventional neutron guide. We are presently in the final stages of the installation of this instrument and our goal is to be ready to perform final alignment of the optics system with neutrons when the reactor starts cycle 441 on March 26. Assuming the present schedule holds, we should have this instrument introduced into the formal user program by the end of the summer.

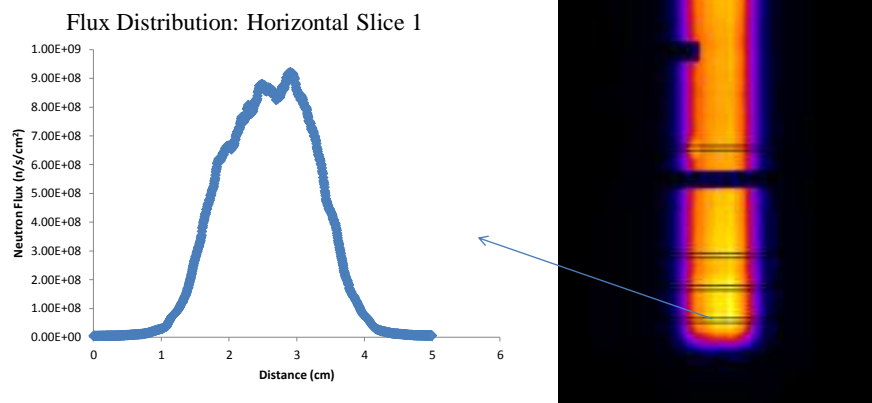


Figure 3: Beam Image and Profile for the IMAGINE Instrument Beam
(Figure courtesy of Kara Beharry and Erik Iverson of ORNL)

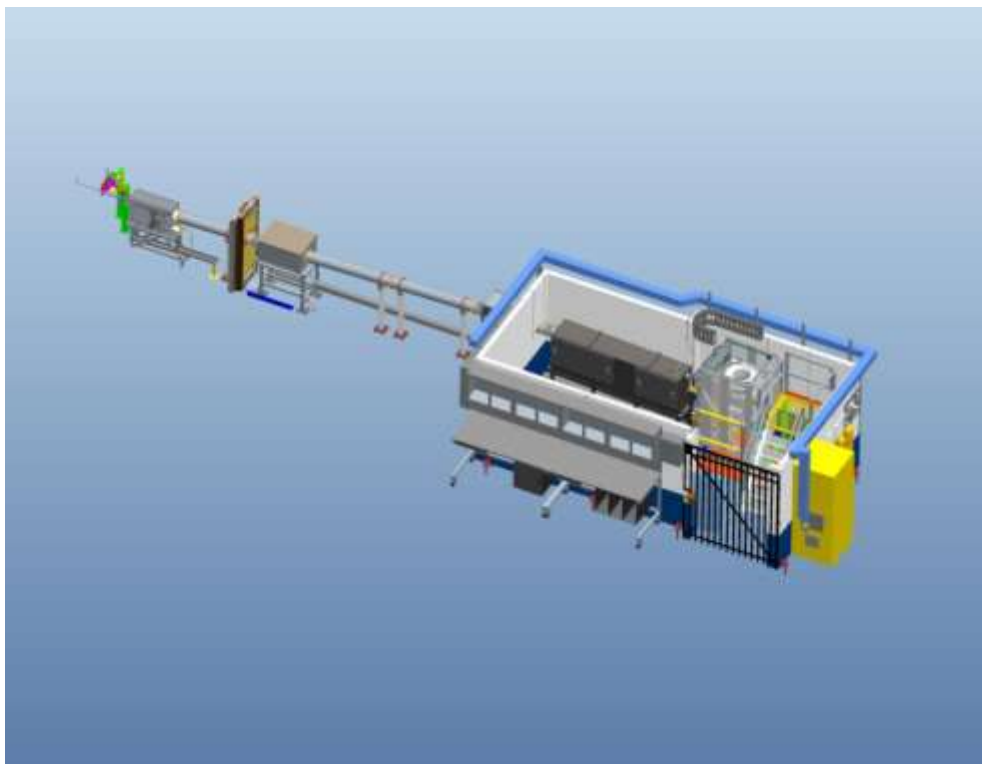


Figure 4: Model of IMAGINE Instrument

6. New Helium Tube Detectors for General Purpose SANS and BioSANS Instruments

The first two instruments that were installed in the Cold Neutron Guidehall were the General Purpose SANS and the BioSANS Instruments. We initially installed 1m x 1m multiwire detectors in these instruments similar to those used at the NIST reactor. However, the HFIR cold neutron beams were too intense for these detectors and attenuators had to be used for many experiments to reduce the beam intensity. A project was initiated in 2009 to replace these detectors with new 1m x 1m GE He-3 tube detectors. The new detector for the General Purpose SANS instrument was installed during the summer of 2011 and the installation of the new detector for the BioSANS instrument has just been completed and will see beam for the first time when the reactor restarts on March 26th. The new detectors allow the use of the full cold neutron beams and depending on the experiment, this gives us a factor 5 to 10 increase in the beam intensity at the sample position.

7. HFIR Future

The possibility of a second cold source and guidehall for HFIR remains in consideration. An early conceptual layout of such a facility is shown in Figure 5. This cold source and guidehall would be tied to the HB-2 beam tube which is the most intense neutron beam available at HFIR. A cold source located on this beam line would have the potential for a factor of 4 performance improvement over the existing cold beam lines at HFIR and would nearly double the number of neutron user instruments at HFIR.

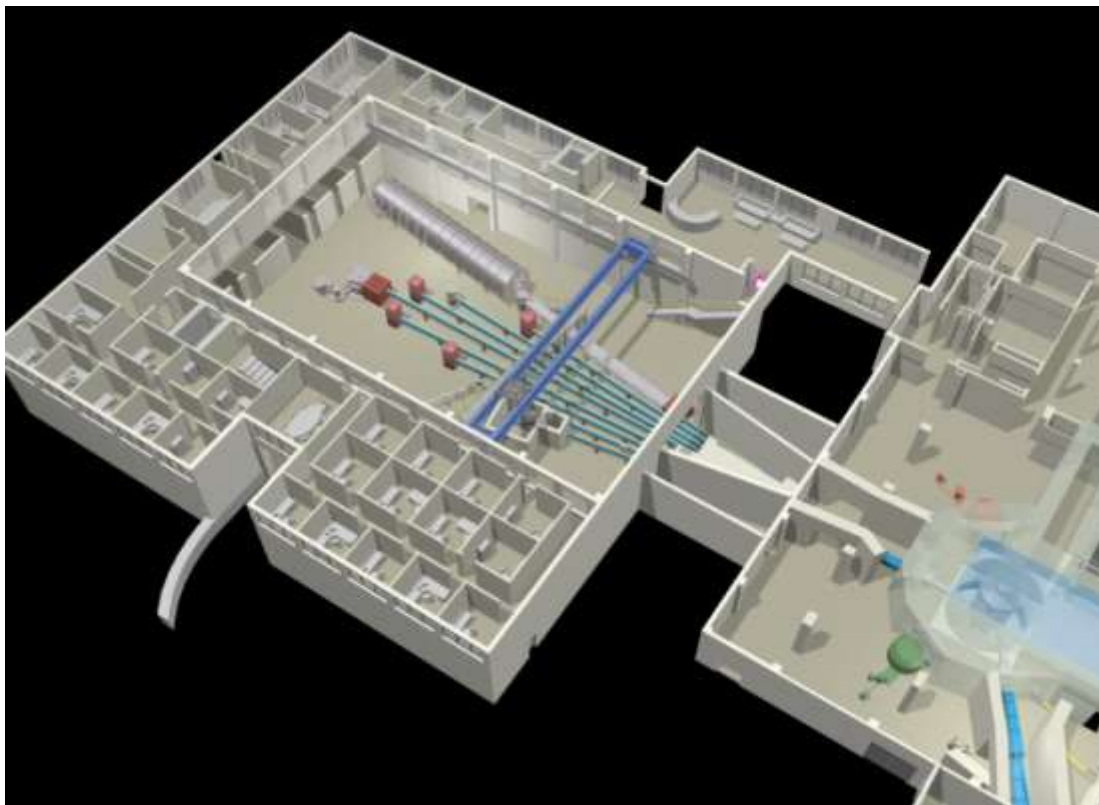


Figure 5: Concept for Second HFIR Cold Source and Guidehall

Neutrons for Service of the Society

Gabriele Hampel, Stephan Zauner
Universität Mainz, Institut für Kernchemie
Fritz-Strassmann-Weg 2, D-55128 Mainz, Germany

Heiko Gerstenberg
TU München – Forschungs-Neutronenquelle Heinz Maier-Leibnitz (FRM II)
Lichtenbergstraße 1, D-85748 Garching, Germany

Bernard Ponsard
SCK•CEN, BR2 Reactor
Boeretang 200, BE-2400 Mol, Belgium

Abstract

Today, the public media have an important impact on the public beliefs, opinions and attitudes and also on political decisions. This was demonstrated very efficiently by the media coverage following the Fukushima accident. Similarly the public debate in modern media and in particular the internet certainly affects the acceptance and even the future of research reactors. On the other hand the internet provides an ideal forum to inform the public about the applications of research reactors and their social benefits.

Neutrons produced in research reactors deliver an important service to the society, this is the basic message of the internet page “research-reactors.eu” which was initialized and realized commonly by the research reactors TRIGA Mainz (Germany), BR2 Mol (Belgium) and FRM II Munich (Germany). This presentation summarizes the content of this web-page.

Introduction

Public beliefs, opinions and attitudes have an important impact on the acceptance of power reactors and political decisions and can also affect the future of research reactors. As compared to power reactors, research reactors are not used to produce electrical energy, but are instead applied as neutron sources for research, medical, and industrial applications, as well as for education and training. An easily available and improved information distribution on the benefits generated to society by research reactors offer a better understanding to the public and help to increase the acceptance of research reactors.

There are many advantages of using internet web pages, such as the content published on a web page is immediately available to a global audience of users at every time. The product is advertised and the customer is able to look up various product specification sheets and find some additional information. Various announcements for many users can be distributed very fast. Finally the internet is supposed to be the primary source for possible customers to check whether or not a particular technical problem may be tackled by neutron based production or analysis.

The web page “neutrons for service of the society” aims to use these advantages to present the possible options research reactors can offer to the public.

Neutrons for service of the society

Neutrons produced in research reactors deliver a service to the society; this is the message of the internet page “research-reactors.eu” which is operated by the research reactors TRIGA **M**ainz, Germany, BR2 **M**ol, Belgium, and FRM II **M**unich, Germany. Regarding the founder the short form of this webpage is MMM. The visitor of the web page receives information about the applications and services of the research reactors joint on the web page. He is supported to decide which one of the research reactors offers the best options and infrastructure for his particular application. A comparison of the available applications at the three research reactors operating the web page and the differences of the three reactor types are visible.

The aim of MMM is to offer interested parties the possibility to identify suitable irradiation conditions for their projects. This internet page allows users to access the necessary information quickly and conveniently. Contact information is provided, and the requirements for irradiation are mentioned. Potential applications of neutrons produced at the facilities in Mainz, Mol and Munich include: Radioisotope production for medical, industrial and research applications, neutron transmutation doping (NTD) of Si, neutron activation analysis (NAA), material research, irradiations in medicine (cancer therapy) as well as education and training.

The internet page is written in English and German and separated in 9 buttons: home, news, services, members, contact, about us, links, references, and the button for the choice of the language.

The Homepage (fig. 1) gives a short introduction and summarizes the characteristic data as reactor power and the available neutron flux densities for each of the three facilities.

Under “***news***” the facilities present actual information which might be interesting for customers or the public, for example the start of operation of a reactor after revision or a symposium which is open for the public.

“Services” gives an overview on the current medical and technical applications of the research reactors, as well as educational and training opportunities offered. In tables the applications are summarized for the TRIGA Mainz, BR2 and FRM II.

The button “Member” provides separated fields for the research reactors in Mainz, Mol and Munich. Here, a detailed description of the research reactors and specific information about the services of the research reactor are given. For each facility the page starts with a description of the research reactor. On the left buttons for the different applications are listed, which offer the information by clicking the button (see figure 2 to 4).

“Contacts” includes the addresses of the facilities and the contact persons. “About us” informs about the cooperation between the research reactors to create a community for the industrial applications of neutron sources.

“Links” include an easy connection to the home pages of the facilities in Mainz, Mol and Munich and also to some other organizations as the IAEA, Deutsch-Schweizerischer Fachverband für Strahlenschutz.

“References” summarized some publications which might be useful for interested persons.

The MMM page has also an intranet platform which is protected by a password. It can be used for exchange of data and information between the facilities in Mainz, Mol and Munich for protocols, presentations etc.

Examples for applications with benefit for the society

The applications of the low power TRIGA Mainz are focused on education and training, neutron

activation analysis and the production of short lived isotopes. High flux reactors as the FRM II and the BR2 offer services in transmutation doping of silicon and the production of medical isotopes. The mentioned applications of all three reactors have high commercial relevance and benefit for the society due to the following reasons:

Education and training deliver important elements in nuclear science technology, and research infrastructures. Training of personnel is crucial for a safe operation, maintenance, regulation and improvement of reactors and other facilities associated with nuclear power activities, and to manage and direct nuclear technology's development and nuclear science research. The basis for advances in power reactor safety is well-educated scientists and engineers. Development of high-technology applications in fields such as materials science, fluid dynamics and biomedical science, where neutron sources are needed, can profit through utilisation of research reactors. Due to the dismantling of power and research reactors, radiation protection and knowledge in the handling of radioactive materials becomes even more important.

The NAA is a qualitative and quantitative analytical technique for the determination of trace elements in a variety of complex sample matrices. It is the most simple and the most widely used application of research reactors. In addition, many results of trace element identification can be directly linked to potential economic benefits. Therefore, NAA is one of the main applications of research reactors from the commercial point of view. The main advantages of the NAA technique are the very low detection limits for many elements, a non-destructive analysis and the low amount of sample mass. In many cases it is a fast multi-element analysis with turnaround times between a day and a few days. Due to its inherent sensitivity and accuracy, NAA has been extensively applied to environmental sciences, nutritional and health related studies, biology, medical, geological and geochemical sciences, material sciences, archaeological studies, forensic studies, etc. In addition, NAA has a role in the quality assurance of chemical analysis.

The NTD of silicon is a commercially attractive application at the research reactors in Munich and Mol. The basic material for the semiconductor industry is silicon, doped with small quantities of host atoms (e.g. phosphor) in order to provide the desired semiconductor characteristics. The NTD is based on the transmutation of ^{30}Si into ^{31}P : Caused by the capture of thermal neutrons Si-31 is produced which decays into P-31 with a half-life time of 2.62 hours. The NTD provides the highest quality in doping uniformity (e.g. for power electronics).

Isotope production for medical use remains one of the most important commercial and beneficial applications of research reactors with high power such as the FRM II and BR2. Mo-99/Tc-99m – the by far most important radioisotopes in nuclear medical diagnostics - is gained as fission products resulting from the irradiation of uranium targets. For this purpose dedicated irradiation channels exhibiting high thermal neutron flux densities $> 1\text{E}14 \text{ cm}^{-2}\text{s}^{-1}$ and well established handling procedures are required at the producing research reactors. Due to the short half-lives of Mo-99 (66 h) and Tc-99m (6h), the quick delivery of the irradiated targets to the chemical processors separating the desired isotopes from the target and finally to the hospitals is of crucial importance. Each step in the production process needs experts from respective disciplines, laboratory facilities equipped for radioactivity handling and other supporting infrastructure. So far BR2 is the only reactor out of the MMM group to offer target irradiation for Mo-99/Tc-99m. At FRM II a project team is designing a corresponding irradiation facility which is supposed to be available starting from 2015. Further relevant radioactive isotopes produced at FRM II and BR2 for medical purposes in nuclear medicine are Xe-133, Ir-192, I-125, I-131, Er-169, Lu-177, W-188 / Re-188 for therapy and Sm-153, Re-186 and Sr-89 for pain palliation of bone metastases. The production of the radioactive isotope for alpha-targeted therapy (especially Ac-227) is currently being developed in

BR2. Alpha emitters are suitable for tumour therapy, and because of their short range and high ionization effects, a target-selective irradiation of tumour cells with a lethal effect is possible.

Isotope production is also important for technical applications. Short lived isotopes as Na-24, K-42, Mn-56, Hg-203, Br-82, Ar-41, In-128m or I-128 are produced to check the quality of procedures for example in the chemical industry.

More detailed information can be found on the web page “neutrons for services of the society.

Summary

The MMM web page is used to advertise the use of research reactors for industrial purposes. Interested parties are invited to look up various services and products offered by research reactors. The customer can explore information in as much detail as wanted, a general overview or information more in depth. News are provided timely and a download of descriptions for several applications and important publications will be possible in future

The web page is open for other research reactors if any member of MMM agrees such extension.



Figure 1: Homepage Neutrons for Services of the Society (MMM)



Figure 2: Services of the TRIGA Mainz, University of Mainz, Germany

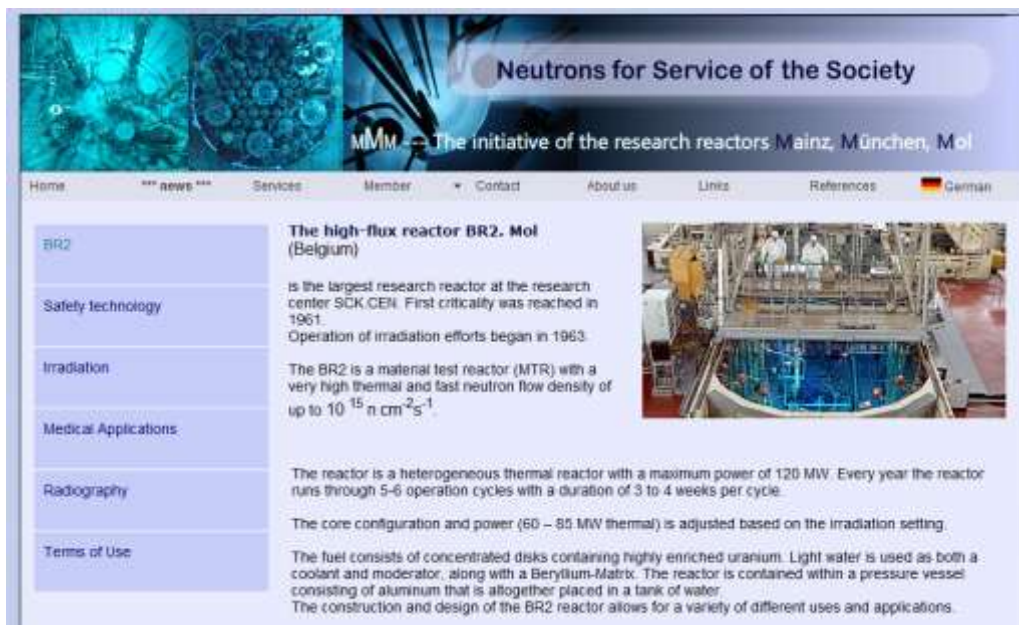


Figure 3: Services of the BR2, SCK•CEN, Mol, Belgium



Figure 4: Services of the FRMII, TU Munich, Germany

PRODUCTION AND DETERMINATION OF ^{75}Se BY NEUTRON ACTIVATION METHOD FOR SELENIUM REMOVAL STUDIES

E. ORUCOGLU

*Istanbul Technical University, Faculty of Mines,
TR-34469, Maslak, Istanbul, Turkey*

S. HACIYAKUPOGLU

*Istanbul Technical University, Energy Institute,
TR-34469, Maslak, Istanbul, Turkey*

ABSTRACT

The importance of selenium pollution, due to its toxicity for living species and its bioaccumulation feature in aqueous environment, has getting growing awareness day by day. According to water standards, the level of the selenium in the water resources should be less than 10 $\mu\text{g/L}$. Although this value is so small, it can be dangerous for aquatic species. That is why, the accurate and precise determination of selenium is very important.

Selenium can disperse to the environment from different processes like mining activities, burning of coal and other fossil fuels, irrigation facilities, industrial applications, nuclear accidents, nuclear waste disposal sites. ^{79}Se radioisotope is one of the components of nuclear wastes and should be taken into consideration in radioactive waste management due to extremely long half-life and potential migration ability through environment.

One of the most important analytical methods used for selenium determination, the neutron activation method, was used in this study to produce ^{75}Se radioisotopes supplying sufficient low activities. Pure selenium dioxide compound was irradiated in central irradiation tube of ITU TRIGA MARK II research reactor of Istanbul Technical University. Pure gold foils were used in irradiations as flux monitors. Thermal and epithermal neutron fluxes were determined by using cadmium covers. Selenium removal from polluted waters was investigated with batch adsorption experiments; for this reason solutions prepared with this irradiated material were added onto modified bentonite composites. The amount of produced ^{75}Se radioisotopes and the activities of the solutions prepared with radioactive selenium compounds were determined by using high resolution gamma spectroscopy system and GAMMA-VISION-32 software. Results showed that the selenium adsorption performance of modified composites can be effectively determined by relative activity measurements of adsorption solutions including ^{75}Se .

1. INTRODUCTION

One of the antioxidant elements, selenium, can be harmful for living species when its excess amount is taken into body, due to its toxicity. Additionally, researchers revealed that the amount of selenium around or below the selenium limits in water, determined as 10 $\mu\text{g/L}$ for drinking water by world health organization, has a poisonous effect on the aquatic species due to bioaccumulation and biomagnifications property of the element [1-3]. Mining activities, fossil fuel combustion and phosphate fertilizing activities are the main sources of selenium enrichment in the water or soil [1]. Another potential hazard of selenium can originate from nuclear power plants. ^{79}Se radioisotope is one of the interested radionuclide in nuclear waste disposal due to its long half life and potential migration ability. It is mainly produced in nuclear reactors by fission of uranium-235 and can be found at significant levels in spent nuclear fuel and waste materials resulting from fuel reprocessing [4]. In the literature there are many studies investigating selenium removal by using various treatment methods as ion exchange, adsorption, precipitation, nanofiltration/reverse osmosis, chemical reduction, biological treatments [1]. In the adsorption studies specifying selenium removal, iron, aluminium, clay and modified clay minerals were used as adsorbents and Inductive Coupled Plasma Mass Spectroscopy, Atomic Adsorption Spectroscopy, Extended X-ray Absorption Fine Structure, X-ray Absorption Near Edge Structure Spectroscopy and High Resolution Gamma

Spectroscopy (HRGS) methods were used for determination of selenium [5, 6, 7]. Usage of ^{75}Se as adsorbate and HRGS system for determination of ^{75}Se gave accurate and precise results in many studies [7, 8, 9]. The other advantage of ^{75}Se usage is its appropriate half-life (119.769 days) and easy production possibility from ^{74}Se by neutron activation [10].

In this study, in order to investigate the usage possibility of ^{75}Se radionuclide in selenium removal applications from aqueous media, firstly it was aimed to produce ^{75}Se by irradiation of the selenium dioxide compound at ITU TRIGA MARK II nuclear research reactor by neutron activation method. Next, it was intended to measure the ^{75}Se activities of solutions that were prepared from the irradiated compounds by HRGS system. Then, batch adsorption experiments with ^{75}Se solutions and Resadiye organo-inorgano-sodium bentonite composite were executed and the activities of the solutions obtained before and after adsorption were measured by HRGS system.

2. Material Method:

2.1 ^{75}Se radioisotope production

To prepare adsorption solutions, weighted and sealed selenium dioxide compound (SeO_2 , Fluka, 99% purity) and gold (Au) foil flux monitor (99.9918 % purity, 0.001 inch thickness, Reactor Experiments Inc.) were irradiated together in central irradiation tube of TRIGA MARK II nuclear research reactor at Istanbul Technical University at 250 kW for 1h.

2.2 Radioactivity measurements

All radioactivity measurements were implemented in Low Level Radioactivity Measurement Laboratory in the Istanbul Technical University Energy Institute. GAMMA-X HPGe coaxial n-type germanium detector having copper lined lead shield (10 cm) was used to determine ^{75}Se radioisotope activities of the adsorption samples and gold foils activities representing neutron fluxes in the reactor. The detector, with the integrated digital gamma spectrometer (DSPEC jr. 2.0), has 45.7 % efficiency and 1.84 keV full width at half maximum for 1.3 MeV of ^{60}Co . In the measurements, statistical confidence level and range were adjusted to 1σ and 8K, respectively. Counting times were changed from 5 min up to 10 hour, depending on the activities of samples. Peak areas of ^{75}Se at 121.12 and 136.0008 keV gamma-rays in the spectrums and peak areas of Au at 411.80205 keV gamma-ray in the spectrums were determined by using GAMMA VISION-32 software program [10, 11]. ^{152}Eu standard point source was used in energy and efficiency calibrations [12].

2.3 Neutron flux determination

In order to determine the activity of the solutions prepared by using irradiated SeO_2 compound, thermal and epithermal neutron fluxes of the reactor were determined by irradiation of two weighted gold foils inside and outside of a cadmium cover (15 mm diameter and 1.016 mm thickness, Reactor Experiments Inc.) in pneumatic transfer system of TRIGA MARK II nuclear research reactor at Istanbul Technical University at 250 kW for 10 min. Activities that were necessary to determine the cadmium ratio (CR), which presents the ratio of activities of flux monitors inside and outside of a cadmium cover, were calculated by using the equation (1)

$$A_0 = \frac{P \cdot \lambda \cdot e^{\lambda \cdot t_d}}{I \cdot \varepsilon \cdot (1 - e^{-\lambda \cdot t_m})} \quad (1)$$

where A_0 is the activity of the element at the end of the irradiation, λ is the decay constant, t_d is decay time, P is the counts accumulated in the peak during the counting time (t_m), I is the gamma-ray intensity and ε is the counting efficiency. The epithermal neutron flux was determined by using the activity of the monitor inside the Cd-cover as given in equation (2),

$$\Phi_{\text{epi}} = \frac{(P_{\text{epi}}/t_m) \cdot M \cdot e^{\lambda \cdot t_d}}{m \cdot I_{\text{epi}} \cdot N_A \cdot a \cdot (1 - e^{-\lambda \cdot t_i}) \cdot \epsilon} \quad (2)$$

The thermal neutron flux was determined by using the CR and epithermal neutron flux as given in equation (3),

$$\Phi_{\text{th}} = \frac{\Phi_{\text{epi}} \cdot (CR - 1) \cdot I_{\text{epi}}}{\sigma_{\text{th}}} \quad (3)$$

In the equations, Φ_{epi} is the epithermal neutron flux, Φ_{th} is the thermal neutron flux, t_i is the irradiation time, N_A is Avogadro's number, M is the atomic mass of the element, I_{epi} is the resonance integral of radionuclide and a is the abundance of the isotope yielding the radionuclide to be measured.

2.4 ^{75}Se activity determination

The ^{75}Se activities of solutions before and after adsorption were calculated by inserting the experimentally obtained thermal and epithermal neutron fluxes into the equation (4)

$$A_0 = \left[N_A \frac{m \cdot a}{M} \cdot (\sigma_{\text{th}} \cdot \Phi_{\text{th}} + I_{\text{epi}} \cdot \Phi_{\text{epi}}) \cdot (1 - e^{-\lambda \cdot t_i}) \right] \quad (4)$$

where m is the amount of irradiated selenium in solution. Since flux determination and isotope production experiments were executed at different locations in reactor, results were also corrected for location. Minimum detectable activity of ^{75}Se for the experimental conditions at 121.12 keV was determined according to the classical ORTEC Method [11].

2.5 Adsorption experiments

Selenium, the investigated element in this study, has anionic species in aquatic environment and bentonite, one of the clay minerals that are proposed as buffer material in radioactive waste management systems, has negative surface charges. So, raw bentonite could not adsorb anionic selenium species effectively [13], therefore in adsorption a modified product of Resadiye organo-inorgano-sodium bentonite (oim-Rsb) was used. ^{75}Se adsorption experiments were implemented by using batch adsorption method in shaker bath (Nuve ST402). In this frame, 1 mM stock solution was prepared with irradiated SeO_2 compound. In the experiments, oim-Rsb composites were contacted with radioactive solutions in polycarbonate centrifuge tubes satisfying 10 g/L solid/liquid ratio and shaken horizontally in water bath for 24 h at 25 °C. Then they were centrifuged (Hereaus Labofuge A) at 5000 rpm for 5 min and 4 mL representative solutions were pipetted (Brandt Transferpette) from both stock and adsorption solutions for gamma spectrometric measurements. To improve accuracy of the results, adsorption experiments were also duplicated. Representative solutions were counted at HRGS system for 136.0008 keV photopeak of ^{75}Se . Since the activities of the stock and adsorption solutions were different at the moment of separation time and measurement time, the decay corrections for all samples were done by using the equation (5)

$$A_0 = A \cdot e^{\lambda \cdot t} = \frac{P}{t_m} \cdot e^{\lambda \cdot t} \quad (5)$$

In this equation, A_0 is activity of the representative solution at the moment of separation of adsorbent from solution and A is the activity of the solution at measuring time. P is number of counts in net area of the peak, t_m is counting time and λ decay constant of the nuclide [14]. Decay corrected ^{75}Se activity data, which are directly proportional with ^{75}Se concentration, were used in calculations of selenium adsorption efficiencies of adsorbent material oim-Rsb composite (V_A):

$$V_A = \frac{C_0 - C_F}{C_0} \cdot 100 \quad (6)$$

where, V_A is the adsorption efficiency, C_0 is the initial concentration (M) of adsorbed material, C_f is the concentration (M) of adsorbed material remained in solution at the end of adsorption [15]. C_0 and C_f are determined experimentally by using the measured ^{75}Se activities in stock and remained adsorption solutions.

3. Results and Discussion

In the study, in order to calculate the ^{75}Se and ^{198}Au radionuclide activities the 121.78 and 411.116 keV photopeaks efficiencies of ^{152}Eu were used; the determined efficiencies were 0.373 % and 0.176 % respectively. By using results of measurements of CR and related equations, thermal and epithermal neutron fluxes of the reactor were calculated as $2.84 \cdot 10^{12}$ and $1.38 \cdot 10^{12} \text{ n} \cdot \text{cm}^{-2} \cdot \text{s}^{-1}$ respectively. Experimental results showed that approximately 15 % of the irradiated ^{74}Se was activated. Minimum detectable activity of ^{75}Se for the experimental conditions was determined as 3.34 Bq. The activity of the starting adsorbing solution used in adsorption experiments was found as $1317 \pm 1 \text{ Bq/4mL}$; this value changed depending on solution concentration and decreased in accordance with increasing adsorption efficiency. Since stock and adsorption solutions activities were directly related with ^{75}Se concentration, they can be used in adsorption efficiency calculations; therefore the necessary ^{75}Se concentrations were calculated by using count rates of ^{75}Se radionuclide as given in Figure 1. According to the results of adsorption experiments the ^{75}Se adsorption efficiency of oim-Rsb composite samples varied between 97-100 %.

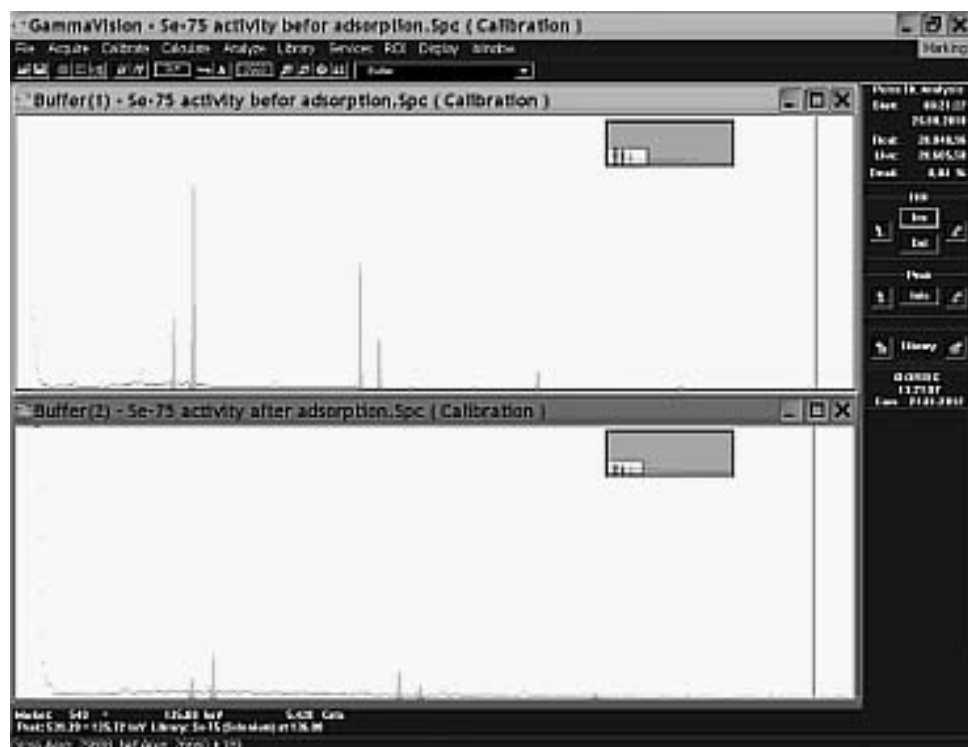


Fig 1. ^{75}Se photopeaks in spectrums of solutions before and after adsorption

When the results obtained in this study were taken into consideration, it can be said that selenium can be easily irradiated in the research reactor in a relatively short time. The irradiated compound will have low activity for satisfying safer working conditions; this will also prevent working with highly activated ^{75}Se sources to dilute and to prepare solutions including ^{75}Se radiotracer for adsorption solutions. And furthermore the results confirmed the usage possibility of irradiated selenium compound for selenium removal studies.

Acknowledgements

This study is part of the project funded by ITU Research Foundation (Project No. 33041). Authors are grateful to ITU TRIGA MARK II reactor staff for their support during irradiations.

4. References

1. Lenz, M., Lens, P.N.L., 2009, "The essential Toxin: The Changing Perception of Selenium in Environmental Sciences", *Science of the Total Environment*, 407, pp. 3620 – 3633.
2. EPA/600/R-01/077, 2001, "Selenium Treatment/Removal Alternatives Demonstration Project", Mine Waste Technology Program Activity III, Project 20, 133 p.
3. Lemly, A. D., 2004, "Aquatic Selenium Pollution is a Global Environmental Safety Issue", *Ecotoxicology and Environmental Safety*, 59, pp.44–56.
4. Wang, W., Guan, Y., He, M., Jiang, S., Wu, S., Li C., 2010, "A Method for Measurement of Ultratrace ^{79}Se with Accelerator Mass Spectrometry", *Nuclear Instruments and Methods in Physics Research B* 268, pp.759–763
5. Peak, D., Saha, U. K., Huang, P. M., 2006, Selenite Adsorption Mechanisms on Pure and Coated Montmorillonite: An EXAFS and XANES Spectroscopic Study, *Soil Sci. Soc. Am. J.*, 70, pp.192–203.
6. Rovira, M., Gimenez, J., Martinez, M., Martinez-Llad, X., Pablo, J., Marti, V., Duro, L., 2008, "Sorption of selenium(IV) and selenium(VI) onto natural iron oxides: Goethite and hematite", *Journal of Hazardous Materials*, 150, 279–84.
7. Missana, T. Alonso, U., García-Gutiérrez, M., 2009, "Experimental study and modelling of selenite sorption onto illite and smectite clays", *Journal of Colloid and Interface Science*, 334, pp.132–138.
8. Dhillon, K.S., Dhillon, S.K., 1999, "Adsorption–desorption reactions of selenium in some soils of India", *Geoderma*, 93, pp. 19–31.
9. Montavon, G., Gu, Z., Lützenkirchen, J., Alhajji, E., Kedziorek, M.A.M., Bourg, A.C.M., Grambow, B., 2009, "Interaction of selenite with MX-80 bentonite: Effect of minor phases, pH, selenite loading, solution composition and compaction", *Colloids and Surfaces A: Physicochem. Eng. Aspects*, 332, pp. 71–77.
10. Firestone R.B., 1998, "Table of Isotopes [electronic resource]", Coral M. Baglin, editor; S.Y. Frank Chu, CD-ROM editor, 8th ed., update New York, Wiley.
11. ORTEC, 2003, Gamma Vision-32 A66-B32 Software Users Manual.
12. DKD-K-36901-000386, 2006, "Calibration certificate", Isotope Products Laboratory, Valencia, California.
13. Orucoglu, E., 2011, "Modification of Resadiye Bentonite by Using Organic and Inorganic Cations and Investigation of ^{75}Se Radioisotope Adsorption on the Modified Products", PhD Thesis, Istanbul Technical University, 281 p.
14. Loveland, W.D., Morrissey, D.J., Seaborg, G.T., 2006, "Modern Nuclear Chemistry", John Wiley & Sons, New Jersey.
15. Inglezakis, V. J., Pouloupoulos S. G., 2006. "Adsorption, Ion Exchange, and Catalysis", Elsevier Science, 614 p.

ENHANCED NAA SERVICES THROUGH NETWORKING, AUTOMATION, QUALITY ASSURANCE AND QUALITY CONTROL

D. RIDIKAS¹ AND P. ADELFGANG²

International Atomic Energy Agency (IAEA)

¹*Department of Nuclear Sciences and Applications and* ²*Department of Nuclear Energy*
Wagramer strasse 5, PO Box 100, 1400 Vienna, Austria

ABSTRACT

Although the number of research reactors (RRs) is steadily decreasing, more than half of them are still heavily underutilized, and in most cases, underfunded. The decreasing and rather old fleet of RRs needs to ensure the provision of useful services to the community, in some cases with adequate revenue generation for reliable, safe and secure facility management and operations. Enhancement of low and medium power RR utilization is often pursued by increasing the neutron activation analysis (NAA) activities. In this paper we will present the strategy and concrete actions how NAA as one of the most popular RR applications can contribute to the above goals in particular through a) RR coalitions and networks, b) implementation of automation in different stages of NAA c) QA/QC, including dedicated proficiency tests. We also show that despite the IAEA's efforts, some of the NAA laboratories still perform poorly in proficiency tests, do not have formal QA/QC procedures in place, have not implemented automation to process large number of samples or lack of clear marketing strategies. Some concrete actions are proposed and outlined to address these issues in the near future.

1. Introduction

Over the years, the IAEA has stimulated the orientation of NAA groups worldwide on fields of application in which large amounts of samples may exist for analysis. Whereas the markets for NAA laboratories may have been identified and quality may have been established, an underestimated problem remains the absence of automation, which limits tremendously the analytical capacity. The level of automation in most NAA laboratories does not compare to what modern industry provides for alternative techniques such as X-ray Fluorescence Spectroscopy (XRF), Atomic Absorption Spectroscopy (AAS) and Inductively Coupled Plasma (ICP) Spectroscopy. Data processing in NAA often requires an unequal amount of human intervention since the existing software packages were never designed for routine service applications. Equally, commercially available sample changers do not fit for handling the NAA sample vials. In most of the cases the NAA service requests have to be rejected not because of lack of RR availability, but because of limited capacity in automation and data processing. It emphasizes the relevance and urgency to support the development of NAA automation procedures and implementation thereof at different stages such as automatic sample changers both for irradiation and measurements, more efficient use of detectors, automated data handling and analysis procedures, faster quality control process and reporting software. A number of major requirements for the attractive, efficient, and reliable NAA will be discussed in this paper, namely enhanced networking and cooperation in the field of NAA, implementation of automation and QA/QC for the entire NAA process at different stages of realization, and development of specific marketing strategies.

2. RR Coalitions and Networks

Among a number of related efforts [1], during the last 4 years the IAEA has been promoting networking, coalitions and regional collaboration to improve the efficient and sustainable utilization of research reactors (RRs) [2]. A number of RR coalitions and networks have been

developed with IAEA support as a new model to better utilize RR and facilitate access for the Member States without such facilities. The coalition/network concept involves putting in place cooperative arrangements among RR operators, user entities, customers and other stakeholders. Ideally, a strong partnership is formed leading to increased utilization of individual RRs through collective efforts, including improved self-sustainability and self-reliability. As shown in Fig. 1 (also see Table 1), six such networks collectively offered their services to regional and international users, including the countries without RRs. With the Central Africa RR Network (CARRN), created in July 2011 in Accra (Ghana), the efforts of RR Coalitions and Networks currently involve 42 Member States (25 with RRs and 17 without such facilities) [3]. In the final project coordination meeting of RER4032 on “Enhancing the Sustainability of Research Reactors and their Safe Operation through Regional Cooperation, Networking and Coalitions”, held in December 2011 in Vienna, an initiative to create a new RR coalition, involving mainly the Commonwealth of Independent States (CIS), was supported. The official inception of this new network is expected in 2012 within the framework of a new regional TC project RER1007.

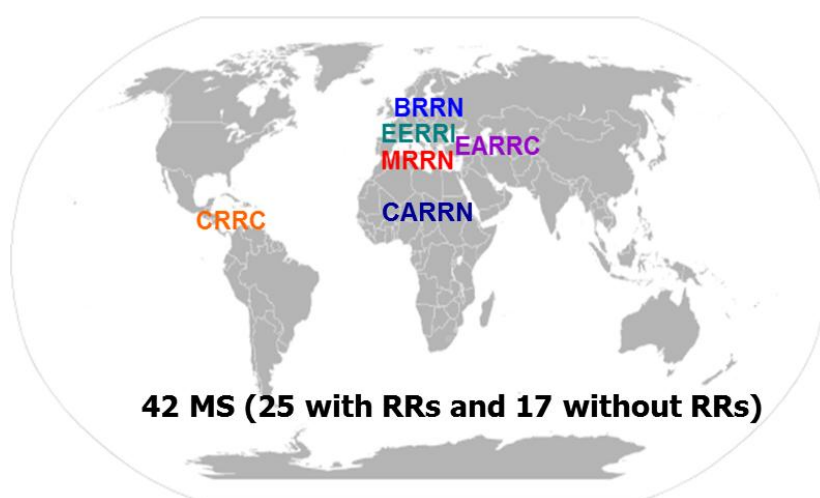


Figure 1: IAEA supported RR coalitions and networks (also see Table 1).

As it is indicated in Table 1, NAA is a joint activity of 4 RR coalitions out of 6. In detailed work-plans of these networks the following actions related to NAA have already been scheduled: in collaborative way provide NAA services to the partners without RRs, share of good practices and knowledge among NAA laboratories, periodically participate in NAA proficiency tests, implement modernization and automation of NAA laboratories, ensure and implement QC/QA procedures, seek for laboratory accreditation and joint marketing strategies within the network.

RR coalition/network (year of creation)	Participating Member Sates	Major joint activities
BRRN – (2009) Baltic RR Network	Denmark, Estonia, Finland, Germany, Latvia, Lithuania, Norway, Poland, Russian Federation, Sweden	<ul style="list-style-type: none"> • Education and training • Irradiation services including NAA • Neutron beam applications • Waste and decommissioning issues
CRRC – (2009) Caribbean RR Coalition	Colombia, Jamaica, Mexico	<ul style="list-style-type: none"> • NAA
CARRN – (2011) Central Africa RR Network	Algeria, DRC, Ghana, Madagascar, Morocco, Niger, Nigeria, Sudan, Zambia	<ul style="list-style-type: none"> • Education and training • NAA
EARRC – (2009) EurAsia RR Coalition	Czech Republic, Hungary, Kazakhstan, Ukraine, USA, Uzbekistan	<ul style="list-style-type: none"> • Mo-99 production via (n, gamma)

EERRI – (2008) Eastern European RR Initiative	Austria, Czech Republic, Hungary, Poland, Romania, Serbia, Slovenia	<ul style="list-style-type: none"> • Education and training • Radioisotope production • Neutron beam applications • Material irradiation and tests
MRRN – (2009) Mediterranean RR Network	Algeria, Azerbaijan, Bulgaria, Egypt, France, Greece, Italy, Montenegro, Morocco, Portugal, Slovenia, Syria, Tunisia, Turkey	<ul style="list-style-type: none"> • Education and training • NAA • Neutron radiography

Table 1: Regional Member State representation and major areas of joint activities of RR coalitions and networks.

In summary, although some noticeable results have been obtained in initiating and supporting RR coalitions, much more work needs to be accomplished in order to achieve the objective of increase utilization of individual RRs through collective effort, on a self-sustainable and self-reliant basis. In addition to their individual strategic plans, the coalition partners need to put into place coalition-based common strategic and management plans as a group. They also need to pursue more detailed market analysis and business development to identify specific pay-back opportunities through sustainable commercial activities, through complementary marketing and delivery of irradiation products and services, education and training among other potentially revenue generating applications of RRs.

3. IAEA Collaborating Centre for NAA Based Methodologies

The IAEA Collaborating Centres (CC) are, in general, scientific institutions such as laboratories, universities, research facilities, etc., that receive public recognition by the IAEA and have been designated to collaborate with the IAEA in a variety of fields, such as food safety, environmental protection, water resources and human health. In line with the objectives of the IAEA, IAEA-CCs are expected to further the research, development and training in the peaceful applications of nuclear science and technology. In this regard, the Reactor Institute Delft (RID) of Delft University of Technology was inaugurated in May 2009 as an IAEA Collaborating Centre for Neutron Activation Based Methodologies of RRs. The collaboration involves education, research and development in (i) Production of reactor-produced, no-carrier added radioisotopes of high specific activity via neutron activation; (ii) NAA with emphasis on automation as well as analysis of large samples, and radiotracer techniques; and, as a cross-cutting activity, (iii) Quality assurance and management in research and application of RR based techniques and in RR operations.

Concrete activities in the area of NAA are ensured through:

- Regional thematic training courses such as (but not limited to) NAA, and metrology in nuclear analytical methods; to be held either at RID or, via RID's staff expert service, in Member States' institutions;
- Hosting scientific visitors and research fellowship training with emphasis on automation and conduct and logistics of large-scale projects;
- Expert services to assist Member States „on-the-spot“ in improving their facilities;
- Transfer of knowledge and expertise in large sample analysis for realizing new dedicated facilities elsewhere, as well as in providing opportunities for researchers using the Delft facility as a benchmark, and in providing opportunities to use the large sample facility for specific projects in the applied fields;
- Quality assurance and management in research and application of RR based analytical techniques.

Given its demonstrated sustainability, the Delft University of Technology recently approved a plan identified by the acronym OYSTER (Optimized Yield - for Science, Technology and

Education - of Radiation) for installing a new compact reactor core with new type of fuel elements which, together with a power increase from 2 MW to 3 MW and a cold neutron source in one of the radial beam-tubes. OYSTER will also boost the research based on neutron activation and, consequently, the IAEA-CC will benefit for it too [4].

4. New Coordinated Research Project on Development of an Integrated Approach to Routine Automation of NAA

In December 2009 the IAEA has organized a Consultancy Meeting on “Preparation of Guidelines on Implementation of Routine Automation in Advanced Neutron Activation Analysis Laboratories”, which was attended by 6 international experts representing 5 Member States. During this meeting issues related to routine automation of NAA laboratories were discussed in detail. Among the experts there was unanimous agreement that there are significant opportunities to increase the measurement capacity in less advanced NAA laboratories through automation. The following points summarize the current situation as it pertains to the majority of NAA laboratories and provide a guide to those areas that need to be addressed as a matter of priority to enable the widespread adoption of automated systems:

- Enhancement of RR utilization via NAA is seriously hampered by the lack of automation both in hardware and software, and most RR-based NAA laboratories worldwide are facing this problem.
- A lack of advanced training currently constrains several aspects of the effective use of NAA, including in the areas of marketing, the quality management of projects with a large number of samples and the implementation of advanced technology.
- There are no commercially available automated solutions for data processing and management after gamma-ray spectrum analysis.
- Irradiation stage: there are no automated irradiation facilities with sample changers commercially available.
- Measurement stage: only one company currently offers an automatic sample changer specifically for NAA.

In addition to these major observations, the meeting adopted the following recommendations, satisfying the stated objectives of enhancing RR utilization in Member States, promoting cooperation between different RR centers and end-users, and enhancing NAA capabilities in particular.

- Continue efforts to promote and realize automation in NAA laboratories so as to increase opportunities for enhanced RR utilization. Promote automation through the dissemination of good practice documents.
- Continue support of k0-IAEA and any improvements developed in response to Member State end-user requests. A modular approach of this tool was recommended to be implemented.
- Create an internet based platform to provide a means for the exchange of information on automated irradiation facilities and on sample changer constructions.
- Continue support for training workshops and fellowships through the period of installation and commissioning of automated systems so that the NAA laboratory can assure the continued functioning of the systems beyond the term of the Agency's support, i.e. ensure the transition toward self-sustainability.
- Provide training courses for NAA laboratory staff to fill the increased capacity arising from automation. Courses would include: marketing; commercial outreach and finding applications and stakeholders for NAA services; and planning and organization of large scale NAA projects.

As a result of the above meeting, the IAEA through a comprehensive questionnaire initiated the collection of detailed information related to the specifications and automation status of NAA laboratories world-wide. More than 30 replies have been obtained so far from various RR facilities world-wide, both from developing as well as from developed Member States. Preliminary analysis of already received questionnaires indicates that only a few groups world-wide have demonstrated that automation in NAA is feasible, both with respect to hardware (e.g., sample changers) and software (e.g., integrated modules for converting peak areas in element amounts).

All this information was further analyzed in the consecutive IAEA Consultancy Meeting that took place in June 2011 in Vienna (Austria). The meeting participants (7 international experts representing 7 Member States) advised and assisted the IAEA on the draft design of the new CRP on “Development of an Integrated Approach to Routine Automation of NAA”, that has been submitted and approved in December 2011. The main objective of this new CRP is to coordinate activities on the implementation of automation processes for NAA technique at RR centers. The CRP will have a modular structure in developing and implementing the hitherto missing tools for automation approach, both hardware and software, including data processing and analysis reporting, cover some of the design principles, interaction with and control of sample changers; this all with quality assurance procedures as a cross-cutting component. It will strengthen the optimization and competitiveness of the NAA process by harmonized automation hardware and software. The pursued harmonization will also render in a network of NAA laboratories and experts from different countries. Finally, it is expected that the CRP would contribute to enhanced RR utilization, increased NAA capacity, additional revenue generation with more end-users serviced including countries without RRs, and increased cooperation between different RR centers. The project kick-off meeting is already scheduled for July 2012. Participation of close to 20 NAA laboratories is expected.

5. NAA Proficiency Tests in support of QA/QC

An optimized and effective utilization and safety of research reactors (RRs) in support of the socio-economic development in AFRA Member States is the overall objective of the IAEA Technical Cooperation project RAF 4/022 (2009-2013). One of the projected roads towards this objective is the provision of services to third parties by RR affiliated nuclear analytical laboratories or newly created RR networks, in particular using NAA. Obviously, the reported results of these laboratories should meet or even exceed the end-users' requirements, and be in compliance with international standards to ensure global acceptance. In this respect Member State's laboratories participating in RAF 4/022 are expected to boost the quality and trustworthiness of their results, by implementing the theoretical and practical guidelines made available by the IAEA via the various activities in this and previous projects. The degree of trueness and precision of the measurement results is thus expected to improve. Participation in inter-laboratory comparisons is an independent and objective approach to verify this.

In 2010-2011 the IAEA has facilitated and supported 11 analytical laboratories, representing 11 Member States in Africa, to participate in the Wageningen Evaluating Programs for Analytical Laboratories (WEPAL, accredited as proficiency testing provider by the Dutch Council for Accreditation under Ref. No. R002) [5]. Participants were invited to join two rounds of WEPAL inter-laboratory comparisons for both soil-related (ISE) and plant-related (IPE) materials [4]. Fig. 2 illustrates some selected results of a well-performing laboratory and poorly-performing NAA laboratory respectively. The results are presented in terms of relative bias points. In general, it is expected that most of the relative bias points, which stand for $[(laboratory\ value - mean\ value) / mean\ value * 100 \ %]$, would fall within, say, 20 % limit to be qualified as a “well-performing” laboratory.

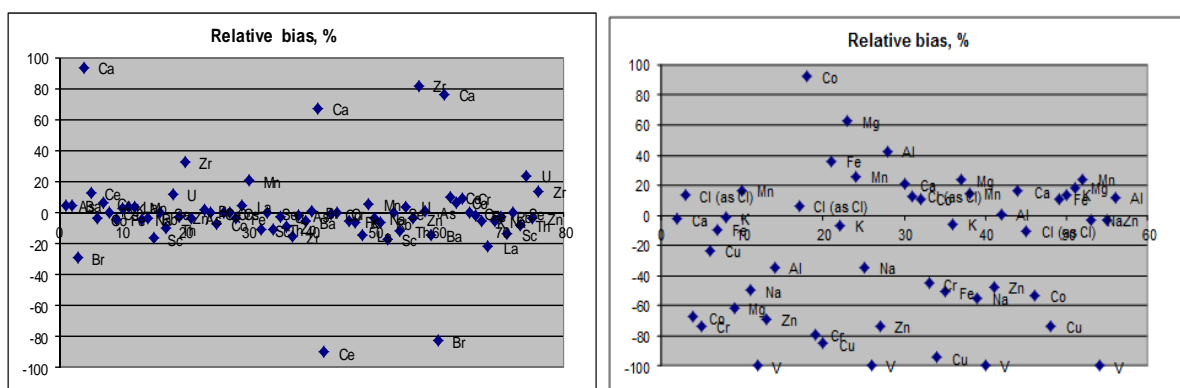


Figure 2: Example for relative bias (%) of “well-performing” (on the left) and “poorly-performing” (on the right) NAA laboratory for multi-elemental determination of composition using soil-related samples.

In brief, these inter-laboratory comparison exercises have provided extremely valuable information on the performance of 11 analytical laboratories, participating in the RAF 4/022 project. The following resumes most of the findings:

- 1 participant was not able to report any result even though the samples were dispatched for two consecutive rounds.
- 3 participating laboratories reported satisfying results for both the soil (ISE) and botanical (IPE) materials in both rounds; 1 participant also performed well but only for botanical materials.
- 6-7 participating laboratories have analytical difficulties resulting in less satisfying/poor performance. This is very worrying given the potential impact of results reported currently and in the past.
- It seems that these less satisfying performing laboratories have no systematic mechanism for independent verification of measurements/calculations and/or of the validity of the results reported.
- The less satisfying/poor performing laboratories apparently did not take any action for improvement of their performance, by whatever means, after receiving the first round reports from the inter-comparison provider and continued performing poorly for the second round.
- All participating laboratories tend to schedule the reporting – and maybe also the execution of the analyses - as tight as possible to the reporting deadline, whereas ample time (~3 months) is available to perform the necessary work.

It is clear that current situation is unacceptable, and urgent measures should be taken to improve the performance of the poorly-performing laboratories. Through the follow up workshop on detailed analysis of these proficiency tests, dedicated training courses and individual expert missions, the IAEA is already assisting the African Member State laboratories in the identification of potential sources of errors, methods for monitoring the occurrence thereof and opportunities for correcting the effects. The IAEA has also arranged repeated proficiency tests to examine that after different measures and joint efforts the situation has improved.

In addition to African Continent, similar proficiency tests have been initiated and are presently ongoing in Europe and Latin America. Taken all together, the effort currently involves more than 30 NAA laboratories world-wide with regional follow up workshops already planned in order to perform detailed analysis of these proficiency tests and share good practices among the participating teams.

6. Summary

Neutron activation analysis (NAA) has all the potentials of demonstrating the relevance of a nuclear research reactor via its application in programs of social-economical relevance and by providing services, at a competitive price, to third parties such as governmental bodies, NGOs and industry, including countries without such capabilities. Still, despite the continuous IAEA's efforts, some of the NAA laboratories do not succeed in this due as they are operating at limited capacity, do not have strict QA/QC procedures implemented, require modernized equipment (both hardware and software) and properly trained staff to install and implement routine automation stages of NAA, do not have well defined marketing strategies, etc. Therefore, quite some efforts have recently been and should be still undertaken with support of the IAEA (e.g. in Africa and Latin America regions) to address the above issues, including a) creation of partnerships with industry by third party oriented NAA services to emphasize the social-economical role of RRs, b) offer the IAEA's Analytical Quality Control services (AQCS) in continuous improvement of the intrinsic quality of their analysis results, leading to accreditation, c) propose continuous training courses and workshops with emphasis on customer oriented services. Some assistance also is offered on individual basis as might be country-laboratory specific. This paper aimed to inform about the most recent IAEA's efforts related to the support of RR-based NAA laboratories through coalitions and networks, technical cooperation and coordinated research projects, promotion of NAA services to the Member States without such facilities, implementation of routine automation and QA/QC procedures, development and implementation of facility-specific marketing strategies, publication of NAA related state-of-the-art documentation and guidelines.

7. References

- [1] IAEA Project D2.01: Enhanced Utilization and Applications of Research Reactors. http://www-naweb.iaea.org/napc/physics/research_reactors/index.html. Accessed in March 2012.
- [2] Ridikas D, et al., (2011) New Opportunities for Enhanced RR Utilization through Networks and Coalitions, Proceedings of the International Conference on Research Reactors: Safe Management and Effective Utilization, 14-18 November 2011, Rabat, Morocco. In print by the IAEA.
- [3] The IAEA Research Reactor Data Base (RRDB). <http://nucleus.iaea.org/RRDB/>. Accessed in March 2012.
- [4] Bode P, et al., (2011) IAEA Collaborating Centre for Neutron Activation Based Methodologies of Research Reactors, Proceedings of the International Conference on Research Reactors: Safe Management and Effective Utilization, 14-18 November 2011, Rabat, Morocco. In print by the IAEA.
- [5] Wageningen Evaluating Programs for Analytical Laboratories (WEPAL). <http://www.wepal.nl/>. Accessed in March 2012.

MYRRHA

A FLEXIBLE FAST SPECTRUM IRRADIATION FACILITY

P. BAETEN, R. FERNANDEZ, D. DE BRUYN, G. VAN DEN EYNDE,
E. MALAMBU, H. AÏT ABDERRAHIM
Belgian Nuclear Research Centre (SCK•CEN)
Boeretang 200, B-2400 Mol – Belgium

ABSTRACT

MYRRHA (Multi-purpose hYbrid Research Reactor for High-tech Applications) is an experimental accelerator driven system (ADS) currently being developed at SCK•CEN in replacement of its material testing reactor BR2. The MYRRHA facility, currently developed with the aid of the FP7-project 'Central design team', is conceived as a flexible fast spectrum irradiation facility, which is able to run in both subcritical as critical mode. This implementation of MYRRHA will allow for fuel developments for innovative reactor systems, material developments for GEN IV systems and fusion reactors, doped silicon production, radio-isotope production and fundamental science applications at the high power proton accelerator.

Next to these applications, MYRRHA will demonstrate the ADS full concept by coupling the accelerator, spallation target and subcritical reactor at reasonable power level to allow operational feedback, scalable to an industrial demonstrator and allow the study of efficient transmutation of high-level nuclear waste. Since MYRRHA is based on the heavy liquid metal technology, namely lead-bismuth eutectic (LBE), it will be able to significantly contribute to the development of Lead Fast Reactor (LFR) technology and will play the role of European Technology Pilot Plant in the roadmap for LFR when operating in critical mode.

Within this paper, the latest configuration of the MYRRHA system is described.

1 Introduction

Since its creation in 1952, the Belgian Nuclear Research Centre (SCK•CEN) at Mol has always been heavily involved in the conception, the design, the realization and the operation of large nuclear infrastructures. One of the flagships of their nuclear infrastructure, is the BR2 reactor^[1], a flexible irradiation facility known as a multipurpose materials testing reactor. BR2 is operational since 1962 and is, after being refurbished twice, licensed for operation until 2016 with a possible ten-year extension until 2026. Since 1998 SCK•CEN is working on the design of a multi-purpose flexible irradiation facility, MYRRHA, that can replace BR2.

MYRRHA has started from the ADONIS project (1995 – 1997), which was the first project at SCK•CEN where the coupling between an accelerator, a spallation target and a subcritical core was studied. ADONIS was a small irradiation facility, having the production of radioisotopes for medical purposes as its single objective. In 1998, the ad-hoc scientific advisory committee advised extending the purpose of the ADONIS machine to become a material testing reactor for material and fuel research, to study the feasibility of transmutation of minor actinides and to demonstrate the principle of the ADS at a reasonable power scale. Since 1998, the project is called MYRRHA.

MYRRHA is designed as an accelerator driven system (ADS) for R&D applications and consists of a proton accelerator delivering its beam to a spallation target coupled to a subcritical core. In 2005 MYRRHA consisted of a proton accelerator delivering 350 MeV * 5 mA to a windowless spallation target coupled to a subcritical fast core of 50 MW_{th}. This 2005 version is the "MYRRHA – draft 2" design^[2]. This 2005 design was used as a starting base

within the FP6 EUROTRANS integrated project^[3], which resulted in the XT-ADS^[4] (Experimental Demonstration of the Technical Feasibility of Transmutation in an Accelerator Driven System) design, where a linear proton accelerator delivers a 600 MeV * 3.2 mA beam into the spallation target. The reactor power of XT-ADS was 57 MW_{th}.

The XT-ADS design was taken as a starting point for the work performed in the FP7 CDT project^[5], which resulted in the current design of the MYRRHA reactor. This design is referred to as MYRRHA-FASTEF (MYRRHA Fast Spectrum Transmutation Experimental Facility) and is described in this paper.

2 The current MYRRHA design

MYRRHA is a pool-type ADS cooled by lead-bismuth eutectic (LBE). While MYRRHA is a pool-type design, the reactor vessel houses all the primary systems and the primary coolant. The vessel is closed by the reactor cover. The diaphragm, located within the reactor vessel, divides the LBE coolant in a hot, low pressure upper pool and a cooler, high pressure lower pool. It serves as the support structure for the major internal components and foresees feedthroughs to the cold plenum. Figure 1 shows a section of the MYRRHA-FASTEF reactor with its main internal components.

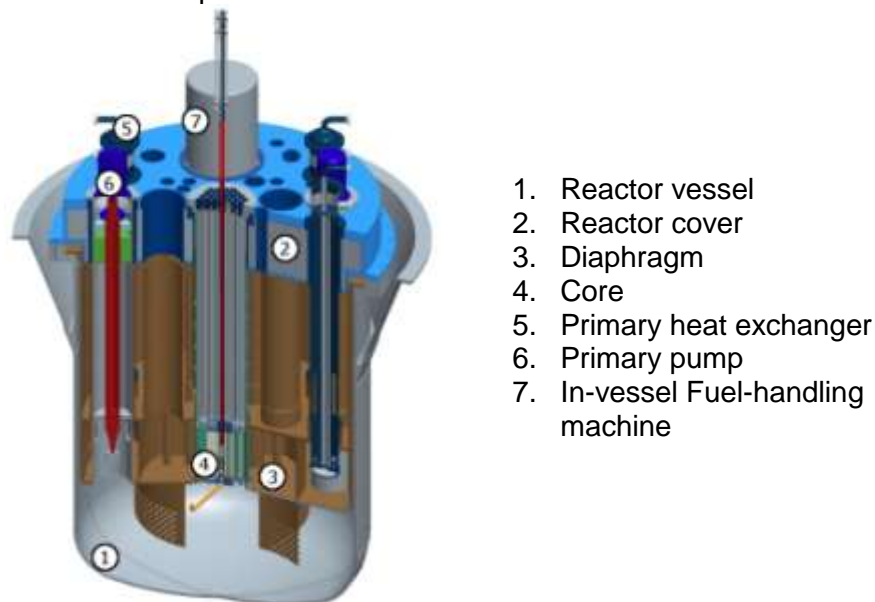


Figure 1 – Vertical cut of MYRRHA

While the room situated directly above the core will be occupied by a lot of instrumentations and experiments, fuel handling will be done from underneath the core. The fuel assemblies (FA) will be kept in place under the core support plate by buoyancy. There are two in-vessel fuel-handling machines, each covering one side of the core, based on the well-known principle of rotating plugs (SCARA robots). A ultrasonic sensor will be used to identify the FA's.

2.1 Accelerator

The accelerator is the driver of MYRRHA while it provides the high energy protons that are used in the spallation target to create neutrons which in turn feed the subcritical core. The accelerator must be able to provide a proton beam with energy of 600 MeV and a maximum current of 4 mA, which will be delivered to the core in continuous wave mode. The beam is delivered to the core from above through a beam window.

Accelerator availability is a crucial issue for the operation of the ADS. A high availability is expressed by a long Mean Time Between Failure (MTBF), which is commonly obtained by a combination of over-design and redundancy. On top of these two strategies, fault tolerance must be implemented to obtain the required MTBF. Fault tolerance will allow the accelerator to recover the beam within a beam trip duration tolerance after failure of a single component. In the MYRRHA case, the beam trip duration tolerance is 3 seconds. Within an operational

period of MYRRHA the number of allow beam trips exceeding 3 seconds must remain under 10, shorter beam trips are allowed without limitations. The combination of redundancy and fault tolerance should allow obtaining a MTBF value in excess of 250 hours.

At present proton accelerators with megawatt level beam power in CW mode only exist in two basic concepts: sector-focused cyclotrons and linear accelerators (linacs). Cyclotrons are an attractive option with respect to construction costs, but they don't have any modularity which means that a fault tolerance scheme cannot be implemented. Also, an upgrade of its beam energy is not a realistic option. A linear accelerator, especially if made superconducting, has the potential for implementing a fault tolerance scheme and offers a high modularity, resulting in the possibility to recover the beam within a short time and increasing the beam energy.

A basic layout of the MYRRHA accelerator is provided in Figure 2, aiming at maximizing its efficiency, its reliability (or MTBF) and its modularity.

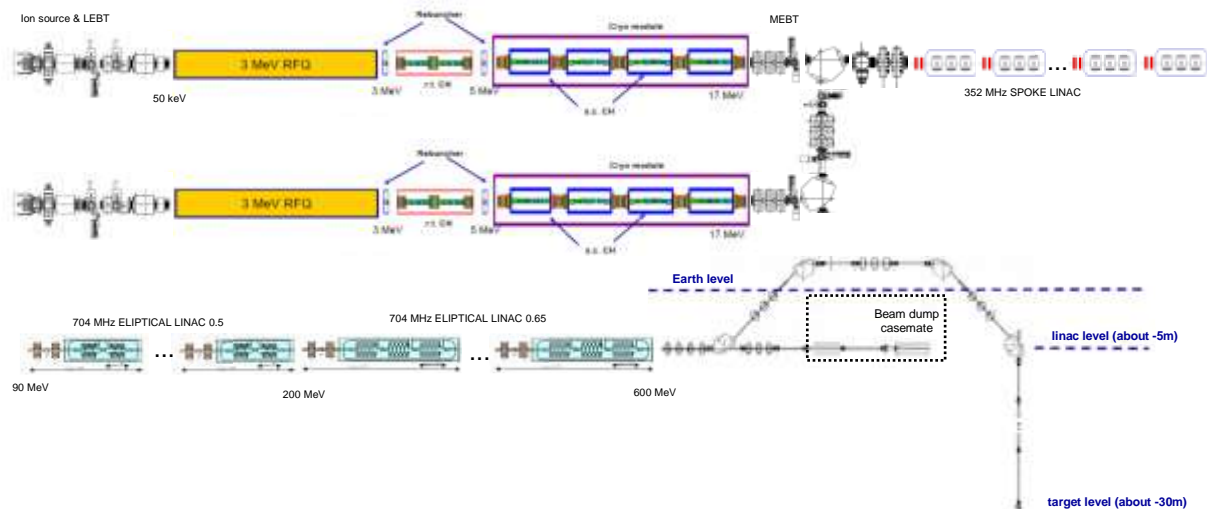


Figure 2 – Schematic layout of the reference design of the MYRRHA accelerator

2.2 The core and spallation target

The reactor core consists of mixed oxide (MOX) fuel pins, typical for fast reactors. 151 hexagonal positions can be taken by fuel assemblies, control and scram rods (in the critical configuration), the spallation target (in subcritical configuration) and in-pile test sections (IPS). When MYRRHA is operating in subcritical mode, the central position is always taken by the spallation target. Thirty seven positions are available for IPS: these positions are accessible from the top and have the possibility to house on top extra out-of-pile equipment to create other irradiation conditions. Figure 3 shows a critical core configuration.

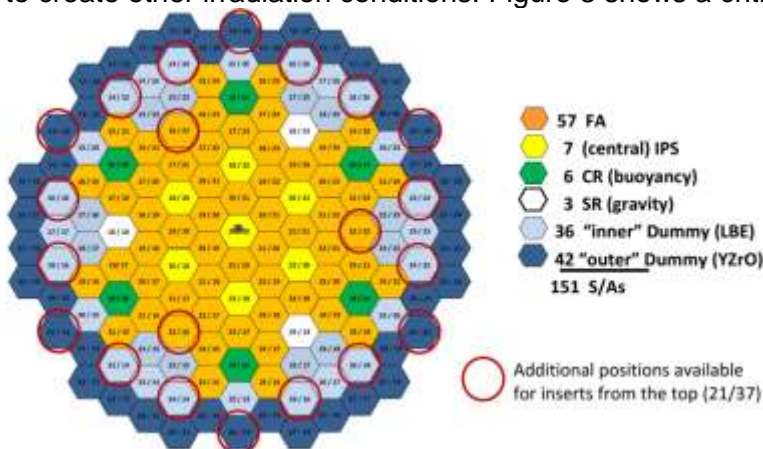


Figure 3 – Cut in the MYRRHA-FASTEF core

The requested high fast flux intensity has been obtained optimizing the core configuration geometry (fuel rod diameter and pitch) and maximizing the power density. We will be using, for the first core loadings, 15-15Ti as cladding material instead of T91 that will be qualified progressively further on during MYRRHA operation. Thanks to the use of LBE as coolant, it permits to lower the core inlet operating temperature down to

270 °C. Consequently the risk of corrosion is decreased and the core ΔT might be increased. This together with the adoption of reliable and passive shut down systems will permit to meet the high fast flux intensity target.

In subcritical mode the spallation target assembly, located in the central position of the core, brings the proton beam via the beam tube into the central core region. The assembly evacuates the spallation heat deposit, guarantees the barrier between the LBE and the reactor hall and assures optimal conditions for the spallation reaction. The assembly is conceived as an IPS and is easily removable or replaceable. When switching to critical mode, the spallation target is removed from the reactor and the control and shutdown rods are inserted in place.

When operating in critical mode, MYRRHA is equipped with two redundant, passive and diverse shutdown systems. One system has also the control function is constituted by rods inserted by buoyancy (in a passive way) from the bottom of the core. The other is constituted by rods inserted from the top by pneumatic means fail safety (loss of gas causes the rod insertion) and enhanced by a ballast.

2.3 The cooling system

The primary, secondary and tertiary cooling systems have been designed to evacuate a maximum thermal power of 110 MW. The 10 MW more than the nominal core power account for the power deposited by the protons, for the power of in-vessel spent fuel and for the power deposited in the structures by γ -heating. The average coolant temperature increase in the core in nominal conditions is 140 °C with a coolant velocity of 2 m/s. The primary cooling system exists of two pumps and four primary heat exchangers.

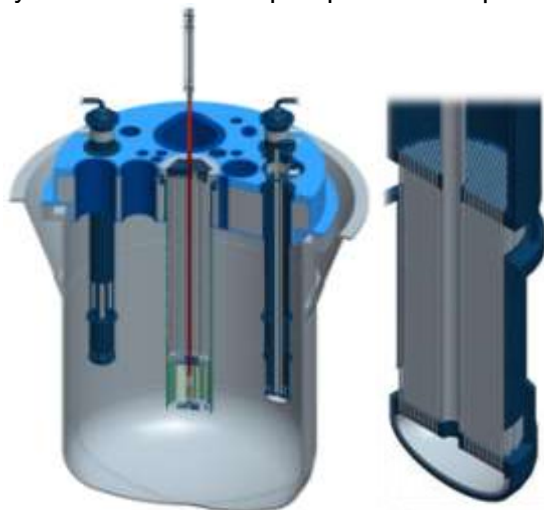


Figure 4 – Heat Exchangers

The primary pumps shall deliver the LBE to the core with a mass flow of 4750 kg/s (453 l/s per pump). The working pressure of the pump is 300 kPa. The pump will be fixed at the top of the reactor cover, which is supposed to be the only supporting and guiding element of the pump assembly.

The main thermal connection between the primary and secondary cooling system is provided by the primary heat exchangers (Figure 4). The heat exchangers are from the shell and tube, single pass and counter-current type, using pressurized water as secondary coolant. A feed-water pipe guides the secondary coolant from the top of the heat exchanger to the lower dome. The walls separating LBE and water plena (feed-water

tube, lower dome and upper annular space) are double walled to prevent the total collapse of the whole water inventory into the primary pool.

The secondary cooling system uses saturated water/vapour as heat transfer medium. In this way the secondary cooling system operates at lower pressure and lower water flow than with single phase pressurized water. This offers the ability to reduce the dimensions of piping and heat exchangers and mitigates the consequences in case of a primary heat exchanger tube rupture or a secondary cooling pipe rupture. The secondary cooling system consists of 4 independent loops, one for each primary heat exchanger.

For each of the 4 secondary loops, a tertiary loop is foreseen in order to release the heat from the secondary loop to the atmosphere. The tertiary system is an air cooling system, where on this moment 2 options are considered: air cooled condensers for both active as passive cooling or air cooled condensers for active cooling and isolation condensation systems for passive cooling.

In case of the unlikely event of loss of the primary flow (primary pumps failure), the primary heat exchangers aren't able to extract the full heat power. In such cases, the beam must be shut off in the subcritical case and the shutdown rods inserted in the critical case. The decay

heat removal (DHR) is achieved by natural convection. Ultimate DHR is done through the reactor vessel coolant system (RVACS, reactor vessel air cooling system) by natural convection.

3 Further developments

In the following years, a lot of R&D must be performed in order to support the design work and the safety analysis of the facility presented in this paper.

First of all, it is essential to perform the necessary R&D to support the qualification of the MOX fast driver fuel and the investigation of structural and cladding material behaviour in reactor conditions.

Then, the main goal of the material R&D and qualification programme is to provide reliable material property data for the design and licensing of FASTEF. Within the MYRRHA project as a whole, it is preferred to consider industrially available and qualified materials, rather than to develop and optimize new materials. Based on the available material properties, 15-15Ti, T91 and 316L have been selected as the candidate materials. Austenitic stainless steels, including 15-15Ti and 316L, have been used in the construction of fast, sodium-cooled, reactors and are well characterized for nuclear applications. However, due to the innovative character of FASTEF, further investigation on the material behaviour and performances must be done. On this moment, four overlapping activities regarding material R&D are performed: a) identification of the material issues for design and licensing, b) development of test and evaluation guidelines for structural materials characterisation, c) assessment of material properties and finally d) development of testing infrastructure.

Finally, for a long-term operation of a LBE cooled ADS, chemistry control and monitoring is crucial for the reactor. A LBE chemistry and conditioning R&D programme handles about the LBE technology related to the chemical control of the coolant and the purification of the evaporated gasses. Several issues have been identified for this programme: a) development of oxygen sensors to measure the dissolved oxygen concentration in the coolant, b) conditioning of the LBE to minimize dissolution of structural materials and core internals and to prevent formation and precipitation of oxides, c) filtration and trapping of impurities in the LBE, d) evaporation and capture of volatile and/or highly radiotoxic elements from the cover gas and finally e) removal of LBE or dissolved constituents from among others components and test samples.

Conclusion

SCK•CEN is working to replace its aging flagship facility BR2 by a new flexible irradiation facility MYRRHA. MYRRHA is a flexible fast spectrum irradiation facility that can work in both subcritical as critical mode.

MYRRHA is planned to be operational by 2024. As a fast spectrum irradiation facility, it will address fuel and material research for innovative reactor systems, radioisotope production, both for industrial and medical purposes, and several industrial applications, like Si-doping.

References

- [1] BR2 Reactor, (<http://www.sckcen.be/en/Our-Research/Research-facilities/BR2-Belgian-Reactor-2>)
- [2] H. Aït Abderrahim, D. De Bruyn *et al.*, "MYRRHA Project – Technical Description", SCK•CEN Report reference AND/HAA/DDB/3900.B043000/85/07-17bis, April 2007.
- [3] EU Integrated Project EUROTRANS, contract nr. FI6W-CT-2004-516520.
- [4] D. De Bruyn, S. Larmignat, A. Woaye Hune, L. Mansani, G. Rimpault and C. Artioli, "Accelerator Driven Systems for Transmutation: Main Design Achievements of the XT-ADS and EFIT systems within the FP6 IP-EUROTRANS Integrated Project", International Congress on Advances in Nuclear Power Plants (ICAPP'10), San Diego (California, USA), June 13-17, 2010, American Nuclear Society (2010).
- [5] D. De Bruyn, P. Baeten, S. Larmignat, A. Woaye Hune and L. Mansani, "The FP7 Central Design Team Project: Towards a fast-spectrum transmutation experimental

facility", International Congress on Advances in Nuclear Power Plants (ICAPP'10), San Diego (California, USA), June 13-17, 2010, American Nuclear Society (2010).

THE MASURCA CRITICAL FACILITY REFURBISHMENT AND THE DESIGN OF THE FUTURE GENESIS PROGRAM IN SUPPORT TO THE ASTRID PROTOTYPE

B.AUTRAN¹, F.MELLIER²

**(1) CEA, DEN, DER, Masurca Operation and Refurbishment Laboratory
(2) CEA, DEN, DER, SPEX Experimental Laboratory**

C.E.A, Cadarache, France,

(1) bernard.autran@cea.fr, (2) frederic.mellier@cea.fr

Key words: MASURCA, Fast reactor, Neutron, ASTRID, GENESIS, Refurbishment, Facility, Mock-up, Seismic strengthening, Ventilation, Nuclear, Ageing.

As a result of an investigation carried out in 2009 about the role and the importance of MASURCA to meet the needs of 4th generation fast neutron reactors, the CEA decided, at the beginning of year 2010, to proceed to the refurbishment of the facility. After an important renovation phase, the future programs will be conducted within the framework of ASTRID project and GENESIS R&D program on innovative sodium cooled reactors.

HISTORY

Started up in 1966, MASURCA mock-up is a “zero” power reactor (5kw) dedicated to the studies of Fast Neutron Reactors (FNRs) and development of measurement techniques.

From 1966 till the middle of the 90s, programs were mainly focused on sodium-cooled cores. The RZ and PLUTO programs (1966-1977) first contributed to the development of calculation tools used for PHENIX and SUPERPHENIX design. Then the PRE-RACINE and RACINE programs (1978-1984) extended the study to heterogeneous cores. The programs that followed, BALZAC (1984-1988), completed the knowledge in the field of control rods. Lastly the CONRAD program (1989-1993) was aimed at investigating large axial heterogeneous cores.

The recent programs have been carried out under the terms of the French 1991 law on the management of long-lived radioactive wastes (the “Bataille” act). These were essentially conducted within axis 1 “Partitioning and Transmutation”:

- The CIRANO program (1994-1997) contributed to the study of Pu burner reactors and addressed the “sodium void” issue,
- From 1998 to 1999 based on ECRIX experiments in the PHENIX reactor, the COSMO program investigated the principle of transmutation in moderated target,
- Lastly, from 2000 to 2004, the behaviour of accelerator driven system (ADS) was thoroughly studied during the MUSE-4 project.

In 2006, the loading of “gas” core to validate the new neutronic control system of the facility marked the beginning of experiment in support of the 4th generation systems.

FACILITY

The MASURCA facility is the French facility acronym for mock-up breeder-reactor in CADARACHE.



Figure 1: MASURCA aerial photo

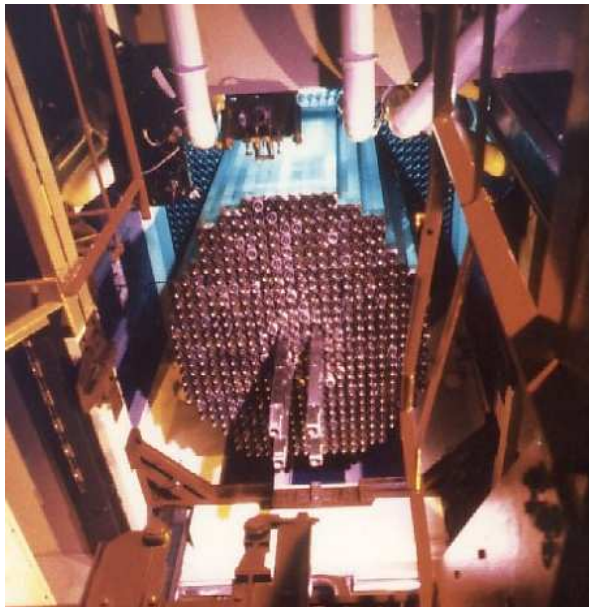
MASURCA (fig. 1) is composed of four blocks;

- Reactor building,
- Storage building
- Staff and Control Room building,
- Auxiliary building.

Its staff is about 30 people, including a team for experimental test.

REACTOR

This reactor, like “Meccano[®] toys” style assembly, may hold cores with volumes of up to 6 m³ (fig. 2). It is made up of square-section tubes, individually loaded with fuel strips, or platelets, or with coolant, representative of the fast- or epithermal-neutron lattices being investigated.



The core materials are contained in rodlets (with parallelepipedic or cylindrical shape) with a square or circular section of ½ inch for the sides and 4 to 24 inches in height. These rodlets are arranged according to basic pattern which is reproduced several times and put into a wrapper tube with a square section of 4*4 inches and about 3.8 meters long. Tubes are then hung onto a vertical plate support by a concrete structure. The core is cooled by air and is surrounded by a biological shielding made of heavy concrete.

Figure 2: MASURCA Core

MEASUREMENT

The MASURCA design enables measurement devices to be located in all areas of interest:

- Activation foils can be put anywhere in each tube,
- Two perpendicular radial channels and several axial channels can be opened throughout the core in order to introduce various detectors (fission or gamma chambers, activation foils and TLDs) or neutron sources,
- Several counters can be distributed inside the core to monitor the flux and thus the reactivity.

PERIODIC SAFETY REVIEW

With time, the safety level of any facility is intended to be kept at least as it was at start up. Maintenance programs are performed in that purpose but, when getting older, the facility is becoming slightly less reliable due to ageing of non-removable components. A more substantial way to outdate the safety level of a facility is the increase of regulation requirements with time. These convergent processes of ageing on one hand and tightening on the other hand make sooner or later the facility no more able to meet safety requirements. Before this moment arises, shut down or renewal has to be considered.

As early as February 2000, the French Safety Authority (ASN) informed the CEA that it was necessary to conduct a safety review of the reactor, the previous such review dating from 1988 and several reactor items now being obsolescent. Consequently, priority in 2005 was given to continuing the periodic safety review of the facility and carrying out a certain amount of renovation work. The Advisory Committee for reactors should therefore in March 2006 be reviewing the steps taken to enable MASURCA to operate on a long-term basis.

In conclusion of the permanent group on MASURCA facility, Safety authorities accepted the refurbishment proposed by the CEA. After engineering studies and best-cost estimate studies, the CEA decided in 2010 to engage the upgrade of the facility. In September 2010 the French government confirmed its support, for a 600 MWe Astrid prototype (Gen IV program).

This program includes the development of the reactor itself and the refurbishment of MASURCA facilities to qualify innovative core design (low void core).

Refurbishment of MASURCA is needed to reach new safety standards requirements. Safety studies concern the most sensitive points:

- Designing of the confinement barriers
- Management of internal risks (criticality, fire, flood...)
- Management of external risks (earthquake, airplane crash...)
- Incidental and accidental situation analysis (with radiological impact).

Improvements are necessary for this 45 years old facility to increase the safety level.

Experiment instrumentation is although being update, with new experimental devices, new experimental room and a new control room.

Seven years are necessary to finalize the project. The refuelling of the reactor is planned in 2018.

An extensive refurbishment program is undertaken which includes;

- Civil engineering works to build a new material storage building with earthquake resistance, based on 3D computations and withstanding Maximum Historically Likely Earthquake,
- Improving confinement of reactor building,
- Changing ventilation system core and building,
- Changing power supplies by two independent lines,
- Upgrading mechanical loading machinery,
- Fire detection and protection system,
- Radioactivity monitoring and alarms,
- Installing a new control room,
- Transferring the fissile element inside the new storage building.

Most of the work will end in mid 2017. The total refurbishment final cost is about 50 M€. Recent events placed the focus on seismic update due to Fukushima Stress test analysis and increase the level above requirements of the safe shutdown earthquake (level 9). Safety authorities ask the CEA to empty the old storage of material as soon as possible, with a milestone set to end 2013.

PROJECT DESIGN

The initial expertise done, the project was built according to the safety objectives described above in main fields: confinement (static, dynamic), loading handling, radiological, energy supply reliability, fire detection/remediation and seismic strength of the facility. The resulting actions of refurbishment to be fulfilled are the following :

Confinement: Increasing the tightness of the reactor building by fixing the leak of the containment vessel. Replacing the crossing instrumentation throw the building. Changing door seals of the airlock.

Ventilation devices: Total replacement of the old system (ventilators for the core and reactor building) by a two separate systems able to sustain low pressure in the building and air cooled in the core. The difficulty originates from the fact that refurbishment activities present risk of contamination. Thus, a worksite's ventilation system has to be run during operation. Temporary bypasses are used to maintain ventilation while replacing the pipes and other parts. The second difficulty is to evaluate the pressure drop in tube. To solve this problem we have build a pressure drop facility to perform measurement on different tube designs.

Machinery loading: Refurbishment of mechanical equipment, pilot rod and control rods drive system, replacement of equipment parts due to obsolescence and ageing effect. Renewals of the travelling fuelling machine by a new computerised system in replacement of the old relay automatism with old synchro/resolver position feed back. Updating all the documentation.

Utility supply reliability: Replacement of all electrical wires (power and monitoring) to fireproof grade, of the electricity power supply by two geographical separate ways. Automatic monitoring of the starting up of ventilation devices following an incidental power cut.

Monitoring system: Renewal of the reactor control room to new standard, replacement of the computerized monitoring for fire detection, radiological control, flooding, electricity supplying, ventilation pressures and flow rate now able to give a detailed description of the facility state and allowing some remote action to put back the facility in a safe condition. Complete renewal of the monitoring and remote command for the fuelling machine. The difficulty originates from the fact that refurbishment activities are conducted during maintenance operating and control. Thus, a provisional control room is necessary to monitor safety system, and has to be run during renewal operation of the reactor control room.

Reactor shutdown system: Renewal of the reactor safety Instrumentation and Control (I&C) systems with Safety-oriented Design of components to perform control rod dropping in a very short time inside the core. This system include neutron flux rate monitoring to prevent reactivity excursion and power. The chain although control several security concerning the emergency stop. Two independent lines contribute to ensure the safety of this function.

Fire fighting: Creation, throughout the facility, of so-called fire compartments designed to sustain a fire and to mitigate its propagation (2 hours) before being brought under control.

New storage building: The purpose is, for the new building, to withstand a Safe Shutdown Earthquake. It includes the assembly room devoted to tubes construction, bench-mounting and the material storage racking.

ORGANISATION AND TIME SCHEDULE

The project was managed by a dedicated CEA project team (7 persons) in charge of the refurbishment itself and of the coordination with the day to day facility operation and the experimental programs. The operator keeps the control on the safety management of the facility including the refurbishment work safety as well as the experimental programs execution. He also brings a logistic support to the workers (clothes, control, wastes, etc.).

The engineering is carried out by ASSYSTEM Company.

The end date for the project is middle of 2017. At this time we will reload the core devoted to GENESIS experiments.

IMPORTANT MILESTONE

Milestone	Date
JP0 : Engineering contractor (MOE)	06/01/2012
JP1 : Study details review	J0 + 16 months
JP2 : Start fissile material transfer	J0 + 12 months
JP3 : Start of EXE phase	J0 + 31 months
JP4 : End fissile material transfer	J0 + 30 months
JP5 : 1er Concrete (New Storage Building)	J0 + 38 months
JP6 : Start for performances testing	J0 + 53 months
JP7 : End of contractor mission (and commissioning)	J0 + 66 months

FUTURE EXPERIMENTAL PROGRAMS

- OBJECTIVE AND MOTIVATION

Experimental neutron physics programs are an essential component of the general data and code validation process, which consists in assessing and quantifying calculation errors and uncertainties for a given application domain. These experiments are essential, as they ultimately contribute to the demonstration that plant design, operation and safety criteria are fulfilled.

Over the past twenty years, this validation process at CEA has evolved from a rather global approach to a very analytical one, in which every effort is made to separate the individual physics phenomena in order to identify the various possible sources of errors. Detailed and systematic analyses of calculation-vs.-measurement (C/E) discrepancies, using sensitivity and perturbation techniques, have lead to a better understanding of the underlying physics phenomena, from which recommendations for improvements in the data and/or models could be derived [1].

As a consequence, “reference” neutronic simulations are now capable of accurately modeling classical fast reactor subassemblies and cores. In particular, they no longer suffer from a number of modeling approximations, a posteriori corrections and ad hoc factors that characterized the older methods.

Nevertheless, Gen-IV fast system design studies have led to subassembly and core concepts that are significantly different from “classical” sodium-cooled concepts like PHENIX and SUPERPHENIX reactors [2, 3]. The specific systems under consideration are large size, pool-type, plutonium-fuelled SFRs designed to achieve a high conversion ratio without radial blankets and a low, possibly even negative, sodium void reactivity effect (SVRE). The French “CFV” concept [4], in particular, include design solutions (a reduced sodium-to-fuel volume fraction, an internal fertile plate, a sodium plenum and an absorber plate at the top of sub-assemblies above the plenum sodium) that make this design innovative (fig. 3) and very challenging to calculate even for state-the-art neutron physics simulation codes. Therefore, validation experiments are required to demonstrate that important physics phenomena are properly accounted for in the simulations, and that numerical predictions are within targeted error bands.

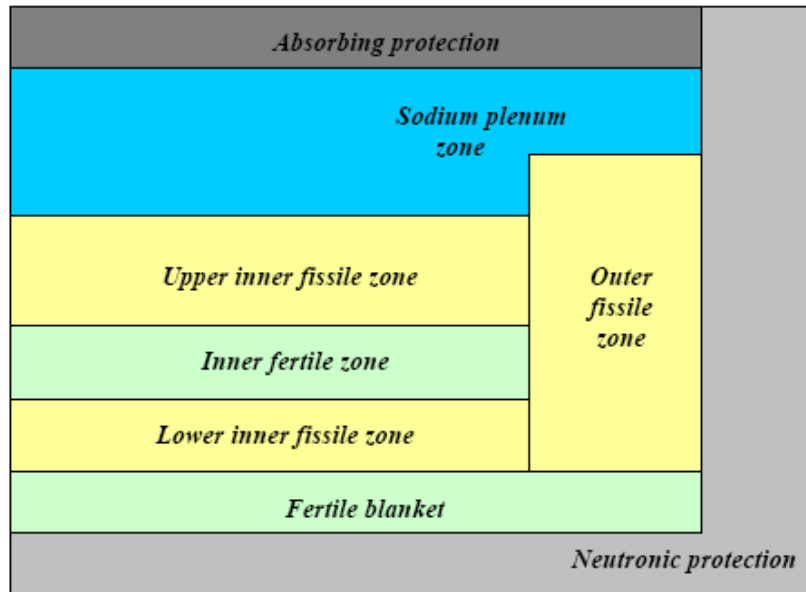


Figure 3 : Core geometry of the ASTRID/CFV design (from [4])

- RATIONALE OF FUTURE EXPERIMENTAL PROGRAMS

The purpose of future programmes in the MASURCA facility is to obtain experimental data needed for the design and safety assessment of these innovative sodium-cooled fast reactor core concepts. Taking advantage of the flexibility of the MASURCA facility and its fuel stock, various configurations representing or bracketing the situations of interest can be studied, usually in a progressive, analytic approach allowing to investigate separate-effect experiments as well as combined-effect experiments, both representative of the particular situations found in the “actual” reactor core concept. The rationale is to go progressively from a “simple” reference core to more complex cores, by introducing one variation at a time, so that individual and cumulative effects can be assessed.

In a first phase, next programme should support the ASTRID project and more especially the evolutionary core design named CFV (low void sodium effect core) [4]. This design has the objective to lead to a zero and even negative void sodium effect by including:

- a plenum sodium,
- an upper absorbing zone located above the plenum,
- an internal fertile plate,
- inner and outer fissile zones with different heights.

One of the major objectives of the programme in MASURCA to be defined, the GENESIS program, will be to consolidate calculations of void sodium configurations corresponding to incidental situations. A number of sodium density reduction and voiding experiments will be simulated over a central zone, in which the sodium simulation elements will be replaced by void elements, while preserving the overall geometry (core height in particular). Different configurations, including design options described above, will be studied, involving axial sections of various sizes and positions.

In a first step, it is envisaged to load a reference core consisting of an homogeneous PuO₂-UO₂ core, surrounded by lower and upper fertile blankets (~30 cm). The purpose of this “classic” core will be to calibrate experimental techniques and calculation tools, more especially for void sodium measurements. From this, major modifications will be set-up :

- the upper fertile blanket will be replaced by a sodium plenum. Different variants with several plenum heights will be set-up.

- an internal fertile plate will be introduced below the fissile zone mid-plane. Once again, different axial positions of the plate, from ~ -5 to -10 cm, and thicknesses in the range ~ 20 to 25 cm, will be investigated.
- an absorbing protection above the plenum sodium will be then arranged.

Complementary configurations including modelling of the fuel fission gas plenum volume and with different heights of the inner and outer fissile zones should be also investigated. The study of reactivity worth of absorber rods in this new type of configurations will be also carefully investigated.

Next phases, could then include new reflectors, innovative absorbers, modelling of incidental situations as well as phases devoted to future power reactors.

At the moment, preliminary calculations have been performed to study feasibility of first experimental configurations envisaged (figure 1) and to optimize representativity of physical parameters to be measured. Further studies should help to define more precisely the needs for new simulation elements, the dimensions of experimental zones, the chaining of different configurations with time, the measurements to be carried out during each phases and the overall schedule of the program.. This work will be pursued in the coming years taking into account the future evolutions of ASTRID prototype core design and needs linked to the development of future power SFRs.

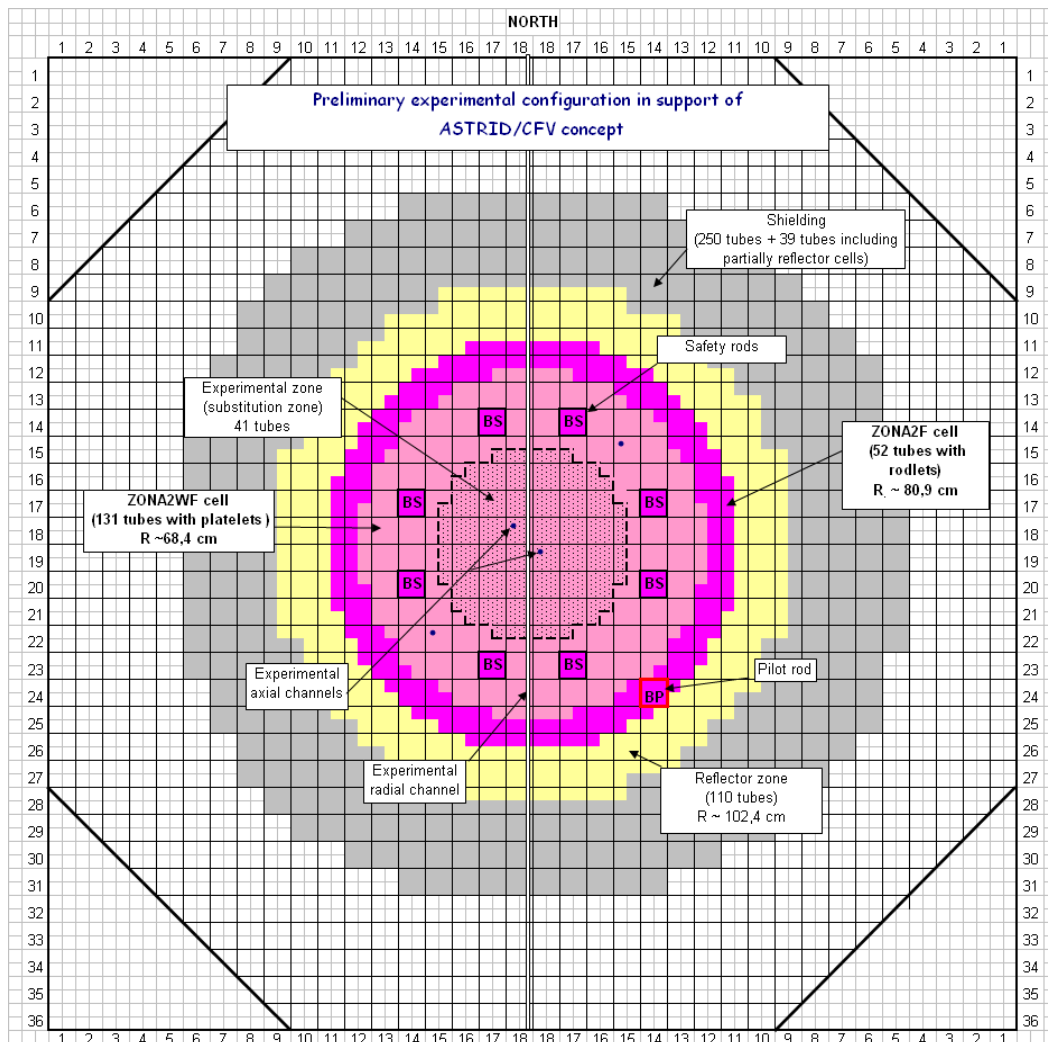


Figure 4: Preliminary picture of an experimental configuration in MASURCA in support of ASTRID/CFV core concept

A comprehensive measurement programme is planned in each phase. Main measurements of interest will include:

- - criticality,
- - fission rate distributions, more especially in axial direction, by miniature fission chambers moved inside an internal channel arranged in fissile tubes,
- - complementary axial reaction rate distributions by foil activation,
- - capture-to-fission ratios by activation foils inside the tubes,
- - reactivity variation measurements using different techniques (multiplication methods, compensation by an absorber rod, return to critical configuration)

Measurements of spectral indices, neutron relative importance, kinetics parameters will be also conducted on a limited number of configurations.

An essential objective of the programme is to obtain high quality results. The measurements should therefore be sufficiently diverse and numerous to obtain reduced experimental uncertainties.

Renovation of existing experimental equipments (detectors, electronics modules, mechanic devices for handling of detectors, acquisition systems, analysis tools, databases ...) and development of new ones is fully part of the renovation project. Inventory of equipments needed for this ambitious program is already in progress.

CONCLUSION

The organisation was set up by the CEA. Renovation of MASURCA has been started with the objective of performing new experimental programs at the dawn of 2017/2018.

One of our key focuses is to work on conditioning and transfer to empty the storage fissile material according our safety requirements. Draft design studies have been started in January 2012 and the first detail framework that provides direction for the renewal should be send in the middle 2013.

Definition of future experiments in support of ASTRID prototype, the GENESIS program, is on going. This activity should increase in the coming years.

REFERENCES

[1] BLAISE Patrick, SANTAMARINA Alain, BERNARD David et al., The VVQ&UQ process for neutronics code package: issues on nuclear data assimilation and transposition for the current and future nuclear systems, Second Workshop on Verification and Validation for nuclear systems analysis, Beach Cove Resort, North Myrtle Beach, SC, USA, 24-28 May, 2010

[2] RIMPAULT & al., "Towards GEN-IV SFR design: Promising ideas for large advanced SFR core designs", Proc.Int.Conf. PHYSOR'2008, Interlaken, Switzerland, September 14-19, 2008

[3] LE COZ Pierre (CEA), SAUVAGE Jean-François (EDF), SERPANTIE Jean-Pol (AREVA), Sodium-cooled fast reactors: The Astrid plant project, ICCAPP 2011, Nice, France, 2-6 May, 2011

[4] SCIORA Pierre & al., "Low sodium effect core design applied on 2400 MWth SFR reactor", ICCAPP 2011, Nice, France, 2-6 May, 2011

LAUNCHING OF A NEW RESEARCH REACTOR PROJECT IN KOREA

S.I. WU, I.C. LIM, S.Y. OH and J.J. HA

Division of Reactor Project Engineering, Advanced Reactor Development Institute

Korea Atomic Energy Research Institute

ABSTRACT

In order to cope with the growing demand of radio-isotopes including Mo-99 and the neutron silicon doping service, the Korea government has decided to construct a new research reactor, which will be a second middle class research reactor less than 15 MW in thermal power. The decision was determined based on the findings of a feasibility study conducted jointly by KDI (Korea Development Institute) and KAERI (Korea Atomic Energy Research Institute). The NRR project will be officially launched on March 2012 and has a 60 months planned period for all activities, from design to commissioning. Through this project, the roll of HANARO will be changed to a neutron beam facility and the NRR will take over the neutron irradiation service function independent from HANARO.

1. Introduction

This paper intends to introduce the background, launching and future plans of the New Research Reactor Project in Korea. The Korea, Ministry of Education, Science and Technology (MEST), has taken a significant initial step toward the construction of a new research reactor, which is a step toward the self-sufficiency in terms of medical and industrial radioisotope supply and to build up Korean research reactor technologies. As a first step, the MEST has signed an implementation agreement for a “New Research Reactor Development and Demonstration Project” with the local governments and KAERI on February 14th, 2012[1]. The four entities have agreed to fully cooperate for the success of this project to construct a reactor and its utilization facilities which is located near Busan city, the south-eastern part of the Korean peninsula.

MEST will be responsible for coordinating this project by providing its support for stable government financial subsidies, and the local governments will be responsible for land preparations including the purchase of land for this project and setting up infrastructures for utilities including the electric power and raw water line, while KAERI will be responsible for all the procedures such as development, design, licensing, installation, and commissioning to complete the new research reactor project. In the future, the new research reactor will greatly provide the ultimate solution for the domestic supply of medical radio-isotope and will have the capacity to provide some radio-isotopes to the Asian region. The reactor will be also equipped with the capability to provide silicon doping services, which will contribute to the energy saving via the use of efficient power semiconductor device. It is expected that the new research reactor will increase the contribution of nuclear technology to the people in Korea and help the development of technologies for a safer and more efficient research reactor.

2. Background

HANARO, which is a research reactor with a thermal power of 30 MW, has been operating since 1995. The reactor was designed for multi-purpose use in various science and engineering fields such as material irradiation, nuclear fuel irradiation, neutron scattering including cold neutron source, neutron

radiography as well as neutron transmutation doping for silicon. It was intended to enhance the neutron science research area, and utilization of HANARO. The technologies obtained from during its design, construction, operation, and the strong, continuous support from the Korean government, have made HANARO into a well utilized multi-purpose research reactor.

Meanwhile, Korea has been trying to build a new research reactor since 2009. In order to cope with the following three reasons; The first one is that although HANARO is successfully being used for neutron scattering experiments, material and fuel tests for power reactor application, RI production, silicon doping, neutron activation analysis, and neutron radiography, the user's demands to use the research reactor are increasing over the capacity of HANARO. The second reason is in order to cope with the growing demand of the radio-isotopes including Mo-99 and the neutron silicon doping service. Finally, the third reason is to enlarge its capability of the research reactor engineering field. Even if Korea has developed many kinds of technologies in design and utilization of the research reactor but there is still the lack of experience in plate type fuel as well as bottom-mounted control rod drive mechanism.

On the other hand, the project feasibility was confirmed in June of 2011 by a study conducted by the Korea Development Institute (KDI), which is a national research institute supporting the Ministry of Strategy and Finance. The feasibility study has reviewed in such kind of the maturity of technologies required, economic effects due to the cost and benefits of the project, and strategic needs from a national wide point of view. The feasibility report provided a positive result and therefore the Korean National Assembly finally adopted the financial support for the new research reactor. Thus, in 2011, Korea has decided to build a new research reactor to fill the self-sufficiency of RI demand, to increase the NTD capacity and to develop and validate technologies related to the research reactor. The project will start officially from the 1st of Apr. 2012 considering its contribution to the public, industry and research reactor technology development.

3. Design Feature & Utilization

This project includes the installation of a reactor, RI production/research facility, LEU target production facility for Mo-99 production, NTD facility and a radioactive waste treatment facility. The major design characteristics of the reactor in the conceptual stage are summarized in Tab 1.

Tab 1: Design features and requirements of the new research reactor

Item	Value	RIs	No.	Dia. (cm)	Flux (n/cm ² s)
Reactor Power	~15 (MWth)	Fission Mo and other Fps	4	5~8	~2x10 ¹⁴
Reactor Type	Pool type	Ir-192, P-33, Lu-177, Co-60 (Medical purpose)	4	4~6	~3x10 ¹⁴
Neutron Flux (Max)	> 3.0x10 ¹⁴ n/cm ² s	I-131, I-125, Cr-51, Re-186, Sm-153	3	4~6	>1x10 ¹⁴
Operation day	~300/year	HTS and PTS for Short half-life RI2	1 1	3	~1x10 ¹⁴
Life Time	50 year	Others for research purpose	4~5	3	~5x10 ¹³
Fuel	LEU U-Mo plate type (~8.0 g/cc)	6" ingot	2	~17	~1x10 ¹³
Reflector	Beryllium	8" ingot	3	~22	~1x10 ¹³
Coolant & Flow Direction	H ₂ O & Downward Forced Convection	12" ingot	2	~32	~1x10 ¹³
Reactor Building	Confinement				

The new research reactor will be the first reactor in the world which will use U-Mo fuel in full scale. Also, the adoption of bottom-mounted CRDM will make it easy to load and unload RI targets into irradiation holes. In view of safety, it will be equipped with a secondary shutdown system, an automatic seismic trip system, a post accident monitoring system, the emergency control room and the emergency diesel generator in an appropriate size.

The major isotopes to be produced in the new research reactor will be Mo-99, I-131, I-125 and Ir-192. Their production capacities will be respectively 100,000, 3,000, 100 and 300,000 Ci per year. The technologies to produce I-131, I-125 and Ir-192 have been already established. However, the technology to produce Mo-99 will be developed in parallel with the facility development. Considering these, the target for Mo-99 production in the first year is to fulfill the national demand and its capability will be expanded year by year. The production capability for other major isotopes is expected to reach its capacity from the beginning. [2]

As for the silicon doping, the installation of 6" and 8" irradiation rigs will start from 2017. However, the installation of 12" ingot rigs will be made in conjunction with the large diameter ingot irradiation technique development and the availability or needs of 12" ingot irradiation. When the planned installations are finished, the doping capacity will reach 150 tons per year. The surplus in the RI production may be exported to regional countries, which will help to maintain the world Mo-99 production capacity. The increase capacity in RI production and NTD will also contribute to the development of the RI and power device industry in Korea.

4. Site Evaluation

4.1 Site Selection

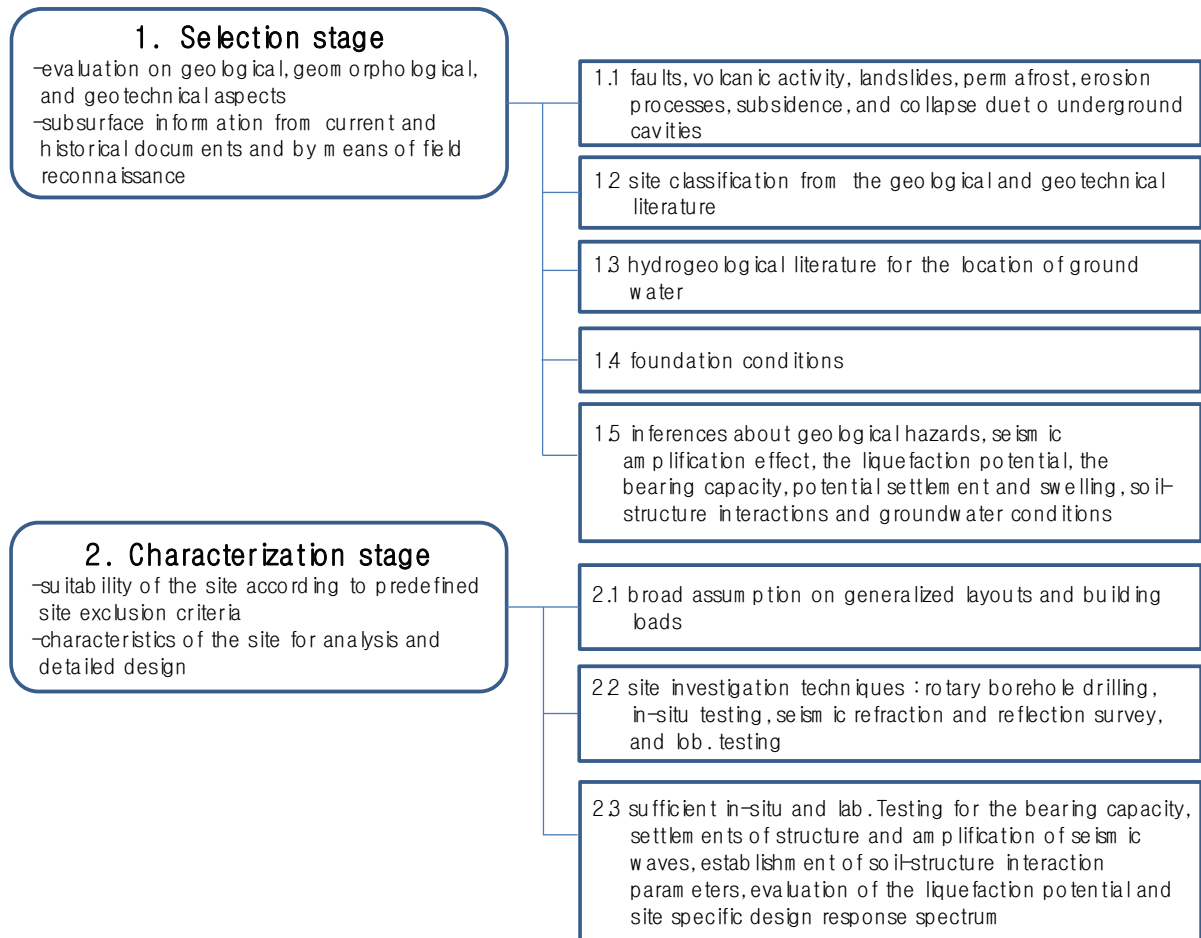
Local governments have been informed on a plan to build a new research reactor. Nine local governments applied and their proposals were evaluated by a site selection committee using established criteria. In parallel, a preliminary site evaluation to review the geologic, seismic and hydrologic conditions of the proposed sites was conducted.

The preferred site was selected as a candidate site through evaluations by the site selection committee, which was formed in July 2010, from nine local autonomous bodies that have expressed their wish to host a new research reactor. The preferred site has several existing nuclear power plants in operation. Thus, it is expected that there is no difficulty in the site characteristics and in the public acceptance as well. In addition, the site is very close to Busan which is the second largest city in Korea and has an international airport and a harbor which will provide good accessibility for people as well as easy transportation of products.

4.2 Site Evaluation Plan

The site investigation and evaluation will be performed according to the general and specific requirements of the NS-R-3 [3] as well as the requirements of the Nuclear Safety and Security Commission which is the regulatory body in Korea. The objective of the IAEA NS-R-3 is intended to provide the requirements for the elements of a site evaluation for a nuclear installation so as to characterize fully the site specific conditions pertinent to the safety of a nuclear installation. The evaluation procedure will be divided into two stages, a selection stage and characterization stage such as described in Tab 2. The site investigation work will start from June 2012 and the site evaluation report will be issued by the end of May 2013. The report will be used to be an input data for the Site Characteristics of Preliminary Safety Analysis Report (PSAR), which will be prepared to get the construction permit from the regulatory body.

Tab 2: Phased Site Evaluation Procedure



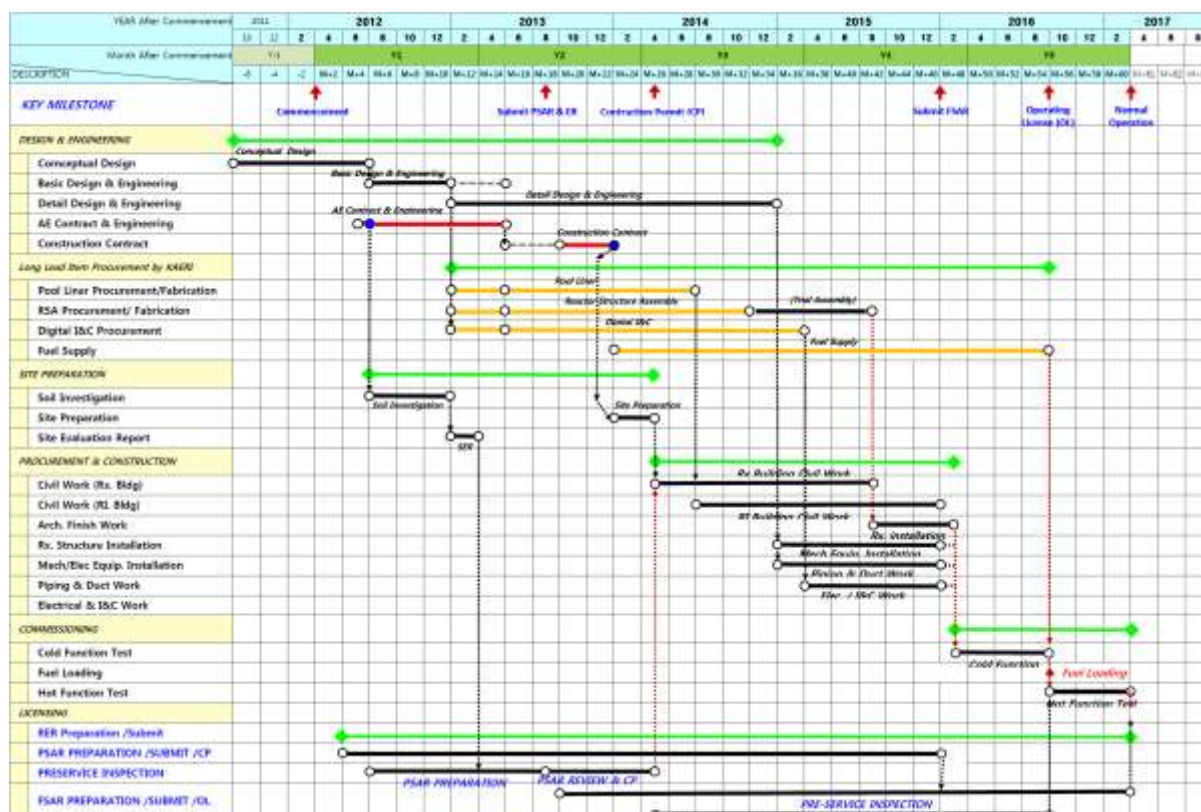
5. Project Schedule

The New Research Reactor project will be officially launched in the beginning of March 2012 and a 60 months period is planned for all activities, from design to commissioning. The detailed project schedule is shown in Tab 3.

The conceptual and basic design will be finished by the end of 2012. In parallel with the detailed design, which will be started from the beginning of 2013, the PSAR will be prepared according to the result of the basic design as a byproduct material. In order to get the construction permit, the PSAR will be submitted to the regulatory body by July 2013 and the construction permit is expected to be issued by March 2014. The FSAR will be submitted by the end of 2015 and, the fuel loading and the initial criticality will be achieved in Sept. 2016. Normal operation will start in Feb. 2017.

The design of the new research reactor will comply with the Korean Nuclear Law, regulatory requirements and guidelines. In addition, the regulatory submittals will adhere to internationally applicable standards and guidelines such as the IAEA safety standards. In parallel with the IAEA guidelines, the technical requirements and criteria for such kind of industrial codes and standards are applied to the safety design of this project to complement the detailed technical requirements.

Tab 3: Project Schedule



6. Concluding Remarks

Korea has taken a significant initial step toward the construction of a new research reactor, which is a step toward the self-sufficiency in terms of medical and industrial radioisotope supply and to build up Korean research reactor technologies. In the future, the new research reactor will greatly provide the ultimate solution for the domestic supply of medical radio-isotope and will have the capacity to provide some radio-isotopes to the Asian region. The reactor will be also equipped with the capability to provide silicon doping services.

Through this project, the New Research Reactor will be used for providing the national demand for RI production, irradiation service and technology validation relating to the research reactor. The new research reactor equipped with improved safety features will serve as a regional reactor whose benefit can be shared with neighboring countries in the Asian region. After completion of the construction of the new reactor, the roll of HANARO will be changed to a neutron beam and material irradiation facility and still provide a function to backup the RI production and NTD. The New Research Reactor will be a large scale national facility which will be used for 50 years and will take the irradiation service function independent from HANARO. The new application techniques could be devised in its life time of 50 years. Thus, the flexibility of the reactor and systems which will allow the installation of future demand will be considered during the design and engineering stages.

7. References

- [1] http://www.koreatimes.co.kr/www/news/tech/2012/02/129_104833.html
- [2] I.C. LIM, 'Plan of New Research Reactor Construction in Korea', ICRR-2011, 2011
- [3] Site Evaluation for Nuclear Installation, IAEA Safety Standards Series, No. NS-R-3

THE PRE-LICENSING OF A MULTI-PURPOSE HYBRID RESEARCH REACTOR FOR HIGH-TECH APPLICATIONS “MYRRHA”

N. HAKIMI, C. DAMS, A. WERTELAERS, V. NYS, M. SCHRAUBEN,
R. DRESSELAERS

*Nuclear Facilities & Waste Department and Security & Transport Department,
Federal Agency for Nuclear Control (FANC-AFCN)
Rue Ravenstein 36, 1000 Brussels, Belgium*

ABSTRACT

The Belgian Nuclear Research Centre in Mol has been working for several years on the design of a multi-purpose flexible irradiation facility in order to replace the ageing BR2, a multipurpose materials testing reactor (MTR), in operation since 1962.

MYRRHA, a flexible fast spectrum research reactor is conceived as an accelerator driven system (ADS), able to operate in sub-critical and critical modes. It contains a proton accelerator of 600 MeV, a spallation target and a multiplying medium with MOX fuel, cooled by liquid lead-bismuth (Pb-Bi).

Since February 2011, the Belgian Nuclear Research Centre has engaged in a “pre-licensing” process with the regulatory authority for an estimated period up to mid 2014.

The paper presents on the one hand the objectives of the pre-licensing phase as well as its implementation process and on the other hand, two implementing instruments which have been developed by the regulatory authority providing guidance to the designer of MYRRHA in order to meet the pre-licensing phase objectives. The first instrument is a strategic note for the design and operation of MYRRHA where as the second instrument is a guidance document for the format and content of a design options and provisions file (DOPF). Both instruments have been developed taking into account that MYRRHA is an irradiation facility using a Generation IV nuclear power system's type technology (liquid metal cooled fast neutron reactor).

The strategic note overview aims to cover the safety approach as well as the security requirements and safeguards obligation applicable to MYRRHA. In particular, in the strategic note, a specific attention has been paid in order to ensure that a safety, security and safeguards integrated approach will drive the development of the MYRRHA design.

The safety approach focuses on the safety goals and the minimum safety objectives set by the regulatory authority for this innovative design. The DOPF overview presents its objectives and structure resuming the suggested logic and the links between the different design steps.

With these two instruments in hand, the designer will, with the help of selected and justified safety design options, have the opportunity to demonstrate at the end of the pre-licensing phase, that his design is mature for a licensable facility, e.g. into a facility design that aims at reaching the safety goals, meets, at the minimum, safety objectives set by the regulatory authority and fulfils the security requirements and safeguards obligation.

1. Introduction

For large projects aiming at the construction and operation of complex nuclear installations or relying on new technologies, it is desirable that the regulatory authority follows, during a pre-licensing phase, the project development of the prospective applicant. So, the regulatory authority can in a timely manner communicate its expectations from the future installation in

terms of nuclear safety, security and safeguards. Such a pre-licensing phase is always initiated by the prospective applicant (requester) on a voluntary basis. Looking at the overall licensing process, two phases could be distinguished: a pre-licensing phase and a licensing phase. This paper covers the pre-licensing phase of MYRRHA, initiated by the Belgian Nuclear Research Centre (SCK.CEN) on February 2011 for an estimated period up mid 2014.

2. Scope of MYRRHA

The Belgian Nuclear Research Centre in Mol has been working for several years on the design of **a multi-purpose flexible irradiation facility in order to replace the ageing BR2**, a multipurpose materials testing reactor (MTR), in operation since 1962.

MYRRHA, a flexible fast spectrum research reactor is conceived as an accelerator driven system (ADS), able to operate in sub-critical and critical modes. It contains a proton accelerator of 600 MeV, a spallation target and a multiplying medium with MOX fuel, cooled by liquid lead-bismuth (Pb-Bi).

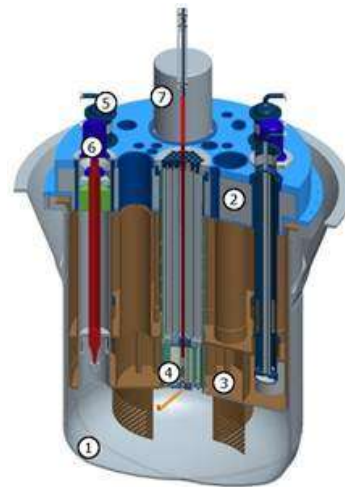


Fig. 1: The MYRRHA reactor
(1: Reactor vessel; 2: Reactor cover;
3: Diaphragm; 4: Core barrel;
5: Heat exchanger; 6: Pump; 7: In-Vessel Fuel
Handling Machine)

3. The pre-licensing phase for MYRRHA: objectives and process description

The objectives of the pre-licensing phase are described in [1]. They provide a well defined framework for future exchanges between the requester and the regulatory authority.

The objectives of the pre-licensing phase are:

1. Identification, by the regulatory authority, of the necessary and/or desirable improvements of the regulatory framework in case the existing regulatory framework is not sufficient for such a new type of facility.
2. Development, by the regulatory authority, of the safety¹ objectives and security requirements² that it expects the future facility to meet.
3. The description, by the requester, of the safety options and security provisions that he applies to his future facility to meet, at the minimum, the objectives and requirements of the regulatory authority. These safety options include the national and international experience feed-back on significant incidents and accidents.
4. The assessment, by the regulatory authority, of the level the design achieves the expected objectives and requirements. This assessment applies to the technologies and to the processes, but also to the tools which must provide evidence that the safety options are met e.g. assessment methodologies for safety, computer codes, as well as the security requirements.

¹ In this paper, nuclear safety encompasses radiation protection

² This includes for example the development of a specific DBT "Design Basis Threat"

5. The development, by the requester, of answers and justifications to specific Focus Points³ he identified himself and/or identified by the regulatory authority to demonstrate that the future installation can meet the expectations of the regulatory authority.

The objectives of the pre-licensing phase are not the detailed analyses of the safety report and / or other specific documents that will later accompany the formal construction and operation license application. The same applies to data on physical protection and safeguards.

The final objective of this pre-licensing phase is to converge, through an iterative process, to a fixed design of the installation for which it is demonstrated that the safety options, security requirement and safeguards obligation implemented by the requester meet the objectives and requirements of the regulatory authority.

The pre-licensing process consists of different activities, some carried out in parallel and others, sequentially. These various activities are:

1. Provision to the regulatory authority, by the requester, of any document and information which allows the regulatory authority to have the latest evolutionary design as envisaged by the designer.
2. Analysis, by the regulatory authority, of the regulatory framework and existing standards, both nationally and internationally and assessment of their adequacy to the new facility.
3. Consultation with other regulatory authorities of countries involved in similar phases for projects of advanced technology or innovative.
4. Gathering, by the regulatory authority, of information and know-how available and accessible for such technologies as envisaged by the designer.
5. Setting, by the regulatory authority, of safety objectives, security requirements, safeguards obligation, regulation and standards which the facility must meet at the minimum as well as more ambitious safety objectives.
6. Completion, by the requester, of the safety options and security provisions to meet these requested levels of safety and security and indication of the way safety options are implemented.
7. If needed, writing, by the regulatory authority, of thematic guidance on matters that deserve a deeper insight, e.g. the requirements and methodologies to be followed in terms of resistance against earthquakes.
8. Identification, by the requester and by the regulatory authority, of particular Focus Points in connection with safety and security, and justification by the designer that the concept used is able to answer satisfactorily to these specific concerns. This justification can be made by the available and sufficiently successful experience feed-back, by theoretical analyses based on methodologies and tools validated and reliable, and / or by the results of research and development programs specific and representative of these concerns.
9. Information exchange and consultation, by the regulatory authority, with the scientific council of the FANC-AFCN on safety items listed above.
10. Writing, by the regulatory authority, of a report with its conclusions to the pre-licensing phase. These conclusions are not binding for the regulatory authority during the later licensing phase. These conclusions have always to be put in the real and judiciary

³ A Focus Point (FP) is an issue which is new or not mature enough (i.e. there are still significant uncertainties associated), specific to MYRRHA, and which has an impact on the safety of the facility (i.e. can jeopardize any of the three safety functions: control of reactivity, the guarantee to the heat removal and the confinement of the radioactive products). The tools and methodologies used to guarantee the fulfilment of the safety functions will be also addressed in these FPs. Some findings observed in a FP could become a shortcoming in the design or in the design process that, if not corrected, could lead to significant risk to the public, to workers or to the environment.

context applicable during the pre-licensing phase. Nevertheless, taking into account these conclusions, by the prospective applicant for a construction and operation license, provides a solid basis, in case of an identical real and judiciary context, for sufficient confidence in such a later process.

4. The strategic note of the regulatory authority on the design and operation of MYRRHA

The strategic note [2] is the first instrument developed by the regulatory authority in support to the pre-licensing phase. Its objectives are to recall the regulatory framework and to present and comment the safety, security and safeguard philosophy.

4.1. The existing regulatory framework

The basis of the Belgian regulation regarding radiation protection and nuclear safety can be found in the General Regulation on the Protection of the Population, the Workers and the Environment Against the Danger of Ionizing Radiation (GRPIS, [3]) and in the recently published Royal decree on safety rules for nuclear installations [4]. This latter royal decree is the transposition into Belgian law of the European Directive 2009/71/Euratom ‘Nuclear Safety’ and of the WENRA reference levels [5]. In addition, the European EIA (Environmental Impact Assessment) Directive 85/337/EG of June 27, 1985 is applicable. The security and safeguards regulatory framework is derived from the relevant international/European conventions, treaties, agreements and protocols (national laws and royal decrees).

4.2. The safety philosophy

The safety philosophy is elaborated by considering that MYRRHA is an irradiation facility using a Generation IV nuclear power system's type technology (liquid metal cooled fast neutron reactor).

The safety philosophy includes the information necessary to translate the safety principles, requirements and guidelines into safety options needed to select the technical and operational provisions (e.g. equipments and operational procedures). This set of technical and operational provisions build the “safety architecture”.

The MYRRHA design, materialized by the “safety architecture”, has to meet the safety objectives and aims at reaching the safety goals. This demonstration goes through an iterative process and has to be provided through an assessment carried out by the designer and documented in a Design Options and Provisions File “DOPF” [6] (see §5).

Safety Principles, Requirements and Guidelines: The fundamental safety objective endorsed by the regulatory authority is the one stated in the IAEA Safety Fundamentals Principles standard [7] namely “To protect people and the environment from harmful effects of ionizing radiation”. Objectives for the design of MYRRHA must address the applicable fundamental principles.

Besides these fundamental principles, specific safety principles felt to be particularly relevant for the MYRRHA design are: Taking advantage of inherent safety characteristics; Utilizing passive safety systems; Safety independence of experimental devices; Defence in depth for accident prevention, control and mitigation and Risk-Informed Design.

In addition, general and specific applicable IAEA safety requirements standards shall be followed by the designer, taking into account the specificity of MYRRHA. Similarly, general and specific applicable IAEA safety guides standards shall be considered by the designer as the first option when compared to alternative guidance.

Safety goals and minimum safety objectives:

The design and operation of MYRRHA should warrant a high level of safety. This means that the expected level of safety is:

- Reach, at least, a level as high as the level of PWRs designed according to the WENRA objectives for new power plants [8] and PWRs currently under construction (generation III+)
- Tend to the highest level that can be expected for new reactor designs – i.e. generation IV

The regulatory authority considers that GEN IV safety goals [9] shall be the goals retained for the MYRRHA design, taking into account its specificity.

The regulatory authority also considers that WENRA safety objectives for new power plants shall be the minimum objectives to be met by the MYRRHA design, taking into account its specificity.

4.3. The security philosophy

The security objective is: « Protect the nuclear materials, nuclear installations and other radioactive materials and installations associated against malicious acts by putting in place a physical protection system to prevent of malicious acts by means of deterrence and by protection of sensible information, to manage attempt of malicious acts or malicious acts by an integrated system of detection, delay and response and to mitigate the consequences of malicious acts.»

The security fundamentals of Ref. [10] are the basis of the regulation concerning the physical protection [11 & 12] and will lead to the security requirements. On the basis of these security fundamentals, security requirements are derived and address on the one hand the categorization of nuclear material and the corresponding security ranking and on the other hand, the Design Basis Threat (DBT).

The nuclear material is first divided into three categories. These categories are the three nuclear material categories (I, II, III) and determined on the basis of the type of the nuclear material, its content of fissile isotopes, its quantity and radiation intensity because of the risk it represents regarding the nuclear proliferation. To every category of nuclear material corresponds a security ranking (« Top secret – Nuc »; « Secret – NUC »; « Confidential – NUC »). This security ranking is attributed to every one of the categories of the nuclear material on the basis of its radiological risk, or the nuclear proliferation that an inappropriate use of this material might cause or, also, because of its attractiveness.

Starting from the State's current evaluation of the threat, a DBT is derived. To define the DBT, the set of threats described in the State's Threat Assessment are refined to take into account particular requirements. To make the transformation from Threat Assessment to DBT, rigorous analysis and decision-making are essential.

This threat assessment is obtained by the collaboration between OCAD/OCAM⁴ and FANC-AFCN. Based on this threat assessment a sectoral DBT is developed. This DBT has to be translated by the operator into a site specific DBT, based on the local information and elements. This site specific DBT has to be validated by FANC-AFCN. The operator has to use this DBT to elaborate and evaluate his physical protection system.

⁴ OCAD/OCAM is the Belgian agency for threat assessment

4.4. The safeguards philosophy

In view of the prevention of the proliferation of nuclear weapons, the safeguards objectives are recalled in the strategic note:

- Verify that nuclear material declared to be used for peaceful purposes are not diverted to non peaceful applications.
- Verify that the declared basic technical characteristics of an installation correspond to the reality on the field.
- Verify the absence of undeclared nuclear materials and activities.

Any person or undertaking setting up or operating an installation for the production, separation, reprocessing, storage or other use of source material or special fissile material has to declare to the Commission the basic technical characteristics of the installation, using the relevant questionnaire, in Annex I of the EURATOM regulation 203/2005.

Each Member State being a party to Additional Protocol 1999/188/Euratom, shall designate a site representative for each site on its territory who shall provide to the Commission a declaration containing a general description of the site, using the questionnaire in Annex II of the Erratum regulation 203/2005.

The declaration of the basic technical characteristics of new installations shall be communicated to the Commission in accordance with Article 3(1) at least 200 days before the first consignment of nuclear material is due to be received.

For new installations with an inventory or annual throughput of nuclear material of more than one effective kilogram, all relevant information relating to the owner, operator, purpose, location, type, capacity and expected commissioning date shall be communicated to the Commission at least 200 days before construction begins.

4.5. Safety, Security and Safeguards Integrated Approach

An integrated safety, security and safeguards approach is essential to guaranty that the safety architecture is not be in contradiction with any of the security fundamentals and safeguards obligation.

Thus, when a first process aiming at reaching a safe design is finalized, a second process should be initiated that aims to fully comply with the security requirements and safeguards obligation.

This second iterative process should be such that:

- Any security design proposal should not jeopardize the safety level of the facility while meeting the security requirements and safeguards obligation.
- Any design modifications, for safety reasons or not, should be such that it does not jeopardize the security level of the facility and be in accordance with the safeguards obligation.

The security process should clearly identify when security requirements could lead to an antagonism between the security architecture and the safety architecture. The proposed solution should clearly reflect this specificity. A traceable management of the documentation should be implemented in such a way that, in the future, any modification that will be made, takes into account this specificity.

5. The guidance document for the format and content of a design options and provisions file “DOPF”

A second instrument developed by the regulatory authority to guide the prospective applicant in documenting his assessment during the pre-licensing phase is a guidance document for the format and content of a Design Options and Provisions File “DOPF” [6].

The DOPF, which is submitted and updated by the future applicant during the pre-licensing phase, will present and justify the safety and security architecture derived from stated safety options and security requirements and taking into account the safeguards obligation. The DOPF will also provide indications about the measures implemented to approach the safety goals and meet the defined safety objectives. The DOPF should address in particular all Focus Points identified and analyses so far in the design of MYRRHA.

The DOPF guidance document is organized in six volumes to ease the presentation and the assessment. The following structure is suggested (see Fig 2.):

- *Volume 1: Purpose and description of the facility*
- *Volume 2: Approach to the nuclear safety*
- *Volume 3: Design Options and selected provisions*
- *Volume 4: Justification of design options against the objectives and related goals*
- *Volume 5: Management system for safety of the installation*
- *Volume 6: Security and Safeguards Integrated Approach*

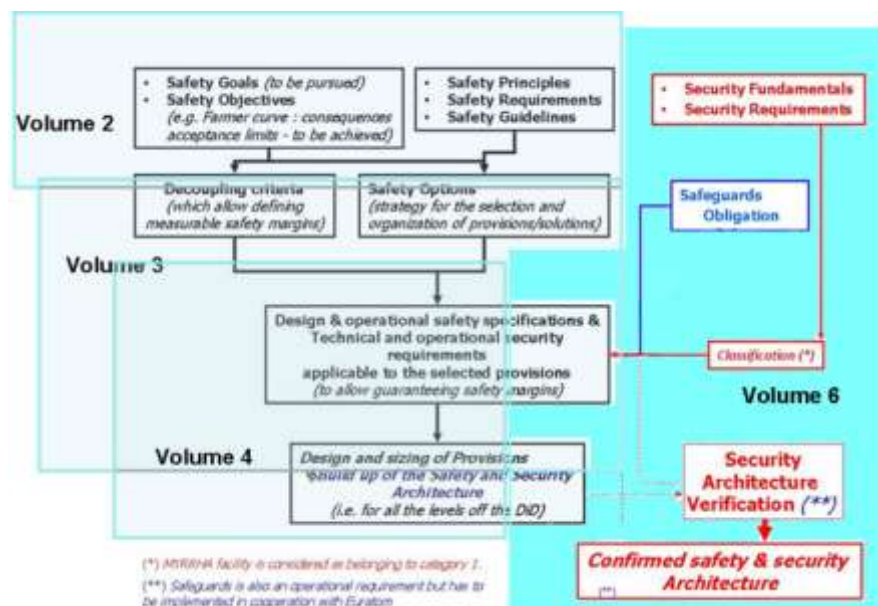


Fig. 2 – Content and concatenation for the volumes the Design Options and Provisions File “DOPF” for MYRRHA

6. Conclusions

Within the context of the MYRRHA project, the Belgian regulatory authority has defined a “pre-licensing” process which was initiated by the Belgian Nuclear Research Centre (SCK.CEN) in February 2011. This process is supported by two instruments namely a strategic note and a guidance document on the format and content of a Design Options and Provisions File (DOPF), both presented in this paper. With these tools in hand, the prospective applicant, with the help of selected and justified safety design options and security provisions, will have the opportunity to demonstrate at the end of the pre-licensing phase, that his design is mature.

7. References

- [1] FANC, 2011-04-09-MSC-5-3-2-FR, Description d'un processus de « Pre-licensing » pour un projet de construction d'une nouvelle installation nucléaire majeure, revision 1.
- [2] 2011-10-13-NH-5-4-3-EN, revision 0, "MYRRHA Strategic Note"
- [3] Royal Decree of July 20, 2001 concerning the General Regulation on the Protection of the Population, the Workers and the Environment Against the Danger of Ionizing Radiation (GRPIS)
- [4] 30 November 2011, Royal decree on safety of nuclear installations, (published on 21.12.2011)
- [5] WENRA Reactor Safety Reference Levels January (2008)
- [6] 2011-10-12-NH-5-4-3-EN, revision 0, "Guidance for the format and content of the Design Options and Provisions File"
- [7] IAEA, Fundamental Safety Principles Series No. SF-1, 2006
- [8] WENRA statement on safety objectives for new nuclear power plants (November 2010)
- [9] GIF/RSWG/2007/002 - Basis for the Safety Approach for Design & Assessment of Generation IV Nuclear Systems Revision 1 November 24, 2008
- [10] IAEA Nuclear Security Series No. 13, Nuclear Security Recommendations on Physical Protection of nuclear material and nuclear facilities, 2011
- [11] Law of 15th of March 1994 modified by the laws of 2th of April 2003 and of 30 March 2011 and the fourth 8 November 2011 Royal decrees on physical protection, on categorization, on security attestations and on documents
- [12] Law of 11th of December 1998 modified by the law of the 30 March 2011

ASSESSING THE ROLE OF RESEARCH REACTORS AND RELATED INFRASTRUCTURE IN THE DEVELOPMENT OF A NUCLEAR POWER PROGRAMME

E. Bradley

*IAEA - Research Reactor Section, Division of Nuclear Fuel Cycle and Waste Technology
VIC, A-1400, Vienna Austria*

D. Ridikas

IAEA – Physics Section, Division of Physical and Chemical Sciences

M. Yagi, M. Ferrari

IAEA - Integrated Nuclear Infrastructure Group, Division of Nuclear Power

B. Molloy

IAEA - Nuclear Power Engineering Section, Division of Nuclear Power

ABSTRACT

Throughout the second half of the 20th century, many countries saw research reactors as an essential step towards building their first nuclear power plants. Times have changed; industrial experience and globalisation now significantly facilitate the exchange of information and collaborative resource development and software modelling, and simulation, is widely available. While there is no clear evidence that a research reactor is a prerequisite for nuclear power, the infrastructure developed to support the construction, regulatory approval, operation, maintenance and eventual decommissioning of a research reactor can help a country introduce nuclear power. The Agency's 'milestones approach' identifies 19 distinct national infrastructure issues to be addressed by countries starting nuclear power programmes. During 2012, the IAEA will undertake a comprehensive assessment, based on the milestones approach, to enable Member States to make informed decisions on how best to apply an existing research reactor and related infrastructure or whether to consider a new research reactor facility as a stepping stone to the development of a national nuclear power programme. This paper will discuss the background of this work, completed and planned actions as well as related activities on-going at the IAEA.

1. Introduction

Based on questions received from Member States, the IAEA began to explore the role of RRs in the introduction of nuclear power during the 2010-2011 programme cycle. A number of consultancy meetings were held, primarily with representatives of the RR community. The response from this community indicated that RRs do in fact play a role in existing nuclear power programmes in many countries and have potential relevance to on-going or future efforts to introduce nuclear power.

Throughout the second half of the twentieth century, many countries saw research reactors (RRs) as an essential step towards building their first nuclear power plants (NPPs). Times have changed; industrial experience and globalization now significantly facilitate the exchange of information and collaborative resource development. Nonetheless, in certain

situations and provided that additional applications of the RR are well planned, an RR can still be a useful step towards nuclear power.

RRs fulfil diverse needs, including medical and industrial isotope production, elemental analysis, silicon doping, neutron beam based science and applications, education and training, scientific research, and technology development (this includes support for existing and advanced nuclear power technologies). While an RR is not a prerequisite for nuclear power, the infrastructure developed to support the construction, regulatory approval, operation, maintenance and eventual decommissioning of an RR can help a country to introduce nuclear power. The infrastructure necessary for an RR is similar to that required for an NPP but often differs in scale. In addition, certain RR capabilities directly or indirectly support the development and implementation of nuclear power. Experience from managing nuclear material at RRs promotes a better understanding of the infrastructure and issues that need to be addressed in the field of nuclear power.

Because the countries that now have nuclear power had access to operating RRs before commissioning their first NPPs, several countries currently seeking to embark on nuclear power programmes for the first time are also considering either building their own RRs or joining an existing RR coalition as a stepping stone towards nuclear power. In Morocco, for example, staff with experience from a project to build a new RR are now directly involved in their country's nuclear power planning. In contrast, the United Arab Emirates has taken a different approach and contracted its first NPPs without having previously operated an RR.

Countries considering the introduction of nuclear power may find that the experience gained from running an RR and managing nuclear material helps to facilitate studies that will allow them to make a knowledgeable decision about the long-term commitments required for nuclear power. The Agency's 'Milestones approach' identifies 19 distinct national infrastructure issues to be addressed by countries considering the introduction of nuclear power programmes [1]. Having an RR or other nuclear facility may mean that a country has already made progress on some of the issues such as safeguards accountancy, nuclear security and regulatory oversight.

In particular, an existing RR programme and supporting infrastructure, when managed in accordance with international standards and accepted practices, can help in developing the infrastructure, experience and expertise of interest to a country's nuclear energy programme implementing organization (NEPIO). Treaties, legal frameworks, emergency response preparedness, and waste management policies and plans are examples of RR programme infrastructure of potential interest to a NEPIO. Similarly, experience derived from operating and regulating an RR, managing its fuel cycle, training its staff, assuring safety, continuously improving programmes, and managing a large capital project provides the NEPIO with an important reserve of domestic knowledge to draw on. The pool of experienced staff within the RR operating organization, regulatory authority and associated government agencies is a source of beneficial domestic expertise as a country begins to form a NEPIO. In Slovenia, for example, practically all nuclear professionals in the country began their career or attended practical training courses at the RR at Podgorica, Montenegro. In Malaysia, technical staff from an electric utility are being trained by RR operators in preparation for introducing nuclear power.

Conversely, countries with underutilized or shut down RRs that are not managed in accordance with international standards and accepted practices may have legacy issues to overcome before they can introduce nuclear power. Dysfunctional infrastructure, institutional inertia, as well as laws, practices, policies and protocols unsuitable for commercial nuclear power may have to be revised to match the needs of a nuclear power programme. In this case, a prior RR programme might turn out to be a burden for the NEPIO, albeit one that must be addressed in any case.

The NEPIO will complete comprehensive reviews of all the issues to be covered before each milestone can be attained. The infrastructure, experience and expertise gained from one or more RRs that have been safely and reliably operated, effectively utilized and well maintained could help in attaining milestones for several of the 19 issues specified by the Agency.

2. Selected issues for which research reactor programmes can pave the way for nuclear power

2.1. National position

The foundations of a country's national position on nuclear power are significantly different to those on which a national RR programme might rest. Government support may (and does) exist for RR programmes in countries politically opposed to nuclear power. For example, in Australia a new RR called the Open Pool Australian Light Water (OPAL) Reactor started operation in 2007, even though national policy there excludes nuclear power. Similarly in Germany, which established a nuclear power phase-out policy in 2000, the FRM-II RR at the Technical University in Munich was subsequently commissioned in 2005.

However, despite the apparent lack of linkage, many key infrastructure requirements related to Milestone 1 for a country's national position on nuclear power will have typically already been considered within the scope of an RR programme. This experience could help develop an understanding within a NEPIO, energy ministry or a public utility of:

- The need to ensure the safety, security and non-proliferation of nuclear material;
- The need to adhere to appropriate international legal instruments;
- The need to develop a comprehensive legal framework covering all aspects of nuclear law, which includes safety, security, safeguards and nuclear liability and other legislative, regulatory and commercial aspects;
- The need to have an effective, independent, competent regulatory body;
- The need to develop and maintain national human resource capabilities within both government and industry to successfully manage, operate, maintain and regulate nuclear facilities and nuclear material as well as preserve knowledge and expertise.

Similarly, in implementing the actions recommended for Milestone 2 for a country's national position on nuclear power, governments will benefit from the experience of an RR programme, but any measures adopted as part of the latter will likely have to be revised to support nuclear power. Examples include:

- The expansion of an existing regulatory body;
- The establishment and maintenance of an effective State system of accounting for and control of nuclear material to facilitate the implementation of the State's safeguards commitments;
- An established policy for the nuclear fuel cycle, including arrangements for secure supplies of fuel, safe and secure transportation and storage of new and spent fuel, and long term waste management;
- Established legal, organizational and financial arrangements for decommissioning and radioactive waste management;
- Programmes for the security of nuclear materials and facilities;
- Programmes for radiation protection and emergency preparedness and response;
- Adopted international standards for environmental protection.

2.2. Nuclear Safety

The operator's prime responsibility for safety is as important for an RR as it is for an NPP, as is the need for the government and all other stakeholders to appreciate what this means in practice. In particular, similarly stringent safety requirements must be implemented by both

RR staff and nuclear power staff. The need for an effective regulatory body is just as important in both cases and is considered in a later section of this paper.

In most cases, countries with effectively utilized, well maintained and reliable RRs will be able to easily demonstrate that programmes are implemented consistently with fundamental safety principles and other internationally recognized safety standards. Nuclear power newcomer countries with established RR programmes that are operated and maintained in accordance with such standards will generally already be participating in the global nuclear safety regime.

With respect to Milestone 1 for nuclear safety, relevant aspects of an RR programme may help a NEPIO achieve specific objectives. Examples include domestic expertise and experience in fostering and maintaining a nuclear safety culture, stakeholder involvement and participation in the global nuclear safety regime. The NEPIO will have to ensure that the safety culture is adequate for introducing nuclear power and take any necessary actions to instil a safety culture in stakeholders not normally involved with RRs, e.g. utilities, industrial organizations and energy related government agencies (as opposed to those agencies involved in science and research).

With respect to Milestone 2, the requirements relate more specifically to nuclear power and the need to ensure that the relevant stakeholders adopt the proper practices and culture. However, expertise and experience from government organizations responsible for RRs, from the RR regulator and from operating organizations could be used by the NEPIO to help ensure that all nuclear safety related objectives are satisfied.

2.3. Legislative Framework

Countries with an active RR programme are likely to have an existing legislative framework that may provide an adequate basis for the legislative framework needed to support nuclear power. Many international legal instruments that are necessary for nuclear power are also necessary for an RR programme. In any case, national legislation should comprehensively cover nuclear safety, security, safeguards and liability for nuclear damage.

A number of elements related to Milestone 1 will typically already exist for an RR programme, but must still be reviewed by the NEPIO for possible revision to support nuclear power. Examples include:

- Established and effectively independent regulatory authorities and legislation dealing with
 - a system of licensing, inspection and enforcement,
 - radioactive material and radiation sources,
 - the safety of nuclear installations,
 - emergency preparedness and response,
 - transport of nuclear material,
 - radioactive waste and spent fuel,
 - nuclear liability and coverage,
 - safeguards,
 - export and import controls, and
 - physical protection;
- Legislation dealing with the roles of the national government, local government authorities, the public and other stakeholders;
- Legislation dealing with fuel cycle issues in general and the ownership of nuclear material;
- Provision for the development of human resources to ensure the continued integrity of the nuclear programme;
- The commitment to use nuclear technology and techniques for peaceful purposes.

Likewise, for Milestone 2, elements of the required legislation for nuclear power will have been developed to support RRs but will likely have to be revised. Examples include:

- Appropriate national legislation pursuant to the relevant non-proliferation undertakings of the State;
- Legislation that specifies the allowed ownership of nuclear facilities and nuclear materials; the legislation establishes clear responsibilities and liabilities for the operation of nuclear facilities and safeguarding of nuclear material;
- Legislation that establishes an effectively independent regulatory body with full authority to implement the functions assigned to it by the enabling legislation.

2.4. Regulatory Framework

A country embarking on a nuclear power programme will consider how to efficiently build on the national infrastructure already in place for radiation, waste and transport safety. Expanding the existing regulatory body for an RR so that it can also act as the regulator for an NPP may be the best way to utilize existing facilities and human resources that are likely to be limited in many countries.

With respect to Milestone 1, many fundamental elements of a regulatory framework will be in place to support an existing RR programme but must still be reviewed by the NEPIO for possible revision to support nuclear power. Examples include:

- Designation of an effectively independent regulatory body, with clear authority and adequate human and financial resources;
- Regulations for licensing, review and assessment, inspection, enforcement and public information;
- Authority to obtain technical support as needed;
- Authority to implement international obligations, including IAEA safeguards;
- Provisions for stakeholder and public information and interactions;
- Compatibility with the existing regulatory framework for radiation, waste and transport safety.

Similarly for Milestone 2, a number of important issues would be familiar to a regulatory body established for RRs, but will also likely have to be revisited for nuclear power. Examples include:

- Safeguards;
- Nuclear and radioactive materials transportation, handling and storage;
- Radiation protection;
- Waste management, including disposal;
- Codes and standards developed or adopted for:
 - The import/export, transportation, storage and handling of nuclear and other radioactive material;
 - Radiation protection;
 - Waste management;
 - Emergency preparedness and response.

2.5. Security and Physical Protection

Nuclear security requires the concerted effort and commitment of all organizations involved in the planning, design, construction and operation of a nuclear research or power reactor. It is critical that these organizations acknowledge the importance of nuclear security and embrace a nuclear security culture. With respect to Milestone 1, an existing RR programme should demonstrate a country's commitment to a strong nuclear security culture. The NEPIO will work to ensure that the existing security culture is adequate for the introduction of nuclear power and take any necessary actions to instil a security culture in stakeholders not normally involved with RRs, e.g. utilities, industrial organizations and energy related government agencies (as opposed to those agencies involved in science and research).

With regard to Milestone 2, several conditions should already exist in countries with a well-managed RR programme. As is the case above, existing programmes will likely have to be revised to support nuclear power. Examples include:

- Legislation providing appropriate authorities for security and physical protection;
- Protocols and programmes for local and national law enforcement;
- Programmes for the definition of sensitive information, protection requirements and associated penalties;
- Laws providing for penalties for malicious acts, illegal possession and trafficking of materials, as described in international legal instruments;
- Programmes for the careful selection and qualification of nuclear programme staff with access to facilities or sensitive information.

3. Utilisation Planning

Careful consideration is essential before committing to start a new RR programme to avoid unnecessary burdens, underutilization and the significant legacy issues currently faced by many RRs worldwide. While a new RR programme can, over time, serve to facilitate the introduction of nuclear power just like an existing RR programme, experience suggests that the support provided by a new or existing nuclear power programme is inadequate on its own to sustain long-term RR operation. Most nuclear utilities develop customized training programmes, and nuclear engineers make up only a minor proportion of the workforce at an NPP [2].

The decision to embark on an RR programme and the decision to introduce nuclear power are similar in that both involve long-term commitments related to facility construction, operation, decommissioning and the ultimate disposition of all waste. A major difference between the two, however, is the funding of operation, maintenance, waste management and decommissioning. Nuclear power plant financing and funding requirements are typically at least an order of magnitude greater than those of an RR. Even more important is the fact that NPPs generate revenues to cover these costs, while most RRs are funded and operated with government funds. In other words, most of RRs will never be financially self-sustaining and therefore require government financial support throughout the entire period of operation and decommissioning.

The utilization plan for an NPP is straightforward. It should safely operate as consistently as possible with sustainable programmes and procedures. For RRs, utilization planning is less straightforward. Underutilized RRs may struggle to justify and secure adequate funding to be properly maintained. This makes it harder to ensure adequate safety, security and environmental stewardship. A robust utilization programme and strategic plan can help to ensure sustainable funding to fulfil a country's or region's long-term needs in terms of research, education and training, isotope production and other RR products and services. An RR constructed without a thorough utilization analysis could be faced with reduced utilization and funding cuts. Therefore, a robust utilization plan based on well quantified and justified needs is indispensable from the very beginning of planning RR activities [3].

An RR constructed mainly or solely to support the introduction of nuclear power may lose its principal value after the first NPPs are commissioned because a nuclear power programme can be sustained without national RRs. For example, nuclear power continues in Spain and Sweden although all RRs have been shut down there. Also, following the breakup of the former Soviet Union and the division of Czechoslovakia; Armenia, Slovakia and Lithuania (until 2009) have maintained nuclear power without domestic RRs.

On the other hand, some countries with nuclear power are reconsidering the role of their RRs. For example, plans to shut down an RR at Imperial College, London, were reconsidered at least in part to support human resource development for an expected

expansion of nuclear power. Also, construction of a new training reactor is being considered in Sweden.

Figure 1 illustrates that practical or vocational training is an important component of nuclear education and infrastructure development for nuclear power. In addition, formal training and education programmes must be established for people throughout the full range of a country's nuclear power infrastructure, i.e. students, engineers, operators, inspectors, regulators, managers and even the general public. Access to RRs — particularly those designed to support training programmes — can help satisfy both formal and vocational education needs. Such access could be through a domestic RR or partnership in a regional RR coalition.

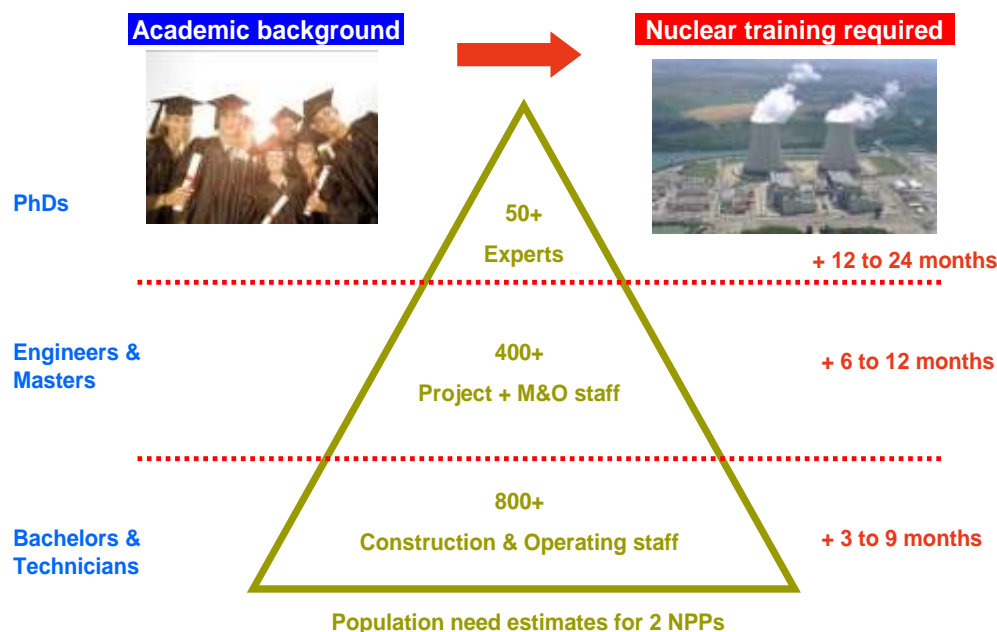


FIG. 1: The need for basic academic qualifications (on the left) and supplemental specialized nuclear training (on the right) for staff at all required levels for building, operating and managing a first NPP with two reactor units. (M&O = operation and maintenance) Source: AREVA, France.

France uses a range of training methods that includes software applications, training RRs and dedicated simulators. The combination of these different tools provides a comprehensive understanding of reactor design, physics phenomena, operation and safety principles. In this context, the ISIS RR of the French Atomic Energy and Alternative Energies Commission (CEA)'s National Institute for Nuclear Sciences and Technology (INSTN) in Saclay has been refurbished and adapted to be used exclusively for nuclear training. It now provides more than 100 hands-on training courses annually for nuclear and non-nuclear engineering students, reactor operators, safety authorities and nuclear industry specialists both from France and other countries. The Czech Republic uses a similar approach. Figure 2 illustrates training courses at the VR-1 training RR of the Czech Technical University (CTU) in Prague.

RR regional coalitions help countries that would like to support their nuclear power programmes with training at RRs but are unable to justify operating domestic RRs. Coalitions allow access to existing RRs in other countries to help develop the necessary human resources and skills with little delay [2]. Such shared access can allow countries without RRs of their own to take advantage of other countries' established infrastructure, including their competence in nuclear technology and their mature safety and security cultures.

RRs are well suited to this role. Many have utilization programmes specifically developed for nuclear related training and education and are often very willing to accommodate the needs of other countries. Austria, for example, has no nuclear power programme, but the RR in Vienna is a founding member of the Eastern European RR Initiative (EERRI) and supports the nuclear education and training programmes of other countries, including training NPP operators. Another example is in Jordan, where the Jordan University of Science and Technology is using a web-based video system (internet reactor concept) to permit its nuclear engineering students to complete exercises and experiments as if they were present in the control room of a RR at the North Carolina State University in the USA.



FIG.V-2: Training courses at the VR-1 training RR of the Czech Technical University (CTU) in Prague.

Other examples include:

- The TRIGA Mark II reactor located at the University of Mainz, Germany. Here, a broad range of courses are offered related to nuclear engineering, including reactor operation and reactor physics, nuclear chemistry and radiation protection.
- The AGN-201K reactor at the Kyung Hee University, Republic of Korea. Between January 2009 and December 2010, 12 courses were completed at this reactor for 128 nuclear engineering students from 7 universities.
- The IPR-R1, TRIGA Mark I reactor at the Nuclear Technology Development Centre in Belo Horizonte, Brazil. Most of Brazil's NPP operators and other technical staff have been trained at the IPR-R1 reactor. As of December 2010, more than 250 nuclear energy workers were certified by an operator training course on RRs. This course was designed as part of the first phase of the power reactor operator training programme.

Additional data for selected RR training programmes that support existing nuclear power programmes are provided in Table 1.

Table 1. Role of RRs in education and training for nuclear power utilities, support industry and safety authorities

Country – Research Reactor	Number of staff trained			
	2008	2009	2010	2011
Austria*, TRIGA Mark II, 250 kW	15	15	15	8
Brazil, IPEN/MB-01, 0.1 kW	0	23	0	37
Czech Republic**, VR-1, 5 kW	13	31	51	33
France, ISIS reactor***, 700 kW	290 (i=11%)	310 (i=17%)	350 (i=32%)	400 (i=30%)
France, MINERVE, 0.1 kW	40	40	40	60
Germany****, AKR-2, 0.002 kW	41	50	44	25
Italy, TRIGA Mark II, 250 kW	0	47	47	24
Malaysia, TRIGA Mark II, 1000 kW	20 ⁺	-	10 ⁺⁺	-
Slovenia, TRIGA Mark II, 250 kW	51	41	32	70

* *For utilities in Slovakia*

** *For utilities in the Czech Republic and Slovakia*

*** *Depending on the specific objectives, training course durations range from 3 to 24 hours (i = percentage of international students)*

**** *For 9 other countries*

+ *17 engineers from a utility, 3 lecturers from a university*

++ *All lecturers from a university*

4. IAEA Activities

During 2012, the IAEA will continue to explore this topic during a Technical Meeting planned for December. During this meeting, IAEA will compile input from selected RR and non-RR stakeholders including NPP operators, technical support organisations, regulators and/or other competent authorities for comparison with feedback already received from the RR community. The objective is to obtain practical examples based on demonstrated experience from existing programmes. Significant inconsistencies will be reconciled as appropriate and IAEA will publish a report for use by relevant decision makers in the Member States. This report may either update, reinforce, or correct the findings of the RR community summarised in this paper. Finally, this work will compliment related activities to assist Member States with new RR projects, improved utilization and other, nuclear technology related human resource and skill development.

5. Conclusion

The support infrastructure, experience and expertise fostered by an existing, well utilized and effectively managed RR programme can contribute to the knowledge a country needs in order to make informed decisions regarding nuclear power. In particular, a competently managed RR programme will be backed up by national laws, international legal instruments and organizational infrastructure with features similar to those required for sustaining nuclear power. RRs can foster domestic safety and security cultures that are difficult to achieve in the absence of active programmes and the day to day hands-on experience that these entail. In addition, RRs can support an existing or new nuclear power programme, particularly with regard to training, research and technical support.

On the other hand, a poorly managed RR programme can add a significant burden to the efforts of a NEPIO. In some cases, existing infrastructure will have to be significantly revised to address the needs of a nuclear power programme. Thorough assessments by the NEPIO and other national oversight organizations will determine the best path forward.

Countries have benefited in the past from RRs before launching nuclear power programmes. Today they can benefit from the RR capabilities offered through partnerships with others, via a regional RR facility or a coalition. In these cases, the capabilities of the existing reactor, the approach to nuclear safety and security, and the value and relevance of its training programmes can be evaluated in advance to ensure its application will address the specific needs of the NPP operator, regulator or other relevant organisation.

For those countries which choose to construct a new RR as a stepping stone towards nuclear power, identifying other uses for the facility will help to ensure its long-term viability. A robust utilization plan, developed with input from a broad community of potential users and customers, will be reflected in high levels of utilization, the availability of necessary funding, and long-term safe, sustainable and environmentally responsible operation of the facility.

Based on questions and requests from the Member States, the IAEA is working to develop practical guidance on the role of RRs in the introduction of nuclear power to assist policy makers and other key decision makers.

6. References

- [1] IAEA, Milestones in the Development of a National Infrastructure for Nuclear Power (IAEA Nuclear Energy Series No. NG-G-3.1), Vienna, 2007.
- [2] IAEA, Human Resources for Nuclear Power Expansion (Supplement to Nuclear Technology Review 2010 (IAEA document GC(54)/INF/3) 2010.
- [3] IAEA, Specific Considerations and Milestones for a Research Reactor Project (IAEA Nuclear Energy Series), Vienna (in print).

STATISTICAL METHODS FOR NEUTRON MULTIPLICATION FACTOR DETERMINATION IN DEEPLY SUBCRITICAL STATES ON SUBCRITICAL ASSEMBLY YALINA-THERMAL.

S. SADOVICH, V. BURNOS, YU. FOKOV, H. KIYAVITSKAYA
Joint Institute for Power and Nuclear Research – Sosny, Minsk, Belarus

Abstract

Determination of neutron multiplication factor in subcritical systems plays an important role in accelerator-driven systems (ADS) operation. Statistical methods (alpha-Rossi and alpha-Feynman are the most famous) are widely used for these purposes, although originally were designed for the critical zero-power reactors. In this work several kinds of statistical methods (alpha-Rossi, alpha-Feynman, Bennett's method, Babala's method) as well as their modifications were investigated and applied for neutron multiplication factor determination on subcritical assembly Yalina-thermal for different configurations in wide range of subcriticality 0.7-0.975.

The results were compared with calculated values using MCNP and results obtained from PNS method and source-jerk method. For all investigated configurations chain-length distribution was calculated. Based on these results features of application of statistical methods in highly subcritical systems are given.

It was shown that combination of the statistical methods with multiplying source method, spatial correlation factor and neutron source characteristics should be used for deeply subcritical states. In this case measured values agree well with calculated results.

1. Introduction

The number of radioactive decays emitted by a radio-active medium per unit time is Poisson distributed. However, in a multiplying media (reactor core) this distribution will be disturbed due to fission process in the system. Techniques based on investigating the deviation from the pure Poisson distribution in such systems are called neutron noise methods. They are important tools for reactivity measurements both in power reactors and in future accelerator-driven subcritical (ADS) systems.

The most applies methods are Rossi-alpha, Feynman-alpha and their modifications, which have been used in many reactor systems. Being developed for critical or near critical systems these methods can be used also for sub-critical reactors. However, for highly sub-critical systems neutron noise signal becomes complex and its interpretation becomes difficult. Several new theories are being developed to describe these methods in a more sophisticated way with special attention to spatial, spectral and temporal effects [1-2].

In this investigation statistical methods were applied for deep sub-critical systems with k -effective from 0.7 to 0.975. Using MCNP4c kinetic parameters were calculated for all configurations and compared to results, obtained using source-jerk and PNS methods.

2. Subcritical assembly Yalina-Thermal

The YALINA facility is a zero-power, sub-critical assembly driven by a conventional neutron generator. It is located in the Joint institute for power and nuclear research – Sosny in Minsk, Belarus. This facility was designed for the purpose of investigating the static and dynamic neutronics properties of accelerator driven sub-critical systems and studying transmutation reactions involving minor-actinide nuclei [3].

The YALINA facility contains two sub-critical assemblies Yalina-Thermal and Yalina-Booster. These assemblies are shown on the figure below.

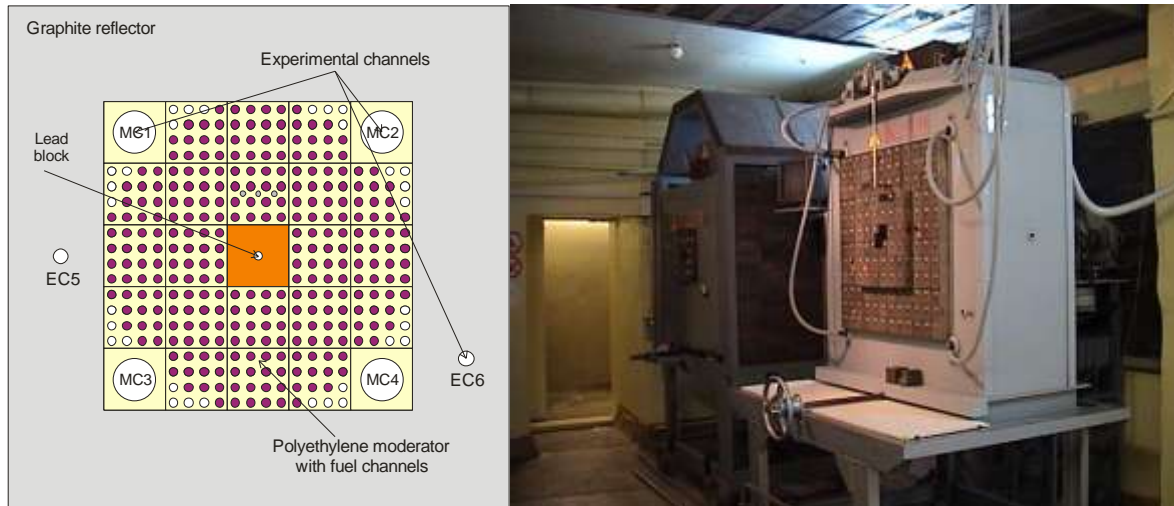


Fig. 1: Yalina-Thermal (outline) and Yalina-Booster.

Yalina-Thermal's core is a rectangular parallelepiped 40.0-cm wide, 40.0-cm long, and 57.0-cm high assembled from polyethylene blocks with channels to place the fuel pins. The central part of the sub-critical assembly is a neutron producing lead target. The core is surrounded by graphite reflector. There are four channels that are 55 mm in diameter for accommodating neutron flux monitoring detectors at the boundaries of the core and two experimental channels located in the graphite reflector. The fuel rods that are loaded into the core consist of UO_2 dispersed in a matrix of magnesium oxide. The ^{235}U enrichment of the EK-10 uranium fuel rods (UO_2) equals 10%.

Various fuel loading configurations are possible with this facility. To change the reactivity during these studies two options were used: extraction fuel pins from the core and insertion boric absorber. Two configurations with $k_{\text{eff}} \approx 0.8$ but different composition of core are shown below.

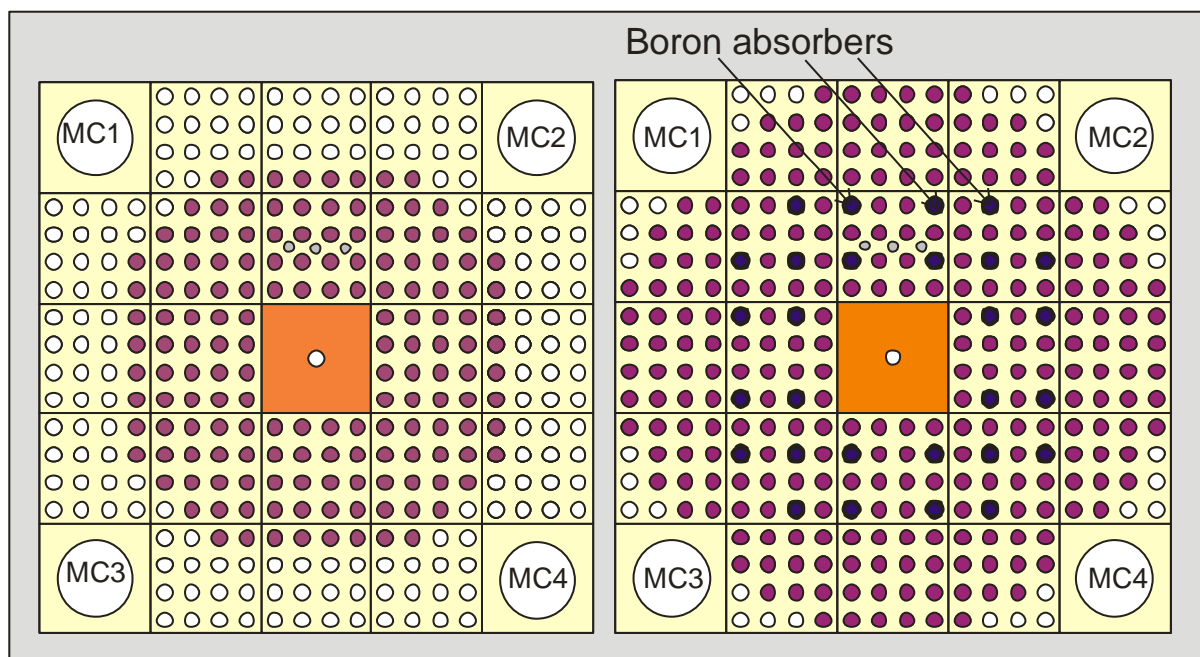


Fig. 2: Configurations with $k_{\text{eff}} \approx 0.8$.

K-effective values as well as effective delayed neutron fraction using k-ratio method were calculated using MCNP4c [4]. Dependencies of these characteristics on number of fuel rods in the core are shown on Figure 3 and Figure 4.

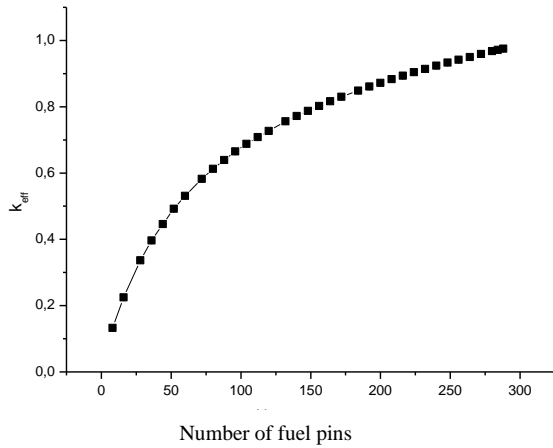


Fig. 3: Dependence k_{eff} on number of fuel rods in the assembly for ENDF/B VI.6

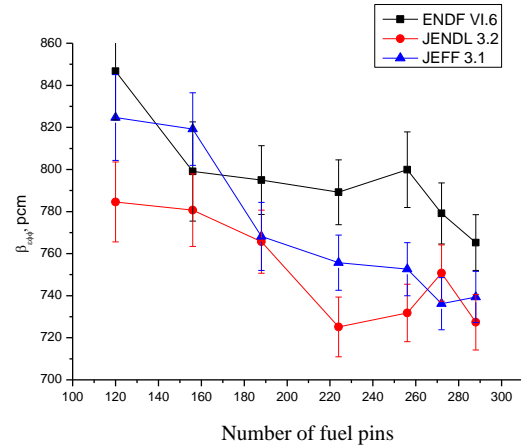


Fig. 4: Dependence β_{eff} on number of fuel rods in the assembly for different nuclear data libraries.

3. Reactivity measurements

3.1. Chain length distribution

Numerous methods for measuring subcriticality in multiplying systems have been proposed over the past years of reactors operation. One general class of these methods is based on neutron noise theory [5], in which correlated pairs of neutrons belonging to the same fission chain are of interest. In order to detect correlated pairs it is necessary that the chain length and detector efficiency will be high enough [6].

A neutron chain is defined as all the neutrons in the system related to common ancestor or initiating source neutron. In a multiplying system the source neutrons can be neutrons from external sources, internal sources and delayed neutrons. Although delayed neutrons are generated from precursors that appeared from fission events in a main chain, the time associated with their appearance are significantly greater than the average lifetime of a prompt neutron.

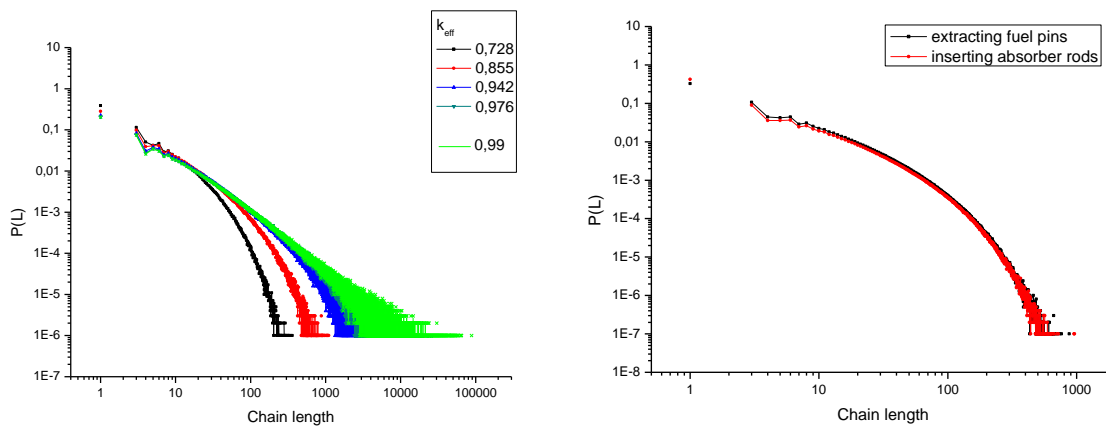


Fig. 5: Chain-length distribution for different configurations of Yalina-Thermal.

Using MCNP4c code probabilities to observe fission chains in the system were calculated for all configurations. The probabilities P to observe chain length L in the system are shown on the Figure 5.

It should be noted that configurations with identical k -effective but different composition of the core have different probability to observe chain with the same length. For configurations shown on the Figure 2 difference is about 10%.

The more k-effective is the larger chain length can be observed in the system. On Figure 5 chain distribution is also provided for hypothetical configuration with k-effective equal to 0.99. For critical system there is non-zero probability to observe infinity fission chain.

3.2. Statistical methods

Rossi-alpha method is widely used to determine the subcritical reactivity of a system [7]. The method was originally introduced by Bruno Rossi in his studies of cosmic-particle cascades, later coined as shower, where detection of coincidences was used to indicate the occurrence of cosmic particles. It based on the measurement of the covariance function of the detector counts in the system. It can be shown that probability $p(t)$ to detect a neutron in the interval dt around time t after the detection of a neutron at $t=0$ is:

$$n(t) = F\varepsilon + \frac{\varepsilon D_v k_p^2}{2(1-k_p)l} e^{-\alpha t},$$

where F is average rate of fission, ε is efficiency of the detector, D_v is Diven factor, k_p is k-effective prompt, t is time and $\alpha = \frac{\beta_{eff} - \rho}{\Lambda}$.

In this terms $\frac{\varepsilon D_v k_p^2}{2(1-k_p)l}$ is correlated amplitude, $F\varepsilon$ is uncorrelated or random component.

Feynman-alpha method is based on deviation of the counts of neutron detector from a true Poisson distribution due to presence of fissile material. Usually this deviation is denoted Y as:

$$\frac{\sigma(c)^2}{\bar{c}} = \frac{\overline{c^2} - \bar{c}^2}{\bar{c}} = 1 + Y,$$

where \bar{c} is average number of counts in time interval T [7]. It can be shown that Y is a function of ΔT (the time base used in the measurement).

$$Y = \frac{\varepsilon D_v}{\rho_p^2} \left(1 - \frac{1 - e^{-\alpha T}}{\alpha T} \right).$$

Figure 6 shows Rossi- α histograms normalized to the mean count rate for different configurations of the Yalina-Thermal. Figure 7 shows Feynman- α histograms for different configurations.

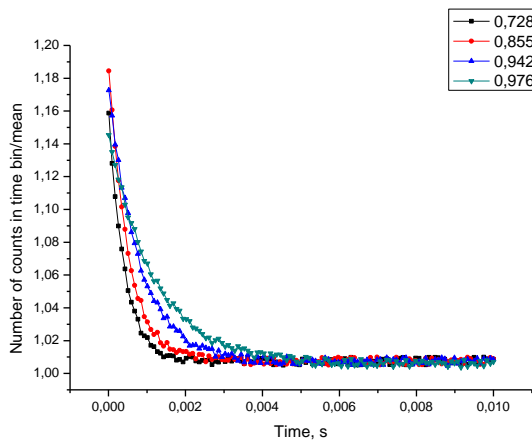


Fig. 6: Rossi- α histograms normalized to the mean count rate for different configurations.

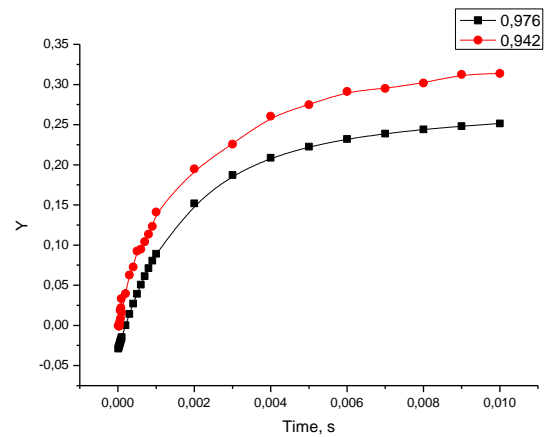


Fig. 7: Feynman- α histograms for different configurations.

Figure 8a and Figure 8b show dependence alpha parameter on rho for two different ways of reactivity changing as it was described above.

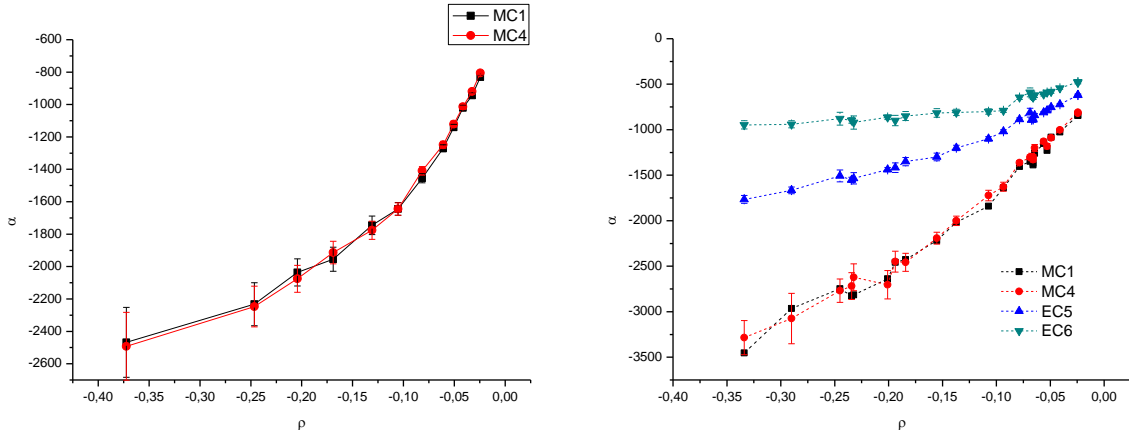


Fig. 8: Dependence alpha parameter on rho for different compositions of core.

With calculated correction factor as proposed in [8], plots in experimental channels EC5 and EC6 fit well but value of alpha is quit different compare to results in experimental channels MC1 and MC4. It should be noted that experimental channels EC5 and EC6 located in reflector and MC1 and MC4 are in the core. Also, in case when fuel pins are extracted from the core, the position of detectors in MC1 and MC4 becomes closer to reflector than to the core and two point kinetic model should be used to explain this difference.

Method proposed by Bennet is quit similar to Feynman-alpha method and based on calculation of second moment of difference in consecutive samples [7]. Then with expression

$$W = \frac{\varepsilon D_v}{\rho_p^2} \left(1 - \frac{1.5 + 0.5e^{-2\alpha T} - 2e^{-\alpha T}}{\alpha T} \right) \text{ kinetic parameters can be received.}$$

Babala proposed to use the time distribution of the length of the intervals between samples from detector [7]. In this case:

$$p_{cc}(t)dt = C_1(t)dt + C_2(t)dt \cdot e^{-\alpha t}, \text{ where}$$

$$C_1(t) = 4F\varepsilon \left[\frac{(\gamma + 1) + (\gamma - 1)e^{-\alpha t}}{(\gamma + 1)^2 - (\gamma - 1)^2 e^{-\alpha t}} \right]^2$$

$$C_2(t) = \frac{8F\varepsilon\gamma^2}{\sigma((\gamma + 1)^2 - (\gamma - 1)^2 e^{-\alpha t})t^2}$$

$$\gamma = \sqrt{1 + 2 \frac{\varepsilon D_v}{\rho_p^2}}$$

Typical Babala's distributions are shown on the Figure 9.

Table 1.

Results from different methods of multiplication factor determination.

k-effective MCNP	ρ/β_{eff} , [\$]	Source jerk method, [\$]	PNS method,[\$]	Rossi- α , [\$]	Feynman- α ,[\$]
0.97614±0.00006	-3.17±0.04	-3.12±0.1	-3.16±0.06	-3.20±0.08	-3.19±0.11
0.94261±0.00006	-7.51±0.08	-6.90±0.3	-7.12±0.12	-7.18±0.63	-7.20±0.51
0.85539±0.00006	-20.61±0.16	-23.1±1.9	-27.7±0.9	-33±2	-38±2
0.72867±0.00006	-44.86±0.24	-50.2±2.2	-48.4±1.1	-56±3	-59±3

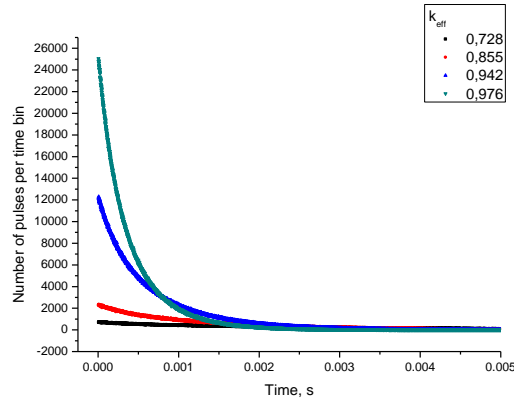


Fig. 9: Babala's distributions for different configurations.

Fitting of these plots is very intricate task, while there are several solutions with different values of fitting parameters but close goodness of fit. It can be explained by complex fitting equations. Summary for statistical methods PNS, source jerk method and calculated values are shown in table 1.

4. Conclusion

Statistical methods can be reliable methods for reactivity measurements in near critical configurations. Using spatial correction factors these methods can be used for systems with k -effective equal up to 0.95. For sub-criticalities less than 0.9 Rossi- α and Feynman- α noise methods did not reproduce the results from PNS and source jerk methods, even taking into account expressions proposed for very deep subcriticalities. It can be explained by two zone complex system (core and reflector).

Acknowledgments

The authors are grateful to Dr. Yousry Gohar from Argonne National Laboratory for significant discussion and support.

References

1. A.G. Shokodko, Drawbacks of classical theory of α -Rossi method and its alternative. Atomic energy, 2002 vol 93
2. V.A. Grabeznoi, V.V. Dulin, G.M. Mikhailov, O.N. Pavlova, α -Rossi determination of deeply subcritical states of multiplying media. Atomic energy, Vol. 101, No 2, 2006.
3. V.V. Burnos et al., "YALINA Sub-critical Test Bed for Neutron Generation and Experimental Studies in the Area of ADS Technology," Preprint, Integrated Institute of Power Engineering and Nuclear Research – Sosny, Minsk-Sosny, Belarus, 2006.
4. M. M. Bretscher, Evaluation of reactor kinetic parameters without the need for perturbation codes. Proc. Int. Mtg. Reduced Enrichment for Research and Test Reactors, Jackson Hole, WM (1997).
5. M. M. R. Williams, Random processes in nuclear reactors. Oxford: Pergamon, 1973.
6. Steven D Nolen, Gregory D Spriggs Estimation of the neutron chain-length distribution in subcritical systems using a point Monte Carlo code Annals of Nuclear Energy Volume 28, Issue 5, March 2001, Pages 509–512.
7. R. Urig, Statistical Methods in Nuclear Reactor Physics [in Russian], Atomizdat, Moscow (1974).
8. J.-L. Muñoz-Cobo, C. Berglöf, J. Peña, D. Villamarín, V. Bournos, Feynman-alpha and Rossi-alpha formulas with spatial and modal effects. Annals of Nuclear Energy Volume 38, Issues 2–3, February–March 2011, Pages 590–600
9. R. Urig, Statistical Methods in Nuclear Reactor Physics [in Russian], Atomizdat, Moscow (1974).

DEVELOPMENT, VALIDATION AND QUALIFICATION OF NEUTRONICS CALCULATION TOOLS FOR SMALL REACTORS – APPLICATION TO THE JHR, CABRI AND OSIRIS REACTORS

J.P. HUDELOT, A.C. COLOMBIER, C. D'ALETTO, J. DI SALVO, L. GAUBERT,
O. GUETON, O. LERAY, P. SIRETA, C. VAGLIO-GAUDARD, M. VALENTINI
CEA, DEN, DER/SPRC, Cadarache, F-13108 Saint Paul les Durance, France

ABSTRACT

OSIRIS and JHR (Jules Horowitz reactor) are respectively the present and future reactors of irradiation of CEA. CABRI is a reactor of CEA Cadarache devoted to the study of reactivity injection accidents. The studies of definition, development, realization and safety of these reactors require the development of complete systems of calculation covering different areas: neutronics, photonics, cycle, thermal hydraulics.

Each experimental reactor being a single object, the Laboratory of Nuclear Projects of CEA Cadarache is in charge of the development and validation of calculation forms for neutronics (N) and photonics (P): *ANUBIS* for OSIRIS reactor, *HORUS3D/N* and P for the JHR reactor, Monte Carlo calculation scheme for the CABRI reactor.

This paper describes the standard and generic process of validation and qualification of calculations forms for experimental reactors, based on the "VV&Q process". It details the main results and uncertainties obtained from the numerical and experimental validation phases for JHR, OSIRIS and CABRI reactors

1. Introduction

OSIRIS and JHR (Jules Horowitz Reactor) are respectively the present and future reactors of irradiation of CEA. CABRI is a reactor of CEA Cadarache devoted to the study of reactivity injection accidents.

The studies of definition, development, realization and safety of these reactors require the development of complete systems of calculation covering different areas: neutronics, photonics, cycle, thermal hydraulics.

Each experimental reactor being a single object, the Laboratory of Nuclear Projects of CEA Cadarache is in charge of the development, validation and qualification of calculation forms for neutronics (N) and photonics (P): *ANUBIS* for OSIRIS reactor, *HORUS3D/N* and P for the JHR reactor, Monte Carlo calculation scheme for the CABRI reactor.

This paper describes the standard and generic process of validation and qualification of calculations forms for experimental reactors. It details the main results and uncertainties obtained for JHR, OSIRIS and CABRI reactors.

2. Approach to the development of a calculation form

The estimate of the physical phenomena throughout a calculation requires the establishment of a reliable calculation chain containing: geometric and material balance data of reactors, physical models, equations, numerical methods, nuclear data base and computers [1].

To carry out studies of design, demonstration of safety and operation for reactors, industrial codes must meet constraints of speed of execution, not available to existing data with calculators and reference methods of resolution of the transport such as the Monte Carlo methods. As a result, they are generally based on deterministic numerical methods and simulations implying some simplifications.

Therefore it is important to demonstrate the reliability of the results obtained with the simulations, i.e. to control with precision the physical phenomena investigated in the core of the reactor. To do this, calculation codes are included in a more general package called "calculation form", consisting of:

- a nuclear data library (cross sections, fission yields, radioactive decay constants...)
- a chain of calculation modules
- recommendations on calculation parameters (flux solver options, energy and space mesh, self-shielding strategy,...)
- an application domain, associated with biases and uncertainties applicable to each calculated physical parameter

3. The validation and qualification process

To meet the needs of users, a rigorous approach of Verification - Validation - Qualification (VVQ) is applied systematically to all calculation forms. Figure 1 presents the synthesis of the validation-qualification process, in line with the needs expressed by final users of the calculation form.

The verification step ensures the proper functioning of the calculation algorithms.

The validation step consists in comparing the calculation results with the ones given by a reference calculation most often based on a Monte Carlo code. It allows quantifying biases related to modelling and numerical methods adopted.

The qualification step confronts the results of the calculation to experimental data representative of the studied cases. It allows setting the uncertainties due to the technological data and nuclear data. Therefore, a crucial step in this phase is to identify or to specify accurate and representative experimental programs.

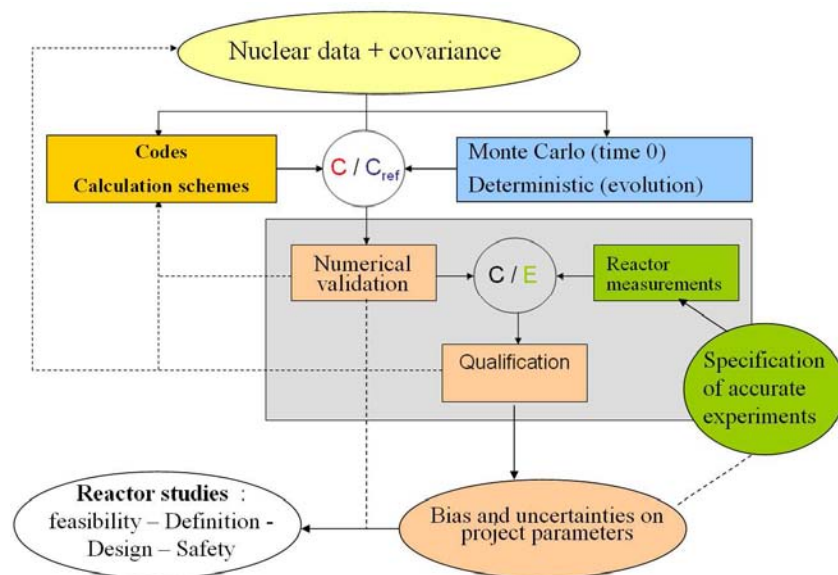


Fig 1: validation-qualification process in line with the needs expressed by final users

In terms of calculation scheme, the deterministic way generally uses a two-level scheme based on two neutronics codes (An example of application of this two-level scheme is given in section 4):

- the APOLLO2 code [2] solves the Boltzmann equation in 2 dimensions : for SN or Pij assembly calculation, or for heterogeneous and unstructured core calculations with the method of characteristics [3]

- the CRONOS2 code [4] solves the diffusion equation in 3 dimensions

The TRIPOLI4 [5] continuous Monte Carlo code is used as a reference for validation purpose.

For all calculations, the most recent European JEFF3.1.1 nuclear data library is used [6].

4. The ANUBIS calculation form for OSIRIS

For operation and safety needs, the ANUBIS form aimed at replacing the former calculation form for OSIRIS that was based on the older generation of codes.

ANUBIS is a two-level scheme based on the Apollo2 and Cronos2 codes, answering several needs for operation and design: loading plan of the reactor, calculation of safety parameters and calculation of parameters for operation (mass balance, depletion, flux, power, reactivity effects, critical position of the rods, cycle length, ...).

The relevant criteria for the design of the calculation scheme were the following ones: 3-dimension depletion calculations, output for the relevant parameters, control of biases and uncertainties, optimized balance between computation time and accuracy.

The two-level scheme for ANUBIS is illustrated in figure 2. First the macroscopic cross-sections, collapsed into a 6 energy-groups mesh and homogenized on the fuel assembly are stored in a library, called SAPHYB, that is further used as nuclear constants (for a given burn up) for the CRONOS2 code. Note that a home-made interface called NEFTIS allows automating the pre-processing of the core loading and of the CRONOS2 scheme and outputs, based on SAPHYB libraries. More details on the calculation scheme can be found in reference [7].

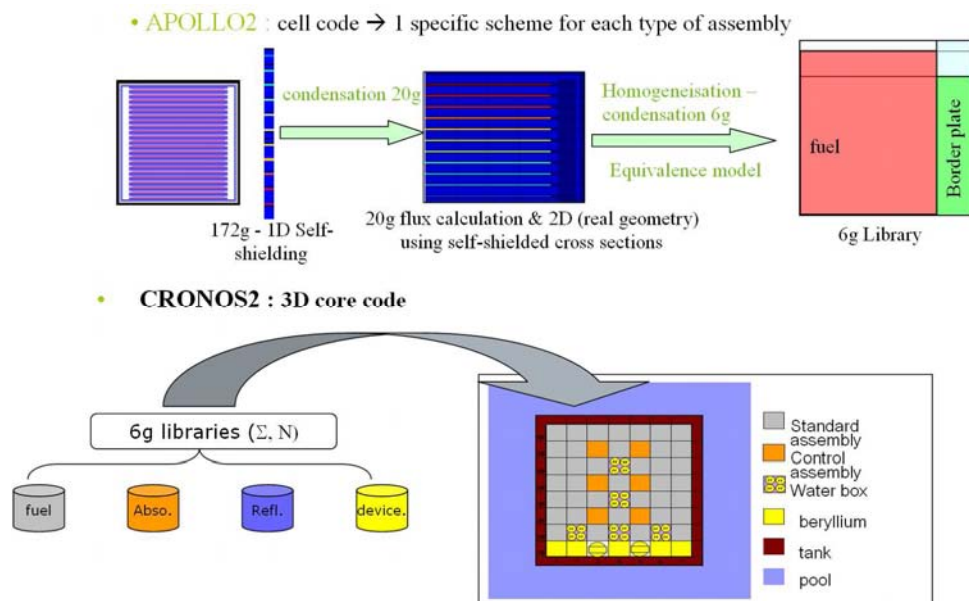


Figure 2: illustration of the two-level scheme for ANUBIS

The validation of the ANUBIS scheme is performed in comparison with a reference TRIPOLI4 calculation for time zero, and with 2D Apollo2 complete core calculation using the method of characteristics (MOC) for evolution [8]. Note that those two reference schemes can also be used to reach detailed and very local performances (power, gamma-heating, gas production, instrumentation, ...) of devices loaded in OSIRIS (see figure 3).

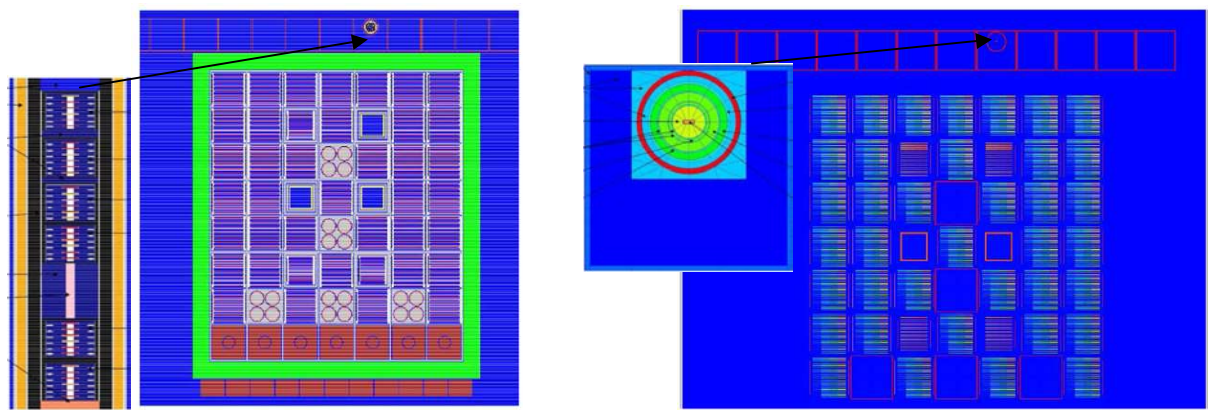


Figure 3: example of Tripoli4 scheme (left side) and 2D Apollo2-MOC scheme (right side), loaded with fully detailed device in the reflector zone (north part of the reactor)

In the end, the qualification process is based on specific experiments in the ISIS mock-up and on OSIRIS critical states and cycle length measurements. It leads to the uncertainties shown in figure 4, which suit target uncertainties dealing with operation and safety.

Uncertainties on relevant parameters

Reactivity BOL : ± 800 pcm
 Reactivity EOL : ± 500 pcm
 Absorber weight : $\pm 14\%$
 Local power: $\pm 10\%$
 Thermal and fast flux
 Fuel ass. $< \pm 10\%$
 Beryllium $< \pm 15\%$

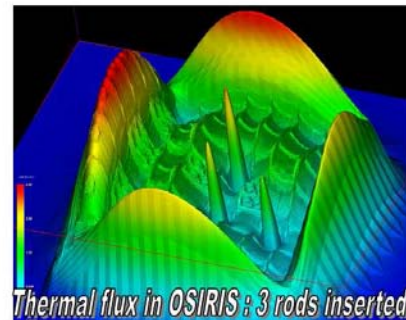


Figure 4: uncertainties on major relevant parameters with the ANUBIS form – example of calculated thermal flux distribution in the OSIRIS core

5. The HORUS3D/N calculation form for JHR

For JHR reactor, the HORUS3D/N and P forms must allow designing studies of the different phases of the project with uncertainties and biases controlled through the VVQ process. Performances in terms of applicable biases and uncertainties are defined at each phase of the project, based on extended numerical validation actions and on accurate qualification. The experiments related to the qualification come from:

- the VALMONT program in the MINERVE facility of CEA Cadarache, in which the reactivity worth of relevant samples for JHR were measured through the oscillation technique
- the AMMON program [9] in the EOLE facility of CEA Cadarache, where the core is loaded with 7 JHR real fuel assemblies. Several core configurations were defined to fit with representative situations of operation or accident of JHR.
- The ADAPh program on the EOLE and MINERVE facilities, during which gamma-heating was measured using thermoluminescent detectors, to qualification HORUS3D/P

HORUS3D/N particularly needs to fit with the very complex geometry of the different elements (control rods, fuel elements, devices and reflector) of the JHR core. This implicated

specific developments (iso-parametric finite element method [10]) in the CRONOS2 code and scheme to be able to model JHR in 3D.

Also note that a home-made interface called GAIA allows automating the pre-processing of the core loading and of the CRONOS2 scheme and outputs, based on SAPHYB libraries.

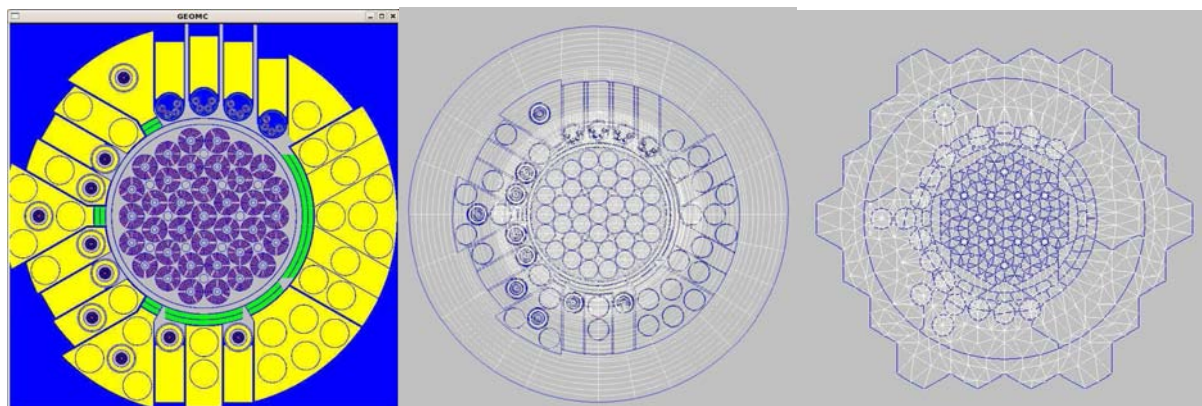


Figure 6: TRIPOLI4 (left), 2D APOLLO2-MOC (centre) and 3D CRONOS2 (right) calculation schemes for HORUS3D/N V4.0 form

The following table gives the best-estimate biases and uncertainties – from validation step and elementary qualification on the Valmont program - applicable to the key-parameters using the latest version HORUS3D/N V4.0. The target uncertainties on those parameters forecasted after the AMMON program interpretation are also given in the last column.

Key parameters	Best estimate bias and uncertainty HORUS3D/N V4.0	target uncertainties after AMMON
Reactivity	-550 pcm \pm 1200 pcm	\pm 500 pcm
Plate power peak	\pm 8%	\pm 5%
Absorber worth	+3.1% \pm 8.4%	\pm 5%
Thermal and fast flux	\pm 4% (*)	\pm 10%
Gamma-heating in core	+25% \pm 15%	\pm 15%

(*) uncertainty due to nuclear data only

Table 1: bias and uncertainties for HORUS3D/N V4.0; target uncertainties after the AMMON program interpretation

6. The calculation scheme for CABRI

For the CABRI reactor, the Monte Carlo Tripoli4 calculation scheme allows predicting accurately the relevant neutronics parameters: neutron flux and power, gamma-heating, experimental pin/core coupling, kinetic parameters, temperature coefficient [11]. Figure 7 show the description of CABRI (with water loop) in real geometry using the Tripoli4 code.

This calculation scheme proved its capability to estimate the experimental pin/core coupling within the experimental uncertainties. Furthermore, it was possible to well reproduce the power transients inside Cabri using the calculated kinetics parameters and temperature coefficients. Finally, the scheme also helped to dimension all new instrumentations (chambers, dosimeters) for core characterization in the frame of future experiments in Cabri.

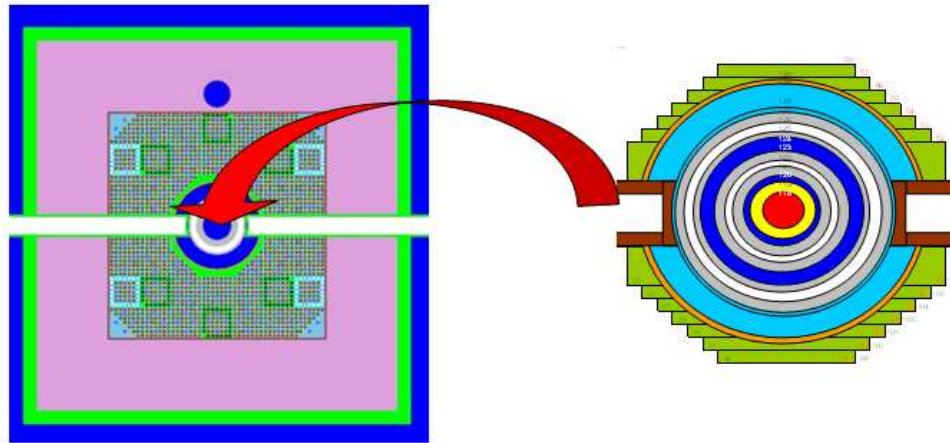


Figure 7: description of the CABRI core with Tripoli4; zoom on the water loop (left)

7. Conclusions

The Laboratory of Nuclear Projects of CEA Cadarache develops accurate calculation forms for all kinds of experimental reactors. Modern and accurate calculation codes and tools help to fit with the complexity of those reactors, in terms of geometry and heterogeneity.

The generic Validation and Qualification process applied to these forms ensures that the calculations respect the target uncertainties defined by the final users for all the relevant neutronics parameters, and that potential biases are controlled.

This know-how has already been successfully adapted to several types of irradiation reactors such as JHR, CABRI, OSIRIS or naval propulsion reactors.

8. References

- [1] P. Blaise, D. Bernard, « L'apport des maquettes critiques pour la physique es réacteurs de puissance : données nucléaires et codes de calcul », Revue Générale Nucléaire, Année 2011 n°6, ISSN 0335-5004, p.23-28
- [2] R. Sanchez et al., "APOLLO2 A user-oriented, portable, modular code for multigroup transport assembly calculations", Nuclear Science and Engineering, vol. 100, pp. 352-362
- [3] A. Santamarina et al. APOLLO2.8: a validated code package for PWR neutronics calculations, ANS 2009, topical Meeting ANFM 2009, p. 1/18
- [4] JJ. Lautard et al., "CRONOS, a modular computational system for neutronics core calculations", IAEA topical meeting, 1990, Cadarache, France
- [5] JP. Both et al., A survey of TRIPOLI4, 8th International Conference on radiation shielding, Arlington, (Texas, USA), 1994
- [6] A. Santamarina, D. Bernard, « The recommended JEFF-3.1.1 File and CEA2005V4 library for accurate neutronics calculations », JEFF Report OECD/NEA 2009
- [7] O. Guéton et al., Validation and qualification of the ANUBIS scheme used for safety assessment and operation management of the OSIRIS reactor, IGORR12 Conference, Beijing (China), October 28-30, 2009

- [8] J. Di Salvo, The OSIRIS reactor neutronic reference calculation scheme based on the method of characteristics, PHYTRA1 Conference, Marrakech (Morocco), March 14-16, 2007
- [9] C. Vaglio-Gaudard et al., "Monte Carlo interpretation of the AMMON experiment for the experimental validation of the JHR reactor calculation ", PHYSOR 2012 Conference, Knoxville, Tennessee (USA), April 15-20, 2012 (to be published)
- [10] C. Döderlein et al., The 3D neutronics scheme for the development of the Jules-Horowitz-Reactor, PHYSOR 2008 Conference, Interlaken, Switzerland, September 14-19, 2008
- [11] O. Guéton et al., Neutronics computations in support of the CABRI core safety analysis, IGORR12 Conference, Beijing (China), October 28-30, 2009

IMPROVED NEUTRON LEAKAGE TREATMENT ON NODAL EXPANSION METHOD FOR SMALL REACTORS

Antonio Carlos Marques Alvim, Fernando Carvalho da Silva and Aquilino Senra Martinez

Programa de Engenharia Nuclear, COPPE/UFRJ
Av. Horácio Macedo, 2030, Bloco G - Sala 206 - Centro de Tecnologia
Cidade Universitária, Ilha do Fundão, 21941-914 - Rio de Janeiro, RJ
aalvim@gmail.com; fernando@con.ufrj.br; aquilino@imp.ufrj.br

ABSTRACT

For quick and accurate calculations of spatial neutron distribution in nuclear power reactors 3D nodal codes are usually used aiming at solving the neutron diffusion equation for a given reactor core geometry and material composition. However such codes are not directly applied to small reactors, due to high neutron leakage from the small reactor core. The models used to represent the neutron leakage in conventional 3D nodal codes are not good enough to be applied to small reactors.

This paper deals with an alternative method to represent the neutron leakage to be used in conjunction with the nodal expansion method (NEM). The proposed method was implemented into a computational system which, besides solving the diffusion equation, also solves the depletion equations governing the gradual changes in material compositions of the core due to fuel burnup. Results confirm the effectiveness of the method for practical purposes in small reactors.

Key Words: High leakage, nodal expansion method, power density, research reactors

1. INTRODUCTION

The neutron distribution has to be frequently calculated in research or multi-purpose small reactors. This calculation is validated with experimental measurements of the thermal, epithermal and fast neutron fluxes in different channels of irradiation. Even the neutron population varies along the reactor operation period, depending on time variation of the nuclide distribution, which in turn varies with the spatial distribution of the depletion rate. So, one is fully justified to use a quasi-static approximation [1], in which the reactor cycle is divided into certain time intervals, during which the neutron fluxes are held constant. Therefore, in this case, the stationary diffusion equation and the burnup equations are solved, in each of the defined time intervals for the reactor operation period.

There are a lot of methods to solve the neutron diffusion equations for a given reactor core, but determining factors that affect the quality of a system for calculating the neutronic parameters of the reactor core are the precision and speed with which the operational performance of the reactor is predicted. For power reactors the most popular method is the nodal expansion method (NEM) [2]. An example of application of this method is the CNFR code (Portuguese acronym for National Reactor Physics

Code) [3] that consists of three main modules, which generate nuclear data for fuel elements, 3D nuclear power distributions and characteristic parameters calculation of the nuclear reactor.

However codes based on NEM are not directly applicable to small and research reactors due to the treatment of neutron leakage from reactor core. Low leakage is usually considered in such treatments. Because that, the present paper deals with an alternative technique to represent higher neutron leakage. This method was introduced in CNFR to solve the space dependent neutron diffusion equation and was shown to be very accurate for small reactors.

We aim at applying CNFR, with appropriated leakage treatment for small reactors, to RMB (Portuguese acronym for Brazilian Multi-purpose Reactor), which is a multi-purpose open pool type reactor with a nominal power of 50MW and to other Brazilian research reactors. There are four research reactors in Brazil, namely: IEA-R1, IPR-R1, ARGONAUTA and IPEN/MB-01.

IEA-R1 is pool type research reactor having light water as moderator and coolant, having graphite as reflector. IPR-R1 is a light water cooled research reactor fueled with uranium metal 20% enriched in ^{235}U and having zirconium hydride (U-ZrH) as moderator. ARGONAUTA was the first research reactor built Brazil, with maximum power of 5kW, while IPEN/MB-01 was the first research reactor totally designed and built in the country having square lattice geometry with active dimensions of $39 \times 42 \times 54 \text{ cm}^3$, with an array of 28×26 fuel rods and 48 guide tubes used to insert control rods and instrumentation. Right now, two small reactors are under construction, one of them is RMB. The RMB reactor is been designed mainly for radioisotope production.

In section 2, a brief comment on the nodal expansion method (NEM) is presented. Section 3 presents the treatment for leakage used in conventional codes. Section 4 presents the alternative method for neutron leakage treatment, and section 5 shows the results obtained. The conclusions are presented in section 6.

2. NODAL EXPANSION METHOD

The nodal expansion method (NEM) has been applied to solve neutron diffusion equations for decades. There have been some variants of NEM [2] since its appearance. One of them is the analytical NEM, e.g., the nodal integration method (NIM) [4]. Other variant is the semi-analytic NEM [5]. Basic difference between them lies in the expansion of the fission source in the transverse integrated equations, which is done only in the semi-analytic method.

The majority of nodal diffusion codes employ the diffusion equation integrated in a transverse area for given direction. From this integration, the transverse leakage is obtained. These codes use a second order polynomial to represent the transverse leakage term.

The Nodal Expansion Method divides the reactor core into contiguous parallelepipeds called nodes. Since NEM requires that the nodes be homogeneous, special models are adopted to deal with cross-sections that are no longer uniform inside the node, due to burnup and control rod motion [3]. With these special models, nodes remain homogeneous and core nodalization, which was previously established, is maintained.

The NEM method uses partial interface currents and has as its starting point the neutron continuity equation and Fick's Law. The nodal balance equation, from which

one obtains average nodal fluxes $\bar{\phi}_g^n(t_\ell)$ for each time t_ℓ , results from integration of the continuity equation in the volume $V_n = a_x^n a_y^n a_z^n$ of a node n and subsequent division of the integrated equation by this volume, i.e.

$$\sum_{u=x,y,z} \frac{1}{a_u^n} [\bar{J}_{gur}^n(t_\ell) - \bar{J}_{gul}^n(t_\ell)] + \Sigma_{tg}^n(t_\ell) \bar{\phi}_g^n(t_\ell) = \sum_{g'=1}^2 \left\{ \frac{\chi_g}{k_{eff}} \nu \Sigma_{g'}^n(t_\ell) + \Sigma_{gg'}^n(t_\ell) \right\} \bar{\phi}_{g'}^n(t_\ell) \quad (1)$$

where the cross sections involving capture and fission, which because of the burnup gradient [4] vary spatially within the node.

2.1 – Nodal Coupling Equations

The nodal coupling equations are obtained from Fick's law, integrating these equations in the area transverse to direction u, and subsequent division of the integrated equations by this area, i.e.

$$\bar{J}_{gus}^n(t_\ell) = \bar{J}_{gus}^{+n}(t_\ell) - \bar{J}_{gus}^{-n}(t_\ell) = -\bar{D}_g^n(t_\ell) \frac{d}{du} \bar{\psi}_{gu}^n(u, t_\ell) \Big|_{u=u_s^n}, \quad (2)$$

for $u = x, y, z$ and $s = r, l$.

$\bar{\psi}_{gu}^n(u, t_\ell)$ is obtained by integrating the diffusion equation in the transverse area to direction u. The transverse integrated diffusion equation, mentioned above is written as:

$$-\bar{D}_g^n(t_\ell) \frac{d^2}{du^2} \bar{\psi}_{gu}^n(u, t_\ell) + \Sigma_{tg}^n(t_\ell) \bar{\psi}_{gu}^n(u, t_\ell) = \sum_{g'=1}^2 \left\{ \frac{\chi_g}{k_{eff}} \nu \Sigma_{fg'}^n(t_\ell) + \bar{\Sigma}_{gg'}^n(t_\ell) \right\} \bar{\psi}_{g'u}^n(u, t_\ell) - L_{gu}^n(u, t_\ell) - d_{gu}^n(u, t_\ell) \quad (3)$$

Where $L_{gu}^n(u, t_\ell)$ is the transverse leakage and $d_{gu}^n(u, t_\ell)$ is the cross section difference [3]. There has been some variants of NEM [2], since its appearance, to solve eq. (3). One of them is the analytical NEM, e.g., the nodal integration method (NIM) [4]. This method solves the transverse integrated equations analytically, approximating only the transverse leakage and the cross section difference term. Other variant is the semi-analytical NEM [5], which makes use of polynomial expansions for the transverse leakage, fission source, scattering and the cross section difference term, thus uncoupling the energy groups. According to the original NEM, $\bar{\psi}_{gu}^n(u, t_\ell)$ are calculated using a fourth order polynomial expansion [2].

3. TREATMENT OF LEAKAGE IN CONVENTIONAL CODES

All the NEM based nodal codes, including CNFR, use second order polynomial expansions to approximate $L_{gu}^n(u, t_\ell)$, for every node in the reactor (active core and reflector), in the form:

$$L_{gu}^n(u, t_\ell) = \bar{L}_{gu}^n(t_\ell) + \sum_{k=1}^2 \alpha_{kgu}^n(t_\ell) h_k(u/a_u^n), \quad (4)$$

where

$$\bar{L}_{gu}^n(t_\ell) \equiv \frac{1}{a_v^n} [\bar{J}_{gvr}^n(t_\ell) - \bar{J}_{gvl}^n(t_\ell) + \frac{1}{a_w^n} [\bar{J}_{gvr}^n(t_\ell) - \bar{J}_{gvl}^n(t_\ell)] , \quad (5)$$

$$\alpha_{1gu}^n(t_\ell) = \frac{1}{2} \{L_{gur}^n(t_\ell) - L_{gul}^n(t_\ell)\} \quad (6)$$

and

$$\alpha_{2gu}^n(t_\ell) = \bar{L}_{gu}^n(t_\ell) - \frac{1}{2} \{L_{gur}^n(t_\ell) + L_{gul}^n(t_\ell)\} \quad (7)$$

with $L_{gus}^n(t_\ell) \equiv L_{gu}^n(u_s^n, t_\ell)$ for $u = x, y, z$ and $s = r, l$.

4. NODAL METHOD APPLICABLE FOR SMALL REACTORS

In this work, we have used for all nodal surfaces in the core and reflector, except by those reflector node surfaces at the external surface of the reactor, the following expression for $L_{gur}^m(t_\ell)$:

$$L_{gur}^m(t_\ell) = \frac{a_u^n \bar{L}_{gu}^m(t_\ell) + a_u^m \bar{L}_{gu}^n(t_\ell)}{a_u^n + a_u^m}, \quad (8)$$

where m is the node adjacent to node n .

But in those reflector node surfaces at the external surface of the core, the following expression was used

$$L_{gus}^n(t_\ell) = \{\bar{\psi}_{gu}^n(u_s^n, t_\ell) / \bar{\phi}_g^n(t_\ell)\} \bar{L}_{gu}^n(t_\ell). \quad (9)$$

5. RESULTS

To demonstrate the efficiency of the nodal method developed applied to small reactor calculations, so that we can apply it to the RMB reactor, we used the FDR-2 ship reactor, whose configuration and nuclear data were taken from reference [6]. Table 1 shows the multiplication factor for different positions of control rod bank, from fully withdrawn (position 0/8) to fully inserted (position 8/8), calculated by the nodal method. The same table presents the CPU time of the nodal calculation, in the case of 3x3 nodes per assembly, in accordance with reference [6]. In addition, we also introduce the multiplication factor calculated using finite differences with a mesh of $0.5 \times 0.5 \times 0.5 \text{ cm}^3$, the CPU time for each case and the relative deviation between the nodal and the finite difference calculations.

Table 1 Multiplication factor for each control bank position.

Bank position	Nodal Method		Finite Difference		Relative deviation in k_{eff} (%)
	k_{eff}	CPU time (s)	k_{eff}	CPU time	
0/8	1.1086696	1.08	1.108445	3h 48min	0.02
1/8	1.1023437	1.03	1.102035	2h 09min	0.03
2/8	1.0913593	0.98	1.091019	4h 35min	0.03
3/8	1.0748512	0.81	1.074476	5h 46min	0.03
4/8	1.0515517	0.92	1.051129	3h 23min	0.04
5/8	1.0208039	1.06	1.020317	4h 12min	0.05
6/8	0.9894788	1.36	0.988981	3h 43min	0.05
7/8	0.9735736	0.33	0.973094	3h 52min	0.05
8/8	0.9699907	1.03	0.969568	2h 35min	0.03

In addition, we performed a nodal calculation, with 50x50 nodes per assembly, for the case 0/8 in order to demonstrate the consistency of the method developed. The multiplication factor of 1.1085189 was obtained with a relative deviation of 0.007% and CPU time of 1h 47min. This shows that the nodal method developed is in fact a consistent method.

Reference [6] presents a graph of the multiplication factor versus control rod bank position (cm) for different methods. Then, to show that results obtained with this method show the same behavior, we present in fig.1 a graph similar to the one of reference [6].

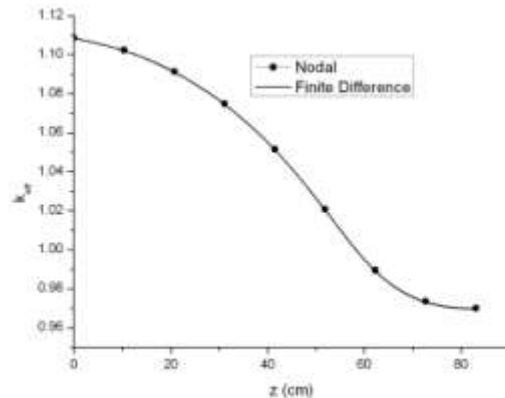


Figure 1 Multiplication factor control bank curve.

6. CONCLUSIONS

The novel treatment of the transverse leakage term in our code has successfully produced very good results for the FDR-2 ship reactor, for several insertion control rod positions, with a maximum relative deviation from a finite difference calculation in k_{eff} of only 0.05%. A fine mesh nodal calculation, with 50x50 nodes per assembly, for the case 0/8 was done to demonstrate consistency of the method. A multiplication factor of 1.1085189 was obtained with a relative deviation of 0.007%. We conclude that this transverse leakage treatment, developed to treat small reactors was successful, producing accurate results for the reactor in which it was tested, with a CPU time much smaller than a conventional finite difference code.

7. REFERENCES

1. W. M. Stacey, *Nuclear Reactor Physics*, Wiley-VCH, Weinheim, Germany (2004)
2. H. Finnemann, F. Benneritz and M. R. Wagner, "Interface current techniques for multidimensional reactor calculations" *Atomkernenergie* **30**, 123 (1977)
3. F. C. Silva, A. C. M. Alvim and A. S. Martinez, "An Alternative Solver for the Nodal Expansion Method Equations" *PHYSOR 2010 – Advances in Reactor Physics to Power the Nuclear Renaissance*, Pittsburgh, Pennsylvania, USA (2010)
4. H. D. Fischer and H. Finnemann, "The Nodal Integration Method – A Diverse Solver for Neutron Diffusion Problems" *Atomkernenergie-Kerntechnik*, **30**, 229 (1981)
5. H. K. Joo, C. M. Kim, J. M. Noh and S. Kim, "A Semi-Analytic Multigroup Nodal Method", *Annals of Nuclear Energy*, **26**, 699 (1999)
6. H. Siewers and W. Jager, "Comparison of coarse-mesh methods for benchmark and realistic reactor problems" *Atomkernenergie*, **30**, 107 (1977)

MODERN APPROACHES FOR THE GENERATION OF LOW ENERGY NEUTRON SCATTERING CROSS SECTIONS

A. I. Hawari

*Nuclear Reactor Program, Department of Nuclear Engineering, North Carolina State University
P.O. Box 7909, Raleigh, NC, 27695, USA*

ABSTRACT

The process of neutron moderation and thermalization is a fundamental physical phenomenon in nuclear science and engineering applications. In nuclear fission reactors, the moderation of prompt fission neutrons (e.g., in water) and their thermalization are the basic catalyst for the fission reaction in the uranium fuel. Upon thermalization, the neutron energy spectrum tends towards a pseudo-equilibrium state with an average energy that is defined by the temperature and structure of the moderator. Moreover, in research reactors, the physics of thermalization represents the fundamental working principle for the design of various cold and ultracold neutron sources. In addition, low energy neutron interaction physics also describes the operation of filters that may be used in thermal and cold neutron beams.

The neutron thermalization process is quantified using material specific thermal neutron scattering cross sections. In recent years, progress in computational capabilities has made it possible to implement modern predictive techniques to estimate the basic data that are needed to calculate the thermal neutron scattering cross sections in various materials. This includes techniques such as *ab initio* (i.e., first principles) and molecular dynamics (MD) simulation methods. *Ab initio* techniques are able to calculate inter-atomic forces using a quantum mechanical approach. The generated force information can then be used to describe the lattice dynamics of the atomic system and to derive the excitation spectrum that sets the thermal scattering cross sections. Classical MD techniques utilize a similar philosophy. However, due to the classical nature of the calculation, it represents a computationally less demanding approach. This also implies that it can be useful in addressing more complicated atomic systems such as ones where the atomic structure has been disrupted due to exposure to radiation.

Furthermore, in some cases, the utilization of such modern techniques allows the generation of more complete thermal neutron scattering data libraries accounting for effects that may have been cumbersome to capture in the past. This includes the ability to avoid the traditionally invoked incoherent approximation and to explicitly treat coherent inelastic scattering effects. As a result, new and improved thermal neutron scattering data libraries are now available for a variety of materials and at various temperatures. Among these are reactor moderators and reflectors such as graphite and beryllium (with coherent inelastic scattering), cold and ultracold neutron media such as solid methane and solid deuterium, and neutron beam filters such as sapphire and bismuth.

1. Introduction

Low energy or “thermal” neutrons are characterized by energies that are on the order of the excitation (vibration, rotation etc.) energy in the medium in which they interact. Furthermore, their de Broglie wavelength is on the order of the separation distance in solids. Consequently, such neutrons are highly sensitized to the atomic binding details of the system that surrounds them including its structure and dynamics. In fact, the structural and dynamic properties of the atomic system are sampled through scattering interactions between the system’s atoms and molecules and the neutrons.

The scattering of low energy neutrons in an atomic system is generally described using thermal neutron scattering cross sections. Traditionally, the cross sections are quantified

based on Born scattering theory combined with Fermi's Golden and the assumption of an extremely short range (delta function) nuclear potential [1]. The outcome of this approach, is an expression for the double differential scattering cross section given by

$$\frac{d^2\sigma}{d\Omega dE} = \frac{1}{4\pi} \frac{k'}{k} \left(\sigma_{coh} S(\vec{\kappa}, \omega) + \sigma_{inc} S_s(\vec{\kappa}, \omega) \right), \quad (1)$$

where $S(\kappa, \omega)$ is known as the scattering law, κ is the scattering vector, ω is the frequency, k and k' represent the magnitude of the wave vector of the incident and scattered neutron respectively, σ_{coh} is the bound atom coherent scattering cross section, and σ_{inc} is the bound atom incoherent scattering cross section. In general, S is composed of two terms as follows

$$S(\vec{\kappa}, \omega) = S_s(\vec{\kappa}, \omega) + S_d(\vec{\kappa}, \omega), \quad (2)$$

where S_s is known as the self-scattering law, which accounts for non-interference (incoherent) effects, while S_d is the distinct scattering law and accounts for interference (coherent) effects. Examination of Eq. 1 shows that the thermal neutron scattering cross section depends on two factors: first, the neutron-nucleus interaction as represented by the bound atom cross sections, and second, a factor that represents the dynamics of the scattering system (i.e., the collection of atoms) as represented by the scattering law.

Frequently, the calculations of the thermal scattering cross section invoke the incoherent approximation where S_d is set equal to zero in Eq. 2. Based on this assumption, Eq. 1 is developed to give [2]

$$\frac{d^2\sigma}{d\Omega dE'} = \frac{1}{4\pi} \frac{k'}{k} \left[\sigma_{coh} + \sigma_{incoh} \right] S_s(\vec{\kappa}, \omega). \quad (3)$$

However, for some important neutronic materials such as graphite and beryllium, this assumption can introduce uncertainties that reach nearly 20% in the calculated total inelastic scattering cross section. Various methods can be used to remedy this effect by estimating S_d and introducing it into the expression for thermal neutron scattering cross sections. If the atoms are assumed to be bound by harmonic forces, an expansion can be performed to allow the decomposition of the coherent and incoherent double differential scattering cross section into elastic and inelastic components. In crystalline materials, this expansion is known as the phonon expansion. Assuming that the largest contribution to the scattering law is due to the creation or annihilation of a single phonon, the thermal neutron scattering cross section (including the S_d coherent inelastic contribution) can be written as

$$\frac{d^2\sigma}{d\Omega dE'} \cong \frac{1}{4\pi} \frac{k'}{k} \left(\sigma_{coh} \left(\sum_{p=2}^P S_s \right)_{incoh} + \sigma_{coh} \left({}^1S_s + {}^1S_d \right)_{exact} \right), \quad (4)$$

where 1S_d is the distinct scattering law for 1-phonon scattering [3].

2. Methods for Generating the Scattering Law

As indicated above the scattering law, S , is an inherent property of the material in which the neutrons are interacting. Consequently, it can be estimated based on atomistic models of the material. For crystalline solids, the formulation for calculating the scattering law is reduced to require the phonon density of states for a given material [e.g., see Ref. 2]. In this case, modern methods that depend on ab initio density functional theory (DFT) for the estimation of inter-atomic forces combined with a dynamical matrix approach can be used to calculate S [4]. This represents a significant departure from past techniques that may have depended on simplistic atomistic models and fitting to experimental data to arrive at such

information. However, the use of DFT simulations (and its variants) allows the application of a predictive approach for the eventual generation of S , which expands substantially the ability to generate the thermal neutron scattering cross sections to many materials, (e.g., moderators, filters etc.) that may be of interest to nuclear reactor design and utilization.

More recently, the application of classical molecular dynamics (MD) techniques has also been initiated to estimate the scattering law of materials [5]. In this case, the forces between atoms are calculated based the choice and parameterization of appropriate potential functions [6]. The advantage of this approach over, e.g., the use of a dynamical matrix methodology is the ability to treat imperfect materials that may contain irregularities in the lattice structure. Furthermore, the MD approach is inherently suited for estimating the scattering law for materials that may be in the liquid or gaseous states. Information regarding the density of states and the scattering law can be extracted by calculating velocity and density autocorrelation functions, respectively, for the atoms in the systems. However, as the calculations are classical in nature, elements of the thermal scattering phenomenon such as detailed balance and recoil effects are not typically captured. Therefore, quantum mechanical correction procedures are introduced to account for such missing phenomena [7,8]. The final outcome of this approach is a methodology that can treat the calculation of the scattering law of a given material in a general fashion including the calculation of the S_d component to relax the incoherent approximation.

3. Thermal Neutron Scattering Data

Based on the above discussion, DFT combined with the dynamical matrix approach and MD methods were used to generate the thermal neutron scattering cross section for neutron moderators/reflectors, neutron filters and neutron source materials that are of interest in research reactor applications. Two important materials of interest in this work are graphite and beryllium. Both of these materials are strong coherent scatterers where the incoherent approximation is known to introduce noticeable biases. Consequently, the calculations were performed by combining the fundamental input (i.e., the phonon density of states) that was generated using DFT and dynamical matrix methods with Eq. 3 (i.e., the incoherent approximation) and Eq. 4 to account for the S_d component of the scattering law. This data can be seen in Fig. 1, which gives the total inelastic scattering cross section for both materials. Moreover, graphite as used in nuclear reactors belongs to a certain type of graphitic materials known as reactor-grade graphite. This type of graphite generally has a density ranging between 1.5 g/cm^3 to 1.8 g/cm^3 in comparison to ideal graphite with a density of 2.25 g/cm^3 . The decrease in density is mainly due to the large porosity content of reactor grade graphite. Figure 1 also shows results for graphite with a porosity content of 10% and 30% that were generated based on MD methods [9]. As it can be seen, the introduction of porosity substantially improves the agreement between the calculated data and the measured cross sections for reactor-grade graphite.

DFT and dynamical matrix techniques can be used to generate the thermal neutron scattering cross sections for thermal neutron filters. While current practices in research reactor beam design favor the utilization of curved neutron guides to separate the thermal neutrons from higher energy components in the neutron beam. The use of neutron filters to perform this function remains prevalent in reactors where the implementation of curved guides may not be possible. In this case, two very popular filters are single crystal sapphire and single crystal bismuth (usually used as in-beam gamma-ray filter) that are usually implemented at room temperature. Figure 2 shows the total inelastic scattering cross section for these materials [10]. In both cases the calculations were performed within the limits of the incoherent approximation (i.e., Eq. 3).

Another class of materials that is of interest to research reactor applications is cryogenic moderators that serve as cold and ultracold neutron sources. As an example of that, MD techniques were used to study solid methane in its various phases to understand the impact of temperature dependent phase changes on its eventual performance as a cold neutron source [11]. Figure 3 shows the total inelastic scattering cross section for solid methane.

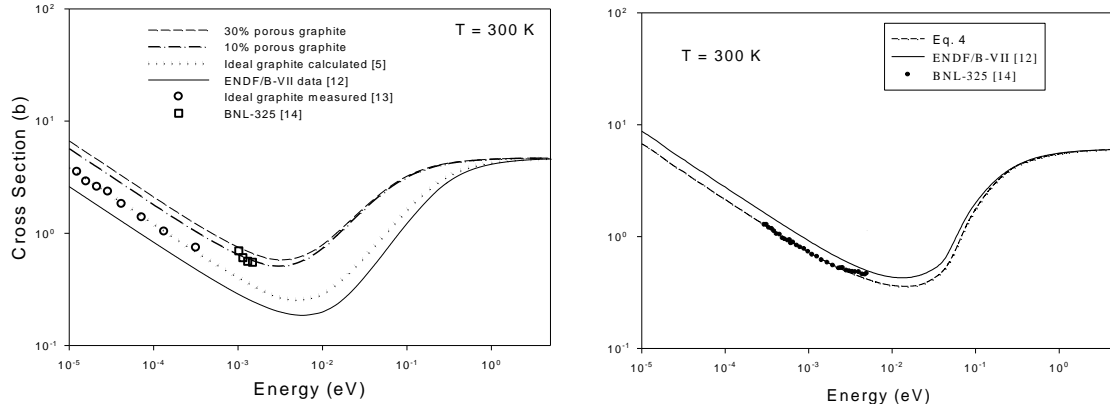


Fig. 1. The total inelastic scattering cross sections for graphite (left) and beryllium (right). The data shows the impact of the incoherent approximation for both materials and porosity for graphite.

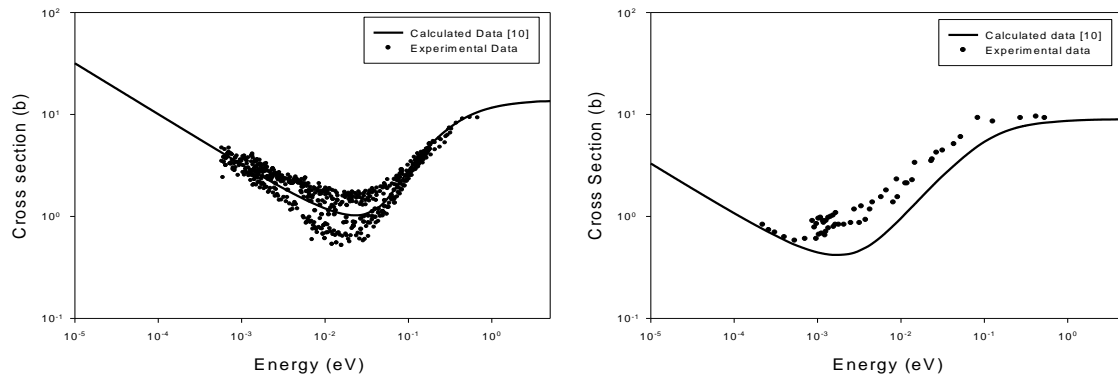


Fig. 2. The total inelastic scattering cross sections for sapphire (left) and bismuth (right) at 300 K.

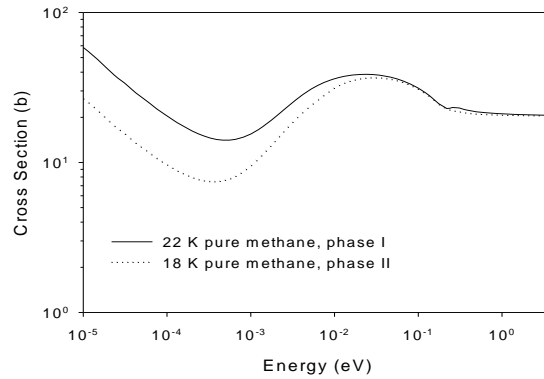


Fig. 3. The total inelastic scattering cross sections for phase I and II of solid methane.

4. Conclusions

As it can be seen from the above discussion, nowadays various computational techniques have become available to generate the needed input for the calculation of the thermal neutron scattering cross sections. These techniques are of a general nature and, if needed, can quite easily overcome the handicaps of past methods (e.g., the incoherent approximation). In addition, the techniques take advantage of sophisticated atomistic simulations approaches based on DFT and MD that are predictive in nature, that can treat matter in all of its usual states (solid, liquid and gas), and that allow the treatment of irregular materials. The generated results present data for various materials some of which are note

presented as part of the standard ENDF libraries such as reactor-grade graphite, sapphire and bismuth. Furthermore, work is currently underway to finalize a thermal neutron scattering data library for solid deuterium, which is being considered as an ultracold neutron sources at various facilities including the North Carolina State University PULSTAR reactor.

Acknowledgement

This work has been supported by the US Department of Energy through various NERI and NEUP grants and contracts.

References

- 1) G. L. Squires, "Introduction to the Theory of Thermal Neutron Scattering," Cambridge University Press, UK, 1977.
- 2) R. E. MacFarlane, "New Thermal Neutron Scattering Files for ENDF/B-VI, Release 2," LA-12639-MS, Los Alamos National Laboratory, 1994.
- 3) A. I. Hawari, and I. I. Al-Qasir, "Graphite Thermal Neutron Cross Section Calculations Including Coherent 1-Phonon Effects," PHYSOR-2008: International Conference on the Physics of Reactors, Nuclear Power: A Sustainable Resource, Interlaken, Switzerland, 2008.
- 4) A. I. Hawari, I. I. Al-Qasir, V. H. Gillette. B. W. Wehring. And T. Zhou, "Ab initio Generation of Thermal Neutron Scattering Cross Sections," PHYSOR 2004: The Physics of Fuel Cycles and Advanced Nuclear Systems-Global Developments, Chicago, IL, USA, 2004.
- 5) B. D. Hehr, and A. I. Hawari, Transactions of the American Nuclear Society, 98 (2008) 1126.
- 6) B. D. Hehr, A. I. Hawari, and V. H. Gillette, Nuclear Technology, 160 (2007) 251.
- 7) B. D. Hehr, and A. I. Hawari, Transactions of the American Nuclear Society, 102 (2010) 509.
- 8) B. D. Hehr, "Development of the Thermal Neutron Scattering Cross Sections of Graphitic Systems using Classical Molecular Dynamics Simulations", Ph.D. Dissertation, North Carolina State University, Raleigh, NC, USA, 2010.
- 9) A. I. Hawari, and V. H. Gillette, Transactions of the American Nuclear Society, 106 (2012).
- 10) A. I. Hawari, I. I. Al-Qasir, and K. K. Mishra "Accurate Simulation of Thermal Neutron Filter Effects in the Design of Research Reactor Beam Applications," PHYSOR-2006: Advances in Nuclear Analysis and Simulation, Vancouver, Canada, 2006.
- 11) A. Petersen, and A. I. Hawari, "Molecular Dynamics Simulations of Phase I and II of Solid Methane and Inelastic Neutron Scattering," AccApp'11, Tenth International Topical Meeting on Nuclear Applications of Accelerators, Knoxville, TN, USA, 2011.
- 12) M. B. Chadiwick, et al., Nuclear Data Sheets, 107 (2006) 2931.
- 13) A. Steyrel, and W. D. Trustedt, Z. Physik., 267 (1974) 379.
- 14) D. J. Hughes, and R. B. Shwartz, Neutron Cross Sections-BNL 325, Second Edition, 1958.

NEUTRONICS CORE OPTIMISATION OF THE JULES HOROWITZ REACTOR

L. WONG

*Nuclear Operations, Australian Nuclear Science and Technology Organisation
New Illawarra Road, Lucas Heights 2234, NSW, Australia
lindee.wong@ansto.gov.au*

B. POUCHIN

*Service du Réacteur Jules Horowitz, Commissariat à l'Energie Atomique et aux Energies Alternatives
CEA Cadarache, 13108 St Paul Lez Durance Cedex, France
bernard.pouchin@cea.fr*

ABSTRACT

The Jules Horowitz Reactor (JHR) is a materials testing reactor currently under construction at the Cadarache site of the Commissariat à l'Energie Atomique et aux Energies Alternatives (CEA). Within the reactor core, it is envisaged that experimental devices will be placed within the vacant positions in the core rack for irradiation under fast flux. Thus, the current configuration of the core has been optimised for a hard neutron spectrum. However, depending on the experimental device loading in the core, this fast flux optimisation in the core may not be necessary. Instead, in this situation, it is more economical to thermalise the flux and increase the cycle duration.

A neutronics study using TRIPOLI-4 was performed to locate positions within the JHR core in which neutron moderating materials, beryllium or water, could be placed, in order to increase the reactivity in the core. These positions include the experimental device positions at the centre of the fuel assembly, and inter-assembly or outer periphery positions which are currently designated to be filled by aluminium cylinders. The impact of these materials on the experimental device performance within the core and in the reflector and the flux distribution within the core was analysed. Operating cycle gains of several full power days were identified.

1. Introduction

The Jules Horowitz Reactor (JHR) is a 100 MW, water moderated materials test reactor [1]. JHR will host a variety of experimental facilities, located within the core and in the beryllium reflector. The in-core experimental devices, such as CALIPSO, are designed for material irradiation under fast flux, and can be located in several positions at the centre of a fuel assembly, between fuel assemblies, as well as in fuel assembly sized positions. In the reflector, experimental facilities such as ADELIN and MADISON, as well as Mo-99 irradiation facilities are planned. The facilities in the reflector are designed to utilise the thermalised neutron region of JHR.

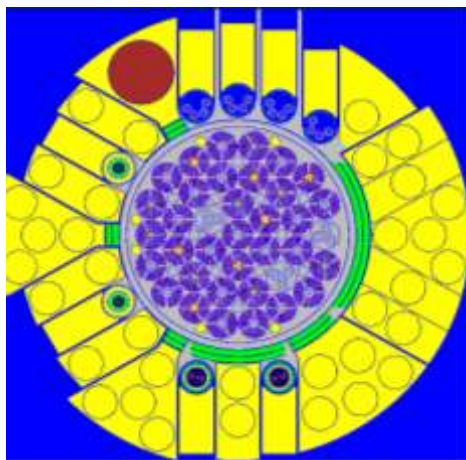
Due to varying usage and demands from the experimental facilities, it may be possible to increase the thermalisation of the flux in the JHR core, in order to increase the duration of the operating cycle and thus reduce the costs of fuel. Currently in the absence of in-core experimental facilities, the in-core positions are designated to be filled with aluminium rods. This paper presents a neutronics study which was performed to analyse the effect of replacing these aluminium rods with beryllium rods or water. This study considers the reactivity impact, as well as the resulting changes to the power profile of the JHR core and the performance of the experimental facilities.

2. Concept and Geometry

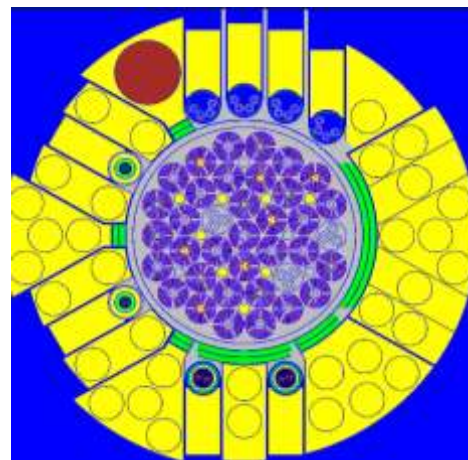
There are four groups of irradiation positions within the JHR rack where beryllium or water can replace aluminium rods (yellow spots in fig. 1):

1. 6 outer periphery positions located in the core rack between the outer ring of fuel assemblies and the reflector, with a diameter of 2.9 cm (fig. 1a).
2. 8 inter assembly positions, with a diameter of 3.0 cm (fig. 1b).
3. 7 positions located at the centre of fuel assemblies, with a diameter of 3.2 cm (fig. 1c).
4. 3 positions for large diameter experimental devices, located in fuel assembly positions, with a diameter of 8.6 cm (fig. 1d).

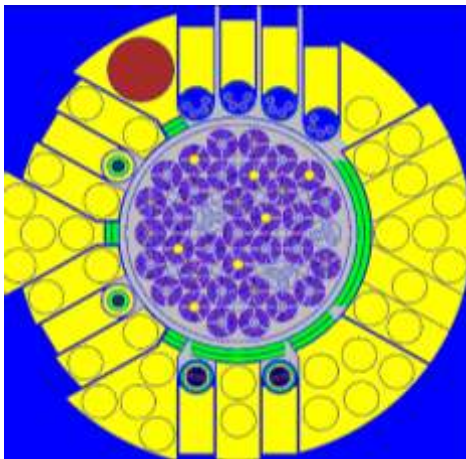
For each group, beryllium or water volumes were modelled at every position along the active length of the core (60 cm).



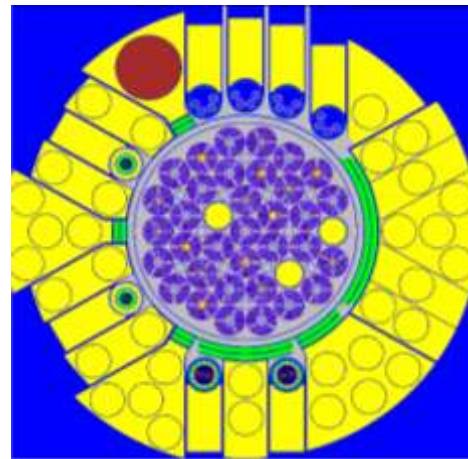
(a) Outer-periphery positions



(b) Inter-assembly positions



(c) Central fuel assembly positions



(d) Fuel assembly positions

Fig. 1 : Available irradiation positions within the core rack, highlighted in yellow

3. Methodology

The reactivity effects and flux distributions were evaluated using a full core model of JHR. The neutronics calculations were performed using TRIPOLI-4, version 4.7 [2], which is a three dimensional particle transport code, which solves the neutron transport equation using the Monte-Carlo method. TRIPOLI-4 calculations were performed using the CEAV5 library, which is based on JEFF-3.1.1 cross sections [3].

The addition of neutron moderating volumes in the core alters the power distribution in the core, at times creating localized areas of high power. One criterion to assess the viability of the core optimisation configurations is to compare the power distributions, normalised over the volume of each plate with thermal hydraulics limits.

The normalized average plate power density (N_i) is related to the volume of the plate (V_i) as follows:

$$\sum(N_i \cdot V_i) / \sum V_i = 1$$

The actual power from the plate (P_i) is obtained by the following equation:

$$P_i = N_i \cdot P_{\text{tot}} \cdot (V_i / \sum V_i)$$

where P_{tot} is the total power of the core. The normalized average power density limit in a plate is 1.88.

4. Results and discussion

Position	Material	$\Delta\rho$ (pcm)	Equivalent 100 MW days	Max. Av. Normalised Plate Power Density
Outer periphery	Be	249	1.1	1.51
Inter assembly	Be	836	3.8	1.61
Central fuel assembly	Be	672	3.1	1.50
Fuel assembly	Be	1901	8.6	1.88
Outer periphery	H ₂ O	61	0.3	1.51
Inter assembly	H ₂ O	824	3.7	1.73
Central fuel assembly	H ₂ O	883	4.0	1.82
Fuel assembly	H ₂ O	-996	-4.5	2.00

Table 1: Reactivity difference and normalised plate power density of Be and H₂O configurations in core rack

As seen in Table 1, there are six viable core configurations which increase the reactivity of the core, with power densities within the limiting value. Be in the outer periphery, inter assembly and central assembly positions result in reactivity changes ($\Delta\rho$) equivalent to gaining 1.1 (249 pcm), 3.8 (836 pcm) and 3.1 days (672 pcm) of 100 MW operation, respectively. The reactivity gain of H₂O in the inter assembly and central assembly positions are similar to Be, with 3.7 days (824 pcm) and 4.0 days (883 pcm) of 100 MW operation, respectively. H₂O in the outer periphery positions contributes only 0.3 days of 100 MW operation (61 pcm), significantly smaller than the impact of Be.

Apart from the central assembly position, the addition of Be in the core results in a higher increase in reactivity than the addition of the equivalent volume of H₂O. This is attributed to the higher thermal neutron absorption cross section of H₂O. The significance of this effect is observed with the large decrease in reactivity when H₂O is placed in the fuel assembly positions.

Considering the power distribution criterion, the additional moderation in the core causes the thermal flux, and hence fission rate, to be skewed towards the fuel plates surrounding the additional moderation in the core. The H₂O and Be in the fuel assembly positions were found to have large power hot spots which exceed the limiting value. In addition, H₂O in the central fuel assembly positions causes power hot spots at the fuel plates in the centres of the fuel assemblies where the water is located (fig. 2b), with the maximum plate power density of this configuration close to the thermal hydraulic limit.

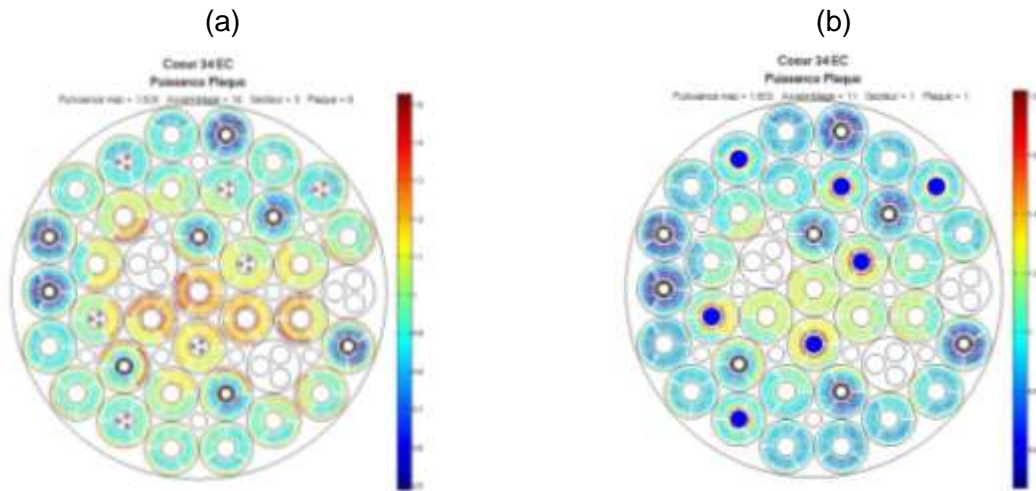


Fig. 2 : Power distributions of (a) the reference core, and (b) core containing water in the central fuel assembly positions.

The Be and H₂O core configurations result in lower performances of the in-core facilities due to reduced fast flux in the core, as well as a lower flux at the reflector devices because of a shifted thermal flux distribution which peaks closer to the centre of the core. For the reflector devices, the impact of the core thermalisation is a reduction in power by up to 7.5%. For the in-core CALIPSO device, the presence of H₂O and Be in the outer periphery and inter-assembly positions reduces the fast flux by up to 3.5%.

Optimisation of fuel assembly positions

Table 1 shows that H₂O in the fuel assembly positions results in a large, negative $\Delta\rho$, however, for smaller sized H₂O volumes positioned in the JHR core, the $\Delta\rho$ is positive. An analysis was performed to optimise the radius of the H₂O volume in the fuel assembly position in order to obtain a reactivity gain with small normalized plate powers, as obtained for the other small radii H₂O core configurations. In this configuration, the remainder of the fuel assembly position is filled with aluminium.

The results of the sensitivity analysis show that the negative reactivity worth of the water volume becomes smaller as the radius of the water volume decreases (fig. 3). However, a reactivity gain was never attained for the water volumes in the fuel assembly positions. The smallest reactivity loss (10 pcm) was obtained with a water radius of 16mm.

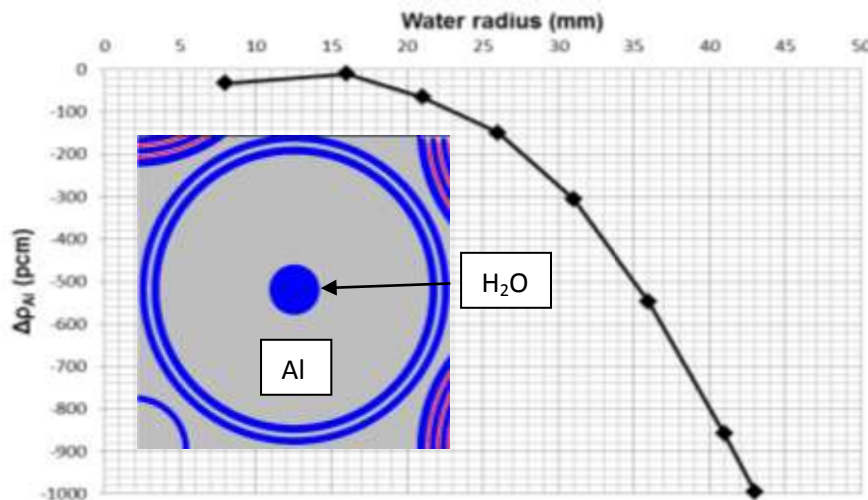


Fig. 3: $\Delta\rho$ as a function of the radius of the water volume in the fuel assembly position.

Optimisation of central assembly positions

The study of H₂O in the central assembly position showed an increase in reactivity of 883 pcm, however, with a high maximum normalised plate power density of 1.82 (fig. 2b). An optimisation study was performed to find the ideal width of water in the central assembly position, which maximises reactivity gain and while having a lower power density. This was performed by introducing aluminium cylinders of varying radii in the central assembly position. The initial study of H₂O in the central assembly position corresponds to a case without an Al cylinder (Al radius of 0 mm and water width of 18.5 mm).

The results displayed in fig. 4 show that the largest reactivity gain is achieved with the initial study of H₂O occupying the entire central assembly position, without an Al cylinder. This result is similar to the optimisation study of the fuel assembly positions, which found the smallest reactivity loss with a water radius of 16 mm. The reactivity effect and maximum plate power decreases with decreasing water width (and increasing Al cylinder radius). Thus, it is possible to gain reactivity equivalent to 2 to 3 days at 100 MW, while limiting the power hot spots in the core.

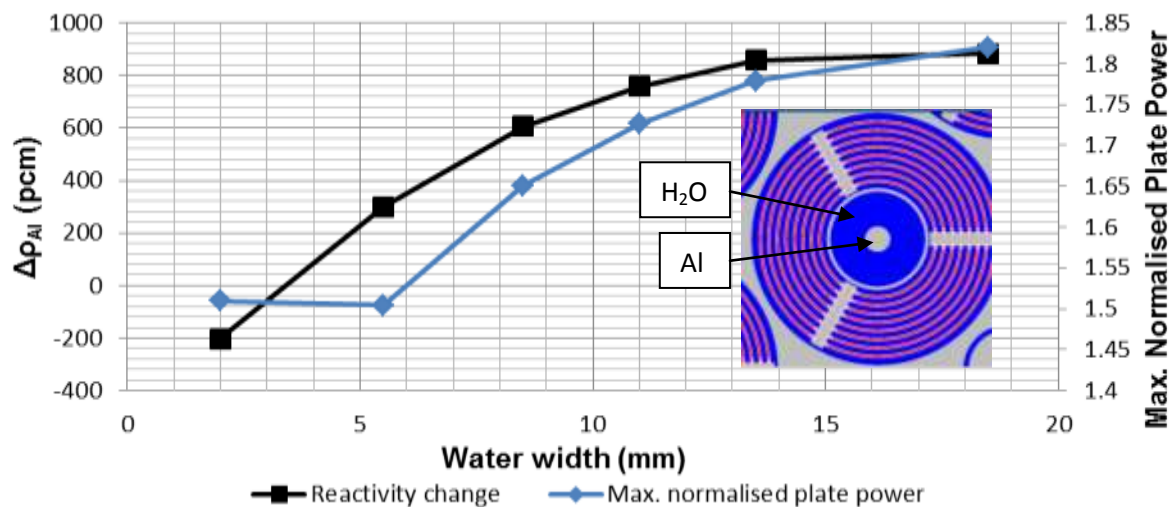


Fig 4: $\Delta\rho$ as a function of the width of water in the central fuel assembly position.

5. Conclusion

This preliminary study of JHR core optimisation shows that Be and H₂O volumes in potentially vacant positions in the outer periphery, inter assembly and central assembly positions of the core rack result in positive reactivity changes. For Be, this is equivalent to gaining 1.1, 3.8 and 3.1 days of 100 MW operation, respectively. For H₂O in these positions, the reactivity gain is 0.3 days, 3.7 and 4.0 days of 100 MW operation. These core configurations meet the requirements for maximum normalised fuel plate and fuel assembly power, while slightly reducing the performance of the experimental facilities in the core and reflector. Additional studies will be pursued to further optimise the core with various combinations of water volumes in the vacant positions of JHR.

6. References

- 1) RRFM meeting 2010, Marrakech, 21-25 March 2010, "The Jules Horowitz Reactor Project: A new Material Testing Reactor working as an international user-facility for the improvement of scientific skills within nuclear R&D"
Daniel Iracane, Patrick Lemoine, Christian Gonnier, Gilles Bignan, French Atomic Energy Commission /Nuclear Energy Directorate.
- 2) O. PETIT et al.,
TRIPOLI-4 User Guide, ISSN 0429-3460, January 2008
- 3) C. JOUANNE
Rapport Technique DEN/DANS/DM2S/SERMA/LLPR/RT/10-4933/A
Notice d'identification de la bibliothèque CEAV5 pour TRIPOLI-4.7

USE OF MONTE-CARLO CODE MORET 5 FOR RESEARCH REACTOR SAFETY ANALYSIS

Y. CHEGRANI, V.TIBERI, L. HEULERS

*Institut de Radioprotection et de Sûreté Nucléaire
B.P. 17, 92262 Fontenay-aux-Roses, France*

E-mail of the corresponding author: yacine.chegrani@irsn.fr

ABSTRACT

This paper presents the use of the IRSN developed continuous-energy Monte Carlo code MORET 5 [1] in French research reactor safety assessment. Three research reactor configurations have been studied. Two of these cases – ORPHEE and Jules Horowitz reactors (JHR) - focused on the assessment of accidental reactivity insertions involved in the analysis of BORAX-type accident (BORAX [2] is an accidental transient due to a reactivity rush leading to a core melting and a steam explosion). ORPHEE study consisted in re-evaluating the worth of reactivity insertions caused by the neutron beam channels ruptures. The purpose of JHR study was to evaluate the worth of the reactivity insertion due to a control rod ejection. Both these results were widely used to direct the conclusions of the safety assessment. Basic calculations with MORET 5 allow obtaining k_{eff} evaluations for each configuration. But in order to fully extend the capabilities of this code to answer reactor safety specific issues, some developments have been performed in the 5.A.1 version of the MORET code. Thus, this version allows computing kinetic parameters, essential to the understanding of the reactivity accident progress. In order to validate this new functionality in MORET 5.A.1, the last chosen research reactor case deals with the validation of kinetic parameters models against measurements on the Brazilian reactor IPEN. The results obtained on IPEN allowed highlighting the needed improvements to increase the accuracy of kinetic parameters computation, in particular to better assess the power transient in the core. These calculations confirmed that MORET 5 is a convenient and reliable tool for the neutronic safety analysis of research reactors.

1. Introduction

The Institut de Radioprotection et de Sûreté Nucléaire (IRSN) is the French Technical Support Organisation to the Nuclear Safety Authority. As such, one of its missions is to lead the safety analyses on all national nuclear facilities. This activity may require the use of computation codes to assess the robustness of the safety demonstration, especially the core behaviour. Throughout the evolution of nuclear technology, the effort on simulation tools development was focused on standard nuclear power plants (the codes were mainly supported by the applicants). Thus, neutronic deterministic tools were adapted to standard PWR geometries and benefit from the tremendous amount of operational feedback for calibration, to balance the simplifications in cross section libraries and physical representation. On the other hand, research and experimental reactors have the particularity of being unique objects, geometrically and chemically, which often makes the use of industrial PWR oriented tools un-practical. This is why IRSN uses the home-made, criticality oriented, point-wise Monte Carlo code MORET 5 and started developments to extend its application to reactor physics. The assets of such a code are numerous: both chemistry and geometry can be defined without any simplification in order to have a realistic modelization, input decks benefits from an easy writing syntax, output capabilities of the code allow to obtain information in every part of the geometry.

2. MORET 5

MORET code has been developed since the early seventies. Since the MORET 4 version, the code is a main component of the French well-known criticality package CRISTAL used by

the major actors of the French nuclear industry. Before the release of the 5th version of the code, MORET needed to be coupled with a cell code (like APOLLO2, DRAGON or SCALE) that provides multi-group libraries or to use the old Hansen and Roach cross sections (16 energy groups binning). The point-wise root has been implemented in the MORET 5.A.1 version from 2007[1]. This version benefits also from various improvements increasing the flexibility and improving the handling of very complex geometries useful for reactor modelling. MORET 5 offers a very straightforward description of the geometries, based on a combination of simple volumes (prisms, cylinders, spheres, cones combined in usual logical operations) allowing geometric revolution and rotation, and of chemical media, with the ability to select isotopes information from various nuclear data evaluations (JEFF-3, ENDFB VI ...).

Besides, MORET includes the following five simulation methods in addition to the natural simulation method: Stratified, MKIJ, Importance, Super-History and Wielandt. Then, when using the natural, Super-History and Wielandt methods, the MORET code enables the use of an alternative to the conventional simulation of the neutron paths (the Woodcock tracking method), which improves the computation time for heterogeneous systems containing a large number of volumes. This wide variety of simulation methods offers users, including design engineers, experts and researchers, the possibility of comparing results and making a better assessment of the configurations being studied.

More recently, kinetic parameters estimators have been implemented into MORET 5 along with powerful output capabilities based on SCORE definition that give users flexibility and a wide possibilities in the results analysis. Also, tests have been added to help users to determine the keff-stationnarity and to determine the initial transient suppression ([1] and [3]).

This overall flexibility of the code fills another specific need. Indeed, in addition to providing an independent tool for safety assessments, it enables to carry out sensitivity studies to investigate any relevant parameters, by making the edition of input data (geometry, materials, chemistry, tallies etc.) easier. This way, for instance, the bias induced by a certain library or specific isotopes, or the difference between two core layouts can be evaluated. The whole validation of these developments is reaching its final stage. However, MORET 5.A has already been used to support, in addition to the use of other Monte Carlo codes, two reactor safety analyses on JHR and ORPHEE. The use of a zero-power reactor benchmark from the IRPHEE handbook served as an intermediate validation point through the optimisation of the kinetic parameters calculation.

3. Cases of application

3.1 ORPHEE core analysis

This first analysis has been carried out in the frame of the second decennial safety review of ORPHEE research reactor, located near Paris. It is a 14MW neutron source reactor composed of nine HEU-Aluminium fuel plates cooled in light water, internally reflected by a beryllium bloc and surrounded by a heavy water tank. The external reflector is equipped with nine neutron channel beams, two cold sources and one hot source. The design of this reactor is complex, considering the intricate geometry and the chemical diversity of its components.

Neutronic calculations have been carried out during the design phase (70's) with a two-group diffusion code and have not been updated since. The safety report and the section related to the accidental reactivity insertions in particular, referred to those out-dated values concerning the reactivity worth of the neutron beam channels.

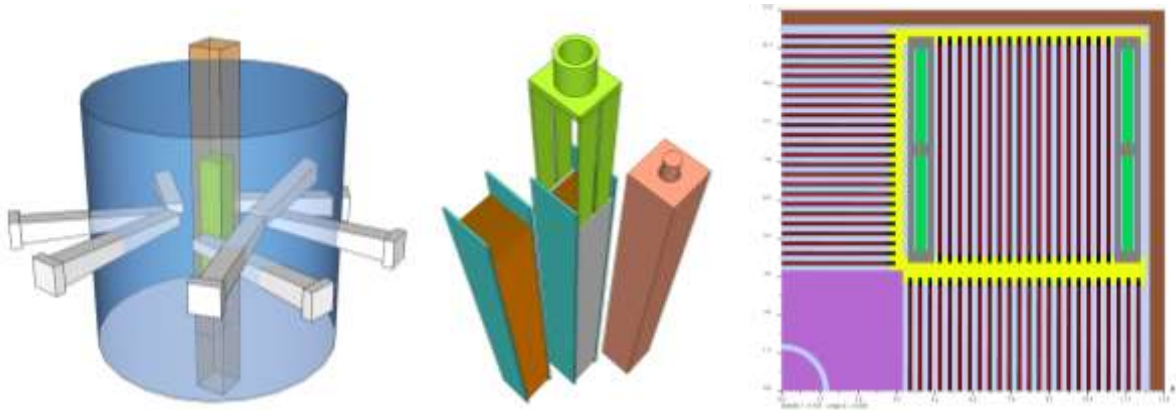


Figure 1: Representations of ORPHEE. Reactor (left), 3 unique subassemblies (middle), MORET 2D visualisation of 1/4 core (right)

The safety assessment carried out by IRSN required calculations, which were performed with MORET 5. The reactor has been fully and easily represented by creating reference modules and instantiating them to reproduce the core (Figure 1). First, the model of the reactor was validated by achieving excellent results in comparing the MORET 5 calculated critical height of the control blades against operation data. MORET 5 was proven fit to accurately describe this type of cores. The investigation of the reactivity worth of the channels was then carried out by simulating the postulated step-wise reactivity insertion, as shown on the schematics below (Figure 2).

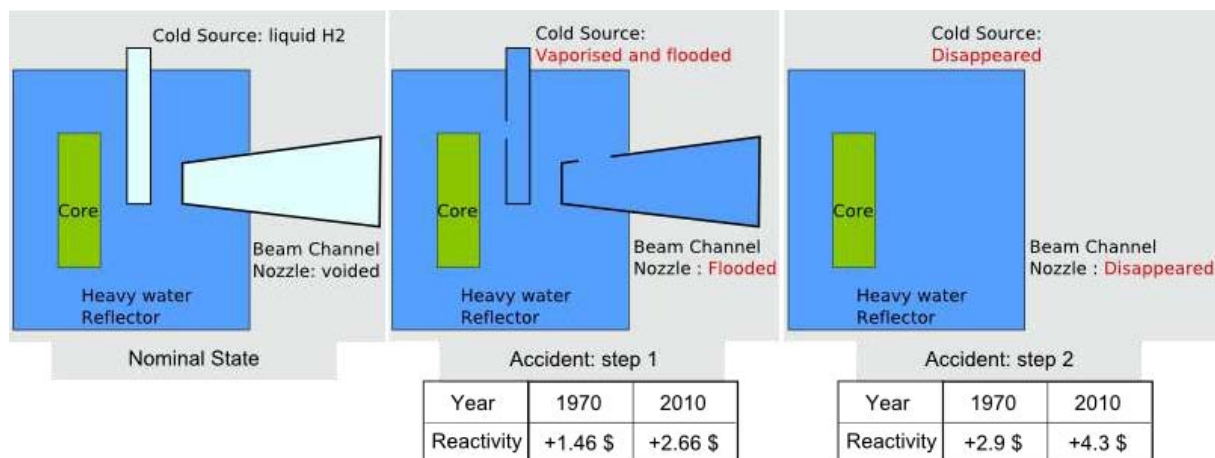


Figure 2: diagram of reactivity insertion scenario in ORPHEE and relative reactivity calculations during design phase (1970) and with MORET 5 (2010)

The tables above demonstrate that the reactivity worth of the BORAX initiator were largely under-estimated during the design phase. The use of a 3D precise modelling tool and up-to-date nuclear data enabled highlighting this discrepancy, and improving the safety level of this facility by advocating increased examination frequency in order to reduce the risk of fault appearance.

3.2 JHR core analysis

The Jules Horowitz Reactor is a Material Testing Reactor currently in commissioning in southern France. Recently, neutronic studies have been carried out by the applicant in the frame of the BORAX accident, in order to evaluate the worth of the reactor control rods, which ejection is the accident initiator, and to present a reference design value for the safety report. The results were obtained via a deterministic code (APOLLO2-CRONOS), using cell-

averaged cross sections condensed from a custom-made multi-group library, in a simplified core layout.

Part of IRSN assessment was the analysis of the conservatism of the provided value considering the calculation methodology implemented by the applicant. The relevant parameters that can influence the result of such calculation have been identified in order to be investigated through sensitivity studies:

- The cross section libraries
- The core configuration (geometry, fuel age, control rod positions)

Once again, the complexity of the core design (subassemblies, experimental positions and layout) was easily handled thanks to the modular capabilities of MORET 5 (Figure 3). The user friendly syntax also enabled to vary cross-section libraries separately for each isotope. These capabilities joined with the GUI platform “Promethee” [8] enables to launch multiple parametric calculations in a single run.

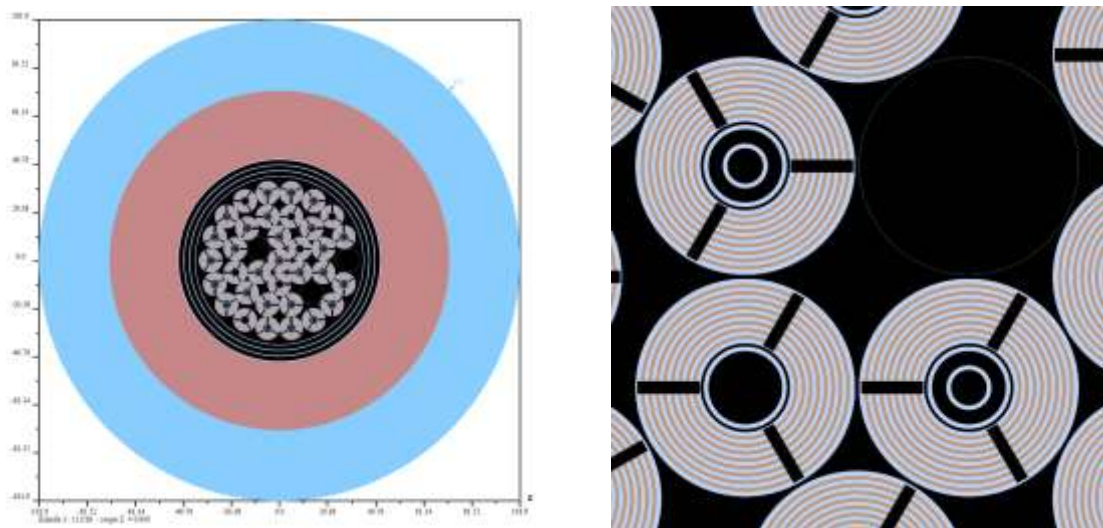


Figure 3: JHR representation in MORET 5: whole core (left), zoom on subassemblies (right)

Calculations performed with MORET 5 on the reference configuration provided by the applicant lead to comparable results regarding the heaviest control rod (2000 pcm).

Results on a configuration very similar (geometry and chemical composition) to the one used by the applicant were shown to be very sensitive to the aluminium cross section. The use of ENDF-B-VII and JEFF3.1 libraries lead to 700 pcm discrepancy on the k_{eff} of which 62% are due to the Aluminium27. The second part of the sensitivity study consisted in verifying the conservatism of the reference core configuration by seeking a more pessimistic one in terms of control rod worth. While keeping the core critical, calculations were carried out to test configurations that could potentially be more pessimistic. For all but one tested core layouts, the heaviest control rod worth was inferior to the value provided by the applicant for the reference configuration. The one layout that led to a higher control rod worth (2700 pcm) was notified to the applicant as to be avoided during reactor operation.

3.3 IPEN/MB-01 experimental benchmark

This third example of IRSN's use of MORET 5 aimed at testing a kinetic parameter calculation model under development [2]. Kinetic parameters calculations (effective delayed neutron fraction, β_{eff} , and effective prompt neutron lifetime, Λ_{eff}) require the knowledge of the adjoint flux and the delayed neutron spectrum.

Two versions of the code (here named 5.A and 5.B) have been used to evaluate the effect of one particular modification to the delayed neutron spectrum. The adjoint flux is approximated in both versions (ref) by the following function:

$$\Phi^*(r, E, \Omega) = \begin{cases} \nu_f \text{ (mean number of neutrons per fission)} & \text{if there is fission} \\ 0 & \text{if there is no fission} \end{cases}$$

In version 5.A, prompt and delayed neutron spectra are identical whereas in version 5.B all delayed neutrons are generated with 0.5MeV of energy. In MORET 5, kinetic parameters are calculated inline and provided as a standard result, along with the k_{eff} .

This particular IRPHE [5] benchmark has been selected because of the accuracy and reliability of the experimental method used to measure kinetic parameters. The results were obtained through a Macroscopic/Microscopic noise method. IPEN/MB-01 is a zero-power reactor located in Brazil, composed of 680 LEU oxide fuel pins and 48 control rods in a square lattice. The layout of the reactor is fairly simple, which made its description in MORET 5 an easy task thanks to the network grid capabilities.

The MORET 5 model of this reactor has been validated by comparing the calculated critical heights with experimental data. The same task was performed in parallel with MCNP5 as a reference Monte Carlo code. MCNP was also used to compute the kinetic parameters via an application of the perturbation theory [6].

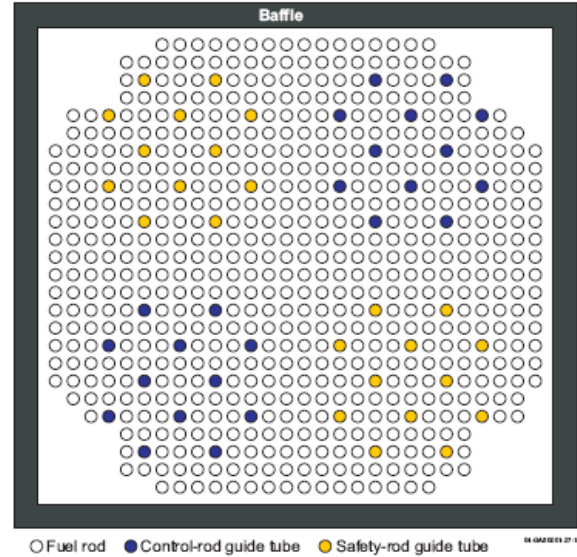


Figure 4: core layout of IPEN as presented in Benchmark

	Experiment	MORET 5.A.1	Δ_{exp}	MORET 5.B.1	Δ_{exp}	MCNP5	Δ_{exp}
$\Lambda_{\text{eff}} (\mu\text{s})$	31.96 ± 1.06	34.73 ± 0.02	8.7%	34.6 ± 0.02	8.3%	32.31 ± 6.2	-1.1%
$\beta_{\text{eff}} (\text{pcm})$	750 ± 5	689 ± 3.5	-8%	745 ± 3.3	-0.6%	776 ± 31	3.5%

Table 1: comparative results of kinetic parameters calculations

The results obtained (Table 1) demonstrate that the reference MCNP calculation is accurate, although the uncertainties are higher. Regarding MORET results, there is a noticeable improvement in the β_{eff} calculation thanks to the modification of the delayed neutron spectrum. However, the results of Λ_{eff} calculation are not influenced by this modification. This is due to the fact that Λ_{eff} is not a function of the delayed neutron spectrum.

From the safety point of view, this study leads to consider that the method of kinetic parameters estimation implemented in MORET 5 is suited for the analysis of experimental reactors. However, developments are under way to take into account a proper delayed neutron spectrum and a better estimation of the adjoint flux, which can also influence the β_{eff} . For the time being, this level of accuracy is a solid basis towards improvements of the models.

4. Conclusions

The Monte Carlo MORET 5 code, developed by IRSN and originally dedicated to criticality, has been chosen to perform neutronics calculations in support to the safety analysis in research and experimental reactors physics. The developments performed in the last version of the code (MORET 5.A and soon MORET 5.B) extend its capabilities from criticality studies to reactor cases. The current status of the code already enables to simulate very complex geometries and reactor materials, and to study variations of several parameters (including bias calculations).

Other applications are carried out in order to develop and optimize new outputs, such as the power distribution calculations. It is currently possible to calculate power distribution, but it implies post-processing raw data (reaction rates in separate volumes etc.) and externally reconstructing the core layout, which is source of error. Work is underway to implement a proper and definite method to be able to include the power distribution in the standard output for the next versions of the code (MORET 5.B probably).

5. References

- [1] *MORET 5 – Overview of the new capabilities implemented in the multigroupe/continuous-energy version*, ICNCN 2011, Loïc Heulers & al.
- [2] IRSN guidelines document: http://www.irsn.fr/FR/Larecherche/publications-documentation/collection-ouvrages-IRSN/Documents/BORAX_texte_VA_290811.pdf
- [3] *Calculating the kinetic parameters in the continuous energy Monte Carlo code MORET*, A. Jinaphanh & al.
- [4] Initial transient suppression in Monte Carlo Criticality calculations using statistics based on keff or Shannon entropy, Physor 2012, A. Jinaphanh & al.
- [5] *NEA-1765/05: International Handbook of Evaluated Reactor Physics Benchmark Experiments, Chapitre LWR/Réacteur IPEN/MB-01*, NEA/NSC/DOC (2006)1, March 2009 Edition (OECD/NEA)
- [6] *Monte Carlo calculation of the effective neutron generation time*, B. Verboomen, W. Haeck, P. Baeten, , Annals of Nuclear Energy 33 (2006) 911-916
- [7] *MCNP5 delayed neutron fraction (β_{eff}) calculation in training reactor VR-1*, Svetozar Michalek, Jan Hascek, Gabriel Farkas
- [8] <http://promethee.irsn.org/doku.php>



Wednesday 21 March
2012

IN-PILE CALORIMETRY: A THERMAL POINT OF VIEW.

C. REYNARD-CARETTE, J. BRUN, M. CARETTE, M. MURAGLIA, A. JANULYTE,
Y. ZEREGA, J. ANDRE.

*Aix-Marseille Univ, LISA, équipe IPCN, Centre St Jérôme, Avenue Escadrille Normandie-Niemen,
bâtiment MADIREL, 13397 MARSEILLE cedex 20, France*

A. LYOUSSI, G. BIGNAN, J-P. CHAUVIN, D. FOURMENTEL, C. GONNIER, P.
GUIMBAL, J-Y.MALO, J-F. VILLARD.

*Commissariat à l'Énergie Atomique et aux Énergies Alternatives
CEA Direction de l'Énergie Nucléaire, Centre de Cadarache
13108 Saint-Paul-Lez-Durance, France.*

E-mail: christelle.carette@univ-amu.fr

Keywords: Calorimetry, Heat Transfer, In-pile Instrumentation.

ABSTRACT

This paper focuses on the in-pile calorimetric method used to quantify the heating due to radiation energy deposit. A discussion of thermal aspects associated to this method is developed by considering a brief state of the art. The different thermal modes (adiabatic-isothermal, simply adiabatic, isoperibol ...) of calorimeters are presented. Calorimetric configurations tested in research reactors are shown. The calibration procedure performed under non irradiation conditions and under irradiation conditions is summarized. The approaches used to determine the response of the calorimeter and its thermal behaviour are discussed.

1. Introduction

Nuclear heating represents a key parameter in the nuclear field. It is involved at different steps in the design of various cooling systems dedicated to evacuate the thermal energy induced by the nuclear reactions and transferred to the irradiated materials:

- before the construction of nuclear plants or research reactors in order to satisfy safety and radioprotection requirements [1],
- during irradiations in order to impose specific wanted thermal hydraulic conditions inside the in-pile experimental channels of research reactors to better understanding phenomena during accelerated ageing of materials or fuel irradiations [2],
- after irradiations in order to take into account residual power for spent fuel storage, transportation, reprocessing [3].

The occurrence of this parameter is due to several complex photon and neutron interactions with matter (fission, capture, elastic and inelastic scattering, nucleus recoil, slowing down of charged particles, ...) which depend especially on the nature, geometry, density, and composition of the matter, on the neutron and photon energy spectra, on the temperature and on the sample size [4]. The comparison between numerical and experimental results indicates that this parameter is in general numerically underestimated [5]. For instance, F. Malouch showed that the discrepancy between calculations by a TRIPOLI-4 3D Monte Carlo Code and measurements by calorimetry is about -15% at the OSIRIS core mid-plane and about -20% to -25% at the edges [6]. Consequently, an accurate prediction of this parameter is still difficult and the improvement of its determination is needed. Then, numerical models require in particular better nuclear data (neutron flux, photon flux, spectra, cross section data) and new experiments testing several material samples are necessary. Thus, at present online measurements during irradiations in MTRs are developed to obtain accurate experimental conditions inside the experimental channels. For instance a new experimental mobile device, called CARMEN, designed in the framework of the IN-CORE program [7], will be used to the online mapping of the experimental conditions inside the core and reflector channels at the start-up of the JHR reactor. This device will couple several sensors in two mock-ups dedicated respectively to neutron and photon measurements [8-9]. The nuclear

heating will be quantified by means of a permanent differential calorimeter and a gamma thermometer. A thermal approach is carried out under non irradiation conditions. Studies of calorimetric cells are performed for different thermal hydraulic conditions in order to better understanding the thermal behaviour of the sensor and to improve its characteristics. Numerical and experimental tools were and are developed [10-14]. This paper discusses the in-pile calorimetric method according to thermal aspects.

2. Calorimetry

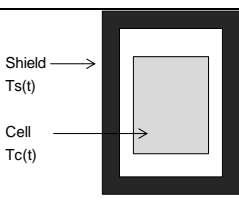
2.2 Thermal modes

A calorimeter is an instrument dedicated to determine heat in various scientific fields: for example heat generated by reactions, transformations.

For the nuclear field, Gunn divided this method into four categories according to its application [14-16]. The first category corresponds to the radionuclide calorimeters which include radioactive source, are used for the investigation of several parameters: activity (disintegrations per unit time), half-life, or disintegration or residual power. The second one and the third one are associated to external sources. They are used as reference measurement methods to calibrate other sensors. The last one corresponds to the in-reactor (or in-pile) calorimeters. This calorimeter category is devoted to the studies of the nuclear energy transferred to specific samples during in-pile experiments for engineering purposes of structural materials or for measurements of local experimental operating conditions.

In general a calorimeter is divided into two parts (cf. Table 1) [18]. The first part corresponds to a calorimetric vessel/cell which includes the sample and the associated instrumentation. The instrumentation is mainly reduced to thermocouples to quantify the transferred nuclear energy by means of a temperature difference measurement and to subsidiary elements to calibrate the sensor such as resistive heaters. The second part is the calorimetric shield/jacket.

Two groups of calorimeters exist and depend on a specific thermal aspect: the heat exchanges with its surroundings. These exchanges can be determined by the value of the temperature gradient between the cell and the shield. When the gradient is equal to zero, the calorimeter is an adiabatic calorimeter. In that case, heat transfer does not occur between the calorimetric cell and the shield. When the temperature gradient is different from zero, heat transfer exists and the calorimeter is called non isothermal calorimeter or heat flow calorimeter. Furthermore, each calorimeter group can be divided according to the stationary state of the shield temperature ($T_s(t)$). The table 1 summarizes the calorimeter classification.

Diagram	Gradient condition	Group	Temperature conditions	Classification
	$\nabla T = 0$	Adiabatic	$dT_s/dt = 0$	Adiabatic-isothermal
			$dT_s/dt \neq 0$	Adiabatic-nonisothermal or simply adiabatic
	$\nabla T \neq 0$	Non isothermal	$dT_s/dt = 0$	Isoperibol
			$dT_s/dt = 0$ and $dT_c/dt = 0$	Permanent
			$dT_s/dt \neq 0$	Scanning

Tab1: Calorimeter classifications

In-pile calorimeters correspond mainly to a permanent non isothermal calorimeter. This is due to two main reasons. Firstly, an adiabatic calorimeter requires a very high thermal insulation to eliminate heat exchanges with its surroundings. This can be realized by means of vacuum loop, various shields, and heat loss compensation system. Then contrary to a simply adiabatic one which accumulates energy (continuously sample temperature increasing), the permanent non isothermal calorimeter can remain in the experimental channel to perform continuously measurements.

2.2 Geometry configurations

At present, two kinds of calorimetric configurations for in-pile measurements exist: a single calorimeter and a differential calorimeter. The single calorimeter consists of one cell [1, 2, 4] containing a sample such as stainless steel, molybdenum, aluminum or iron.

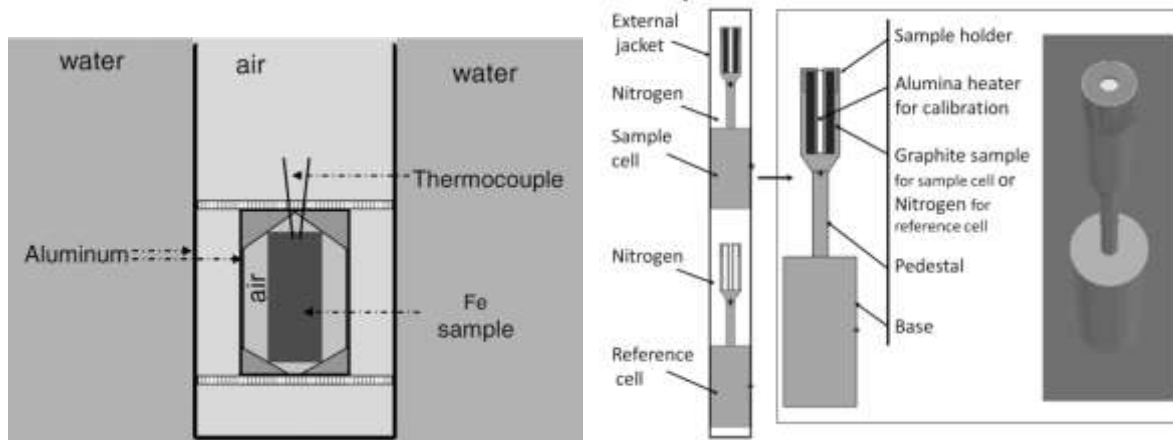


Fig2: Two examples of calorimeter: single calorimeter [4] (on the left), and differential calorimeter (on the right) [10].

A differential calorimeter has at least two identical cells located in a common jacket. Some cells contain samples (graphite). The others are empty and are used as reference to avoid thermal disturbances due to nuclear flux gradients and to remove the nuclear energy transferred on the cell structure. In the OSIRIS reactor Malouch used a calorimeter with four juxtaposed cells [6] while Carcreff tested a calorimeter with a two superposed cells [19]. The drawback of this superposed configuration is the associated operating protocol. In fact, to quantify nuclear heating at a specific location in an experimental channel, the calorimeter has to be moved to put the reference cell at the same previous location of the sample cell. This displacement allows the elimination of the influence of the vertical nuclear flux gradient.

2.3 Thermal calibration

The in-pile calorimeters are often calibrated out-pile. The calibration consists of simulating nuclear energy by injecting heat into the sample by Joule effect [1, 10, 14, 20].

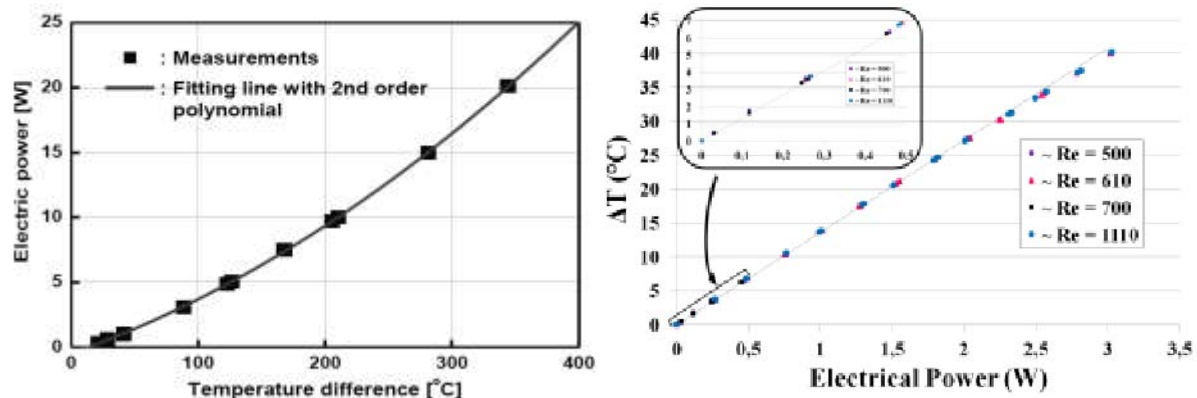


Fig1: Two examples of calibration curve: single calorimeter for an electrical power from 0W to 20 W [1] (on the left), differential calorimeter for a lower power < 3.1 W (on the right) [14].

This method is used even if the out-pile energy deposit shape (in volume) does not correspond to the in-pile one (in surface) and even if the energy deposit is located only into the sample. The calibration curve obtained under non irradiation conditions has to be corrected for in-pile measurements according to the nuclear heating level inside the experimental channel to take into account the thermal radiative mode which becomes non-negligible [19]. The heat losses increase and the linearity of the sensor response is lost [4]. At present a new experimental set-up called BETHY is designed in the frame of the IN-

CORE program in order to study the response of an instrumented calorimeter [14] (sensitivity, temperature field, heat flux/heat losses, transfer coefficient,...) under non irradiation conditions versus various thermal and hydraulic parameters (temperature gradient, flow regime, heating) reproducing specific JHR experimental channel characteristics.

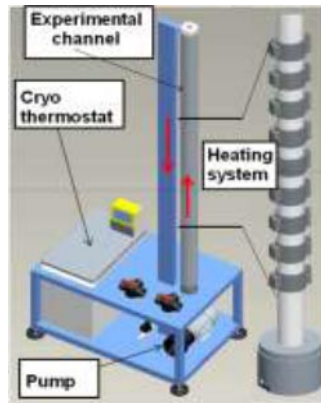


Fig2: Diagram of the thermal hydraulic testing set-up called BETHY.

3. Thermal calorimeter behaviour

When a permanent single heat flow calorimeter has a relatively simple geometry with an isothermal sample surface and an isothermal external shield surface, the temperature field can be determined by a 1D thermal analytical approach [4, 13] and the determination of the thermal resistance between the sample and the shield can be used to define the sensor sensitivity. Whereas when the calorimeter geometry is more complex with specific boundary conditions, numerical and experimental works are needed to design the calorimeter.

The thermal calorimeter behavior can be studied numerically, by taking into account only the domain corresponding to the calorimeter cell and the calorimeter shield. The gas trapped in the calorimetric jacket can be considered static, thus the convective mode is neglected inside the calorimetric shield. Consequently, the thermal behavior is obtained by solving the classical heat energy law reduced to four terms (corresponding to the source, the accumulation, and the conductive and radiative transfers) [10]. In the case of calibration under non irradiation conditions, the source term is applied only on the heating element area. In the case of in-pile simulations, the source term is applied on the whole meshed domain and it has to integrate the nuclear flux profile and the material behavior versus neutron and gamma interactions [12]. The associated boundary conditions depend on the calorimetric mode. For a non isothermal calorimeter, the boundary conditions represent the convective heat exchanges between the calorimetric shield and its surroundings. The thermal exchange coefficient has to be used. This coefficient can be defined owing to thermal empirical laws (correlations) giving the Nusselt number versus the Reynolds number and the Prandtl number for a forced convective cooling flow for example. For a complex geometry, the computational domain needs to be meshed by finite elements for accurate results. Parametric studies can be conducted versus the nature of the cooling flow, the calorimeter geometry, the calorimeter size [11-12], the calorimeter materials and the calorimeter sample. The temperature field inside the sensor is analyzed to ensure safety configurations (no melting, no boiling on the external surface of the shield). Moreover the temperature field inside the sensor is studied to choose the thermocouple locations in order to have the better sensitivity. In the case of a permanent non isothermal differential calorimeter with a part of the calorimetric cell in contact with the calorimetric shield, the sensitivity depends on the heat flux density evacuated by the contact surface and on the thermal resistance. To improve the sensitivity, the heat losses have to be decreased [14]. For a low nuclear heating, the sensitivity can be increased by minimizing the conductivity of the gas [10].

4. Conclusions

Various calorimetric modes exist. However in the case of in-pile calorimeters, the permanent non isothermal mode is mainly achieved to quantify the nuclear energy transferred by the interactions between neutrons, radiations and material sample in research reactor experimental channels. Two geometric configurations of calorimetric cell are used. The sensor calibration can be performed out of pile. A large range of the imposed electrical power is required to obtain the most suitable calibration curve taking into account the radiative transfer otherwise a corrective term has to be applied. Complementary thermal studies have to be conducted in order to optimize the sensor characteristics.

5. Acknowledgements

The IN-CORE program and these analytical works are supported by FEDER, Conseil Régional PACA, and Ville de Marseille.

6. References

1. **Measurements of Nuclear Heating Rate and Neutron Flux in HANARO CN Hole for Designing the Moderator Cell of Cold Neutron Source**, M-S. Kim et al., Proceedings of IGORR 2005
2. **Simulation of the In-Core Calorimeter Experiment in the SAFARI-1 Reactor**, B.M Makgopa, M. Belal, ANIMMA International Conference, 7-10 June 2009, Marseille, France
3. **Merci-Mosaic: Experimental tools for residual power measurement in the Osiris reactor**, Ch. Blandin et al. IGORR 2009
4. **Evaluation of nuclear heating of small samples in a research reactor core**, M. Varvayanni, N. Catsaros, M. Antonopoulos-Domis, Annals of Nuclear Energy 35 (2008) 1414–1420.
5. **Qualification of a gamma-ray heating calculation scheme for the future Jules Horowitz material testing reactor (RJH)**, D. Blanchet et al., 2008. Ann. Nucl. Energy 35, 731–745.
6. **Development and Experimental Validation of a Calculation Scheme for Nuclear Heating Evaluation in the Core of the OSIRIS Material Testing Reactor**, F. Malouch, ISRD14, 22-27 May 2011
7. **In core Instrumentation for Online nuclear heating Measurements of Material Testing Reactor**, C. Reynard et al., RRFM Transactions 2010, Marrakech, Morocco.
8. **Combined analysis of neutron and photon flux measurements for the Jules Horowitz Reactor core mapping**, D. Fourmentel et al., ANIMMA 2011, June 2011, Gant, Belgium.
9. **Advanced methodology and instrumentation for accurate on line measurements of neutron, photon and nuclear heating parameters inside Jules Horowitz MTR Reactor**, A. Lyoussi et al., RRFM/ IGORR 2012, Prague, Czech Republic.
10. **Numerical and Experimental Calibration of a Calorimetric Sample Cell Dedicated to Nuclear Heating Measurements**, J. Brun et al., IEEE Transactions on Nuclear Science, publication accepted.
11. **Numerical study of heat transfer in a radiometric calorimeter dedicated to nuclear heating measurements**, C. Reynard-Carette et al., RRFM Transactions 2011, Rome, Italy.
12. **Numerical parametric study of heat transfer in a non adiabatic calorimeter without or with nuclear heating deposit**, O. Merroun et al., NURETH 2011, Toronto, Canada.
13. **Numerical study of the geometry impact on the heat transfer in a radiometric calorimeter dedicated to nuclear heating measurements**, M. Muraglia et al, RRFM Transactions 2012, Prague, Czech Republic.
14. **Heat transfer during out-pile calibration of a calorimeter used for nuclear heating measurements: influence of convective boundary conditions**, J. Brun et al., RRFM Transactions 2012, Prague, Czech Republic.
15. **Radiometric calorimetry: A review**, Gunn, S. (1964), NIM 29(1), 1-24.
16. **Radiometric calorimetry: A review 1970 supplement**, Gunn, S. (1970), NIM 85(2), 285 - 312.
17. **Radiometric calorimetry: A review: 1976 supplement**, Gunn, S. (1976), NIM 135(2), 251 - 265.
18. **Theory of calorimetry**, W. Zielenkiewicz and E. Margas, Kluwer Academic Publishers, 2004.
19. **Development, calibration and experimental results obtained with an innovative mobile calorimeter (CALMOS) for nuclear heating measurements**, H. Carcreff et al., ANIMMA 2011, June 2011, Gant, Belgium.
20. **CALMOS: Innovative Device for the Measurement of Nuclear Heating in Material Testing Reactors**, H. Carcreff, ISRD14, 2011, Omni Mount Washington Resort, USA

ADVANCED METHODOLOGY AND INSTRUMENTATION FOR ACCURATE ON LINE MEASUREMENTS OF NEUTRON, PHOTON AND NUCLEAR HEATING PARAMETERS INSIDE JULES HOROWITZ MTR REACTOR

A. LYOUSSI, D. FOURMENTEL, J-F. VILLARD, J-Y.MALO, P. GUIMBAL,
H. CARCREFF*, C. GONNIER, G. BIGNAN, J-P. CHAUVIN
*French Alternative Energies and Atomic Energy Commission: CEA
Nuclear Energy Division*

*CEA/DEN/CAD/DER, Centre of Cadarache, 13108 Saint-Paul-Lez-Durance, France
(*)DEN/DANS/DRSN/SIREN, Centre of Saclay. 91191, Gif-Sur-Yvette, France*

C. REYNARD-CARETTE, J. BRUN, O. MERROUN, M. CARETTE, M. MURAGLIA,
A. JANULYTE, Y. ZEREGA, J. ANDRE
Aix-Marseille Univ, LISA, équipe IPCN, Centre de Saint Jérôme,
Avenue Escadrille Normandie-Niemen bât. Madirel, 13397 Marseille Cedex 20, France

E-mail: abdallah.lyoussi@cea.fr

Keywords: Instrumentation, measurement, neutron, photon, nuclear heating, MTR

ABSTRACT

Research and development on fuel and material behaviour under irradiation is a key issue for sustainable nuclear energy in order to meet specific needs by keeping the best level of safety. These needs mainly deal with a constant improvement of performances and safety in view to optimize the fuel cycle and hence to reach nuclear energy sustainable objectives.

The new Material Testing Reactor -MTR- JHR (Jules Horowitz Reactor) currently under construction at CEA Cadarache research centre in France will offer a real opportunity to perform R&D programs regarding needs above and hence will crucially contribute to the selection, optimization and qualification of existing and innovative materials and fuels for current and future Nuclear Power Plants –NPP- needs.

To perform such accurate and innovative experiments in MTR, irradiation devices that contain material and fuel samples are necessary to be set up inside or beside the reactor core. These experiments require beforehand in situ and on line sophisticated measurements to accurately determine parameters such as thermal and fast neutron fluxes and nuclear heating in order to precisely monitor and control the conducted assays.

The paper will present an advanced measurement methodology based on combination of neutron detection (fast and thermal) by using innovative detectors associated to nuclear heating measurement carried out with suitable calorimeter device.

Such innovative developments are made in the frame of a collaborative program between CEA and Aix-Marseille University called IN-CORE¹ [1-3].

Main principle of measurement methodology, specific measurement devices and their performances and limitations are discussed. Recent analytical and simulation results are also presented.

1. Introduction

An innovative and original collaborative research program IN-CORE is under progress between CEA and Aix Marseille University since 2009 and is performed in the frame of common research laboratory LIMMEX². This research program deals with different aspects of radiation measurements and advanced analysis methodologies to reach more accurately specific and crucial physical parameters

¹ Instrumentation for Nuclear radiations and Calorimetry On-line in REactor

² Laboratoire d'Instrumentation et de Mesures en Milieux Extrêmes which roughly means « Instrumentation and measurements in extreme medias »

inside Jules Horowitz Material Testing Reactor –JHR/MTR such as fast and thermal neutron flux, gamma flux and nuclear heating.

In such type of reactors i.e. MTRs, experiments are conducted in specific irradiation devices, which are introduced inside or beside the core of the reactor, and containing material or fuel samples. These experiments require in situ measurements to monitor and control the conducted assays [4].

The increasing of performances and capacities of calculation/simulation tools in particular in the field of material and fuel studies naturally induce increasing of scientific requests. This implies the continuous improvement of experimental capacity and related instrumentation and measurement methods e.g. to switch (to jump) from *in-situ/post-irradiative* measurements to *on-line* combined measurements with a very good level of declared uncertainties. Regarding these new challenges, different programs have been carried out to perform significant innovative developments for MTRs in instrumentation and measurement fields.



Fig. 1: General view of the future Jules Horowitz material testing reactor JHR.
-Up to 20 simultaneous experimental channels are expected-

IN-CORE initiative belongs to these programs and is dedicated to enhance capacity and increase performances offered by MTRs reactors in general and Jules Horowitz in particular by using an updated and advanced instrumentation and performing new devices, and ad hoc analytical and experimental methodologies to reach in different JHR irradiation channels (Fig. 1) specific and pertinent physical parameters with the best uncertainty levels [5-6].

Actually, the challenge deals with advanced on-line measurements of several parameters within experimental channels such as specific power deposit ($W.g^{-1}$), neutron and gamma flux [7] by using new and/or upgraded in pile instrumentation and measurement methods satisfying both safety requirements and scientific criteria. In so doing, two main complementary objectives are pursued:

- 1- Study and development of innovative technological device(s) sharing different existing sensors (neutron and photon detectors, calorimeters). A combined analysis of the different measurement results should reduce the final uncertainties on radiation and nuclear heating measurements [2].
- 2- Analytical/theoretical approach on heat transfer in radiometric differential calorimeter. The aim of these studies is to develop numerical and experimental tools to improve, predict and adapt the response of the calorimeter under various physical and geometrical conditions [3].

The ultimate and global aim is to finally design a suitable experimental mobile device for accurate mapping of the JHR experimental channels.

2. Advanced radiation mapping by using ad hoc experimental device CARMEN³

According to objective 1 described above, different kinds of potential radiation detectors have been carefully studied in view to choose suitable ones to perform such accurate on-line measurements [2]. Neutron detectors as well as photon ones have been selected according to expected flux levels, to signal to noise ratio that could be encountered and to their effective sensitivity in such specific environment. Consequently, we intend to use:

- fission chambers with different neutron converter isotopes (^{235}U , ^{242}Pu) and Self Powered Neutron Detector -SPND- for neutron measurements [8], [9], [10],

³ Calorimétrie en Réacteur et Mesure des Emissions Nucléaires stands for « Calorimetry in Reactor and Nuclear Radiation Measurements »

- ionization chamber and Self Powered Gamma Detector -SPGD- for photon measurements,
- Differential calorimeter and Gamma Thermometer -GT- for nuclear heating measurements.

In MTRs, thermal neutron measurements are generally carried out by using Self Powered Neutron Detectors (SPND) and/or Fission Chambers (FC) thanks to their robustness, to the large variety of emitters/fissile neutron converters and to their low γ -sensitivity particularly for FC [21]. The most usual emitters for SPND are rhodium, vanadium and platinum [13], [14]. For CARMEN-1 experiment we choose rhodium SPND according to MTR's measurement feedbacks (OSIRIS, BR2 [9]).

For fission chamber detectors, we select ^{235}U as thermal neutron converter isotope due to the accurate knowledge of its nuclear data, to the relatively high level of its thermal fission cross section and the wide experience we have with such type of detectors. Hence, using both Rh-SPND and ^{235}U -FC in the same device will lead us to figure out an interesting thermal neutron measurements comparison between two kinds of detectors based on two neutron conversion reactions i.e. (n_{th}, γ) and ($n_{\text{th}}, \text{fission}$) for SPND and FC respectively.

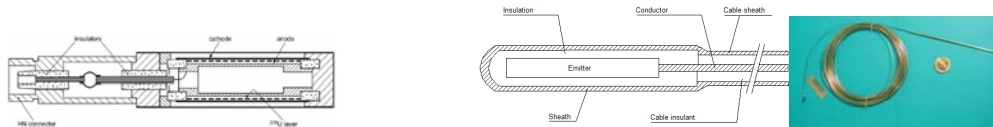


Fig 2: ^{235}U -FC and Rh-SPND are both used for thermal measurements in CARMEN-1 assay

For fast neutron flux measurements, a new on-line detection system called FNDS for Fast Neutron Detector System -FNDS [8] has been selected to be used in CARMEN-1 device. This system developed by the CEA and the SCKCEN consists in a FC with ^{242}Pu as fast neutron converter deposit associated to a specific data analysis unit [22], [15], [16]. Thermal neutron flux contribution integrated by such ^{242}Pu -FC will be estimated by ^{235}U -FC. Time evolution of ^{242}Pu converter due to neutron captures and fissions is computed by FNDS system to accurately adjust and determine the sensitivity of such ^{242}Pu -FC.

An original and new approach in the present MTR experiment program consists also in photon measurements which are performed by using a recently developed detector called SPGD for Self Powered Gamma Detectors using a specific gamma sensitive emitters; lead and/or bismuth [10], [11]. We decided to use a qualified SPGD with Bi-emitter [10], [11]. Furthermore, photons could also be measured by ionization chamber detector, hence we figure out a new No-Deposit-FC as γ -ionization chamber to be tested for direct gamma flux measurement on the one hand and to experimentally be qualified to reach the gamma contribution to foreground signal in FC on the other hand.

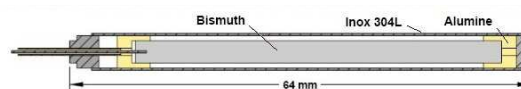


Fig. 3: General description of Bi-SPGD

Finally, the last but not the least parameter that will be measured is nuclear heating. Two sensors have been selected to perform such measurements: Differential Calorimeters -DC- and Gamma Thermometers -GT- [17], [18]. Appropriate graphite DC adapted to the level of nuclear heating in the OSIRIS reflector (2 W/g maximum) has been designed and manufactured. In order to reduce measurement uncertainties, three different methodologies are expected to be used and compared.

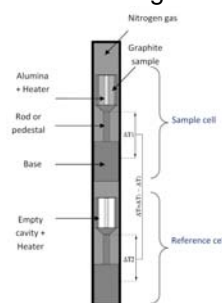


Fig. 4: Differential calorimeter used in CARMEN-1 experiment [3].

Detectors and sensors described above have been suitably associated in a measurement device called CARMEN-1⁴ (Fig. 5) that has been tested and qualified in OSIRIS MTR reactor at CEA-Saclay (France) in January 2012. The measurements consist on mapping irradiation channels in the reflector of OSIRIS core to measure in different locations neutrons, photons and nuclear heating. In fact two variant of CARMEN-1 device have been carried out; CARMEN-1N for neutron measurements and CARMEN-1P for photon measurements.

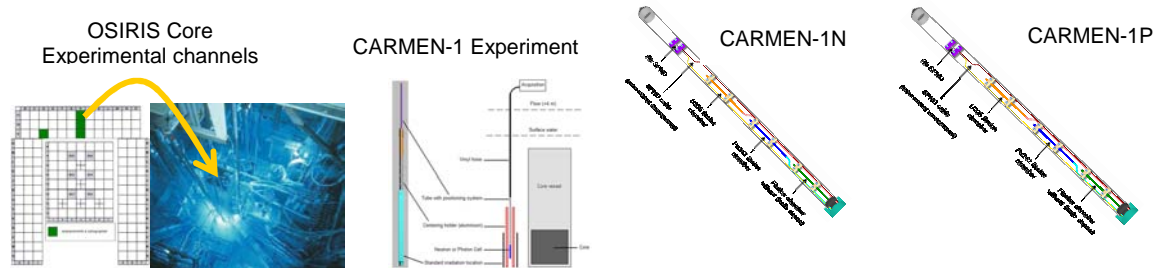


Fig. 5: CARMEN-1N, CARMEN-1P tested and qualified in OSIRIS MTR reactor.

As seen before, for the same parameter to be measured e.g. neutron or photon flux, different kinds of detectors are expected to be used in view to reduce final uncertainty on the one hand and to cross qualify each measurement by combined analysis on the other hand.

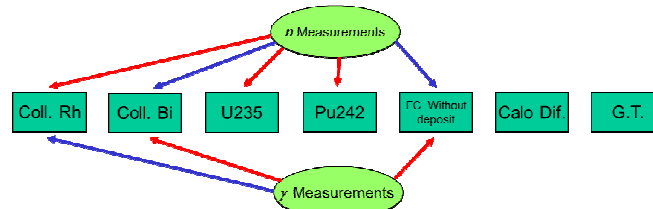


Fig. 6: Several detectors are used to reach same parameter. Red and blue arrows indicate respectively the primary and the secondary channel/tool for parameter measurement.

Thus, the combined analysis approach uses these different measurement results as described in the flowchart bellow.

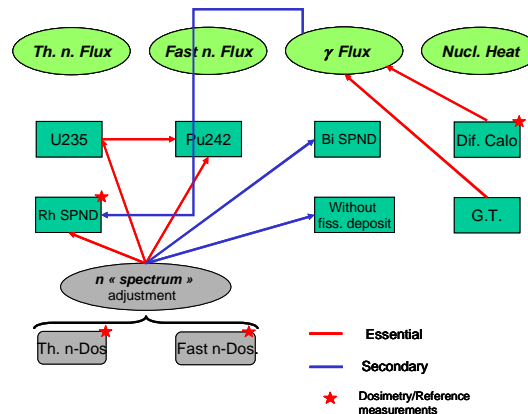


Fig. 7: Measurement results are folded together to be cross qualified and to improve uncertainty budget. Red and blue narrows have the same meaning as described above.

3. Analytical studies for thermal and calorimetric measurements

As specified in § 1 the second main objective of IN-CORE program deals with analytical approach on heat transfer in radiometric differential calorimeter [20] in view to improve its performances under specific constraints (geometrical and physical) inside harsh media (high temperature, high radiation level/high dose rate) such the JHR core environment. Indeed, the goal is to improve knowledge and

⁴ French acronym for « CALorimétrie en Réacteur et Mesure des Emissions Nucléaires »

measurement quality of this key parameter i.e. nuclear heating by reducing final uncertainties thanks to the optimization of the calorimeter and advances in simulation tools and analysis methodologies.

This is progressively performed, firstly by comprehensive analysis of heat transfer phenomena inside the calorimeter itself and with its surrounding media (cooling water) and secondly via interpreting the data sets resulting from in pile simulations [1], [3], [19], [24].

The differential calorimeter is supposed to be in non-adiabatic mode. The calorimeter [3], shown in Fig. 4 corresponds to a simple robust design made by two superposed twin cells contained in a cylindrical stainless steel tube filled with nitrogen gas. The upper cell includes alumina tube containing a resistance and a cylindrical head, which contains the graphite sample acting as radiation absorber due to its relative high atomic density ($\sim 1,134 \cdot 10^{23} \text{ at.cm}^{-3}$), a cylindrical aluminium base and a pedestal/rod which is placed between the head and the base. The lower one contains an empty cavity filled with nitrogen gas and is used as reference cell. Each cell is instrumented via two thermocouples. The first one is imbedded into the top of the pedestal and the second one into the base center allowing a differential measurement of temperature for each cell. The operating mode used is a permanent mode with a heat exchange between the calorimeter and its surroundings (water bath during calibration or water flow during irradiation). The heat generated following the power deposit (W.g^{-1}) in each cell, due primarily to radiation interactions (photons/gammas and neutrons) with atoms/nuclei in structural elements of the cells, is transferred through the base to the reactor coolant at the outside surface of the stainless steel cylindrical can [1].

Heat transfer inside the calorimeter mainly occurs by conduction mode at low temperature in the structural elements of the calorimeter. Hereafter, the heat transfer model is described for two distinct cases. The first one corresponds to the calorimeter calibration under non irradiated conditions. In that case the calorimeter is inserted in water bath with a constant temperature bulk (Figure 8-a) (ISIS reactor pool at CEA/Saclay) without water flow or inserted inside a forced convective liquid bath [19], [23]. The nuclear power deposit (nuclear heating) in graphite sample is simulated by mean of a Joule effect heater element within the alumina. The produced heat is then diffused to the base of the cell through the pedestal/rod. The second model concerns heat transfers in irradiated medium where the calorimeter is exposed to nuclear radiation flux and its structural materials are entirely 3D-heated. This implies that the heat generated should be taken as a spatial distribution according to axial ordinate (the radial gradient is neglected) [1], [3]. Moreover, the thermal radiative mode has to be added for high levels of nuclear heating. Figure 8-b describes schematically the experiment done inside OSIRIS MTR research reactor at CEA-Saclay [18].

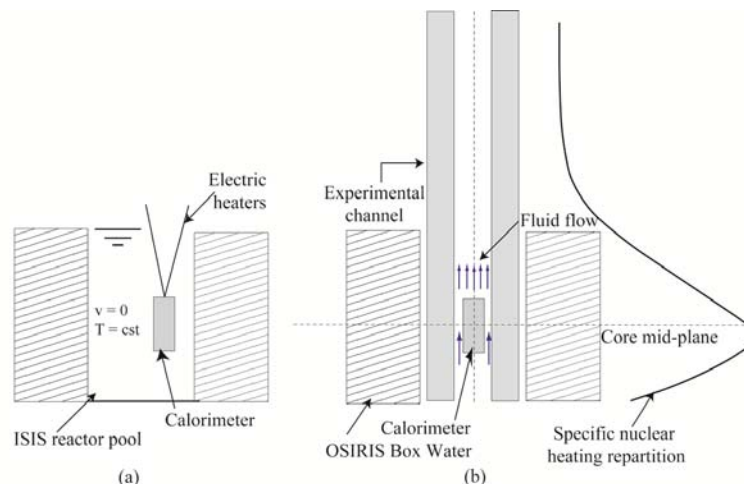


Fig. 8: (a) Calibration experiment under non irradiated conditions; (b) the calorimeter inside an experimental channel under irradiated conditions [3].

These analytical and parametrical studies lead to several and very interesting results (temperature field, heat flux, heat losses) and conclusions that allowed on the one hand to the optimization of the first version of calorimeter device that has been used in CARMEN-1 experiment and on the other hand to figure out an original smart device called BETHY⁵ presented in Fig 9. This unit will be dedicated

⁵ French acronym : « Banc d'Etudes Thermo Hydrauliques ».

firstly to thermal analytical/smart studies and secondly to thermohydraulic ones to figure out an innovative advanced calorimeter dedicated to nuclear heat measurements inside JHR reactor core thanks to CARMEN-1 experiment feedbacks and advances in simulation tools and knowledge of nuclear heat multi origin contribution and heat transfer experiences.

Fig. 9: Conceptual design of BETHY test bench

IN-CORE program is a real opportunity for scientists, engineers and researchers from CEA and University (Aix Marseille University) to share knowledge, competences and know-how to perform innovation and advanced multipurpose experiments in view to face real scientific and technological challenges in the field of nuclear instrumentation and measurement. Such collaborative works have permitted to design, to carry out and to successfully perform a multi-parameters experiment CARMEN-1 inside OSIRIS reflector. At the same time analytical studies on heat transfer in radiometric differential calorimeter are pursued to improve the design of a calorimeter which will be used for JHR mapping experiments. These sensors will be use in association with appropriate nuclear radiation detectors to also reach precisely neutron (thermal and fast) and photon flux.using a future device called CARMEN-2.

IN-CORE research program is supported by European funds of regional development called FEDER and "Conseil Regional PACA" and "Ville de Marseille". It is also co funded by CEA/JHR program. CARMEN-1 experiment campaign has been carried out in OSIRIS reactor at CEA/Saclay: DEN/DANS/DRSN/SIREN.

- [1] C. Reynard et al. " Numerical study of heat transfer in a radiometric calorimeter dedicated to nuclear heating measurements". RRFM 2011,20- 23 mars 2011, Rome, Italy.
- [2] D. Fourmentel JF. Villard, A. Lyoussi et al. « Combined analysis of neutron and photon flux measurements for the Jules Horowitz Reactor core mapping" ANIMMA 2011 Ghent (Belgium). 6-9 June 2011
- [3] O. Merroun et al. "Heat Transfer in a non adiabatic calorimeter: numerical parametric study without and with nuclear heating deposit" The 14th NURETH meeting, Toronto, Ontario, Canada, September 25-29, 2011.
- [4]] C. Gonner et al. "Developments status of irradiation devices for the Jules Horowitz Reactor, RRFM, Transactions 2008.
- [5] G. Bignan, D.Iracane, "The Jules Horowitz Reactor Project:" A new High Performances European and International Material Testing Reactor for the 21st century"- Nuclear Energy International publication (NEI) -Dec 2008
- [6] D. Iracane et al. "Materials subjected to fast neutron irradiation, Jules Horowitz Reactor: a high performance material testing reactor", Comptes Rendus. Physique Vol. 9, 2008, pp. 445–456.
- [7] D. Iracane, JF. Villard "Advanced Instrumentation for Irradiation Experiments in Material Testing

- Reactors", Proceedings of ANIMMA2009, Marseille (France) June 7_10, 2009.
- [8] B. Geslot, L. Vermeeren, et al. "New measurement system for on line in core high-energy neutron flux monitoring in materials testing reactor conditions", Review of Scientific Instruments, Vol. 82, 033504, 2011.
- [9] L. Vermeeren, M. Weber, "Self-powered neutron detector qualification for absolute on-line in-pile neutron flux measurements in BR2", Reactor Dosimetry in the 21st Century, pp. 219-225, 2003.
- [10] L. Vermeeren, H. Carcreff et al. "Irradiation tests of prototype self-powered neutron and gamma detectors", 2nd International Conference ANIMMA, June 2011, Ghent (Belgium).
- [11] M. Alex et al. "Development of bismuth self-powered detector", Nuclear Instruments and Methods in Physics Research – Section A, Vol. 523(1-2), pp. 163-166, 2004.
- [12] H. Carcreff, "CALMOS: Innovative Device for the Measurement of Nuclear Heating in Material Testing Reactors", 14th international symposium on Reactor Dosimetry, Bretton Woods (USA), May 2011.
- [13] W.H. Todt, "Characteristics of self-powered neutron detectors used in power reactors", European Nuclear Society, Berne (Switzerland) World Nuclear Congress. Transactions Vol. III, pp. 312-323, 1998.
- [14] J. Ma, "Self-powered detectors for power reactors: an overview", 27th annual conference of the Canadian Nuclear Society, 7 p., 2006.
- [15] P. Filliatre et al. "Reasons why Plutonium 242 is the best fission chamber deposit to monitor the fast component of a high neutron flux", Nuclear Instruments And Methods in Physics Research – Section A, 593 (3), p. 510-518, 2008.
- [16] P. Filliatre et al. "Joint estimation of the fast and thermal components of a high neutron flux with a two on-line detector system", Nuclear Instruments And Methods in Physics Research – Section A, 603 (3), p. 415-420, 2009.
- [17] S. Solstad, R. Van Nieuwenhove, "Instrument capabilities and developments at the halden reactor project", Nuclear Technology, Vol. 173, N°1, 1-19 8, 2011.
- [18] H. Carcreff, V. Clouté-Cazalaa, L. Salmon, "Development, calibration and experimental results obtained with an innovative mobile calorimeter (CALMOS) for nuclear heating measurements", 2nd International Conference ANIMMA, June 2011, Ghent (Belgium).
- [19] Julie Brun et al. « Numerical and Experimental Calibration of a Calorimetric Sample Cell Dedicated to Nuclear Heating Measurements", J. Brun et al., IEEE Transactions on Nuclear Science, ANIMMA2011 special Edition, publication accepted.
- [20] C. Reynald, A. Lyoussi et al. In-Pile Calorimetry : A thermal point of view, RRFM-IGORR 2012 , Prague, Czech Republic, March 18-22, 2012.
- [21] L. Vermeeren, S. Breaud, P. Filliatre, B. Geslot, C. Jammes and al. "Experimental Verification of the Fission Chamber Gamma Signal Suppression by the Campbelling Mode", IEEE Transactions on Nuclear Science, 2011, Vol. 58 , PP. 362 – 369
- [22] J-F. Villard, M. Schyns, "Advanced In-Pile Measurements of Fast Flux, Dimensions and Fission Gas Release", Nuclear Technology, 2011 , Vol. 173 , PP. 86 – 97
- [23] Heat transfer during out-pile calibration of a calorimeter used for nuclear heating measurements: influence of convective boundary conditions, J. Brun et al., RRFM Transactions 2012, Prague, Czech Republic.
- [24] Numerical study of the geometry impact on the heat transfer in a radiometric calorimeter dedicated to nuclear heating measurements, M. Muraglia et al, RRFM Transactions 2012, Prague, Czech Republic.

OPERATING AN IRRADIATION EXPERIMENT USING NEW NEUTRON TRANSPORT SIMULATIONS AND ENHANCED ANALYSIS OF GAMMA-SPECTROMETRY MEASUREMENTS: APPLICATION TO THE GRIFFONOS DEVICE IN THE OSIRIS REACTOR

F.CHEVALLIER, F.DOLCI
CEA, DEN/DANS/DM2S/SERMA
Gif sur Yvette, 91191, France

L.MARCHAND, PH DELACOUR, L. SALMON, X.TIRATAY
CEA, DEN/DANS/DRSN/SIREN
Gif sur Yvette, 91191, France

ABSTRACT

Driving a fuel rod irradiation ramp in the GRIFFONOS device (in the Osiris MTR¹) requires a numerical relation between the fission power of the fuel rod and the neutron flux measured by SPNDs² detectors. This relation is obtained using neutron transport calculations. It is checked during a pre-irradiation stage and can be tuned in order to drive more precisely the following main irradiation phase. A new neutron transport calculation scheme, based on CEA neutron transport code APOLLO2, has been developed for the Remora 3 experiment which took place in 2010. Results showed that the agreement between calculated and measured activities inside the fuel rod was considerably improved using this new method. These results show that simulations based on the new neutron flux solver: the method of Characteristics, implemented in APOLLO2 code can properly describe an irradiation in the GRIFFONOS device and enable an accurate experiment driving.

1. Introduction

In order to have a better understanding of the high burn-up fuel behaviour under transient operating conditions, an experiment called Remora 3 [1] was performed in 2010 in the OSIRIS reactor [2], a Material Testing Reactor located at CEA/Saclay Research Center. This test was performed at the periphery of OSIRIS reactor core in the GRIFFONOS irradiation loop. This device is driven according to its distance from the core, in order to obtain the required level of linear power density in the irradiated rod.

The GRIFFONOS device is equipped with neutron SPNDs² detectors that measure neutron flux during irradiation experiments. They allow online power control thanks to the use of P/ϕ ratios (ratios between fission power produced by the irradiated rod and neutron flux inside SPNDs), which are calculated at any distance to the reactor core using a neutron transport calculation scheme. This mathematic relation is checked after a pre-irradiation stage by comparing calculated activities of short-lived γ -emitters in the fuel rod and measured ones. For the Remora 3 experiment, a new scheme of neutrons simulation using the Method of Characteristics implemented in the CEA APOLLO2 determinist neutron transport code has been developed. It was intended to improve both P/ϕ predictions and some fuel data used for γ -spectra analysis.

¹ MTR : Material Testing Reactor

² SPND : Self Powered Neutron Detector

2. Neutron transport simulations in the GRIFFONOS device

Neutron transport simulations play a key role both for pre-irradiation and irradiation stages. They are performed with the APOLLO2 [3] neutron transport code and DARWIN [4] code for the depletion of isotopic concentrations.

For the experiment, these codes were used to obtain:

- the neutron flux profile at the periphery of the OSIRIS reactor and fission power in the fuel rod (for the prediction of P/ϕ coefficients);
- the radial fission rate profiles and isotopic density profiles inside the rod (for fine interpretation of γ -spectrometry measurements);
- the reaction rates (for the depletion of the isotopic composition of the rod and for γ -activity calculations).

2.1. New neutron calculation scheme in the GRIFFONOS device

A well-adapted spatial mesh is used to model the OSIRIS reactor and the GRIFFONOS device at several distances to the OSIRIS core. This geometry is obtained as a horizontal section of the reactor at the core mid-plane (Figure 1). It shows a portion of the OSIRIS core, the core vessel, the GRIFFONOS device surrounded by water. The rod is segmented in concentric rings in order to compute the radial reaction rate density profile and to take into account correct isotope depletion.

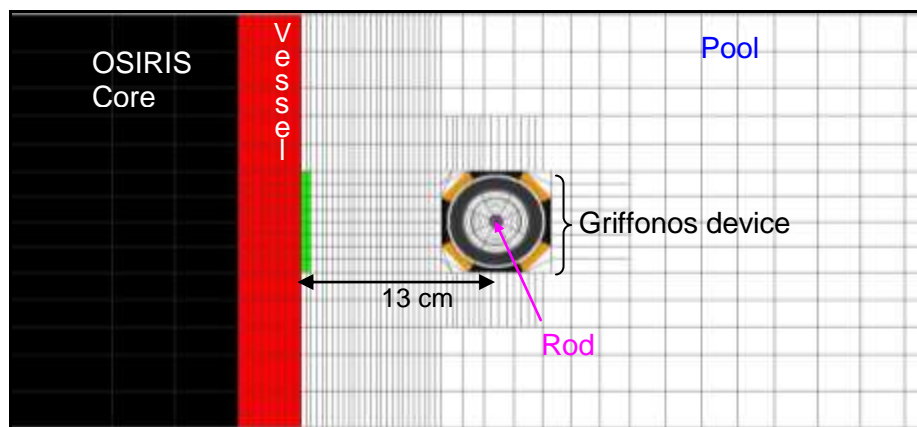


Figure 1: Example of calculation geometry used for the simulation of the GRIFFONOS device, with OSIRIS reactor core (black), vessel (red), water (white) and SPNDs (orange).

With this geometry, the neutron flux coming from the Osiris core and from the rod can be simulated taking into account all physic effects on neutron transport.

In order to obtain reliable predictions of neutron flux and reaction rates in the irradiated rod, the calculation scheme requests several steps:

- In a first step, the isotopic composition of the rod after its irradiation in PWR is determined. Simulation of the rod inside a fuel bundle used in PWR is provided by the APOLLO2 code. Neutron flux is calculated in the rod as a function of its burnup. Using these data and the real power history of the rod as inputs, the PEPIN code can calculate isotopic concentrations and activities of nuclei inside the rod.
- In a second step, neutron flux must be calculated with high accuracy in the environment of the experiment in the OSIRIS reactor. The APOLLO2 Method of Characteristics [3,5] is used to determine the neutron flux in the fine mesh geometry shown in Figure 1. Linear description of the angular neutron flux gives a good description of the neutron flux profile outside the OSIRIS core where neutron flux gradient is strong. The cross section data library used is based on the up-to-date JEFF3.1.1 [6] evaluation with the XMAS energy mesh (172 groups). The spatial meshing and tracking parameters have been optimized. Thanks to the Method of Characteristics described above, a mesh size of around 0.1 cm in water and 0.01 cm between tracks is enough to ensure a fast

convergence and do not overload CPU and memory capacities. Convergence of the neutron flux solver is required with a relative precision of 10^{-5} on eigenvalues.

2.2. Outputs of the simulation

Key data needed for online monitoring of fission power during the irradiation and for precise analysis of γ -spectrometry measurements are deduced from neutron calculations.

In order to run the experiment with accuracy, a pre-irradiation stage was performed. During this first step, the rod was irradiated at several distances to the OSIRIS core. For each distance, neutron flux ϕ was given by SPNDs detectors. These values, combined with P/ϕ ratios provided by neutron simulations enable to calculate online fission power.

One of the key outcomes was the determination of radioisotopes activities of the very few fuel pellets facing SPNDs. The first step was the computation of activities of these γ -emitters according to the estimated fission power level history of the rod. This was performed by the depletion code PEPIN which computes new isotopic composition from reaction rates calculated using the enhanced calculation scheme and estimated fission power level history.

After this pre-irradiation stage, fuel rod γ -spectrometry measurements were performed. These activities from neutron calculations can be compared to experimental activities. The second step consisted in calculating the ratio A_M/A_C between measured and computed activities of these γ -emitters. This ratio is directly related to the P/ϕ coefficients assessed by the neutron transport calculations. Therefore it enables to tune the operating irradiation conditions of the following main irradiation stage in order to be as close as possible to the irradiations power requirements.

Another A_M/A_C ratio is calculated at the end of the main experiment phase to check the whole irradiation experiment.

3. Gamma-spectrometry measurements and analyses

Two spectrometry acquisition campaigns were performed on the Remora 3 fuel rod to support the irradiation program: one after the pre-irradiation stage and one after the main irradiation stage. Shortly after the end of each irradiation stage, the GRIFFONOS device was transferred to the Osiris 'hot cell'. The fuel rod was carefully introduced into a waterproof container dedicated to gamma spectrometry and neutron radiography. Such a container enables to protect the fuel sample rod while limiting any distortion effects during sample examinations. The container was then transferred to the γ -spectrometry measurement bench in the Osiris pool [7]. The γ -spectrometry bench displaces the container in front of a mechanical shutter collimator which defines the size of the gamma beam and therefore spatial resolution and counting rates during the acquisition. As the γ -spectrometry device grants high accuracy position of the moving lift stage, it is therefore possible to scan slice after slice the whole fuel rod length or to focus the acquisition on a few fuel pellets area.

A first step of the gamma spectrometry campaign consisted in the γ -scanning of the rod's whole length leading to axial count rate distributions of many nuclides, with half-life between 2.3 days to 30 years. Among them, one ($^{140}\text{Ba-La}$ 1596 keV) is an image of the relative mean power axial distribution. These data also helped to identify the very few fuel pellets directly located in front of SPNDs during the irradiation stage. In a second step, local γ -scanning was run on these pellets in order to get a high statistic spectrum for precise quantitative analysis (figure 2). The third and last acquisition step consisted in the gamma scanning of an activity standard for quantitative calibration.

Determination of activities from the γ -spectrum needs special care in order to reach lower uncertainties. Basically, activity of a radioisotope $A_{i, E}$ is calculated from the γ -peak at the energy E as following:

$$\mathcal{A}_{i,E} = \frac{\tau_{i,E}}{\eta_E \cdot I_{i,E}}$$

where:

- subscript i is relative to a given nuclide;
- $\tau_{i,E}$ is the nuclide counting rate at a given energy (experimental),
- $I_{i,E}$ is the gamma emission probability relevant to the chosen energy (tabulated);
- η_E is the photons' detection efficiency. This parameter was calculated from a few steps process. The analysis of the Remora 3 spectrum provided an experimental relative photons' detection efficiency curve. This relative curve, built from selected γ -peaks, represents the ratio between relative γ -counting rates and emission probability as a function of energy. This curve is then transposed to an absolute one knowing an absolute photons' detection efficiency. The latter was determined from a γ -spectrometry measurement of an activity standard and from photons' transmission factors of both the activity standard and the Remora 3 fuel rod. The transmission factor of the activity standard is known, the one for Remora 3 fuel rod's was calculated from the geometry and media of the experimental configuration, and, in order to reach high accuracy, from nuclides radial profiles and material compositions of the pellets obtained from the neutron calculations presented in part 2.

For multi-gamma emitters, the activity of the nuclide is calculated as a weighted mean of activities $\mathcal{A}_{i,E}$ from a set of selected peaks.

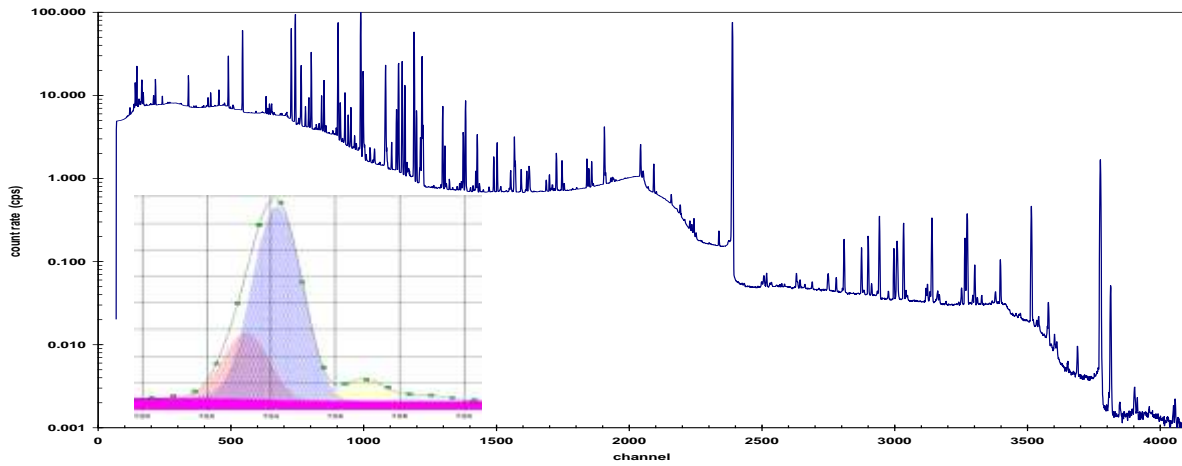


Figure 2: Example of spectrum

Spectrum analysis was complex, with many γ peaks and interferences (figure 2). So, after a first run with the main γ -peaks, showing a good agreement between computed and measured activities, the spectrum analysis was refined, with an optimized treatment for each peak, in particular for those interfering.

After the first irradiation stage, the analysis process led to quantify 33 nuclides, including 2 short live heavy nuclei, 23 short live fission products and 8 long live fission products (present before irradiation).

After the second irradiation stage, the analysis process led also to quantify 33 nuclides, with the same distribution into nuclide categories as above. Volatile fission products (Cs, Te-I), which migrated or were considered so in a conservative approach, were also quantified but were not taken into account to determine the $\mathcal{A}_M/\mathcal{A}_C$ ratio.

4. Comparison between calculated and measured activities

The comparison between calculated and measured activities was carried out for the two irradiation stages.

After the pre-irradiation stage, the most coherent $\mathcal{A}_{i,M}/\mathcal{A}_{i,C}$ set of short-lived fission products (^{95}Nb , ^{95}Zr , ^{99}Mo , ^{103}Ru , ^{131}I , ^{132}Te , ^{132}I , ^{140}Ba , ^{140}La , ^{147}Nd) was selected to estimate the ratio $\mathcal{A}_M/\mathcal{A}_C$. This set is also a part of the most precisely measured nuclides. The $\mathcal{A}_M/\mathcal{A}_C$ ratio was estimated to be: 0.97 ± 0.04 [$2\sigma_{\text{exp}}$]. This value can be compared with the one obtained with the old calculation scheme: 0.85. This means that the P/ϕ coefficients calculated with the new modeling of the GRIFFONOS device leads to a much better accuracy than the previous one. As the correcting factor is used to adjust P/ϕ coefficients needed to drive the main irradiation stage of a GRIFFONOS irradiation, this also means that the new simulation reduces strongly the importance of the pre-irradiation stage in the driving of the main irradiation one.

After the main irradiation stage, the second comparison between calculated and measured activities led to select a conservative set of most coherent and non volatile short-lived fission products (^{95}Nb , ^{95}Zr , ^{99}Mo , ^{140}Ba , ^{140}La , ^{147}Nd), to estimate the $\mathcal{A}_M/\mathcal{A}_C$ ratio. The new $\mathcal{A}_M/\mathcal{A}_C$ ratio was estimated to be: 0.99 ± 0.04 [$2\sigma_{\text{exp}}$] showing that simulations based on the new neutron flux solver can properly describe an irradiation in the GRIFFONOS device.

5. Conclusion

P/ϕ coefficients are needed to drive an irradiation in the GRIFFONOS device. Reliable predictions of these coefficients were difficult to obtain because of the presence of a large amount of reflector between the core of the OSIRIS reactor and the rod. The Method of Characteristics developed in the APOLLO2 neutron transport code, with the linear description of the neutron flux, has been able to produce those predictive P/ϕ coefficients with a better accuracy than the ones obtained with the previous scheme. The new simulation, leading to a tuning factor close to one, reduces the importance of the pre-irradiation stage for the driving of the main irradiation.

6. Acknowledgements

Authors acknowledge Xavier Wohleber who first developed the methodology used to drive GRIFFONOS experiments, using successively a pre-irradiation stage followed by a main irradiation one, and who initiated efforts to improve the $\mathcal{A}_M/\mathcal{A}_C$ obtained for the pre-irradiation phase.

7. References

- [1] Th Lambert and coll "REMORA 3: the first instrumented fuel experiment with on-line gas composition measurement by acoustic sensor", Animma, 6-9 june 2011, Ghent
- [2] "The OSIRIS Reactor", CEA/Saclay Center.
http://den-dans.extra.cea.fr/en/Phoce/Vie_des_labos/Ast/ast_sstheme.php?id_ast=66
- [3] "APOLLO2 year 2010". R. Sanchez, I. Zmijarevic, M. Coste-Delclaux, E. Masiello, S. Santandrea, E. Martinolli, L. Villatte, N. Schwartz, N. Guler. Nuclear Engineering and Technology, 42, 5 (2010), 474-499.
- [4] B. Roque, N. Thiollay, P. Marimbau, A. Barreau, A. Tsilanizara, C. Garzenne, F. Marcel, H. Toubon, C. Garat, "Experimental validation of the code system DARWIN for spent fuel isotopic prediction in fuel cycle applications", PHYSOR, Seoul, Korea, October, 7-10, 2002.
- [5] S. Santandrea, J.C. Jaboulay, P. Bellier, F. Fevotte, H. Golfier, "Improvements and validation of the linear surface characteristics scheme", Annals of Nuclear Energy, 16 décembre 2008
- [6] A. Santamarina, D. Bernard, Y. Rugama: "The JEFF-3.1.1 Nuclear Data Library," JEFF Report 22 (2009).
- [7] L. Marchand "La spectrométrie gamma en réacteur expérimental : un moyen essentiel d'étude des combustibles nucléaires", Journées de spectrométrie gamma et X 1993, Saint-Rémy-lès-Chevreuse, 12-14 oct.1993

HEAT TRANSFER DURING OUT PILE CALIBRATION OF A CALORIMETER USED FOR NUCLEAR HEATING MEASUREMENTS: INFLUENCE OF CONVECTIVE BOUNDARY CONDITIONS.

J. BRUN, C. REYNARD-CARETTE, M. CARETTE, M. MURAGLIA, O. MERROUN,
A. JANULYTE, Y. ZEREGA, J. ANDRE.

*Aix-Marseille Univ, LISA, équipe IPCN, Centre St Jérôme, Avenue Escadrille Normandie-Niemen,
bâtiment MADIREL, 13397 MARSEILLE cedex 20, France*

A. LYOUSSI, G. BIGNAN, J-P. CHAUVIN, D. FOURMENTEL, C. GONNIER, P. GUIMBAL,
J-Y.MALO, J-F. VILLARD.

*Commissariat à l'Énergie Atomique et aux Énergies Alternatives
CEA Direction de l'Énergie Nucléaire, Centre de Cadarache
13108 Saint-Paul-Lez-Durance, France.*

E-mail: julie.brun1@etu.univ-provence.fr

ABSTRACT

The present works concern experimental studies on the response of a permanent calorimetric sample cell under non irradiation conditions by heating by Joule Effect. The influence of the flow rate is tested for a large range of electrical power (< 3.1 W) in a water bath regulated at 23°C. A linear calibration curve is obtained in the case of a laminar flow ($Re < 1200$). Furthermore, a new instrumented jacket allows the heat loss measurements by using fluxmeters. At present, the heat transfer repartition along the external vertical surface of the jacket can be determined experimentally.

1. Introduction

To have a better understanding of the accelerated ageing of various nuclear materials and of new nuclear fuels behaviour under irradiations, experiments are performed in particular in MTRs such as Jules Horowitz Reactor (JHR). Before and during these studies, accurate nuclear and thermal data and operating conditions are required. Consequently, a new instrumentation device for online measurements of relevant parameters inside the JHR experimental channels (nuclear heating, neutron flux or gamma flux) is currently designed in the frame of the collaborative research program called INCORE "Instrumentation for Nuclear radiations and Calorimetry Online in Reactor" [1]. This new device which is composed of several sensors will be used at the starting of JHR [2, 3]. This paper concerns especially one sensor of this device: a calorimeter. Calorimetry is a usual measurement technique used to quantify the nuclear heating inside nuclear reactor channels [4, 5]. This paper presents studies performed in the case of a permanent differential calorimeter, previously designed by the CEA for a specific nuclear heating level inside OSIRIS reactor (from 0.1 to 13 W/g) [6], which allows continuous measurements. Analytical studies under non irradiation conditions on heat transfer associated to an in-pile calorimeter sample cell have been carried out [7-11]. These conditions allow easier parametric experimental studies with a more instrumented cell in order to improve the understanding of the thermal sensor behaviour and then to adapt its response for a wider nuclear heating range occurring into the JHR channels according to the reactor power and the channel location (core, reflector). This paper focuses on experimental studies dedicated to the determination of the out-pile calibration and the quantification of the heat losses (key parameter influencing the sensitivity). The calorimetric sample cell response is presented for a wide electrical power range imposed with a new instrumented jacket. The influence of the flow boundary conditions on the sensitivity is determined and the heat losses are discussed.

2. Experimental Setup

This first section presents the calorimeter, the experimental set up and the operating protocol.

2.1. Calorimeter presentation

The studied in-pile calorimeter is a heat flow calorimeter which thermally exchanges with its surroundings and reaches a stationary thermal state.

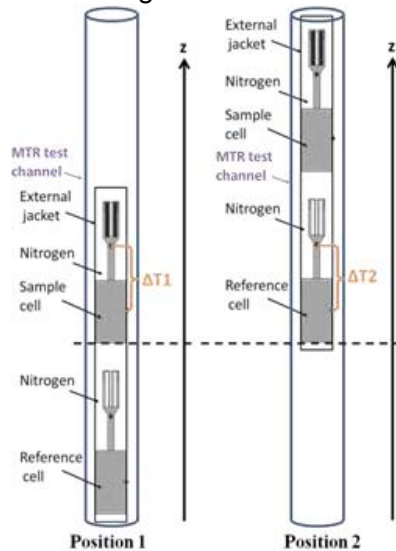


Fig 1. Diagram of the measurement principle of the in-pile calorimeter.

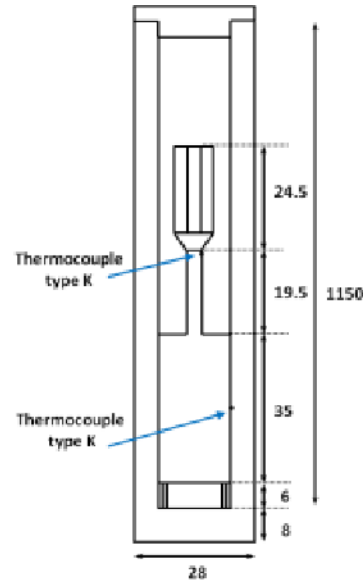


Fig 2. Diagram of the calorimetric sample cell.

Moreover it is a differential sensor because it consists of into two superposed twin cells (cf. Fig1.). The first one, denoted the sample cell, contains a graphite sample. Its response is induced by the nuclear heating of the sample and of the cell structure. The second one, called the reference cell, is used to determine the nuclear heating deposited only on the cell structure and then to deduce the nuclear heating of the sample. Consequently, the calorimeter response is obtained by a temperature difference between these two cells ($\Delta T_1 - \Delta T_2$) taken respectively at the same vertical location to cancel the vertical flux gradient influence (cf. Fig. 1.). In this paper, studies under non irradiation conditions are reduced to the calorimetric sample cell because of the behavior of each twin cell is quite similar [12]. Each calorimeter cell can be described from top to bottom by three parts which are called respectively in the following sections: the head (containing the graphite sample and an electrical heating element), the rod, and the base (in contact with the jacket ensuring the heat transfer) [7]. Temperature measurements are performed by two thermocouples (type K, 0.25 mm in diameter) located respectively in the center of the upper part rod and in the middle height of the base surface (cf. Fig. 2.).

2.2. Presentation of the experimental set up

The set up described on Fig.3 is composed of: a thermostated circulating bath, an instrumented calorimetric sample cell, a data acquisition system, a power supply and a computer. This water bath is used to simulate a cooling flow inside a vertical experimental channel. It can be controlled in temperature (a set point equal to 23°C is chosen for these experiments) and an upward laminar liquid flow can be imposed.

In order to improve the understanding of associated thermal phenomena, an instrumented calorimetric sample cell has been designed. This new cell consists of the calorimetric sample cell presented above inserted inside an instrumented closed jacket filled with nitrogen at atmospheric pressure. The instrumented jacket is made of brass, with external and internal diameters respectively equal to 28 mm and 17 mm. This jacket contains fifteen calibrated

thermocouples (type K) located according to a vertical line on its external surface. They are spaced of 5 mm and used to measure the vertical temperature gradient. Moreover this jacket contains three heat flux sensors glued on three different external areas to quantify heat losses: on the upper horizontal surface (10 mm in diameter, a sensitivity equal to $0.683 \mu\text{V}/(\text{W}/\text{m}^2)$), in front of the thermocouple line at the head and rod level (50 mm in length and 5 mm in wide with a sensitivity equal to $1.77 \mu\text{V}/(\text{W}/\text{m}^2)$) and on the lower horizontal surface (20 mm in diameter, a sensitivity equal to $1.95 \mu\text{V}/(\text{W}/\text{m}^2)$). This instrumented calorimetric sample cell is immersed in the cylindrical channel of the water bath. The resistive heater ($R = 2.8 \Omega$) located inside the calorimetric sample cell head is connected to the power supply to reproduce an energy deposit inside the graphite sample (from 0 to 3 W). The data acquisition system (Compact DAQmx, National Instruments) contains various input and output modules, dedicated respectively to current, tension, temperature and thermal flux measurements. It is connected to a computer using Signal Express software in order to visualize and record data.

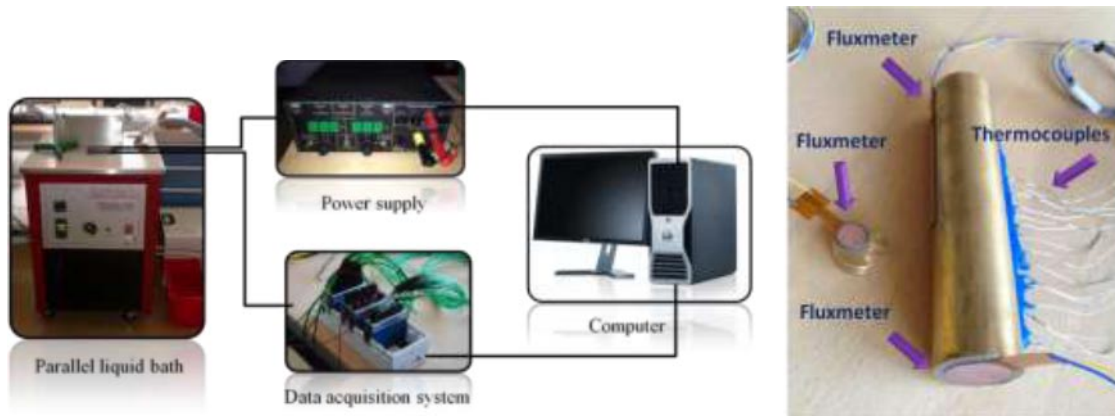


Fig 3. Diagram of the experimental set up (on the left) and picture of the calorimetric sample cell (on the right).

2.3. Operating procedures

For these studies specific external (flow velocity) and internal (heating by Joule effect) conditions are imposed to the calorimetric sample cell and its response is measured.

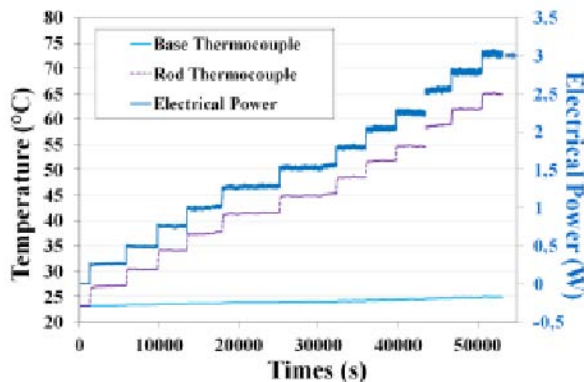


Fig. 4. Electrical power and temperatures versus time ($Re = 610$).

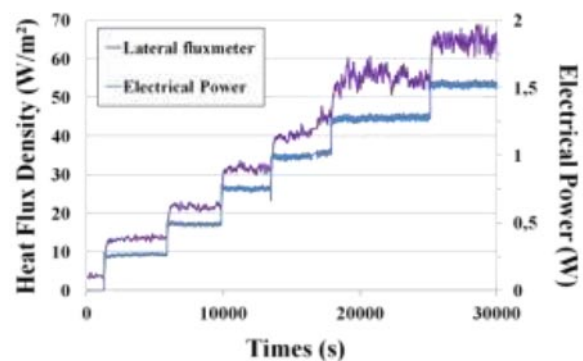


Fig. 5. Lateral heat flux density and electrical power versus time ($Re = 610$).

For each flow velocity, an electrical power range from 0 to 3W with an increment equal to 0.25 W is applied. Each value of the current intensity is tested during one hour. Fig. 4. gives the imposed electrical power (on the right axis) and the temperatures of the two thermocouples associated to the sample cell (on the left axis) versus time for a Reynolds number equal to 610. Fig. 5. shows the thermal flux measurements by the lateral fluxmeter. This curve allows the determination of the lateral heat losses through the jacket.

This operating protocol has been applied for a Reynolds number from 500 to 1110.

3. Influence of the coolant flow on the calorimeter behaviour

From the presented data in the previous section, the average temperature, flux and current intensity measurements are calculated for each power increment and when the stationary state is established and for each flow rate. Then for each condition, the mean temperature difference between the rod and the base thermocouples (ΔT_1 , cf. Fig.1.) is plotted versus the mean electrical power (cf. Fig. 6).

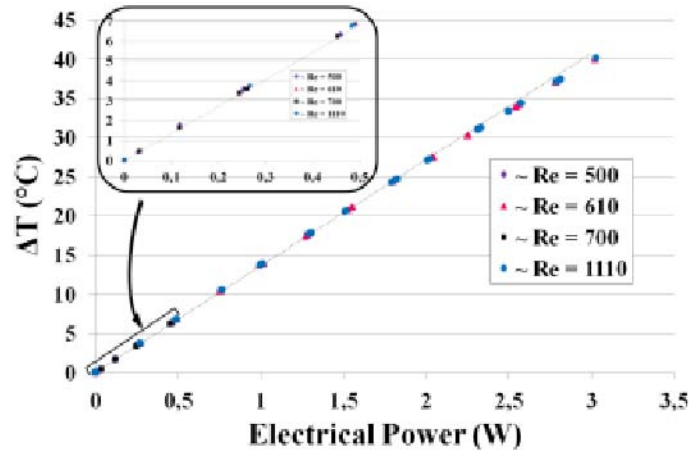


Fig. 6. Calibration curve of the calorimetric sample cell for four Reynolds numbers.

This curve corresponds to the calibration curve and allows the determination of the calorimeter sensitivity. These results show that the sensor temperature difference increases linearly versus the injected electrical power and does not depend on the flow rate.

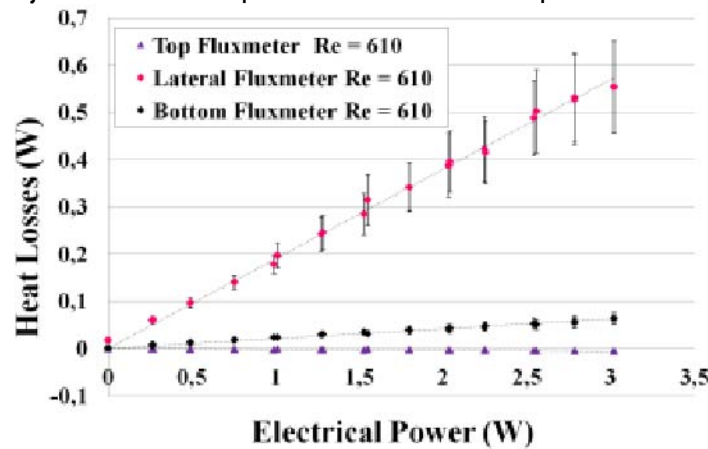


Fig. 7. Heat losses versus electrical power.

These results confirm previous works obtained for a shorter power range [7]. This allows the extension of the sample cell behaviour. The sensitivity, $d(\Delta T)/dP$, is equal to $13.4^{\circ}\text{C}/\text{W}$. This value is slightly lower than the one obtained for the smaller power range ($<0.5 \text{ W}$). On the one hand, this may be due to the new instrumented jacket which has a smaller thickness and consequently may lead to more heat losses at the head and rod levels, on the other hand it may be induced by the increasing of the thermal radiative transfer at higher temperature which involves heat losses.

At present, with the new jacket, the mean heat losses versus the electrical power can be determined for the three different areas. An example for a Reynolds number equal to 610 is given on Fig. 7. The mean heat losses are linear versus injected energy for the three areas. The higher heat losses correspond to the lateral surface in front of the head and the rod, and are equal to 19%. The heat losses through the bottom surface of the jacket are approximately equal to 2%. Finally, the upper fluxmeter data confirm that the top surface

heat exchanges are very low. The sensor sensitivity could be improved if the lateral heat losses were decreased. For instance, a new gas with a lower thermal conductivity could be used.

4. Conclusions and Outlooks

These experimental works have shown that the calibration curve remains linear when the range of the injected electrical power is increased (0-3W). Then, the tested flow rates for a laminar regime have no effect on the sensitivity of the calorimeter sample cell. Moreover, a new instrumented jacket has been tested and is validated for the thermal flux measurements. Consequently, the heat losses can be quantified. The analysis of a specific Reynolds number equal to 610 has shown that the lateral heat losses are relatively important (19% of the injected power).

The heat losses will be measured for various other flow rates. The electrical power range will be extended in order to determine the influence of the radiative transfer on the calibration curves (regression order). These experimental works will be used to adapt our numerical model (developed previously only in the case of a natural convection exchanges). Moreover the new numerical model under forced convection will take into account the radiative transfer.

5. Acknowledgements

INCORE program is supported by FEDER, Ville de Marseille and Conseil Régional PACA.

6. References

1. **In core Instrumentation for Online nuclear heating Measurements of Material Testing Reactor**, C. Reynard et al., RRFM Transactions 2010, Marrakech, Morocco.
2. **Combined analysis of neutron and photon flux measurements for the Jules Horowitz Reactor core mapping**, D. Fourmentel et al., ANIMMA 2011, June 2011, Gant, Belgium.
3. **Advanced methodology and instrumentation for accurate on line measurements of neutron, photon and nuclear heating parameters inside Jules Horowitz MTR Reactor**, A. Lyoussi et al. RRFM/ IGORR 2012, Prague, Czech Republic, March 2012.
4. **Measurements of Nuclear Heating Rate and Neutron Flux in HANARO CN Hole for Designing the Moderator Cell of Cold Neutron Source**, M-S. Kim, S-Y. Hwang, H-S.Jung and K-H. Lee, IGORR Transactions 2005, Gaithersburg, USA.
5. **Benchmark of heat deposition measurement techniques in the SAFARI-1 reactor using MCNP5**, B.M Makgopa, M. Belal, RRFM Transactions 2009, Vienna, Austria.
6. **Development, calibration and experimental results obtained with an innovative mobile calorimeter (CALMOS) for nuclear heating measurements**, H. Carcreff et al., ANIMMA 2011, June 2011, Gant, Belgium.
7. **Numerical and Experimental Calibration of a Calorimetric Sample Cell Dedicated to Nuclear Heating Measurements**, J. Brun et al., IEEE Transactions on Nuclear Science, publication accepted.
8. **Numerical study of heat transfer in a radiometric calorimeter dedicated to nuclear heating measurements**, C. Reynard-Carette et al., RRFM Transactions 2011, Rome, Italy.
9. **Numerical parametric study of heat transfer in a non adiabatic calorimeter without or with nuclear heating deposit**, O. Merroun et al., NURETH 2011, Toronto, Canada.
10. **Numerical study of the geometry impact on the heat transfer in a radiometric calorimeter dedicated to nuclear heating measurements**, M. Muraglia et al, RRFM Transactions 2012, Prague, Czech Republic.
11. **In-pile calorimetry: a thermal point of view**, C. Reynard-Carette et al., RRFM-IGORR, Transactions 2012, Prague, Czech Republic.
12. **CALMOS: Innovative Device for the Measurement of Nuclear Heating in Material Testing Reactors**, H. Carcreff, ISRD14, 2011, Omni Mount Washington Resort, USA.

REVIEW OF RETROSPECTIVE DOSIMETRY TECHNIQUES AND THEIR APPLICATION TO EXPERIMENTAL REACTORS

C. DESTOUCHES¹, N. THIOLLAY¹, G. GREGOIRE¹, D. BERETZ¹

¹ CEA², DEN, DER, Instrumentation Sensors and Dosimetry Laboratory

Cadarache, F-13108 Saint-Paul-Lez-Durance, France

J. NOWOSAD²

² Instytut Energii Atomowej POLATOM 05-400 Otwok Swjerk (Poland)

ABSTRACT

Knowledge of neutron induced embrittlement of reactor vessel or of experimental devices is a key issue for the operating time management of material test nuclear reactors, in particular pressurized water reactors. Experimental determination of the thermal and fast neutron fluences or dpa (displacement per atoms) is often technically impossible with the classical dosimetry techniques. The retrospective dosimetry technique can enable this fluence evaluation by measuring the activity of a sample taken from the chosen device for a radio-isotope which concentration is representative of the neutron fluence received. This technique, which makes possible the neutron fluence measurement at any accessible location in the reactor, implies to precisely know the initial concentration of the parent isotope. Sample collection can be done either "in vivo", if the amount of withdrawn material is small enough not to damage the device, or "post mortem" for destructive measurements. Based on existing retrodosimetry experiments conducted in various reactor facilities, a presentation of the method is performed. Then, possible benefits brought by its use on research reactors, such as the future JHR reactor facility (CEA Cadarache center-France), are discussed in the fields of operating life survey of the reactor and the experimental devices, experimental sample instrumentation and decommissioning operations.

1. Introduction

Knowledge of neutron induced embrittlement of nuclear reactor vessels or experimental devices is a key issue for the operating time management of material test nuclear reactors, in particular pressurized water reactors. As positioning of a set of dosimeters directly on the inner face of the reactor vessel is made impossible due to technical and safety limitations, neutron fluence or displacement per atom (dpa) are currently estimated by indirect calculations based on activity measurements performed at another location (surveillance capsule for example). Due to the increasing number of nuclear reactors approaching the fluence operating limit, an accurate fluence determination in a specific location different than the hot spot, a detected metallurgical defect for example, becomes a classical requirement. This requirement is generic to all types of power reactor BWR, PWR and VVER, but with a feature for VVER, where monitoring capsules are located only outside of the tank. Thus, retrospective dosimetry techniques have been applied successfully for years on all types of pressure water reactors, PWR ([1],[2],[3]), BWR [4] and especially on VVER ([5],[6]) with the following objectives: neutron calculation scheme qualification, enhancement of the reactor vessel embrittlement monitoring program, justification of the restart of a reactor after a failure or of the extension of operating time without a effective surveillance programme [6]. As "post mortem" neutron fluence measurements performed on samples after dismantling ([1],[7]) are by definition of low interest for predicting the operating life, the possibility of "in vivo" retrospective dosimetry techniques which do not jeopardize the integrity of the reactor vessel is investigated. In-core conditions (high radiation rate, sample size) make "in situ" measurements impossible. Consequently, this paper will focus on "destructive" methods which have to meet the following constraints:

- 1) Sample collection must be performed from the reactor vessel during an outage without jeopardizing the vessel integrity. Sample location has to be accurately known to get negligible in the final uncertainty.
- 2) Neutron fluence method should be validated and provide fluence level with an uncertainty of less than 10% ($k = 1$).

2. Retrospective dosimetry principle

Retrospective dosimetry principle is based on the intuitive idea to measure the neutron induced activity of a sample (few milligrams) taken from the studied device. This method makes possible to derive the actual local neutron fluence at any accessible location on the reactor vessel and internals, but implies to precisely know the initial content the isotope of interest. Table 1 lists main reactions suitable for this technique based on the following criteria: energy domain response of the cross section, measurability of radiation (energy and intensity of radioactive emission), decay period of measured radio-isotope (dosimeters mainly recall for the last 3 decay periods). Table 1 analysis shows that $^{93}\text{Nb} (n,n')^{93}\text{Nb}^m$ reaction is the optimal reaction in terms of spectrum covering and duration for the vessel steel embrittlement following. The main problem for thermal neutrons fluence determination, one of the aluminium vessel embrittlement initiators, is not the activity measurement, but the fluence derivation process and its representativeness because of the extreme sensitivity of thermal flux to local irradiation conditions.

Reaction	Response Energy Domain	Decay period	“Optimal Memory”
$^{94}\text{Zr} (n, \gamma) ^{95}\text{Zr}/^{95}\text{Nb}$	Thermal	64.0 days	200 days
$^{54}\text{Fe} (n, \gamma) ^{55}\text{Fe}$	Thermal	2.72 years	8 years
$^{58}\text{Fe} (n, \gamma) ^{59}\text{Fe}$	Thermal	44.5 days	150 days
$^{59}\text{Co} (n, \gamma) ^{60}\text{Co}$	Thermal	5.14 years	15 years
$^{98}\text{Mo} (n, \gamma) ^{99}\text{Mo} \rightarrow ^{99}\text{Tc}^m \rightarrow ^{99}\text{Tc}$	Thermal	210 000 years	600 000 years
$^{58}\text{Ni} (n, \gamma) ^{59}\text{Ni}$	Thermal	76 000 years	230 000 years
$^{62}\text{Ni} (n, \gamma) ^{63}\text{Ni}$	Thermal	96 years	300 years
$^{93}\text{Nb} (n, \gamma) ^{94}\text{Nb}$	Thermal	20300 years	61000 years
$^{93}\text{Nb} (n, n') ^{93}\text{Nb}^m$	$E > 0.5\text{MeV}$	16.13 years	50 years
$^{58}\text{Ni} (n,p) ^{58}\text{Co}$	$E > 2\text{-}3\text{MeV}$	70.8 days	7 months
$^{54}\text{Fe} (n, p) ^{54}\text{Mn}$	$E > 2\text{-}3\text{MeV}$	312.14 days	2.5 years
$^{14}\text{N} (n, p) ^{14}\text{C}$	$E > 5\text{ MeV}$	5700 years	17000 years
$^{56}\text{Fe} (n,p) ^{56}\text{Mn}$	$E > 5\text{MeV}$	2.58 hours	7 hours

Table 1: main reactions suitable for retrospective dosimetry

3. The retrospective dosimetry technique

3.1. Description of the technique

Samples can come either from a replaced piece of the studied device such as a screw or from a mechanical collection on the device using milling or grinding processes. A sample collection device applied to the reactor vessel Czech Dukovany reactor vessel [8] is shown in Figure 2 where a drill bit produces chips that are sucked by a pump and collected on a filter (Figure 3). Figure 1 shows the state of the vessel inner wall after removal at the Ringhals facility (Sweden) [9]. Highlights of these samples lie in the knowledge of the location of

sampling and the low mass collected (few hundred milligrams) which, together with a method of collection control, make sure not to damage the coating. One notes also, that only the inner surface of the vessel can be analysed.

Fig. 1 : State of the inner vessel wall after sample collection

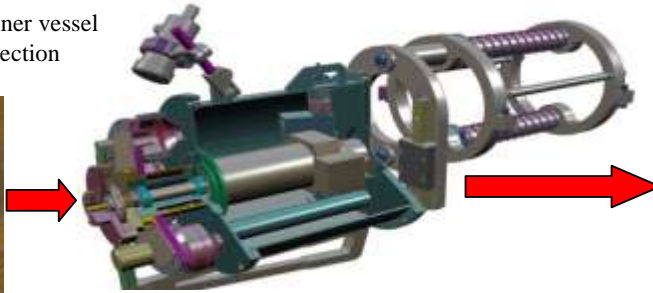


Fig.2 : Sampling device OVZ (Dukovany)

Fig. 3 : collected chip samples



As the direct activity measurement is generally impossible in the solid sample, ample preparation process aims at enabling the activity measurement of the radio-isotope of interest by eliminating the other emitting radio-isotopes and getting a suitable geometry..

The first operation is to extract the isotope to be measured starting with a chemical separation. The first step is the dissolution in a concentrated acid mixture solution (HCl, HNO₃ and HF) [10]. The ion-exchange technique is then used to separate the isotope of interest, more precisely the target ion [11]. At the end of this process, the activity of the remaining solution is ready to be measured either directly on the liquid solution or on a solid state deposit obtained by evaporation. Dissolution and separation processes are optimized to minimize uncertainties associated with the risk of handled material loss. Radioactive tracers are used to ensure consistency in the amount of material at different stages.

The sample activity obtained is measured by conventional techniques: liquid scintillation counter (LSC) for α and β emitters or hyper pure germanium diode with geometry and sensitivity adapted to the measured radiation (X or γ). The uncertainties on activity measurements (ε , given at $k=1$) can be decomposed into three main sources: nuclear data (I_γ , $\varepsilon= 1$ to 5%), counting statistics (background noise, dead time, $\varepsilon= 1\%$ to 20%) and measurement chain calibration ($\varepsilon= 1\%$ to 5%) [11].

The mass (i.e. the number of nuclei) of the prior isotope (an impurity in most of the cases) has to be determined in order to establish a specific activity. Three techniques are available: Inductively Coupled Plasma Mass Spectrometry (ICP-MS [10]), Neutron Activation Analysis (NAA [10]) and Total Reflection of X-ray Fluorescence (TRXRF [12]). They allow the concentration measurement of a few ppm with an accuracy of a few percents [10]. One should note that the radio-isotope of interest content is too low to be measured by any of these methods.

An alternative method for measuring the number of atoms $^{93}\text{Nb}^m$, the Resonance Ionization Mass Spectroscopy method (RIMS) based on the differences between levels of excitation and ionization of $^{93}\text{Nb}^m$ and ^{93}Nb , has been tested in the mid 90's [13]. Authors conclude on the theoretical feasibility of the measurements with selectivity up to ten decades on the $^{93}\text{Nb}^m/^{93}\text{Nb}^m$ ratio. But they also stress out the need of instrumentation improvements and the lack of nuclear data which has prevented them from applying this technique.

The experimental specific activity and its associated uncertainty are finally calculated by the composition of the previous results. Measured values are then compared with calculated ones derived from an activation code based on the resolution of the Bateman equations. In this activation calculation process, the relative irradiation history knowledge is a key point, especially as the dosimeter recalls the information mainly for the last three periods: the shorter the decay period is, the better the knowledge of irradiation history has to be.

3.2. Performances / limitations

Typical uncertainty values obtained from the retrospective dosimetry technique range from 5% to 20% ($k=1$) depending on measurement conditions and sample composition. Following remarks on performances and limitations can be stress out concerning the use of:

Niobium (^{93}Nb (n, n') $^{93}\text{Nb}^m$): decay period (16.1 years) and reaction threshold ($E > 0.5$ MeV) give access to optimal information for neutron induce embrittlement. Nevertheless, niobium content in the steel must be at least of 50 ppm to be measured by ICP-MS, INAA or TRXRF techniques with an acceptable accuracy [10]. Chemical separation of niobium is necessary due to the presence of cobalt which induces an important sample activity. Moreover, the molybdenum/Niobium content ratio must be lower than the unity to allow for a correct measurement and even less than 1% for neglecting the contribution of Mo [7]. Indeed, ^{92}Mo isotope (14.89% of the natural Molybdenum) decays into $^{93}\text{Nb}^m$ with a decay period of 4000 years with unfortunately an approximately known branching ratio.

Iron (^{54}Fe (n, p) ^{54}Mn) - [14]: This isotope, naturally present in every steel alloy, is a good indicator of the fast neutron fluence with interesting threshold (2.5 MeV) and decay period (312.14 days). In most of the cases, presence of other radio-isotopes (such as cobalt) requires a chemical separation of the ^{54}Mn to allow for the activity measurement.

Nitrogen in steel (^{14}N (n, p) ^{14}C) - [15]: Although interesting cross section (80 mbarn) and energy threshold (5 MeV), ^{14}C activity measurement interpretation requires the knowledge of the initial content of nitrogen dissolved in steel (a few tens of ppm) as well as the knowledge of its diffusion law. The use of this reaction requires further analysis to assess the feasibility, especially to reduce uncertainties.

Thermal reactions such as $^{54}\text{Fe}(n, \gamma)^{55}\text{Fe}$, $^{59}\text{Co}(n, \gamma)^{60}\text{Co}$, $^{98}\text{Mo}(n, \gamma)^{99}\text{Mo} \rightarrow ^{99}\text{Tc} \rightarrow ^{99}\text{Tc}^m$, $^{58}\text{Ni}(n, \gamma)^{59}\text{Ni}$, $^{62}\text{Ni}(n, \gamma)^{63}\text{Ni}$ and $^{93}\text{Nb}(n, \gamma)^{94}\text{Nb}$: Their activity measurements are generally easy because of the high level of the thermal cross section. They give information on thermal and low epithermal flux over a period depending on the selected radioisotope decay constant. Nevertheless, sample collection location knowledge is a key point to derive and analyze the neutron fluence because the flux level and the spectrum are very sensitive to the surrounding material: thermal neutron mean free path is of a few millimetres.

4. Application to experimental reactors

Potentialities of retrospective dosimetry technique presented in the previous paragraph lead to study its application in experimental test reactors. First, reactor vessel surveillance can be performed by measurements of some of isotopes present in the material identified by a detailed analysis of the composition. A similar process can be done for the internal devices, as well as for the irradiation devices surveillance. It can be completed by post irradiation retrospective dosimetry on some mechanical pieces withdrawn at specific time. The actual received neutron fluence, given with an uncertainty around 5%, can bring important elements for the operating life justification /extension for irradiations devices by reducing safety margins. Another important issue is, complementarily to a classical dosimetry, the determination of neutron fluence (fast or thermal) in irradiated samples at a location where a classical dosimeter cannot be implemented. For example, this method can give access either to the detailed fluence repartition in the sample or to value at the exact crack location of a metallurgic sample. At last, retrospective dosimetry can be applied to get accurate waste activity estimation in the dismantling operations: the measured fluence at some specific locations can reduce uncertainties on activity calculated for the entire device and optimise their treatment. All these uses can be enhanced if taking into account the design stage of the device conception by addition of a small but well characterised amount of suitable impurities containing isotopes of interest.

5. Conclusions

This paper presents the retrospective dosimetry technique which allows for a measurement at any location accessible from the reactor vessel or internal device based on the activity measurement of a little amount of material. Performances and limitations of this method, dependant on the chosen isotope, make possible the application to experimental reactors for neutron fluence monitoring of the reactor vessel, the experimental capsule or even the irradiated samples themselves with a typical accuracy lower than 10%. This uncertainty can be lowered by taking into account retrospective dosimetry needs in the initial device design (adjunction of specific isotopes). This method has been identified in recent years as a promising technique by scientific and industrial actors ([17],[5]) for the fluence determination improvement. Nevertheless, developments are still needed to reduce uncertainties and to lower isotope detection limits, in particular a special attention has to be paid to alternative measurement techniques (RIMS). Finally, retrospective dosimetry should become a valuable tool completing the existing instrumentation techniques panel use in the experimental test reactor, such as the JHR reactor facility, on the condition of being taken into account in the initial design phase.

6 References

- [1] D. Beretz, C. Destouches and al. « Reaction rates measurement across the pressure vessel of Chooz-A PWR by self-dosimetry technique » *Proceedings of 10th International Symposium on Reactor Dosimetry*,
- [2] A. Vasiliev and al. "Development of a CASMO-4/SIMULATE-3/MCNPX calculation scheme for PWR fast neutron fluence analysis and validation against RPV scraping test data", *Annals of Nuclear Energy* 34 (2007), p. 615-627
- [3] J. Wagemans and al., "A retrospective dosimetry feasibility study for the ATUCHA I", *Proceedings of the 13th International Symposium on Reactor Dosimetry*, Netherlands 2008, p.50-57
- [4] L.R. Greenwood, and al. "Retrospective reactor dosimetry for neutron fluence, helium and boron measurements", *Reactor Dosimetry in the 21st century*, Belgium 2002, p. 32-39
- [5] K. Ilieva and al. "Reactor dosimetry for VVERs: past and future", *Nuclear Engineering International*, August 2010, p.13-19
- [6] S.M. Zatrisky, and al. "Measurement and Calculation of WWER-440 Pressure Vessel Templates Activity for Support of Vessel Dosimetry", *Journal of ASTM International*, Vol.3, No.10 (2006)
- [7] U. Rindelhardt and al., "RPV material investigations of former VVER-440 Geiswald NPP" *Nuclear Engineering and Design* 239 (2009), p. 1581-1590
- [8] M. Ruchar and al. "Sampling of reactor pressure vessel inner cladding for retrospective dosimetry analysis", *18th International Conference on Structural Mechanics in Reactor Technology*, China 2005, p. 725-732
- [9] L.R. Greenwood, and al. "Retrospective dosimetry analyses of reactor Vessel Cladding samples" *International Symposium on reactor Dosimetry - ISR14 – Brettonwoods USA May 2011 – to be published*
- [10] W. P. Voorbraak and al. "Retrospective dosimetry of fast neutrons focussed on reaction $^{93}\text{Nb}(n,n)^{93}\text{Nb}^m$ (RETROSPEC), Euratom - Final report of EC project, Contract No: FIKS-CT-2000-91 2003
- [11] D.A. Skoog., and al. « *Chimie analytique*, 1ère édition » Bruxelles, Éd.De Boeck, 1997, p. 710-714
- [12] N.L. Misra and al. "Determination of trace elements in uranium oxide by Total Reflection X-ray Fluorescence spectrometry" *Spectrochimica Acta Part B* 60(2005) 834-840
- [13] B. Bars, K. Uusheimo, "Experiences with Nb dosimeters for neutron flux measurements", *7th ASTM-EURATOM Symposium on Reactor Dosimetry*, France 1990, p. 331-338
- [14] C.R. Harvey, and al. "Development of Method for the Determination of Mangyrase-54 in long-cooled active steel samples", *Proceedings of 9th International Symposium on Reactor Dosimetry*, Czech Republic 1996
- [15] J. Konheiser and al. "Application of different nuclides in retrospective dosimetry" *International Symposium on reactor Dosimetry - ISR14 – Brettonwoods USA May 2011 – to be published*
- [16] H.M. Lauranto and al. "Hyperfine structure studies of ^{93}Nb by three step resonance ionization spectroscopy" *Spectrochimica Acta Part b* 51 (1996) 175-180
- [17] A. Ballesteros « Open issues in reactor dosimetry » *Progress in nuclear energy* 52 (2010) 615-619

THERMAL HYDRAULIC AND NEUTRONIC CORE MODEL FOR POWER TRANSIENT ANALYSES OF REFLECTOR EXPERIMENTAL DEVICES DURING SHUTDOWNS IN JULES HOROWITZ REACTOR (JHR)

P. CONSOLE CAMPRINI, M. SUMINI

*University of Bologna
Via Risorgimento 2, 48018 Faenza – Italy*

C. ARTIOLI

*National Agency for New Technology, Energy and Sustainable Economic Development (ENEA)
Via Martiri di Monte Sole 4, 40129 Bologna – Italy*

C. GONNIER, B. POUCHIN, S. BOURDON

*Atomic Energy Commission (CEA)
Saint Paul Lez Durance, 13108 – France*

ABSTRACT

The Jules Horowitz Reactor (JHR) is expected to become the most important material testing reactor in the framework of European nuclear research and development. It is designed to exploit a fast in-core spectrum as well as a thermal neutron flux within the experimental locations in the reflector. The latter are mainly used to investigate fuel behaviour under nominal, abnormal and post-failure operating conditions. Since the core power is relatively high (100 MW), the power released within the reflector fuel devices is not negligible. Heat removal is a main topic in nuclear safety and power transient analyses concerning these experimental devices are requested in order to control fuel samples heating.

Here a model of JHR core is implemented by means of the pointwise kinetics code DULCINEE. It takes into account both the neutronic features of the system and the thermal hydraulic properties as far as reactivity feedbacks are concerned. The core power transients are evaluated with respect to normal shutdown and safety shutdown.

Then neutronic coupling between reflector and core is computed by means of the Monte Carlo calculation code TRIPOLI 4.7. Thus power evolution in experimental devices is obtained accounting for four burnup levels during the equilibrium cycle – namely Beginning of Cycle (BOC), Xenon Saturation Point (XSP), Middle of Cycle (MOC) and End of Cycle (EOC). Fission energy is released through different nuclear interactions. Depending on the considered radiation, the yield of energy deposition is different and the time behaviours are specific to particle production mechanisms. Finally neutrons and gammas are considered in terms of energy deposition and contribution to total in-reflector fuel sample power transients during the considered shutdown procedures.

1. Introduction

European nuclear industry challenges are getting more and more focused on material research in order to enhance present power plant performances and prepare for development of next GenIV reactors. Sustainability of nuclear energy is a key feature concerning both the exploitation of existing plants and the role of this important source in future global scenarios. Thus the French Atomic Energy Commission has launched the construction of the Jules Horowitz Reactor (JHR) which is expected to become the most important material testing reactor in Europe for the next decades. The present work has been

performed within the collaborations between the University of Bologna, the Italian National Agency for New Technology, Energy and Sustainable Economic Development (ENEA) and the French Atomic Energy Commission (CEA) in the framework of JHR project and the European research reactor network.

JHR is designed to reach a 100 MW core power in order to achieve high neutron fluxes and it is conceived to perform many experiments at the same time thanks to several irradiation positions. The fast in-core flux is mainly devoted to structural material tests, on the other hand a thermal flux is available within the reflector since different devices are designed to be located there aiming at fuel performance enhancement study.

JHR core is a 60 cm height cylindrical rack in which 37 drilled holes host either 3 “large” experimental positions or 7 “small” device locations. Remaining 27 spaces are devoted to cylindrical plate fuel elements and, particularly, to a uranium silicide metallic fuel 27% U235 enriched. This present analysed starting configuration is expected to be replaced by a UMo metallic fuel 20% 235U enriched. Latter positions are planned also for control rod insertions. In fact 27 hafnium safety devices are necessary both to manage experimental conditions and to secure reactor operations.

All around the core several devices for fuel tests are placed within the beryllium reflector. MADISON is designed to study fuel performances under nominal conditions and it is capable to host 4 UO₂ low enriched LWR fuel pins. ADELIN is expected to investigate abnormal operating parameters up to cladding failure, it is loaded with 1 UO₂ low enriched LWR fuel pin. Conversely, MOLFI device is devoted to molybdenum production for medical purposes. It is fuelled with AIU targets 93% 235U enriched according to present time configuration, a LEU version is still under development.

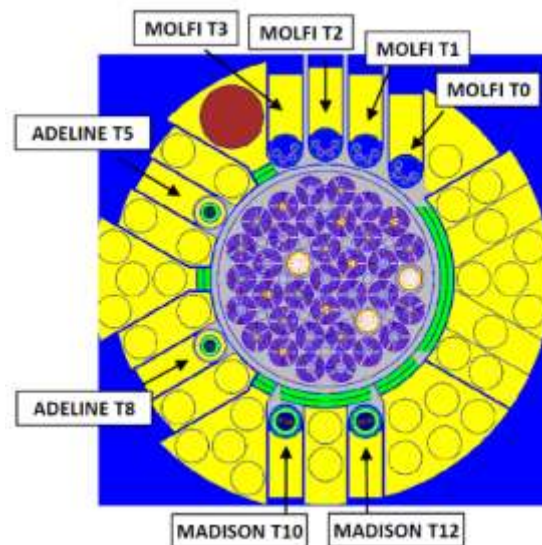


Fig.1 Configuration of JHR reflector devices.

As core power is relatively high, it is worth to consider decay heat removal even for experimental devices charged with fuel, since safety issues during shutdown procedures are main topics in nuclear reactor design and analysis. This simulation has been performed starting from core power shutdown transients concerning four different configurations during equilibrium cycle – namely Beginning of Cycle (BOC), Xenon Saturation Point (XSP), Middle of Cycle (MOC) and End of Cycle (EOC).

2. Shutdown Procedures

The first part of this study has aimed at the calculation of reactor core power evolution during different shutdown procedures. In fact both a normal shutdown (NS) and a safety shutdown (SS) are envisaged in order to assure a proper reactor piloting.

Among the 27 control rods described above, 4 are clustered in a bank – namely the safety rods (SR) – and kept always outside the core except for shutdown. The second bank is

formed by 4 pilot rods (PR) which are placed as close as possible to the core mid-plane. The remaining 19 compensation rods (CR) are used to balance fuel depletion and core poisoning due to fission products buildup.

During normal shutdown, only pilot rods are completely inserted starting from their criticality position which depends on time step in equilibrium cycle. Thus they achieve different reactivity worth.

Safety shutdown is obtained triggering a normal shutdown and inserting the safety rods at the same time from above in order to reach a reactivity effect significantly higher than in the previous shutdown.

3. Model and Methodology

Foremost, the core power evolution during normal and safety shutdown has been evaluated by means of the pointwise kinetics code DULCINEE which was developed by French Radiation Protection and Safety Institute (IRSN).

Power evolution is determined by both control rods reactivity and temperature effects - as far as reactivity feedbacks are concerned.

Kinetics features of the system have been taken into account for the different configurations.

	BoC	XSP	MoC	EoC	Λ
β_{eff}	720 pcm	718 pcm	712 pcm	705 pcm	39,43 μs
β_1 [S]	β_2 [S]	β_3 [S]	β_4 [S]	β_5 [S]	β_6 [S]
0,0404	0,1795	0,1743	0,3794	0,0837	0,1427
λ_1 [s ⁻¹]	λ_2 [s ⁻¹]	λ_3 [s ⁻¹]	λ_4 [s ⁻¹]	λ_5 [s ⁻¹]	λ_6 [s ⁻¹]
0,01330	0,03250	0,12182	0,31651	0,98880	2,94945

Table 1 Standard six families delayed neutron for precursors kinetic parameters (APOLLO2 code).

Thus a specific thermal hydraulic model has been conceived to match the code in-built functions regarding material properties and fuel element shape. In fact proper analogy holds if parameters which influence the time evolution of the systems are coherently chosen. According to that, a simplified and representative fuel plate has been proved to exhibit the requested temperature profile.

Fuel meat length	63.35 mm
Fuel meat thickness	0.61 mm
Cladding thickness	0.38 mm
Plate side thickness	8.42 mm
Fuel plate height	600.00 mm
Hydraulic diameter	3.71 mm
Wet perimeter	16.4 cm
Fuel volume	23.18 cm ³
Cladding volume	28.88 cm ³
Plate sides volume	13.83 cm ³
Coolant volume	91.25 cm ³
Fuel/Cladding surface	760.17 cm ²

Table 2 Equivalent plate dimensions.

Cooling water mass rate	1803 kg/s
Coolant inlet temperature	30.0 °C
Core inlet pressure	9.3 bar
Core outlet pressure	6.3 bar
Core pressure drop	3.0 bar

Table 3 Core T/H features.

Thermal hydraulic analysis and neutronic evolution of the system are strictly connected by the reactivity coefficients listed below.

Moderator coefficient	-19,5 pcm/°C	max value at 40°C
Doppler coefficient	-2,94 pcm/°C	max value at 90°C
Void coefficient	-4,53 10 ⁵ pcm/m ³	for coolant total volume

Table 4 Feedback coefficients

Once power transients computed, the neutronic coupling between the core and the in-reflector devices has been found using the Monte Carlo transport code TRIPOLI 4.7. In fact, the energy deposition due to neutrons and gamma radiation has been obtained both for core fuel elements and for reflector test devices.

After a first order evaluation, in the present work, prompt and delayed effects have been lumped together keeping this approximation conservative. Thus gamma and neutron contributions are considered to vary - as the core power decreases - remaining proportional through the same coefficient.

Moreover the core-to-device power ratio is supposed to rapidly change during transients but it has kept as a constant corresponding to total insertion coupling configuration for both the shutdown procedures.

In order to consider the safety analysis for device cooling issues, the entire equilibrium cycle has been taken into account – namely depletion effects on evolution of flux distribution are considered.

4. Simulation and Results

Starting from control rod insertions and associated reactivity worth, the code DULCINEE allowed to compute the thermal core power evolution.

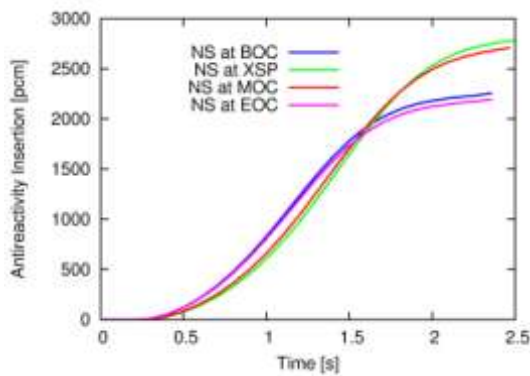


Fig.2 Normal shutdown.

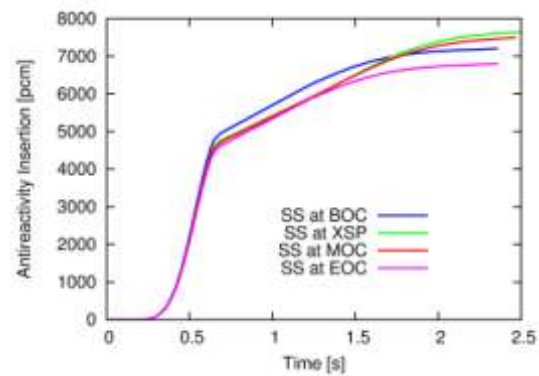


Fig.3 Safety shutdown.

The fuel composition during the equilibrium cycle has been considered since control rods antireactivity injection is influenced by initial criticality insertion.

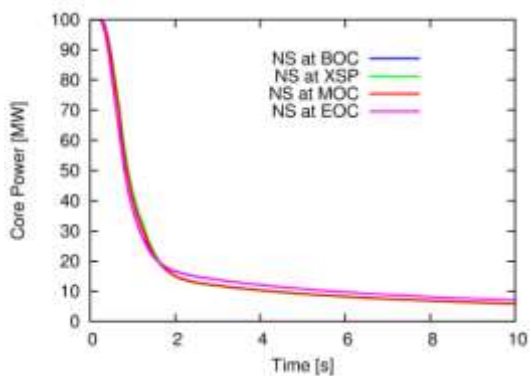


Fig.4 Normal shutdown.

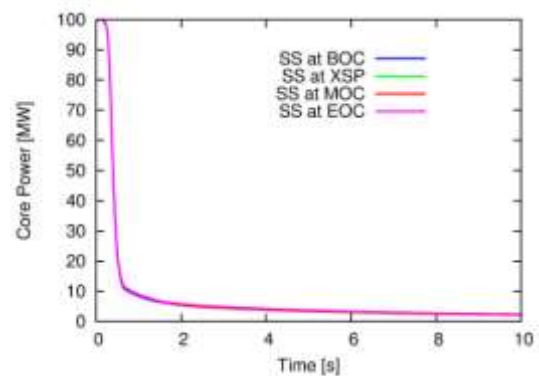


Fig.5 Safety Shutdown.

The data show a slight dependence on burnup for what concerns NS core transients. The higher amount of antireactivity insertion occurring during SS makes it rather independent of time step in equilibrium cycle. Then the more conservative profile has been used for NS evaluations in order to calculate device transients.

Regarding neutronic coupling effects, TRIPOLI 4.7 model has utilized a configuration in which 4 MOLFI, 2 MADISON and 2 ADELIN test devices are placed within the reflector.

An energy deposition ratio referred to nominal power (100 MW) has been evaluated for every test sample in the reflector as all reactions are supposed to be prompt. Results show these coupling coefficients being influenced during equilibrium cycle only for MOLFI as the enrichment is higher. On the other hand MADISON and ADELIN core-device interaction can be thought as constant.

Gamma and neutron contribution ratios do not exhibit significant variation both during cycle and regarding control rod insertions.

		BOC	XSP	MOC	EOC	Neutron	Gamma
MADISON T10	Reference	0,12%	0,12%	0,11%	0,11%		
	After Normal Shutdown	0,12%	0,13%	0,12%	0,11%	84%	16%
	After Safety Shutdown	0,13%	0,14%	0,13%	0,11%		
MADISON T12	Reference	0,12%	0,12%	0,11%	0,11%		
	After Normal Shutdown	0,12%	0,11%	0,10%	0,10%	84%	16%
	After Safety Shutdown	0,12%	0,12%	0,11%	0,11%		
ADELINE T8	Reference	0,05%	0,06%	0,06%	0,06%		
	After Normal Shutdown	0,06%	0,07%	0,07%	0,06%	66%	34%
	After Safety Shutdown	0,06%	0,07%	0,08%	0,07%		
ADELINE T5	Reference	0,05%	0,06%	0,06%	0,06%		
	After Normal Shutdown	0,05%	0,06%	0,06%	0,07%	66%	34%
	After Safety Shutdown	0,06%	0,06%	0,07%	0,07%		
MOLFI T2	Reference	0,62%	0,58%	0,58%	0,67%		
	After Normal Shutdown	0,64%	0,61%	0,61%	0,69%	96%	4%
	After Safety Shutdown	0,76%	0,70%	0,70%	0,81%		
MOLFI T3	Reference	0,62%	0,61%	0,62%	0,66%		
	After Normal Shutdown	0,66%	0,65%	0,66%	0,69%	96%	4%
	After Safety Shutdown	0,76%	0,74%	0,73%	0,79%		
MOLFI T0	Reference	0,62%	0,60%	0,59%	0,68%		
	After Normal Shutdown	0,61%	0,57%	0,57%	0,66%	96%	4%
	After Safety Shutdown	0,70%	0,65%	0,64%	0,76%		
MOLFI T1	Reference	0,61%	0,57%	0,57%	0,68%		
	After Normal Shutdown	0,61%	0,57%	0,57%	0,68%	96%	4%
	After Safety Shutdown	0,72%	0,65%	0,65%	0,79%		
Total	Reference	2,82%	2,71%	2,71%	3,03%		
	After Normal Shutdown	2,87%	2,76%	2,76%	3,07%	94%	6%
	After Safety Shutdown	3,32%	3,13%	3,11%	3,50%		

Table 5 Device-core coupling coefficients.

Then it has been possible to evaluate thermal power transients for every in-reflector device, starting from the core power evolution during different shutdowns and the coupling coefficient listed above. MADISON power evolution can be computed through an average and conservative ratio of about 0,13 %.

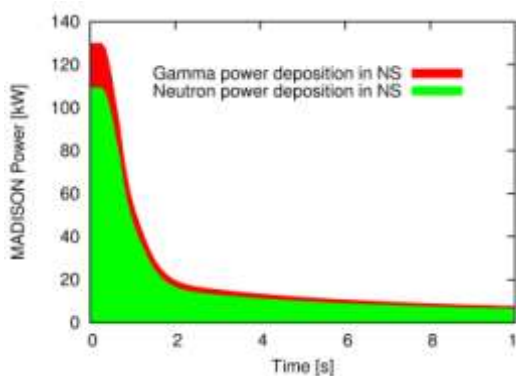


Fig.6 MADISON power (normal shutdown).

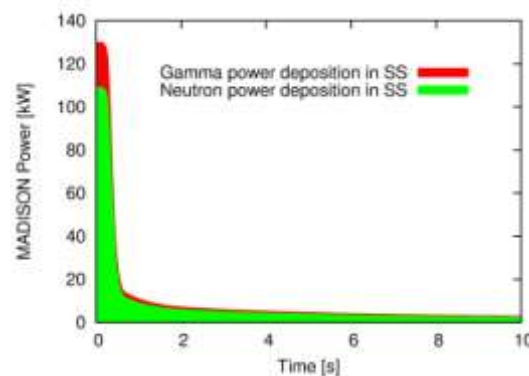


Fig.7 MADISON power (safety shutdown).

A representative ADELIN power transient has been inferred by means of a coupling ratio of about 0,07 %, as follows.

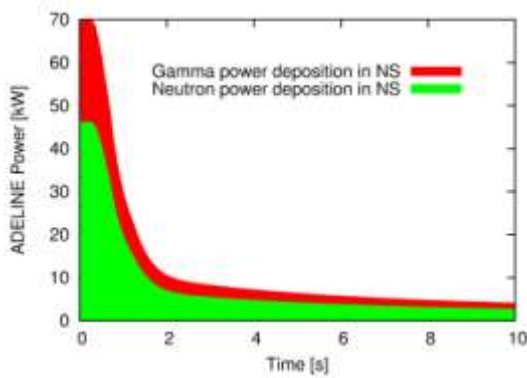


Fig.8 ADELIN power (normal shutdown).

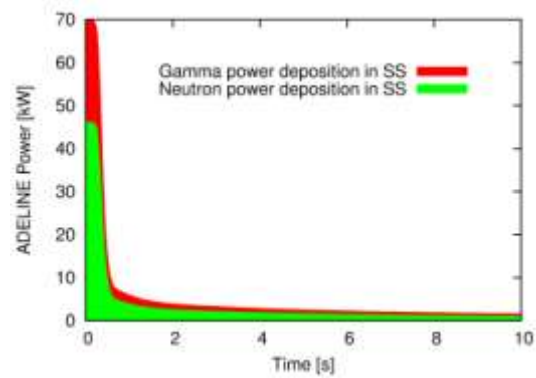


Fig.9 ADELIN power (safety shutdown).

In the same way MOLFI transients have been described by an average coupling coefficient of about 0,8%.

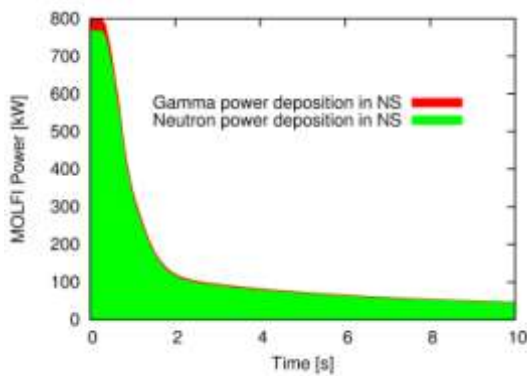


Fig.10 MOLFI power (normal shutdown).

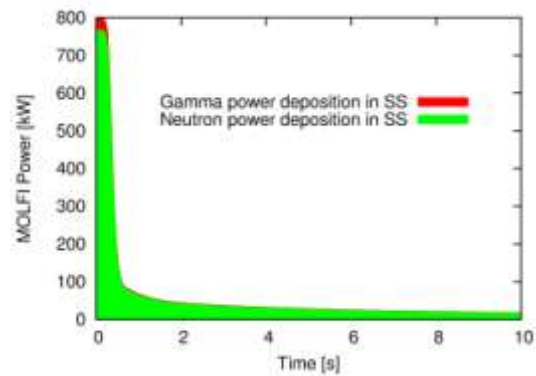


Fig.11 MOLFI power (safety shutdown).

5. Conclusions and Perspectives

In the present work, a simplified model has been conceived in order to properly analyse the thermal power transients within the fuel loaded test samples of Jules Horowitz material testing Reactor (JHR), during normal and safety shutdowns.

Core power evolution has been computed by means of the pointwise kinetics code DULCINEE. Through the Monte Carlo code TRIPOLI 4.7 reflector-core neutronic coupling has been evaluated with respect to MADISON, ADELIN and MOLFI in-reflector test devices. This first approach is supposed to be enhanced considering different time-scale delayed nuclear heating effects and performing several sensitivity calculations concerning particular device neutronic features. The present analysis is aimed at a more detailed description of power evolution within devices in order to be able to better manage and optimise JHR experimental capability.

References

- [1] P. Console Camprini, M. Sumini, C. Artioli, C. Gonner, B. Pouchin, S. Bourdon, *In International Conference on the PHYSICS Of Reactors, PHYSOR*, Knoxville USA (2012)
- [2] D. Iracane, P. Chaix and A. Alamo, "Jules Horowitz Reactor: a High Performance Material Testing Reactor", *C. R. Physique*, **9** (3-4), pp. 445-456 (2008).
- [3] D. Iracane, "Jules Horowitz Reactor, a new Material Testing Reactor in Europe", *In 10th Meeting of the International Group On Research Reactors, RRFM*, Washington USA, (2005).
- [4] P. Roux, C. Gonner, D. Parrat and C. Garnier, "The MADISON experimental hosting system in the future Jules Horowitz Reactor", *In 13th Meeting of the International Group On Research Reactors, RRFM*, Knoxville USA, (2010).

A PRELIMINARY SURVEY ON WORLDWIDE RECENT ACTIVITIES IN RESEARCH REACTORS CENTRES FOLLOWING THE ACCIDENT AT TEPCO's Fukushima-Daiichi NPPs

Y. BARNEA, N. PELD, P. ADEL FANG

Research Reactors Section, NEFW, IAEA.

VIC, PO Box 100, Vienna, Austria

D. RIDIKAS

Physics Section, NAPC, IAEA

VIC, PO Box 100, Vienna, Austria

A.M.A. SHOKR

Research Reactors Safety Section, NSNI, IAEA

VIC, PO Box 100, Vienna, Austria

ABSTRACT

Following the events at TEPCO Fukushima-Daiichi NPP (TEPCO's F-D NPPs) accident, there has been a worldwide initiative to perform complementary safety assessments of nuclear installations. Correspondingly, the community of research reactor (RR) stakeholders, operators and regulators expressed publically their readiness to re-evaluate and update the safety status of the facilities facing a possibility of similar external events. Although the RRs are generating (on average) one thousand times lower energy than NPPs, and consequently their radioactive source term is much smaller, there are several important common safety related topics to be checked and revised (i.e. the seismic design, blackout, safety design scenarios during the loss of ultimate heat sink, accident management, regulations, crisis management, etc.).

As the first immediate step to assist the Member States (MS) regarding the lessons learned from the accident, the IAEA distributed a topic-specific questionnaire. The purpose of this questionnaire was to collect from MS operating RRs, some preliminary information on the types of activities initiated as a result of the unprecedented TEPCO's F-D NPPs accident last March. The questionnaire contained two general questions and three specific questions with multiple proposed answers and it was acceptable to mark more than one answer for each question.

By the end of January 2012, sixty three (63) answers were received, from 35 MS (out of 56 operating RRs). Only one out of four answered the first question by mentioning that no dedicated activity was requested after the TEPCO's F-D NPPs accident. Moreover, one out of five reported revisions in the Design Base Accidents (DBA) list as well as in the Emergency Preparedness Programme (EPP), although only one out of three made changes in the EPP. Finally, two out of three answers indicated no changes in the utilization/operation plan following the lesson learned from the accident. It should be noted that it was not possible to measure the degree of completeness of the activity (i.e., whether the activity is considered, in progress, or completed). The paper's purpose is to present the responds to the questionnaire reflecting the information on the activities initiated by research reactor operators following the TEPCO's F-D NPPs accident, in order to plan the IAEA follow-up on the subject, within the cross cutting section's activities -CCCGR.

1. INTRODUCTION

As a result of TEPCO's F-D NPPs accident, there has been a worldwide initiative to perform complementary safety assessments of nuclear installations. Correspondingly, the Research Reactors (RRs) community including stakeholders, operators and regulators expressed publically their readiness to re-evaluate and update the safety status of the facilities, facing a possibility of similar external events. Although the RRs are generating (on average) one thousand times lower energy than Nuclear Power Plants (NPPs), and their radioactive source term is significantly lower, there are important common safety topics to be checked (e.g. siting and design provisions against external hazards, design-Basis Accidents and safety margins considered in the safety demonstration, design provisions for ensuring basic safety functions, blackout initiated events, safety of spent fuel storage facilities within the reactor building, and emergency organization/crisis preparedness). In June 2011 the Technical Working Group for Research Reactors (TWGRR)

advised the Agency to present in the International Conference on Research Reactors (Rabat, November 2011), the response of RR operators to the TEPCO's F-D NPPs accident, regarding the safety of their facilities [1].

As a first response the RRS/NEFW, as the Cross Cutting Coordinator Group on RR in the IAEA, distributed a Questionnaire to the MS operating RRs. The Questionnaire, provided in the Annex, contained two general questions and three specific questions with multiple proposed answers. For the specific questions, it was acceptable to mark more than one answer for each question. Due to time limitations and because of the nature of the accident, the targeted RRs were those facilities that potentially cause a higher risk (only RRs with a power level greater than 1 MW were selected). The purpose of this questionnaire was to collect from Member States operating RRs preliminary information on the types of activities initiated as a result of the unprecedented accident. In the preparation of the Questionnaires, the basic ideas from the recommended actions published for the TEPCO's F-D NPP accident [2] (and relevant to RRs) were followed, including:

1. Hardware preparation to protect the safety Systems, Structures and Components (SSCs) from external events;
2. Preparation for variety of power sources;
3. Consideration and preparation for variety of cooling systems;
4. Adequate enhanced Emergency Preparedness Plans (EPPs);
5. Hardware preparation for the AM such as multiple wiring for power source;
6. Training and education of AM;
7. AM for spent fuel storage facilities;
8. Improvement of accident scenarios analysed and human resources development;
9. Reassessment of public information disclosure and information sharing;
10. Detailed evaluation for the seismic design, including updating the database.

The first results are available in the Proceedings of the International Conference on Research Reactors: Safe Management and Effective Utilization, 14-18 November, 2012, Rabat, Morocco [3].

2. RESPONDING ORGANIZATIONS

By the end of January 2012, sixty three (63) answers were received, from thirty five (35) MS (out of 56 operating RRs). Ten (10) answers were received from non-operating organization (i.e. regulators), six (6) replies were received from RRs with the maximum nominal power smaller than the targeted threshold of 1 MW, one (1) answer was received from a project manager of a RR under construction and one (1) reply was from a decommissioned reactor. At this preliminary stage, the decision was to include in the report all the replied Questionnaires. It should be mentioned that following the answers, it is impossible to measure the degree of completeness of the activity reported (i.e. whether the activity is considered, in progress, or completed).

3. RESULTS PROCESSING

The results received on the first general question: *What was done in your organization following the F-D event*, are depicted as a pie chart in [Fig. 1](#). The chart indicates that 74 per cent of organizations surveyed launched some dedicated activities (all colours except blue) following the TEPCO's F-D NPP accident. Considering the specific activities performed, many organizations (red & orange & light blue & light green) reported a short re-evaluation of the DBA list in the Safety Analysis Report (SAR) and/or a revision in the EPP. Further comprehensive activities, such as including a complete re-evaluation of the SAR and of the EPP were reported by a smaller number of organizations (green & orange & light green), as these considerable changes are usually requested and approved by the regulatory bodies, and therefore are included in a long term and complex process. The rest of the answers (purple & turquoise) are mentioning unspecified activities of revision the systems and/or the emergency procedures, which can indicate that the activities are not yet completely defined.

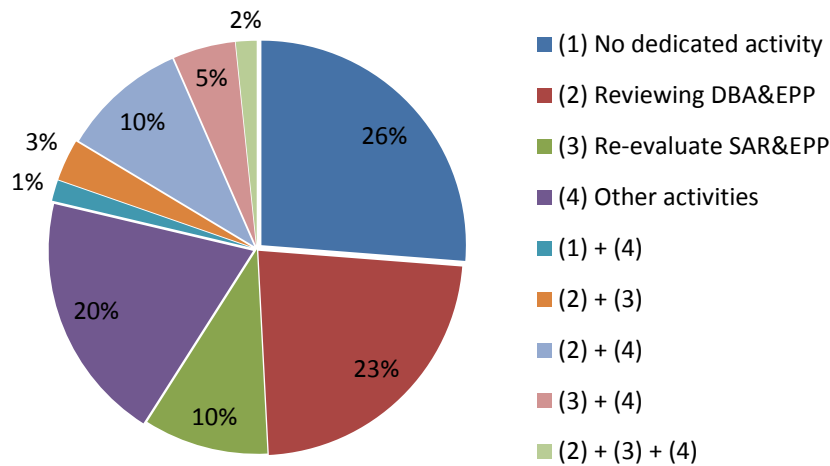


Fig. 1: Share of replies to the question: *What was done in your organization following the TEPCO's F-D NPP accident?*

The second general question: *Considering the social impact and the public acceptance of RRs in your country, following the TEPCO's F-D NPP accident, how would you describe the impact of this event*, was answered in many different ways, ranging from “no impact” to “serious consequences”. Due to the (expected) diversity of the answers, the results will be analysed and published in an upcoming planned future activity (see Chapter 4).

On the specific question: *Considering that the new Safety Assessment (SA) includes re-evaluation of the SAR and the safety margins, how can you describe the outcome of your actions*, the various answers are presented in Fig. 2. Although only 5 per cent (blue) included, or intend to include, new Postulated Initiating Events (PIE's), 20% (red) of facilities included in revised analyses a combination of accidental External Events, e.g. earthquake blackout, flooding & fire, etc. Moreover, 11 % of the replies (turquoise) are indicating that they included, or intend to include in the updated SAR, additional new PIE's and to perform analyses of accidents resulted from combinations of external events. A very important result of the survey is that 10 % (green) of the replies mentioned to include, or intend to include, new or updated database on the magnitude and probability of the external events. It should be noted that these considerable changes in the SAR require approval by the regulatory bodies, and therefore are completed in a longer timeframe. Additional 8 % (pink) reported to accomplish, or intend to do, all the process mentioned above which will be probably followed by a license renewal.

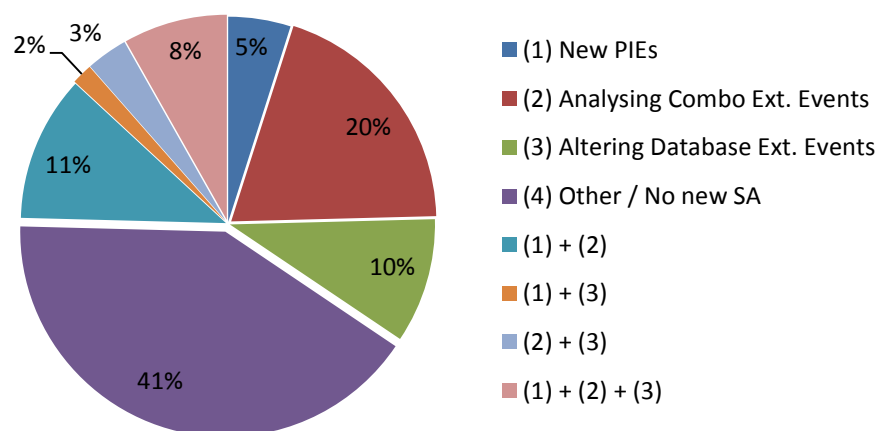


Fig.2: Share of replies to the question: *How would you describe the outcome of the new Safety Assessment?*

On the specific question: *considering the RR Utilization/Operation plan, what was revised following the TEPCO's F-D NPPs accident?* The replies are depicted in [Fig 3](#). Considering the answers received, 8 % (green) reported the revision of the Ageing Management programme only, 2 % changed also the OLC's (orange). 2 % revised only the Safety Assessment of the experimental devices (red), 7 % (red) changed the Maintenance programme only and another 10 % (light green) reported the changed of both. Some organizations (blue & light blue) decided to revise only the Operating Limiting Conditions (OLC's), and some (red & pink) performed only new Safety Assessment. The other 59 % of the answers indicated that no action was taken in this context.

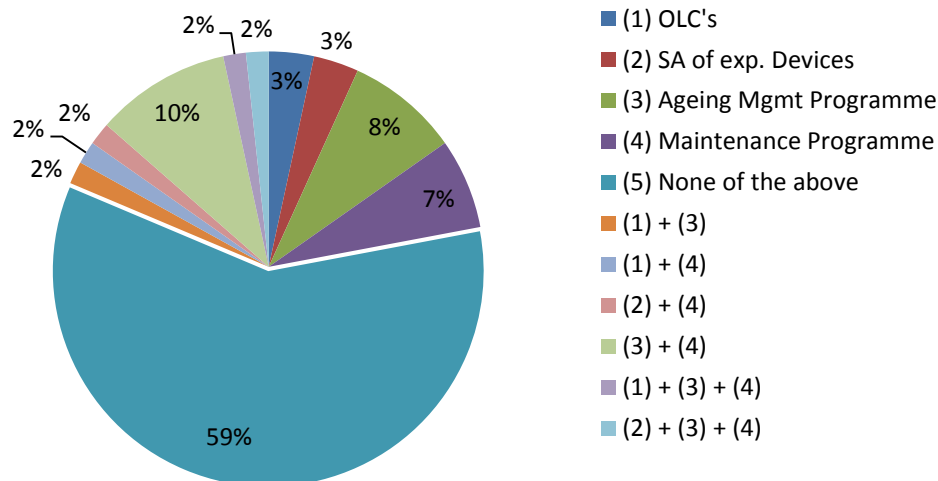


Fig. 3: Share of replies to the question: *What in the RR utilization/operation plan was revised after TEPCO's F-D accident?*

Finally, the fourth question refers to the Emergency Preparedness Plan (EPP): *considering the RR EPP, what was asked for to be done following the TEPCO's F-D NPP event*, and the answers are displayed in [Fig 4](#). The answers indicate that 17 % of the organizations revised the Emergency Response Programme (ERP), 10 % (blue) prepared new Emergency Proceedings and 3 % (green) upgraded the Emergency Equipment. Some of the answers reported combined activities of the above mentioned (orange & light blue and pink), where the most popular activity done by 14 % (light blue) was to revise the ERP, and to upgrade the equipment needed for the emergency response accordingly. Nevertheless, 46 % decided not to change their existing EPP. Once again, it should be mentioned and emphasized that changes in EPPs require approval by the regulatory bodies and therefore assumed to be completed in a longer term.

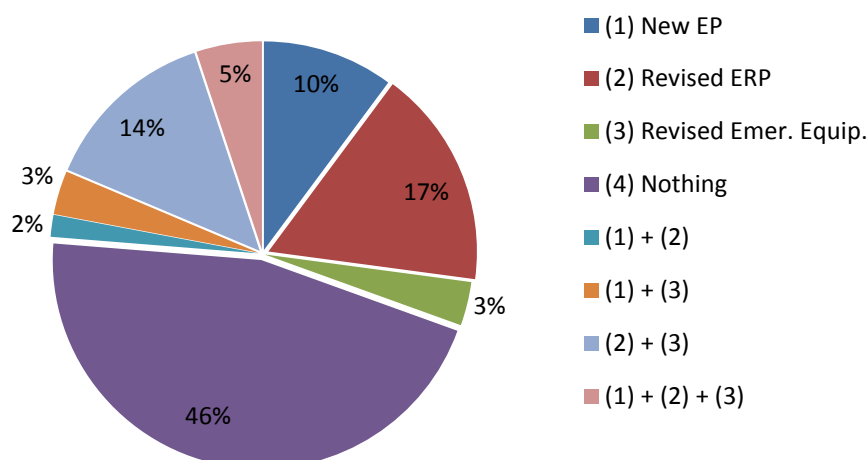


Fig.4: Share of replies to the question: *Considering the RR EPP, what was asked to be done following TEPCO's F-D accident?*

4. CONCLUSIONS

Considering the surveillance, it is concluded that the replies to the questionnaire demonstrate that following the TEPCO's F-D NPPs accident, many and various activities were initiated worldwide in the RR's facilities, regardless that the accident happened in a Nuclear Power Plant. Although, analysing the answers, it is presently impossible to determine whether the activities were concluded or not, the answers reflect an adequately reasonable, mature and serious reaction of the RRs community, following this unprecedented accident. In order to study further the activities performed, the IAEA Cross Cutting Coordinated Group are organizing in May 2012 a Technical Meeting on *Implications of TEPCO's F-D NPP on the Safety of Research Reactors*. Moreover, upon request from Member States, future safety and operation review missions will be also implemented to support Member States in addressing the implications of F-D accident to their RRs. Finally, in the upcoming months, as additional data will be received by the Agency, a further examination of the survey results will be performed, in order to draw the conclusions about the IAEA follow-up activities related to this subject.

5. REFERENCES

- [1] INTERNATIONAL ATOMIC ENERGY AGENCY, Summary of TWGRR Meeting-2011, RRS/NEFW, Working Material, July 2011.
- [2] ATOMIC ENERGY SOCIETY of JAPAN, (QandA_gb@aesj.or.jp), Lessons Learned from the Accident at the Fukushima Daiichi Nuclear Power Plant, Technical Analysis Subcommittee Committee for Nuclear Safety Investigation May 9th, 2011.
http://www.aesj.or.jp/en/release/gbcom_kyokun_EN_20110530.pdf
- [3] <http://www-pub.iaea.org/iaeaameetings/38299/International-Conference-on-Research-Reactors-Safe-Management-and-Effective-Utilization>.

Acronyms:

AM - Accident Management
CCCGRR - Cross Cutting Coordinated Group on RR.
DBA - Design Base Accidents
EPP - Emergence Preparedness Programme
ERP - Emergency Response Plan
F-D - Fukushima-Daiichi
IAEA - International Atomic Energy Agency
IGORR - International Group on Research Reactors
MS - Member States
MW - megawatts
NEFW - Division of Nuclear Fuel Cycle and Waste Technology
NPP - Nuclear Power Plant
NSNI – Division of Nuclear Safety of Nuclear Installations
OLC - Operating Limiting Conditions
PIE - Postulated Initiating Event
RR - Research Reactors
RRFM - Research Reactor's Fuel Management
RRS - Research Reactors Section
SA - Safety Assessment.
SAR - Safety Analysis Report
SSC - System, Structure and Components
TEPCO - Tokyo Electric Power Company
TWGRR -Technical Working Group on Research Reactors

ANNEX

Part A: General questions

1. What was done in your organization following the F-D event?

- ☐ No dedicated activity (e.g. as it was considered an event specific only to NPPs).
- ☐ Short re-evaluation of the Design-Basis Accidents (DBA's) and the Emergency Preparedness Plan (EPP).
- ☐ A complete re-evaluation of the Safety Analysis Report (SAR) and EPP.
- ☐ Other dedicated actions (please elaborate).

2. Considering the social impact and the public acceptance of RRs in your country, following the March 11 accident, how would you describe the impact of the F-D event?

Part B: Specific questions

3. Considering that the new Safety Assessment (SA) includes re-evaluation of the SAR and the safety margins, how can you describe the outcome of your actions?

- ☐ Included new Postulated Initiating Events (PIE's), e.g., no available power supply, etc.
- ☐ Included a combination of accidental External Events, e.g., earthquake & total loss of electrical power supply, flooding & fire, etc.
- ☐ Included new or updated database on the magnitude and probability of external events.
- ☐ None of the above (In this case, pls. describe your activity).

4. Considering the reactor Utilization/Operation plan, what was revised following the F-D event?

- ☐ The Operating Limiting Conditions.
- ☐ The SA of high pressure and temperature experimental devices (e.g., criteria of design, PIEs, etc.)
- ☐ The Ageing Management programme.
- ☐ The maintenance programme concept.
- ☐ None of the above (In this case, pls. describe your activity)

5. Considering the reactor EPP, what was asked for to be done following the F-D event?

- ☐ New/Update of Emergency Procedures. (e.g., classification, action levels, planning zones, etc.)
- ☐ Revision of the Emergency Response Plan.
- ☐ Revision/modification of the Emergency Equipment.
- ☐ None of the above. (In this case, pls. describe your activity).

REASSESSMENT OF RESEARCH REACTORS – THE APPROACH IMPLEMENTED BY IRSN BASED ON THE SO-CALLED “GRADED APPROACH” AND TAKING INTO ACCOUNT THE FIRST LESSONS LEARNED FROM THE FUKUSHIMA EVENTS

C. DE BELLABRE, J. GALLET, T. BOURGOIS

*Institut de Radioprotection et de sûreté Nucléaire
B.P. 17, 92262 Fontenay-aux-Roses, France*

Among its mission, the “Institut de Radioprotection et de Sûreté Nucléaire” (IRSN) carries out the safety assessment of French research reactors in support to the French nuclear safety authority (ASN). In this framework, IRSN develops safety approaches for research reactors, based on those applied for nuclear power plants but adapted to the level of risk associated to research reactors and taking into account specificities of each type of research reactor. These approaches are mainly based on IAEA safety standards, with a special attention concerning the application of the so-called “graded approach”; these approaches also take into account experience acquired by IRSN for years in the framework of the Jules Horowitz reactor (JHR) licensing process and of the safety periodic reviews of OSIRIS reactor, high flux reactor operated by the ILL (RHF), ORPHEE reactor, CABRI reactor and EOLE/MINERVE reactors.

Besides these French activities, IRSN has developed its activities in the community of countries where research reactors are operated. In this regard, collaboration has been established with the Moroccan CNESTEN who operates a 2 MW TRIGA reactor and who is willing to develop TSO capabilities. IRSN has also proposed, in reply to a request of the Dutch Ministry of Economic Affairs, Agriculture & Innovation, a set of safety requirements for the building of the new PALLAS reactor in Petten. Finally, IRSN is also acting as a technical support to the Jordan nuclear regulatory commission (JNRC) for the Preliminary safety report review of the Jordan research on test reactor (JRTR) designed by the Korean company KAERI.

After the events which occurred in March 2011 in Japan, IRSN has lead studies which aim at identifying reactors that, because of their characteristics and their risk level, need a review of their conception. This work has been achieved examining on the one hand the sensibility of facilities to core cooling loss and electrical power supply loss, on the other hand the sensibility of facilities to external hazards. It has been carried out on the basis of the knowledge acquired on French research reactors but also on foreign ones. Finally this work allowed to define precise classification criteria for research reactors based on the graded approach reviewed in the light of the Fukushima events.

1. Introduction

There are currently about 200 functioning research reactors, operated in 60 countries. Only 40 have a power greater than 5 MW. Research reactors can be divided into five distinct families:

- the Material Testing Reactors (MTR): they are dedicated to the study and the test of materials that will be used for nuclear power plant components or fuels. Some of them also produce radioisotopes for medical or industrial use. They are the most powerful research reactors (until several hundred MWatts) and generally are open pool type, which enables easy experimental device handlings and core reshuffling. HBWR in Norway and OSIRIS and the JHR in France are MTR.
- the reactors providing neutron beams: they are mainly dedicated to fundamental research on condensed matter. Their core is surrounded by channels feeding neutron beams. Their power is several MWatts and they are open pool type. OPAL in Australia, FRM II in Germany and the RHF in France are of this type.
- the critical mock-ups: they are devoted to neutronic investigation. Their power is very low (several Watts) and they are cooled by water or by air. BR-1 in Belgium and MASURCA and EOLE in France are of this type.

- the test reactors: they are used to simulate accidents and study the behaviour of an instrumented fuel pin. CABRI and PHEBUS in France are of this type.
- the education reactors: they are used to training future operators or students, their power is several MWatts. TRIGA reactors are of this type

All the reactors have specific objectives and thus have different designs. Therefore the safety stakes are not the same for each reactor. Their safety demonstration can be achieved by applying the graded approach concept.

2. Graded approach concept for Research Reactors safety analysis

The graded approach concept is presented in the IAEA draft safety guide DS351 (reference 1, still under development). It provides support for the application of the safety requirements for research reactors throughout the various stages of a research reactor's lifetime (site selection, site evaluation, design, construction, commissioning, operation and decommissioning).

The graded approach concept indicates that the level of analysis required to demonstrate the compliance with the safety requirements can be deeply reduced depending on the safety issues and the reactor design. Research reactors have specific characteristics compared with nuclear power plants that allow the application of graded approach. They generally have:

- a low operating power (no need to produce steam for electricity): the most powerful research reactors have a few hundred MW power compared with the nuclear power plants thermal powers of a few GW;
- short operating cycles (need for a high neutron flux): the research reactors operating cycles are a few dozens of days compared with the nuclear power plants (NPP) operating cycles of one or two years;
- circuits with low pressure and low temperature (no need to produce steam for electricity): the research reactors primary circuits temperatures and pressures are less than 70 °C and 10 bars compared with the NPP primary circuits temperatures and pressures of 300 °C and 150 bars.

In terms of safety issues, this implies that:

- the amount of fission products in the core, that depends on the operating power and cycles, is low (low potential accident consequences),
- the core decay heat, that depends on the amount of fission products, is often low enough to be removed by natural convection coolant mode on the long range (no need to analyse decay heat removal active systems).

In conclusion, the graded approach concept proposes to implement safety features with a level of robustness related to the expected consequences in case of their failure.

3. Application of the graded approach to the post-Fukushima stress tests analysis on Research Reactors

3.1 Presentation of the post-Fukushima stress tests

Considering the accident at the Fukushima nuclear power plant in Japan, the European Council of 24/25 March, 2011, requested that the safety of all EU nuclear plants should be reviewed (reference 2), on the basis of a comprehensive and transparent risk and safety assessment (called "stress tests"). These "stress tests" are defined as targeted reassessments of the safety margins of nuclear power plants and are developed by ENSREG (European Nuclear Safety Regulators Group), on the basis of the proposals made by WENRA (Western European Nuclear Regulators' Association).

ENSREG proposed a methodology that has to be applied by the EU operators to achieve their stress tests (reference 2). It consists mainly in:

- an evaluation of the response of the nuclear power plant when facing a set of extreme situations envisaged:
 - 1) earthquake more important than the design basis one
 - 2) flooding more important than the design basis one
 - 3) loss of electrical power, including station black out
 - 4) loss of the ultimate heat sink
 - 5) combination of both losses of electrical power and ultimate heat sink.
- a verification of the robustness (available design margins, diversity, redundancy, structural protection, physical separation, etc.) of the safety-relevant systems, structures and components (SSCs) necessary to prevent and/or mitigate these situations. Any potential weak point and cliff-edge effect shall be noted.
- independently from this analysis result, an assessment of the means necessary to manage a loss of core cooling function and a loss of cooling function in the fuel storage pool. Means to protect from and to manage loss of containment integrity should also be assessed.

All operational states of the plant shall be considered.

The stress tests conclusion should report any potential for modifications likely to improve the considered level of defence-in-depth, in terms of improving the resistance of components or of strengthening the independence with other levels of defence.

3.2 Analysis of the post-Fukushima stress tests applied to the French Research Reactors

Although these stress tests have been developed for NPPs, the French safety authority asked all the French nuclear operators, including research reactors operators, to realise this analysis. This has been achieved by adapting the methodology to the research reactors safety stakes, applying the graded approach concept. The methodology applied by IRSN to assess the stress tests for the French research reactors is presented hereafter.

First of all, the different states of the installation that could lead to a cliff-edge effect in terms of radiological consequences on the public and the environment have to be identified. The situations leading to these states, that should be absolutely prevented and then on which the stress-tests will focus, are called “feared situations”.

The French research reactor operators have defined a “feared situation” as a situation that has not been considered in the design of the radiological consequences mitigation systems (i.e. the last containment barrier) or in the emergency planning. As a reminder, these ones have been designed considering a total core meltdown under water. Therefore, for pool type reactors, the “feared situations” considered by the operators are core uncovering, stored fuel elements uncovering and core meltdown under water with failure of the last containment barrier.

IRSN considers that all the situations leading to non negligible radiological releases (i.e. leading to a dose of several mSv for the public or to long term consequences for the environment) have to be defined as “feared situations”. Then, for pool type reactors, core meltdown under water should be considered. For very low power reactors, the only “feared situation” is the fall of a heavy component on the core or on stored fuel elements, that would scatter nuclear material in air.

It has to be noticed that the methodology applied by the French research reactor operators finally led them to consider all the situations leading to non negligible radiological releases.

Then the SSCs absolutely necessary to avoid a “feared situation”, so called “prevention key SSCs”, have to be identified. For the simplest pool type reactors that can be cooled by natural convection coolant mode, the uncovering of the fuel elements in the pool shall not occur if the walls of the pool remain intact and if water is added to compensate evaporation. The core meltdown under water will be avoided if the reactor is shut down and the flap valves

(used for connecting the reactor pool with the primary circuit so that the core is cooled by natural circulation) open¹. Therefore, for this type of reactor, the “prevention key SSCs” are:

- the pool walls,
- the emergency supply water means to compensate evaporation: their type depends on the estimated grace period before the core uncovering occurs; this period is estimated in the part related to the analysis of the installation behaviour in case of the loss of electrical power and ultimate heat sink,
- the reactor shutdown system,
- the flap valves,
- the core itself to ensure that its geometry will enable a sufficient cooling,
- the SSCs that could jeopardize the previous SSCs in case of failure.

The following analysis consists in assessing the robustness of these “prevention key SSCs” for different situations.

Robustness of the installation against extreme external events

As required by ENSREG, it is first necessary to ensure that the design of the installation is sufficient to withstand a design basis earthquake or flooding. Then, the plant compliance to its design requirements has to be checked. These two steps are covered by the “classical” safety analysis.

Then the range of external event severity for which a “prevention key SSC” is likely to be lost (directly or indirectly, for example by the fall of a heavy component) shall be assessed. The plausibility of such an event, taking account of the installation location, has to be discussed. This shall be done on the basis of the external events calculation uncertainties.

If necessary, the “prevention key SSCs” have to be strengthened. Their robustness shall also be assessed considering the events induced by extreme external events such as fires, flooding induced by earthquake, nearby installation explosion, etc.

Robustness of the installation against losses of electrical power or/and ultimate heat sink

Sequential losses of the different electrical power sources (off-site power sources, ordinary back-up generators and other back-up sources) have to be considered. Same approach is applied for the different ultimate heat sinks.

For each postulated loss, it is necessary to present design provisions, ensure that they are sufficient and ensure the plant conformance to its design requirements. It is crucial to assess how long the installation can withstand without any external support before a “feared situation” occurs. Actions that need to be realised by the external support shall be presented. When this delay is too short to allow external support to come (IRSN considers that at least some days should be required), the robustness of the implied electrical power source has to be assessed. It shall especially withstand extreme external events.

Contrary to the NPPs case, the total loss of electrical power or ultimate heat sink is not a severe situation for most of the research reactors; i.e. it does not lead quickly to a “feared situation”. Indeed, for pool type reactors that can be cooled by natural convection coolant mode, there is no “prevention key SSC” that needs an electrical power source. The pool itself is an important ultimate heat sink, which generally allows a delay of several weeks without

¹ There is no core meltdown if the reactor cooling is sufficient. It means that the primary and secondary circuits could be considered as “key SSCs” instead of the components necessary to the reactor shutdown and the natural circulation cooling. However the installation would not be considered in a safe state if the shutdown was not ensured.

external support before fuel elements are uncovered. In this case, the emergency supply water means can be provided by the external support team.

Robustness of the severe accident management means

“Feared situations” are now postulated. If they exist, actions to stop such a situation shall be identified. For example, adding water if fuel elements are uncovered. The possibility to achieve them considering the radiological conditions and the needed components shall be assessed. The means necessary to monitor the main parameters of the installation (to control the “prevention key SSCs” state) and limit the radiological releases shall also be identified. All these systems are called “mitigation key SSCs”. Their robustness and their electrical supply robustness shall be assessed. They shall especially be operational after an extreme external event.

It is then necessary to ensure that severe accidents will be manageable if a situation not considered as a “feared situation” occurs (for example a criticality accident in the reactor building).

4. Conclusion

The post-Fukushima “stress tests” carried out on the research reactors, applying the graded approach principle, have shown the crucial characteristics that should be assessed to evaluate their robustness in case of extreme situations. The need for review the design of a research reactor should therefore be assessed on the basis of these characteristics.

First, the severity of the “feared situation” consequences (i.e. installation design basis accidents and excluded situations in the “classical” safety analysis) should be considered, considering the public location and the environment around the installation.

Second, the number of “prevention key SSCs” should be considered. It directly depends on the installation design. Concretely, the characteristics to take into account are:

- the need for active systems to remove the reactor decay heat,
- the simplicity of the pool design, i.e. the number of penetrations whose failure could lead to the core uncovering,
- the number of equipments that could directly jeopardize the reactor in case of failure (e.g. experimental devices, heavy equipments above the core).

Then, the sensibility of the site to extreme external events should be considered.

Finally, the grace period before a “feared situation” occurs in case of an extreme event and the proximity and the means of external support enabling to prevent a “feared situation” in case of an extreme event should be assessed. Concretely, this leads to take into account the size of the pool and the presence or absence of a robust significant water amount next to the installation.

5. References

- [1] *Draft safety guide DS351 The Use of a Graded Approach in the Application of the Safety Requirements for research reactors*, 2010
- [2] *Declaration of ENSREG of 13 May 2011, in response to the request of the European Council on 25 March 2011*

European Research Reactors after the Accident at Fukushima Daiichi

Gabriele Hampel

Chairman of the Association for Research Reactors (AFR)

Universität Mainz -Institut für Kernchemie

Fritz-Strassmann-Weg 2 - D-55128 Mainz - Germany

Abstract

The accident at the Japanese nuclear power plant Fukushima Daiichi, caused by the devastating tsunami on the 11th March 2011, has raised questions worldwide, especially in Germany, about the safety of nuclear energy. Stress tests were then developed in order to increase the safety level of the nuclear facilities. How are the research reactor facilities in the European countries affected by these discussions and regulatory measures? What is the role of research reactors after Fukushima? These questions were discussed for the research reactors associated in the AFR. AFR is the German acronym for an association of research reactors founded in 1959. Reactor managers of European research reactors meet continuously to exchange experience and knowledge and to support each other. Typically, the meetings are held in the German language. Permanent participants are the countries Austria, Belgium, France (Grenoble), The Netherlands (Delft) and Switzerland. The topic of the last two AFR meetings was the impact of Fukushima for the different research reactor facilities and the situation regarding the stress test. The situation until spring 2012 is summarised in this contribution.

1. Introduction

The public debate surrounding atomic energy after the Fukushima accident has led to closer inspection by authorities of commercial power plants. These safety features include: protection from earthquakes, floods and other important precautions for accident control, such as emergency power diesel, accident management procedures and venting and hydrogen recombinations. Discussions took a broad look at the safety concept in other scenarios that occurred at Fukushima. Worldwide stress tests were then developed in order to increase the safety level of the nuclear facilities.

How are the research reactor facilities in the European countries affected by these discussions and regulatory measures? Are there differences in the stress test for the different European countries? What is the role of research reactors after Fukushima? These questions were discussed for the research reactors associated in the AFR.

AFR (Arbeitsgemeinschaft für Betriebs- und Sicherheitsfragen) is the German acronym for an association of research reactors founded in 1959. Reactor managers of European research reactors meet regularly to exchange experience and knowledge and to support each other. Typically, the meetings are held in the German language. The chairman of the association rotates every two years. Permanent participants are the countries Austria, Belgium, France (Grenoble), The Netherlands (Delft) and Switzerland. From time to time, the Czech Republic, Hungary and Finland take part in the meetings and in 2011, the first joint meeting was held together with the French association of research reactors CER (Club d'Exploitants des Réacteurs).

The topic of the last AFR meetings was the impact of Fukushima for the different research reactor facilities. In most cases, stress tests will be carried out for the facilities with a thermal power of 100 kW and more; the only exclusion is the 250 kW TRIGA Mark II reactor of the Atomic Institute in Vienna, Austria. Also, Zero power reactors in Germany and Switzerland and research reactors currently undergoing dismantling are not affected by stress tests until now.

2. The content of the stress test

The stress test includes the topics of flooding, earthquakes, tornados, terrorist attacks, the importance of cooling systems and vessels and combined events.

The basic criteria of nuclear safety technology is described by the vitality of the facility as “reactivity”, “decay heat” and “release of radioactivity” and also the adherence to the safety limit of 50 mSv for nuclear accidents. In the stress tests, these criteria (vital functions of the research reactor) are proven. It must be demonstrated that the reactor is robust enough and complies with requirements after an accident, also for a combination of the events. The questionnaire includes the following parts:

1. natural events as earthquakes, flooding, extreme weather situations and combined events
2. civilian events, such as airplane crash, including the burning of kerosene, leakages, release of gas and terrorist attacks (confidential)
3. other events, such as station blackout, loss of emergency power for long periods, loss of cooling
4. discussion of actions in emergency cases in difficult situations (possibilities of emergency aid when the infrastructure is destroyed)

The questionnaire is not the same for each research reactor of the AFR. It depends on the reactor type and the European country, all of which must be described. In most cases, terrorist attacks were not included.

3. The situation in the different European countries

3.1 Germany

Especially in Germany, the Fukushima Daiichi accident aroused again the debate about the risks of the peaceful use of nuclear energy and the safety of nuclear power plants. The German government has ordered an inspection of all German power reactors. Therefore, from the reactor safety commission (RSK), a questionnaire was developed for safety inspections of the German power reactors published in April 2011. The aim was to check, if – in addition to hazardous incidents and accident scenario of the power reactor - radioactivity could be released on a grand scale. With reference to a change of the German Atomic Law in June 2011, it was decided by the Federal Council of Germany, that the stress test should be extended to all nuclear facilities including research reactors with a thermal power higher than 50 kW.

Therefore, the three German research reactors FRM II, BERII and the TRIGA Mainz had to participate in the stress test while excluding German Zero power reactors. The FRM II is a high flux reactor, the MTR research reactor BERII is operating at a maximum power of 10 MWth and the inherent TRIGA Mark II in Mainz has a maximum power of only 100 kWth. Therefore the stress test is different for each of these three reactor types although all are located in the same country. For the FRM II and BERII external experts reviewed the documents of the stress tests. Due to the low power and the inherent safety the authority for the TRIGA Mainz decided that it is not necessary to involve external experts to review the stress test in this case.

The three German facilities hand over the answers to the questionnaire their respective authorities which forwarded the documents to the RSK until end of October 2011. The response of the RSK is expected for end of March 2012.

FRM II, Munich

At the time of the Fukushima accident, the FRM II was not in operation since its intended revision continued until October 2011. The experts called by the authority of the FRM II are from TÜV Süd, Germany. They developed a questionnaire for appropriate events for the FRM II directly after the Fukushima accident and in addition performed special inspections on-site.

Nevertheless, due to the decision that all German research reactors had to participate in the stress test, FRM II has to answer the questionnaire (of 150 pages) which was created by the RSK for the power reactors in Germany. Since the FRM II is a new and very modern research reactor the questions could be answered to a large extent using the documentation of FRM II. In the end, the document for the stress test includes about 600 pages and was submitted to the authority at the beginning of October 2012 and to the RSK at the end of October. The assessment is still going on.

During the Fukushima accident, personnel of FRM II informed the public about the situation in Japan, participated intensively in public debates, and spoke to all public media such as TV, radio and newspaper.

BERII, Germany

During the Fukushima accident, the BERII was also in revision with a longer break necessary because of changes at the cold neutron source and the installation of a new conical beam port.

After the Fukushima accident and the assignment of the stress test for German power reactors, already in April 2011 the authority of the BERII inspire a similar safety check for the BERII. The base was the RSK questionnaire focused on the special situation of the BERII research reactor in comparison to a power reactor. The crash of an airplane was discussed controversial since the debate was influenced by the discussion of the public regarding a new airport in the south of Berlin and the route of the plans.

The document of the stress test for the BERII was reviewed by external experts. As result they summarised that the BERII has passed the stress test. The whole experts report is published in the internet [2].

From time to time the stress test of the BERII is content in the debate of the Berlin House of Representatives. Also, unserious reports were published in the German TV which effected discussions about the safety of a welding line at a divider in the reactor tank of the BERII. This situation caused a longer revision break for the BERII. Now, it is expected that the BERII will start operation again end of February 2012.

TRIGA Mainz

In August 2012, the TRIGA Mainz was informed by their authority that the facility has to take part in the German stress test. Due to its inherent safety and its low power of maximum 100 kW, the questionnaire for power reactors was not practical for the TRIGA Mainz. A reduced questionnaire of 10 pages developed by the RSK, was chosen for the stress test of the TRIGA Mainz. It includes the same 4 subjects as presented in paragraph 2, but in a shorter form compared to the FRM II.

Due to the low power of the TRIGA Mainz, a cooling after operation is not necessary and also if all cooling systems would fail, an active cooling is not necessary. Without water in the reactor pool and without any convection the maximum fuel temperature would be 300°C far below the melting point of aluminium of 660°C.

The worst case scenario was the crash of a large airplane. It was assumed that the building and the reactor tank would be fully damaged and all fuel elements destroyed. This part could be answered with the support of the TRIGA Vienna, since this scenario was the content of a diploma thesis, entitled "Accident Scenarios with Environmental Impact of the TRIGA Mark II Reactor Vienna" at the Atominstitut in 2009 [1]. The influence of a kerosene fire was analysed to estimate its effect on the properties of the Zirconium-Hydrogen matrix of the TRIGA fuel.

During the period of the Fukushima accident, scientific personnel of the TRIGA Mainz offered their expertise to inform the public about the situation in Fukushima in public debates and using all public media.

Research reactors in dismantling and/or temporary storage

The discussion continues as to whether research reactors in the stages of dismantling and/or in temporary storages should take part in the stress test. Until now, there has been no final decision by the German government, but it is expected that the stress test will be established also for these facilities. Most research reactors undergoing dismantling have already removed their fuel and the no-fly-zones for airplanes were annulled as decided, for example, for the VKTA Rossendorf. As a consequence, the crash of an airplane would have to be examined in a stress test for these facilities.

3.2 France: Institut Max von Laue – Paul Langevin (ILL)

Following the nuclear accident at the Fukushima Daiichi nuclear power station, the French nuclear safety authority (ASN) decided to launch additional safety assessments at all French nuclear bases. On 5th May 2011, the ILL was requested to carry out an additional safety review known as stress-test and entitled "*Specifications for the complementary safety assessment of nuclear installations in the light of the Fukushima accident: risks of flooding, earthquake, loss of power supply and loss of cooling, in addition to operational management of accident situations*". The results are published in the internet under <http://www.ill.eu/index.php> [3].

In summary, the additional safety assessment performed at ILL confirms the robustness of the installation in terms of its critical safety functions. The multiple failure scenarios studied fall outside the installation's design basis, given their extremely low probability of occurrence and/or the levels of stress never performed so far before envisaged in the safety assessments. Nevertheless, ILL proposes some changes and improvements which were also published on the internet. Since ILL is renewed totally regarding earthquakes most important is the case of a flood hazard. As a result a new emergency reactor control room capable of managing the extreme combined earthquake and dam burst scenario will be constructed.

3.3 The Netherlands: HOR Delft

In the Netherlands, all nuclear plants (including Urenco and Covra) will perform a stress test besides the only nuclear power plant in Borssele. This means that both the research reactors in Petten and Delft are performing the stress test.

The research reactor (MTR) at the Reactor Institute Delft, an university reactor used where possible, the European ENSREG recommendations for the stress test. As the actual impact to the environment of the reactor during a calamity is very limited in contrast to high power reactors, the stress test is mainly focused on the consequences of a total damage of the facilities. The most severe case, which is a plane crash, is evaluated. Even in this case the total doses for the public will stay below the legal limits for evacuation. The stress report is delivered to the authority in the Netherlands at the end of February 2012.

3.4 Belgium: BR2 Mol

The nuclear installations at SCK•CEN are operated according to the national regulations and legislation in force. These regulations involve regular internal inspections and safety reviews, license granting, monitoring and review by the Federal Agency for Nuclear Control (FANC), and operational inspections by its Technical Support Organisation (Bel V) to evaluate the safety level of the installations and the organisation. The framework of the periodic safety reviews for all installations of the SCK•CEN assures that the most recent requirements with regard to safety are taken into account. Nevertheless it is important to take into account the feedback and lessons learned from the major recent events that occurred at Fukushima Daiichi and to verify the safe operation and the emergency preparedness of the installations in the light of these events. SCK•CEN is therefore performing, at request of FANC, a re-evaluation of the safety margins for presupposed situations where its installations might be exposed to extreme events in agreement with the definition of the “Stress Test” by the authorities. The overall safety objective of the evaluation is the prevention or mitigation of release of radioactive material, in severe accident conditions, to the environment and the public. The safety approach used in the design of the installation to achieve this is defence-in-depth, which consists in a hierarchical deployment of different levels of equipment and procedures in order to maintain the effectiveness of physical barriers placed between radioactive materials and workers, the public or the environment, in normal operation, anticipated operational occurrences and, for some barriers, in accidents at the plant. A list of initiating events will be considered for the “Stress Tests”. Realistic combinations of different initiating events and failures will also be investigated. The effects and consequences of these initiating events on the nuclear installation and especially on the structures, systems and components responsible for the assurance of the safety functions will be examined. For the BR2 reactor in particular, the impact of following initiating events and related loss of safety functions is under evaluation: earthquake, flooding, other extreme natural events as forest fire, air plane crash, other manmade events, influence of neighbouring facilities, loss of safety

functions and combination of events, accident and severe accident management, etc. The aim is to finalize a report on SCK•CEN “Stress Tests” by the end of October 2012 [4].

3.5 TRIGA Vienna, Austria

The 250 kW TRIGA reactor of the Atominstitut Vienna needs not to take part in any stress test. The knowledge of this facility was already used to inform the public about the situation of the Fukushima reactor. Therefore, with the support of the scientific staff, an information centre was established by students at the Atominstitut, which collected and interpreted the news 24 h hours a day. With the help of this centre, the scientists of the TRIGA Vienna were able to inform seriously the public through numerous interviews for TV, radio and the printed press. As a result the Atominstitut is accepted today as a centre of nuclear expertise in Austria, an anti-nuclear country without nuclear power plants [5].

4. Summary

For all research reactors belonging to the AFR, stress tests have been/will be carried out for the facilities with a thermal power of more than 100 kW. The only exclusion is the 250 kW TRIGA Mark II reactor of the Atomic Institute in Vienna. Also, Zero power reactors in Germany and Switzerland and research reactors already being dismantled are not affected by stress tests until now. The content of the stress tests includes natural events such as earthquakes, flooding, extreme weather situations and combined events, other events such as station blackouts, loss of emergency power for long periods, loss of cooling, discussion and actions in emergency cases in difficult situations. Only in Germany also civilian events such as crash of an airplane, including the burning of kerosine, leakages and release of gas were included in the stress test.

Another aspect includes discussions on the utilisation of research reactors after the accident, their acceptance in the society, and the support of research projects in competition to accelerator facilities. Education, training and research in nuclear safety will become more important, as well as a differentiated consideration between power and research reactors. It may be important for the future of research reactors to demonstrate that neutron from such facilities can provide an excellent service to society (www.research-reactors.org).

References

- [1] Villa, M., Haydn, M., Steinhauser, G., Boeck, H., 2010. Accident scenarios of the TRIGA Mark II reactor in Vienna. Nucl. Eng. Des. 240, 4091-4095.
- [2] <http://www.parlament-berlin.de:8080/starweb/adis/citat/VT/17/DruckSachen/d17-0074.pdf>
- [3] <http://www.ill.eu/index.php>
- [4] Reference: B.Ponsard, personal communication, January 23, 2012.
- [5] G. Steinhauser et al; Information management of the Fukushima reactor accident in Austria by the Vienna University of Technology; Disaster Advances (2012), in press.

ASSESSMENT OF THE CONSEQUENCES OF THE FUKUSHIMA ACCIDENT ON THE GERMAN ENERGY POLICY

IGORR/RRFM PRAGUE 2012

Joel Guidez

DEN/DIR CEA Saclay 91190 Gif sur Yvette France

CEA Councilor at the French embassy in Berlin from 01/11/2009 to 31/08/2011

ABSTRACT

The nuclear power generated in Germany in 2010 was 139 TWh. This production was provided by 15 of the 17 reactors still in operation and represents 22.4% of the total electricity production in Germany in 2010. At the end of 2010, a law was taken authorizing the extension of the power plants' service life from 8 years (oldest reactors), to 14 years for the others.

Germany is the country that has had the quickest and most resounding reaction to the Fukushima accident. Four days after the tsunami, a moratorium was imposed by the government by shutting down the 7 oldest reactors that means about 30% of the German nuclear power available. This paper takes stock of the moratorium a few days after the accident, the foundation of the ethics commission and its report released in May, as well as the first stress tests carried out and related report also released in May. An explanation is then given on the content of these reports and on the package of laws adopted on June 30, by the Bundesrat, in accordance with these reports. At the end, eight reactors will never restart and the nine remaining reactors are legally scheduled to stop operating. The last one will stop in 2022.

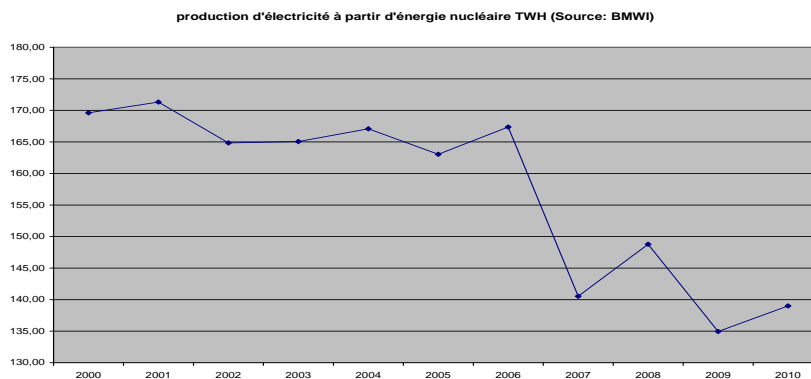
This document analyzes the initial consequences of these decisions. Firstly in terms of production and power grid, the renewable energy development was intensified but the accelerated construction of a program of thermal power plants was also decided. Secondly, the first consequences on the German energy industry and on the cost of energy are presented.

Finally, explanations are given on the launch of a major research program to develop renewable energy, energy storage methods and energy efficiency.

To conclude, the law on the extension of the power plants' service life will therefore have survived only three months. The transition to renewable energies by nuclear power plants, which was to have taken place due to this law, will be carried out mainly through a program of accelerated construction of thermal power plants.

Background to nuclear power generation in Germany

The nuclear power generated in Germany in 2010 was 139 TWh. This production was provided by 15 of the 17 reactors still in operation. It represents 22.4% of the total electricity production in Germany in 2010. This production was 170 TWh in the 2000s. Graph No. 1 below illustrates the downward trend.



Electricity production from nuclear energy, TWh (Source: BMWi)

This decrease is due in 2010, to the shutdown of two of the ten power plants extending through 2010 due to technical problems, and the operation at reduced power of some of the other plants. They had reached their quota and were awaiting a governmental decision as to the extension of their useful life, which did not come until December (amendment to the law on nuclear power: "Atomgesetz"). They only returned to full power operation in early 2011, following the law authorizing the extension of the plants' service life from 8 to 14 years.

In 2011, with the shutdown of seven reactors in March 2011, the nuclear production was only 108,4 TWh, that represents 17,7% of the German electrical production.

Government reaction following the Fukushima accident

Following the earthquake and tsunami that hit Fukushima on March 11, the government decided, as of Tuesday March 15, to adopt a 3-month moratorium on its own legislation to extend the service life of plants.

This period should be used to perform safety tests reinforced on all German power plants, with respect to the exceptional events.

In practice, this moratorium has led to the immediate shutdown of the seven oldest plants that had exceeded their initial operating, i.e. one third of the available German nuclear capacity.

The three-month moratorium led to preparing an extremely tight schedule of actions:

- The government set up an ethics commission which was put in charge of searching for a social consensus with respect to the decision to abandon nuclear energy and the corresponding consequences. It had to draw its conclusions by late May.
- The government instructed the reactor safety commission (RSK) to submit a report, on May 17, on the technical reviews of the 17 German power plants' resistance to extreme events.

On the basis of this report and that of the ethics commission, Chancellor Angela Merkel planned the following schedule:

June 6, presentation of the legislative package (nuclear Act) to the cabinet and implementation of parliamentary sessions.

June 8: full day of hearing of the environmental commission on the entire energy package (getting out of nuclear power and accelerating the energy transition).

June 9: first parliamentary reading of the Bundestag (National Assembly)

late June: vote on the legislative package

It shall be noted that this precipitation is specific to Germany and seems to be due to the lack of legal basis for the moratorium. Indeed the nuclear act had been adopted by the parliament even though the moratorium had not been voted and had only been decided by the government. Other European countries gave themselves the time to carry out genuinely technical work, with an analysis of the stress test and final conclusions, planned for December 2011.

Results of the ethics commission's work

This commission, consisting of 17 well-known figures and 28 experts from various backgrounds, rendered its report on May 30. It concluded that Germany can replace nuclear energy with technologies that present less risk for society. In this context, it advocates abandoning nuclear energy within 10 years.

It poses all the problems relating to this choice: climate protection, energy safety, dependence on imported fossil fuels, increase in energy costs, importing "nuclear" electricity, grid problems, etc.

It recommends more intensive research, in particular for energy savings and storage. It should be noted that this committee recommended continuing research in the nuclear field (safety and waste) as well as for fusion, the bearer of great hopes.

Lastly, the commission would like nuclear safety to become a component of the European policy, in particular to prevent the grid from being powered by power plants whose safety criteria would be inferior to those applied in Germany.

Results of the first stress tests performed on German reactors

The final report was written in a very short imposed time frame. In particular the operator only had two weeks to answer all questions asked by the safety authority on the government's request. Similarly, all the findings had to be summarized in less than three weeks.

All this is evident in the final version of the report, which is rather disappointing and does not offer any proposals or conclusions. There is only an estimate of the margins with respect to the initial conditions retained in the safety reports, for a certain number of exceptional events...

However, this report did show, for the 7 reactors affected by the moratorium, an inferior protection against aircraft crashes, which retrospectively allowed their permanent closure to be substantiated.

Review of the "energy" package of laws adopted on June 30

The legislative package adopted is composed of eleven legal texts, endorsing an accelerated nuclear withdrawal ending in 2022 and an accelerated transition toward renewable energy, which should cover 80% of the electricity production by 2050. The main points covered are as follows:

- The 7 reactors affected by the moratorium and the Krümmel reactor (already shutdown for several years) will not be brought back into operation. The nine remaining reactors will stop between 2015 and 2022.
- Renewable energies will be developed in a massive way, particularly offshore wind power which will reach a capacity of 25 GWe by 2030 for an estimated cost of 75 billion euros.
- In the short term gas and coal power plants shall ensure the necessary transition
- Federal planning of the infrastructures required for the network development is being implemented.
- Energy efficiency will be enhanced.
- No additional energy imports shall be undertaken.

Economic consequences for German energy companies

Four German electricity producers are destabilized by these measures, which are costing them dearly (loss of production of eight reactors and supplies to be furnished for the dismantling). In addition, for the remaining reactors, the fuel tax has been maintained while it had been established as a compensation for extending the service life of the plants stemming from the new Atomgesetz 2010 law. Finally, the results of the European stress test could lead to other extra costs.

For example, RWE with a turnover of €53 billion in 2010 is the largest producer of electricity in Germany and a European energy heavy weight. Its shares crashed by 43%, and its indebtedness is now deemed excessive. A new boss arrived on August 8 with specific tasks of debt reduction, selling off assets and significant restrictions on investment.

Similarly, Eon announced on August 10, a huge quarterly loss of 1.5 billion Euros, while over the same period last year, Eon announced €1.7 billion of profits.

Major restructuring is announced along with a loss of 11,000 jobs.

In this context Eon (court of Hamburg) and RWE (court of Munich) have brought a lawsuit against the government for the tax on nuclear fuel (originally linked to the extension of the power plants' service life.) Customs offices reimbursed Eon €96M and RWE €74M at the end of October.

Moreover, Vattenfall and Eon want to bring action against the Federal Government, to claim billions of euros for damages and interest, for infringement to their property rights.

For the nuclear industries located in Germany (uranium enrichment, fuel or equipment manufacture, research reactors, etc.) political pressure has been brought to bear and will continue to be felt in the coming years, aimed at their closure. Export guarantees may also be called into question. Restructuring is in progress at AREVA GmbH.

However these same industries are also reorganizing to take advantage of the potential linked to renewable energy in particular for offshore sites as well as for the work on networks and storage. These are indeed the fields in which Germany wants to be at the forefront in the years to come. In this respect, it should be noted that Siemens, which had anticipated this turning point, is winning major contracts in these areas.

Production policy to compensate for the loss in the nuclear field

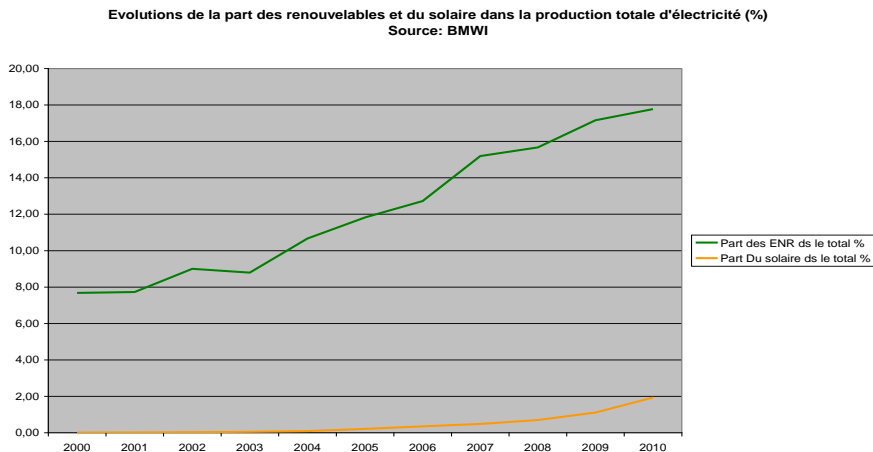
- Compensation in the short term on the grid

The 8 reactors shut down correspond to approximately 30% of the installed nuclear capacity, i.e. approximately 8% of the German electricity generation.

It had some excess capacity, which in particular, by running the fossil energy facilities at a maximum, enabled the demand to be met in the spring. However, a certain rebalancing of imports/exports with France was noticed nevertheless.

- Compensation in the medium term

This involves replacing within ten years, the 23% of electricity generated by nuclear plants in 2010. Since 2000, when renewable energies accounted for 8% of production, production (%) the overall rise was about 1% per year during the last ten years (see above graph N° 2) . But in 2011, the renewable energy production reached 121,8 TWh . It represents 19,9% of the German electricity production, and for the first time , more than nuclear production.



Developments of renewable energies and solar power in overall electricity

This progression will lead to many challenges: problems of cost (solar energy), of physical limitations (for the land-based wind and biomass energy) and of instability of the network.

So now no-one thinks that an acceleration of the renewable program , mainly with offshore wind projects, would enable the required replacement in the allotted time.

A major program has thus been launched to install the required complement in the form of fossil-fuel thermal power plants: 12.8 GW under construction by 2013, then an additional 10 GW by 2020. Compliance with the construction schedules for these plants, as well as offshore projects will be essential to ensure compensation during peak periods.

The attached table shows the developments in forecast capacities until 2023 (excluding renewable and nuclear energy)

Variation in production capacities excluding renewable energies and nuclear power (in GW)	2012-2014		2015-2023	
	new capacities	capacities discontinued	new capacities	capacities discontinued
coal	+ 8.03	- 1.08	+ 5	- 2.2
lignite	+ 2.74	- 2.02	-	- 2.7
gas	+ 1.734	0	+ 5	-3.7
hydroelectric	+ 0.195	0		
other	+ 0.139	- 0.232		
Total (excluding renewable energies and nuclear power)	+ 12.8 GW	- 3.3	+ 10 GW	- 8.6
balance	+ 9.5 GW		+ 1.4GW	

- Compensation in the long term

In the long term Germany aims to jointly reduce consumption and continue to increase renewable energies (up to 80% in 2050).

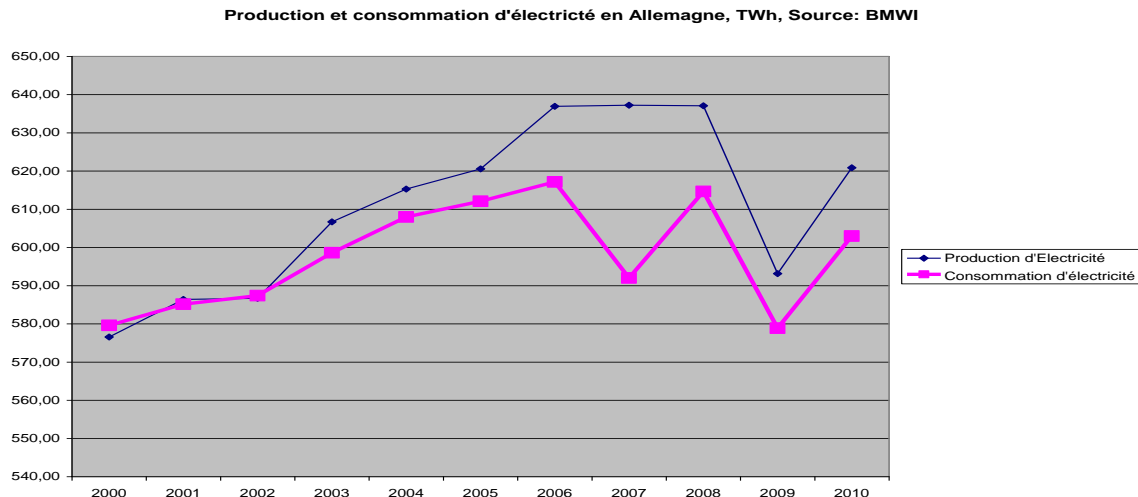
This poses significant problems in terms of cost and feasibility, but also in terms of storage, network stability and energy savings. This last point will, however, be facilitated by an additional increase in the cost of electricity, already, predictable.

In conclusion, there is no change to the long-term policy to move away from nuclear power and replace it essentially with renewable energies. Quite simply the transition, which was to be provided by extending the service life of nuclear power will largely, be provided by this scheduling of 22.8 GW from thermal power plants.

Towards an increase in energy costs and a drop in consumption

The graph below (graph No.3) of electricity consumption developments in Germany shows an end to the on-going rise and the start of the decline from 2006.

In 2011 , the global production was 611,4 TWh and the global consumption 607 TWh.



Electricity production and use in Germany, TWh, Source: BMWI

The private German individual already pays in 2010, his power 24 EC/KWh compared to 13 in France. (Source: Eurostat, BMWI). Major investments for future renewable energies and the network will continue to be largely covered by the consumer's bill. Energy savings will therefore be associated with an increasingly expensive energy.

As an example, in 2009, a German used 7,070kWh on average per year and a Frenchman 7,740kWh/year. .

Remember that the official target is a 50% reduction of energy consumption by 2050.

Towards an acceleration of research

A new program for research was presented on August 3 by the ministers for the 2011/2014 period. 3.5 billion euros are devoted to energy research, which represents an increase of 75% compared the 2006/2009 period. This program incorporates the major themes already being studied, but with a marked increase in the budgets assigned. 80% of this budget is devoted to energy efficiency and renewable energy.

Conclusion

The law on the extension of the power plants' service life will therefore have survived only three months. The transition to renewable energies by nuclear power plants, which was to have taken place due to this law, will eventually be carried out primarily through a program of accelerated construction of thermal power plants.

The early withdrawal of the Germans from nuclear energy accentuates a certain divergence between the energy policies with France, and will lead to the need to manage problems related to this divergence.

Conversely, it represents a tremendous opportunity in terms of research, for collaboration between the two countries in many new areas, where an acceleration of the results has now become vital.

HOW RESEARCH REACTORS CAN COPE WITH FUKUSHIMA-TYPE EVENTS

A. DOVAL, C. MAZUFRI

Nuclear Engineering Department, Nuclear Projects Division, INVAP S.E.

Av. Cmdt. Luis Piedrabuena 4950, 8400 S. C. de Bariloche, Argentina

ABSTRACT

While the first attempts to identify the key lessons from the Fukushima accident are being carried out, some undoubted facts can be mentioned: there is no evidence of major human errors as in the previous accidents (namely, U. S. Three Miles Island and Chernobyl) and the initiating event was of an extraordinary magnitude, causing a long term loss of the normal power supply producing the failure of each defence-in depth barriers with the final release of radioactive material to the atmosphere.

While a Beyond Design Basis Accident (BDBA) is normally analysed in terms of dose to the public and frequency of occurrence (probabilistic analysis), to consider that the BDBA occurs due to and together with a catastrophic situation adds a severe stress component worse than the dose in itself, giving the analysis a new perspective.

The objective of this work is to present an overview of the different Engineered Safety Features that can cope with one of the basic safety functions "removal of the residual heat" for different designs of research reactors depending on their power.

The assessment of the evolution and consequences of a combined long term power blackout with a LOCA event, clearly identify as a BDBA, and the way this can be managed by passive means, is also presented.

1 Introduction

There is no doubt that the Fukushima accident gave rise to a new assessment of initial events, particularly external events, not only for the NPPs safety analysis but for research reactors, as well. However, there is no need to reach such extreme conditions to face these scenarios. Extraordinary situations following an earthquake, such as the sudden flooding of the primary pump room and/or the electric board or the volcano ashes, could result in the unavailability of the residual heat removal equipment, either due to the loss of the coolant pumps or due to the loss of the cooling towers/heat exchanger, for example. So, it is realistic to think that future safety reviews will require facing such type of scenarios to identify which are the Engineered Safety Features that can manage this kind of events, focusing on the "residual heat removal" basic function.

To proceed with this analysis, first a list of reactor types, based on the fission power or on power density, will be presented together with the relevant ESFs for each case. Following, a list of the key issues observed at Fukushima and how RR could manage these issues will be assessed and, finally, the analysis of the sequence of events of the Fukushima BDBA for a "generic" high power reactor of 20 MW, will be discussed.

2 Engineered Safety Features - ESF

The basic purpose of reactor safety is to comply with the Safety Objectives, mainly, "to protect individuals, society and the environment from harm by establishing and maintaining in nuclear installations effective defences against radiological hazards maintain the integrity of the multiple barriers to fission product release", following IAEA guidelines [1].

This implies to fulfil the three basic safety functions, also stated by IAEA guidelines:

- shut down the reactor and maintain it in a safe shutdown state for all operational states or Design Basis Accidents (DBA);
- provide for adequate removal of heat after shutdown, in particular from the core;
- confine radioactive material in order to prevent or mitigate its unplanned release to the environment.

To maintain the integrity of the multiple barriers to fission product release and cope with potential human and mechanical failures, several levels of protection are implemented. The classical five levels “defence-in-depth concept” foresees protections against damage to the plant and to the barriers themselves. The five levels are **(i)** Prevention of deviations, **(ii)** Control by detection, **(iii)** Control of the consequences, **(iv)** Control of severe conditions and **(v)** Mitigation of the radiological consequences.

The safety functions that cope with accidental conditions (Level 3 of defence in depth) are fulfilled by Engineered Safety Features (ESFs) of the plant.

The need for ESFs is always determined by the analysis of accidents that could occur. It is possible that, for a particular design, the analysis performed for the Safety Analysis Report demonstrates that some ESFs considered “usual” are not needed. They include both safety systems and components of safety related systems that perform selected safety functions.

Following the IAEA safety Standards [1] and regarding only the ESF related to the residual heat removal function, a research reactor should have:

- ✓ Residual/Emergency Core Cooling system (RECCS);
- ✓ Emergency Make-up Water System (EMWS);
- ✓ Emergency Electrical Power Supply (EEPS)

Typically, there are also components or subsystems that perform the selected safety function, they are:

- Reactor Pool Pressure Boundary;
- Provisions for Flow and Pressure decrease;
- Check or Flap Valves;
- Siphon effect breakers;
- Core Cooling System Pressure Boundary;

The role of these ESF related to residual heat removal is:

- **Residual/Emergency Core Cooling System – RECCS:** The main function is the removal of the heat from the core once the reactor has been shutdown in the event that the Primary Cooling System is not running and core cooling by natural circulation is not feasible, yet.
- **Emergency Make-up Water System – EMWS:** This system has the function of compensating the loss of water from the pool in case of a LOCA in order to maintain the core under water. Depending on the total power and the maximum heat flux in the reactor this system may be either neglected, specified as a passive system, or powered by the On-site Emergency Power Supply.
- **Reactor pool coolant boundary:** It has the overall safety function of keeping available sufficient amounts of reactor coolant. In the long term, the pool coolant inventory defines the time till the operator action is required to manage the accidental sequence.
For a tank-in pool type reactor, it has an additional function as the EMWS injects water to the PCS from the pool inventory until the removal of the decay heat is compatible with natural circulation.
- **Provisions for Flow and Pressure decrease:** For the open pool type designs it provides a coast-down flow compatible with the decay power until natural convection establishes ensuring the adequate cooling of the core. Flywheels, pressurized tanks or Pony motors, are selected to ensure this function. Depending on flow direction this component allows either a delay for flow reversal, (for downward flow), or postpones the natural circulation regime, for the upward flow option.

For the pressurised tank-in pool design the flow coast-down is not enough as a slow pressure decrease is also required and most demanding. For this type of reactors this feature, flow and pressure decrease, provides the cooling condition until the RECCS starts running.

- **Valves for Natural Circulation:** The function is to connect the PCS line/s to the reactor pool and they have the safety function of allowing natural circulation to remove the residual heat of the core only after the PCS pump coast-down is complete. In other words, these valves are designed to deal with a black-out scenario.
- **Siphon-effect breakers:** Calibrated orifices in the inlet and outlet pipes of the cooling systems entering the pool will avoid the total drainage of the pool in case of a major pipe rupture of the systems and outside the pool (LOCA).
In some designs flap valves also play the role of siphon effect breakers while considering redundant flap valves at two different heights of the PCS pipes inside the reactor pool will cope with the combination of LOFA + Black-out events.
- **Core cooling System Pressure Boundary:** This is considered an ESF in case the pressure boundary design has to be conservative enough to turn its failure in an unlikely event, ensuring that a failure within the DBA scenario will not develop in a larger rupture, namely the Leak-Before-Break and Break Preclusion.
For some designs this ESF is supplied by the **Core Chimney and Inlet pipes inside the pool**. The safety function of these components is to serve as a containment for water to cool the core in the event of drainage of the reactor pool by, e.g. the rupture of the tangential irradiation tube during operation and with the irradiation tube blind flange removed from its location.

3 Research Reactors Types

There are several ways of grouping research reactors, this time the core power was adopted as the figure of merit although the power density plays an important role depending on the period of time considered. For the short-term analysis the power density results more demanding for the safety point of view while the total power (accumulated energy in the system) is the variable to be taken into account for the long term analysis.

A major classification corresponds to **open pool** and **tank-in pool** reactors and depending on core power the reactors can be grouped into low, medium or high power reactors. Commonly, high power reactors with high power densities require a pressure vessel and they are identified as **tank-in pool** reactor types. The difference with an **open pool** basically remains in the operating pressure (around 2 absolute bars in the core against some tens of bars) which marks the need or not of on-site power.

Low power

Normally, for this group of reactors the coolant flowing downwards is the more appropriate direction providing adequate cooling of the core. The power is limited, mainly, for the event of a pump stop. After reactor shutdown, a flow reversal occurs during the transition to shutdown cooling mode (natural circulation). This flow reversal, together with the low working pressure, restricts the power that can be achieved. Typical power densities for this group are lower than 100 kW/l. A flap valve for natural circulation after reactor shutdown and a proper water inventory results enough to remove the residual heat in case of a total black-out for long periods.

Medium power

The core power considered within this group is higher than 10 MW, typically, around 30/40 MW and up to 70 MW, with power densities higher than 100 kW/l. The maximum power that could be removed depends, also, on the power density or, more precisely, on the

maximum heat flux. This is the reason why reactors of up to 70 MW, like Osiris reactor, can be cooled using this scheme.

In general, the forced flow in this type of reactors is in the upward direction ensuring that there is no flow reversal when main pumps stop. For the event of a total black out, a fly-wheel in the cooling pumps and flap valves in the outlet pipes will provide the proper heat removal in the short term, changing from forced convection towards natural circulation. Additionally, a core chimney surrounding the core not only enhances the natural circulation but provides, also, physical independence of the reactor pool in case a break in the tangential beam occurs

In the long term an adequate ratio of power reactor/water inventory in the pool together with the emergency water injection by gravity, will allow the proper management of the event.

High power reactors

For this range of powers and compact cores, i.e., high power densities, the tank-in pool design is commonly adopted. Normally, they require forced coolant flow for some hours after shutdown to remain safe. To ensure the coolant flow, batteries or diesel generators are maintained to power the emergency coolant pumps operation. After that period the reactor is in a safe condition as long as the fuel remains covered with water.

Unlike the open pool type, the cooling of core is independent of the flow direction taking the corresponding advantages of each direction but, on the other hand and due to pressurization, some additional systems are required to avoid the sudden depressurization of the core cooling systems.

A general conclusion would be that, for the short term, the on-site power supply is required for the tank-in pool designs.

4 Key Issues to be observed

Clearly, research reactors do not have the same heat removal concerns as NPPs. They have a much lower heat load, much lower operating temperature and much shorter operating cycle. However, in the light of recent event some questions arise regarding if safety systems of RRs will function after a severe earthquake and if combined initiating events can happen.

• EMERGENCY POWER SUPPLY

Fukushima issue: *The loss of offsite power due to the earthquake and onsite AC power due to the tsunami, resulted in a complete station blackout which, in turn, led to fuel overheating and damage*

Low and medium power reactors have a large ratio of water inventory to power so; they do not need electricity to overcome a failure in the electrical power supply. In the short term the cooling of the reactor is ensured by a coast-down flow compatible with the decay power, (pump fly-wheel) until natural convection establishes (flap valve) and remains for longer time periods. However, high power reactors (tank-in pool designs) require the actuation of the RECCS for some period after shutdown before the core can be cooled by natural circulation.

For the long term, the pool coolant inventory defines the time till the operator action is required to manage the accidental sequence. Rough calculations show that to heat-up and evaporate a water amount of $\approx 50 \text{ m}^3$ (i.e. a pool of 3.5m \varnothing and 5m of water column height) for a reactor power of 20 MW, give almost 1 month to evaporate the water above the core and it still remains covered. For a tank-in pool type reactor, that amount of coolant has an additional function as the EMWS takes water from the pool into the primary cooling system until the removal of the decay heat is compatible with natural circulation.

- **FRESH WATER SUPPLY**

Fukushima issue: The unavailability of a large amount of fresh water for the cooling system after the earthquake caused an unprecedented emergency response, sea water injection.

For RRs, the unavailability of a large quantity of fresh water, in case of an emergency, cannot be considered as a mayor issue due to the large water inventory and the low rate of evaporation. For low power reactors the pool water generally is enough and no EMWS is required, some designs (medium power) include stored onsite water by the EMWS which can provide passive injection from gravity to supply water to the reactor core.

- **SPENT FUEL POOLS**

Fukushima issue: Some radioactivity releases from the Fukushima plant might be caused from the spent fuel pools. Lack of cooling (loss of power supply) combined with the elevated location (damaged from hydrogen explosions) and earthquake-induced water leakage have aggravated the accident.

In research reactor, the stored energy and radioactive inventory are orders of magnitude lower than in a NPP. Additionally, the dispersed fuel used in research reactor has a significantly different behaviour in term of fission product retention. Some research reactors have the spent fuel pools of stainless-steel lined and built into the concrete structure seismically qualified besides a large ratio of water inventory to power.

- **SUMMARY OF KEY ISSUES AND THE RR MANAGEMENT**

It is assumed that the loss of the off-site power supply is the major key issue and new regulation will seek to verify and assess the capability of the plant to mitigate Fukushima-like scenarios and take appropriate actions if vulnerabilities are identified. Table 1 summarizes the key issues of a Fukushima-like event and how research reactors can manage them.

As an example, in the next section a combined initial event of total black-out with LOCA event is analyzed for a medium power reactor.

Key issue	Fukushima	Low Power	Medium Power	High Power
Emergency power supply	Lost	Not necessary • Flap valves for NC • Reactor pool water inventory	Not necessary • Pump fly-wheel • Flap valves for NC • Core chimney • Reactor pool water inventory	For short/medium term: • On-site power (diesel generators) For the long term: • Flap valves for NC • Reactor pool water inventory
Fresh water supply	Sea water injection	Pool water inventory	Passive EMWS	On-site power for the EMWS (diesel generators)
Spent FE pool	Failed	Pool water inventory SS lining	Auxiliary Pool water inventory SS lining	Auxiliary Pool water inventory SS lining

Table 1: Key issues and ESF for different types of RRs

5 Analysis of a combined Black-Out + LOCA events

The present analysis was motivated in the light of Fukushima observations. It is not unreasonable to think that after an earthquake of such large magnitude as that occurred in Japan, the electric power supply interrupts and a break in any of the cooling pipes takes place. The assessment was performed for a reactor of 20 MW and 250 kW/lt considering the break of a pipe of 250mm of diameter.

The coolant flows upwards, the main pumps have inertia fly-wheels and the amount of water in the reactor pool is more than 50 m³. Figure 1 shows the evolution of the pool water level and the heat removal mechanisms are indicated at different points.

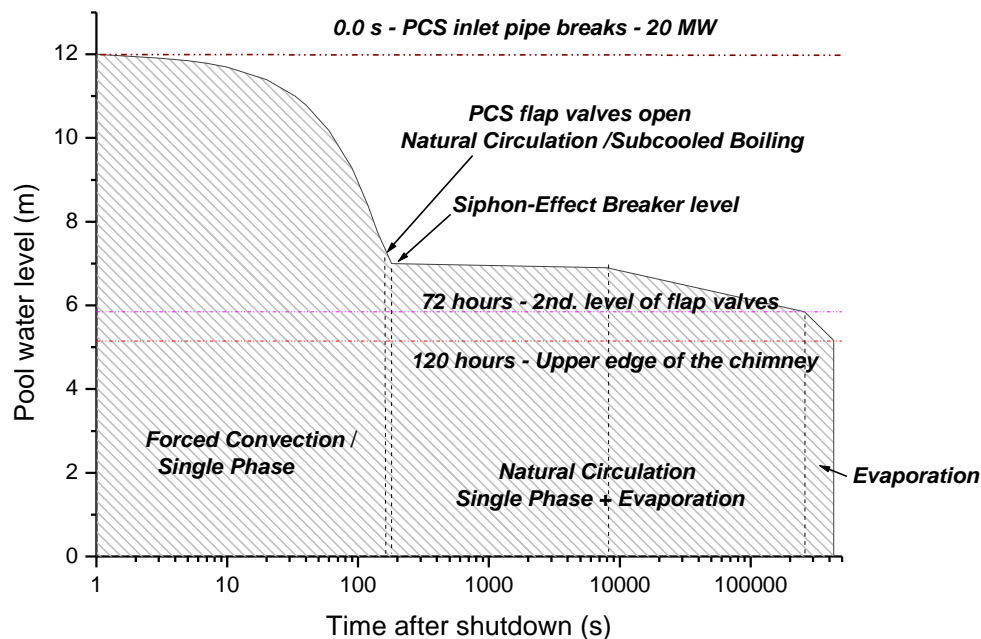


Figure 1: Evolution of pool water level and heat removal mechanisms for LOCA + Black-out

From Figure 1 it can be seen that residual heat removal is always fulfilled but more important is to notice that the accident can be managed only by the passive features of the design; no additional emergency power supply is needed.

When a tank-in pool design is analyzed active components, such as the pumps in the residual and emergency core cooling system or in the emergency make-up water systems, require on-site emergency power supply. Different alternatives, such as smaller diameter of PCS pipes, must be analyzed in order to avoid or reduce the requirements of an emergency power supply.

6 Conclusions

Fukushima accident has opened a new discussion regarding the safety features of research reactors and how this kind of accidents can be managed. This paper presents a list of ESF that has been analysed for different types of research reactors with power ranges from some MW up to some tens of MWs.

A combination of a black-out event plus a LOCA, bounding a Fukushima-like scenario, for an open pool reactor of 20 MW, was generically assessed showing that it can be managed properly by means of passive systems and components and that there is no need of any emergency power supply.

7 References

- [1] INTERNATIONAL ATOMIC ENERGY AGENCY, Safety of Research Reactors, IAEA Safety Standards Series No. NS-R-4, IAEA, Vienna (2005).

STATUS UPDATE ON CONVERSION TO LEU-BASED ^{99}Mo PRODUCTION IN SOUTH AFRICA

G. BALL

*Technology Division, NTP Radioisotopes (Pty) Ltd
Church Street West Extension, PO Box 582, Pretoria, 0001 – South Africa*

ABSTRACT

The 20 MW SAFARI-1 research reactor and NTP ^{99}Mo production facilities at Pelindaba, South Africa continue to produce and distribute significant quantities of ^{99}Mo to service the world nuclear medicine market. Over a number of years a significant effort has been expended by NTP Radioisotopes (Pty) Ltd and its parent company, Necsa, towards the conversion of uranium targets, reactor fuel and the ^{99}Mo production process from HEU- to fully LEU-based.

Developmental work on the conversion to a LEU target and associated ^{99}Mo production process commenced in 2007 and steady progress was made towards the goal of full conversion with various landmark successes having been achieved along the way. Finally, in December 2010, the first large scale batch of fully LEU produced ^{99}Mo was shipped to the United States for use in the production of $^{99\text{m}}\text{Tc}$ generators and subsequent multiple patient diagnostic procedures. These technical and commercial achievements were the culmination of many years of work by various highly skilled people and organisations.

In this paper the challenges and successes over the past 5 years are summarised and views on the future challenges being faced regarding the completion of the conversion to LEU are expressed.

1. Introduction

The SAFARI-1 research reactor is owned and operated by the South African Nuclear Energy Corporation (Necsa). It was commissioned in 1965 and has a designed thermal power of 20MW. Since commissioning, it has operated with an exemplary safety record. Commercial and research programs at the reactor are supported by an extensive infrastructure, ranging from theoretical reactor physics, radiochemistry and radio-analytical groups, a fuel and target fabrication plant, hot cell facilities for the production of medical and industrial isotopes, a pipe storage facility for the interim dry storage of spent fuel and a disposal site for low and intermediate radioactive waste. For the past ten years SAFARI-1 has operated at a power of 20MW from 300 to 305 days per year, almost exclusively for isotope production purposes.

NTP Radioisotopes (Pty) Ltd, a limited liability company, is a wholly-owned subsidiary company of Necsa. Its primary focus is the production and distribution of various radiochemicals and isotopes to both the medical and industrial sectors. NTP also produces various radiopharmaceuticals such as a variety of cold kits, its locally developed NovaTec-PTM $^{99\text{m}}\text{Tc}$ generator, ^{18}F based PET products and ^{131}I capsules and solutions.

Necsa and NTP have ardently supported the principles of the Reduced Enrichment for Research and Test Reactor (RERTR) programme for many years and have actively worked towards converting both SAFARI-1 to LEU fuel and the ^{99}Mo production process to LEU

targets within the technical and commercial constraints facing it [1]. It should also be noted that despite the recent international crises with regards to ^{99}Mo production and supply, NTP continued to develop and industrialise its LEU-based ^{99}Mo production process while ensuring the complex development programme did not influence routine ^{99}Mo supplies.

During the past 2 years, significant milestones were achieved several of which are outlined in this paper. In particular, the first ever commercial sized batch of FDA approved LEU-produced Mo-99 was produced and shipped to the United States in December 2010 for use in $^{99\text{m}}\text{Tc}$ generators and subsequent human patient diagnostic procedures..

Although the many technical challenges involved in LEU-based ^{99}Mo production have successfully been addressed, various others have yet to be overcome in order to complete the conversion process.

2. ^{99}Mo Production Plant

The ^{99}Mo production process was developed at NTP in the late 1980's and early 1990's. During 1993 the production batch sizes were 20Ci (6 day calibrated) and this was progressively scaled up to 100Ci to 200Ci in 1994 and it was during this year that the first ^{99}Mo commercial sales to export markets commenced. The pilot production plant which was used for the hot process development phase, as well as during the early years of commercial production, was shut down in 1995. The experience gained in the pilot plant phase proved invaluable in the later design and construction of the large-scale production lines and a significantly improved production process, the first of which was commissioned in 1995 and the second in 2000.

The facility used for isotope production (including ^{99}Mo) was originally designed for and operated as a Post Irradiation Examination (PIE) plant. After completion of the PIE work in the plant in the late 1980's the plant was substantially modified to accommodate large-scale isotope production requirements. Due to the flexibility of the of the plant layout, the original hot cells were decommissioned and decontaminated, removed and new purpose-built hot cells were designed, manufactured and commissioned. Substantial changes were also made to the liquid handling and gaseous filtration systems. All work was carried out or, in isolated cases managed, entirely in-house.

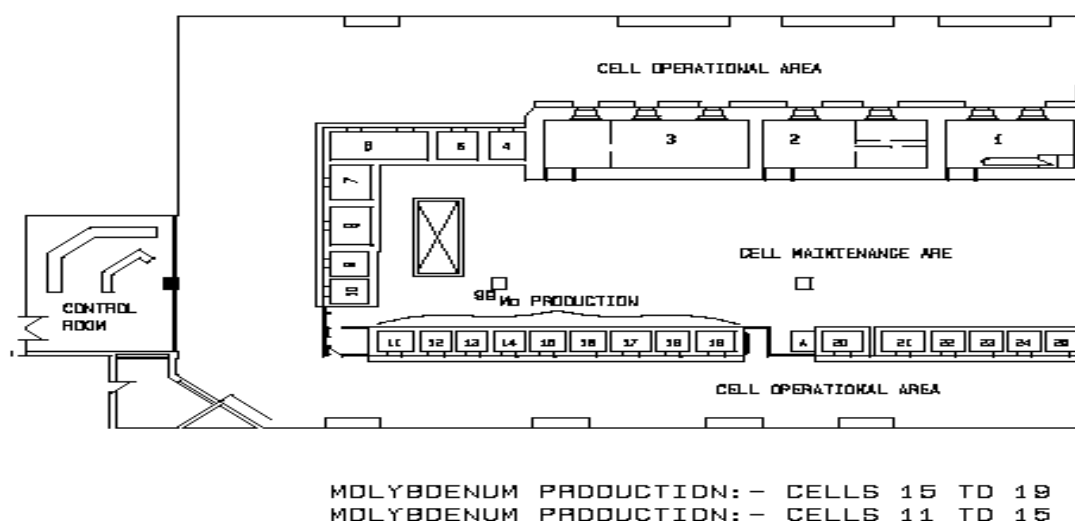


Figure 1: Schematic Layout of Hot Cell Facility

The facility consists of 3 large concrete-shielded and 22 smaller lead-shielded hot cells (See Figure 1). The extensive infrastructure also includes liquid waste handling and intermediate

storage facilities for various radioactivity levels; four ventilation and filtration systems (and additional specialised such systems for the dissolver cells); solid waste handling and other support facilities.

The dissolution, extraction, purification and dispensing operations are spread over various hot cells in order to minimise the risk of cross contamination and provide an uncluttered and spacious environment in which to perform each step of the process. Two types of hot cells are used in each production line i.e. a special dissolver cell containing additional shielding, specialized ventilation and liquid waste systems in order to handle the highly radioactive target plates and four standard cells housing the rest of the production processes. For redundancy and production continuity risk mitigation, currently the facility has two separate production lines for ^{99}Mo production and has dual dissolvers in each line.

The radiochemical production facility is operated for 51 out of every 52 weeks. This high level of operational availability is due to the availability of two production lines and extensive maintenance and upgrade programmes.

3. Conversion of the NTP ^{99}Mo Production Process

NTP has been producing ^{99}Mo from 45% enriched uranium for over 17 years and consequently has a wealth of experience and knowledge of its process and plant. It was this experience and knowledge base that was used to expedite the project to convert to fully LEU-based ^{99}Mo production. In order to minimise the changes required to target, irradiation, handling and processing technology, a low enriched uranium aluminium dispersion target was selected.

From 2008, numerous cold and hot development runs were performed. These were followed by formal process validation runs, both for NTP as the producer of LEU ^{99}Mo and for $^{99\text{m}}\text{Tc}$ generator manufacturers. The timeline of events is summarized in the table below.

Table 1: Timeline of events for NTP's ^{99}Mo production process conversion

Date	Event
2007	Theoretical feasibility study performed
2008	Cold and depleted uranium experiments performed
October 2009	SA Nuclear Regulator approval received for Hot Test Phase Hot Test Phase commenced
March/April 2010	Process validation production runs performed
June 2010	Submission to SA Nuclear Regulator for routine LEU ^{99}Mo production Submission to Medical Regulators commenced
July 2010	Customer tests and validation runs commenced
September 2010	SA Nuclear Regulator approval received for routine LEU ^{99}Mo production
September 2010	US FDA approves LEU ^{99}Mo for a customer in the US
December 2010	First large scale commercial FDA approved batch of LEU ^{99}Mo produced and shipped to US for patient use
June 2011	Routine commercial supply of LEU ^{99}Mo commenced to some customers

After the completion of developmental work to optimise ^{99}Mo extraction efficiencies, the yields obtained from LEU ^{99}Mo production runs are equivalent to those achieved using HEU. It must, however, be pointed out that the batch sizes have decreased by approximately 10% due to the ^{235}U loading in the LEU targets being lower than for HEU as a result of uranium density restrictions in the dispersed target. LEU-produced ^{99}Mo continues to conform to the British and European pharmacopeia's requirements.

The figure below indicates the distribution of LEU ^{99}Mo production runs (as a percentage of total LEU runs) performed in six monthly periods over the past 2½ years. Other than the initial developmental runs performed in the latter half of 2009, there has been a steady increase in the number of LEU production runs performed during each of the six month periods over the past 24 months.

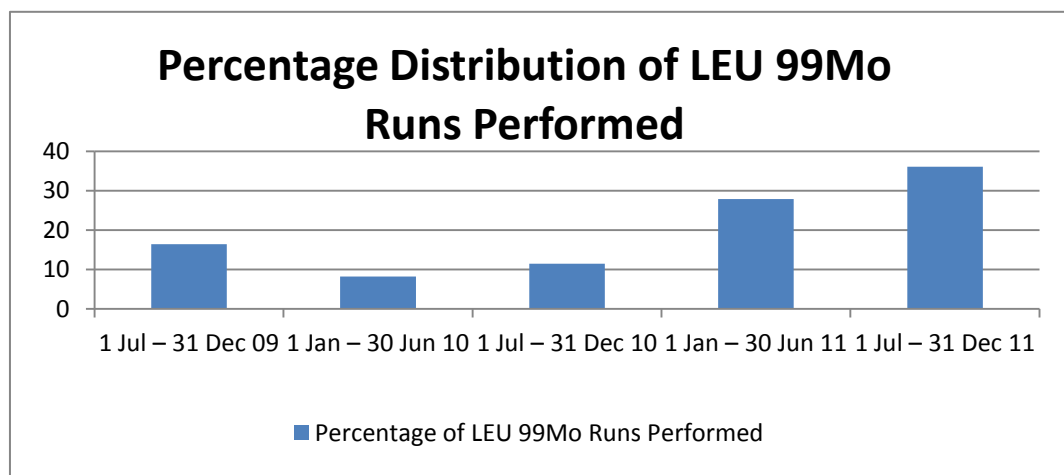


Figure 2: Percentage of LEU ^{99}Mo Runs Relative to Total LEU ^{99}Mo Runs

Of all the LEU production runs to date, 28% and 36% were performed during the first and second halves of 2011 respectively.

Initiatives have also commenced in an attempt to regain the lost production capacity experienced due to the lower ^{235}U loading in the LEU targets. This will initially be addressed by considering changing the current LEU target dimensions. Going forward, the possibility of using a higher density target is being investigated.

Several steps of process optimisation and improvement have also been necessary by the target manufacturer in order to produce LEU dispersed targets that comply with the more stringent specifications which developed due to the experience gained in producing LEU ^{99}Mo .

4. Challenges to Conversion

Putting the technical issues aside, there are various other challenges which have to be addressed in order to convert from HEU to LEU ^{99}Mo production. Some of these are mentioned below:

Customer Appetite for LEU ^{99}Mo

It is a significant, costly and time consuming exercise for a $^{99\text{m}}\text{Tc}$ generator producer to qualify themselves for LEU ^{99}Mo . Although most customers understand the international drive to reduce the enrichment of uranium used in the civil sector, they have no real urgency to convert and as a result their response is mixed. Currently the benefit to customers of LEU ^{99}Mo is minimal if any at all. Even though customers appreciate that the production cost for LEU ^{99}Mo is higher, they are generally not prepared to pay an increased price.

Medical Regulators

Medical regulators require that a new Drug Master File (DMF) be prepared and submitted for LEU ^{99}Mo . This DMF, together with the validation data provided by the $^{99\text{m}}\text{Tc}$ generator

producers, is then put through a formal review process. The challenge is that, not only does this take time, but it has to be done by the regulator of each country in which the ^{99m}Tc generators are sold. Only after approval is obtained from each of the regulators can the generator producer start manufacturing and distributing their generators produced using LEU ^{99}Mo . This results in long lead times to complete the validation and review process and has to be completed by all generator manufacturers in all countries to which their product is distributed.

Logistics

There are significant challenges associated with production planning arising from customer requirements, cGMP issues and general downstream effects. Due to the current routine production and supply of HEU ^{99}Mo and the requirement to minimise the impact of LEU ^{99}Mo production runs on current supply, production planning is becoming increasingly complex. Customers have rigid requirements regarding their ^{99}Mo supply due to the downstream effects on generator producers of untimely or lower than ordered activity. As a result, in some circumstances, it is impossible to produce LEU ^{99}Mo on the day and in quantities which the customer requires due to the detrimental impact on HEU ^{99}Mo production. Also, due to cGMP requirements, complexities exist with regard to ensuring that the HEU and LEU production runs are separated to prevent any cross contamination.

^{131}I Production

A further complication affecting conversion to LEU is that fission ^{131}I is also produced from the same targets as ^{99}Mo . The entire process which has to be gone through for the qualification of LEU ^{99}Mo also must be performed for LEU produced ^{131}I . The production challenges to this are also significant.

Manufacture

To increase uranium loading in the target in order to, at least, regain the lost ^{99}Mo production capacity is a significant problem to overcome. If achievable, it will be the result of a joint effort between target manufacturers, reactor operators and ^{99}Mo producers, based on a detailed investigation of manufacturing processes and product specifications.

5. Conclusions

Significant progress has been made towards the conversion from HEU to LEU ^{99}Mo production at Necsa/NTP. In fact, increasing numbers of customers have started accepting LEU ^{99}Mo for test and qualification purposes. Routine commercial supply of the product also commenced in July 2011 and this is evidenced by the steady increase in the number of LEU production runs performed over the past few years.

The challenges raised in the paper will continue to be addressed and solutions sought. NTP remains committed to completing the full conversion of its ^{99}Mo process and switching entirely to LEU production but will do so in a responsible manner and will not place undue risk on the security of supply of approved ^{99}Mo .

6. References

- [1] G. Ball, "Status of Conversion of the South African SAFARI-1 Reactor and ^{99}Mo Production Process to Low Enriched Uranium", Proceedings of the XXXII International Meeting on Reduced Enrichment for Research and Test Reactors, Lisbon, Portugal, 10-14 October 2010.

Irradiations of HEU Targets in MARIA RR for Mo-99 Production

G. Krzysztoszek

National Centre for Nuclear Research, A. Sołtana 7, 05-400 Otwock, Poland

G. Krzysztoszek : g.krzysztoszek@ncbj.gov.pl

Abstract

The high flux research reactor MARIA is operated at the National Centre for Nuclear Research. It is a water and beryllium moderated reactor of pool type with graphite reflector and pressurized channels containing concentric tube of fuel element. Due to the shutdown of the NRU reactor (Canada) and plans for scrambling the HFR reactor (Holland) in the half of 2009 a decision was taken on cooperation between IAE and COVIDIEN which was aimed to initiate an irradiation of high-enriched uranium plates in MARIA reactor for production of molybdenum Mo-99. There was developed the Mo-99 irradiation and transport technology in MARIA reactor facility and then its expedition to the processing factory in Petten (Holland).

The positive opinion of the Nuclear Safety Committee of IAE and approvals released by the National Atomic Energy Agency were received in the end of December 2009.

Before regular irradiation the program for checking and testing full installation was carried out.

The number of licenses needed for the transport of irradiated uranium plates from MARIA reactor in Poland through Germany to Holland were received.

During irradiation through February 2010 - February 2012 we have received very good results confirmed by production facility in Petten.

1. Introduction

Due to the shutdown of the NRU reactor (Canada) and plans for scrambling the HFR reactor (Holland) in the half of 2009 a decision was taken on cooperation between IAE and COVIDIEN which was aimed to initiate an irradiation of high-enriched uranium plates in MARIA reactor for production of molybdenum Mo-99. There was developed the Mo-99 irradiation and transport technology in MARIA reactor facility and then its expedition to the reprocessing factory in Petten (Holland). The physics calculation, safety analyses, technical projects of equipment for irradiation and transport inside the reactor facility and loading to the special transport container (MARIANNE) were made.

After receiving the positive opinion of the Nuclear Safety Committee of IAE and approvals released by the National Atomic Energy Agency there were made channel for uranium plates' irradiation, equipment for plates' transport from the reactor core to the shielding container MARIANNE. It was accomplished the program for checking and testing full installation which included:

- loading unloading and transport of plates within the boundary of reactor pools,
- reloading of the dummy plate's to the shielding container,
- irradiation of the plates' dummies (Al) in the reactor,
- monitoring of container leak-tightness,

The number of licenses needed for the transport of irradiated uranium plates from MARIA reactor in Poland through Germany to Holland were received. The irradiation of uranium plates has been taken place in the MARIA reactor from February 2010.

2. MARIA research reactor description

The research reactor MARIA is operated at the Institute of Atomic Energy POLATOM (IAE). The multipurpose high flux research reactor MARIA is a water and beryllium moderated

reactor of a pool type with graphite reflector and pressurised channels containing concentric six-tube assemblies of fuel elements. It has been designed to provide high degree of flexibility. The fuel channels are situated in a matrix containing beryllium blocks and enclosed by lateral reflector made of graphite blocks in aluminium cans, *FIG.1*. The MARIA reactor is equipped with vertical channels for irradiation of target materials, a rabbit system for short irradiations and six horizontal neutron beam channels.

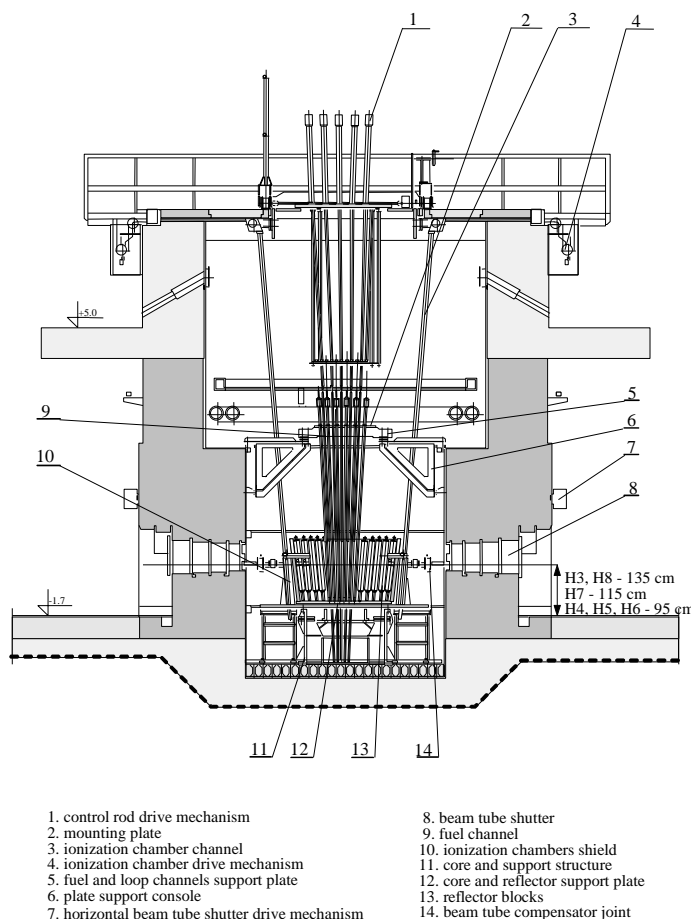


FIG. 1. Vertical cross-section of MARIA RR.

The main characteristics and data of MARIA reactor are as follows:

- nominal power 30 MW (th),
thermal neutron flux density $4.0 \cdot 10^{14} \text{ n / cm}^2 \cdot \text{s}$,
- moderator H_2O , beryllium,
- cooling system channel type,
- fuel assemblies:
 - material $\text{UO}_2\text{-Al alloy}$
 - enrichment 36 %
 - cladding aluminium
 - shape six concentric tubes
 - active length 1000 mm
- output thermal neutron flux
at horizontal channels $3 \div 5 \cdot 10^9 \text{ n / cm}^2 \cdot \text{s}$

The main areas of reactor application are as follows:

- production of radioisotopes,
- testing of fuel and structural materials for nuclear power engineering,
- neutron radiography,
- neutron activation analysis,
- neutron transmutation doping,
- research in neutron and condensed matter physics.

3. Developing the uranium targets irradiation technology, safety analysis, measurements and tests

In the period from June 2009 up to January 2010 the technology and safety analyses of irradiation and shipment of uranium was developed and also a number of tests and measurements were conducted. They included the hot test in which several test plates were irradiated.

Technology for irradiation and handling of uranium plates comprise of:

- Irradiation of plates and initial cooling in the irradiation channel
- Calorimetric measurement of heat generation in the capsule with plates
- Transport of plates into the hot cell
- Handling operations in the hot cell
- Loading of plates into the transport cask MARIANNE

Calculations and safety analyses at steady states are as follows:

- Calculations of molybdenum activity
- Neutronic calculations
- Thermal-hydraulic calculations at steady states
- Activity of fission products and thermal power of the uranium plate batch
- Cooling of uranium plates in the capsule for irradiation during natural convection in the air
- Shielding calculations and an assessment of radiological hazard for personnel pending reloading – transport operations

Program of examinations and installation tests consist of:

- Hydraulic measurement of channel for irradiation of capsules containing the mock-ups of plates
- Cold trials of reloading and transport operations with a batch of dummy plates
- Calibration measurements of calorimeter for measuring of thermal power of 4 plate batch
- Measurement of axial distributions of the neutron flux density in the capsule containing dummy plates
- Measurements of the heat balance in molybdenum installation with the dummy plates
- Test irradiation of uranium plates and their dispatching
- Measurements of temperatures of uranium plates in the air

The main assumptions have been taken into account while developing the uranium targets irradiation technology for the production of the molybdenum in the MARIA reactor and are as follows:

- Irradiation is held in containers, containing 4 plates each, loaded into the molybdenum channel,
- Irradiation of the containers with plates is held in installations which are converted fuel channels of the MARIA reactor,
- The nominal flow of coolant is maintained in the irradiation installation because of high thermal flux and the possibility of the molybdenum channel location change,

- Preliminary cooling of uranium plates after irradiation is held in the installation to irradiation as part of the procedure of removing of the residual heat generated in fuel of the MARIA reactor,
- The transport of the containers with plates into the hot cell involves the change of conditions of cooling the containers with plates as well as uranium plates (handling operations in the hot cell are conducted in the air),
- The total activity of fission products in uranium plates during transport operations in the hot cell is ca. 100 kCi,
- The plates are loaded into a special shielding container MARIANNE and transported to COVIDIEN company for processing at the laboratory in Petten (Netherlands).

4. Mo-99 production in the MARIA reactor - current state

In the period March 2010 to January 2012, 34 irradiation cycles in the MARIA reactor were conducted. In all cycles were irradiated 500 plates.

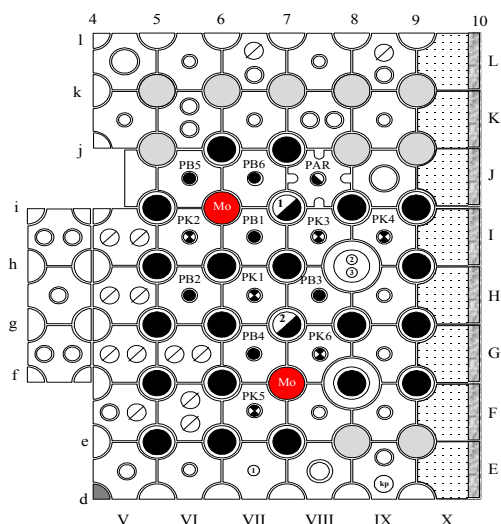


FIG. 2. A typical configuration of the MARIA reactor core with molybdenum channels.

Irradiations were conducted in three different locations of molybdenum channels (f-7, h-7 and i-6) and different configurations of the core, introduced in FIG.2. The typical configuration of the core for irradiations of molybdenum channels is shown in Fig.2.

The details of irradiation cycles of uranium plates in the Maria reactor are presented below:

- | | |
|--|---------------------|
| – time of irradiation | – 120 ÷ 145 [hours] |
| – average power | – 180 ÷ 200 [kW] |
| – Mo-99 activity at the end of irradiation (EOI) | – 7000 ÷ 8000 [Ci] |

The technological parameters of MARIA RR core are shown in FIG.3.

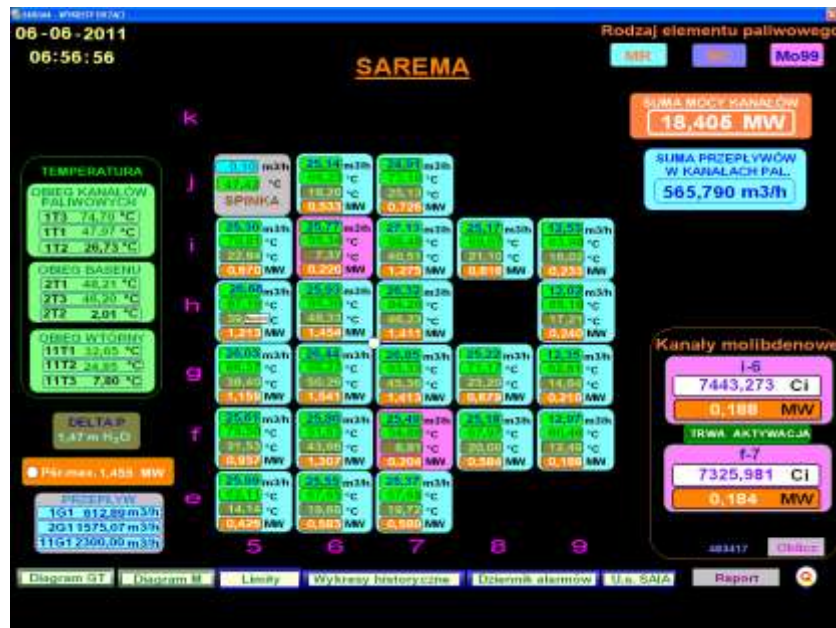


FIG. 3. Diagram of MARIA RR core.

The programme of HEU targets irradiations in 2012 connected with 10 cycles is shown in FIG.4.

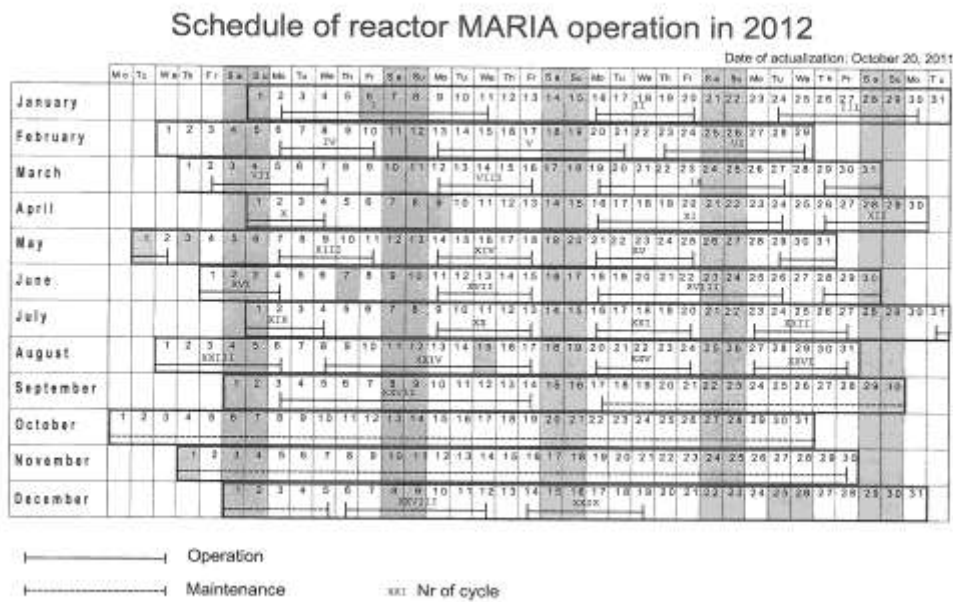


FIG. 4. Schedule of reactor MARIA operation in 2012.

5. Possibilities of increasing Mo-99 production in the MARIA reactor

The substantial rise in the production is possible by increasing the number of molybdenum channels or increasing the number of containers with uranium plates in the channel.

5.1 Increasing the number of molybdenum channels in the MARIA reactor

Installation of molybdenum channels in the MARIA reactor core is connected with the need to increase the mass of fuel (U-235). The enlargement of the core causes increasing of the total reactor power and also the flow of coolant has to be ensured by additional fuel elements and molybdenum channels. Operation of the reactor with one molybdenum channel required increasing the power in the range of $13 \div 19\%$ whereas with two molybdenum channels $18 \div 22\%$. According to results of calculations the installation of another molybdenum channel in the h-8 position would cause enlargement of the core by adding next fuel element and the increasing of the reactor power by at least 25%. In the current state of the reactor ensuring the appropriate flow of coolant through channels is a more difficult task. Planned in the second-half of 2012 modernization of the cooling channels circuit (exchange of pumps, change of their configuration) would make it possible to enlarge of the MARIA reactor core. The modernization of the circuit will be conducted as a part of the program of conversion MARIA reactor from HEU to LEU fuel. Adding another molybdenum channel in the MARIA reactor core would make it possible to increase the Mo-99 yield by 50% in comparison to current state.

5.2 Increasing the number of the containers with uranium plates (up to 3)

The height of the fuel zone of the MARIA reactor (1000 mm) makes it possible to irradiate simultaneously 3 containers with 12 uranium plates in the molybdenum channel.

The assumption was made that the modification of the molybdenum channel means increasing the number of containers in the channel and placing the containers in such a way that they are symmetrical in relation to the maximum of the neutrons flux in the channel.

Total efficiency of Mo-99 production grows in the version with three containers up to 135% in relation to the version with two containers.

The total thermal power generated in the channel reaches the value of 300 kW compared with 220 kW in the version with 2 containers.

6. Conclusion

The realization of the molybdenum program confirmed the correctness of the irradiation technology and handling operations in the reactor pools and in hot cell as well as the loading operation into the transport container MARIANNE. Experience acquired made it possible to implement additional technical and organizational solutions, which increased the certainty and shortened the time of handling operations not violating adopted operating procedures.

The achieved very good results of production was an important step in increasing of commercial products and services of MARIA research reactor.

MARIA research reactor has still possibilities of increasing Mo-99 production by increasing the number of molybdenum channels or increasing the number of containers with uranium plates in the channel.

Also the number of irradiation cycles with molybdenum channels can be increased 3 times.

OECD-NUCLEAR ENERGY AGENCY'S POLICY APPROACH FOR A RELIABLE SUPPLY OF ^{99}Mo

Dr. RON CAMERON, CHAD WESTMACOTT
Nuclear Development Division, OECD – Nuclear Energy Agency
12 Bd des Iles, Issy-les-Moulineaux, 92130, France

ABSTRACT

The OECD Nuclear Energy Agency (NEA) established the High-level Group on the Security of Supply of Medical Radioisotopes (HLG-MR) to examine the reasons for the lack of security of supply of molybdenum-99 (^{99}Mo) and its decay product, technetium-99m ($^{99\text{m}}\text{Tc}$) and to develop a policy approach to address the challenges to reliable supply. This paper describes the key findings of the HLG-MR and its policy approach, which provides the steps necessary to ensure a long-term secure supply of ^{99}Mo and $^{99\text{m}}\text{Tc}$. This policy approach is the result of two years of intensive examination of the supply chain. It includes ways to send strong price signals across the supply chain, ensuring international coordination of supply availability, improving communication and demand side management and establishing a mechanism for reviewing its implementation. The HLG-MR is continuing its work, focusing on: a) the implementation of the policy approach by all producing and consuming nations (including issuing guidance documents on how to implement full-cost recovery and outage reserve capacity) and, b) examining the cost and supply impacts of converting to ^{99}Mo produced from low enriched uranium targets.

1. Introduction

At the request of its member countries, the OECD Nuclear Energy Agency (NEA) established the High-level Group on the Security of Supply of Medical Radioisotopes (HLG-MR) in 2009. During its first mandate (June 2009-2011), the HLG-MR examined the major issues that affect the short-, medium- and long-term reliability of molybdenum-99/technetium-99m ($^{99}\text{Mo}/^{99\text{m}}\text{Tc}$) supply and then developed a policy approach to move the supply chain to a sustainable basis and ensure security of supply.

At the end of the first mandate, HLG-MR members and other nuclear medicine stakeholders recognised that continued action was required to implement the HLG-MR policy approach. Thus, the NEA agreed to a second mandate for the HLG-MR (July 2011-2013). The objectives of the second mandate are to work towards increasing the long-term security of supply of ^{99}Mo and $^{99\text{m}}\text{Tc}$, especially through the implementation of the HLG-MR policy approach and its associated recommendations.

This paper will focus on the importance of implementing the HLG-MR policy approach, and will describe the work being done during the second mandate to encourage the long-term secure supply of medical isotopes. It only will briefly touch on the findings of the first mandate and the developed policy approach; however, additional detail can be found in the various publications of the NEA, especially the “final report” of the first mandate, *The Supply of Medical Radioisotopes: The Path to Reliability* (OECD/NEA, 2011a).

2. The importance of making changes in the supply chain

The $^{99}\text{Mo}/^{99\text{m}}\text{Tc}$ supply chain was the subject of global attention during the shortages of 2009 and 2010, when the two largest producing reactors experienced extended shutdowns. Since then, these reactors have come back on line and ^{99}Mo irradiation capacity returned to levels seen before the supply shortage. In addition, a few research reactors joined the supply chain

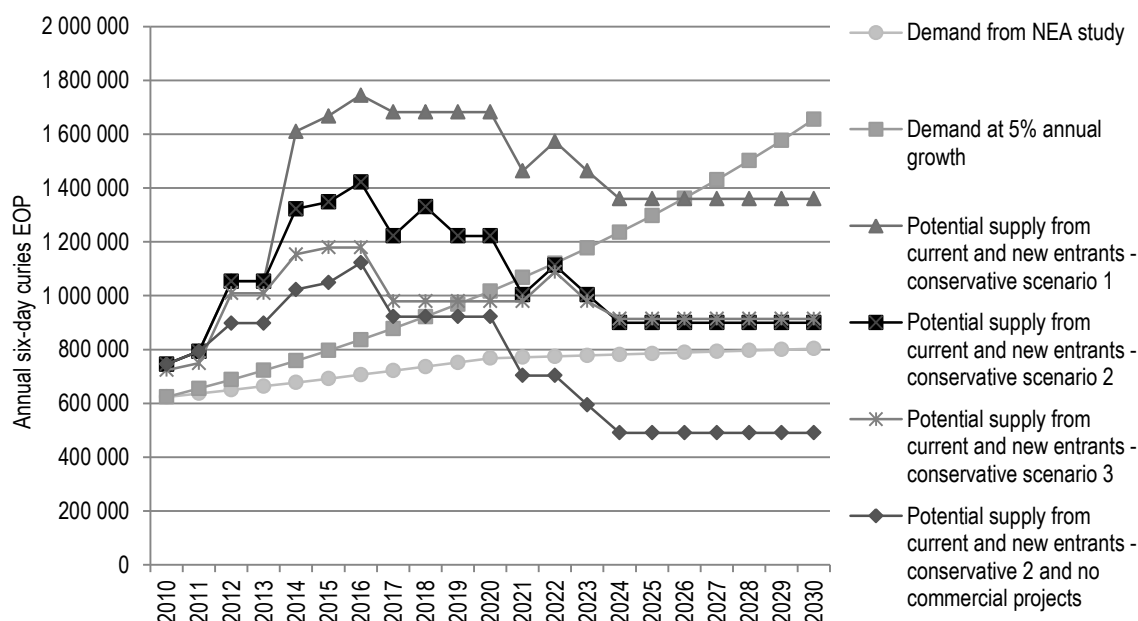
(supplementing the small historical fleet) or expanded production beyond domestic needs during and following the shortages.

While this is positive news, the current capacity remains fragile and further supply shortages could be expected. A number of the producing reactors in the current ageing fleet are scheduled to be removed from the supply chain over the next decade. Coupling these shutdowns with growing demand (OECD/NEA, 2011b), supply could be insufficient as early as 2016, even considering the reactors that have recently joined the supply chain.

Given the supply situation, a number of stakeholders are suggesting new projects to produce $^{99}\text{Mo}/^{99\text{m}}\text{Tc}$. If all the proposed projects went forward, there would appear to be no concern over future supply. However, there are a number of economic, technical and political reasons why this projection may not materialise. A key factor is that governments have indicated that they require ^{99}Mo production to be done on a commercial basis, as they are no longer interested in subsidising the industry at the reactor level

Recognising these challenges, forecasts of supply with various project scenarios are presented in Figure 3. Even if some of the projects do move forward, there could be a shortage in the coming decades as the current fleet stops producing ^{99}Mo and demand continues to increase; in addition, the level of capacity that would be available as back-up would be greatly reduced. Most troubling is the bottom line in the figure, which forecasts supply if all the projects that require some form of commercial funding do not proceed; a likely possibility if changes do not occur in the supply chain.

Figure 3: Potential supply versus demand based on conservative scenarios



The HLG-MR policy approach is meant to address the key barriers to ensuring sufficient infrastructure (irradiation and processing). The supply problem is at its root a policy failure, which established an economic structure that does not support the long-term investment necessary. The HLG-MR policy approach sets out three key themes that are addressed by six principles and a number of supporting recommendations (see Annex 1 for the principles and recommendations). The three themes are:

1. Economic return needs to be improved, especially for reactors.
2. Outage reserve capacity needs to be sourced, valued and paid for.
3. All supply chain participants need to make the necessary changes.

To address these three themes, the policy approach's main recommendations are:

1. Implement full-cost recovery in the supply chain.
2. Apply the outage reserve capacity system, as proposed in the policy approach.
3. Undertake regular reporting of progress to implementation and ensure on-going discussion among the international supply chain participants.

To ensure the long-term security of supply, these changes (and the full policy approach) need to be implemented by all countries that have an impact on the global market – either as a producer or a consumer of $^{99}\text{Mo}/^{99\text{m}}\text{Tc}$. In addition, the changes should occur by June 2014 (three years after the release of the approach) to ensure the necessary move to a more commercial-based industry.

3. Implementing full-cost recovery

A key action under the second mandate is to provide guidance on the implementation of the HLG-MR policy approach. In this light, the HLG-MR's Full-cost Working Group developed a document to provide guidance to reactor and alternative production technology (e.g., cyclotrons, accelerators) operators on how to undertake full-cost identification and implement full-cost recovery. Processors and other supply chain participants should already be applying this principle given their commercial nature.

Full-cost recovery means that all costs associated with providing ^{99}Mo -irradiation services are identified and covered through the prices set for those services. It should include both operational and capital costs; both easily identifiable direct costs and allocated indirect cost. The full-cost recovery methodology is not a price-setting mechanism; it defines the cost elements and allocation methods, but it does not dictate the value of those costs nor prices that would be expected or required under full-cost recovery.

The basic steps of the full-cost identification methodology are to: 1) identify all the costs at the reactor facility; 2) allocate the direct costs to the irradiation services; and 3) allocate the indirect costs according to the agreed upon methodology. Figure 1 provides an overview of the cost elements examined in the full-cost identification methodology.

The overall methodology for determining the costs of ^{99}Mo irradiations services is provided by the following equation:

$$\text{Full Cost for } ^{99}\text{Mo} = wA + y_m(x_rB + C) + zD + E$$

Where:

- A = Capital costs
- B = General overhead costs of the entire site
- C = General operational costs of the reactor
- D = Decommissioning
- E = Specific ^{99}Mo irradiation costs

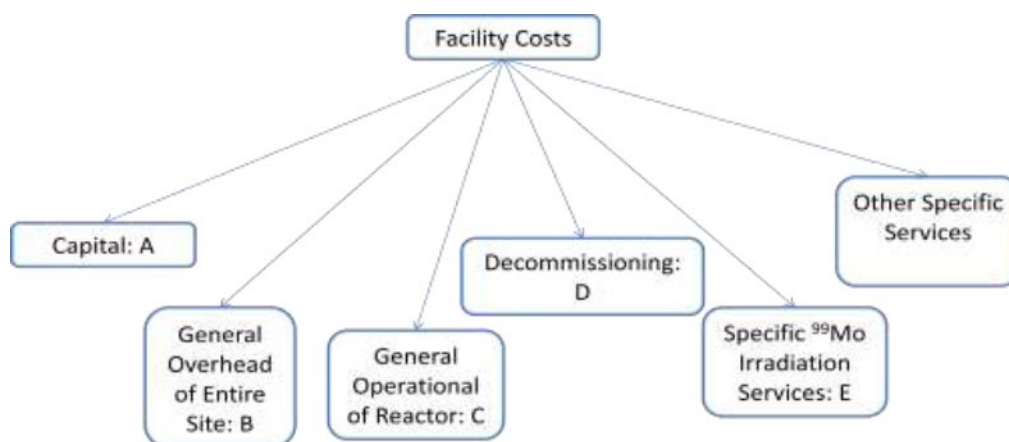
and where the proportionality constants are defined by usage parameters.

Additional details are provided in the full-cost recovery guidance document, available on the HLG-MR webpage for use by operators of research reactors and other $^{99}\text{Mo}/^{99\text{m}}\text{Tc}$ production technologies (see www.oecd-nea.org/med-radio).

The implementation of full-cost recovery is essential for all producers that supply the global market, otherwise there will be distortions that could jeopardise the long-term economic sustainability of the irradiation providers and thus jeopardise the long-term supply security of $^{99}\text{Mo}/^{99\text{m}}\text{Tc}$. In addition, it should be recognised by all consumers within the global market that the price increases expected by the application of full-cost recovery should flow through the supply chain and should be reflected in the costs of the final medical procedure, to be reimbursed appropriately by the health care system. As shown in the *Economic Study* (NEA,

2010), the final impact on end-users should be reasonably small; however, the increases are necessary to ensure reliable supply.

Figure 1: Overview of full-cost identification methodology



A supporting tool to the guidance document is an Excel workbook that puts the concepts and formulas described into a usable format (accessible on the HLG-MR webpage).

The HLG-MR policy approach also noted that outage reserve capacity (ORC) should be sourced and paid for by the supply chain. The provision of ORC is not an item included in the full-cost recovery methodology as ORC could be considered a product that is offered separately from irradiation services. However, it is expected that full-cost recovery should also be applied to the provision of ORC within a reactor.

The HLG-MR will be releasing a guidance document (by the end of 2012) on how to implement the proposed outage reserve capacity system. Some details are already available in the final report of the first mandate (OECD/NEA, 2011a).

4. Ensuring that all supply chain participants are making necessary changes

The policy approach also calls for a periodic review of the supply chain to verify that supply chain participants are implementing (or are in progress to implement) the policy approach. It was agreed by stakeholders that the NEA Secretariat would undertake the review of the supply chain, based on input from key supply chain participants.

The review is essential to be able to determine whether the HLG-MR policy approach, especially the principles related to full-cost recovery, outage reserve capacity and governments' role, is being implemented. The review serves as the HLG-MR's "enforcement mechanism". To ensure that the policy approach succeeds, all stakeholders need to have confidence that the actions they are taking are being matched by all other players and this review will increase awareness among all supply chain participants, including consumers.

The review will recognize those supply chain participants that are implementing or making good progress toward full implementation of the HLG-MR policy approach; it would also highlight those players that are not making sufficient efforts to implement the policy approach. In this context, the report will serve as a labelling tool, providing information for customers and governments on those participants that are encouraging long-term supply security.

The first review is expected to be released by spring 2013, allowing an assessment of progress half-way through the implementation period recommended in the policy approach.

5. Additional objectives of the HLG-MR Second Mandate

The HLG-MR is continuing its work, focusing on: a) the implementation of the policy approach by all producing and consuming nations (including issuing guidance documents on how to implement full-cost recovery and outage reserve capacity) and, b) examining the cost and supply impacts of converting to ^{99}Mo produced from low enriched uranium (LEU) targets.

In addition, the objectives of the second mandate include maintaining transparency on global developments, continuing communication with the supply chain and end users, evaluating implementation progress and providing additional information and analysis where necessary.

As noted above, a key activity of the second mandate is to determine the impacts of converting to LEU targets on the security of supply of medical radioisotopes. This conversion has been agreed to by all major ^{99}Mo -producing nations. The overall goal of the study is to use a micro-economic assessment of the impact on an individual facility within the supply chain to develop a macro-economic assessment of the impacts on the whole market supply chain. Economic and capacity models of the supply chain are being developed and analysis undertaken of various conversion scenarios and their impact on the ^{99}Mo supply chain structures, in comparison to a reference case. The results of the study will be available at intervals over the next year and half, with the first findings expected to be publically available in the summer of 2012.

Another key issue for the forthcoming period will be to allow the market to move to full-cost recovery, while allowing the producers of ^{99}Mo from LEU to be able to compete on an equal basis with those producing using HEU. Dealing with these transitions will be a key part of the focus of the HLG-MR during its second mandate.

6. Conclusion

While the current situation may leave many thinking that there is no longer any concern for supply, this is not the reality; the underlying problem – that of an economically unsustainable structure – has not been fully corrected. The NEA, HLG-MR members, and other stakeholders are working hard to make the necessary changes, and we need to continue working. If the changes in the policy approach are not implemented, we will likely be faced again with supply shortages within the decade.

References

OECD/NEA (2011a), *The Supply of Medical Radioisotopes: The Path to Reliability*, OECD, Paris. ISBN 978-92-64-99164-4, 169 pages

OECD/NEA (2011b), *The Supply of Medical Radioisotopes: An Assessment of Long-term Global Demand for Technetium-99m*, OECD, Paris. 61 pages

OECD/NEA (2010), *The Supply of Medical Radioisotopes: An Economic Study of the Molybdenum-99 Supply Chain*, OECD, Paris. ISBN 978-92-64-99149-1, 123 pages

Annex: Principles and supporting recommendations

The following principles and supporting recommendations are explained in more detail in *The Supply of Medical Radioisotopes: The Path to Reliability* (www.oecd-nea.org/med-radio).

Principle 1: All ^{99m}Tc supply chain participants should implement full-cost recovery, including costs related to capital replacement.

Commercial arrangements in the supply chain, including contracts, must recognise and facilitate the implementation of full-cost recovery in order move towards achieving economic sustainability.

Principle 2: Reserve capacity should be sourced and paid for by the supply chain. A common approach should be used to determine the amount of reserve capacity required.

Supply chain participants, both public and private, should both continue and improve annual co-ordination efforts through the Association of Imaging Producers and Equipment Suppliers (AIPES) or another similar mechanism to ensure the appropriate use of available capacity, recognising a minimum necessary volume level at all $^{99}\text{Mo}/^{99m}\text{Tc}$ producing facilities. New entrants to the supply chain should join these co-ordination efforts.

Processors should voluntarily hold at every point in time outage reserve capacity equal to their largest supply (n-1 criterion), which can come from anywhere in the supply chain as long as it is credible, incremental and available on short notice.

Reserve capacity options should be transparent and verifiable to ensure trust in the supply chain. Reactor operators, processors and generator manufacturers should review the current contracts to ensure that payment for reserve capacity is included in the price of ^{99}Mo .

Principle 3: Recognising and encouraging the role of the market, governments should:

- establish the proper environment for infrastructure investment;
- set the rules and establish the regulatory environment for safe and efficient market operation;
- ensure that all market-ready technologies implement full-cost recovery methodology; and
- refrain from direct intervention in day-to-day market operations as such intervention may hinder long-term security of supply.

Governments should target a period of three years to fully implement this principle, allowing time for the market to adjust to the new pricing paradigm while not delaying the move to a secure and reliable supply chain.

Governments should:

- in co-operation with health care providers and private health insurance companies, monitor radiopharmaceutical price changes in order to support the transparency of costs;
- periodically review payment rates and payment policies with the objective of determining if they are sufficient to ensure an adequate supply of ^{99m}Tc to the medical community;
- consider moving towards separating reimbursement for isotopes from the radiopharmaceutical products as well as from the diagnostic imaging procedures.
- encourage continued supply chain participation in $^{99}\text{Mo}/^{99m}\text{Tc}$ production schedule co-ordination efforts, including making such participation mandatory if voluntary participation wanes or commitments are not respected.
- monitor levels of outage reserve capacity maintained by the market and, if found to be below the set criterion, consider regulating minimum levels.

- where required, support financial arrangements to enable investment in $^{99}\text{Mo}/^{99\text{m}}\text{Tc}$ infrastructure using various forms of public-private partnerships with appropriate returns.
- consider $^{99}\text{Mo}/^{99\text{m}}\text{Tc}$ production capacity requirements when planning multipurpose research reactors to ensure that the required capacity is available. However, the funding of the ^{99}Mo -related capacity development should be supported through the commercial market.

Principle 4: Given their political commitments to non-proliferation and nuclear security, governments should provide support, as appropriate, to reactors and processors to facilitate the conversion of their facilities to low enriched uranium or to transition away from the use of highly enriched uranium, wherever technically and economically feasible.

Governments should consider encouraging as well as financing R&D related to LEU target conversion through participation in International Atomic Energy Agency (IAEA) efforts or by other means. They should address enriched uranium (LEU and HEU) availability and supply during and after conversion. They should also examine options to create a market justification to using LEU targets to ensure a level playing field between producers. In the meantime, they should consider financially addressing the price differential of ^{99}Mo produced with LEU targets in order to achieve agreed upon non-proliferation goals.

Governments should encourage the development of alternative (non-HEU) technologies to facilitate the diversity of the supply chain, wherever economically and technologically viable.

Principle 5: International collaboration should be continued through a policy and information sharing forum, recognising the importance of a globally consistent approach to addressing security of supply of $^{99}\text{Mo}/^{99\text{m}}\text{Tc}$ and the value of international consensus in encouraging domestic action.

Domestic and/or regional action should be consistent with the proper functioning of the global market.

The IAEA and its partners are encouraged to carry on international dialogue and efforts to ensure that safety and security regulations, and their application, relating to $^{99}\text{Mo}/^{99\text{m}}\text{Tc}$ production, transport and use are consistent across international borders. Regional (e.g. European Union) and domestic efforts towards facilitating transport and use of $^{99}\text{Mo}/^{99\text{m}}\text{Tc}$ in a safe and secure manner should continue.

Industry participants could consider international collaboration to achieve other goals as well, such as harmonisation of targets.

Principle 6: There is a need for periodic review of the supply chain to verify whether $^{99}\text{Mo}/^{99\text{m}}\text{Tc}$ producers are implementing full-cost recovery and whether essential players are implementing the other approaches agreed to by the HLG-MR, and that the co-ordination of operating schedules or other operational activities have no negative effects on market operations.

This policy approach sets the foundation for consistent and comprehensive steps forward to ensure the long-term security of supply of the vital medical radioisotopes molybdenum-99 and its decay product, technetium-99m.

TEPCO's Fukushima-Daiichi accident impact stakeholders: requirements from Russian Federation RRs

Alexander Sapozhnikov

Federal Environmental, Industrial and Nuclear Supervision Service of Russia,
109147 Moscow, Taganskaya, 34, Russia

ABSTRACT

The report is dedicated to arrangements of the complementary target safety assessments of Nuclear Research Installations (NRIs)¹ in the Russian Federation, when facing a set of potential extreme situations. Their preliminary results are being discussed in line with safety requirements in force.

1. Introduction.

The first complementary target inspections concerning emergency preparedness and response at NRIs in the Russian Federation were executed in 2004. Since then Federal Environmental, Industrial and Nuclear Supervision Service of Russia (Rostekhnadzor) permanently control the emergency preparedness and emergency response at NRIs to enhance safety culture. In view of preliminary lessons learned from TEPCO's Fukushima-Daiichi NPP accident that happened on 11 March 2011 the complementary target safety assessments have been arranged at NPPs and NRIs in Russian Federation with purpose to evaluate facilities robustness² at extreme external impacts, which can cause severe beyond design basis accident³ (stress- tests). The Rostekhnadzor has developed programmes of safety assessments regarding to NPPs and NRIs. The programmes take into account proposals on scope that have been developed by Western European Nuclear Regulator's Association (WENRA) and recommended by European Nuclear Safety Regulators Group (ENSREG) to operators of NPP European Union [1]. This assessment includes inspections by Rostekhnadzor, the OOs' complementary safety assessments of NRIs for external extreme impacts, and evaluation of the results by Rostekhnadzor. The complementary safety assessment («stress tests») of NRIs in the Russian Federation is being carried out now and has not finished yet. The preliminary results of safety assessment in compliance with the Federal Norm, Rules and Regulations in the field of nuclear energy use (FNR) are given below.

2. Arrangements of “stress-tests” at NRIs in the Russian Federation.

At present the Rostekhnadzor conducts the state safety regulation and supervision at 70 civil NRIs operated by 19 organizations. These organizations are governed and recognized as the Operating Organization by following governmental structures: the Ministry of Education and Science of Russian Federation (7 OOs), the Ministry of Industry and Trade of Russian Federation (1 OO), the State Corporation “Rosatom” (11 OOs).

The Rostekhnadzor has sent to the mentioned above governmental structures the proposals to carry out the programme of “stress-tests” in the OOs managed by them. At first the stress-tests shall be done at NRIs in operation with power level more than 1 MW (in terms of IAEA - facilities

1 NRIs – nuclear facility consisting of research reactor (RR) or critical assemble (CA) or subcritical assemble (SCA) and complexes of structures, systems, components and experimental facilities with incorporated workers (personnel) within territory defined by design (NRI site) for utilization of neutrons and ionizing radiation for research purposes.

2 robustness - quality to withstand a possible scenarios of extreme external impacts taking into account available design margins, diversity, redundancy, structural protection, physical separation, etc.

3 severe accident - beyond design basis accident that is being accompanied with the loss of facility fundamental safety functions, integrity of fuel cladding and subsequent fuel degradation and release of radioactivity outside of protective barriers in quantities exceeding the limits prescribed by safety norms.

threat category). Basing on conservative approach for safety assessment no predictive severe accident can be predicted for NRIs with power level less than 1 MW. The list of NRIs with potential radiological hazards (power more 1 MW) is given in the Table 1. Moreover one research reactor BR-10 (Obninsk) has been finally shutdown in 2002 for further decommissioning. The research reactors listed in table are situated at 8 sites. At all sites the programmes of safety enhancement are being carried out including technical measures and organizational arrangements that address to compliance with up-to-day safety requirements established in licensing basis.

№	Title RR,	IAEA code	OO, place	Put in operation	Type of RR, power (MW)
1.	VK-50	RU0043	Dimitrovgrad	1965	BWR-prototype, 220
2.	PIK	RU0016	Gatchina	Commissioning	Tank, 100
3.	SM-3	RU-0024	Dimitrovgrad	1961	Tank, 100
4.	MIR.M1	RU-0013	Dimitrovgrad	1966	Channels in the pool, 100
5.	BOR-60	RU-0027	Dimitrovgrad	1969	Tank, LMR type, 60
6.	WWR-M	RU-0008	Gatchina	1959	Tank, 18
7.	WWR-TS	RU-0019	Obninsk	1964	Tank, 15
8.	IVV-2M	RU-0010	Zarechnyi	1966	Pool, 15
9.	RBT- 10/2	RU-0020	Dimitrovgrad	1984	Pool, 10
10.	IR-8	RU0004	Moscow	1957	Pool, 8
11.	IRT-T	RU-0014	Tomsk	1967	Pool, 6
12.	RBT-6	RU-0022	Dimitrovgrad	1975	Pool, 6
13.	IRT-MEPH	RU-0005	Moscow	1967	Pool, 2,5
14.	IBR-2	RU-0036	Dubna	1984	Pulse, 0,05- stationary , 1,5 – peak

Tab 1: NRIs with operational power more than 1 MW

The Rostekhnadzor recognized necessity of implementation “stress-tests” at NRIs in the following scope:

- Protectability of the facility when facing a set of extreme external impacts of nature and man- induced origin including beyond its design basis.
- Emergency preparedness tobdba at full loss of NRI power supply;
- Emergency preparedness tobdba at loss of primary ultimate heat sink;
- Emergency preparedness to severe accident.

Basing on result of “stress-tests” the evaluation of necessity to correct safety requirements to NRIs is being carried out.

3. The reference level to analyse accidents at NRIs in the Russian Federation.

Evaluation of potential accidents at NRI is one of the major issues of expert review of safety. The current licensing basis is listed in references [2]. The analysis of possible accidents is carrying out on the basis of following safety requirements of documents that will be used as references below:

- General Provisions for Nuclear Research Installations Safety, NP-033-11;
- Nuclear Safety Regulations for Research Reactors, NP-009-04;
- Requirements to Contents of Safety Assessment Report for NRIs, NP-049-03;
- Rules for Design and Safe Operation of Equipment and Pipelines of Nuclear Power Installations, PNAE G-7-008-89 (version 2008);
- Standards on Strength Analysis of Equipment and Pipelines of Nuclear Power Installations, PNAE G-7-002-86;
- Seismic Building Design Code, SNiP II-7-81 (version 2011);
- Consideration for External Impact of Natural and Man-induced Origin on Nuclear Energy Facilities, NP-064-05;
- Requirements to Content of Plans of Actions for Personnel Protection in Case of an Accident at Nuclear Research Installations, NP-075-06;
- Regulation for Compliance Evaluation for Equipment, Accessories, Materials and Half-finished Products Delivered to Nuclear Facilities, NP-071-06.

In line with the requirements of NP-033-11 the design of each NRI contains a list of initiating events for the design basis accidents (DBAs), a list of beyond design basis accidents (bdbas),

and assessment of an accident probability and its sequence. The OO using conservative deterministic analysis of defence-in-depth concept have justified the list of initiating events, possible ways of accident progression and radiation consequences accordance with requirements to DBAs and BDBAs analysis established in NP-049-03. According to requirements of NP-049-03, NP-064-05 all external impacts peculiar to area of NRI location and having potential frequency 10^{-6} per year and more have been taken into consideration in the design ground and justified in the SAR of NRI. In line with NP-033-11 the modifications of NRIs that have been done before or are in progress now provide:

- efficiency of safety systems at extreme conditions of fire, flooding of internals ect;
- technical methods and means of implosion protection and fire protection of the equipment and premises.

At the facilities where the water radiolysis is essential and potential accumulation of explosive mixture exist due to oxyhydrogen gas in normal operation and in accident the protection is provided by organizational measures and technology systems: monitoring of explosive gas concentration, ventilation, gas adsorption and separation, burner of oxyhydrogen gas. OO shall carry out the comprehensive analysis of taken measures for extreme external impacts.

The limits established by the FNR "Radiation Safety Codes, NRB-99/2009" restrict radiation dose rate to personnel, public and impact to environment during operation and accidents. The basic dose limits for normal operation of NRI are followings: occupational dose limit is 20 mSv/a in average for any consecutive 5 years but annually not more 50 mSv, public dose limit is 1 mSv/a in average for any consecutive 5 years but annually not more 5 mSv. In case of accident the intervention level for urgent protective actions for public: sheltering - 5 mSv, evacuation - 50 mSv.

The following probabilistic criteria are established in the FNR "Nuclear Safety Regulations for Research Reactors" (NP-009-04) and the FNR NP-033-11 accordingly:

- Probability of the reactor core melting shall not exceed 10^{-5} 1/a per facility;
- Probability of extreme radioactivity release requiring decision on public protection shall not exceed 10^{-7} 1/a per facility.

In IAEA documents the following risk assessments are used: for severe accident - 10^{-4} and for public effect - 10^{-6} 1/a per facility.

In order to assess radiation consequences of severe accident the failures' chains have been determined that constitutes the most probable way of accident transition to severe accident. For this scenario the time has been evaluated before fuel degradation. During this time personnel can be able to use measures for accident mitigation by switching on emergency cooling systems and emergency coolant injection. At that case the probability of extreme radioactivity release will be less than 10^{-7} .

4. Preliminary results of supplementary safety assessment («stress tests») of NRIs in the Russian Federation.

4.1. Protectability from extreme external impacts of nature and man- induced origin.

In line with NP-033-11 safety systems of NRI shall be capable to execute the safety functions in the scope established by the design in view of impact of natural phenomena and external man-induced events, typical for the region of NRI site, including possible mechanical, thermal, chemical and other impacts at design basis accidents.

Seismic impact

According to the seismic zoning plan of the Russian Federation territory that is attached to the document "Seismic Building Design Code", SNiP II-7-81 (version 2011) sites of NRIs belong to aseismic zones where the design earthquake (DE) is less than 5 units on MSK-64 scale and the safe shutdown earthquake (SE) is less than 6 units of measure of the intensity on 12-units seismic scale MSK-64⁴ (excluding zone of one facility location, where values of seismic loads are justified insufficiently).

⁴ The design (basis) earthquake (DE) - earthquake with average recurrence till 100 years, and the safe shutdown earthquake (limit for calculation) (SE) - earthquake with average recurrence till 10000 years, are used to estimate a seismic loads.

In line with requirements of NP-033-11 the safety class of NRI systems and elements, including experimental devices, is an obligatory attribute at formation of other classifications of NRI elements being established in normative documents including seismic stability. The equipment of NRIs is being classified according to requirements of PNAE G-7-008-89 (version 2008) including the following: "Designs of equipment and pipelines shall fulfill requirements of these Rules and requirements of the "Standards on strength analysis of equipment and pipelines of nuclear power installations" (PNAE G-7-002-86). The last document establishes the requirement to fulfill a seismic estimation for NRI elements and determines the methodology of assessment depending on equipment impact on safety of the NRI.

To evaluate seismic loads on the reactor building, main equipment, and pipelines with isolation valves in primary circuit DE= 5 units and SE= 6 units on MSK-64 scale have been accepted accordingly. The purpose of calculations of DE impact consists in prevention of partial or full loss of operational properties by the construction. The purpose of calculations of SE impact consists in prevention of global failure of construction or its parts that present a threat to personnel. To evaluate margin of safety of the reactor building, main equipment, and pipelines beyond the NRI design basis the calculations of seismic loads have been carried out based on the floor accelerograms and response spectrums at the fixing points of equipment at parameters when SE= 6 units MSK-64. The most mechanical stresses were assessed as following:

- In the components of the reactor building - less than 60 % to prescribed values;
- In the components of fixing points (reactor tank, heat exchangers, tank of coolant reserve) - less than 40 % to prescribed values;
- In pipelines of primary circuit - less than 60 % to prescribed values.

The margins of safety at seismic loads that are beyond design basis exist in value 1-2 MSK-64 scale (excluding SM-3 and MIR.M1).

Flooding

The Russians NRIs sites do not subject to impact of tsunami, tidal, and storm surge. The other possible cause of flooding were identified and analyzed: emergency situation at hydro engineering complexes like breaking of dam, heavy rainfalls and waterspout. For all facilities it was confirmed that in the worst case specific for site there is no impact to safety at flooding.

Other extreme natural and man- induced origin events and their combinations

The executed assessments have confirmed protectability of all NRIs at the external impacts that have been identified in the NRIs design basis. At the same time for some facilities the additional evaluations of the robustness of the reactor building shall be carried out beyond the design basis due to effects linked to whirlwind (tornado) and extreme heavy snowfall. The programme of "stress-tests" at NRIs envisages study of effect linked to combinations of external impacts that can be important for evaluation. That is being done now including events of very small probability. For example, taking into account prohibited area for flying above the territory of scientific centers the evaluated probability of airplane fall on the NRI building is 10^{-9} - 10^{-11} per year. In view of negligible value of event probability this impact was assessed in stress-tests only for new facility PIC but shall be assessed further for other NRIs.

There is no straight requirement in the FNR to consider combinations of external impacts in the NRIs design basis. Thereupon a holistic analysis of combinations of external impacts shall be included in enhancement safety action plan of OOs: it is recommended to OOs to carry out comprehensive analysis of safety systems to withstand mechanical, thermal and other impacts during accidents.

4.2. Emergency preparedness tobdba at full loss of NRI power supply

In line with requirements of NP-033-11 the NRIs' designs:

- Include necessary auxiliary safety systems providing power supply and supply of other safety system by working fluids and environmental conditions for their operation;
- Include rating of power supply reliability depending on classification of equipment important

to safety, acceptable time of break in power supply, type of internal backup power sources (heat station, diesel generators, storage battery);

- Justify that emergency back-up sources provide safety functions in case of DBA and BDBA at safety systems.

The heat removal from reactors, reactor spent fuel pools and spent fuel storage facilities at site of NRIs is available during the time sufficient to achieve safe shutdown conditions in case of superposition of full loss of off-site power sources and failure of one of the emergency back-up sources. The determined design decisions provide extended cooldown of the reactor core by natural circulation of coolant in primary and secondary circuits at loss of all sources of power supply, including reserve sources. As a result of preliminary stress-tests at some threat category facilities OOs shall develop proposals to provide them by supplementary equipment (additional diesel generators, monoblock pumps), which will exclude transition to severe accident during BDBA with full loss of off-site power sources and multiple failure of NRI equipment, that will enhance robustness of facility beyond its design basis. The emergency back-up sources shall be in earthquake-resistant design and shall be equipped with automatic fire-fighting at extreme external impacts of natural phenomena and man-induced events to enhance robustness of safety functions.

4.3. Emergency preparedness to BDBA at loss of primary ultimate heat sink

The heat removal from the reactor cores, reactor spent fuel pools and spent fuel storages to ultimate heat sink - atmosphere, is arranged by system of service water, secondary coolant system, and other systems depending on specific reactor design. All Russian NRIs possess inherent safety characteristics. Evaluation of BDBA at loss of primary ultimate heat sink did not discover any severe accidents resultant radiation exposure to population exceeding prescribed limits and does not require any urgent off-site protective actions at initial stage of emergency.

At the powerful threat category facilities the result of assessments shows that to exclude transition of BDBA with loss of primary ultimate heat sink to severe accident the supplementary equipment (diesel generators) shall be installed to provide power supply of elements that fulfill emergency function of primary ultimate heat removal during emergency.

4.4. Preparedness to severe emergencies

In line with requirements of NP-033-11 was confirmed the following:

- The most RRs have been equipped by a reserved control point (secondary control room) that can be used in case if the main control point is not available to control NRI. In some cases the last one shall be improved taking into account BDBA.
- Emergency plans have been developed, coordinated, approved and provided with necessary material resources taking into account radiation consequences of possible accidents.
- All facilities were equipped by autonomous system providing registration and storage of information, necessary for investigation of DBA, and retaining operability under conditions of design basis and beyond design basis accidents;
- Measures in case of natural disasters, internal and external impacts, including fires and accidents at NRIs have been developed.

According to requirements of FNR "Requirements to content of plans of actions for personnel protection in case of an accident at nuclear research installations", NP-075-06, those OOs, which managed a few NRIs at one site, have developed and implemented at each facility the Emergency Plan that is constituent of the General Emergency Plan of the OO site. The preliminary assessments show that personnel will have got enough time to withstand an accident and core cooldown before damage to the fuel becomes unavoidable (time interval 7-25 hours depending on facility). It was revealed the OOs' needs in additional equipment to control and mitigate severe accident. This additional equipment includes diesel - generators, lines for coolant recovery to the pool from receiving vessels/chamber, communication and information systems (internal, external), in some cases improved emergency ventilation/filtration systems. It is reasonable in research center operating powerful facilities to develop equipment for seismic control to shutdown and cooldown NRIs in proper time in case of seismic event. Such system already exists at site of the reactor PIC.

5. Evaluation of necessity to improve safety requirements.

The complementary target inspections have not discovered any significant deviations from safety requirements of Russian Federation. It was Intended further improvement of interdepartmental information exchange, strengthening of safety requirements to enhance NRI efficiency to withstand accident and provide safety functions at combination of extreme external impacts of nature and man-induced origin (to enhance robustness of the safety-relevant SSC and the effectiveness of the defence-in-depth concept). The following issues can be discussed to strengthen NRIs' safety requirements as a result of preliminary finding of the stress-tests:

- to determine seismic rating of safety-relevant systems, structures and components (SSC);
- to develop regulations to control and mitigate severe accident at threat category NRIs on the basis of IAEA recommendations [3] .

Operating organizations (licensees) should refresh SAR and operating documentations of NRIs when stress-tests will be finished and the Rostekhnadzor will complete their review.

6. Conclusion

The Rostekhnadzor programme of stress-tests of NRIs in the Russian Federation retains holistic approach to evaluation DBAs, BDBAs and severe accidents at NRIs.

Safety of NRIs in the Russian Federation is secured by up-to-day requirements of Federal norms and rules in the field of nuclear energy use that are being harmonized with recommendation of IAEA and other international organizations.

No any significant safety gaps have been discovered where the lack of scientific and technical data could cause a weakness in safety regulation and safe utilization of NRIs.

In case of impact of extreme external natural phenomena and man-induced events the robustness of the safety-relevant systems, structures and components (SSC) of operated NRIs and the effectiveness of the used defence-in-depth concept are in line with safety requirements of national standards. The national reference basis can be strengthened by improvement requirements to seismic categorization of SSC and development of regulations to control and mitigate severe accident.

The international nuclear law has to be strengthened based on lessons learned from TEPCO's Fukushima-Daiichi NPP accident.

References

- [1] The proposal by the WENRA Task Force about "Stress tests" specifications (21 April 2011) (<http://www.wenra.org/extra/pod/>).
- [2] The list of legislative acts and normative documents related to sphere of activity of Federal Environmental, Industrial and Nuclear Supervision Service of Russia P-01-01-2009, the order of Rostekhnadzor from 17 March 2010 № 178.
- [3] Generic Procedures for Response to a Nuclear or Radiological Emergency at Research Reactors, EPR-RESEARCH REACTOR 2 01 1, IAEA, Vienna, 2011

PRESENT STATUS AND FUTURE PLAN FOR THE EXPERIMENTAL FAST REACTOR JOYO

YUKIMOTO MAEDA

*Experimental Fast Reactor Department, Oarai R and D Center, Japan Atomic Energy Agency
4002 Narita, Oarai, Ibaraki, 311-1393, Japan*

ABSTRACT

The experimental fast reactor Joyo is the first sodium-cooled fast reactor in Japan. Thirty years of successful operation of Joyo and the related post irradiation examination (PIE) facilities have contributed valuable irradiation data on fuels and materials. In 2003, the Joyo core was upgraded to the high performance MK-III core to provide a more robust and capable irradiation test facility not only for FBR development but also for other fields. In order to utilize the high neutron flux which has become possible, enhancements of the irradiation capabilities of Joyo are being considered for multipurpose utilizations.

The Great Eastern Japan Earthquake and tsunami which occurred on March 11, 2011 did not cause serious damage to Joyo: however, it is presently temporarily shut down for in-vessel inspection and restoration work related to the damage of the on-line irradiation test device MARICO-2. The resumption work was recently started officially, and Joyo will play an important role as a fast neutron irradiation facility after its restart.

1. Introduction

The experimental fast reactor Joyo at the Oarai Research and Development Center of the Japan Atomic Energy Agency (JAEA) is the first sodium-cooled fast reactor in Japan. Its first operation was as a breeder core. Then, its core was converted from the MK-I breeder core to the MK-II Irradiation test core and irradiation tests were commenced from 1983. In 2003 after completing the 35th duty cycle operation of the MK-II core, Joyo was upgraded to the high performance MK-III core to provide a more robust and capable irradiation test facility not only for FBR development but also for other fields such as LWRs, fusion reactor, and non nuclear industries. Joyo is presently temporarily shut down due to the damage of the on-line irradiation test device MARICO-2, and the resumption work was recently started officially.

2. Plant description and irradiation test devices

The main reactor parameters of the MK-III irradiation core are shown in Table 1 and its core configuration is shown in Figure 1. The MOX fuel region is divided into two radial fuel composition zones to flatten the neutron flux distribution. The fissile plutonium (Pu) content ($^{239}\text{Pu} + ^{241}\text{Pu}$) / (U + Pu) is about 16 wt% in the inner core fuel and about 21 wt% in the outer core fuel. Both the inner core and outer core fuels have the same uranium enrichment of 18 wt%. The active core is cylindrical and about 80cm in equivalent diameter and 50cm in height. There is a radial reflector region of stainless steel (SUS) surrounding the core which is about 25cm thick. Shielding subassemblies (S/As) with B_4C are loaded in the outer two rows of the reactor grid. Two of six control rods were shifted from the third row to the fifth row to provide the positions for loading instrumented type irradiation test S/As in the high flux region of the fast neutron field. All six of the control rods have the same poison-type design. The poison

section contains B₄C enriched to 90 wt% in ¹⁰B, and there is a stainless steel follower section below it.

Tab 1: Main reactor parameters of Joyo

Items		Specification
Reactor Thermal Output	(MWt)	140
Max. No. of Irradiation Test S/As	---	21
Core Diameter	(cm)	80
Core Height	(cm)	50
²³⁵ U Enrichment	(wt%)	18
Pu Content	(wt%)	≤30
Pu Fissile Content (Inner/Outer Core)	(wt%)	~16/21
Neutron Flux Total	(n/cm ² ·s)	5.7×10 ¹⁵
Fast (E>0.1MeV)	(n/cm ² ·s)	4.0×10 ¹⁵
Primary Coolant Temp. (Inlet/Outlet)	(°C)	350/500
Operation Period	(days/cycle)	60
Reflector/Shielding	---	SUS/B ₄ C
Max. Excess Reactivity (at 100 °C)	%Δk/kk'	4.5
Control Rod Worth	%Δk/kk'	≥7.6

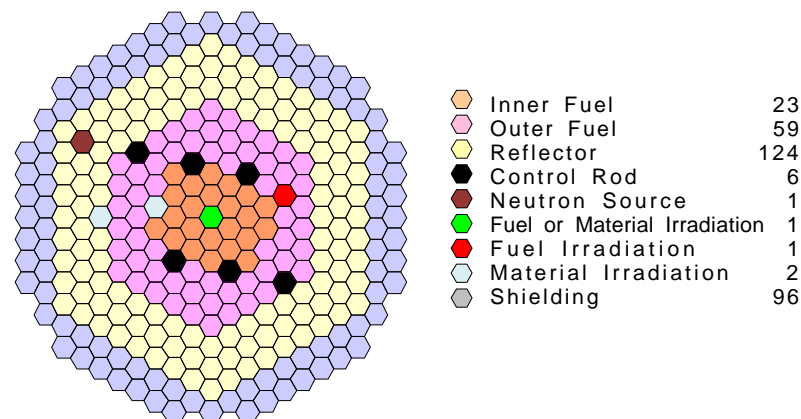


Fig 1. Core configuration of Joyo MK-III

Joyo has two primary sodium loops, two secondary loops and an auxiliary cooling system as shown in Figure 2. The sodium enters the core at 350 °C at a flow rate of 1,350 tons/h/loop and exits the reactor vessel at 500 °C. The maximum outlet temperature of a fuel S/A is about 570 °C. The intermediate heat exchanger (IHX) separates radioactive sodium in the primary system from non-radioactive sodium in the secondary system. The secondary sodium loops transport the reactor heat from the IHXs to the air-cooled dump heat exchangers.

The MK-III core provides the maximum fast neutron flux of 4.0×10¹⁵n/cm²s. This is the highest level of fast neutron flux among irradiation test facilities worldwide. Irradiation test fields and irradiation test devices of Joyo are shown in Figure 3. Irradiation tests require specific devices to perform them effectively. Joyo utilizes six types of irradiation test devices; the first four are for on-line irradiation and the last two are for off-line irradiation. (1) Instrumented test assemblies (INTAs) have an on-line monitor to obtain irradiation data during reactor operation. Each INTA is equipped with a fission product (FP) gas pressure gauge, flow velocity meter, thermocouple and neutron detector. (2) MARICO is able to control irradiation temperature of test specimens during irradiation. (3) EXIR is also an irradiation temperature control device but it is installed in the safety vessel. (4) UPR is a structure material irradiation device irradiated in the upper core field. (5) The un-instrumented fuel irradiation subassemblies (UNISs) are irradiation rigs for irradiating test fuel pins, and classified into mainly three types, A, B, and C according to test purposes. Type-A contains both test fuel pins and driver fuels

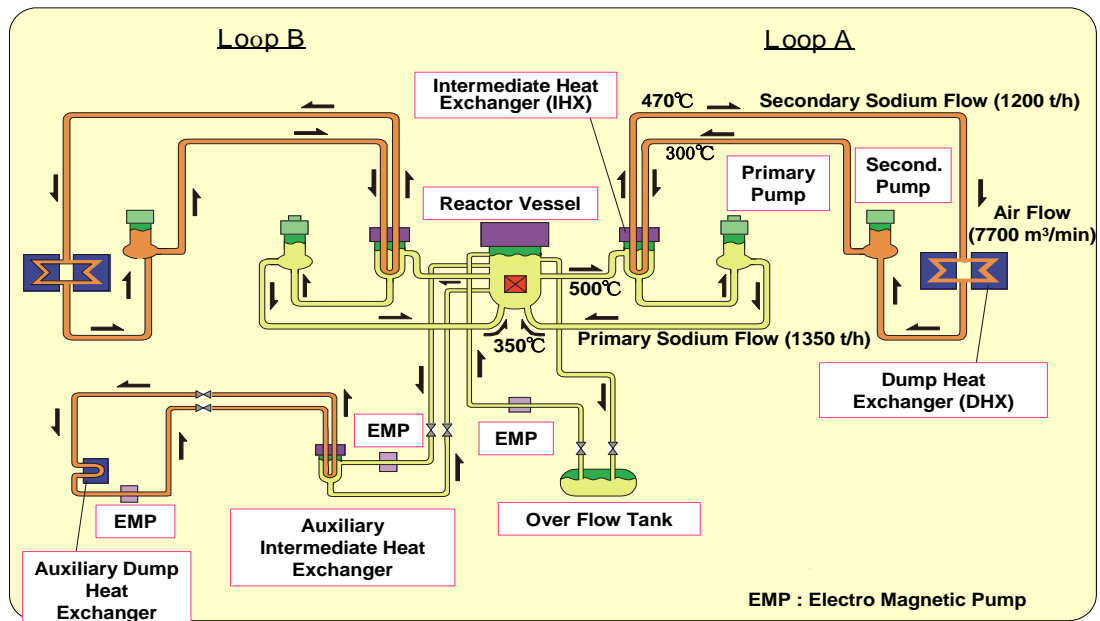


Fig. 2 Joyo heat transport system

used for high linear power irradiation testing. Type-B is a compartment type rig which can be reloaded in the core after interim examinations. In addition, it can be used for parametric irradiation testing since the coolant flow rate in each compartment can be set separately. Type-C is used to obtain irradiation data of fuel pin bundle behavior. Materials irradiation rigs are classified into three types according to the materials tested. CMIR is used for core materials, SMIR is used for structural materials and AMIR is used for absorber materials. All these rigs are compartment type like UNIS-B. Any shape of test specimens can be encapsulated and installed in the compartments. These material irradiation rigs can be reloaded in the reactor core after interim examinations. Series of these devices have contributed to obtainment of valuable irradiation data on fuels and materials. The development of irradiation devices will be continued to meet with future irradiation needs.

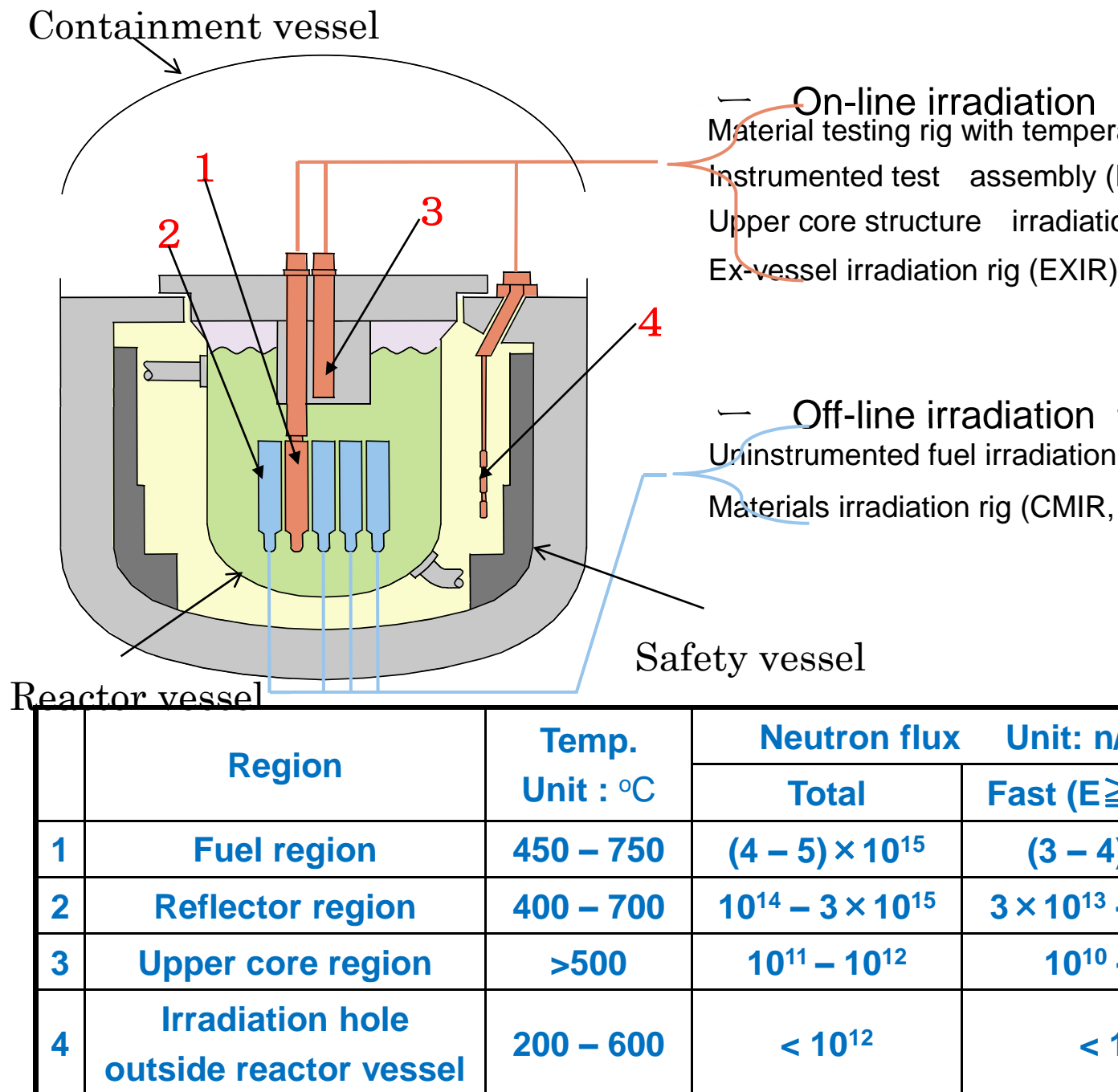


Fig. 3 Irradiation test devices and irradiation fields in Joyo

3. Enhancement of irradiation capability

The upgrading program of irradiation capability is being promoted to use Joyo in multiple R&D fields. This program has two main aims. The first is an expansion of the temperature range and the neutron energy spectrum to meet irradiation needs for the existing light water reactors (LWRs) or future energy systems such as Generation-IV reactor and fusion reactors. The second is to provide the additional functionality to be able to run transient tests or short-term irradiation tests while achieving the high plant availability factor required for the major irradiation test to high burn-up or high dpa. Enhancement of irradiation capability in Joyo is summarized in Figure 4.

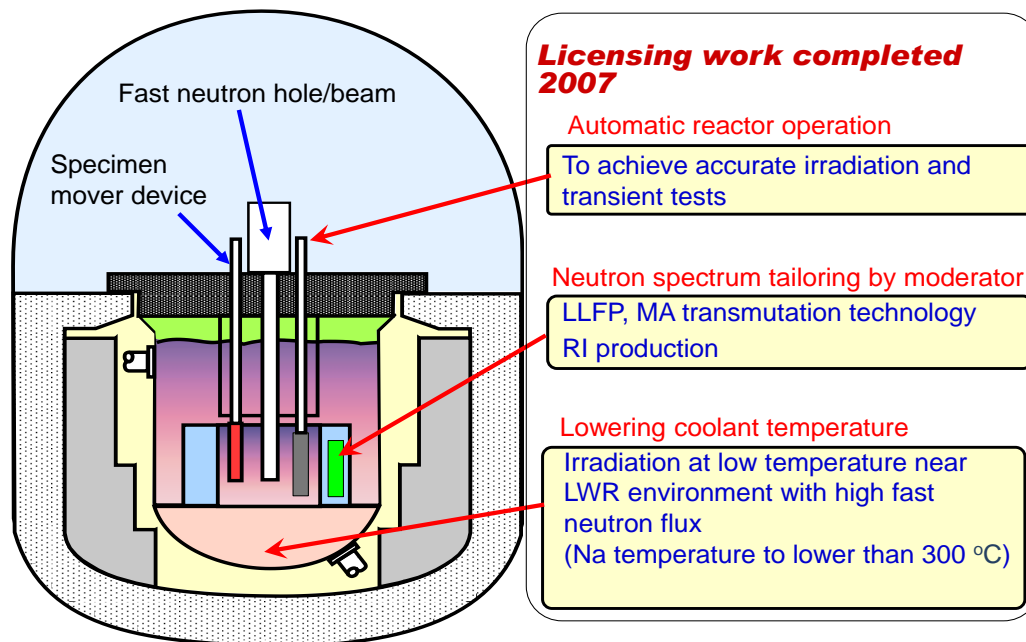


Fig. 4 Enhancement of irradiation capability

The following items describe expansion of the irradiation capability of Joyo for innovative irradiation testing applications.

(1) Neutron spectrum tailoring

In order to conduct irradiation tests of LWR materials or the transmutation tests of long-lived fission products (LLFPs), the creation of a slow neutron irradiation field by loading neutron moderating S/As in the radial reflector region is being considered. Seven SUS reflector S/As are replaced with moderator and target S/As. Beryllium (Be) and zirconium hydride ($\text{ZrH}_{1.65}$) are moderator candidates from the viewpoint of temperature resistance and transmutation performance. The moderator S/As can tailor the neutron spectrum so that the slow neutron flux ($E < 1\text{keV}$) is increased by approximately 10-fold and then the LLFP transmutation rate becomes several times larger than that of a research LWR.

(2) Lower coolant temperature

Irradiation tests in the LWR temperature range (320 – 370 °C) with high fast neutron flux can be conducted by lowering the coolant temperature. In the MK-III operation, the inlet temperature of the reactor vessel is 350 °C. The irradiation at low temperature can be attained by changing the inlet coolant temperature to less than 300 °C and lowering the overall coolant temperature. Assuming that the inlet temperature is 290 °C a fast neutron flux of about $2 \times 10^{15} \text{ n/cm}^2\cdot\text{s}$ can be obtained at 370 °C.

(3) Specimen mover device

In order to simulate a large transient overpower to establish the capability of the fuel pin and conduct cyclic irradiation tests, a specimen mover device is under development. Neutron flux and linear heat rate are changed by a factor of approximately 100 by moving the specimen up and down while keeping the reactor power constant. The linear heat and neutron flux change ratio can attain values of approximately 40 W/cm/min and $2 \times 10^{14} \text{ n/cm}^2\cdot\text{s/min}$.

(4) Fast neutron hole/beam

For a short term irradiation test without restriction of the duty cycle operation (60 days), a fast neutron irradiation hole/beam is under investigation. The neutron flux has been calculated in 100 energy groups using the two-dimensional transport code DORT. A fast neutron flux of $4 \times 10^9 - 4 \times 10^{15} \text{ n/cm}^2\cdot\text{s}$ can be obtained by installing the irradiation hole in the core center.

4. Restoration of equipment following damage to the MARICO-2

An in-pile creep rupture experiment was conducted from 2006 to 2007 to evaluate the creep rupture strength of oxide dispersion strengthened (ODS) ferritic steel. The irradiation test device named MARICO-2 (material testing rig with temperature control) which was developed to control the irradiation temperature within ± 4 °C was applied for this experiment. 24 ODS specimens which were pressurized by helium gas were installed into MARICO-2. During the irradiation, the temperature was successfully maintained at the target value. 14 ODS specimens were ruptured and all were detected and identified. After the completion of the irradiation test, work in preparation to separate the test assembly from the upper structure of MARICO-2 was done to unload the test rig from the reactor vessel. However, the separation work was not done completely and the rotation plug was rotated without noting that MARICO-2 was not fully separated. As this event might have resulted in damage to MARICO-2 and the reactor components, an in-vessel observation was carried out to investigate the damage inside the reactor vessel. In-reactor vessel observation of a sodium fast reactor has to be conducted under severe conditions such as high temperatures (~ 200 °C) and high radiation doses (~ 400 Gy/h), while retaining the primary sodium coolant in the reactor vessel (R/V) to remove decay heat. In-reactor vessel observation equipment has to be designed to not only tolerate these severe conditions but also to be capable of being inserted into the sealed R/V through the fixed holes in the rotating plug to access the observation area. Therefore a radiation-resistant fiberoptic was used for the observation equipment, and the observation was conducted in order to investigate foreign materials on the top of the S/As and to investigate the condition of the upper core structure (UCS) bottom face where the sodium level was -50 mm, that is 50 mm below the top of the S/As.

In-reactor vessel observations were successfully conducted and the information was obtained on the following items: (1) When MARICO-2 had not been completely separated, it was rotated, and the upper part of the test S/A was bent onto the in-vessel storage rack. (2) The sodium flow regulating grids and guide tubes on the bottom of the UCS were deformed. (3) No loose parts were found on the top of the S/As.

This event has necessitated the replacement of the damaged UCS and retrieving the bent test S/A of MARICO-2 before Joyo can be restarted. Procedures for the restoration work have been established. Figure 5 outlines the steps for Joyo resumption of operation. The length of the bent part of the test S/A is approximately 200 mm, and it cannot be retrieved through the existing hole in the rotating plug such as the fuel exchange hole. Therefore, it is planned to retrieve the bent test S/A through the bigger hole which will be formed after the damaged UCS is pulled out. Replacement of the highly radioactive UCS is an important subject for the development of handling equipment. In order to evaluate the radioactivity of the UCS, gamma dose rate measurements inside the R/V were conducted under the condition at the sodium level of -50 mm below the top of the S/As. The results are being used for the shielding design of the cask of the UCS. This resumption work was recently started officially with a completion target in 2014.

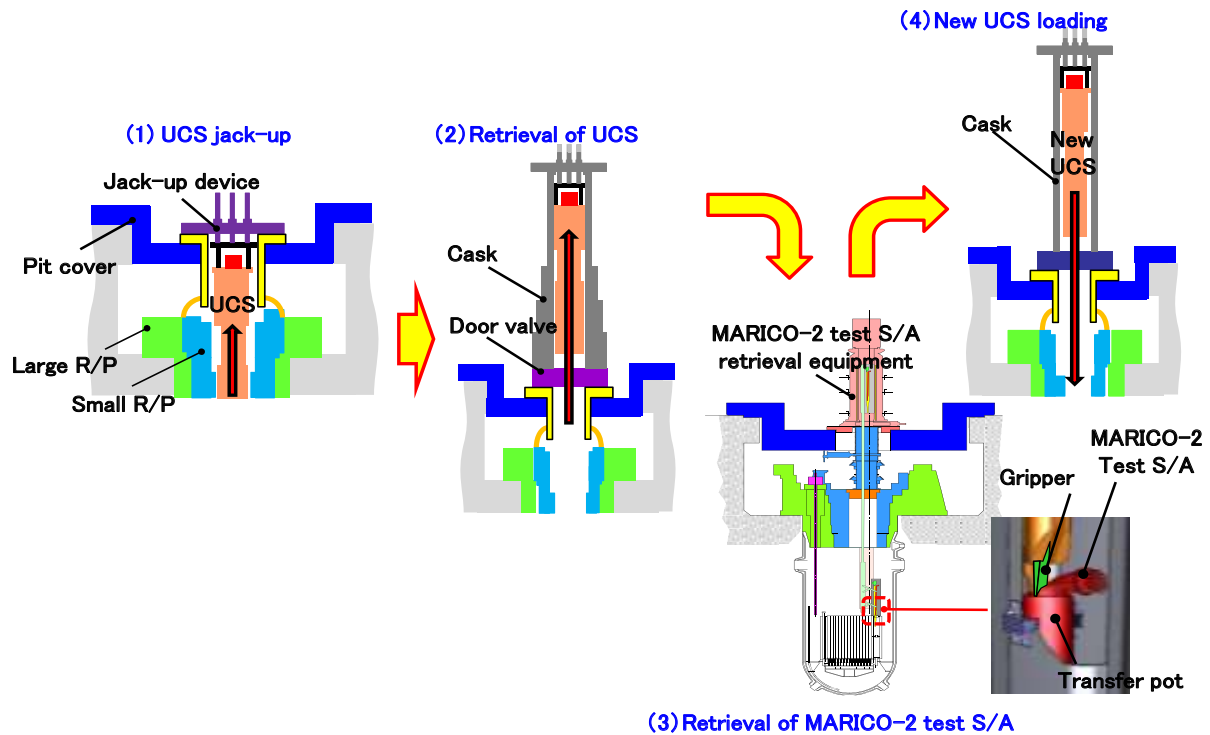


Fig. 5 Outline for step in Joyo resumption of operation

5. Impact of the Great Eastern Japan Earthquake on Joyo

The Great Eastern Japan Earthquake which occurred on March 11, 2011 had a seismic intensity of upper 5 (on the Japanese seismic scale) at the Oarai site; however, no serious damage occurred to Joyo. As shown in Figure 6, Joyo is located on a hill about 38m above sea level: there would not be any flooding of the facilities and equipment even if such an enormous tsunami as struck the Fukushima nuclear power plant hit the coast at the Joyo site. Additionally, sea water is not used for cooling in Joyo as generated heat is cooled by air. Reviewing the seismic design of Joyo had been carried out before March 2011 based on the geological survey in response to revision of the “Regulatory Guide for Reviewing Seismic Design of Nuclear Power Plants.” The provisional safety of the seismic design of Joyo has been confirmed for larger earthquakes by calculations using new seismic force. Revision of the Joyo seismic design will continue based on the findings of the Great Eastern Japan Earthquake.

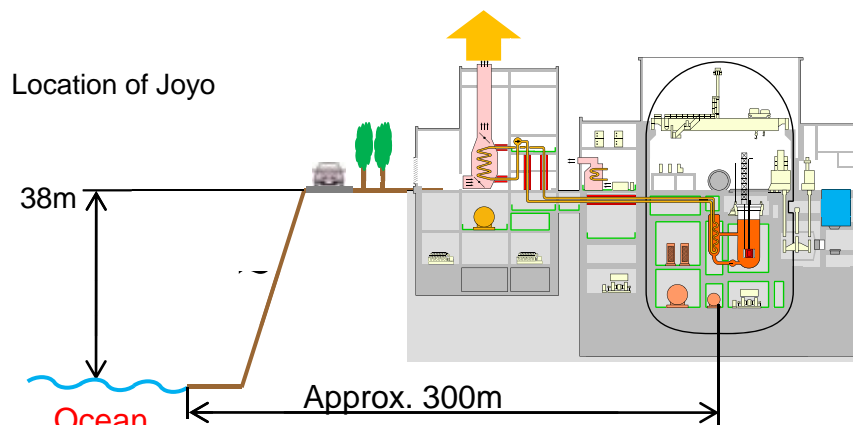


Fig. 6 Location of Joyo from the ocean

As the reactor has been shut down since the MARICO-2 was damaged in 2007, decay heat removal was not necessary for Joyo. The plant was maintained for 8 days by its emergency diesel generators due to the loss of external power supplies. As sodium is used as a coolant, even if all power supplies are lost in Joyo during reactor operation, the core melt accident will not occur since decay heat can be removed by natural circulation as shown in Figure 7.

Based on the accident at the Fukushima nuclear power station, strengthening of measures to prevent a severe accident and implementation of thorough accident management measures are required in nuclear power plants. Though accident management is not required for research reactors, measures to ensure spent fuel pool water and emergency power supplies should be in place depending on the situation of each reactor.

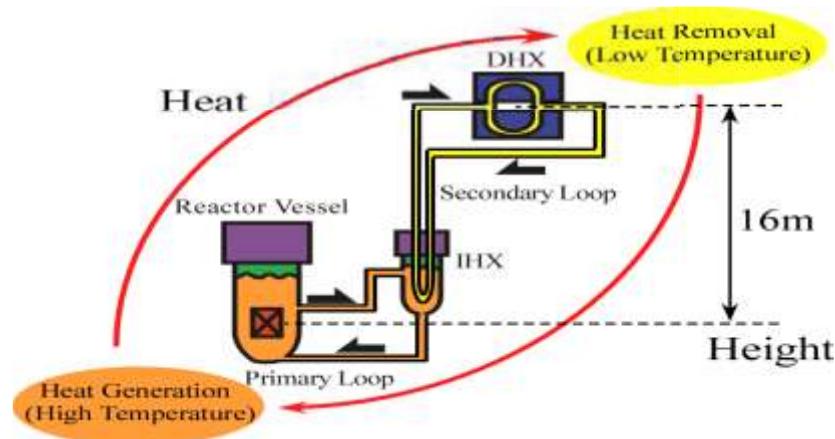


Fig.7 Cooling by natural circulation

The present safety regulations governing nuclear power plants in Japan are mandated under the “Act on the Regulation of Nuclear Source Material, Nuclear Fuel Material and Reactors” and “The Electricity Business Act.” The Nuclear and Industrial Safety Agency (NISA) within the Ministry of Economy, Trade and Industry (METI) is responsible for these regulations. On the other hand, safety regulations for research reactors are mandated under the Ministry of Education, Culture, Sports, Science and Technology (MEXT). From April 2012 a new Nuclear Regulatory Agency will be launched in the Ministry of the Environment which will have jurisdiction over the regulations for both nuclear power plants and research reactors. It is likely that the regulations for research reactors will not significantly change at least initially; however, in the future they might be affected by the regulations of the nuclear power plants.

The review of the Framework for Nuclear Energy Policy is being carried out within the Atomic Energy Commission based on the accident at the Fukushima nuclear power plant. This review is expected to be concluded in the summer of 2012. It is including discussion of the nuclear fuel cycle and FBR development. However, JAEA considers that the significance of Joyo will not be changed. Plans will be made to use Joyo for multiple R&D fields as a fast neutron irradiation facility by the upgrading program of irradiation capability. Joyo will be restarted after completion of the restoration work and various irradiation tests will be carried out as a fast neutron irradiation facility.

6. Conclusion

Joyo provides the highest level of fast neutron flux among reactors worldwide. An upgrading program is being promoted to pioneer new irradiation testing applications. These improvements of irradiation capability are expected to promote international collaborations and utilization by external users through sharing the infrastructure for high-quality irradiation tests.

7. References

- [1] Maeda Y., et al., "Distinguished achievements of a quarter-century operation and a promising project named MK-III in Joyo," Nuclear Technology Vol. 150, No.1, 2005, pp.16-36.
- [2] Isozaki K., et al., "Upgrade of cooling system heat removal capacity of the experimental fast reactor Joyo," Nuclear Technology Vol. 150, No.1, 2005, pp.56-66.
- [3] Aoyama T. et al., "Transmutation of Technetium in the Experimental Fast Reactor 'Joyo'," Journal of Nuclear and Radiochemical Sciences, Vol. 6, No. 3, pp. 279-282, 2005.
- [4] Sekine T., "Utilization of High Neutron Flux Experimental Fast Reactor 'Joyo' for Fusion Material Research," Consultancy Meeting on Role of Research Reactors in Material Research for Nuclear Fusion Technology, IAEA, 2010.

CURRENT STATUS OF JRR-3 - AFTER 3.11 EARTHQUAKE IN JAPAN -

YOJI MURAYAMA, MASAJI ARAI and TAKESHI MARUO

Department of Research Reactors and Tandem Accelerator

Nuclear Science Research Institute, Japan Atomic Energy Agency

2-4, Sirakata-shirane, Tokai-mura, Naka-gun, Ibaraki 319-1195 - Japan

ABSTRACT

JRR-3 at Tokai site of JAEA was in its regular maintenance period, when the Great East Japan Earthquake was taken place on 11th March 2011. The reactor building with their solid foundations and the equipment important to safety survived the earthquake without serious damage and no radioactive leakage has been occurred. Recovery work is planned to be completed by the end of this March. At the same time, check and test of the integrity of all components and seismic assessment to show resistance with the 311 earthquake have been carried out. JRR-3 will restart its operation after completing above mentioned procedures.

1. Introduction

JRR-3 (Japan Research Reactor No.3) has suffered the great earth tremor not previously experienced when the Great East Japan Earthquake has occurred on March 11, 2011. At that time, JRR-3 was in a periodic inspection and the reactor was not operated but many maintenance people have worked in the reactor building. All workers and JAEA's staff have evacuated successfully just after feeling the strong earthquake. Although commercial electric supply was stopped, necessary minimum facilities were continuously operated with emergency electric generators. There has been checked that no injured person and no increase of radiation dose.

2. Description of JRR-3

JRR-3 is a light water cooled and moderated swimming pool type research reactor with nominal thermal power of 20MW. Figure 1 shows the layout of JRR-3 buildings and facilities. Reactor building contains reactor facilities such as a reactor pool, cooling system, I&C system etc. Neutrons coming from the core are transported to a neutron guide hall and several neutron beam experiments are carried out in the hall. Secondary cooling tower receives heat generated in the core and emitted it to the atmosphere. Air with minor radioactivities in the reactor building is filtered and exhausted to the air through an exhaust stack.

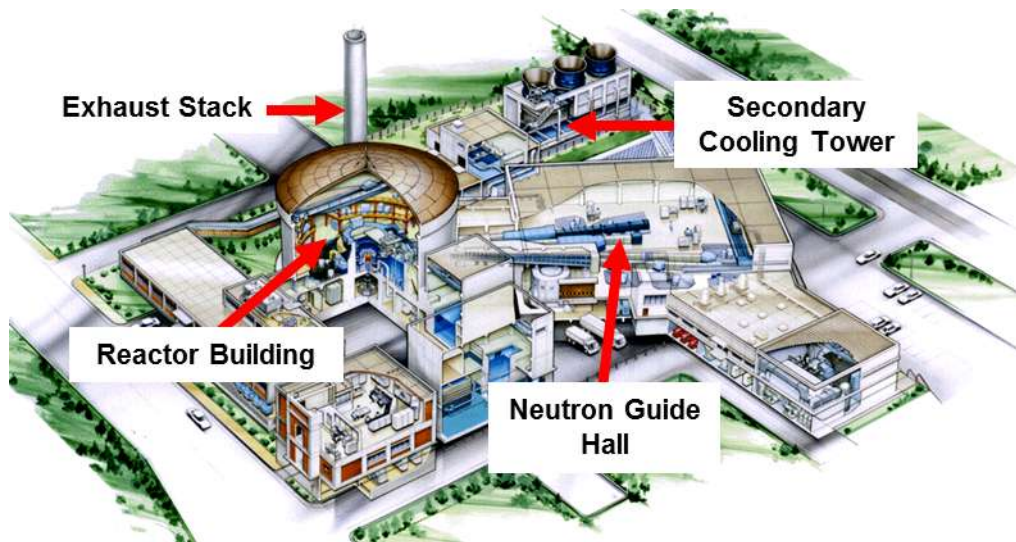


Fig.1 Layout of JRR-3 buildings

3. Damage check

It is very important to confirm immediately whether nuclear fuel materials and reactor confinement system are damaged or not. During the aftershocks for a few hours, the reactor pool, nuclear fuels and their storage facilities were checked visually and confirmed to keep their soundness. Although several small cracks were shown on the internal wall of reactor building, they did not result in adverse effect on the integrity of confinement and there was no release of radioactive materials to environment.

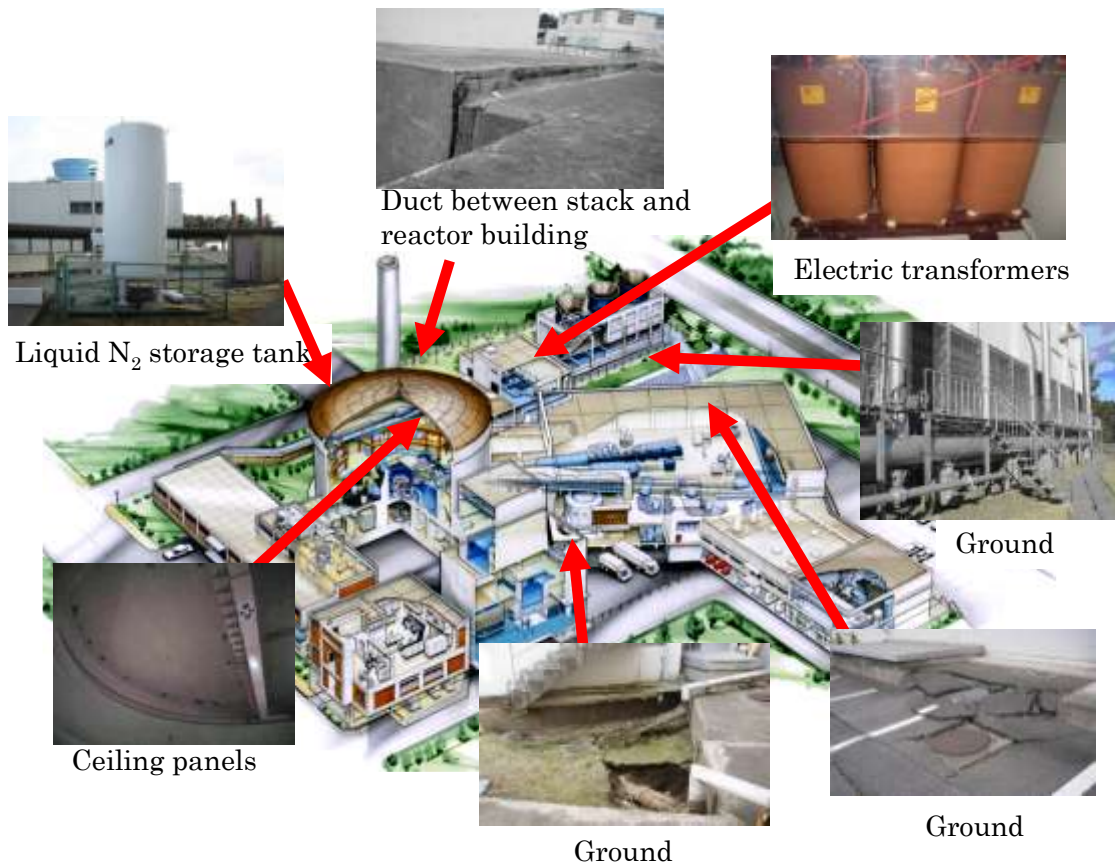


Fig.2 Some damages of JRR-3 observed after 311 earthquake

Some damages visually observed are shown in Fig. 2. Ground around the buildings was sunk about 40cm. The buildings themselves did not sink since they are built on the bedrock. According to the ground sinking, an exhaust duct leading from the reactor building to a stack was slightly damaged at a connection. A liquid nitrogen storage tank, used for feeding nitrogen to experimental facilities, and electric transformers for secondary cooling system were also damaged and leaned. Some of the ceiling panels in the reactor building were dropped.

4. Recovery work

Recovery works have been carried out as shown in Fig.3. They will be completed by the end of this March.









	Damage	After Recovery
Ground sinking - around cooling tower		
Ground sinking – around neutron guide hall		
Flexible pipe for exhaust system, contained in a duct connecting the reactor building to the stack		
Ceiling panel in the reactor building		

Fig.3 Recovery work

5. Regulatory procedure to re-start the reactor

As the 311 earthquake measured larger seismic acceleration than that of seismic design of JRR-3, regulatory body has demanded us to evaluate soundness of reactor facilities and report it. Two types of evaluation have been required such as a) check and test of all of the structure, systems and components (SSCs), and b) seismic analysis. Moreover, in the light of experience of Fukushima Daiichi Nuclear Power Station, impacts of tsunami with 15m-high waves and station blackout were required to be assessed.

5.1 Check and test for evaluation of facilities soundness

Check and test have been carried out as shown in Fig. 4. So far, soundness of the SSCs needed for reactor re-operation has been confirmed. All of the check and test will complete by the end of this March.



(a) Check of primary cooling system



(b) Check of experimental facilities

Fig.4 Check and test of all of the SSCs

5.2 Seismic analysis for evaluation of facilities soundness

Seismic analysis has been carried out in order to confirm the JRR-3 would have been resistant with the 3.11 earthquake adequately. Simple structures such as reactor building, roof etc. have been assessed as sound enough. Complex structure such as reactor pool is in evaluation. Analysis of other components such as fuel elements, control rod driving mechanism shows there would be no damage.

5.3 Impact of tsunami and station blackout

Impact on the facilities caused by 15 meter tsunami that hit the Fukushima Daiichi Nuclear Power Station was evaluated. As the JRR-3 is located at the attitude of 19 m, there is no need to take particular countermeasures. For reference, about 5m-high waves have been observed in Tokai site.

JRR-3 is operated with the thermal power of 20 MW. When a station blackout occurs, the reactor shuts down automatically. The maximum surface fuel temperature reaches to 123 C and then decreases gradually [1]. This shows that integrity of core is sufficiently kept even in a station blackout. Pool water evaporates very slightly and it takes about 40 days before the fuels are exposed in the air.

5. Conclusion

Damages by the 3.11 earthquake would not diminish the safety of the JRR-3. Recovery work mainly for ground sinking has been carried out smoothly. SSCs needed for reactor re-operation have been checked to be reusable without major repair. Seismic assessment shows almost SSCs are soundness, and only reactor pool is under analysis. We are planning to start a service after the regulatory body confirms the soundness of the facility.

Acknowledgement

The authors want to express great appreciation to the staff of JRR-3 operation division for their dedicated work for recovery from the 3.11 earthquake.

References

[1] M. Arai, Y. Murayama and S. Wada: "Current Status of JRR-3 -After 3.11 earthquake in Japan-", 2012 JAEA/KAERI Joint Seminar on Advanced Irradiation and PIE Technologies, Mito, March 28– 30, 2012 (in printing)

OVERVIEW OF ARGONNE PROGRESS IN TECHNOLOGY DEVELOPMENT FOR (1) CONVERSION OF ^{99}Mo PRODUCTION TO LOW ENRICHED URANIUM AND (2) IMPLEMENTING DOMESTIC PRODUCTION OF Mo-99

G. F. VANDEGRIFT, K. ALFORD, A. J. BAKEL, J. P. BYRNES, S. D. CHEMERISOV, D. BOWERS, A. V. GELIS, L. HAFENRICHTER, A. HEBDEN, J. JERDEN, M. KALENSKY, J. KREBS, E. O. KRAHN, V. MAKARASHVILI, K. J. QUIGLEY, N. A. SMITH, D.C. STEPINSKI, P. TKAC, A. J. YOUKER

*Chemical Sciences and Engineering Division, Argonne National Laboratory
9700 S. Cass Ave., Argonne, IL 60439 – United States of America*

ABSTRACT

The Global Threat Reduction Initiative (GTRI)--Reactor Conversion program supports the conversion of domestic and international civilian research reactors and isotope production facilities from the use of high enriched uranium (HEU) to low enriched uranium (LEU) fuel and targets. The main technology components of the program are: (1) the development of advanced LEU fuels, (2) design and safety analysis for research reactor conversion, and (3) development of targets and processes for the production of ^{99}Mo without using HEU. Argonne supports the conversion of international ^{99}Mo production by (1) developing frontend processes that will allow the use of high density-LEU-foil targets to be used in the alkaline processes being used in the production of ^{99}Mo with HEU targets by the current producers, (2) cooperating with ICN and Y-12 to perform LEU-foil-target qualification experiments in Pitesti, Romania, and (3) working with the IAEA Working Group for Conversion Planning for ^{99}Mo Production Facilities from HEU to LEU. Argonne is also supporting the development of three U.S. domestic non-HEU-based technologies for production of ^{99}Mo . These three technologies are: (1) electron-linac-accelerator production from the γ/n reaction on ^{100}Mo in cooperation with NorthStar Medical Radioisotopes, LLC and Los Alamos National Laboratory (LANL), (2) production of fission-product ^{99}Mo from an aqueous homogeneous reactor in cooperation with Babcock and Wilcox Technical Services Group (BWTSG), and (3) D/T-accelerator-driven production of fission-product ^{99}Mo in an aqueous uranyl-salt solution target in cooperation with the Morgridge Institute for Research and LANL. A brief discussion of each technology under development and Argonne's role in development activities will be discussed in this paper.

1. Introduction

The Global Threat Reduction Initiative (GTRI)--Conversion Program develops technology necessary to enable the conversion of civilian facilities using high enriched uranium (HEU) to low enriched uranium (LEU) fuels and targets. For the non-HEU production of ^{99}Mo , GTRI has three goals:

- Assisting current producers to convert from HEU to LEU targets for production of ^{99}Mo
- Assisting potential producers of Mo-99 to do so without the use of HEU
- Accelerating the establishment of a reliable, commercial U.S. domestic supply of the critical medical isotope ^{99}Mo produced without the use of HEU

Argonne National Laboratory (Argonne) is involved in both (1) assisting current producers convert to LEU targets and (2) assisting in the development of a U.S. domestic production of ^{99}Mo .

The conversion of conventional HEU uranium-aluminide dispersion targets to LEU for the production of ^{99}Mo production requires approximately five-times the uranium in a target to maintain the ^{99}Mo yield per target. Under GTRI, Argonne is supporting conversion of current Mo producers from HEU to LEU targets by developing two frontend options to the current processes to allow the use of LEU-foil targets. [1] Because of the high density of uranium in

uranium-metal foils compared to that in dispersion-fuel meats, these LEU foil targets will allow equal or greater ^{99}Mo production than is now produced with HEU-dispersion targets. Both the frontend-process options under development have two major goals. The first goal is to produce a Mo-product solution from the LEU-foil frontend that will be compatible with current purification operations and that will, with the same number of targets irradiated, provide the same or higher yield of ^{99}Mo at the end of processing. The second goal is to deliver a product solution that is of the same or higher Mo purity than the current solution and is of equal or better compatibility with current purification process.

In the first frontend option, the LEU foil (contained in a thin (10-15 μm) Ni fission-recoil barrier is removed from the annular target and dissolved in nitric acid. After dissolution, the solution will be fed to a small column of titania sorbent, where Mo will be sorbed on the column with minor amounts of other feed components. The column will be washed with nitric acid and then water; then Mo will be stripped into a sodium hydroxide solution. In the second option, the LEU-foil target uses a 40- μm aluminium fission recoil barrier. Once the Al/U foil is removed from the target, the Al layer is dissolved in base to expose the uranium surface. This is followed by a low-temperature, low-pressure procedure employing electrolytic oxidation of the uranium metal into an aqueous bicarbonate solution. After precipitation of uranium, carbonate, and alkaline-insoluble fission and activation products from the solution by the addition of calcium oxide, the Mo solution can be fed into the current purification processes.

Argonne is also assisting in the development of three technologies for domestic production of ^{99}Mo without the use of HEU.[2,3,4] These three technologies are: (1) electron-linac-accelerator production from the γ/n reaction on ^{100}Mo in cooperation with NorthStar Medical Radioisotopes, LLC and Los Alamos National Laboratory (LANL), (2) production of fission-product ^{99}Mo from an aqueous homogeneous reactor in cooperation with Babcock and Wilcox Technical Services Group (BWTSG), and (3) D/T-accelerator-driven production of fission-product ^{99}Mo in an aqueous uranyl-salt solution target in cooperation with the Morgridge Institute for Research and LANL.

2. Frontend Processes for Conversion to LEU-Foils

These two frontend options were discussed in a recent paper presented at the 2011 RERTR meeting.[1]. Each option is discussed separately below.

2.1 Nitric-Acid Dissolution followed by Mo Recovery on a Titania Column

In the first frontend option, the LEU foil (contained in a thin (10-15 μm) Ni fission-recoil barrier is removed from the annular target and dissolved in nitric acid. In the dissolution, the uranium, nickel, and all fission and activation products are dissolved. The resultant solution (~0.5L) will be ~7 mM Mo, ~450 g-U/L, and the nitric-acid concentration after dissolution will be ~1 M. After dissolution, the solution will be fed to a small column of titania sorbent, where Mo will be sorbed on the column with minor amounts of other feed components. The column will be washed with nitric acid and then water; then Mo will be stripped into a sodium hydroxide solution.

The nitric-acid-dissolver system was designed to allow the dissolution of up to 250 grams of irradiated uranium foil and associated Ni fission-recoil barrier at ambient pressure. Components of the dissolver system are currently being tested so that the design can be optimized in preparation for a full-scale demonstration. The key design criteria that this dissolver system must incorporate are listed below.

- All water vapour, reaction products, and fission gases must be contained within the dissolver system at a maximum temperature of 125°C and 2 atmospheres of pressure (absolute) under both normal and off-normal (loss of cooling during reaction) conditions.
- The acid feed system must be designed so that the thermally hot LEU foil (hot from decay heat) can be immersed in nitric acid without losing solution due to instantaneous boiling.
- All dissolver system components must be designed for remote operation in a hot-cell facility.

- Gas-trap components must be designed to trap/neutralize all nitrogen oxide and acid gases (NO , NO_2 , HNO_2 , HNO_3) as well as trap iodine gas for possible extraction of economically important iodine isotopes (noble fission gases will be passively contained).
- Our future plans for this year are to:
 - Cooling system (heat exchange) tests will continue. Tests will be performed for both normal and off-normal (loss of cooling air flow) conditions.
 - Dissolution experiments on DU foils (up to 250g) will begin soon to quantify how the exothermic dissolution heat and loss of NO_x influence the overall performance of the system (loss of dissolver solution, loss of acidity).
 - Iodine trapping and recovery tests will continue (Cu, silver based traps).
 - The system will be tested in a manipulator mock-up facility to ensure that the dissolver system can be easily operated in a production scale inside a hot cell.
 - A full-scale demonstration with irradiated LEU is being planned. Both target dissolution and Mo-99 recovery processes will be tested.

Titania based sorbents have been identified as supports for separation of Mo from concentrated uranium solutions.[4-9] They offer high capacity, remarkable K_d values, and are slightly affected by the presence of uranium. Adsorption of metal ions on inorganic supports such as alumina or titania is often slow and tends to take several hours or days to reach equilibrium in batch contacts. Slow adsorption kinetics relative to mass transfer rates lead to slow development of constant mass transfer pattern. Non-equilibrium adsorption/desorption can introduce large errors to column designs, sorbent capacity, and estimation of system parameters. In this study, a non-constant pattern mass-transfer-zone (NCP-MTZ) method was applied to the design and optimization of Mo separation using a titania column. In this approach, batch tests were conducted to estimate isotherm parameters, and breakthrough column experiments were utilized to determine particle diffusivity (D_p) for each sorbent. Once the intrinsic parameters were determined, VERSE (Versatile Reaction and Separation—developed by Purdue University, IN, USA) simulations were carried out to estimate mass transfer zone (MTZ) at various linear velocities and loading times. Determination of MTZ lengths allows design of process separation column. Key designs were verified experimentally, through loading and breakthrough experiments, to verify D_p , MTZ, and column designs. For recovery of Mo from a 500-mL solution containing 450 g-U/L uranyl nitrate and 7 mM Mo in 1 M HNO_3 , a 2.5 cm ID by 8-cm long column should be sufficient. The recovery operation should be completed in about 1 hour. Laboratory tests using slightly irradiated uranium foils have shown ~96% recovery of Mo. The fates of other radionuclides in the solution are:

- The majority of radionuclides, including uranium, iodine, alkaline earths (Ba and Sr), transition metals (Cd, Rh and Ru) and lanthanides (Ce, Nd) report in the eluent and wash streams.
- The fission products found in Mo product stream are Te and I (~ 8% from fission + growing-in from Te), as well as < 3% of Ru, Rh, Sb and Zr.
- Te (~ 50%), Sb (>90%), and Zr (~80%, likely as a precipitate) remain on the sorbent.

2.2 Electrochemical Dissolution of LEU Foils in Sodium Bicarbonate

In the second option, the LEU-foil target uses a 40- μm aluminium fission recoil barrier.[10] Once the Al/U foil is removed from the target, the Al layer is dissolved in base to expose the uranium surface. This is followed by a low-temperature, low-pressure procedure employing anodic oxidation of the uranium metal into an aqueous bicarbonate solution. After precipitation of uranium, carbonate, and alkaline-insoluble fission and activation products from the solution by the addition of calcium oxide, the Mo solution can be fed into the current purification processes. A prototypical 50 g-U dissolver is now being tested; once parameters are optimized, a 250 g-U hot-cell-compatible dissolver will be fabricated and demonstrated.

3. Development of U.S. Domestic non-HEU Production of ^{99}Mo

Argonne is assisting in the development of three technologies for domestic production of ^{99}Mo without the use of HEU.[2,3,4] These three technologies are: (1) electron-linac-

accelerator production from the γ/n reaction on ^{100}Mo , (2) production of fission-product ^{99}Mo from an aqueous homogeneous reactor, and (3) D/T-accelerator-driven production of fission-product ^{99}Mo in an aqueous uranyl salt solution. A summary of the technology and Argonne's R&D are described in separate sections below.

3.1 Accelerator Production through the γ/n reaction on ^{100}Mo

NorthStar Medical Radioisotopes, LLC in cooperation with Argonne and Los Alamos National Laboratory, is developing this technology.[3] During 2011, two demonstrations are planned—a thermal and production test. In the thermal test, a two-sided target containing 25 1-g natural-Mo discs will be irradiated to produce ~1kW/disc. The target will be He-cooled; the objective of this test is to demonstrate the adequacy of the target holder and He-cooling. Later in the year, a short production test will be run to produce ~20 Ci of ^{99}Mo . The objective of this test is to produce commercially significant quantities of ^{99}Mo , to process these disks, and test the TechneGen™ with commercially significant production of $^{99\text{m}}\text{Tc}$. Another important parameter for this test is the measurement of yields for side-reaction by-products in the Mo-99 product.

3.2 Solution Reactor Production of ^{99}Mo

Argonne is assisting Babcock and Wilcox Technical Services Group (BWTSG) to develop the Medical Isotope Production System (MIPS) to produce commercially ^{99}Mo . Effort is in three areas: (1) understanding MIPS solution chemistry and radiolytic gas formation during reactor operation, (2) developing the Mo-recovery system for the MIPS, and (3) developing a Mo-purification step for the ^{99}Mo recovered from the MIPS using the LEU-Modified Cintichem process. Argonne has developed design parameters for the full-scale Mo-recovery column using a 110 μm titania sorbent and the mini-SHINE/MIPS experiment is providing data and for understanding the radiation chemistry in an irradiated uranyl nitrate solution.[2]

The mini-SHINE/MIPS experiments will be performed using the Argonne linac with an electron/x-ray/neutron convertor to produce neutrons that will produce fissioning in solution. The solution will be either a 150 g-U/L LEU uranyl nitrate or 90-150 g-U/L uranyl-nitrate or uranyl-sulphate solution. In phase-1, the convertor will be tantalum, and the target solution will have a volume of five L; this will generate a fission power density of up to 0.05 W/mL (1/20 of that foreseen for the MIPS and 1/10 of that foreseen for SHINE. In Phase-2, the convertor will be depleted uranium, and the solution will be 10 to 20 L; this will generate a fission power density of up to 0.5 W/mL (1/2 of that foreseen for the MIPS and equal of that foreseen for SHINE. The volumes of the actual MIPS and SHINE units will be much larger however--200 to 500 L. These experiments have four major objectives:

1. Quantitate the production rate and composition of radiolytic gases generated during operation of the system under varying conditions of power density, solution temperature, and start-up conditions.
2. Provide information on changes of solution composition (peroxide concentration, iodine and nitrogen speciation, pH, conductivity, solids formation), vs. time, temperature, and fission power.
3. Demonstrate Mo-recovery from the irradiated solution hours after end of irradiation.
4. Produce 2 Ci of ^{99}Mo for shipment to a $^{99\text{m}}\text{Tc}$ -generator producer for testing.

3.3 Accelerator-Driven Production of Fission-Product ^{99}Mo through Neutron Irradiation of an Aqueous Solution of Uranyl Sulphate

Argonne is supporting the development of the SHINE technology for producing ^{99}Mo by (1) use of the Argonne mini-SHINE/MIPS to provide operational data for the SHINE target solutions for both nitrate and sulphate media with uranium concentrations relevant to SHINE target solution concentrations, (2) design of the production-scale Mo-recovery system, (3) performing column verification studies at Argonne, (4) developing solution clean-up schemes for sulphate media and (5) providing technical assistance for developing a robust commercial accelerator system and target-processing/Mo-recovery facility.

4. Acknowledgements

The submitted manuscript has been created by UChicago Argonne, LLC, Operator of Argonne National Laboratory ("Argonne"). Argonne, a U.S. Department of Energy Office of Science laboratory, is operated under Contract No. DE-AC02-06CH11357. The U.S. Government retains for itself, and others acting on its behalf, a paid-up nonexclusive, irrevocable worldwide license in said article to reproduce, prepare derivative works, distribute copies to the public, and perform publicly and display publicly, by or on behalf of the Government.

This work was supported by the U.S. Department of Energy, Office of Nuclear Energy, under Contract DE-AC02-06CH11357. Argonne National Laboratory is operated for the U.S. Department of Energy by UChicago Argonne, LLC.

5. References

- [1] Vandegrift, G. F., Stepinski, D., Jerden, J., Gelis, A., Krahn, E., Hafenrichter L., and Holland, J., GTRI PROGRESS IN TECHNOLOGY DEVELOPMENT FOR CONVERSION OF ^{99}MO PRODUCTION TO LOW ENRICHED URANIUM, proceedings of the 2011 International RERTR Meeting AND TEST REACTORS, Santiago Chile, October 23-27, 2011.
- [2] Chemerisov, S., Youker, A. J., Hebden A., Smith, N., Tkac, N., Jonah, C. D., Bailey, J., Makarashvili, V., Micklich, B., Kalensky, M., Vandegrift, G. F., DEVELOPMENT OF THE MINI-SHINE/MIPS EXPERIMENTS, Proceedings of Mo-99 2011—MOLYBDENUM-99 TOPICAL MEETING, SANTA FE, NEW MEXICO, USA, December 4-7, 2011.
- [3] Tkac, P., Chemerisov, S., Makarashvili, V., Vandegrift, G. F., and Harvey, J., DEVELOPMENT ACTIVITIES IN SUPPORT OF ACCELERATOR PRODUCTION OF ^{99}MO PRODUCTION THROUGH THE γ/N REACTION ON ^{100}MO , Proceedings of Mo-99 2011—MOLYBDENUM-99 TOPICAL MEETING, SANTA FE, NEW MEXICO, USA, December 4-7, 2011.
- [4] Youker, A. J., Pei-Lun Chung, P. L., Tkac P., Quigley, K. J., Makarashvili, V., Bowers, D. L., Chemerisov, S., and Vandegrift, G. F., SEPARATION, PURIFICATION, AND CLEAN-UP DEVELOPMENTS FOR MIPS AND SHINE, Proceedings of Mo-99 2011—MOLYBDENUM-99 TOPICAL MEETING, SANTA FE, NEW MEXICO, USA, December 4-7, 2011.
- [5] Bakel, A. J., Aase, S. B., Leyva, A. A., Quigley, K. J. and Vandegrift, G. F., THERMOXID SORBENTS FOR THE SEPARATION AND PURIFICATION OF ^{99}MO , Proceedings of the 2004 International RERTR Meeting, Vienna, Austria, Nov. 7-12, 2004.
- [6] Allen J. Bakel, Dominique C. Stepinski, George F. Vandegrift, Argentina Leyva, Artem V. Gelis, Andrew H. Bond, and Heather Mayes, PROGRESS IN TECHNOLOGY DEVELOPMENT FOR CONVERSION OF ^{99}Mo PRODUCTION--BATAN'S (INDONESIA) CONVERSION PROGRAM, PROGRESS IN THE CNEA (ARGENTINA) LEU FOIL/BASESIDE PROCESS, AND DEVELOPMENT OF INORGANIC SORBENTS FOR ^{99}Mo PRODUCTION, Proceedings of the 2005 International RERTR Meeting, Boston, USA, November 6-10, 2005.
- [7] Allen J. Bakel, Dominique C. Stepinski, Artem Guelis, Andrew Hebden, Argentina Leyva, Lohman Hafenrichter, Pauline Gentner, and George F. Vandegrift, PROGRESS IN TECHNOLOGY DEVELOPMENT FOR CONVERSION OF ^{99}MO PRODUCTION FROM HEU TO LEU TARGETS - DEVELOPMENT OF NEW SEPARATION SCHEMES, AND NEW PROCESSING EQUIPMENT, Proceedings of the 2006 International RERTR Meeting, Cape Town South Africa, November 26 – November 1, 2006.
- [8] Ziegler, A., Stepinski, D., Krebs, J., Chemerisov, S., Bakel A., and Vandegrift, G. F., MO-99 RECOVERY FROM AQUEOUS-HOMOGENEOUS-REACTOR FUEL—BEHAVIOR OF THERMOXID SORBENTS, Proceedings of the 2008 International RERTR Meeting, Washington D.C., USA, October 5-9, 2008.
- [9] Vandegrift, G. F., Stepinski, D., Ziegler, A., Krahn, E., Fortner, J., Quigley, K., Mertz, C., Chemerisov, S., Jerden J., Hebden, A., Guelis, A., and Bakel, A., OVERVIEW OF ARGONNE PROGRESS IN DEVELOPING LEU-BASED PROCESSES FOR THE

PRODUCTION OF MO-99, Proceedings of the 2009 International RERTR Meeting, Beijing, China, November 1-5, 2009.

- [10] Gelis, A., Wiedmeyer, S., and Vandegrift, G. F., PROGRESS IN DEVELOPING ELECTROCHEMICAL DISSOLUTION OF LEU FOILS, Proceedings of the 2010 International RERTR Meeting, Lisbon Portugal, October 10-14, 2010..

NEUTRONIC CALCULATIONS IN SUPPORT OF RESEARCH REACTOR OPERATION FOR MOLYBDENUM-99 PRODUCTION

D. HERGENREDER

Nuclear Engineering Division INVAP SE- Argentina

M. A. GAHEEN

*Egypt Second Research Reactor (ETRR-2), Egyptian Atomic Energy Authority (EAEA)
13759 Abou Zabal – Egypt*

ABSTRACT

Neutronic calculations were performed in support of research reactor operation to irradiate uranium plates for ^{99}Mo production. The core neutronic model was tested and verified using critical positions. The excess reactivity was also calculated from critical positions showing that the operation cycle meet the irradiation requirement. The calculation was done for the core with and without loading of uranium plates. In addition, two figures were developed to help the operators to understand and evaluate the reactor availability. These figures show as a function of operation hours, the maximum allowable time to prompt restart the reactor after unexpected trip and the reactor dead time.

1. Introduction

The production of the ^{99}Mo requires fixed operation cycle and continuous irradiation without unplanned shutdown. When the reactor operation fulfills these requirements the ^{99}Mo production could be delivering on fixed days of the week. The first requirement can be met by nuclear design [1]. That is, the core shall be capable to operate without refueling requirement during the irradiation cycle of the uranium plates to produce ^{99}Mo . The second requirement of continuous irradiation shall be met by minimizing the number of trips during the uranium plates irradiation by a complete reactor maintenance plan.

In case of unexpected trips like that produced, for example, by short interruption of the external power supply, the reactor auxiliary systems can be restarted again promptly. The reactor operators have a time that could vary between 25 minutes and more than 3 hours, depending on the state of the core cycle (beginning, middle, or end of cycle) and the operation time before trip, to bring the reactor critical again and increase the reactor power to the required level. If the reactor operators do not success with the reactor start up before the ^{135}Xe (xenon-135) build up, it is necessary to wait for a minimum time between 0 and 36 hours, depending on the state of the core cycle and the operation time before trip. Both times, the time to restart the reactor before ^{135}Xe build up and the waiting time to restart after the ^{135}Xe concentration decrease are presented in figures as function of the core excess reactivity and the operation time before trip.

The neutronic calculations support Egypt Second Research Reactor (ETRR-2) operation by providing excess reactivity information and time figures to restart the reactor after a trip ensuring the success of the uranium plates irradiation. The training of the reactor operators also helps to take benefit from these calculations.

2. Methodology

The CITVAP code used to carry out the core neutronic is a new version of the CITATION-II code [2], developed by INVAP's Nuclear Engineering Division. The code was developed to improve CITATION-II performance. In addition, programming modifications were performed for its implementation on personal computers. The code solves 1, 2, or 3-dimensional multi-group diffusion equations in rectangular or cylindrical geometry. Spatial discretization can also be achieved with triangular or hexagonal meshes. Nuclear data can be provided as microscopic or macroscopic cross section libraries [3, 4].

In this paper the following calculations were performed to support in core irradiation of uranium plates for ^{99}Mo production:

- Verification of the core neutronic model using control rod critical positions.
- Prediction of the cycle length (excess reactivity calculation).
- Maximum allowable time to restart the reactor promptly after a trip.
- Minimum waiting time for ^{135}Xe decay to restart the reactor.

The most important fission product that poisons the reactor core is the ^{135}Xe . Although the fission production of this isotope ceases when a reactor shutdown, it continues to be produced as a result of the decay of ^{135}I (iodine -135) present in the system. The ^{135}Xe negative reactivity continues increases exceeding the core excess reactivity [5]. If the operator fails to restart the reactor before the core reaching this status, the operator should wait for ^{135}Xe decay. The two critical times are calculated using the well known equations of ^{135}I and ^{135}Xe production from fission in a nuclear reactor [6]:

$$\frac{\partial I(t)}{\partial t} = -\lambda_I I(t) + \gamma_I \Sigma_f(t) \phi(t)$$

$$\frac{\partial Xe(t)}{\partial t} = -\lambda_{Xe} Xe(t) - \sigma_a^{Xe} Xe(t) \phi(t) + \lambda_I I(t) + \gamma_{Xe} \Sigma_f(t) \phi(t)$$

Where:

$I(t)$ and $Xe(t)$ are the ^{135}I and ^{135}Xe concentrations as function of time respectively,

λ_I and λ_{Xe} are the time decay constants for ^{135}I and ^{135}Xe respectively,

γ_I and γ_{Xe} are the production yield from fission for ^{135}I and ^{135}Xe respectively,

Σ_f and ϕ are the fission cross section and the neutron flux respectively, and

σ_a^{Xe} is the absorption cross section for the ^{135}Xe .

These equations are solved with an excel spreadsheet, by integration of time differentials where $\Sigma_f = 0.072 \text{ cm}^{-1}$ (average Value) and ϕ is an average flux of $1 \times 10^{14} \text{ n/cm}^2\text{s}$. The equilibrium ^{135}Xe concentration is equivalent to -3300 pcm.

3. Results

After approximately two days of continuous operation at a stable power, the ^{135}Xe concentration reaches the equilibrium and the control rod movement compensated the core fuel burn up. In this condition it is possible to verify the core calculation model by calculating the core reactivity using in the calculation model the critical positions as function of the core burn up. The core burn up is obtained experimentally by integration of the reactor power during the operation time. The expected result is line or points without a clear trend. Fig. 1 shows the results of verification of core neutronic model where it is possible to observe a maximum deviation less than 500 pcm between model and critical positions (zero pcm).

During the commissioning of the irradiation of uranium plates in the ETRR-2 core, the control rods were calibrated with dummy plates (aluminum plates instead of uranium plates) and uranium plates in the core. This leads to two sets of experimental values obtained by the asymptotic period method. Taking into account the critical positions, it is possible to obtain the core excess reactivity by adding the reactivity worth of the rod portions that are inserted in the core. Fig. 2 shows the core excess reactivity as function of the core burn up. The end of cycle is reached when the excess reactivity is 1000 pcm. This margin allows the reactor operators to compensate operation transients and gives time margin to restart the reactor after a trip at near the end of cycle. By extrapolation of the excess reactivity as function of the core burn up until 1000 pcm, it is possible to identify the end of cycle and the remaining operation time.

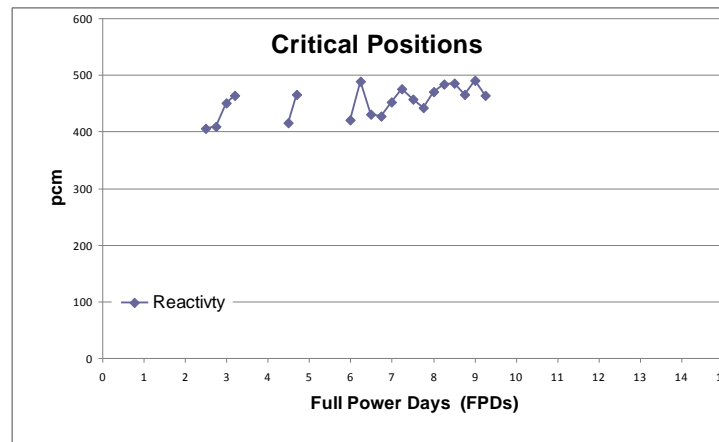


Fig. 1. Verification of core neutronic using critical positions

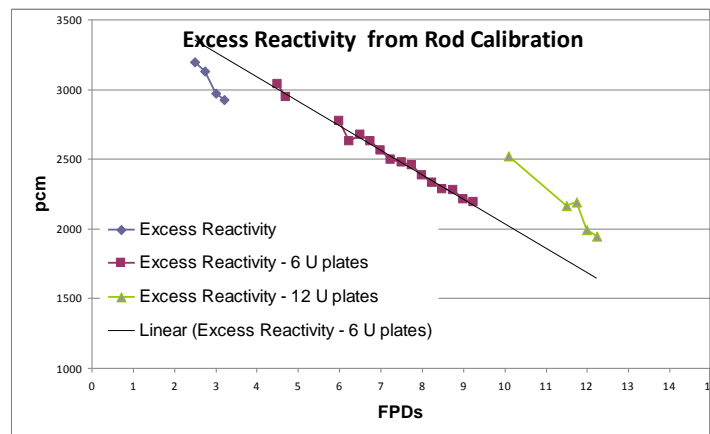


Fig. 2. Core excess reactivity and cycle length prediction

In order to help the reactor operators about the maximum allowable time to restart the reactor after unplanned shutdown, Fig. 3 was developed. The time is function of key parameters namely the reactor operation hours before shutdown and the core excess reactivity. This time is flux dependent (but is assumed full power conditions) and it is independent of the core configuration. Typical values for core excess reactivity at BOC, MOC, and EOC (beginning, middle, and end of cycle) are 3000, 2000, and 1000 pcm respectively.

In case the operators could not restart the reactor after the trip, it is important to know the minimum waiting time required for ^{135}Xe decay. The knowing of this time will help to minimize the shutdown time. This time is also flux dependent and independent of the core configuration. Fig. 4 shows the minimum waiting time required to resume the reactor after the trip and ^{135}Xe buildup.

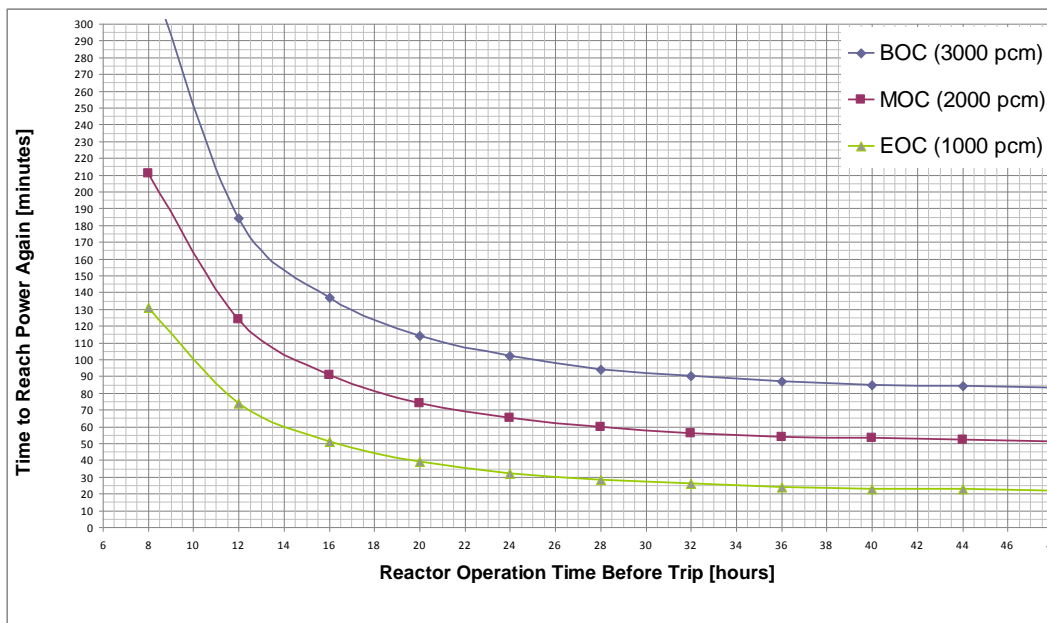


Fig. 3. Maximum allowable time to restart the reactor promptly after a trip

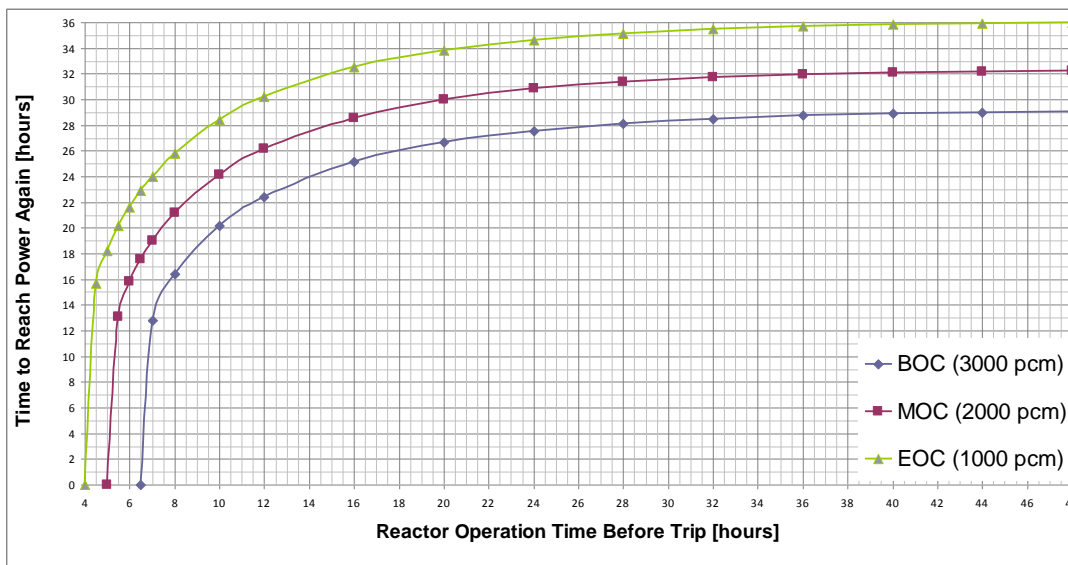


Fig. 4. Minimum waiting time for ^{135}Xe decay to restart the reactor

4. Conclusions

The results show that the core neutronic model is accurate enough for the cycle length prediction. Two figures were developed showing maximum allowable time to restart the reactor and minimum waiting time for ^{135}Xe decay. The obtained curves are useful to have minimum time of outage and reliable operation for ^{99}Mo production. The calculation support is important to reach a successful operation and isotope production, as it was done at the end of year 2011 in the ETRR-2 and the Radioisotope Production Facilities. The training of the reactor operators is always essential to benefit from these calculation figures.

5. References

- [1] International Atomic Energy Agency, "Safety Assessment of Research Reactors and Preparation of the Safety Analysis Report," Safety Series No. 35-G1, IAEA, Vienna, December 1994.
- [2] T. B. Fowler, D. R. Vondie, "Nuclear Core Analysis Code: CITATION," ORNL-TM-2496, July 1969.
- [3] Ignacio Mochi, "INVAP's Nuclear Calculation System," Science and Technology of Nuclear Installation, Vol. 2011, Article ID 215363, 7 pages, 2011.
- [4] MTR – PC USER MANUAL, INVAP's Nuclear Engineering Division.
- [5] J. R. Lamarsh, A. J. Baratta, "Introduction to Nuclear Engineering," Third Edition, Prentice Hall, Upper Saddle River, New Jersey 07458, 2001.
- [6] J. R. Lamarsh, "Introduction to Nuclear Reactor Theory," Addison-Wesley Eds., 1966.

RADIOISOTOPES PRODUCTION FOR MEDICAL USE: PRELIMINARY DESIGN OF THE JULES HOROWITZ REACTOR FACILITIES

JP COULON, M. ANTONY, S. GAILLOT,
*CEA, DEN, Cadarache,
F-13108 Saint Paul Lez Durance, France*

A. ALBERMAN
*CEA, DEN, Saclay,
F-13108 Saint Paul Lez Durance, France*

ABSTRACT

This paper describes the status of the radioisotopes production design studies for medical use which is part of the Jules Horowitz Reactor (JHR) under construction at CEA (Commissariat à l'Energie Atomique et aux Energies Alternatives) Cadarache in France. It focuses on the molybdenum 99 (^{99}Mo) irradiation systems and associated facilities. Most of the ^{99}Mo consumed worldwide is produced in research reactors by irradiation of uranium targets. Technetium 99m ($^{99\text{m}}\text{Tc}$), the ^{99}Mo daughter product, is the most commonly used medical radioisotope in the world. Following the recent radioisotope supply shortages, efforts have been undertaken to secure the ^{99}Mo supply. JHR is to contribute sustainable ^{99}Mo security of supply in Europe for the long term, by providing a production capacity of 25% of Europeans needs on an average basis, and up to 50% in peak production. The ^{99}Mo production will be one important issue of JHR starting operations. Production start-up is foreseen in continuity of the OSIRIS reactor which is planned to shut down within this decade.

1 Introduction

The production of molybdenum 99 (^{99}Mo), and its decay product, technetium 99m ($^{99\text{m}}\text{Tc}$), the most widely used medical radioisotope for diagnostic purposes, is important for public health. As a matter of fact, disruptions in the supply chain of these medical isotopes, which have half lives of 66 hours for ^{99}Mo and 6 hours for $^{99\text{m}}\text{Tc}$, can lead to cancellations or delays in important medical testing services. Unfortunately, supply reliability has declined over the past decade, due to unexpected or extended shutdowns at the few ageing ^{99}Mo producing research reactors and processing facilities. These shutdowns have created global supply shortage. As an answer, the Jules Horowitz Reactor (JHR) under construction at CEA Cadarache in France took into account this new major challenge.

In this paper, we very briefly present an overview of JHR project. Then, after describing the new issues for radioisotope production for medical use, we will present the JHR initiatives and its organisation to answer them. Furthermore, an overview of the technical studies which are undertaken in the framework of JHR program will be outlined.

2 JHR project

The Jules Horowitz Reactor (JHR) is a Material Testing Reactor currently under construction at CEA (Commissariat à l'Energie Atomique et aux Energies Alternatives) Cadarache in France. It will represent a major research infrastructure for scientific studies dealing with material and fuel behaviour under irradiation. The reactor will perform Research and

Development programs for the optimization of the present generation of Nuclear Power Plants (NPPs), support the development of the next generation of NPPs and also offer irradiation possibilities for future reactors. The reactor will also be devoted to medical radioisotope production. [R1].

JHR will offer irradiation experimental capacities to study material and fuel behaviour under irradiation. JHR will be a flexible experimental infrastructure to meet industrial and public needs. It is designed to provide high neutron flux, to run highly instrumented experiments and to operate experimental devices with environmental conditions (pressure, temperature, flux, ...) relevant for water reactors, or specific environments (eg. gas, sodium) related to other thermal or fast reactor concepts.

As a modern research infrastructure, JHR will contribute to the development of expertise and know-how, and to the training of the next generation of scientists and operators. The JHR is designed to meet these technical objectives. Another important objective is its contribution to secure the production of radioisotope for medical application [R2]. It is a major challenge of the JHR.

The construction of JHR is undergoing on and some major milestones have been achieved in 2011 regarding, for example the construction of buildings. Figures 1 and 2 show the evolution of the construction of the Reactor Building and the construction of the Nuclear Auxiliary Building from beginning of 2011 to beginning of 2012.



Figure 1: Nuclear Auxiliary and Reactor Building in January 2011
Reactor criticality is scheduled for 2016.



Figure 2: Nuclear Auxiliary and Reactor Building in January 2012

3 The Supply of Medical Radioisotopes

Following the 2009 - 2010 $^{99}\text{Mo}/^{99\text{m}}\text{Tc}$ supply shortages where the Canadian and Dutch reactors were subject to extended shutdowns, many initiatives have been carried out to provide solutions for sustainability of radioisotope production. Amongst them is the NEA High Level Group on the Security of Supply of Medical Radioisotopes (HLG-MR). The collective efforts of HLG-MR members and nuclear medicine stakeholders have allowed for a comprehensive assessment of the areas of vulnerability in the supply chain and an identification of the issues that need to be addressed. The Group suggested policy approach based on six principles:

- All participants in the supply chain should implement a full cost-recovery;
- Reserve capacity to cope with unexpected supply shortages should be sourced and paid by those in the supply chain;
- Governments have to play their role in setting the proper environment for safe and efficient market operations;
- Governments should support the conversion of research reactors to use low enriched uranium (LEU) targets for molybdenum 99 production;

- Governments and participants to the supply chain should collaborate internationally to ensure a globally consistent approach to addressing the security of supply issues;
- Periodical reviews of progress have to be organised to check the implementing of an economically sustainable supply chain.

In this particular context, efforts on each principle expressed by the NEA HLG-MR have been undertaken by JHR project to secure the ^{99}Mo supply. The list below presents the action of the project on each topic:

- JHR is working on developing a new economic model with the objective of implementing of the full cost recovery;
- JHR is to contribute sustainable ^{99}Mo security of supply in Europe for the long term, by providing a production capacity of 25% of Europeans needs on an average basis, and up to 50% in peak production. The ability to manage reserve capacities represents an asset to cope with unexpected supply shortages at regional or worldwide scale;
- CEA received from the French government, an exceptional funding for JHR through the French national grant for investing in the future. Part of this funding is dedicated to secure radioisotope capacity production in JHR;
- JHR is preparing to irradiate LEU targets;
- From the last two principles, JHR will participate in the global approach toward the security of supply, as well as the implementation of an economically sustainable supply chain.

4 Project Management

As an answer to this matter of public health concern, JHR has built up, as from the beginning of 2011, a project for radioisotope production for medical use. The project is managed by a technical manager who has in charge the running, the coordination and the development of technical aspects of the project, as well as the control of the resources. The following part presents the organisation which has been put in place.

The JHR radioisotope production project was created to plan, organize, secure, and manage resources to achieve specific goals:

- Production targets, associated to an industrial scheme operation;
- Start of the production in continuity of the OSIRIS reactor (industrial scale irradiation of targets currently scheduled by 2018);
- Management of scope, schedule, and budget.

During 2011, the dedicated organisation began to be effective in order to:

- Define the perimeter of the project: Documents such as, management plans, specifications were finalised;
- Plan the project: All project activities or tasks were listed with their necessary interfaces. Periodically, the project team meets together, in order to up-date the data;
- Execute the project: The project team has begun to be built during 2011. In this phase, the project manager has defined the resources needed and how much budget he can obtain for the project. The project manager then assigned those resources and allocated budget to various tasks in the project;
- Control the project: The updating of the tasks is done monthly;
- Close the project: The final outcome of the project was defined as the beginning of the industrial irradiation of the targets in JHR.

From a technical standpoint, the project has set up a specific organisation. As a summary, the project is also organized around these main technical points:

- Studies and manufacturing of the irradiation devices and associated equipments;
- Interfaces with the reactor (core, reflector, pools), the cooling systems and cubicles;
- Support to operations (tools, cranes, casks...);
- Interface with the other experiments;
- Production schedule taking into account reactor availability and experimental constraints;

- Nuclear safety licensing of the complete irradiation process of the UAI targets in JHR;
- Tests and start-up of the production.

The main defined milestones are the following:

- Preliminary design using the feedback experience of research reactors as OSIRIS (France) or HFR (Netherlands). Two steps are identified for this phase. Firstly, a review at the end of 2011 – beginning of 2012 is underway. Secondly, by 2012, a specific evaluation will be done for the developments made for the LEU aspects;
- Detailed studies with a formal technical review before official launch of the production of devices, cooling circuits and tools. For the time being, this detailed conception review is forecast at 2013;
- Define an economic model for JHR ^{99}Mo production. Work on this topic has begun. Many contacts with all participants of the supply chain (uranium target manufacturers, reactor operators, processors, $^{99\text{m}}\text{Tc}$ generators manufacturers) has been underway;
- Manufacturing of the devices, of the circuits and tools with factory acceptance. This process will take more than 2 years;
- Tests and beginning of production.

5 Technical studies

One first technical question handled is related to the shape of the irradiated target. The consideration of LEU targets, as substitute to HEU targets, leads to an update of the input data of the project. Up to the present, these data are not fully established. Therefore, all studies should be included when the final characteristics of the UAI LEU target are determined. In the meantime we worked on the design HEU which allowed us to begin to size some systems that will be needed. In this paper, we briefly focus on some technical topics.

Preliminary neutronic calculations have been made with different configurations (HEU or LEU targets, locations in the beryllium reflector, number of targets per device, type of equipments material,...) in order to obtain the following data : neutron flux, linear power, ^{99}Mo production. The main objective of these calculations was to check our ability to get a sufficiently high thermal neutron flux density of $1.10^{14} \text{ n.cm}^{-2}.\text{s}^{-1}$ or higher.

Part of these results represents entrance data for thermo hydraulic calculations on the heat removal from the targets under irradiation. These calculations are very important for both operational and safety approaches. Studies made in 2011 allowed us to check the heat removal from targets and to roughly define the main cooling circuit. These results gave the operation points of the normal cooling circuits. Further thermo hydraulic calculations will be necessary in 2012 to detail cooling systems.

About irradiation devices, it has been defined that they will be located in the JHR beryllium reflector. In order to increase the JHR means of radioisotopes production, without decreasing the global experimental capacity, the design of the JHR reflector was redefined by the beginning of 2011. Consequently, the irradiation devices will be placed on displacement systems in order to achieve the loading and unloading operations out of the neutron flux. Four locations are devoted to the ^{99}Mo production. The displacement systems should be well interfaced with reactor structures. They should be very robust. The irradiation devices are connected by hoses to a dedicated cooling circuit, As radioisotopes production is an industrial process, equipment dedicated to this activity should be reliable for use over several decades. It will be one of the main criteria in the detailed studies phase.

Concerning tools for operation, many preliminary design studies were undertaken on the target holders, on the tables for target handling, on the tools for hot cells and shielding casks. At the end of 2011, a review process on the preliminary definition studies was carried out. The conclusions will be available beginning of 2012 and injected as entrance data for the detailed studies.

6 Nuclear safety

The nuclear safety studies are very important in the initial conception phase of the project. In 2011, CEA has initiated preliminary safety analysis work. One important issue to be considered is the cooling of targets in the various operating conditions, including incidental situations. After the preliminary definition review, the detailed conception should take into account in an iterative way the results of the 2011 studies.

In 2011, CEA has also made studies related to nuclear safety in the following areas:

- Nuclear Pressure Equipments;
- Calculations of the radiological consequences.

7 Future prospects

Preliminary 2011 studies have been focused on JHR ability to produce 25% of European needs on an average basis, and up to 50% in peak production. Studies will be carried out in 2012 in connection with the decision to irradiate LEU targets.

The next period, until 2013, will be devoted the detailed studies for irradiations devices, circuits and tools. Finally and above all, project will also emphasize on the studies about nuclear safety and on the thermo hydraulic issues.

8 References

[R1] The Jules Horowitz Reactor: a new high performances Europeans MTR with modern experimental capacities : toward an international centre of excellence, RRFM 2012, Bignan G., Bravo X., Lemoine P.-M., CEA, France

[R2] The Jules Horowitz Reactor MOLY system. Towards a concept proposal according a large Molybdenum production capabilities, IGORR, September 19-24, 2010 Knoxville TN USA. S. Gaillot et Al, CEA, France

Burn up calculations and validation by gamma scanning of a TRIGA HEU fuel

R. KHAN, S. KARIMZADEH, H. BÖCK, M. VILLA, T. Stummer

*Vienna University of Technology
Atominstitut
Stadionalle 2, 1020-Vienna, Austria*

ABSTRACT

The TRIGA Mark II research reactor operated by Atominstitut is one of the few TRIGA reactors which still utilizes several High Enrich Uranium (HEU) Zirconium-Hydride (U-ZrH) fuel elements. Its current core is a completely mixed core with three different types of fuel elements including one HEU type with 70% enrichment and a stainless steel cladding. The present paper calculates the burn up of the FLIP (Fuel Lifetime Improvement Program) fuel using the burn up code ORIGEN2 and validates the theoretical results by high resolution gamma spectrometry using a unique fuel scanning device (FSD) developed at the Atominstitut especially for TRIGA fuel. For this purpose a FLIP fuel element was removed from the reactor core and stored in the reactor tank for an optimal cooling period. The fuel element was then transferred into the fuel scanning device to determine the Cesium-137 isotope distribution along the axis of the fuel element. The comparison between theoretical predictions and experimental results is the highlight of the present paper.

1. Introduction

The 250 kW TRIGA Mark II research reactor at the Atominstitut (ATI) is the only operating nuclear facility of Austria. In this reactor the fuel elements FE(s) are arranged into six concentric circular rings denominated A to F resulting in a cylindrical core. This core is surrounded by an Aluminum encased annular graphite reflector. Penetrating through the graphite reflector to the core are four beam tubes, one thermal column and a neutron-radiography collimator to allow various neutron beam experiments as shown in Figure 1. The whole core structure is submerged into a tank with about 20 m³ of light water. The current operating core is loaded with 83 FE(s) with three different specifications. One of these three types are the FLIP (= Fuel Lifetime Improvement Program, type 110) fuel elements, presently there are eight FLIP FE(s) in the current core. The objective of this paper is to compare the burn up calculations and its experimental confirmation of one selected FLIP FE. The FLIP fuel contains 70% enriched U and is clad with standard SS (FE type 104). Further it also contains 1.6 w/o erbium homogeneously mixed inside the fuel as burnable poison alloyed with 91 wt-% zirconium. Erbium-167 has a large absorption cross section near 0.5 eV. When the fuel temperature increases, the thermal neutron spectrum is hardened and an important fraction of the thermal neutron population is shifted into the region of the erbium absorption resonance. The presence of erbium thus augments the negative temperature coefficient [1]. The geometrical dimensions and material composition of the TRIGA HEU fuel is listed in the Table 1.

Due to proliferation risks associated with HEU fuel, the Vienna University of Technology has planned to return its HEU fuel back to US under the US DOE Spent Fuel Return Program. For this purpose detailed studies of the spent fuel is necessary including fuel burn up and shielding procedures which is presented in this paper. The paper describes the burn up calculation using the burn up code ORIGEN2 and its experimental validation through a gamma spectroscopic experiment.

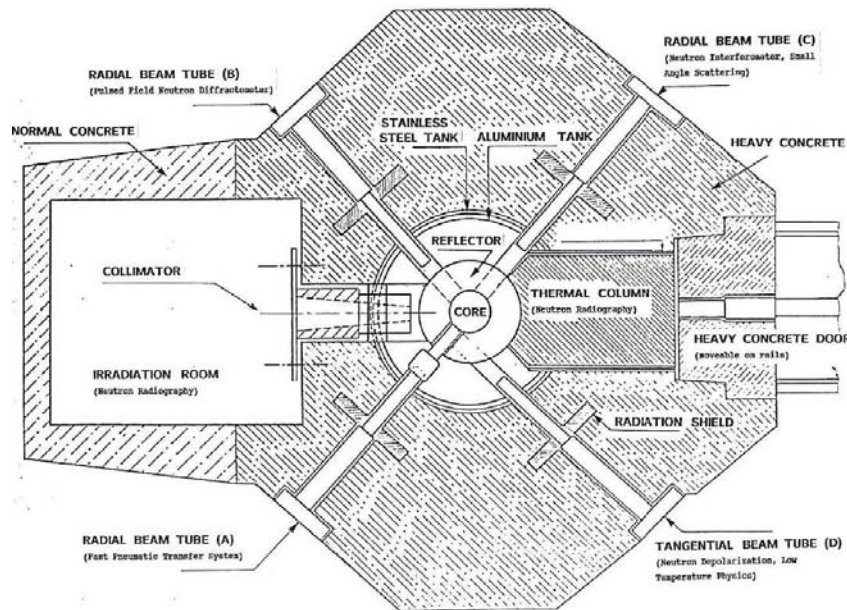


Fig. 1 Top view of the TRIGA Mark II research reactor at ATI

Fuel element type	FLIP fuel
Fuel moderator material	U-ZrH1,65
Uranium content (wt. %)	8.5
Enrichment (%)	70
Erbium content (%)	1.6
Average ^{235}U content (g)	136
Diameter x length of fuel meat (cm)	3.63 x 38.1
Graphite reflector length (cm)	8.81
Cladding material	304 SS
Cladding thickness (mm)	0.51

Table 1: Geometrical & material specifications of the FLIP FE

The burn up is a measure of the total amount of thermal energy generated per unit quantity of heavy element (U) loaded into the core. The burn-up is expressed in units of MWd / (kg U) [2]. This work calculates an average burn up and isotopic composition of the irradiated FLIP FE employing the ORIGEN2 reactor physics code. These theoretical results are confirmed experimentally through a gamma spectroscopic experiment using an improved TRIGA fuel scanning device. Applying the theoretical and experimental results, the axial burn up distribution is evaluated in this work.

To perform the FLIP fuel scanning experiment, one FE (ID no. 7302) was removed from the core on 7.1.2010 and stored into the in pool storage rack for an extended cooling time. The axial fuel surface dose rate was used to measure every month to determine the optimal possible dose rate for the fuel scanning experiment. This experiment was delayed as the electronic part of the fuel scanning device was modified. Finally the FE was measured on 10.6.2011 for its axial Caesium distribution. The irradiation history of the FE no. 7302 is given in Table 2.

FE ID no.	Action	Date	Position
7302	Loaded to core	07.10.1974	B03
	Remove from core	28.01.1985	In pool fuel storage
	Charged into core	03.08.1988	F07
	Reshuffle	27.07.2001	F21
	Removed from core	07.01.2010	In pool fuel storage

Tab 2: Irradiation history of the FLIP FE ID no. 7302

For burn up calculation, the energy production (MWd) was extracted from the log books [3]. Using these MWds, the full Power Days (FPD) for B03, F07 and F21 positions were determined. These burn-up days (FPD) were used to calculate the power of FE 7302. Using the Full Operating Length (FOL) in days and power at FPD, the power at FOL is determined and given in the Table 3. The full length power at FOL is applied to ORIGEN2 to calculate the burn up and material composition of irradiated FLIP FE 7302.

From	To	FOL (days)	FE Position	Burn up (MWD)	FPD (Days)	MW at FPD	MW at FOL
07.10.1974	27.01.1985	3767	B03	104.02	416.11	0.003136	0.000347
03.03.1988	26.07.2001	4766	F07	151.80	607.21	0.001689	0.000542
27.07.2001	07.01.2010	3117	F21	94.79	379.14	0.001528	0.000534
08.01.2010	June 2011	0	Out	0	0	0	0

Tab 3: Irradiation history calculations from log book for FLIP FE 7302

2. Burn up Calculations

The ORNL isotope generation and decay simulating burn up code ORIGEN2 was selected for the burn up, the isotopic composition and the activity calculations of the TRIGA spent FLIP FE [4]. The standard ORIGEN2 package does not include TRIGA specific libraries. Therefore in this work, the FLIP TRIGA fuel element has been modelled using the available PWR cross-section and fission product yield libraries.

2.1 ORIGEN2 Model

This code was selected because it can simulate the build-up and decay of nuclides during irradiation. ORIGEN2 uses a matrix exponential method to solve a large system of coupled-, linear-, first-order ordinary differential equations with constant coefficients [5]. Based upon full operation length, the overall irradiation history of the FLIP FE was divided into equal steps. The step length was set to 300 days and a weighted average power was applied to all irradiation steps. The irradiation power history of this FE is shown in Table 3.

An ORIGEN2 model for the selected FLIP FE was developed to calculate the average burn up and its relevant material isotopic composition. The ORIGEN model requires: 1) material inventory, 2) library selection and 3) fuel irradiation history. The material inventory of the FLIP FE was taken from the fuel shipment documents [6]. As ORIGEN2 is not equipped with a TRIGA reactor library the PWR library was found appropriate for TRIGA type reactors and was applied to this ORIGEN2 model. The fuel irradiation part of the model is of key importance because it plays an important role in the accuracy of the model, the fuel history was carefully extracted from the reactor operation log books [3].

3. Gamma Spectroscopic experiments

The gamma spectroscopic measurement of the FLIP fuel was performed in the ATI reactor hall. An adequate shielding was provided to the system by the fuel transfer cask. About 2 to 3 μSv dose rates were measured at the cask surface and the working station. The experimental setup consists of the fuel transfer cask, the fuel inspection unit, a beam collimator and a High Purity Germanium (HPGe) detector which is shown in the Figure 2.

The FLIP FE to be measured was transferred in the reactor pool into the transfer cask to provide sufficient shielding to the fuel transfer process. Then, the fuel transfer cask was raised out of the reactor tank and transferred to the fuel scanning device located at the reactor hall floor. This fuel transfer cask was then positioned on top of the fuel scanning device where the fuel can be moved vertically with an adjustable speed. The upgraded fuel scanning device is controlled by a computer program; the fuel can be moved in equal vertical steps of one centimetre by adjusting the spectrum recording time, an optimal recording time of 300 seconds was determined [7].

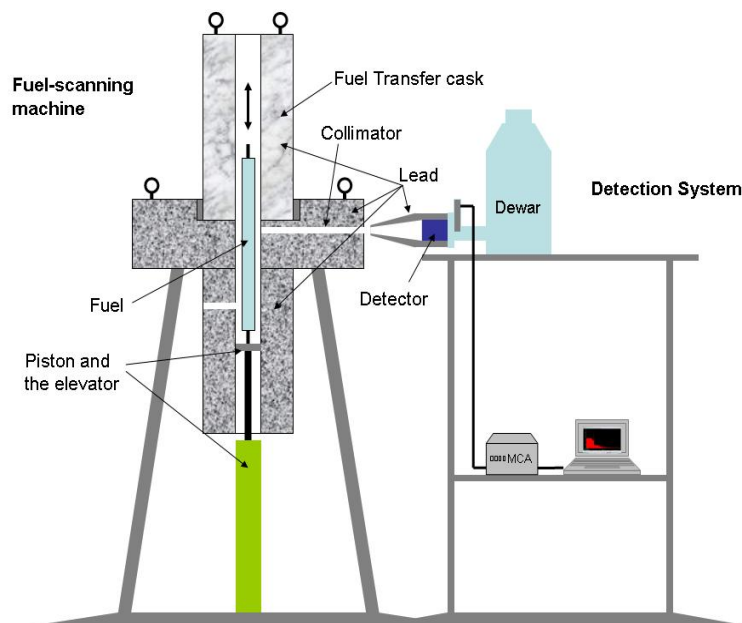


Fig 2: The experimental set up developed at Atominstitut [7]

4. Results and Discussions

There is no direct experimental technique to determine the burn up of an intact irradiated fuel element, the different fission products are used as burn up indicators. This paper determines the burn up of the spent FLIP fuel through the measurement of Caesium-137. The irradiation length described in Table 2 and 3 results in 2.8706 MWd burn up which corresponds theoretically to $2.377\text{e}11$ Bq (6.423 Ci) of Cs-137. The gamma scanning experiment measures the Cs-137 activity as $2.779\text{E}11$ Bq (7.51 Ci), which is 14.5% more than the calculated value. One possible reason for this difference is the PWR cross section used actually for TRIGA fuel. The other possibility could be due to some error in the long irradiation history. Figure 3 presents the axial distribution of Cs-137 along the length of the measured HEU FLIP FE. The axial Cs-137 profile (i.e. maximum in the centre and decreases along the length) follows the axial flux distribution. The two peaks at the upper and lower end of the FE shows the effect of two axial graphite reflectors at both ends of the fuel meat (see Figure 3).

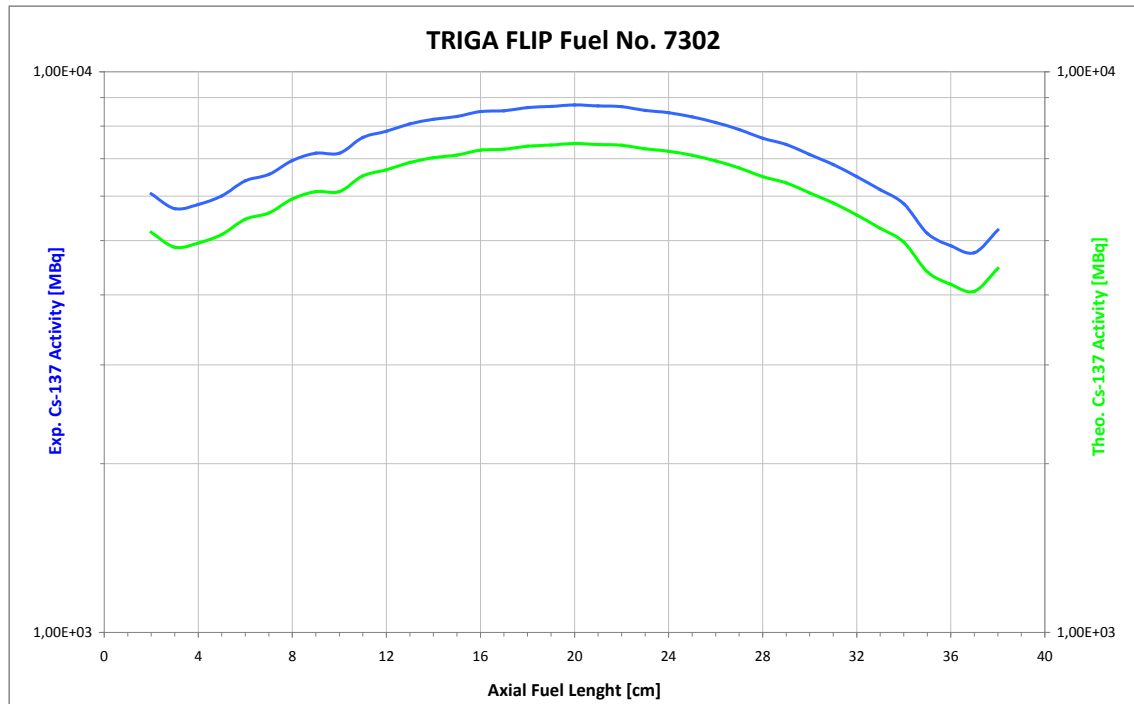


Fig 3: The comparison of the experimental Cs-137 with the ORIGEN2

5. References

1. S. T. Keller: "Modelling the Oregon State University TRIGA Reactor Using the Attila Three-Dimensional Deterministic Transport Code", Master Thesis, Oregon State University, 2007.
2. Matsson and B. Grapengiesse: "Developments in Gamma Scanning of Irradiated Nuclear Fuel", Applied Radiation and Isotopes, Vol 48, Issues 10-12, Oct-Dec 1997.
3. Reactor Operation Log books of the TRIGA Mark II: "Atominsitut, Vienna University of Technology, 1962-2009.
4. A. Persic, M. Ravnik, S. Slavic, T. Zager: "TRIGLAV A Program Package for Research Reactor Calculations", IJS-DP 7862, ver. 1, March 2000.
5. S. Ludwig: "Revision to ORIGEN2 – Version 2.2", Oak Ridge National Laboratory, May 23, 2002.
6. General Atomics: "Shipment documents from General Atomics", GA-USA, 1962-1988.
7. S. Karimzadeh et al.: "Gamma Spectrometry Inspection of TRIGA MARK II Fuel Using Caesium Isotopes", Nuclear Engineering and Design, Volume 241, Issue 1, January 2011, Pages 118-123.

POSSIBILITY OF A REPRESENTATIVE SFR FUEL PIN IRRADIATION AT THE JHR

T. STUMMER

*Institute of Atomic and Subatomic Physics, Vienna University of Technology
Stadionallee 2, 1020 Wien - Austria*

M. Blanc

*CEA, DER, CPA
Cadarache, F-13108 Saint-Paul-lez-Durance - France*

B. Pouchin

*CEA, DEN, SRJH
Cadarache, F-13108 Saint-Paul-lez-Durance - France*

ABSTRACT

While the main workload of JHR program will be the ongoing support of the current reactor fleet, its high flux and hard neutron spectrum core design were chosen to allow for experimental programs for the development of GEN IV type reactors. The near term goal for the reactor start up is the support of the ASTRID program and one of the options under investigation is a close to representative SFR fuel pin irradiation experiment in the JHR core. This requires the use of strong neutron screens inside the core, which is costly in terms of reactor reactivity, roughly equivalent to a fully inserted control rod, under very tight space constraints. The study is based on the already developed CALIPSO device and investigates the effect of different incorporated screen materials on radial flux distribution and the linear heat rate. Among the results one is that the commonly used screen materials Cd and Hf are unlikely to be useable because of too low melting temperature or too low shielding efficiency. The investigated replacement candidates are Gd, Eu_2O_3 , Dy and B_4C . Additionally there are strong incentives to place the experiment as far as possible in the periphery of the core although this would make the enrichment of the U in the sample necessary.

Introduction

Neutron physics calculations were done last year at the Jules Horowitz Reactor [2] to highlight options and limits for experiments supporting fast reactor research programs with JHR. One of the options and the topic of this paper is a close to representative SFR fuel pin irradiation in the JHR core. This requires the use of strong neutron screens inside the core, which is costly in terms of reactor reactivity, roughly equivalent to a fully inserted control rod, under very tight space constraints. Preliminary work presented last year [6] indicated that the originally preferred shielding materials, Cd and Hf, are not suitable because of either too low melting temperature or too low shielding efficiency. In this paper the effects of the replacement candidates, Gd, Eu_2O_3 , Dy and B_4C , on the radial flux distribution and the linear heat rate at beginning of irradiation are given for a sample SFR fuel pin. The reactivity cost of such an experiment depending on the position in core is presented as well together with the resulting change of linear power in the sample.

Concept and Geometry

According to the current JHR core design (fig 1), there will be seven fuel elements with a central irradiation channel with a usable diameter of 3.3 cm and three irradiation positions with a diameter of 9.6 cm, which replace a fuel element in the core. For this study a pre-existing device, CALIPSO [4], intended for material irradiations inside a fuel element was adapted with various neutron screens to give an estimate for the resulting neutron spectrum and the reactivity costs on reactor operation. CALIPSO has a NaK cooling loop for high temperature / high power experiments and provides room for a single sample fuel pellet with a diameter of 9.5 mm and about 4 mm screen thickness with an outer device diameter (in core) of 33.1 mm. In the here considered model both the shield and the fuel pin sample cover the full active core height of 60 cm. For the calculations four positions were chosen: two near the centre of the core (101 and 103), one in the outer fuel element ring (313) and one in the reflector close to the core (C313) as a low reactivity cost fall back option. The position 103 was included in case the available space in the centre of a fuel element would prove insufficient for the needed shield thickness and cooling.

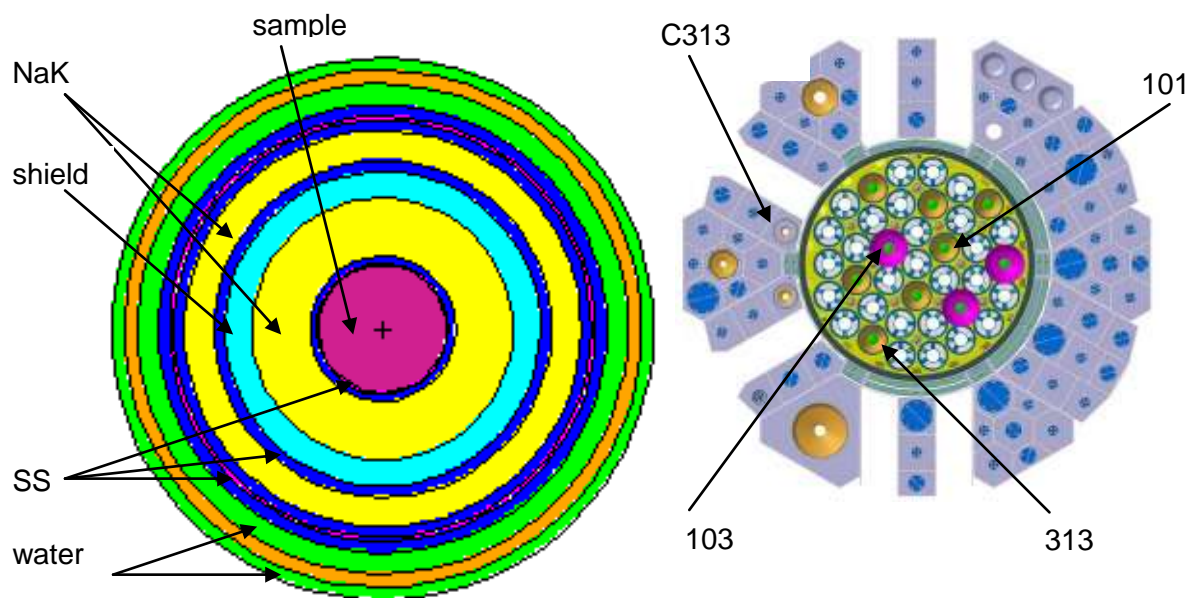


Fig 1: Assumed irradiation positions and device cross section

Methodology

All the JHR calculations were done with TRIPOLI-4 [3] based on the standard CEA JHR core model with the JEF2.2 neutron library wherever possible. The cross sections for isotopes not or incorrectly included in JEF2.2 were taken from ENDF6.4 and several full core simulations with JEFF3.1.1 were run to insure there were no large differences (<3%). In order to get an acceptable statistical accuracy, both the radial fission power distribution and the maximum linear fission power of the sample are averaged over a 20 cm long part in the centre of the core. All other results are averaged over the full 60 cm height. To get the maximum values in the centre of the core the form factor of the axial neutron flux (1.25) can be used on the total average. The reactivity effects, overall flux distribution and fission rate in the sample were calculated with the full core model for all cases. Besides variations of the shield material and thickness, several cases with enriched U were calculated to improve the results for placement in the periphery of the core. As shielding material, the focus was on Eu_2O_3 as it was already used in a similar case at ORNL [5] and the originally preferred Hf and Cd turned out to be unsuitable. Additional examples with Gd, Dy and B_4C are also presented. As a

reference sample serves a 9.43 mm thick (UPu)O_{1.97} rod with a effective density of 10.5 g/cm³ and the following isotopic composition (17.4% PuAm +depleted U):

	238Pu	239Pu	240Pu	241Pu	242Pu	241Am	235U	238U
at%	0.62	8.25	5.16	1.43	1.81	0.14	0.21	82.39

Tab 1: sample actinide composition

The basis for SFR reference case was calculated by V. Brun-Magaud and L Buiron [1] with ERANOS. The average total core flux is given as 2.5×10^{15} n/s/cm² and the spectrum is shown in fig 2. The gamma heating values provided are TRIPOLI results corrected for lacking cross sections according to a previous study of gamma heating in JHR experimental devices [7], but they still carry a 2 sigma uncertainty of 15%.

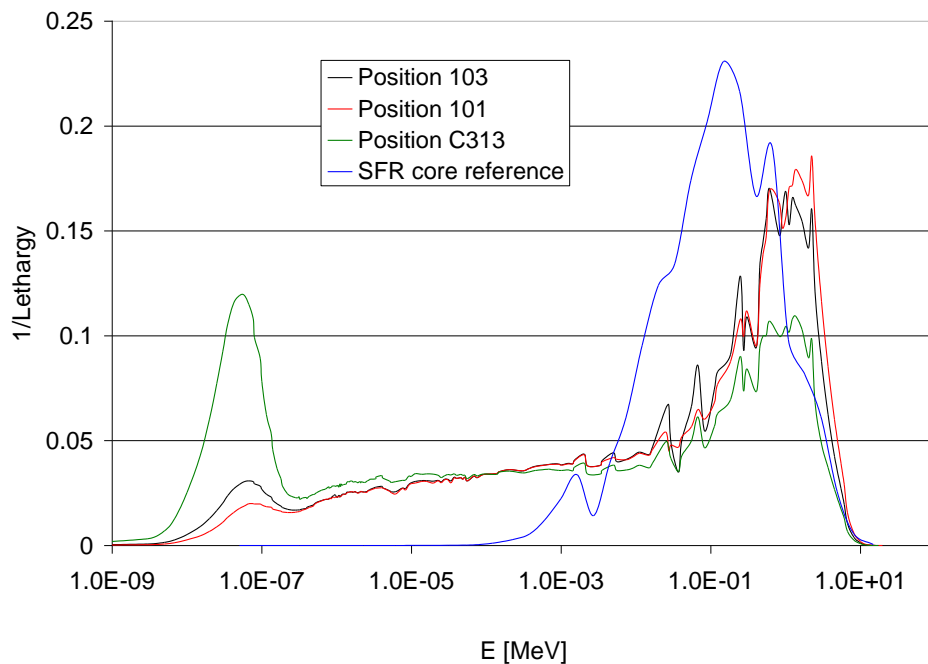


Fig 2: unshielded neutron spectra at the experimental positions

Results

As seen in figure 2 above the fuel element (27% enriched U₃Si₂) in position 101 acts as thermal neutron shield for the device, increases the fast flux and reduces the reactivity cost for the reactor (table 2). This combined with the fact that 7 in-fuel element positions are available versus 3 fuel element replacements, such a setup would be preferable if the experiment is to be placed inside the core.

One of the key problems of utilizing MTRs for FR fuel research is generating a similar radial power profile in the fuel sample while keeping the fission rate comparable due to the strong self shielding effects in the thermal and low epithermal neutron energy ranges and the usually lower overall neutron flux in MTRs. Figure 3 on the next page compares the relative radial fission power in the central 20 cm of the sample for various screen materials at 3 mm thickness in position 101 to give a first impression of their suitability from the neutronic point of view. The device allows adding another mm of screen to either flatten the profile further or to increase the reactor life time of the screen. Interestingly the Europia and natural boron carbide shielded cases give a flatter fission power distribution than the SFR reference spectrum but the other materials could be suitable as well.

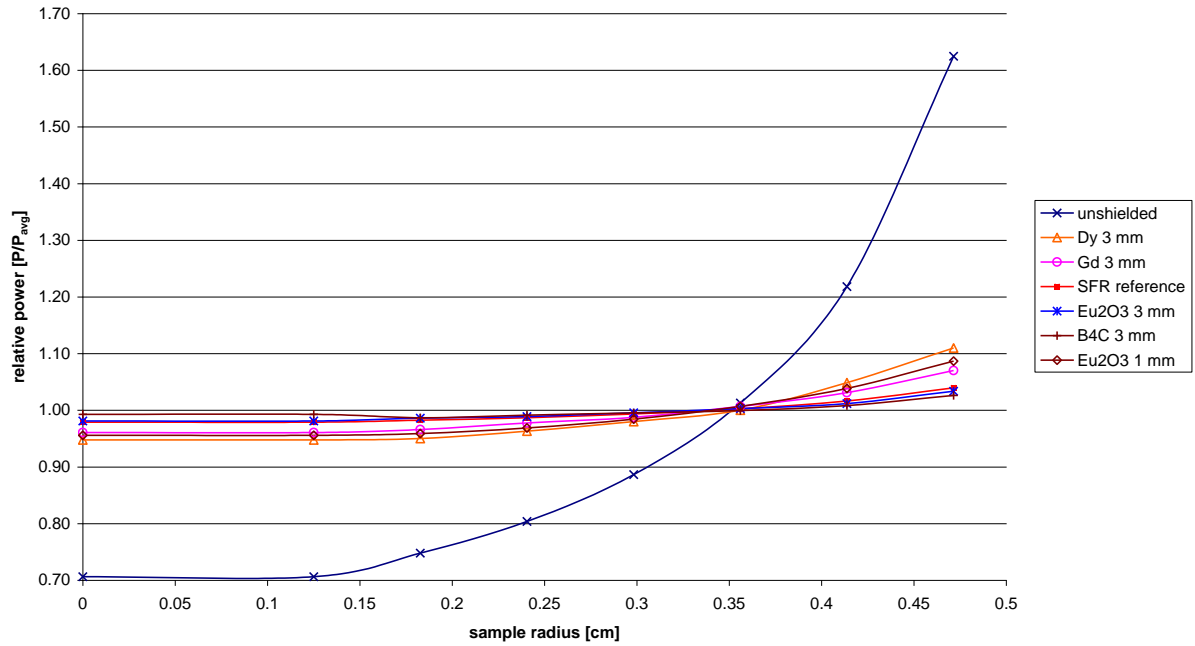


Fig 3: radial power distribution in sample depending on shield material.

Position	101	103	313	C313
Δ reactivity [pcm]	-1020	-1020	-380	-70
reduced cycle length [%]	18-27	18-27	7-10	<2
avg. lin. fission heating [W/cm]	261	240	159	45
avg. lin. gamma heating [W/cm]	128	122	80	32
fast/thermal ratio	358	211	324	71
total neutron flux [n/s/cm ²] inside shield	6.44E+14	5.66E+14	3.95E+14	9.94E+13

Table 2: Reactivity cost of a full core height 3 mm Eu₂O₃ shield depending on position.

In table 2 above the effect of the experiment placement on the core and the linear power in the sample is shown for a 3 mm Europa screened device. To put the above values in context: depending on the power of operation (70 or 100 MW) the reactivity necessary for one day of operation is between 150 and 220 pcm with 25-26 days between scheduled refueling. The lost reactivity has to be made up by either increasing the core moderation or in extreme cases inserting additional fuel elements. Generally speaking a position at the periphery of the core would reduce the effect of the experiment on the core (but increase it on nearby reflector positions) but would reduce the available neutron flux and with it the available fission heating. While this can be countered somewhat by enriching the U in the sample, it is limited to about a factor 2 for 20% enrichment without additionally sacrificing the neutron screen/radial power distribution. Still with the axial neutron flux form factor of 1.25 and gamma heating, 400 W/cm peak linear power should be in reach for all in-core positions with a 3 mm Eu₂O₃ screen or equivalent if U enrichment is used.

Conclusions

Overall approximating a SFR like radial fission and peak power distribution in a single fuel rod experiment is possible in the JHR core but only at considerable reactivity and hence economic costs. To minimize the costs the experimental device should be placed as far as possible in the periphery of the core and enriching the uranium in the sample to reach adequate fission rates should be considered.

From a purely neutron shield strength point of view all discussed materials, Gd, Eu_2O_3 , Dy and B_4C , would be sufficient. The final selection of the material can therefore be based solely on engineering concerns. At current point of development the favorites are Eu_2O_3 or B_4C . The problems with the first are the lack of experience with it in France and radioprotection concerns due its high energy gamma productions combined with isotope half-lives of 10-15 years. For the later the concerns are the high He production and the effects of depletion during the up to 400 efpd duration of the experiment.

For a follow up study, which should incorporate depletion calculations for both the neutron shields and the sample, further definition of the problem by the fuel developers would be necessary, especially in regards to the maximally acceptable divergence between the SFR and the JHR cases for the radial and linear power distribution at both start-up and during the time evolution.

References

1. L. Buiron et al., "Minor actinides transmutation in SFR depleted uranium radial blanket, neutronic and thermal hydraulic evaluation", *Proceedings GLOBAL 2007*, Boise, Idaho USA, September 9-13 2007.
2. G. Bignan et al., "The Jules Horowitz Reactor: A new European MTR (Material Testing Reactor) open to International collaboration: Description and Status", *Proceedings RRFM 2011*, Rome, Italy, March 20-24 2011.
3. O. Petit et al., "TRIPOLI-4 User's Guide", ISSN 0429-3460, January 2008.
4. D. Moulin et al., "Thermal assessment of the CALIPSO irradiation device for the Jules Horowitz reactor", *Proceedings IGORR 2010*, Knoxville, TN, USA, September 19-23 2010.
5. R. J. Ellis et al., "Analysis of a fast spectrum irradiation facility in the high flux isotope reactor", *PHYSOR 2008*, Interlaken, Switzerland, September 14-19 2008.
6. T. Stummer et al., "APPROXIMATION OF FAST REACTOR SPECTRA AT THE JHR", *Proceedings RRFM 2011*, Rome, Italy, March 20-24 2011.
7. D. Blanchet, "Développements méthodologiques et qualification de schémas de calcul pour la modélisation des échauffements photoniques dans les dispositifs expérimentaux du futur réacteur d'irradiation technologiques Jules Horowitz (RJH)" Thèse Université Blaise Pascal, June 2006.

SIMULATION OF THE TIME-EVOLUTION OF OXIDE LAYERS SURROUNDING CLADDING-MEAT CONTACT FAULTS (NON-BONDS) AND THEIR THERMAL-HYDRAULIC IMPLICATIONS

H. BREITKREUTZ, W. PETRY

*Forschungs-Neutronenquelle Heinz Maier-Leibnitz (FRM II), Technische Universität München
Lichtenbergstr. 1, 85747 Garching bei München – Germany*

ABSTRACT

Contact faults between cladding and meat, so-called non-bonds, may have noticeable consequences on the thermal-hydraulic behaviour of fuel plates as they form a strong barrier for the heat flux from the fuel into the cladding and therefore deflect the heat to the opposite side. Furthermore, due to the resulting increased heat fluxes in some parts of the plate, the presence of such faults may lead to a drastic growth of the oxide layer, finally leading to oxide flaking.

The time evolution of the oxide layer and the resulting impact on the thermal hydraulics of such a break-up are simulated for different fault sizes and meat materials using a CFD code. The effects have been calculated for small demonstration samples. It is shown that there is a notable dependence of the resulting (surface) temperatures and heat fluxes as well on the irradiation time as on the thermal conductivity of the fuel. Fuels with low thermal conductivities, e.g. monolithic UMo, generally perform worse than fuels with high thermal conductivity, especially regarding fuel temperatures. However, the oxide layer build-up and effects caused by this generally expose smaller differences between the different fuels than what is expected if no oxide layer is present.

1. Introduction

Contact faults between cladding and fuel, so-called "non-bonds" (Fig 1), occur during the production process of fuel plates. These contact faults represent a strong barrier for the heat flux from the meat into the cladding, therefore their number and size is generally limited by the production quality criterions for the plates. Nevertheless, such non-bonds occur regularly. Starting from a certain size, the "minimum relevant fault size" (MRFS), non-bonds notably change the thermal-hydraulic behaviour of fuel plates [1], that is the cladding surface heat flux and the temperature on the cladding as well as in the meat. Therefore, non-bonds have been subject to large calculational [2,3] and experimental [4,5] efforts since long time. In a broader frame-work, the tensile tests and interface characterisations currently conducted by a number of working groups [6,7,8,9] also contribute to the understanding of the evolution and growth of non-bonds by determining the bond-strength between cladding and meat.

In this paper, we will discuss the time-evolution of oxide layers as simulated with a modern CFD code, ANSYS CFX 13 [10]. The only free parameter in these simulations is the material of the fuel zone, more precisely its thermal conductivity. All other parameters remain fixed, i.e. we will act on the assumption of a static contact fault which does not change in size and which forms a perfect barrier for the heat flux all over its extent. Of course, the latter is a very conservative restriction and might in the future be replaced by a more realistic assumption like heat conduction through a gas-filled hole. Fig 1 shows a sketch of a fuel plate with a contact fault and the expected effects for the heat flux and the surface temperatures: On the side of the non-bond ("fault side"), temperatures will be lower than expected due to the reduced

heat flux, while on the side opposed to the fault ("good side"), increased heat fluxes and higher temperatures are expected.

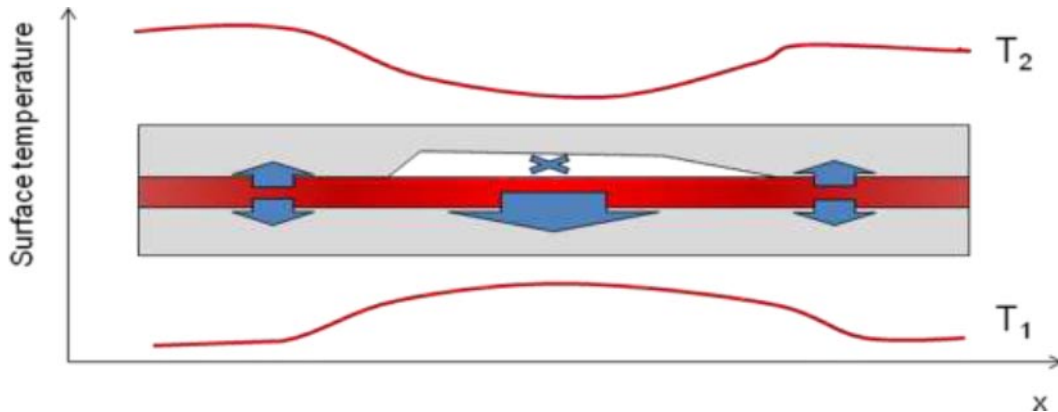


Fig 1: Sketch of surface temperatures (red lines) and heat fluxes (blue arrows) due to a contact fault between cladding (grey) and fuel (red)

All analysed contact faults are located somewhere inside the active zone, i.e. not close to the unheated frame surrounding the fuel in the plate. It was shown before, that such contact faults are worse than those close to the frame [1]. No defects smaller than $0.5 \times 0.5 \text{ mm}^2$ are analysed in this work as this is already below the MRFS for cladding related effects (see Fig 2).

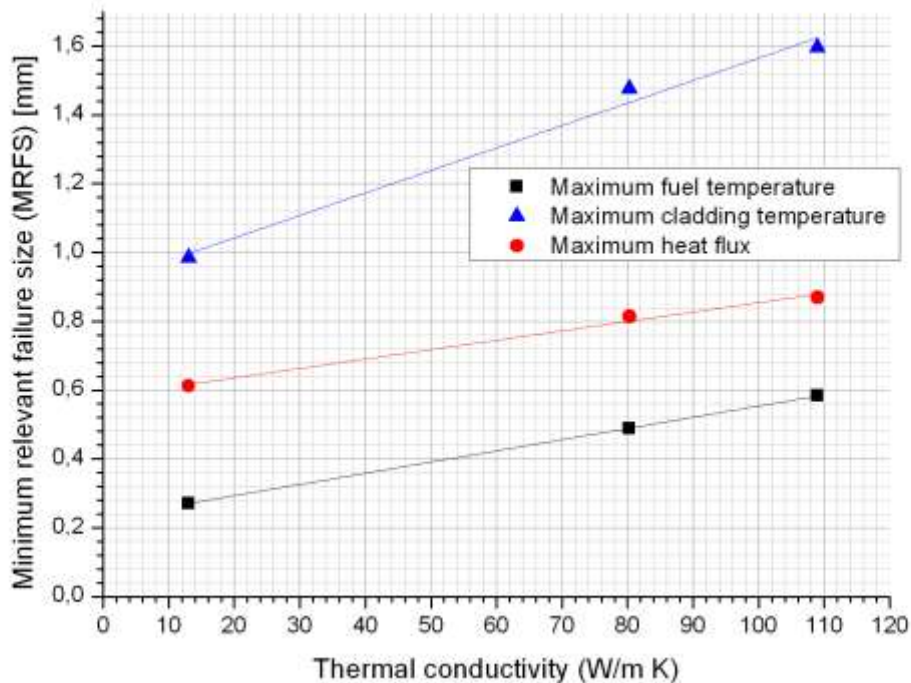


Fig 2: Minimum relevant fault size (MRFS) as calculated in [1] for normal faults: Starting from this size, non-bonds notably change the thermal-hydraulic behaviour of the fuel plate. The MRFS depends on the regarded quantity, i.e. the maximum fuel temperature, the maximum cladding surface temperature or the maximum heat flux. Generally, the MRFS increases with the thermal conductivity. Regarding an analysis of the influence of contact faults on the thermal hydraulic behaviour, the lowest relevant of the three shown MRFS has to be taken into account.

2. Methodology

The following boundary conditions were applied for all calculations:

- Plate: 2 × 380µm Al 6061-Cladding, 600µm meat
- Coolant: H₂O, 15.9m/s, 2.2mm channel width, 310K (37°C / 99°F), 2.7% turbulence, fully developed turbulent flow, pH 6, 2.3 bar pressure at the outlet
- Oxide layer: Boehmite, 2.25 W/(m·K) (1.3 btu/(h·ft²·°F/ft) [2,11])
- Undisturbed heat flux (2 cases):
 - 350 W/cm² (equivalent 3.6 × 10¹⁴ fissions/(cm³·s) for this geometry, 1.9 × 10²¹ fissions/cm³ after 60 days)
 - 450 W/cm² (equivalent 4.7 × 10¹⁴ fissions/(cm³·s) for this geometry, 2.4 × 10²¹ fissions/cm³ after 60 days)

Three different fuels will be analysed: U₃Si₂ dispersed in Aluminium with an uranium density of 3.0g/cm³, U8Mo dispersed in Aluminium with an uranium density of 8.0g/cm³, and monolithic U8Mo. The relevant properties of these fuels are given in table 1. Temperature dependencies are taken into account as far as they are known [12,13].

Fuel material	Thermal cond.	Density U <=> Total
U ₃ Si ₂ disperse	109 W/(m·K)	3.0g U/cm ³ <=> 5.2 g/cm ³
U8Mo disperse	82.1 W/(m·K)	8.0g U/cm ³ <=> 10.0 g/cm ³
U8Mo monolithic	13.0 W/(m·K)	15.9g U/cm ³ <=> 17.3 g/cm ³

Tab 1: Used thermal-hydraulic properties (at BOL if not quoted otherwise)

No temperature feedback or burn-up effect on the fission rate is respected, i.e. the fission rate in the meat is assumed to be constant over the whole time, so that the expected heat flux is constant, too.

2.1. Oxide thickness calculation

The time- and surface temperature dependent thickness of the oxide layer is calculated by the iterative formalism presented in [2] (see also [4,5]):

$$d_{\text{Oxide}}(t_{\text{irr},k}, T_{\text{surf},k}) = 11.25 \cdot 10^{-3} \cdot (\psi_{k-1} + t_{\text{irr},k})^{0.778} \exp\left[-\frac{4606}{T_{\text{surf},k}}\right] \quad (1)$$

$$\psi_{k-1} = (\psi_{k-2} + t_{\text{irr},k-1}) \cdot \exp\left[5920 \cdot \frac{T_{\text{surf},k-1} - T_{\text{surf},k}}{T_{\text{surf},k-1} \cdot T_{\text{surf},k}}\right] \quad (2)$$

In this formula, the irradiation time $t_{\text{irr},k}$ for timestep k has to be entered in hours, the surface temperature $T_{\text{surf},k}$ in Kelvin and the resulting thickness d_{Oxide} is given in meters. Due to the assumed coolant pH of 6, this value has to be multiplied by 2.7 afterwards as the original formula is tailored for a pH of 4.7 to 5.0 and a more alkaline environment panders to the growth of an oxide layer. All unknown values in the first iteration steps, i.e. those with negative indices k , are 0. The formalism is valid for heat fluxes between 315 and 630 W/cm² and is accurate to about 25%.

Measurements will be necessary to ensure that the presented formalism is applicable to the calculations presented here in all aspects.

2.2. General implementation

The calculations were achieved by using a set of Perl scripts, which remotely control CFX and perform the data analysis. Every timestep can be subdivided in five general steps:

1. Start CFX, calculate steady state solution
2. Export heat fluxes and temperatures from CFX
3. Analyse results from (2), process data
4. Calculate oxide thickness based on (2) and length of timestep
5. Update CFX model with new oxide thickness
6. Next timestep (\Rightarrow 1)

Steps 1 and 2 are handled completely by CFX, everything else (including the execution of stages 1 and 2) is handled by the Perl scripts.

Care has to be taken about the selected time stepping to avoid oscillations in the solution for surface heat fluxes and temperatures that seem to have a straightforward physical explanation but in fact are nothing more than numerical artefacts caused by the usage of the explicit Euler method: If the change of the oxide layer in one timestep is too large, this will lead to a heat flux that is flowing around this thermal resistance in the next step, causing disproportionately higher temperatures in the area surrounding the thick oxide spot. In turn, in the next timestep, this will lead to an even stronger growth of the oxide layer in those surrounding regions, pushing the heat flux back to the spot with the originally thick oxide (which is now thinner than in the neighbourhood). This way, an oscillation of the solution is produced, which will finally lead to unrealistically high heat fluxes, but could still be physically explained. A timestepping of about four days after a finer resolution for the first ten to twenty days where the growth is more rapid yielded reasonable results.

2.3. CFX implementation

The contact faults were modelled using thin interfaces in CFX 13. They were implemented as a very thin layer with varying thermal conductivity, which was assumed to be infinite where thermal contact was established and zero at the location of the fault.

The oxide layer was modelled using thin interfaces, too. This means that the oxide layer was not resolved by the mesh but only included by means of a thermal resistance at the fluid-solid-interface. This also means that no matter how large the oxide layer grows, plate deformation and cladding-material consumption are not taken into account, i.e. the cladding thickness of the original Al 6061 stays constant. This is a reasonable assumption as long as $d_{\text{Oxide}} \ll d_{\text{Cladding}}$ and as long as the heat conduction in the oxide layer can be treated in 1D. As the oxide layer normally starts to flake off from the fuel plate surface at thicknesses of 50 - 75 μm at the latest [2], this thickness $d_{\text{Oxide,critical}}$ can be regarded as a cut-off criterion for calculations.

Furthermore, as $d_{\text{Oxide}} \ll d_{\text{Cladding}}$, we consider our assumption to be valid within a certain range of uncertainty, especially regarding the fact that the calculated oxide thickness suffers from the before-mentioned 25% uncertainty anyway.

According to [2], the expected aluminium metal consumption would be approximately 80% of the oxide thickness, so we must hold $d_{\text{Oxidecritical}} \ll 1.254 \cdot d_{\text{Cladding}}$, which equates to a worst case ratio

$$\frac{d_{\text{Oxidecritical}}}{1.254 \cdot d_{\text{cladding}}} = 0.15.$$

That is well smaller than unity and small enough for the purpose of the calculations presented here.

CFX 13 currently does not allow to specify varying thicknesses for thin interfaces, therefore the thermal conductivity κ_0 of the Boehmite was varied accordingly: From Fouriers law in 1D follows for the temperature difference due to the oxide layer

$$\Delta T = -q \left(\frac{d_{\text{Oxide}}}{\kappa} \right). \quad (3)$$

As the thickness of the interface $d_{\text{Oxide}} = d_0$ is fixed due to the requirements of CFX, a new thermal conductivity κ' was introduced and used in the above formula, which is calculated by

$$\kappa' := \kappa_0 \frac{d_0}{d_{\text{Oxide,real}}}. \quad (4)$$

The reference thickness d_0 was set to $1\mu\text{m}$ but is in fact arbitrary as it cancels out if (4) is inserted in (3) with $\kappa = \kappa'$ and $d_{\text{Oxide}} = d_0$.

3. Results

Two different expected heat fluxes, 350 W/cm^2 and 450 W/cm^2 were regarded. In the following plots, all temperatures, heat fluxes and oxide thicknesses marked with "distance from centre" are recorded along the white line shown in Fig 3, from the centre of the fault perpendicular to plate surface and flow direction.

It is easily understandable that the oxide layer will build up fastest on the cladding side opposed to the non-bond ("good side"), as it suffers from high heat fluxes and therefore rather high temperatures. In the following, this thicker oxide layer will act as an obstacle for the heat flux, forcing the heat to flow to areas with thinner oxide layer. Therefore, with the build-up of the oxide layer, the situation eases regarding heat flux and surface temperature. Accordingly, the situation regarding those two quantities is worst at BOC (begin of cycle).

On the other side, the oxide layer will finally lead to higher temperatures in the fuel itself. Naturally, the oxide layer will grow to its final thickness at EOC (end of cycle). Depending on the thickness, the probability for flaking will grow the highest at EOC.

3.1. Exemplary time evolution for monolithic U8Mo, 450 W/cm²

First, one special case, monolithic U8Mo with a desired heat flux density of 450 W/cm² is regarded to explain the time evolution of oxide layers, heat fluxes and temperatures in general. In addition, this is the worst case that is analysed in this work and therefore deserves special attention. Fig. 4 shows how the oxide layer will develop during the irradiation time, recorded along the white line in fig. 3, for a rather large 5x5mm² fault.

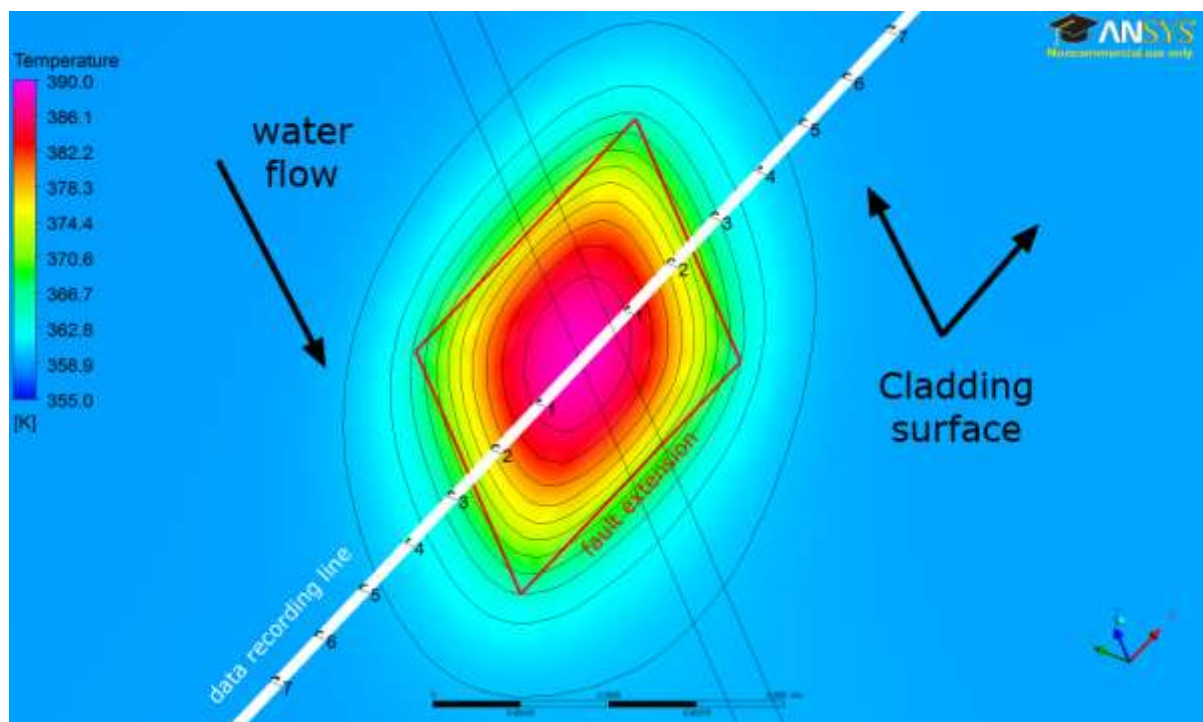


Fig 3: Example solution: Cladding surface temperatures for a failure size of 5x5mm² and an expected heat flux of 350 W/cm² after 1 day. The red square shows the dimension of the failure. Water comes in from above. The white line indicates where data was taken for the following plots.

The main effect of the oxide layer growth can be identified when Fig 5 is regarded: The top half shows the heat flux on the fault side, the lower half shows the good side. It can easily be observed how the growing oxide layer pushes the heat flux to the surrounding area and even more around the fault itself to the backside. As an effect of this rerouting, surface temperatures at the thermally most loaded places drop and the growth of the oxide layer is slowed down.

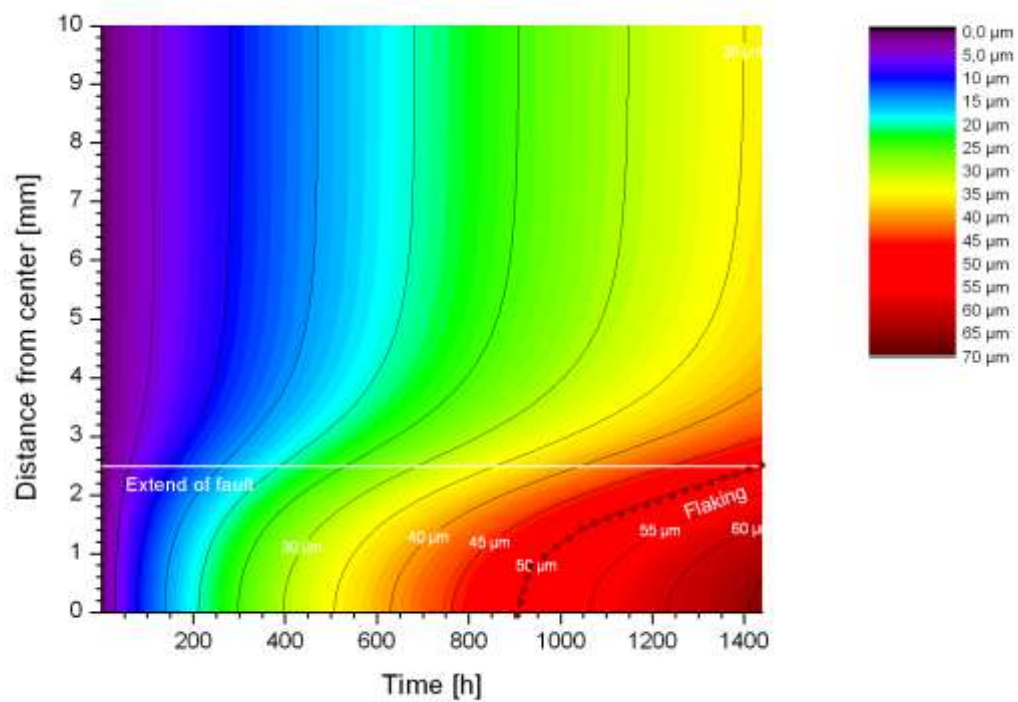


Fig 4: Growth of oxide layer for monolithic UMo, expected $450\text{W}/\text{cm}^2$ on the cladding surface opposing a $5\times 5\text{mm}^2$ contact fault.

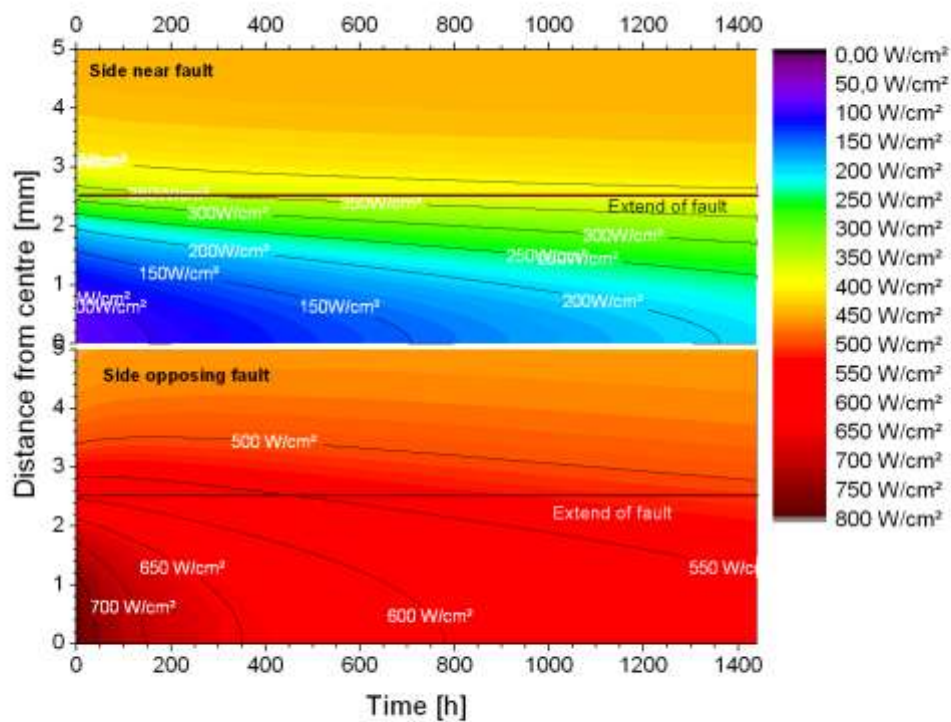


Fig 5: Development of the surface heat flux along the white line in Fig 3 for monolithic U8Mo, $450\text{ W}/\text{cm}^2$ expected heat flux, $5\times 5\text{mm}^2$ fault size. Top: Fault side of cladding, bottom: good side. The oxide layer pushes the heat flux back to the expected shape.

The oxide layer in this case reaches 50 μm thickness already after about 900h of irradiation. So, oxide flaking is very likely to occur. Naturally, the maximum tolerable irradiation time increases with decreasing surface temperatures, i.e. lower heat fluxes, which corresponds to smaller defect sizes. The maximum oxide layer thickness directly over the centre of the fault depending on the irradiation time and the fault size is shown in Fig 6. It is easily visible that starting from a given fault size, flaking is very likely to occur, and the larger the fault size, the sooner it will happen.

The maximum fuel meat temperature is depicted in Fig 7. It must be emphasized, that these calculations are based on the assumption of perfect thermal isolation due to the contact fault and are therefore very conservative. From the comparison with Fig 6, it can be concluded that meat temperatures larger than about 650K - 700K are unlikely to occur as flaking will start at about that time. However, regarding current production limits (1.35mm), no temperatures higher than 550K have to be expected. Furthermore, for the special case of FRM II, a constant expected heat flux of 450 W/cm² is neither present nor awaited.

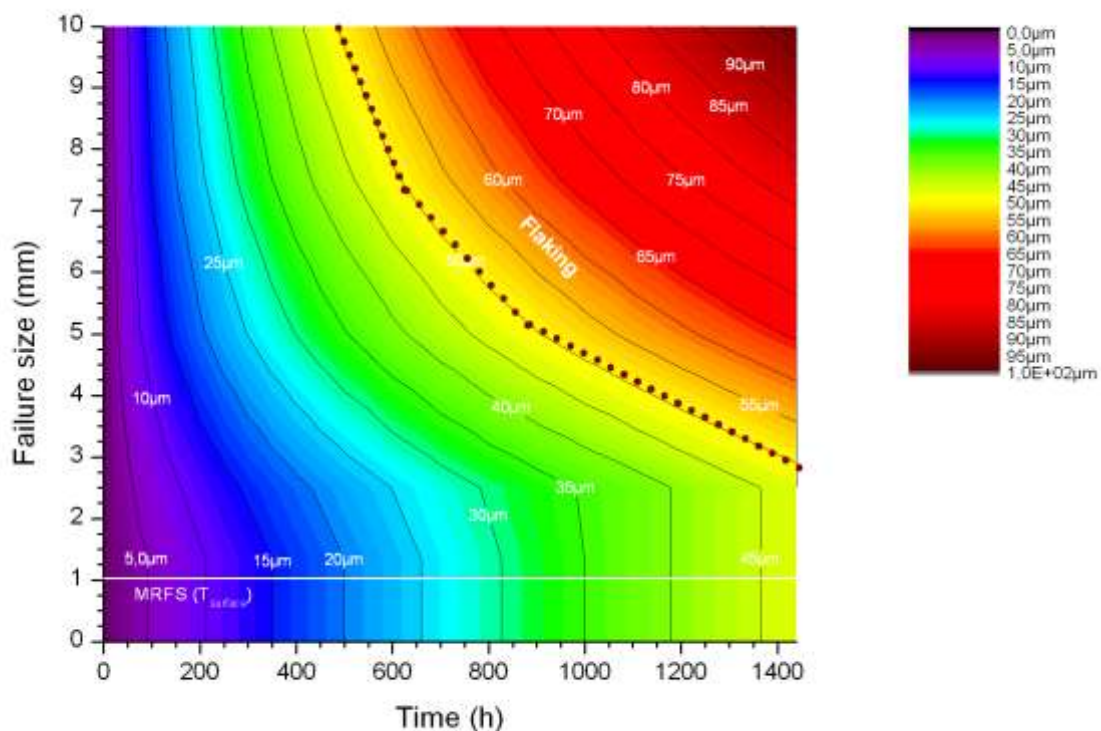


Fig 6: Maximum oxide layer thickness for monolithic UMo with 450 W/cm² expected heat flux depending on fault size (one side length) and irradiation time.

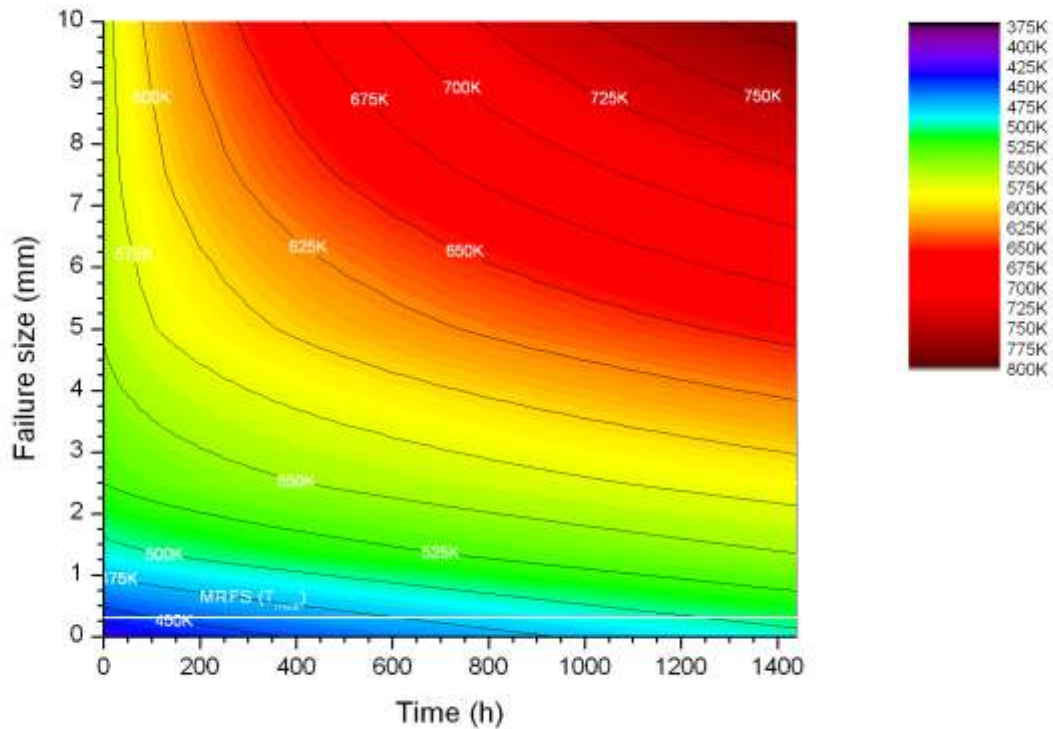


Fig 7: Maximum meat temperature for monolithic UMo with 450 W/cm² expected heat flux, depending on fault size (one side length) and irradiation time.

3.2. Case 1: 350 W/cm² expected heat flux

In the following, not single scenarios like in 3.1 but only worst case consequences will be discussed, i.e. heat flux and surface temperature at BOC as well as oxide layer thicknesses and meat temperatures at EOC.

3.2.1. Begin of cycle

It is assumed that no oxide layer is present at the beginning of a cycle. Therefore the following results are a generalization of what was shown in [1, Fig. 5], this time for 350 W/cm² instead of ~200 W/cm². Fig 8 shows the calculated surface temperatures, Fig 9 shows the heat fluxes on the good cladding side (lower surface in Fig. 1) depending on the thermal conductivity. The fault side shows comparably lower temperatures and heat fluxes.

As could be expected from [1], there is a slight dependency on the thermal conductivity κ of the meat material, where a higher κ means lower temperatures and heat fluxes, as it permits the heat to better flow around the fault. The marked MRFS are taken from [1]. Although the wall temperatures reach up to 396K for a 1cm² fault in monolithic UMo, no boiling would occur at the specified pressure of 2.3bar (boiling temperature 412K).

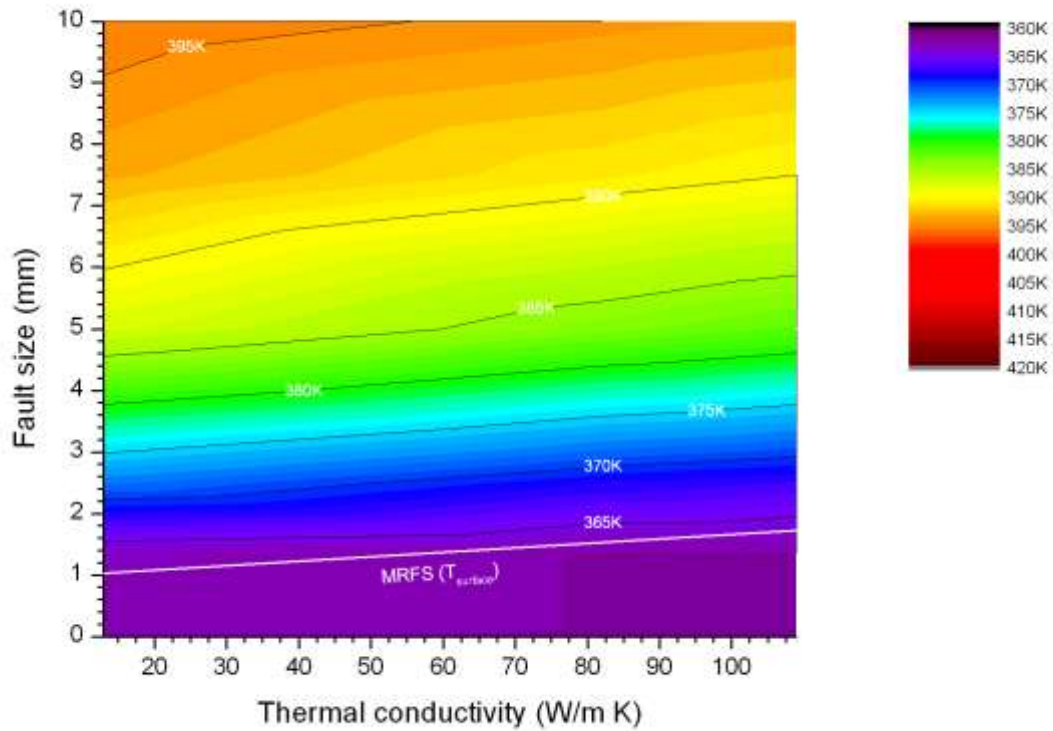


Fig 8: Maximum cladding surface temperatures for expected 350 W/cm², depending on the thermal conductivity of the meat material and the size of the fault (one side length)

The corresponding heat fluxes are shown in Fig 9. Obviously, the maximum heat flux tends to $2 \times q_0$ for $A_{\text{fault}} \rightarrow \infty$. This limit is approached slower if the thermal conductivity of the fuel is higher. This finding was already discussed in detail in [1] and is therefore not further analysed here.

3.2.2 End of cycle after 60 days / 1440h / 1.81 GJ/cm²

Regarding the maximum oxide layer thickness shown in Fig 10, the higher surface temperatures on the good side caused by comparably higher heat fluxes due to lower thermal conductivity of the meat leads to an increased oxide layer growth for material with lower κ . This was already visible in the MRFS, and shows up again in terms of the flaking threshold being reached for lower fault sizes for low- κ fuels. Nevertheless, the flaking threshold is only reached for intolerably large non-bonds in all cases.

The effect is much more pronounced when the maximum meat temperature after 1440h of irradiation is regarded as shown in Fig 11: Here the low κ is not only expressed in terms of an increased oxide layer growth, but additionally in form of elevated temperatures resulting from Fourier's law. This explains the considerably stronger κ -dependence of the result in Fig 11. However, it can be safely concluded, that with the specified fission density, the meat temperature is not the relevant criterion regarding the safety of the assembly as the oxide layer will start to flake off much before critical temperatures are reached, even under the assumption of perfect thermal isolation due to the non-bond and even with unrealistically large faults of up to 1cm².

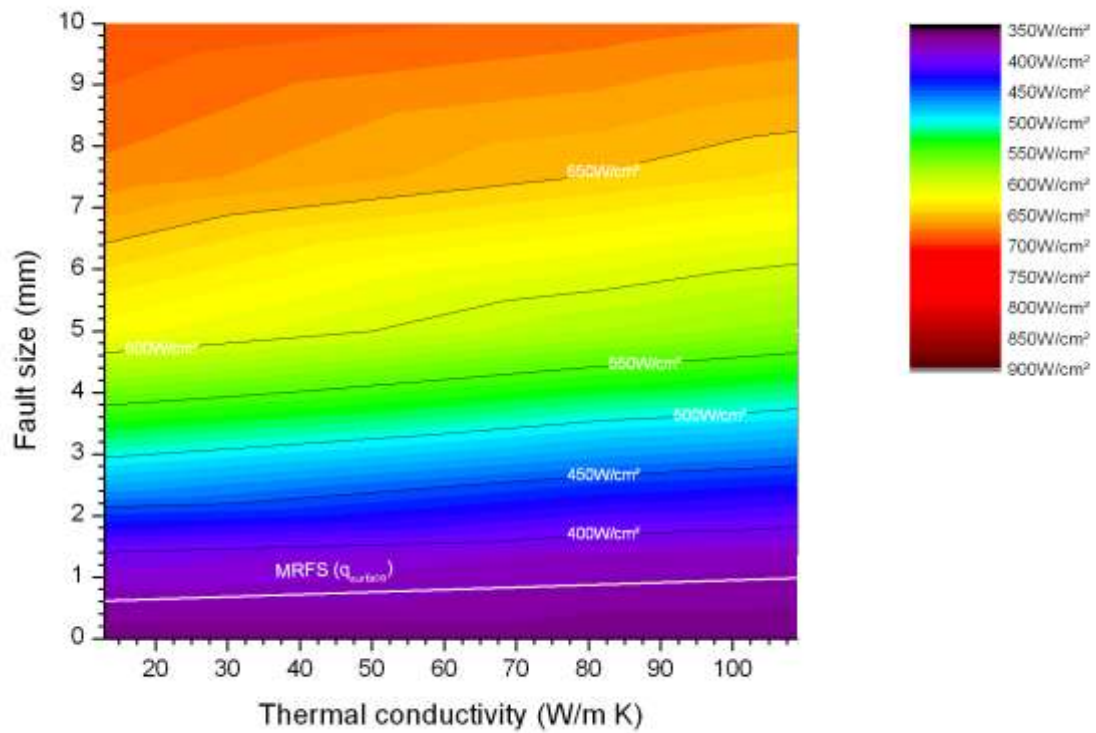


Fig 9: Maximum cladding heat flux for expected 350 W/cm^2 on the surface opposed to the side of the fault, depending on the thermal conductivity of the meat material and the size of the fault (one side length).

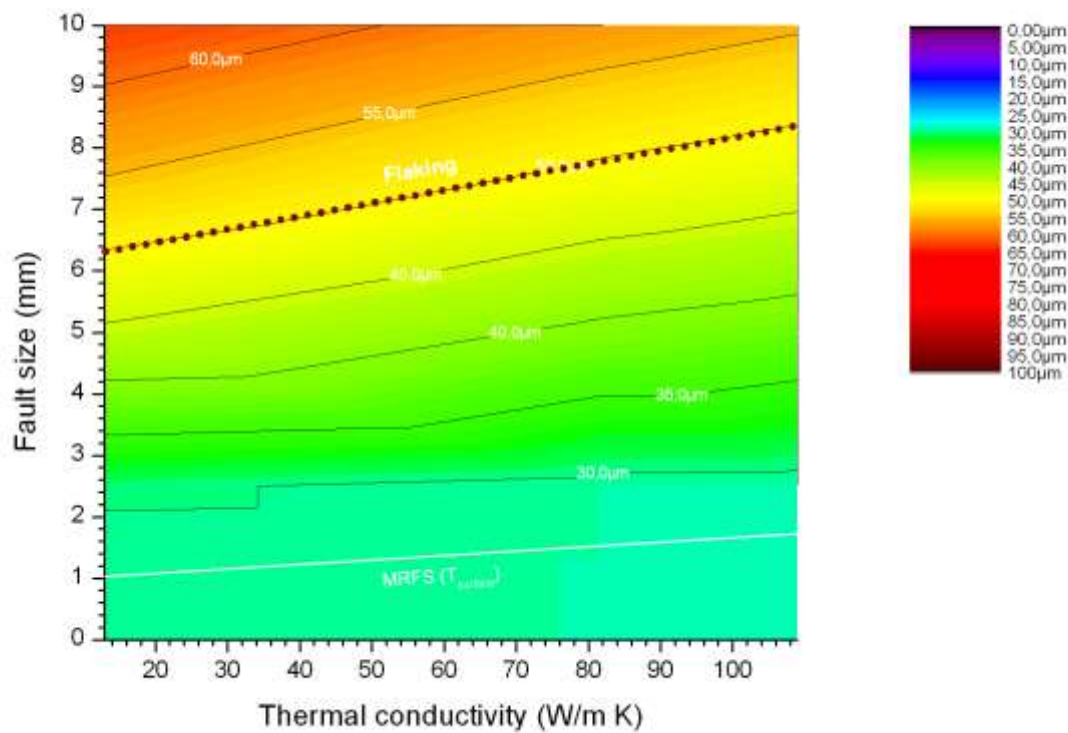


Fig 10: Maximum oxide layer thickness depending on thermal conductivity of the meat and the fault size (one side length) after 1440h irradiation time. Expected heat flux 350 W/cm^2 .

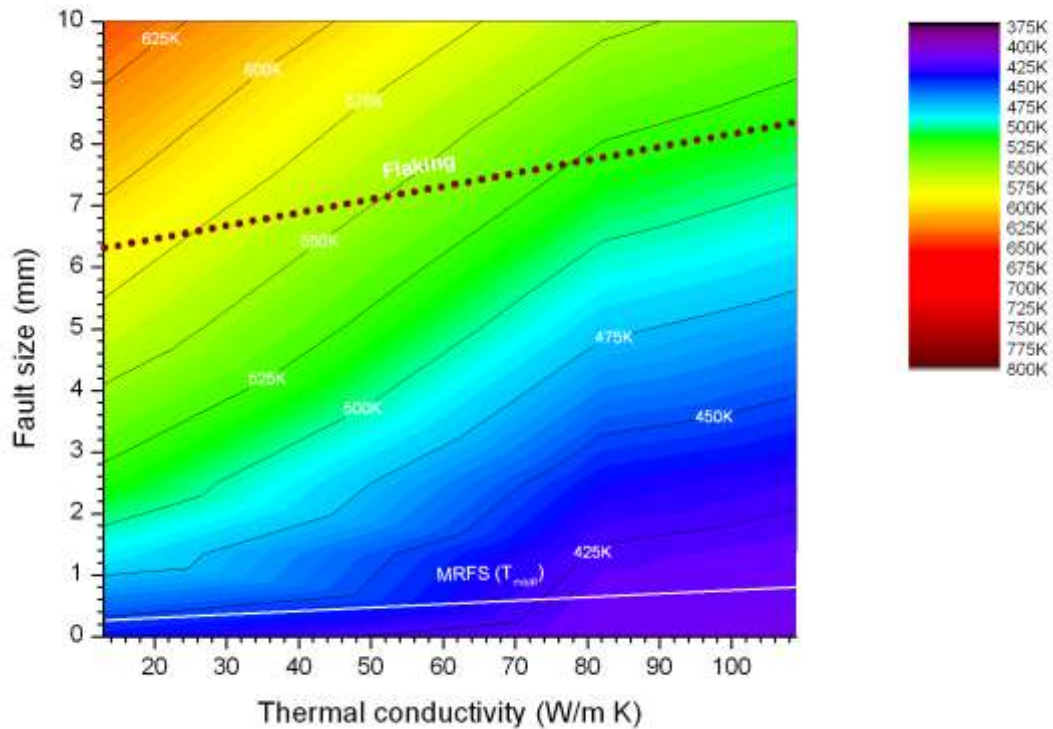


Fig 11: Maximum meat temperature after 1440h irradiation depending on fault size (one side length) and thermal conductivity of the meat. Expected heat flux 350 W/cm².

3.3. Case 2: 450 W/cm² expected heat flux

In general, the conditions at an expected heat flux of 450 W/cm² just resemble those discussed before but in a tightened version. Therefore, discussion is kept short in this section and only new findings are discussed.

3.3.1. Begin of cycle

Surface temperatures are shown in Fig 12. They are generally about 15K to 20K higher than in case 1, with increasing difference for higher heat fluxes due to the disproportionately lower heat transfer coefficient. The heat fluxes are shown in Fig 13. For very large non-bonds, they are high enough to raise the surface temperatures above the limit for subcooled boiling. As the simulations presented here do not include multi-phase phenomena, the heat fluxes in Fig 13 above the boiling line have to be considered to be inaccurate.

3.3.2 End of cycle after 60 days / 1440h / 2.33 GJ/cm²

Maximum oxide thicknesses after 1440h are shown in Fig 14, maximum meat temperatures at EOC in Fig 15. Due to the subcooled boiling discussed above, a part of the results shown in these figures is equally questionable, but as discussed in section 3.1, surface temperatures and heat fluxes drop quickly after the beginning of the irradiation. In addition, the relevant areas lie well above the oxide flaking line.

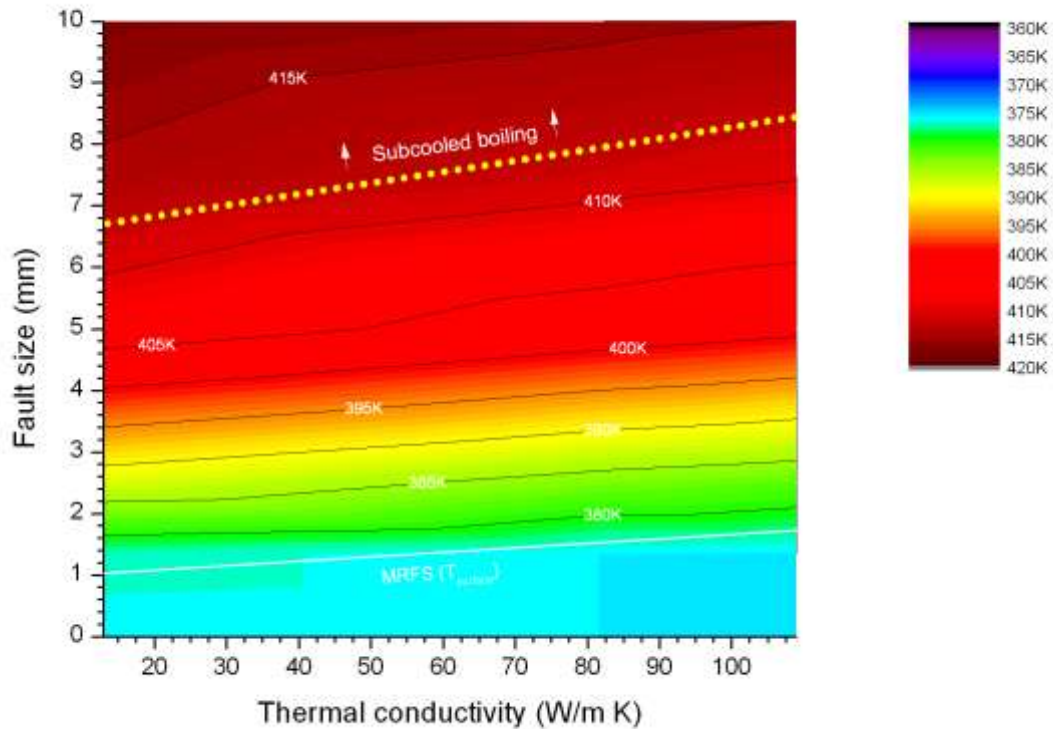


Fig 12: Maximum cladding surface temperatures for expected 450 W/cm², depending on the thermal conductivity of the meat material and the size of the fault (one side length).

Generally, flaking is likely to occur even for very small fault sizes with such high fission rates under the conditions analysed in this paper. In addition, the meat- κ -dependence is much smaller in this case than it was in case 1. This is due to the fact that the κ -dependence of the oxide layer thickness generally increases with larger fault sizes, and in this case the flaking fault size limit is rather low.

3.4. Influence of the thermal conductivity of the oxide layer

One interesting side note is the effect of the thermal conductivity of the oxide layer itself, which until now still is not fully known: While it is true that a lower thermal conductivity of the oxide layer leads to higher fuel temperatures, it is seldom regarded that a lower κ leads to a stronger heat flux barrier for hot spots caused by non-bonds, therefore stronger diverting the heat flux, which results in comparably lower surface temperatures and therefore a slower oxide layer growth. In a last consequence, this will extend the possible irradiation time interval if it is limited by oxide layer flaking. However, the slower growth and therefore smaller thickness will not compensate the fuel temperature increase caused by the lower thermal conductivity of the oxide compared to the conditions for better conducting oxide.

Thinking this the other way round, i.e. if Boehmite in water really has a higher thermal conductivity than in its dry state, and if the heat transfer coefficient stays the same, this means that the heat fluxes due to non-bonds were underestimated in this work. In that case, thicker oxide layers, earlier flaking and higher meat temperatures would have to be expected.

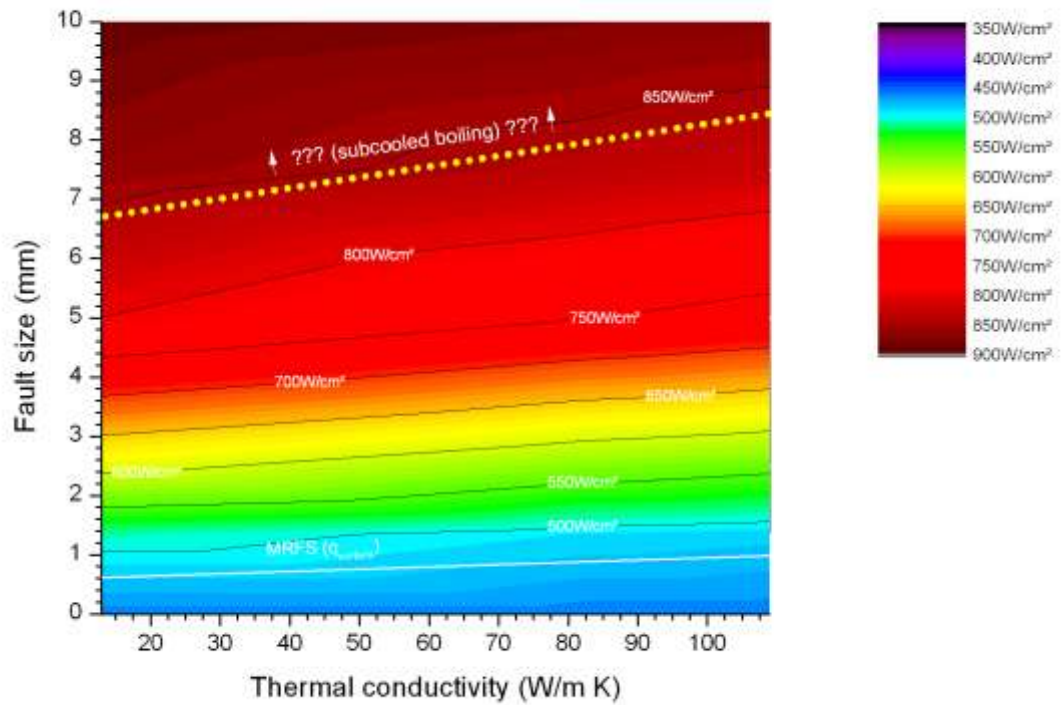


Fig 13: Maximum cladding heat flux for expected 450 W/cm² on the surface opposed to the side of the fault, depending on the thermal conductivity of the meat material and the size of the fault (one side length).

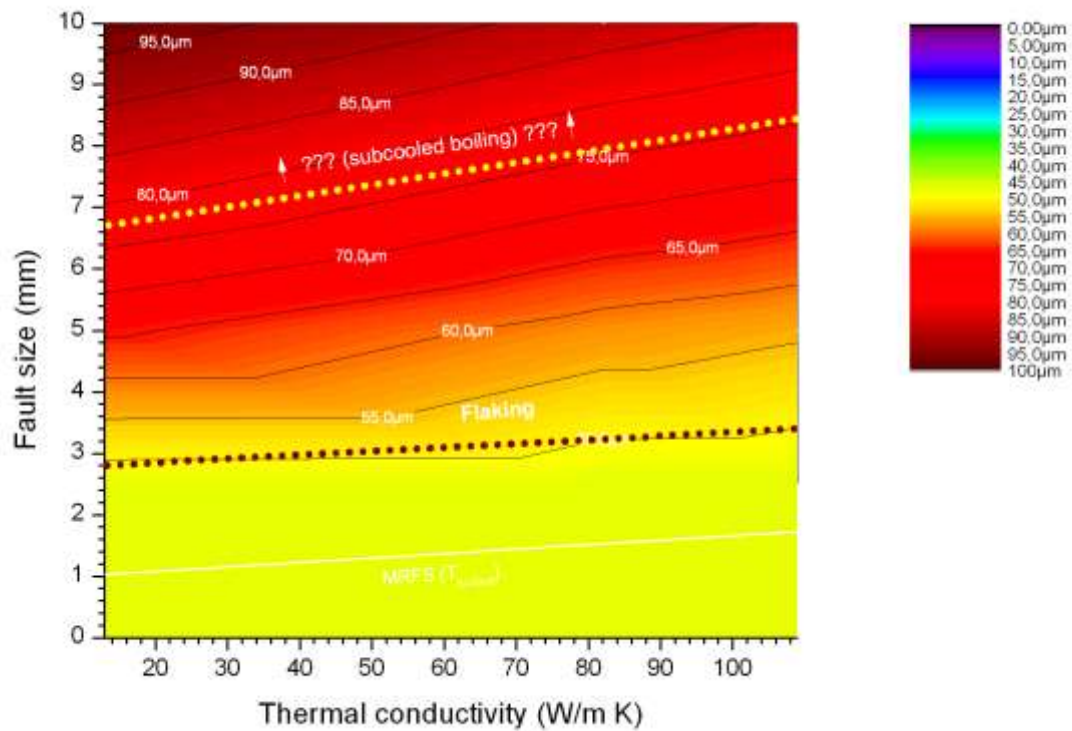


Fig 14: Maximum oxide layer thickness depending on thermal conductivity of the meat and the fault size (one side length) after 1440h irradiation time. Expected heat flux 450 W/cm².

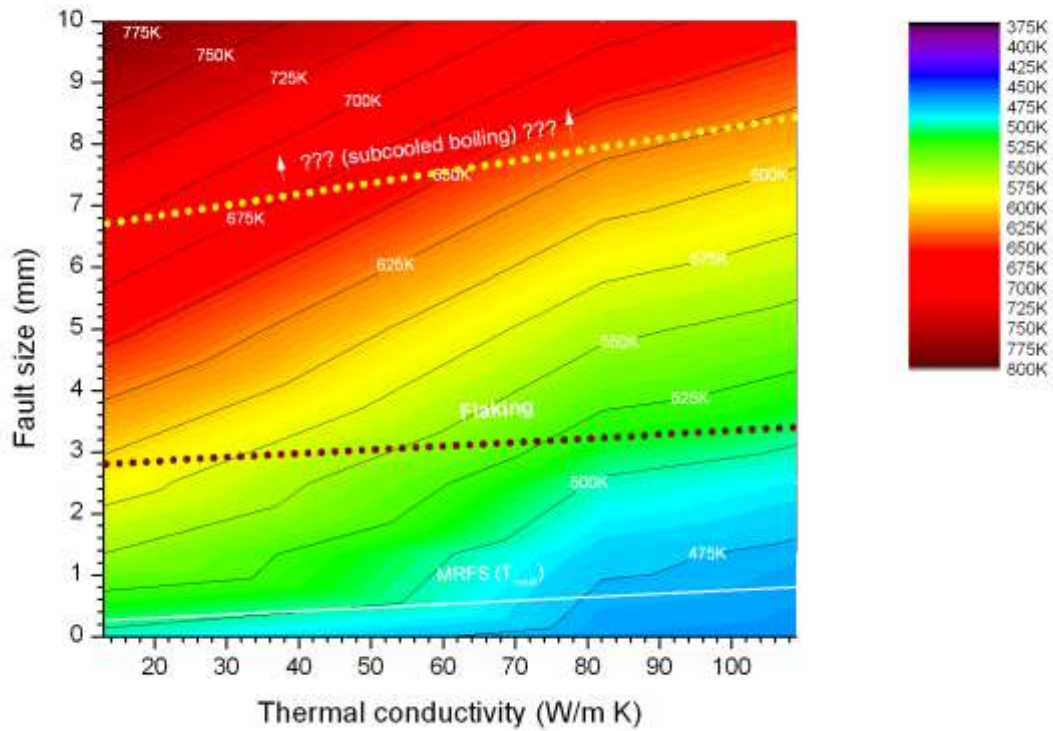


Fig 15: Maximum meat temperature after 1440h irradiation depending on fault size and thermal conductivity of the meat. Expected heat flux 450 W/cm².

4. Conclusions and outlook

It could be shown that the higher the expected heat flux, the lower is the dependence of the oxide layer build-up on the thermal conductivity of the fuel, especially regarding the thickness where flaking is possible. With increasing heat fluxes and irradiation time, this dependency gets smaller and smaller, as the influence of non-bonds with small sizes on the relevant thermal-hydraulic parameters is generally lower. This decrease probably continues with rising heat fluxes until the flaking limit is reached even for samples without non-bonds or with faults below the MRFS, where the thermal conductivity for a homogeneously heated plate is irrelevant regarding the oxide layer anyway.

Even though it was shown in [1] and in this work that the thermal conductivity of the meat plays a significant role regarding heat fluxes and surfaces temperatures at BOC if non-bonds are present, this dependency vanishes with increasing irradiation time due to the build-up of oxide layers. Therefore, it can be concluded, that the difficulties regarding oxide layer build-up and flaking in recent irradiation tests of monolithic UMo plates cannot be explained by the mechanisms analysed in this paper alone but that other effects not taken into account here must be involved.

Acknowledgements

This work was supported by a combined grant (FRM0911) from the Bundesministerium für Bildung und Forschung (BMBF) and the Bayerisches Staatsministerium für Wissenschaft, Forschung und Kunst (StMWFK).

References

- [1] Harald Breitzkreutz, Winfried Petry: Thermal-hydraulic effects of cladding-meat contact faults. Transactions of RERT 2011, Santiago, Chile, 11/2011
- [2] Howard A. McLain: HFIR fuel element steady state heat transfer analysis, revised version. Technical Report ORNL-TM-1904, Oak Ridge National Laboratory (ORNL), TN, USA. 12/1967
- [3] John R. Kirkpatrick: Calculation for HFIR fuel plate non-bonding and fuel segregation uncertainty factors. Technical Report K/CSD/TM-79, Oak Ridge Gaseous Diffusion Plant, TN, USA. 10/1990. DOI 10.2172/6434595.
- [4] G.L. Yoder, N.C.J. Chen, D.K. Felde, W.R. Nelson, R.E. Pawel: The effect of aluminium corrosion on the Advanced Neutron Source Reactor fuel design. Nuc. Eng. Des. 136 (1992) 401-408
- [5] R.E. Pawel, G.L. Yoder, D.K. Felde, B.H. Montgomery, M.T. McFee: The Corrosion of 6061 Aluminium Under Heat Transfer Conditions in the ANS Corrosion Test Loop. Oxidation of Metals 36 (1991), Nos. 1/2, 175-194
- [6] Stefan Dirndorfer: Tensile tests on monolithic two metal layer systems for research reactor fuels. Diploma Thesis, Technische Universität München, 2/2010.
- [7] D.E. Burkes, D.D. Keiser, D.M. Wachs, J.S. Larson, M.D. Chapple: Characterization of monolithic fuel foil properties and bond strength. Transactions of RRFM 2007.
- [8] C. Liu, M.L. Lovato, W.R. Blumenthal: Interfacial Strength of Al/Al and Al/Zr/Du-10wt%Mo subject to different loading modes. Transactions of RERT 2011, Santiago, Chile, 11/2011
- [9] N.A. Mara, J. Crapps, T. Wynn, K. Clarke, P. Dickerson, B. Mihaila, D.E. Dombrowski: Nanomechanical behaviour of U-10Mo/Zr/Al fuel assemblies. Transactions of RERT 2011, Santiago, Chile, 11/2011
- [10] ANSYS CFX Reference Guide (Release 13.0) (2011).
- [11] G. Ervin Jr., E.F. Osborn: The system $\text{Al}_2\text{O}_3\text{-H}_2\text{O}$. J. Geology, 59 (1954) 381-394
- [12] R. Hengstler, L. Beck, H. Breitzkreutz, C. Jarousse, R. Jungwirth, W. Petry, W. Schmid, J. Schneider, N. Wieschalla: Physical properties of monolithic U8wt%-Mo. J. Nuc. Mat. 402 (7/2010), p. 74-80. DOI 10.1016/j.jnucmat.2010.04.024
- [13] S.H. Lee, J.M. Park, C.K. Kim: Thermophysical Properties of U-Mo/Al Alloy Dispersion Fuel Meats. Int. J. of Thermophysics, 28 (10/2007), p.1578-1594. DOI 10.1007/s10765-007-0212-0

OPERATIONAL EXPERIENCE WITH LEU IRT-4M FUEL AFTER THE CONVERSION OF LVR-15 REACTOR

M. Koleska, J. Ernest, J. Zmitkova, M. Marek
Department of Reactor Services, Research Centre Rez
Husinec – Rez 130, 250 68 Rez – Czech Republic

V. Broz
Department of Reactor Operation, Research Centre Rez
Husinec – Rez 130, 250 68 Rez – Czech Republic

ABSTRACT

LVR-15 is 10 MW tank-type LWR research reactor situated in the Research Centre at Rez near Prague, Czech Republic. Since February 2010 the reactor had successfully undergone a conversion from HEU IRT-2M fuel to LEU IRT-4M fuel. The conversion was successfully finished within the criticality experiment in September 2011. This paper summarizes operational experience with LEU IRT-4M fuel gained during the conversion and operation of fully LEU cores.

1 Introduction

The LVR-15 research reactor successfully finished the last step of conversion from HEU to LEU fuel in September 2011. This final step was a criticality experiment organized within the preparation for cycle K132 after 16 cycles operating both, the HEU and the LEU, types of fuel. Since operation of the first fully LEU core, the reactor successfully finished 5 more cycles. The FIG. 1 shows the milestones of the conversion starting with the last HEU core and ending with the last mixed core.

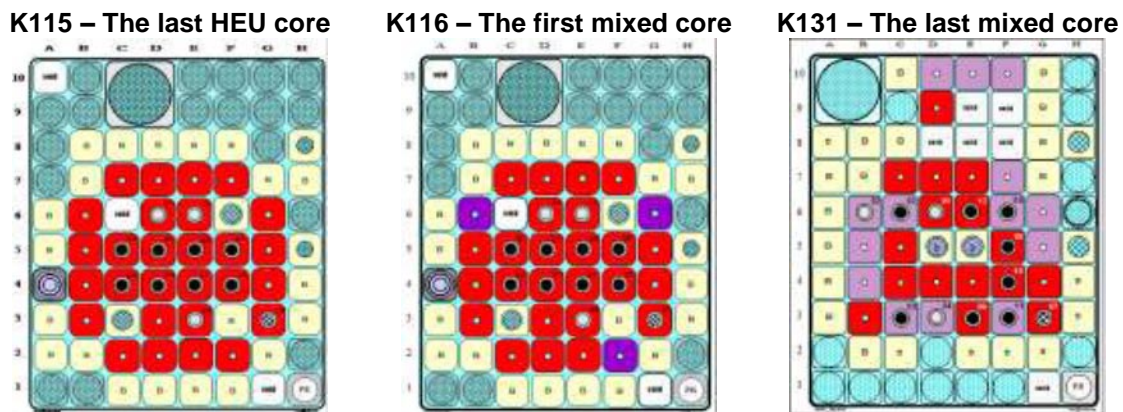


FIG. 1 Important cores of the conversion

2 The criticality experiment

The conversion of the LVR-15 reactor was planned to be performed through the operation of mixed cores using HEU and LEU fuel, with intended finish in March 2012. Due to the planned transport of the spent HEU fuel back to Russia in 2013, the conversion plan was slightly modified and accelerated. The criticality experiment was planned and performed as a result of the acceleration. The experiment had two parts where both, fresh and spent, LEU fuel was used.

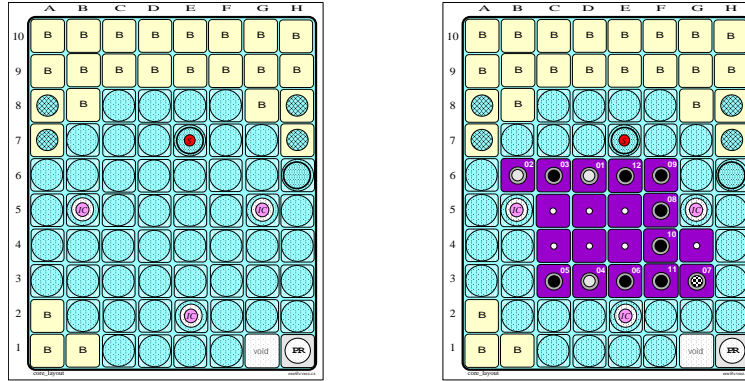


FIG. 2 Criticality experiment, step I – initial and final configuration

TABLE 1 Overview of criticality experiment, step I

No.	FAS	CALCULATED K_{EF} (NODER)	CALCULATED K_{EF} (MCNP)	MEASURED K_{EF}
1	8	0.6705	0.6595	0.630
2	12	0.7425	0.7408	0.673
3	14	0.8626	0.8615	0.842
4	15	0.9122	0.9111	0.880
5	16	0.9503	0.9478	0.950
6	17	0.978	0.9758	0.964
7	18	1.0025	0.9999	0.986
8	19	1.0162	1.0134	reactor critical

The goal of the first part of the experiment was to build a compact core configuration using fresh and spent fuel. It started with a fully unloaded core with beryllium blocks placed in peripheral positions as shown in the FIG. 2. In the first two steps, six-tube FAs with control rods were inserted. In the next steps only standard FAs were loaded. The first criticality with LEU fuel was achieved during step 8 with 19 FAs loaded (TABLE 1). The first part of the experiment showed a good agreement between experiment and calculation performed by the operational diffusion code NODER. Also the MCNP calculation performed with enhanced model of LVR-15 gave comparable results.

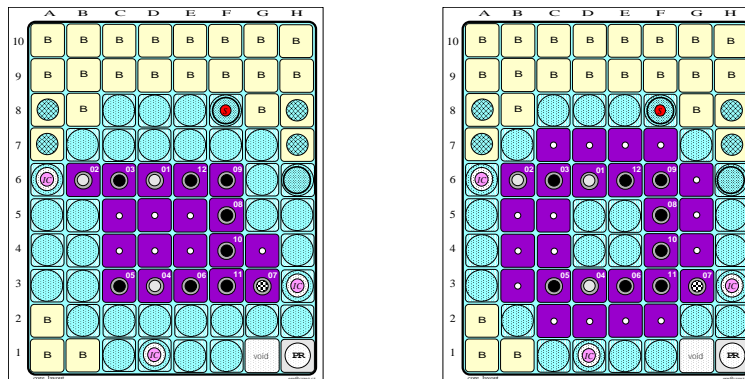


FIG. 3 Criticality experiment, step II – initial and final configuration

TABLE 2 Overview of criticality experiment, step II

No.	FAs	CALCULATED K_{EF} (NODER)	CALCULATED K_{EF} (MCNP)	MEASURED K_{EF}
1	19	0.8634	0.8629	0.881
2	22	0.9297	0.9313	0.951
3	24	0.9644	0.9630	0.978
4	26	0.9850	0.9831	0.992
5	27	0.9990	0.9941	0.999
6	28	1.0114	1.0046	reactor critical

The goal of the second part was to build the configuration with central trap. It started by rearranging the compact configuration and creating the central irradiation trap (FIG. 3, TABLE 2). In this part only fresh and spent standard FAs were loaded to the core. The criticality was achieved during the 6th step. Results obtained by operational code NODER and MCNP are again in a good agreement with experimental data.

3 Evolution of operational characteristics during LEU cycles

Since the end of the conversion, the reactor has finished five cycles. During these cycles, the rising mean fuel burnup was compensated only by movement of beryllium blocks toward the core and by the exchange of fuel position. Compact beryllium reflector was almost finished with cycle K136. Evolution of LEU configurations is shown in the FIG. 4. The evolution of key operational characteristics is shown in the TABLE 3.

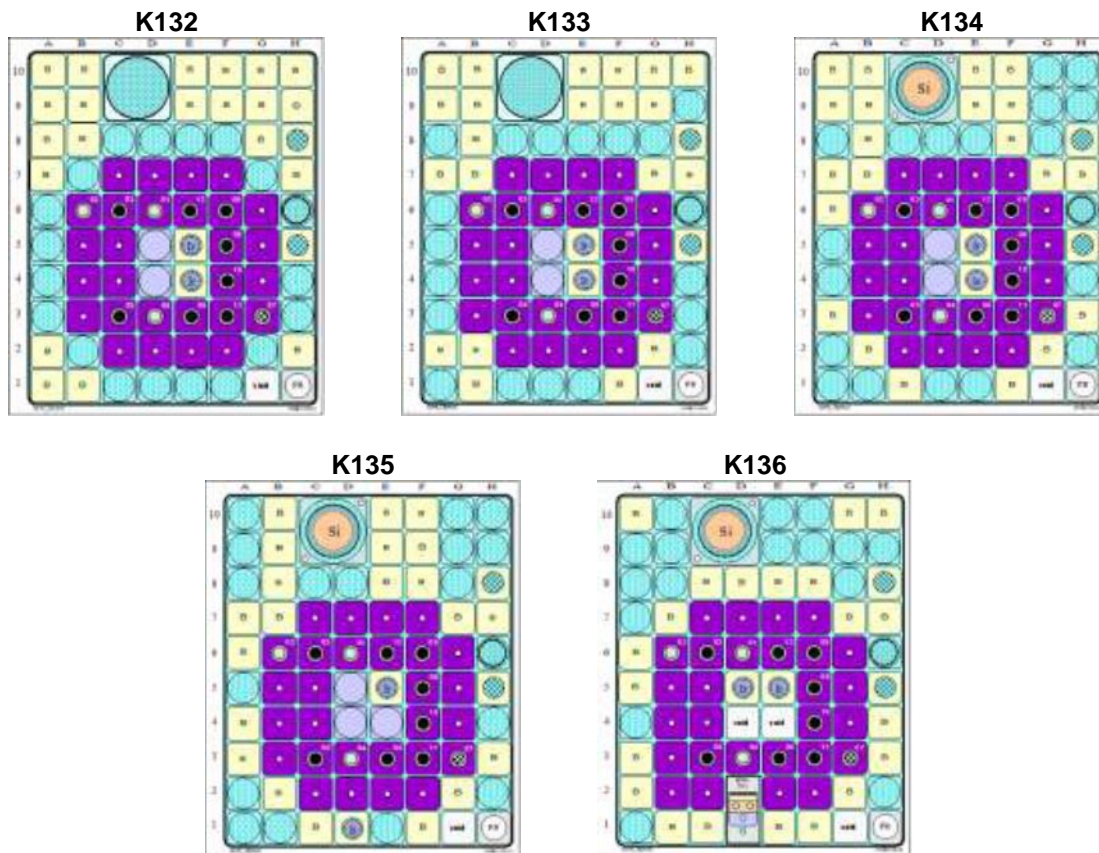


FIG. 4 Evolution of LEU cores

TABLE 3 Evolution of key operational characteristics

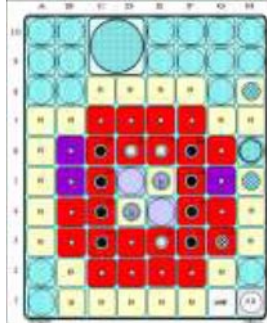
	LENGTH (DAYS)	WORK (MWd)	EOC BURNUP			REACTIVITY			THERMO HYDRAULICS	
			8-TUBE FA	6-TUBE FA	AVERAGE	CR WEIGHT	PPR	KSS	Q [M ³ /HOD]	ΔT
K132	13.94	138.97	21.53	12.31	17.86	20.88	7.11	2.66	893.70	10.70
K133	23.94	231.34	27.38	18.60	23.88	21.20	6.77	2.84	914.50	10.50
K134	20.93	206.84	32.49	24.42	29.26	20.66	8.47	2.21	904.80	10.61
K135	6.90	69.69	34.21	26.35	31.09	20.74	6.36	2.98	803.50	11.95
K136	15.36	153.43	39.26	32.02	36.38	22.70	8.96	2.28	847.70	11.30

Compared to the HEU cores, key parameters of the core remained after the conversion almost the same. Lower burnup is a logical consequence of the way the conversion was performed and is consistent with the operation of HEU fuel. Key reactivity parameters, such as control rod weight, initial reactivity excess (PPR) and compensating ability of the system (KSS) also remained within the same range. The biggest difference between HEU and LEU was caused by different thermo hydraulic parameters of the new fuel, so the minimal flow rate could be reduced for almost 50%.

4 Evolution of irradiation conditions

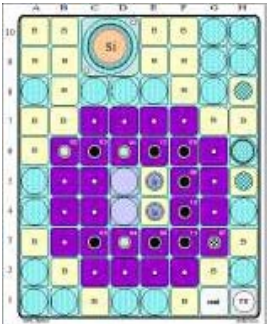
During first LEU cycles, the operation of the reactor was optimized for production of ¹⁹²Ir and ⁹⁹Mo from IRE targets and irradiation of silicon crystals. During the cycle K136 started operation of the TW3 rig dedicated to the fusion devices. At the end of the cycle K136 was also performed test with rig CHOUCA.

TABLE 4 Irradiation conditions in central trap and DONA in mixed core K124



ENERGY	NEUTRON FLUX (N.CM ⁻² .S ⁻¹)				
	D5	D4	E4	E5	C,D-9,10 (DONA)
< 0.625 eV	1.54E+14	1.74E+14	1.65E+14	1.73E+14	3.69E+13
0.625 eV - 5.53 keV	6.85E+13	7.35E+13	7.30E+13	7.38E+13	5.05E+12
5.53 keV - 0.821 MeV	7.59E+13	7.16E+13	7.96E+13	7.24E+13	3.73E+12
0.821 MeV - 20 MeV	8.85E+13	5.20E+13	9.47E+13	5.23E+13	2.70E+12

TABLE 5 Irradiation conditions in central trap and DONA in LEU core K134



ENERGY	NEUTRON FLUX (N.CM ⁻² .S ⁻¹)				
	D5	D4	E4	E5	C,D-9,10 (DONA)
< 0.625 eV	1.54E+14	1.59E+14	1.45E+14	1.43E+14	3.67E+13
0.625 eV - 5.53 keV	7.54E+13	7.70E+13	7.83E+13	7.62E+13	4.45E+12
5.53 keV - 0.821 MeV	8.39E+13	8.41E+13	7.37E+13	7.60E+13	3.60E+12
0.821 MeV - 20 MeV	9.41E+13	9.63E+13	5.11E+13	5.08E+13	3.09E+12

The influence of the fuel exchange on irradiation conditions is represented in TABLE 4 and TABLE 5. The TABLE 4 shows neutron spectra in one of the first mixed cores with only three LEU FAs in peripheral position. A comparison of results for the central trap

(D4, D5, E4, E5) in these two configurations gives a slight decrease in the thermal neutron flux with an increase in the fast region of the spectra. Irradiation conditions in DONA irradiation device used for irradiation of silicon crystals have not changed.

The mean power in IRE targets production increased with the conversion for 4.2%. Irradiation conditions suitable for material test experiments are shown in the FIG. 5. Results were obtained for the rig CHOUCA placed for the trial irradiation in A1 position at the end of the cycle K136. This test proved sufficient neutron flux and radiation heating for further successful operation of the rig in similar configuration of the core.

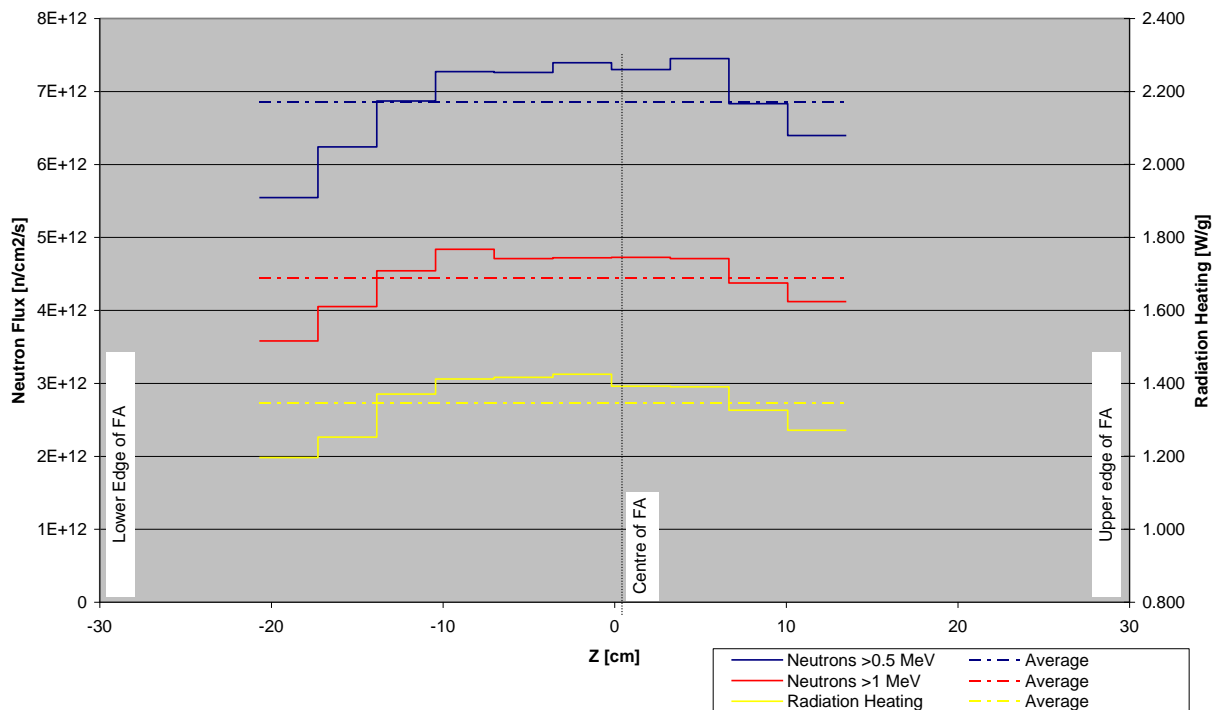


FIG. 5 Irradiation conditions in rig CHOUCA for core K136

The irradiation experience obtained after the conversion is coherent to the common experience with hardening the neutron spectra after the conversion to the LEU fuel. The common value of thermal neutron flux decrease gives 5 – 10%.

5 Acknowledgements

The work done during the conversion was financially supported by the US Department of Energy and by project FI-IM4/0291 of the Ministry of Industry and Trade, Czech Republic.

6 References

- [1] M. Miletić and J. Ernest, "Program výstavby konfigurace AZ K132 reaktoru LVR-15." PP 7801.10, Řež, 2011.
- [2] M. Vinš, M. Kolečka, P. Mühlbauer, Z. Lahodová, J. Ernest, and J. Zmítková, "Výpočtové stanovení ozařovacích podmínek pro vybrané pozice reaktoru LVR-15 s nízkoobohacenou aktivní zónou s palivem IRT4M." CVR 050, Řež, 2011.

CER & AFR: A Coalition for a Successful Future for Research Reactors in Europe

Gabriele Hampel (AFR)

*Universität Mainz -Institut für Kernchemie
Fritz-Strassmann-Weg 2 - D-55128 Mainz - Germany*

Jérôme Estrade(CER)

*CEA/DER/SRJH
Centre de Cadarache – 13108 Saint Paul lez Durance - France*

André Chabre (CER)

*CEA/DEN/DISN
Centre de Saclay - 91191 Gif sur Yvette - France*

Abstract

Networking and the establishment of coalitions between research reactors are important to guarantee a high technical quality of the facility, to assure well educated and trained personnel, to harmonize the codes of standards and the knowledge of the personnel as well as to enhance research reactor utilization.

In Europe, the research reactors are connected in the Research Reactors Operators Group (RROG), a working group of the European Atomic Energy Society (EAES). In addition, country-specific working groups have been established for many years, such as the French research reactor Club d'Exploitants des Réacteurs (CER) and the community of German speaking research reactors aligned in the Arbeitsgemeinschaft für Betriebs- und Sicherheitsfragen an Forschungsreaktoren (AFR). These groups meet regularly to exchange experiences in all areas of operating, managing and utilization of research reactors.

Due to the dismantling of many power and research reactors and the public debate about nuclear energy after the Fukushima accident, networking between the facilities in Europe becomes even more important. To enforce the tasks and position of the research reactors in Europe, for a first time CER and AFR had a mutual meeting with members of the French research reactor CER and members of the AFR in Cadarache in 2011. Topics such as principles, functions, and tasks of the AFR and CER were introduced. Both the research reactors in France, as well as those in the AFR serve as intense neutron sources for physical, chemical, biological, and medical uses, and also for many other fields in the applied sciences.

1. Introduction

Research reactors are intense neutron sources delivering neutrons for a broad variety of research and development, industrial, technical and medical applications as well as education and training. The research reactor environment is dynamic and adaptable which delivers a base for future applications of research reactors which is connected not only to nuclear power plants but also to nuclear research center, and generates new developments, projects and undertakings. Radioisotope production for medical use remains one of the most important commercial applications of research reactors, in particular in the case of dedicated large-scale production facilities due to the availability of high neutron fluxes and dedicated irradiation channels. Technical applications at research reactors include neutron transmutation doping (NTD) of silicon, isotope production, neutron activation analysis (NAA), neutron radiography and tomography, as well as fuel and materials testing. Due to

their high flexibility research reactors can be used very effectively for different projects on fundamental and applied science in a variety of fields: condensed matter physics, chemistry, biology, nuclear and particle physics, materials science and medical research. Neutron beams are a type of non-destructive radiation with properties that make them an extremely versatile and unique analytical probe. Hence, neutrons are a powerful tool for investigating nature at all levels, from testing theories about the evolution of the Universe to elucidating on the complex processes of life.

The international community of expertise is requested more and more frequently, to communicate and work together, in the framework of a global economy. The entire range of research reactors should be used as effectively as possible: While low power research reactors are being most easily available and particularly appropriate for training and education and some special and individual experiments, high flux reactors with a high performance are being more complex to implement but enable to carry out analytical experiments as well as experiments in incidental and accidental situations which are important for safety reasons.

For a future in Europe, the research reactors have to participate at the process of globalisation. The experience feedback of Fukushima and the energy policies of the European countries can have an effect on the future of research reactors. They require more than in the past of openings towards the outside to promote their activities, improve their availability and their use for the society. It is also necessary to set-up new coalitions. In this context, the joint AFR and CER meeting is an example to encourage and develop relationship between users and research reactor operators. These exchanges can also offer a good opportunity to open cooperations between single facilities. The AFR-CER coalition should be on the basis of mutual benefit, equality and reciprocity.

2. CER and AFR - a brief summary

2.1 AFR

The acronym AFR stands for, in English, “Community for the Operation and Safety of Research Reactors”. The community was created in 1959 for the purpose of the exchange of experience between facilities in technical applications, while also taking into account the specific interests of each reactor. Since 1976 the AFR belongs to the German Atomic Forum. Requirements for the research reactors, as decided by the regulatory bodies, are discussed, as well as guidelines which were developed for power reactors and adapted to research reactors.

Members of the AFR are all “German-speaking” research reactors in Belgium, Germany, Austria, the Netherlands, Switzerland, as well as the European research reactor at the Institute Laue Langevin, Grenoble, France, and partly the reactor facilities of the Czech Republic and Hungary. In the AFR high flux research reactors, MTR research reactors, TRIGA reactors and zero power reactors are represented. As summarised in Table 1 the AFR includes at the moment 12 research reactors in operation (excluding Czech and Hungarian facilities) and 4 research reactors in decommissioning.

The youngest research reactor of AFR is the FRM II which started operation in 2004 and has a similar fuel element as the HFR Grenoble. The oldest research reactor in the AFR being still in operation is the TRIGA Vienna which started operation in 1962. The elder research reactors in Rossendorf and Munich (FRM) and also the research reactors of similar age as the FRJ-2 Jülich and the FRG-2 Geesthacht are in decommissioning meanwhile.

The AFR research reactors in operation are used as intense neutron sources for education and training, medical and technical purposes and basic research in physical, chemical and biological subjects. While education and training are typical applications for low power research reactors, such as the zero power reactors or the TRIGA reactors in Mainz and Vienna, the production of radioisotopes for medical and technical use, and silicon transmutation doping for solar cell

manufacture are important commercial applications of the high-flux research reactors in Munich and Mole. The beam ports and irradiation facilities of the research reactors in Berlin, Delft, Munich, Grenoble, Mainz and Vienna deliver intense beams of neutrons to a suite of high-performance instruments and can be used for some special applications which are unique in the way they are carried out.

The members of AFR meet twice a year at one of the reactor facilities for an exchange of experience and knowledge regarding all aspects of the research reactors as technical procedures, licensing matters, fuel cycle, waste management, documentation, managing research reactor operation or dismantling, utilisation issues of the reactors etc. The agenda includes the summary of important conferences, meetings, publications or other events regarding research reactors. AFR has also formed subgroups, one for security and one to answer questions regarding dismantling of research reactors which presented their work at the AFR meeting. Guests can be invited to talk about special subjects, which was the case for many years regarding the spent nuclear fuel management. Every meeting has its main topic, the last one was – besides the discussions following the accident of Fukushima - the presentation of the AFR in the intra- and internet which is now in preparation and will be open to the public in 2012.

AFR delivered a platform for exchange and support between the members which is used in the past for education and training, delivery of technical equipment due to different reasons, support in evaluations and documentations.

No.	Name	Thermal power in MW	Moderator	Reflector	Operation period
High flux research reactors					
1	FRM II	20 MW	D ₂ O	–	since 2004
2	HFR Grenoble	57 MW	D ₂ O	–	since 1971
MTR reactors					
3	HOR Delft	2 MW	H ₂ O	BeO	since 1963
4	FRM München	4 MW	H ₂ O	–	1957 – 2000
5	BER II Berlin	10 MW	H ₂ O	Be	since 1973/1991*
6	FRG-1 Geesthacht	15 MW	H ₂ O	Be	1963 – 2010
7	FRJ-2 Jülich	23 MW	D ₂ O	D ₂ O	1962 – 2006
8	BR2 Mol	100 MW	Be / H ₂ O	Be / H ₂ O	since 1963
TRIGA reactors					
9	TRIGA Mainz	100 kW	Zirconium Hydrid H ₂ O	Graphite	since 1965
10	TRIGA Vienna	250 kW	Zirconium Hydrid H ₂ O	Graphite	since 1962
Zero power reactors					
11	PROTEUS, PSI	1 kW	Polyethylhene	Graphite	since 1968
12	TU Dresden	2 W	Polyethylhene	–	Since 1978/2005*
13	Stuttgart	100 mW	Polyethylhene	Graphite	since 1964
14	Ulm	100 mW	Polyethylhene	Graphite	since 1965
15	Furtwangen	100 mW	Polyethylhene	Graphite	since 1973
WWR-SM (Russian type)					
16	RFR Rossendorf	10	H ₂ O	Be	1957 - 1991

Table 1: Research reactors of the AFR (status 2011); * year of complete refurbishment.

Most important and the basis of AFR is the mutual assistance between the individual facilities since the beginning until today, which guarantees a safe operation and technical support whenever it is necessary and has established friendships between the AFR members over the years.

2.2 CER

CER stands for Club d'Exploitants des Réacteurs. It is the association of French research reactors representing all types of research reactors from zero power up to high flux reactors. CER was formed in 1990 and today a number of 12 research reactors meet twice a year for an exchange of experience. Members are the reactor facilities in Cadarache, Saclay, Valduc, Grenoble and Marcoule (see Fig. 1). These reactors primarily belong to the French atomic energy commission (CEA¹) located on the Saclay, Cadarache, Marcoule and Valduc research centres. The club also includes the high-flux reactor (HFR) of the Laue-Langevin Institute (ILL) in Grenoble and reactors belonging to the Areva Group. About 1,700 highly-qualified staff from these sites is directly involved in operating these reactors.

The different types of research reactors, the different conditions of operation, their status (under construction, in operation, in final shutdown situation for dismantling) are a great opportunity to exchange on the problems of operations during “the life” of a reactor. So, the sustainability of the equipments, the consideration of the constraints of dismantling and maintenance in the conception phase for the new facility, the optimization of organizations in all the phases of life of the installation are subjects which are discussed and can be benefited for all.

Each year, the highlights of these facilities are presented to the members. The last two years, the main highlights were:

- Phenix reactor operating in 2009, a last series of tests could be performed to collect essential data on the effects of degraded operating conditions in this type of reactor,
- The Jules Horowitz Reactor (JHR) and the RES facility, currently under construction, are two challenging projects for the Cadarache Centre. Similarly, opening the JHR to the international scientific community is a great step forward for future users,
- The difficulties in procuring radionuclides in 2008 led the Osiris teams to double their efforts in producing molybdenum to meet medical demands,
- There are still numerous requests to use neutron beams for fundamental research and the continued renovation of the Orphee and HFR facilities means we can ensure the durability of our tools to meet such demands,
- Last of all, the French “grand loan” (public bond) will breathe new impetus into the design of Generation IV reactors, which includes refurbishment of the Masurca reactor as part of core design support.

During these meetings, 2 or 3 subjects are discussed in this group. For example:

- Exchange about the new requirements (regulations, standards, guideline) for the nuclear facilities in the framework of the periodic safety review or during implementation of new equipments: good practice to take into account the new requirements, to maintain the adequacy between the operating documents and current status of the System, Structures and Components important to safety. The practically continuous upgrading of facilities is also an important issue in guaranteeing the future of our experimental reactors,
- Feedback of experience : technical and operational problems, ageing management, exchange about obsolescence management (I and C, radioprotection sensors..), exchange about analysis of failure mode and generic impact,

¹ Commissariat à l'Energie Atomique et aux Energies Alternatives

- Personnel training accreditations and authorizations: description of the processes authorizations, periodicity of recycling, organization of the internal exercises (safety / security: periodicity, themes, objectives), good practice for the installations which definitely shutdown (repositioning of the teams of operators, waste management, preparation of the new organisation..., Periodic test and maintenance program : development of predictive maintenance (vibration monitoring for the pump, implementation of specific instrumentation for develop in-service inspections..), good practice for recording and analysis the results of maintenance and periodic test operation

In conclusion, the interests of this club are to promote:

- Technical exchanges between the different operators to improve the manners to operate by sharing the feedback of experience; different items could be exchanged (maintenance, ageing program, training, commissioning test for new facilities, instrumentation, etc.)
- Exchange on method of neutron and thermal hydraulic calculations: methodology to evaluate Gamma heating (measurements and evaluation),
- The development of instrumentation to measure gamma and neutron flux
- Cooperation in education includes the opportunity for young students to collaborate in joint research activities



Fig. 1 Location of the French “fleet” of research reactors including OSIRIS/RJH: Materials testing reactor; EOLE/MINERVE : Mock-up in support to LWR studies; MASURCA: Mock-up in support to SFR studies; ISIS/AZUR/MINERVE: Education and training; ORPHEE/RHF: fundamental research reactor; CABRI/SILENE: Reactor for safety studies; RES : prototype reactor

3. The CER and AFR coalition - a perspective for Europe

A goal of the coalition between AFR and CER is a greater exchange of ideas, information, and experience between European countries in consideration of their close geographic proximity of the European nations. The number of research reactors has decreased in Europe in recent years. Therefore, it is important to form a broad common network with the aim to maintaining the competence of research reactors at the highest level, to present development and utilization of research reactors as neutron sources for science, research, and technology on a high international

level and to receive a common standard for research reactor in Europe. Possibilities and advantages offered by the AFR-CER coalition are described in the following:

i. Exchange on “know-how” and experience

The coalition offers the members of AFR and CER the possibility to exchange experience and knowledge in all areas of operating a research reactor, to discuss technical problems, safety, and radiation protection measures. Also, topical subjects are discussed, such as nuclear incidents and their consequences for the research reactors, for example, with regard recently to the Fukushima-Daiichi accident in 2011.

Due to the decrease of research reactors in Europe and the close distances in Europe, it is essential and more effective to have such debates in the AFR-CER coalition.

ii. Analysis, comparison and harmonisation of European and international standards

The technical standard, the quality of the utilisation, research and also of the management of research reactors can be improved by intercomparison programmes. Due to the contacts in the coalition such programmes can be defined, carried out and the results can be analysed. As a result, a high quality of the applied technique will be established. It also advances the work towards harmonization of technical codes and standards on the European level.

iii. Education and training for reactor personnel

The basis for a safe and reliable operation and a highly utilization of the research reactor is well-educated personnel including the technicians, engineers, manager and scientists. Continuous education and training is necessary in order to maintain the competence, and to have the knowledge to improve and develop the technique and other facilities connected with the research reactor. Contacts and exchange possibilities for the personnel from different research reactors and common education and training opportunities are an alternative to motivate the personnel and to improve the qualification level. This is already practiced successfully in some bilateral co-operations between research reactors of the AFR (e.g. Vienna and Mol or Mainz and Munich for the training of reactor operators). In some cases, different languages could cause problems, however with an extension of the education and training programme within the AFR-CER coalition, this would support the setting up in Europe of an approach on harmonisation in education, qualifications and knowledge of the research reactor personnel.

iv. Networking

Networking and research reactor coalitions provide the chance to offer complex services in a wide range of activities to the public, i.e. government, industry and other potential partners. A single reactor cannot offer this alone and a synergistic benefit can only be gained from the joint efforts of the coalition. Coalitions also allow coordinating the reactor operating shutdown periods and sharing the irradiation and experimental capacities. Due to the close geographic distances, networking is important for all European nations and can be advanced by the CER-AFR coalition.

v. Public relation

Another objective of the joint effort is to create a forum between the public and the research reactor community about nuclear energy and research. It is important to establish a clear understanding between the risks involved in the operation of research reactors, and those involved in the operation of commercial power plants. It is a dialogue that, after the tragic accident at Fukushima, needs to be brought to the attention of all parties. The accident has created changes in the atomic energy

community, and impacted each European nation to a certain extent. As a consequence, an objective dialogue between the public and the research reactor community about the uses of research reactors and the use of neutrons in the fields of medicine, science, and technology should be created and openly debated in the international community. This dialogue will be more effective and powerful in an international co-operation, such as the CER-AFR coalition. Such a coalition will be able to demonstrate the potential of research reactors to the public and also at international conferences, workshops seminars etc. to a larger national and international audience.

4. Future perspectives

The CER-AFR coalition delivers an extension of the network between European research reactors. The members themselves have the possibility to decide about the content and future of the coalition. The success will also depend on the formation of bilateral collaborations between members of the AFR and CER, which could serve as a basis not only for a broad coalition between the research reactors of the AFR and the CER, and also be the beginning of an international cooperative effort between the research reactors of many European countries. It would support the tasks and responsibilities of the RROG in the future and help to build an efficient network between research reactors in Europe. This is one of the topics which will be discussed on the next joint meeting in March 2012 at the FRM II in Munich, Germany.

Ten Years of IAEA Cooperation with the Russian Research Reactor Fuel Return Programme

S. Tozser, P. Adelfang and E. Bradley
International Atomic Energy Agency,
PO Box 100, 1400 Vienna – Austria

ABSTRACT

The Russian Research Reactor Fuel Return (RRRFR) Programme was launched in 2001. Over the duration, the programme successfully completed 43 safe shipments of 1.6 tons of fresh and spent HEU fuel from different countries using Russian fuelled research reactors to the country of origin. The IAEA has been a very active supporter of the RRRFR Programme since its inception. Under the auspices of the RRRFR Programme, the Agency has been ensuring a broad range of technical advisory and organizational support to the HEU fuel repatriation, as well as training and advisory assistance for supporting RR conversion from HEU to LEU. The presentation gives an overview of the RRRFR programme achievements with special consideration of the IAEA contribution. These include an overview of the shipments' history in terms of fresh and spent fuel, as well as a summary of experiences gained during the shipments' preparation and termination. The presentation focuses on technical advisory support given by the IAEA during the programme implementation, captures the consolidated knowledge of the unique international programme and shares the most important lessons learned.

1. Introduction

The preparation for the Russian Research Reactor Fuel Return (RRRFR) programme started in December 1999 [1], when at the IAEA General Conference in September 1999, U.S. Energy Secretary, Bill Richardson announced that the US was prepared to work with Russia and the IAEA to manage and dispose of Russian-origin HEU RR fuel remaining in a number of countries. Between 1999 and 2000, this then led to a series of tripartite meetings organised by the IAEA to review the situation regarding fresh and spent Russian origin RR fuel in various locations around the world. The primary goal was to advance nuclear non-proliferation objectives by eliminating stockpiles of HEU and encouraging eligible countries to convert their research reactors from HEU to low enriched uranium (LEU) fuel upon availability, qualification and licensing of suitable LEU fuel. Then it was decided that the IAEA should send a letter to targeted member states to assess their interest in participating in a fuel return programme.

Thus, the IAEA took the initiative in the RRRFR programme, when in October 2000 the IAEA's Director General sent a letter to the governments of relevant countries for the elimination of HEU fuel from Soviet RRs. Fourteen out of sixteen responses were favourable, that concerned 20 RRs, which led to the launching of the RRRFR programme in 2001.

2. Shipments accomplished

Since the first shipment made in August 2002, the RRRFR programme successfully completed 43 shipments of 1.6 tons of fresh and spent HEU fuel from different countries using Russian fuelled research reactors to the country of origin.

2.1 Fresh RR HEU fuel shipments

In the case of fresh shipments from 2002 to 2010 under contract agreement by the IAEA, 21 shipments representing a total amount of about 600 kilograms of fresh HEU were returned safely to the Russian Federation. The shipments are listed in Table 1 in chronological order. The first actual step in the implementation of the RRRFR programme was in 2002 when the Serbian Government decided to shut down the RA reactor permanently in Vinča [2], and to participate in the international nuclear non-proliferation efforts to minimize HEU in international commerce. Thus the Republic of Serbia was the first IAEA Member State to return fresh HEU fuel to the Russian Federation that followed further twenty shipments.

Table 1. Fresh RR HEU fuel returned to Russia under IAEA contracts

No.	Country	Facility	Container used	Mode of transport	U-mass [kg]	Actual Finish
1	Serbia	RA, Vinča	TK-S16	Air transport	48.0	2002-08-08
2	Romania	WWR-S Magurela	TK-S16	Air transport	14.0	2003-09-30
3	Bulgaria	IRT-2000, Sofia	TK-S16	Air transport	17.0	2003-12-23
4	Libya	IRT-1 Tajura	TK-S16	Air transport	17.0	2004-03-07
5	Uzbekistan	WWR-SM Tashkent	TK-S16	Air transport	3.0	2004-09-09
6	Czech Republic	LWR-15, Rez	TK-S16	Air transport	6.0	2004-12-21
7	Latvia	IRT-M, Salaspils	TK-S16	Air transport	3.0	2005-05-25
8	Czech Republic	CA, CTU Prague	TK-S16	Air transport	14.0	2005-09-27
9	Libya	IRT-1 Tajura	TK-S16	Air transport	3.0	2006-07-25
10	Poland	MARIA	TK-S16	Air transport	39.8	2006-08-10
11	Czech Republic	Rez	TK-S16	Air transport	0.2	2006-10-15
12	Germany	RRR	TK-S16	Air transport	268.0	2006-12-18
13	Poland	MARIA	TK-S16	Air transport	8.8	2007-08-28
14	Vietnam	Dalat	TK-S16	Air transport	4.0	2007-09-17
15	Romania	Pitesti	TK-S16	Air transport	30.0	2009-06-28
16	Hungary	BRR	TK-S16	Air transport	18.6	2009-07-06
17	Czech Republic	Rez	TK-S16	Air transport	12.2	2010-06-18
18	Belarus	Minsk. Pamir fuel	TK-S16	Air transport	46.7	2010.11.29
19	Ukraine	Sevastopol	TK-S16	Air transport	25.1	2010.12.29
20	Ukraine	KINR	TK-S16	Air transport	9.8	2010.12.29
21	Ukraine	Kharkov 1 st	TK-S16	Air transport	15.7	2010.12.29

Last update: 2012-02-07

TOTAL 603.7

The features of fresh shipments can be summarised as follows:

- Shipments were accomplished under IAEA contracts (tripartite contracts where the Agency was the customer for the benefit of the consignor's country under the Technical Cooperation Project of "Repatriation, Management and Disposition of Fresh and/or Spent Nuclear Fuel from Research Reactors").
- The transport mode at each shipment was air-transport (AT);
- TUK 16S, Russian type containers were used; and
- Nearly the same preparatory and licensing procedures (including tripartite contract conditions), as well as shipment scenario was applied at each shipment.

2.2 Spent RR HEU fuel shipments

In contrast to the relatively simple and “standardised” fresh fuel shipments, shipment of the spent nuclear fuel (SNF) assemblies requires a more extensive preparation, including package design approvals, site preparation to be able to serve the transport containers, circumspect transport route and mode selection, trans-boundary shipment approvals (if the facility country don’t have common border with the RF) to transport SNF through the territory of a third country.

Table 2 shows shipments carried out under the RRRFR programme in chronological order. Since 2006, altogether 22 shipments from RR sites to RF were safely and successfully accomplished that mean a total amount of about 987 kg HEU SNF removal. The first, so called “pilot shipment” was accomplished in January 2006 followed by three other SNF transports from Uzbekistan. Russian type TUK-19 casks were used for the first four shipments, while later the newly developed Skoda type VPVR/M casks were also used for the shipments.

Table 2. Spent RR HEU fuel returned to Russia

No.	Country	Facility	Container used	Mode of transport	U-mass [kg]	Actual Finish
1	Uzbekistan	WWR-SM Tashkent	TUK-19	RW	10.0	2006-01-10
2	Uzbekistan	WWR-SM Tashkent	TUK-19	RW	13.0	2006-02-14
3	Uzbekistan	WWR-SM Tashkent	TUK-19	RW	14.0	2006-03-20
4	Uzbekistan	WWR-SM Tashkent	TUK-19	RW	26.0	2006-04-15
5 ^(*)	Czech Republic	Rez	VPVR/M	RW	80.0	2007-11-29
6	Latvia	Salaspils	TUK-19	RW	14.4	2008-05-12
7	Bulgaria	Sofia	VPVR/M	RW	6.3	2008-07-04
8	Hungary	BRR	VPVR/M	PR-RW- <u>SV</u> -RW	154.5	2008-10-10
9	Kazakhstan	Alatau	TUK-19	RW	17.3	2008-12-25
10	Kazakhstan	Alatau	TUK-19	RW	16.6	2009-03-01
11	Kazakhstan	Alatau	TUK-19	RW	18.8	2009-04-01
12	Kazakhstan	Alatau	TUK-19	RW	21.0	2009-05-01
13	Romania	Magurele	TUK-19	AT	23.7	2009-06-29
14 ^(*)	Poland	EWA	VPVR/M	PR-RW- <u>SV</u> -RW	190.1	2009-09-13
15	Libya	Tripoli	TUK-19	AT	5.2	2009-12-21
16 ^(*)	Poland	EWA, MARIA	TUK-19, VPVR/M	PR-RW- <u>SV</u> -RW	139.2	2010-03-18
17 ^(*)	Poland	MARIA	TUK-19	PR-RW- <u>SV</u> -RW	49.5	2010-05-23
18 ^(*)	Ukraine	KINR	VPVR/M	PR- <u>RW</u>	55.9	2010-05-25
19 ^(*)	Poland	MARIA	TUK-19	PR-RW- <u>SV</u> -RW	38.6	2010-07-24
20 ^(*)	Poland	MARIA	TUK-19	PR-RW- <u>SV</u> -RW	37.5	2010-10-10
21	Belarus	Minsk. Pamir	VPVR/M	RW	42.0	2010-10-24
22 ^(*)	Serbia	Vinča RA	TUK-19, VPVR/M	PR-RW- <u>SV</u> -RW	13.2	2010-12-17
TOTAL					986.8	

Last update: 2012-02-27

(*) = IAEA involvement; PR = Public Road (highway, truck); RW = railway; SV = seagoing vessel; AT = air transport

As it can be seen from Table 2 the transport modes show also a kind of “developments”. In the beginning the railway mode was licensed only, later (due to transit difficulties in a third country) in 2008, the sea transport than finally the air transport was applied in 2009. Now it can say that RR SNF assemblies can be transported by all modes. However it should be noticed that the TUK-19 type package still have only license for air shipment (Type “B” package according to the IAEA TS-R-1 [3]), while the VPVR/M

package is under an air shipment licensing procedure in RF to get, as the first in the world the Type “C” package design certificate [4].

Regarding SNF shipment preparation and termination, it means a very challenging and more painstaking preparation and implementation. Although the main steps are similar to the fresh HEU fuel, but is much more complex, more expensive and time consuming especially when the SNF should be transported through the territory of one or more transit countries. There is no way to apply a unified preparatory procedure, since each shipment requires special preparation. It should be pointed out that some procedural modules (fuel characterisation, safeguards control, loading procedures, package preparation to transport, etc.) and supplementary equipment (spacers, transport flask) can be applied for future shipments.

Preparation and termination procedures are beyond the scope of this paper (these matters are well described in IAEA-TECDOC-1632 [5]), but the main features of the SNF shipments can be summarised as follows:

- The legal frameworks as well as the contracting solutions look different from country to country. With the exception of the Vinča SNF removal, the main stakeholder to support and coordinate the shipments as well as the primary contractor was in all cases the US DOE NNSA. In the case of the Vinča SNF removal the coordination and primary contracting role was ensured by the IAEA.
- Each shipment is unique. It is not possible to give one set of general procedural rules (site preparation, licensing, etc.) for all shipments. However some procedural modules and supplementary equipment developed for previous shipments can be applied in future shipments.
- Special attention should be devoted to non-technical issues such as licensing matters, managerial activities, implementation of good communication process among the stakeholders.
- The site and SNF conditions significantly influence the preparatory works, therefore the results of the site survey as well as the fuel characterization play determinative role to define the site modification (upgrading) packing technology and mode (put the fuel assemblies as they are in a container or encapsulate prior to loading in the transport container) as well as application of supplementary equipment (filter system, transport flask, drying and vacuuming systems, etc.).
- The selection of the transport route and the modes of transport, including assigning reloading places from one vehicle onto another (if needed) are based on a case study where all circumstances of the transport with a stressed consideration to the safe and secure transport conditions are evaluated, and the best alternative is selected.
- Preparation entails serious planning and staff training.
- Typically a multinational team from four-five countries have to support the facility’s operators at fuel loading (not taking into account radiation and physical protection services of transit countries).
- It is typical also that along the entire transport route significant radiation protection and defence forces are mobilised to secure the shipment operation.

3. IAEA contribution and support activities

Under the auspices of the RRRFR programme, the Agency has been ensuring a broad range of technical, advisory and organizational support to the HEU fuel repatriation, as well as training and advice to support RR conversion from HEU to LEU since core conversion is mandatory for reactors to participate in the RRRFR programme. Particularly the Department of Nuclear Energy and the Department of Nuclear Safety and Security as well as the Department of Technical Cooperation and of course the Office of Procurement Services, play a key role in arranging fresh and spent fuel shipments, assisting in the planning of fuel return projects, and providing technological support for member states (MSs) participating in the RRRFR programme. This section provides an overview of the IAEA’s contribution in the RRRFR programme and summarises the support it provides to the MSs.

In general, the Agency's role in supporting projects like the RRRFR programme is threefold: (1) verification made by Safeguards; (2) standardization ensured by published IAEA Safety Standards (e.g. Nuclear Safety-, Transport-, Emergency preparedness-, Waste management standards, etc.); and (3) technical cooperation ensuring multidisciplinary backing for MSs throughout technical cooperation mechanisms. The first two supports are a continuous Agency service for the MSs. From RRRFR programme's viewpoint the third group plays a significant role through which programme specific supports have been provided.

Regarding technical cooperation mechanisms with regard to the RRRFR programme the support activity of the Agency can be divided into four groups:

- Traditional support
- Programme specific technical cooperation
- Advisory support
- Collecting and dissemination practices

3.1 Traditional support

The traditional support is typically an integral part of a TC project launched by the Agency that means in general: outlining a project, organising technical meetings, conducting fact finding missions, equipment and service procurements (issuing call for bids, contracting, procurements and appraisal of deliverables), etc. Some of the most significant IAEA cooperation with regard to RRRFR programme support are as follows:

- Organising bilateral and multilateral meetings (nearly hundred meetings were organised including the organisation of the first serial of the tripartite initiative meetings in 1999 -2000);
- Fact find missions between 2001-2004 (15 RR sites in 11 countries were surveyed);
- Agency is one of the contracting parties in case of fresh HEU shipments (21 contracts with its entire procurement support from the issuing call for bids to the deliverables' evaluations);

3.2 Programme specific technical cooperation

Within the framework of IAEA's Technical Cooperation projects two significant subject specific projects were launched: (1) Skoda VPVR/M cask procurement; (2) Vinča (Serbia) SNF return programme.

3.2.1 Skoda VPVR/M cask procurement

Transporting a large quantity of SNF stored at many of Russian origin RRs required to develop suitable new capacity packages for the RRRFR programme to haul all of the stored SNF with one shipment from some facilities (at the beginning 16 pcs. TUK-19 casks were available), and in addition ensure further transport package alternatives with an improved cask loading technology to meet the needs of the different RR site and SNF conditions stored at a facility. To assist in resolving this demand, the IAEA agreed to use their procurement system to send out a call for bid and procure enough casks to meet the foreseen shipment needs. After the bidding procedure the VPVR/M cask system of Skoda (Czech Republic) was selected from six international cask vendors. The Skoda proposal not only met all of the scope requirements, but also provided additional benefits to the programme: had NRI's offering to provide to the RRRFR programme their six VPVR/M casks after completing the transfer of their SNF to Russia.

The IAEA procured ten high capacity dual purpose (transport/storage) containers under a 4 million Euro contract. The complex procurement and implementation included outlining the technical requirements,

evaluations of bids, contracting, quality inspections, evaluation of the results of the so called “dry run” and “wet run” tests [6].

Thus, due to this procurement the programme has now 16 VPVR/M casks and 16 TUK-19 casks. A comparison table of casks’ utilisation is presented in Table 3 [7].

Table 3. Comparison table of casks’ utilization

Cask	Casks available, since	Total No. of shipment used	Total No. of cask used	Total No. of FAs shipped	Total HEU mass
TUK-19	16 pcs, Jan 2006	16	275	1100	357 kg
VPVR/M	16 pcs., May 2008	8	86	3096	623 kg

3.2.2 Vinča (Serbia) SNF return programme

The first TC project after the re-admittance of the country was started in 2001 that was then followed by several specific projects. The strategic objectives of these projects were firstly to survey the Vinča site, identify the real conditions of the SNF as well as stabilize its conditions (prevent as much as possible the escalation of further degradation) and achieve a long term safe and stable state [8].

From 2004 the IAEA, the Nuclear Threat Initiative (NTI), the US-DOE and the European Union provided funds to cover the Vinča RA Reactor SNF removal¹. With such financial support, upon the invitation of the IAEA, in May 2005 an international consultancy meeting was held in the Vinča Institute. The main goal was to draft the outlines of an international bid for the removal and transportation technology of the seriously corroded and leaking SNF assemblies in the storage pool adjacent to the reactor building. At the conclusion of this meeting an international tender was issued by the IAEA in the summer of 2005. An RF consortium was selected and an international tripartite contract between the IAEA, RF consortium and the Vinča Institute was signed in September 2006 for the safe removal of SNF from the Vinča RA Reactor and return to the RF (Vinča SNF return programme).

For the implementation of the tripartite contract consistently with the TC management principle a special PMO was appointed by the Agency to coordinate the programme implementation in all respect. During the programme performance, 16 technical officers, and two technical experts were assigned to the Project Management Unit at Vinča site. Thus, the Agency not only contracted, but provided a general coordinative managerial support, as well as an overall technical backing for the operating organisation and the officers of the regulatory body [9].

The project was completed as planned in December 2010: 8030 SNF was removed representing more than two-and-half tonnes of highly radioactive spent fuel [10]. This transport was the largest single shipment of SNF made under the RRRFR programme, and also this project became the largest and most complex TC project in the history of the IAEA with a total budget of over USD 55 million.

3.2.3 Advisory support

Advisory support was provided either upon demand by a regulatory body or a stakeholder involved in the shipment preparation:

- **Support provided upon the demand of a regulatory body.** The goal was to assist and advice the regulatory body to review the safety documentation prepared for a shipment, and assist onsite inspection. This support mainly was ensured in the form of a safety mission, as well as follow up missions with the involvement of external experts. During these missions the items reviewed were focused on QA/QC, training and education programs, and their implementation in the practice, as

¹ In 2004, a so called Vinča Institute Nuclear Decommissioning programme (VIND) was launched objective of which covers not only SNF removal but includes RA Reactor decommissioning, radioactive waste management and on-site radiation protection logistic.

well as on applied radiation protection measures, waste- and emergency preparedness programs. The communication mechanism was always an issue in reviewing and implementing the lessons learned. Altogether four missions were conducted three of which concerned the Vinča project [11].

- **Support provided upon demand of a stakeholder.** This technical and advisory support was mostly case specific interactions requested by the operating organisations and/or stakeholders (contractual parties or even authorities). This contribution encompassed mainly the following four activity fields: (1) feasibility consideration and technology selection; (2) documentation preparatory support, (3) licensing support (local and trans-boundary licensing supports), (4) on-site technical review and advisory support to implement equipment [12].

3.2.4 Collecting and dissemination practices

Regional lessons learned workshops. As the first shipments were completed, experts were brought together to share their experience and knowledge with those who would be dealing with fresh and spent fuel shipments in the future under the umbrella of RRRFR programme. In 2005, the IAEA in cooperation with the US DOE initiated a yearly regional workshop on “Russian Research Reactor Fuel Return Programme Lessons Learned”. The primary objective was – and still is – to bring together the core players in the preparation and accomplishment of shipments, and sharing experiences on lessons learned so that others may benefit in the future. Accordingly the invited participants represent facility operators from 16 countries², regulatory bodies, stakeholders ensuring financial and coordination support for the programme, as well as companies actively being involved in the programme completion on a contractual basis.

Table 4 shows the history of the Regional Workshops. Although the meeting indicated in the second row was a workshop on “International Legal Framework Applicable for Shipment of Russian-origin Research Reactor Spent Fuel to the Russian Federation” that replaced the annual regional workshop in 2007, but its main feature was gathering experience. Thus altogether six workshops on lessons learned were organised.

Table 4. History of the Regional Workshops on RRRFR programme Lessons Learned¹

No	Place	Date	Participants
1	Belgrade, Serbia	October 2006	75 participants from 15 countries
	Poina-Brasov, Romania ⁽¹⁾	April 2007	43 participants from 10 countries and EU
2	Rez, Czech Republic	May 2008	97 participants from 17 countries
3	Varna, Bulgaria	June 2009	88 participants from 17 countries
4	Poina-Brasov, Romania	May 2010	71 participants from 16 countries
5	Jackson, WY-USA	June 2011	95 participants from 17 countries
6	Lake Balaton, Hungary	Scheduled for 2012	

(1): It was a Workshop on “International Legal Framework Applicable for Shipment of Russian-origin Research Reactor Spent Fuel to the Russian Federation” organised by the IAEA in cooperation with the European Union.

Regarding the workshop scenario, workshops traditionally consist of a series of review lectures given by the leading experts, followed by status reports from facilities, and round table discussions of relevant problems and tasks. The main benefit of the workshop is to exchange experience and methods for effective performance of RRRFR, to discuss, consider technical, legal, logistical, administrative and other experiences obtained during the programme implementation, as well as draw conclusions and lessons learned for improving safety, radiation protection and physical protection while shipping fresh and spent fuel. Experience shows that the annual workshop on lessons learned is an important tool in collecting and

² Belarus, Bulgaria, Czech Republic, Germany, Hungary, Kazakhstan, Latvia, Poland, Romania, Russian Federation, Serbia, Slovenia, Ukraine, USA, Uzbekistan, Vietnam

disseminating information. After the first three-four workshops it was a common understanding the Lessons Learned Workshops ensure a stand-alone forum to exchange experiences (applied practices, methods, developed and implemented special auxiliary equipment, tools, etc.) and lessons learned, as well as capturing the consolidated knowledge of this unique international historical programme.

IAEA-TECDOC booklets issued for support RRRFR programme objectives. The IAEA-TECDOC publications mean another effective tool to disseminate practical information and experiences. On the basis of the gathered experience during RRRFR programme's implementation the Agency issued four booklets to support the programme implementation. They are:

- B. Yuldashev and J. Thomas: Technical and Administrative Preparation for Shipment of Russian-origin Research Reactor Spent Fuel to Russian Federation. IAEA Guideline document. Vienna, Austria. February 2007. This guideline document provides key information for the planning and return of Russian-origin SNF or materials containing HEU to the RF.
- IAEA-TECDOC-1593: Return of Research Reactor Spent Fuel to the Country of Origin: Requirements for Technical and Administrative Preparations and National Experiences. July 2008. This IAEA-TECDOC is a proceedings of technical meeting held in Vienna, August 2006 summarising shipment experiences 32 shipment preparation and operation experiences made under the umbrella of USA Foreign Research Reactor Spent Nuclear Fuel (FRRSNF) acceptance programme and RRRFR programme.
- IAEA-TECDOC-1632: Experience of Shipping Russian-origin Research Reactor Spent Fuel to the Russian Federation. November 2009. This IAEA-TECDOC is an extended summary and account of the experience obtained from the completion of international projects on return SNF to the RF from RRs in Uzbekistan, Czech Republic, Latvia, Bulgaria and Hungary;
- Draft of IAEA-TECDOC: Legal Aspects of Spent Nuclear Fuel Repatriation to Russian Federation - Lessons Learned. The need for a multilateral approach to reviewing both national and international legal obligations connected with the international transport of the SNF was first raised in the context of LL workshop held in Belgrade 2006. The TECDOC focuses on the national and international legal aspects of SNF fuel to the RF from RRs located in a number of States in central and Eastern Europe.

4. Look into the Future

The Agency will continue to support RRRFR programme. This support encompasses the core conversion efforts of RRs since core conversion being is mandatory for reactors to participate in the RRRFR programme. A status review of the foreseen shipments intending to be accomplished under the umbrella of the RRRFR programme is shown in Table 5.

As it can be seen after the core conversion six RR SNF shipments are still due between 2012-2016. Three postponed shipments from Germany are hanging, shipment dates of which are not scheduled yet. Also three fresh HEU shipments are still due. Service contract for Kharkov (Ukraine) was signed in October 2011, the shipment is due in March 2012, the remaining fresh at MARIA in Poland is scheduled by the end of 2012, but the fresh HEU from Minsk (Belarus) still not scheduled yet.

Table 5. Status review of the foreseen shipments

Location	Facility name	Type	Power	Core conversion		Due shipments
				Start	End	
Due HEU SNF shipments						
Kiev, Ukraine	WWR-M	Tank type	10MW	Jan 2011	2013	March 2012
Taschkent, Uzbekistan	WWR-SM	Pool type	10 MW	March 2008	Nov. 2009	December 2012
Rez, Czech Republic	LVR-15	Tank type	10 MW	Febr 2010	Sept 2011	December 2012
Budapest, Hungary	BRR	Tank type	10 MW	Sept 2009	Dec. 2012	December 2014
Dalat, Vietnam	Dalat RR	Pool	500 kW	–	–	December 2012
Svierk, Poland	MARIA	Pool type	30 MW	July 2012	Jan 2014	2016
Germany, Rossendorf	–	–	–	–	–	3 postponed SNF shipments (no scheduled date yet)
Due HEU fresh shipments						
Kharkov, Ukraina	–	–	–	–	–	March 2012
Svierk, Poland	–	–	–	–	–	December 2012
Minsk, Belarus	–	–	–	–	–	No scheduled date yet

5. Summary and conclusions

The RRRFR programme was launched in 2001. The programme has successfully completed 43 shipments of 1.6 tons of fresh and spent HEU fuel from different countries using Russian fuelled research reactors to the country of origin. Since the programme inception the IAEA, in cooperation with US DOE, Russian Federation, European Union, and a number of individual Member States has provided important overall technical support in the effort to return HEU RR fuel to the RF.

In this cooperation, the Agency utilizes all its mechanisms available through its regular Agency programme and Technical Cooperation Programme to advance Member States and the international non-proliferation efforts to eliminate stockpiles of HEU fuel. The Agency's contribution overlaps a broad range of technical, advisory and organizational support from usual Agency services (safeguards, standardization, procurement, meeting organizing) with the programme specific supports. With regard to the RRRFR programme, the following two contributions by the Agency should be emphasised: (1) procurement of ten high capacity of dual purpose (transport/storage) containers; (2) Complex support of Vinča (Serbia) SNF return programme, which resulted (i) the largest single shipment of SNF made under the RRRFR programme, and also (ii) the largest and most complex TC project in IAEA's history total budget over USD 55 million.

The Agency initially contributed in collecting and disseminating practices when, in cooperation with the US DOE, initiated in 2005 to organise annually a Regional Workshop on Lessons Learned. The primary objectives were – and still are - to bring together the core players in the preparation and completion of shipments, and sharing the lessons learned, so that others may benefit in the future. And also, on the basis of that experience the Agency issued four TECDOCs to support proactively the programme implementation. Experience shows that the annual lessons learned workshops as well as the TECDOCs are important tools in collecting and dissemination practices.

The Agency's contribution in implementing the RRRFR programme includes a wide-range of professional support, which is provided almost immediately on the demands of the stakeholders. The

continuous advice and expertise contributed greatly to the smooth shipment preparations and operation, and helped to ensure that all the 43 shipments were accomplished safely according to schedule. In summarising, the following may be concluded:

- Special attention should be devoted to „non technical” issues such as managerial activities, licensing matters and implementation of good communication process among the stakeholders. It is important that all activities are well planned, controlled and documented.
- While the fresh shipment operations can be implemented on a more or less standardised way, in case of SNF shipment some procedural modules and supplementary equipment developed at previous shipments can be applied for future shipments. Each SNF shipment preparation and operation is unique.
- While the IAEA fulfilled its advisory and coordination assistance, the Agency unintentionally played the role of a mediator amongst the stakeholders, which consequently yielded additional Agency support: a kind of “charity mission” to resolve conflicts between core actors and strengthen trust issues amongst the contractual parties.

References

- [1] P. Adelfang, I.N. Goldman, E. Bradley and D.O. Jincuk: IAEA Cooperation with RERTR and Spent Fuel Return Programmes: a Retrospective and Future Look. 30th International Meeting of RERTR, October 5-9, 2008. Washington D.C., USA.
- [2] M. Pešić, O. Šotić, W. H. Hopwood Jr.: Transport of HEU Fresh Fuel from Yugoslavia to Russian Federation, Nuclear Technology & Radiation Protection, Vol. XVII, No. 1-2, 71-76 (2002).
- [3] IAEA-TECDOC-1593: Return of Research Reactor Spent Fuel to the Country of Origin: Requirements for Technical and Administrative Preparations and National Experiences. Proceedings of a technical meeting held in Vienna, August 28-31, 2006. Vienna, Austria, July 2008.
- [4] S.V. Komarov at all: Licensing Air and Trans-boundary Shipments of Spent Nuclear Fuel. CN-187 - International Conference on the Safe and Secure Transport of Radioactive Materials, Vienna, 17-21 October 2011.
- [5] IAEA-TECDOC-1632: Experience of Shipping Russian-origin Research Reactor Spent Fuel to the Russian Federation. November 2009, Vienna, Austria.
- [6] M. Tayack at all: Development of new transportation/storage system for use by DOE Russian Research Reactor Fuel Return Program. Packing, Transport, Storage & Security of Radioactive Material. 2010 vol. 21. No. 2 pp 111-121.
- [7] F. Svitak: Experience Gained from Skoda VPVR/M Cask Use for RRRFR programme. Regional Workshop on RRRFR Program Lessons Learned. 7-10 June 2011, Jackson Hole, Wyoming US.
- [8] E. Bradley, M. Pešić, J. Kelly, P. Adelfang, I. Goldman and D. Jinchuk: Repatriation of Vinča RA reactor spent fuel. PATRAM (Packaging, Transport, Storage & Security of Radioactive Material) Journal, 2009, Vol 20, No 2, pp 55-59.
- [9] S. Tozser at all: IAEA’s Technical Advisory Support of Vinca’s SNF Repatriation in the Final Preparatory Stage of the Shipment. RRFM-2011, Rome, Italy, 20-24 March 2011.
- [10] O. Šotić, R. Pešić: Nuclear Fuel Shipments for the Republic of Serbia. RRFM-2011, Rome, Italy, 20-24 March 2011.
- [11] J.P. Boogaard, H. Abou Yehia: IAEA’s Safety Review of Vinča’s Spent Nuclear Fuel Repackaging Operation. RRFM 2010. 21 -25 March 2010, Marrakech, Morocco.
- [12] S. Tozser, P. Adelfang, J. Boogaard, J. Kelly and O. Sotic: Status Report on the SNF Repatriation Project from Vinca Institute. RERTR-2010, October 10-14, 2010, Lisboa, Portugal.



Poster

USE OF SPECIALIZED MEASURING SYSTEMS FOR RADIATION MONITORING AT MR RESEARCH REACTOR IN NRC “KURCHATOV INSTITUTE”

V.G. VOLKOV, A.V. GERASOV, Y.A. ZVERKOV, A.V. LEMUS,
S.G. SEMENOV, S.Y. FADIN, A.V. CHESNOKOV, A.D. SHISHA

*Scientific & Technical Department “Rehabilitation”, National Research Centre “Kurchatov Institute”
1, Kurchatov Sq., 123182 Moscow – Russia*

ABSTRACT

In 2011 NRC “Kurchatov Institute” started dismantling the systems and equipment of its 50-MW research reactor MR – a channel-type reactor submerged into a water pool and equipped with nine loop-type facilities. Long and intensive operation of the MR reactor itself and its loop-type facilities resulted in elevated radioactive contamination of systems and equipment and in high gamma radiation fields, which existed in the reactor rooms by the moment of its final shutdown. This radiation situation largely complicates the performance of required operations, and also caused considerable difficulties in 2008–2010, while the reactor was being prepared for decommissioning. Works in high radiation fields are conducted with the application of remote-control techniques and devices allowing the dose burden on the personnel to be reduced. Towards this end, specialized measuring systems were developed, which allow the personnel to monitor the radiation conditions, make measurements and obtain necessary data by means of remote control.

1. Introduction

Between 2008 and 2010, NRC “Kurchatov Institute” has completed preparatory works for decommissioning of its 50-MW research reactor MR and in 2011 started dismantling its systems and equipment [1]. This reactor has been launched in 1964 and finally shut down in 1993. In construction terms, MR was a multi-loop channel-type reactor submerged in a water pool. It was equipped with nine loop-type facilities cooled by water, steam-water mixture, gas or liquid metal. Systems and equipment of the reactor and its loop-type facilities were installed in over 70 technological rooms all located in a single building – that is, their arrangement was very dense.

As a result of long-term and intensive operation, systems and equipment of both the reactor and its loop-type facilities have received considerable radioactive contamination, which has produced high gamma radiation fields (~20 mSv/h and more) in the technological rooms by the moment of reactor final shutdown. This radiation situation in the rooms largely complicates the performance of required operations. Working in high radiation fields requires the application of remote-control techniques and devices allowing the dose burden on the personnel to be reduced. Towards this end, specialized measuring systems allowing the personnel to monitor the radiation conditions and make necessary measurements by means of remote control were developed and are currently in place. These systems make it possible to: monitor radiation in the working area online; timely detect and diagnose various high-level gamma sources; and identify nuclear fuel and fission products’ availability. The same systems are used for remote-control process operations performed with the BROKK robotics: with BROKK-90 robot used to explore high-level sources, and BROKK-50, -90, -160, -180, -330 and -440 robots – for these sources’ extraction, fragmenting (when necessary) and packaging into containers.

2. Specific features of radiation monitoring at MR reactor

Radiation monitoring at MR reactor is performed by the basic system and the auxiliary system. The basic system uses standard dosimetric devices, such as threshold detectors equipped with light and sound alarms, and portable devices for aerosol activity monitoring.

This system assures continuous radiation monitoring by measuring gamma dose rates and volumetric activity of radionuclides in the air of all the reactor and loop-type facilities' rooms. When necessary, this system could be supplemented with portable threshold detectors to be installed near working areas.

The auxiliary system is based on specialized radiometric, spectrometric and other systems used to enhance monitoring efficiency and response rate in the course of actual work. These specialized systems include: Gamma Pioneer radiometry complex [2]; Gamma Locator portable spectrometer system [3]; Gamma Visor portable system producing gamma images [4]; and a system of video cameras.

Gamma Pioneer radiometry complex is equipped with an integral detector, a collimated detector and a video camera with high optical resolution. The first one allows dose rates ranging from 0.4 mSv/h to 8.5 Sv/h to be measured. The second measures gamma radiation fluxes within its collimation angle, thus making it possible to identify the contribution of any specific direction to the total radiation flux. This radiometry complex is equipped with a detector signal data-processing unit. The complex can communicate with operator control unit by either radio or cable. The control unit monitor displays a video image of the explored object together with the measuring results, which are recorded. The complex is installed on BROKK-90 robot, so it can be used for remote gamma/video scanning of various high-level objects (such as reactor loop-type channels, metallic canisters with radioactive waste extracted from storage cells during their survey, and other objects). The BROKK-90 robot is controlled and steered towards the objects to be explored on a remote basis, using the pre-installed system of video cameras connected with the operator control unit. The radiometry complex measuring detectors are steered to the target on the basis of video image transmitted to the operator control unit from these video cameras.

Portable spectrometer system Gamma Locator includes: a spectrometric collimated gamma detector; a colour video camera coupled with the collimator; and a control unit. The spectrometer system uses three mutually replaceable detectors. Two of them are based on scintillator-photodiode optical couple with CsI(Tl) scintillators of different sensitivity. The third is a semi-conductor detector CdZnTe registering the characteristic radiation of uranium in the spectra emitted by explored objects, thus allowing the presence of uranium to be identified in these objects with the help of dedicated methodology. This spectrometer system is connected with the operator control unit by cable, so it can be used for remote survey of reactor loop-type channels, canisters or containers with radioactive waste and other high-level items.

The portable system producing gamma images – Gamma Visor – is intended for exploring various high-level objects and producing visual gamma images of their radioactive contamination. Compared with previous similar devices, this portable Gamma Visor has a rotating coding aperture producing gamma images in mask/anti-mask positions. The system can be controlled remotely, due to the cable connecting it with its operator control unit.

These specialized systems allow the operating personnel to solve a variety of tasks connected with more details or more complete data required on: current radiation conditions in technological rooms and working areas; high-level gamma radiation sources available in these rooms; character and composition of their radionuclide contamination; and other parameters. These systems can be used both together and separately, depending on the specific task to be solved and the data to be obtained.

3. Radiation monitoring during the works in the MR central hall

Available experience shows that radiation conditions in contaminated rooms, where works are being performed, usually depend on many factors, such as: contamination level and geometry of rooms; contamination level and positioning of equipment; nuclide composition of contamination; and some others. During the works their respective contributions to radiation situation can vary. This circumstance requires analysis of available gamma radiation sources and their respective contributions to the total dose rate. For this purpose, the specialized systems described in the previous chapter can be used quite efficiently. In particular, the works in the MR central hall have considerably deteriorated the radiation conditions there – the dose rate in this hall at 1-meter height from its floor was 30–50 μ Sv/h average. This was

due to partial opening of the plate floor and the storage pool containing high-level working and loop channels, as well as to the need to accommodate contaminated robots used in certain works and radioactive waste containers in the same hall. Deteriorated radiation conditions required certain corrective measures to be taken in order to reduce the dose burden on the personnel. Towards this end, the whole central hall was scanned with Gamma Locator system. This scanning has made it possible to identify all gamma radiation sources influencing the radiation situation and to estimate their respective contributions to the total dose rate (Fig. 1).



Fig. 1. Estimated contributions from various gamma radiation sources to the radiation situation in the MR central hall, $\mu\text{Sv/h}$

Analysis of scanning results has shown that the dose rate contributions from the opened plate floor, storage pool and waste containers were decisive. Consequently, in order to improve the radiation conditions, it was decided to: rearrange the equipment and waste containers; decontaminate the equipment and the contaminated spots detected on the central hall floor; and install a shady shielding made of lead sheets. These measures have partially improved the radiation situation in the central hall – the dose rate there at 1-meter height from its floor decreased to 15–20 $\mu\text{Sv/h}$. This made it possible to identify the safest personnel paths and temporary workplaces with acceptable radiation conditions in this hall. Similar approach was also used to organize and perform dismantling operations in the technological rooms accommodating loop-type facilities. Towards this end, all these rooms and equipment they contained were first scanned using the systems described above. Analysis of scanning results has shown that the equipment was contaminated unevenly. However, considerable level of this contamination coupled with high density of equipment positioning has made it impossible to select the dismantling sequence, which would be the best optimum from the viewpoint of improving the radiation conditions in these rooms. For this reason, the scanning results were used to select the most efficient equipment dismantling and cutting methods allowing these works to be performed on a remote-control basis, with the lowest possible dose burden on the personnel.

4. Radiation monitoring of working and loop channels' extraction from the MR storage pool

MR operating lifetime has lead to accumulation of above 150 working and loop channels stored in the storage pool in the reactor central hall. These channels represent long elements of reactor and loop facility equipment and differ by their structures. Parts of these channels that have operated in the reactor core were subject to intensive neutron radiation, while the rest were contaminated with fission and activation products. As a result, dose rates at 1-meter distance from some channels were as high as 0.3 Sv/h. This circumstance considerably complicated these channels' extraction from the storage pool, fragmentation and removal from the central hall.

These works were performed in several stages and used the specialized systems described above. For this purpose, the above systems were deployed on prescribed spots near the storage pool, and then the channels were successively extracted from the storage pool by the central hall crane and measured as follows. First, these channels were scanned by Gamma Pioneer radiometer system. During the scanning, video images of channels being scanned, together with the results of their integrated and collimated detector measurements, were displayed on the control unit monitor and recorded by video-recorder. Gamma images of radioactive contamination of scanned channels superposed with their visual images were produced by portable Gamma Visor system (Fig. 2a). After that, on the basis of analysis of scanned results and measured spectra, activity distribution along each channel was identified using the methods developed specifically for this purpose (Fig. 2b).

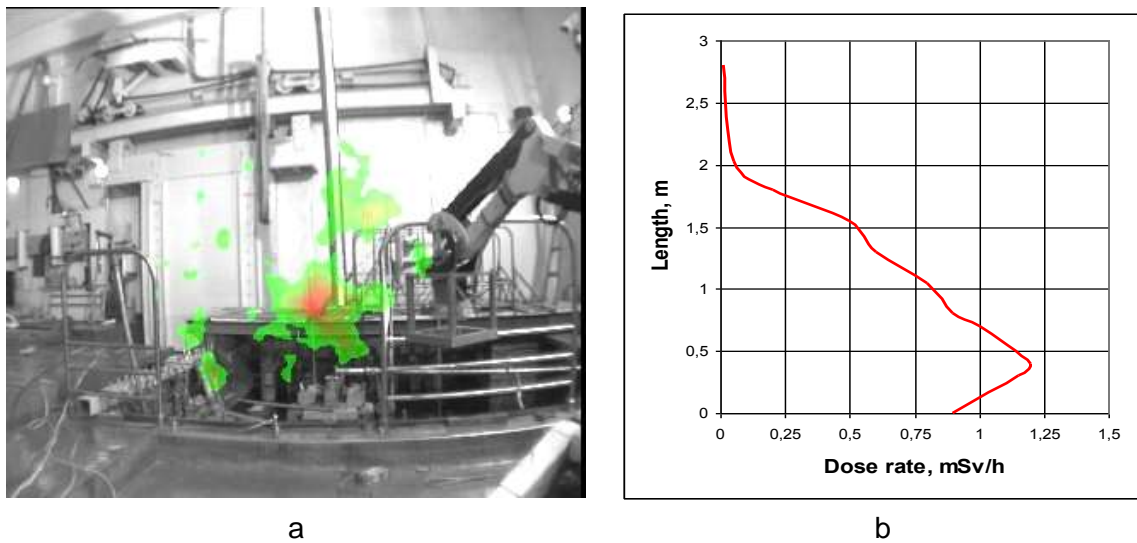


Fig. 2. Gamma image of one channel superposed with its video image (a) and activity distribution along the channel (b)

The nuclide composition of contamination in scanned channels was identified on the basis of their radiation spectra measured by Gamma Locator spectrometer system. Results analysis has shown a considerable extent of unevenness in the activity distribution along the channels, with the highest levels registered in the parts that have been inserted in the reactor core. The basic dose-forming radionuclides are ^{60}Co and ^{137}Cs , however in the spectra measured in some channels other radionuclides – such as ^{94}Nb , for instance – were also detected.

Analysis of activity distribution along channels, as well as of their gamma images, has made it possible to identify the spots, where the channels should be cut to separate their high-level parts, which required packaging into special canisters.

After that, the patterns of further fragmentation of cut-of parts were developed to allow optimal container packaging of all fragments with account of their respective activities.

Channel cutting, fragmentation and container packaging operations were subject to remote control and were performed by BROKK robots equipped with all necessary attachable implements (Fig. 3). Robots' steering towards channel cutting or fragmenting spots, as well as channel fragments' sorting depending on their activities, were based on the results measured by the above specialized systems.



Fig. 3. Cutting and fragmentation of channels using BROKK robotics

5. Conclusion

NRC “Kurchatov Institute” is performing pre-decommissioning and equipment dismantling works at MR research reactor in conditions of high radiation fields. In order to reduce and control the operating personnel exposure during these works, a radiation monitoring system was developed and now in place onsite. This system applies both standard and portable specialized devices to measure the parameters responsible for radiation conditions. The portable specialized devices were developed specifically for performing radiometric, spectrometric and other measurements, and for obtaining the necessary data by means of remote control. These devices allow online monitoring of radiation conditions in working areas and timely detection and diagnostics of various high-level gamma radiation sources, including detection of nuclear fuel and fission products’ availability.

The same devices are successfully used to control BROKK robotics, which extract, fragment (when necessary), sort and package the detected gamma sources into containers, which is done on the basis of measured results and visualized activity distributions.

Combined application of robots and these specialized portable remote-control devices allows dose burdens on the personnel to be reduced to by 2 mSv/year – while the established limit makes 20 mSv/year.

Use of specified portable devices could be also helpful and efficient during research reactor operation, for example, in the course of maintenance or repairing of their equipment and systems.

6. References

- [1] Volkov V.G., Zverkov Yu.A., Kolyadin V.I., et al. Preparation for decommissioning of MR research reactor in the RRC “Kurchatov Institute”. – Atomic Energy, 2008, vol. 104, issue 5, p. 259–264 (in Russian).
- [2] Stepanov V.E., Smirnov S.V., Lemus A.V., et al. Application of collimated radiometer system mounted on the robot for inspection of SNF storage of MR research reactor in the RRC “Kurchatov Institute”. – Atomic Energy, 2010, vol. 109, issue. 3, p. 162–165 (in Russian).
- [3] Stepanov V.E., Smirnov S.V., Ivanov O.P., et al. Remotely-controlled collimated detector to measure the distribution of radioactive contamination. – Atomic Energy, 2010, vol. 109, issue 2, p. 82–84 (in Russian).
- [4] Danilovich A.S., Smirnov S.V., Stepanov V.E., et al. Application of portable gamma camera for the control on extraction of the radioactive wastes from temporal storage at the territory of the RRC “Kurchatov Institute”. – In: Proc. of ICEM05/DECOM05 (Scotland, Glasgow, 2005), Abstract Book, p. 97.

METHODOLOGY FOR GAP MEASUREMENT IN THE FUEL ELEMENT FABRICATED AT IPEN

M. DURAZZO, D. GOMES da SILVA, L. R. SANTOS, E. F. URANO de CARVALHO,
H. G. RIELLA,

Nuclear and Energy Research Institute – IPEN/CNEN-SP

Av. Prof. Lineu Prestes, 2242 – Cidade Universitária – São Paulo, SP - CEP: 05508-000, Brazil

ABSTRACT

The use of radioisotopes in medicine is certainly one of the most important social uses of nuclear energy. The Nuclear and Energy Research Institute - IPEN occupies a special position in the history of nuclear medicine in Brazil as a producer of radioisotopes. Due to the serious international crisis in the supply of this material, Brazil has decided to build a new nuclear research reactor, the Reator Multipropósito Brasileiro – RMB (Brazilian Multipurpose Reactor), in order to assure the supply of radioisotopes to the Brazilian market. Since 1988, IPEN has fabricated the fuel for the research reactor IEA-R1. It was decided that the new reactor RMB will use the same type of fuel that is used in the IEA-R1 research reactor, with an increase in uranium concentration from 3.0 to 4.8 g/cm³ using silicide technology. These new fuel elements will operate in conditions more severe than those currently found in the IEA-R1. Thus, it becomes necessary to develop a methodology to measure the gap between fuel plates inside the fuel element, in order to generate quantitative data to ensure that the cooling channels dimensions of the fuel element meet the specification. Currently, as the IEA-R1 fuel element is operating at low power, it requires just a gap checking with a gauge-type device. However, under the more severe operating conditions of the new higher power reactor RMB, a quantitative gap measurement is necessary to ensure the perfect performance of the fuel element. This paper describes a methodology and its device to perform the gap measurement.

1. Introduction

The use of radioisotopes in the medicine certainly is one of the most important social uses of the nuclear energy. Distributed for hospitals and clinics by the whole country, radiopharmaceutical products assist more than three million patients a year. The Nuclear and Energy Research Institute - IPEN occupies a special position in the history of the nuclear medicine in Brazil, developing and producing radiopharmaceuticals starting from radioisotopes produced in the nuclear research reactor IEA-R1, being responsible for 98% of the current total demand. The Brazilian demand for radiopharmaceuticals has been growing continually through the years, in a regime of approximately 10% a year.

The recent serious world crisis in the supply of radioisotopes caused serious impact in Brazil. To face that situation, Brazil decided to build a new nuclear research reactor, denominated Reator Multipropósito Brasileiro – RMB (Brazilian Multipurpose Reactor), with larger power than the current reactor of IPEN, in order to guarantee the supplying of radioisotopes to the Brazilian market [1].

Since 1988 IPEN has been manufacturing the fuel for the IEA-R1 reactor of IPEN, being the unique Brazilian manufacturer of this type of fuel [2,3,4]. It was decided that the new reactor RMB will use the same type of fuel than the reactor IEA-R1, increasing the uranium concentration to $4,8 \text{ g/cm}^3$ with the uranium silicide technology, in a first stage, and possibly to 7 g/cm^3 with the U-Mo alloy technology, in a second stage. The new fuel elements for the RMB reactor will operate in much more severe conditions than the ones found now in the IEA-R1 reactor of IPEN. The minimum channel gap is one of the parameters in the calculations for the hot channel and for this reason the tolerances are in most cases included in the thermodynamic calculation and the safety report. Then, a work was started seeking to develop and to implement in IPEN a methodology to measure the gap between fuel plates in the fuel element, generating quantitative data that will guarantee the dimensions of the cooling channels. Now, due to the low operational request of the fuel element operating in the IEA-R1 reactor, which has low power, just verification with pass-not-pass type calibers is enough to guarantee the dimensions of the cooling channels.

The quantitative data for cooling channels dimensions were obtained during the fuel element assembling process through a device fitted to the roll swaging machine that fix the fuel plates to the side plates. These measures will be part of dimensional analysis to qualify the fuel element. The determination of this parameter by means of this device will allow greater assurance in relation to the distance between the fuel plates and thus ensure the proper use of the fuel element within the core of the nuclear reactor. This paper presents a methodology for measuring the distance between the fuel plates, giving a metrological report with the dimensions for the cooling channels of the fuel element.

2. Methodology

2.1 Fuel Element Assembly

IPEN routinely manufactures fuel elements for its research reactor IEA-R1 and in this work the distances between fuel plates were determined in this fuel element. The current configuration of the IEA-R1 reactor core incorporates 25 fuel elements in a 5x5 matrix. The fuel elements are formed by assembling 18 fuel plates, which are spaced allowing the passage of water that serves as a coolant and moderator. The fuel plates consist of a meat containing fissile material, which is fully covered with an aluminum cladding. They are manufactured by adopting the traditional picture frame assembly technique and rolling to the proper thickness. Powder metallurgy techniques are used in manufacturing the fuel plate meat, which are composed of dispersions. Several types of dispersions can be used, where powders of uranium compounds, such as U_3O_8 , U_3Si_2 or UMo alloys, are mixed with aluminum powder, which is the structural material used as the matrix of the fuel meat. Figure 1 shows views of the fuel element fabricated at IPEN, with the 18 fuel plates arranged parallel to each other. The distance between the fuel plates define the dimensions of cooling channels.

The fuel element is assembled by fixing the fuel plate to the side plates, which have grooves where the fuel plates are fitted. The fixation is made by roll swaging. A swage wheel is placed over the side plate contact lip

and a force is applied, as shown in figure 2A. The swage wheel is dislocated along the side plate groove length and the fuel plate is mechanically fixed by deforming the side plate contact lip (figure 2B). One side of the fuel plate is fixed and the swaging head is rotated to starting fix the other side of the fuel plate. The swaged connections are tested to assure that a minimum pullout load capacity of 27 N per millimeter of the side plate length is maintained. After the fuel assembly is swaged, the end nozzle and handle pin are attached.



Fig 1 – Fuel element fabricated at IPEN (A) and details of the cooling channels (B)

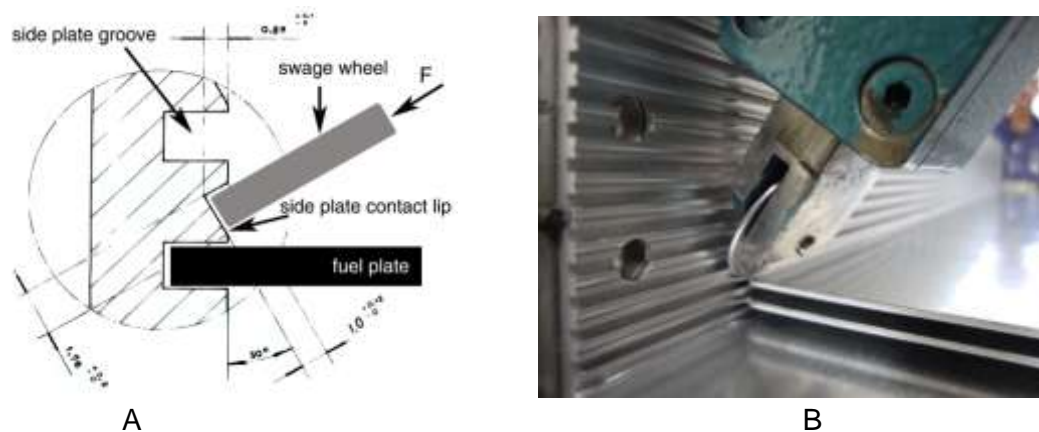


Fig 2 – Fuel element swaged joint (A) and roll swaging operation (B)

2.2 Measuring Device

The quantitative determination of the distance between fuel plates is made during the fuel element assembly. In the case of the IEA-R1 research reactor, according to the request in the fuel design, the spacing between fuel plates is 2.89 ± 0.25 mm. Figure 3 shows photographs illustrating the roll swaging machine. A system to measure coordinates in XYZ axes was installed in this machine. In conjunction with this coordinate system it was assembled a probe attached to the Z axis of the machine. Figure 4 shows photographs illustrating the measurement system installed in the roll swaging machine. It is possible to control the position of the probe in the X and Y axis and to perform the measurement in the Z axis. The probe repeatability is ± 0.025 mm.

2.3 Measuring Methodology

The measurements are performed in 21 points over every swaged fuel plate. The measurement positions are the same used to determine the fuel plate thickness, as established in the production routine. The fuel

plate thickness measurement locations are very well defined, with the coordinates of seven determinations in the X axis and three determinations in the Y axis, as shown in figure 5.



Fig 3 – Views of the roll swaging machine



Fig 4 – Measurement system installed in the roll swaging machine

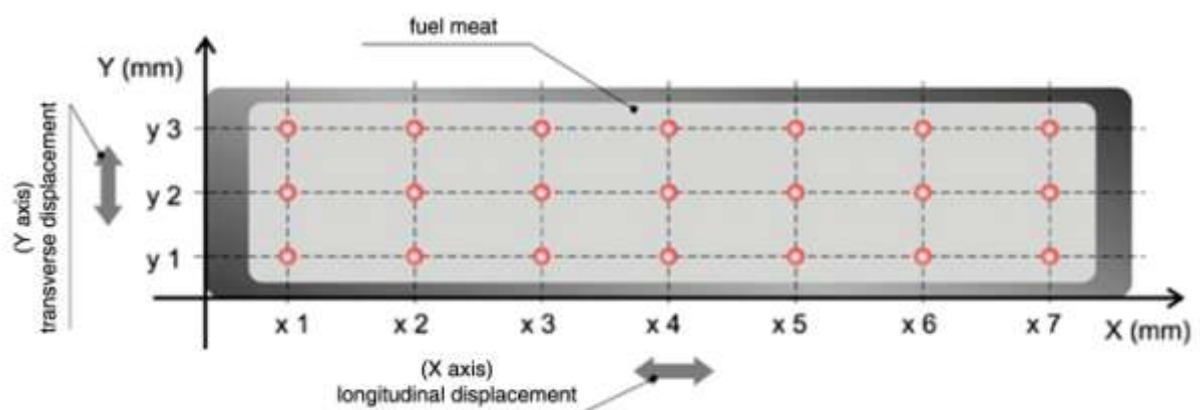


Fig 5 – Measurement positions, the same used to measure plate thickness

After swaging each fuel plate, the measurements are performed in the 21 specific points used in determining the thickness of the fuel plate mounted. All measurements are collected by a computer, which processes the data and calculate the distance between the plates in the 21 measuring positions, once

knowing the thickness of the plate in the 21 measured points. After swaging one fuel plate, the reference zero is taken from the central point of the end of the fuel plate previously mounted (position x7y2 according to the figure 5).

3. Results

The methodology was applied for measuring the cooling gaps of a fuel element (IEA 224) during a routine fuel fabrication under realistic fabrication conditions. The results are presented in table 1.

Tab 1: Results for gap dimensions determined with the proposed measuring methodology

Gap Number	Gap Dimension (mm)		
	maximum	minimum	mean
1	3.00	2.76	2.88 ± 0.07
2	3.00	2.65	2.86 ± 0.09
3	3.03	2.68	2.86 ± 0.10
4	2.85	2.65	2.76 ± 0.05
5	3.01	2.65	2.81 ± 0.10
6	3.14	2.73	3.00 ± 0.11
7	2.76	2.64	2.65 ± 0.03
8	3.11	2.67	2.94 ± 0.12
9	2.76	2.64	2.68 ± 0.04
10	3.11	2.68	2.93 ± 0.10
11	2.91	2.64	2.78 ± 0.08
12	3.14	2.71	2.96 ± 0.09
13	3.03	2.73	2.84 ± 0.07
14	3.05	2.73	2.89 ± 0.09
15	2.96	2.69	2.80 ± 0.06
16	3.14	2.89	3.00 ± 0.06
17	2.92	2.64	2.74 ± 0.09

4. Conclusion

The development of a device and the related procedure to perform the gap measurement in the fuel element fabricated at IPEN for the IEA-R1 research reactor was completed successfully. The generated data seems to be consistent. The next step is to fabricate full sized dummy fuel element according to the new RMB reactor design and to apply this methodology to do the gap measurement.

Acknowledgements

The authors wish to express their gratitude to the Fundação de Amparo à Pesquisa do Estado de São Paulo – FAPESP, for financial support for this work through the FAPESP Project 2009/18633-4. The authors are also grateful for the support received from the IAEA.

5. References

- 1 – OSSO Jr, J. A.; TEODORO, R.; DIAS, C. R. B. R.; BEZERRA, R.R.L.; VILLELA, J. L.; CORREIA, PERROTTA, J. A.; PEREIRA, G. A.; ZAPPAROLI Jr, C. L.; MENGATTI, J. “Brazilian strategies to overcome molybdenum crisis: present and future perspectives of the Multipurpose Research Reactor”.

In: INTERNATIONAL TOPICAL MEETING ON RESEARCH REACTOR FUEL MANAGEMENT, 15TH, March 20-24, 2011, Rome, Italy.

- 2 – DURAZZO, M.; SALIBA SILVA, A. M.; SOUZA, J. A. B.; URANO DE CARVALHO, E. F.; RIELLA, H. G. "Current status of U_3Si_2 fuel elements fabrication in Brazil". International RERTR Meeting. Prague, Czech Republic, September 23-27, 2007.
- 3 – SALIBA SILVA, A. M.; DURAZZO, M.; URANO DE CARVALHO, E. F.; RIELLA, H. G. "Fabrication of U_3Si_2 Powder for Fuels used in IEA-R1 Nuclear Research Reactor". Materials Science Forum, Vol. 591-593 (2008) pp 194-199.
- 4 – SALIBA SILVA, A. M.; URANO DE CARVALHO, E. F.; RIELLA, H. G.; DURAZZO, M. "Research Reactor Fuel Fabrication to Produce Radioisotopes". RADIOISOTOPES – APPLICATIONS IN PHYSICAL SCIENCES. INTECH - Open Access Publisher. Croatia, 2011, pp. 21-54.

ELASTIC-PLASTIC THERMO-MECHANICAL ANALYSES OF AN AL-U10MO FUEL ELEMENT

BRIAN W. LEITCH, NING WANG

*Reactor Safety Division, Atomic Energy of Canada
Chalk River Laboratories, Ontario, K0J 1J0, Canada*

ABSTRACT

Previous investigations [1a,1b] of a three-dimensional (3-D) finite element model of a U-10Mo/Al fuel element had focused on the thermal response of the element to internal heat generation. As the fuel was consumed and the thermal properties changed during the heat-generation process, the temperature of the fuel and the aluminum fuel cladding was determined for a number of different thermal boundary conditions of external temperature and film coefficients. Using these temperature values, the stress/strain condition of the fuel and the fuel cladding were estimated by applying isothermal, elastic material properties to the 3-D model. Following this preliminary study, temperature dependent material properties have been determined for the U-10Mo/Al fuel and aluminum cladding and have been used to update the linear elastic material models. Results have shown that for a geometrically-perfect fuel element, the cladding can easily sustain the mechanical stresses created by the heat and swelling of the U-10Mo/Al fuel. Scoping analyses were performed to determine the effect of manufacturing errors such as misalignment of the fuel core and the aluminum cladding. Experimental internal pressure burst tests have been performed on the aluminum cladding and similar internal pressure loadings were applied to the 3-D aluminum cladding finite element model which had elastic-plastic material properties. The non-linear 3-D cladding model produced very large strains and deformations at pressure values very similar to the experimental test pressures and provided confidence in the aluminum non-linear material values. A further refinement to the 3-D cladding model will be the incorporation of a failure strain criterion to more accurately model the rupture behavior of the cladding. Future enhancements to the 3-D fuel pin model are the addition of modeling procedures to simulate the welding of the end-plug to the cladding. The subsequent residual stresses of the welding process will have an influence on the overall response of the fuel pin. The validation of the residual stress modeling technique will be confirmed experimentally using neutron diffraction.

1. Introduction

Previous analyses [1,1b] of the Nuclear Reactor Universal (NRU) mini-element fuel rod had investigated the thermal response and the corresponding stress behaviour using linear elastic material and boundary conditions. Time-dependent heat generation was considered in [2], Figure 1, and a unique internal friction technique [3] was used to determine the temperature-dependent elastic material properties of the U-Mo fuel, Figure 2.

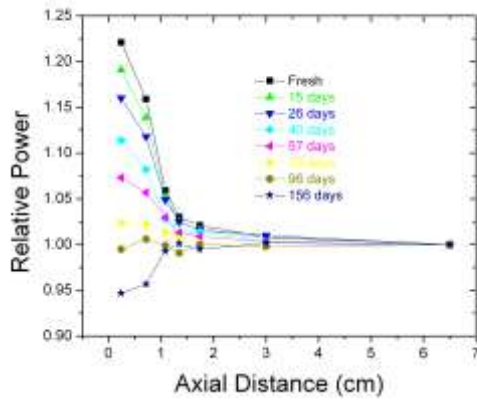


Fig 1. Mini-Element Power/Time History [2]

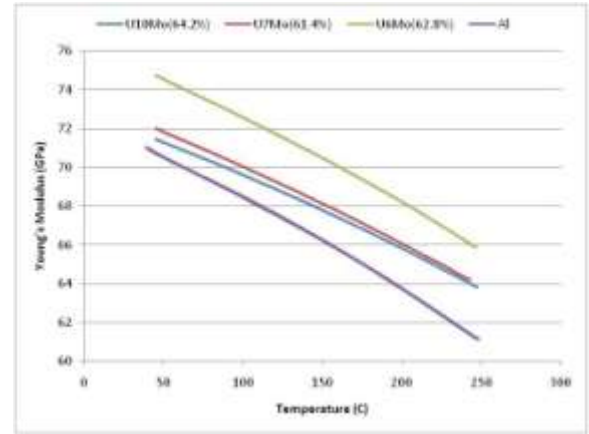


Fig 2. U-Mo and Aluminum Temperature Dependent Young's Modulus [3]

These previous analyses of the NRU mini-element have extended to investigate the effect of different thermal properties on the temperature response and non-linear, temperature-dependent mechanical material properties.

2. Varying thermal behaviour

It is known [4] that the thermal conductivity [1a] of the U-Mo changes as the fuel is consumed and transmuted. The thermal conductivity of the fuel is shown in Figure 3.

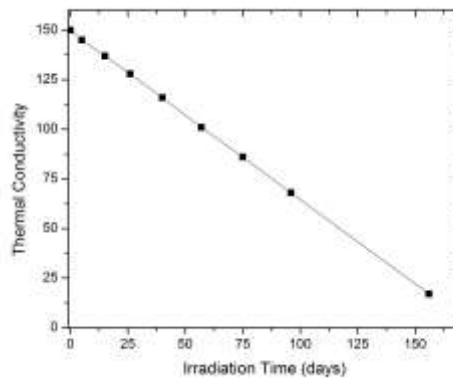


Fig 3. U-Mo thermal conductivity [1a]

The thermal conductivity at the end of the cycle was estimated using the linear relationship of previous values. This results in relatively high fuel temperatures at the end of the cycle. The element temperature at 90 days is shown in Figure 4 and the estimated temperature at 156 days of irradiation is shown in Figure 5. As can be seen there is significant rise in temperature that is a direct result of the low thermal conductivity value at 156 days.

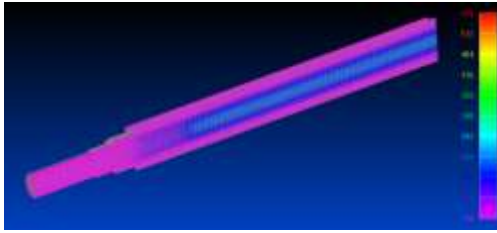


Fig 4. Temperature distribution at 90 Days of irradiation. Maximum 232°C

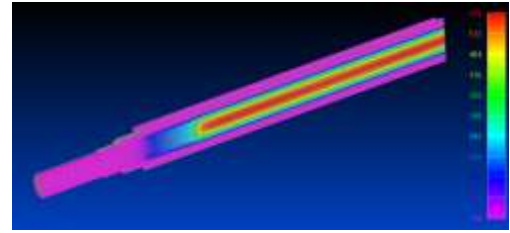


Fig 5. Temperature distribution at 156 days of Irradiation. Maximum 583°C

In these analyses, a static fluid is assumed to surround the mini-element and has a uniform temperature of 100°C. This far-field temperature was assumed to interact with the mini-element through a fixed-value, film boundary co-efficient acting on the external surface of the mini-element. This external thermal boundary condition imposed on the model may be unrealistic. While the reduction in the thermal conductivity would allow the fuel temperature to increase, it seems unlikely that the maximum fuel temperature of 583°C, Figure 5, would be attained while the external mini-element surface remains at 100°C without the surrounding fluid beginning to boil and changing phase. A conjugate heat transfer within a computational fluid dynamics analyses is necessary to address this issue.

3. Stress analyses

Temperature-dependent elastic-plastic material properties [5] of the 1060 Aluminum were used in the finite element model and shown in Figure 6. For the present, it is assumed that the material properties are consistent to a strain of 25%. (Further refinements to the material properties will be to define the temperature dependent failure strain.)

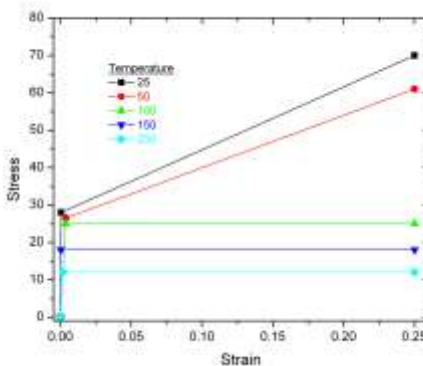


Fig 6. Temperature dependent Al stress/strain relationship [5]

The ANSYS finite element program [6] was used to perform the thermal and mechanical analyses. Applying the temperature distribution from the previous thermal analysis, the mechanical stress analysis was performed. The subsequent maximum principal stress distribution for 90 days is shown in Figure 7 and for 156 days in Figure 8.

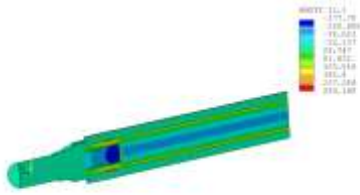


Fig 7. Maximum principle stress at 90 days of irradiation. Max cladding value 20 MPa

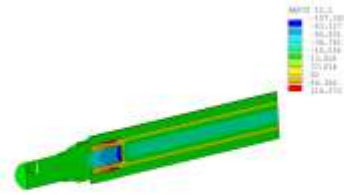


Fig 8. Maximum principle stress at 156 days of irradiation. Max cladding value 50 MPa

As can be seen, the maximum principle stress values in the cladding are lower than the ultimate tensile stress value of the aluminum material. There are higher stress values around the end plug location where the fuel is compressing the end plug. These cladding results indicate that the stresses are acceptable for the imposed boundary and geometry conditions considered in the analyses. The finite element models are generated using the ideal geometry of the component and does not take into account any dimensional relationships viz. extrusion/machining tolerances. For example, if the fuel was to be manufactured eccentrically that would produce thinner cladding on one side of the element. Such a condition is examined next.

4. Offset fuel distribution

To simplify the analyses, the U-Mo fuel was not modeled and internal pressure was applied to the inside surface of the aluminum cladding to simulate the expansion of the fuel. The aluminum cladding was generated assuming the fuel meat was extruded with a center offset of 0.5 mm. This fuel offset creates a thinner wall thickness on one side of the mini-element and a corresponding thicker wall section on the opposite side. For the moment, only a symmetrical fuel offset has been considered. Internal pressure was applied and the von Mises stress distribution is shown in Figure 9. The maximum value occurs near the cooling fin located on the thinner wall section and illustrates the stress concentration effect of the thinner wall thickness. Further analyses are being considered to examine (optimize) the effect of manufacturing tolerances on the behaviour of the fuel element.

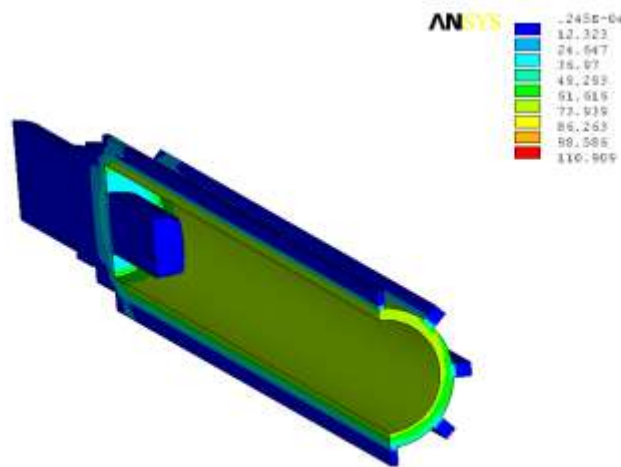


Fig 9. von Mises stress distribution in an offset cladding

5. Aluminum elastic-plastic analyses

A series of experimental tests were performed on mini-element fuel cladding to determine the internal pressure required to rupture the cladding. Again for these analyses, the fuel was removed and internal pressure loads were applied directly to the cladding. Eccentric fuel extrusion was not simulated for these analyses. Internal pressure values were increased until the analysis failed to converge due to numerical instabilities in the computational solution. Figure 10 shows the model just prior to convergence failure. Figure 11 show a typical experimental burst test.

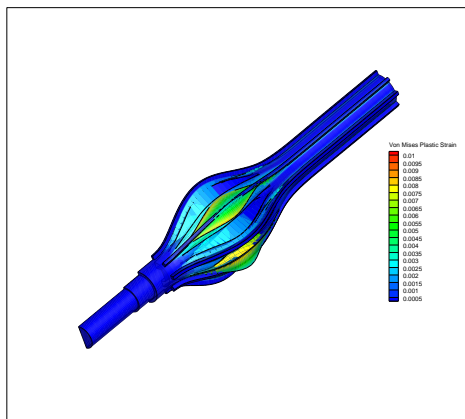


Fig 10. 3-D model strain results just prior to convergence failure



Fig 11. Mini-element burst test

The numerical burst pressure is reasonably close to the experimental pressure values ($\approx 10\%$). These experimental tests are a good benchmark for the numerical simulation of the aluminum material properties and the cladding behaviour. Further refinement of the aluminum elastic-

plastic material properties, i.e., incorporation of a failure criterion, will narrow the difference between the experimental and numerical results.

6. Future analyses

The current 3-D models of the mini-elements assume that the end plug and the fuel cladding are integral. While the fuel meat and the cladding are bonded together during the extrusion process, the end plug is welded to the cladding as shown in Figure 12. Although the aluminum material has a fairly rapid creep relaxation, the welding process will induce a residual stress/strain in the mini-element that will have an influence on the structural behaviour. Future enhancements to the 3-D fuel pin model are the addition of modeling procedures to simulate the welding of the end-plug to the cladding. The subsequent residual stresses of the welding process will have an influence on the overall response of the fuel pin. The validation of the residual stress modeling technique will be confirmed experimentally using neutron diffraction.

At present the cooling fins are circumferentially-orientated in an axial-radial plane. It may be more thermally efficient if the cooling fins were in a spiral pattern to induce turbulence and promote better thermal cooling and allow higher burn-ups to be achieved. It is hoped to use 3-D rapid-prototyping techniques to extract the 3-D analyse models and use these to perform experimental tests that will then feed back into the analytical models.

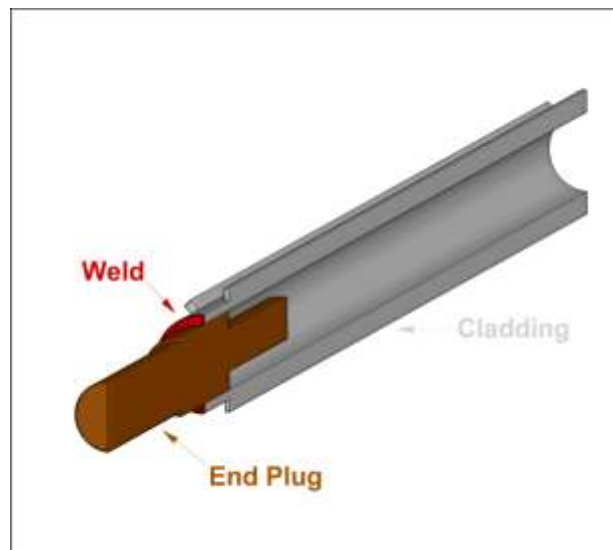


Fig 12. Weld location where the end plug is attached to the cladding

7. Acknowledgement

The authors would like to thank Dr. R.S. Dickson for kindly allowing us to use a picture of his experimental burst test.

8. References

- [1a] A.F. Williams, B.W. Leitch and N. Wang, "A Microstructural Model of the Thermal Conductivity of Dispersion Type Fuels with a Fuel Matrix Interaction Layer", RRFM 2011, Rome, Italy, 2011 March 20-24
- [1b] B.W. Leitch, D. Sears, A.F. Williams and N. Wang, "Thermo-Mechanical Analyses of NRU Mini-Element Fuel Rod", RERTR2010, Lisbon, Portugal, 2010 October 10-14
- [2] D.F. Sears, B.W. Leitch, G.W. Edwards, K. Colon, I.P. Swainson, R.B. Rogge and R.L. Donaberger, "Effect of burnup and irradiation temperature on crystalline phase evolution in Al-UMo dispersion fuel", RERTR 2009, Beijing, 2009 November 1-5
- [3] N. Wang, B.W. Leitch, L. Fu and A.D. Davidson, "Measurements of Elastic Modulus of Hot-extruded U-Mo/Al Dispersion Fuel", RERTR 2011, Santiago, Chile, 2011 October, 23-27
- [4] J.C. Wood et al., "Advance in the Manufacturing and Irradiation of Reduced Enrichment Fuels for Canadian Research Reactors", Proceedings of the International Meeting of Reduced Enrichment for Research and Test Reactors, Tokai, Japan, 1983 October 24-27
- [5] J.G. Kaufman, Properties of Aluminum Alloys, The Aluminum Association, ASM International, 2006 November
- [6] ANSYS Inc, Pittsburgh, OH, USA

A Method of High Flux Engineering Test Reactor Operation

Li GuangHui

Nuclear Power Institute of China ,Chengdu, 61000, China

Correspondence e-mail address: jimily@126.com

Abstract: This paper introduces the work method of HFETR (High Flux Engineering Test Reactor)operation department in such fields as reactor operation, maintenance test, operator training and incident management .This method, which is based on the laws and regulations about research reactor which are published by the administrative department of China, has been improved though the lessons learnt from big accidents that have happened in reactors all over the world and the experiences gained from a long period of HFETR operation. This paper also gives some examples to explain how this method works in the practice. After all these years, it's clear that this method can ensure the safety of HFETR and the method is valid.

Keyword: HFETR; operation;

1 preface

HFETR operation management experience from is not standard to comparatively perfect stage of development. Along with the relevant state regulations about the research reactor issued, under the help of the national nuclear security administration, have been perfect the system and operation procedures, etc., so that HFETR management to a new level, which ensure the safety of the reactor operation and the successful completion of all tasks. This paper summarizes the HFETR operation, test, maintenance, personnel training, event management methods of work.

2 reactor operation

2.1 operational limits and conditions

This reactor in strict accordance with “Operational limits and conditions of HFETR” which been approved by State Bureau of Nuclear Safety.Its main requirement as follows:

(1) Safety limits

All kinds of process variables limit in the reactor operating within the limit has proven to be safe. Safety limits from the final design and analysis of the reactor accident in export. In any conditions, and will never allow exceed safe limits.

This reactor safety limits include the scope is: maximum thermal power reactor; Fuel element the highest surface wall temperature; Fuel element minimum burned down; Reactor minimum inlet pressure; Reaction of the biggest introducing rate; Introducing the biggest step representation positive reactivity.

(2) operational condition

A whole set of regulations about equipment functions and performance mission ,which approved by the national nuclear security department.

(3) the set values of Safety system

To prevent more than safety limit is worth state, is expected to happen in running events and

accident when working on automatic protection device start triggers. Reactor automatic shut-down amplifier. Generally take runtime values within the scope of the rate of 20%.we can see the detail from table 1.

(4)Normal operation limit

The normal operation of the reactor process parameters value range, in over that abnormal warning system give the signal. Generally take runtime values within the scope of the rate of 10%. we can see the detail from table 1.

(5)Monitoring requirements

The system safety inspection and supervision, control requirements. To check the frequency, methods and treatment measures are specific provision.

Table 1: HFETR safety the set values system

Protection parameter name	Normal operation value	Safety the set values system	Channel number
Small power reactor	/	103	3
Reactor cycle	/	$\geq 15s$	3
Reactor power	$\leq 110\%PH\ MW$	$\leq 125\%PH\ MW$	3
Reactor thermal power	$\leq 110\%PH\ MW$	$\leq 120\%PH\ MW$	2
A water into the heap of flow	$\geq 90\%t/h$	$\geq 80\%t/h$	3
Reactor inlet pressure	$\geq 90\%MPa$	$\geq 80\%MPa$	3
Export reactor pressure	$\geq 90\%MPa$	$\geq 80\%MPa$	2
Reactor exit temperature	$\leq 71\ ^\circ C$	$\leq 75\ ^\circ C$	2
γ value of 16N	$\leq 110\%PH$ Corresponding γ value of 16N $\mu R/S$	$\leq 125\%PH$ Corresponding γ value of 16N $\mu R/S$	1
Outside power supply voltage	$\geq 75\%U$	$\geq 75\%U$	4
Damage detection system γ	$\leq 500\ cps$	/	1
delayed neutron	$\leq 25\ cps$	/	1
Secondary water wastewater monitoring	$\leq 80\ Bq/l$	/	1

3 System prepare

3.1 components of the load

By calculating personnel according to the operation power and running task, loading according to calculation, make loading plan. After technical director approval, the scheme plan was introduced by calculating personnel to operation personnel, so that the operation personnel can understand the basic situation of loading plan, and puts forward problems and calculation with researchers discuss, deepen our understanding of the plan, clear some problems needing attention. At the same time also can put forward to that occurred in the past in the use of the reactor ,some conditions are discussed and analyzed. So, can make the operation staff to grasp some about the reactor's internal state

information, be helpful for safe operation. on one hand, also can make the calculation staff know the actual operation situation, improved calculation method, the result to accord with the actual approach.

3.2 maintenance is introduced

Before the operation, need to organize overhaul will work. By the chief of all professional maintenance overhaul introduces to operation personnel about equipment changes, and in running the problems to be pay attention to. Operation people also can put forward the problems and discussed, ensure operators in the operation of equipment of facts are fully understood.

3.3 pour the implementation of the fuel

According to the loading plan, the mechanical group responsible for writing pour fuel program, after technical management group check and simulation operations, and implementation pour fuel work before get approval by room leadership. In the process of pour fuel accordance with the relevant instruction, put into the corresponding instrument and meter to supervise the reaction of the change, and to the manufacturing shift supervisors by the monitoring. Mechanical group poured fuel procedures according to the relevant rules, to ensure accuracy and safety when pour fuel.

3.4 pre-critical test

After completing loading fuel, and through the check and correct, must be pre-critical test. The experiment of shut-down system ,instruments, and protection signal , the set values for inspection and test must be before. Request pulse count device, small power protection, cycle protection, power measurement instrument and the two sets of independent work normally. In the test in strict accordance with “the HFETR safety set ”requirement and the approved pre-critical test procedures and control reactive into amount and introducing rate.

In complete critical test, reactor before block, it is necessary to check the reactor core loading. Inspection team in the reactor core of technology by room director, and science and technology leadership office, supervisor's office, security division, quality, mechanical group. Signature onthe loading chart after Check and correct in the reactor core.

3.5 protection function test

Before reactor start-up, also need the security check of the power supply system, and the test of the protection system, to ensure the normal operation of the function in the reactor.

3.6 reactor with power operation

In the operation of the reactor, the reactor safety is responsible for his supervisors. supervisor's full control and schedule post, the effective implementation of the rules and regulations, to ensure the safety of the operation reactor.

In Operation, the position of the officer on duty operation parameters monitoring and analysis, and make record, operator may at any time to ask operation conditions and check. When an exception occurs, the officer on duty should report his supervisors, and timely analysis and processing. For some more serious abnormalities or equipment failure, his supervisors can notify relevant personnel carries on the analysis, the research and treatment. If necessary, report to the room led. Likely to endanger the safety of the abnormal situation, the officer on duty can suspending the reactor, to ensure the safety of the reactor.

The operation of the special work, order form technical administration tasks related team orders, each team must implement.

Some important operation, such as: reactor system to prepare, reactor startup, power conversion, reactor system suspending, reactor system security check, and outside power lose electric events

processing according to relevant operating card operation.

On may cause changes in the pile of reactive various operating and test of prior estimate should be reactive disturbance, and take the necessary measures to prevent it.

3.7 reactor for suspending

After Reactor suspended, check all control rod into the bottom and confirmed that reactor already safety for suspending.

According to the situation of the residual heat, when excess power less than 0.5% pH, the reactor can get into uncontinuous cooling. Before uncontinuous cooling, we must ensure that the flow of pour into the reactor more than 480 t/h. before the main cold system pressure relief , open pipe main valve put, confirmed that out of the water, make siphon damaged between main line and the pressure vessel.

4 reactor maintenance

The reactor maintenance adopt the the method of combining, which contain preventive maintenance, routine maintenance inspection , maintenance and repairs fault . That is a times each year about two months clearance to take preventive maintenance; For the fault occurred during operation, ensure the safety of the premise, the fault equipment timely make emergency repair; if time for clearance is short, we take routine inspection and maintenance, and the fault equipment repair.

4.1 the preventive maintenance

(1) to determine the maintenance plan

In view of its are responsible for all professional equipment, according to the relevant regulations and set up the annual maintenance plan. And for some working conditions is special equipment, with many years of practical situations, rationally adjust.

In addition, each time before shut-down amplifier, according to the operation condition of equipment, and connecting with the annual maintenance plan involved the content work out the stage maintenance plan. After authorization by the leadership, the technology group is responsible for organizing and implementation.

(2) the implementation of maintain

In the implementation of maintain process, for some important or large equipment, professional group put forward for maintenance to technical management group a day earlier , the technology management group use the work order notice the control centre room. After supervisor's approval, professional maintenance charge in control centre room for equipment to stop service procedures. After take safety measures to equipment out of service, repair work be conducted. Repair process, all professional in strict accordance with the related regulations execute maintenance.

4.2 maintenance acceptance

Equipment maintenance, after the completion of the maintenance, technology management leadership group, the maintenance, the person in charge of the acceptance of his supervisors on duty team acceptance. If there need to research institute of equipment acceptance level, the competent director, science and technology department, security branch, quality branch, technology management group, leadership on duty, maintenance of acceptance of his supervisors team acceptance.

When acceptance provides professional maintenance report that contains the failure causes of equipment or system, method of treatment, validation data and maintenance record, etc. After the acceptance by acceptance group fill in acceptance report. Through the acceptance, the director for

equipment maintenance service procedure, recovery equipment normal state.

4.3 fault repair

If happen malfunction of facilities During operation, under the premise that the reactor safety guarantee, the supervisor's organization concerned personnel analysis, make the determination of reasonable scheme, remove the faults. After the completion of the equipment maintenance, the maintenance of his supervisors make the acceptance, then the equipment can put into use. Operation personnel will put equipment fault imagination, maintenance , check and acceptance situation in run log on record. Professional should make detailed records about equipment failure and overhaul.

All professional according to the operation of equipment and situations prepare spare parts. In equipment operation, the regular inspection tour to grasp equipment operation. Operators in operation to make regular inspection tour of some important equipment, if found problem, the organization concerned personnel for processing, ensure the normal operation and safety of the reactor.

5 the spentfuel storage

spentfuel elements in the preservation in storage pool, and through calculation, storage conditions meet nuclear safety regulations safety requirements. The pool of storage environment regular cleaning, prevent sundries falling into the pool. Regularly to get pool water samples check, to decide that if the purification system need to run.

6 operation personnel training

Running the training of workers take guide teacher guiding the way of learning.

Choose the guide teacher who responsibility is strong, technology is good ,and the teacher must be advanced operator or supervisor's work in the reactor as two or more years.

6.1 training

Reactor operator training process is divided into follow practice, monitoring operation, on duty practice three stages.

6.1.1 trainee stage

Trainee from assigned to operator post began to practice. Under the guidance of the guide teacher to learn professional knowledge, learning theory basis of nuclear reactor, nuclear security and protection dose. Learning the drawings and related system operation procedures ,making themself understand the system process flow. Also to participate in the field study of reactor startup and running. After qualified the expiration examination can turn to the next stage to study.

6.1.2 monitoring operation stage

Trained person under the guidance of guiding teacher to do further learning about drawing material and operating rules, and gradually learn to actual operation. And according to the reactor operators license system requirements, assessment by related subject's test evaluation, such as electrical, loop system, physics, automatic control and manipulate thermal, operator independent part on duty. Qualified person can turn into the next study stage.

6.1.3 practice on stage

This phase is training the trainee independent operation ability, and learn to analyze the abnormal situation occurred when the reactor operating, making them can handle general events. In the custody of the guarding personnel can accept and ratification of the operation orders, accumulate experience of reactor operation.

Person that experienced in the above each phase of the training, and obtains the national nuclear security administration issued license, can be in control on the position of independent member on duty.

Senior manipulate member and shift supervisor's training also need after the various stages of training process, and require a wider range of knowledge, the analysis judgment and the ability to handle events more strong. After examination and appraisal of the corresponding, obtain corresponding post qualification, can be put in the corresponding positions.

6.2 retraining

To improve the quality of the personnel training is one of the most important work. Through retraining can make people keep its competent for his own work ability, especially the ability of handling the abnormal situation.

Retraining the work mainly through sent people to schools off-job learning, hold related experts lectures, regular exchange of experience running in research institute, institute of organization operation experience and technology exchange, in addition to the operation of the reactor and other personnel technical exchanges.

Through the training and retraining, make the operation personnel quality enhances unceasingly, in operating conditions more complex and running more heavy task, still can guarantee the safety of the reactor operation.

7 event management

7.1 events of treatment

When there is an operating events, processing according to the supervisor's instruction and report to the leadership. When necessary, the supervisor or leadership organization concerned personnel earnestly analyze the cause of the event, make effective corrective actions. Technology management according to the relevant regulations of the requirements, report the incident to the relevant departments.

7.2 corrective measures of execution

After getting information from superior department, operation department is responsible for the implementation of corrective actions and check corrective measures the implementation effect, according to the rules, to fill in "the research reactor running events trailer card", and submitted to the security division, finally accept security, quality, science and technology department witness and acceptance. Related documents and material of the events saved by technical management group.

7.3 event handling experience feedback

After the event handling, and organize related team and personnel to the cause, processing, consequences, prevention measures of the event are fully discussed, learning and make everybody deepen understanding, and improve the analysis and processing of events ability. This process is also as an important content of personnel training.

8 summary

The above is the preliminary summary of work experience in HFETR operation management. With the change of operation conditions and running mission, in specific management work, also need to constantly improve and summarize the management method, and according to the other safety of the reactor experience feedback, improve the operation of the reactor level and guarantee the safe operation of the HFETR.

References

- [1] Duan Tianyuan, operational limits and conditions of HFETR
- [2] Liu Rong, The operation system of HFETR
- [3] Yang Shuchun, Event management of HFETR

DULCINEE. Beyond neutron kinetics, a powerful analysis software

G. Ritter, R. Berre, L. Pantera. Poster presented by F. Jeury.

CEA/Nuclear Energy Division/ Cadarache Nuclear Research Center/Reactor Studies Department

Abstract— The CABRI experimental reactor is located at the Cadarache nuclear research center, southern France. It is operated by the Atomic Energy Commission (CEA) and devoted to IRSN (Institut de Radioprotection et de Sûreté Nucléaire) safety programmes. It has been successfully operated during the last 30 years, enlightening the knowledge of FBR and LWR fuel behaviour during Reactivity Insertion Accident (RIA) and Loss Of Coolant Accident (LOCA) transients in the frame of IPSN (Institut de Protection et de Sûreté Nucléaire) and now IRSN programmes devoted to reactor safety. This operation was interrupted in 2003 to allow for a whole facility renewal programme for the need of the CABRI International Programme (CIP) carried out by IRSN under the OECD umbrella.

When the facility comes back to experiments, checking core safety criteria will be needed on a day to day basis. This operation is based on calculations with DULCINEE, the neutron kinetics toolbox and SCANIR, dedicated to criteria characterization. The purpose of this poster is to illustrate the contents of DULCINEE, its inputs and outputs and major improvements.

The poster and this paper include a description of the facility, a reminder of the upgrade to the safety case including core commissioning and a comprehensive description of the DULCINEE software.

Index Terms— RIA, Core, ^3He , Neutron kinetics, Power, software.

I. THE CABRI FACILITY

The experiments to be performed in the CABRI facility will now be confined to a new pressurized water loop. This device is located at the heart of a pool type reactor (cf. fig. 1). The experimental fuel rod will then stand a powerful neutron flash during the core driven power transient. A vertical channel symmetrical across the core allows the hodoscope, a unique neutron camera, to monitor the course of fissions in the experimental rod along the experiment.

The core is made of 1488 stainless steel clad fuel rods with a 6% ^{235}U enrichment. The reactivity is controlled via 6 bundles of 23 Hf rods. The reactivity worth for these solid control rods is $\sim 19\%$.

The active part of the core is the size of a small refrigerator.

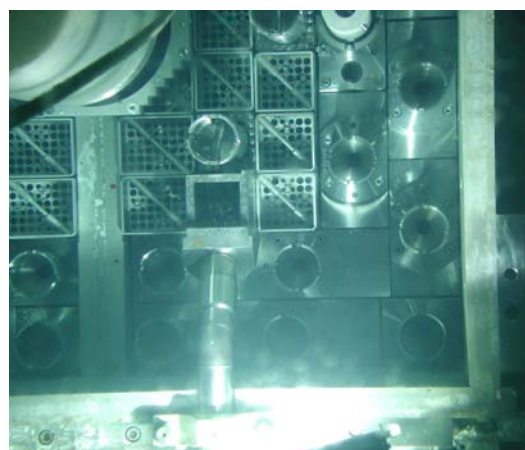
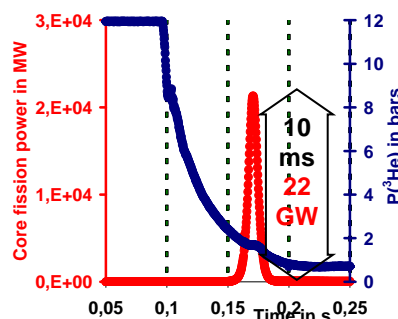


Fig. 1. $\frac{1}{4}$ CABRI core at unloading. Center up-left.

The key feature of the CABRI core is its reactivity injection system. This device allows 96 tubes filled with ^3He (major gaseous neutron absorber with a thermal neutron capture cross section $\sigma_{\text{He-3}(n,p)\text{T}}$ at least 50 times larger than Hf) up to a maximum pressure of 15 bars and located among fuel rods to depressurize very fast into a discharge tank. The absorber ejection translates into an equivalent reactivity injection possibly reaching 4% within a few 10ms. The power consequently bursts from 100 kW up to $\sim 20\text{GW}$ (cf. fig. 2) in a few ms and decreases just as fast due to the Doppler effect and other delayed reactivity feed-backs.



D:\V\Projets\BEP-CABRI\Cratons\cours\seminaire\1_FHe_Pce_E_SUREP4.xls

Fig. 2. Typical CABRI ^3He pressure and core power during a transient.

G. Ritter, R. Berre, L. Pantera. F. Jeury DENCAD/DER CEA Cadarache, B¹ 223. 13108 St Paul Lez Durance. France. (Corresponding author. Phone +33 (0)442 25 41 80. Guillaume.Ritter@CEA.Fr)

The CABRI International Programme was decided in order to realize tests representative of PWR accidental conditions.

The facility is now being modified in order to have a pressurized water cooling in the test section instead of the previous sodium coolant.

Installing water cooling for the test rod will allow to be representative of PWR's, essentially during the post rod failure phase when there can be fuel-coolant interactions. It will be used to test future high burn up or alternate fuels like MOX (Mixed Oxide) and to re-assess current safety margins.



Fig. 3. The basket : support structures for the new CABRI water loop.

Figure n° 3 before shows what volume it takes to put a pressurizer, a pump, a couple of heat exchangers and a few valves.

The core fuel rods are steel clad to allow them to withstand the numerous power bursts performed in the facility. There have been about 700 pulses since the beginning. The feed core fuel rods safety case was upgraded during the facility refurbishment.

II. FEED CORE FUEL RODS SAFETY CASE

In 2008, the core safety case was upgraded. It maintained the prescription for a preliminary computation before each new test campaign because the power transients to be realized had different features. This analysis also allowed a sharper physics characterization of the core behavior during transients. The core model is identical but reactivity insertion parameters are determined by the ^3He pressure that will generate the expected power sequence. This power sequence needs to be

evaluated and the resulting safety criteria also.

The CABRI reactor is a world unique facility for its reactivity injection system (cf. figure n°4 below). The main feature of this device is to allow an accurate control of reactivity injections. Opening the valves delivers a fast ^3He ejection causing a reactivity injection resulting in the burst of power (e.g. 3,5 \$ within 0,12 s as in figure n°2 prev. page).

There are two options for ^3He depressurization, a long breath or a quick blow, depending on the aperture tuned on adjustable valves for each way.

The design of a test basically depends on two criteria : The energy released during the power pulse and the transient duration at half peak power. These performance metrics are used to determine which conditions must be met with the ^3He reactivity injection system. Afterwards, an investigation is performed to make sure these parameters comply with the facility safety.

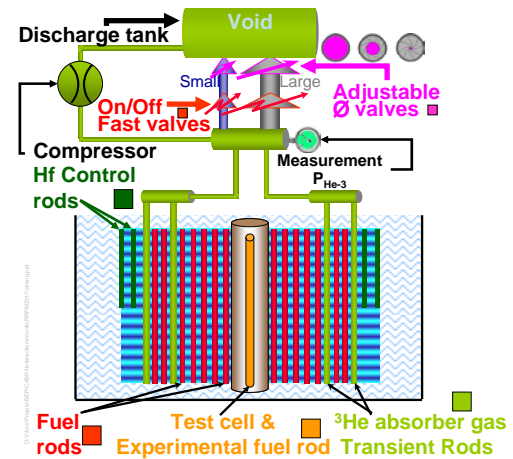


Fig. 4. Principle of operation of the CABRI facility.

The assessment of core power comes from point kinetics. The time wise reactivity worth corresponding to ^3He ejection off the core can be evaluated with a combination of functions $\rho(t) = \rho(P_{\text{He}}) \otimes P_{\text{He}}(t)$ where $\rho(P_{\text{He}})$ is given by a Monte-Carlo core computation with TRIPOLI 4 [3] and $P_{\text{He}}(t)$ is a preliminary measurement of ^3He pressure in actual test conditions but without core operation.

The DULCINEE neutron kinetics code converts the reactivity $\rho(t)$ into a pulse of core power.

The core safety is now based on the evaluation of three parameters and each must be evaluated with the maximum margins [6]. The fuel temperature must not exceed 2810°C, the clad strain must not go beyond 3.6% and the maximum clad temperature must be lower than 1300°C.

Before any new test campaign, the envelope safety parameters are computed according to the maximum expected conditions during the campaign. The computation of safety criteria is made with SCANAIR, the thermal hydraulics and thermal mechanics code from IRSN [2] dedicated to fuel rod characterization during power transients. This code was adapted to a routine production use by experimentalists under

MS Windows environment and this upgrade provides a large flexibility for test preparation. The main input to SCANAIR is the fission power in the hot rod and it is generated by DULCINEE.

A unique database containing ~700 previous tests power records can be used to interpolate the power plot of an upcoming pulse but it may not be fully envelope. As a consequence, the core power commissioning will produce ~100 pulses with increasing experimental parameters (essentially the energy delivered to the system) in order to almost reach the safety limits from below and use it later as an absolute maximum.

The design of these 100 commissioning power bursts will be made according to a dedicated experimental approach. Key experimental parameters will be increased one after the other within a preferred pattern so that the resulting energy does not move beyond core safety. This progressive approach will be validated by neutron kinetics computations with DULCINEE.

III. DULCINEE : A MIGHTY LADY

This neutron kinetics computer code was developed in the 1970's with fortran 77 essentially by P. Dutraive and B. Brun (CEA) [4]. It was designed to characterize the behaviour of a nuclear core with low pressure coolant (water, sodium ...) during several types of transients like the main following :

- Reactivity initiated transients (RIA, LOF)
- Ramps
- Overpower
- LOCA

The thermal hydraulics can process single or double phase flows in forced convection. It operates in the axial direction and can accommodate either upward or downward flow. Pressure and flow rate are computed according to the local void fraction with dedicated correlations.

Heat transfer in the rod is modeled from the inside to the outside. Several types of regions can be described (fuel/gap/clad). The physics properties of each region can be tabulated as a function of the temperature.

The code can accommodate plate or rod geometries according to the type of core design.

The core is modeled with 2 regions : 1 hot channel and the remaining average channels.

In the late 80's, a fractured fuel model was inserted allowing a better validation against experimental temperatures. It was successfully validated against the CAPRI experimental Thermal-Hydraulics programme realized at CEA-Grenoble in the late 1970's.

It is based, as for neutron kinetics, on the following coupled equations

$$\frac{dn(t)}{dt} = \frac{\rho - \beta}{\ell} n(t) + \lambda C(t)$$

$$\frac{dC(t)}{dt} = \beta \frac{n(t)}{\ell} - \lambda C(t)$$

Where

λ : Precursor decay constant (s^{-1})

β : Delayed Neutron fraction (pcm)

ℓ : Neutron generation lifetime (s)

n : neutron density ($\propto P$) n/cm^3

ρ : Reactivity (\$ or pcm)

C : precursor density p/cm^3

CABRI : $\beta=758\text{pcm} - \Delta 27.7\mu\text{s} - \text{Doppler}=103\text{pcm.K}^{-1/2}$

DULCINEE uses feedback parameters that were computed with TRIPOLI 4. It includes the instant Doppler effect and all delayed phenomena like clad expansion or coolant density. The delayed neutron fraction β and generation lifetime ℓ were computed with MCNP [5]. The resulting values are now consistent and have successfully been tested with DULCINEE against experimental data acquired during the sodium loop past programs (several hundred power bursts in the past 40 years).

After this temperature step, the neutron feedbacks can be integrated and provide the overall system reactivity.

Eventually, the reactivity or the core power can be given from the solution of the above mentioned neutron point kinetics equations system. This system can be used either in a straight way (a reactivity input providing a power output), or in the reverse fashion (a power input providing a reactivity output).

The time step is incremented and an ulterior situation is computed.

This well-known routine is called the quasi-static method as the point kinetics equation is based on a sequence of stationary thermal conditions.

It was used until 2008 with "handmade" input files. The input jobs were based on former punched cards formats. It basically handled 2 types of inputs; either experimental data records after several signal processing routines or a hand built power or reactivity plot according to the engineers will.

IV. ERGONOMICS AND SAFETY

Using the code required a full knowledge of all possible hypotheses and computational steps. Any alternative data processing or use of the code requested heavy improvements and anyway a comprehensive training for any newcomer. Moreover, fast pulse tests preparation relied on converting experimental parameters like initial pressure and valve aperture into the corresponding power plot. This feature had to be developed to test the core behaviour against new safety criteria.

It was decided to preserve the physics part of DULCINEE but

to secure interfaces and to develop new features for inputs and outputs so that the risk of mistake and the efficiency would meet better standards.

For that reason, about 20 routines were made and gathered within 9 options around the neutron kinetics solver, each of these options bearing a high flexibility. Model based data, that is all inputs relative to the core geometrical description including physics properties were set apart so that the transient can be the only new input to the calculation.

The 9 computation options either correspond to a reactivity input or to a power input. It can also be sorted in so called "standard" or "safety" calculations. A "safety" calculation will produce a ^3He pressure and power output that can be used to determine safety criteria with SCANAIR from IRSN, which means it has the right format and includes the necessary conservatism. The hot rod power features are computed in SCANAIR to evaluate the three safety parameters presented in the previous paragraph (i.e. T_{fuel} , T_{clad} and ϵ_{clad}). The steps exposed before to assess the safety of any upcoming experiment include several added margins. Most of this legitimate conservatism is concentrated in a large overestimation of the core power. This approach maximizes the energy deposited in the rod, which is the driving parameter for clad temperature.

Inputs come from measurements without any specific data processing. The filtering, format, range, and selection issues are all included. It can also be produced by any external computation. Eventually, the design of an experiment can now directly generate the external reactivity plot that causes the power transient. Use of the code is thus much easier and safer.

V. EXTERNAL REACTIVITY GENERATION

External reactivity plots used to generate a power transient either came from the reverse kinetics translation of previous pulses or from an adaptation by the engineer.

The time wise reactivity worth corresponding to ^3He ejection off the core is now evaluated with a combination of functions:

- $\rho(t) = \rho(P_{\text{He}}) \otimes P_{\text{He}}(t)$ where
- $\rho(P_{\text{He}})$ is given by a Monte-Carlo core computation with TRIPOLI 4 [3] and
- $P_{\text{He}}(t)$ corresponds to ^3He pressure

The term $P_{\text{He}}(t)$ is a preliminary measurement of ^3He pressure in actual test conditions but without core operation. It can also be computed with the following analytical law.

$$\frac{p(t)}{p(0)} = \frac{1}{(Bt + 1)^\alpha}$$

with :

$$\alpha = 2\gamma / (\gamma - 1) \text{ and } \gamma = C_p / C_v, \gamma = 1.66 \text{ for Helium}$$

B = a term characterizing the valve aperture and fitted to the experiments.

The analytical law exposed above shows $P_{\text{He}}(t)$ and thus $\rho(t)$ only depends on the initial pressure and the valve aperture. The helium pressure is of course used as a combination of terms the aim of which is to make the link between actual ^3He concentration and reactivity. It means the air pollution in helium and the gas temperature are also important hypotheses. An attempt to better describe the physics of ^3He depressurization was proposed in [8]

The ^3He bound reactivity is also tight to experimental parameters like both valves aperture and delay between small and large depressurisation channels which are included as inputs in the code.

The control of core reactivity during a transient starts with ^3He depressurisation and ends with the control rods automatic insertion. This last term is thus also included at the end of the $\rho(t)$ transient model.

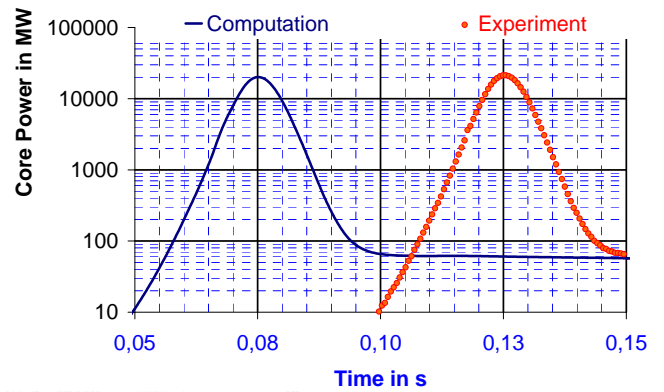


Fig. 5. Agreement between computation and experiment for DULCINEE

Figure 5 before shows the very good agreement between computation and experiment for the DULCINEE kinetics tool during a 10 ms duration typical fast pulse. The "experiment" plot corresponds to the measurement of an ion chamber whereas the "computation" plot corresponds to a reactivity driven DULCINEE computation. The time offset is artificial and only helps both curves be discerned.

VI. ^3He REACTIVITY WORTH ASSESSMENT

The reactivity as a function of ^3He pressure has been computed with TRIPOLI 4 Monte Carlo whole core computations and with DULCINEE in the reverse kinetics option. It has been successfully validated against past measurements. This validation first compared the computed hafnium rods criticality level to the measurement for several ^3He pressures in a statics approach and it also provided an assessment of the ^3He reactivity worth in a dynamics approach. Both methods showed a good and coherent agreement as presented in figure 6 below [7].

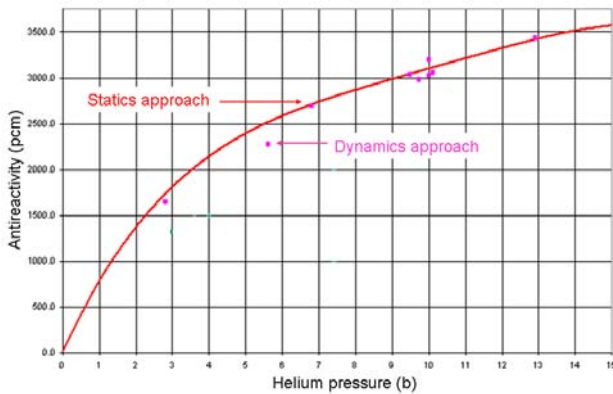


Fig. 6. Agreement between computation and experiment for TRIPOLI 4

As a consequence, the uncertainty on $\rho(t)$ basically depends on the gas concentration in the core that is to say $P_{He}(t)$. This pressure comes from a measurement either made during previous experimental campaigns (actual test with a power burst) or in preparation of an upcoming test (system depressurization without core operation). These records fit the analytical formula presented in chapter V.

VII. JAVA GRAPHICS USER INTERFACE

Starting from fortran punched cards type inputs and a bunch of ascii output files the upgrade towards a graphics User Interface was not frivolous luxury.

This interface now has 2 main entry panels: the model and the transient description.

The model panel has several tags corresponding to the geometrical and physics characteristics of the system. Each field has an adjacent definition with corresponding unit. There is no risk to fail the job because of a wrong format.

The transient description has 1 tag per option. Each option requires either scalar data like initial power or an input file fetched through a drag and drop mode. Corresponding records are documented with a description of the file format, content and units.

The output provides a synthetic view of main computation parameters like execution time and input hypotheses. It also gives the output main results like maximum power, integrated energy and peak duration at half height.

A plot of key physics indicators (reactivities including 3He , Doppler and other feedbacks, power, 3He pressure) eventually provides a straight view of the computation.

VIII. CONCLUSION

This paper presented the current upgraded version of the neutron point kinetics software DULCINEE. A broad description of the CABRI facility reminds to what the code can be applied.

The driving motivation to improve the code is safety and the new core safety criteria were detailed.

The software physics content is described as well as the main improvements, including the reactivity generation routine from experimental parameters and its JAVA Graphics User Interface.

REFERENCES

- [1] Neutron Commissioning in the New CABRI Water Loop Facility. G. Ritter, O. Guéton, F. Mellier, and D. Beretz. IEEE TRANSACTIONS ON NUCLEAR SCIENCE, VOL. 57, NO. 5, OCTOBER 2010.
- [2] SCANAIR reference documentation. version V_6_1. A.Moal F.Lamare J.C.Latché E.Fédérici V.Bessiron. February 18th, 2008
- [3] TRIPOLI-4 VERSION 4 USER GUIDE. Odile PETIT, François-Xavier HUGOT, Yi-Kang LEE, Cédric JOUANNE, Alain MAZZOLO. Rapport CEA-R-6169.
- [4] DULCINEE CODE. Dutraive, P. ; Fabrega, S. ; Millot, F. CEA Internal report CEA-N—1378. 1970 Jan. 01.
- [5] Forrest B. Brown, et al., "MCNP Version 5," Trans. Am. Nucl. Soc., 87, 273 (November 2002).
- [6] UPSCALING CABRI CORE KNOWLEDGE FOR A NEW SAFETY CASE. J. ESTRADA, G. RITTER, D. BESTION, J-CH. BRACHET, Y. GUÉRIN, O. GUÉTON. RRFM Conference 2009 Vienna.
- [7] CABRI Études de coeur. Cinétique rapide. French Nuclear Society. Reactor physics section technical meeting. 10/21/2009 Paris. O. Guéton, G. Ritter.
- [8] Safety of experiments prior to a test campaign and associated reactivity injection characterization. G. Ritter, Th. Cadiou, A. Rondeaux. Research Reactor Fuel Meeting 11th Conference, Roma, Italy, March 20-24, 2011.

Validation of the 3-D VENTURE and MCNP UMLRR Core Models used in Support of the WPI Fuel Transfer Project

DR. JOHN R. WHITE, RUSSELL GOCHT, MICHAEL PIKE, and JEREMY MARCYONIAK
Nuclear Engineering Program, UMass-Lowell, Lowell, MA 01854

ABSTRACT

This paper overviews recent efforts to validate a set of new 3-D VENTURE and MCNP models of the UMLRR core. Several inter-comparisons of the two models as well as direct comparison to measured data from the reactor at two burn states (BOL and after about 50 MWD of operation) were made. In most cases, good to excellent agreement was achieved with both models -- and, with successful validation, both the VENTURE and MCNP models can now be utilized with confidence within a variety of on-going and future projects.

Introduction

Upon closing of the Worcester Polytechnic Institute (WPI) research reactor, the slightly used WPI fuel elements were transferred to the University of Massachusetts Lowell for use in our on-campus 1 MW pool-type research reactor.¹ Although the WPI and UMass-Lowell research reactor (UMLRR) elements have similar geometries and both contain low enriched uranium (LEU) fuel, the material composition of the fuel meat is different -- the WPI fuel plates contain uranium-aluminide fuel (UAl_x -Al) and the UMLRR plates have uranium-silicide fuel (U_3Si_2 -Al). In addition, the U235 loading is 167 g for the WPI element vs. 200 g for the UMLRR assembly and there are also some small differences in meat thickness, plate thickness, water gap thickness, etc. Thus, because of the number of variations to consider, a formal comparison and safety evaluation for combined use of the UMLRR and WPI fuel elements within the reactor is needed before the WPI fuel can be used -- and a series of reactor physics and thermal analysis computations are required to perform the desired comparative analyses.

At UMass-Lowell, the VENTURE code, with few-group cross sections generated by a series of SCALE modules, has traditionally been the primary tool used to do 2-D and 3-D core physics studies, with focus on computing reactivity effects and spatial power distributions within a variety of core configurations. A set of consistent 2-D and 3-D VENTURE models was generated in 1999 for support of the conversion of HEU to LEU fuel in the UMLRR. The actual conversion was successfully completed in August 2000 and the models generated at that time²⁻³ have proved to be adequate for predicting the overall core physics behavior within the UMLRR for the last 10+ years.

However, after a detailed review of the existing VENTURE models, it became clear that some updates were needed to support the WPI fuel transfer project and that some additional analytical capabilities that are not available with the deterministic VENTURE models would be highly desirable. In particular, we identified several changes that could be made that would simplify the VENTURE model, make it more useful, and improve upon the overall accuracy of the computational results. In addition, it was decided that a detailed MCNP model of the UMLRR was needed to support a variety of analyses associated with its various experimental facilities (since few-group diffusion theory is not particularly useful for these tasks). Thus, the decision was made to overhaul the existing deterministic VENTURE models and to generate a new detailed 3-D stochastic MCNP model of the UMLRR core and surrounding experimental facilities. Burnup was achieved by coupling MCNP spatial analysis to ORIGEN2 temporal analysis using MCODE so that both the deterministic and stochastic models could simulate the behavior of the system with both fresh and burnt fuel configurations. This paper overviews the various UMLRR configurations that were modeled and addresses the steps taken to validate the new physics models generated as part of this work.

The M-1-3 and M-2-5 UMLRR Core Configurations

The 1 MWth UMass-Lowell Research Reactor (UMLRR) contains a 7x9 grid of fuel assemblies, graphite reflector elements, irradiation baskets, and corner posts. It also has two grid locations reserved for an external neutron source and a low-worth regulating rod for fine reactivity control. Four large control blade assemblies are used for gross reactivity control and for reactor shutdown. The reactor is enclosed on four sides by an aluminum core box and a large pool of water surrounds the system on three sides, with a 3 inch lead shield and large graphite thermal column on the remaining side. The original system also had a set of six beam ports along the axial centerline of the core. A specific arrangement of fuel elements, graphite reflector blocks, and radiation baskets makes up a particular core configuration.

In August 2000 the UMLRR converted from the use of HEU uranium-aluminide fuel to LEU uranium-silicide fuel (see Refs. 2-3). The basic layout for the LEU startup core arrangement, including the six beam ports and thermal column, is sketched in Fig. 1. This reference configuration is referred to as the M-1-3 core and it contains 19 full fuel assemblies and 2 partial assemblies arranged roughly in the center of the 7x9 grid. Directly in the middle of the core is a central irradiation zone known as the flux trap. Note that, when referring to a given location, the row and column indices shown in the sketch are used (e.g. the flux trap is contained in location D5). Also, when referring to the four large control blades, the blades are numbered consecutively starting in the lower left region of Fig. 1 and increasing in a clockwise direction. Thus, Blade 1 is in the lower left, Blade 3 in the upper right, etc., as viewed from the perspective of Fig. 1.

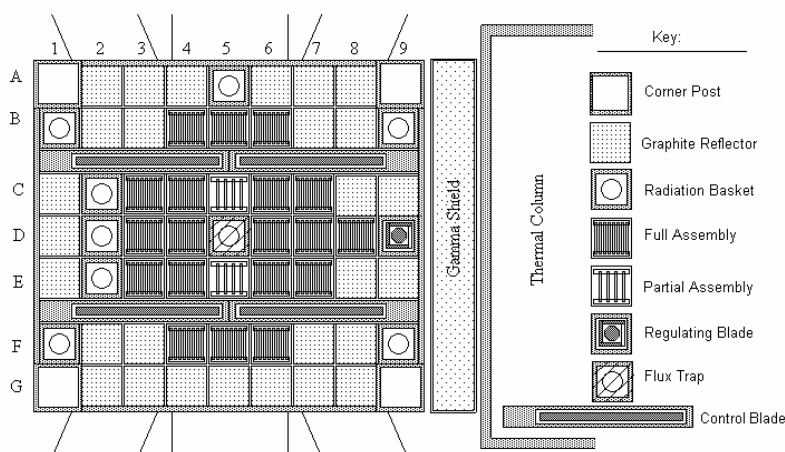


Fig. 1 LEU startup core layout for the UMLRR (M-1-3 core).

During startup testing in Fall 2000, a series of reactivity evaluations and flux profile measurements were taken within the beginning-of-life (BOL) M-1-3 configuration to support routine operation of the new LEU core. Now, 10+ years later, these experimental results are still important since they can be used to help validate any new models that may be developed.

In late 2001, a new ex-core fast neutron irradiation facility⁴ was installed within the UMLRR pool. The fast neutron irradiator (FNI) replaced the three beam ports on the side of the core next to row A. The FNI was purposely placed outside the core for relatively easy access to the large experimental location and to minimize any effect on core operation during its use. This new facility required some changes to the actual in-core assembly configuration -- to optimize performance of the FNI and to counter reactivity effects caused by the composite facility changes. The resulting configuration, including the FNI grid and shield blocks, is referred to as the M-2-5 configuration and this is also the current operating layout for the UMLRR (February 2012). This post-FNI configuration is sketched in Fig. 2.

During the approximately 11-year period since startup (Aug. 2000 through June 2011), the LEU core accumulated about 1100 MWhr of total burnup (i.e. equivalent to about 46 full power days at 1 MW operation). Also of note is that the M-1-3 core had less than 4 MWD of burnup when the new M-2-5 configuration was installed. Thus, most of the operating history to date has been associated with a single core layout -- that is, the M-2-5 configuration.

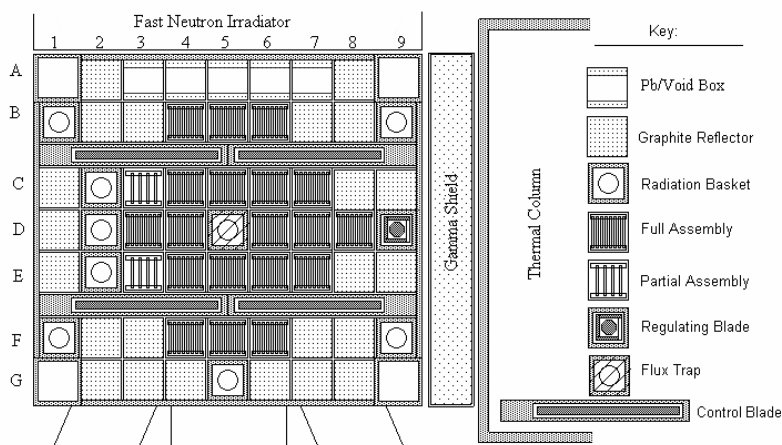


Fig. 2 Post-FNI configuration for the UMLRR (M-2-5 core).

From a model validation perspective, the BOL M-1-3 model represents a fresh core and it has the most measured data available (reactivity evaluations and some thermal flux mappings) to support model evaluation -- thus, this configuration is the easiest and best to use for initial model validation. Also of interest is the initial M-2-5 configuration, but only reactivity evaluations (i.e. measured blade worth curves) are available for this configuration. However, because of the low burnup level (less than 4 MWD), approximating this configuration with fresh fuel densities gives a good representation of reality. In contrast, for the current configuration with its nearly 50 MWD cumulative burnup, fuel depletion calculations are required to achieve a reasonable representation of the core physics. However, since the VENTURE and MCNP models after 50 MWD of burnup essentially represent current operations, this also presented an opportunity to perform additional measurements within the reactor. In particular, selected reactivity worths measurements associated with various bayonet insertions and fuel element interchanges were made in July 2011 and compared to predictions with the new computational models.

Calculational Results and Model Validation

The three configurations noted above have been fully modeled in both codes and comparisons to measured data have been performed. There were four primary comparisons made as part of the validation effort, as follows:

1. Prediction of the "critical" k_{eff} for each of the three critical configurations.
2. Comparison of the computed and measured total worths for each of the five control blades for each configuration. Also of interest here is an estimate of the excess reactivity for each configuration.
3. Comparison of some selected axial thermal flux profiles from the computational models with measured data for the M-1-3 core.
4. Comparison of some selected reactivity worth measurements within the initial M-1-3 startup core and in the current M-2-5 configuration with nearly 50 MWD of burnup.

Each of these comparisons is discussed separately in the following subsections.

Prediction of the "Critical" k_{eff} : The critical configurations for the M-1-3 startup core, the M-2-5 BOL core, and the July 2011 M-2-5 core with nearly 50 MWD of burnup, all give consistent results for the "critical" reactivity level of the system, as summarized in Table 1. As seen here, the VENTURE results have a rather large, but consistent, negative bias of about

2.0-2.5% $\Delta k/k$, but the predicted critical MCNP k_{eff} values are very close to unity for all the cases, indicating that these models can predict the absolute reactivity level of the UMLRR with good accuracy (the MCNP calculations used 20×10^6 histories with $1\sigma = 0.0002 \Delta k/k$). The cause of the large reactivity bias for the VENTURE model is not apparent, but it does not seem to affect the usefulness of the model for a wide range of other parameters (see below).

Table 1 Summary results for several critical configurations within the UMLRR.

Model Description	Blades 1-4 Location (inches out)	Regulating Blade Location (inches out)	VENTURE K_{eff}	MCNP K_{eff}
BOL M-1-3	15.3	8.0	0.980	0.995
BOL M-2-5	14.9	10.0	0.978	0.999
M-2-5 at 50 MWD	16.3	7.7	0.975	0.996

Prediction of Blade Worths: Estimating the reactivity worth associated with each of the four large control blades and the low-worth regulating blade within the UMLRR was another main component of the model evaluation process. Unfortunately, however, the discussion of the blade worth results is somewhat cumbersome for several reasons -- mostly because of the relatively large uncertainty that exists in the resultant “measured or experimental” differential and integral worth curves (e.g. see the discussion in Refs. 2-3). Thus, the comparisons here are not as “clean” as desired and are more qualitative in nature than quantitative -- with focus on obtaining the proper blade worth distribution among the four blades, along with a reasonable estimate of the absolute magnitude of the total worth of each blade.

Table 2 Computed vs. measured blade worths for three UMLRR configurations.

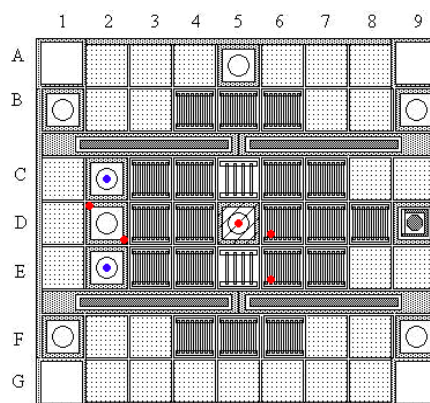
	M-1-3 BOL Core Total Worth (% $\Delta k/k$)			M-2-5 BOL Core Total Worth (% $\Delta k/k$)			M-2-5 at 50 MWD Total Worth (% $\Delta k/k$)		
Blade #	Expt.	VENT	MCNP	Expt.	VENT	MCNP	Expt.	VENT	MCNP
Blade 1	2.63	2.95	3.00	2.82	2.91	2.76	2.55	2.86	2.73
Blade 2	2.47	2.80	2.75	2.19	2.35	2.40	2.23	2.29	2.40
Blade 3	3.32	3.32	3.42	3.19	3.16	3.42	3.64	3.06	3.19
Blade 4	3.20	3.43	3.55	3.93	3.72	3.83	4.19	3.74	3.71
Total Blades 1-4	11.6	12.5	12.7	12.1	12.1	12.4	12.6	12.0	12.1
Excess K_{eff} Blades 1-4	2.82	3.22	3.44	3.46	3.45	3.46	2.41	2.71	2.60
Regulating Blade	0.28	0.44	0.38	0.30	0.45	0.38	0.31	0.45	0.38

From the summary data in Table 2, generally good agreement to within 10-15% is apparent for most of the calculated vs. experimental results for the four large control blades -- and, considering the observed uncertainty in the experimental approach, this is actually not bad. In addition, all the expected trends are predicted quite nicely with the various VENTURE and MCNP models. For example, the fuel and graphite/water reflector arrangement suggests that, for the M-1-3 BOL core, there should be a slight tilt in the flux and blade worth distribution in the direction of Blades 1 and 4, with an additional slight shift towards Blade 4 (lower right portion of Fig. 1). Thus, for the BOL M-1-3 core, we would expect the worths for Blades 1 and 2 to be comparable, with Blade 1 worth a little more than Blade 2. Similarly, Blades 3 and 4 should have comparable worths, with Blade 4 having the largest reactivity effect of all the blades. For the M-2-5 configurations, roughly the same worth distribution is expected, but the asymmetry should be magnified significantly because of the movement of the partial

assemblies to the left side of the core (Col. 3 instead of Col. 5) and the replacement of five graphite reflectors in Row A with Pb-void elements (i.e. compare Figs. 1 and 2). Thus, for this configuration, Blade 2 is expected to have the lowest worth and Blade 4 the highest, with the difference being much larger than for the M-1-3 layout. These expected trends are exactly as observed in Table 2, which gives good confidence in the ability of the computer models to predict these effects.

Concerning the regulating blade worths, the VENTURE and MCNP values are consistently high relative to the measured values. Here the VENTURE values are 45-55% high and MCNP over predicts the worths by 25-35%. However, it is important to note that the absolute differences are rather small and the uncertainty in the measured value is not negligible.

Axial Thermal Flux Profiles in the M-1-3 Core: A mix of gold foils (blue) and copper wires (red) were used to perform thermal flux mapping in selected locations of the M-1-3 LEU startup core as illustrated in the UMLRR core map shown here. Cadmium-covered and bare gold foils were used to provide an absolute determination of neutron fluence rate, while copper wires provided an axial flux distribution at the chosen locations. The irradiation was performed at a power level of 100 watts for 30 minutes. The wires and foils were then removed and counted on a gamma spectrometer, and the measured flux distribution data were then normalized to a nominal power level of 1 MW and compared to the results from the VENTURE and MCNP computational models for the M-1-3 core with the BOL critical blade configuration.



Summary results from these comparisons are shown in Fig. 3. The individual small circles on these curves represent the experimental values of the absolute thermal flux, the dots with the 1σ error bars are associated with the MCNP results, and the solid lines represent the VENTURE predicted flux profiles. The top two plots highlight the two copper wires in the D2 position, with relatively good agreement in both cases. The results for the wires in the two fuel assemblies are shown in the middle plots and, as apparent, the MCNP simulation over predicts the thermal flux in these regions by as much as 20-25%, whereas the VENTURE results are quite good. Finally, the bottom curve in Fig. 3 shows the computed and measured thermal flux profiles in the center of the flux trap assembly in location D5. The agreement here is also quite reasonable for both cases with a good representation of the axial shape but, again, the MCNP results slightly over predict the flux magnitude by roughly 10-15%.

Finally, we should note that there is not a lot of information available about the uncertainty in the measurements that were taken back in August 2000 (only nominal flux values are available). This is unfortunate, since it is difficult to draw quantitative conclusions about the validity of the computer models without some idea as to the uncertainty in the experimental data. One concern, for example, is that the irradiations were performed at a power level of approximately 100 W and the measured data were then scaled to 1 MW -- thus, even a small error in this "approximate" power level could account for a magnitude difference in the measured and computed results. Overall, however, the five experimental and computed axial profiles for both models show good qualitative agreement, with the VENTURE results giving somewhat better magnitude comparisons to the nominal experimental data.

Selected Reactivity Worth Comparisons: As a final indicator of the general reliability of the UMLRR computational models, a number of measured reactivity worth results were also compared with those computed using the MCNP models for the BOL M-1-3 core and for the M-2-5 configuration after nearly 50 MWD burnup. The majority of the tests involve the insertion of an empty (air-filled) bayonet into one or more specific locations. However, one test in the M-1-3 core also measured the worth of a water-filled bayonet in the flux trap.

Finally, the worth associated with the replacement of a burnt fuel element in location D6 with a fresh uranium-silicide assembly was also compared. Table 3 summarizes these reactivity worth comparisons -- where we note that a full set of VENTURE comparisons are not given here, since its homogenized flux trap and radiation basket geometries are not appropriate for these type of calculations (this is one of the main reasons for developing the MCNP model).

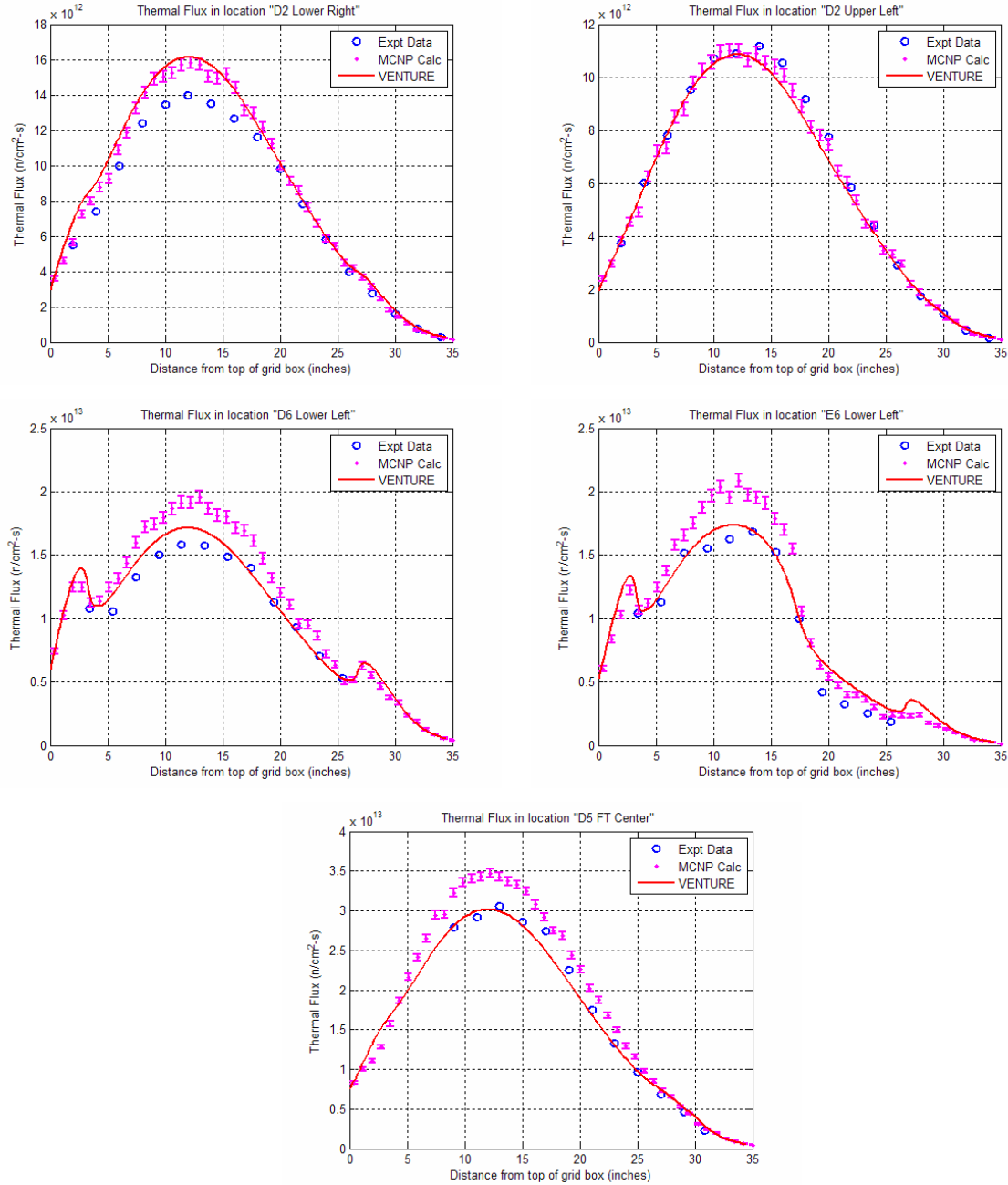


Fig. 3 Calculated vs. measured axial thermal flux profiles at various locations (M-1-3).

In these comparisons, it is important to emphasize that the 1σ uncertainty in the MCNP computations is about 0.02% $\Delta k/k$, and this is a large uncertainty when the absolute actual $\Delta k/k$ is less than 0.10%. In addition, as noted above, there is also a fair amount of uncertainty in the blade worth curves which were used to get the "measured" reactivity worths. Thus, the best we can hope for here with these small worth measurements is to be "in the ballpark" with the correct direction for the reactivity change. For the larger worths, however, a more quantitative comparison is indeed possible.

Table 3 Computed vs. measured reactivity worth results for selected configurations.

Case #	Description of the Experimental Configuration	M-1-3 BOL Core Reactivity Worths (% $\Delta k/k$)		M-2-5 at 50 MWD Reactivity Worths (% $\Delta k/k$)	
		Measured	MCNP	Measured	MCNP
1	air-filled bayonet in flux trap (D5)	0.25	0.20	0.11	0.14
2	water-filled bayonet in flux trap (D5)	0.03	0.06	--	--
3	air-filled bayonet in radiation basket (D2)	-0.01	-0.07	--	-0.05
4	air-filled bayonet in radiation basket (C2)	--	--	-0.00	-0.02
5	air-filled bayonets in both C2 and D2	--	--	-0.02	-0.08
6	air-filled bayonets in C2, D2, and E2	--	--	-0.02	-0.08
7	interchange fresh fuel assembly with the burnt fuel element in D6	--	--	0.10	0.10

Well, as apparent from Table 3, the measured and calculated reactivity worths are indeed “in the ballpark”. In general, small measured reactivities map to small computed values and the correct direction of the change is consistently predicted. For the larger changes, as apparent for Case 1 for example, the magnitude of the change is also well predicted within our uncertainty constraints. In addition, for Case 7, it was estimated that the burnup associated with the fuel element in location D6 was approximately 2.75 MWD, which gives a reduction of slightly over 3 grams of U235 relative to a standard fresh fuel assembly. Thus, by replacing this burnt element with a fresh assembly, one would expect a positive reactivity addition associated with about 3 grams of fissile material near the center of the core. As apparent from Table 5, the reactivity effect was indeed positive and the predicted magnitude was the same as the measured result. For comparison, a VENTURE calculation for this fuel interchange perturbation gives 0.13% $\Delta k/k$, which is also in excellent agreement with the measured value.

Summary/Conclusion

The current validation effort has looked at critical blade heights, total blade worths, selected thermal flux profiles, and some reactivity worth measurements in both the M-1-3 and M-2-5 cores. In all cases, the computational results are reasonable and they consistently exhibit the expected behavior of the system. There are some areas that could use improvement (such as the negative reactivity bias in VENTURE and the over-prediction of some of the thermal flux profiles with MCNP), but generally, the comparisons have been quite favorable. Thus, both the VENTURE and MCNP models have successfully passed their first set of validation tests. Of course, model validation is a never-ending process -- so we plan to continually evaluate the real predictive capability of these computer models as they are used to support future operations within the UMLRR facility.

References

- Decommissioning status for the WPI reactor at URL: <http://www.nrc.gov/info-finder/decommissioning/research-test/worcester-polytechnic.html>.
- J. R. White, et. al., “Calculational Support for the Startup of the LEU-Fueled UMass-Lowell Research Reactor,” Advances in Reactor Physics and Mathematics and Computation, Pittsburgh, PA (2000).
- J. R. White and L. Bobek, “Startup Test Results and Model Evaluation for the HEU to LEU Conversion of the UMass-Lowell Research,” 24th International Meeting on Reduced Enrichment for Research and Test Reactors, San Carlos de Bariloche, Argentina (2002).
- J. R. White, et. al., “Design and Initial Testing of an Ex-Core Fast Neutron Irradiator for the UMass-Lowell Research Reactor,” ANS Radiation Protection and Shielding Topical Conference, Santa Fe, NM (2002).

METHODS FOR VERIFYING ACCURATE MEASUREMENTS IN RESEARCH REACTORS

M. A. GAHEEN

*Egypt Second Research Reactor (ETRR-2), Egyptian Atomic Energy Authority (EAEA)
13759, Abou Zabal – Egypt*

ABSTRACT

Accurate measurements are fundamental to operation and power control of any Research Reactor (RR). In this paper, methods for verifying accurate measurements in research reactors are proposed and discussed. The cross-calibration test is proposed for calibration verification of temperature instrumentation. The second method is for accurate core flow verification based on initial measurements of core pressure drop. A power monitoring system based on ^{16}N (Nitrogen-16) measurement is also described to verify the accurate relationship between indicated power and actual core power. These verification methods are discussed with practical examples and experiments. It is shown that the application of these methods complies satisfactory with the operational requirements.

1. Introduction

The instrumentation used in a RR can be classified as nuclear instrumentation and process or non-nuclear instrumentation. Nuclear instrumentation is used to detect the neutron flux a low level to maximum power level [1]. The measured neutron flux is calibrated to provide an indicated power that can be related to the actual power within the core. Accurate relationship between indicated and actual power can be obtained by the methods of thermal power. This later methods require accurate measurements of temperatures and flow rates [2]. Process instrumentation comprises those process measurements that involve temperature, flow, and pressure parameters. The nuclear and process measurements are sent to protection system and/or monitoring and control system [1].

In this paper, methods are proposed for verifying accurate measurements of temperatures, core flow, and core power in research reactors. The cross calibration method is proposed for calibration verification of temperature instrumentation. The cross-calibration is a test for verifying the calibration of a number of detectors that measure the same process parameters. Its basic principle of operation is to record the reading of detectors, average these readings, and calculate the deviation of each detector from the average, less any outlier(s) [3]. The second method is for accurate core flow verification based on initial measurements of core pressure drop. As will be shown, the core pressure drop is function of the core coolant temperature and core flow. The accurate core flow should results in a core pressure drop within these initial measurements. Linearity and thermal balance should provide a confidence in the measured core power. The operation for increasing the core power is performed in steps. Making thermal balance in each, linearity and calibration of nuclear instrumentation can be verified [4]. The calibration constant allows obtaining the relation between measured local flux and core power. However, the calibration constant is depending on neutron detector location, configuration of fuel elements and/or reflectors, and control rod positions. ^{16}N measurement can provide independent method for corroborating or correcting the obtained power from neutron detectors [1, 5, 6].

These methods for verifying accurate measurements in research reactors are presented and discussed with practical examples and experiments performed at Egypt Second Research Reactor (ETRR-2).

2. RR measurements and instrumentation

In this section, the research reactor measurements and instrumentation are described and discussed. In Fig 1, the nuclear and process measurements of interest are shown in the schematic view of a typical open pool RR plant. The cooling system consists of two core cooling loops and pool cooling system with interconnection flow between core and pool cooling systems as can be found in some RR plants [7].

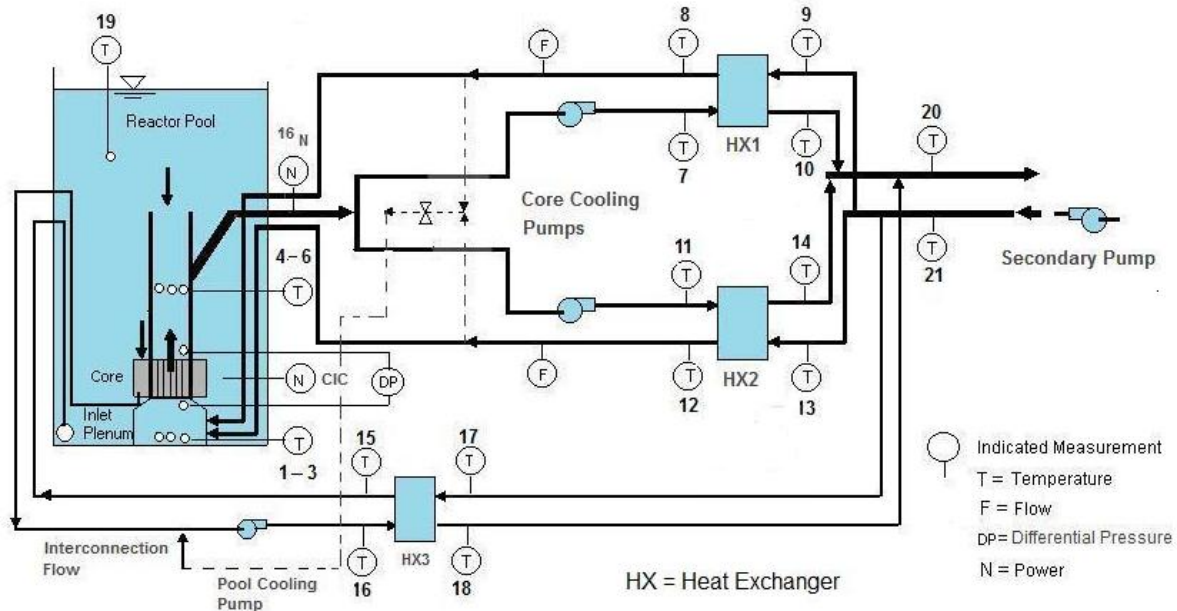


Fig. 1. Schematic view of a typical open pool RR plant

Temperatures (T) are measured with RTDs (Resistance Temperature Detectors), which use platinum elements, have very high sensitivity, linearity and precision. RTDs can be used safely up to temperatures of 500°C, and in general have larger time constant than thermocouples [1]. The temperature is indicated through a measurement of the resistance $R(T)$ of the element [8]:

$$R(T) = R_0 (1 + a T) \quad (1)$$

Detectors used are platinum 100 RTD type ($R_0 = 100 \text{ ohm}$ and $a = 0.00385$), specified in accordance to DIN 43760 Class A with maximum allowable deviation of $\pm 0.13 \text{ ohm}$. Each core inlet (outlet) coolant temperature measurement assembly includes two platinum 100 detectors. The first detector is used for inlet (outlet) coolant temperature measurement. The second detector is used for core coolant Differential Temperature (DT). Each coolant temperature measurement includes platinum 100 detectors are connected to RTD and to current converters to provide a 4 - 20 mA output current. The current is wired to protection system and/or monitoring and control system [1].

Despite the several techniques of flow measuring, the most common type of flow meters use differential pressure transmitters to measure the difference in pressure caused by orifice plates or venture tubes placed in the piping system. Accuracies of the order of 3 % are easily achievable, and the instruments are simple and extremely reliable, therefore suitable for safety systems [1]. The subsystem is calibrated to evaluate the Flow (F) as a function of the Differential Pressure (DP) where maximum flow and operation temperature should be specified:

$$F = \text{constant} \sqrt{DP} \quad (2)$$

It is also important to notice that the differential pressure can be measured in other locations like in the reactor core itself. The reactor core is a restriction to the flow, and it causes a differential pressure. This signal known as core DP is usually used in the reactor protection system. Most of them are used to assure that there is coolant flowing in the system. Differential pressure through the core is measured by means of differential pressure transmitters. Transmitters used are of the capacitive sensor type and develops a 4 - 20 mA current output. Maximum inaccuracy must be equal or lower than 0.2 % of full span [1].

Compensated Ionization Chambers (CIC) is used to measure the core neutron flux. The main reason to monitor neutron flux in a RR is that it is proportional to the power density, and this is the variable which operators are concerned about. The detector is located out of the reactor core, and the quantity measured is often the leakage flux. This will reduce radiation hazard to the detector and also limit the effect of gamma induced current [1]. The measured neutron flux is calibrated with the thermal power measurements verifying linearity and accurate relationship between indicated and actual core power. The core power is calculated using measured core flow and Differential Temperature (DT_{Core}) and power transferred to the pool (P_{Pool}). The losses through the pool and the piping can be neglected and core power is calculated as [4]:

$$P_{Core} = 1.16 (\text{Core Flow} \times DT_{Core} + P_{Pool}) \pm 0.08 \quad (3)$$

Where $P_{Pool} = \text{Pool Flow} \times \text{pool heat exchanger primary side inlet and outlet temperature difference}$ (about 7 % of core power). This method has the advantage of its fast estimation of the core power and therefore set of calibration points can be obtained. However, possible temperature non-uniformity between RTDs used in measuring the outlet core temperature is the main disadvantage of this method.

The second method of thermal balance requires some hours of power operation (about 6 hours). The core power is calculated using the measured flow (F) and heat exchanger primary side inlet and outlet temperatures (T_i HX and T_o HX respectively) as follows:

$$P_{Core} = \rho_{o1} C_{p1} F_1 (T_i HX_1 - T_o HX_1) + \rho_{o2} C_{p2} F_2 (T_i HX_2 - T_o HX_2) + \rho_{o3} C_{p3} \text{ Pool Flow } (T_i HX_3 - T_o HX_3) \quad (4)$$

The subscripts 1, 2, and 3 denote, respectively, core cooling loop 1, core cooling loop 2, and pool cooling system. The water density (ρ) and specific capacity (C_p) is calculated as function of the heat exchanger average temperature using the equations [9]:

$$\rho = 2.080 \times 10^{-5} T^3 - 6.668 \times 10^{-3} T^2 + 0.04675T + 999.9 \quad (5)$$

$$C_p = 5.2013 \times 10^{-7} T^4 - 2.1528 \times 10^{-4} T^3 + 4.1758 \times 10^{-2} T^2 - 2.6171T + 4227.1 \quad (6)$$

^{16}N activity is produced by the activation of ^{16}O (oxygen-16) within the reactor core, through the nuclear reaction: $^1_0\text{n} (\text{neutron}) + ^{16}_8\text{O} \longrightarrow ^{16}_7\text{N} + ^1_1\text{p} (\text{proton})$. The ^{16}N level is therefore proportional to the reactor integral flux, or the integral power. Hence a detector that is located near a core coolant discharge line can be used to monitor the activity ^{16}N level and hence the core power:

$$\text{Power} = \text{conversion parameter} \times ^{16}\text{N current (PA)} \quad (7)$$

The conversion parameter of this power measuring system is provided first using thermal power measurements. This approach provides a method for corroborating or correcting the obtained power from neutron detectors [1]. However, it should be recognized that the power signal from a ^{16}N detector will be delayed relative to the true core power by the time required for the coolant to flow from the core to the detector location (^{16}N activity is measured by a gamma ionization chamber).

3. Verification methods and results

3.1 Cross-calibration test

The cross-calibration of RTDs in a RR plant is based on the assumption that, at isothermal plant conditions, the average temperature of a sufficient number of RTDs reflects the true temperature of the process. The isothermal plant condition is achieved when the cooling pumps are operated without power for a time enough to assume that all RTDs are at the same temperature. Any significant departure from this assumption can cause errors in the results of cross-calibration. The test may include the RTDs used in measuring inlet and outlet temperature of the core, heat exchangers, and cooling tower and reactor pool temperature. Table 1 shows results from a typical cross-calibration test. In the example in Table1, the temperatures for the whole plant RTDs are averaged, and the result is subtracted from each individual temperature to identify the deviation (Dev) of each RTD from the average. If the deviation of any RTD element exceeds a predetermined value (e.g. ± 0.8 °C or ± 0.4 °C), the RTD element measurement is excluded from the average. Normally, the accepted deviation value of the temperature instrumentation used in protection and power control is lower than deviation of the instrumentation used in monitoring [3]. In cross-calibration test, the RTDs that are excluded (from the average) are referred to as outliers. An outlier is either replaced, recalibrated, or a new calibration table is developed for the outlier using the cross-calibration data.

The calibration of core DT instrumentation can be also verified since the output reading of core DT instrumentation should be 0.0 °C during this test.

RTD No.	Whole plant RTDs		Average of whole Plant less one outlier (*)		Average of whole plant less two outliers (**)	
	T °C	Dev °C	T °C	Dev °C	T °C	Dev °C
1	29.6	-0.12	29.6	-0.07	29.6	-0.11
2	29.5	-0.22	29.5	-0.17	29.5	-0.21
3	29.4	-0.32	29.4	-0.27	29.4	-0.31
4	29.6	-0.12	29.6	-0.07	29.6	-0.11
5	30.6	0.88	Outlier	0.92	Outlier	0.89
6	29.0	-0.72	29.0	0.67	Outlier	0.71
7	29.7	-0.02	29.7	0.03	29.7	-0.01
8	29.7	-0.02	29.7	0.03	29.7	-0.01
9	29.5	-0.22	29.5	-0.17	29.5	-0.21
10	29.6	-0.12	29.6	-0.07	29.6	-0.11
11	30.1	0.38	30.1	0.43	30.1	0.39
12	29.9	0.18	29.9	0.23	29.9	0.19
13	29.7	-0.02	29.7	0.03	29.7	-0.01
14	29.8	0.08	29.8	0.13	29.8	0.09
15	30.0	0.28	30.0	0.33	30.0	0.29
16	29.8	0.08	29.8	0.13	29.8	0.09
17	29.6	-0.12	29.6	-0.07	29.6	-0.11
18	29.8	0.08	29.8	0.13	29.8	0.09
19	29.8	0.08	29.8	0.13	29.8	0.09
20	29.8	0.08	29.8	0.13	29.8	0.09
21	29.6	-0.12	29.6	-0.07	29.6	-0.11
Average	29.72	0.00	29.67	0.00	29.71	0.00

(*): Predetermined deviation value is 0.8 °C

(**): Predetermined value is 0.4 °C

Table1: Results of cross calibration test

3.2 Initial measurements of core DP

Initially, during the commissioning, the core DP measurements were made in the pre-operational tests and with the reactor running at power. As shown in Fig. 2, the core pressure drop is function of the core coolant temperature (average temperature) and core flow. The accurate core flow for a given core average temperature should results in a core pressure drop within these measurements. As shown in Fig. 3, the initial measurements of core pressure drop (the accurate measurements) are within the two dashed lines (less than $\pm 2\%$). The variation in core flow can be obtained through the interconnection flow valve. The core DP has the advantages of its sensitivity to small variation in core flow as shown in the test points $+ 2\%$ and $\pm 0.3\%$ and can be calibrated directly by measuring known pressure values. This verification method can be also applied for each core cooling loop (50 % of nominal core flow).

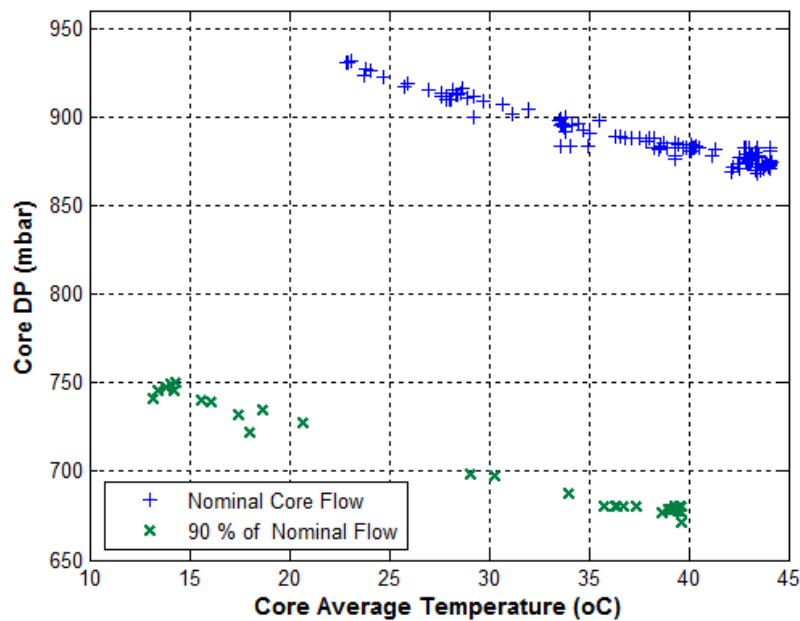


Fig. 2. Initial core DP versus core average temperature and core flow

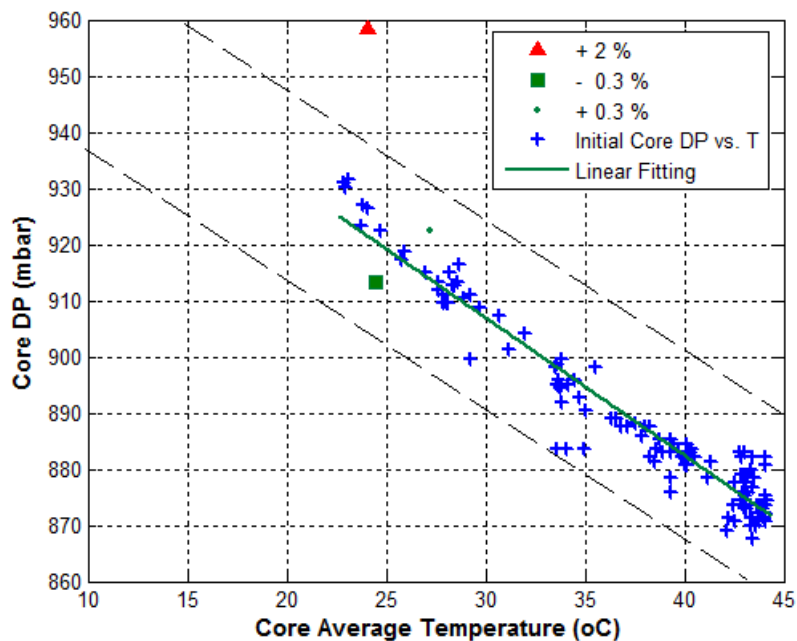


Fig. 3. Accurate measurements of core flow (between the dashed lines)

3.3 ^{16}N measurement

The operation for increasing the core power is performed in steps. In one step, the thermal balance can be done using the temperature and flow instrumentation. Accurate power measurement can be verified by linearity and obtained power from thermal balance as shown in Fig.4 for ^{16}N detector. The dashed line is the linear power (%) versus ^{16}N current (PA) using a conversion parameter of 0.005763. The ^{16}N is power monitoring system based on ^{16}N measurement. Also, during operation for shutting down, the accurate power measurement can be verified.

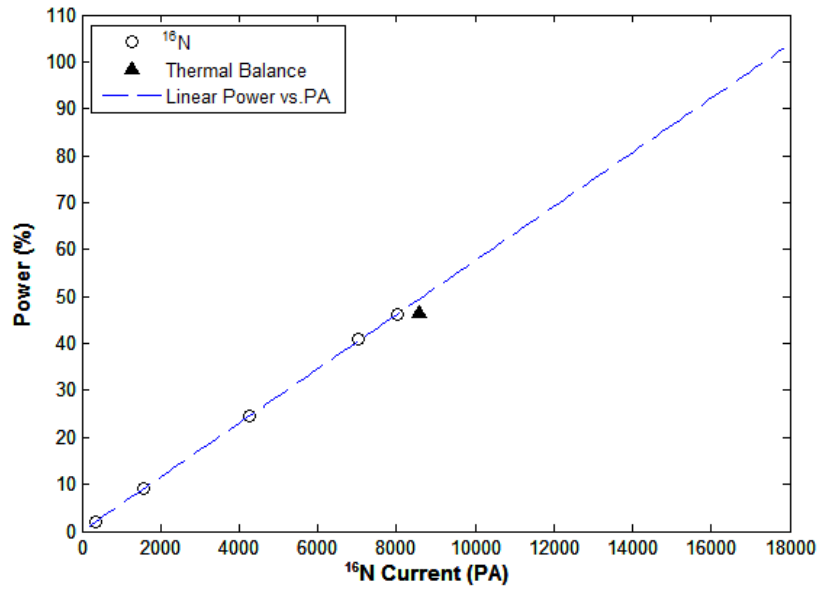


Fig. 4. Power vs. ^{16}N current

CIC calibration constants are altered upon CIC movement, changes in the configuration of fuel elements and/or reflectors, and modification of control positions. Using the power obtained from ^{16}N measurement the CIC can be calibrated or corrected. The quotient between the average reading of every CIC (nv) and the average ^{16}N reading (MW) allows obtaining the calibration constant (nv/W) of every CIC. Fig. 5 shows the CIC readings versus power from ^{16}N measurement and thermal power (Eq. 3). The deviation between the two methods of power measurement is less than 2 %.

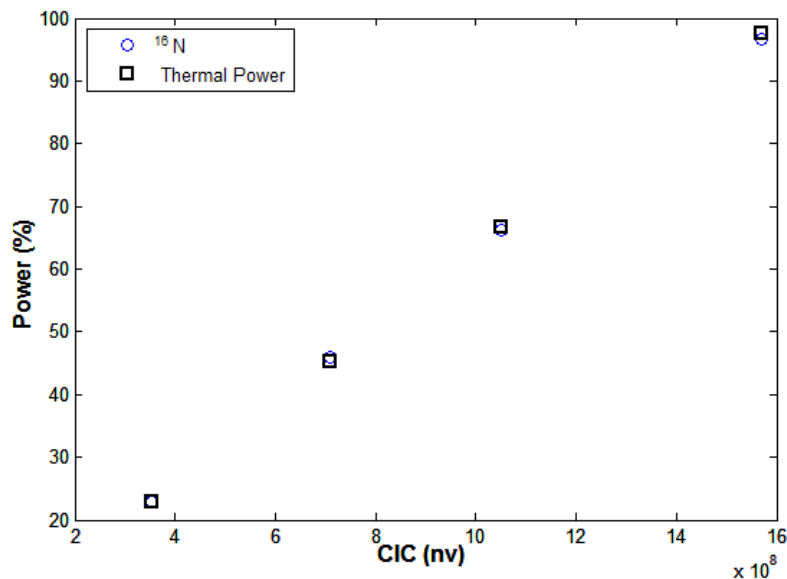


Fig. 5. CIC readings versus ^{16}N power and thermal power

4. Conclusions

Methods for verifying accurate measurements of temperature, core flow, and power in research reactors are described and discussed. Each method is giving confidence that the parameter being measured is within that approved by its conditions of operations. It can be concluded that the application of these methods is simple and can be done during reactor start up, power operation, or shutting down i.e. normal procedures of operation. The methods of calibration verification comply satisfactory with the operational requirements and thus it is proposed for use in similar RR plants.

5. References

- [1] International Atomic Energy Agency, "Research reactor instrumentation and control technology," IAEA –TECDOC-973, Vienna, October 1997.
- [2] A. Z. Mesquita, H. C. Rezende, "Thermal methods for on-line power monitoring of the IPR-R1 TRIGA Reactor," *Progress in Nuclear Energy*, Vol. 52, pp. 268-272, 2010.
- [3] H. M. Hashemian, "Maintenance of Process Instrumentation in Nuclear Power Plants," Springer-Verlag Berlin Heidelberg, 2006.
- [4] G. Gennuso, A. Doval, "steps for power rise," Procedures No. 767-5420-3PPCG-011-10, 23 November 1997.
- [5] J. E. Moorman, P. A. Beeley, J.P. Highton, "A Review of Four Methods for the Independent Monitoring of Core Power in the Jason Argonaut Reactor," IAEA-SM-360/50P, Research Reactor Utilization, Safety and Management, Symposium held in Lisbon, Portugal, 6–10 September 1999.
- [6] R. Blaumann, J. M. Longhino, F. Sánchez, E. Lopasso, F. Lezczycynski, D. Ferraro, F. Brollo, C. Fernández, "RA-6 reactor conversion and neutronic tests of the new silicides fuel core," International Meeting on Reduced Enrichment for Research and Test Reactors (RERTR), Beijing, China, 1-5 November 2009.
- [7] Gee Y. Han, "Mathematical Dynamic Modeling and Thermal-Hydraulic Analysis of HANARO," *International Communication of Heat and Mass Transfer*, Vol. 28, pp. 651-660, 2001.
- [8] Alan S. Morris, "Measurement and Instrumentation Principles," Butterworth-Heinemann, 2001.
- [9] J. A. W. Gut, J. M. Pinto, "Modeling of plate heat exchangers with generalized configurations," *International Journal of Heat and Mass Transfer*, Vol. 46, pp. 2571-2585, 2003.

HORIZONTAL CHANNEL FOR NEUTRON RADIOGRAPHY AND TOMOGRAPHY IN LVR-15 RESEARCH REACTOR

L. VIERERBL, J. ŠOLTÉS, Z. LAHODOVÁ, M. KOŠTÁL, M. VINŠ

*Research Reactors, Nuclear Centre Řež Ltd.,
Husinec-Řež near Prague, 250 68, Czech Republic*

ABSTRACT

The LVR-15 reactor is a light water research reactor, which is situated in Nuclear Centre Řež Ltd., Řež near Prague. The reactor operates as a multipurpose facility with maximal thermal power of 10 MW. It has ten horizontal channels. One of them, not used up to now, is prepared for neutron transmission radiography and tomography. The method is based on absorption and scatter of thermal neutrons in the analysed sample. The channel leads neutrons from the reactor core with 3 m long and 100 mm in diameter tube. For the neutron radiography, collimated beam of thermal neutrons is necessary to prepare. Around the irradiation box, shielding for gamma and neutron radiation will be used for radiation protection purposes. Measurement of neutron fluence in the beam outlet with free channel is presented. Measurement results are compared with MCNP calculations. Next calculations of neutron fluence and gamma dose rate were made for design of filters inside the channel and shielding around the irradiation box.

1. Introduction

The LVR-15 reactor [1] is a light water moderated and cooled tank nuclear research reactor with forced cooling. It is situated in Nuclear Centre Řež Ltd., Řež near Prague. The nominal reactor thermal power is 10 MW and it operates as a multipurpose facility. It offers services in many fields: material research, production of radioisotopes for medical and industrial purposes, irradiation of silicon single crystals, neutron activation analysis, neutron capture therapy, neutron diffraction etc.

The reactor is equipped with ten horizontal channels, see Fig. 1. One of them is an epithermal neutron beam, used mainly for boron neutron capture therapy (BNCT), others use thermal neutrons for neutron diffraction, prompt gamma neutron activation analysis (HC3) and similar methods.

Horizontal channel HC1 have not been regularly used up to now. In 2011, project was started to adapt the channel for neutron radiography and tomography. The final goal (2015) is to build up the workplace for non destructive testing, diagnostics and 3D imaging with neutron radiography and tomography. In the paper, design of filter inside the channel and design of outer shielding around the irradiation box is described, which is the first stage of the project.

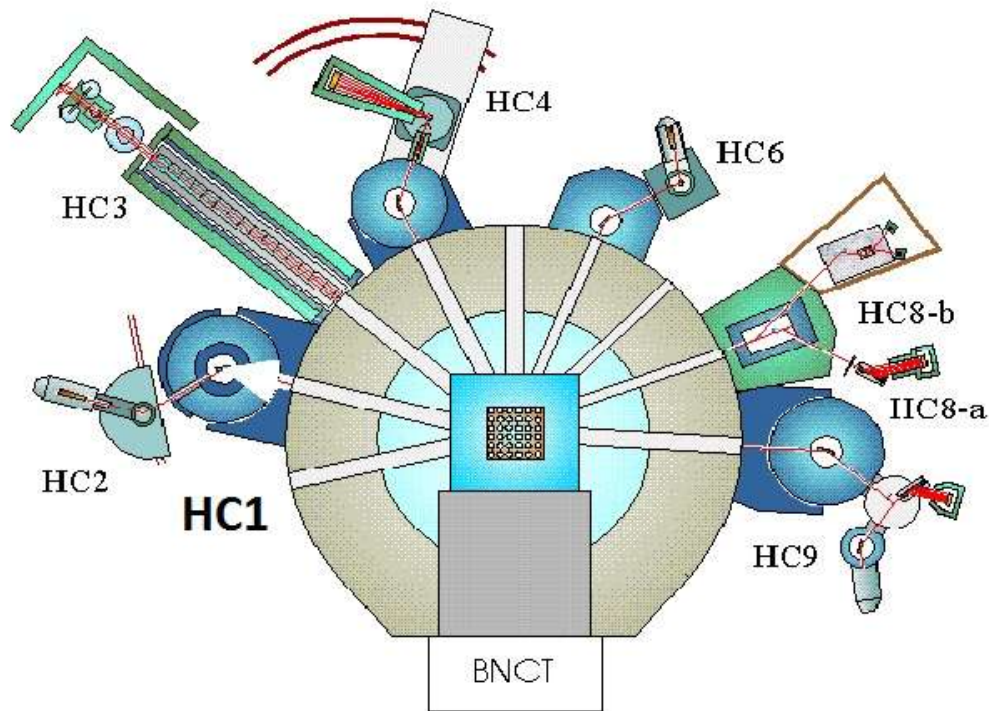


Fig. 1. Arrangement of horizontal channels in the LVR-15 reactor

2. Parameters of the free channel

Neutrons from the reactor core pass through cylindrical tube to the beam outlet, which is about 3 m from the reactor core and has a diameter of 10 cm. In the first step, neutron fluence and spectrum and gamma dose rate were evaluated for the free channel (i.e. empty, without filter).

Neutron fluence and spectrum was calculated by MCNPX code (red line in Fig. 2) and verified by measurement with activation detectors (blue dotted line in Fig. 2). The detectors were $\phi 10 \text{ mm} \times 0.1 \text{ mm}$ foils. Ten types of activation detectors were used: Au, W, La, Cu, Fe, In and Ni without cadmium cover and Au, W, La, Cu with 1 mm cadmium cover. Detectors were irradiated for 1 hour, then induced activities of the detectors were measured [2]. The neutron spectrum was evaluated [3] with the SAND II unfolding code using the IRDF90 dosimetry library. Measured values of neutron fluence rate for free channel and four energy groups are in Table 1.

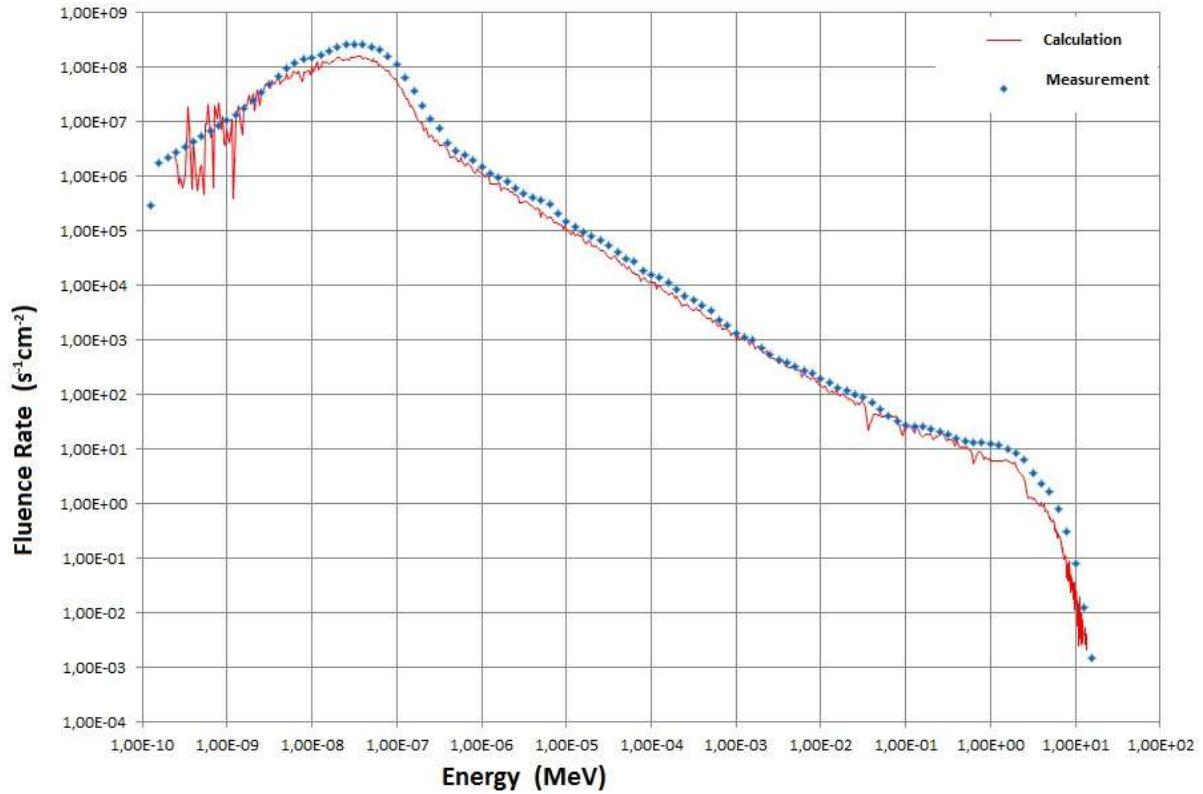


Fig. 2. Neutron spectrum for free channel in the outlet point

Table 1. Neutron fluence for free channel in the outlet point for 4 energy groups

Neutron energy	Neutron fluence rate (cm ⁻² .s ⁻¹)
< 0.501 eV	3,03E+09
0.501 eV - 10 keV	1,43E+09
10 keV - 1 MeV	5,48E+08
> 1 MeV	3,25E+09

Gamma dose rate was evaluated by MCNPX code with result of 5300 Gy/h for free channel in the outlet point.

3. Design of the filter

Ideal beam for neutron radiography and tomography is collimated beam of thermal neutrons with sufficient fluence rate. In real case always fast neutrons and gamma radiation are present. Evaluated values of fast neutron fluence rate and gamma dose rate for free channel are too high. In this case an outer shielding satisfying radiation protection demands would be too massive (mass, space, cost). Therefore a filter inside of the channel is usually used. The filter should suppress fast neutrons and gamma radiation and transmit thermal neutrons (thermal neutron filter). For this purpose are used different materials such as quartz, bismuth, aluminium, silicon, lead and sapphire [4], [5].

For HC1 filter design we consider on materials: silicon and bismuth single crystals and polycrystalline aluminium. Fig. 3 shows MCNPX calculated neutron spectrum for four versions of the filter. The thermal neutron parts of the spectra are a little underestimated due to particular single crystal properties (e.g. [4]).

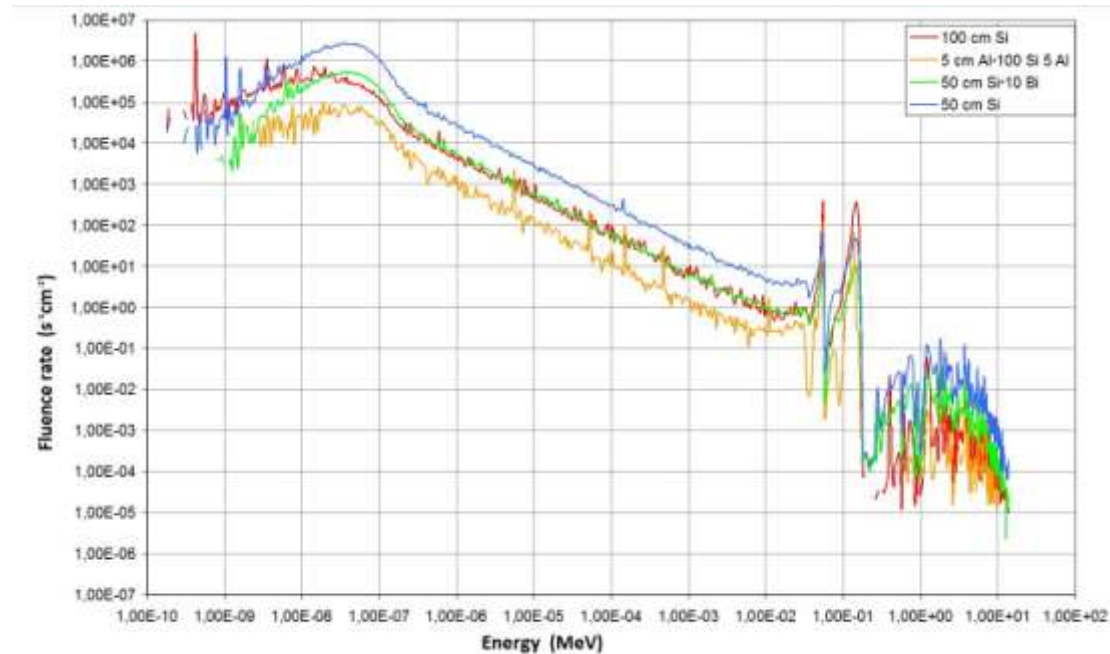


Fig. 3. Neutron spectrum for different filters in the outlet point

4. Design of the outer shielding

Outer shielding was designed mainly from borated polyethylene (30 cm) and lead (6 cm), see Fig. 4. Dose rates from neutrons and photons were calculated by MCNPX code in several points and with different filters. Table 2 gives example of results for point P1 and four filters. In the table “primary photons” are generated in reactor core, “secondary photons” come from interaction of neutrons with sample and shielding.

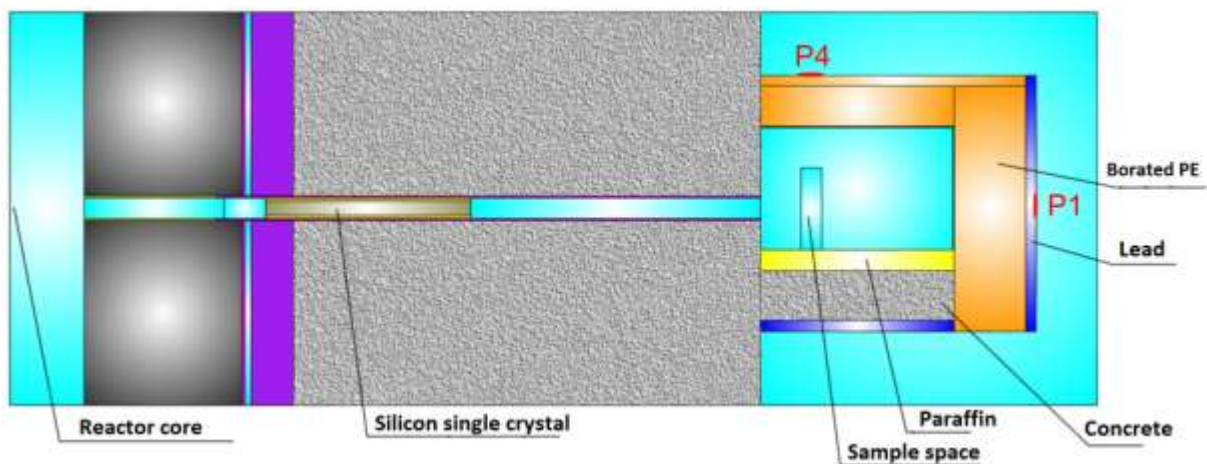


Fig. 4. Calculation model of HC1 with filter and outer shielding

Table 2. Dose rates in point P1

Filter	Dose rate ($\mu\text{Sv/hod}$)		
	Neutrons	Primary photons	Secondary photons
100 cm Si	2.1	171.1	27.9
50 cm Si	146.5	2624.5	197.5
50 cm Si + 10 cm Bi	28.9	68.5	22.8
5 cm Al + 100 cm Si + 5 cm Al	0,7	25.9	2.3

5. Conclusion

For horizontal channel HC1, design of the filter is based on 100 cm Si single crystal and outer shielding on borated polyethylene (30 cm) and lead (6 cm). Total neutron fluence rate on the beam outlet for free channel was calculated and measured with result of $9 \cdot 10^9 \text{ s}^{-1} \text{ cm}^{-2}$ with uncertainty of 15 %. Thermal neutron fluence on the beam outlet with designed filter is estimated about $10^8 \text{ s}^{-1} \text{ cm}^{-2}$. Parameters of the beam should allow neutron radiography and tomography with space resolution of 0.1 mm and sensitivity for hydrogen concentration in the sample about 0.1 %.

6. Acknowledgement

This work was performed within the scope of research project ALFA No. TA01010237 supported by Technology Agency of the Czech Republic.

7. References

- [1] NRI Rez, 2008. Research Reactor LVR-15, <http://www.nri.cz/eng/rsd_services.html>
- [2] ASTM E181-98, 2003. Standard Test Methods for Detector Calibration and Analysis of Radionuclides.
- [3] ASTM E944-08, 2008: Standard Guide for Application of Neutron Spectrum Adjustment Methods in Reactor Surveillance.
- [4] M. Adib and M. Kilany, J. Rad. Phys.& Chem. 66 (2003) p.81.
- [5] D.F.R. Mildner and G.P. Lamaze, J. Appl. Cryst. 31 (1998) p.835.

IN-CORE OPTICAL THERMOMETRY FOR THE FUTURE LORELEI LOCA TEST DEVICE OF THE JULES HOROWITZ REACTOR (MTR)

L. RAMIANDRISOA, G. CHEYMOL

*CEA Saclay, DEN, DANS/DPC
F-91191 Gif-sur-Yvette – France*

N. HORNY, T. DUVAUT

*GRESPI, Université de Reims Champagne Ardenne
Campus Moulin de la Housse, 51100 Reims – France*

V. VANDENBERGHE

*CEA Saclay, DEN, DANS/DMN
F-91191 Gif-sur-Yvette Cedex – France*

C. GONNIER

*CEA Cadarache, DEN, CAD/DER/SRJH
F-13108 St-Paul-lez-Durance – France*

ABSTRACT

In many experiments lead in Material Testing Reactors the temperature is a key parameter for understanding the behaviour of nuclear materials and its estimation depending on the localization in the reactor may not be easy. The Light-water One Rod Equipment for Loca Experimental Investigations (LORELEI) test device which will be implemented on the Jules Horowitz Reactor (MTR) illustrates this difficulty. In this device the CEA will simulate a Loss Of Coolant Accident (LOCA) transient. The aim is essentially to analyse cladding materials behaviour in such a hard environment where steam oxidation is enhanced by temperatures exceeding 800°C. The ability to gauge the fuel rod temperature with a precision of $\pm 10^\circ\text{C}$ and in real time (1Hz) would constitute a great advantage for understanding and modelling the phenomena. This paper aims at explaining how such a sensor can be developed.

1. Introduction

One of the most accidental scenarii considered in Nuclear Power Plant design is the LOCA. It implies a large break on the primary circuit inducing a violent pressure decrease from nominal value (~ 150 bars for LWR) to few bars. This depressurization at nominal temperature ($\sim 300^\circ\text{C}$ for LWR) results in fast ejection of a two phase flow at the break and in a steam environment in the core. The core dewatering makes the fuel clads overheat (800 up to 1200°C). They are unable to resist to the generated high internal pressure. At around 700 - 800°C (or higher, depending on the inner pressure) they may burst and fission products may be released into the reactor building. The oxidation of the clads by steam at high temperature weakens the cladding material which becomes more brittle.

This typical accident will be simulated on one rod placed inside LORELEI test device at the Jules Horowitz Reactor core periphery. The ambient irradiation in this MTR is mixed: the dose rate exceeds 1 kGy/s and neutron flux $10^{13} n_{\text{fast}}/\text{cm}^2/\text{s}$. The cumulated dose during test sequence will be about 1 GGy and fluence near $10^{19} n_{\text{fast}}/\text{cm}^2$. The test device LORELEI (figure 1) will consist of a holder fitted with the rod, cooled by a water channel and surrounded by the test device structures (thermal insulation, inox tubes...). In order to create a simplified LOCA the water channel will be partially emptied and replaced by 2-3 bars hot steam. As the fuel rod overheats the surrounding shell will be artificially heated in order to reproduce more or less the adiabatic conditions of one rod in a LWR core centre.

A track of the fuel clad temperature in the midrod would allow a better understanding of the burst phenomena. But the traditional use of thermocouples is prohibited especially in this

case. The first reason is due to the high sensitivity of the clad: the thermocouple would create a cold point which would systematically disturb the burst conditions. The second reason relates to the reliability of thermocouples. Thus one may try to design a non contact real time measurement: the CEA plans to integrate in the LORELEI test device an optical thermometric sensor deported by fibre. Inserted in the test device a few millimetres away from the fuel rod, an optical fibre will transmit the clad thermal radiation far from the damaging neutrons and γ radiations. A pyrometric analysis helped by preliminary known properties of cladding material will deduce the corresponding temperature.

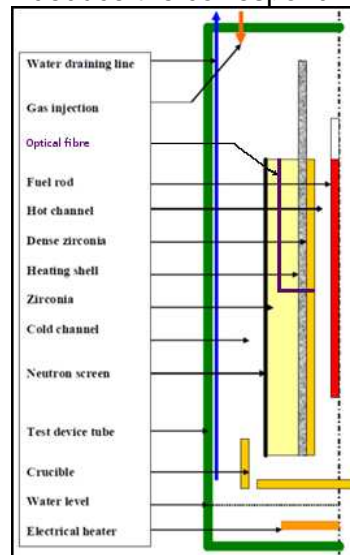


Figure 1: LORELEI's diagram. The dotted line is the rotational symmetry axis.

2. Optical fibre in severe environment

The collected signal must be taken away from the JHR core in order to be numerically interpreted: the outset will be insured by an optical silica fibre. The choice of this technology is motivated by its less intrusive aspect and its potential resistance against irradiation. Designing an optical fibre for application in LORELEI involves determining the dimensions of its core and its cladding, their respective chemical compositions (doping agents), the nature of the protective coating and designing the sight system toward the fuel rod. One must be careful with the fibre bending when it goes far from the sight system: through the test device structures the fibre core dimension must be small enough.

The silica glass suffers from severe irradiation mixed with high temperature.

Neutrons and γ irradiation creates crystallographic defects in silica. Combined with pre-existing ones the irradiation generates parasite signals and absorption. Many authors have studied defect types and their relation to the luminescence/absorption phenomena observed in nuclear environments [7], [1] and [5]. With the exception of Cerenkov radiation which decreases as the wavelength increases as λ^{-3} on the whole spectra, luminescence and absorption occur within limited spectral ranges. Thus the windows 800 to ~ 1200 nm and possibly 1400 to 1600 are free for use. The "hole" at around 1300 nm is due to silica luminescence at 1270 nm and to OH absorption at 1380 nm. Irradiation also reduces the fibre transmission creating a Radiation Induced Attenuation (RIA). As observed in previous experiments like COSI in 2008 [3] for a pure silica core fibre the higher the wavelength in the near infrared range the higher the RIA. The ability to measure at the end of the second window depends on the chosen detector sensitivity.

Since it is not placed on the clad but few millimetres away, the fibre extremity does not reach in LORELEI more than 800°C but it is high enough to suspect local potential deterioration of the silica. If the sight system includes some lenses or porthole(s), they must be resistant to peaks of at least 800°C .

Few articles address the combined influence of irradiation and temperature. It seems that relatively high temperatures may cure some silica defects. At the present time we think about either a pure silica core or an F-doped silica core both with metallic coating.

3. Pyrometry methods

The raw optical signal collected and transmitted by the fiber must be cleared of luminescence parasites. Once it has been deconvolved by the detector transfer function the signal can be treated. The pyrometry is established by Planck's law:

$$L(\lambda, T) = \frac{C_1}{\lambda^5} \frac{1}{e^{\frac{C_2}{\lambda T}} - 1} \text{ [W/m}^2\text{/sr/m]} \quad [a]$$

This physical law describes the maximal spectral radiance L a body can emit according to its temperature T and the measurement wavelength λ . C_1 and C_2 are constants. The ideal body (or blackbody) is a fictive object able to emit the exact thermal radiation predicted by this law at a given temperature. In order to retrieve the temperature at given radiance and wavelength one can simply inverse the formula (monochromatic pyrometry):

$$T = \frac{C_2}{\lambda \ln\left(\frac{C_1}{L(\lambda, T)\lambda^5} + 1\right)} \text{ [K]} \quad [b]$$

Transfer function and fibre transmission can be determined through calibration. A real body is less easy to describe. To quantify its deviation from blackbody, a coefficient called emissivity (noted ε) is introduced. The emissivity depends on many parameters [6], [9] either quantifiable or not.

The first obvious emissivity parameters are the nature of the observed surface, the wavelength and the temperature. But in general only experimental analysis can reach a conclusion on the importance of the last two parameters.

Secondly the emissivity depends more qualitatively on the precise state of the surface. Even a thin oxide layer, a solid phase transition or little roughness is likely to modify the outline of emitted thermal radiations. In general apparition of roughness tends to make the emissivity uniform and close to 1 (blackbody).

The pyrometry needs precise information about emissivity values of the studied surface [2] and this parameter may be in some cases very difficult to obtain experimentally. Although some literature lists experimental data on typical metals or dielectrics, if their experimental conditions differ even a little, then an accurate comparison cannot be made. Moreover the emissivity may also vary during experiments making the analysis more difficult. Some pyrometry methods try to partially get round this problem [4], relying on relative emissivity values: the bichromatic one uses 2 wavelengths whose emissivity values ratio must be known whereas the multispectral one only requires the spectral emissivity coarse shape.

4. Experiment

As seen above the use of pyrometry requires a preliminary study of the clad emissivity: depending on this knowledge we have more or less a choice of pyrometry methods. Our first experiment thus aims at determining as precise as possible the emissivity of a zircaloy-4 clad without irradiation for a given temperature. We try to compare the clad spectra to a blackbody one at the same temperature. If the transmitting system is conserved, the spectral emissivity is the ratio of both spectra. We must be cautious with the precision of this comparative method because the emissivity uncertainty is strongly dependent on both temperatures uncertainties:

$$\frac{\Delta\varepsilon}{\varepsilon} = \left(\frac{dF_C}{F_C} + \frac{dF_B}{F_B}\right) + \frac{C_2}{\lambda T_C} \frac{dT_C}{T_C} + \frac{C_2}{\lambda T_B} \frac{dT_B}{T_B} [\%] \quad [c]$$

Just above the first term is the power total uncertainties, clad and blackbody. T_C is the clad temperature and T_B the blackbody one: even if we have tried to do $T_C = T_B$ the blackbody and clad temperature uncertainties are not necessarily the same (numerical application in 4.2).

4.1. Materials

For clad spectra we use an experimental facility named EDGAR 2 located at the CEA Saclay centre to simulate the LORELEI device but without irradiation. EDGAR 2 was initially designed for mechanical studies especially burst phenomena during LOCA clad overheat. It consists of a holder for a half meter long clad surrounded by a protective moving inox shell with 5 silica portholes. Air (ambient) or steam (a little hotter than 100°C) can be blown into the vessel. Once the clad is clamped by holder it is heated by an electric current (maximum about 1000 A) thanks to Joule's effect. The PID (Proportional Integral Derivative) control is

made by a pyrometer IMPAC IGAR 12-LO whose sight uses one of the vessel portholes. The pyrometer indications are more or less confirmed in static conditions by a reference K-thermocouple placed in the inner midclad. The clad sample is a 490 mm long piece of rod in Zircaloy-4: its diameter is about 9.6 mm and its thickness about 570 μm . Because of the air/steam environment at high temperature the clad becomes quickly covered with a thin oxide layer (ZrO_2) reaching several micrometres in few minutes.

For the blackbody spectra we use a SR70-32 cylinder-shaped cavity source (CI-System). The temperature range reaches 900°C.

Our optical system is made of two identical silica lenses. The focusing plane makes an agreement between short (800 nm) and long (1700 nm) wavelengths. A multimode fibre SMA - FC/PC (silica core of 200 μm and Number of Aperture 0.2) carries the signal into a spectrometer. The spectrometer is an ANDO OSA AQ6315.

4.2. Results and perspectives

In figure 2 we overlay the spectra issued from the clad sample (blue) at the temperature indicated by the reference thermocouple 720°C and the blackbody (green) settled to the same temperature.

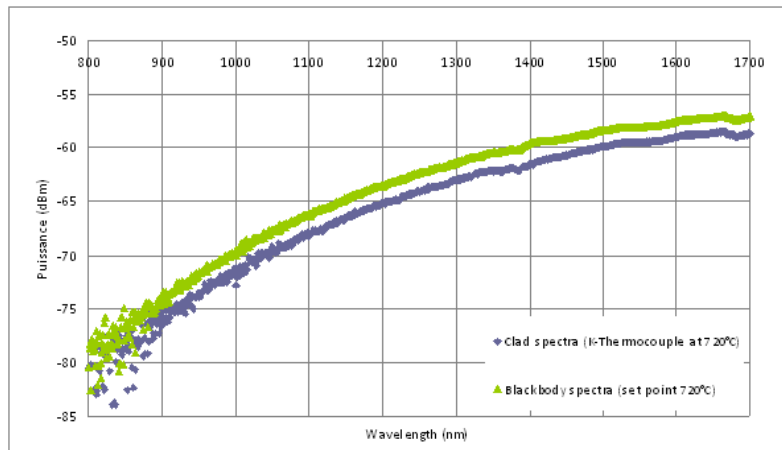


Figure 2: Comparison between clad and blackbody spectra

The following graph (figure 3) plots the emissivity shape according to the wavelength deduced from the ratio between both curves.

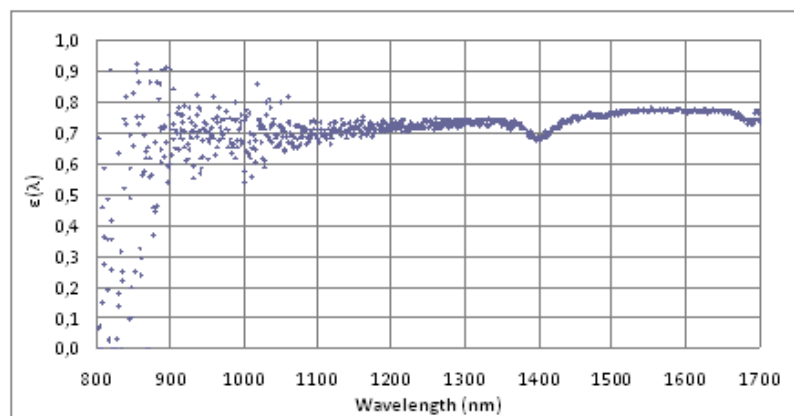


Figure 3: Ratio between clad and blackbody spectra

The signal is lost in the noise at wavelengths shorter than 1100 nm. Between 1100 and 1700 nm the signal is cleaner but some accidents around 1380 and 1650 nm on the curve betray some technical problems with the spectrometer. Globally the emissivity is flat and turns at around 0.7 and 0.8 which are close to literature values [8]. The preliminary results appear promising but the useful spectral range must be enlarged to shorter wavelengths and the theoretical uncertainties reduced as much as possible.

Because of the bichromatic uncertainties relationship, the technical specification of $\pm 10^\circ\text{C}$ for the temperature measurement is respected if the levels of both emissivity uncertainties are limited (no power noise) [4]:

$$\frac{dT}{T} = \frac{\lambda_1 \lambda_2}{|\lambda_1 - \lambda_2|} \frac{T}{C_2} \left(\frac{d\varepsilon_1}{\varepsilon_1} + \frac{d\varepsilon_2}{\varepsilon_2} \right) [\text{K}] \quad [\text{d}]$$

The table 1 gives values with $\lambda_1 = 1.0 \mu\text{m}$ and $\lambda_2 - \lambda_1 = 0.5 \mu\text{m}$ at 700°C .

$\frac{d\varepsilon_1}{\varepsilon_1} + \frac{d\varepsilon_2}{\varepsilon_2} [\%]$	0.5	1	2	4	8	16
$\frac{dT}{T} [^\circ\text{C}]$	1.0	2.0	3.9	7.9	15.8	31.6

Table 1: Numerical applications of [d]

The blackbody uncertainty is $\pm 3^\circ\text{C}$. The inner thermocouple value is most probably higher than the surface temperature but we cannot estimate to what extent. Nevertheless the K-thermocouple uncertainty is $\pm 5.4^\circ\text{C}$. Under the equation [c] with no power noise the emissivity uncertainty is at least 15.5% at 800nm and decreases to 7.3% at 1700nm. This precision is far too low to allow a bichromatic measurement according to [d] and our standards (table 1).

We have to enhance the temperature knowledge for example by modelling heat transfer between inner and outer clad. In short term we will change both spectrometer and blackbody source to respectively improve the spectra registration (noise) and to enlarge the aperture diameter (practical reason). In midterm we must optimize the thermocouple location.

5. Conclusions

The study of emissivity is the first point to describe for an in-depth design of a LORELEI pyrometric sensor. For the moment we want to measure as precisely as possible the spectral emissivity ($< 2\%$) in order to respect the technical specification of $\pm 10^\circ\text{C}$ for the clad temperature measurement. The next step will compare the performances of the various pyrometry methods with their corresponding wavelengths in temperature monitoring for any Zircaloy-4 fuel rod without irradiation. If any of the methods are successful we will integrate the fibre constraints (core composition and diameter, luminescence parasite signals, differential RIA...) and its sight system into our study.

6. References

- [1] B. Brichard, P. Borgermans, A. F. Fernandez, K. Lammens, and M. Decretton. Radiation effect in silica optical fiber exposed to intense mixed neutron-gamma radiation field. *Ieee Transactions On Nuclear Science*, 48(6):2069–2073, December 2001.
- [2] François Cabannes. *Température de surface: mesure radiative*. Techniques de l'Ingénieur, 1996.
- [3] G. Cheymol, H. Long, J.F. Villard, and B. Brichard. High level gamma and neutron irradiation of silica optical fibers in cea osiris nuclear reactor. pages 1 –5, 2007.
- [4] T. Duvaut, D. Georgeault, and J. L. Beaudoin. Multiwavelength infrared pyrometry: Optimization and computer simulations. *Infrared Physics & Technology*, 36(7):1089–1103, December 1995.
- [5] S. Girard. *Analyse de la réponse des fibres optiques soumises à divers environnements radiatifs*. PhD thesis, Université Jean Monnet de Saint Etienne, 2003.
- [6] Philippe Hervé. *Mesure de l'émissivité thermique*. Techniques de l'Ingénieur, 2005.
- [7] T. Kakuta, K. Sakasai, T. Shikama, M. Narui, and T. Sagawa. Absorption and fluorescence phenomena of optical fibers under heavy neutron irradiation. *Journal of Nuclear Materials*, 258-263(Part 2):1893 – 1896, 1998.
- [8] P.M. Matthew, M. Krause, M. Dean, and M.H. Schankula. Emittance of zircaloy-4 sheath at high temperatures in argon and steam atmospheres. 1989.
- [9] Dominique Pajani. *Thermographie*. Techniques de l'Ingénieur, 2001.

IMPACT OF THE NEW JAPANESE NUCLEAR DATA LIBRARY (JENDL-4.0) ON THE CRITICALITY OF RSG GAS (MPR-30) REACTOR

Tagor Malem SEMBIRING

*Center for Reactor Technology and Nuclear Safety, National Nuclear Energy Agency (BATAN)
Kawasan PUSPIPTK Gd. No. 80, Serpong, Tangerang Selatan 15310 - Indonesia*

Peng Hong LIEM

*Nippon Advanced Information Service (NAIS Co. Inc.)
416 Muramatsu, Tokai-mura, Naka-gun, Ibaraki 319-1112 - Japan*

ABSTRACT

Benchmark calculations of the new JENDL-4.0 nuclear data library on the first criticality experiments of the Indonesian multipurpose reactor, Reaktor Serba Guna G.A. Siwabessy (RSG GAS, former name MPR-30) has been conducted using a continuous energy Monte Carlo code, MVP-II. It was found that the latest nuclear data showed high accuracy where in average only 0.27 % overestimation in predicting the criticality, while the older version, i.e. JENDL-3.3 produced 0.35 % overestimation in average. It can be concluded that the latest nuclear data improved significantly.

1. Introduction

Accurate neutronic parameters are very important in the design and safety analysis of a research reactor. The calculation method and neutron cross-section data play an important role to obtain an accurate neutronic parameter. For the calculation method, the Monte Carlo calculation is the best option for improving the accuracy of the calculated neutronic parameters. Furthermore, the use of recent nuclear data is an answer to get higher accuracy for the calculated parameters.

The Japanese Evaluated Nuclear Data Library, JENDL-4.0 [1], is the most recent evaluated nuclear data which covers 406 materials (405 nuclides and 1 natural element) with the incident neutron energy range from 10^{-5} to 20 MeV. Unlike the previous release (JENDL-3.3 [2] or older), thermal neutron scattering data for typical moderator materials are now included, such as beryllium metal and water used in the present benchmark as the reflector and moderator materials, respectively.

This paper deals with the accuracy of the JENDL-4.0 in benchmarking the first criticality experiments of the Reaktor Serba Guna G.A. Siwabessy (RSG GAS, previous name MPR-30). The research reactor uses beryllium metal and light water as its reflector and neutron moderator materials. In this benchmark, the high-fidelity continuous energy Monte Carlo code, MVP-II [3] was used in the criticality calculations for several important criticality conditions during the first criticality experiment series. The results of this benchmark are expected to contribute to the estimation of accuracy of the nuclear data for research reactors which use low enriched uranium (<20 %) fuel, light water moderator and beryllium reflector, as well as to provide suggestions for the future improvement of the nuclear data.

2. Criticality experiments

The Indonesian multipurpose research reactor, RSG GAS, is a beryllium-reflected, light-water-moderated and -cooled, 30 MWth (max.) tank-type reactor. The first criticality of the reactor was achieved in July 29, 1987 [4]. RSG GAS has five transition cores (smaller cores) before a full core configuration (commonly called typical working core (TWC) which consists of 40 standard fuel elements and 8 control fuel elements) can be achieved in the sixth core. As a part of the commissioning work, a series of reactor physics experiments has been done on the transition cores especially for the first core. These efforts have been aimed to check and fulfill the safety and operational requirements. In the present benchmark analyses, several criticality configurations were selected from the un-burnt first core configurations.

The criticality experiments have been conducted as follows:

1. Estimation of the number of standard and control fuel elements required for the first criticality. It was expected that the first criticality (with small excess reactivity) would be achieved with 6 control fuel elements, 8 ± 1 standard fuel elements while all control rods were withdrawn.
2. Six control fuel elements were loaded in the core with the absorber plates were all fully inserted. The ^{252}Cf neutron source was inserted into the E-7 grid position to initiate fission chain reactions, and then loading of standard fuel elements was done step by step. At each loading step, the inverse multiplication rates were plotted for four control rod configurations to estimate the critical loading.
3. The first criticality was not achieved at the 8-th loading of standard fuel elements and the 9-th fuel element was inserted (RI-20 into grid position F-7). As seen in Fig.1, the first criticality was achieved in this loading step where the regulating rod position of 475 mm gave the first criticality condition for the first core of RSG GAS reactor.
4. After the first criticality, as seen in Fig. 2, loading of fuel elements and reflector elements were conducted to achieve a full core configuration with sufficient excess reactivity for one core cycle.

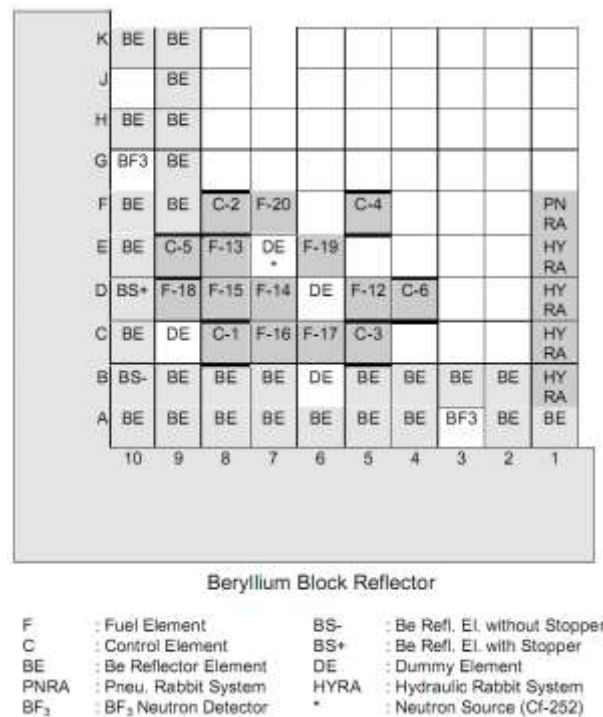


Fig 1. First criticality core configuration of RSG GAS first core
(empty lattices contain water)

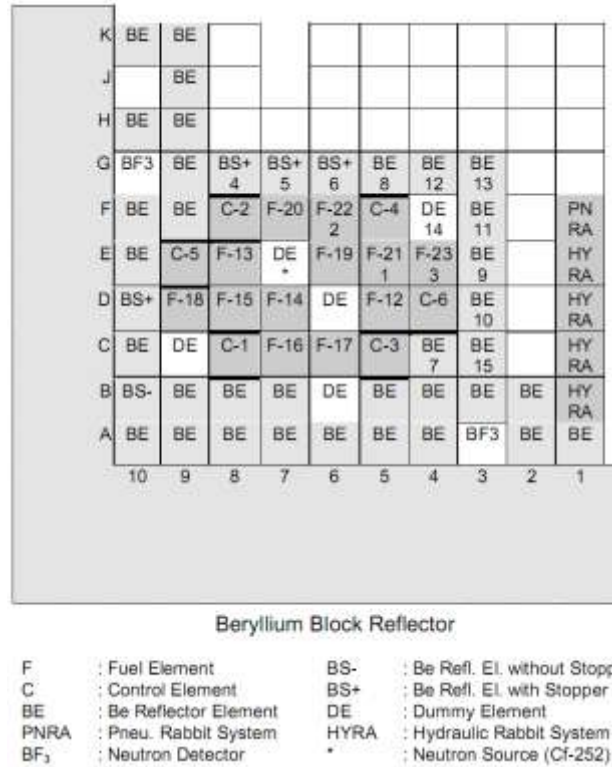


Fig 2. Full core configuration of RSG GAS first core (plain numbers in the core show loading step of fuel, Be reflector and dummy elements after first criticality; empty lattices contain water)

3. Calculation methods

The calculations have been conducted using a continuous energy Monte Carlo code, MVP-II. The active part ($7.71 \times 8.1 \times 60 \text{ cm}^3$) of both standard and control fuel elements were modeled as their exact geometry and dimensions while the top and end-fitting of the elements were modeled in an approximate manner since their geometry are very complicated, that is, the structure materials were homogenized with water by volume weighting. Exact modeling approach was also taken for the active parts of the beryllium reflector elements, beryllium block elements and irradiation positions.

The movable control rods (absorber blades) were modeled as their exact geometry and dimensions. Consequently, 60 cm water layer above the core had to be included in the calculation to provide enough space for the absorber blades when a control rod was fully withdrawn. Approximately 30 cm water layers were included below the core bottom support, and around the beryllium block and element reflectors. Vacuum boundary conditions were imposed on the outer boundary of the reactor system.

All MVP-II calculations in the present benchmark were conducted with JENDL-4.0 library for room temperature of 300 K. The measured critical effective multiplication factors (k_{eff}) were corrected when the core isothermal temperature was not identical with 300 K. The total number of batches (generations) was 10,000 where each batch consists of 10,000 histories, i.e. the total number of effective histories is 100 millions. Initial 100 batches were skipped to guarantee the fundamental mode had been achieved before statistical evaluation of the k_{eff} and other tallies were conducted. Under this calculation conditions, the fractional standard deviation for k_{eff} is less than 0.01 % for all cases.

4. Results and discussions

Table 1 shows the comparison between experiment data and Monte Carlo results for first criticality and excess reactivity of RSG GAS first core. The first criticality predictions by Monte Carlo method were very close to the experiment data, especially the one with JENDL-4.0 library (slightly over-estimation of C/E by about 0.25 %). The previous version, i.e. JENDL-3.3 library produced a slightly higher C/E but still below 0.35 % differences. In the table, the core excess reactivity and control rod worth are also shown and compared. These two were estimated from control rod calibration results and not direct measured values. On top of that, no correction concerning the control rod interference effects were taken into account.

Core configuration		Experiment data	JENDL-4.0	JENDL-3.3
First criticality (9 FEs, 6 CEs, RR=475 mm)	k_{eff}	1.0	1.00243	1.00342
	C/E		1.002	1.003
Full core (9 FEs, 6 CEs, CRs all up)	k_{eff}	1.09242 ^{a)}	1.09854	1.09979
	C/E		1.006	1.007
Full core (9 FEs, 6 CEs, CRs all down)	k_{eff}	n.c. ^{b)}	0.918801	0.919104
	C/E		-	-
Control rods worth	$\Delta\rho(\%)$	17.80 ^{c)}	17.81	17.88
	C/E		1.000	1.004

a) $\beta_{eff} = 0.00765$, estimated from control rod calibration results

b) n.c. = not conducted

c) Shim rod bank compensation method, measured by reactivity meter, summation of single control rod worth

Table 1: The calculation results with experiment data for first criticality and excess reactivity of RSG GAS first core

Table 2 shows the comparison between Monte Carlo results with several critical conditions of the RSG GAS first core occurred during control rod calibrations. These critical conditions were achieved when the calibrated rod was fully inserted and the other rods were in a certain bank position.

Calibrated rod / grid position (calibrated rod position / other rod bank position)		Experiment data	JENDL-4.0	JENDL-3.3
JDA05 / C-5 (600 mm / 288 mm)	k_{eff}	1.00008 ^{a)}	1.00342	1.00403
	C/E		1.003	1.004
JDA06 / C-8 (600 mm / 290 mm)	k_{eff}	1.00008	1.0026	1.00361
	C/E		1.003	1.004
JDA07 / D-4 (600 mm / 282 mm)	k_{eff}	1.00008	1.00277	1.00364
	C/E		1.003	1.004
JDA01 / E-9 (600 mm / 284 mm)	k_{eff}	1.00008	1.00231	1.00302
	C/E		1.002	1.003
JDA04 / F-5 (600 mm / 290 mm)	k_{eff}	1.00008	1.003	1.00374
	C/E		1.003	1.004
JDA03 / F-8 (600 mm / 293 mm)	k_{eff}	1.00008	1.00281	1.00347
	C/E		1.003	1.003

a) $\beta_{eff} = 0.00765$

Table 2: The calculation results with several critical conditions of RSG GAS first core occurred during control rod calibrations

The measured critical conditions shown in the table were already corrected for the Joule effect (which turned out to be negligible) of the primary cooling pumps. It can be observed from the table that Monte Carlo results using JENDL-4.0 library gave excellent C/E agreement with experiment data (C/E over-estimation of 0.27 % in average). JENDL-3.3

library results systematically produced slightly higher C/E but again still below 0.35 % differences.

5. Conclusions and future works

From the present benchmark calculations, it was found that the latest nuclear data library, JENDL-4.0, showed high accuracy where in average only 0.27 % overestimation in predicting the criticality, while the older version, JENDL-3.3, produced 0.35 % overestimation in average. It can be concluded that the latest nuclear data improved significantly.

We are also conducting the same benchmark calculations for other world-widely used latest nuclear data libraries (ENDF/B-VII.0 [5] and JEFF-3.1 [6]). Still more works are needed to identify the source of improvement of the new JENDL-4.0 library. These include sensitivity analyses to investigate the dominant nuclides, nuclear reactions and their energy ranges for this particular system.

References

- [1] K. Shibata et al. (2011) JENDL-4.0: A New Library for Nuclear Science and Engineering. J. Nucl. Sci. Technol. 48, 1-30.
- [2] K. Shibata et al. (2002) Japanese Evaluated Nuclear Data Library Version 3 Revision-3; JENDL-3.3. J. Nucl. Sci. Technol. 39, 1125-1136.
- [3] Y. Nagaya et al. (2004) MVP/GMVP-II: General Purpose Monte Carlo Codes for Neutron and Photon Transport Calculations based on Continuous Energy and Multigroup Methods. *JAERI 1348*.
- [4] Batan (1989) Multipurpose Reactor G.A. Siwabessy Safety Analysis Report, Rev. 7.
- [5] M.B. Chadwick et al. (2006) ENDF/B-VII.0: Next Generation Evaluated Nuclear Data Library for Nuclear Science and Technology. Nucl. Data Sheets 107, 2931-3060.
- [6] A. Koning et al. (2006) JEFF Report 21: The JEFF-3.0 Nuclear Data Library. OECD.

PRELIMINARY THERMOHYDRAULICS DESIGN OF LORELEI AN EXPERIMENTAL DEVICE OF JHR

F. S. NITTI

*Brasimone Research Centre, ENEA
Bacino del Brasimone, 40032 Camugnano – Italy*

S. BOURDON, C. GONNIER, P. ROUX,
J. ESTRADÉ, G. BIGNAN

*Cadarache Research Centre, CEA Technology
13115 St. Paul les Durance – France*

L. WONG

*Australian Nuclear Science and
Organisation (ANSTO)*

ABSTRACT

In the Jules Horowitz Reactor (JHR) experimental facilities will be available, including the Light water One Rod Equipment for LOCA Experimental Investigations (LORELEI) device. In this work the thermohydraulics design of the LORELEI facility was developed with the code CATHARE-2. The objective of the work was: to define a 3D geometry of the facility and to verify the capacity of the system, under natural circulation, to remove the power generated both by the fuel rod (up to 400 W/cm) and by gamma irradiation heating on the structures, during the re-irradiation phase before the simulation of the high temperature transient. A parametric calculation modifying several geometrical parameters was performed. The parameters that should be varied were evaluate with an analytical approach. A final geometry of the facility, able to work in natural circulation condition up to the maximum power was selected. Further calculation was performed to analyze the correlation between the accumulation of steam and the geometries of device, at constant power.

1. Introduction

In the Jules Horowitz Reactor (JHR) experimental facilities will be available, including the Light water One Rod Equipment for LOCA Experimental Investigations (LORELEI) device, which is dedicated to Loss Of Coolant Accident (LOCA) transient studies on a single fuel rod. The objective of the test device is to evaluate the thermomechanical properties and radiological consequences of LOCA phenomena on a LWR fuel rod. The main operating conditions consist of, [1]: 1) Re-irradiation Phase: Before the LOCA transient, the test device is operated as a capsule at a temperature below of saturation value (330,85 °C), in natural circulation, at 13 MPa; 2) Dry-out Phase: It is simulated by a gas injection that allows the emptying of test device to a low pressure value; 3) Heat-up Phase: It will occur at a rate of 10 to 20°C/s and will be monitored by tuning the power in the fuel; 4) Quenching Phase: It will be simulated by a water injection at the bottom of the test device.

In this work the thermalhydraulics design of the LORELEI facility was developed with the code CATHARE-2. The objective of the work was: to define a 3D geometry of the facility and to verify the capacity of the system, under natural circulation, to remove the power generated both by the fuel rod (up to 400 W/cm) and by gamma irradiation heating in the structures. The study consisted of three main steps: definition of a 3D geometry of the facility; definition of a numerical model and development of thermohydraulics calculations.

2. The geometry of the facility and the numerical model

In normal operating conditions the LORELEI device operates with pressurized water in natural circulation, moving the nuclear thermal power generated from a hot source to a cold sink.

Essentially the system is composed of two concentric cylinders with the internal cylinder containing the fuel rod (the hot source) and the external cylinder in contact with a pool (the cold sink). The annular chamber between the rod and the internal cylinder is the hot channel, the annular chamber between the two cylinders is the cold channel. The connection between the hot and cold channel consist of 4 holes located on a plane and separated 90° from each other. However in reality, the system will be composed of cylindrical layers of different materials, which meet different needs in the normal and safety operating conditions. The schematic cross section with utilized materials and an axonometric view of the device is displayed in the fig.1.

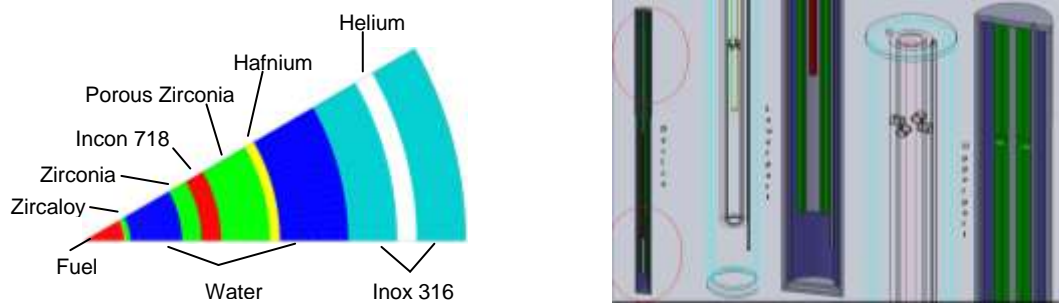


Figure 1 Schematic cross section and axonometric view

The numerical calculations were performed with CATHARE-2 code V2.5_2, a two-phase thermohydraulic code with a 2-fluids and 6-equations model. The input data required for these calculations were: geometries; material physical properties; local pressure drop coefficients and boundary conditions. Typical calculation parameters used were: number of meshes 474; meshes length from 1mm to 10 mm; boundary conditions: pressure 13 MPa, temperature 50 °C on the external wall of device. The required operating conditions for the system are: fluid temperature below the saturation value; cladding temperature above the saturation value, to guarantee nucleation conditions at the wall; a sufficient margin for the Critical Heat Flux (CHF).

Different geometries were analyzed modifying three parameters: the internal radius of the first external wall (r_1); the length of the device above the fuel rod (L) and the thickness of the gas gap between the two external walls (t_2). In tab.1 the data of main cases analyzed are displayed.

	r_1 [mm]	L [mm]	t_2 [mm]	Max Power on Fuel Rod [W/cm]	Gamma-Power [W]	DNBR _{min}
G0	30.54	700	2	300	-	1.30
G4	50.54	1200	1.24	400	-	2.67
G5	52.04	1200	0.5	400	$3.98 \cdot 10^4$	2.73

Table 1 Data of main cases analyzed

3. Thermal power in fuel rod

The first calculation is related to the initial geometry, case G0. The simulation showed that the system operates with the flow temperature below the saturation value only with a

generated power less than 100 W/cm. With a higher power, a lot of steam is accumulated in the upper part of the cold channel. It is necessary to increase the heat exchanged with the cold sink. With fixed surrounding conditions, the heat exchanged depends on the fluid flow which, at fixed power supply, depends on geometrical characteristics of the walls. A parametric calculation was performed. Keeping constant the geometry of internal cylinder of device, the heat exchange with surrounding is correlated to the geometry of the external cylinder: internal and external radius of first wall (r_1 , r_2), internal and external radius of second wall (r_3 , r_4), gas gap between the walls t_2 and the length L . In order to evaluate which parameters should be varied and the magnitude of the variation, an approximate correlation between the heat exchange and geometrical parameters was developed, [2].

The external wall of the device is composed of two concentric cylinders with a gas gap, however, due to the small width, the convective circulation is not taken into account and the gas gap is considered as a conductive material. Arranging the correlations of convective and conductive heat transfer it is possible to have an expression of the heat flux as a function of geometric parameters, of conductive and convective coefficients and of temperatures of fluids on both side of the wall:

$$Q = \frac{2\pi L r_1 r_4 h_i h_e}{r_1 h_i + r_4 h_e + r_1 r_4 h_i h_e \left[\frac{1}{k_a} \ln \frac{r_2}{r_1} + \frac{1}{k_b} \ln \frac{r_3}{r_2} + \frac{1}{k_c} \ln \frac{r_4}{r_3} \right]} (T_i - T_e) \quad (1)$$

Assuming some simplified hypotheses it is possible to evaluate the variation of the Global Heat Transfer Coefficient (GHTC) in equation (1), with the variation of geometrical parameters. Starting with the stable operating condition (100 W/cm), a study was performed to obtain an appropriate global heat transfer coefficient, modifying only the physical dimensions of the device, with the goal of obtaining the same stable conditions with a higher linear power supplied. Utilizing the results of the calculation obtained with a power of 100 W/cm, average values for temperatures, density, viscosity, specific heat, conductivity and thermal expansion coefficient, in the cold channel above the rod, were assumed. Assuming that these average physical parameters remain constant, it is possible to calculate the change in the GHTC with the variation of the geometric parameters. Fig.2 displays the variation of GHTC with the variation of geometrical parameters that give a higher variation of GHTC.

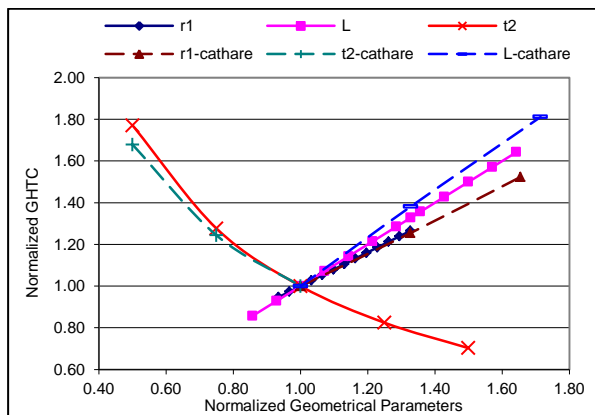


Figure 2 Normalized GHTC as a function of Normalized geometrical parameters. By correlation and by CATHARE.

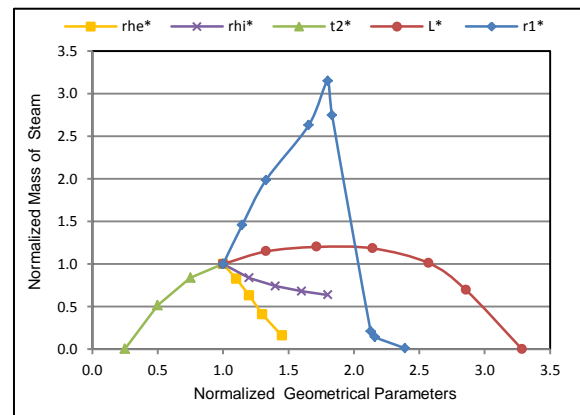


Figure 3 Variation of mass of steam with variation of geometrical parameters at constant power, 300 W/cm

The values on the Cartesian axes are normalized to the initial reference values, case G0: $k^* = k / k_{in}$; $r_1^* = r_1 / r_{1in}$; $L^* = L / L_{in}$; $t_2^* = t_2 / t_{2in}$ (2). The curves show the percentage increase of the heat flux removable from the device, keeping constant the physical condition of the fluid and varying each geometrical parameter one by one. Predictably the gas gap t_2 has a large impact on the variation of GHTC, due to the low conductivity of the gas. To verify the reliability of these graphs, further calculations with different geometries, obtained modifying the three parameters, were performed. In fig.2 the variation of normalized GHTCs obtained from the code calculation is displayed.

The maximum power that the system should nominally be able to handle is 400 W/cm, four times the initial reference value. The single variation of a geometrical parameter is not enough to guarantee an increase of heat transfer by a factor of four. Therefore a combined variation is necessary. The effect of a combined variation can be evaluated with the hypothesis of principle of superposition of effects and the variation of GHTC can be evaluated by means the correlation: $k^* = k_{r1}^* k_L^* k_{t2}^*$ (3). The choice of which parameters should be varied must be driven in direction of maximization of the heat exchanged, keeping the system simple, compact and easy manufacture. However the geometrical parameter variation is limited by the space available for the facility (max length 2200 mm and max external diameter 129 mm were assumed in this study). Therefore, assuming the maximum values possible for length L and internal radius r_1 , the gas gap thickness was calculated. Fixed L and r_1 , from (2) the normalized value were calculated, and from the diagrams of fig.2, the normalized heat transfer coefficients: k_{r1}^* , k_L^* were determined. Knowing the GHTC required, from (2) the normalized value was calculated and from (3) the normalized heat transfer coefficients k_{t2}^* and thus, from the diagram, the gas gap normalized thickness t_2^* , and then t_2 . The calculation with the new geometric parameters, case G4, showed good thermohydraulic behaviour of the system up to 400 W/cm, without a significant amount of steam production. In fig.4 the temperature distribution and void fraction behaviour in the fluid are displayed. The diagram shows a small quantity of steam in the hot-channel along the rod, thus nucleation phenomena appear in the fluid.

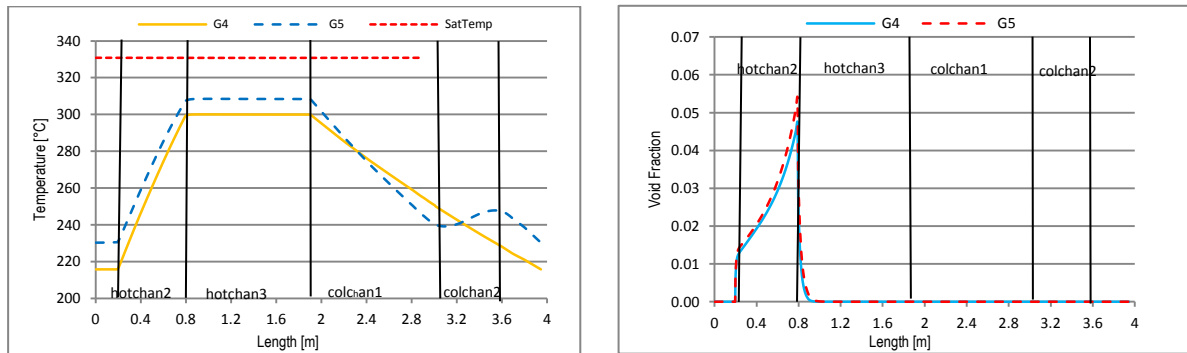


Figure 4 Temperature and void fraction behaviour for the geometries G4, G5

4. Thermal Power due to Gamma Heating

The amount of the gamma-power and its linear distribution was evaluated considering the neutron flux distribution coming from the reactor core. The gamma-power distribution is centered at the middle of fuel rod and it extends of 200 mm above and below of the rod. The thermohydraulic calculation in the case G4, considering also the gamma-power in the structures, showed a flow with the presence of steam in the upper part of the cold channel. The total heat power due to gamma irradiation resulted of about $3.98 \cdot 10^4$ W distributed on a

length of 1 m, therefore it is a linear power distribution of the same order of magnitude of the linear power in the rod. Thus the total power, in the fuel rod and in the structures, is eight times to that of the initial reference geometry, G0. Hence it is necessary to change once more the geometry of the device, case G5. Adopting the same procedure presented in the previous paragraph the appropriate gas gap thickness was evaluated. The gas gap reduction was obtained by increasing the internal radius of the wall. In fig.4 temperature distribution in the fluid and the void fraction are displayed. The selected geometry showed a good operative conditions for the Critical Heat Flux (CHF). The Departure from Nucleate Boiling Ratio (DNBR) resulted of 2,73.

5. Further calculations

The thermohydraulic calculations in all geometries analyzed showed an accumulation of steam in the upper part of the cold channel. The amount of steam accumulated changes for different geometries at constant power. The calculations showed the presence of an annular flow in the upper part of cold channel, thus the condensation of vapour is due to the heat exchanged between the two phases of the fluid. The rate of condensation, depends on physical parameters, geometries and above all by velocities and temperatures [3,4]. Therefore the rate of condensation increases with the reduction of the liquid temperature and with the increase of the steam velocity, i.e. increasing the exchange with the surrounding and reducing the dimension of the cold channel, respectively. Further calculations with different geometries were performed to analyze these phenomena, and the impact on the accumulation of mass of steam in the cold channel. The new geometries were obtained starting from the basic geometry G0 and modifying the parameters r_1 , L , t_2 and the internal (r_{hi}) and the external (r_{he}) radii of the hot channel wall. In fig.3 the variation of the mass of steam with the variation of geometrical parameters, at constant power is displayed. The values on the axis are normalized to the reference geometry G0. The curves displayed on the diagram show the action of the two opposite effects, the heat exchange with the surrounding and between the two phases, on the mass of steam accumulated.

6. Conclusions

The thermalhydraulic study outlined that the thermal power that can be removed from the test device, mainly depends on the external geometrical parameters of the system: r_1 ; L and t_2 . With an analytical approach and a parametric calculations, modifying the defined geometrical parameters, a final geometry of the facility which is able to work in natural circulation, and with the flow in single phase conditions, up to the maximum power of 400 W/cm, was selected. Further calculations to analyze the correlation between the mass of steam accumulated and the geometry underlined: the increase of r_1 and L causes an increase of mass of steam up to a certain geometrical value, after this value, the steam mass decreases; the reduction of t_2 causes a reduction of mass of steam; the increase of internal (r_{hi}) and external (r_{he}) radius of the hot channel wall causes a reduction of mass of steam.

References

- [1] "Jules Horowitz Reactor, Status Report 2006-2007" – CEA
- [2] "Preliminary Thermohydraulics Design of the LORELEI Device with CATHARE" - F. S. Nitti
Accordo di Programma ENEA-MSE-2011- Rapporto tecnico NNFISS-LP2-045
- [3] "CATHARE 2 V2.5_2. – Description of the Base Revision 6.1 Physical Laws Used in the 1D,0D and 3D Modules" DER/SSTH/LDAS/EM/2008-044 CEA
- [4] "Convective Boiling and Condensation"- J. G. Collier, J.R. Thome –C. Press Oxford-2001

FORCED CONVECTIVE HEAT TRANSFER CHARACTERISTICS IN A THIN RECTANGULAR CHANNEL FOR DOWNWARD AND UPWARD FLOWS

Daeseong Jo, Jonghark Park, Heetaek Chae, Byungchul Lee

*Division for Research Reactor Core and System Design, Korea Atomic Energy Research Institute
Daedeok daero 989-111, Yuseong-gu, Daejeon, 305-353, Korea*

ABSTRACT

An experiment apparatus was built to investigate forced convective heat transfer characteristics for water flowing downward and upward through a thin rectangular channel. The thin rectangular channel heated from both sides had a width of 54mm, a length of 640mm, and a gap of 2.35mm. Experiments were carried out for $500 < Re < 54000$ and $2.1 < Pr < 6.9$. Results showed that there was no difference of the heat transfer characteristics between upward and downward flows. The transient between laminar and turbulent flow regions around Re of 5000 was observed. For the turbulent flow region, Nusselt number was proportional to $Re^{0.8543}$, and it was proportional to $Re^{0.4063}$ for the laminar flow region. As a result, a new correlation developed from the present experiment investigation resulted in a lower heat transfer coefficient compared to Colburn (1933), Dittus and Boelter (1930), Sieder and Tate (1936), and Sudo et al. (1985).

1. Introduction

Many open pool-type research reactors, where the cores are submerged in reactor pools, operate with downward core cooling. Downward core cooling has advantages such as accessibility to the pool top due to low pool top radiation, a simple locking system of the fuel assemblies and irradiation blocks, easy handling of the irradiation targets and fuel assemblies, and less flow resistance during shutdown rod insertion. However, it also has a major disadvantage from a thermal hydraulic design point of view. For open pool-type research reactors with downward core cooling, the hydraulic static head from the top of the reactor to the pool surface determines the inlet pressure. Since a lower inlet pressure results in lower NPSH (net positive suction head) and ONB (onset of nucleate boiling) at lower power, which are not desirable in a thermal hydraulic core design, the pool should be deep enough for a sufficient inlet pressure. During normal operation, the coolant flows downward through the core to remove the heat generated from the core. However, the coolant flows upward through the core if primary cooling pumps do not run or fail. In this case, the heat released from the core should be removed by natural convection. Therefore, heat transfer characteristics through fuel channels for both upward and downward flows are important to understand reactor safety and design purposes.

Convective heat transfer through pipes and channels has been studied for the past several decades, and many correlations are available. In 1930, Dittus and Boelter proposed a convective heat transfer correlation for turbulent flows ($10000 < Re < 12000$ and $0.7 < Pr < 120$) in pipes [1]. The correlation is recommended for only rather small differences between the wall and coolant temperatures. A few years later, in 1936, Sieder and Tate developed another correlation that accommodates larger temperature differences by taking account of the variation of viscosity with fluid bulk and wall surface temperatures [2]. The Sieder-Tate correlation is valid for $Re > 10000$ and $0.7 < Pr < 16700$. Both the Dittus-Boelter and Sieder-Tate correlations are still widely and extensively used for many applications. In 1945, Colburn et al. proposed a similar correlation to the Dittus-Boelter correlation, but considered properties at film temperature [3]. The film temperature is the arithmetic mean of the bulk and

wall surface temperatures. The existing correlations for turbulent forced convection heat transfer proposed by Colburn, Dittus-Boelter, and Sieder-Tate are listed below:

$$\text{Dittus-Boelter} \quad : \quad Nu = 0.023 Re_b^{0.8} Pr_b^{0.4}$$

$$\text{Sieder-Tate} \quad : \quad Nu = 0.027 Re_b^{0.8} Pr_b^{1/3} (\mu_b/\mu_w)^{0.14}$$

$$\text{Colburn} \quad : \quad Nu = 0.023 Re_f^{0.8} Pr_f^{0.3}$$

Levy et al. (1959) experimentally investigated heat transfer to water in thin rectangular channels (2.54 × 63.5 mm). The range of Re covered from 6000 to 200000. They concluded that the heat transfer coefficient obtained in a rectangular channel was considerably lower than that obtained in a circular pipe. Moreover, the comparisons against Colburn, Dittus-Boelter, and Sieder-Tate correlations showed that the heat transfer coefficient measured was lower than those predicted by the correlations [4]. Recently, Sudo et al. (1985) studied single-phase convective heat transfer characteristics between upward and downward flows through a narrow rectangular channel (2.25 × 40 mm). The range of Re was from 100 to 40000, and the range of Pr was from 3.5 to 10. Unlike Levy et al.'s experimental study, Sudo et al. (1985) found different heat transfer characteristics between upward and downward flows. The downward flows resulted in a lower heat transfer coefficient than that with the upward flows. In addition, different transitions from the turbulent to laminar regions were observed for upward and downward flows. Although they observed differences from the previous experimental study, the heat transfer coefficients for both upward and downward flows were considerably lower than those predicted by Colburn, Dittus-Boelter, and Sieder-Tate correlations [5].

Since there are few heat transfer experimental data in thin rectangular channels, and some data conflict with each other, the heat transfer characteristics in a rectangular channel heated from both sides have been experimentally investigated for upward and downward flows in this paper. The wall temperatures measured and predicted by other correlations were compared. The heat transfer characteristics were expressed as a function of Nu, Re, and Pr. The experimental data obtained by the present study are compared with Sudo et al.'s experimental data, and a new heat transfer correlation that is applicable to a rectangular channel is proposed.

2. Description of test facility

Heat transfer experiments in a thin rectangular channel were performed at the RCS Thermal Hydraulic Loop located at KAERI (Korea Atomic Energy Research Institute). The RCS Thermal Hydraulic Loop is available for various thermal hydraulic experiments from single phase heat transfer up to CHF (critical heat flux) experiments. The loop consists of a circulation pump, a mass flowmeter, a preheater, steam-water separator, pressurizer, and heat exchanger as shown in Fig.1. Since the loop was originally designed for high pressure, a level tank was installed on the top of the pressurizer to control the system pressure below 2.0 bar instead of using the pressurizer. The top of the level tank is open to the atmosphere. A test section designed for the present experiment was connected to the inlet and outlet of the loop. Since the flow directions of the present study were upward and downward, the flow path from the inlet of the loop was controlled by four actuator-type ball valves. The test section consists of upper and lower plenums and a thin rectangular channel. The total length of the rectangular channel was 1200mm (heated 640mm and unheated 280mm at each end) as shown in Fig.2. The rectangular channel has a thickness of 2.35mm and a width of 54mm. The width of the heater is 50mm. The heater made of inconel 625 directly heats the water on one side, and is insulated by an alumina insulator on the other side. Each heater has 10 thermocouples (TC) installed at the back to measure centerline temperatures in the axial



Range

3. Data reduction

The inside wall temperatures are estimated by the temperatures measured on the back of the heater.

$$T_{W,i} = T_{W,o} - \frac{q'' t}{2k}$$

where $T_{W,i}$ is the inside wall temperature on the flow channel side
 $T_{W,o}$ is the outside wall temperature on the insulator side
 q'' is the average heat flux
 t is the thickness of the heater
 k is the thermal conductivity of the heater

Since a uniform heat flux in the axial direction is applied, the average heat flux is expressed as $q'' = \frac{Q_e}{\text{total heated area}}$. Before performing any test, the electric power Q_e applied and thermal power Q_{th} transferred from the heater to the coolant must to be compared to evaluate the power loss. The thermal power can be evaluated by measuring the coolant temperatures at the inlet and exit of the test section as $Q_{th} = (\dot{m} C_p |T_{in} - T_{out}| \times \text{total heated area})$. The thermal power is evaluated as approximately 7% lower than the electric power for upward and downward flows.

4. Results

In Fig.3, the wall temperatures measured are compared with those predicted by the correlations [1,2,3]. As can be seen, the measurements are higher than the predictions. This means that the heat transfer coefficient obtained by the present experiment is lower than the existing correlations. Although Dittus-Boelter correlation is relatively simpler than the others, it agrees well with the experimental data. Therefore, the heat transfer coefficient is evaluated with $Pr^{0.4}$. The experimental data for upward and downward flows are shown in Fig.4. There is no difference in the heat transfer characteristics between the upward and downward flows. If Re is larger than 5000, the flow region is turbulent. If Re is smaller than 3000, the flow region is laminar. For the turbulent flow region, Nusselt number was proportional to $Re^{0.8543}$, and it was proportional to $Re^{0.4063}$ for the laminar flow region. At a low Re of around 500, Nusselt number is approximately 6.35. A new set of convective heat transfer correlations proposed in the present study are listed below:

$$Nu = 0.0104 Re_b^{0.8543} Pr_b^{0.4} \quad \text{for } Re \geq 5000$$

$$Nu = (0.0038 Re_b - 4.016) Pr_b^{0.4} \quad \text{for } 3000 \leq Re < 5000$$

$$Nu = 0.2866 Re_b^{0.4063} Pr_b^{0.4} \quad \text{for } 500 \leq Re < 3000$$

The convective heat transfer correlation for Re larger than 5000 has $\pm 16\%$ error, and for Re smaller than 3000 has $\pm 25\%$ error to meet 95% confidence level: 95% of experimental data exist within the error bounds.

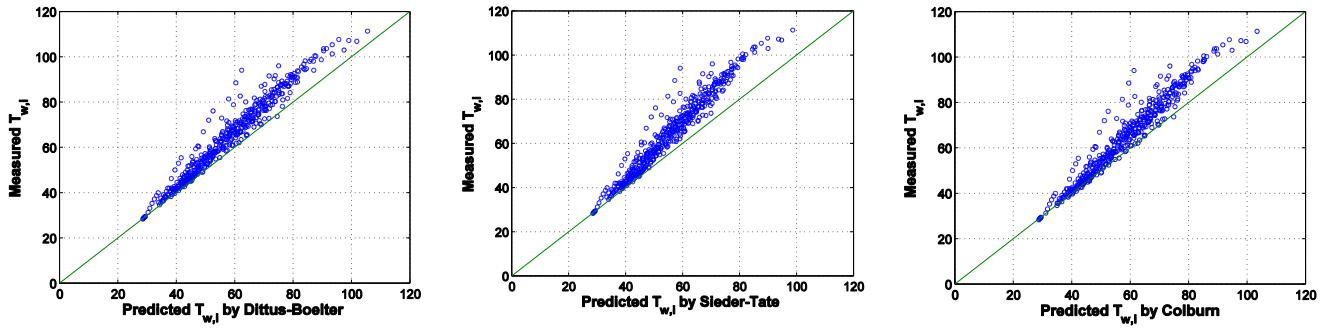


Figure 3. Temperature measured vs. predicted

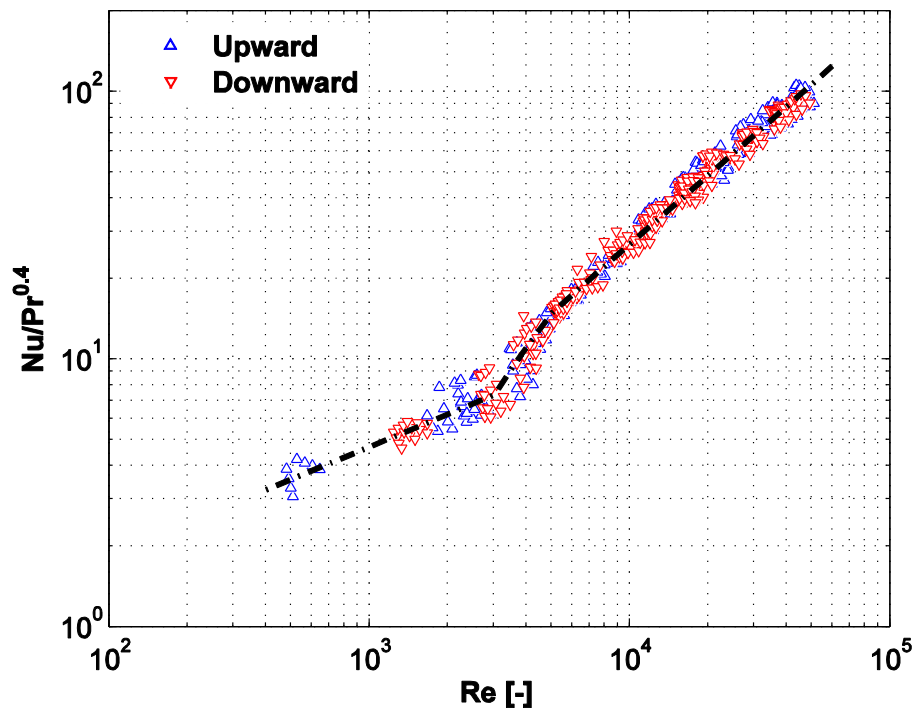


Figure 4. Experimental data with proposed correlations

5. References

- [1] Dittus, F.W., Boelter, L.M.K., 1930. Heat transfer in automobile radiator of the tubular type. University of California at Berkley Publ. Eng. 2, 443-461
- [2] Sieder, E.N., Tate, G.E., 1936. Heat transfer and pressure drop of liquids in tubes. Industrial and Engineering Chemistry 28, 1429-1435.
- [3] Colburn, A.P., 1933. A method of correlating forced convection heat transfer data and a comparison with fluid friction. Trans. AIChE J. 29, 174-210.
- [4] Levy, S., Fuller, R.A., Niemi, R.O., 1959. Heat transfer to water in thin rectangular channels. Journal of Heat Transfer 1, 129-143.
- [5] Sudo, Y., Miyata, K., Ikawa, H., Ohkawara, M., Kaminaga, M., 1985. Experimental study of differences in single-phase forced-convection heat transfer characteristics between upflow and downflow for narrow rectangular channel. Journal of Nuclear Science and Technology 22, 38-48.

EFFECTS OF BURNABLE ABSORBERS ON THE FUEL FABRICATION AND IRRADIATION PERFORMANCE OF U-MO DISPERSION FUEL

HO JIN RYU, JONG MAN PARK, CHANG KYU KIM, YOON SANG LEE,
CHUL GYO SEO

*Korea Atomic Energy Research Institute
Daedeokdaero 989-111, Yuseong, Daejeon 305-353 – Republic of Korea*

YEON SOO KIM

*Argonne National Laboratory
9700 S Cass Ave, Argonne, IL 60439 – USA*

ABSTRACT

The future utilization of U-Mo/Al dispersion fuel in the HANARO requires the use of burnable absorbers due to the high uranium density of U-Mo fuel compared to conventional silicide fuel. Ceramic compounds such as Er_2O_3 , B_4C and CdO have been incorporated in the U-Mo/Al or U-Mo/Al-Si samples for the irradiation tests in the HANARO (KOMO) in order to investigate the performance of burnable absorber materials. Single or mixtures of the burnable absorber powder were added to the mixture of U-Mo powder and Al powder according to the neutronic calculations for the KOMO irradiation tests. Possible chemical reactions of the absorber materials with Al or U were analyzed by thermodynamic calculations. Microstructural observations after the hot extrusion into fuel meat rods and after irradiation did not reveal notable differences from other dispersion fuel rods without a burnable absorber. The thickness of the interaction layers between U-Mo and Al(-Si) measured by post-irradiation examinations showed that the addition of burnable absorbers is effective in reducing the initial power peaking of U-Mo dispersion fuel as expected in the theoretical estimation.

1. Introduction

In order to develop a high density U-Mo fuel, KAERI has performed a series of irradiation tests at HANARO research reactor, i.e., the KOMO test[1,2]. The possible purposes of the future conversion from U_3Si dispersion fuel to U-Mo dispersion fuel include the extension of fuel life cycle, increase in available numbers of irradiation holes, and more flexibility of the back end option of spent fuel. Uranium loadings ranging from 4.5 to 5.5 gU/cm^3 will be the target density for the possible conversion of rod-type dispersion fuel for HANARO. Neutronic calculation for the KOMO tests revealed that a small amount of burnable absorber would be needed to control initial power peaking in the full size U-Mo fuel due to the high uranium density. Therefore, it is necessary to investigate the performance and stability of burnable absorber materials when added in the U-Mo/Al dispersion fuel. In this study, the effects of ceramic compounds such as Er_2O_3 , B_4C , CdO and Gd_2O_3 , which have been incorporated in the U-Mo/Al or U-Mo/Al-Si samples for the irradiation tests at HANARO, were studied in terms of fuel fabrication and irradiation performance of U-Mo/Al dispersion fuel.

2. Irradiation tests

Centrifugally atomized U-7wt.%Mo powder was used for the fabrication of the rod-type U-Mo dispersion fuel meats for the KOMO irradiation tests. In order to investigate the effects of Er_2O_3 , a U-7wt.%Mo dispersion fuel rod with a uranium density of 4.5 gU/cm^3 was prepared for the KOMO-2 irradiation test which was performed from Jan. 9, 2003 to Jan. 27, 2004[3]. 4 wt% of Er_2O_3 was added in the mixture of U-7Mo and Al powder before compaction. Fig. 1 shows an SEM image of the extruded dispersion fuel rod with 4 wt% Er_2O_3 . The linear power

and B.O.L. temperature of the Er_2O_3 added rod were calculated as 92.6 kW/m and 180.2°C, respectively. Average burnup was calculated as 60.8 at.%U-235 and the maximum local burnup was 71.2 at.% of U-235. After cooling in the pool for about three months, PIE was performed in the IMEF (Irradiation Material Examination Facility) facility. When optical micrographs of the U-7Mo dispersion fuel with Er_2O_3 was compared with the 4.5 g-U/cc U-7Mo dispersion fuel rod without Er_2O_3 at the same burnup of 62at%, less interaction layers on U-7Mo were found in the U-7Mo dispersion fuel with Er_2O_3 as shown in Fig. 2. The interaction layer growth at the U-Mo/Al interface depends on the fuel temperature during irradiation. Because the addition of burnable absorbers controls the initial power peaking, the interaction layer growth could be reduced.

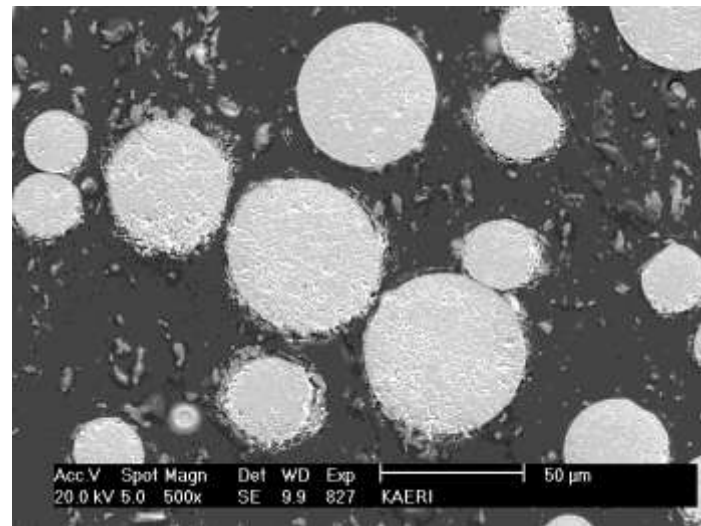


Fig. 1. An SEM image of U-7Mo/Al (4.0 gU/cc) with 4 wt% Er_2O_3

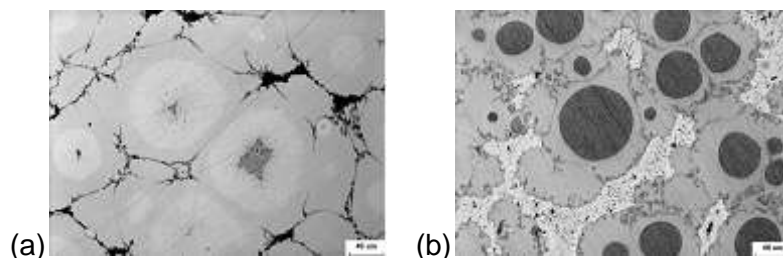


Fig. 2. Optical micrographs of 4.5 g-U/cc U-7Mo dispersion fuel rods with 62at% burnup at the center of fuel meat; (a) U-7Mo without Er_2O_3 (b) U-7Mo with Er_2O_3 .

The KOMO-4 irradiation test which was performed for 132 EFPD from Dec. 22, 2008 to Jan. 3, 2010[4]. Average burnup was calculated to be 47.1 at.% U-235 and the maximum local burnup was 55 at.% U-235. A 5 gU/cm³ U-7wt.%Mo/Al-5wt.%Si dispersion fuel rod with 0.2 wt% Cd and 0.1wt% B was prepared in order to investigate the effects of burnable absorbers. For the chemical compounds for Cd and B, cadmium oxide(CdO) and boron carbide (B_4C) were used, respectively. The linear power and B.O.L. temperature of the Er_2O_3 added rod were calculated as 89.6 kW/m and 175.1°C, respectively. Fig. 3 shows the average linear power histories with burnup for fuel rods in the KOMO-4 irradiation test at a specific position. The fuel rod with burnable absorbers, which is Rod-10, has lower initial power, while the other fuel rods present an initial power peaking behavior. Again, the as-fabricated microstructure shows a sound distribution of U-Mo particles and the CdO and B_4C particles were difficult to identify in the image shown in Fig. 4. Fig. 5 shows cross section images of the irradiated fuel rod with CdO and B_4C at local burnup of 48 at%U-235. No microstructural abnormality was observed in the irradiated fuel rod.

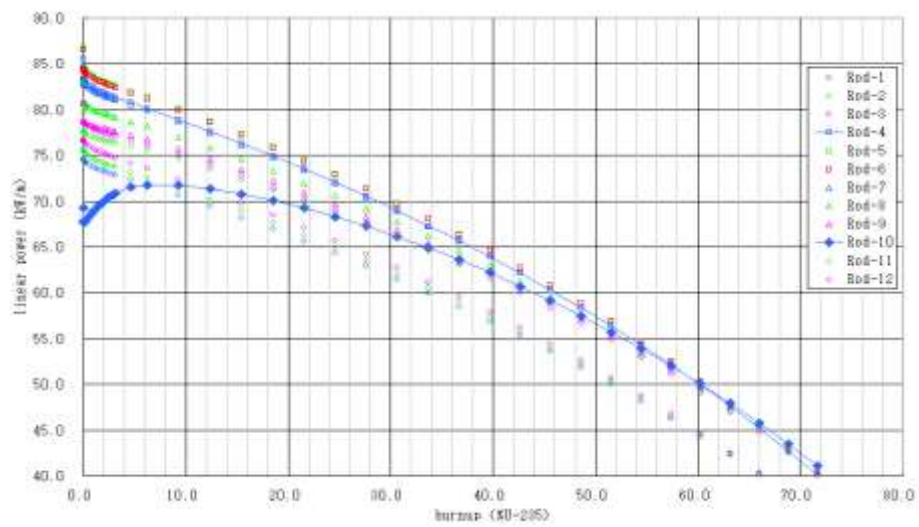


Fig. 3. The average linear power histories with burnup for fuel rods in the KOMO-4 irradiation test (Rod-10: the fuel rod with burnable absorbers)

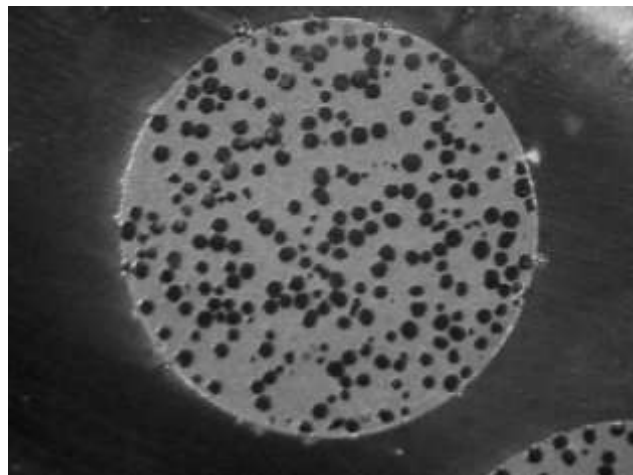


Fig. 4. A cross section image of a U-7Mo/Al-5Si fuel rod with 0.2 wt% CdO and 0.1wt% B₄C.

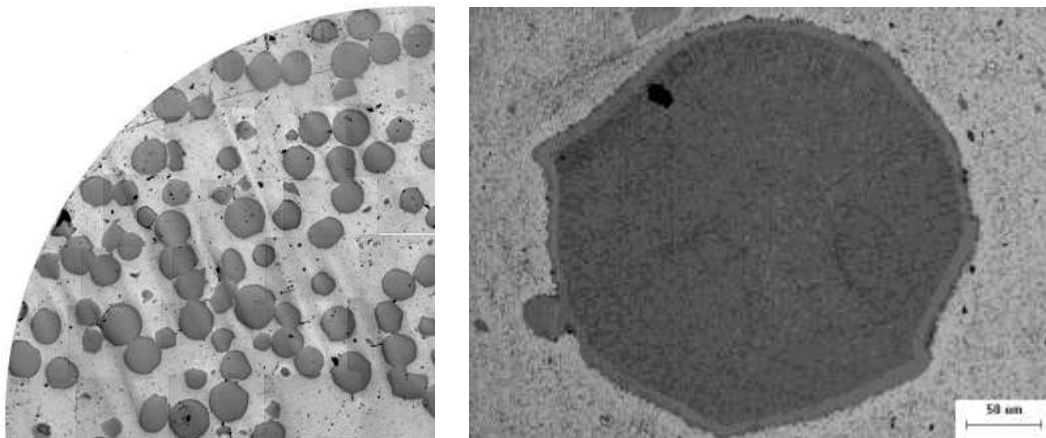


Fig. 5. Metallographic cross sections of a KOMO-4 irradiated fuel rod with CdO and B₄C at a discharge burnup of 48 at%U-235.

The KOMO-5 irradiation test for the full size U-Mo fuel rods was started from May 23, 2011 and the fuel rods will be discharged after reaching 60% burnup in average in late May 2012[5]. For the full length (700 mm) U-Mo/Al-Si and U-Mo-X/Al-Si (X=Ti or Zr) dispersion fuels, Si content in matrix was fixed to 5 wt% and burnable absorber materials (Cd, B, Er) were added to the matrix. 0.1wt% of Cd and 0.2wt% of B were added as chemical forms of CdO and B₄C into a U-7Mo/Al-5Si fuel rod, a U-7Mo-1Zr/Al-5Si fuel rod, and a U-7Mo-1Ti/Al-5Si fuel rod, while for another U-7Mo/Al-5Si fuel rod, 1 wt% of Er₂O₃ was added in addition to CdO and B₄C. Fig. 6 reveals that the distribution of B is uniform in a fuel rod containing B₄C powder in the dispersion fuel meat. It means that powder mixing technique is recommendable for the addition of burnable absorber powder.

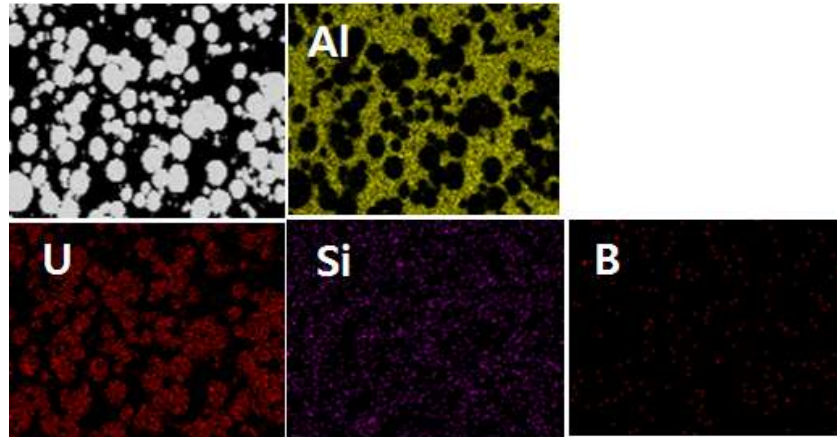


Fig. 6. X-ray elemental mapping of U-7Mo/Al-5Si with 0.1wt%CdO+0.2wt%B₄C

3. Out-of-pile tests

Thermal conductivities of U-7Mo/Al dispersion samples with 5 wt% burnable absorber powder were measured and compared with U-7Mo/Al dispersion sample without burnable absorber. 5 wt% of Gd₂O₃, Dy₂O₃, Er₂O₃ powder were added to U-7Mo/Al powder mixtures and extruded into dispersion samples. Fig. 7 presents the thermal conductivities of the samples from 25°C to 500°C. The thermal conductivities of all samples increased with temperature. Although slightly reduced thermal conductivities were measure in some samples with burnable absorber powder, the differences were not considered so large to affect the fuel performance significantly.

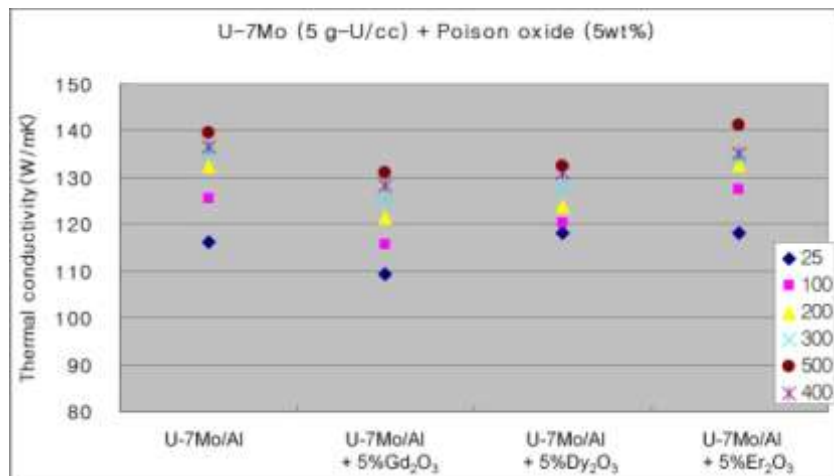


Fig. 7. Thermal conductivities of U-7Mo/Al samples with 5wt% burnable absorbers from 25°C to 500°C

Recently, because the thermodynamic stability of CdO was questioned[6], the Gibbs free energy of the CdO-Al reaction was calculated as shown in Fig. 8(a). It was found that CdO tends to be reduced to metallic Cd as a result of the reaction with Al. During the hot working process at temperature high than 400°C, the metallic Cd, with a low melting point of 321°C, can be liquefied. When a simulated U-7Mo/Al with 5wt% CdO sample were heated to 500°C and annealed for 1 hour, the formation of liquid Cd phase was confirmed from the resulting microstructure(Fig.8(b)). Because the solubility of pure Cd in Al is very low (0.02 at%), the liquid Cd does not absorbed in the Al. Therefore, CdO would not be a proper form for addition of Cd in the U-Mo/Al dispersion fuel.

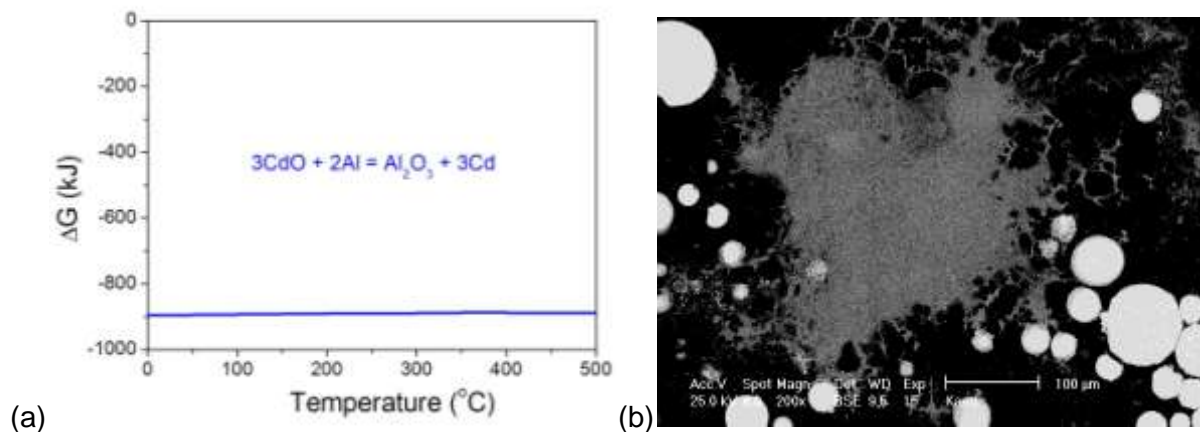


Fig. 8. (a) Gibbs free energy calculation of a CdO-Al reaction, and (b) Microstructure of U-Mo/Al with CdO after annealing at 500°C for 1 hour.

4. Conclusions

Ceramic compounds such as Er_2O_3 , B_4C and CdO have been incorporated in the U-Mo/Al or U-Mo/Al-Si samples for the irradiation tests at the HANARO (KOMO-2, KOMO-4, KOMO-5) in order to investigate the performance of burnable absorber materials. The addition of burnable absorbers was found effective in reducing the initial power peaking of U-Mo dispersion fuel as expected in the theoretical estimation. Microstructural observations after the hot extrusion into fuel meat rods and after irradiation did not reveal notable differences from other dispersion fuel rods without a burnable absorber. Thermal conductivities of U-7Mo/Al dispersion samples with 5 wt% burnable absorber powder did not show significant differences. When possible chemical reactions of the absorber materials with Al were analyzed by thermodynamic calculations, it was found that CdO would not a proper form to be used in the Al matrix.

ACKNOWLEDGMENTS

This work is supported by the National Nuclear R&D Program of Ministry of Education, Science and Technology of Korea.

References

- [1] C.K.Kim et al. 2000 RERTR Meeting, Las Vegas, Nevada, USA, October 1-6, 2000.
- [2] C.K.Kim et al. 2002 RERTR Meeting, Bariloche, Argentina, November 3-8, 2002.
- [3] C.K.Kim et al. 2004 RERTR Meeting, Vienna, Austria, November 7-12, 2004.
- [4] J.M.Park et al. 2010 RERTR Meeting, Lisbon, Portugal, October 10-14, 2010.
- [5] H.J. Ryu et al. 2011 RERTR Meeting, Santiago, Chile, Oct. 23-27, 2011.
- [6] M.Meyer, Personal communications, 2011.

A MEASUREMENT OF HOMOGENEITY OF SIMULATED RESEARCH FUEL PLATE USING REAL TIME X-RAY

Y.S. LEE, H.I. LEE, D.B. LEE, Y.J. JEONG, J.M. PARK

*Research Reactor Fuel Development, Korea Atomic Energy Research Institute.
989-111 Daedeok-daero, Yuseong-gu, 305-353, Daejeon-Korea*

ABSTRACT

During fabrication of a high density fuel plate such as U-Mo dispersion fuel, quality control is very important to secure the integrity of the fuel elements. One of the quality control items is homogeneity of the uranium distribution in the fuel plate. To check the homogeneity of the fuel plate, x-ray radiography has been used. In this paper, we introduce the results by measuring the homogeneity of a simulated fuel plate by using a real time x-ray radiography system. Even though the real time x-ray beam profile was not even, comparable results using a conventional x-ray film densitometer method were achieved. Therefore, the procedure of homogeneity measurement methods for the dispersion fuel plate was successfully developed by using an RTR system.

1. Introduction

In KOREA, there is a plan to build a new research reactor for isotope production. KAERI has started installation of the plate fuel fabrication lines and development of quality control systems for the new research reactor last year. During fabrication of a high density U-Mo fuel plate, quality control is very important to secure the integrity of fuel element. One of the quality control items is homogeneity of the uranium distribution in the fuel plate. To check the homogeneity, the conventional method has been the use of an x-ray radiography using film[1]. KAERI established a real time x-ray radiography systems(RTR) to inspect welding areas of a pin type research reactor fuels of HANARO. In this paper, confirmation of whether a real time x-ray system can be also applicable to inspect the homogeneity of the plate type dispersion fuel was discussed.

The simulated fuel plate was fabricated in ANL, which was made of stainless steel powder mixed with aluminium powder instead of U-Mo powder. The dimension of the simulated plate is about 600 mm in length, 100 mm in width, 1.27 mm in thickness. The fuel meat thickness of the mixture is 0.5 mm.

By using the simulated plate, the homogeneity of the mixture using RTR following the ANL/RERTR/TM-15 procedures[2] was inspected. For the inspection of homogeneity, measuring the gray value of an x-ray image with digital radiography software was introduced instead of measuring the film density with a densitometer which has been used conventionally.

2. Equipment and experimental procedures

The real time x-ray radiography system consists of an x-ray generator, image intensifier, CCD camera, digital image processor software, and display monitor as shown in Fig. 1. The x-ray generator has a 90 kV microfocus x-ray tube Kevex with a spot size of 4 μ m. The simulated fuel plate is made with a mixture of stainless steel powder and Al powder by rolling shown in Fig. 2. The step wedge has 6 steps of which the thickness is 0.05, 0.1, 0.15, 0.2, 0.25, 0.3 respectively as shown in Fig. 3.

The x-ray image of the plate was taken under the condition of 50 kV, 0.05 mA. The FOD(Focus to Object Distance) was 80 mm, and FDD(Focus to the image Detection Distance) was 500 mm.

As shown in Fig. 4, the beam intensity expressed by gray value on the x-ray sing RTR is high in the center area of the image intensifier, and low in the peripheral area of the image

intensifier. The image intensifier has a type of concave lens, so it causes some image distortion, and there is uneven gray value on the screen. In order to measure the gray value consistently, we took an x-ray on the designated positions. In the case of a step wedge, 6 shots on the center of each step for the step wedge were taken.

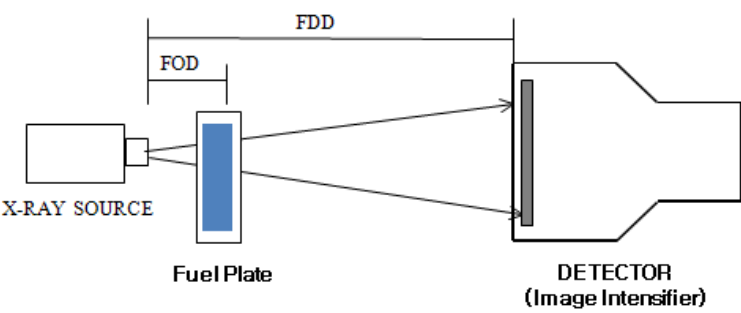


Fig. 1 Real time x-ray radiography inspection system

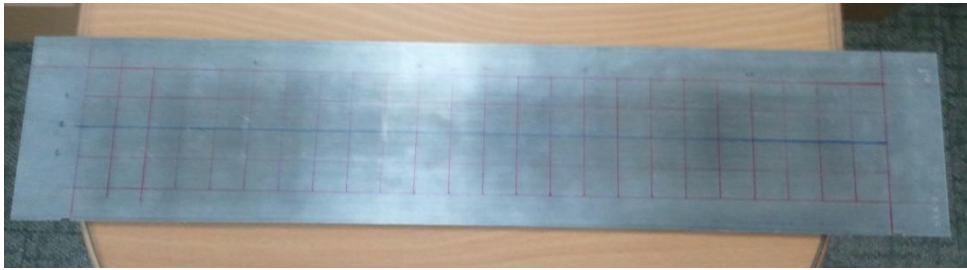


Fig. 2 The simulated fuel plate made with a mixture of stainless steel powder and Al powder



Fig. 3 Step wedge made of stainless steel foil

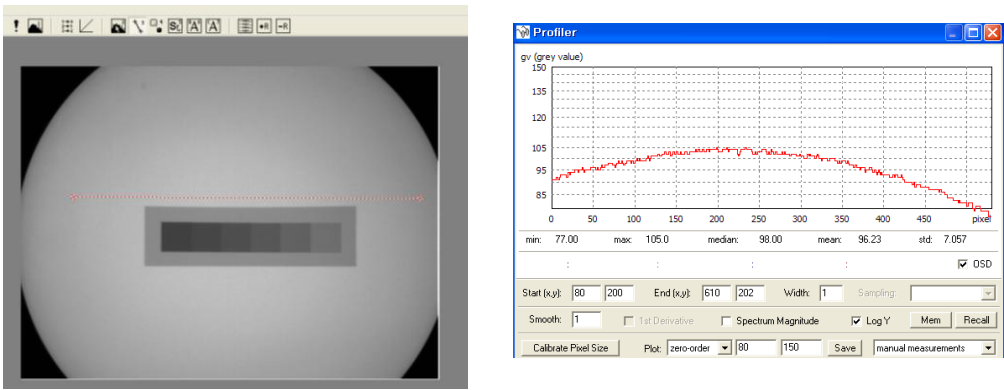


Fig. 4 Beam Profile of Real Time X-ray Radiography System

We took an x-ray at every 25 mm length on the fuel plate meat region. The total number of inspection points amounted to 69, longitudinally 23 column positions and vertically 3 row positions.

At first, the pixel calibration was made with a step wedge image as shown in Fig. 5. Using the gray level profiler mode, the length of one step was adjusted at 10mm, and it was possible to read the pixel size. Conventional method of the density measurement for the homogeneity of the plate is to measure the film density with a digital densitometer whose spot diameter is 2 ~ 3 mm. To make it equivalent for the 3 mm diameter spot size, a 2 x 2 mm square area was taken as shown in Fig. 6. In this area, there are total of 4096 gray values for each pixel, the mean value of the gray values can be obtained.

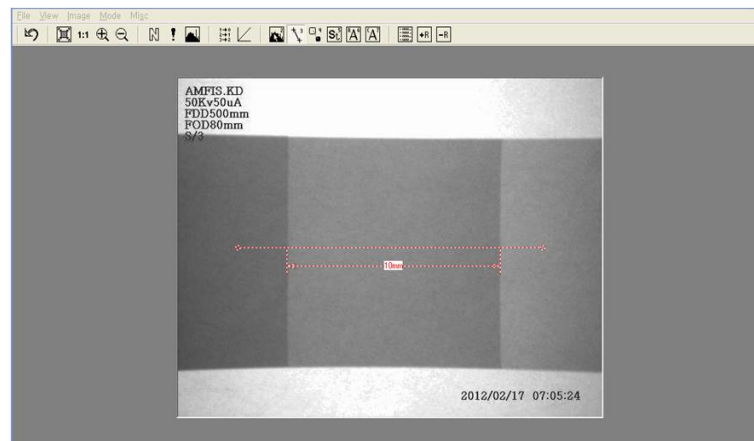


Fig. 5 Pixel calibration set to the 10 mm length for one step wedge.

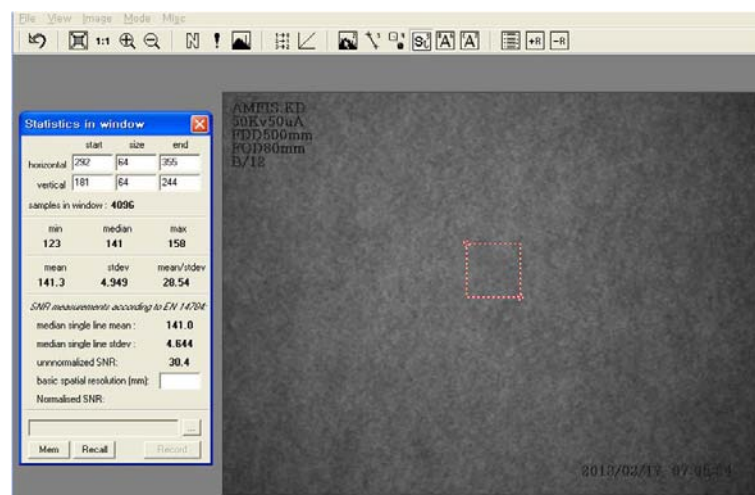


Fig. 6 The spot size for the density measurement

3. Results

The average gray value reading for each step of the wedge is plotted on the ordinate vs. the step wedge thickness on the vertical on a linear graph as shown in Fig. 7. Fig. 8 shows the gray value variations through the longitudinal direction of the fuel meat region. The average, maximum and minimum values were obtained from 3 measurements in each of the 23 columns of the x-ray image of the fuel plate region. The average, maximum and minimum values of the equivalent thickness of the simulated fuel plate were 0.188 mm, 0.21 mm(+11.7%), 0.17

mm(-9.6%). The allowable variation is usually $\pm 24\%$. The calculated equivalent thickness should be 0.2 mm, but the measured equivalent thickness of the simulated plate was 0.188 mm.

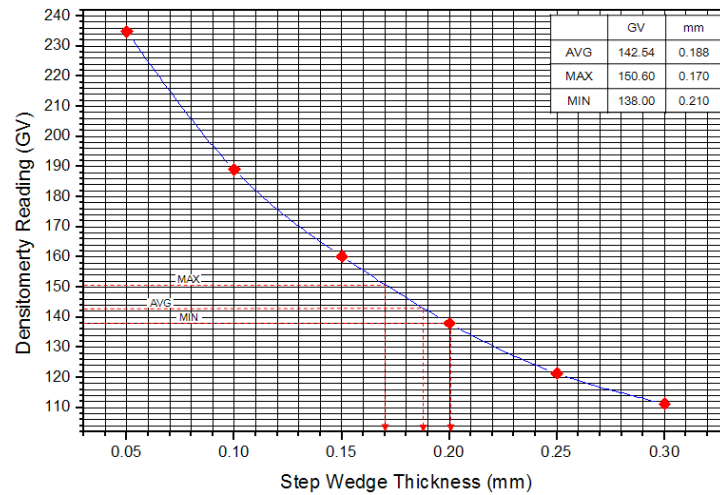


Fig. 7 Calibration curve for the measurement of equivalent thickness of the fuel density

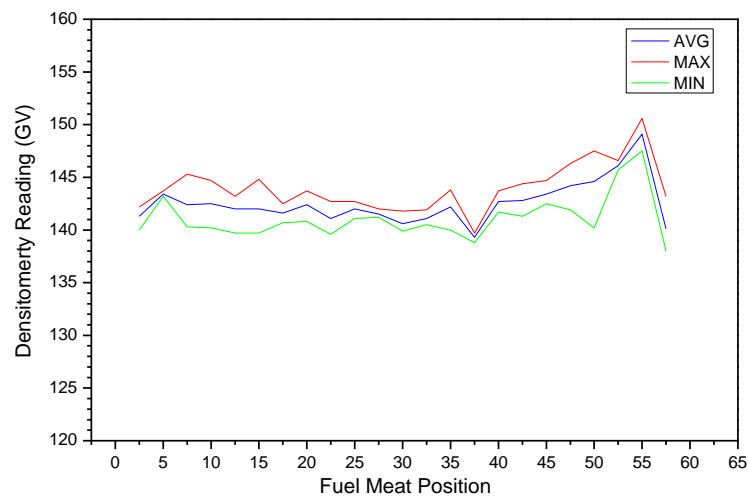


Fig. 8 The gray value distribution on the fuel meat region

4. Conclusions

In this paper, we introduced a real time x-ray radiography to measure homogeneity on the dispersion fuel plate. Even though the real time x-ray beam profile was not even, the procedure of measuring the gray value of the x-ray image of the simulated fuel plate and equivalent thickness of the fuel plate were developed. The average equivalent thickness was 0.188 mm, and the variation of the equivalent thickness was +11.7% to -9.6%. The results were comparable to the conventional x-ray film densitometer measurements. Therefore, the procedures of homogeneity measurement methods for the dispersion fuel plate were successfully developed by using a real time x-ray radiography.

References

- [1] F.B.J. FERRUFINO, et al, "Quantitative Determination of Uranium Homogeneity Distribution in MTR Fuel Type Plates", RRFM2011.
- [2] T.C. Wiencek, "Summary Report on Fuel Development and Miniplate Fabrication for the RERTR program 1978 to 1990", 1995. 8, ANL.

AN EXPERIMENTAL FACILITY TO QUALIFY THE CALIPSO MOCK-UP AND NAK PROCESSES FOR THE JULES HOROWITZ REACTOR

Damien J. MOULIN, Fabrice DELASSALLE, Laurent AYRAULT

*CEA, DEN, Department of Nuclear Technology,
F-13108 Saint-Paul-Lez-Durance, France.*

ABSTRACT

The CALIPSO device is a NaK liquid metal loop for material irradiation in the core of the Jules Horowitz Reactor. Its detail design was achieved and a hard mock-up which is composed of the main part containing liquid metal is currently being assembled.

In the same time, a new experimental facility called SOPRANO was developed and built at the CEA Cadarache centre.

Two main objectives have been assigned to this facility. The first one is to qualify the mock-up in realistic conditions and thus to get experimental feedback to carry on the development of CALIPSO. The second one is to test tools and methods concerning NaK operations aiming to validate processes for the Jules Horowitz Reactor.

After a short recall on the CALIPSO irradiation device, this paper will present the test section containing the mock-up. Then, it will detail the different components of the SOPRANO facility: the operating platform, the water cooling and gas conditioning circuits, the electricity and data acquisition system. Finally, the operations with the main tools such as the handling cask, the fluid transfer system and the cleaning section will be explained.

1. Introduction

The CALIPSO device is a NaK liquid metal loop for material irradiation in the core of the Jules Horowitz Reactor. Its design and thermal performances have been presented in previous congresses (1) (2). The manufacturing of an out-of-pile hard mock-up is under way. In the same time a new experimental facility called SOPRANO was developed and built at the CEA Cadarache centre.

Two main objectives have been assigned to the SOPRANO facility. The first one is to qualify the mock-up in realistic conditions and thus to get experimental feedback to carry on the development of CALIPSO. The second one is to test tools and methods concerning NaK operations aiming to validate processes for the Jules Horowitz Reactor.

After a short recall on the CALIPSO irradiation device, this paper will present the test assembly containing the mock-up, the different components of the SOPRANO facility and the main NaK operations.

2. The CALIPSO test device

The overall length of CALIPSO is 6800 mm and its outer diameter is 33 mm in the lower part so that it can fit into the central hole of JHR fuel elements. An annular electromagnetic pump is located above the active zone in the containment rig. An electrical heater is situated in the NaK just above the pump and a heat-exchanger at the lower part of the sample-holder, below the active zone. The containment rig is a double wall shell that fits to the core mechanical structures. A sample-holder is plugged into the containment rig through the circular opening situated in the upper part. It holds the material samples and experimental instrumentation (Figure 1), (Figure 2).

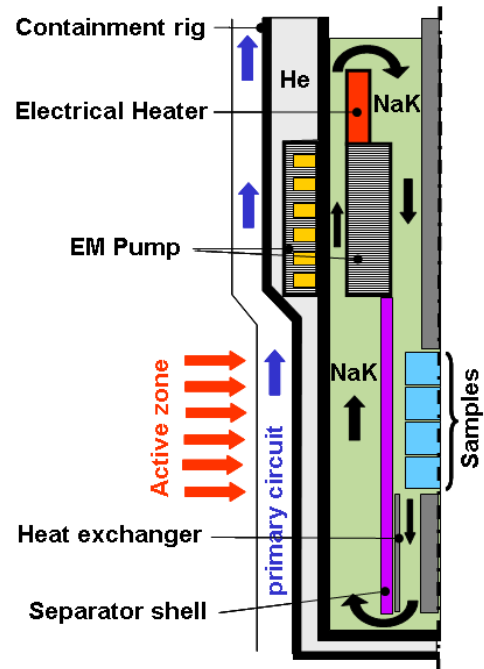


Figure 1 : Operating principle of CALIPSO

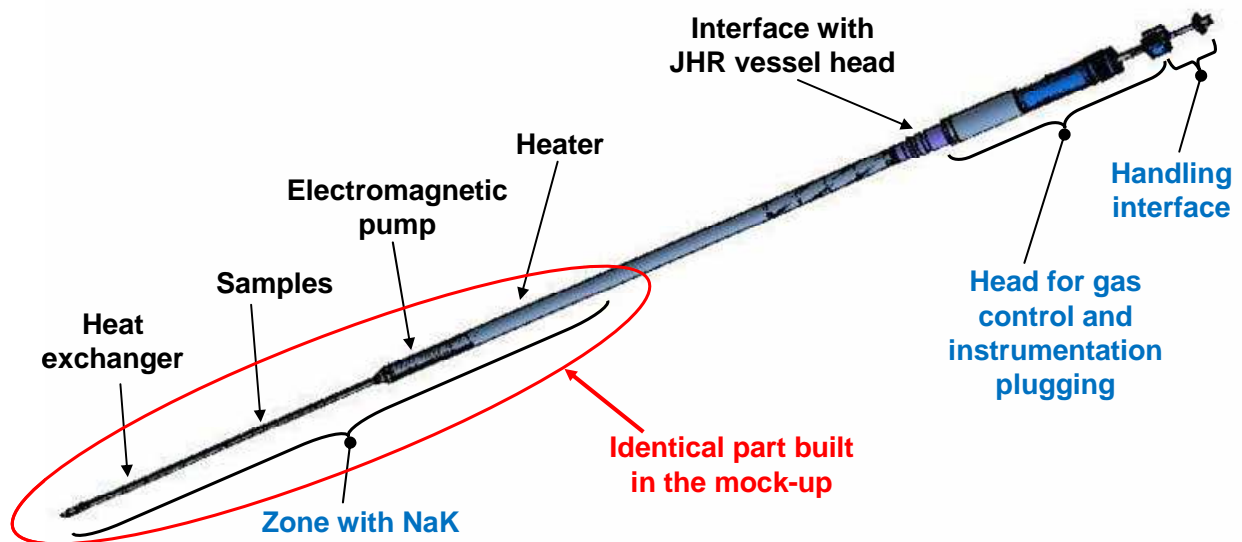


Figure 2 : General view of CALIPSO

3. The experimental assembly and the mock-up

Performing experimental tests on a representative mock-up of CALIPSO implies some evolution of the actual design and specific components have to be added to the assembly. The mock-up of CALIPSO consists in the bottom part of the actual test device. It is composed of all the components entering into the NaK loop with the same geometry. The rest of the mock-up was designed in order to reduce the total length and to respect the safety request.

The mock-up of CALIPSO is placed into a water box composed of a flow channel shroud surrounded by a safety shell (Figure 3). The steel tube of the safety shell is 40 mm thick and is intended to prevent people injuries in case of explosion due to NaK - water interaction (Figure 4). This assembly is about 4 m long and 40 cm large.

The geometry of the water channel around the mock-up is the same as the one in the JHR core.

To simulate nuclear heating, an 18 kW electrical heating rod replaces the actual sample holder.

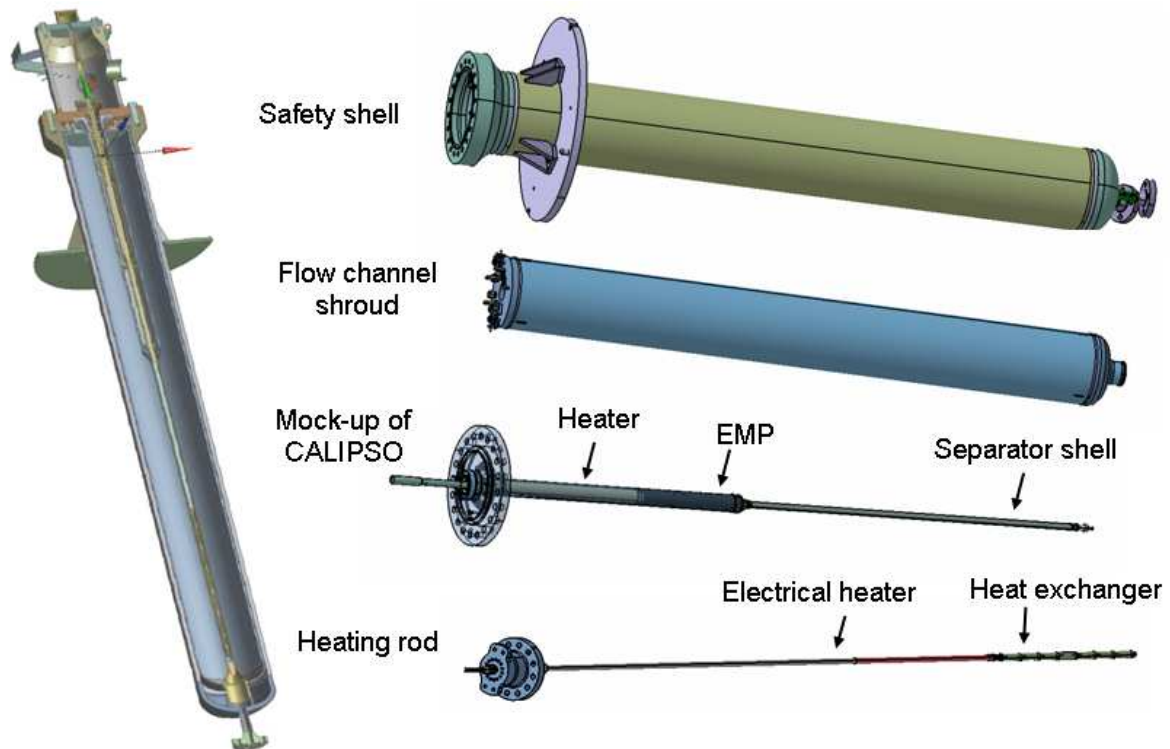


Figure 3 : The CALIPSO mock-up and the water box



Figure 4 : The safety shell

4. The SOPRANO facility

The SOPRANO facility was designed and built to perform experimental testing on the mock-up of CALIPSO and to allow operations with NaK.

It is composed of an operating platform (Figure 5) with different components and circuits. Its steel structure is mainly sized to support the test assembly.

A water circuit is connected to the bottom of the test assembly to cool the mock-up in the same conditions as the primary circuit of the JHR.

Because of its high reactivity with oxygen, NaK liquid metal needs inert gas cushion. A fluid control panel is installed near the test area to provide inert gas to the different NaK containments and equipments through flexible lines.

A 50 kW electrical supply is necessary to the mock-up and surrounding equipments. The CALIPSO mock-up is also largely instrumented with thermocouples to measure temperature of NaK and component structures. To process and control the signal of the different sensors, a reliable data acquisition system is installed near the platform.

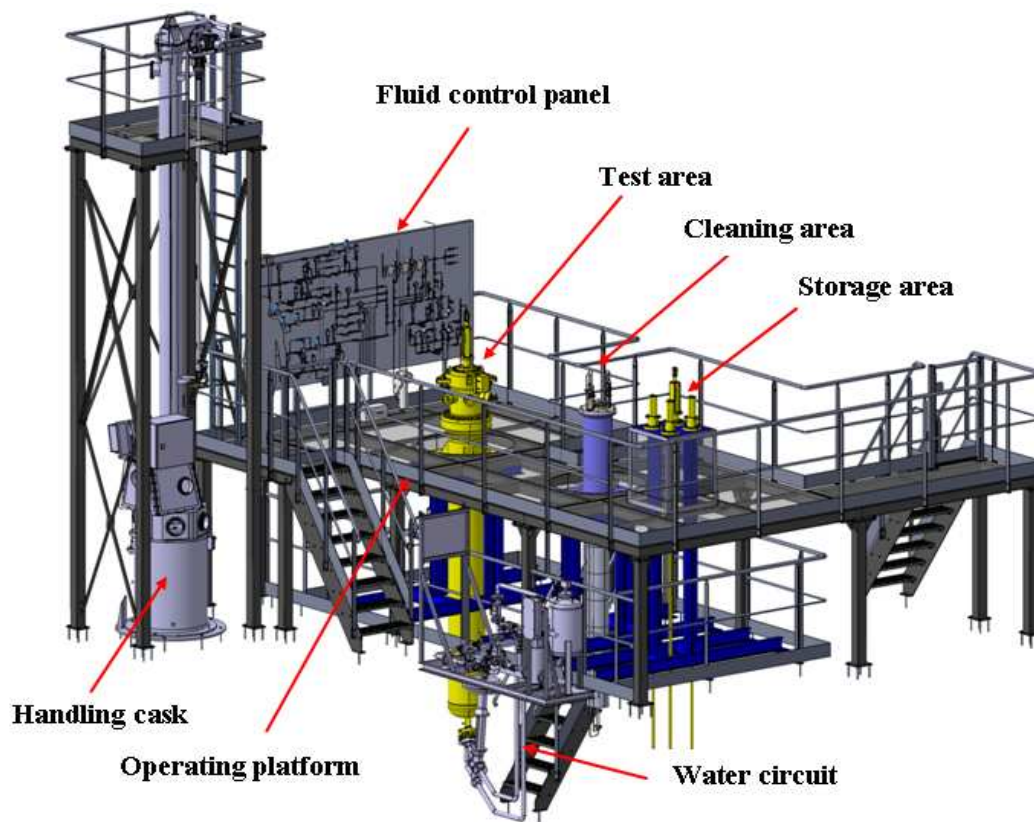


Figure 5 : The operating platform



Figure 6 : The platform under construction

5. Procedure with NaK

One of the NaK characteristics is its high chemical reactivity with components such as oxygen, water, organic materials and halogen. Therefore it is necessary to always use inert gas cushion in NaK containment. Moreover, to prevent pollution of NaK, equipments have to be carefully cleaned and dry before their contact with NaK.

A specific handling cask is used for maintenance operation of the test assembly and for transfer operations with the cleaning area. This cask is composed of the glove box surmounted by a 4,6 m long tube including an electrical lifting winch. During handling operation, the cask is filled with inert gas.

NaK can be poured into the mock-up via a feeder with calibrated volumes and a rod-shaped tool plugged onto the test area. The same tool is also intended to be used to empty the mock-up. Fresh NaK and waste NaK containers are also provided.

A cleaning area is supplied to get rid of the few grams of residual NaK on the heating rod or filling-emptying tool after their removal from the test area. The process consists in a controlled NaK / water chemical reaction into the cleaning container while venting the produced gases. Then, rinsing and drying phases are successively done. Finally the cleaned equipment is moved onto the storage rack.

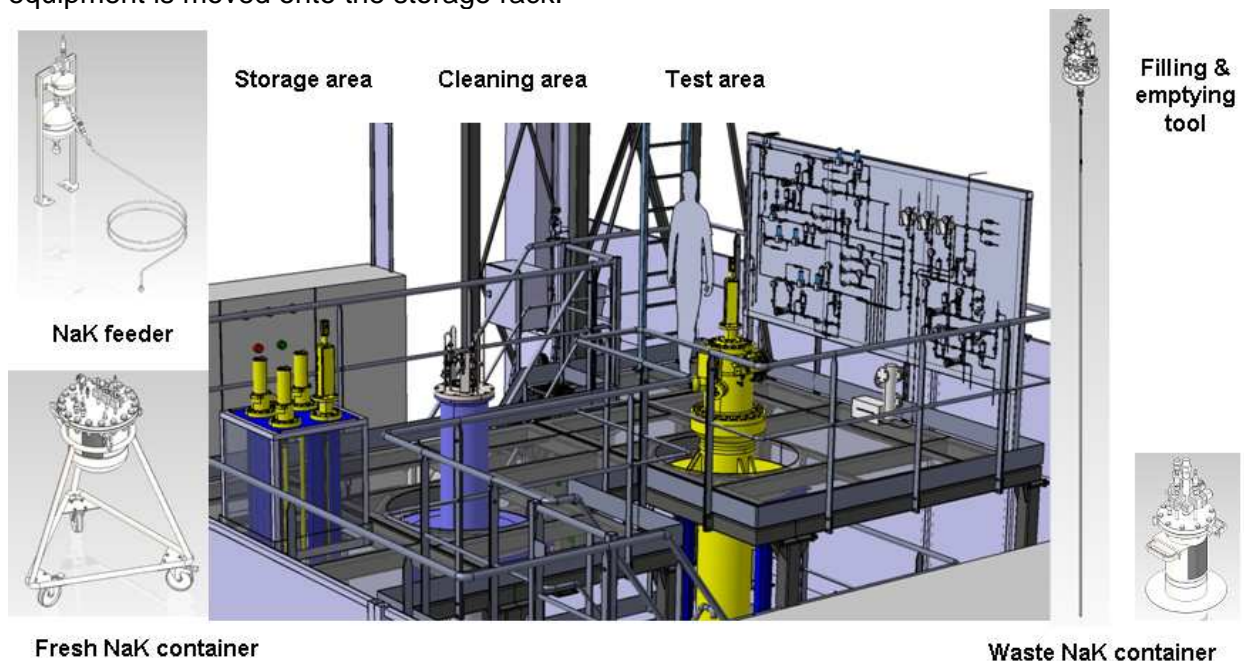


Figure 7 : Equipments used into the NaK processes

6. Conclusion

The manufacturing of the mock-up of CALIPSO has already provided very useful feedbacks to improve the design of the actual irradiation test device. However, the ultimate validation will be drawn from the experimental testing of the mock-up in the SOPRANO facility. The qualification program includes components testing and comparison with thermal calculations. In the same time, tools for the NaK processes will be validated before their adaptation into the JHR facility.

7. References

- (1) D. Moulin, C. Biscarrat, S. Christin, G. Laffont, A. Morcillo, E. Pluyette, F. Rey, " Design of a flowing-NaK experimental device for in-core irradiation in the Jules Horowitz Reactor", *European Nuclear Society RRFM 2009, Vienna, March 22-25, 2009*
- (2) D. J. Moulin, S. Christin, Ch. Biscarrat, "Thermal assessment of the CALIPSO irradiation device for the Jules Horowitz Reactor", *IGORR 13, Knoxville, TN, USA, September 19-24, 2010*

Jules Horowitz Reactor Project. Fuel irradiation device through engineering process description.

S.Gaillot⁽¹⁾, T.Dousson⁽²⁾, S.Vitry⁽¹⁾, S.Gay⁽¹⁾, C.Garnier⁽¹⁾

(1) CEA, DEN, DTN-STPA-LCIT, bat 204, Cadarache, F-13108 Saint-Paul-lez-Durance, France

Phone : + 33 (0) 442253165 - Email : stephane.gaillot@cea.fr

(2) CEA, DEN, DER-SRJH-LEDI, bat 225, Cadarache, F-13108 Saint-Paul-lez-Durance, France

Phone : + 33 (0) 442253791 - Email : thierry.dousson@cea.fr

ABSTRACT

To answer to the needs of the customers in terms of selection, qualification and behaviour of fuels and materials under neutron flux, Material Testing Reactors (MTR) types are used. These experimental reactors propose high performances in core in terms of fast neutron flux permitting to accelerate the irradiation processes on materials (as ageing phenomenon) but also permitting in the reflector to check, under pre-defined power scenarios, the behaviour (as PCI phenomenon [^a]) of fuel samples issued of nuclear power plants.

The irradiation devices used for the tests of fuel rods allow reproducing at small scales the conditions of the studied nuclear reactors (as LWR type). Exposed to the neutron flux of the reactor, they allow the test of samples under representative or more severe experimental conditions. The irradiations carried out can be performed on a short duration period (a few days) or on a long phase (several years) to study e.g. the corrosion phenomena of the claddings under flux.

The experimental loop is generally composed, in the reactor pool, of an irradiation device linked through under water lines to a cooling circuit (located in an experimental area close to the core) allowing reproducing the thermal-hydraulic conditions (as LWR) in the test channel of the device.

The irradiation device, containing the active part, consist in metallic structures envelopes working under temperature and pressure conditions but also designed to limit the neutron absorption (use of zircaloy material). Located in the reactor, the device must satisfy adapted safety rules and depending of the fluid activity, satisfy to the French regulation constraints (as ESPN type [^a]). Design studies are carried out according thermo-mechanical rules specific to nuclear power plants (as RCC-M, MRX [^a]).

Concerning the irradiations performed with experimental vocations, the devices and in particular the test channel and the rod can be strongly instrumented allowing the on-line following of the required phenomena (thermal-hydraulics, deformations (creeping, swelling,...)).

The experimental process allowing in core setting and the use of irradiation device is generally the result of a long process of several years including physical studies and safety analyses, design engineering studies, critical components qualification, manufacture and controls.

The paper describes part of this process applied to a typical fuel irradiation device for JHR.

Key words: material research reactor (MTR), irradiation device, engineering process, technologies.

^a cf. glossary,end of document

1. Introduction:

1.1 JHR Facility: key characteristics and performances

The Jules Horowitz Reactor (JHR-Materials Testing Reactor) is under construction in the south of France (CEA, Cadarache, Bouches du Rhone). This Nuclear Facility is dedicated to perform irradiations of materials, fuels in support of actual (LWR) and futures power plants (Gen.IV, fusion). It allows also producing radioisotopes for medical applications, namely Mo-99. This facility will offer to the international community interesting irradiation capabilities (15 dpa/year at 100MWth) for core materials samples, high thermal neutron fluxes in the reflector for irradiation of fuels samples (corresponding to 8 times the neutron flux in a PWR). It will allow also a high flexibility in terms of experimental conditions, several irradiation locations in the core, in the reflector in fixed and also on movable locations (systems permitting to modify the distance between the sample and the core using pre-defined moving scenario). For different experimental issues, several Thermal Hydraulics conditions can be obtained (LWR (P&B) [°], HTR, SFR,...). The irradiation devices in the reflector are cooled by the water of the reactor pool in natural or forced convection regimes, depending of the experimental thermal load.

In addition, some supports utilities (storage pools, hot cells, non-destructive equipments (Xrays, gamma imaging systems) are integrated in the facility in order to propose to the customers a complete offer in terms of irradiation services.

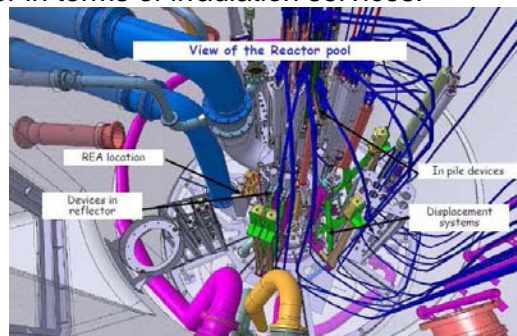


Fig.1: view of the JHR reactor pool

1.2 Typical fuel irradiation scenario for power transient tests

The main goal of these tests is to check the behaviour of an irradiated fuel rod generally representative of a power plant fuel sample during experimental phases as power transients. The device is placed in the Beryllium reflector on a displacement system. The typical experimental scenario is the following:

- Pre-irradiation of the rod during a few days (12h to 1week) at low power (100W.cm^{-1} with 200W.cm^{-1}) with representative PWR thermal-hydraulic conditions: 155bar, 320°C.
 - heat balance before ramp test,
 - power increase with kinetics of $200\text{W.cm}^{-1}.\text{min}^{-1}$ with $660\text{W.cm}^{-1}.\text{min}^{-1}$,
 - power plateau for 3 to 12 hours. Heat balance at high power,
 - device removing to backward position with drive power decrease,
 - cooling, transfer of the device and non destructive examinations realization (GAMMA spectrometry, X-rays).

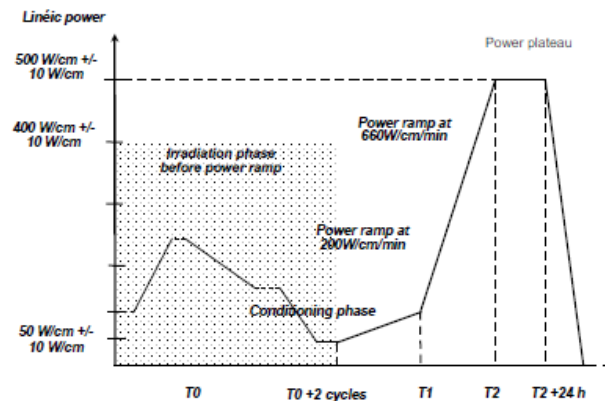


Fig.2: typical transient of power ramp test

2. Engineering process description:

In order to reach these objectives, adapted processes are applied to take into account the specificities of the devices. These processes are of iterative nature and concern various fields:

- the experimentation field characterizing the external customers' requirements which concern the neutron and thermal hydraulics performances. These input data are considered in terms of design of devices (capsule, loop), location in the reactor (in core or in the reflector), materials pre-selection and instrumentation definition (on the device and on the loop),
- the cell of licensing defining the safety options and the requirements in terms of regulation that the equipment must satisfy,
- the operation staff defining the constraints related on the implementation and the use of the equipment in the facility during the various phases of works (in particular, definition of the handling tools, storage equipment),
- engineering field having charges of the technological issue with the equipment, the thermo-mechanical dimensioning of the components, the qualification of the critical components, the industrialization, the manufacturing controls (fabrication and assembling phases) and the start-up on site.

This process of studies, manufacture and start-up for a new experiment requires a long time (several years) implying all the actors around the reactor.

2.1 First step : input data determination

▪ *Experimental issue*

To answer to the experimental objective describes above for the realization of a power ramp on an irradiated rod, the first studies take generally into account the experience feedback in Europe on research reactors (working or stopped): OSIRIS, SILOE in France, HALDEN in Norway, SCK-CEN in Belgium, HFR in the Netherlands or STUDEVICK in Sweden. The first thermal hydraulic and neutron calculations are carried out to define the working experimental field :

- determination of the neutron flux on the sample, the linear power and the gamma heating. Analyzes evolutions during the reactor cycle .
- determination of the cooling flow acceptable for the rod during normal conditions. Determination of the thermal hydraulic criteria and the margins regarding boiling parameters (REC) [a],
- analyzes of instrumentation equipments:
 - on the rod (temperature, deformation),

- in the test channel (TH measurements and thermal balance),
- on the sleeve (neutron measurements),
- operation scenario studies and interface determination with the facility.

▪ **Safety issue**

Application of the safety report requirements of the facility,

- application of a CEA technical guide dedicated to irradiation devices utilization,
- identification of the off-normal scenarios. Thermal hydraulics analyses and preliminary safety options definition. Identification of requirements regarding the design of the irradiation device (shells, barriers, screens,...).

According to the guide on the experimental devices, consequences analyzes of various types of scenarios:

- radiological impact following the failure of the device and/or the circuit,
- mechanical impact on the core and on safety systems due to failure of the device,
- neutron effect on the core as a consequence of device removing.

The results of these analyses allow defining the number of barriers and protective systems to implement. The conclusions also make it possible to define the level of mechanical calculations to be taken into account for the thermo-mechanical studies of the components having a function for safety or a role in the availability of the facility. These studies are carried out by using dedicated thermo mechanical codes (as RCC-M(R) X for design & manufacture rules of equipments used for experimental reactors, [1]).

▪ **Regulation and Quality issues**

The standards applied are French or European levels (NF, EN).

The quality process respect the ISO9001 standard and Nuclear Facilities Quality order (AQ-08-84). Concerning the Nuclear pressure containments, the French order ESPN is applied. The applicable codification (e.g. N2, cat.IV) can have for consequence increased controls during manufacturing phase (e.g voluminal control of the weldings), hydraulic tests, periodical inspections (<40months) based on visual and non destructives exams, and pressure requalification tests (every 10 years).

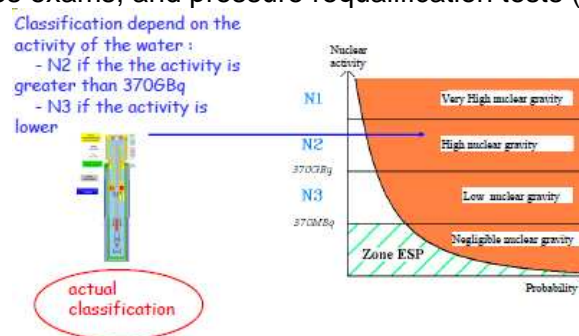


Fig.3: ESP(N) regulation application

2.2 Second step: preliminary design and studies.

The first phases of engineering process are reminded herewith:

- feasibility phase,
- preliminary design phase. Conceptual design report (APS^[a]) production.

On the basis of preliminary data, the main technological options of the fuel irradiation loop are defined.

- **Description of the sample:**

The sample considered for the standard experiment can be a PWR fuel UO_2 rod with a 600 mm long fissile stack and either being fresh or pre-irradiated.

The sample can be instrumented with a fuel centreline thermocouple (C type) and a cladding thermocouple (K type). In some cases for fission products (FP) tests, two capillary tubes connected to the top and the bottom free volumes of the rod will be used to sweep the gases (fission gases) released by the fuel and to route them to the fission product laboratory in the JHR experimentation area (called CEDE [a]). The instrumented sample is maintained in the test section through a sample holder (see fig.4).

In order to increase the flexibility of the device, studies are also performed on the internal structures design regarding the possibility to take into account BWR rods samples (diameter up to 12.3mm).

Note: Current studies are performed in order to increase the number of irradiation phases during a cycle. In this case, the instrumentation on the rod will be reduced and specific equipments will be used in order to load and unload the rod under water in the reactor pool (under water transfer system).

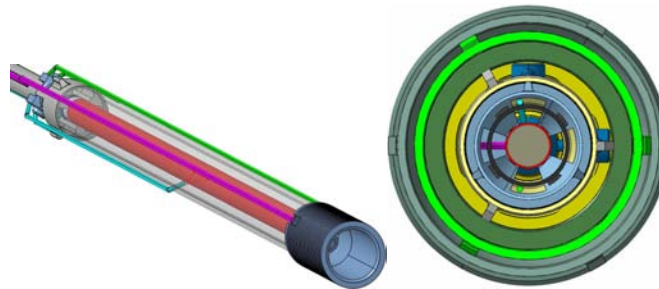


Fig.4: view of the sample holder and test section

- **Description of the loop**

The loop is typically composed of two parts:

- An in-pile section subjected to the flux, the low and high extensions, the instrumentation lines, the device head, the fluid connectors, FP line and electrical equipments, flexible connections, the pool experimental and the Fission Products penetrations (if necessary) (see fig.5):

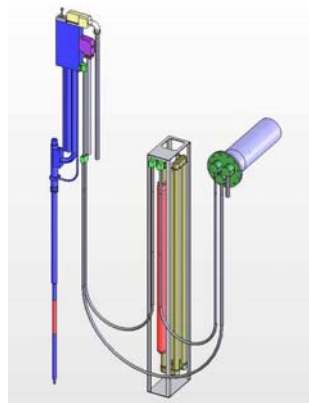


Fig.5: view of a typical irradiation device
(in-pile equipments and flexible connections)

- a grounded section including the fluid circuit, connections to fixed parts of the facility (fluids, utility fluids, utility waste, ventilation and electrical equipments), and Instrumentation and controls (I&C) modules.

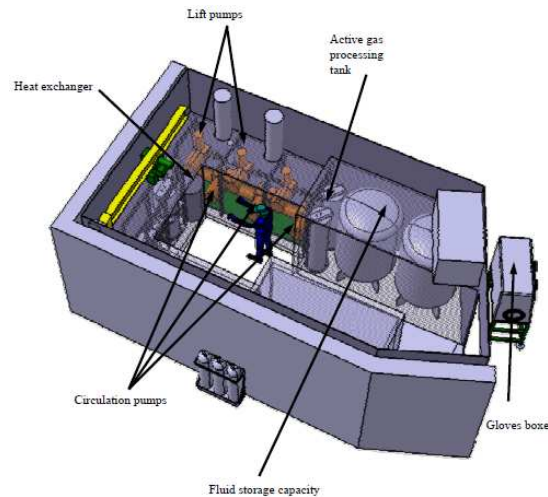


Fig.6: view of the experimental cubicle

2.3 Third step : simulation (hydraulics, thermal, thermo-mechanical)

Once the data input established, thermal hydraulics studies engaged and safety options defined, the thermal-mechanical dimensioning of the structures which have a safety functions (barrier) is carried out according to the rules of the RCC-MRX in normal and off-normal conditions. During these studies, the dimensioning criteria are checked.

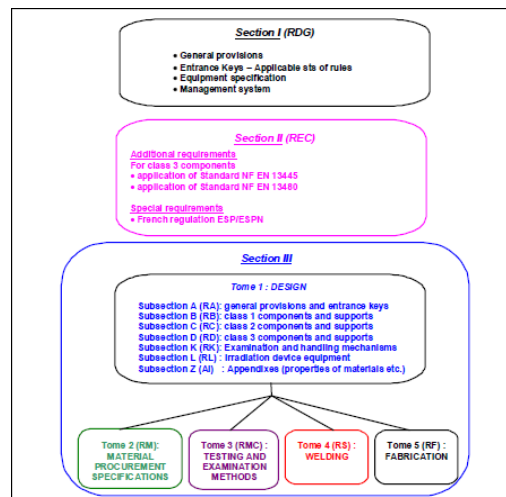


Fig.7: RCC-MRX outlines (illustration)

Other studies are performed in order to design and to assess the assembling of internal components of the device.

• **Example of study of the sealing joint of the head of the device**

The device of irradiation is composed of various vessels contained the ones with the others for which sealing's are to be guaranteed:

- an internal vessel containing the instrumented experimental rod. It is made up of the internal envelope of the force tube, of the high part of the instrumentation holder and

the caps of the sample holder. This vessel contains the fluid circulating at high pressure and temperature,
 - the tightness system between the various constitutive parts is ensured by seals:

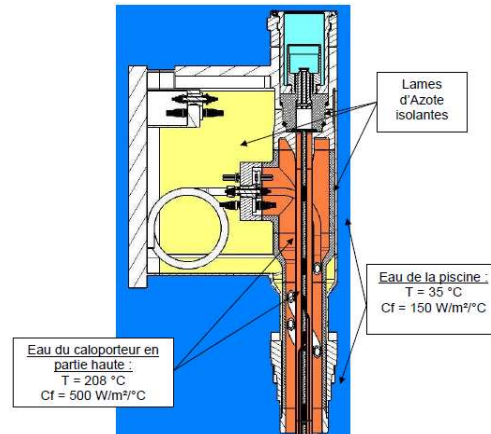
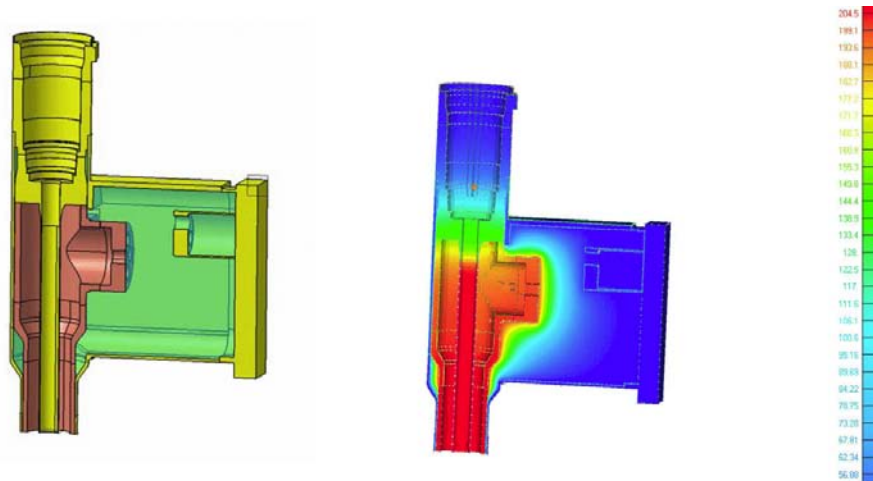


Fig.8: description of the head device

The choice on the technology of these seals (metallic, elastomer) depend on the conditions of temperature in normal and off-normal conditions. Other considerations related to the operation of the device (loading and un-loading operations in hot cells) can also influence the choice of the system to use. A thermal study made it possible to define the thermal cartography of the head of device in order to estimate them temperatures seen by the seals.



software used: CATIA v5 (CAD design code), FEMAP-NASTRAN (thermo mechanical code).

Fig.9: CAD simulation of the head of the device & thermal map simulation

The first results obtained imply to optimise the geometries in order to improve the cooling of this zone:

- geometry modification in the zone close to the seals (reduction in the volume of water) and reduction of natural convection exchange between the fluid and the wall (anti-convective geometry consideration). Positive impact on the working temperature of seals (-10%),
- modification of the gas gap geometry between the internal and external tube in order to limit the thermal barrier function.

On the basis of thermal study carried out, a thermal-mechanical study made it possible to estimate the stresses in this zone and to calculate the differential expansions between the parts. The results obtained require to use differential systems of dilation (as metallic bellows).



Fig.10: metallic bellow

2.4 Fourth step : mock-up and components qualifications

Technical and technological studies are performed up to a level of detailed design report. In parallel, some items can result in producing mock-up of certain components to confirm the studies of simulation or to assess the manufacture issue:

Description	Out of pile test	In pile test
Qualification of innovating components (connectors, sensors,...)	X	
Behaviour test of the sealing joint in normal and off-normal conditions. thermal and pressure tests.	X	
Mock-up testing critical aspects of operation process. Cold checking of the kinematics of a sample holder: loading, unloading phases.	X	under water transfer system and/or JHR hot cell

Table.1: qualification tests (illustration)

2.5 Fifth step: industrialization (external supplier support), manufacture and controls.

In parallel of the simulation phase, technological feasibility studies are carried out in order to check the manufacturing specificities of the components and/or to evaluate the manufacturing processes:

- industrial suppliers research and analyzes of their technical capabilities to manufacture the device, of organization to deal with manufacture, the tests and the start-up of an experimental irradiation loop,
- studies and manufacture of critical components,
- manufacture and assembly of the components of the loop in external factories (industrial suppliers),
- controls in factories: conformity with the technical specifications, checking of the quality of manufacture,
- first tests of performance (thermal, hydraulic, pneumatic, electrical).



Fig.11: example of welding operation on instrumentation

2.6 Sixth step: In pile assembling and tests, start-up.

This phase contains different operations:

- transport and assembly of the loop in the facility,
- connection with the existing utilities (fluid, electric, effluent, I&C) and tests of performance,
- test of start-up: tests of tightness, cold hydraulic tests, tests in temperature with heating simulating rod, test of performance of heat exchangers,
- test of start-up with fuel rod : global checking of the experimental performances of the loop,
- pressure acceptance tests according ESP(N) regulation.

At this state, the experimental loop is ready to operational service for commercial irradiation programs.

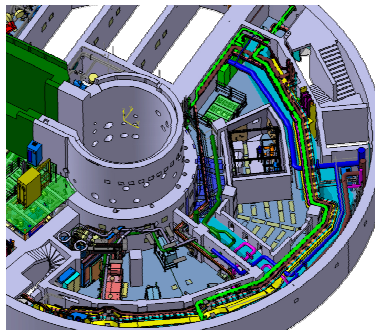


Fig.12: JHR experimental area. Bunker integration

3 Conclusion :

The study and the start-up of an experimental loop for fuel rod irradiation program require the implementation of a process consist in physical studies, safety analyses and engineering issues, long and complex leading to many iterations between the experimentation and the engineering parts. The constraints of operation (equipment working under pressure, temperature, irradiated sample), result in complying with strict rules in terms of design and quality of realization (designing, calculating, manufacturing, controls according to RCC-MRX), of safety (application of the Safety Report) and regulation (ESP (N) and Quality order).

The required experimental objectives lead to study, design and to implement devices making it possible to perform on line during the irradiation phase, measurements on the experimental rod (fuel and clad temperature evolution), deformation phenomena (elongation, swelling) and also in the fluid (thermal heat balance).

Operation constraints, based on the precise analysis of the phases of work of the device in the facility make it possible to identify the needs for tools, control and interfaces between the device and the facility in order to facilitate its preparation, its use, and its storage.

RRFM/IGORR 12

European Research Reactor conference
PRAGUE, Czech Republic, 2012, March 18^h to 22^d

4 References:

[1] NA3 manufacturing practices.

MTR+I3 European Program (2006-2009).

[2] The ADELINe irradiation loop in the Jules Horowitz MTR

Testing a LWR fuel rod up to the limits with a high quality level experimental process

12th International Group on Research Reactors (12th IGORR) . CIAE-Beijing, P.R. China, October 28-30, 2009.

Glossary:

- APS: Conceptual Design Phase,
- CEDE: Experimental Area in the Nuclear Building,
- ESPN: Regulation concerning Nuclear Equipments working under Pressure,
- LWR (P&B): Light Water Reactors (Pressurized or Boiling types),
- PCI: Pellet Clad Interaction,
- RCC-MX: Design and thermal mechanical rules concerning Mechanical Equipments used to experimental Nuclear reactors,
- RCC-MRX: Merge of RCC-MX (applied to Experimental reactors) & RCC-MR (applied to fast breeder reactors),
- REC: Critical Heating Ratio,

EVALUATION AND MODELLING OF THE THERMAL NEUTRON FLUX IN SAMPLES IN THE CAROUSSEL CHANNELS OF THE TRIGA MARK I IPR-R1 REACTOR USING MONTE CARLO (MCNP) CODE

J. A. D. SALOMÉ¹, C. A. M. DA SILVA¹, C. PEREIRA¹, B. T. GUERRA¹, M. A. DE B. C. MENEZES², A. L. COSTA¹, M. A. F. VELOSO¹ AND V. V. A. SILVA^{1,2}

*1- Departamento de Engenharia Nuclear, Universidade Federal de Minas Gerais
Av. Antônio Carlos, 6627 – PCA1 – Anexo Engenharia – Pampulha
CEP 31270-90 Belo Horizonte, MG, Brasil*

*2 – Centro de Desenvolvimento da Tecnologia Nuclear/Comissão Nacional de Energia Nuclear –
CDTN/CNEN,
Av. Presidente Antônio Carlos, 6627 – Campus UFMG, 31270-900, Belo Horizonte, MG, Brazil*

ABSTRACT

The IPR-R1 is a reactor type TRIGA, Mark-I model located at Nuclear Technology Development Centre (CDTN) sponsored by Brazilian Nuclear Energy Commission (CNEN), at Belo Horizonte City, Brazil. It is a light water moderated and cooled, graphite-reflected, open-pool type research reactor. This reactor has a Rotary Specimen Rack (RSR) at the outside the reactor core where is possible to irradiate samples in forty different positions (channels).

The reactors type TRIGA (Training, Research, Isotopes, General Atomics) have been used in research, training of personnel and materials analysis, achieving excellent results. The most research analysis performed in TRIGA reactor is represented by the technique of neutron activation (NAA). The mechanism is irradiating the sample with a flux of neutrons and then measure the activity produced by gamma spectrometry.

The MCNP5 code (Monte Carlo N-Particle transport code – version 5) was applied to simulate the IPR-R1 reactor core. The thermal neutron flux through the samples in eleven irradiation channels was evaluated to investigate the effects of sizes samples variation on the thermal neutron flux inside each sample. These channels were characterized as representative channels of the neutron flux distribution in the RSR. The simulations are compared with experimental results and good agreement has been obtained for the most channels as it is being presented in this work.

The core was configured in the MCNP using a cylinder that contains water, fuel elements, radial reflectors, central tube, control rods and neutron source. Around the core is the rotary rack with adequate groove to insert the samples to irradiation.

Keywords: neutron flux, reactor TRIGA IPR-R1, neutron activation analysis.

1. Introduction

The reactor TRIGA IPR-R1 is installed at the CDTN, Belo Horizonte, since 1960. It is a research reactor cooled and moderated with light water demineralized and its fuel is an alloy of uranium and zirconium hydride moderator (U-ZrH) containing 8% to 8.5% by weight of uranium enriched at 20% ²³⁵U. This reactor has the following main applications: neutron activation analysis, nuclear plants operators training and nuclear applications and thermo-hydraulic. The IPR-R1 had several different configurations of its core. Consequently, some studies were performed with the goal of characterizing the neutron flux in its irradiation devices [1-6].

The IPR-R1 core has a radial cylindrical configuration with six concentric rings (A, B, C, D, E and F) containing 91 positions able to host either fuel rods or other components like control rods, reflectors and irradiator channels. The core has 59 fuel elements cladding with aluminum, 4 fuel elements cladding with stainless steel, 23 radial reflectors elements, 3 control rods (shim, safety and regulating), 1 central thimble, and 1 neutron source. The fuel elements have three axial sections with upper and lower reflector (graphite), and the central portion filled with fuel (UZrH). The radial reflectors elements are covered with aluminum and filled with graphite having the same dimensions of the fuel elements. Boron carbide and aluminum cladding compose the control rods. In the center of the reactor, there is an aluminum tube (central thimble) to irradiation of experimental samples. This tube is removable and when it is not in use, the reactor pool water fills its volume. Furthermore, the core has an annular graphite reflector with aluminum cladding. Such annular reflector has a radial groove where a rotary rack is assembled for insertion of the samples to irradiation. In such rotary rack is possible to place the samples in 40 different channels (positions) around the core. Moreover, tangent to annular reflector, there is a pneumatic tube where the samples also can be inserted to irradiation. Figure 1 shows the radial and axial core configuration [7].

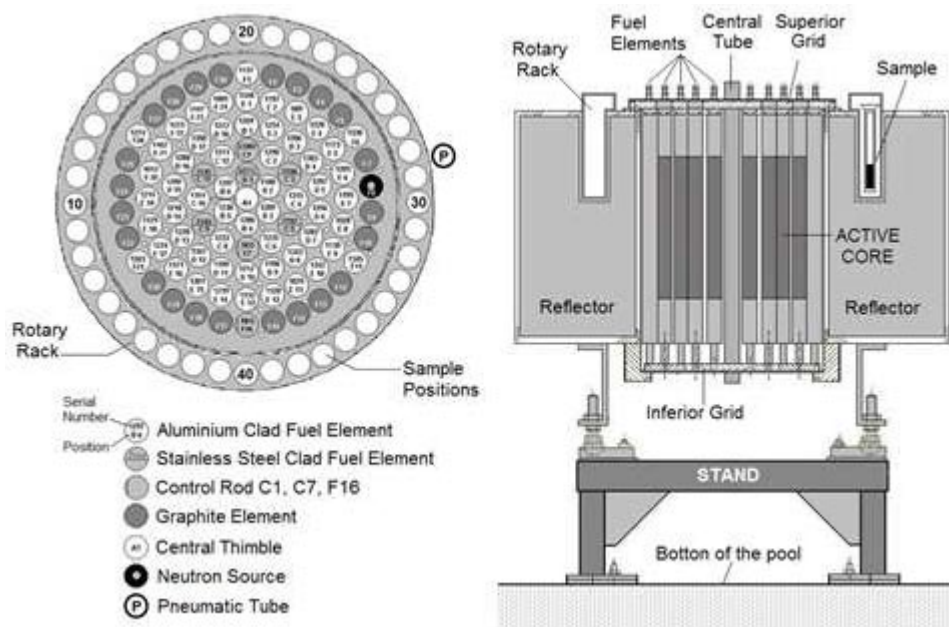


Fig. 1 - Current horizontal and vertical cross-sections of TRIGA IPR-R1 reactor core

In 1995, the k_0 method was established at CDTN/CNEN [8]. Since then, this method has been responsible for 90% of all neutron activation analysis demand. To apply this method, it is necessary to determine the parameter f (ratio of thermal to epithermal neutron fluxes) [8] where the samples are irradiated. Thus, the evaluation of the neutron flux became indispensable in the application of k_0 method. In order to contribute for the use and validation of k_0 method, studies have developed a theoretical method to calculate the thermal neutron flux in devices where the samples are irradiated [7, 8]. Now, using the same methodology, it simulates the effects of irradiating some samples in the IPR-R1. The aim is to evaluate the effects of size samples variation about the value of the thermal neutron flux inside the samples. To model the validation, the simulations are compared with experimental results obtained by the teams of Dr. Maria Ângela Menezes Correia de Barros, CDTN/CNEN, that worked together Dr. Radojko Jacimovic, researcher at Jozef Stefan Institute, University of Ljubljana [4].

2. Methodology

2.1 Configured Model

The reactor model was developed using MCNP5 code where 500 active cycles were calculated with 10000 neutrons per cycle. The simulated model was based on previous studies [3-6] where the reactor core has the same features of the IPR-R1 geometry described before. The core was configured considering a cylinder containing water, fuel elements, radial reflectors, central tube (or central thimble), control rods and neutron source. Each rod has a coordinate value. They were filled according to their individual characteristics. Around the core is located the RSR which has grooves to insert the samples to irradiation. The configured core is inside the pool. The RSR is in outside of the pool and it is filled with air. Figures 2 and 3 illustrate the axial and radial views of the simulated model, respectively [9].

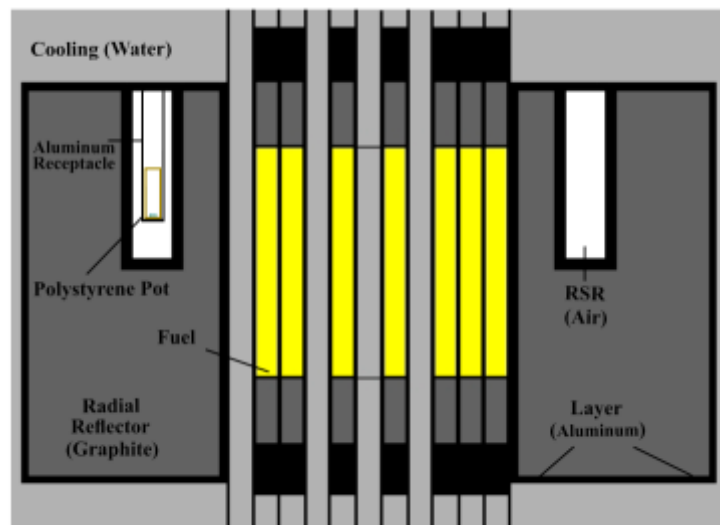


Fig. 2 - Axial view of the IPR-R1, considered in this research with MCNP5

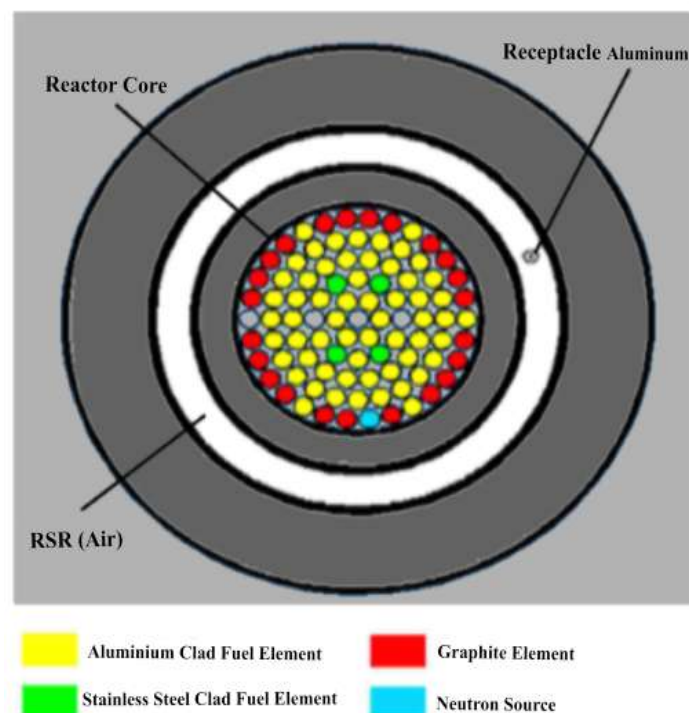


Fig. 3 - Radial view of the IPR-R1, considered in this research with MCNP5

2.2 Configured Samples

The modeled samples were composed of an alloy of aluminum and gold, the percentages of each material were 99.9% and 0.1%, respectively, with geometry type disc, with diameters of 6.0 mm. The thicknesses of samples are presented in Table 1.

Sample	Thicknesses (x) (mm)
A1	0.1
B1	0.2
B2	0.2
C1	0.3
C2	0.3
D1	4.3

Tab 1: Thicknesses of the configured samples

In addition, it was assumed that the samples were within three capsules being the first one of aluminum, the second one composed of polystyrene and the third of polyethylene. The Table 2 presents the cylinders dimensions which are inside of RSR [6]. This model was adopted to be compared to experiments performed at CDTN.

Cylinder Material	Inner Radius (cm)	Radial Thickness (cm)	Height (cm)
Aluminum	1.50	0.10	20.0
Polystyrene	1.10	0.30	7.90
Polyethylene	0.48	0.07	0.55

Tab 2: Dimensions of the simulated cylinders inside Rotary Specimen Rack

Within each sample, to reduce the variance, has been placed a DXTRAN sphere. In the sample A1, the DXTRAN sphere was positioned in the center of the sample. The inner and outer radii of the sphere DXTRAN measure, respectively, 0.0025 and 0.005 cm. The sphere DXTRAN of sample B1 was placed in the upper half of the sample. The dimensions of DXTRAN sphere of sample B1 are the same as sample A1.

Inside the sample B2, the DXTRAN sphere was positioned in the center of the cell, the inner and outer radii measure, respectively, 0.0025 and 0.01 cm. The DXTRAN sphere of sample C1 was positioned in the upper third of the sample. The dimensions of DXTRAN sphere of sample C1 are the same as sample A1.

Within the sample C2, the DXTRAN sphere was positioned in the center of the cell, the inner and outer radii measure, 0.0025 and 0.015 cm.

Finally, inside the sample D1, was placed a DXTRAN sphere also at the center of the element, its dimensions are equal to the case of the sample A1.

Figure 4 shows a schematic representation (off scale) of all samples simulated. It has been showing the location of DXTRAN sphere inside each case. The value of thickness x is 0.1 mm.






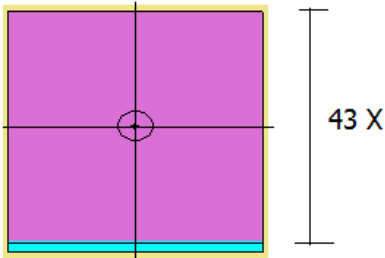
SAMPLE	Schematic of the thickness	SAMPLE	Schematic of the thickness
A1		C1	
B1		C2	
B2		D1	

Fig. 4 - Schematic of the thicknesses of the samples

2.3 Results

In all simulations was obtained the thermal neutron flux and they were compared with experimental data obtained in the research [4]. Table 3 presents the estimated relative errors from MCNP code (R^*) for all simulated samples. According to the literature [10], values of R^* fewer than 10%, generally, produce reliable results.

	SAMPLE					
Channel	A1	B1	B2	C1	C2	D1
	R^* (%)	R^* (%)	R^* (%)	R^* (%)	R^* (%)	R^* (%)
1	6.43	5.49	9.74	7.29	5.78	3.23
3	6.24	5.23	5.48	6.29	5.90	3.21
7	5.33	5.28	5.95	7.81	5.57	3.22
10	5.89	9.14	6.52	5.73	7.29	3.36
24	6.40	6.39	6.16	8.74	7.65	3.20
25	7.05	7.31	5.27	5.79	7.66	3.10
29	14.66	5.87	5.29	8.01	5.80	3.27
34	6.64	9.37	8.77	6.84	6.18	3.40
35	6.21	6.47	5.57	6.91	7.78	3.25
38	5.27	5.64	6.29	8.39	5.62	3.28
40	5.44	6.12	5.58	5.67	5.72	3.26

Tab 3: Estimated relative errors from MCNP code (R^*)

Table 4 shows the estimated values for the thermal neutron flux in the samples volumes and the error related to experimental results.

Channel	Experimental values [7]	SAMPLE											
		A1		B1		B2		C1		C2		D1	
		Value	Error (%)	Value	Error (%)	Value	Error (%)	Value	Error (%)	Value	Error (%)	Value	Error (%)
1	6.69	6.69	0.04	6.03	9.91	7.74	-15.67	6.22	7.08	6.67	0.36	6.37	4.78
3	6.55	6.12	6.56	5.60	14.45	6.49	0.87	5.96	8.95	6.13	6.41	6.44	1.64
7	6.35	6.65	-4.71	6.57	-3.43	6.67	-5.11	6.41	-0.93	6.64	-4.52	6.70	-5.58
10	5.99	6.25	-4.37	7.06	-17.85	6.32	-5.49	6.56	-9.53	6.86	-14.52	6.65	-10.95
24	6.94	7.50	-8.02	6.91	0.48	6.87	1.00	6.97	-0.44	7.19	-3.54	6.73	3.01
25	6.45	6.62	-2.67	6.87	-6.49	6.75	-4.69	6.37	1.29	7.12	-10.33	6.68	-3.60
29	7.32	7.12	2.77	6.45	11.88	6.57	10.22	5.97	18.50	6.88	6.02	6.87	6.17
34	7.3	6.63	9.22	6.54	10.46	6.08	16.72	6.74	7.60	6.89	5.68	6.35	12.95
35	7.18	6.37	11.29	6.53	9.06	6.62	7.78	5.63	21.65	7.33	-2.07	6.42	10.62
38	6.58	5.74	12.78	6.10	7.33	7.53	-14.50	6.60	-0.24	6.52	0.88	6.43	2.29
40	6.16	5.99	2.77	6.58	-6.88	6.55	-6.35	6.50	-5.49	6.66	-8.17	6.59	-6.98

Tab 4: Experimental and calculated thermal neutron flux ($\text{ncm}^{-2}\text{s}^{-1}$) $\times 10^{11}$

As can be verified in the Table 4, most of results were within expected in according with the literature [4] and [11] which allows deviations of up to 15%. However, some atypical values were found. In sample B1, channel 10, the error was -17.85%. In sample B2, channels 1 and 34, the errors were -15.67% and 16.72%, respectively. In sample C1, channels 29 and 35, the errors were 18.50% and 21.65%.

3. Conclusions

In this work, the MCNP5 code was applied to simulate the IPR-R1 reactor core and to evaluate the thermal neutron flux through samples in eleven irradiation channels in the RSR.

Evaluating the errors related to experimental results in the considered channels it was possible to conclude that the most calculations presented values within the expected.

However, some investigations and improvements in our model are necessary to achieve better results, especially for those channels where atypical results were observed.

Acknowledgments

The authors are grateful to CAPES, CNPq, FAPEMIG and CDTN/CNEN for the support.

4. References

- [1] C.A.B. Santoro, **Determinação do espectro de nêutrons no reator TRIGA pelo método de ativação**. Master thesis, Instituto de Pesquisas Radioativas, Escola de Engenharia, Universidade Federal de Minas Gerais, Belo Horizonte, 1975.
- [2] R.R.R. Guimarães, **Levantamento das distribuições dos fluxos de nêutrons térmicos e rápidos no núcleo do reator IPR-R1**. Master thesis, Departamento de Engenharia Nuclear, Escola de Engenharia, Universidade Federal de Minas Gerais, Belo Horizonte, 1985.
- [3] H.M. Dalle, C Pereira, R.G.P Souza, **Neutronic calculation to the TRIGA Ipr-R1 reactor using the WIMSD4 and CITATION codes**. Annals of Nuclear Energy 29, 901–912, 2002.
- [4] M.A.B.C. Menezes, R. Jaćimović. R.C.O. Sebastião, A.S. Leal, R.M.G.P. Souza, **Experimental and modelling thermal neutron fluxes characterization of the carousel irradiation channels in the TRIGA MARK I IPR-R1 reactor, Brazil** (*in press*).
- [5] D.M. Zangirolami, A.V. Ferreira and A.H. Oliveira, **Specific Induced Activity Profile at the Rotary Specimen Rack of IPR-R1 TRIGA Reactor**. Brazilian Journal of Physics, vol. 39, no. 2, June, 2009.
- [6] H.M. Dalle, **Simulação do reator TRIGA IPR-R1 utilizando métodos de transporte por Monte Carlo**. Doctor thesis , Faculdade de Engenharia Química, Universidade Estadual de Campinas, Campinas, (2005)
- [7] B.T. Guerra, C.A.M. da Silva, C. Pereira, A.H. Oliveira, A.L. Costa, M.Â.B.C. Menezes, **Thermal Neutron Fluxes Characterization in the Irradiation Channels of the IPR-R1 using Monte Carlo Method**, European Research Reactor Conference, Rome, Italy, 20-24 March, paper A0124, 2011.
- [8] M.A.B.C. Menezes, C.V.S. Sabino, M.B. Franco, G.F. Kastner, E.R.H. Montoya, **k_0 -Instrumental neutron activation analysis establishment at CDTN, Brazil: a successful story**, *Journal of Radioanalytical and Nuclear Chemistry*, v. 257, pp. 627-632, 2003.
- [9] B.T. Guerra, C.A.M. da Silva, C. Pereira, M.A.B.C. Menezes, R. Jaćimović, A.H. de Oliveira, **Neutron Flux Evaluation in the Irradiation Channels of the IPR-R1 TRIGA Research Reactor Using Monte Carlo Method**, International Nuclear Atlantic Conference, Belo Horizonte, Brazil, 24-28 October, 2011.
- [10] J.F. Briesmeiter et al., **MCNP-4B - A General Monte Carlo N-Particle Transport Code-Version 4B**, Los Alamos National Laboratory, LA-12625-M. 1997.
- [11] T. Madi et al., **Experimental and Monte Carlo evaluation of the neutron flux of an assembly with two AmBe sources**, *Radiation Protection Dosimetry*, 115 (1-4), 412-414. 2005.

AN INITIAL VERIFICATION AND VALIDATION STUDY OF CFD NUMERICAL SIMULATIONS OF THE IPR-R1 TRIGA REACTOR

V. V. A. SILVA^{1,2}, F. L. A. SCHWEIZER^{1,2}, A. A. C. SANTOS, A. Z. MESQUITA

Serviço de Tecnologia de Reatores, CNEN/CDTN¹

Av. Presidente Antônio Carlos 6627, CEP 31270-901, Belo Horizonte – Brazil

C. PEREIRA, A. L. COSTA, M. A. F. VELOSO

Departamento de Engenharia Nuclear, UFMG²

Av. Antônio Carlos, 6627, PCA 1 – Anexo Engenharia, CEP 31.270-901, Belo Horizonte – Brazil

R. MIRÓ AND G. VERDÚ

ISIRYM, Universitat Politècnica de València

Camí de Vera, s/n 46022, Valencia – Spain

ABSTRACT

The Computational Fluid Dynamics (CFD) presented itself as an accurate tool to perform analysis in fluid flows. As expected, Nuclear Reactor Analysis is a field of study in which fluid dynamics analysis is fundamental in almost all aspects since the majority of nuclear reactors use water as coolant and/or moderator. However, due to numerical approximations and, sometimes, lack of precise methods to solve special cases, the results obtained by use of a CFD code must be carefully investigated. In this work we present the simulation of IPR-R1 TRIGA reactor located in the Nuclear Technology Development Center (CDTN/CNEN) using the open-source CFD system OpenFoam and an additional validation scheme. Steady-state calculations were performed simulating the reactor operating at 50kW. Best practices guidelines (BPG) have been applied in CFD simulation to set boundary conditions, time step, turbulence models, numerical schemes and convergence criteria. Some simplifications in reactor geometry and in reactor core were introduced due to computational power constraints. The important step to validate the simulation was performed in two different ways. The first and common way was comparing the simulation results to another CFD – ANSYS CFX 13.0 - running both at the same conditions and the same meshes. These two results are then compared to experimental data obtained from the reactor operating at the same conditions. The second and more systematic approach consisted in apply the ASME Verification and Validation (V&V) standard. The objective of this approach is to quantify the degree of accuracy in the simulation of the chosen variables: the inlet and outlet core temperatures and fuel temperature. The results show that OpenFoam is able to simulate the IPR-R1 TRIGA with good degree of accuracy and the V&V standard is a promising methodology to quantify numerical results obtained from CFD computations.

1. Introduction

In 2012, the TRIGA IPR-R1 reactor starts its 62th operational year. After years collecting experimental data, it's possible to use this set of information to validate some computational simulations of it using two different Computational Fluid Dynamics (CFD) codes, namely ANSYS CFX [1] and OpenFOAM [2]. To compare the two softwares results, the same simplified mesh representing the TRIGA reactor was used on both simulations. The mesh quality is a key issue to perform verification and validation; nevertheless, an elementary analysis was performed in order to establish an initial methodology that can be applied to a future mesh representing the TRIGA IPR-R1 reactor in detail.

2. Simulation settings

The simplified mesh was constructed using the *ANSYS Meshing* software. It models six fuel rods with one centred and five surrounding it. The mesh has around 250,000 cells being most of them tetrahedral (227,000). The biggest and the smallest element have 100 and 50 mm, respectively. The space among fuel rods at the core was modelled with 10 layers and these were extruded with an expansion factor of 5. Fuel elements on faces have 4 parallel layers (inflation) with the biggest element having 25 mm and the smallest with 2 mm. It is worth noting that *OpenFOAM* is projected to work with hexahedral meshes making mandatory the use of orthogonal corrections during the solving time.

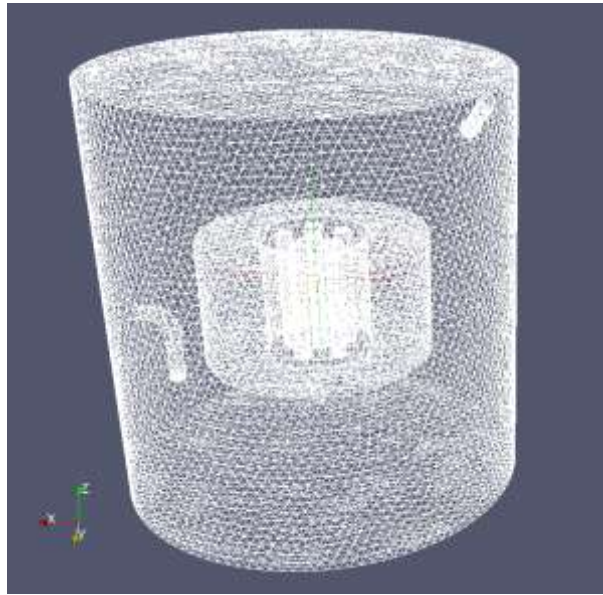


Fig 1: Complete Mesh

The mesh width is the same of the reactor while the pool size is smaller. This simplification is to avoid spending time calculating physics for elements which have small or almost no impact in results on a qualitative analysis. Table 1 summarizes the simulation set-up.

Reactor power	250 kW
Water mass inlet	40 m ³ /h (12 kg/s)
Turbulence model	k- ϵ
Inlet temperature	300 K
Pool surface pressure	<i>ANSYS-CFX</i> : Atmosphere pressure <i>OpenFOAM</i> : Wall at 275 K
Spatial discretization	2 nd order
Time step	fixed
Convergence criteria	10 ⁻⁴ RMS
Analysis type	<i>ANSYS-CFX</i> : steady-state <i>OpenFOAM</i> : transient

Table 1: Simulation set-up

The simplification is also justified by the steady-state problem characteristics. To reach the steady-state, the simulation must run for an additional time and, for each physics parameter changed, it must be repeated.

2.1 ANSYS-CFX

The simulation run in a grid of 6 computers quad-core with 4 Gb RAM for each node. The pool water was initially at 27°C and the pool walls were all set to adiabatic. The top pool which is in contact to the reactor room atmosphere had the free slip boundary condition. There were no significant differences between the room's temperature and the pool's water temperature. A fluid flow of 12 L/s was specified from an inlet located at the wall in the upper part of the pool to the outlet located at the bottom of the pool. All of these initial conditions were defined based data measured during the reactor operation [3].

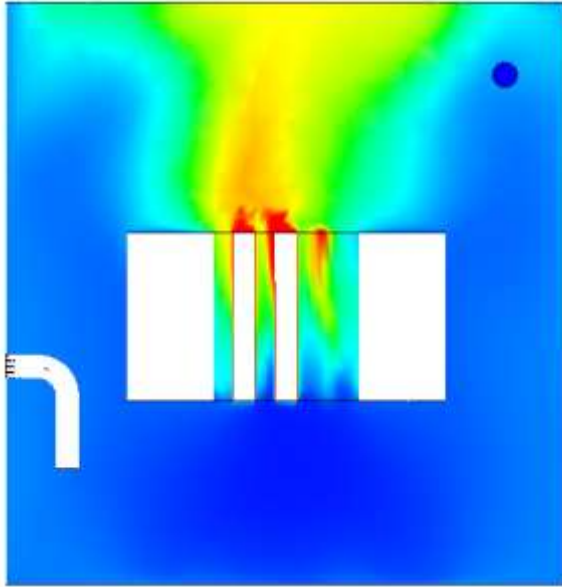


Fig 2: Temperature at steady-state on CFX

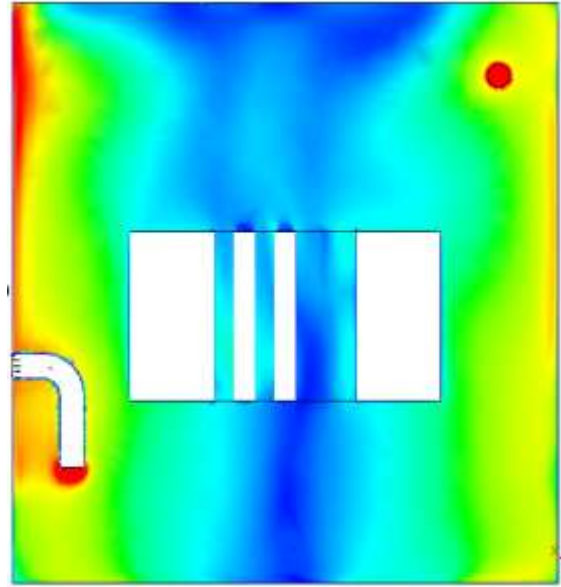


Fig 3: Fluid velocity at steady-state on CFX

Figure 2 clearly shows the water heating near the fuel rods and its diffusion to the top of the pool. The natural convection can be seen in Figure 3, with the fluid being faster near the walls and at the inlet and outlet.

2.2 OpenFOAM

OpenFOAM offers a standard solver called *buoyantBoussinesqPimpleFoam* which is aimed to transient simulations of an incompressible fluid in a turbulent flow. This solver uses the $k-\epsilon$ model for turbulence [4] and takes into account the hydrostatic pressure. The boundary conditions were the same of CFX simulation except for the top pool, which was modelled experimentally as a fixed value of temperature of 2°C. The reason for this unrealistic situation – the room temperature is the same of the atmosphere and the lowest temperature ever recorded is exactly 2°C - is to force the heat transfer at the top pool. It is possible to see the cool water surface in Figure 4.

The full power of 250kW was divided among the six fuel rods and modelled as constant since OpenFOAM has no standard boundary condition that accepts a specific function temperature gradient on the cells surfaces. The convergence criteria were the closest possible to those used in ANSYS-CFX simulation.

Martínez-Lians et al. [5] simulated the same reactor operating at 50 kW power and considering a more complex mesh with about 10 times more elements. The results presented are quite similar to the results obtained in both simulations performed in this work. The main difference is in the fluid heating, as expected, smaller. It is possible to observe convection flow and the heat diffusion through the coolant.

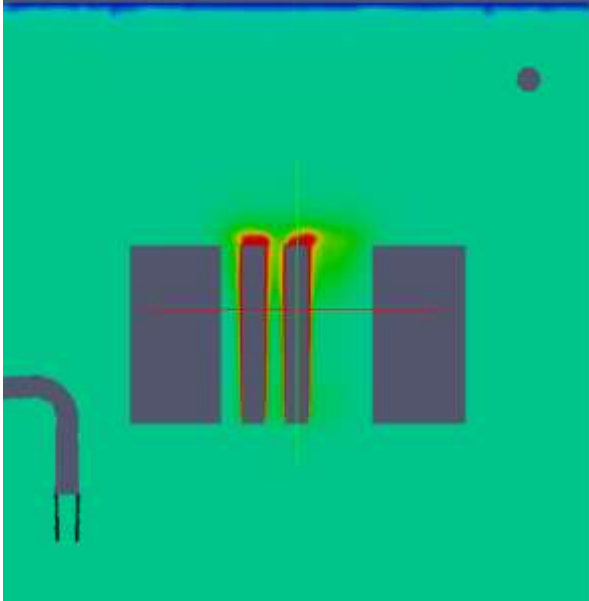


Fig 4: Transient fluid heating on OpenFOAM

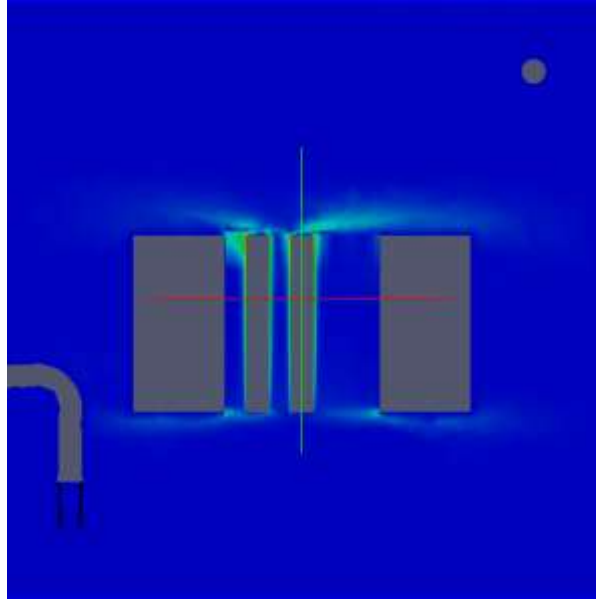


Fig 5: Transient fluid velocity on OpenFOAM

3. Verification and Validation (V&V)

Verification and Validation are a standard methodology largely applied in computational dynamics field. Oberkampf [6] defines the Verification and Validation objective as the guarantee of accuracy and reliability in computational fluid dynamics simulations. In the present work, the main axis of interest relies on validation of the experiments through the validation metrics.

A validation experiment is a special type of experiment, in which the main purpose is determining the validity of a computational model and its predictive accuracy. With this statement in mind it is easily seen that, to be able to validate two different experiments and check their results, the computational model must be as similar as possible to the experiment. In other words, the mesh must be the same, the physical model must address the same physical phenomena, boundary conditions must be equivalent and, obviously, the spatial points where simulation data is collected, must corresponding with those experimentals.

Considering these assumptions, an initial verification and validation scheme was developed. At this point, more emphasis was given to the verification step. Being a first approach to check experiments which are, essentially, qualitative, it is of fundamental importance to verify if the computational models are the correct implementation of conceptual models and if the code can be properly used for an analysis. Despite being the bases of the V&V methodology, it is not simple to perform this task. The *ANSYS-CFX* does not offer the source code, what makes verification only indirectly possible through a careful analysis of the source documentation. *OpenFOAM*, however, comes with all sources available, what makes straightforward to check the computational model implementation, at least in part: the mathematical model is easily checked, but, the implementation verification demands a deep C++ language understanding. So, the approach chosen heavily relies on the CFD codes

robustness, being indirectly checked through source code analysis to *OpenFOAM* and documentation analysis for *ANSYS-CFX*.

The validation metrics are only meaningful when performing a complete simulation. For the present case, makes no sense to validate the simulations since it is only qualitative. However, this initial study aims to prepare a set of rules to the application of V&V methodology to the next complete simulations. Among the many aspects included in the validation assessment, the focus was set to the spatial convergence, which is mainly a mesh issue. Experimental data will be presented carrying the uncertainties of it.

In order to determine the spatial convergence, the well known approach of using successively finer grids was chosen. The ASME Verification & Validation 20 [7] provides a standard way to progressively refine the meshes and how to compare one to another. The information obtained gives quantitative information about the simulation and grid quality.

This simplified approach of Verification & Validation standard is a first proposal to evaluate in a quantitative and standard way the results of the next simulations that will be performed to totally simulate the TRIGA IPR-R1 reactor.

4. Conclusions

The qualitative analysis doesn't allow any conclusion on simulation validation. However, it is the first step to be taken in order to choose the best solver to this heat transfer problem in a turbulent incompressible fluid. Since *ANSYS-CFX* and *OpenFOAM* have different interfaces and completely different ways to set-up and process the simulation, the step of carefully chose the solver is crucial to run simulation on them and be able to compare the results. The results of these simulations confirmed that the physics modelling of each software are comparable.

The *OpenFOAM* simulation convergence was an issue. Due to the hexahedral mesh characteristic, a non orthogonality criteria had to be used increasing the simulation time.

Further work is to simulate the complete TRIGA IPR-R1 geometry in both softwares and validate the results with operational data. Moreover, the fuel heat function should be modelled as specified in TRIGA User Manual as a cosine function. Although easily made in *ANSYS-CFX*, the *OpenFOAM* approach forces the implementation of a new boundary condition.

The simplified Verification and Validation methodology will be applied on both simulations for the guarantee of the simulation accuracy.

5. References

- [1] ANSYS® Academic Research, Release 14.0, Help System, Coupled Field Analysis Guide, ANSYS, Inc.
- [2] H. Jasak, A. Jemcov, Ž. Tuković, "OpenFOAM: A C++ library for complex Physics Simulations", International Workshop on COUPLED METHODS IN NUMERICAL DYNAMICS, Dubrovnik, Croatia, September 19th-22st 2007.
- [3] A. Z. Mesquita, "Investigação experimental da distribuição de temperaturas no reator nuclear de pesquisa TRIGA IPR-R1", Ph.D thesis, Faculdade de Engenharia Química, Universidade Estadual de Campinas, Campinas, Brazil, april 2005.
- [4] H. K. Versteeg, W. Malalasekera, "An Introduction to Computational Fluid Dynamics – The finite volume method", book, second edition, Pearson Prentice Hall, 2007.
- [5] M. Martínez-Lianes, R. Miró, P.A. L. Reis, C. Pereira , A. L. Costa, A. Z. Mesquita, S. Chiva and G. Verdú, "Steady-state modelling of flow conditions of a TRIGA reactor using the

CFD code ANSYS CFX”, 2011 International Nuclear Atlantic Conference – INAC 2011, Belo Horizonte, Brazil.

[6] W. L. Oberkampf, T. G. Trucano, “Verification and validation in computational fluid dynamics”, Progress in Aerospace Sciences, 38 (2002), pages 209-272.

[7] V&V 20 - Verification and Validation in Computational Fluid Dynamics and Heat Transfer, ASME, 2009.

THERMAL HYDRAULIC ANALYSIS OF THE BRAZILIAN MULTIPURPOSE REACTOR BY RELAP5 CODE

H. V. SOARES, A. L. COSTA, C. PEREIRA, M. A. F. VELOSO, V. V. A. SILVA

Departamento de Engenharia Nuclear, Universidade Federal de Minas Gerais

Av. Antônio Carlos, 6627 – PCA1 – Anexo Engenharia – Pampulha

CEP 31270-90 Belo Horizonte, MG, Brasil

Instituto Nacional de Ciências e Tecnologia de Reatores Nucleares Inovadores/CNPq, Brasil

I. D. ARONNE

Centro de Desenvolvimento da Tecnologia Nuclear/Comissão Nacional de Energia Nuclear – CDTN/CNEN, Av. Antônio Carlos, 6627, CEP 31270-90 Campus UFMG, Belo Horizonte, Brasil

ABSTRACT

The Brazilian Multipurpose Reactor (BMR) has being planned as an open pool multipurpose research reactor, using low enriched uranium fuel, with a neutron flux higher than 2×10^{14} n/cm²/s. The reactor core will be compact, using Materials Testing Reactor (MTR) fuel assembly type, with planar plates and will be cooled and moderated by light water, using beryllium, heavy water and light water as reflectors. Its power will be about 30 MW. The BMR is designed to perform three main functions: radioisotope production (mainly molybdenum); fuel and material irradiation testing to support the Brazilian nuclear energy program; and provide neutron beams for scientific and applied research. This work presents a thermal hydraulic model for the BMR reactor using the RELAP5 code and results of simulations of steady state and transient operations. The transient considered was the loss of electric power accident. Such accident can be very serious for the research reactor when the plant doesn't have a reliable standby power supply system. Such transient event induced a large reduction of mass flow rate in the core and consequently the core and pool coolant temperatures increased slowly reaching the saturation point as can be seen by the results presented in this paper.

1. Introduction

The characteristics of the Australian research reactor Opal projected by Argentina and built in Australia were considered as initial references for the Brazilian Multipurpose Reactor (BMR) project lead by the Brazilian Nuclear Energy Commission (*Comissão Nacional de Energia Nuclear - CNEN*). The BMR will be constructed and operated to attend the present Brazilian need for a multipurpose neutron source mainly to supply the demand of radioisotopes, carry out material tests and develop scientific, commercial, and medical applications with the use of neutron beams.

In the present work, a thermal hydraulic nodalization for the RMB core using the RELAP5/MOD3.3 and the most important components of the pool loop and core loop circuits are presented. Steady state simulation and a transient have been performed. The thermal hydraulic system code RELAP5 has been developed for best estimate transient simulation of light water power reactor systems during postulated accidents. Recent works have demonstrated that the code can be also used with good results for thermal hydraulic analysis of research reactors as it can be verified in the present literature [1 - 9].

2. Main Characteristics of the Brazilian Multipurpose Reactor

The BMR will be an open pool multipurpose research reactor using low enriched uranium fuel, with a neutron flux higher than $2 \times 10^{14} \text{ n}/(\text{cm}^2\text{s})$. The reactor core will be compact using MTR fuel assembly type with planar plates and will be cooled and moderated by light water. Table 1 presents the main characteristics of BMR. Figure 1 shows the model of the present concept of the BMR reactor [10] that was based in the Australian research reactor Opal [11]. The BMR pool is cylindrical with 12.8 m of high and 5.6 m of diameter.

Reactor	
Nominal Power	30 MW
Moderator and coolant	Light water
Reflector	H ₂ O, D ₂ O, Beryllium
Thermal and fast neutron flux in the core (higher than)	$2.0 \times 10^{14} \text{ neutrons.cm}^{-2}.\text{s}^{-1}$
Core	
Flow direction in core	Upwards
Control rods drive location	Below core
Grid array	5 x 5
Dimensions	0.51 x 0.55 x 0.815 m
Number of fuel and control elements	23 / 6
Absorbing material	Ag-In-Cd
Fuel assembly type	MTR (LEU)
Nuclear fuel	U ₃ Si ₂ -Al enriched at 20%
Fuel density	4,8 gU/cm ³

Tab 1: General characteristics of BMR

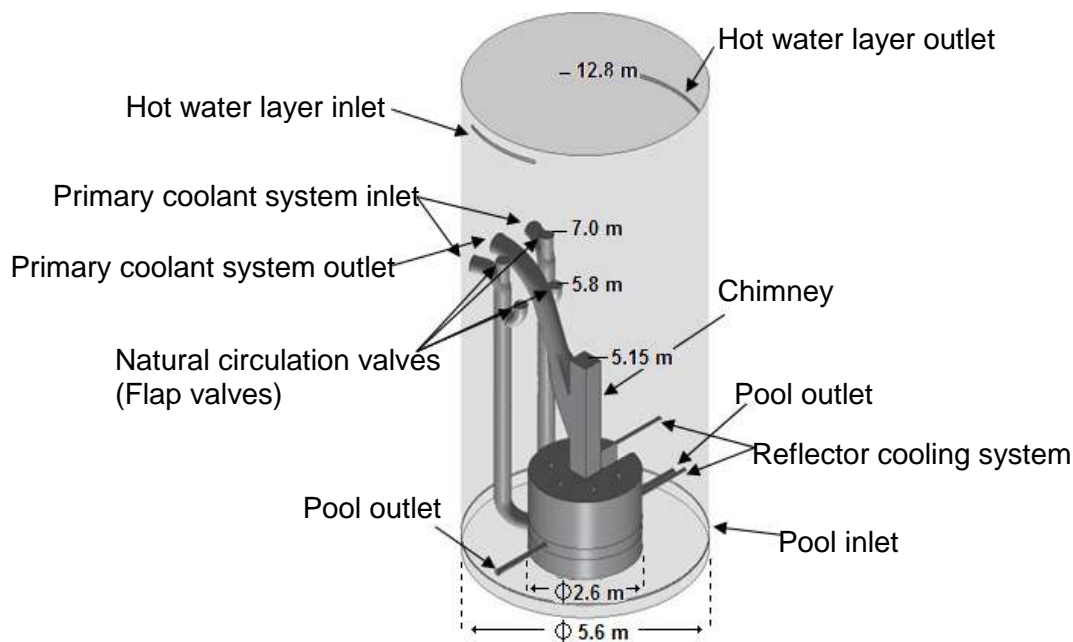


Fig 1. BMR present concept

A heavy water tank surrounds three quarters of the chimney in the core area working as a reflector and enabling the extraction of neutron beams and placement of materials for irradiation. In the remaining quarter there is beryllium that also works as a reflector. The heavy water temperature will be controlled by a dedicated cooling system.

The whole core structure will be located within a square cross-section “core chimney” which forms part of the primary cooling circuit. The core will be cooled by a flow of demineralised light water moving upwards through the core. In normal operation, the coolant is pumped through the core and then via pipes to a heat exchanger before returning to the core inlet.

The reactor cooling has four circuits: Hot Water Layer (HWL), Primary Cooling System (PCS), Reactor and Service Pools Cooling System (RSPCS) and Reflector Cooling System (RCS).

3. RELAP5 model

Figure 2 shows the RELAP5 nodalization for the BMR. The reactor pool was modeled using two pipes components (100 and 130) composed by twenty volumes each one. The heat generated by reactor in the one side of the pool (100) allows water circulation inside the pool through of the cross junctions between the pipes. The service pool was modeled using a pipe component (150) with twelve volumes. Volume 140 is a branch component that represents the upper pool surface, which is in contact to the atmosphere. Volume 190 is a time dependent volume that simulates the atmosphere on the top of pool surface.

The Reactor and Service Pools Cooling System (RSPCS) removes heat from the irradiation rigs in the reactor pool. The system comprises two pipes inside the pool, the long term pool cooling pipe (component 202) and a pipe (component 204). Components outside the pool are: a decay tank (components 222-226), a main pump (component 230), heat exchanger (component 234 - primary side), a three-way valve (simulated by valves 209 and 211) and associated components. The position of the three-way valve defines which of the two lines is connected to the pumping equipment to perform forced circulation. The rigs cooling branch has a pipe (component 204) that extends from the irradiation rig plenum below the reflector vessel and passes through the reactor pool boundary at level +7.00 m inside the pool. From there, it is connected to the three-way valve and then to the decay tank.

The Primary Cooling System (PCS) comprises components 300 through 360 which are inside the pool and components 400 through 460 which are outside the reactor pool. Component 300 represent the core inlet lower plenum which conducts the light water to the core (component 316). The core has one hydrodynamic channel with only one Heat Structure (HS) associated to it representing all fuel plates. The heated water goes through the components 320 and 330 where it is mixed with a small downward flow coming from the pool through the chimney (component 340). This flow corresponds about 10% of the total outlet flow of the PCS.

In order to allow the establishment of natural circulation when the PCS pumps are not in operation, four flap valves are located in a line returning to the pool (component 360). One set of valves is located at level +7.00 m (components 363 and 364) and the other set, at level +5.80 m (367 and 368). These are both above the upper edge of the chimney at level +5.15 m (component 340). The lower flap valves will open, thus creating the natural circulation cooling flow path. Valves 363 and 367 are of type trip valves and 364 and 368 are of type check valves. Both valves behave as on/off switch. Trip valves will open if the pool coolant level decreases up to +7.00 m. The check valves work obeying static pressure/flow-controlled check valve (by hysteresis effect) between the components connected to the valves. Only one of the two valves is required to provide sufficient flow to remove core decay heat.

The main components outside the pool of PCS are: a tank for nitrogen-16 decay (components 402-406), two parallel primary cooling pumps (components 410 and 412), the main heat exchanger (component 430 - primary side), valves (components 407, 409, 423 and 425), and piping components. The Reflector Coolant System- RCS is composed by a heavy water tank (component 500) and its heat exchange circuit (component 530- primary side and component 910- secondary side).

The area located on level -5.00 m (under the pool ground level) accommodates the pumps of the cooling systems, heat exchangers and associated components of both circuits PCS and RSPCS. The point kinetics model was used to estimate the fuel power in the simulations.

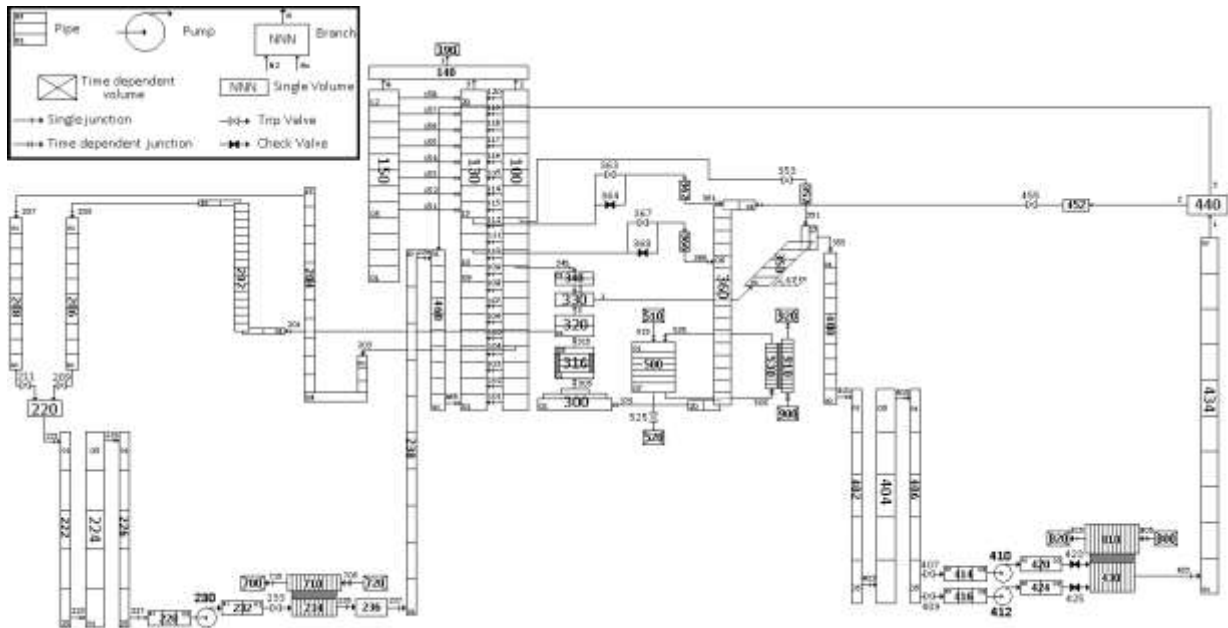


Fig 2. BMR nodalization for RELAP5

4. Steady state calculation

Several thermal hydraulic parameters in the BMR like: energy balance, the pool and the core mass flow circuits, the heat transfer in the heat exchangers and the heat generated in the core and in the pool, pressure drop in the core, core and pool temperature, and other parameters have not been defined in this project and frequently there are changes on their values and definitions. Experiments involving these parameters have not been carried out, therefore, there are not experimental data to compare with the results of RELAP5. However, the mass flow rate and temperature in the core has been defined [10] based in the Opal reactor and they have been used in the RELAP5 input. Table 2 shows the steady state calculations with RELAP5 performed at 30 MW and the comparison with some references values [10]. As it can be seen in Table 2, the coolant temperature in core inlet/outlet showed very good agreement with the reference.

Parameters	Reference	RELAP5	Error (%)*	Acceptable Error (%)
Core coolant temperatures (inlet/outlet)	311 K / 320 K	311 K / 320 K	0.0/0.0	0.5
Pool coolant temperatures (inlet/outlet)	306 K / ---	307.02/ 312.33K	0.39	0.5
Mass flow rate from pool to core by chimney	83.3 kg/s	83.1 kg/s	0.24	2.0
Core mass flow rate (inlet/outlet)	750 / 833 kg/s	748 / 831 kg/s	0.18 / 0.19	2.0

*Error = $100 \times (\text{calculation} - \text{experimental}) / \text{experimental}$

Tab 2: Reference and calculated results for 30 MW power condition

5. Transient calculation

5.1 Analysis of the loss of electric power

Postulated Initiating Events (PIEs) are events that have the potential to challenge the safety limits of the plant. They are the initiators of fault sequences. The primary causes of a PIE may be equipment failure and operator errors (both within and external to the reactor facility) and human-induced or natural events.

Following the guidance of the IAEA, a set of PIEs is assembled for assessment against the design of the Replacement Research Reactor. This list covers all aspects of the design, operation and utilization of research reactors [11].

Loss of electric power supplies is itself not an initiating event, but, in general, regulations require analysis of the behavior of the facility under loss of electric power. When the reactor has a reliable standby power supply system (e.g. appropriately qualified diesel generators), it is only necessary to analyze loss of normal power. When reliability of the system cannot be assured, loss of standby power needs to be evaluated as well. Low power reactors that can be cooled by natural circulation may not have a standby power supply beyond uninterruptible power systems (batteries) for instrumentation and control. Higher power MTRs may have diesel generators and rely on their functioning for decay heat removal [12].

For this simulation in the RELAP5 code, six trips were actuated at the same time in order to simulate the accident. As a consequence of such trips, actuation of the PCS pumps (410 and 412) and RSPCS pump (230) were turned off; stopped the secondary flow rates in all heat exchangers of reactor: RSPCS (710), PCS (810) and RCS (910) in its time dependent junctions 705, 805 and 905, respectively.

All transient events started at 10,000 seconds, after the simulation of steady state at 30 MW. Figure 3 shows evolution of the mass flow rate in the chimney outlet, core outlet and PCS outlet during 1×10^6 s of simulation. The details shows the mass flow rate evolution enlarged; it is possible to see perfectly that mass flow rate in the PCS outlet (350-01) is canceled due to isolation of this circuit. The inertia of the PCS pumps flywheel provided a slow coast down in the its mass flow and at about 500 s after the loss of electric power to occur, the mass flow in chimney inlet changes its direction, of downwards to upwards. This fact occurred due the mass flow interruption in PCS outlet and therefore the hot water generated in core rises and flow out by chimney causing the natural circulation. Automatically, the flap valves (364 and 368) open providing the cooling in reactor core. The natural circulation mass flow rate is very small, about 12 kg/s, but it is enough to cool fuel elements and to transfer this heat to the pool.

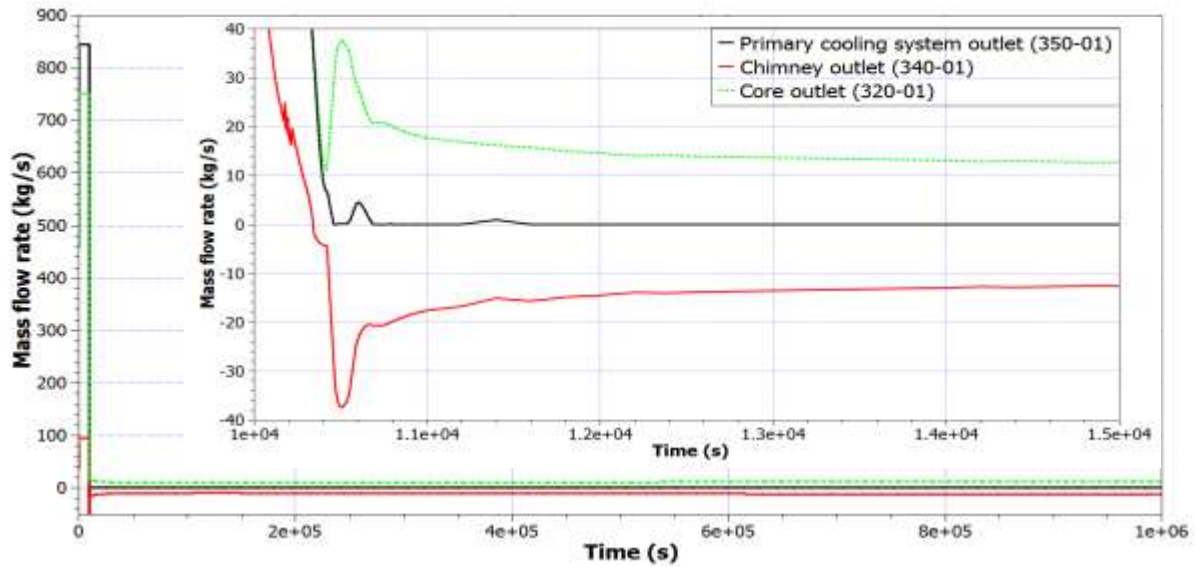


Fig 3. Mass flow rate evolution to natural circulation mode

To simulate the First Shutdown System (FSS) action (insertion of all control plates in core) using the RELAP5, it was inserted \$10 of negative reactivity in 0.5 seconds of calculation, when the mass flow in core inlet decrease below 50% of steady state value. In the accident analyzed, this happened at about 60 seconds after the PCS pumps trip, as it can be verified in Fig. 4. The coolant temperature in the core outlet and cladding surface temperature (mid-height) reached about 340 K and 379 K, respectively, after 60 seconds of transient. However, after the reactor shutdown, both temperatures dropped abruptly to new steady state values.

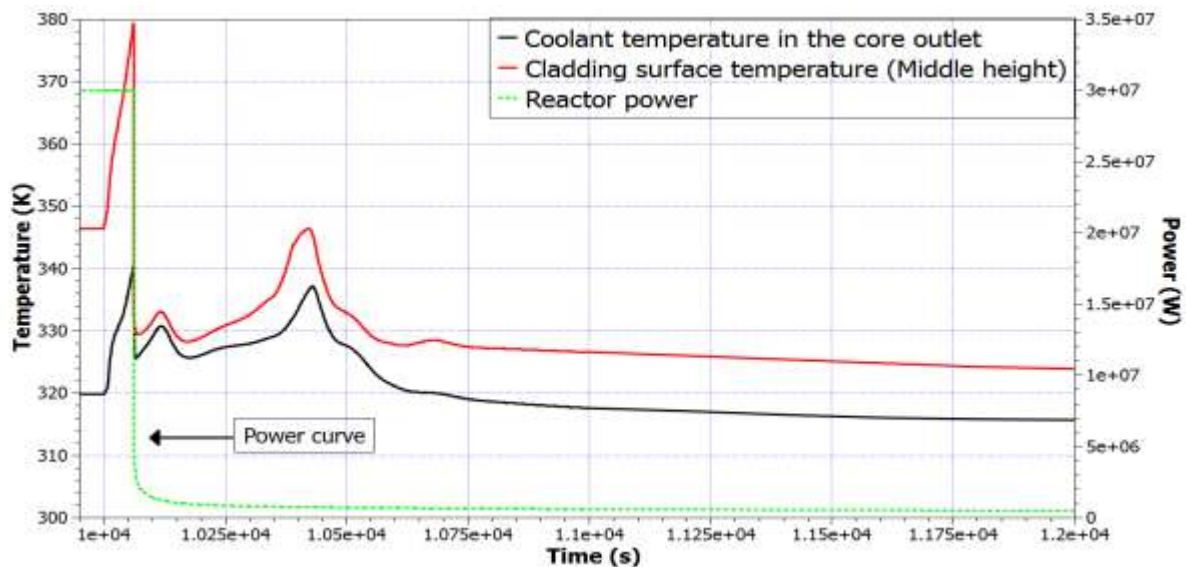


Fig 4. Coolant and cladding temperatures and reactor power evolution

Figure 5 shows the evolution of coolant temperatures at the bottom, middle and top of the pool (pipe 100 in the nodalization). As it can be seen, after the beginning of the event, the pool temperature began to increase and, 1,060,000 s (~294 hours or ~12 days) after the accident, the coolant temperature in the pool middle and top reached the saturation point. Differences between the coolant temperature in the middle and the top of the pool were not observed. The difference of temperatures between the bottom and the top increased after the event showing that the middle and the top receive and accumulate more power than the bottom pool in natural circulation due the large thermal inertia of the heavy water tank inventory, which absorb the heat of the pool bottom coolant.

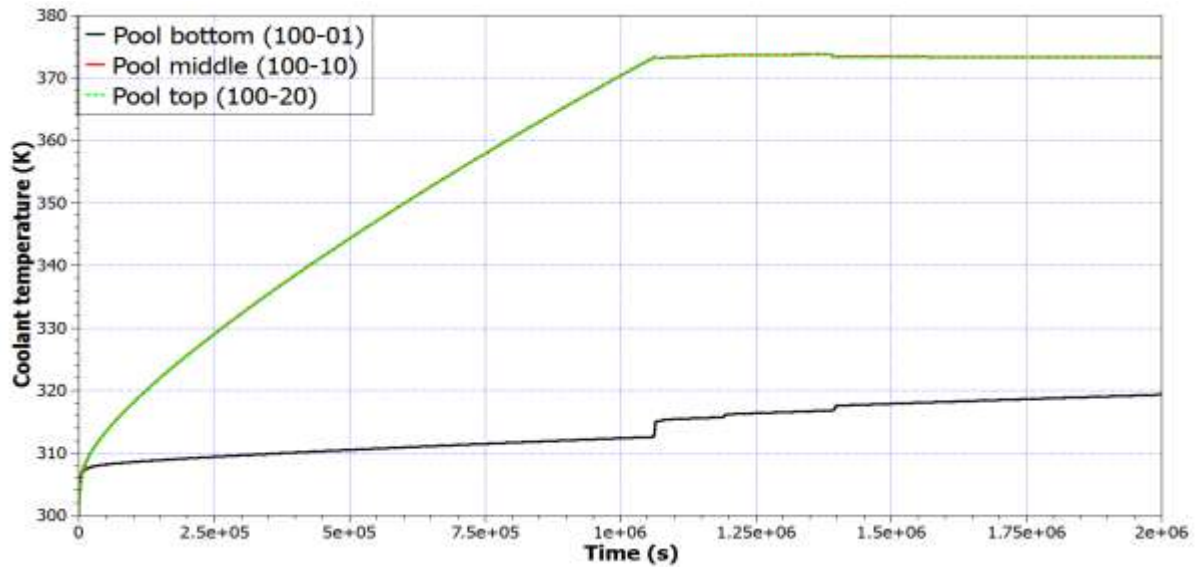


Fig 5. Pool coolant temperature evolution

6. Conclusions

The BMR thermal hydraulic model was presented in this work using the RELAP5 code. After several simulations, the steady state operation condition was reached at 30 MW with all thermal hydraulic parameters in stable behavior. Thereafter, a loss of electric power accident was simulated. Such transient event induced a large reduction of mass flow rate in the core and consequently the core and pool coolant temperature increased slowly. During 60 s after the transient, the temperature of the fuel assembly cladding increased very fast but remains below the onset of nucleate boiling value (~ 393 K) and the coolant in the core outlet didn't reach the saturation temperature. The action of FSS caused the safe shutdown of the reactor. However, at about 1,060,000 s of calculation, the pool coolant reached the saturation point. The check valves opened correctly showing that the natural circulation mode was established keeping the core cooled during the loss of electric power event.

Acknowledgments

The authors are grateful to CAPES, CDTN/CNEN, FAPEMIG and CNPq for the support.

References

- [1] M. Adorni, "Accident Analysis in Research Reactors", *Laurea Thesis*, University of Pisa, Italy, 2007.
- [2] A. R. Antariksawan et al., "Validation of RELAP/SCAPSIM/MOD3.4 for research reactor applications", In: *13th. International Conference on Nuclear Engineering*, Beijing, China, pp. 1-8 2005.
- [3] C. B. Davis, "Applicability of RELAP5/MOD3.2 to research reactors" In: *IAEA Regional Training Workshop on Safety Analysis Methodology and Computer Code Utilization*. KINS, Daejeon, South Korea, 2002.
- [4] B. Di Maro et al., "Analysis of a pump trip in a typical research reactor by RELAP5/MOD 3.3", In: *Proceedings of ICAPP'03*, Cordoba, Spain, paper 3215, 2003.
- [5] A. L. Costa et al., "Thermal hydraulic analysis of the IPR-R1 TRIGA research reactor using a RELAP5 model", *Annals of Nuclear Energy*, Vol. 240, pp.1487-1494, 2010.
- [6] T. Hamidouche et al., "Dynamic calculations of the IAEA safety MTR research reactor benchmark problem using RELAP5/3.2 code", *Annals of Nuclear Energy* 31, pp. 1385-1402, 2004.
- [7] A. Khedr et al., "The effect of code user and boundary conditions on RELAP calculations of MTR research reactor transient scenarios". *Nuclear Technology & Radiation Protection* 1, pp. 16–22, 2005.

- [8] B. Končar and B. Mavko, "Modelling of Low-pressure Subcooled Flow Boiling using the RELAP5 Code", *Nuclear Engineering and Design*, Vol. 220, pp. 255-273, 2003.
- [9] P. A. L. Reis et al., "Assessment of a RELAP5 model for the IPR-R1 TRIGA research reactor", *Annals of Nuclear Energy*, Vol. 37, pp.1341-1350, 2010.
- [10] CNEN, "Geração de seções de choque para o primeiro núcleo do Reator Multipropósito Brasileiro", Relatório técnico: RMB-10100-RD-003.00, Brazil, 2010.
- [11] ANSTO, "Preliminary safety analysis report for ANSTO replacement research reactor facility", Australia, 2001.
- [12] IAEA, "Safety Analysis of Research Reactors", Vienna, 2008.

LEONIDAS E-FUTURE II: CHARACTERISTICS OF THE FRESH FUEL PLATES

H. PALANCHER¹, X. ILTIS¹, A. BONNIN¹, F. CHAROLLAIS¹, P. LEMOINE²

¹CEA, DEN, DEC, Cadarache, F-13108 Saint-Paul-Lez-Durance – France

²CEA, DEN, DISN Saclay, F-91191 Gif sur Yvette – France

S. VAN DEN BERGHE, A. LEENAERS, E. KOONEN

SCK•CEN, Boeretang 200, B-2400 Mol - Belgium

B. STEPNIK³, C. JAROUSSE⁴

³AREVA-CERCA, Les Berauds, B.P. 1114, F-26104 Romans Cedex – France

⁴AREVA-CERCA, 10, Rue Juliette Récamier, F-69456 Lyon Cedex 06 - France

Y. CALZAVARA, H. GUYON

ILL, 6 rue Jules Horowitz, B.P. 156, F-38045 Grenoble Cedex 09 - France

ABSTRACT

After the observation of blistering of fuel plates in the E-FUTURE experiment, but with a clear indication of the positive trend with increasing Si content, the LEONIDAS group decided to launch a second selection irradiation, called E-FUTURE II. This experiment will be performed on plates with higher Si content (up to 12 wt%) and modified Si distribution in the matrix. To optimise the manufacturing process for such plates, four types of plates were first fabricated with natural uranium (NU). They differ by their Si content in the matrix (7.3, 10 or 12 wt%) and by the characteristics of the powders constituting the matrix (Al(Si) alloy powders or mixtures of Al + Si powders). Samples coming from these four plates underwent an additional heat treatment, aimed to enhance Si diffusion. These different types of plates and the annealed samples were characterized by optical microscopy, SEM+EDS (with image analysis) and high energy X-ray diffraction, to compare the main following characteristics: the Si-rich diffusion layer (SiRDL) thickness, the coverage rate of the U(Mo) particles by this layer, its elementary and crystallographic composition and the fraction of Si remaining in the matrix. The results are compared to E-FUTURE ones and discussed, as a basis for the definition of the E-FUTURE-II irradiation grid.

1. Introduction

The European LEONIDAS project (collaboration joining SCK•CEN, ILL, CEA and AREVA-CERCA) is currently leading a qualification program of the U(Mo) dispersion LEU fuel for the European high performance research reactors: RHF (Grenoble), BR2 (Mol) and later on JHR (Cadarache) [1, 2]. A first experiment in BR2, called E-FUTURE, has tested 4 full size fuel plates made of 8g_U/cc U(Mo) atomized powder dispersed in an Al matrix with Si addition (4 and 6 % Si) at a maximum heat flux of 470 W/cm². The mean and maximum burnup reached were respectively about 48 % and 70 % ²³⁵U without cladding failure. The Post Irradiation Examinations have shown a local abnormal swelling in the highest burnup region (above 60-65% ²³⁵U), but with a clear positive evolution from 4 % to 6 % Si [3, 4].

On the basis of these results, the LEONIDAS project has decided to launch a new selection irradiation with higher Si content (>6%Si) in the matrix. The objective of this new irradiation, called E-FUTURE II, remains to finetune and select the optimal fuel plate characteristics for the subsequent BR2 mixed curved fuel element irradiation test. Two new target values have been selected, 7%Si and 12%Si, in order to define new boundaries of a Si concentration range to be tested in pile in similar conditions as E-FUTURE for the U(Mo) dispersion fuel qualification [5]. It has also been decided to preferentially introduce silicon in the form of an

AlSi alloy powder rather than a mixture of Si and Al powders. The better behavior of the fuel under irradiation with an AlSi alloy (vs a mixture of powders) is expected because of an optimized spatial dispersion and finer size distribution of the Si precipitates. The matrix microstructure developed by the use of an AlSi alloy should lead to an enhancement of the Si effect (the Si availability is expected to be more efficient during the fabrication but also during irradiation by fission product recoil induced diffusion). As the use of such a high Si content in the matrix of the fuel plates had never been tested by AREVA-CERCA before and as addition of Si is known to harden the material, the LEONIDAS project decided to perform a preliminary study of fabrication feasibility with natural U(Mo) powders dispersed in either Al7Si alloy, Al12Si alloy, Al10Si powder mixture or Al12Si powder mixture¹. Initially, only two plates were expected to be inserted in the basket of E-FUTURE II. In order to define and to support the choice of the LEU plates for the E-FUTURE II experiment, fresh fuel characterization was performed on NU plates by CEA. In addition to this first task, CEA decided to apply different thermal treatments (425°C/2h and 425°C/4h) to investigate an expected silicon diffusion enhancement.

This paper details first characterizations performed by CEA on the as-fabricated and on the further annealed NU E-FUTURE II samples². Then results are compared with those obtained on E-FUTURE fresh fuel plates. Finally the consequences of this work and their impact on the definition of the E-FUTURE II experiment will be discussed.

2. Plates characteristics

Four full size plates were fabricated by AREVA-CERCA, using atomized Natural U7Mo powder dispersed in different Al+Si matrices (made of either AlSi alloy powders or mixture of Al and Si powders), the fuel meat being clad with AG3NE alloy. The uranium loading of the plates is 8 gU.cm⁻³. For the manufacturing of the alloy based plates, it was necessary to separately anneal the AlSi alloy powders to precipitate the Si and soften the powder [6]. During the manufacturing, the NU plates were annealed in the same conditions (thermal treatment (TT): 2 hours at 425°C).

At CEA Cadarache, pieces of these fuel plates were cut to obtain at least 3 samples per fuel plate. The two first were used for analyses of the as-fabricated fuels and the last one underwent an additional thermal treatment (TT) of 2 hours at 425°C to assess the effect of a longer TT at low temperature on the silicon thermal induced diffusion towards U(Mo) particles.

The plates are identified as follows: Si content (wt%) – type of Al-Si powder (M for mixture, A for Alloy) – thermal treatment (temperature, duration). Table 1 recaps the main characteristics of the examined NU plates.

Al-Si Matrix characteristics		Thermal treatment		Plate identification
Si content (wt%)	Production method	Duration (hours)	Temperature (°C)	
10	Mixture	2	425	10-M-425_2
7.3	Alloy	2		7-A-425_2
12	Mixture	2		12-M-425_2
12	Alloy	2		12-A-425_2
10	Mixture	2+2		10-M-425_4
7.3	Alloy	2+2		7-A-425_4
12	Mixture	2+2		12-M-425_4
12	Alloy	2+2		12-A-425_4

Table 1: Characteristics and identification of the analyzed samples (E-FUTURE II NU plates)

¹ The notation 'AlxSi mixture powders' stands for the mixture of Al and Si powders with a Si content of x%.

² This paper details only the results obtained on samples annealed with an additional TT of 425°C/2h. Exhaustive results (with the ones gathered on samples annealed 425°C/4h) will be given in a future paper [10]

3. Characterization methods

Optical Microscopy (OM) and Scanning Electron Microscopy combined with energy dispersive spectrometry (SEM-EDS) investigations were first performed on fuel plate cross sections for the samples annealed at 425°C during 2 hours and on pieces polished parallel to the cladding for samples annealed during 4 hours. The microstructural analyses have been focused on the characterization of the Si-rich diffusion layers (SiRDL) which have grown around U(Mo) particles. The SEM-EDS measurements were basically performed using the methodology and criteria developed for studying the E-FUTURE plates [7]: about twenty particles fulfilling the defined criteria were analysed per sample.

Image analysis algorithms have been upgraded, compared to the E-FUTURE plate analysis, to evaluate the coverage rate of particles coated with a SiRDL. The procedure can be described as follows:

1. detection of the SiRDL boundaries (in between the matrix and the U(Mo) core) by grey level segmentation,
2. Measurement of the distance between these two boundaries (i.e. the SiRDL thickness) perpendicularly to the SiRDL skeleton at 360 different points (one per degree),
3. For these 360 points, determination of the number of points (X) whose the distance (thickness) is above 0.3 μm (considered as a threshold value because being twice the pixel size),
4. calculation of the coverage rate ($X/360$).

The macroscopic crystallographic composition of the NU fuel plates has been characterised using high energy X-ray diffraction (HE-XRD). Measurements have been performed on the ID15B beamline at the ESRF synchrotron light source (Grenoble, France) [8-9].

4. Results

a. U(Mo)/Al(Si) plates, annealed at 425°C for 2 h

Both microscopy observations and diffraction experiments demonstrate that the four plates which underwent a TT at 425°C during 2 hours exhibit the main characteristics:

- Low gamma-to-alpha transformation of the U(Mo) particles,
- Presence of a SiRDL around U(Mo) particles,
- Significant amount of Si precipitates still present in the Al(Si) matrix.

4.a.1. Si precipitates in the matrix

The amount of Si remaining in the matrix as precipitates has been quantified by HE-XRD: values are gathered in table 2. For the applied TT, the microstructure of the matrix (mixture or alloy) does not seem to have a direct influence on this quantity (compare for example the Si precipitates fraction in the plates 12-M-425_2 and 12-A-425_2).

OM examinations and Si X-ray maps (see Figure 1) confirm the expected significant difference in the Si precipitates characteristics between plates containing an Al(Si) alloy powder and those made with a mixture of Al and Si powders [6]. In the first case, numerous small precipitates are homogeneously distributed in the matrix (cf. Figure 1b), whereas in the second case, large and scattered particles are encountered (cf. Figure 1a).

A large number of U(Mo) particles in the plates made with Al(Si) alloy powder clearly show a silicon precipitate free zone (PFZ) of around 6 μm wide in the matrix surrounding them. This is not the case in the plates made with a mixture of Al and Si powders, where large Si precipitates are more numerous. These larger precipitates, randomly distributed in the matrix, are also often found close to or in contact with a U(Mo) kernel surface, but

nevertheless have not been consumed in a reaction with the U(Mo) during the fuel plate manufacturing process or even under the most demanding annealing conditions. This appears to indicate that the thermal diffusion of the Si from these large particles is much slower than for smaller precipitates, which can be understood in view of the much larger surface-to-volume ratio of the latter. This allows a much more effective use of the Si inventory of the matrix in the case of alloys. One can assume that a similar reasoning will apply to the fission product recoil driven diffusion in pile.

Plate designation	Si precipitates in the matrix (weight fraction of the AlSi matrix)	SiRDL characteristics		
		Mean thickness (μm)		Coverage rate (SEM) (%)
		HE-XRD	SEM	
10-M-425_2	7.1	0.7	1.2 ± 1.0	78 ± 5
7-A-425_2	3.4	0.7	1.2 ± 0.7	84 ± 5
12-M-425_2	8.6	0.8	1.6 ± 0.8	98 ± 5
12-A-425_2	8.4	0.8	1.3 ± 1.0	83 ± 5
10-M-425_4	5.6	1.0	1.7 ± 1.1	98 ± 5
7-A-425_4	2.1	1.0	1.6 ± 0.7	99 ± 5
12-M-425_4	6.3	1.3	1.7 ± 0.4	93 ± 5
12-A-425_4	4.8	1.5	2.1 ± 1.3	94 ± 5

Table 2: Fraction of Si in the matrix and SiRDL characteristics for E-FUTURE II NU plates

4.a.2. SiRDL characteristics

OM examinations and Si X-ray maps confirm that SiRDLs are present on almost the complete particle circumference. This result, illustrated by Figure 1 for 12 wt% Si plates, is also valid for the two other ones, with lower Si contents.

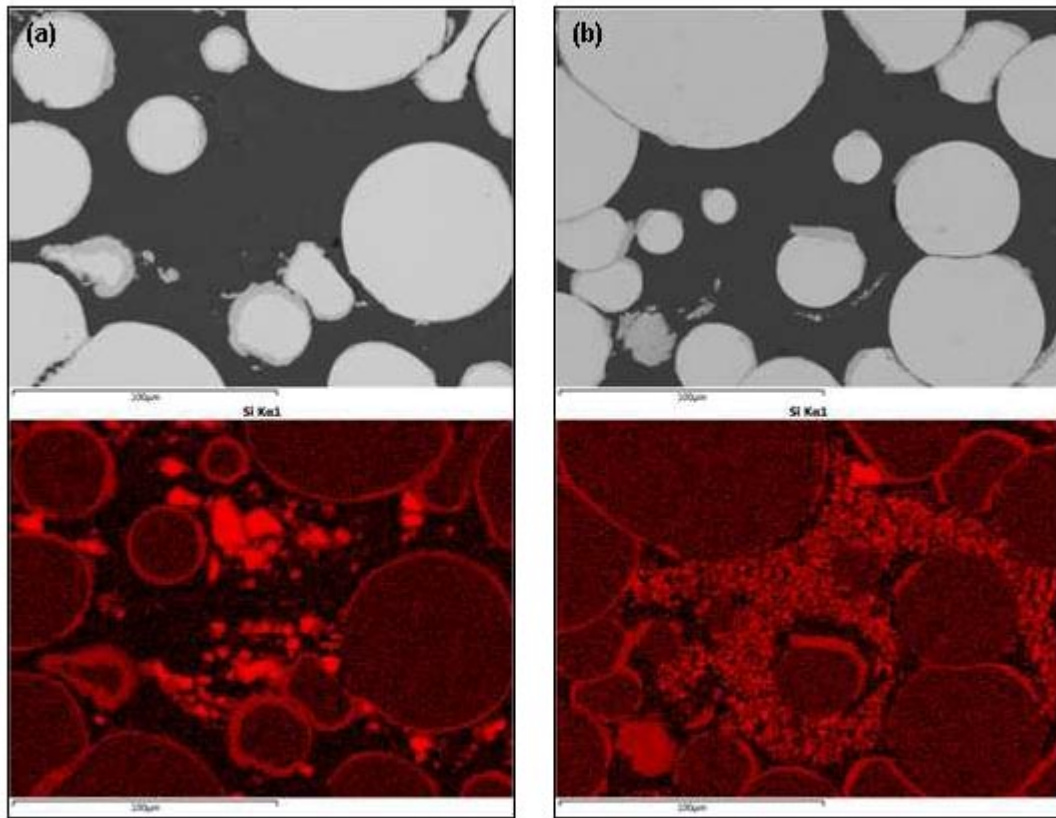


Figure 2: SEM+EDS examination (BSE image + Si X-ray map) of (a) NU-12M-0, (b) NU-12A-0 plates

Figure 1: SEM+EDS examinations (BSE image+Si X-ray map) of 12-M-425_2 (a) and 12-A-425_2 (b)

Table 2 and Table 3 respectively gather the results of image analysis performed on SEM images (given SiRDLs characteristics) and the results of EDS measurements (about 20 points per plate). The Si mean content in the SiRDL appears to be slightly higher than 50 at.% in the four cases. Taking into account the standard deviation of the measurements, one can statistically conclude that the silicon concentration is quite equivalent for all plates.

Plate designation	Mean [Si] (at.%)	Standard deviation (at.%)	Minimum [Si] (at.%)	Maximum [Si] (at.%)
10-M-425_2	52.8	1.8	49.3	56.2
7-A-425_2	53.2	1.5	50.9	56.2
12-M-425_2	54.9	2.9	48.5	59.8
12-A-425_2	53.9	1.9	49.5	56.5
10-M-425_4	50.9	1.2	47.6	52.9
7-A-425_4	50.7	2.3	47.3	54.5
12-M-425_4	49.3	3.9	33.6	53.4
12-A-425_4	51.6	1.7	46.9	54.0

Table 3: Si content in SiRDL as measured by EDS in E-FUTURE II NU plates

The SiRDL mean thickness has been determined by HE-XRD measurements (see Table 2) according to a methodology previously well described in [8-9]. The SiRDL thickness is found to be around 0.7-0.8 μm for the 4 plates. These XRD analyses highlighted also the presence of two crystallographic phases in this protective layer: $\text{U}(\text{Al}, \text{Si})_3$ and a distorted form of U_3Si_5 [10].

The SiRDL mean thickness, assessed by microscopy, is found to be slightly more than 1 μm in the four plates. Like for the EDS composition measurements, taking into account the

statistical dispersion of the thickness values, one can conclude that this thickness is globally the same for the four plates. Same conclusion can be drawn for the coverage rate, which is at least of the order of 80% in the four plates.

As expected, the SiRDL thicknesses obtained by HE-XRD are systematically below those derived from SEM/EDS analyses, but values deduced from XRD analysis must be considered as more representative of the 'true' average SiRDL thickness because of less statistical and geometric bias [9]. It must be finally stressed that both techniques are in agreement to show that the composition of the different (matrix) fuel plates does not influence strongly the measured SiRDL thicknesses.

b. U(Mo)/Al(Si) plates, annealed at 425°C for 4 h

4.b.1. Si precipitates in the matrix

HE-XRD measurements have shown the decrease of the remaining Si precipitates weight fraction in the matrix after this second annealing. It must be underlined that this decrease is definitely stronger for fuel plates produced with an alloyed Al(Si) matrix (see Table 2). OM and SEM/EDS studies have also confirmed that, provided the Si precipitates size was not strongly affected by this additional thermal treatment, the thickness of the free precipitate zone appears to have increased systematically in the plates made with an alloyed matrix (see Figure 2b). For other fuel plates, the occurrence of this FPZ is less obvious, particularly due to the presence of the larger Si particles close to U(Mo) particles (see Figure 2a).

4.b.2. SiRDL characteristics

In the four fuel plates, the SiRDL thickness has clearly increased after the second annealing step (see Table 2). It is worth noting that the Si concentration inside the SiRDL has only very slightly decreased and remains close to 50 at%. To be more specific, SEM/EDS analyses have revealed a systematic slightly reducing Si concentration when scanning a SiRDL from the U(Mo) core to the Al(Si) matrix.

Moreover, the coverage rate of U(Mo) particles by a SiRDL has also improved for all fuel plates.

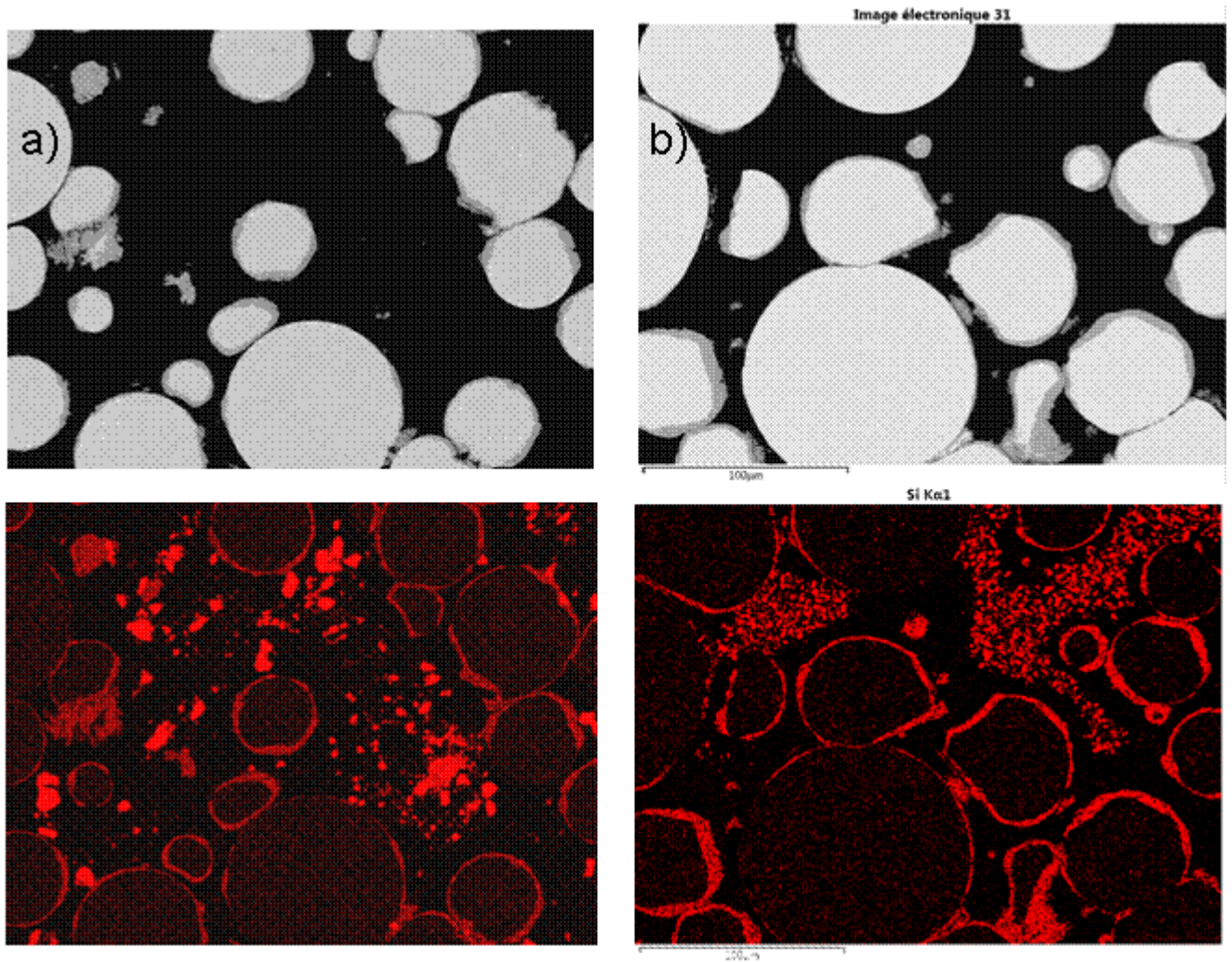


Figure 2: SEM+EDS examinations (BSE image+Si X-ray map) of 12-M-425_4 (a) and 12-A-425_4 (b)

4.b.3. Conclusion

Both HE-XRD and SEM/EDS examinations of samples annealed at 425°C during 4 hours demonstrate that this thermal treatment has promoted an enhanced Si diffusion from the matrix towards the U(Mo) particles especially with the alloy Al(Si) matrix based plates. As a consequence, the SiRDL characteristics (thickness and coverage rate) have been significantly improved without a large Si concentration decrease in the SiRDL.

The use of enhanced post manufacturing thermal treatments for improving the SiRDL characteristics has been more widely investigated: this process has been evaluated as an alternative to previously developed Si coating techniques [11-12]. The results of this work will be available soon [10].

5. Discussion

a. Comparison with E-FUTURE fresh fuel characteristics

In the framework of the E-FUTURE experiment, four U(Mo)/Al(Si) fuel plates were manufactured. Using the identification code defined previously, they can be labelled as: 4-M-425_2 (4112), 6-M-425_2 (6101), 4-M-475_2 (4201), 6-M-475_4 (6311). As for E-FUTURE II NU plates, E-FUTURE plates were characterized by SEM/EDS and HE-XRD [7, 9].

The main conclusions derived from the analysis of the fresh E-FUTURE fuel plates are reported in Table 4. They can be summed up as follows:

- In the plates annealed at 425°C during two hours, SiRDLs were systematically thinner than those reported in this work whatever the considered technique. Their Si content was however quite high (about 50 at%). A slightly higher destabilization ratio in the U(Mo) particles of E-FUTURE plates must finally be mentioned. Indeed, an average value of 15 % has been found for the $U\alpha$ _ratio in E-FUTURE II NU plates that underwent a TT of 2 h at 425°C. The choice of $U\alpha$ _ratio as a tracer of U(Mo) particle destabilisation has been justified elsewhere [9].
- The use of higher temperatures for TT (475°C) has firstly lead to a high destabilization ratio in U(Mo) particles. $U\alpha$ _ratio above 30% are readily obtained after short TT (2 hours). These values are significantly higher than the ones measured on E-FUTURE II NU plates annealed 4 h at 425°C (about 20 %).
Secondly, it can be concluded that, although annealing the fuel plates at high temperatures has enabled an increase in the SiRDL thickness (see fuel plate 6-M-475_4 (6311)), the Si concentration in the SiRDL has dramatically dropped. Moreover, this decrease is followed by an increase of Al concentration and U(Mo)/Al interaction products (UAl_4 and $U_6Mo_4Al_{43}$ with poor in-pile behaviors) are likely to grow [13,14,15].
With a TT at 425°C during 4 h, the growth of the SiRDL is enhanced but without inducing a significant decrease of Si content in the SiRDLs [10].

Plate designation	Si precipitates in the matrix (weight fraction of the AlSi matrix)	SiRDL characteritics			U(Mo) particles destabilisation (Uα_ratio,wt%)
		Mean thickness (μm)		Si fraction in the SiRDL obtained by EDS/EPMA (at%)	
		HE-XRD	SEM		
4-M-425_2 (4112)	3.2	0.2	0.7	53	19
6-M-425_2 (6101)	4.2	0.4	0.6	38	23
4-M-475_2 (4201)	2.1	0.4	0.8	33	34
6-M-475_4 (6311)	2.7	0.8	1.3	36	42

Table 4: Main Characteristics of the E-FUTURE fresh fuel plates [7,9].

b. Definition of the E-FUTURE II irradiation experiment

Depending on the duration of the thermal treatment, this work confirms that two alternative microstructures can be produced using AlSi alloys:

- The first includes thinner Si-rich layers but numerous small Si precipitates remaining in the matrix (UMo dispersed in Al12Si alloy with 2 hours TT),
- The second exhibits characteristics closer to those obtained with a coating process: optimised Si-rich layers (thicker and allowing a better coverage of the UMo particles) but with less Si precipitates in the matrix (i.e. UMo dispersed in Al12Si alloy heat treated 425°C 4h). Note that these features are even more pronounced when increasing the TT durations to 6 h [10]. However any additional thermal treatment is a important penalty for the manufacturing process.

No definitive conclusions on the in-pile performances of each microstructure can be postulated [16]. To select the best microstructure, an irradiation test is required: this is the goal of E-FUTURE II.

Therefore, it has been agreed by all partners (LEONIDAS and US/GTRI) that it is worthwhile to extend the E-FUTURE II experiment to 4 plates. After LEU plate manufacturing was completed, the four following plates were selected for testing in BR2 [17]:

- One plate with a matrix based on Al7%Si alloy powder (no additional thermal treatment) as a direct comparison with the Al6%Si blended E-FUTURE plate,
- Two plates with an Al12%Si alloy based matrix, with two different microstructures tailored by thermal treatment, i.e. one plate without additional thermal treatment and another one with additional thermal treatment (425°C, 2h). The additional TT of 425°C 2h has been preferred (to the one of 425°C 4h) to avoid the negative influence of long thermal treatments on the fabrication yield.
- A plate with a matrix based on an Al12%Si mixture of powders (no additional thermal treatment) to be compared to the Al12%Si alloy one.

6. Conclusion

The main conclusions of this work made by CEA on the fresh NU fuel plates (with and without additional heat treatment) can be summarized as follows:

- Characteristics of the Si-rich layer (thickness, coverage of UMo particles, Si concentration) in the as-fabricated plates: only very small differences can be noticed between the 4 NU plates, either between the Al7Si alloy and the Al12Si alloy, or between the Al12Si alloy and the Al12Si blended powders.
- Characteristics of the Si microstructure (size distribution and spatial dispersion of the Si precipitates) in the as-fabricated plates: large differences can be noticed between the plates manufactured with Al-Si alloy and Al-Si powder blends. Large numbers of small Si precipitates ($< 5\mu\text{m}$) remained after fabrication in the Al-Si alloy based plates. Less, but bigger Si particles can be seen in the Al-Si blend based plates.
- Comparison with E-FUTURE plates: the SiRDL Si concentrations in as-fabricated E-FUTURE II precursor plates and in the E-FUTURE 6%Si 425°C -2h are quite similar, while Si-rich layers are nearly twice as thick. Moreover, much more Si remains in the matrix of E-FUTURE II plates with 10 and 12%Si, than in E-FUTURE fresh ones: the E-FUTURE II irradiation will thus also provide an evaluation of the role of this Si reservoir on the behaviour of UMo fuel plates.
- Influence of an additional thermal treatment: An increase of the average thickness of the SiRDL (with a [Si] still around 50%at) up to about a factor of 2 can be observed for the Al12Si alloy sample after an additional heat treatment at 425°C-2h in comparison with the as-fabricated ones.

Based on these results, the E-FUTURE II experiment has been extended to 4 plates (Al7%Si alloy, Al12%Si alloy, Al12%Si alloy with additional TT of 425°C 2h and Al12%Si powder mixture). The irradiation is scheduled to start in March 2012 in BR2.

7. Acknowledgments

J. Sanchez is warmly thanked for preparing the samples before their characterization and for performing the heat treatments. We are also grateful to H. Rouquette, N. Tarisien and C. Tanguy for performing SEM+EDS characterizations and image analyses.

References

- [1] E. Koonen, H. Guyon, P. Lemoine, C. Jarousse, D.M. Wachs, J. Roglans-Ribas, “*Dispersed U(Mo) fuel qualification road map for the BR2 and RHF Reactors*”, Proceedings of RRFM 2009, Vienna, Austria, March 22-25, 2009.
- [2] F. Fréry, H. Guyon, E. Koonen, S. Van den Berghe, P. Lemoine, F. Charollais, C. Jarousse, D. Geslin, “*LEONIDAS U(Mo) Dispersion fuel qualification program: progress and prospects*”, Proceedings of RERTR2010, Lisbon, Portugal, October 10-14, 2010.
- [3] S. Van den Berghe, Y. Parthoens, E. Koonen, F. Charollais, P. Lemoine, Y. Calzavara, H. Guyon, C. Jarousse, D. Geslin, D. Wachs, D. Keiser, A. Robinson, G. Hofman, Y.S. Kim, “*Results of the Non-Destructive Analyses of the E-FUTURE U(Mo)-Al(Si) Fuel Plates of the LEONIDAS Program*”, Proceedings of RERTR 2011, Santiago, Chile, October 23-27, 2011.
- [4] A. Leenaers S. Van den Berghe, E. Koonen, F. Charollais, P. Lemoine, Y. Calzavara, H. Guyon, C. Jarousse, B. Stepnik, D. Wachs, A. Robinson, « *LEONIDAS E-FUTURE : Results of the Destructive Analyses of the U(Mo)-Al(Si) Fuel Plates* », this conf.
- [5] F. Charollais, P. Lemoine, Y. Calzavara, H. Guyon, E. Koonen, S. Van den Berghe, B. Stepnik, C. Jarousse, D. Geslin, Proceedings of RERTR2011, Santiago, Chile, 2011.
- [6] A. Leenaers ,S. Van den Berghe, A. Robinson and C. Detavernier, *Al-Si matrix : mixture or alloy - an annealing study*, Proceedings of RERTR2011, Santiago, Chile, 2011.
- [7] X. Iltis, F. Charollais, M.C. Anselmet, P. Lemoine, A. Leenaers, S. Van den Berghe, E. Koonen, C. Jarousse, D. Geslin, F. Frery, H. Guyon, Proceedings of RERTR 2010, Lisbon, Portugal, Oct. 10-14, 2010.
- [8] A. Bonnin, H. Palancher, V. Honkimäki, R. Tucoulou, Y. Calzavara, C.V. Colin, J-F. Béar, N. Boudet, H. Rouquette, J. Raynal, C. Valot, J. Rodriguez-Carvajal, Zeit. Krist. Proc. (2011) 1, 29-34.
- [9] H. Palancher, A. Bonnin, V. Honkimäki, T. Buslaps, *et al.*, J. Alloys and Compounds, accepted, 10.1016/j.jallcom.2012.02.010; A. Bonnin, H. Palancher, F. Charollais, M.C. Anselmet, V. Honkimäki, P. Lemoine, Proceedings of RRFM 2011, Rome, Italy, March 20-24, 2011.
- [10] H. Palancher, A. Bonnin, X. Iltis, F. Charollais, M. Grasse, B. Stepnik, T. Zweifel, V. Honkimäki, in preparation.
- [11] S. Van den Berghe, A. Leenaers, E. Koonen and L .Sannen, Adv. Sc. Techn. 73 (2010), 78-90.
- [12] H.J. Ryu, J.S. Park, J.M. Park, C.K Kim, Nucl. Eng. and tech. 43 (2010) 159-166.
- [13] B. Yao, E. Perez, D.D. Keiser Jr., J.-F. Jue, C. R. Clark, N. Woolstenhulme, Y. Sohn, J. Alloys and Compounds, 509 (2011) 9487– 9496
- [14] J. Gan, D.D. Keiser Jr., B.D. Miller, D.M. Wachs, T.R. Allen, M. Kirk, J. Rest, J. Nucl. Mater. 411, (2011) p. 174-180
- [15] H. Palancher, Ph Martin, V. Nassif, R. Tucoulou, O. Proux, J.L. Hazemann, O. Tougait, E. Lahera, F. Mazaudier, C. Valot, S. Dubois, J. Appl. Crystallogr. 40 (2007) p.1064–1071; F. Mazaudier, C. Proye, F. Hodaj, J. Nucl. Mater., 377 (2008) p 476-485; M.I. Mirandou, S.N. Balart, M. Ortiz, M.S. Granovsky, J. Nucl. Mater., 323 (2003), p. 29-35; E. Perez, D.D. Keiser Jr., and Y.H. Sohn, Metallurgical and materials transaction, 42A (2011), 3071-3083
- [16] G. Hofman, Proceedings of RERTR2009, Beijing, 2009.
- [17] B. Stepnik, M. Grasse, D. Geslin, C. Jarousse, F. Charollais, P. Lemoine, Y. Calzavara, H. Guyon, E. Koonen, S. Van Den Berghe, « *LEONIDAS UMO dispersion fuel qualification program: progress and perspectives highlight on the e-future ii fuel plate manufacturing* », this conf.

ANALYSIS OF REACTIVITY INDUCED ACCIDENTS IN MTR CORE FOR VARIOUS PROTECTION SYSTEM PARAMETERS

M. A. GAHEEN, F. MAHMOUD BADRY, S. ELARABY
*Egypt Second Research Reactor (ETRR-2), Egyptian Atomic Energy Authority (EAEA)
13759, Abou Zabal – Egypt*

M. NAGUIB ALY, M. E. NAGY
*Department of Nuclear Engineering, Alexandria University
21544, Alexandria – Egypt*

ABSTRACT

Analysis of Reactivity Induced Accidents (RIA) in a MTR (Material Testing Reactor) core is presented for various engineering and design parameters of Reactor Protection System (RPS). The PARET code was used to model the RPS parameters and calculate peak core power and peak fuel clad temperature. Typical RPS as described in IAEA-TECDOC-973 for research reactor instrumentation and control technology has been simulated. The RIA initiating events include insertion of excess reactivity, accidental extraction of fixed experiment, and uncontrolled withdrawal of a control rod. The peak core power and peak clad temperature were plotted for each initiating event with variation in shutdown setting, instrumentation delay time, dropping or insertion time, and shutdown margin. As results, useful figures were obtained, which describe the importance of each of these RPS parameters to limit the clad temperature well below the melting temperature.

1. Introduction

The safety analysis of MTR research reactors usually entails the simulation of several selected cases of RIA. The analysis of RIA is performed to ensure that the fuel clad temperature is below the melting temperature. It is not only required for new reactors but also when replacement of reactivity control devices, removal or insertion of experimental apparatus, and installation of new core components with new characteristics [1, 2]. The analysis should be performed with conservative characteristics of the RPS [3].

The intent of this paper is to perform analysis of RIA for a typical MTR core with a simple and validated code. The code should be capable of simulating the reactivity accidents applicable to MTR cores and the RPS engineering and design parameters. The PARET code was selected for performing the analysis, which is designed for use in predicting the course and consequences of non-destructive transients in small reactor cores [4]. The analyzed initiating events are: (1) insertion of excess reactivity of 1 \$ (prompt critical condition), (2) accidental extraction of in-core experiment, and (3) uncontrolled withdrawal of control rod. The analysis includes variation in shutdown setting, delay in instrumentation, dropping or insertion time (e.g. control rod dropping time), and shutdown margin.

1. RPS description

The RPS is an independent and reliable system that monitors the safety variables and initiates appropriate protective actions if any of such variables reaches the safety setting. This system brings the reactor to a safe condition in the event of incidents and accident conditions. In Fig. 1, the RPS main components and units to protect the core against RIA are shown [5].

The power channel measures the evolution of neutron flux during power operation range. This range allows neutron flux monitoring beyond 1.5 times full power. Three redundant and independent power channels are included in the RPS. The detector is a Compensated Ionization Chamber (CIC). The resulting current is proportional to the thermal neutron flux [5]. The ConDitioning Unit (CDU) performs the interface between the detector and the instrumentation system. There are three redundant conditioning units, each one works with only one Trip Unit (TU) of the three redundant trip units. Hence, there is a direct one-to-one correlation between each conditioning unit and each trip unit. The Safety Setting Input Units (SSIUs) are three redundant devices, one for each trip unit. Each SSIU has the Safety System Settings (SSS) required by its related trip unit. Appropriate values for these SSS are defined by an authorized operator. There are two redundant voting units working in parallel applying logic two out of three to the three redundant inputs produced by the three trip units [5]. Two Final Actuation Logic (FAL) units using logic one out of two are for actuation of the first shutdown system (scram) shown in Fig. 2. In scram condition, the Magnetic Coupling (MC) between the rod and the pneumatic cylinder is disconnected and the motor is released. When the comprised air valves are open, fast insertion (500 ms) of the absorbing plate inside the core is ensured.

In case of failure of the first shutdown system, some research reactors have second shutdown system independent of the first and using different means of operation. The second shutdown system uses insertion of neutron absorbing solution between core and reflector or partial dumping of heavy water reflector in 15 s [6].

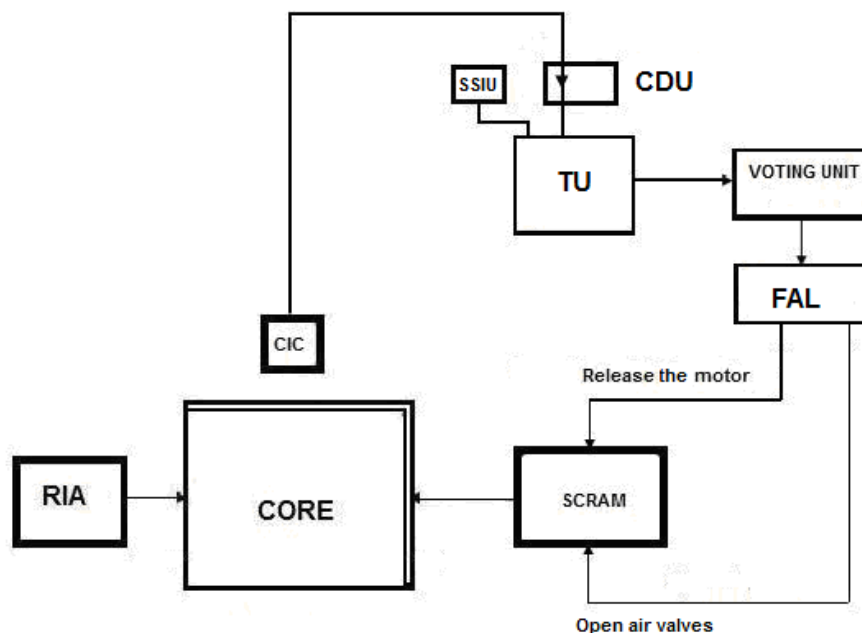


Fig.1. RPS main components and units to protect the core

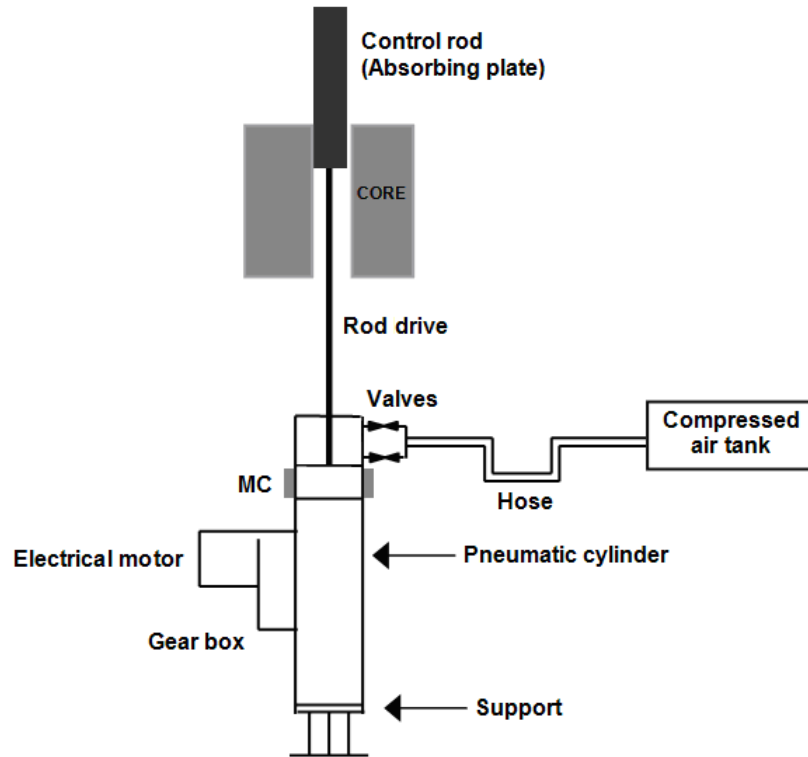


Fig.2. First shutdown system

3. Modeling

The PARET code was used to simulate RIA in a typical MTR core. It is a code developed by Argonne National Laboratory to provide a coupled thermal hydrodynamic and point kinetics capability specifically for use in predicting the course of and consequence of nondestructive accidents in research and test reactor cores [7]. The PARET code is built basically on three models (Kinetics model, thermal model, and hydrodynamic model). A description of the modeling approach is given in [4, 7].

A two-channel model was used in the PARET code with one channel assumes to have the hottest fuel plate in the core and the second channel representing the reminder of the core. Axial power distribution along the plate has been represented by 21 mesh points. The fuel plate has peak to average ratio of 1.311 and a maximum peaking factor of 3 was defined as the total peaking factor. Analysis of RIA for various protection system parameters has been performed by varying one parameter individually and keeping the others constant. In all simulation runs it is assumed that all the control rods are out of core and only shutdown due to over power is enable. The main operation and design parameters of the MTR core are given in Table 1.

The modeling of reactivity insertion includes ramp insertion of $1 \text{ } \$/\text{s}$, accidental extraction of a fixed experiment of $1.65 \text{ } \$$ ($2.887 \text{ } \$/\text{s}$), and uncontrolled withdrawal of a control rod of about $4.5 \text{ } \$$. In case of accidental extraction of fixed experiment the model assume that the maximum allowable worth of fixed experiment is extracted from the core with velocity of 1.4 m/s . The uncontrolled withdrawal of control rod is modeled considering the S shape of reactivity worth versus position as shown in Table 2.

Parameters	Value
Total fuel volume (m ³)	0.0184
Meat dimensions (mm × mm × mm)	0.7 × 64 × 800
Hot channel total peaking factor	3 (maximum)
Inlet core temperatures (°C)	20
Coolant channel mass flux (kg/s.m ²)	5090
Coolant channel between two plates (mm)	2.7
Total cross section flow area (m ²)	0.1056267
Fuel heat capacity (J/°k/m ³) (T in °C)	1638T+1632×10 ³
Clad heat capacity (J/°k/m ³) (T in °C)	1242T+2069×10 ³
Fuel thermal conductivity (W/mK)	15
Clad thermal conductivity (W/mK)	180
Delayed neutron fraction	0.00705
Prompt neutrons generation time (s)	75×10 ⁻⁶
Coolant temperature coefficient (\$/°C)	-0.0154
Void coefficient (\$/%)	-0.241
Fuel temperature coefficient (\$/°C)	-0.002482

Table 1: Main core operation and design parameters

Time	Extraction ^a	Reactivity ^b
(s)	(%)	(\$)
0	20%	0
1	40%	1.211
2	60%	3.031
3	80%	4.244
4	100%	4.474

a: percentage of extraction of the control plate.

b: The control rod is extracted from the 80% inserted position

Table 2: Control rod worth considering S shape of reactivity versus position

4. Results and discussion

From previous description of RPS units and components, four important parameters have been studies:

2. RPS Shutdown Setting (SS).
3. Instrumentation Delay time (IDT).
4. Control rod dropping or Insertion Time (IT).
5. Shutdown Margin (SM).

Fig. 3 and Fig. 4 show the peak core power and peak clad temperature, simulated by PARET, when parameters of RPS are varied. The simulated initiating events, insertion of 1\$, accidental extraction of fixed experiment, and uncontrolled withdrawal of a control rod are denoted respectively by 1, 2 and 3. The first protection system parameters are normalized to the typical values of SS = 110 %, IDT = 25 ms, IT = 500 ms, and SM = 10 \$ [2]. Except the shutdown setting, the peak core power and peak clad temperature for initiating event 1 are approximately

constant independent of the protection parameters. For initiating events 2 and 3, it can be observed that the instrumentation delay time is the most important parameter to limit the clad temperature. The rod dropping time is less important than instrumentation delay time. It can be also observed that increasing shutdown margin more than the minimum limit (4 %) will decrease power and clad temperature significantly.

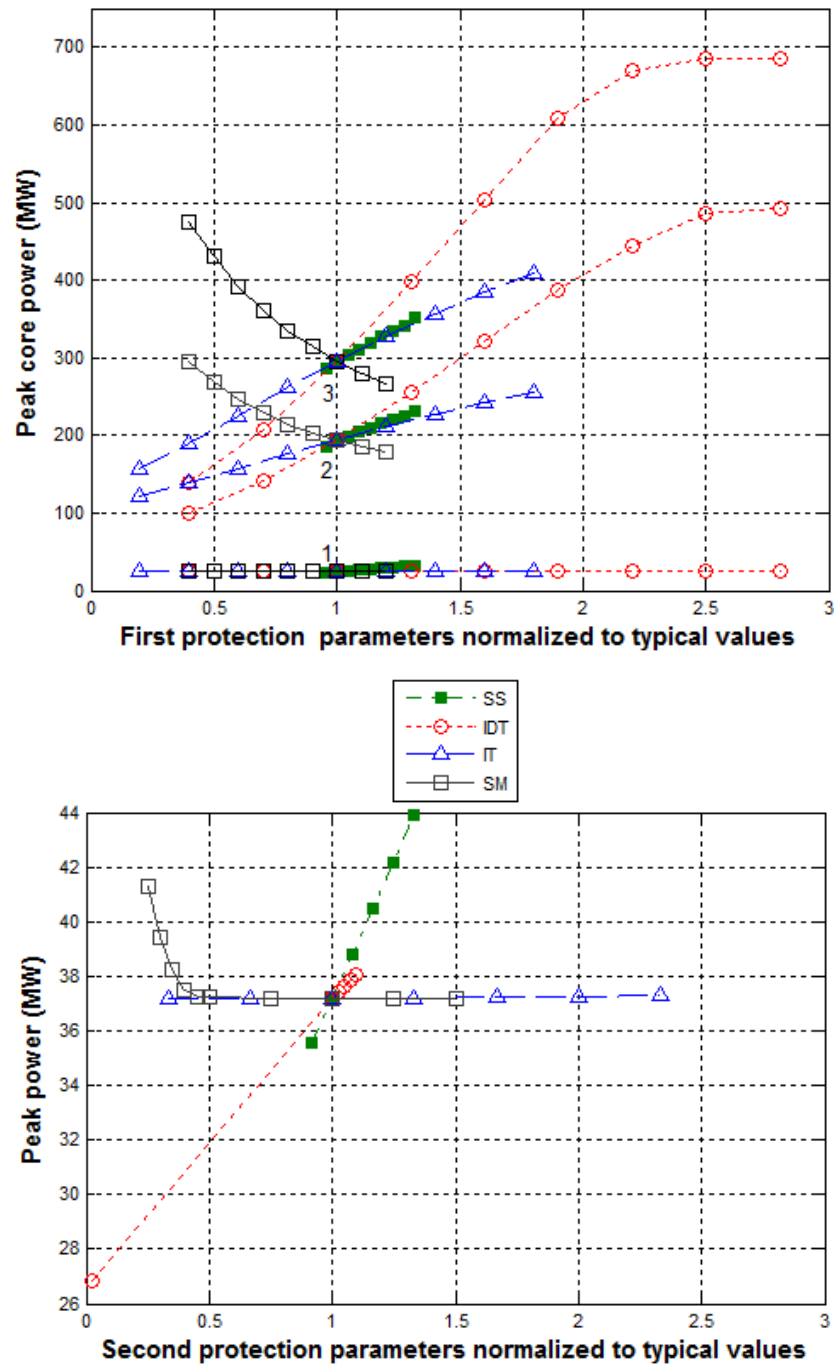


Fig.3. Peak core power with variation in protection parameters

The typical values of second protection parameters are $SS = 120\%$, $IDT = 1025\text{ ms}$ (including 1 s delay between detection of scram failure and actuation of the second shutdown system), $IT = 15\text{ s}$, and $SM = 4\text{ \$}$ [8]. Therefore, the insertion of 1 \$ is only considered in the analysis. The peak power and peak clad temperature increase linearly with the shutdown setting and instrumentation delay time. Variation in the insertion time almost has no variation in results. It can be observed that the peak power and peak clad temperature increase only for shutdown margin below 2 \$.

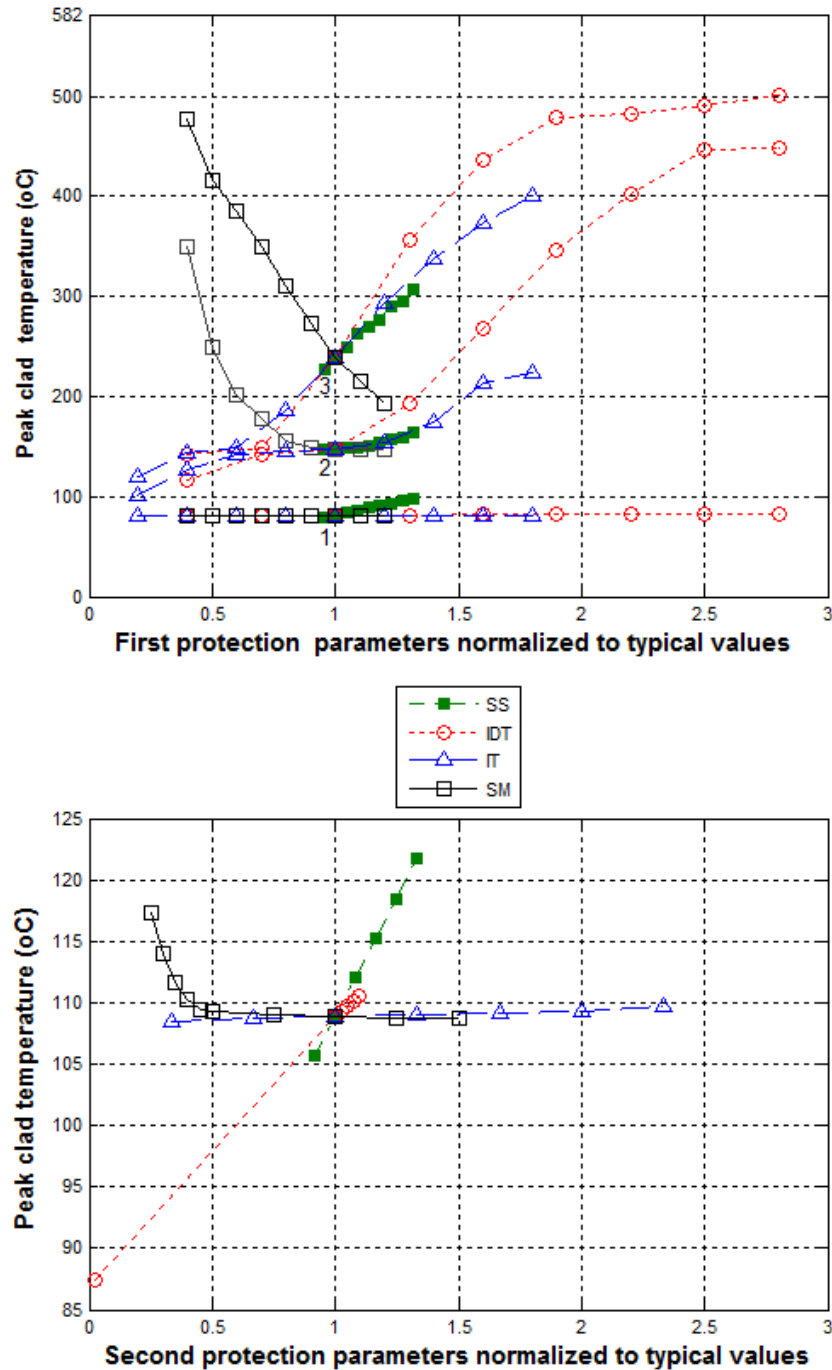


Fig. 4. Peak clad temperature with variation in protection parameters

The results given in Table 3 are the new peak power and peak clad temperature (between brackets) when the values of protection parameters are the conservative values usually used in the RIA analysis.

Initiating event	Parameter	Variation	Peak core power (MW)	Peak clad temperature (°C)
First protection parameters				
(1) Insertion of 1 \$	SS	110 – 120% (+0.9 %)	24.5 (26.7)	81.3 (86.2)
	IDT	Approximately constant independent of the parameter		
	IT			
	SM			
(2) Experiment Extraction	SS	110 – 120 % (+0.9 %)	193.5 (204.7)	148 (148.7)
	IDT	25 – 40 ms (+60 %)	193.5 (321.6)	148 (268.7)
	IT	500 – 800 ms (+ 60 %)	193.5 (241.7)	148 (213.2)
	SM	10 – 4 \$ (- 60 %)	193.5 (296)	148 (349)
(3) Control rod withdrawal	SS	110 – 120 % (+0.9 %)	294.5 (311.3)	238.8 (263)
	IDT	25 – 40 ms (+60 %)	294.5 (503.5)	238.8 (437.3)
	IT	500 – 800 ms (+ 60 %)	294.5 (384.5)	238.8 (374.3)
	SM	10 – 4 \$ (- 60 %)	294.5 (474.1)	238.8 (477)
Second protection parameters				
(1) Insertion of 1 \$	SS	120 – 130 % (+0.8 %)	37.2 (38.82)	108.8 (112)
	IDT	1025 – 25 ms (*)	37.2 (26.82)	108.8 (87.5)
	IT	Approximately constant independent of the parameter		
	SM	4 – 1.4 \$ (- 65 %)	37.2 (38.2)	108.8 (111.7)

(*) when the second shutdown is actuated as the first

Table 3: New peak power and peak clad temperature when using conservative values

5. Conclusions

RIA in a MTR core has been simulated for various RPS parameters, namely, shutdown setting, instrumentation delay time, rod dropping or insertion time, and shutdown margin. The results concerning the first protection system are discussed for each initiating event reaching the following conclusions:

1. For insertion of 1\$, the scram setting is the only parameter varying the peak core power and clad temperature.

2. Instrumentation delay time is the most important parameter for the insertions $> 1\%$ (accidental extraction of fixed experiment and uncontrolled control rod withdrawal).
3. The insertion time is less important than instrumentation time.
4. With increasing the shutdown margin more than the minimum value (4 %), the peak power and clad temperature are significantly decreased.

The second protection system is capable to limit the clad temperature against insertion of 1 %.

6. References

- [1] R. Waldman, A. Vertullo, "Reactivity Accident Analysis in MTR Cores," International Meeting on Reduced Enrichment for Research and Test Reactors (RERTR), Buenos Aires, Argentina, Sep 28-Oct. 1, 1987.
- [2] International Atomic Energy Agency, "Research Reactor Core Conversion Guidebook," Vol. 3. Analytical Verification, IAEA-TECDOC-643, Vienna, April 1992.
- [3] I. H. Bokhari, "Analysis of Accidents at the Pakistan Research Reactor-1 Using Proposed Mixed-Fuel (HEU and LEU) Core," Nuclear Technology, Vol. 148, pp. 369-376, 2004.
- [4] C. F. Obenchain, "PARET-A program for the analysis of reactor transients," Idaho National Engineering Laboratory, Report IDO-17282, 1969.
- [5] International Atomic Energy Agency, "Research reactor instrumentation and control technology," IAEA-TECDOC-973, Vienna, October 1997.
- [6] Australian Nuclear Science and Technology Organization, "Summary of the Preliminary Safety Analysis Report (PSAR) for the ANSTO Replacement Research Reactor Facility," www.ansto.gov.au, 2001.
- [7] W. L. Woodruff, "A Kinetics and Thermal-Hydraulic Capability for the Analysis of Research Reactors," Nuclear Technology, Vol. 64, pp. 196-206, 1984.
- [8] E. Villarino, S. Gomez, V. Ishida, "Neutronic Design of the First Core of the Replacement Research Reactor," Proceedings of International Conference on Research Reactor Utilization, Safety, Decommissioning, Fuel and Waste Management, Santiago, Chile, 10–14 November 2003.

NUMERICAL STUDY OF THE GEOMETRY IMPACT ON THE HEAT TRANSFER IN A RADIOMETRIC CALORIMETER DEDICATED TO NUCLEAR HEATING MEASUREMENTS

M. MURAGLIA, C. REYNARD-CARETTE, J. BRUN,
M. CARETTE, A. JANULYTE, Y. ZEREGA, J. ANDRE

*Aix-Marseille Univ, LISA, Equipe IPCN,
13397, Marseille Cedex 20, France*

A. LYOUSSI, G. BIGNAN, J-P. CHAUVIN, D. FOURMENTEL, C. GONNIER,
P. GUIMBAL, J-Y. MALO, J-F. VILLARD

*Commissariat à l'Énergie Atomique et aux Énergies Alternatives
CEA Direction de l'Énergie Nucléaire, Centre de Cadarache
13108 Saint-Paul-Lez-Durance, France.*

E-mail : magali.muraglia@univ-amu.fr

ABSTRACT

This work presents a first study of the impact of the geometry of a calorimeter used for nuclear heating measurements on heat transfer from theoretical and numerical points of view.

More precisely, we compare the heat transfer and the sensitivity of a simple calorimeter with a complex calorimeter composed with a single graphite cell.

1. Introduction

On-line accurate nuclear heating measurements in Material Testing Reactor - MTR - is still a real challenge regarding improvement of experimental parameters knowledge and hence for present and future reactor generation. Thus, IN-CORE program "Instrumentation for Nuclear radiations and Calorimetry Online in REactor", involving the LISA laboratory (Aix-Marseille Université, France) and the CEA research institute (French Atomic Energy and Alternative Energies Commission) - Jules Horowitz Reactor (JHR) program [1], is aimed to design a suitable mobile device, composed by several sensors/detectors, dedicated for online measurements of relevant physical parameters (nuclear heating, neutron flux, etc...). In this paper, we focus especially on one sensor of this device: a differential graphite calorimeter dedicated to the nuclear heating measurement [2]. In order to optimize the sensor design, to calibrate it, and to study the internal and external heat transfer, experimental and numerical works of the calorimeter response under non radioactive conditions have been performed in [3, 4, 5]. However, the effect of the calorimeter geometry and the effect of the external flow, on the heat transfer and on the sensitivity which are key parameters for the sensor, are still open questions relevant for the optimization of the device. Thus, the objective is to derive a 2D model describing the coupling between the heat transfer in the complex geometry of the calorimeter with the external flow dynamics governed by the Navier-Stokes equation and to develop a numerical code to solve this model. This paper is a first step of this work and concerns the impact of the geometry on the heat transfer and on the sensitivity. We compare the numerical response of a complex calorimeter with one cell to the theoretical response of a simple calorimeter.

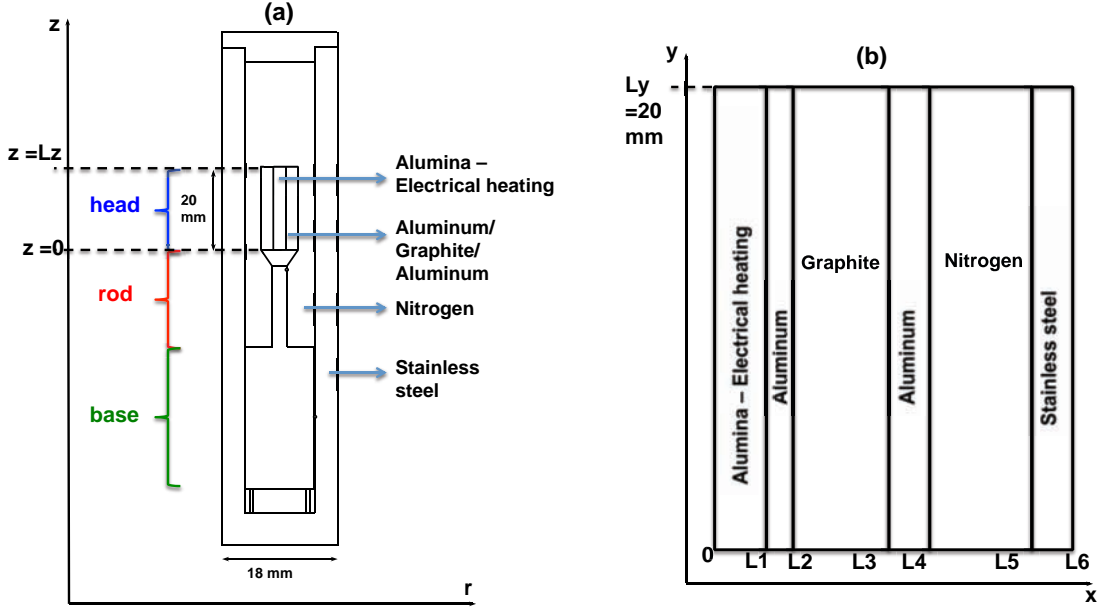


Figure 1: (a) Diagram of the complex calorimeter with one graphite cell used in [6] (cylindrical geometry). (b) Diagram of the simple calorimeter solved theoretically (cartesian geometry).

2. Heat transfer in a complex calorimeter with one cell

Fig.1-a presents the diagram of the complex calorimeter with one graphite cell which can be described from top to bottom by three parts: the head (containing an electrical heating element), the rod and the base. The head is composed by graphite, aluminum and alumina and is laid under nitrogen. The jacket of the calorimeter is made of stainless steel. In order to give some insight on the geometry impact, the heat transfer inside the calorimeter is studied from a numerical point of view. We use a model already validated for convective boundaries [5]. In this model, the heat equation in 2D axi-symmetrical geometry is reduced to a conductive term and to a source term only into alumina area corresponding to the heat induced by Joule effect, the nitrogen cavities are considered as static gas cavity. The following equation is considered:

$$\rho_i c_{p_i} \partial_t = \frac{1}{r} \partial_r (\lambda_i r \partial_r T) + \partial_z (\lambda_i \partial_z T) + S \quad (1)$$

where ρ_i is the mass density ($kg.m^{-3}$) of a given material i , c_{p_i} is its heat capacity ($J.kg^{-1}.K^{-1}$). λ_i is the thermal conductivity ($W.m^{-1}.K^{-1}$) of material i and its temperature dependance is taking into account in the model. Finally, S represent the electrical power ($W.m^{-3}$) injected into the alumina part. The boundaries conditions correspond to adiabatic conditions on the horizontal upper and lower surface of the jacket and to convective conditions along the vertical external jacket surface. The convective exchange between the calorimeter jacket and its surroundings is determined by applying a thermal correlation to deduce the heat transfer coefficient[7]. This model is solved using 2009 CASTEM code based on finite element schemes allowing to take into account the complex geometry of the calorimeter presented on Fig.1-a. Thus, the temperature profile in the head of the calorimeter is obtained numerically for a range of electrical power applied at the middle of the head. As shown on Fig.2-a, the temperature profile depends strongly on the electrical power injected: more powerful is, higher the temperature inside the alumina part is. The temperature profile is naturally affected by the different materials: whereas alumina, graphite and aluminum are good conductoor, the temperature decreases quickly inside the nitrogen which dissipates well energy. Finally, the reached temperature at the

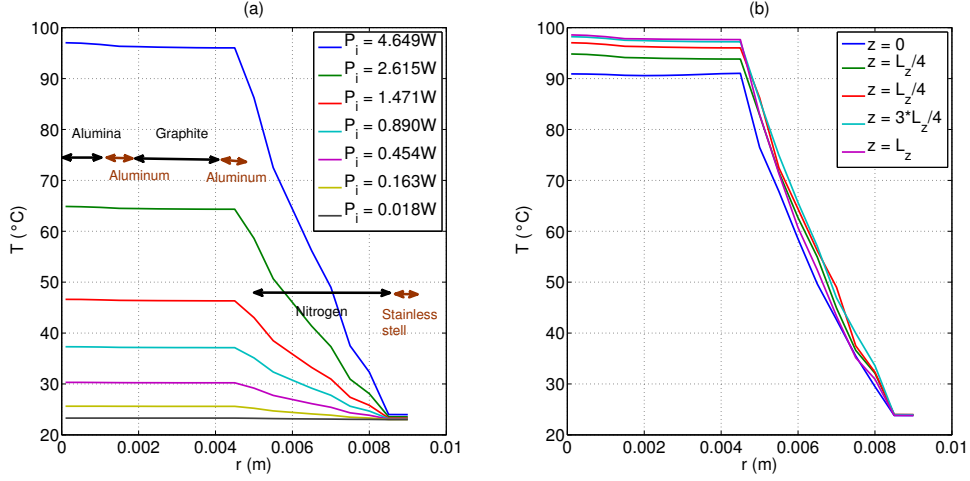


Figure 2: (a) Numerical temperature profiles obtained in the head of the complex calorimeter for different values of the injected electrical power. (b) $P_i = 4.649W$. Numerical temperature profiles obtained for the complex calorimeter at different vertical positions in the head.

edge of the calorimeter is close to the ambient temperature ($\sim 23^\circ C$). Let us note that the temperature reaches, at the heart of the alumina, for high value of the injected electrical power, can be supported by the device, in particular by the aluminum (melting point at $660^\circ C$). Moreover, a key parameter for the calorimeter is its sensitivity which can be defined as $S_e = \partial T / \partial P_i$ and which represents the capability of the sensor to measure a small fluctuation of the injected electrical power. Fig.4-b shows that for the complex calorimeter $S_e = 15.9^\circ C.W^{-1}$.

The heat transfer is affected by the geometry of the calorimeter. Indeed, as shown on Fig.2-b which presents profile temperatures in the head at different vertical positions (see Fig.1-a) for $P_i = 4.649W$, the temperature is smaller around $z = 0$ than at the top of the head, letting the heat drains out through the rod of the sensor.

3. Analytical study of a simple geometry

In order to see how the geometry can affect the heat transfer, we focus now on a simple geometry for the calorimeter presented on Fig.1-b. In fact, in this simple geometry, we gaze only the head of the calorimeter still composed by an alumina part where the electrical power is injected and two aluminum, a graphite, a nitrogen and a stainless steel parts. The heat transfer inside this simple calorimeter is studied from a theoretical point of view. In first approach, we describe this calorimeter in a 2D cartesian geometry supposing, thanks to the tiny size of the head, the cylindrical effects are negligible. Thus, the temperature profile inside the calorimeter is known theoretically by solving the stationary 1D heat equation in a cartesian geometry :

$$\partial_x (\lambda_i \partial_x T) = -S \quad (2)$$

where periodic conditions are applied for the y direction ($T(x, 0, t) = T(x, L_y, t)$). The calorimeter is supposed to be isothermal, thus, for the x direction, constant boundary conditions are imposed ($T(-L_x, y, t) = T(L_x, L_y, t) = 23^\circ C$). We suppose that the electrical power is injected only in the alumina area. We solve Eq.(2) material by material and we connect each area using the continuity of the flux and of the temperature. Thus the temperature profile at saturation (*i.e.* during the permanent regime) in the alumina is :

$$T_{alumina}(x) = -\frac{S}{2\lambda_{alumina}}x^2 + B_{alumina} \quad (3)$$

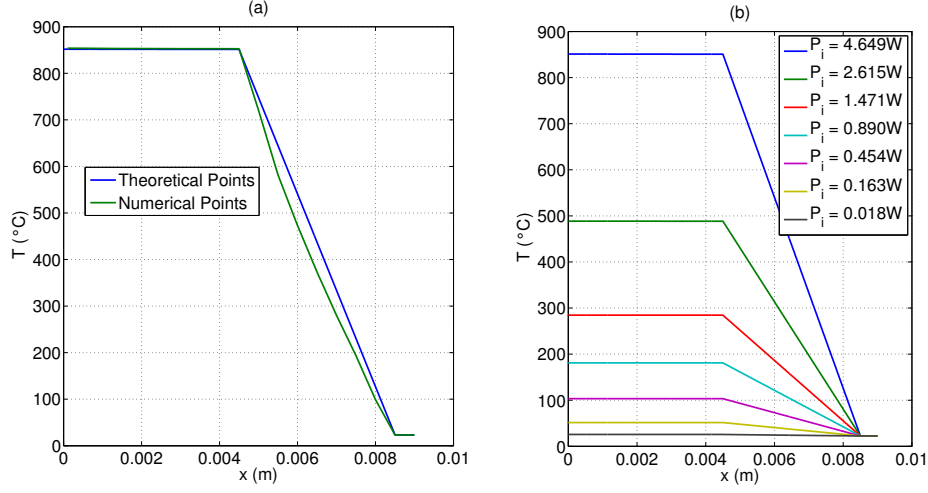


Figure 3: (a) $P_i = 4.649W$. Validation of the theoretical solution with the numerical response of the simple calorimeter. (b) Analytical temperature profiles obtained for the simple calorimeter and for different values of the injected electrical power.

For other material i , we found at saturation regime:

$$T_i(x) = A_i x + B_i \quad (4)$$

where $A_i = -(L_1 S)/\lambda_i$ obtained by the flux continuity and coefficients B_i are calculated from the temperature continuity.

In order to validate the theoretical study, we compare, for a fixed electrical power injected in alumina ($P_i = 4.649W$), the analytical response of the calorimeter given by Eqs.(3-4) with the temperature profile obtained numerically with 2009 CASTEM code using the simple calorimeter (Fig.1-b) in 2D axi-symmetrical geometry. Fig.3-a shows a good agreement between theoretical and numerical points and shows also that the cylindrical effects can be neglected in a first approach. Fig.3-b shows the theoretical temperature profiles obtained using Eqs.(3-4) for different values of injected electrical power P_i . The comparison between Fig.2-a and Fig.3-b demonstrates that the geometry impacts strongly the heat transfer inside the geometry: the temperature reaches inside the alumina area is higher in the simple calorimeter than in the complex one. Indeed, as shown on Fig.4-a which presents the numerical temperature map inside the simple calorimeter at saturation, the periodic condition imposed on the y direction stops heat evacuating by the y direction. As a consequence, the temperature inside the alumina part is higher. Let us note that the melting point of the aluminum is for $660^\circ C$, thus the simple calorimeter can not assume high injected electrical power. Moreover, Fig.4-b compares the sensitivity of the two calorimeters and shows that the geometry impacts strongly the response of the sensor: the simple calorimeter has clearly a better sensitivity than the complex one.

4. Conclusion

We have studied the response of two calorimeters with different geometries. The first calorimeter, due to its complex geometry, is solved using the 2009 CASTEM code. The second calorimeter, with a simple geometry, is solved analytically. The theoretical study of the simple calorimeter has been validated. This study shows that geometry has an impact on the heat transfer and on the sensitivity of the sensor. Indeed, the complex calorimeter evacuates heat through the rod, is suitable for high injected electrical power and its sensitivity is weak. Regarding the simple calorimeter, due to periodic conditions imposed in the y direction, the heat is only evacuated radially. This calorimeter is not

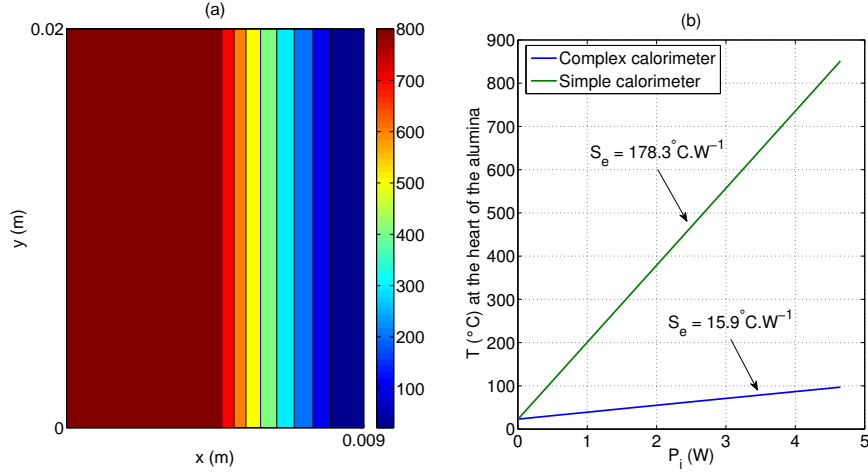


Figure 4: (a) $P_i = 4.649W$. Numerical temperature map inside the simple calorimeter at saturation. (b) Temperature at the heart of the alumina at the alumina for the two calorimeters

suitable for high injected electrical power and its sensitivity is adapted to measure small fluctuation of injected electrical power.

Acknowledgements

The IN-CORE program is supported by FEDER, Conseil Régional PACA and Ville de Marseille

References

- [1] In core Instrumentation for Online nuclear heating Measurements of Material Testing Reactor, C. Reynard et al., RRFM Transactions 2010, Marrakech, Morocco.
- [2] Development, calibration and experimental results obtained with an innovative mobile calorimeter (CALMOS) for nuclear heating measurements, H. Carcre et al., ANIMA 2011, June 2011, Gant, Belgium.
- [3] Numerical study of heat transfer in a radiometric calorimeter dedicated to nuclear heating measurements, C. Reynard-Carette et al., RRFM Transactions 2011, Rome, Italy.
- [4] Numerical and Experimental Calibration of a Calorimetric Sample Cell Dedicated to Nuclear Heating Measurements, J. Brun et al., IEEE Transactions on Nuclear Science, publication accepted.
- [5] Numerical parametric study of heat transfer in a non adiabatic calorimeter without or with nuclear heating deposit, O. Merroun et al., NURETH 2011, Toronto, Canada.
- [6] Heat transfer during out pile calibration of a calorimeter used for nuclear heating measurements : Influence of convective boundary conditions, J. Brun et al., RRFM/IGOR 2012, Prague, Czech Republic.
- [7] Oleg G. Martynenko Pavel P. Khramtsov, Free-Convective Heat Transfer, Springer, 2005.

HEU AND LEU FUEL MANAGEMENT AT THE DALAT NUCLEAR RESEARCH REACTOR

V.L. PHAM, N.D. NGUYEN, B.V. LUONG, V.V. LE,
T.N. HUYNH, M.T. NGUYEN AND K.C. NGUYEN

*Nuclear Research Institute
01 Nguyen Tu Luc Street, Dalat City – Vietnam*

ABSTRACT

The Dalat Nuclear Research Reactor (DNRR) is a pool type research reactor which was reconstructed in 1982 from the old 250 kW TRIGA-MARK II reactor. During reconstruction, some structures of the former reactor such as the reactor aluminium tank, the graphite reflector, the thermal column, the horizontal beam tubes and the radiation concrete shielding were retained. The reactor core, the control and instrumentation system, the primary and secondary cooling systems, the spent fuel storage as well as other associated systems were newly designed and installed. The core was loaded by Russian WWR-M2 fuel assemblies (FAs) with 36% enrichment. The reconstructed reactor reached its initial criticality in November 1983 and attained its nominal power of 500 kW in February 1984. From 1984 to 2007 the reactor was operated with core loaded with HEU FAs. In this period four fuel reloading were executed. From 2007 to 2011 the reactor was operated with mixed core loaded with HEU and LEU FAs. In this period two fuel reloading were executed. In 2011 the reactor operation with mixed core was terminated. HEU and LEU irradiated FAs were discharged from the core and put in interim storage in reactor pool. Then all irradiated HEU FAs were transported and put in spent fuel storage for cooling. The core was prepared for restart-up with LEU fuel. Restart-up and commissioning plan with full LEU fuel core were realized. The first working core with 92 fresh LEU FAs was created. Return of irradiated HEU FAs to the Russian Federation is planned in 2013. This paper presents the HEU and LEU fuel management at the DNRR.

1. Introduction

The DNRR is a pool type research reactor which was reconstructed from the 250 kW TRIGA-MARK II reactor. During reconstruction, some structures of the former reactor such as the reactor aluminium tank, the graphite reflector, the thermal column, the horizontal beam tubes and the radiation concrete shielding were retained. The reactor core, the control and instrumentation system, the primary and secondary cooling systems, the spent fuel storage as well as other associated systems were newly designed and installed. The core was loaded with VVR-M2 fuel assemblies with 36% enrichment [1]. The reconstructed reactor achieved first criticality in November 1983 with 69 fuel assemblies and attained its planned nominal power of 500 kW in February 1984. The vertical section of the reactor is shown in Figure 1. On the supporting base located at the end of upper cylindrical shell in reactor pool there are 24 piercing holes provided to hold 24 pits for interim storage of irradiated or spent fuel assemblies as well as of other objects removed from the core. Each pit can contain 3 fuel assemblies placed vertically. This interim storage is capable of containing 72 fuel assemblies. Next to the reactor pool in the same concrete shield structure, there is spent fuel storage. It was the old bulk-shielding experimental tank, kept from the former TRIGA reactor. For the present reactor, this tank is coated with stainless steel and

filled with demineralised water. The capacity of the spent fuel storage is to contain 300 fuel assemblies.

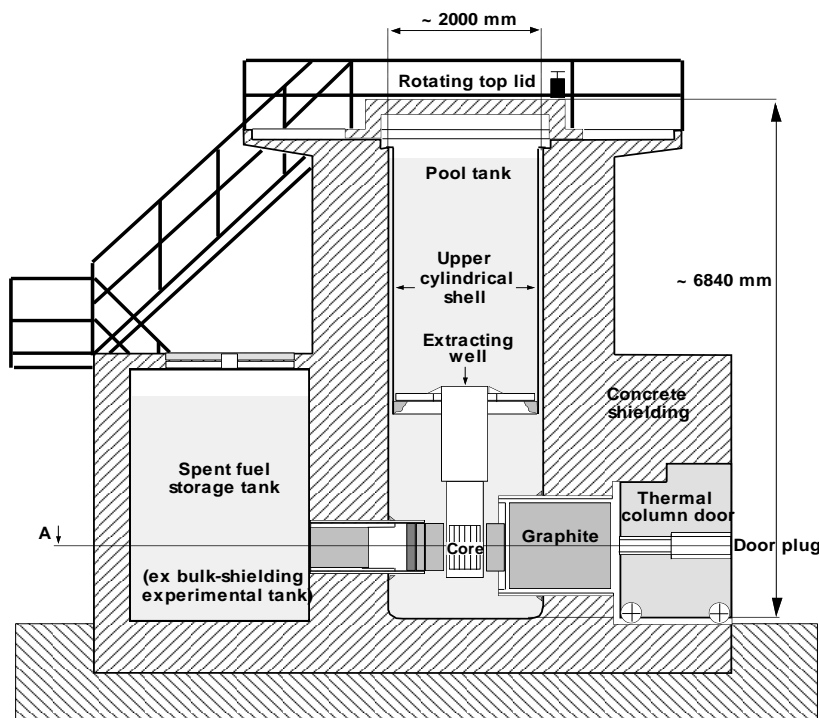


Fig 1. Vertical section view of the reactor

2. HEU Core management of the Dalat Nuclear Research Reactor

The first fuel reloading was executed in April 1994 after more than 10 years of operation with 89 HEU FAs. The 11 new HEU FAs were added in the core periphery, at previous beryllium element locations. After reloading the working configuration of reactor core consisted of 100 HEU FAs. Second reloading for Dalat Nuclear Research Reactor was realized in March 2002. The 4 new HEU FAs were added in the core periphery, at previous beryllium element locations. After reloading the working configuration of reactor core consisted of 104 HEU FAs [2]. The third fuel reloading by shuffling of HEU FAs was executed in June 2004. The shuffling of 16 HEU FAs with highest burn up in the centre of the core and 16 HEU FAs with low burn up in the core periphery was done. The working configuration of reactor core kept unchanged of 104 HEU FAs. In waiting for execution of fuel conversion and saving of fresh HEU FAs, the fourth fuel reloading was executed in November 2006. Only 2 new HEU FAs were loaded in the core periphery, at previous locations of wet irradiation channel and dry irradiation channel. After reloading the working configuration of reactor core consisted of 106 HEU FAs.

3. Realization of mixed Core for the Dalat Nuclear Research Reactor

Based on Contracts for reactor core conversion between USA, Russia, Vietnam and the International Atomic Energy Agency, the 35 fresh HEU FAs were sent back to Russian Federation and the 36 new LEU FAs from Russian Federation have been received in 2007. The characteristics of HEU and LEU FAs is shown in Table 1.

Parameter	HEU VVR-M2	LEU VVR-M2
Enrichment, %	36	19.75
Average Mass of ²³⁵ U in FA, g	40.20	49.70

Fuel Meat Composition	U-Al Alloy	UO ₂ +Al
Uranium Density of Fuel Meat, g/cm ³	1.40	2.50
Cladding Material	Al alloy	Al alloy
Fuel Element Thickness, mm	2.50	2.50
Fuel Meat Thickness, mm	0.70	0.94
Cladding Thickness, mm	0.90	0.78

Tab 1: The characteristics of HEU and LEU FAs

The first mixed core configuration has been created on 12 September, 2007. The 8 HEU FAs with highest burnup were removed from the core periphery positions. The 8 HEU FAs from second ring counted from neutron trap were moved to the core periphery positions. The 2 HEU FAs from locations of wet irradiation channel and dry irradiation channel were moved to 2 positions in second ring. The 6 new LEU FAs were added in 6 positions in second ring. The 2 wet irradiation channels were added in 2 positions of previous locations of wet irradiation channel and dry irradiation channel. After reloading the working configuration of reactor core consisted of 104 FAs (98 HEU FAs and 6 new LEU FAs). The second mixed core configuration has been created on 20 July, 2009. The 6 HEU FAs with highest burnup were removed from the core periphery positions. The 6 HEU FAs from second ring counted from neutron trap were moved to the core periphery positions. The 6 new LEU FAs were added in 6 positions in second ring. After reloading the working configuration of reactor core consisted of 104 FAs [3]. The working core configuration of DNRR with 12 LEU FAs and 92 HEU FAs is shown in Figure 2.

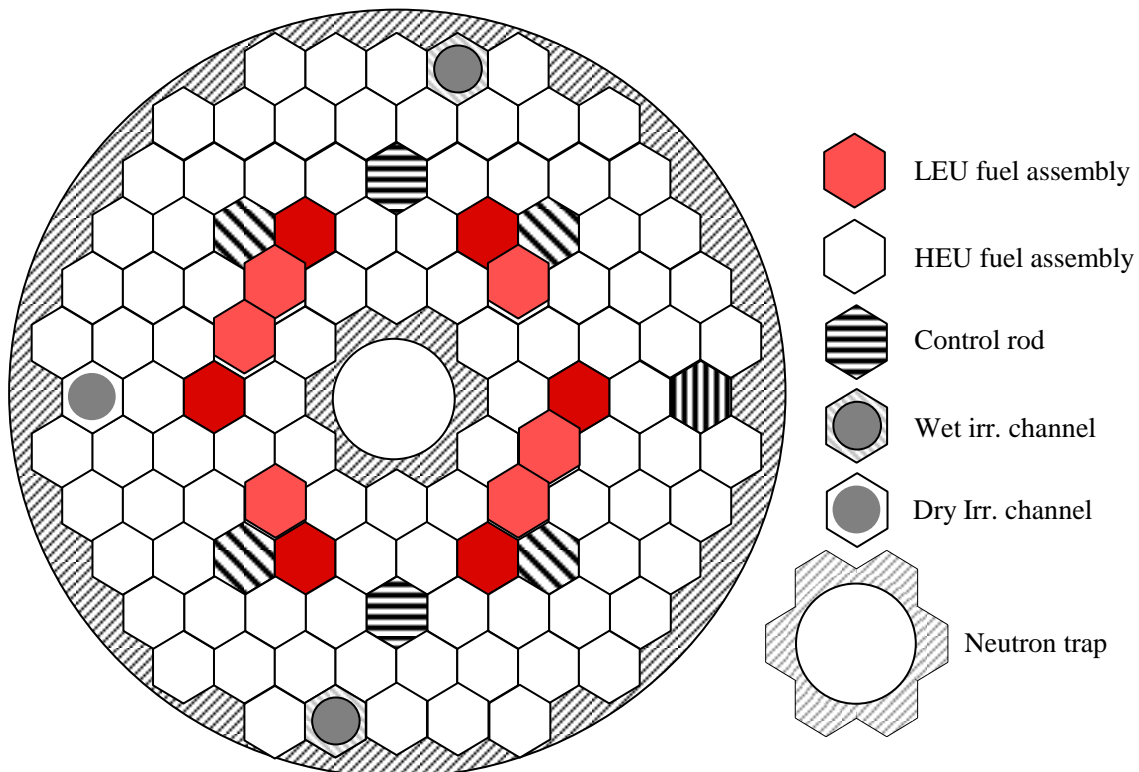


Fig 2. Working core configuration of DNRR with 12 LEU FAs and 92 HEU FAs

4. Realization of Full LEU Core for the Dalat Nuclear Research Reactor

The LEU core design commenced by establishing several possible cores and roughly analyzing to get some main safety and utilization characteristics such as shutdown margin, radial power peaking factors, and neutron performance at some irradiation positions. Contract for nuclear fuel manufacture and supply for Dalat Nuclear Reactor among JSC TVEL, Russia and Vietnam Atomic Energy Institute, Vietnam and Battelle Energy Alliance, LLC, USA have been realized in fourth quarter of 2010. The 66 new LEU FAs from Russian Federation have been received. Capacity of reactor bridge crane was upgraded from 3.6 ton load to 5 ton load. All FAs were discharged from the core to interim storages of fuel in reactor pool in August 2011. Then all HEU FAs were transported from interim storages in reactor pool to spent fuel storage tank in October 2011 for cooling. Figure 3 shows storage of 106 HEU FAs in spent fuel storage tank.



Fig 3. The storage of 106 HEU FAs in spent fuel storage tank

The restart-up and commissioning plan with full LEU core were carried out. The fuel loading of LEU FAs to the reactor core was started on November 24th, 2011. On November 30th, 2011 the reactor was reached criticality with 72 LEU FAs and neutron trap in the centre. Fuel loading for working core was carried out from December 6th, 2011 to December 14th, 2011. Figure 4 shows the working core configuration with 92 LEU FAs and neutron trap in the centre. Test run of reactor at nominal power of 500 kW was realized from 9 to January 13th, 2012. The results of measurements carried out in restart-up and commissioning plan show that the main features of 92 LEU VVR-M2 FA cores are equivalent to those of previous HEU and mixed fuel cores.

5. Conclusions

We have managed HEU fuel and realized DNRR core conversion from HEU to LEU fuel. The preparing works for shipment of HEU irradiated FAs to Russia are going. Return of Russian irradiated highly enriched uranium fuel to the Russian Federation is proposed in 2013.

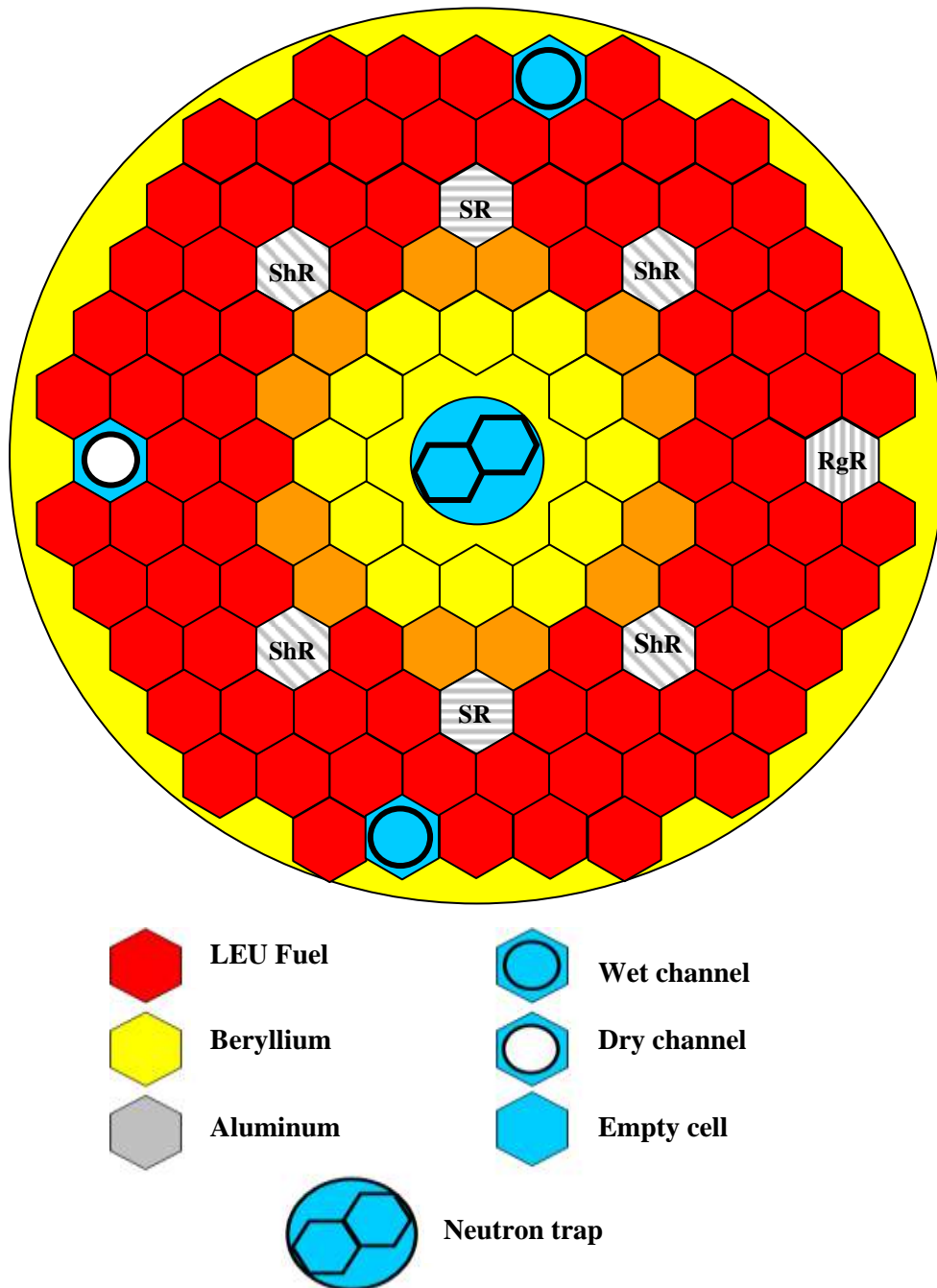


Fig. 4. The working core configuration with 92 LEU FAs
(Orange is partly burnt FAs)

6. References

- [1] "Safety Analysis Report for the Dalat Nuclear Research Reactor", Dalat, 2009.
- [2] Pham Van Lam et al., "Core Management of the Dalat Nuclear Research Reactor", IAEA-CN-100/134, International conference on Research Reactor Utilization, Safety, Decommissioning, Fuel and Waste Management, 10 – 14 November 2003, Chile.
- [3] Pham Van Lam et al., "Realization of mixed core configurations in Core Conversion for the Dalat Nuclear Research Reactor", the RERTR 2009, Beijing, China, November 1-5, 2009.

IMPROVED AGEING MANAGEMENT AND MAINTENANCE SYSTEM FOR THE FIR 1 TRIGA INSTRUMENTATION

I. AUTERINEN, P. KIVELÄ, J. HELIN
*VTT Technical Research Centre of Finland
Otakaari 3, FI-02044 VTT, Espoo – Finland*

H. PALMÉN, M. KATAJISTO
*VTT Expert Services Ltd
Biologinkuja 7, FI-02044 VTT, Espoo – Finland*

ABSTRACT

A management system for ageing management at FiR 1 has been created. Inspection and service procedures are extended and improved. An obsolescence management system for the systems, structures, and components (SSC's) has been created. To improve the ageing management the quarterly and yearly inspections are extended to all SSC's and the data logging is improved to aid the analysis of the ageing process.

To improve the ageing management and maintenance system for the electronic instrumentation all electronic units are labelled individually and registered into an equipment registry system (Efecte). The operational, storage, inspection and maintenance history of each unit is recorded into the system. Based on the stored data a failure statistics is created. The quarterly and yearly inspection programs are revised. As a new procedure the units in operation are imaged with a thermographic camera. The condition of the most critical components, like relays, is studied. The environmental conditions affecting ageing and damaging of the components are surveyed. Temperature and humidity in the reactor control room as well inside the cabinets is followed with a data logger.

Reserve units for the Valmet Elmatic measurement and control system were acquired from recently closed pulp and paper mills. The condition of these units was inspected using visual inspection with high resolution digital cameras. The dust was analysed and the presence of Whiskers was studied. All reserve units are stored in ESD compatible storage boxes. An ESD compatible electronic workshop was established at the reactor for maintenance and inspection of the instrumentation units.

1. Introduction

FiR 1 -reactor is a TRIGA Mark II type research reactor manufactured by General Atomics (San Diego, CA, USA). The FiR 1 started operation in 1962 and reactor power was increased in 1967 from 100 kW to 250 kW. In 1982 the reactor instrumentation was totally renewed. The nuclear channels were purchased from KFKI (Hungary) and the control electronics from Valmet (Finland). In 1996-1997 the reactor building was completely renovated and the ventilation and reactor cooling systems were replaced. The ventilation and cooling are controlled by a ATMOSTECH HVAC system (Finland). The control rod drives have been refurbished at General Atomics in San Diego in 2006 to 2009.

Boron Neutron Capture Therapy (BNCT) work dominates the current utilization of the reactor. The weekly schedule allows still three days for other purposes such as isotope production, neutron activation analysis as well as education and training [1]. The operating

licence of the reactor was extended for the period 2011 to 2023 by the government of Finland in December 2011.

The new nuclear energy legislation in Finland requires that also a research reactor shall have a document describing the management of the ageing management. FiR 1 – ageing management program was created as reported at the RRFM-2011 [2]. When creating that document also the ageing management system is being further developed. Inspection and service procedures are extended and improved. An obsolescence management system for the systems, structures, and components (SSC's) has been created. The SSC's important to safe and reliable operation of the reactor have been identified as well as their degradation processes that affect safety.

2. Role of periodic inspections in the ageing management

To improve the ageing management the quarterly and yearly inspections are extended to all SSC's and the data logging is improved to aid the analysis of the ageing process.

Many systems have been checked even daily and weekly for proper operation, that is that the signal is at proper level, but the devices have never been thoroughly inspected. Previously mainly the nuclear channels and scram logic systems have been thoroughly checked. Now systems like conductivity measurements, pH measurement, tank level measurement, pressure, temperature and flow measurements are added in to the yearly inspection program with systematic testing and inspection of the devices.

3. Improved ageing management and maintenance system for the electronic instrumentation

3.1 Equipment registry system

To improve the ageing management and maintenance system for the electronic instrumentation all electronic units are labelled individually and registered into an equipment registry system (Efecte, Finland). The operational, storage, inspection and maintenance history of each unit is recorded into the system. Based on the stored data a failure statistics is created.

Along with the equipment registry system the documentation of the reactor control system has been improved by creating new a block diagrams of the whole system at different detail level down to single unit level.

3.2 Survey of the environmental and general conditions

The environmental conditions affecting ageing and damaging of the components are surveyed. Temperature and humidity in the reactor control room as well inside the cabinets is followed with a data logger for one year. A thorough inspection of the general condition of all the electronics cabins and the wirings and components has been performed. Some deteriorated fastenings of single components like relays were observed. Risk for whiskers in the control units was identified.

3.3 Improving periodic inspections

The quarterly and yearly inspection programs are revised. As a new procedure the units in operation are imaged with a thermographic camera. The condition of the most critical

components, like relays, is studied. Visual inspections and documentation of the condition of instrument cabins, electronic units, relays and other components are performed.

4. Reserve units for the measurement and control system

Reserve units for the Valmet Elmatic measurement and control system were acquired from recently closed pulp and paper mill. Two full cabins of units were received. The condition of these units was inspected using visual inspection with high resolution digital cameras. The dust was analysed and the presence of Whiskers was studied.

Two display units and a set point unit were readily utilized. All other units in generally acceptable condition were set to reserve. They are stored in ESD compatible storage boxes or in five instrument crates in a storage cabin at the reactor. Before taking them into use they will be inspected in detail.

One valuable addition to our Valmet Elmatic system was a separate test crate with own power supplier.

5. Ensuring maintenance of the nuclear channels

The contacts to the KFKI-RegTron Instrumentation & Measuring Co., Ltd, Budapest, Hungary were updated and a broken electronic card from the nuclear channel units was sent for repair to Budapest. The card was successfully repaired in a timely fashion.

6. Improving the maintenance and inspection environment for the electronics at the reactor

An ESD compatible electronic workshop was established at the reactor for maintenance and inspection of the instrumentation units. ESD carpets have been installed in front of all electronics cabins including the reactor control panel to avoid static electric shocks to the sensitive electronics.

7. Conclusions

The systematic approach of the ageing management system combined with collaboration with specialists in the ageing of electronic components has given impetus to many improvements in the inspection, maintenance and management of the measurement and control system of the FiR 1 TRIGA reactor. The active approach taken has also lead to acquisition of reserve parts for the discontinued Valmet Elmatic measurement and control system.

References

1. Auterinen I, Salmenhaara S.E.J, The 250 kW FiR 1 TRIGA Research Reactor - International Role in Boron Neutron Capture Therapy (BNCT) and Regional Role in Isotope Production, Education and Training, Research Reactors: Safe Management and Effective Utilization - Proceedings of an international conference held in Sydney, Australia, 5-9 November 2007, Proceedings of an International Conference organized by the International Atomic Energy Agency (IAEA), IAEA-CN-156, 2008.
http://www-pub.iaea.org/MTCD/publications/PDF/P1360_ICRR_2007_CD/datasets/I.H.%20Auterinen.html

2. Auterinen I, Kivelä P, Developing Ageing Management for the Fir 1 TRIGA Reactor in Finland, RRFM 2011 Transactions, European Nuclear Society, 2011.

EXPERIMENTAL AND CALCULATED DATA ON CRITICALITY OF URANIUM-ZIRCONIUM HYDRIDE SYSTEMS WITH 21% ENRICHED URANIUM-235

S. Sikorin, S. Mandzik, S. Polazau, T. Hryharovich, Y. Palahina

*Joint Institute for Power & Nuclear Research - Sosny,
National Academy of Sciences of Belarus, 99 Acad. Krasin str., Minsk 220109, Belarus*

ABSTRACT

Experiments on criticality of uranium-zirconium hydride systems were performed on the critical facilities EDELVEIS, GFS, KRISTAL and GIACINT of the Joint Institute for Power and Nuclear Research-Sosny (JIPNR-Sosny) of National Academy of Sciences of Belarus. Critical facilities were designed to simulate different reactor core configurations using different fuel with water and zirconium hydride moderators for development of new reactors of different function and benchmark experiments. The experiments were performed with 21%, 36% and 45% enriched uranium fuels. Water, zirconium hydride, beryllium and stainless steel were used in the reflector. The results of experiments on critical facilities with zirconium hydride have been analyzed by creating detailed calculation models and performing simulations for the different experiments. In addition, the sensitivity of the obtained results for the material specifications and the modelling details has been examined. The critical assemblies with zirconium hydride moderator represent a hexagonally pitched lattice of two types of fuel assemblies and absorber rods. In this paper, the model details, the results for uranium fuel enrichment 21% in different configurations and the results sensitivity for the model details are presented. The analyses used the MCNP and MCU computer programs. In addition, the impact of using different nuclear data files is examined.

1. Introduction

The Joint Institute for Power and Nuclear Research-Sosny of National Academy of Sciences of Belarus has developed several critical facilities for testing various reactor configurations with a zirconium hydride moderator and different nuclear fuels and reflector materials. The experiments were performed with 21%, 36% and 45% enriched uranium-235 fuels. The absorber materials were boron, europium, cadmium. Four critical facilities, EDELVEIS, GFS, KRISTAL и GIACINT, have been developed to test about a hundred critical assemblies with a zirconium hydride moderator of various usage, including:

- uniform heterogeneous uranium – zirconium hydride lattices from hexagonal cassettes with cylindrical fuel rods, 21% and 36%, with and without zirconium hydride, beryllium and stainless steel reflectors, containing absorbers, such as cadmium wire, boron plates and rods;
- nonuniform heterogeneous multi-zone uranium – zirconium hydride lattices from hexagonal cassettes with cylindrical fuel rods, 21%, 36% and 45%, boron absorber plates, boron and europium absorber rods, zirconium hydride, beryllium and stainless steel reflectors, simulating different versions of cores in the mobile nuclear power plant “Pamir 630D”, cooled by dissociative coolant, nitrogen tetroxide $N_2O_4 \leftrightarrow 2NO_2 \leftrightarrow 2NO + O_2$.

Data presented in this paper are based on experimental results, obtained at EDELVEIS, GFS and GIACINT critical facilities with lattices from hexagonal cassettes with cylindrical 21% uranium-235 fuel rods, zirconium hydride moderator, zirconium hydride – stainless steel and zirconium hydride – beryllium reflectors. This paper presents calculation and experimental results.

2. Critical facilities EDELVEIS, GFS and GIACINT

The EDELVEIS critical facility (Fig. 1) was used for experiments with cold critical assemblies with water and zirconium hydride moderators. The technological equipment for these facilities was located in a special room with reinforced concrete walls. The critical facility included a critical assembly, placed on supporting steel structures, a control and protection system and other equipment. The critical assemblies were fabricated from hexagonal cassettes with water and zirconium hydride moderators, placed on steel supporting grid for fixing the cassettes at specified distances, as well as cassettes and units of the reflector. Neutron detectors were placed around the critical assembly in plexiglas hoods. The control rod drives of the regulation and emergency protection system were installed on special sites above and below the critical assembly. The start-up Pu-Be neutron source with remote control was arranged in a special protection container. The critical assembly control board was arranged in a separate room.

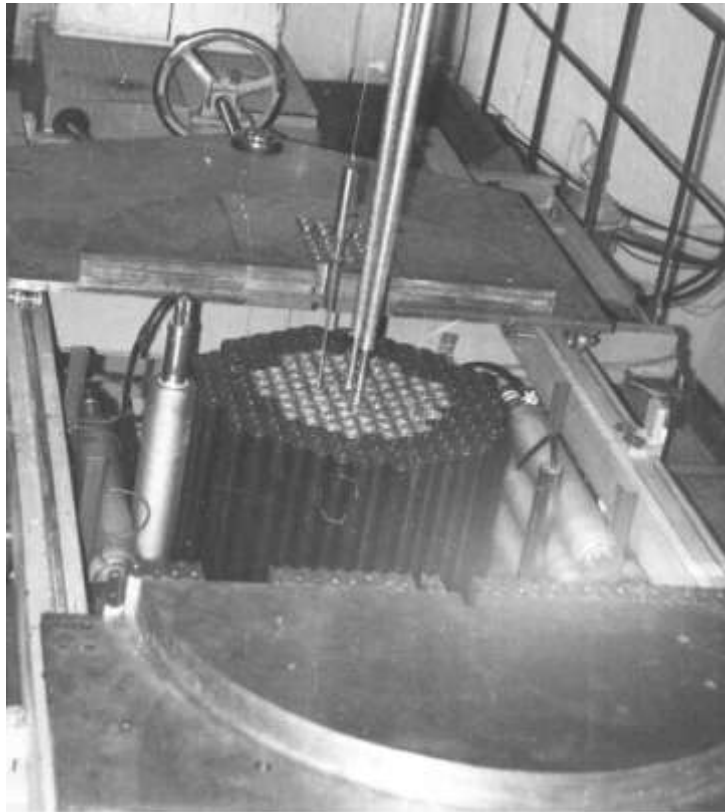


Fig. 1. The EDELVEIS critical facility

The GFS critical facility (Fig. 2) was developed for experiments with cold and hot critical assemblies with zirconium hydride moderator. Its structure was similar to the EDELVEIS critical assembly; however, it allowed experiments heating the critical assemblies to 300 °C. The critical assemblies were made from hexagonal cassettes with zirconium hydride moderator, placed on a steel support grid for fixing these cassettes at specific distances, and cassettes with zirconium hydride and steel units of the reflector. The critical assemblies were located in a tank installed on supporting steel structures. The same tank housed a heating electrical furnace.

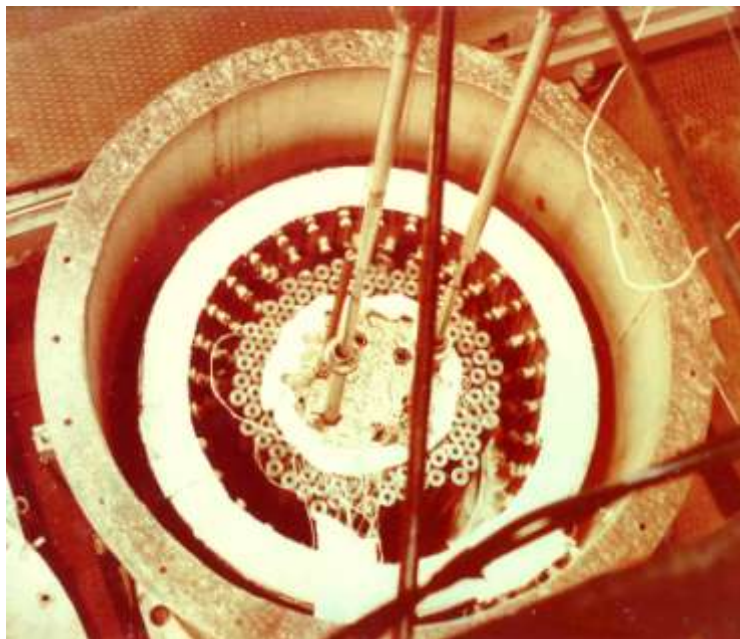


Fig. 2. The GFS critical facility

The GIACINT critical facility (Fig. 3) was designed to make experiments with cold critical assemblies with water or zirconium hydride moderator and also without a moderator. A special hydraulic system is used to perform experiments with water moderator. Otherwise, this facility is similar to the EDELVEIS critical facility.

3. Experimental results

Three experimental configurations with 21% uranium-235 nuclear fuel are discussed.

3.1 Experiments at the EDELVEIS critical facility

This critical facility represented a hexagonal grid, 45 mm pitch, and included fuel cassettes with zirconium hydride moderator, channels for regulation and emergency protection control rods, and cassettes of the zirconium hydride and beryllium moderator.



Fig. 3. The GIACINT critical facility

The cladding of the fuel cassette was a thin-wall hexagonal tube made of 0X18H10T steel, for a 44 mm wrench, and the 0.4 mm wall. The hexagonal tube was connected to the shank. The upper part of the cassette has a head to capture the cassette during handling (use only on the GIACINT critical facility). The hexagonal tube housed 12 hexagonal moderator units from zirconium hydride $ZrH_{1,9}$, each 50 mm high, for a 42,85 mm wrench. The moderator unit had seven holes, 8.2 mm dia., located with 14.5 mm pitch on the triangular grid; these holes housed the channel tubes from 0X18H10T steel, with 8 mm outer dia., and 0.25 mm wall. Each cassette included seven fuel rods. The fuel cassette is shown in Fig. 4. The fuel rod (Fig. 5) includes a fuel core, cladding, two holders, a spring and end parts, i.e., upper and lower plugs. The fuel rod cladding is made from 0X16H15M3B steel, with the 6.2 mm outer dia., and 0.4 mm wall. The fuel core includes tablets, 5.2-5.3 mm dia. and 5-7 mm height, made from uranium dioxide 10.2 g/cm^3 . The uranium-235 enrichment is 21%. The total core height is 500 mm. The uranium-235 mass in the fuel rod is 20.5 g. The core is placed and fixed inside the cladding by means of a spring, fixing devices and end parts. The fuel rod is tightly sealed, by welding the upper and lower plugs to the fuel rod cladding. The total fuel rod length is 651 mm. The fuel rod cladding has a wire coiled, 100 mm pitch, 09X16H15M3B steel, the diameter 0.55 mm, which is welded at the fuel rod ends.

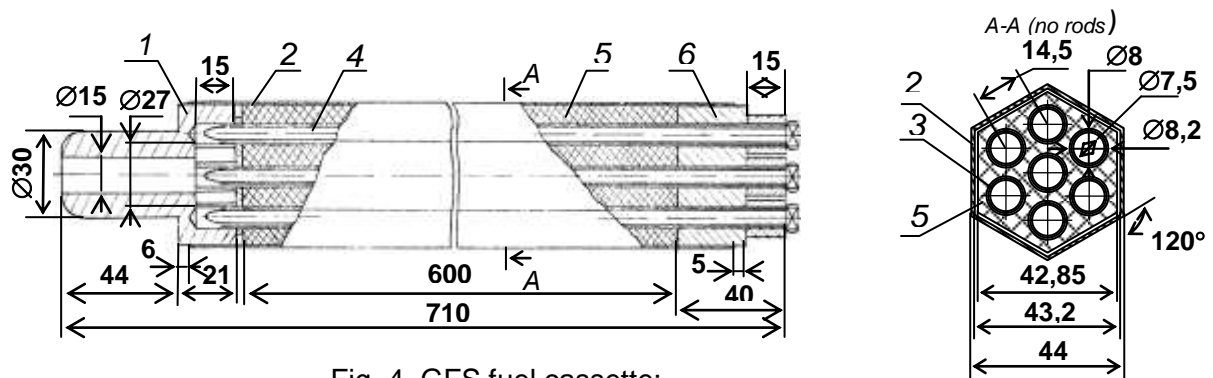
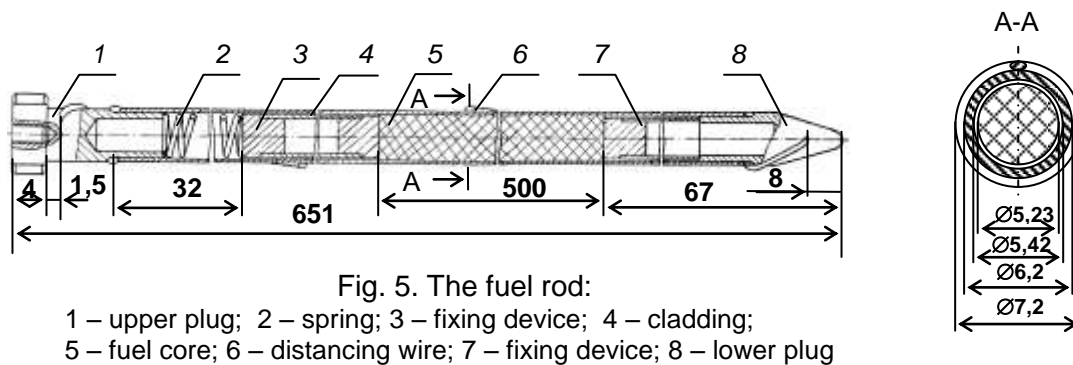


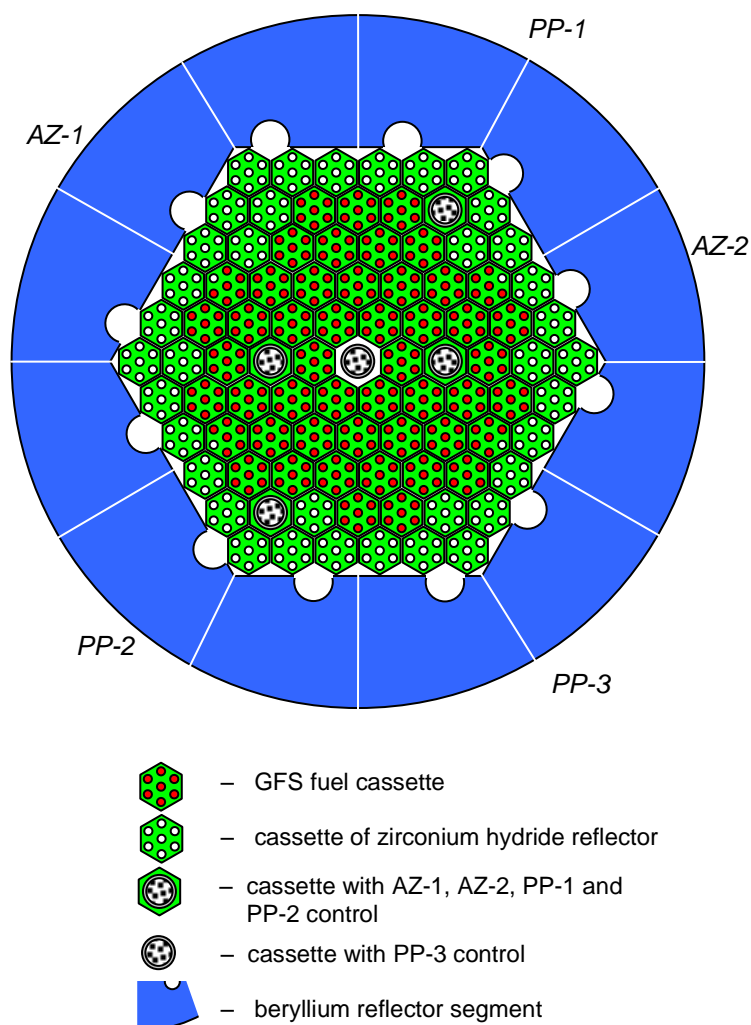
Fig. 4. GFS fuel cassette:

- 1 — shank with the lower tube plate; 2 — body; 3 — casing pipe; 4 — fuel rod;
5 — zirconium hydride units; 6 — upper tube plate



The side reflector of the critical assembly was of the above cassettes with zirconium hydride without fuel rods and segments of the beryllium reflector. The beryllium reflector was assembled from 12 segments. Its assembly represents a cylinder, 714 mm in dia. and 600 mm height, with a hexagonal hole for a 438 mm wrench. Each segment has an axial recession on the edge facing the hexagonal hole. The lower end reflector of the critical assembly included zirconium hydride and lower steel end parts of the fuel rods and fuel cassettes, the supporting grid, 715 mm dia. and 40 mm thick from 12X18H9T steel, and the 1500X1300 mm support plate 140 mm thick, made from Cт3 steel. The upper end reflector of the critical assembly included zirconium hydride and upper steel end parts of the fuel rods and fuel cassettes.

The critical assembly has two emergency protection rods and three regulating control rods. The emergency protection rods are made from tubes, 22 mm dia. and 0.3 mm thick, from X18H10T steel, filled with boron carbide 1.2 g/cm³ over 650 mm length. To move these control rods, the core includes channels from a hexagonal tube made of 0X18H10T steel, 640 mm long, fit for a 44 mm wrench, and 0.4 mm wall, containing hexagonal zirconium hydride $ZrH_{1.9}$ units, for a 42,85 mm wrench, and a central 33.5 mm hole and a tube from X18H10T steel, 33.5 mm dia. and 0.4 mm wall. Two regulating control rods were made from tubes made of X18H10T steel, 26 mm dia. and 0,3 mm wall, filled with boron carbide 1.2 g/cm³ over 510 mm. To move these control rods, channels were arranged in the core similar to emergency protection rods, with an additional tune of X18H10T steel, dia. 32 mm



and 1 mm wall. A third regulating control rod was made of 0X16H15M3B steel, as a tube with 7 mm dia. and 0.35 mm wall, filled with boron carbide 1.2 g/cm^3 over 500 mm. To move this control rod, a tube made of X18H10T steel, 32 mm dia. and 1 mm wall, was arranged in the core.

The critical load was 49 fuel cassettes with 339 fuel rods. This critical assembly configuration is shown in Fig. 6.

3.2. Experiments at the GFS critical facility

This critical assembly is a hexagonal grid, a 45 mm pitch, of fuel cassettes with zirconium hydride moderator, cassettes of the zirconium hydride reflector and steel reflector units. The critical assembly was located in the electrical heating furnace in the tank made of Cт3 steel.

These fuel cassette, fuel rod and reflector cassette are described above. The heating furnace made of Cт3 steel, 840 mm dia. and 930 mm high, included the bottom and the side cylindrical surface. The electrical furnace lid was removed, since the experiments were at room temperature. The furnace heat insulation was 110 mm, made of laminated thin Cт3 stainless steel sheets. The heating furnace with the critical assembly was located in a Cт3 steel tank, 1300 mm dia. and 1280 mm high, with a 5 mm lip and 10 mm bottom. The tank lid was removed during the experiments. The side reflector of the critical assembly was a row of zirconium hydride reflector cassettes and two rows of steel reflector units, representing cylinders made of steel, 44 mm dia. and 660 mm high. The lower end reflector of the critical assembly included zirconium hydride and lower steel end parts of fuel rods and fuel cassettes, a support grid 715 mm dia., made of 12X18H9T steel, a 1500X1300 mm support plate 140 mm thick, made of Cт3 steel, the electrical furnace bottom of Cт3 steel, and the tank bottom, 10 mm thick, made of Cт3 steel. The upper end reflector of the critical assembly included zirconium hydride and upper steel end parts of fuel rods and cassettes.

The critical assembly had two emergency protection rods, two regulating control rods and one compensation rod. The emergency protection and compensation rods and one regulating control rod were made from X18H10T steel tubes, 26 mm dia. and 0,3 mm wall, filled with boron carbide 1.2 g/cm^3 over 650 mm (emergency protection rods) and 575 mm (compensation emergency rod). In order to locate emergency protection and

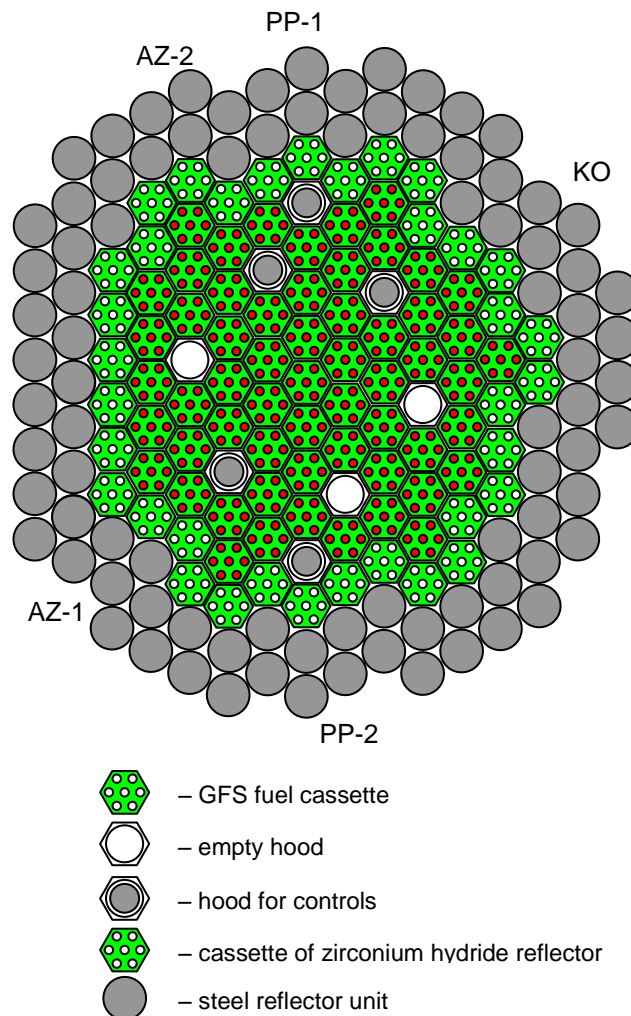


Fig. 7. Cartogram of the critical assembly load at the GFS critical facility

compensation rods, channels were arranged in the core, made of hexagonal 0X18H10T steel tubes, 640 mm in length, fitting to a 44 mm wrench, and 0.4 mm wall; they housed X18H10T steel tubes, 32 mm dia. and 2.5 mm walls. The second regulating control rod included the upper absorbing and the lower dissipating parts. The absorbing part was made as coaxial tubes, from ЭИ435 steel, 33 mm dia. and 0.8 mm wall, as well as 17 mm dia. and 0.5 mm wall; the ring cavity between them was filled with europium oxide 5.3 g/cm^3 over 400 mm. The inner part of the tube, 17 mm dia., was filled with aluminium oxide, 2.1 g/cm^3 . The dissipating part of the regulating control rod was a ЭИ435 steel tube, 33 mm dia. and 0.8 mm wall, filled with aluminium oxide 2.1 g/cm^3 over 417 mm. To operate this regulating control rod, the core had a channel of a hexagonal 0X18H10T steel tube, 640 mm long, fitting a 44 mm wrench, and 0.44 mm wall, which housed a X18H10T steel tube, 40 mm dia. and 2 mm wall. In addition, the core included three channels for locating additional compensation rods, made from a hexagonal 0X18H10T steel tube, 640 mm long, fitting a 44 mm wrench, and 0.4 mm wall, which housed a X18H10T steel tube, 32 mm dia. and 2.5 mm wall.

The critical load was 58 fuel cassettes, with 406 fuel rods. This critical assembly configuration is shown in Fig. 7.

3.3 Experiments at the GIACINT critical facility

This critical assembly is a hexagonal grid, a 45 mm pitch, of fuel cassettes with zirconium hydride moderator, regulating, compensating and emergency protection control channels, cassettes of the zirconium hydride reflector and steel reflector units.

These fuel cassette, fuel rod and reflector cassette are described above. The steel reflector unit is made of 12X18H10T steel and is a weight-and-size simulator of the fuel cassette. The side reflector of the critical assembly includes one row of zirconium hydride cassettes of the reflector and two rows of steel reflector units. The lower end reflector of the critical assembly included zirconium hydride and lower steel end parts of the fuel rods and fuel cassettes and a support plate, 950 mm dia. and 65 thick, made of 12X18H10T steel. The upper end reflector of the critical assembly was from zirconium hydride and upper steel end parts of the fuel rods and cassettes, including also upper end reflector units, 62 mm high from X18H10T steel, installed on the cassettes.

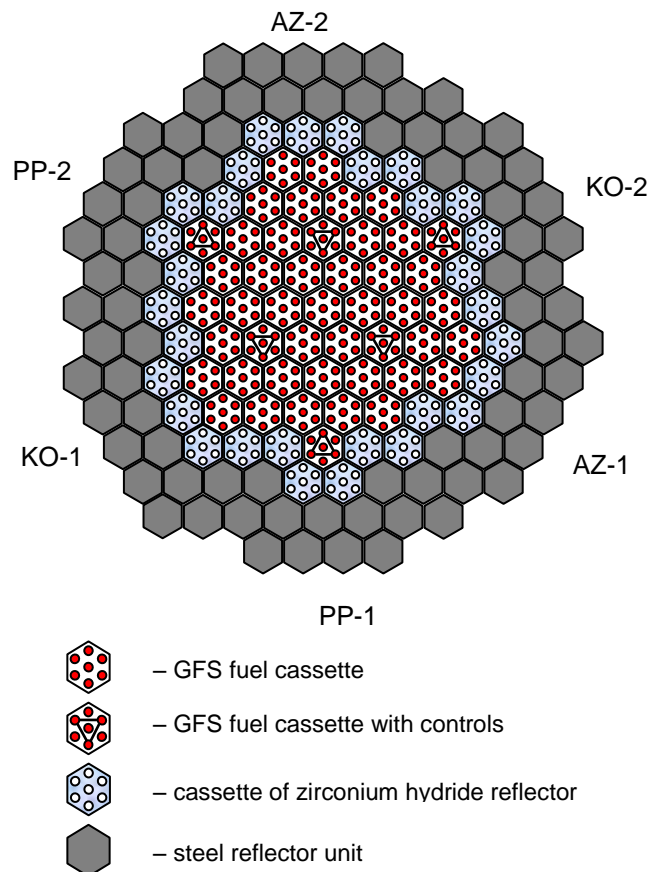


Fig. 8. Cartogram of the critical assembly load at the GIACINT critical facility

The critical load was 46 fuel cassettes with 322 fuel rods. This critical assembly configuration is shown in Fig. 8.

4. Calculation results

Calculations of critical assemblies were made using mathematical codes of MCNP-4A and MCU-RFFI. In creating calculation models of the above uranium – zirconium hydride critical assemblies, in addition to the component parts of the fuel cassettes, emergency protection, compensation and regulating control rods, cassettes, units and segments of the reflector the following design elements of critical assemblies were taken into consideration: the spacing and supporting grids (spacers), electrical heating furnace and critical assembly tank. The effects of the Plexiglas hood with the neutron detector, located behind the side reflector of the emergency protection controlees, and of the reinforced concrete walls, ceiling and floor in the rooms with the critical assemblies were not taken into consideration. The calculation results are given in Table 1.

Nos.	Critical facilities	Number of fuel cassettes /rods	Cassette pitch, mm	Calculated value K_{eff}	
				MCNP-4A	MCU-RFFI
1	EDELVEIS	49/339	45	1.00919 (± 0.00043)	0.9981 (± 0.0007)
2	GFS	58/406	45	1.01142 (± 0.00043)	—
3	GIACINT	46/322	45	1.0197 (± 0.0005)	1.0173 (± 0.0010)

Table 1. Calculated effective neutron multiplication factor, K_{eff}

5. Conclusions

Experiments to test criticality of uranium – zirconium hydride hexagonal multiplying systems with 21% uranium-235 nuclear fuel were performed on the EDELVEIS, GFS and GIACINT critical facilities. The experimental results for the three critical assemblies were evaluated using Monte Carlo calculation codes MCNP-4A and MCU-RFFI and relevant nuclear data libraries. The calculation results matched well the experimental results, except the ones obtained at the GIACINT critical facility, which requires additional studies.

THE DESIGN OF ADDITIONAL SAFETY CONTROL RODS FOR NIRR-1 HEU AND PROPOSED LEU CORES USING MCNP CODE

Y. V. IBRAHIM, S. A. JONAH

Centre for Energy Research and Training, Ahmadu Bello University, Zaria, Nigeria.

ABSTRACT

A Monte Carlo Simulation of additional safety rods for NIRR-1 HEU and LEU cores was carried out using the MCNP5 version 5 Code. Two Additional Safety Control Rods having the same material composition as the main central control rod except for the surface area were studied. The following reactor core physics parameters were determined; neutron flux distribution within the core with safety rods in completely withdrawn position, Control Rod (CR) worth for each rod, core excess reactivity, shutdown margin and some kinetic parameters. Results obtained indicate that it would be feasible to include two additional safety control rods to improve the safety level of MNSR with little or no modification to the existing core configuration.

1.0 Introduction

The Nigeria Research Reactor-1 (NIRR-1) is a low power reactor, which was designed with one central control rod that performs safety and regulatory functions (Jonah et al, 2007; SAR, 2005). Control rods are strong neutron absorbers that can be inserted or withdrawn from the core. They are basically used to compensate for the excess reactivity necessary for long term core operation and also to adjust the power level of the reactor in order to bring the core to power, follow load demands and shutdown the reactor (Stamatelatos, et al, 2007; Varvayanni, et al, 2009).

The design of the NIRR-1 reactor has been carried out in accordance with the Chinese standards with some attention focused on relevant International Atomic Energy Agency (IAEA) standards (IAEA, 2009). However, this design is not fully in conformance with the IAEA safety standards. In particular, the lack of redundancies of control rods and neutronics does not provide for protection against single failure. Even though the reactor is inherently safe due to high negative temperature coefficient of reactivity, which provides self-limiting power excursion characteristics, reactor safety experts have recommended for redundancies in design for reliability of systems important to safety (IAEA, 2005).

In order to address the single point failure of the current Highly Enriched Uranium (HEU) core and consequently improve the safety of the MNSR without any modification to the fuel region in the core, the inner irradiation channels of the reactor has been used to introduce two Additional Safety Control Rods (ASCRs). The control rods introduced will work simultaneously and it is proposed to be controlled by a single mechanical device such that when scrammed into the reactor, they would fall under gravity. Conversion studies of the NIRR-1 from the current HEU to Low Enriched Uranium (LEU) core began in 2006. An input deck was created for the reactor using the MCNP 4C code and benchmarked against experimental results (Jonah et al, 2007). Calculations indicated that it is possible to convert the reactor from 90.2% HEU Al_4 to 12.5% LEU UO_2 fuel (Jonah et al, 2009). Because the conversion to LEU was envisaged, the potential LEU core was also modified with the two Additional Safety Control Rods.

2.0 Description of NIRR-1 Reactor

Detailed description of the reactor can be found elsewhere (Jonah et al, 2007). The reactor was modified to include two additional safety control rods totally inserted in the inner irradiation channels located at angles 0° and 144° as displayed in Figs. 1a-c. The inner irradiation channels are placed 40mm above the bottom of the core through which the ASCRs move to cover a distance of 190mm (i.e. 230mm-40mm) in the core. The total vertical distance travelled by the ASCRs is 192mm. The diameter of each ASCR is 18mm including clad thickness of 0.5mm. The geometric representation of the central control rod and ASCR when fully inserted as simulated by the MCNP is shown in Figs. 2a and b.

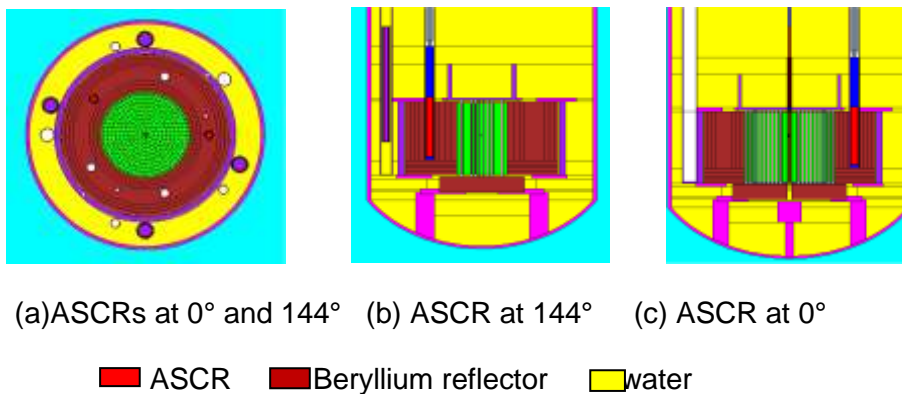


Fig.1 Cross section through the NIRR-1 reactor showing ASCRs

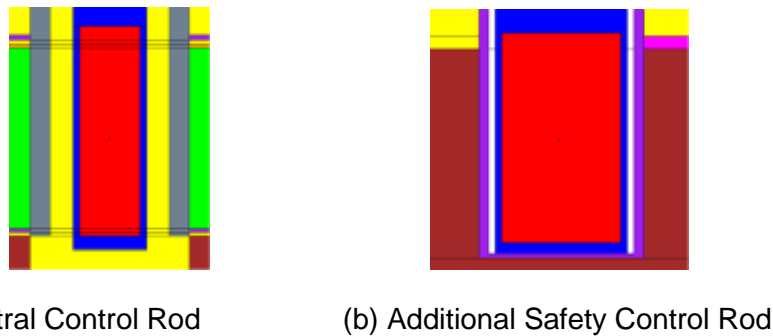


Fig.2 MCNP geometric representation of central and ASCRs

3.0 MCNP Modeling and Simulation

In modeling the ASCR, the dimensions and material composition of the central control were optimized through the introduction an ASCR into one of the unconnected inner irradiation channels. The length of the cadmium was reduced in the case of the ASCR since the level of the irradiation channels are 40 mm above bottom core region. Criticality calculations were then performed with the ASCR in completely inserted position keeping the central control completely withdrawn until a sub-criticality was achieved. Runs performed for nuclear criticality did not give sub-criticality therefore; the absorber's surface area was

increased. This was done up to a maximum diameter of 18mm with 2mm gap between the ASCR and the inner walls of the irradiation channel. Because sub-criticality was not achieved, another ASCR was introduced with the first kept in completely inserted position and the diameter was also increased gradually until sub-criticality was achieved. This was also achieved with a diameter of 18mm for the second rod. The ASCRs were inserted into two unconnected inner irradiation channels located at angles 0° and 144° which were named A and B respectively. The choice to maintain properties of the main control rod was made because of ease of manufacture and good properties of cadmium absorber [Bretscher, 1997; Ismail, 2010; Shoushtari et al, 2010). Reactor safety rods must effectively absorb neutrons since they are mainly used for emergencies.

The 3D- MCNP model of the NIRR-1 was simulated to estimate the nuclear criticality k_{eff} , excess core reactivity ρ_{ex} , control rod worth ρ_w , effective delayed neutron fraction β_{eff} and neutron flux. Neutron transport simulations were performed for a clean cold core (zero burn-up). Criticality calculations were performed using the KCODE option to determine the k_{eff} and corresponding ρ_{ex} with all fuel elements as fission source points. In the analysis 500, 000 neutron particle source histories per cycle were made for 830 criticality cycles including 30 inactive cycles. The inactive cycles were allowed for convergence of k_{eff} and fission distribution. The MCNP criticality calculations were normalized to the steady state full power level. Using the FM card, a value of 2.4 was used for the average number of neutrons per fission at steady state operation which is used in computing the source strength by which all the tallies are scaled.

4.0 Results and Discussion

The result obtained for the nuclear criticality, excess reactivity and control rod worth for the HEU core were compared with measured value to check the effect of the modification of the cross section data at typical pool temperature. The result obtained for HEU and LEU cores are presented in Table 1.

Parameter	Experiment	HEU			LEU		
Rods-out (k_{eff})	-	1.00474 ± 0.0005			1.00474 ± 0.0004		
Main rod-in (k_{eff})	-	0.99714 ± 0.0004			0.99824 ± 0.0004		
A-in k_{eff}	-	1.00165 ± 0.0004			1.00164 ± 0.0004		
B-in k_{eff}	-	1.00169 ± 0.0004			1.00181 ± 0.0004		
ρ_{ex} (mk)	4.99–1.2 = 3.77	4.72 ± 0.05			4.72 ± 0.05		
Rod worth (mk) 7.0		Main	A	B	Main	A	B
		7.59	3.07	3.03	6.48	2.97	2.91
ASCRs worth (mk)	-	6.10			5.88		
Shutdown margin (mk)							
Main CR	3.33	2.87			1.76		
A and B		1.38			1.16		
β_{eff} (mk)	0.0081	0.00834 ± 0.0004			0.00849 ± 0.0004		

Table 1 Calculated neutronics parameters for NIRR-1 HEU and LEU cores.

Table 1 shows some eigenvalues with relative errors for NIRR-1 when rods are out of the core and also the eigenvalues when each of the three rods is fully inserted in the core for HEU and LEU. The worth of each rod was calculated. The worth of main control rod was found to be 7.62mk for the HEU which is quite close to the measured value of 7.0mk (SAR, 2005) and value reported by some authors (Jonah et al, 2007) while that of LEU was found to be 6.48mk which is in agreement with reported value (Jonah et al, 2009). This decrease in rod efficiency is expected for the LEU and can be attributed to the increase in the inventory of ^{238}U in LEU resulting in the hardening of the spectrum. The worth of A and B was

calculated to be 3.07mk and 3.03mk for HEU and 2.97 and 2.91 for LEU respectively. The combined worth for A and B were calculated to be 6.10mk and 2.88mk for HEU and LEU respectively. In both cores, sub-criticality was achieved. During the zero power experiment, the available excess reactivity for NIRR-1 was 4.97mk. Due to licensing condition, a permanent poison of worth (-1.2mk) to bring the value to 3.77mk. The core excess reactivity of 4.72 ± 0.05 is quite close to the measured value.

In the estimation of the effective delayed neutron fraction, two calculations were made. In the first the parameter “totnu yes” and the second “totnu no” were used while rods A and B were withdrawn and the value of the effective delayed neutron fraction obtained are presented in Table 1 for HEU and LEU cores. The effective delayed neutron fraction obtained for the HEU and LEU cores are statistically indistinguishable. This suggests that effective delayed neutron fraction does not significantly depend on the fuel type. This was also observed by some authors (Snoj et al, 2010).

The shutdown margin of 2.87mk obtained for the central control rod for HEU core is quite close to the measured value of 3.33mk (SAR, 2005) and reported value (Jonah et al, 2007). This value is lower for the LEU as expected. The shutdown margin for the ASCRs for HEU and LEU cores were calculated to be 1.38mk and 1.16mk respectively. Again, the same is observed with the ASCRs as you move from HEU to LEU. Using this value calculated for ASCRs in equation 4 implies that in the event of rod stuck situation of the central control rod withdrawn or when the rods are scrammed into the reactor, the power level will drop by 90% and 88% for HEU and LEU cores respectively. The flux magnitudes calculated in the inner and outer channels for HEU and LEU cores are presented in Table 2.

Fuel	Thermal 0.625 eV($\text{ncm}^{-2}\text{s}^{-1}$) $\times 10^{12}$		Epithermal(0.625 eV–0.825 MeV) $\text{ncm}^{-2}\text{s}^{-1} \times 10^{12}$		Fast (0.825–20 MeV) $\text{ncm}^{-2}\text{s}^{-1} \times 10^{12}$	
	Inner	Outer	Inner	Outer	Inner	Outer
HEU	1.16 ± 0.01	0.66 ± 0.01	1.29 ± 0.01	0.19 ± 0.01	0.27 ± 0.01	0.04 ± 0.003
LEU	1.04 ± 0.01	0.62 ± 0.01	1.26 ± 0.01	1.18 ± 0.01	0.26 ± 0.01	0.04 ± 0.003

Table 2 Calculated flux for NIRR-1 HEU and LEU inner and outer irradiation channels.

From the results in Table 2, the calculated thermal neutron flux value in the inner channel for the HEU core was $(1.16 \pm 0.01) \times 10^{12} \text{ n/cm}^2.\text{s}$ at an axial height of -3.32cm. This value is in good agreement with the value of $(1.1 \pm 0.2) \times 10^{12} \text{ n/cm}^2.\text{s}$ (SAR, 2005) measured during the steady state operation at full power (30kW) at commissioning and reported value (Jonah et al, 2007). This value is also consistent with measured data of $(5.4 \pm 0.2) \times 10^{11} \text{ n/cm}^2.\text{s}$ (Jonah et al, 2005) using Al-0.1%Au foil activation detector at a steady state power of 15kW. For the LEU, the calculated value obtained was $(1.04 \pm 0.01) \times 10^{12} \text{ n/cm}^2.\text{s}$ which agrees with reported value (Jonah et al, 2009). Since the ASCRs will remain withdrawn during normal operation, their effect on flux distribution when inserted was not studied. As in accordance with calculations and measurements performed for the main control rod, the integral worths of ASCRs were calculated. Data obtained as the ASCRs are inserted in bank, a plot of reactivity versus depth of insertion for the HEU and LEU cores are shown in Fig. 3.

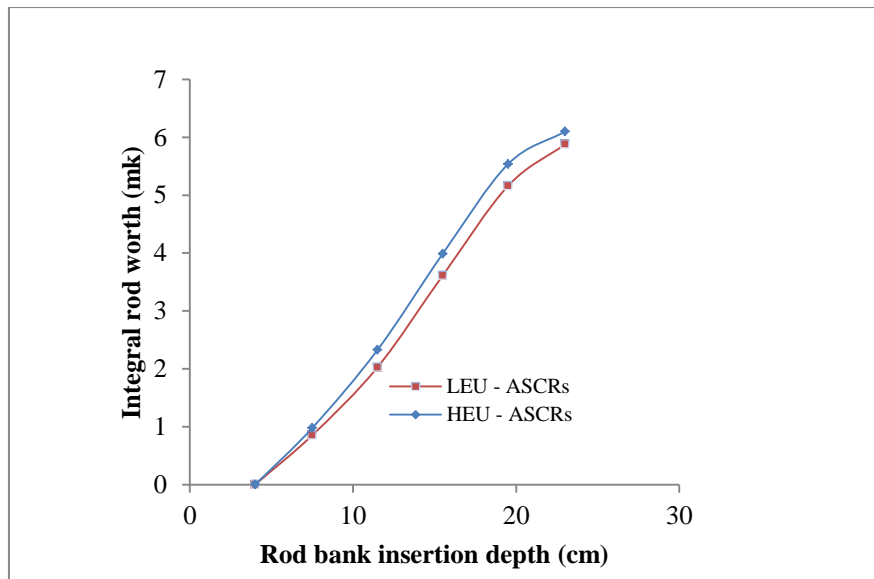


Fig.3 Integral worth of ASCRs versus depth from the bottom of inner channels for HEU and LEU cores.

5.0 Conclusion

The MCNP model of NIRR-1 developed for the conversion of NIRR-1 to LEU was modified to simulate two ASCRs to enhance safety. Neutronics data obtained indicates that it is possible to include two ASCRs with little or no changes to the existing HEU core. Furthermore, the introduction of the two ASCRs has no effect on the neutron distribution in completely out position.

Acknowledgement

This work is supported in part by the IAEA Coordinated Research Project entitled "Conversion of MNSR from HEU to LEU" NIR/13934.

References

- Bretscher, M. M., 1997. Computing Control Rod Worths in Thermal Research Reactors. Reduced Enrichment for Research and Test Reactors Program, ANL/RERTR/TM-29, Argonne, USA.
- International Atomic Energy Agency, 2005. Safety of Research Reactors, IAEA Standard Series, Safety Requirements No. NS-R-4, Austria, Vienna.
- International Atomic Energy Agency, 2009. Report of the Integrated Safety Assessment of Research Reactors Mission to the Nigeria Research Reactor-1, IAEA-TCR-05184, 21-23 December, 2009.
- Ismail, S., 2010. Design of Epithermal Neutron Irradiation Site in the Syrian MNSR. Progress in Nuclear Energy 58, p. 569-572.

- Jonah, S. A., Ibikunle, K, Li Y., 2009. A Feasibility Study of LEU Enrichment Uranium fuels for MNSR conversion using MCNP. *Annals of Nuclear Energy* 36, p. 1285-1286.
- Jonah, S. A., Liaw J. R., Matos, J. E., 2007. Monte Carlo Simulation of Core Physics Parameters of Nigerian Research Reactor-1. *Annals of Nuclear Energy* 34, p. 953-957.
- SAR, 2005. Final Safety Analysis Reportss of Nigerian Research Reactor-1, CERT Technical Report-CERT/NIRR-1/FSAR-01.
- Shoushtari, M. K., Kakavand, T., Sadat Kiai S. M., Ghaforian, H., 2010. Monte Carlo Simulation of Research Reactor with Norminal Power of 7 MW to Design New Control Safety Rods. *Nuclear Instrumentation and Methods in Physics Research B* 268, p. 519-523.
- Snoj, L., Kavcic, A., Zerovnik, G., Ravnik, M., 2010. Calculation of Kinetic Parameters for Mixed TRIGA Cores with Monte Carlo. *Annal of Nuclear Energy* 37, p. 223-229.
- Stamatelatos, I. E., Varvayanni, M., Tzika, F., Ale, A. B. F., Catsaros, N., 2007. Monte Carlo Simulation of the Greek Research Reactor Neutron Irradiation Facility. *Nuclear Instrumentation and Methods in Physics Research B* 263, p. 136 – 139.
- Varvayanni, M., Savva, P., Catsaros, N., 2009. Control Rod Worth Calculations Using Deterministic and Stochastic Methods. *Annal of Nuclear Energy* 36, p. 1718-1725.

An alternative chemical cleaning procedure for blank monolithic U-Mo foils

B. Baumeister^{a)}, W. Schmid^{a)}, F. Kraus^{b)}, W. Petry^{a)}

*a) Technische Universität München, Forschungs-Neutronenquelle Heinz Maier-Leibnitz (FRM II)
Lichtenbergstr. 1, 85748 Garching bei München*

*b) Technische Universität München, Department Chemie, AG Fluorchemie
Lichtenbergstr. 4, 85748 Garching bei München*

Abstract

To prepare a blank monolithic U-Mo fuel foil for cladding application, it is necessary to perform an in-depth cleaning of the foil surface to remove oxides and other pollutants that could affect cladding adhesion. Usually, chemical treatment with HNO_3 solution is used for this purpose. We investigated an alternative chemical treatment based on $\text{NaOH}/\text{H}_2\text{O}_2$ solution and compared its efficiency to the HNO_3 treatment. The surface of DU-10wt.%Mo foils was characterized before and after the chemical treatment optically, by SEM and by EDX. As a result, it was found that the common HNO_3 cleaning method is efficient for oxide removal, but leaves characteristic impurities like Si, Al and C on the foil surface, which originate from the foil fabrication process. The $\text{NaOH}/\text{H}_2\text{O}_2$ cleaning method shows comparable efficiency for oxide removal, but additionally removes the fabrication impurities almost completely.

1. Introduction

Since more than one decade, research worldwide aims to develop a high-density nuclear fuel on the basis of U-Mo alloys [Rer12]. The Technische Universität München (TUM) participates in these efforts in order to convert its high-flux research reactor Forschungs-Neutronenquelle Heinz Maier-Leibnitz (FRM II) from the currently used nuclear fuel U_3Si_2 to U-Mo fuel [Boe04; Roe05]. TUM research activities in this context cover conversion scenarios for FRM II [Bre11; Roe06], U-Mo metallurgy [Jun11] and U-Mo processing [Sch11]. In the field of processing, research at TUM currently focusses on the monolithic plate fuel design, which uses fuel plates with a massive U-Mo core and Al cladding.

An industrial fabrication process for monolithic U-Mo plate fuel is currently being developed [Moo09]. A crucial and error-prone step in this process is the application of the Al cladding to the monolithic U-Mo fuel foil that represents the plate

core by the well-known picture frame technique. A good bonding quality of fuel foil to cladding is required to ensure sufficient fission heat transfer, to retain mechanical stability, and to avoid swelling induced delaminating during fuel plate operation.

A factor that has a major effect on bonding quality is the cleanliness of the interface of the U-Mo foil and the Al cladding material. Surface pollutants or oxides on U-Mo and Al with only a small adhesion to the underlying bulk material strongly reduce the contact area of U-Mo and Al but do not contribute to the adhesion. Thus, overall bonding strength is reduced. Especially the blank U-Mo foil surface is prone to the formation of thick and brittle oxide layers when handled in air due to the rapid oxidation of U in contact with O_2 . A proper in-depth cleaning of the monolithic U-Mo foil shortly before Al cladding application is thus mandatory to ensure sufficient interface cleanliness.

A well-known cleaning method in this respect is bathing the raw U-Mo fuel foil in HNO_3 solution, a procedure which is commonly used but has

hardly been investigated in detail. We examined the oxide layer on U-Mo foils prior and after the treatment with HNO₃ solution and characterized the resulting chemical cleaning effect. Further, we compared the common HNO₃ cleaning method with an alternative method based on basic etching in a bath of aqueous NaOH/H₂O₂ solution.

2. Materials and methods

For our experiments we used monolithic foils of 360 μm thickness consisting of DU-10wt.%Mo (denoting an U-Mo alloy composed of depleted U with 10 wt.% Mo content), which had been provided by Y-12 National Security complex.

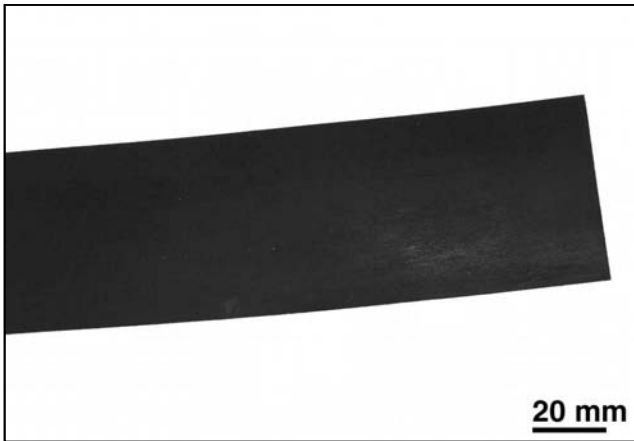


Figure 1: Oxidized DU-10wt.%Mo foil. Clearly visible is the thick black U oxide layer on the foil surface.

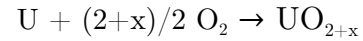
We examined several foil pieces of about 200 mm² in size, which were taken from a larger DU-10wt.%Mo foil and were still in their as-fabricated state (Figure 1). SEM (scanning electron microscopy) was used to study the surface structure and oxide layers while EDX (energy-dispersive X-ray spectroscopy) was used to analyze the elemental composition of the foil surface.

Both analysis methods were used before and after the cleaning procedures to see the effect of the chemical cleaning to the surface and the oxygen concentration. It should be noted however, that the EDX measurement actually does not measure the surface material composition but determines the mean composition of a material volume of 2-3 μm thickness, beginning at the surface. Depending on the thickness of the oxide layer, EDX will thus measure either only the oxide layer

(if oxide layer thickness > 2-3 μm) or both oxide layer and bulk material (if oxide layer thickness < 2-3 μm). Still, oxygen contents of approximately 10 at.% were found even on freshly cleaned surfaces, which may result either from remaining oxide on the foil surface or from the finite oxygen partial pressure in the SEM vacuum chamber.

3. Surface oxide layer and impurities

The uranium oxides expected at the foil surface are UO₂, U₄O₉, U₃O₇, U₂O₅ and U₃O₈ [HoK02], which follow from the chemical reaction [Rit81]:



Depending on the parameter x (usually between 0.2 and 0.4 according to [Rit81]), the non-stoichiometric UO_{2+x} will form one of the oxide states mentioned above. At large time scales, all U oxides become the stable U₃O₈.

Surface structure

From the SEM measurements, we found the surface structure of the untreated DU-10wt.%Mo foils to be rough and irregular (Figure 2), with cracks to be found widely over the measured surface (Figure 3). These cracks are likely to result from the characteristic property of U oxide surfaces, which tend to crack at thicknesses above 75 nm [Lau04], but could also be formed due to the atmospheric conditions in the SEM device. Cross-section studies reveal that the oxide layer shows an average thickness of 3 μm with deviations up to 100 % across the surface (Figure 4).

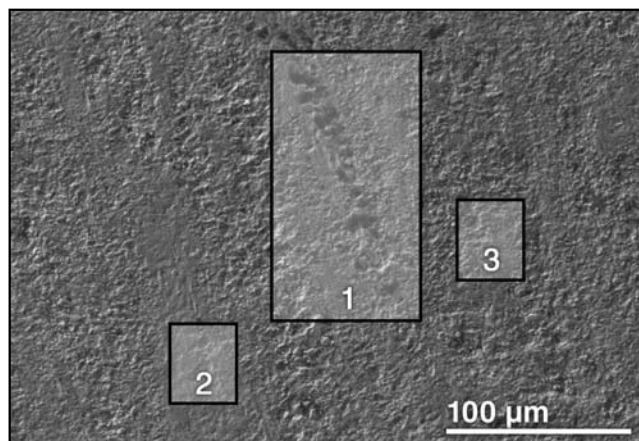


Figure 2: SEM picture of oxidized DU-10wt.%Mo foil surface. One can see the irregularity and roughness of the surface as well as an impurity, consisting mainly of Si, Al and C (area 1).

Oxygen content

By EDX analysis, we determined the surface oxygen content in the oxidized areas 2 and 3 in Figure 2 to be between 35 at.% (area 2, slightly oxidized) and 50 at.% (area 3, strongly oxidized). Due to the variations in oxide layer thickness, one can assume that the measured surface volume element contains no bulk material but only oxides for the large measured oxygen concentrations, and a certain fraction of bulk material for the smaller oxygen concentrations.

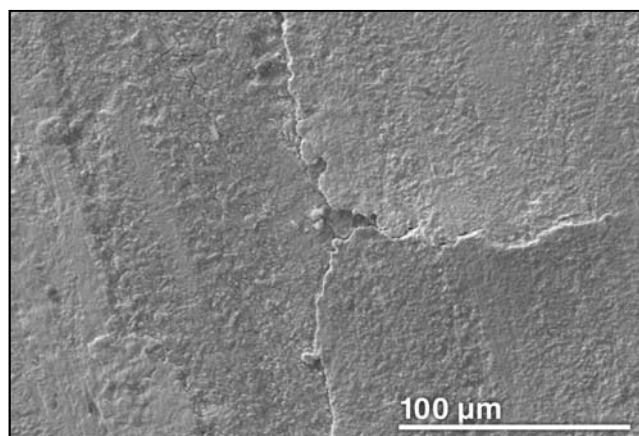


Figure 3: SEM picture of a cracked DU-10wt.%Mo surface. Cracks like the one shown here can be found widely across the analyzed samples.

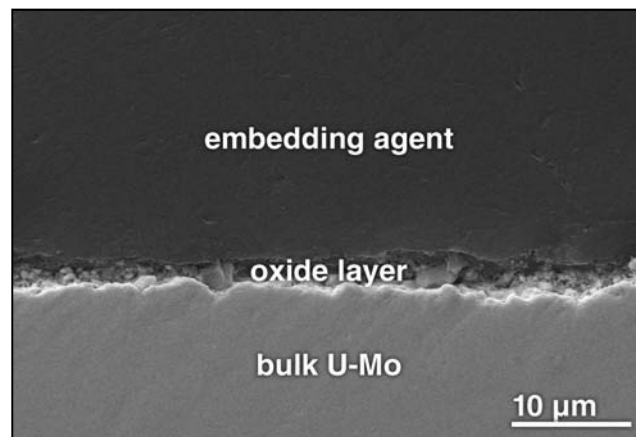


Figure 4: SEM picture of the cross-section of an oxide layer on the surface of a DU-10wt.%Mo foil. The oxide layer has an average thickness of 3 µm and is extremely porous and irregular.

Impurities

Impurities like visible in area 1 in Figure 2, consisting mainly of Si, Al and C, were found in various forms all over the surface, but mostly in the form of elongated grooves (Si and Al). As all grooves are oriented in the same direction, we assume that they result from the foil fabrication process, where the foils were sand-polished and lubricants were used to roll the foil.

4. Chemical treatment

For our experiments, we used the generalized cleaning procedure that is listed in Table 1. The actual chemical cleaning, respectively the etching step, is highly dependent of the type of chemical agent used, its concentration and its temperature and thus described separately in the following sections. As chemical agents we used aqueous solutions of HNO_3 (65 %), H_2O_2 (35 %) and NaOH (aq) (1 M), all of analytical grade.

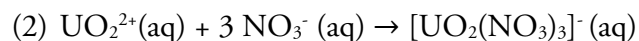
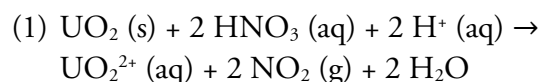
Cleaning with HNO_3 solution

Aqueous solutions of HNO_3 are the most commonly used cleaning agents for U and its alloys because of its suitable oxide dissolution abilities and its tendency to dissolve oxides faster than the underlying bulk metal. Nevertheless, the cleaning process as well as the chosen concentration and temperature of the cleaning solution have to be monitored carefully to avoid damage of the U-Mo bulk material.

Step	Time
Removal of surface pollution like dust, dirt and wetness	0-2 mins
Production of sufficient amounts of cleaning solution with well-defined temperature and concentration	3 mins
Degasifying the cleaning solution with an ultrasonic bath or inert gas	1 min
Chemical etching process of the foil in the cleaning solution	See below
Rinsing the foil with distilled water	10 secs
Inserting the foil into an ultrasonic bath with distilled water	1 min
Inserting the foil into an ultrasonic bath with acetone	1 min
Drying the foil with a clean wiping cloth	30 secs

Table 1: Generalized cleaning procedure for U-Mo foils including the necessary time to gain satisfying results. For the details of the etching step, see text.

The chemical reactions that describe the dissolution of UO_2 or UO_{2+x} in contact with an aqueous HNO_3 solution may be given as:



For the simplicity of the equations, we use NO_2 as the evolving nitrogen oxide species. UO_2 is oxidized to the soluble UO_2^{2+} cation, which subsequently forms the well soluble $[\text{UO}_2(\text{NO}_3)_3]^-$ complex. Immediately after putting the foil into the solution, one can barely see any etching effect, but after half of the etching time, the black oxide layer begins to disappear and will have been fully gone after some more seconds.

In various experiments we found an optimum etching behavior for 6.5 vol.% HNO_3 concentration at 60 °C temperature and 120 s etching time, 19.5 vol.% at 40 °C and 90 s, as well as 32.5 vol.% at 30 °C and 60 s. The total volume of cleaning solution has always been chosen to be 50 ml.

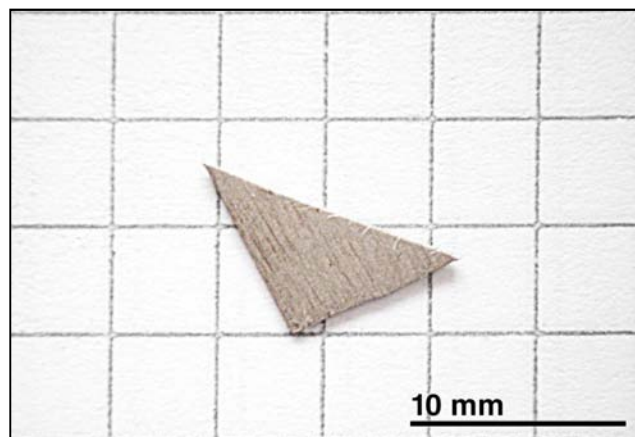


Figure 5: DU-10wt.%Mo foil piece cleaned with HNO_3 solution. On the blank metal surface, one can see a pattern of darker stripes, consisting of impurities.

The impurities mentioned before can still be found on the HNO_3 cleaned foil surface, forming a pattern of dark stripes, as seen in Figure 5 as well as in the SEM picture in Figure 6. The oxygen concentration on the foil surface has decreased to below 10 at.% (which can be attributed either to remaining oxide or to oxygen in the SEM vacuum chamber) and in cross-section SEM pictures no oxide layer can be found anymore.

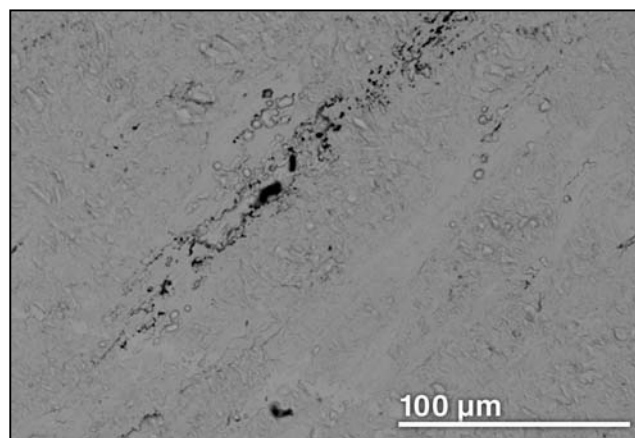
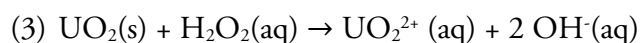


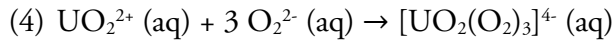
Figure 6: SEM backscattering picture of a DU-10wt.%Mo surface cleaned with HNO_3 solution. The pure U-Mo has a grey color, the dark structure is an impurity, primary consisting of Si.

Cleaning with NaOH / H_2O_2 solution

Another promising cleaning agent according to the literature is a combination of H_2O_2 and NaOH (aq) solutions. The chemical reactions responsible for the cleaning effect in this case are primarily the oxidation of UO_2 to the soluble UO_2^{2+} cation, which is given as:



Due to the high pH value of the NaOH solution, well soluble peroxo compounds are formed in a second reaction, consisting mainly of the $[\text{UO}_2(\text{O}_2)_3]^{4-}$ anion [Jan06]:



In contrast to reactions (1) and (2), this process can be observed as a continuous dissolution of the black oxide layer over the whole etching time, while the cleaning solution will colour itself yellow to orange-yellow due to the high concentration of peroxouranate anions.

For our experiments we used 25 ml of 1M NaOH (aq) with 2.5 ml of 35 vol.% H_2O_2 at room temperature.

Figure 7 shows a $\text{H}_2\text{O}_2/\text{NaOH}$ cleaned DU-10wt.%Mo foil piece which shows no visible pattern of surface impurities any more. An etching time of 120 s is sufficient and will lead to a well-cleaned surface with an oxygen concentration below 10 at.%. Impurities such as Fe and Si are almost fully removed, while carbon still can be found across the cleaned surface.

Fe is effectively removed by NaOH under hydrogen generation and formation of soluble $[\text{Fe}(\text{OH})_6]^{4-}$, whereas it is passivated and hence undissolved with nitric acid. Si does not dissolve in nitric acid due to the formation of a protective SiO_2 layer but is easily dissolved in alkaline conditions forming hydrogen and soluble silicate anions [Hol07].

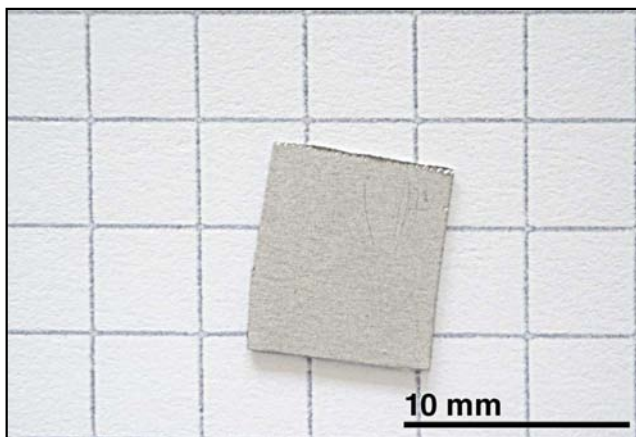


Figure 7: DU-10wt.%Mo foil piece cleaned with H_2O_2 and NaOH solution. Nearly no impurities are visible on the blank metallic surface.

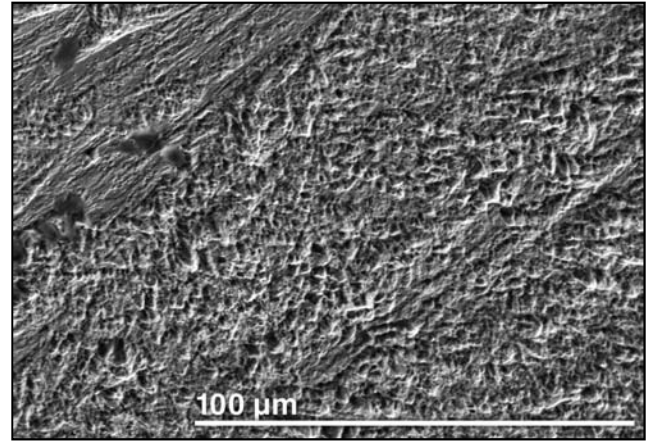


Figure 8: SEM picture of a DU-10wt.%Mo surface cleaned with NaOH/ H_2O_2 solution. One can see the effect the cleaning procedure has on the surface topography.

Re-oxidation behaviour

We found the re-oxidation rate of already cleaned pieces of DU-10wt.%Mo foil in air to be strongly dependent on the surface condition of the foil. We observed, that foils which were mechanically grinded with a grinding paper of roughness $10 \mu\text{m}$ to remove the oxide layer, will much slower form a new black oxide layer by re-oxidation than foils that were cleaned by HNO_3 solution. Foils that were cleaned by $\text{H}_2\text{O}_2/\text{NaOH}$ solution also showed a slower re-oxidation rate than those cleaned by HNO_3 solution, but still oxidized faster than the grinded foil.

We conclude that chemical etching may generally produce a much rougher surface topology on the U-Mo foil than mechanical grinding with a $10 \mu\text{m}$ grinding paper. The chemically cleaned surfaces thus offer much more contact surface to air oxygen and therefore suffer from increased oxidation. We also conclude that etching with HNO_3 solution and with $\text{H}_2\text{O}_2/\text{NaOH}$ solution will produce a similar surface topology, but in opposite to the acid etching process, the alkaline etching may form protective layers on the U-Mo surface which slow down re-oxidation.

5. Conclusion

We found that polluted U-Mo foil surfaces can effectively be cleaned by our generalized cleaning procedure. As chemical cleaning agents, we investigated HNO_3 solution and $\text{H}_2\text{O}_2/\text{NaOH}$

solution. Both agents can efficiently dissolve U oxide layers on the foil surface in reasonable time without notable damage to the underlying bulk material. HNO_3 solution is however not able to remove the impurities found on the U-Mo foil surfaces, while $\text{H}_2\text{O}_2/\text{NaOH}$ solution solves them as well.

6. Acknowledgements

This work was supported by a combined grant (FRM0911) from the Bundesministerium für Bildung und Forschung (BMBF) and the Bayerisches Staatsministerium für Wissenschaft, Forschung und Kunst (StMWFK).

We want to thank Y-12 National Security complex for providing the DU-10wt.%Mo foil material that was used for our experiments. We also want to thank our colleagues R. Jungwirth and C. Steyer for their help in preparing the foil samples for the SEM and EDX analysis. We thank the radiochemistry of the TUM for providing lab space. F.K. thanks the Fonds der Chemischen Industrie for the Liebig stipend.

7. References

- [Rer12] Argonne National Lab. 2012. Homepage of the RERTR programme. [Online] 2012. <http://www.rertr.anl.gov>.
- [Boe04] Böning, K., et al. 2004. Conversion of the FRM II. *8th International Topical Meeting on Research Reactor Fuel Management (RRFM)*. Munich, 2004.
- [Bre11] Breitzkreutz, Harald. 2011. Coupled neutronics and thermal hydraulics of high density cores for FRM II. *PhD thesis*. Garching bei München. Technische Universität München, 2011.
- [HoK02] Ho Kang, Kweon, et al. 2002. Oxidation behavior of U-10 wt% Mo alloy in air at 473–773 K. *Journal of Nuclear Materials*. 2002, Vol. 304, 2-3, pp. 242-245.
- [Hol07] Holleman, Wiberg. 2007. Lehrbuch der anorganischen Chemie, 102. Auflage. Berlin, de Gruyter, 2007.
- [Jan06] Jander, Blasius. 2006. Lehrbuch der analytischen und präparativen anorganischen Chemie, 16. Auflage. Stuttgart, S. Hirzel Verlag, 2006.
- [Jun11] Jungwirth, Rainer. 2011. Irradiation behavior of modified high-performance nuclear fuels. *PhD thesis*. Garching bei München. Technische Universität München, 2011.
- [Lau04] Laue, C. A., Gates-Anderson, D. and Fitch, T. E. 2004. Dissolution of metallic uranium and its alloys. Part I. Review of analytical and process-scale metallic uranium dissolution. *Journal of Radioanalytical and Nuclear Chemistry*. 2004, Vol. 261, 3, pp. 709-717.
- [Moo09] Moore, Glenn A., et al. 2009. Monolithic Fuel Fabrication Process Development at the Idaho National Laboratory. *Topical Meeting on Reduced Enrichment for Research and Test Reactors (RERTR)*. Beijing, 2009.
- [Rit81] Ritchie, A. G. 1981. A Review of the rates of reaction of Uranium with Oxygen and Water vapour at temperatures up to 300°C. *Journal of Nuclear Materials*. 1981, Vol. 102, 1-2, pp. 170-182.
- [Roe06] Röhrmoser, Anton, et. al. 2006. Reduced enrichment program for FRM II, actual status & principal study of monolithic fuel for FRM II. *Proceedings on the 10th International Topical Meeting on Research Reactor Fuel Management, 30.4. - 2.5 2006*. Sofia, 2006.
- [Roe05] Röhrmoser, Anton, et. al. 2005. Reduced Enrichment Program for the FRM-II, Status 2004/05. *Transactions 9th International Meeting on Research Reactors Fuel Management (RRFM), 10. - 13. April 2005*. Budapest, 2005. pp. 119-125.
- [Sch11] Schmid, Wolfgang. 2011. Construction of a sputtering reactor for the coating and processing of U-Mo nuclear fuel. *PhD thesis*. Garching bei München. Technische Universität München, 2011.

NEW REACTOR SAFETY ANALYSIS OF FRM II COMPACT CORE USING TRACE/PARCS

M. DÄUBLER, H. BREITKREUTZ, W. PETRY
*HEUMEU group, Forschungs-Neutronenquelle Heinz Maier-Leibnitz (FRM II)
Lichtenbergstr. 1, 85747 Garching – Germany*

R. MACIAN-JUAN
*Lehrstuhl für Nukleartechnik (NTech)
Boltzmannstr. 15, 85748 Garching - Germany*

ABSTRACT

Currently, several approaches to extend our modelling capabilities to cover FRM II reactor dynamics are being investigated. The USNRC best-estimate, coupled code system TRACE/PARCS, developed for coupled systems analysis of nuclear reactors, is in the process of qualification and has a growing number of international users. As a step towards assessing the feasibility of using TRACE/PARCS for reactor dynamics calculations, a study to determine the achievable accuracy of simulating the FRM II compact core under normal operating conditions at BOL is on-going. The accuracy is quantified by a code-to-code comparison of the calculation results obtained with the in-house X^2 program system for the current compact core fuel assembly with its involute shaped fuel plates. The X^2 program system is used for high-detail 3D, steady-state coupled neutronics and thermal-hydraulics calculations of potential future fuel assembly designs. It couples the burn-up sequence MONTEBURNS - a coupling of MCNPX and ORIGEN - and the computational fluid dynamics code ANSYS CFX.

Available intermediate results of the feasibility study are discussed, i.e. the achievable accuracy of TRACE's thermal-hydraulics model standalone is presented.

1. Introduction

The Forschungs-Neutronenquelle Heinz Maier-Leibnitz (FRM II) in Garching is a reflected compact core research reactor. Its purpose is to generate neutrons for various scientific, medical and industrial applications. Using a single cylindrically shaped fuel assembly, it operates at 20 MW for 60 days. Its current fuel is uranium silicide enriched to 93w%.

Within the context of the possible conversion of FRM II from HEU fuel to less enriched high density fuel, efforts to set up a new calculation system for reactor safety analysis are under way at FRM II. A methodology to analyse FRM II using the best-estimate coupled code technique has been developed and the USNRC coupled best-estimate code system TRACE/PARCS has been chosen to simulate the reactor.

TRACE/PARCS has been developed and is being validated for today's LWR power reactors which differ from FRM II in overall system geometric layout, fuel and structure materials employed, coolant temperatures, system pressures and reactor dynamic behaviour. Consequently, we are performing a detailed feasibility assessment which includes the determination of the achievable simulation accuracy under normal operating conditions at BOL, as well as, the identification of models and correlations in TRACE/PARCS, so that they can be adapted to adequately describe FRM II conditions and behaviour.

Thermal-hydraulic and neutronics models of FRM II under nominal conditions at BOL are studied both independently and coupled. As the cylindrical PARCS model is currently still in a developmental stage, only stand-alone thermal-hydraulic calculations are discussed here.

2. TRACE model

Under normal operating conditions, it is sufficient to model the FRM II's reactor core without its by-pass flows and to represent the remainder of the primary coolant circuit by means of appropriate boundary conditions.

The TRACE thermal-hydraulics model describes the reactor core with fuel assembly resolution, i.e. it consists of a single coolant channel. The resulting nodalization scheme is shown in figure 1. Effective one-dimensional model sections are related to their actual reactor counterparts – head of fuel assembly, fuel plate region and foot of fuel assembly.

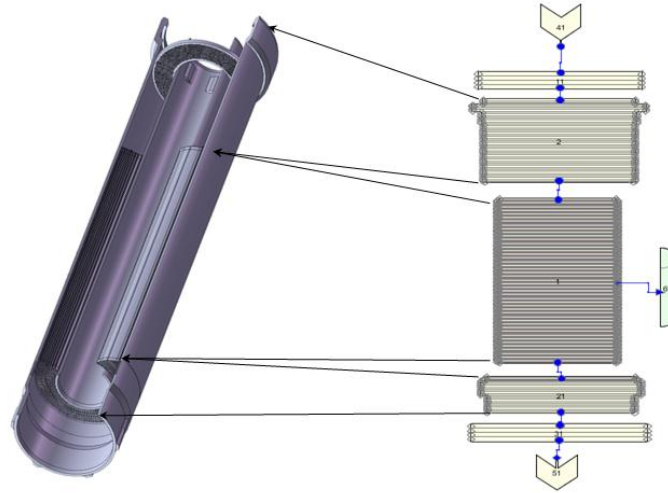


figure 1: TRACE nodalization of FRM II reactor core without by-passes
(CAD fuel assembly model taken from [1])

Input power shapes for the heat structure component used in TRACE to simulate the powered core have been generated by using the existing MCNPX models of the current reactor configuration in the X² program system.

3. Benchmarking of the TRACE model

First, the mass flow dependence of cold zero power core pressure drops was investigated. TRACE calculation results are compared to SIEMENS KWU design data [2] in figure 2 where the mass flow rate through the core $\dot{m} = 274.5 \text{ kg/s}$ corresponds to nominal operating conditions. A very good overall agreement is shown in the figure. The relative difference between SIEMENS reference data and the simulated values increases as the mass flow decreases. However, these remain at an acceptable level.

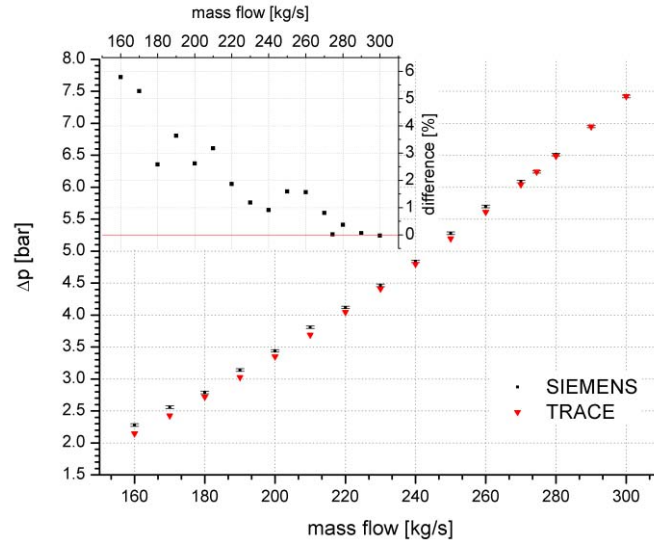


figure 2: Mass flow dependence of cold core pressure drops

Second, the TRACE simulation was benchmarked against the computational fluid dynamics code ANSYS CFX. The FRM II CFX model was taken from the X² program system [1]. To allow for a comparison, 3D CFD results were collapsed such that only an axial dependence remained – just like in the 1D TRACE model. In case of static pressure and coolant temperature, flow area averages were computed which within the finite volume framework of CFX correspond to averages over mesh cell control volumes. Thus, values obtained are actually volume averages for an effective cell of axial height Δz . For surface heat fluxes, clad outside temperatures and fuel centre-line temperatures the values represent the mean along curves of constant z within fuel plate surface and centre plane.

A comparison of TRACE and CFX static pressure profiles within the fuel assembly is depicted in figure 3 where $z = 0$ marks the bottom end of the fuel plate region. The agreement is remarkably good for a comparison of static pressure flow area averages in a truly 3D model with a 1D stream-line model. All significant deviations except for the one observed at the bottom of the fuel assembly may be attributed to the different dimensionality of the models. In case of the fuel assembly bottom, certain structures are included in the TRACE model which have not been implemented in the CFX model yet.

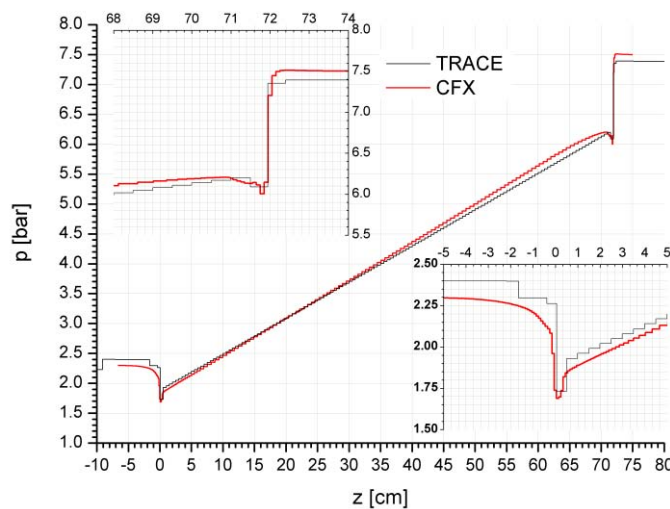


figure 3: Static pressure profile in current fuel assembly at BOL

An examination of the average primary coolant temperature axial profile yields an accumulated temperature difference of 0.15°C at the core outlet. It was found that these are due to unequal versions of the IAPWS steam water data tables and different interpolators employed by TRACE [3, 4] and CFX [5].

From a safety point of view, fuel plate surface heat fluxes play an important role, see figure 4.

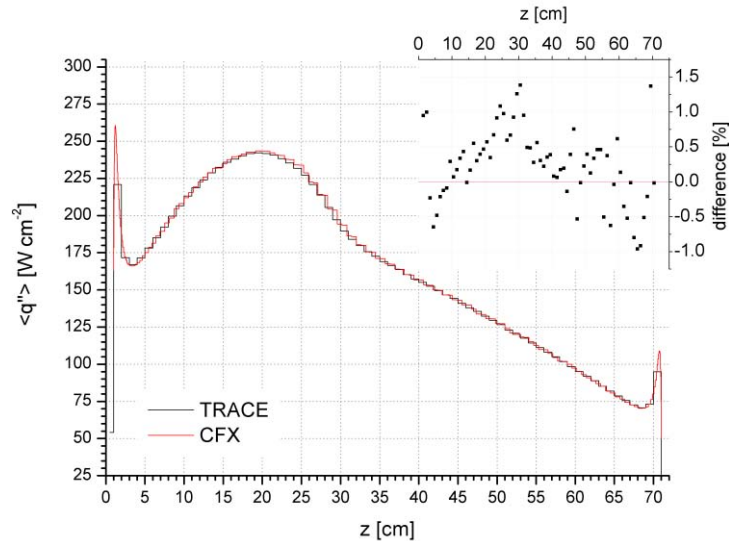


figure 4: Fuel plate surface heat flux profile of current fuel assembly at BOL

Absolute values of the relative deviations from the CFX reference calculation lie well below 2% everywhere. Boundary effects resulting in peaks at both ends of a fuel plate are not completely captured by the simple TRACE model to their full extend.

The temperature differences between clad outside and fuel centre-line also show a very good agreement between TRACE and CFX (see figure 5). When comparing clad outside temperatures and fuel centre-line temperatures as evaluated by TRACE and CFX individually, one observes that CFX predicts lower temperatures than TRACE. Deviations up to 5°C occur.

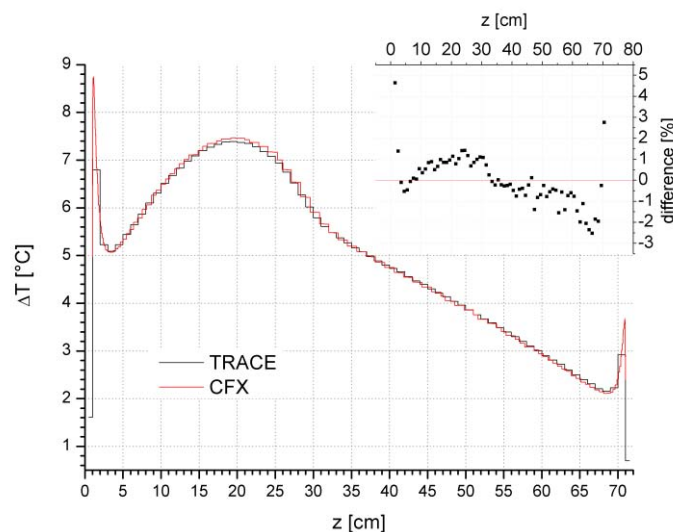


figure 5: Cladding outside to fuel centre-line temperature difference for current fuel assembly at BOL

In the CFX model of FRM II, wall functions are utilized to resolve boundary layers at the fuel plate surfaces and, thus, to treat heat transfer from solid to fluid. Wall function parameters may be translated into heat transfer coefficients [5]. When comparing these with TRACE's coefficients computed based on the Gnielinski correlation for the Nusselt number [3], these turn out to be on average 37% higher leading to lower clad outside and, consequently, fuel centre-line temperatures.

Besides TRACE temperatures being conservative when compared to CFX results, the Gnielinski correlation is the state-of-the-art relationship to compute the Nusselt number for single phase forced convection flows.

4. Conclusion and outlook

The work performed illustrates that employing TRACE to model FRM II is feasible, provided the necessary changes to the code are made. Such changes include the sub-cooled boiling models for the low pressure and low temperature range.

With the development of the PARCS based FRM II neutronics model, the thermal-hydraulic analysis of the reactor will be extended to enable the treatment of numerous off-nominal conditions.

Once both models are fully developed and tested, coupled steady-state runs will be benchmarked against simulation results obtained with the X² program system.

5. References

- [1] Breitzkreutz, Harald: *Coupled Neutronics and Thermal Hydraulics of High Density Cores for FRM II*, Technische Universität München, PhD thesis, 2011
- [2] Giesler, Ehrich Sperber: *Thermohydraulische Kernausslegung*, SIEMENS KWU technical report (A1C-1301735-0), 1996
- [3] U.S. Nuclear Regulatory Commission: *TRACE v5.0p2 Theory Manual - Field Equations, Solution Methods and Physical Models*, 2010
- [4] Information Systems Laboratory Inc. for U.S. Nuclear Regulatory Commission: *RELAP5/mod3.3 Code Manual (Volume 1-8)*, October 2010
- [5] ANSYS Inc.: *ANSYS CFX-Solver Theory Guide. ANSYS CFX Release 12.0*, March 2009

THERMAL CONDUCTIVITY MEASUREMENT OF IRIS-TUM FUEL PLATES (DISPERSE U-8WT.-%-MO)

T. K. HUBER, R. JUNGWIRTH, T. RÖHRMOSER, W. PETRY

*Forschungs-Neutronenquelle Heinz Maier-Leibnitz, Technische Universität München
Lichtenbergstr. 1, 85747 Garching – Germany*

D. STAICU, M. ERNSTBERGER, H. THIELE, A. ZAPPIA

*European Commission, Joint Research Centre Institute for Transuranium Elements
P.O. Box 2340, D-76125 Karlsruhe – Germany*

D. W. WACHS

*Fuel Performance and Design, Idaho National Laboratory
P.O. Box 1625, Idaho Falls, ID 83415 – USA*

C. JAROUSSE, B. STEPNIK

*AREVA-CERCA
Les Berauds, B.P. 1114, 26104 Romans Cedex – France*

P. LEMOINE¹, C. VALOT², F. CHAROLLAIS²

¹CEA, DEN, DISN Saclay, F-91191 Gif sur Yvette – France

²CEA, DEN, DEC, Cadarache, F-13108 Saint-Paul-Lez-Durance – France

ABSTRACT

The thermal diffusivity of ground U-8wt.-%-Mo powder in an aluminium matrix has been measured in the temperature range of 300°C to 400°C. By means of best estimates for the heat capacity and density of this complex compound a thermal conductivity of about 25 W/mK has been determined.

1. Introduction

International research for the qualification of high density fuel for research reactors currently focuses on UMo alloys with 7 – 10 wt% Mo content. In this context TUM in collaboration with CEA and AREVA-CERCA has launched the fabrication of full scale fuel plates made of ground UMo powder, its subsequent irradiation and post irradiation examination (PIE) The Forschungs-Neutronenquelle Heinz Maier-Leibnitz (FRM II) is working on reducing the enrichment of its current HEU fuel to a lower level. Besides calculations [Boe04], [Roe04], FRM II is also actively participating in the development of the needed high density fuels, i.e. UMo [Jar09], [Jun10]. As a candidate for such a fuel, the IRIS-TUM fuel plates have been designed and produced by CERCA-AREVA in collaboration with TUM and CEA [Pet08], [Lee09], [Lee11], [Ren09]. This irradiation campaign is called IRIS-TUM. Its test platesThese contain ground U(Mo) fuel kernels in an aluminium matrix clad in AlFeNi. As one important parameter of this new fuel, the thermal conductivity before and during irradiation has to be determined. Thermal

conductivity enters as a sensitive parameter, which is needed in thermal-hydraulical calculations to correctly determine heat fluxes and meat temperatures. The thermal conductivity is a composition of the thermal diffusivity, the heat capacity and the density. In this paper, we present the first measurement of the thermal diffusivity of the IRIS-TUM non-irradiated samples obtained with the LASER Flash Method [Par60]. In combination with calculated heat capacities and densities the thermal conductivity is deduced from these measurements.

Sample

The IRIS-TUM spare full size plate (8003), which was used for the thermal diffusivity measurements, contains an alloy of 49.2% enriched uranium with 8.1wt.% molybdenum content and a Uranium density of 8gU/cm^3 . The U-8wt.-%-Mo particles are embedded in a pure aluminium matrix with a volume fraction of 41.6% aluminium. AlFeNi is an aluminium alloy containing ~1wt.% Fe, ~1wt.% Ni and ~1wt.% Mg [Pet08].

The meat and the cladding of the test plates have been measured separately. To do so, small parts have been cut from the whole plate. Afterwards, these parts have been polished to remove the cladding on both sides of the meat. The thermal diffusivity has been measured by the LASER Flash method. The measurement set-up requires small samples of ca. $(5 \times 5)\text{mm}^2$, which have been cut from the plates prior to polishing. The AlFeNi samples have been cut from a fresh AlFeNi sheet and had the same dimensions as the meat samples.

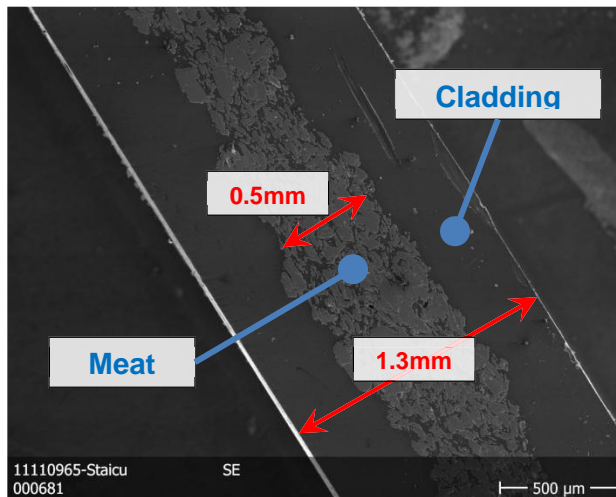


Figure 1: SEM picture of non-irradiated IRIS-TUM sample before measurement.

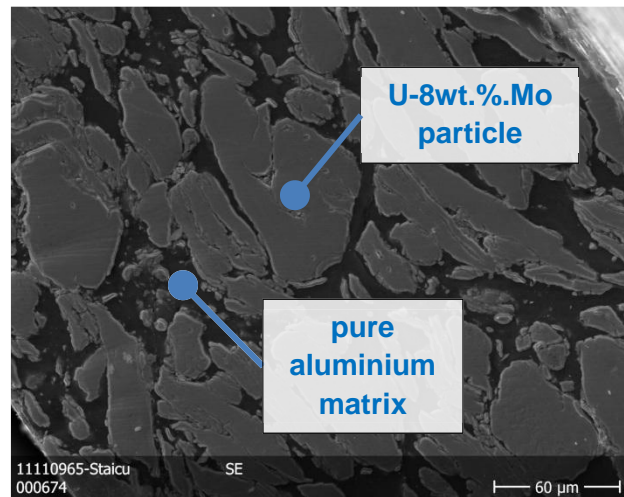


Figure 2: High resolution SEM picture of non-irradiated IRIS-TUM sample before measurement. The picture shows clearly the random shape of the ground powder fuel particles.

Figure 1 shows a cross section of an unpolished IRIS-TUM fuel sample with the meat cladded in AlFeNi. The thickness of the meat without cladding is 0.5mm. Figure 2 is a zoom of the meat region: The fuel particles have a random irregular shape with a particle size up to $250\mu\text{m}$ with an average diameter of $147.3\mu\text{m}$.

2. Determination of the Thermal Conductivity

The thermal conductivity λ cannot be measured directly. However, it is the product of the thermal diffusivity α , heat capacity C_p and density ρ :

$$\lambda = \alpha \cdot \rho \cdot C_p \quad (1)$$

and therefore can be derived from a measurement of those three. The thermal diffusivity is measured with the LASER Flash method. The heat capacity of a composition, as it is the case for disperse IRIS-TUM fuel, can be calculated from the heat capacities of the single components. In the future, this quantity will be measured via calorimetry. The density is calculated in a similar way by now, but will later be measured using Archimedes method.

2.1. Thermal Diffusivity Measurement via LASER Flash Method

Figure 3 shows a schematic drawing of the LASER Flash apparatus [She98], which was used at ITU to determine the thermal diffusivity.

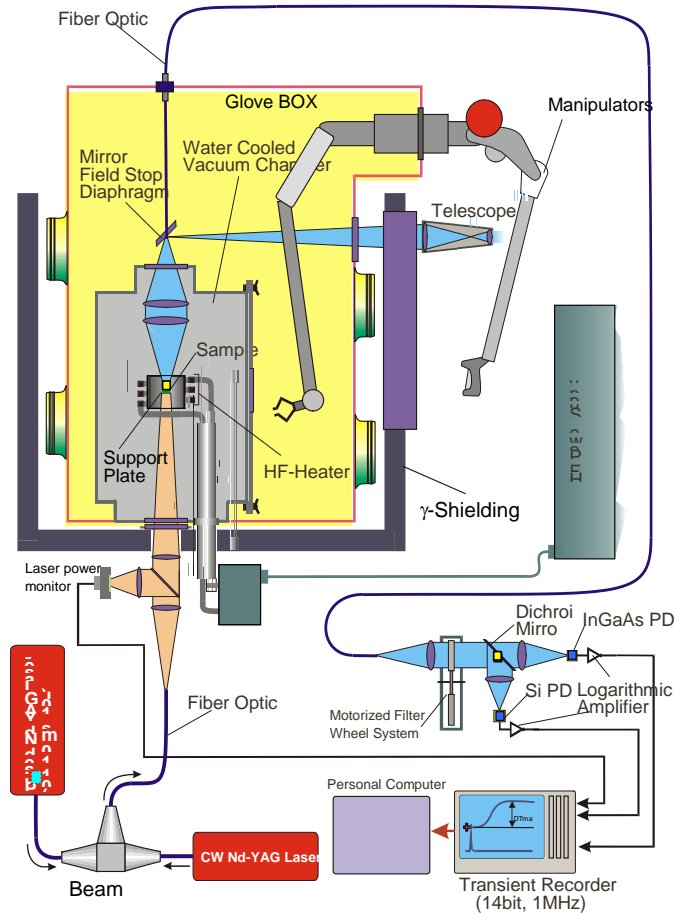


Figure 3: Schematic drawing of the LASER Flash set-up at ITU.

The set-up mainly consists of a LASER, a sample holder and an infrared detector. The Nd-YAG LASER emits very short (10ms), but very intense (60W/cm²) heat pulses. These heat up the sample, which is located in a vacuum chamber with a pressure in the range of 10⁻³ mbar to

minimize conductive heat transfer from the sample surface to the surrounding. The sample can be continuously heated to temperatures between 300°C and 1200°C by a HF induction furnace inside the vacuum vessel. The temperature of the sample is measured contact-free by an InGaAs pyrometer. The infra-red radiation is guided through a lens system and a fibre optic to the InGaAs pyrometer, which is connected to a computer via a fast log amplifier and an A/D converter.

The LASER flash on the front side of the sample induces a temperature rise (between 1K and 10K) in the bulk, which can be observed with the pyrometer on the backside of the sample. Figure 4 shows a typical normalized temperature curve of an IRIS-TUM meat sample. The temperature dependent thermal diffusivity $\alpha(T)$ is obtained by a numerical fit of the steepness of the temperature rise by a function containing an infinite sum of exponential functions. This model already includes heat loss effects [Par60].

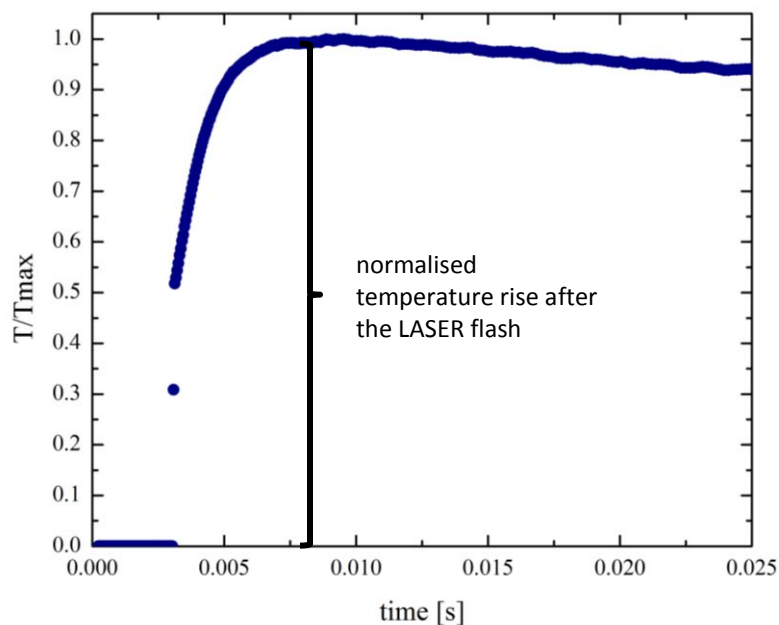


Figure 4: Typical normalised temperature curve of an IRIS-TUM meat sample with the characteristic temperature rise after the LASER flash.

The uncertainty of the thermal diffusivity is a composition of the statistical uncertainty of the curve fitting (5% relative uncertainty), the systematic uncertainties of the plate thickness, which is part of the thermal diffusivity calculation (8% relative uncertainty) and of the temperature measurement (3% relative uncertainty). This yields a total relative uncertainty of 12%. The relative uncertainties of the thermal diffusivity of the cladding have the same composition and values, except the uncertainty due to the plate thickness, which is lower with only 6%. All in all, this adds up to a total relative uncertainty of 9% for the cladding.

The temperature range of the measurement was between 300°C and 400°C. At temperatures over 400°C, an undesired thermal diffusion layer can be generated in the meat between the U-8wt.%-Mo particle and the aluminium matrix. Such a layer would reduce the thermal conductivity of the fuel. Although the measurements were performed slightly below 400°C, Scanning Electron Microscope pictures have been taken of the IRIS-TUM meat sample after the measurement to examine, if such a layer has been produced (see figure 5).

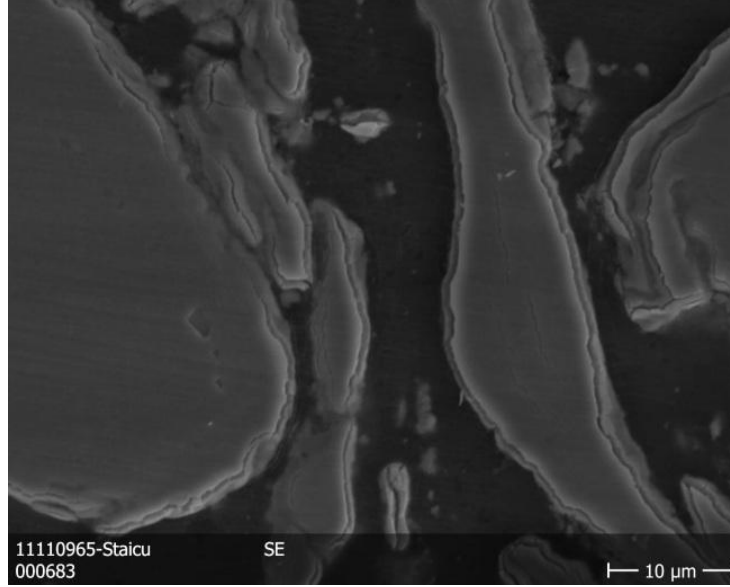


Figure 5: Scanning Electron Microscope (SEM) picture of IRIS-TUM meat sample after measurement.

On the SEM picture a bright area can be seen alongside the U-8wt.%-Mo particle borders. This can be interpreted as an interdiffusion layer accompanied by cracks. However, it has to be noted that the surface of the sample has not been polished again before the SEM picture was taken; therefore, this may only be a surface effect. New SEM pictures will be taken with a polished sample surface to check this effect in the near future.

Thermal Conductivity Calculation

For the calculation of the thermal conductivity, the heat capacity and density have to be calculated as no measured data is available now.

The disperse IRIS-TUM meat can be assumed as a composite of known materials, which are U-8wt.%-Mo and pure aluminium [AMS], [Hen10]. The temperature dependent heat capacity $C_p(T)$ and the density $\rho(T)$ of a composite can be calculated by weighted summation of the heat capacity $C_{p,i}(T)$ and density $\rho_i(T)$ of all constituents n . Thereby the heat capacity is weighted by the mass fraction m_i of the constituents, while the density is weighted by the volume fraction v_i of the constituents. The thermal conductivity $\lambda(T)$ is finally the product of the measured thermal diffusivity $\alpha(T)$ and the calculated heat capacity and density.

$$\lambda(T) = \alpha(T) \cdot \sum_{i=1}^n (v_i \cdot \rho_i(T)) \cdot \sum_{i=1}^n (m_i \cdot C_{p,i}(T)) \quad (2)$$

The porosity needs to be considered in the calculation of the density ($\rho_{\text{porosity}} = 0 \text{ g/cm}^3$) as further constituent and reduces the density and further reduces the thermal conductivity.

3. Results

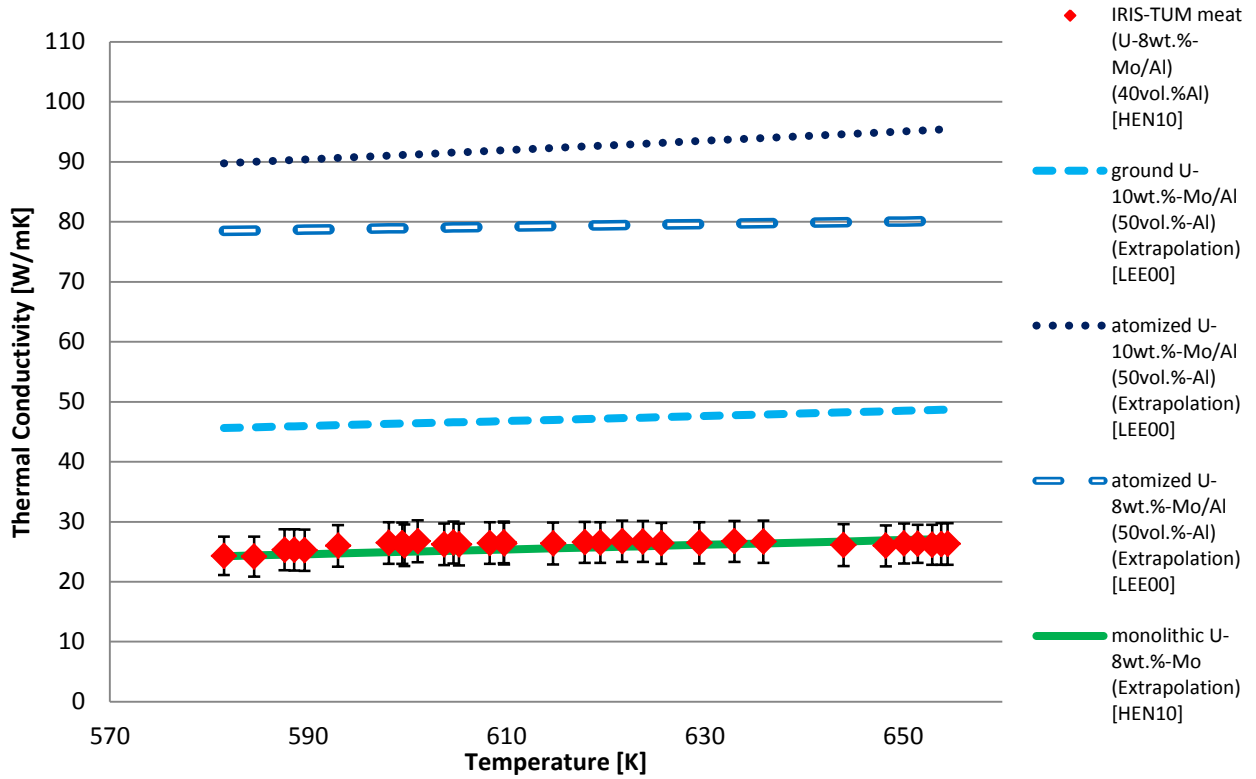


Figure 6: Thermal conductivity of IRIS-TUM meat compared to values for similar disperse meat, measured by S. H. Lee et al. [Lee00].

The thermal conductivity $\lambda(T)$ in the temperature range of 580K to 660K (~310°C to 390°C) of non-irradiated IRIS-TUM meat is given by

$$\lambda(T) = (16.3 \pm 4.8) \cdot 10^{-3} [W/mK^2] \cdot T + (18.2 \pm 3.0) [W/mK]. \quad (3)$$

Compared to disperse fuel with ground U-10wt.%-Mo, measured by S.H. Lee et al. [Lee00] a difference of ~20W/mK can be observed. IRIS-TUM fuel has about 10vol.% less aluminium in the matrix. As pure aluminium has a very high thermal conductivity (~230W/mK, see figure 7) compared to monolithic U-8wt.%-Mo (~25W/mK) [Hen10], the amount of aluminium in the matrix plays a significant role. A further difference is the ~2wt.% less molybdenum (~120W/mK) content in the U(Mo) alloy of IRIS-TUM, which has a similar impact on the thermal conductivity as aluminium. The difference between U-10w.%-Mo and U-8wt.%-Mo can be clearly seen in figure 6, where the impact of the molybdenum content on the thermal conductivity between atomized U-10wt.%-Mo and atomized U-8wt.%-Mo with the same aluminium content in the matrix can be compared directly. This difference alone gives a shift of more than 10W/mK.

Further differences arise from the particle shape: ground powder has a higher porosity than atomized powder due to its random furrowed shape (see figure 2). A higher porosity leads to a decrease of the thermal conductivity, which can also be clearly deduced from figure 6: Atomized powder fuels have a significant higher conductivity than ground powder fuels.

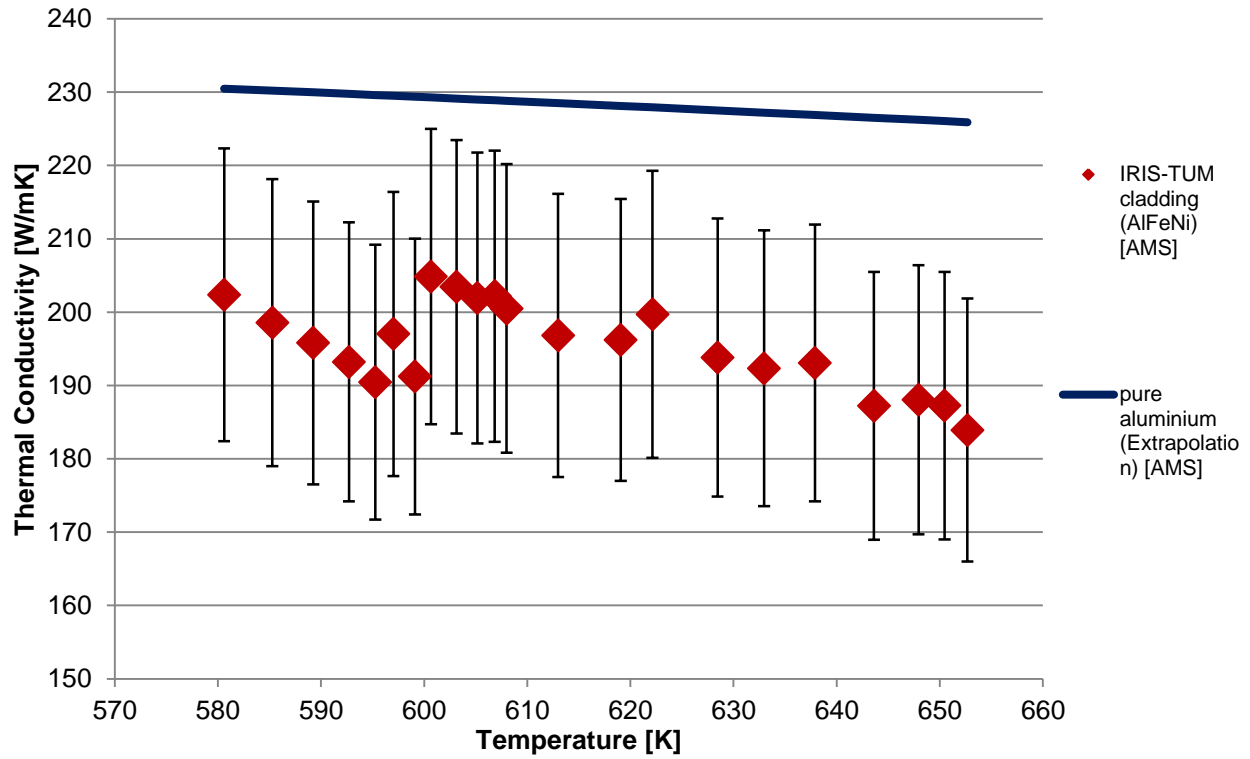


Figure 7: Thermal conductivity of IRIS-TUM Cladding (AlFeNi) compared to pure aluminium [AMS86].

The average value of the thermal conductivity of IRIS-TUM cladding made of AlFeNi in the temperature range from 580K to 660K (~310°C to ~390°C) is given by

$$\lambda(T) = (-0.18 \pm 0.04)[W/mK^2] \cdot T + (304.38 \pm 26.63)[W/mK]. \quad (4)$$

As expected for an aluminium alloy, the value for the thermal conductivity of AlFeNi is about 30W/mK lower than the value of pure aluminium.

4. Conclusion & Outlook

The amount of aluminium in the matrix and the amount of molybdenum in the UMo alloy have significant impact on the thermal conductivity of disperse UMo fuels. Furthermore, the particle shape (atomized or ground powder) causes different porosity levels, which influences the thermal conductivity to a large extent. The impact of an interdiffusion layer will be examined in the future by annealing the IRIS-TUM meat sample at temperatures up to 600°C and re-measuring the thermal diffusivity. The heat capacity and density are currently employed only as calculated values, but will be verified by measurements. The heat capacity will be measured at TUM with a Differential Scanning Calorimeter and the density will be measured with Archimedes' Method.

5. Acknowledgments

This work was supported by a combined grant (FRM0911) of the Bundesministerium für Bildung und Forschung (BMBF) and the Bayerisches Staatsministerium für Wissenschaft, Forschung und Kunst (StMWFK).

6. References

- [AMS86] John E. Hatch, Aluminum Association, American Society for Metals, 1986.
- [Boe04] K. Böning, W. Petry, A. Röhrmoser, and Chr. Morkel, In *Proceedings of the 8th International Topical Meeting on Research Reactor Fuel Management (RRFM)*, 2004.
- [Hen10] R.M. Hengstler, L. Beck, H. Breitzkreutz, C. Jarousse, R. Jungwirth, W. Petry, W. Schmid, J. Schneider, N. Wieschalla, *J. Nuc. Mat.* **402** (2010).
- [Jar09] C. Jarousse, L. Halle, W. Petry, R. Jungwirth, A. Röhrmoser, and W. Schmid, In *Proceedings of the 13th International Topical Meeting on Research Reactor Fuel Management (RRFM)*, 2009.
- [Jun10] R. Jungwirth, X. Iltis et al., In *Proceedings of the International Meeting on Reduced Enrichment for Research and Test Reactors (RERTR)*, 2010.
- [Lee00] S.-H. Lee, J.-C. Kim, J.-M. Park, H.-J. Ryu, and C.-K. Kim, In *Proceedings of the International Meeting on Reduced Enrichment for Research and Test Reactors (RERTR)*, 2000.
- [Lee09] A. Leenaers, S. van den Berghe, F. Charollais, P. Lemoine, C. Jarousse, A. Röhrmoser, and W. Petry, In *Proceedings of the International Meeting on Reduced Enrichment for Research and Test Reactors (RERTR)*, 2009.
- [Lee11] A. Leenaers, S. van den Berghe, W. Van Renterghem, F. Charollais, P. Lemoine, C. Jarousse, A. Röhrmoser, and W. Petry, *J. Nucl. Mater.* **412** (2011) 41-52
- [Par60] W. J. Parker, R. J. Jenkins, C. P. Butler, and G. L. Abbott, *J. Appl. Phys.* **32**, 1679 (1960).
- [Pet08] W. Petry, A. Röhrmoser, P. Boulcourt, A. Chabre, S. Dubois, P. Lemoine, Ch. Jarousse, J.L. Falgoux, S. van den Berghe, and A. Leenaers, In *Proceedings of the 12th International Topical Meeting on Research Reactor Fuel Management (RRFM)*, 2008.
- [Ren09] W. van Rentergham, A. Leenaers, S. van den Berghe, M.-C. Anselmet, F. Charollais, P. Lemoine, and W. Petry, In *Proceedings of the International Meeting on Reduced Enrichment for Research and Test Reactors (RERTR)*, 2009.
- [Roe04] A. Röhrmoser, W. Petry, K. Böning, and N. Wieschalla, In *Proceedings of the 8th International Topical Meeting on Research Reactor Fuel Management (RRFM)*, 2004.
- [She98] M. Sheindlin, D. Halton, M. Musella, C. Ronchi, *Rev. Scient. Instr.* **69**, 1426 (1998).



European Nuclear Society
Rue Belliard 65
1040 Brussels, Belgium
Telephone: +32 2 505 30 50 - FAX: +32 2 502 39 02
rrfm2012@euronuclear.org
www.rrfm2012.org